

Graduate School for Cellular and Biomedical Sciences

University of Bern

Development of Synthetic Research Tools for Structural and Functional Studies of Mitochondrial Carriers and Other Membrane Proteins

PhD Thesis submitted by

Philipp Grossenbacher

for the degree of

PhD in Biochemistry and Molecular Biology

Supervisor

PD Dr. Martin Lochner

Institute of Biochemistry and Molecular Medicine

Faculty of Medicine of the University of Bern

Co-advisor

Prof. Dr. Christoph von Ballmoos

Department of Chemistry, Biochemistry and Pharmaceutical Sciences

Faculty of Science of the University of Bern



Accepted by the Faculty of Medicine, the Faculty of Science and the Vetsuisse Faculty of the University of Bern at the request of the Graduate School for Cellular and Biomedical Sciences

Bern,

Dean of the Faculty of Medicine

Bern,

Dean of the Faculty of Science

Bern,

Dean of the Vetsuisse Faculty Bern

Abstract

Calcium signalling mediates many physiological functions such as regulating cell death/ survival, cell proliferation/ differentiation and gene expression. The calcium signals within cells originate in a release of bivalent calcium cations (Ca^{2+}) from the endoplasmic reticulum (ER), which is the main store of intracellular calcium. The endoplasmic reticulum is a highly dynamic structure within the cell and can tether itself to the plasma membrane or membranes of other organelles in the cell such as the mitochondrion. Even though it is already established that a rise in the intracellular Ca^{2+} concentration signals an increased energy demand, the many relationships between the calcium concentration and the energy metabolism remain unknown.

With the aim to reveal individual players in the calcium regulation pathway and gain insight into their function, different strategies were envisioned as part of a SNF funded Sinergia project, which involves multiple project partners. Two of the envisioned chemical biology strategies involved synthesis of chemical tools. The first strategy required fluorescent antibodies against targets of the calcium signalling/communication machinery for fluorescence microscopy and western blot applications. The second strategy entailed ligands to stabilise the conformation of a Ca^{2+} -controlled mitochondrial solute carrier (mSLC), in order to solve the structure of this particular mSLC by cryo-EM. We designed and synthesised compounds that allow for easy and functional modification of antibodies, rendering them fluorescent whilst remaining functional for fluorescence microscopy and western blot experiments. Furthermore, we have developed synthetic ligands that stabilise a particular conformation of the highly dynamic mSLC Citrin (AGC2, SLC25A13) to aid determination of its structure by cryo-EM.

In several parallel projects, various tool compounds and probes for biochemical investigations were synthesised and biologically evaluated. This comprises inhibitors of the parasite *Echinococcus multilocularis*, pH-dependent fluorescent probes for proteoliposomes and giant unilamellar vesicle (GUV) applications, trifunctional bioorthogonal probes for proteomic and target identification studies, store-operated calcium entry (SOCE) inhibitors and positive allosteric modulators of the G protein-coupled adenosine A_1 receptor.

*There's so much to explore
 There's so much to absorb
And then the atoms that you borrowed
 They are returned to the cosmos*

The One True Colour - Enter Shikari

Danksagung

Mein grösster Dank geht an Martin: Ich danke Dir, dass Du mich in unsicheren Zeiten in Deine Gruppe aufgenommen hast. Den Freiraum und das Vertrauen, dass ich erleben durfte, haben mich massgeblich geprägt und reifen lassen. Viele neue Situation und Veränderungen haben uns vor unerwartete Herausforderungen gestellt, die wir durch grossartige Teamarbeit überwinden konnten. Für Deine wertvolle Unterstützung, wenn immer diese nötig war, bedanke ich mich bei Dir.

Weiter möchte ich mich bei meinem restlichen Thesis Komitee bedanken. Prof. Dr. Christoph von Ballmoos als mein Ko-Betreuer, hat mir immer wieder neue Inputs gegeben und auch zu guten Kollaborationen angeregt. PD Dr. Cristina Müller, als externe Referentin, hat sich die Zeit genommen meine Arbeit zu begutachten und zu evaluieren. Ein weiterer Dank geht an Prof. Dr. Benjamin Gantenbein, der mir als Mentor zugeteilt wurde.

Ein grosses Danke geht and meine Kolleg:innen im IBMM, die mich tatkräftig bei den Themen unterstützten, die ich mit meinem organisch-chemischen Hintergrund noch erlernen musste. Ein grosser Dank an Stefanie Häusler, Maria Essers, Simon Singer & Jean-Sébastien Rougier. Aber natürlich auch an alle anderen Mitarbeiter des IBMMs und des DCBPs, die immer mit Rat und Tat zur Seite standen.

Also, my colleagues in Cambridge shall be thanked, Denis Lacabanne and Edmund Kunji. The collaboration with you was a delight, and I hope that we will continue to work on this fruitful project.

Bei der Gruppe von Britta Lundström-Stadelmann möchte ich mich ganz herzlich bedanken. Trotz einigen Corona bedingten Hürden haben wir es geschafft, vielversprechende Resultate zu generieren. Vielen Dank an Britta Lundström-Stadelmann, Tanja Karpstein, Marc Kaethner, Roman Memedovski, Tobias Kämpfer, Sheena Chaudhry, Matías Preza & Lea Hiller.

Auch der von Ballmoos Gruppe, insbesondere Roman Mahler und Nicolas Dolder, möchte ich danken. Die Zusammenarbeit mit euch war grossartig, und hat mir die Möglichkeit gegeben, neue, komplett andersartige Synthesen zu versuchen.

Ein sehr grosser Dank geht an die Mitglieder der Lochner Gruppe. Vor allem an Luca Dick, mit dem ich die längste Zeit im Labor verbringen, und einige Hochs und Tiefs erleben durfte. Weiter danke ich Achille Schild, Christian Gerber und Jérôme Fischer, den aktuellen Gruppenmitgliedern, sie alle trugen massgeblich zu einer guten Stimmung inner- und ausserhalb des Labors bei. Auch den ehemaligen Gruppenmitgliedern insbesondere Dominic Tscherrig möchte ich danken. Auch den Lernenden, die ich betreuen durfte, gebührt Dank. Jessica Balsiger, Mike Liechti & Nika Tschanz, es war eine Freude mit

euch zu arbeiten, und euch kontinuierlich fortschreiten zu sehen. Dasselbe gilt auch den unzähligen Studierenden und Praktikant:innen, die ich während meiner Arbeit begleiten durfte.

Natürlich danke ich auch meinen Freunden und der Familie, allen voran Vivi: Du warst immer für mich da, konntest mit all meinen mäandernden Gefühlszuständen umgehen und hast mich unterstützt und abgelenkt, wo es nötig war. Hier geht auch ein besonderer Dank an Severin Martz: Zu zweit etwas durchzustehen ist immer einfacher, als allein dazustehen. In dem Sinne haben wir uns gegenseitig immer wieder Motivation und Courage zugesprochen.

Abbreviations

A1R	Adenosine A ₁ receptor
AB	Albendazole
ADC	Antibody drug conjugates
ADP	Adenosine diphosphate
ADPN	Arylene dipropiolonitriles
AGC	Aspartate glutamate carrier
AM	Acetoxymethyl
ATP	Adenosine triphosphate
BFL	BODIPY-FL
Bn	Benzyl
Boc	<i>tert</i> -Butyloxycarbonyl
Brine	Saturated solution of NaCl in water
bs	Broad signal (NMR)
BSA	Bovine serum albumin
Cbz	Benzyl carbonochloridate
Cmpd	Compound
CPM	7-Diethylamino-3-(4'-maleimidylphenyl)-4-methylcoumarin
c-state	Carrier conformation open to cytoplasm
CuAAC	Copper catalysed azide-alkyne cycloaddition
D	Dextro
DAR	Drug-to-antibody ratio
dc	Direct concentration
DCBP	Department of Chemistry, Biochemistry and Pharmaceutical Sciences
DCC	<i>N,N'</i> -Dicyclohexylmethanediimine
DCE	1,2-Dichloroethane
DIPEA	<i>N,N</i> -Diisopropylethylamine
DMF	<i>N,N</i> -Dimethylformamide
DMSO	Dimethylsulfoxid
DTT	1,4-Dithiothreitol
<i>E. multilocularis</i>	<i>Echinococcus multilocularis</i>
EI	Electron ionisation
EmPGI	<i>E. multilocularis</i> phosphoglucose isomerase
EmTDH	<i>E. multilocularis</i> threonine dehydrogenase
ER	Endoplasmic reticulum
ESI	Electrospray ionisation
GAPDH	Glyceraldehyde-3-phosphate dehydrogenase
GUV	Giant unilamellar vesicles
HATU	1-[Bis(dimethylamino)methylene]-1 <i>H</i> -1,2,3-triazolo[4,5- <i>b</i>]pyridinium 3-oxide hexafluorophosphate
HC	Heavy chains (antibody)
HPLC	High performance liquid chromatography
KBL	ketobutyrate CoA ligase
L	Levo
LC	Light chains (antibody)

LHMDS	Lithium bis(trimethylsilyl)amide
mpc	Mitochondrial pyruvate carrier
MS	Mass spectrometry
mSLC	Mitochondrial solute carrier
m-state	Carrier conformation open to mitochondrial matrix
NAD⁺	Nicotinamide adenine dinucleotide in oxidised form
NADH	Nicotinamide adenine dinucleotide in reduced form
NHS	<i>N</i> -Hydroxysuccinimide
NMR	Nuclear magnetic resonance
np	No product
PB	Pacific Blue
PGI	Phosphoglucose isomerase
Qc	Quinazolinecarboxamide
quant.	Quantitative yield
rm	Reaction mixture
rpc	Reverse phase column chromatography
rt	Room temperature
SDS-PAGE	Sodium dodecyl sulphate polyacrylamide gel electrophoresis
SiR	Silicon rhodamine
SNF	Swiss national science foundation
SOCE	Store-operated calcium entry
TBAF	Tetrabutylammoniumfluoride
<i>t</i>-BuOK	Potassium <i>tert</i> -butoxide
TCEP	Tris-(2-carboxyethyl)-phosphine
TDH	Threonine dehydrogenase
TFA	Trifluoroacetic acid
THF	Tetrahydrofuran
TLC	Thin-layer chromatography
TMS	Tetramethylsilane
TRPV	Transient receptor potential cation channel subfamily V
TSA	Thermal shift assay
UV	Ultraviolet
γ-BenGlu	L-glutamic- γ -benzyl ester

Table of Contents

1. Bioorthogonal site-selective conjugation of fluorescent dyes to antibodies: method and potential applications	1
1.1. Introduction	3
1.2. Results and discussion	5
1.3. Conclusions	13
1.4. Experimental section	13
1.5. Supplementary Information.....	23
2. Developing small molecule ligands to stabilise mitochondrial aspartate/ glutamate carrier	67
2.1. Introduction	67
2.2. Aim of this work	76
2.3. Methods and results	77
2.4. Conclusion and outlook	104
2.5. Experimental.....	107
3. Development of various molecular tools.....	255
3.1. New compounds against Echinococcus multilocularis	255
3.2. pH-Dependent fluorophores.....	310
3.3. Trifunctional probe	341
3.4. New SOCE inhibitors	362
3.5. MIPS-521	373
4. Functional design of bacterial superoxide: quinone oxidoreductase	377
5. Summary, conclusion, and outlook.....	400
6. Bibliography	403
7. Curriculum Vitae	A
8. Declaration of Originality	D

1. Bioorthogonal site-selective conjugation of fluorescent dyes to antibodies: method and potential applications

Philipp Grossenbacher,^a Maria C. Essers,^a Joël Moser,^b Simon A. Singer,^a Stephanie Häusler,^c Bruno Stieger,^c Jean-Sébastien Rougier^a and Martin Lochner^{*a}

^aInstitute of Biochemistry and Molecular Medicine, University of Bern, Bühlstrasse 28, 3012 Bern, Switzerland

^bDepartment of Chemistry, Biochemistry and Pharmaceutical Sciences, University of Bern, Freiestrasse 3, 3012 Bern, Switzerland

^cDepartment of Clinical Pharmacology and Toxicology, University Hospital Zurich, University of Zurich, Rämistrasse 100, 8091 Zürich, Switzerland

Keywords: antibodies; fluorescent dyes; Si-rhodamine; synthetic organic chemistry; bioorthogonal conjugation; disulphide bonds; Western blot; immunofluorescence.

Contribution to this study

I was deeply involved in the conception, design, and execution of all the experiments. I performed all post-processing and data analysis, and as first author wrote major parts of the manuscript and prepared all figures. For detailed author contributions see Author contributions.

This work was published in *RSC Advances*: **2022**, 12, 28306-28317, <https://doi.org/10.1039/D2RA05580E>.

Abstract

Antibodies are immensely useful tools for biochemical research and found application in numerous protein detection and purification methods. Moreover, monoclonal antibodies are increasingly utilised as therapeutics or, conjugated to active pharmaceutical ingredients, in targeted chemotherapy. Several reagents and protocols are reported to synthesise fluorescent antibodies for protein target detection and immunofluorescence applications. However, most of these protocols lead to non-selective conjugation, over-labelling or in the worst case antigen binding site modification. Here, we have used the antibody disulphide cleavage and re-bridging strategy to introduce bright fluorescent dyes without loss of the antibody function. The resulting fluorescent IgG1 type antibodies were shown to be effective imaging tools in Western blot and direct immunofluorescence experiments.

1.1. Introduction

The use of antibody drug conjugates (ADCs) has seen a substantial rise in recent times. They offer precise treatment options with less side effects, as the payload is guided by the antibody to its specific target.¹ In the wake of this development, various techniques have been established, moving from highly heterogenic mixtures to precise homogenous conjugate constructs using monoclonal antibodies with specified drug-to-antibody ratio (DAR) and controlled sites of attachment. For instance, unnatural amino acids can be used to engineer bioorthogonal functional groups into the monoclonal antibody, which subsequently enable site-selective and efficient coupling reactions with a variety of modified drugs.²

Traditionally, native antibody modifications have relied on the chemical reactivity of amino acid side chains, and numerous chemical reagents and methods have been developed to conjugate drug molecules to such reactive groups (e.g. the primary amine group of lysine residues).³ Such chemical reagent-based methods often produce heterogeneous mixtures of modified antibodies and involve the risk of over-labelling and altering the antigen binding sites, which results in inactive antibody conjugates. Alternatively, more recent strategies entail the targeting of glycans in native antibodies to guide modifications away from the antigen binding sites.⁴ Thiols are useful functional groups for protein bioconjugation as they react efficiently with widely used and available maleimides. Thiol-containing antibodies can be obtained through cysteine-engineering⁵ or generated by full or partial reduction of disulphide bonds, and reacted site-specifically with maleimide reagents.² A potential drawback of maleimide conjugates is their propensity to undergo retro-Michael addition reactions and transfer their payload onto plasma thiols.⁶ Another viable approach is to specifically target the interchain disulphide bonds, in particular in IgG1 antibodies. In this subtype, four solvent-accessible disulphide bonds can be cleaved by mild, biocompatible reducing agents (e.g. TCEP or DTT) and then re-bridged using various bis-reactive cysteine reagents that carry the payload or functional groups for subsequent conjugation reactions.^{2, 4} Several re-bridging strategies and agents have been developed, including bissulfones,^{7, 8} divinylsulfonamides,⁹ arylene dipropionitriles (ADPN),¹⁰ dibromomethyl heterocycles (C-LockTM),¹¹ dichloroacetone,¹² next-generation maleimides,¹³⁻¹⁵ pyridazinediones¹⁶⁻²² and divinylpyrimidines.²³⁻²⁵

Immunofluorescence applications in general require fluorescently labelled antibodies. Detection of the cellular target can either be achieved directly, using a primary labelled antibody, or indirectly, by using a secondary labelled antibody that recognises the primary (unlabelled) one. Numerous commercial suppliers offer primary or secondary fluorescently labelled antibodies that were raised in different species. The selection of the primary antibody is one of the most important steps to achieve

successful experimental outcome in Western blot and immunofluorescence applications. Despite the wide variety of commercial antibodies, in many cases antibodies against a specific protein of interest are not available and first have to be generated, validated, and depending on the intended application, fluorescently labelled.

The common workflow in immunofluorescence includes the use of a primary antibody that binds specifically to the cellular target, followed by detection of the primary antibody with a fluorescently labelled secondary antibody. While this method works for most applications, there are limitations that negatively affect experimental outcome (**Table 1**). Direct immunofluorescence can provide an alternative in such situations; however, it does not come without technical issues either (**Table 1**).

Method	Advantages	Disadvantages
<i>Direct immunofluorescence</i>	<ul style="list-style-type: none"> • Simplified workflow and shorter sample staining time • No cross-reactivity between secondary antibodies • Best solution for specific staining of multiple targets 	<ul style="list-style-type: none"> • Lower sensitivity for low-abundance targets with limited number of fluorescent dyes that can be attached to primary antibody • Limited number of commercially available fluorescently labelled primary antibodies
<i>Indirect immunofluorescence</i>	<ul style="list-style-type: none"> • Greater sensitivity for low-abundance targets due to signal amplification by secondary antibodies • Numerous inexpensive secondary antibodies commercially available with various dyes and tags attached 	<ul style="list-style-type: none"> • Cross-reactivity between secondary antibodies, in particular when performing multilabel experiments • Reaction of secondary antibodies with endogenous immunoglobulins leading to high background fluorescence

Table 1 Advantages and disadvantages of direct and indirect immunofluorescence

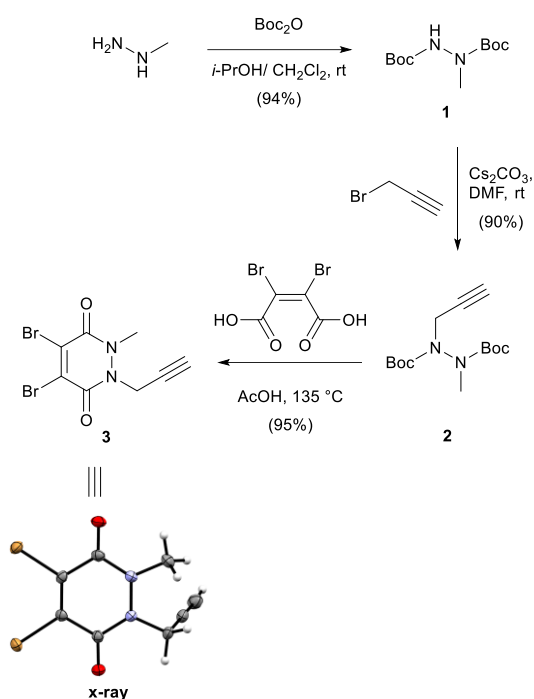
The goal of our study was to provide a practical method to site-specifically label native antibodies with bright fluorescent dyes by targeting the solvent-accessible interchain disulphide bonds. In most

examples such conjugations have been shown on monoclonal IgG1 therapeutic antibody trastuzumab (Herceptin®),^{9, 13-21, 24} and recently monoclonal IgG4 magacizumab.²² In this work, we explored if the modification approach is more widely applicable to other mono- and polyclonal IgG1 antibodies and validated the fluorescently labelled products in Western blot and direct immunofluorescence applications.

1.2. Results and discussion

Chemistry

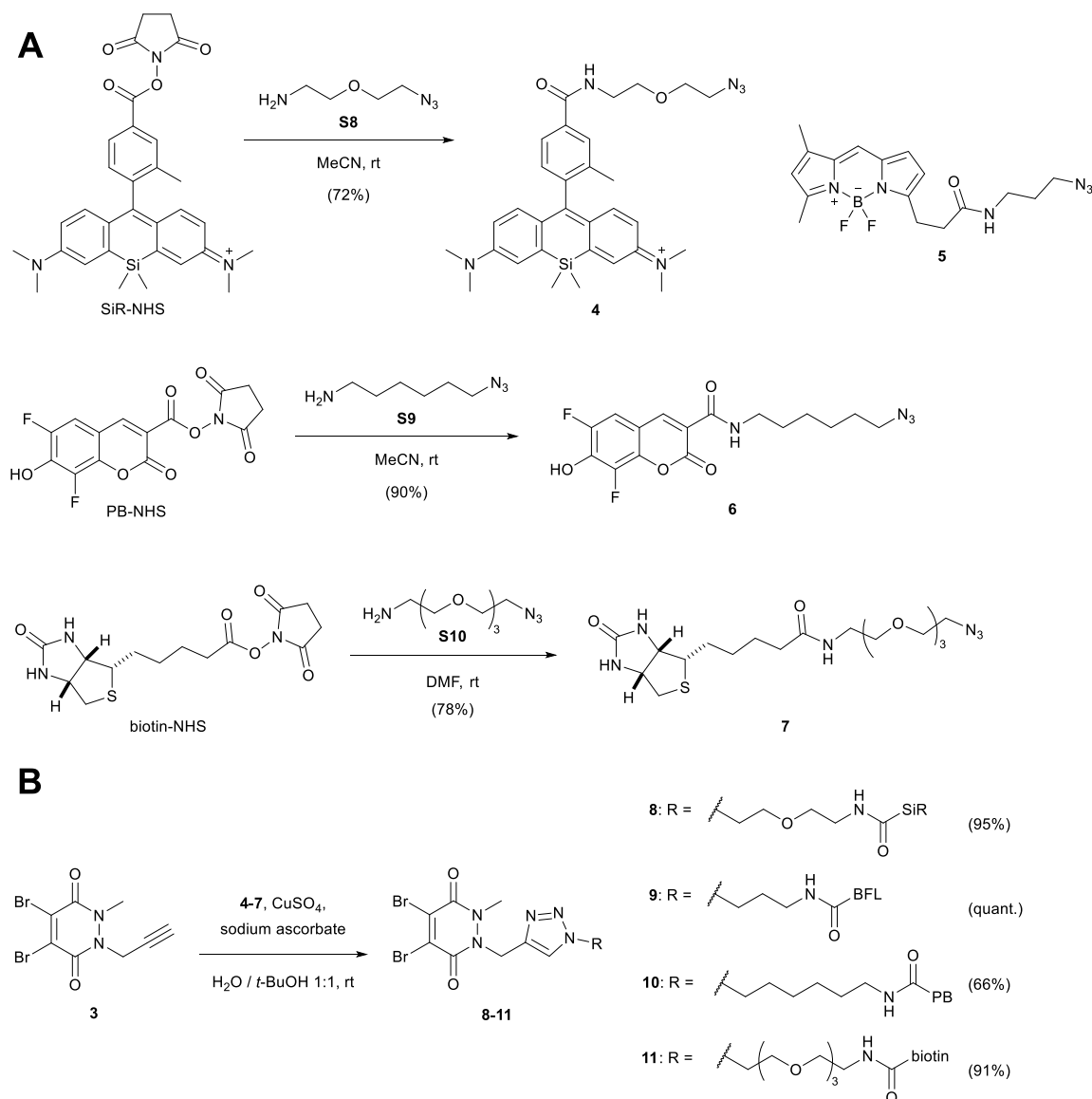
We first synthesised small and versatile re-bridging agent **3**, featuring an alkyne clickable handle for fluorescent dye conjugation, by adapting synthetic routes published for very similar dibromopyridazinediones.^{18, 20, 26, 27} Methylhydrazine was first Boc-protected and then alkylated with propargyl bromide on the remaining free carbamate nitrogen (**Scheme 1**).



Scheme 1 Synthesis of propargyl dibromopyridazinedione **3** and x-ray structure thereof.

This was followed by a one-pot deprotection and cyclisation reaction by heating bis-carbamate **2** with dibromomaleic acid in acetic acid at refluxing temperature.²⁰ Overall, this synthetic route delivered dibromopyridazinedione **3** in 80% yield over three steps as a crystalline solid. We were able to obtain a crystal structure of **3** to confirm the identity of the compound (**Scheme 1**).

We then attached various azido linkers via activated *N*-hydroxysuccinimid (NHS) esters to different fluorescent dyes that emit bright light in the red/far-red (Si-rhodamine, SiR)²⁸ or blue region (Pacific Blue, PB), or to biotin (**Scheme 2, A**). Azide **5** with a bright emission in the green region (BODIPY FL, BFL) was purchased from a commercial supplier.



Scheme 2 A) Attachment of linkers to fluorescent dyes and biotin. **B)** CuAAC-coupling with alkyne dibromopyridazinedione **3**. For the synthesis of SiR-NHS (Scheme S1), biotin-NHS and the azide linkers **S8-S10** see ESI[†]. PB-NHS was commercially available. SiR, Si-rhodamine; PB, Pacific Blue; BFL, BODIPY FL.

The resulting constructs **4-7** were then coupled to pyridazinedione alkyne **3** using standard Cu-catalysed alkyne-azide cycloaddition (CuAAC) conditions, which gave the final re-bridging agents **8-11** in good to very good yields.

Originally, our synthetic plan was to couple the SiR dye with alternative dibromopyridazinediones via NHS-activated esters, rather than using CuAAC coupling chemistry (Scheme S2, ESI[†]). Even though the amide forming reactions were successful, one bromine atom was displaced by the NHS leaving group. We therefore speculate that this side reaction might be a potential generic risk when working with dibromopyridazinediones in the presence of NHS-activated esters, although these undesired products might still work as re-bridging agents.

Anti GAPDH antibody modification

Glyceraldehyde-3-phosphate dehydrogenase (GAPDH) is a key enzyme in the glycolytic pathway. It catalyses the conversion of glyceraldehyde-3-phosphate to 1,3-bisphosphoglycerate in the presence of NAD⁺ and inorganic phosphate. In biochemistry labs, GAPDH is commonly used as house-keeping gene in semi-quantitative or quantitative studies to confirm expression or suppression of proteins of interest in proteomic or genetic studies. Apart from its practical utility and important role in carbohydrate metabolism, several studies have shown that GAPDH also binds single-stranded DNA and in some cases acts as a transcription factor.²⁹ Furthermore, GAPDH can initiate apoptosis but can also function as a mediator of cell survival. Other studies thus point to the fact that GAPDH could be an important marker in age-related neurodegenerative diseases, prostate cancer, and viral diseases.^{30,}

31

For the initial antibody conjugation experiments, we chose a commercially available monoclonal anti GAPDH loading control antibody and followed the reported disulphide re-bridging protocol²⁰ with some slight experimental modifications. The anti GAPDH antibody was incubated with TCEP (10 equiv.) and excess (20 equiv.) dibromopyridazinedione re-bridgers **8-11** in borate buffered saline (BBS) at 4°C overnight (**Figure 1, A**). Isolation of the modified antibodies was conveniently achieved by using spin filter columns. Figures 1B and 1C show a representative analysis of the SiR-modified anti GAPDH antibody by SDS-PAGE. Two strongly fluorescent bands at 25 kDa and 50 kDa were detected, which correspond to the fluorescently labelled light and heavy chains, respectively (**Figure 1, B** lane C-AB).

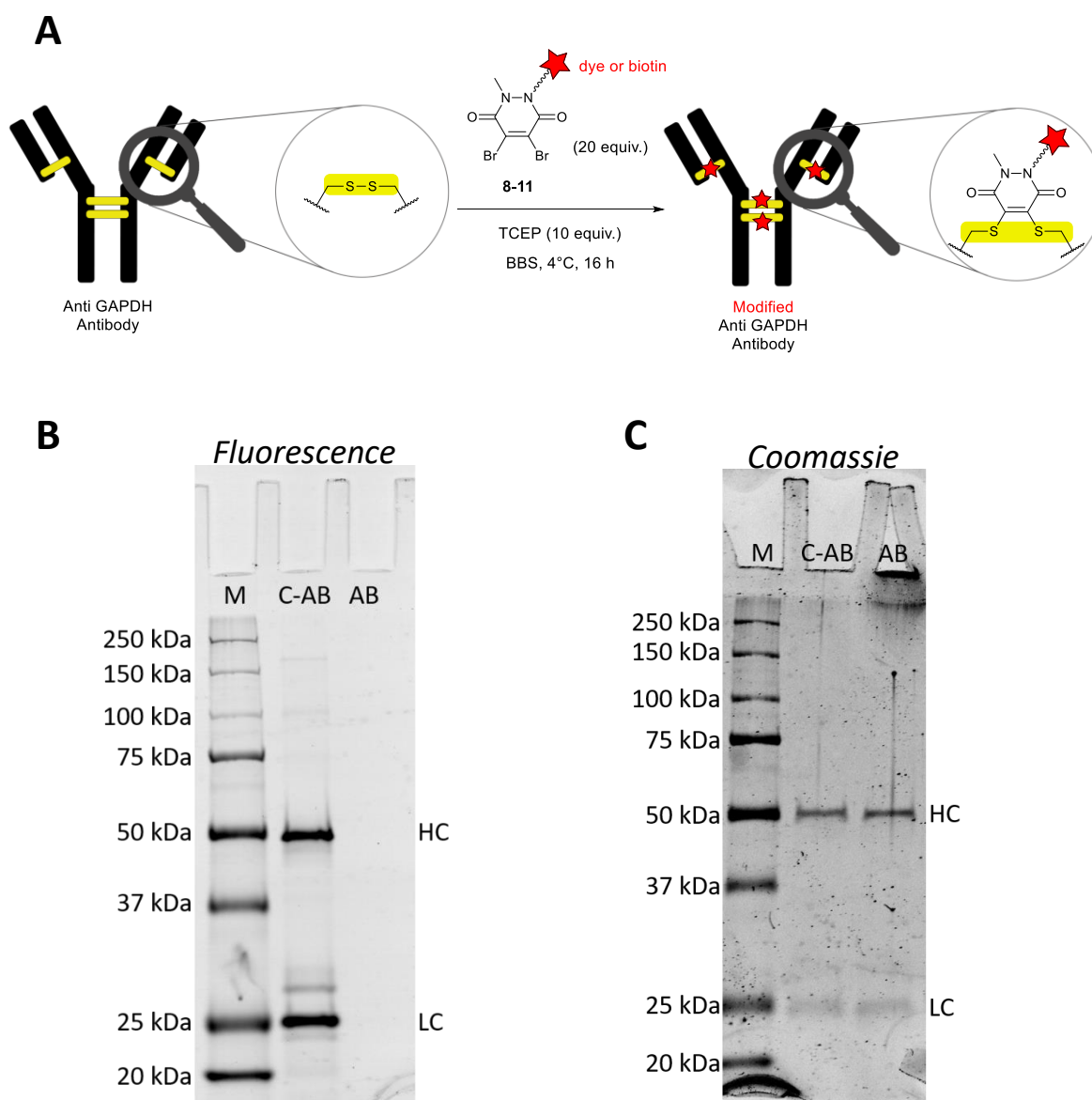


Figure 1 **A)** Modification of anti GAPDH antibody by disulphide bond cleavage and re-bridging with dibromopyridazinediones **8-11**. **B)** Representative SDS-PAGE (reducing conditions) of conjugation reaction of anti GAPDH antibody with SiR-labelled **8**. Detection of protein bands by fluorescence (excitation at 635 nm, Cy5 channel). Bands at 50 kDa and 25 kDa correspond to the heavy (HC) and light chains (LC), respectively. **C)** SDS-PAGE as in **B)**, stained with Coomassie blue dye. Loading concentration of C-AB for in-gel fluorescence **B)** was tenfold lower than for Coomassie gel **C)** to avoid oversaturation of the fluorescence detector. Lanes: M, All Blue Protein Standard; C-AB, SiR-conjugated anti GAPDH antibody; AB, native anti GAPDH antibody.

During the reductive and denaturing SDS-PAGE sample preparation (using 10% mercaptoethanol in the loading buffer and heating), excess thiol presumably leads to disulphide cleavage and antibody fragmentation. The same two bands at 25 kDa and 50 kDa were also detected when a native anti GAPDH antibody sample was prepared analogously for SDS-PAGE and stained with Coomassie (**Figure 1, C** lane AB). Omitting the mercaptoethanol in the SDS-PAGE loading buffer for the SiR-conjugated antibody sample resulted in several fluorescent bands at very high molecular weight at around 250 kDa (Figure S1, ESI[†]), most probably resulting from incomplete linearisation and aggregation. We

therefore deemed the non-reducing SDS-PAGE conditions as less suitable for conjugation reaction control. Due to the very bright fluorescence of the SiR dye, the conjugated antibody SDS-PAGE sample had to be diluted down tenfold to avoid oversaturation of the fluorescence detector (**Figure 1, B**). It is worth noting that at this low sample concentration Coomassie staining was almost unable to detect the same protein bands.

In addition to SDS-PAGE analysis, we have used size exclusion chromatography (SEC) to characterise the antibody conjugation products. The SEC traces of BFL-modified anti GAPDH antibody after re-bridging with dibromopyridazinedione **9** show the same peaks with very similar retention times as SEC traces of native anti GAPDH antibody (Figure S2). This leads us to conclude that the antibody remains intact and a fully re-bridged antibody is obtained. Consequently, it is more likely that the fragmentation of the modified antibodies occurs during the reductive SDS-PAGE sample preparation.

Validation of modified GAPDH antibody and immunofluorescence

To assess the specificity of the modified anti GAPDH antibodies, they were tested in Western blot applications, using mouse cardiomyocytes whole cell lysates (**Figure 2**). After incubation and blotting, SiR- and BFL-modified antibodies were detected directly by fluorescence emission (**Figure 2, A and B**), whereas biotin-modified antibody was visualised by complexing with a streptavidin-Cy5 construct (**Figure 2, C**). In all cases a strong band at around 36 kDa was detected, which is in good agreement with the calculated molecular weight of mouse GAPDH (35.81 kDa).³²

For comparison, we have employed a classical antibody modification method and stochastically modified anti GAPDH antibody with electrophilic, fluorescent reagent SiR-NHS. SDS-PAGE analysis of this directly labelled antibody product revealed the same fluorescent bands for the light and heavy chains (Figure S3A), as for SiR-modified anti GAPDH antibody obtained by re-bridging with dibromopyridazinedione **8** (**Figure 1, B**). It was noticeable, however, that the fluorescence intensity of the directly labelled antibody was markedly lower than of the re-bridged antibody. More importantly, the directly SiR-labelled antibody failed to detect its antigen GAPDH in whole cell lysate (Figure S3B).

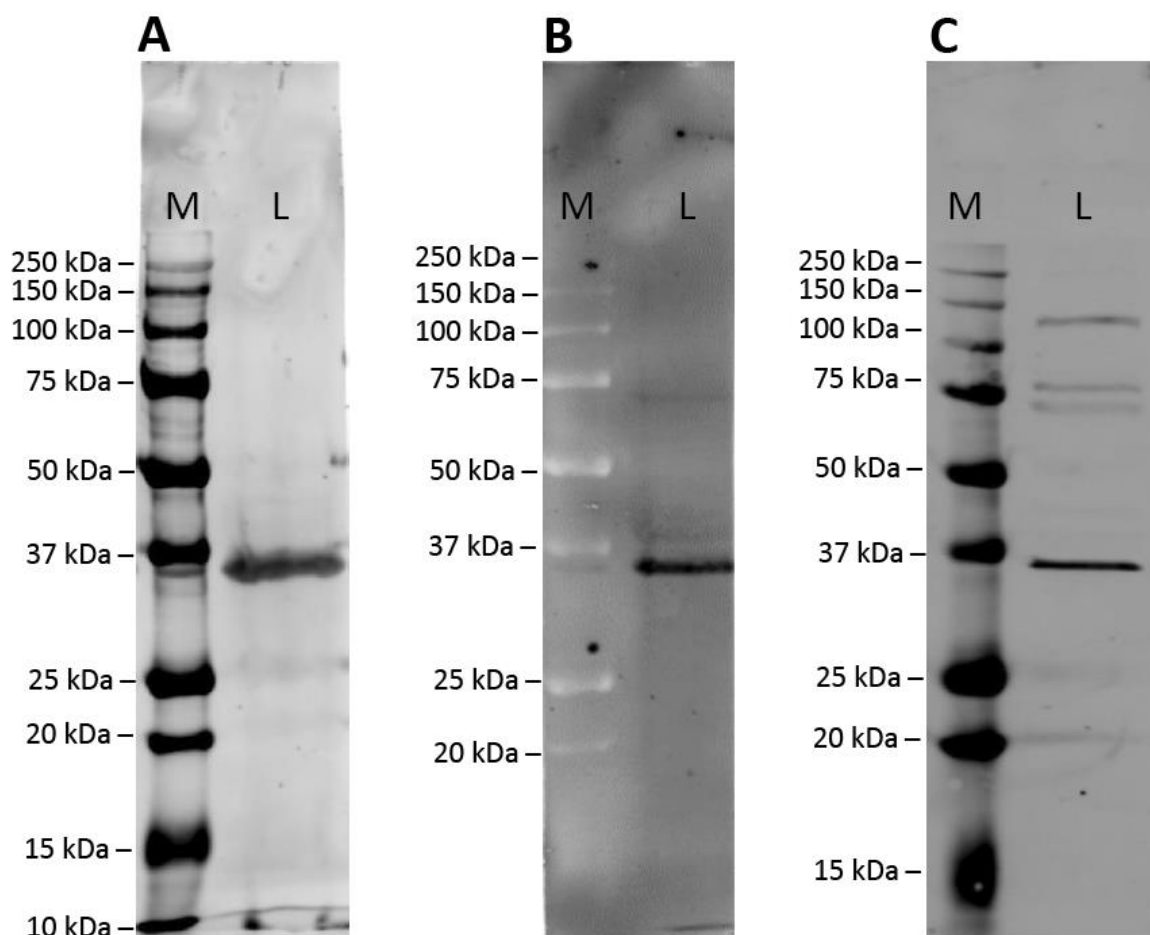


Figure 2 Western blot analysis of mouse cardiomyocyte whole cell lysate using **A**) SiR-modified, **B**) BFL-modified or **C**) biotinylated anti GAPDH antibody. Antibodies were detected directly by fluorescence (**A** and **B**; Cy5 and FITC channel, respectively) or indirectly by complexing with streptavidin-Cy5 construct **C**). The band at 36 kDa corresponds to the molecular weight of mouse GAPDH. Lanes: M, Marker; L, Lysate.

The modified antibodies were then further assessed for their labelling utility in immunofluorescence experiments (**Figure 3**). The images show isolated and fixed mouse cardiomyocytes incubated with modified and native anti GAPDH antibodies. Direct immunofluorescence with SiR- and BFL-conjugated antibodies clearly showed the cytosolic localisation of GAPDH in cardiomyocytes (**Figure 3, A and D**, respectively) compared to control (**Figure 3, C**). Alternatively, labelling with biotinylated antibody and subsequent incubation with streptavidin-Cy5 fusion construct gave the same staining pattern (**Figure 3, B**). Direct immunofluorescence staining was very similar to classical indirect immunofluorescence, using primary native anti GAPDH antibody and fluorescently labelled secondary anti mouse antibody (**Figure 3, E**). In another indirect immunofluorescence control experiment, we have used anti GAPDH antibody, which was re-bridged with alkyne dibromopyridazinedione **3**, as primary antibody and a fluorescent secondary anti mouse antibody for staining (**Figure 3, F**). In this case the staining was again

similar, albeit less strong, compared with direct (**Figure 3, D**) or indirect immunofluorescence (**Figure 3, E**).

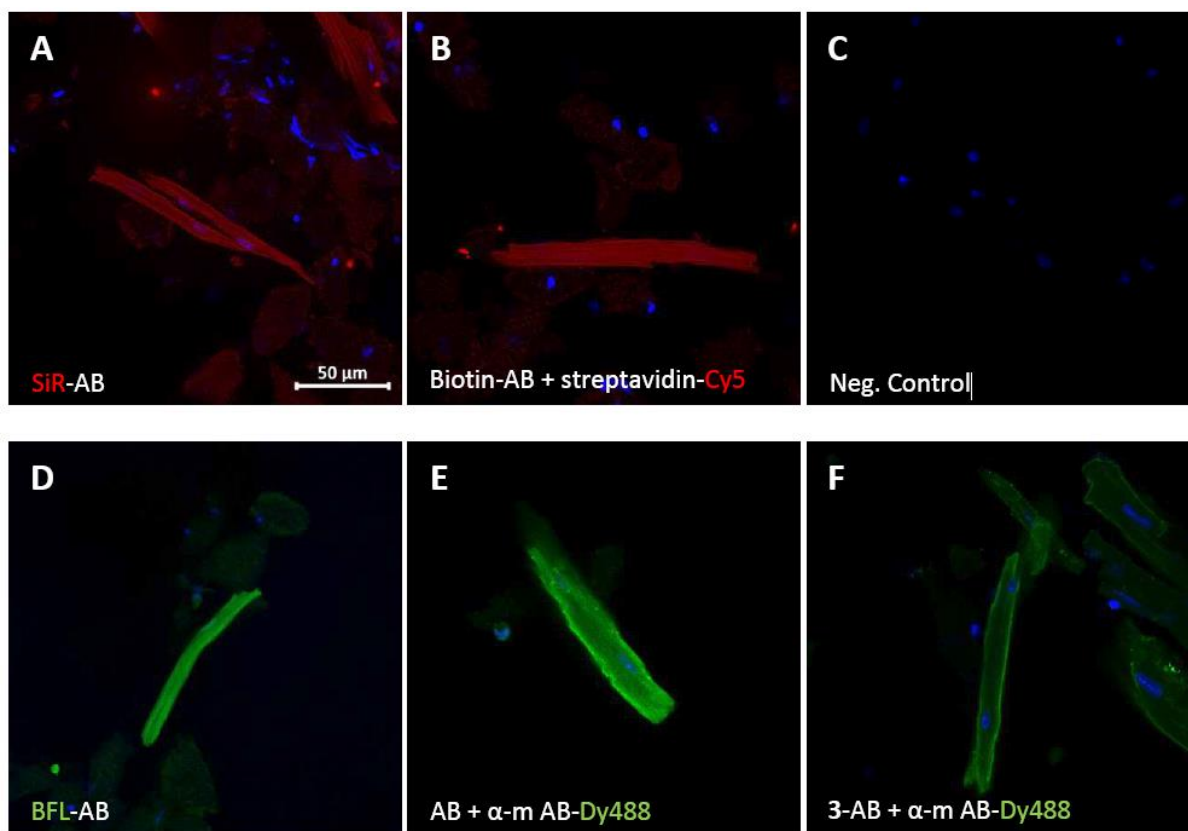


Figure 3 Direct (**A, D**) and indirect (**B, E, F**) immunofluorescence with isolated and fixed mouse cardiomyocytes using conjugated and native anti GAPDH antibodies. **A)** SiR-modified and **B)** biotinylated anti GAPDH antibody. **C)** Negative control (DAPI and Cy5 Scan). **D)** BFL-modified and **E)** native anti GAPDH antibody. **F)** Anti GAPDH antibody re-bridged with alkyne dibromopyridazinedione **3**. Detection of antibodies by fluorescence (**A** and **D**; Cy5 and FITC channel, respectively), by complexing with streptavidin-Cy5 construct **B)** or by secondary goat anti mouse Dy488-labelled antibodies (**E** and **F**). Cell nuclei were stained with DAPI. SiR, Si-rhodamine; BFL, BODIPY FL; Dy488, DyLight® 488; AB, anti GAPDH antibody; α-m AB, anti mouse antibody. Scale bar represents 50 μm.

Modification of other IgG antibodies

We explored the general applicability of the fluorescence modification method with other commercially available or custom-generated IgG antibodies. The targeted antigens included a cytoskeletal protein (β -actin), cardiac ion channels ($\text{Na}_v1.5$, $\text{Ca}_v1.2$, Transient receptor potential cation channel subfamily M member 4 (TRPM4)) and a transmembrane ion pump (Na^+/K^+ -ATPase). The respective IgG antibodies were conjugated with re-bridgers **8** or **9** according to the method shown in **Figure 1, A** and evaluated in Western blot and direct immunofluorescence experiments (**Table 2**).

Entry	Antigen	Antibody Type ^a	Tag ^b	Western Blot ^c	Direct Immunofluorescence ^c
1	GAPDH	IgG1 (m, mc)	SiR	Y	Y
2	GAPDH	IgG1 (m, mc)	BFL	Y	Y
3	GAPDH	IgG1 (m, mc)	Biotin	Y	Y
4	GAPDH	IgG1 (m, mc)	PB	- ^d	- ^d
5	β -Actin	IgG1 (m, mc)	SiR	Y	Y
6	Na _v 1.5	- ^e	BFL	N	Y
7	Ca _v 1.2	IgG ^f (r, pc)	SiR	- ^g	Y
8	Na ⁺ /K ⁺ -ATPase	IgG1 (m, mc)	SiR	N	Y
9	TRPM4	IgG ^f (r, pc)	SiR	Y	N ^h

Table 2 Summary of produced IgG antibody conjugates and their evaluation in Western blot and direct immunofluorescence experiments. ^am, mouse; r, rabbit; mc, monoclonal; pc, polyclonal. ^bSiR, Si-rhodamine; BFL, BODIPY FL, PB, Pacific Blue. ^cY, specific detection or staining of antigen; N, no detection or staining of antigen. ^dSuitable detection system was not available. ^eNo information available from supplier. ^fSubtype(s) not known. ^gWestern blot not attempted with SiR-modified antibody, as native antibody did not give signal. ^hNative antibody did also not give specific staining in indirect immunofluorescence with secondary fluorescent antibody. Experiments in mouse heart sections showed similar inconclusive results for both SiR-modified and native anti TRPM4 antibodies.

In all examples, successful conjugation of fluorescent tags SiR or BFL was evident based on SDS-PAGE of the isolated antibody modification products (Figure S4, ESI[†]). For instance, we obtained a SiR-modified anti β -actin antibody that was able to specifically detect its antigen in a cell lysate (entry 5) and gave very clear staining in direct immunofluorescence with mouse cardiomyocytes (Figures S5 and S6, ESI[†]). Control indirect immunofluorescence using the native anti β -actin antibody and secondary Dy488-conjugated antibody produced very similar signal. For the studied ion channels and ion pump, the method failed to produce tools to detect Na_v1.5, Ca_v1.2 or Na⁺/K⁺-ATPase in cell lysate by Western blot (entries 6-8). However, specific direct immunofluorescence signal was clearly obtained with BFL-modified anti Na_v1.5, SiR-modified anti Ca_v1.2 and anti Na⁺/K⁺-ATPase antibodies (Figures S5 and S6, ESI[†]). It is noteworthy, that the anti Ca_v1.2 staining tool was obtained from a custom-generated polyclonal antibody population. Conversely, modification of polyclonal anti TRPM4 antibody yielded a product that gave a strong and specific signal in Western blot, but direct immunofluorescence was inconclusive (entry 9). In this particular case, TRPM4 detection by indirect

immunofluorescence or fluorescence-assisted cell sorting (FACS), using native polyclonal anti TRPM4 antibody and secondary fluorescent antibody, was not conclusive either.

1.3. Conclusions

The growing field of ADCs has produced several useful antibody conjugation protocols, some of which selectively target the interchain disulphide bridges. We have adapted the dithiol re-bridging dibromopyridazinedione reagents to introduce bright fluorescent dyes and biotin tags site-selectively into IgG1 type antibodies using a straightforward protocol. A further option, which we have not tested experimentally, would be to re-bridge with general reagent **3** and subsequently “click” the tag of choice to the alkyne-modified antibody.

The synthesised anti GAPDH antibody conjugates were shown to give strong and specific signals in Western blot and direct immunofluorescence applications. Our produced modified anti GAPDH antibodies could be further evaluated as potential diagnostic tools in various disease models, where GAPDH was proposed as important marker for cell survival.^{30, 31}

It appears that the thiol re-bridging modification protocol is not generally transferable to other IgG1 antibodies and the source and quality of the native IgG1 antibody seems to play an important role. It is challenging to generate an imaging antibody tool that works equally well and gives specific labelling in both applications (Western blot and direct immunofluorescence), and therefore, modified antibody products must be evaluated carefully for the applications intended. Nonetheless, we have shown that it is possible to start from commercially available monoclonal IgG1 and custom-produced polyclonal IgG antibodies, the latter of which consist of several subtypes having different number and locations of intra-chain disulphide bonds,^{33, 34} and synthetically produce specific ion channel imaging tools for Western blot (β -actin, TRPM4) and direct immunofluorescence (β -actin, Na_v1.5, Ca_v1.2, Na⁺/K⁺-ATPase) applications.

1.4. Experimental section

Chemistry

General remarks. All reactions requiring anhydrous conditions were performed in heat-gun, oven or flame dried glassware under inert atmosphere (N₂, Ar). Silica gel 60 Å (40–63 mm) from Sigma-Aldrich was used for dry loads. Flash column chromatography was performed on a Teledyne Isco CombiFlash® Rf+ with the corresponding RediSep® prepacked silica cartouches unless otherwise stated. Thin layer

chromatography (TLC) was performed on Macherey & Nagel Alugram® xtra SIL G/UV 254 visualization under UV light (254 nm) and/ or (366 nm) and/ or by dipping in anisaldehyde stain and subsequent heating.

Commercial reagents and solvents (Acrôs Organics, Apollo scientific, Combi-Blocks, Fluorochem, Grogg Chemie, Häseler, Sigma-Aldrich) were used without further purification unless otherwise stated. Pacific Blue NHS ester and BODIPY FL azide **5** were obtained from Lumiprobe GmbH. Dry solvents for reactions were distilled and filtered over columns of dry neutral aluminium oxide under positive argon pressure. Solvents for extraction and flash chromatography were used without further purification.

^1H , ^{11}B , ^{13}C and ^{19}F NMR spectra were recorded on a Bruker AVANCE-300 or 400 spectrometers operating at 300 or 400 MHz for ^1H , 96 MHz for ^{11}B , 75 or 101 MHz for ^{13}C and 376 MHz for ^{19}F at room temperature unless otherwise stated. Chemical shifts (δ) are reported in parts per million (ppm) relative to tetramethylsilane (TMS) calibrated using residual signals of the solvent or TMS. Coupling constants (J) are reported in Hz. HRMS analyses and accurate mass determinations were performed on a Thermo Scientific LTQ Orbitrap XL mass spectrometer using ESI ionisation and positive or negative mode by the analytical services (mass spectrometry lab of Prof. Dr. Stefan Schürch) from the Department of Chemistry, Biochemistry and Pharmaceutical Sciences (DCBP) of the University of Bern, Switzerland. X-ray crystal structure determinations were measured, solved, and refined by the service unit of the Department of Chemistry, Biochemistry and Pharmaceutical Sciences of the University of Bern using a Synergy diffractometer. HPLCs were measured on a Thermo-Scientific UltiMate 3000 HPLC with H_2O + 0.1% TFA and MeCN + 0.1 % TFA as eluents on an Acclaim™ 120 C18 5 μm 120Å (4.6 x 150 mm) column.

Di-tert-butyl 1-methylhydrazine-1,2-dicarboxylate (1). To a stirred solution of methylhydrazine (5.7 mL, 5.00 g, 108.52 mmol) in 2-propanol (75 mL) at 27°C Boc-anhydride (60.12 g, 275.48 mmol) was added dropwise over the course of 50 minutes. The mixture was stirred at 27°C for 5 h and then concentrated under reduced pressure. The residue was taken up in EtOAc. The organic layer was washed with water, brine, dried over MgSO_4 , filtered, and concentrated under reduced pressure. The crude was purified by flash column chromatography (cyclohexane/EtOAc gradient from 1:0 to 0:1) to give the desired compound in 94% yield (25.02 g, 101.58 mmol). Physical and spectral data in accordance with literature.²⁰ Colourless solid: Major rotamer, ^1H NMR (300 MHz, CDCl_3) δ 6.47 (s, 1H), 3.08 (s, 3H), 1.45 (s, 18H). Minor rotamer, ^1H NMR (300 MHz, CDCl_3) δ 6.24 (s, 1H), 3.08 (s, 3H), 1.44 (s, 18H). Both rotamers: ^{13}C NMR (75 MHz, CDCl_3) δ 155.88, 81.27, 28.33. HRMS (ESI) calculated for

$[M+H]^+ C_{11}H_{23}N_2O_4^+$ 247.1652, found 247.1658. Calculated for $[M+Na]^+ C_{11}H_{22}N_2NaO_4^+$ 269.1472, found 269.1477.

Di-*tert*-butyl 1-methyl-2-(prop-2-yn-1-yl)hydrazine-1,2-dicarboxylate (2). To a stirred solution of di-*tert*-butyl 1-methylhydrazine-1,2-dicarboxylate (**1**) (0.51 g, 2.06 mmol) in DMF (20 mL) propargyl bromide (80% in toluene, 0.3 mL, 0.32 g, 2.69 mmol) and Cs_2CO_3 (1.04 g, 3.19 mmol) was added. The mixture was stirred at 23°C under an argon atmosphere for 16 h. Then more propargyl bromide (80% in toluene, 0.3 mL, 0.32 g, 2.69 mmol) was added and the mixture was stirred for another 8 h. Subsequently, it was diluted with EtOAc and water. The aqueous phase was extracted with EtOAc. The combined organic layers were washed with brine (3x), dried over $MgSO_4$, filtered, and concentrated under reduced pressure. The residue was taken up in CH_2Cl_2 and was concentrated onto silica gel. The crude was purified by flash column chromatography (cyclohexane/EtOAc gradient from 1:0 to 9:1) to give the desired compound in 90% yield (0.53 g, 1.85 mmol). Colourless solid: Mix of rotamers, 1H NMR (300 MHz, $DMSO-d_6$) δ 4.53 – 3.74 (m, 2H), 3.30 – 3.18 (m, 1H), 3.11 – 2.90 (m, 3H), 1.50 – 1.29 (m, 18H). ^{13}C NMR (75 MHz, $DMSO-d_6$) δ 154.85, 154.16, 153.11, 81.34, 80.72, 80.18, 78.80, 78.65, 74.99, 74.93, 39.39, 38.21, 37.62, 37.46, 36.15, 36.06, 27.81, 27.76, 27.73, 27.69. 1H NMR (400 MHz, at T = 90°C $DMSO-d_6$) δ 4.36 (d, J = 17.5 Hz, 1H), 3.99 (d, J = 17.9 Hz, 1H), 3.08 – 2.97 (m, 4H), 1.53 – 1.32 (m, 18H). HRMS (ESI) calculated for $[M+Na]^+ C_{14}H_{24}N_2NaO_4^+$ 307.1628, found 307.1633.

4,5-Dibromo-1-methyl-2-(prop-2-yn-1-yl)-1,2-dihydropyridazine-3,6-dione (3). To a stirred solution of di-*tert*-butyl 1-methyl-2-(prop-2-yn-1-yl)hydrazine-1,2-dicarboxylate (**2**) (0.90 g, 3.15 mmol) in acetic acid (30 mL) 2,3-Dibromomaleic acid (0.98 g, 3.59 mmol) was added. The mixture was heated to 135°C and stirred for 4 h. The mixture was concentrated under reduced pressure and the residue was taken up in acetone and concentrated onto silica gel. The crude was purified by flash column chromatography (cHex/EtOAc gradient from 1:0 to 1:1) to give the desired compound in 92% yield (0.93 g, 2.91 mmol). A small sample was recrystallised from a mixture of acetone and n-hexane and yielded single crystals of suitable quality for x-ray diffraction analysis (CCDC deposition number: 2171667). Colourless crystals: 1H NMR (300 MHz, $CDCl_3$) δ 4.94 (d, J = 2.5 Hz, 2H), 3.78 (s, 3H), 2.43 (t, J = 2.5 Hz, 1H). ^{13}C NMR (75 MHz, $CDCl_3$) δ 152.87, 152.85, 136.93, 135.16, 75.68, 75.01, 37.17, 34.79. HRMS (ESI) calculated for $[M+H]^+ C_8H_7Br_2N_2O_2^+$ 320.8869, found 320.8872.

***N*-(10-(4-((2-(2-azidoethoxy)ethyl)carbamoyl)-2-methylphenyl)-7-(dimethylamino)-5,5-dimethyldibenzo[*b,e*]silin-3(*5H*)-ylidene)-*N*-methylmethanaminium chloride (4).** To a stirred solution of *N*-(7-(dimethylamino)-10-(4-((2,5-dioxopyrrolidin-1-yl)oxy)carbonyl)-2-methylphenyl)-5,5-dimethyldibenzo[*b,e*]silin-3(*5H*)-ylidene)-*N*-methylmethanaminium chloride (SiR-NHS) (0.029 g, 0.051 mmol) in MeCN (3 mL) was added 2-(2-azidoethoxy)ethan-1-amine (**S8**) (0.059 g, 0.457 mmol).

The mixture was stirred at 21°C for 2 h and protected from light. The mixture was concentrated under reduced pressure. The residue was taken up in CH₂Cl₂, the organic phase was washed with HCl (1 M), brine, dried over MgSO₄, filtered, and concentrated under reduced pressure onto silica gel. The crude was purified by flash column chromatography (CH₂Cl₂/MeOH gradient from 1:0 to 9:1) to give the desired product in quantitative yield (0.030 g, 0.0506 mmol). Purple solid: **¹H NMR** (300 MHz, DMSO-*d*₆) δ 8.69 (t, *J* = 5.5 Hz, 1H), 7.93 (s, 1H), 7.87 (dd, *J* = 7.9, 1.7 Hz, 1H), 7.45 (d, *J* = 2.4 Hz, 2H), 7.27 (d, *J* = 7.9 Hz, 1H), 6.88 (d, *J* = 9.6 Hz, 2H), 6.82 (dd, *J* = 9.7, 2.5 Hz, 2H), 3.68 – 3.60 (m, 4H), 3.50 (t, *J* = 5.7 Hz, 2H), 3.46–3.40 (m, 2H), 3.31 (s, 12H), 2.02 (s, 3H), 0.61 (s, 3H), 0.59 (s, 3H). **¹³C NMR** (101 MHz, DMSO-*d*₆) δ 166.22, 165.77, 153.73, 147.16, 141.30, 139.78, 135.30, 134.60, 128.95, 128.90, 126.04, 124.61, 121.56, 114.57, 68.98, 68.68, 49.99, 40.50, 18.85, -1.04, -1.37. **HRMS** (ESI) calculated for [M-Cl]⁺ C₃₁H₃₉N₆O₂Si⁺ 555.2898, found 555.2878.

***N*-(6-azidoethyl)-5,7-difluoro-6-hydroxy-2-oxo-2H-chromene-3-carboxamide (6).** To a stirred, slightly turbid solution of pacific blue NHS ester (PB-NHS) (0.05 g, 0.15 mmol) in MeCN (10 mL) was added a solution of 6-azidoethanol-1-amine (**S9**) (0.5 M in MeCN, 300 μL, 0.15 mmol, 0.21 g). The reaction mixture was left stirring at 21°C for 24 h, after which it was concentrated onto silica gel. The crude was purified by flash column chromatography (EtOAc/(EtOAc/AcOH 99:1) gradient from 1:0 to 0:1) to give the desired compound in 90% yield (0.049 g, 0.135 mmol). Yellow powder: **¹H NMR** (300 MHz, CDCl₃) δ 9.38 (br. s, 1H), 8.93 (t, *J* = 5.8 Hz, 1H), 8.80 (d, *J* = 1.4 Hz, 1H), 7.29 – 7.20 (m, 1H), 3.48 (q, *J* = 6.7 Hz, 2H), 3.26 (t, *J* = 6.8 Hz, 2H), 1.73 – 1.50 (m, 4H), 1.49 – 1.32 (m, 4H). **¹³C NMR** (75 MHz, CDCl₃) δ 162.16, 160.50, 151.07, 151.06, 148.19, 148.14, 148.10, 147.83, 147.78, 141.03, 141.00, 140.98, 140.95, 140.88, 140.85, 140.61, 140.45, 140.38, 140.21, 137.64, 116.09, 110.30, 110.26, 110.21, 109.99, 110.18, 109.99, 109.94, 51.44, 40.19, 29.20, 28.81, 26.60, 26.45. **HRMS** (ESI) calculated for [M+H]⁺ C₁₆H₁₇O₄N₄F₂ 367.1212, found 367.1212.

***N*-(2-(2-(2-(2-azidoethoxy)ethoxy)ethoxy)ethyl)-5-((3a*S*,4*S*,6a*R*)-2-oxohexahydro-1*H*-thieno[3,4-*d*]imidazol-4-yl)pentanamide (7).** To a stirred solution of biotin-NHS ester (biotin-NHS) (0.1 g, 0.29 mmol) in DMF (10 mL) was added 2-(2-(2-(2-azidoethoxy)ethoxy)ethoxy)ethanol-1-amine (**S10**) (0.146 g, 0.669 mmol) the mixture was stirred under an argon atmosphere for 16 h. The volatiles were removed under reduced pressure. The colourless residue was taken up in CH₂Cl₂ and was concentrated onto silica gel. The crude was purified by flash column chromatography (CH₂Cl₂/MeOH 9:1 gradient from 1:0 to 9:1) to give the desired compound in quantitative yield (0.139 g, 0.313 mmol). Colourless solid: **¹H NMR** (300 MHz, DMSO-*d*₆) δ 7.82 (t, *J* = 5.6 Hz, 1H), 6.39 (d, *J* = 20.1 Hz, 2H), 4.38 – 4.23 (m, 1H), 4.19 – 4.05 (m, 1H), 3.68 – 3.45 (m, 10H), 3.45 – 3.29 (m, 5H), 3.18 (q, *J* = 5.9 Hz, 2H), 3.13 – 3.01 (m, 1H), 2.82 (dd, *J* = 12.4, 5.0 Hz, 1H), 2.57 (d, *J* = 12.3 Hz, 1H), 2.06 (t, *J* = 7.3 Hz, 2H), 1.69 – 1.38 (m, 4H), 1.36 – 1.20 (m, 2H). **¹³C NMR** (75 MHz, DMSO-*d*₆) δ 172.12, 162.73, 69.81, 69.78, 69.71, 69.57,

69.27, 69.18, 61.05, 59.21, 55.43, 50.00, 39.86, 38.45, 35.10, 28.20, 28.04, 25.26. **HRMS** (ESI) calculated for $[M+H]^+$ $C_{18}H_{33}O_5N_6S$ 445.2228, found 445.2221.

***N*-(10-(4-((2-(2-(4,5-dibromo-2-methyl-3,6-dioxo-3,6-dihydropyridazin-1(2*H*)-yl)methyl)-1*H*-1,2,3-triazol-1-yl)ethoxy)ethyl)carbamoyl)-2-methylphenyl)-7-(dimethylamino)-5,5-dimethyldibenzo[*b,e*]silin-3(5*H*)-ylidene)-*N*-methylmethanaminium chloride (8).** To a stirred solution of *N*-(10-(4-((2-(2-azidoethoxy)ethyl)carbamoyl)-2-methylphenyl)-7-(dimethylamino)-5,5-dimethyldibenzo[*b,e*]silin-3(5*H*)-ylidene)-*N*-methylmethanaminium chloride (**4**) (0.034 g, 0.058 mmol) and 4,5-dibromo-1-methyl-2-(prop-2-yn-1-yl)-1,2-dihydropyridazine-3,6-dione (**3**) (0.021 g, 0.066 mmol) in *t*-BuOH (3 mL) and water (3 mL) was added sodium ascorbate (0.005 g, 0.023 mmol) and $CuSO_4 \cdot 5 H_2O$ (0.001 g, 0.005 mmol). The mixture was stirred at 21°C for 3 h. The mixture was concentrated under reduced pressure onto silica gel. The crude was purified by flash column chromatography (CH_2Cl_2 /MeOH gradient from 1:0 to 9:1) to give the desired compound in 95% yield (0.05 g, 0.05 mmol). Blue solid: **¹H NMR** (300 MHz, $DMSO-d_6$) δ 8.61 (t, *J* = 5.4 Hz, 1H), 8.17 (s, 1H), 7.92 (s, 1H), 7.85 (d, *J* = 7.9 Hz, 1H), 7.45 (d, *J* = 2.6 Hz, 2H), 7.27 (d, *J* = 7.9 Hz, 1H), 6.88 (d, *J* = 9.7 Hz, 2H), 6.81 (dd, *J* = 9.7, 2.6 Hz, 2H), 5.33 (s, 2H), 4.55 (t, *J* = 5.1 Hz, 2H), 3.85 (t, *J* = 5.1 Hz, 2H), 3.63 (s, 3H), 3.56 (t, *J* = 5.7 Hz, 2H), 3.42 (q, *J* = 5.5 Hz, 2H), 3.31 (s, 12H), 2.02 (s, 3H), 0.61 (s, 3H), 0.59 (s, 3H). **¹³C NMR** (101 MHz, $DMSO-d_6$) δ 166.24, 165.70, 153.72, 152.42, 152.24, 147.16, 141.33, 140.81, 139.80, 135.68, 135.37, 134.70, 134.52, 128.97, 128.92, 126.04, 124.56, 124.47, 121.55, 114.55, 68.66, 68.29, 54.90, 49.51, 42.45, 40.50, 34.85, 18.87, -1.04, -1.37. **HRMS** (ESI) calculated for $[M-Cl]^+$ $C_{39}H_{45}Br_2N_8O_4Si^+$ 875.1694, found 875.1685.

***N*-(3-(4-((4,5-dibromo-2-methyl-3,6-dioxo-3,6-dihydropyridazin-1(2*H*)-yl)methyl)-1*H*-1,2,3-triazol-1-yl)propyl)-3-(5,5-difluoro-7,9-dimethyl-5*H*-5 λ^4 ,6 λ^4 -dipyrrolo[1,2-*c*:2',1'-*f*][1,3,2]diazaborinin-3-yl)propenamide (9).** 4,5-dibromo-1-methyl-2-(prop-2-yn-1-yl)-1,2-dihydropyridazine-3,6-dione (**3**) (0.016 g, 0.05 mmol) and *N*-(3-azidopropyl)-3-(5,5-difluoro-7,9-dimethyl-5*H*-5 λ^4 ,6 λ^4 -dipyrrolo[1,2-*c*:2',1'-*f*][1,3,2]diazaborinin-3-yl)propenamide (**5**) (0.018 g, 0.047 mmol) was dissolved in *t*-BuOH (2 mL) and H_2O (1 mL). $CuSO_4 \cdot 5 H_2O$ (1 M in H_2O , 2 μ L, 0.002 mmol) and sodium ascorbate (0.003 g, 0.013 mmol) was added to this solution. The mixture was stirred at 23°C for 16 h, under an argon atmosphere and protected from light. The reaction mixture was diluted with MeCN and concentrated onto silica gel. The crude was purified by flash column chromatography (cHex/(EtOAc/MeOH/AcOH 85:10:5) gradient from 1:0 to 0:1) to give the desired compound in quantitative yield (0.034 g, 0.049 mmol). Dark orange powder: **¹H NMR** (300 MHz, $DMSO-d_6$) δ 8.16 (s, 1H), 8.02 (t, *J* = 5.6 Hz, 1H), 7.69 (s, 1H), 7.08 (d, *J* = 4.0 Hz, 1H), 6.35 (d, *J* = 4.0 Hz, 1H), 6.30 (s, 1H), 5.37 (s, 2H), 4.34 (t, *J* = 7.0 Hz, 2H), 3.64 (s, 3H), 3.07 (dd, *J* = 9.6, 6.7 Hz, 4H), 2.47 (s, 9H), 2.26 (s, 3H), 1.94 (p, *J* = 7.0 Hz, 3H). **¹³C NMR** (101 MHz, $DMSO-d_6$) δ 170.92, 159.16, 152.38, 152.25, 140.89, 135.70, 134.72, 132.95, 128.89,

128.19, 125.35, 125.30, 124.14, 120.26, 116.56, 47.35, 42.46, 35.74, 34.81, 33.76, 29.81, 23.95, 14.50, 10.98, 1.14. ¹⁹F NMR (376 MHz, DMSO-*d*₆) δ -143.18 (dd, *J* = 66.5, 33.0 Hz). ¹¹B NMR (96 MHz, DMSO-*d*₆) δ 0.74 (t, *J* = 32.8 Hz). HRMS (ESI) calculated for [M+Na]⁺ C₂₅H₂₇O₃N₈ BBr₂F₂Na 717.0526, found 717.0523.

***N*-(6-(4-((4,5-dibromo-2-methyl-3,6-dioxo-3,6-dihydropyridazin-1(2*H*)-yl)methyl)-1*H*-1,2,3-triazol-1-yl)hexyl)-5,7-difluoro-6-hydroxy-2-oxo-2*H*-chromene-3-carboxamide (10).** To a stirred suspension of 4,5-dibromo-1-methyl-2-(prop-2-yn-1-yl)-1,2-dihydropyridazine-3,6-dione (**3**) (0.051 g, 0.157 mmol) and *N*-(6-azidoheptyl)-5,7-difluoro-6-hydroxy-2-oxo-2*H*-chromene-3-carboxamide (**6**) (0.056 g, 0.154 mmol) and sodium ascorbate (0.004 g, 0.02 mmol) in *tert*-Butanol (2 mL) and water (2 mL) was added a solution of CuSO₄·5 H₂O (1 M, 10 μL, 0.003 g, 10 μmol). The mixture was placed under an argon atmosphere and was stirred for 48 h. The suspension was filtered through a pad of celite and the filter cake was washed with water. The filtrate was discarded. The filter cake was washed with MeCN. The resulting filtrate was then concentrated onto silica gel. The crude was purified by flash column chromatography (EtOAc/(EtOAc/acetic acid 99:1) gradient from 1:0 to 0:1) to give the desired compound in 67% yield (0.071 g, 0.105 mmol). Yellow powder: ¹H NMR (300 MHz, DMSO-*d*₆) δ 12.02 (s, 1H), 8.76 (s, 1H), 8.56 (t, *J* = 5.8 Hz, 1H), 8.16 (s, 1H), 7.74 (d, *J* = 9.6 Hz, 1H), 5.36 (s, 2H), 4.33 (t, *J* = 7.1 Hz, 2H), 3.63 (s, 3H), 3.31 – 3.24 (m, 2H), 1.80 (p, *J* = 7.1 Hz, 2H), 1.49 (p, *J* = 6.6 Hz, 2H), 1.32 – 1.19 (m, 4H). ¹³C NMR (101 MHz, DMSO-*d*₆) δ 160.97, 159.66, 152.38, 152.24, 147.00, 140.92, 140.62, 140.59, 140.54, 135.68, 134.73, 123.91, 115.99, 110.53, 110.32, 109.26, 109.18, 49.38, 42.51, 34.80, 29.47, 28.74, 25.68, 25.44. ¹⁹F NMR (282 MHz, DMSO-*d*₆) δ -135.17, -154.28. HRMS (ESI) calculated for [M+Na]⁺ C₂₄H₂₂O₆N₆Br₂F₂Na 708.9828, found 708.9854.

***N*-(2-(2-(2-(2-(4-((4,5-dibromo-2-methyl-3,6-dioxo-3,6-dihydropyridazin-1(2*H*)-yl)methyl)-1*H*-1,2,3-triazol-1-yl)ethoxy)ethoxy)ethoxy)ethyl)-5-((3*aS*,4*S*,6*aR*)-2-oxohexahydro-1*H*-thieno[3,4-*d*]imidazol-4-yl)pentanamide (11).** *N*-(2-(2-(2-(2-azidoethoxy)ethoxy)ethoxy)ethyl)-5-((3*aS*,4*S*,6*aR*)-2-oxohexahydro-1*H*-thieno[3,4-*d*]imidazol-4-yl)pentanamide (**7**) (0.112 g, 0.252 mmol) was dissolved in a mixture of *t*-BuOH (3 mL) and water (3 mL), using some gentle heating to obtain a clear solution. To this was added 4,5-dibromo-1-methyl-2-(prop-2-yn-1-yl)-1,2-dihydropyridazine-3,6-dione (**3**) (0.089 g, 0.278 mmol), sodium ascorbate (0.005 g, 0.027 mmol) and CuSO₄·5 H₂O (0.002 g, 0.007 mmol). The mixture was stirred at 21°C for 6 h. The mixture was concentrated under reduced pressure. The slight greenish residue was taken up in a mixture of CH₂Cl₂ and MeOH. This mixture was then concentrated onto silica gel. The crude was purified by flash column chromatography (CH₂Cl₂/MeOH gradient from 1:0 to 9:1) to give the desired compound in 91% yield (0.175 g, 0.228 mmol). Pale yellow powder: ¹H NMR (400 MHz, DMSO-*d*₆) δ 8.12 (s, 1H), 7.80 (t, *J* = 5.6 Hz, 1H), 6.38 (d, *J* = 23.7 Hz, 2H), 5.37 (s, 2H), 4.51 (t, *J* = 5.2 Hz, 2H), 4.30 (dd, *J* = 7.7, 5.0 Hz, 1H), 4.16 – 4.08 (m, 1H), 3.80 (t, *J* = 5.3 Hz, 2H), 3.65

(s, 3H), 3.52 – 3.43 (m, 8H), 3.38 (t, J = 6.0 Hz, 2H), 3.17 (q, J = 5.9 Hz, 2H), 3.14 – 3.04 (m, 1H), 2.81 (dd, J = 12.4, 5.1 Hz, 1H), 2.57 (d, J = 12.5 Hz, 1H), 2.06 (t, J = 7.4 Hz, 2H), 1.66 – 1.54 (m, 1H), 1.56 – 1.38 (m, 3H), 1.35 – 1.22 (m, 2H). **^{13}C NMR** (101 MHz, DMSO- d_6) δ 172.09, 162.67, 152.39, 152.24, 140.80, 135.69, 134.73, 124.46, 69.67, 69.61, 69.52, 69.14, 68.56, 61.01, 59.17, 55.39, 54.89, 49.50, 42.41, 39.83, 38.41, 35.08, 34.81, 28.17, 28.02, 25.23. **HRMS** (ESI) calculated for $[\text{M}+\text{H}]^+$ $\text{C}_{26}\text{H}_{39}\text{O}_7\text{N}_8\text{Br}_2\text{S}$ 765.1024, found 765.1024.

Biology

General remarks. Antibodies used were purchased from Invitrogen (anti GAPDH, MA5-15738), Abcam (anti β -actin, ab6276; anti Na^+/K^+ -ATPase, ab7671), Alomone Labs (anti $\text{Ca}_v1.2$, ACC-003) or custom-generated by Pineda antibody services (anti $\text{Na}_v1.5$ and anti TRPM4). All experiments involving animals (mouse hearts) were performed according to the Swiss Federal Animal Protection Law and were approved by the Cantonal Veterinary Administration, Bern, Switzerland. This investigation conforms to the Guide for the Care and Use of Laboratory Animals, published by the US National Institutes of Health (NIH publication no. 85-23, revised 1996).

Buffers used: PBS (Sigma-Aldrich (P5368) dissolved in 1 L Milli-Q water), BBS ($\text{Na}_2\text{B}_4\text{O}_7 \cdot 10 \text{H}_2\text{O}$ 25 mM, NaCl 25 mM, EDTA 0.5 mM, DMSO 2% in Milli-Q water, pH adjusted with aq. HCl to 8.01), SDS-Running Buffer (25 mM Tris, 190 mM glycine, 0.1% SDS), Transfer Buffer (25 mM Tris, 190 mM glycine, 20% MeOH, 0.1% SDS), TBST (20 mM Tris, pH 7.5, 150 mM NaCl, 0.1 Tween 20), 4x loading buffer (0.2 M Tris pH 6.8, 40% glycerol, 20% 2-mercaptoethanol, 8% SDS, 0.002% bromophenol blue in deionised water).

Antibody conjugation through re-bridging

The buffer, in which the antibody was obtained, was exchanged to Borate Buffered Saline (BBS, pH=8.0) using spin filter columns (Amicon® Ultra 2 mL, 30'000 Da molecular weight cut-off, 3 x 15 minutes @ 4000 g). The residue was transferred into a PCR reaction tube. The re-bridging compound **8-11** (20 mM in DMSO) was added in 20-fold excess with respect to the antibody. This mixture was incubated for 1 h at 4°C. Then TCEP (10 mM in water) was added in 10-fold excess with respect to the antibody and the reaction was kept at 4°C overnight. The reaction residue was transferred into a spin filter column (Amicon® Ultra 2 mL, 30'000 Da molecular weight cut-off) and washed with phosphate buffered saline (PBS, pH=7.4) (6 x 15 minutes @ 4000 g). After washing, the modified antibody was diluted to the original concentration with PBS, aliquoted and stored at -20°C.

Stochastic antibody fluorescent labelling

The buffer, in which the antibody was obtained, was exchanged to Borate Buffered Saline (BBS, pH=8.0) using spin filter columns (Amicon® Ultra 2 mL, 30'000 Da molecular weight cut-off, 3 x 15 minutes @ 4000 g). The residue was transferred into a PCR reaction tube. To this a solution of SiR-NHS (10 mM in DMSO) was added in 20-fold excess with respect to the antibody. This mixture was incubated at 4°C overnight. The reaction residue was transferred into a spin filter column (Amicon® Ultra 2 mL, 30'000 Da molecular weight cut-off) and washed with phosphate buffered saline (PBS, pH=7.4, 5 x 15 minutes @ 4000 g and 1 x 15 minutes @ 4000 g). After washing, the modified antibody was diluted to the original concentration with PBS, aliquoted and stored at -20°C.

SDS-PAGE

Polyacrylamide gel were cast from 30% acrylamide solution (Carl Roth, A124.1). For a typical SDS-PAGE experiment the modified antibody in PBS was diluted with 4x loading buffer to obtain a loading of 200 ng per lane. In this dilution the mixture was incubated at 92°C for 30 minutes. A 10% 1 mm polyacrylamide gel was run at 90 V for 15 minutes followed by 120 V up to a total run time of 2.5 h in SDS running buffer. Visualisation was achieved with a Typhoon FLA 9500 fluorescence imager. After the fluorescence analysis, the gel was stained with Coomassie blue staining for 1 h followed by washing with water overnight.

Size exclusion chromatography (SEC)

SEC was conducted on an Agilent 1260 infinity II HPLC with 150 mM phosphate buffer + 0.01% NaN₃, pH = 7 as eluent, using an Agilent AdvanceBio SEC 2.7 µm 300 Å fully porous column (7.8 x 300 mm) and an Agilent AdvanceBio SEC 2.7 µm 300 Å fully porous guard column (7.8 x 50 mm). Proteins were detected by fluorescence and absorption at 215 nm and 280 nm (Figure S2).

Western blot

In a typical Western blot experiment, cardiomyocytes were isolated from mouse heart according to Ozhatil et al.³⁵ and lysed. The lysate was diluted with 4x loading buffer to obtain a loading of 100 µg per lane. In this dilution the mixture was incubated at 37°C for 30 minutes. A 10% 1 mm polyacrylamide gel was run at 90 V for 15 minutes followed by 120 V up to a total run time of 2.5 h in SDS running buffer. The gel was removed and incubated in transfer buffer for 15 minutes. The gel was

sandwiched together with a 0.4 μ M nitrocellulose membrane and was wet-blotted at 90 V for 90 minutes in 0°C transfer buffer. The membrane was then blocked with 3% BSA in TBST for 1 h after which it was rinsed 5x with TBST. Staining of the targets was achieved by incubating the membrane in a solution of the corresponding antibody diluted in TBST + 3% BSA, using a concentration for Western blot application recommended by the manufacturer. Visualisation was achieved with a fluorescence imager (GE Healthcare, Typhoon FLA 9500). The biotin-modified antibody was visualised by co-incubating the membrane with streptavidin-Cy5 (Invitrogen™, SA1011) solution.

Immunofluorescence

Adult mouse heart cardiomyocytes were isolated as described previously³⁵ and plated onto uncoated PCA microscopy chamber slides (Sartstedt, 94.6140.802). The cells were washed twice with PBS 1x and then fixed with 10% PFA for 15 minutes. The cells were washed twice with PBS 1x, blocked with blocking buffer (PBS 1x + 1% BSA + 0.5% TritonX-100 + 10% Goat Serum) for 30 minutes and subsequently incubated overnight at 4°C in incubation buffer (PBS 1x + 1% BSA + 0.5% Triton X-100 + 3% Goat Serum). The incubation buffer contained the corresponding antibody in a concentration for immunofluorescence applications, according to the manufacturer's recommendation. The slides were washed 3x with PBS 1x. For indirect immunofluorescence or biotin detection, secondary antibodies (Abcam, ab96879 (goat anti mouse), ab98462 (goat anti rabbit)) or streptavidin-Cy5 was applied, respectively, in the recommended concentration in incubation buffer for 1 h at 22°C. For direct immunofluorescence using a fluorescent primary antibody, the cells were kept in PBS 1x for 1 h at 22°C. Subsequently, the slides were washed 3x with PBS 1x, applying DAPI (Sigma-Aldrich, D9542) stain in the second wash. The cover slip was mounted with Fluor Save (Calbiochem, 345789). The microscope used was a Zeiss LSM710 with EC Plan-NeoFluor 40x objective.

Author contributions

P. Grossenbacher, B. Stieger and M. Lochner conceived the project. P. Grossenbacher, M. C. Essers, S. A. Singer, B. Stieger, J.-S. Rougier and M. Lochner designed the experiments. P. Grossenbacher, M. C. Essers, J. Moser, S. A. Singer and S. Häusler performed the experiments and data analysis. P. Grossenbacher and M. Lochner wrote the manuscript. All authors edited and approved the manuscript.

Conflict of interest

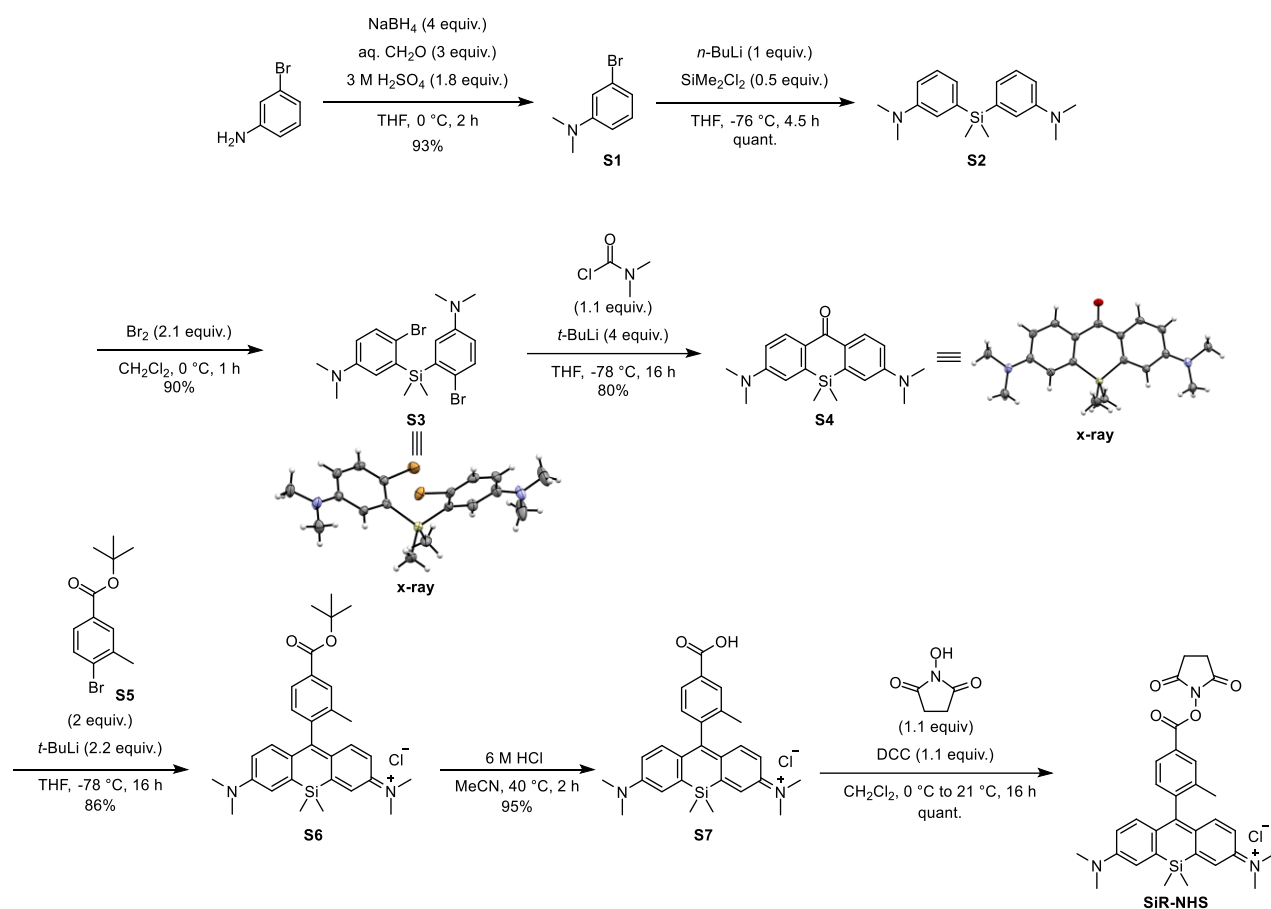
The authors declare no conflict of interest

Acknowledgements

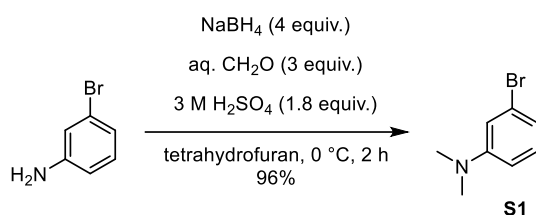
We gratefully acknowledged funding from the Swiss National Science Foundation [CRSII5_180326] to support this work. We thank the Analytical Services from the Department of Chemistry, Biochemistry and Pharmaceutical Sciences, University of Bern, Switzerland, for measuring NMR and MS spectra of synthetic intermediates and final compounds. The X-ray Crystal Structure Determination Service of the same department is acknowledged for measuring, solving, refining, and summarising the structures of compounds **3**, **S3**, **S4** and biotin-NHS. The Synergy diffractometer used was funded in part by the Swiss National Science Foundation through a R'Equip programme [206021_177033].

1.5. Supplementary Information

Synthesis of SiR-NHS ester

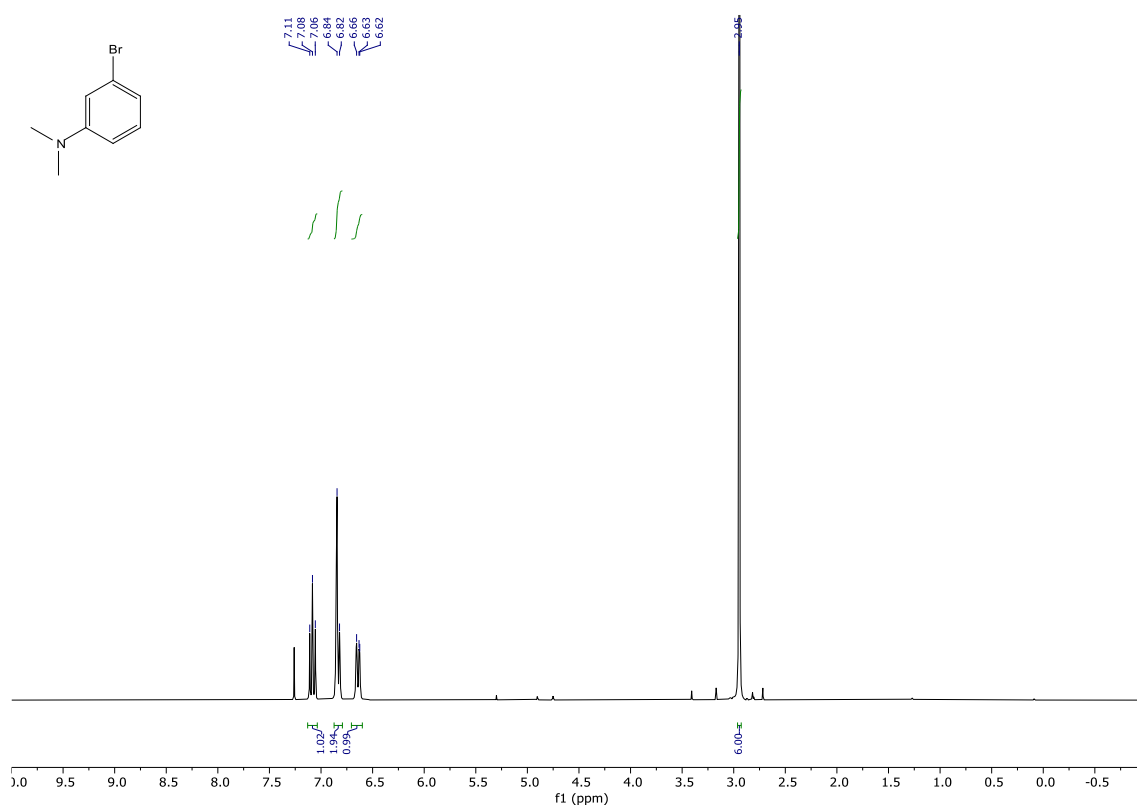


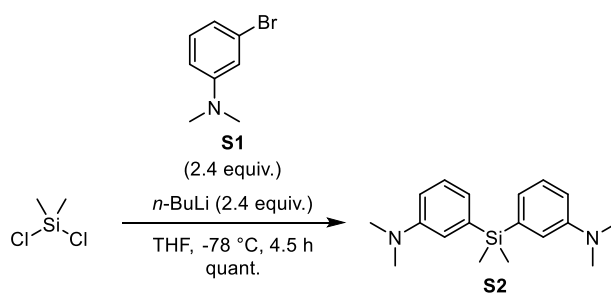
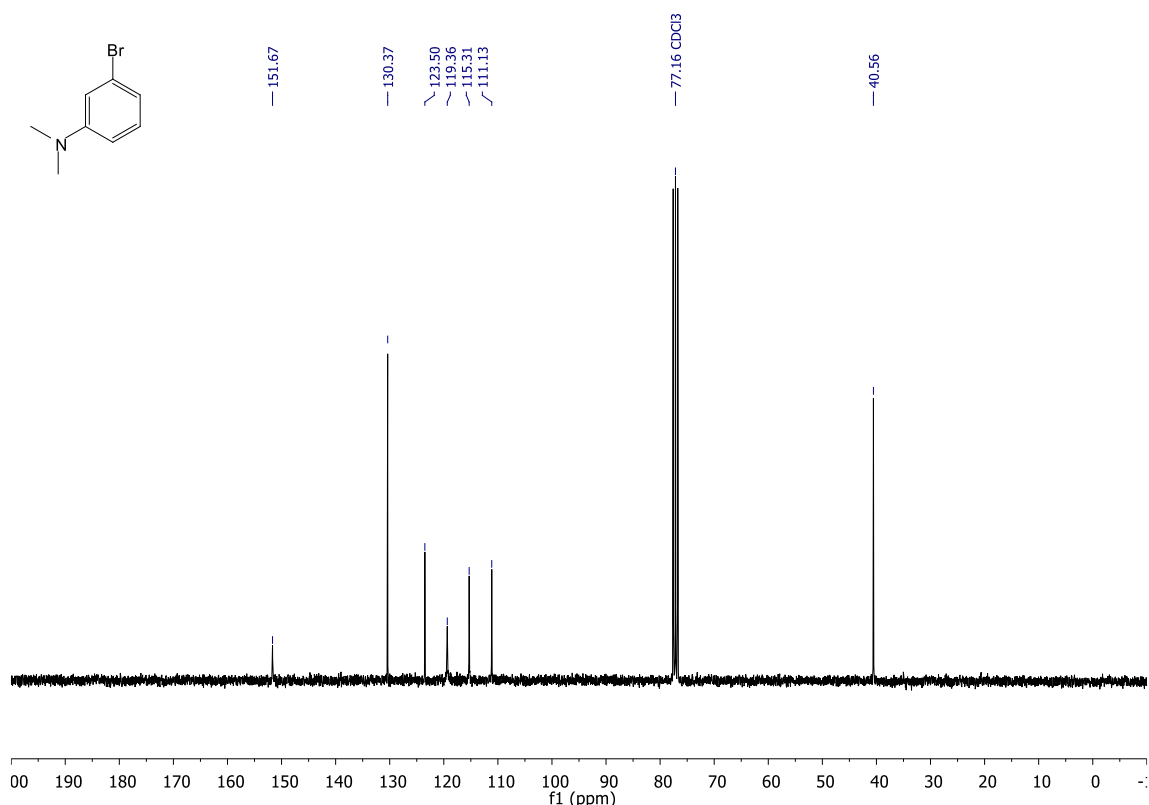
Scheme S1 Synthetic route to SiR-NHS ester.



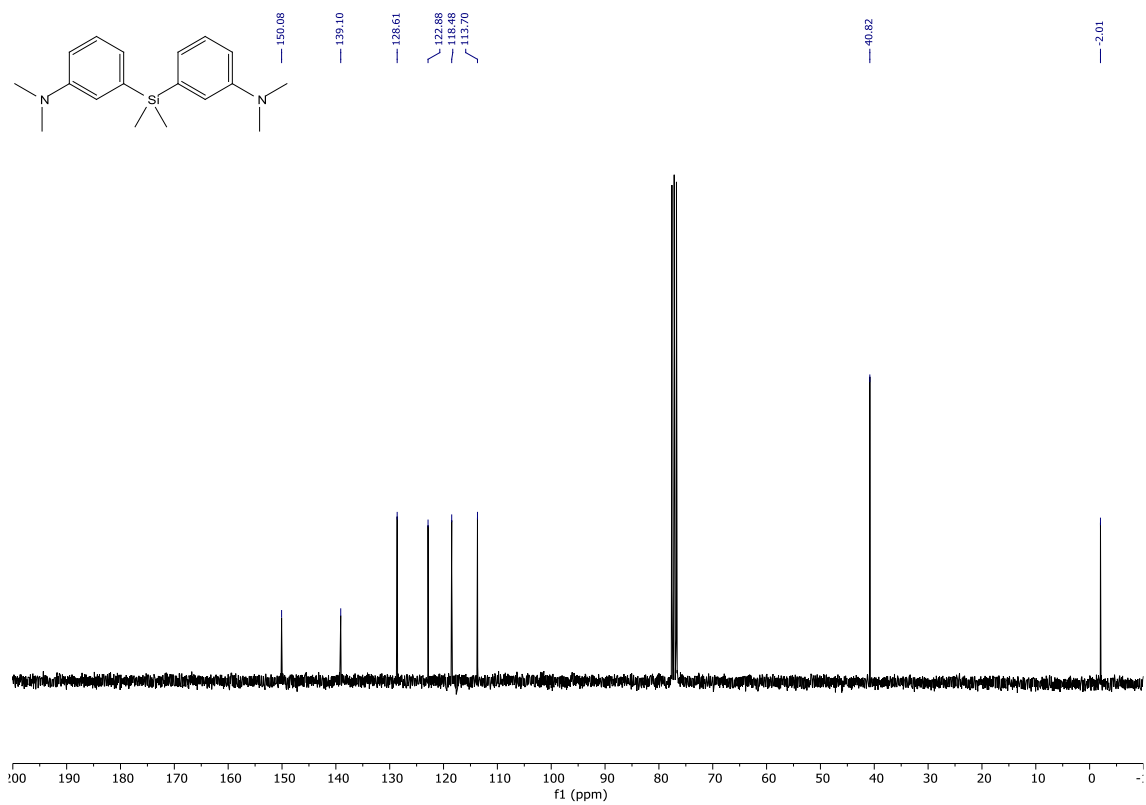
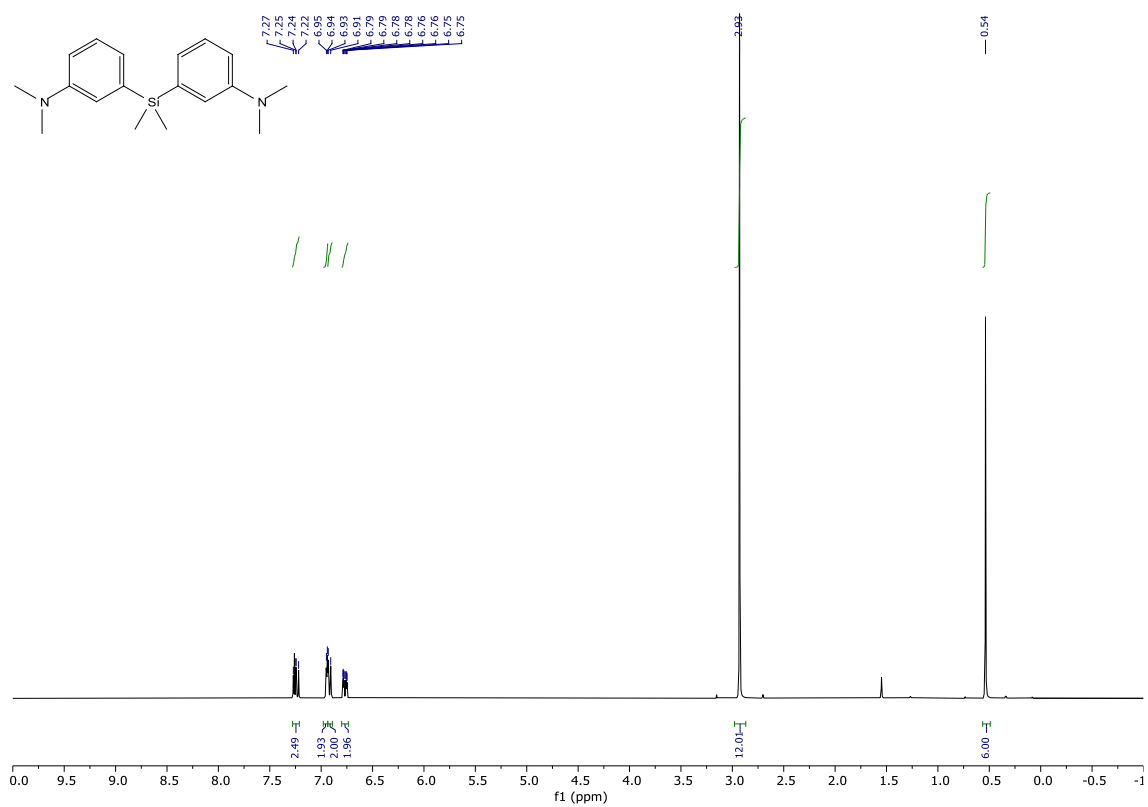
3-bromo-*N,N*-dimethylaniline (S1). To a stirred solution of formaldehyde (37% in water, stabilised with MeOH, 10.4 mL, 4.19 g, 139.67 mmol) in THF (125 mL) was added H₂SO₄ (3 M, 28 mL, 84 mmol). The mixture was cooled to -20°C. 3-Bromoaniline (5 mL, 7.9 g, 45.9 mmol) was added dropwise over the course of 10 min. The resulting flaky suspension was stirred until a clear solution formed. NaBH₄ was added (7.05 g, 186.36 mmol) portion wise over the course of 30 min ensuring that the temperature remained below 0°C during the addition. After the addition, the reaction mixture was slowly warmed to 23°C and stirred for 1 h. The reaction was quenched by adding sat. NaHCO₃ (175

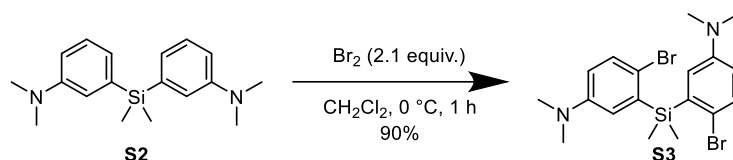
mL) and the mixture was extracted with CH_2Cl_2 (3 x 100 mL). The combined organic phases were washed with brine, dried over MgSO_4 , filtered, and concentrated under reduced pressure. The crude was purified by vacuum Kugelrohrdistillation (1 mbar, 120-145°C). The desired compound was obtained in 96% yield (8.88 g, 44.41 mmol). Physical and spectral data in accordance with literature.³⁶ Yellowish Oil: **^1H NMR** (300 MHz, CDCl_3) δ 7.08 (t, J = 8.1 Hz, 1H), 6.87 – 6.79 (m, 2H), 6.55 (dd, J = 8.9, 2.1 Hz, 1H), 2.95 (s, 6H). **^{13}C NMR** (75 MHz, CDCl_3) δ 151.67, 130.37, 123.50, 119.36, 115.31, 111.13, 40.56. **HRMS** (ESI) calculated for $[\text{M}+\text{H}]^+$ $\text{C}_8\text{H}_{11}\text{BrN}^+$ 200.0069, found 200.0073.



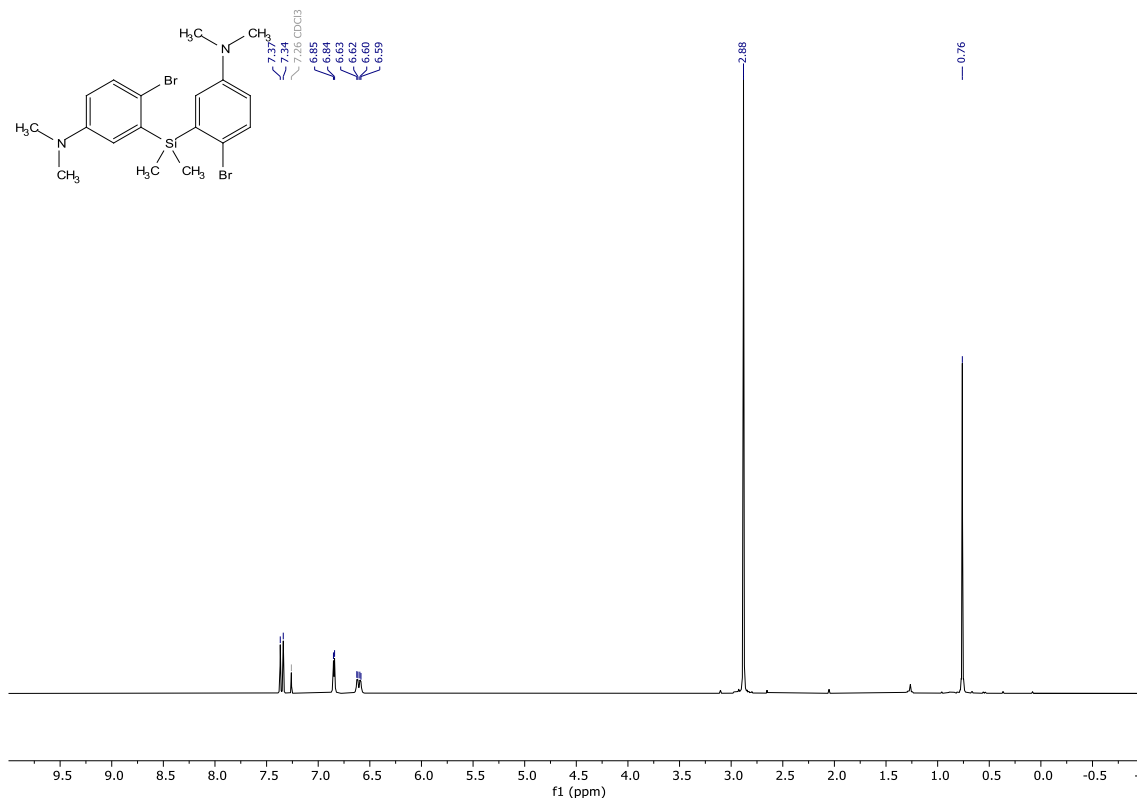


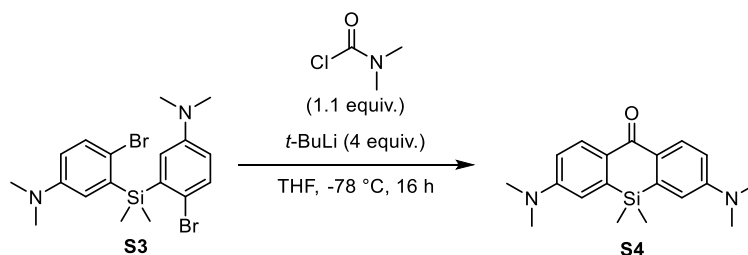
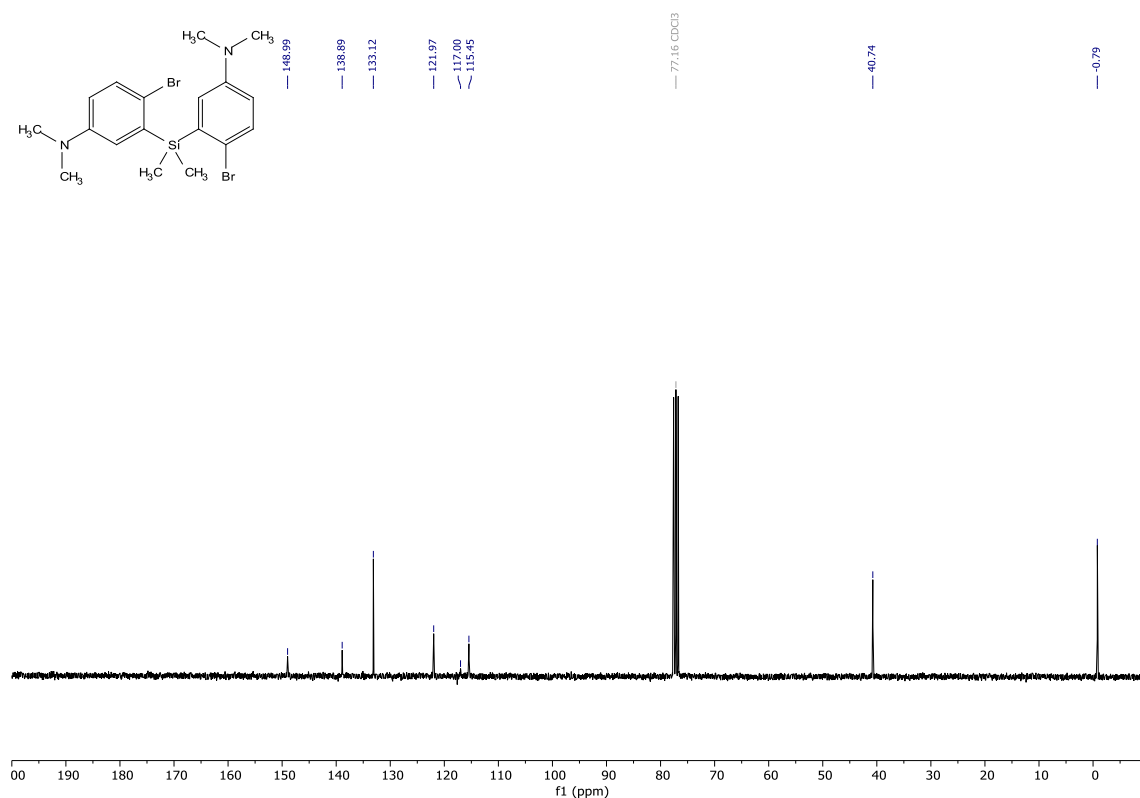
3,3'-(dimethylsilanediyl)bis(*N,N*-dimethylaniline) (S2**).** To a stirred solution of 3-bromo-*N,N*-dimethylaniline (**S1**) (4.009 g, 20.036 mmol) in dry THF (50 mL) under an argon atmosphere at -78°C *n*-BuLi (2.5 M in hexanes, 8 mL, 1.281 g, 20.000 mmol) was added dropwise. After the addition, the mixture was stirred for 30 min at -78°C . Then a solution of dichlorodimethylsilane (1.02 mL, 1.07 g, 8.46 mmol) in dry THF (12 mL), pre-cooled to -78°C , was added dropwise. The mixture was slowly warmed to 22°C and stirred for 4 h. To the reaction mixture was added sat. NH_4Cl (5 mL) and water and it was extracted with EtOAc. The combined organic phases were washed with brine, dried over MgSO_4 , filtered, and concentrated under reduced pressure onto silica gel. The crude was purified by flash column chromatography (CombiFlash, cHex/EtOAc gradient from 1:0 to 9:1). The desired compound was obtained in quantitative yield (2.51 g, 8.41 mmol). Physical and spectral data in accordance with literature.³⁷ Yellowish Oil: ¹H NMR (300 MHz, CDCl_3) δ 7.25 (dd, $J = 8.0, 7.3$ Hz, 2H), 6.94 (d, $J = 2.7$ Hz, 2H), 6.92 (d, $J = 7.1$ Hz, 2H), 6.77 (ddd, $J = 8.3, 2.7, 0.8$ Hz, 2H), 2.93 (s, 12H), 0.54 (s, 6H). ¹³C NMR (75 MHz, CDCl_3) δ 150.08, 139.10, 128.61, 122.88, 118.48, 113.70, 40.82, -2.01. HRMS (ESI) calculated for $[\text{M}+\text{H}]^+$ $\text{C}_{18}\text{H}_{27}\text{N}_2\text{Si}$ 299.1938, found 299.1929.



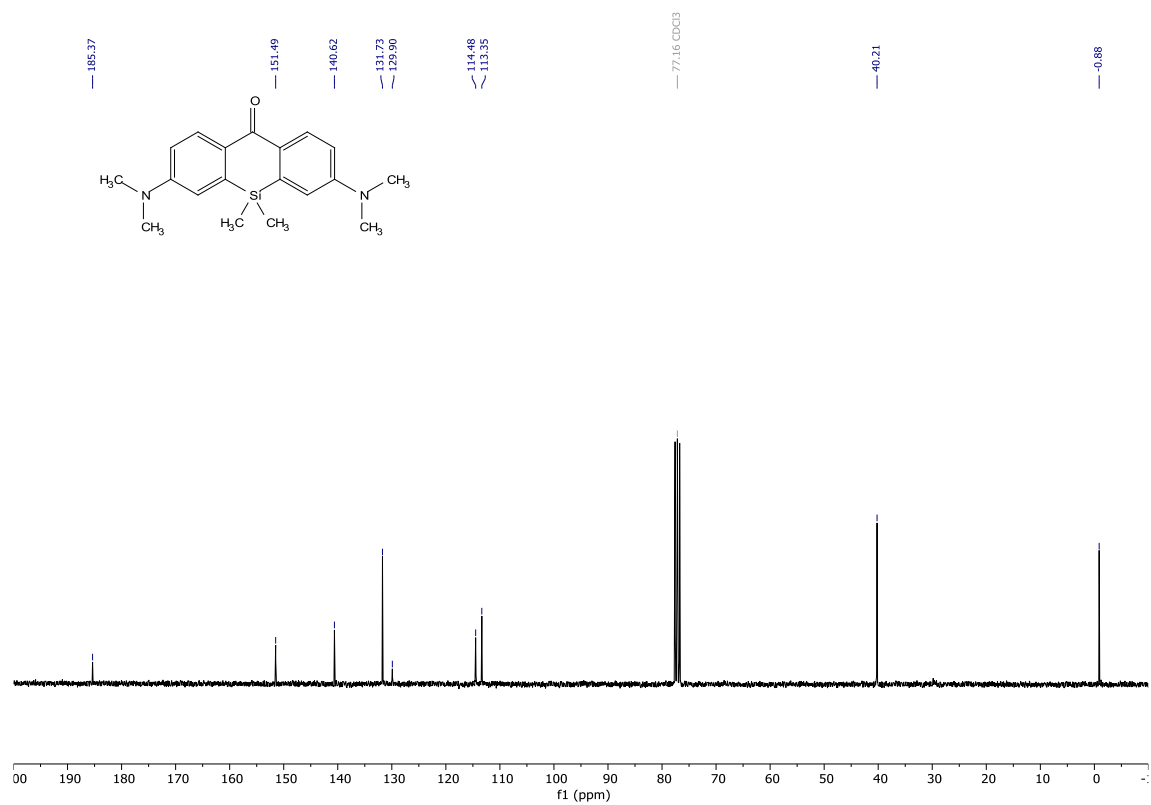
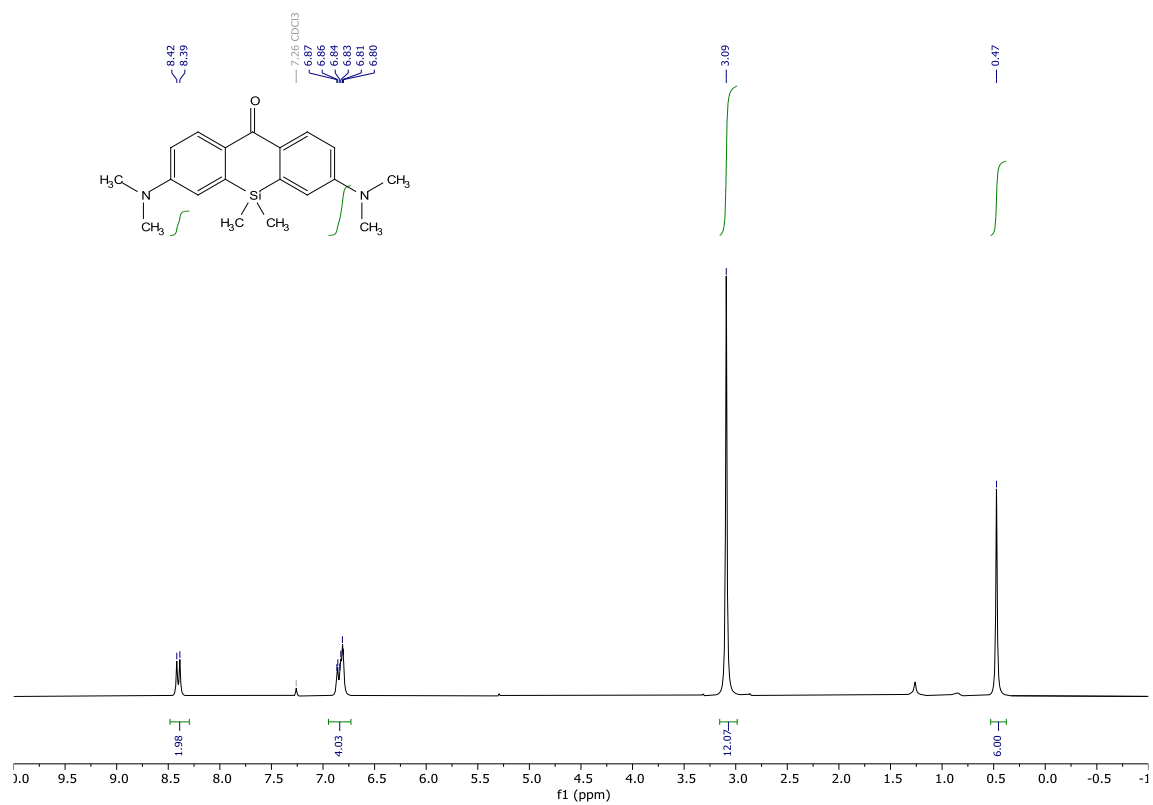


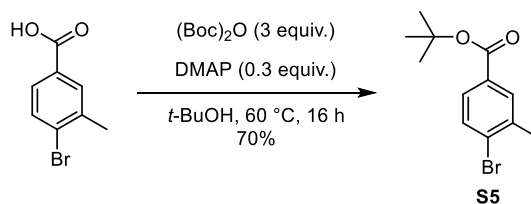
3,3'-(dimethylsilanediyl)bis(4-bromo-*N,N*-dimethylaniline) (S3). To a stirred solution of 3,3'-(dimethylsilanediyl)bis(*N,N*-dimethylaniline) (**S2**) (3.648 g, 12.221 mmol) in CH_2Cl_2 (40 mL) at 0°C was added bromine (1.3 mL, 4.055 g, 25.372 mmol) over the course of 10 min. The resulting solution was stirred for 1 h whilst slowly warming to room temperature. To the mixture was added aq. $\text{Na}_2\text{S}_2\text{O}_3$. Then the mixture was basified with 2 M aq. NaOH until a clear greenish biphasic mixture was formed. The aqueous phase was extracted with CH_2Cl_2 . The combined organic layers were washed with brine, dried over MgSO_4 , filtered, and concentrated under reduced pressure onto silica gel. The crude was purified by flash column chromatography (pentane/ Et_2O gradient 1:0 to 9:1) to give the desired compound in 90% yield (5.003 g, 10.964 mmol). A small sample was recrystallised from pentane and Et_2O to obtain single crystals of suitable quality for x-ray diffraction measurements (CCDC deposition number: 2171687). Physical and spectral data in accordance with literature.³⁸ Colourless solid: **^1H NMR** (300 MHz, CDCl_3) δ 7.35 (d, J = 8.7 Hz, 2H), 6.85 (d, J = 3.2 Hz, 2H), 6.61 (dd, J = 8.8, 3.2 Hz, 2H), 2.88 (s, 12H), 0.76 (s, 6H). **^{13}C NMR** (75 MHz, CDCl_3) δ 148.99, 138.89, 133.12, 121.97, 117.00, 115.45, 40.74, -0.79. **HRMS** (ESI) calculated for $[\text{M}+\text{H}]^+$ $\text{C}_{18}\text{H}_{25}\text{Br}_2\text{N}_2\text{Si}^+$ 455.0148, found 455.0146.



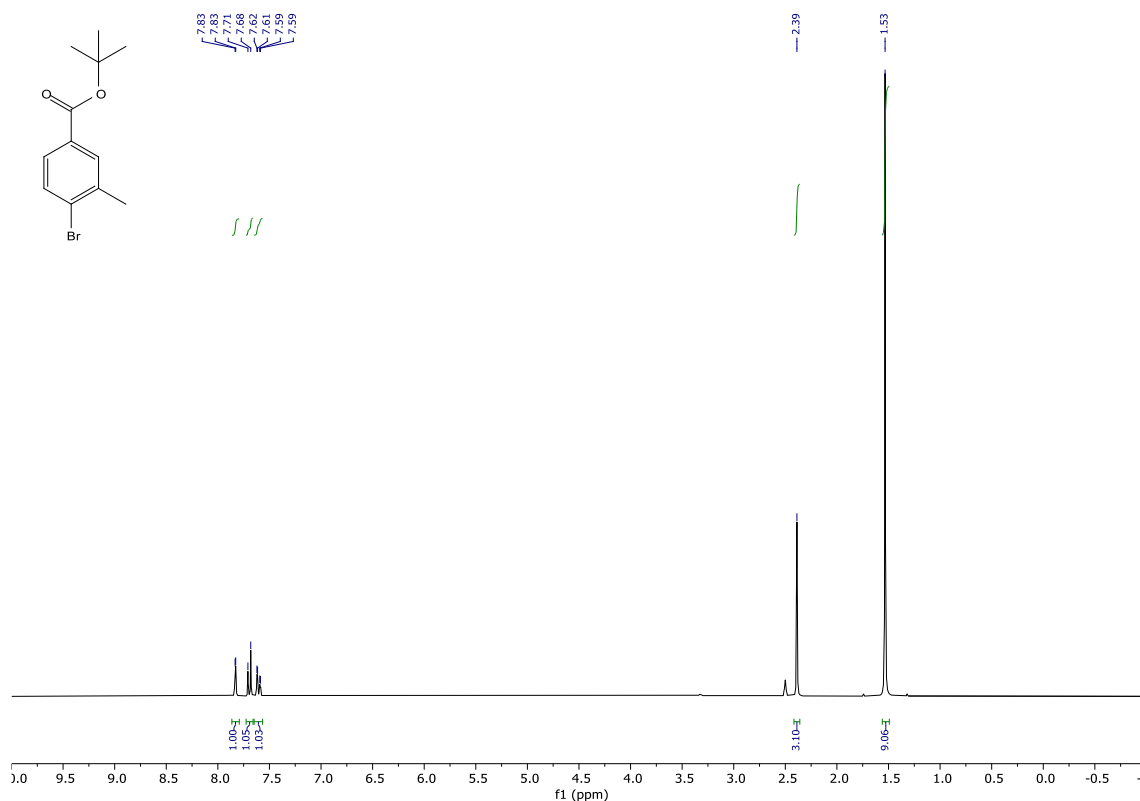


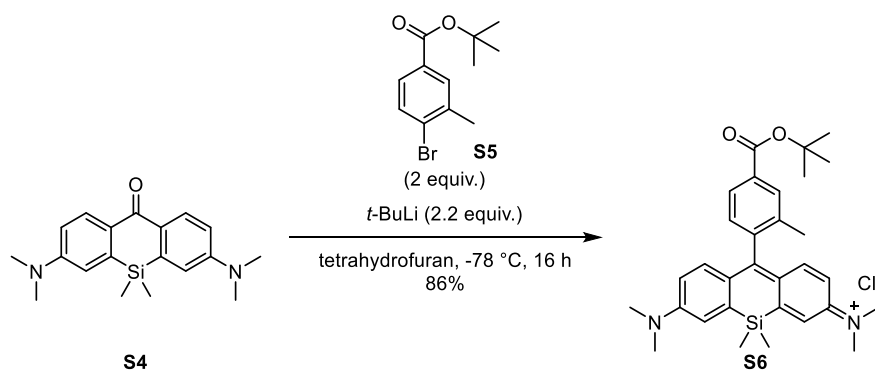
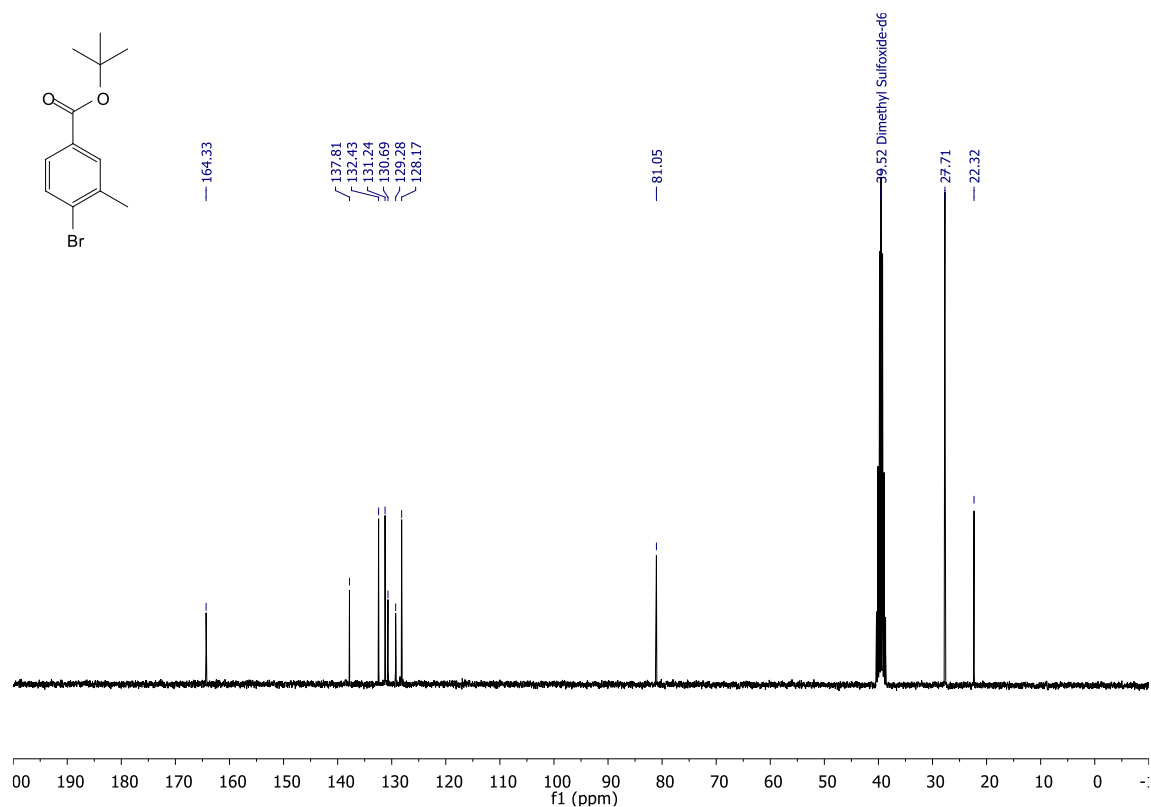
3,7-bis(dimethylamino)-5,5-dimethyldibenzo[*b,e*]silin-10(5*H*)-one (S4). To a stirred solution of 3,3'-(dimethylsilanediyl)bis(4-bromo-*N,N*-dimethylaniline) (**S3**) (0.67 g, 1.47 mmol) in dry THF (30 mL) at -78°C under an argon atmosphere was added *t*-BuLi (1.7 M in pentane, 3.5 mL, 5.95 mmol) over the course of 4 min. The mixture was stirred at -78°C for 1.5 h. Then was added dropwise dimethylcarbonyl chloride (0.15 mL, 0.175 g, 1.629 mmol). The mixture was stirred at -78°C for 16 h while slowly warming to room temperature. To the mixture was added aq. sat. NH₄Cl (6 mL) and it was extracted with CH₂Cl₂. The combined organic layers were washed with brine, dried over MgSO₄, filtered, and concentrated under reduced pressure onto silica gel. The crude was purified by flash column chromatography (cHex/EtOAc gradient from 1:0 to 0:1) to give the desired compound in 80% yield (0.382 g, 1.178 mmol). A small sample was recrystallised from cHex and EtOAc to obtain single crystals of suitable quality for x-ray diffraction measurements (CCDC deposition number: 2171686). Physical and spectral data in accordance with literature.³⁹ Yellow crystals: ¹H NMR (300 MHz, CDCl₃) δ 8.40 (d, *J* = 8.9 Hz, 2H), 6.95 – 6.73 (m, 4H), 3.09 (s, 12H), 0.47 (s, 6H). ¹³C NMR (75 MHz, CDCl₃) δ 185.37, 151.49, 140.62, 131.73, 129.90, 114.48, 113.35, 40.21, -0.88. HRMS (ESI) calculated for [M+H]⁺ C₁₉H₂₅N₂OSi⁺ 325.1731, found 325.1730.





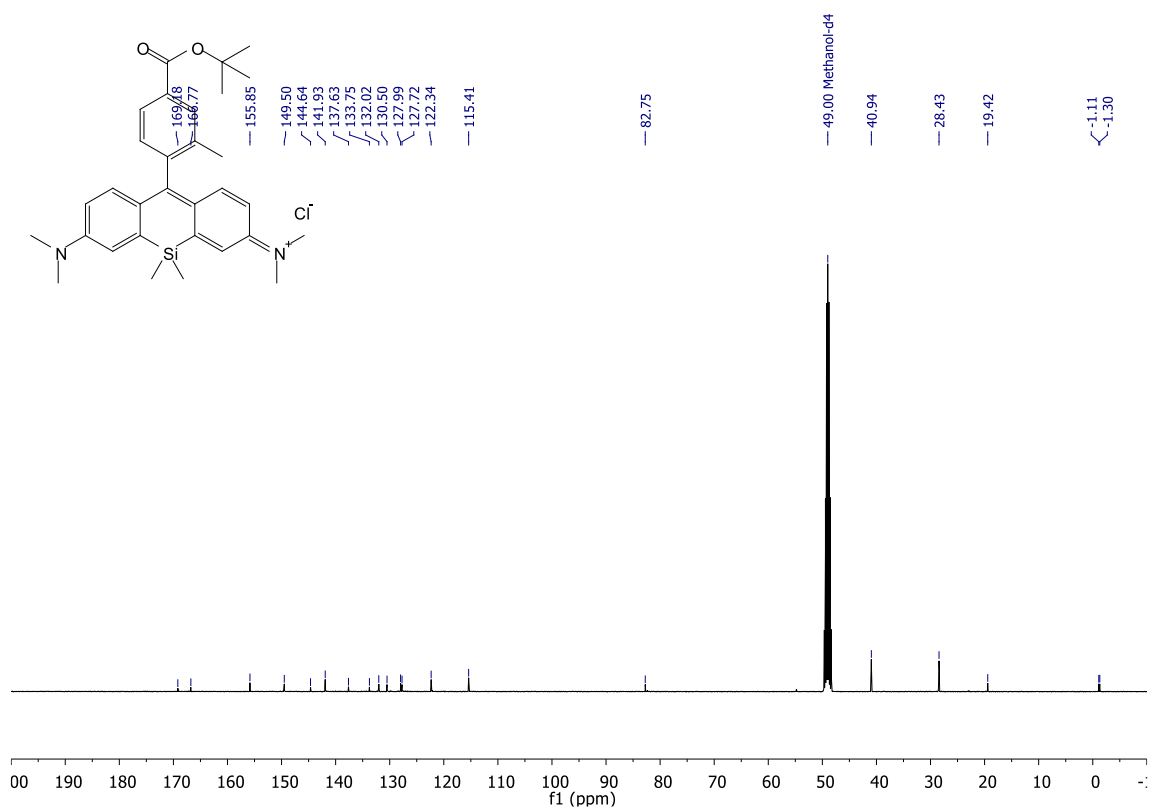
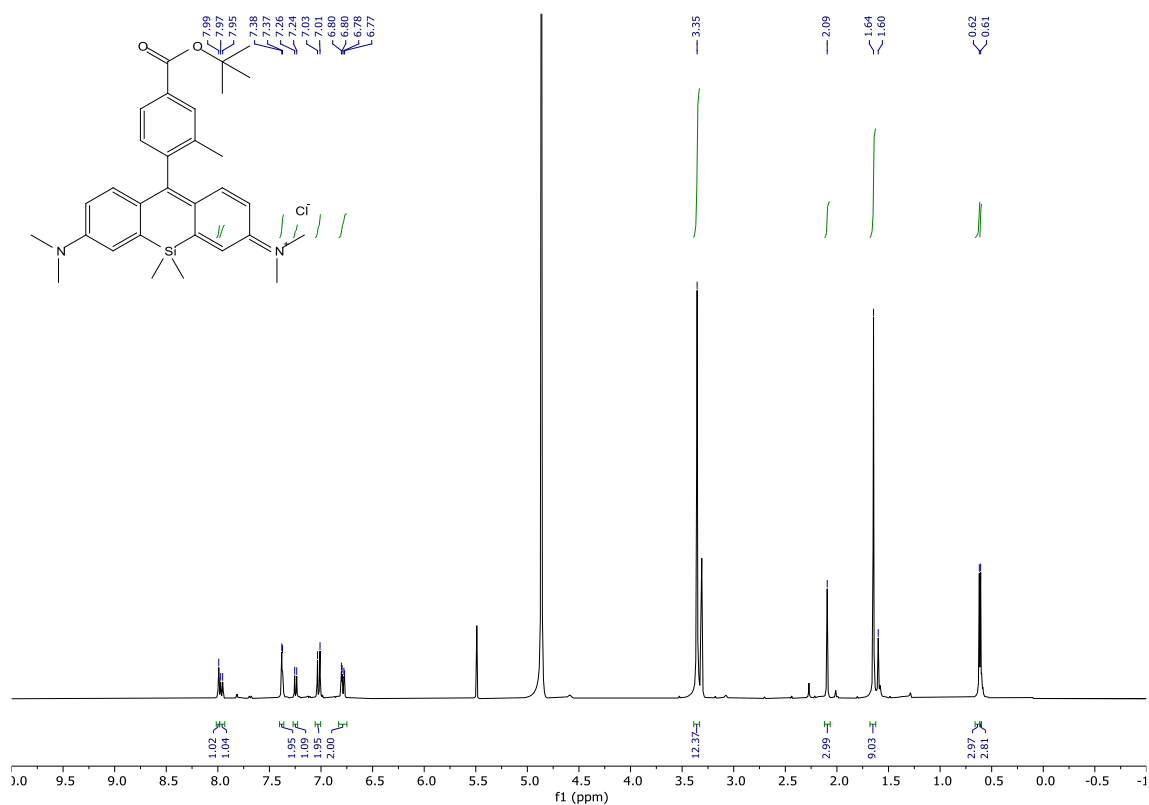
tert-butyl 4-bromo-3-methylbenzoate (S5). To a stirred solution of 4-bromo-3-methylbenzoic acid (3.98 g, 18.52 mmol) in *tert*-Butanol (100 mL) at 60°C was added DMAP (0.627 g, 5.128 mmol). The mixture was stirred for 10 min, then Boc anhydride (12.323 g, 5.646 mmol) in *tert*-Butanol was added dropwise over 30 min. First, the mixture became cloudy, but after the addition of the anhydride the mixture was clear again. It was stirred for 30 min at 60°C. The volatiles were removed under reduced pressure. The colourless solid residue was dissolved in a mixture of aq. NaHCO₃ and CH₂Cl₂. The aqueous phase was extracted with CH₂Cl₂, the combined organic layers were washed with brine, dried over MgSO₄, filtered, and concentrated under reduced pressure onto silica gel. The crude was purified by flash column chromatography (cHex/EtOAc gradient from 1:0 to 0:1) to give the desired compound in 70% yield (3.526 g, 13.002 mmol). Colourless Oil: ¹H NMR (300 MHz, DMSO-*d*₆) δ 7.83 (d, *J* = 1.7 Hz, 1H), 7.69 (d, *J* = 8.3 Hz, 1H), 7.60 (dd, *J* = 8.3, 1.8 Hz, 1H), 2.39 (s, 3H), 1.53 (s, 9H). ¹³C NMR (75 MHz, DMSO-*d*₆) δ 164.33, 137.81, 132.43, 131.24, 130.69, 129.28, 128.17, 81.05, 39.52, 27.71, 22.32. HRMS (ESI) calculated for [M+Na]⁺ C₁₂H₁₅O₂BrNa⁺ 293.0148, found 293.0152.

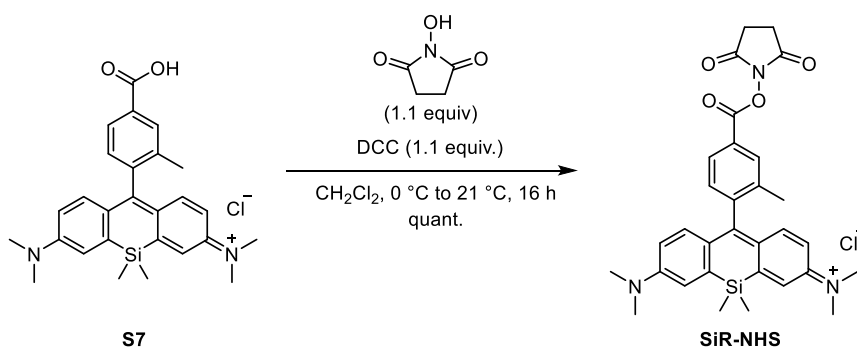




N-(10-(4-(tert-butoxycarbonyl)-2-methylphenyl)-7-(dimethylamino)-5,5-dimethyldibenzo[*b,e*]silin-3(5*H*)-ylidene)-N-methylmethanaminium chloride (S6**).** To a stirred solution of (*tert*-butyl 4-bromo-3-methylbenzoate) (**S5**) (0.90 g, 3.32 mmol) in dry THF (10 mL) at -100 °C was added dropwise *t*-BuLi (1.7 M in pentane, 2.2 mL, 3.74 mmol). The mixture was stirred at -100 °C for 30 min. Then 3,7-bis(dimethylamino)-5,5-dimethyldibenzo[*b,e*]silin-10(5*H*)-one (**S4**) (0.546 g, 1.681 mmol) dissolved in dry THF (25 mL) was added dropwise. The mixture was stirred at -100 °C for 1 h, after which it was slowly warmed to 23 °C and it was stirred for another 24 h. The reaction was quenched by adding aq. HCl (1 M, 75 mL) and the resulting blue mixture was left stirring for 30 min. It was neutralised with Na₂CO₃ until the gas evolution ceased. The mixture was extracted with CH₂Cl₂, the combined organic layers were dried over MgSO₄, filtered, and concentrated under reduced pressure onto silica gel. The crude was purified by flash column chromatography (CH₂Cl₂/MeOH gradient from 1:0 to 9:1) to give the desired compound in 86% yield (0.772 g, 1.443 mmol). Purple solid: ¹H NMR (400 MHz, CD₃OD) δ 7.99 (s, 1H), 7.96 (d, *J* = 7.9 Hz, 1H), 7.38 (d, *J* = 2.8 Hz, 2H), 7.25 (d, *J* = 7.9 Hz, 1H), 7.02 (d, *J* = 9.7 Hz, 2H), 6.79 (dd, *J* = 9.7, 2.8 Hz, 2H), 3.35 (s, 12H), 2.09 (s, 3H), 1.64 (s, 9H), 0.62 (s, 3H), 0.61 (s, 3H). ¹³C NMR (101 MHz, CD₃OD) δ 169.18, 166.77, 155.85, 149.50, 144.64, 141.93, 137.63, 133.75, 132.02,

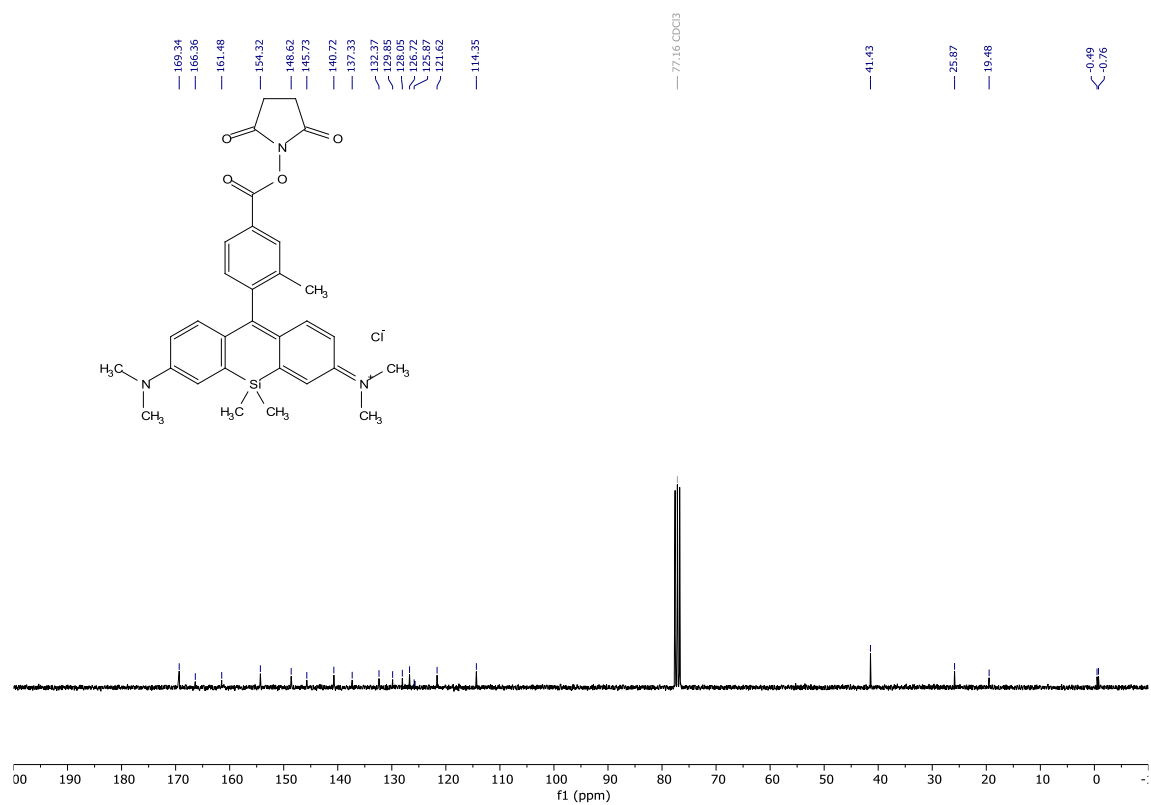
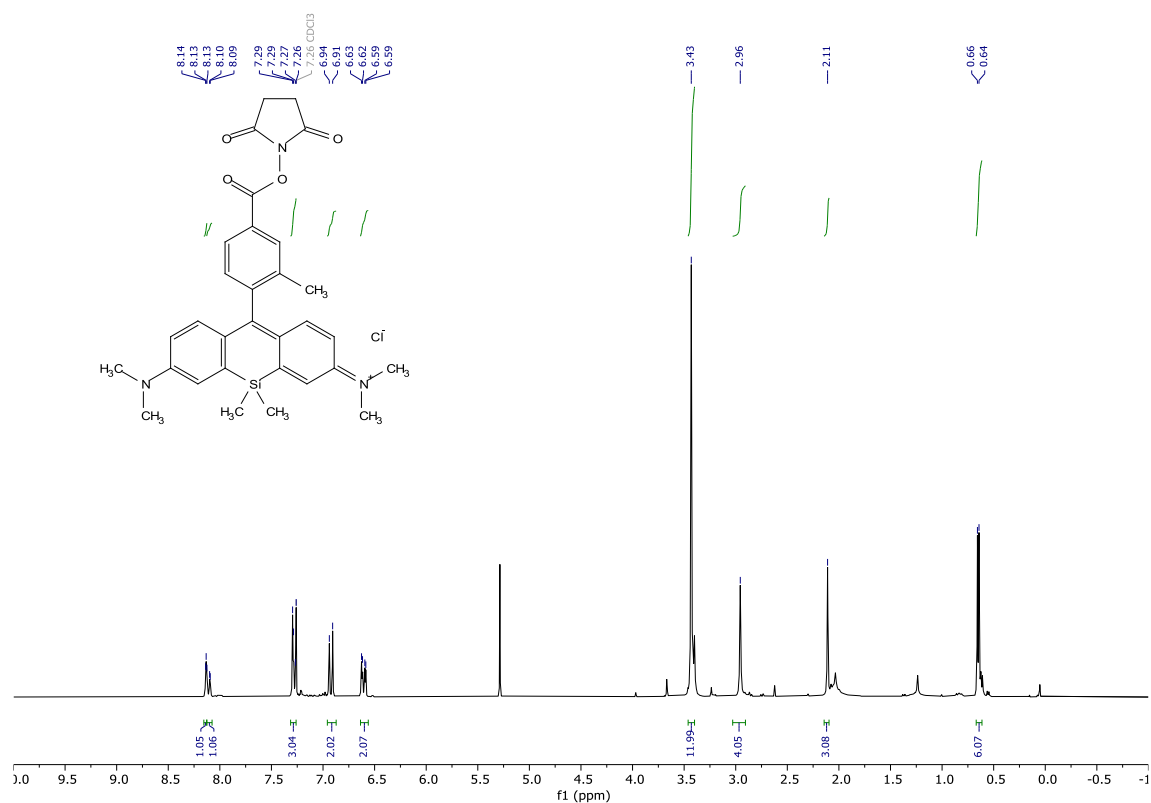
130.50, 127.99, 127.72, 122.34, 115.41, 82.75, 40.94, 28.43, 19.42, -1.11, -1.30. **HRMS** (ESI) calculated for $[M-Cl]^+ C_{31}H_{39}N_2O_2Si^+$ 499.2775, found 499.2779.



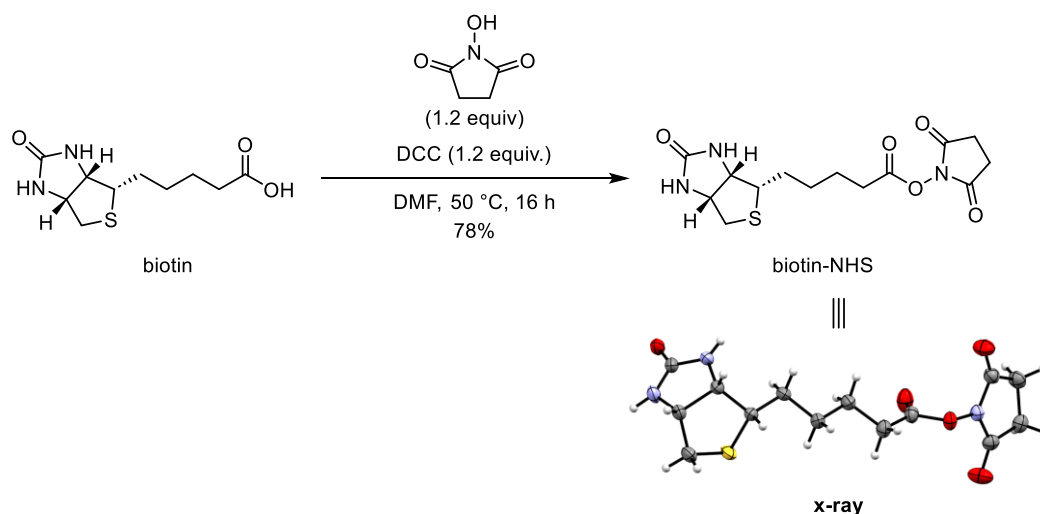


***N*-(7-(dimethylamino)-10-(4-(((2,5-dioxopyrrolidin-1-yl)oxy)carbonyl)-2-methylphenyl)-5,5-dimethyldibenzo[*b,e*]silin-3(5*H*)-ylidene)-*N*-methylmethanaminium chloride (SiR-NHS).** To a stirred solution of *N*-(10-(4-carboxy-2-methylphenyl)-7-(dimethylamino)-5,5-dimethyldibenzo[*b,e*]silin-3(5*H*)-ylidene)-*N*-methylmethanaminium chloride (**S7**) (0.099 g, 0.206 mmol) in dry CH₂Cl₂ (5 mL) at 0°C was added *N*-hydroxysuccinimide (0.037 g, 0.227 mmol) followed by *N,N'*-Dicyclohexylcarbodiimide (0.048 g, 0.234 mmol). The mixture was slowly warmed to 21°C and then stirred for 16 h. The mixture was concentrated under reduced pressure onto silica gel. The crude was purified by flash column chromatography (CH₂Cl₂/MeOH gradient from 1:0 to 9:1) to give the desired compound in quantitative yield (0.118 g, 0.204 mmol). Purple solid: ¹H NMR (300 MHz, CDCl₃) δ 8.16 – 8.06 (m, 2H), 7.31 – 7.26 (m, 3H), 6.92 (d, *J* = 9.6 Hz, 2H), 6.61 (dd, *J* = 9.6, 2.8 Hz, 2H), 3.43 (s, 12H), 2.96 (s, 4H), 2.11 (s, 3H), 0.66 (s, 3H), 0.64 (s, 3H). ¹³C NMR (75 MHz, CDCl₃) δ 169.34, 166.36, 161.48, 154.32, 148.62, 145.73, 140.72, 137.33, 132.37, 129.85, 128.05, 126.72, 125.87, 121.62, 114.35, 41.43, 25.87,

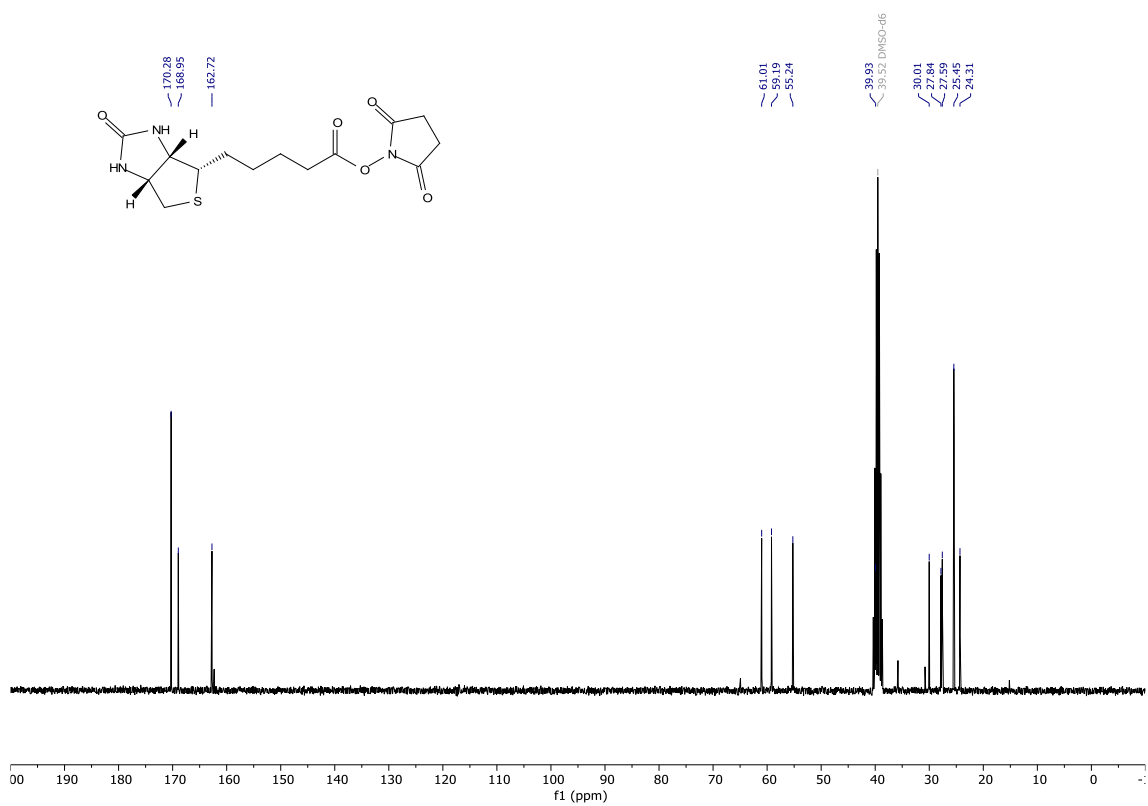
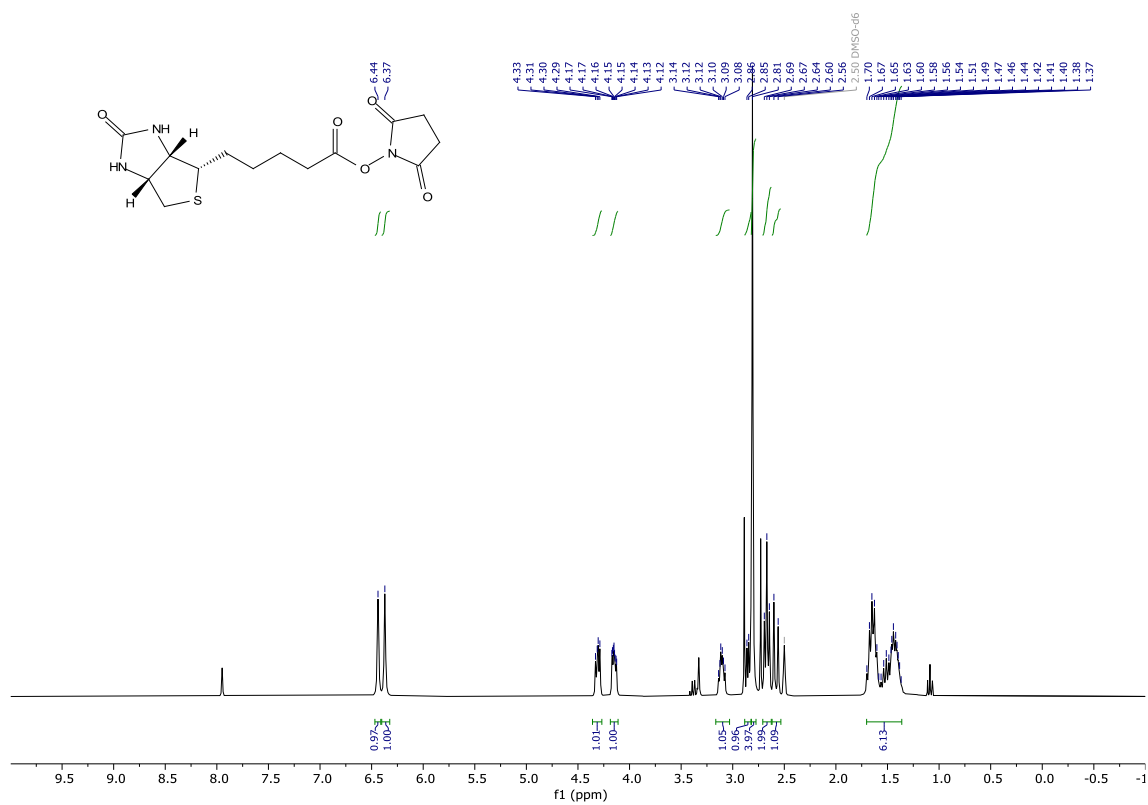
19.48, -0.49, -0.76. **HRMS** (ESI) calculated for $[M-Cl]^+ C_{31}H_{34}N_3O_4Si^+$ 540.2313, found 540.2293. **Purity** (HPLC): 95% UV₂₁₄, 95% UV₂₅₄.



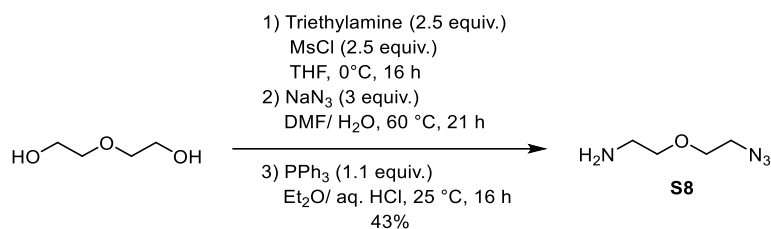
Synthesis of biotin-NHS ester



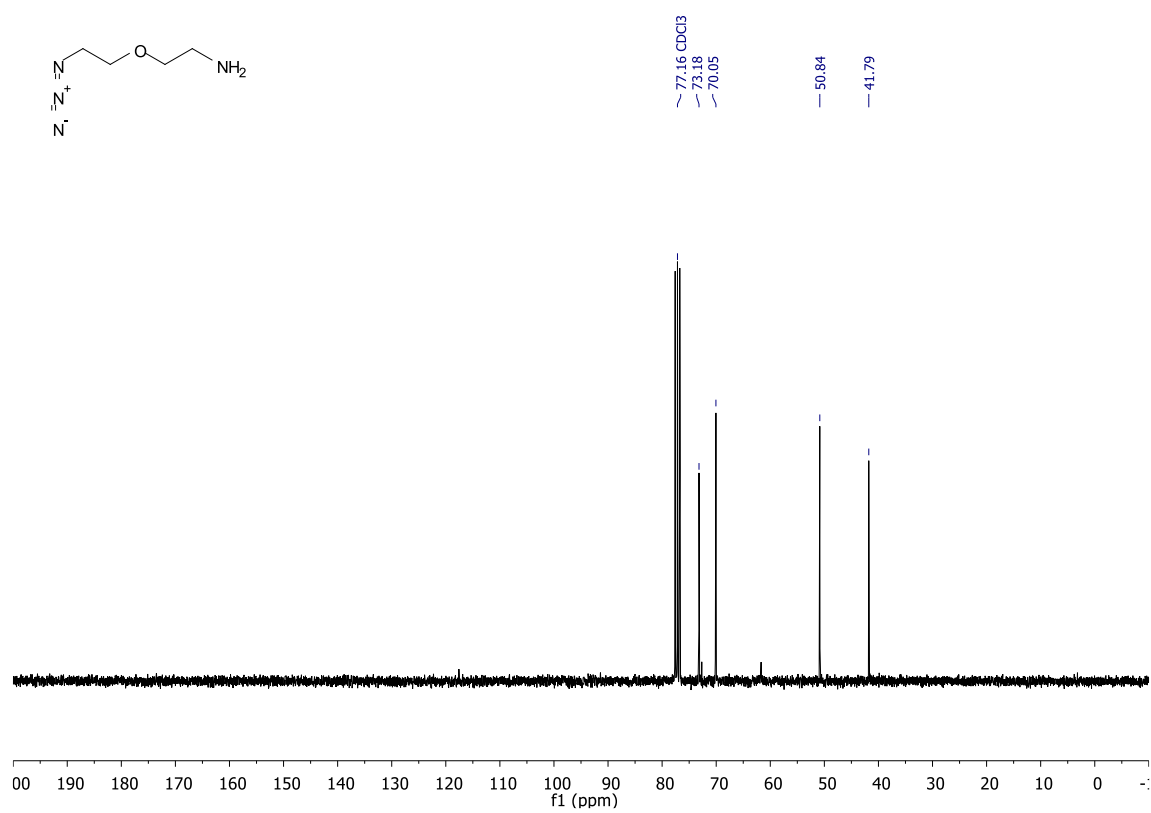
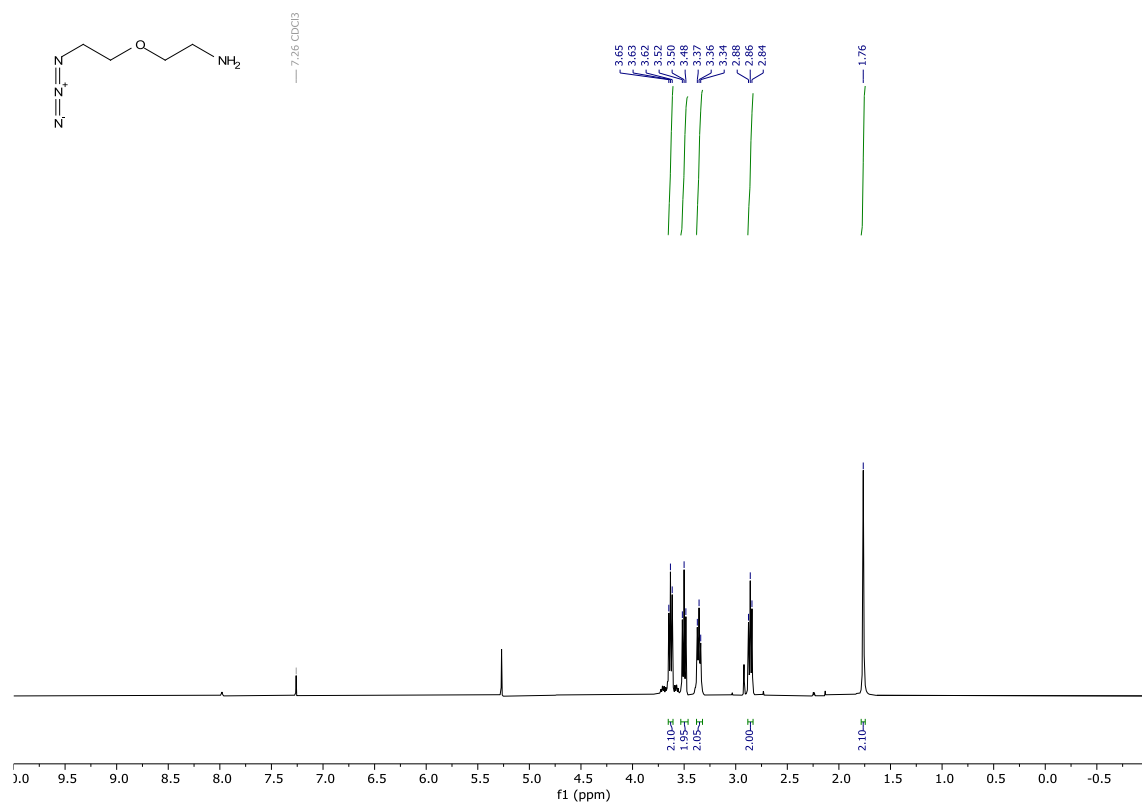
2,5-dioxopyrrolidin-1-yl-5-((3a*S*,4*S*,6a*R*)-2-oxohexahydro-1*H*-thieno[3,4-*d*]imidazol-4-yl)pentanoate (biotin-NHS). Adaptation of described procedure.⁴¹ To Biotin (1.148 g, 4.699 mmol), *N*-Hydroxysuccinimide (0.65 g, 0.565 mmol) and *N,N'*-Dicyclohexylcarbodiimide (1.163 g, 5.639 mmol) was added DMF (50 mL). The atmosphere in the flask was replaced with argon and the mixture heated to 50°C, giving a cloudy suspension. The mixture was filtered through a pad of celite. To the filtrate was added cold (-18°C) Et₂O, resulting in a precipitate. This precipitate was filtered off, washed thoroughly with cold Et₂O and the powder was dried under reduced pressure. This gave the desired compound in 78% yield (1.248 g, 3.654 mmol). A small sample was recrystallised from CH₂Cl₂ and MeOH to obtain single crystals of suitable quality for x-ray diffraction measurements (CCDC deposition number: 2177612). Colourless powder: ¹H NMR (300 MHz, DMSO-*d*₆) δ 6.44 (s, 1H), 6.37 (s, 1H), 4.31 (dd, *J* = 7.7, 4.9 Hz, 1H), 4.15 (m, 1H), 3.11 (m, 1H), 2.85 (d, *J* = 5.1 Hz, 1H), 2.81 (s, 4H), 2.67 (t, *J* = 7.3 Hz, 2H), 2.58 (d, *J* = 12.4 Hz, 1H), 1.70 – 1.36 (m, 6H). ¹³C NMR (75 MHz, DMSO-*d*₆) δ 170.28, 168.95, 162.72, 61.01, 59.19, 55.24, 39.93, 30.01, 27.84, 27.59, 25.45, 24.31. HRMS (ESI) calculated for [M+H]⁺ C₁₄H₂₀N₃O₅S 342.1118, found 342.1113.

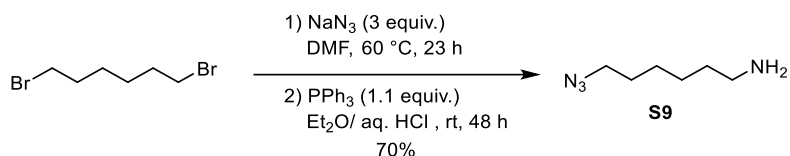


Synthesis of azide linkers

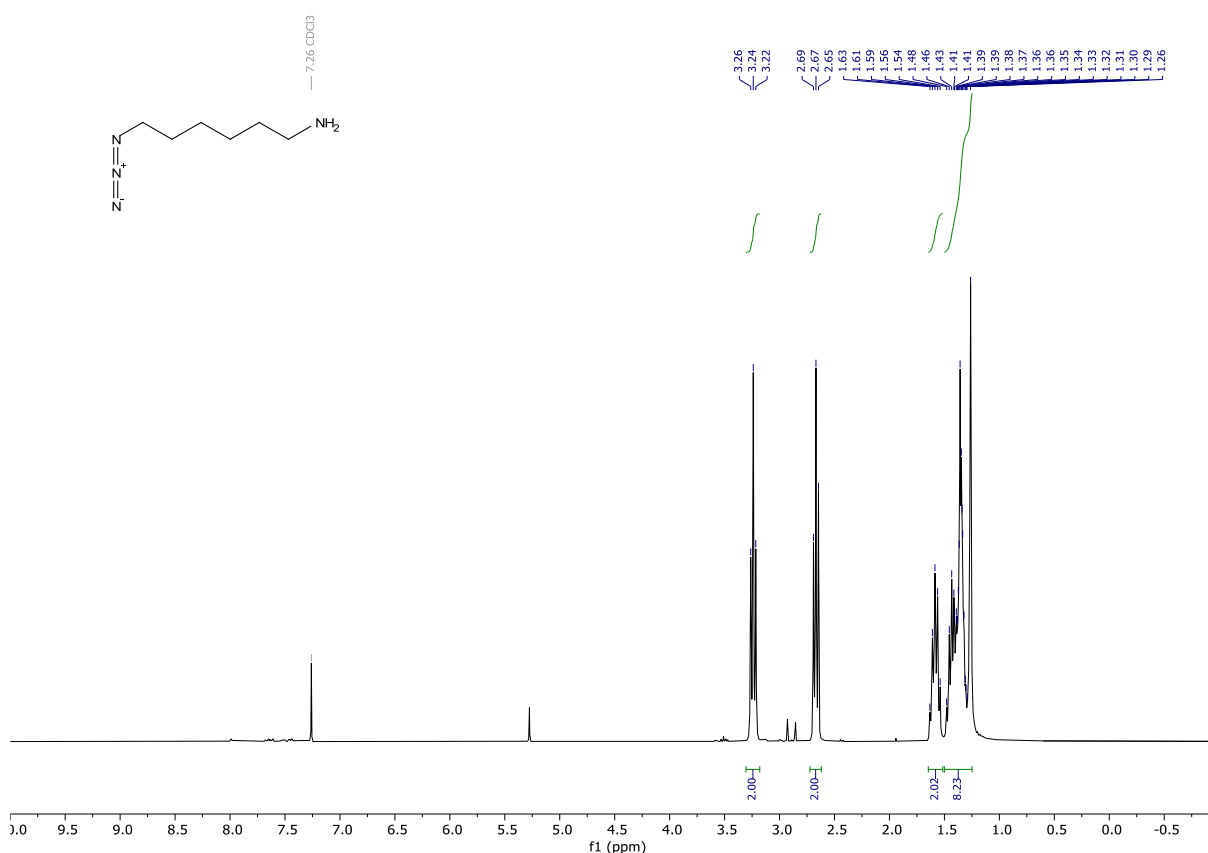


2-(2-azidoethoxy)ethan-1-amine (S8). According to modified literature procedure.⁴² To a stirred solution of diethylene glycol (5.00 g, 47.12 mmol) and methanesulfonyl chloride (9.2 mL, 13.616 g, 118.865 mmol) in THF (55 mL) at 0 °C was added dropwise over the course of 25 min Et₃N (20 mL, 14.6 g, 144.283 mmol) in THF (30 mL). The mixture was slowly warmed to 23 °C and stirred for 16 h. The suspension was filtered, and the filter cake was thoroughly washed with THF. The filtrate was concentrated under reduced pressure resulting in a clear orange oil. This oil was dissolved in a mixture of DMF (40 mL) and H₂O (30 mL). To this mixture sat. aq. NaHCO₃ (15 mL) and NaN₃ (6.404 g, 98.508 mmol) was added. The flask was protected from light and the mixture was stirred for 21 h at 60 °C. The mixture was extracted with Et₂O (6 x 30 mL). The combined organic phases were washed with brine, dried over MgSO₄, filtered, and concentrated under reduced pressure to ca. 30 mL residual volume of Et₂O. To this solution was added aq. HCl (1 M, 40 mL) and then dropwise over the course of 60 min PPh₃ (8.027 g, 31.531 mmol) in Et₂O (40 mL). The reaction mixture was left stirring at 25 °C for 16 h. The organic phase was separated. The resulting aqueous phase was washed with Et₂O (6 x 10 mL). To the aqueous layer was added aq. NaOH (20%, 10 mL). This aqueous mixture was extracted with CH₂Cl₂ (5 x 25 mL). The combined organic layers were washed with brine, dried over MgSO₄, filtered, and concentrated under reduced pressure. This gave the desired compound in 43% yield (2.966 g, 20.430 mmol). Clear yellowish oil: ¹H NMR (300 MHz, CDCl₃) δ 3.63 (t, *J* = 5.0 Hz, 2H), 3.50 (t, *J* = 5.1 Hz, 2H), 3.36 (t, *J* = 4.9 Hz, 2H), 2.88 – 2.83 (t, *J* = 5.1 Hz, 2H), 1.76 (s, 2H). ¹³C NMR (75 MHz, CDCl₃) δ 73.18, 70.05, 50.84, 41.79. HRMS (ESI) calculated for [M+H]⁺ C₄H₁₁N₄O⁺ 131.0927, found 131.0923.

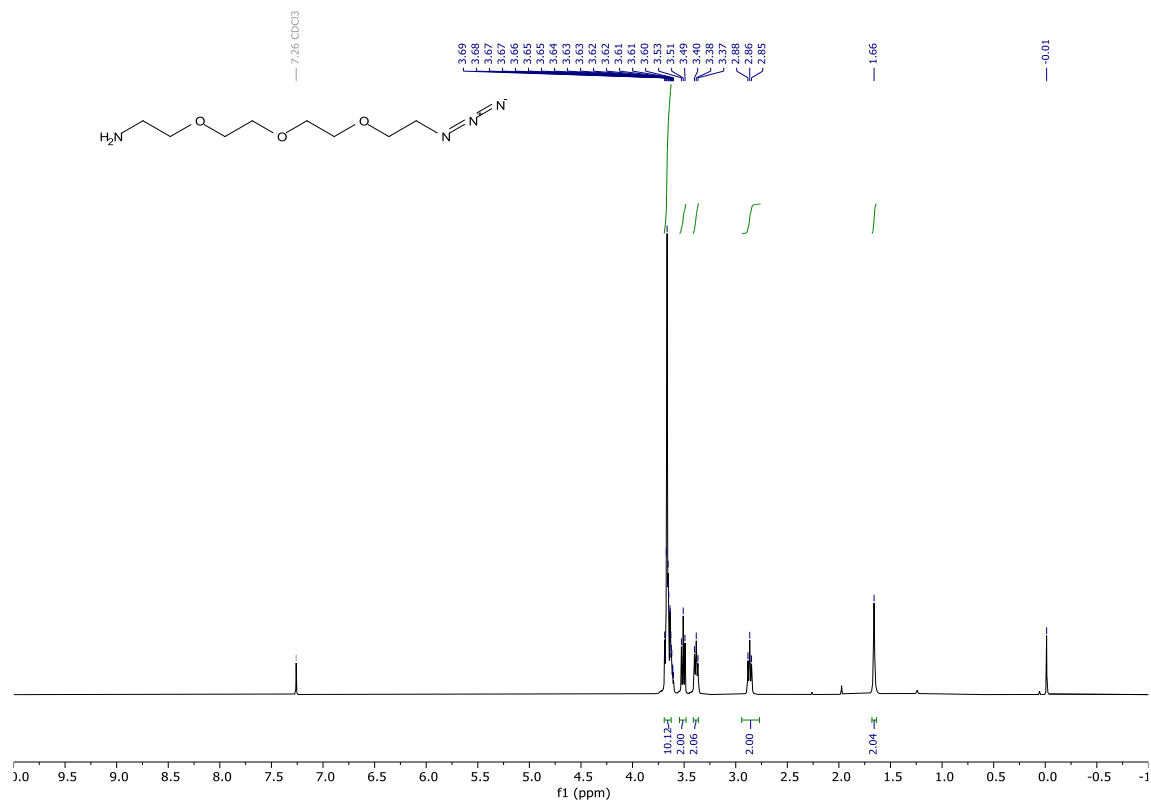


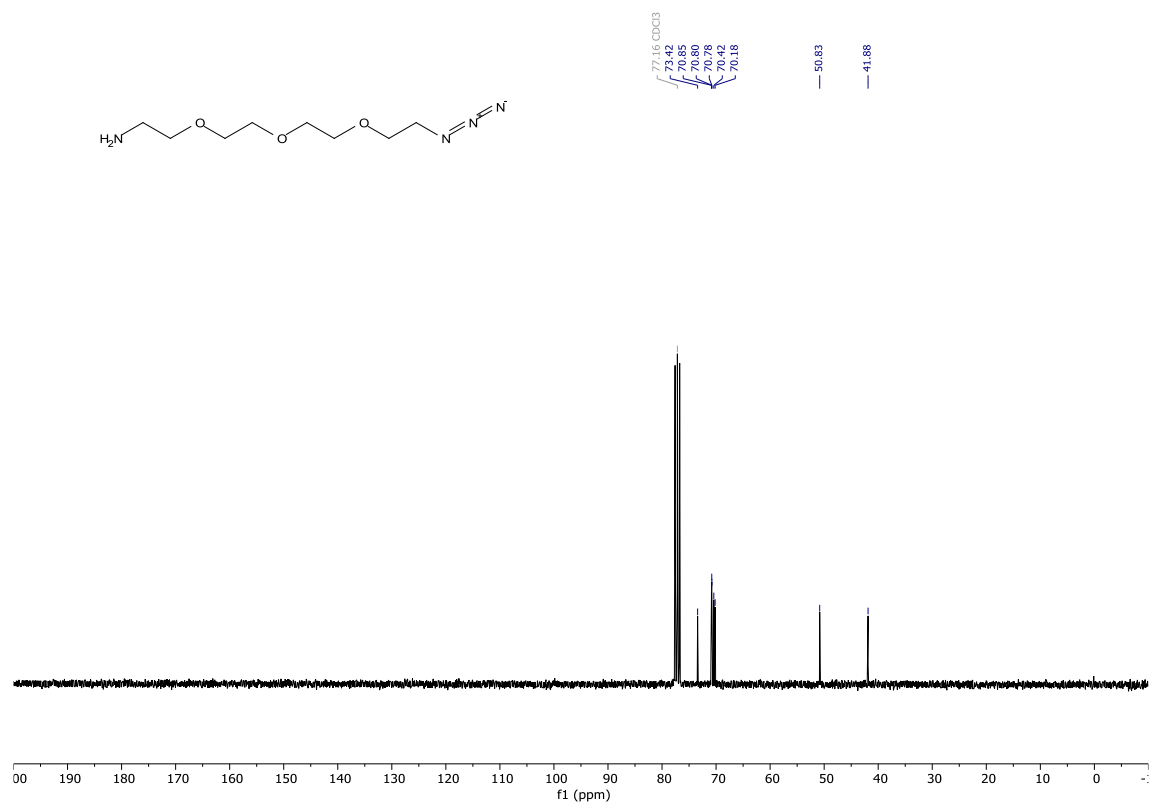


6-azidohexan-1-amine (S9). According to modified literature procedure.⁵⁷ To a stirred solution of 1,6-dibromohexane (4.8 mL, 7.61 g, 31.2 mmol) in dry DMF (80 mL) was added NaN₃ (6.07 g, 93.4 mmol). The mixture was heated to 60°C and stirred for 23 h under an argon atmosphere. To the reaction mixture water (150 mL) was added and the mixture was extracted with Et₂O (4 x 20 mL). The combined organic phases were dried over MgSO₄ and filtered into a round bottom flask. To this flask was added aqueous HCl (1 M, 30 mL), EtOAc (60 mL) and PPh₃ (9.03 g, 34.42 mmol) in portions. First a slight gas evolution was observed, which ceased with the later additions. The mixture was stirred for 48 h under an argon atmosphere. The mixture was diluted with aq. HCl (1 M, 30 mL) and extracted with CH₂Cl₂. The organic layers were discarded and the aqueous layer was basified with aq. NaOH and extracted with CH₂Cl₂. The combined organic layers were washed with brine, dried over MgSO₄, filtered, and concentrated under reduced pressure to give the desired compound in 70% yield (3.109 g, 21.865 mmol). Slight yellow oil: ¹H NMR (300 MHz, CDCl₃) δ 3.24 (t, *J* = 6.9 Hz, 2H), 2.67 (t, *J* = 6.8 Hz, 2H), 1.59 (p, *J* = 6.8 Hz, 2H), 1.50 – 1.20 (m, 8H). ¹³C NMR (75 MHz, CDCl₃) δ 51.49, 42.16, 33.65, 28.91, 26.68, 26.53. HRMS (ESI) calculated for [M+Na]⁺ C₆H₁₅N₄ 143.1291, found 143.1291.

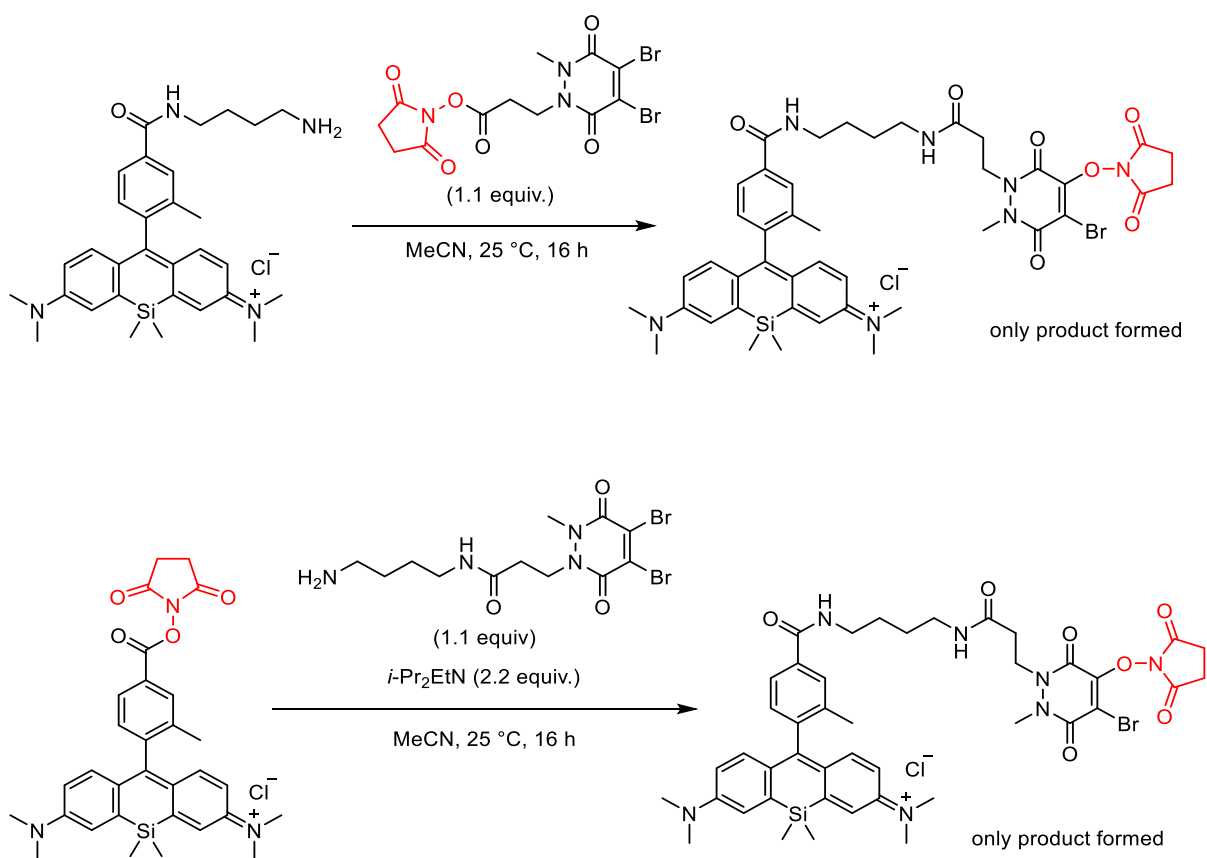


0°C and basified with 2 M aq. NaOH. The aqueous phase was then extracted with CH₂Cl₂, the combined organic layers were washed with brine, dried over MgSO₄, filtered, and concentrated under reduced pressure to give the desired compound in 33% yield (1.731 g, 7.931 mmol). Yellowish oil: **¹H NMR** (300 MHz, CDCl₃) δ 3.69 – 3.63 (m, 10H), 3.51 (t, *J* = 5.2 Hz, 2H), 3.38 (t, *J* = 5.1 Hz, 2H), 2.86 (t, *J* = 5.2 Hz, 2H), 1.66 (s, 2H). **¹³C NMR** (75 MHz, CDCl₃) δ 73.42, 70.85, 70.80, 70.78, 70.42, 70.18, 50.83, 41.88. **HRMS** (ESI) calculated for [M+H]⁺ C₈H₁₉N₄O₃ 219.1452, found 219.1450.





Observed side reactions with NHS-activated esters



Scheme S2 Original coupling strategy to link fluorescent SiR dye with dibromopyridazinediones via NHS-activated esters. Even though the amide bond formation was very efficient, one bromine atom of the dibromopyridazinediones was displaced by the *N*-hydroxysuccinimid leaving group, leading to the shown products. The isolated adducts are most probably a mixture of regioisomers and their NMR and HRMS spectra are in agreement with the depicted structures. HRMS (ESI) calculated for $[M-Cl]^+$ $C_{43}H_{51}BrN_7O_7Si$ 884.2803, found 884.2825.

SDS-PAGE of modified anti GAPDH antibody under non-reducing conditions

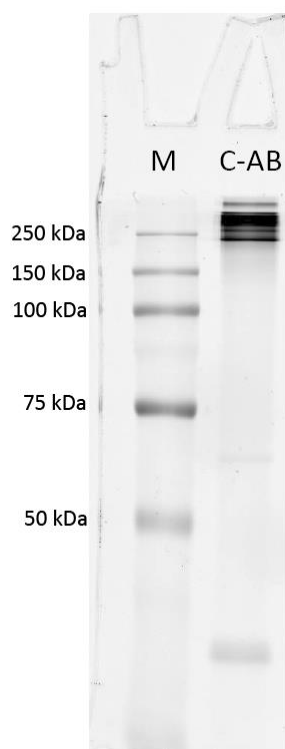


Figure S1 SDS-PAGE of anti GAPDH antibody after re-bridging with SiR-labelled dibromopyridazinedione **8** (lane C-AB) using non-reducing loading buffer (not containing mercaptoethanol). Detection of protein bands by fluorescence (Cy5 channel). Several fluorescent bands at around 250 kDa most probably result from aggregated and incompletely linearised labelled antibodies. Compare to SDS-PAGE of same antibody sample using reducing loading buffer (**Figure 1, B**). Lanes: M, All Blue protein standard; C-AB, SiR-conjugated anti GAPDH antibody.

Size exclusion chromatography (SEC) of BFL-modified anti GAPDH and native anti GAPDH antibodies

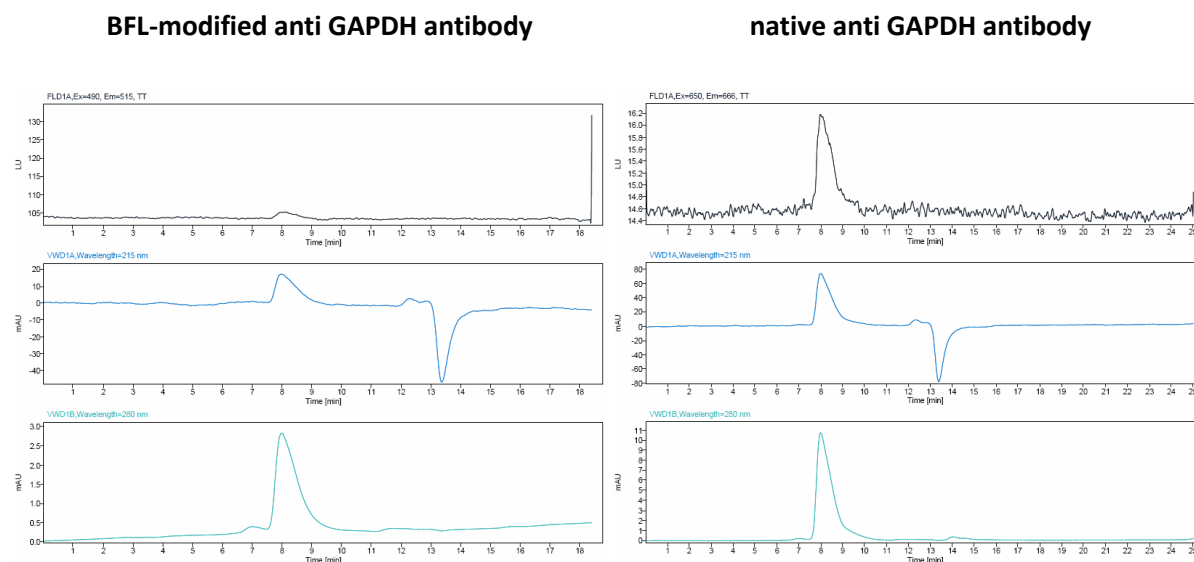


Figure S2 Size exclusion chromatograms of BFL-modified anti GAPDH antibody after re-bridging with dibromopyridazinedione **9** (left traces) and of native anti GAPDH antibody (right traces). Detection of antibodies by fluorescence (top traces, note the different scale of the intensity axes), by absorption at 215 nm (middle traces) and at 280 nm (bottom traces).

Direct conjugation of anti GAPDH antibody

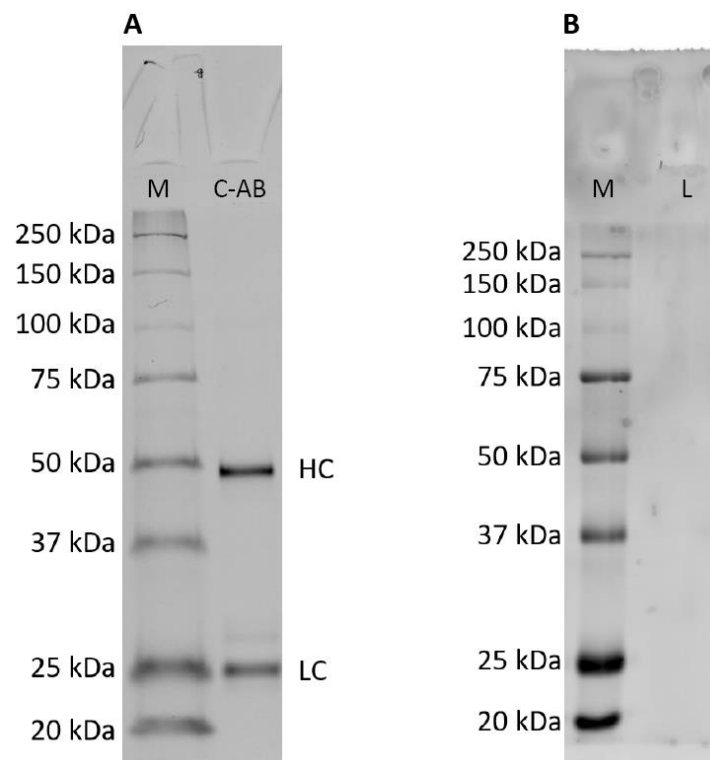


Figure S3 Anti GAPDH antibody was directly labelled with electrophilic, fluorescent reagent SiR-NHS (detailed procedure see *Experimental section*). **(A)** SDS-PAGE of anti GAPDH antibody conjugation product (lane C-AB) detected by fluorescence (excitation at 635 nm, Cy5 channel). Bands at 50 kDa and 25 kDa correspond to the heavy (HC) and light chains (LC), respectively. **(B)** Western blot analysis of mouse cardiomyocyte whole cell lysate (lane L) using directly SiR-labelled anti GAPDH antibody from **(A)**. Detection by fluorescence (Cy5 channel) did not show any protein band at 36 kDa corresponding to mouse GAPDH. M, All Blue Protein Standard.

SDS-PAGE of IgG antibody conjugates

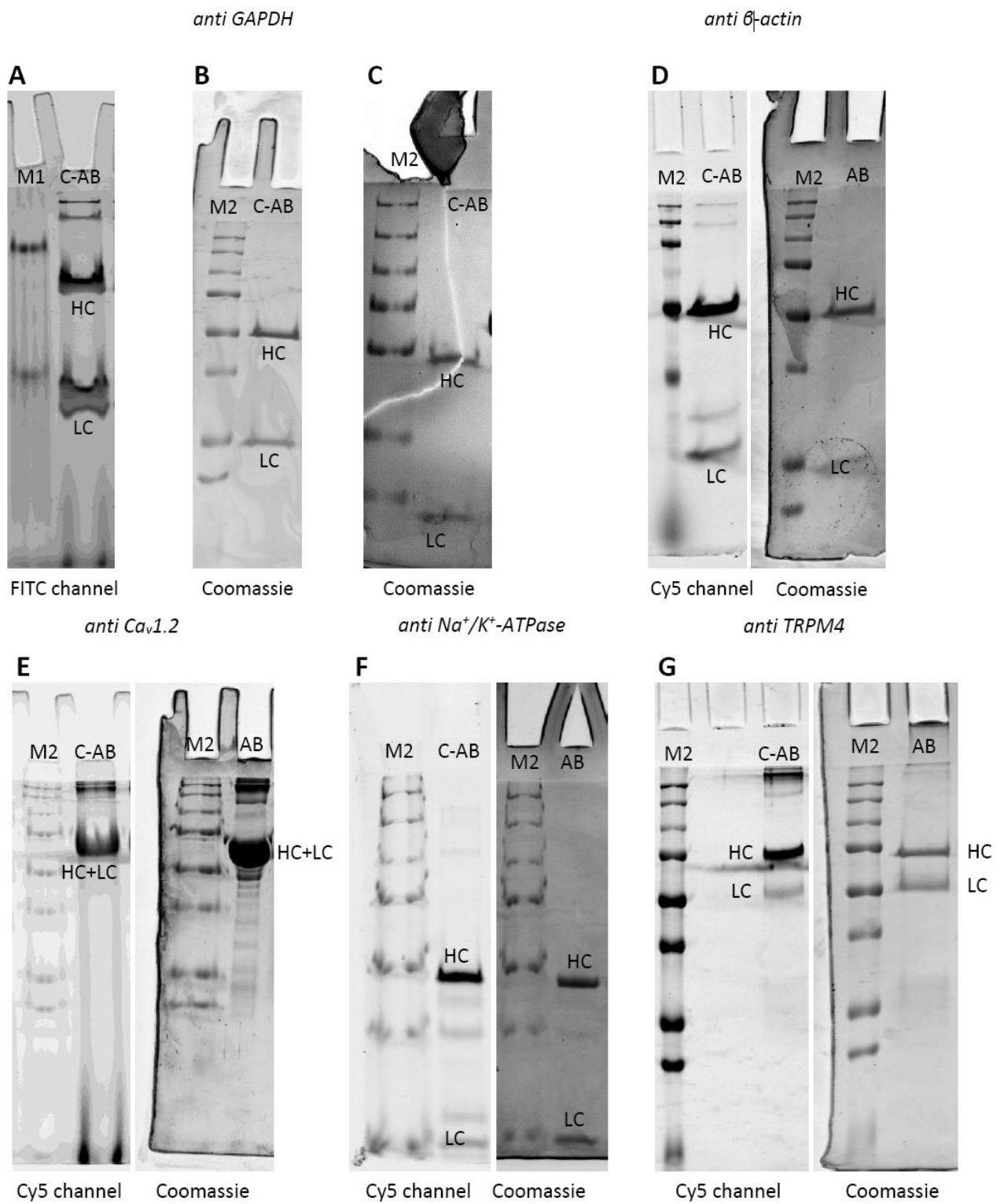
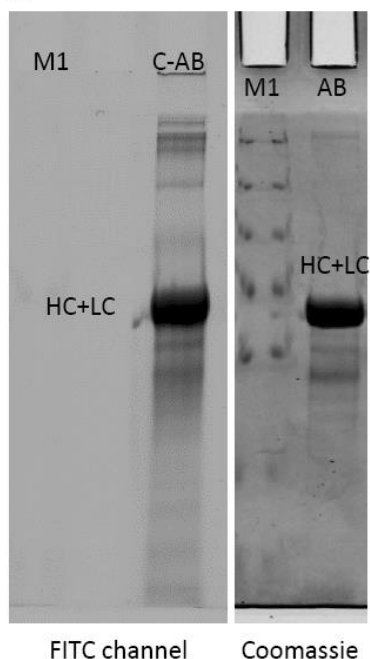


Figure S4



48

Western blot and direct immunofluorescence with IgG antibody conjugates

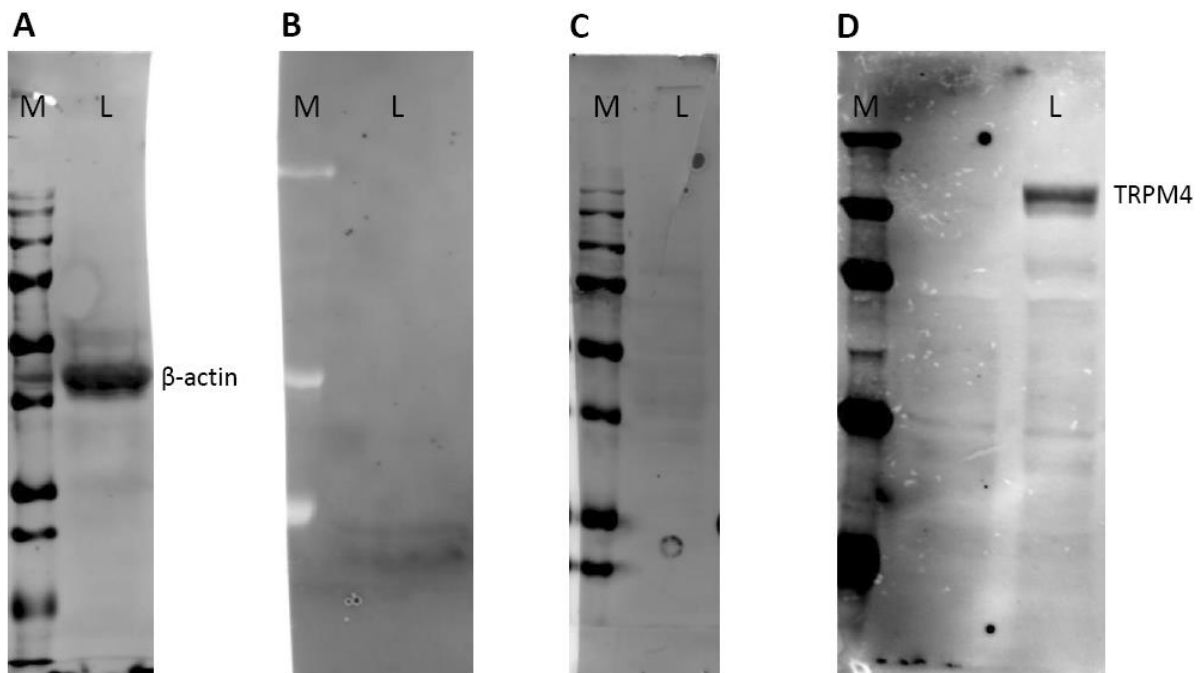


Figure S5 Western blot analysis of mouse cardiomyocyte whole cell lysate using (A) SiR-modified anti β-actin antibody, (B) BFL-modified anti Na_v1.5 antibody, (C) SiR-modified anti Na⁺/K⁺-ATPase antibody or (D) SiR-modified anti TRPM4 antibody. SiR- and BFL-conjugated antibodies were detected directly by fluorescence (Cy5 and FITC channel, respectively). Lanes: M, Marker, L, Lysate.

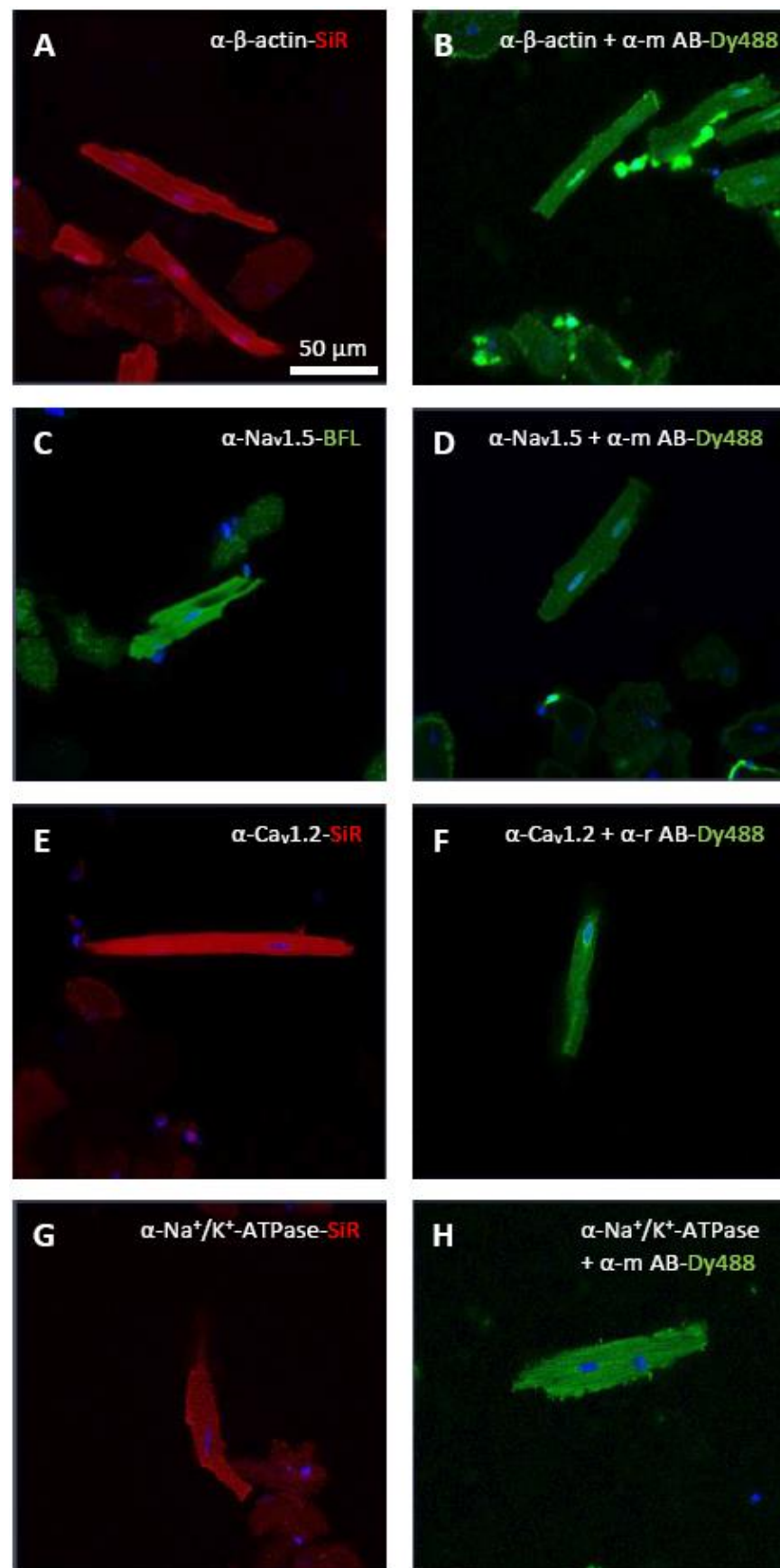


Figure S6

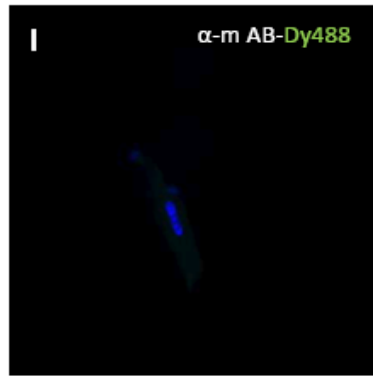
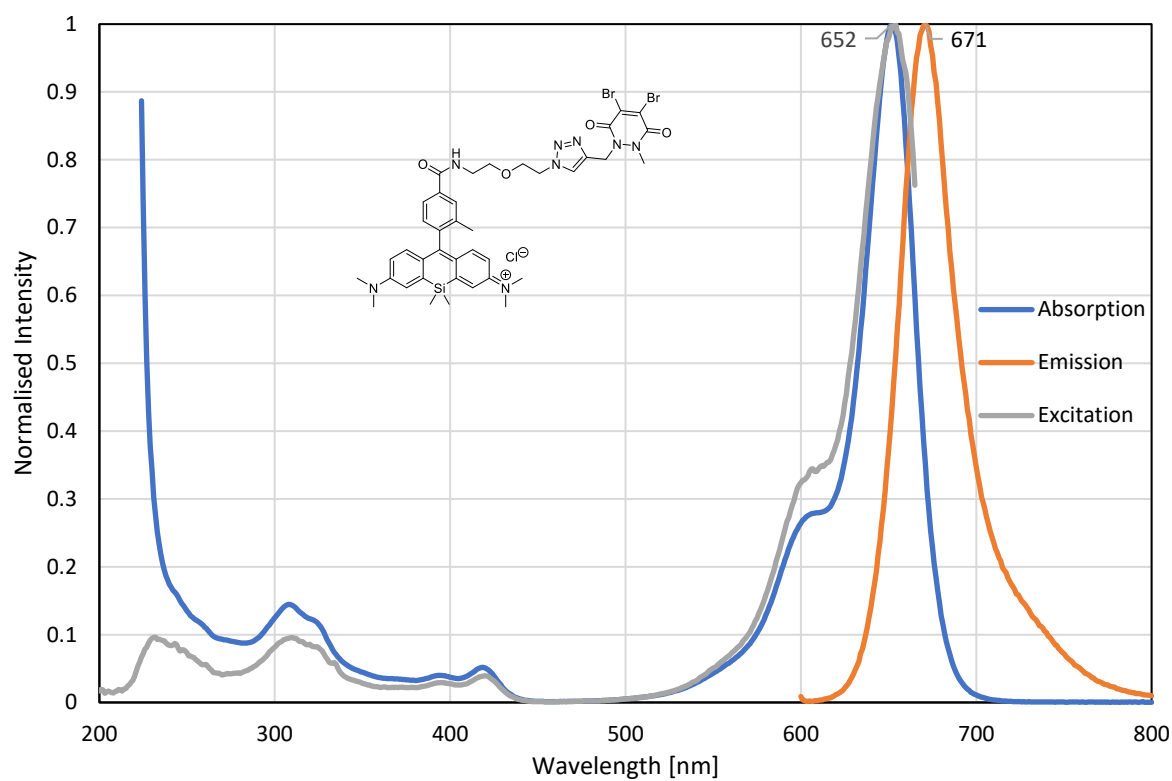


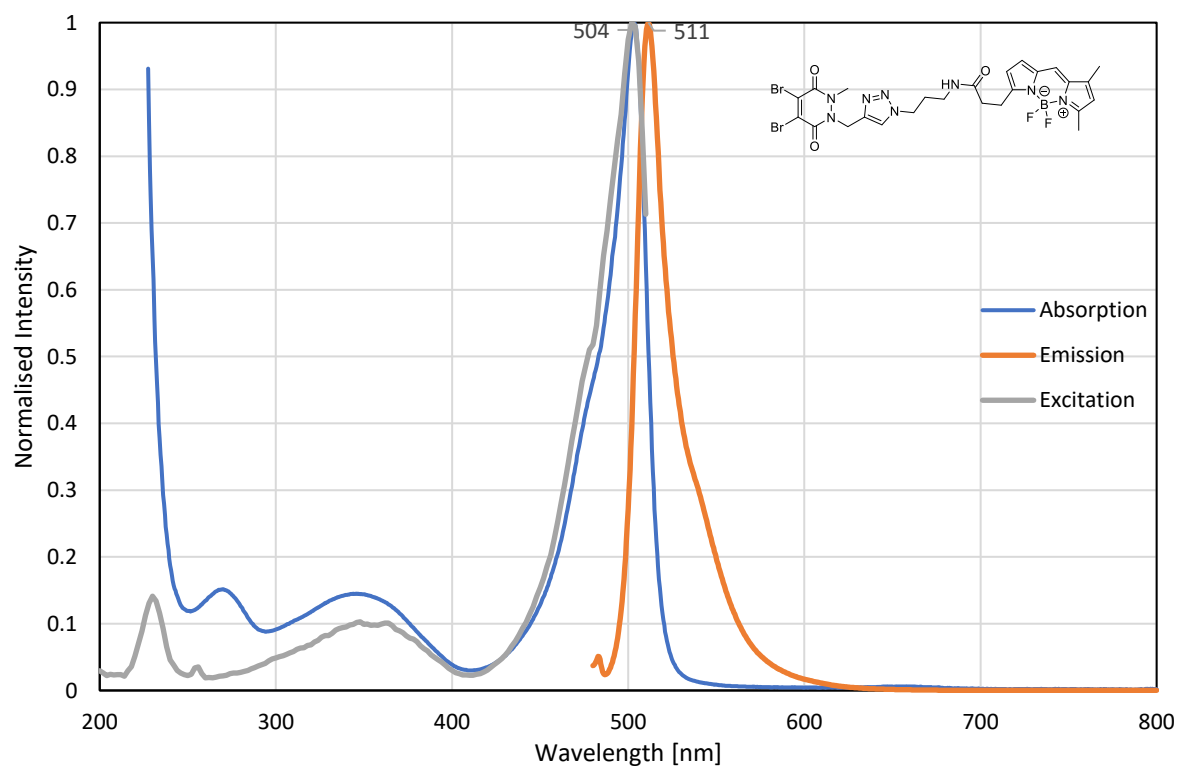
Figure S6 (Continued) Direct (**A, C, E, G**) and indirect (**B, D, F, H**) immunofluorescence with isolated and fixed mouse cardiomyocytes using conjugated and native antibodies. (**A**) SiR-modified anti β -actin antibody. (**B**) Native anti β -actin antibody. (**C**) BFL-modified anti $\text{Na}_v1.5$ antibody. (**D**) Native anti $\text{Na}_v1.5$ antibody. (**E**) SiR-modified anti $\text{Ca}_v1.2$ antibody. (**F**) Native anti $\text{Ca}_v1.2$ antibody. (**G**) SiR-modified anti Na^+/K^+ -ATPase antibody. (**H**) Native anti Na^+/K^+ -ATPase antibody. Detection of primary antibodies by fluorescence (**A, C, E, G**; Cy5 or FITC channel, respectively) or by secondary goat anti mouse or anti rabbit Dy488-labelled antibodies (**B, D, F, H**). (**I**) Control experiment: mouse cardiomyocytes incubated with secondary goat anti mouse Dy488-labelled antibody alone (Cy5, FITC and DAPI channels overlay). Cell nuclei stained with DAPI (blue). SiR, Si-rhodamine; BFL, BODIPY FL; Dy488, DyLight® 488; α -m AB, goat anti mouse antibody; α -r AB, goat anti rabbit antibody. Scale bar represents 50 μm .

Absorption and emission spectra for fluorescent dibromopyridazinediones 8-10

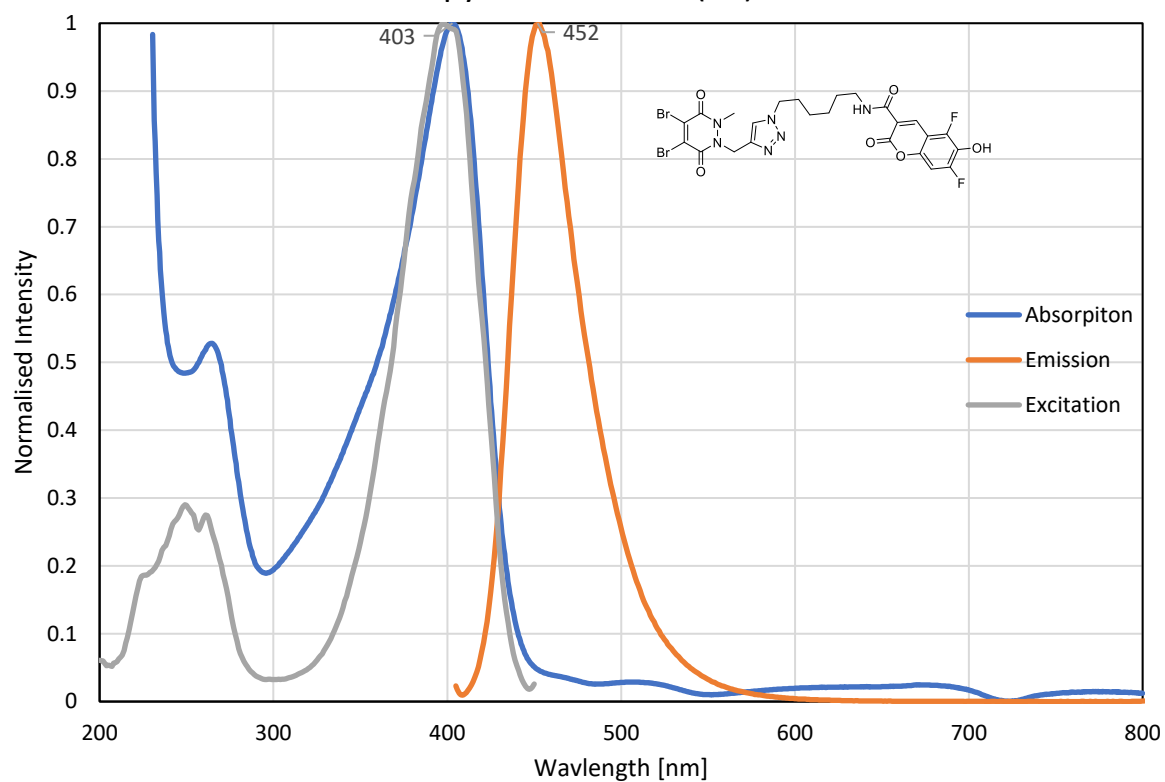
SiR pyridazinedione (**8**)



BFL pyridazinedione (**9**)

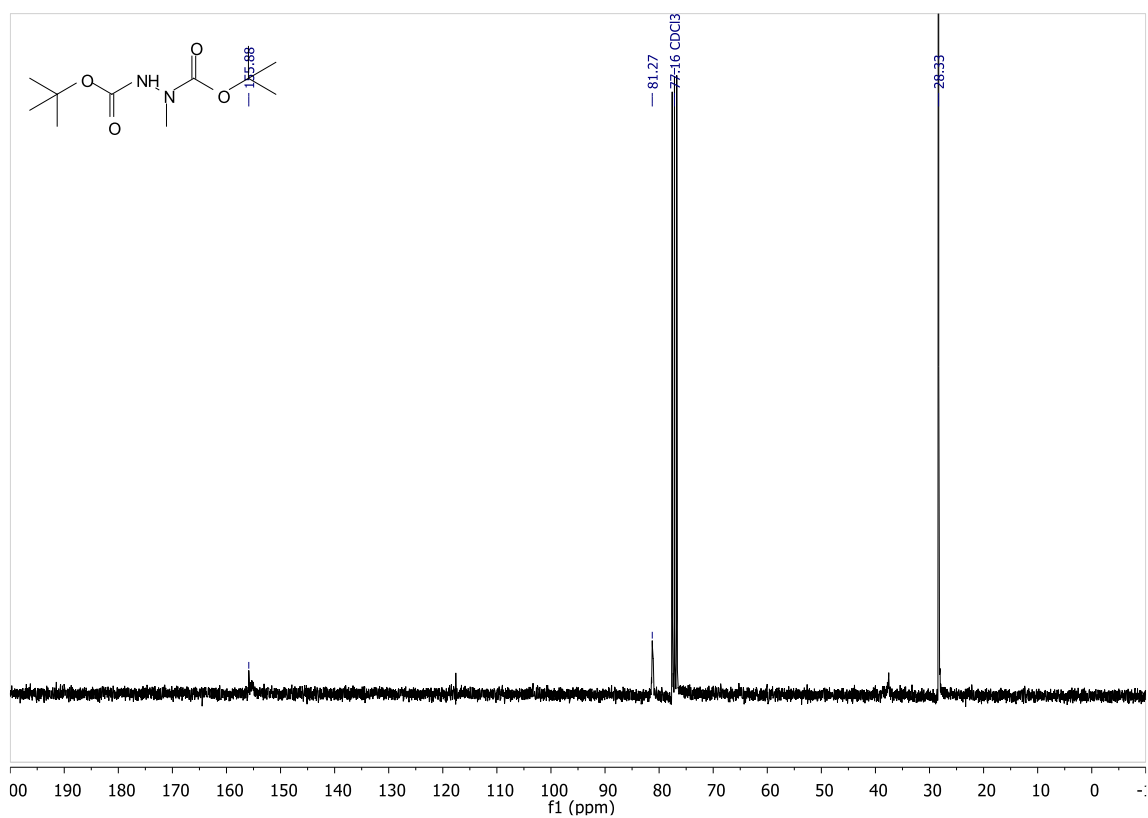
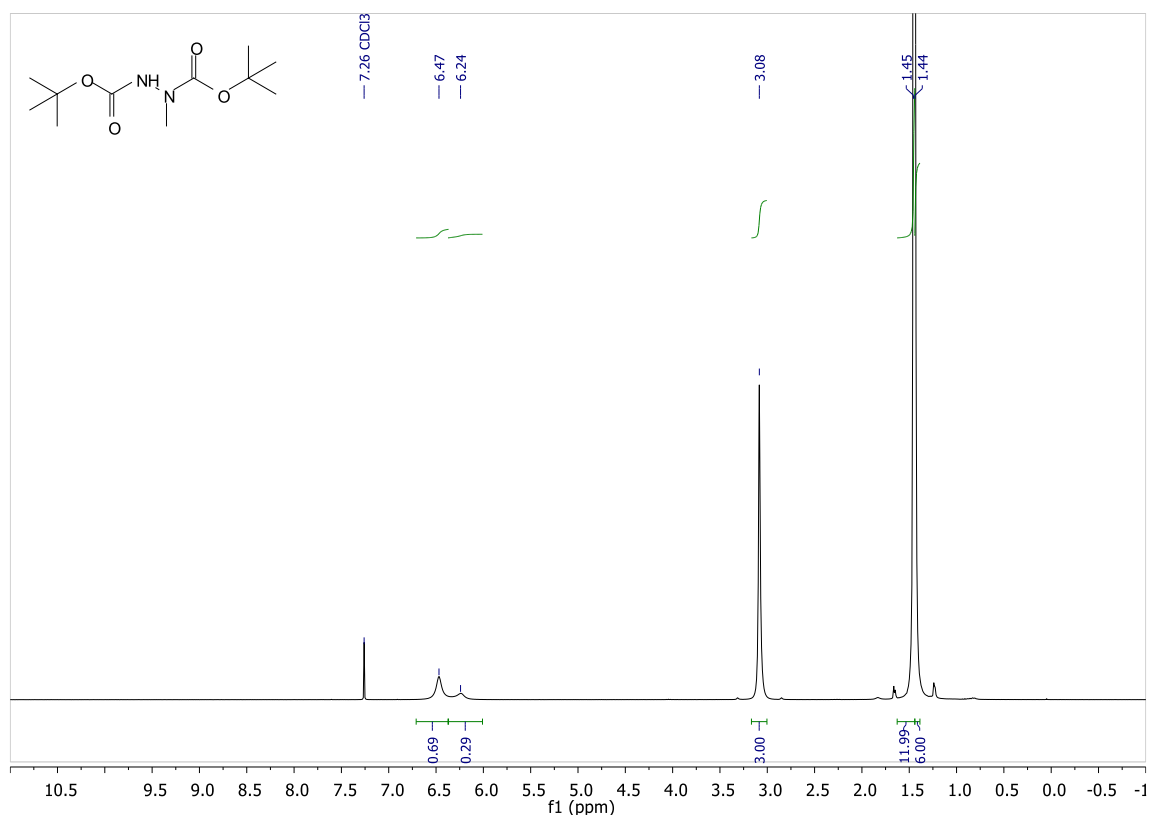


PB pyridazinedione (**10**)

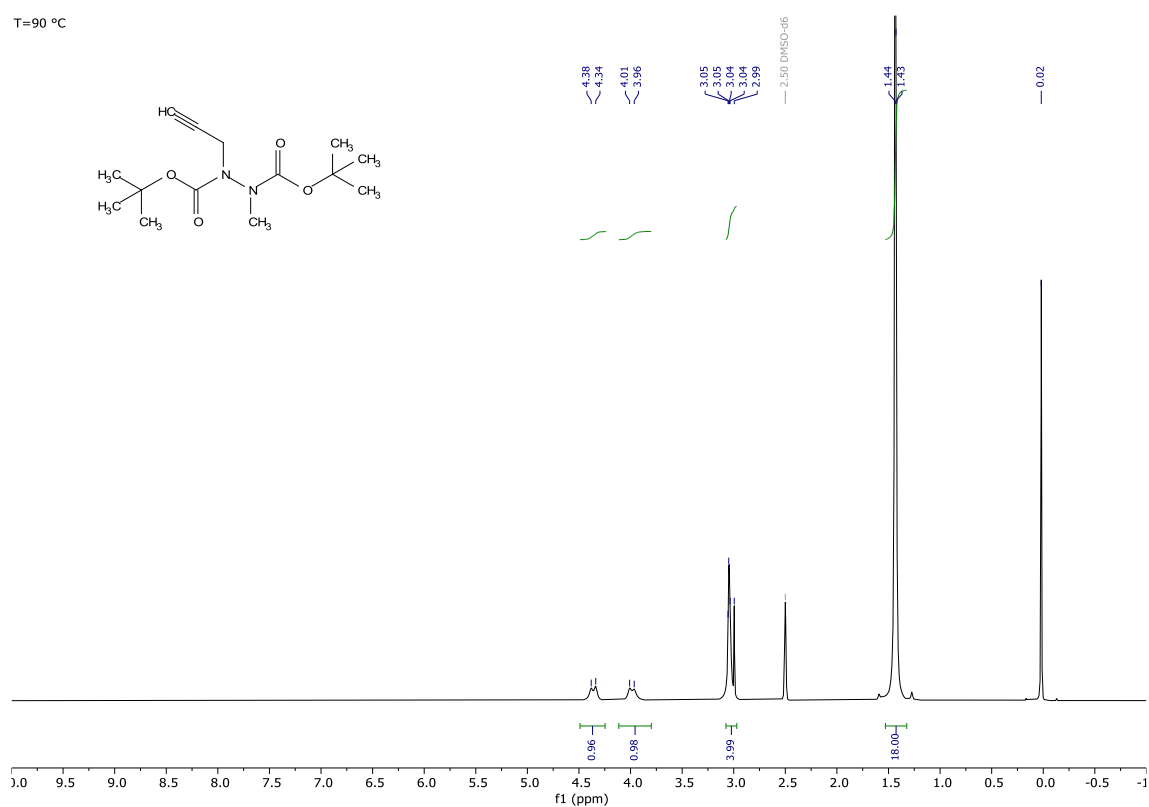
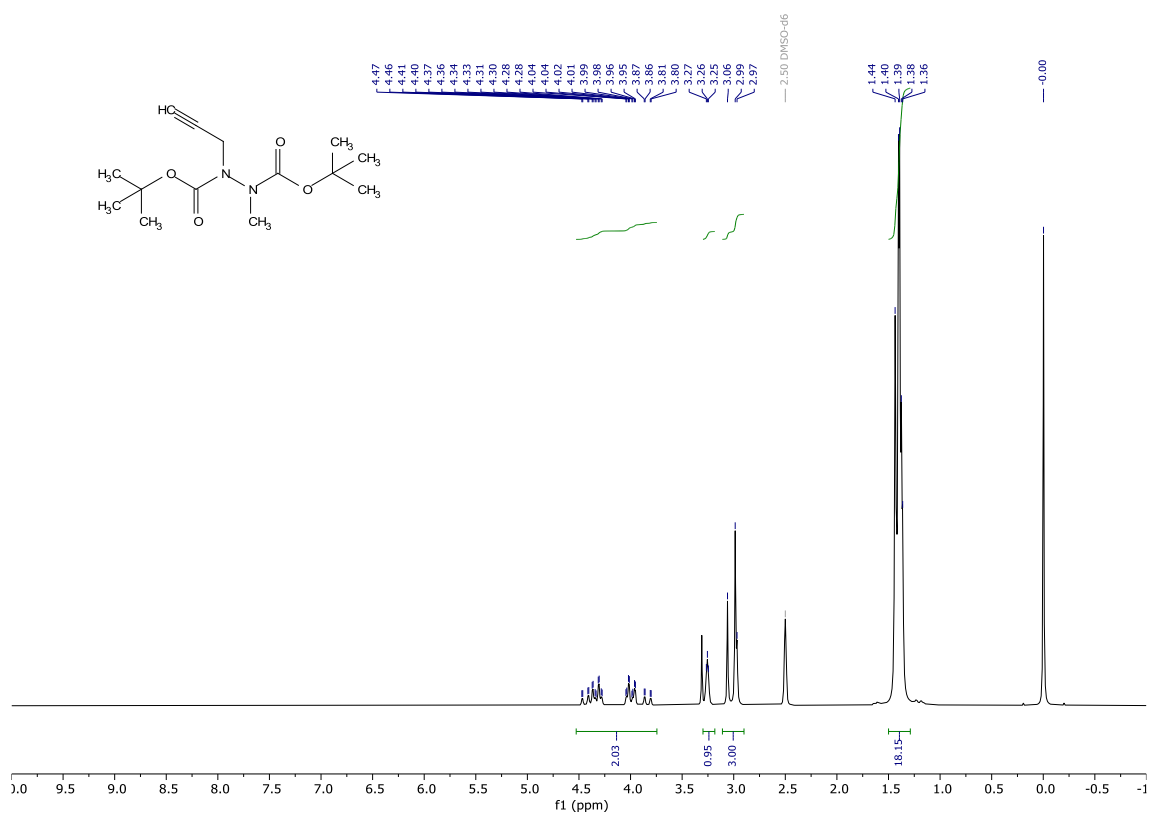


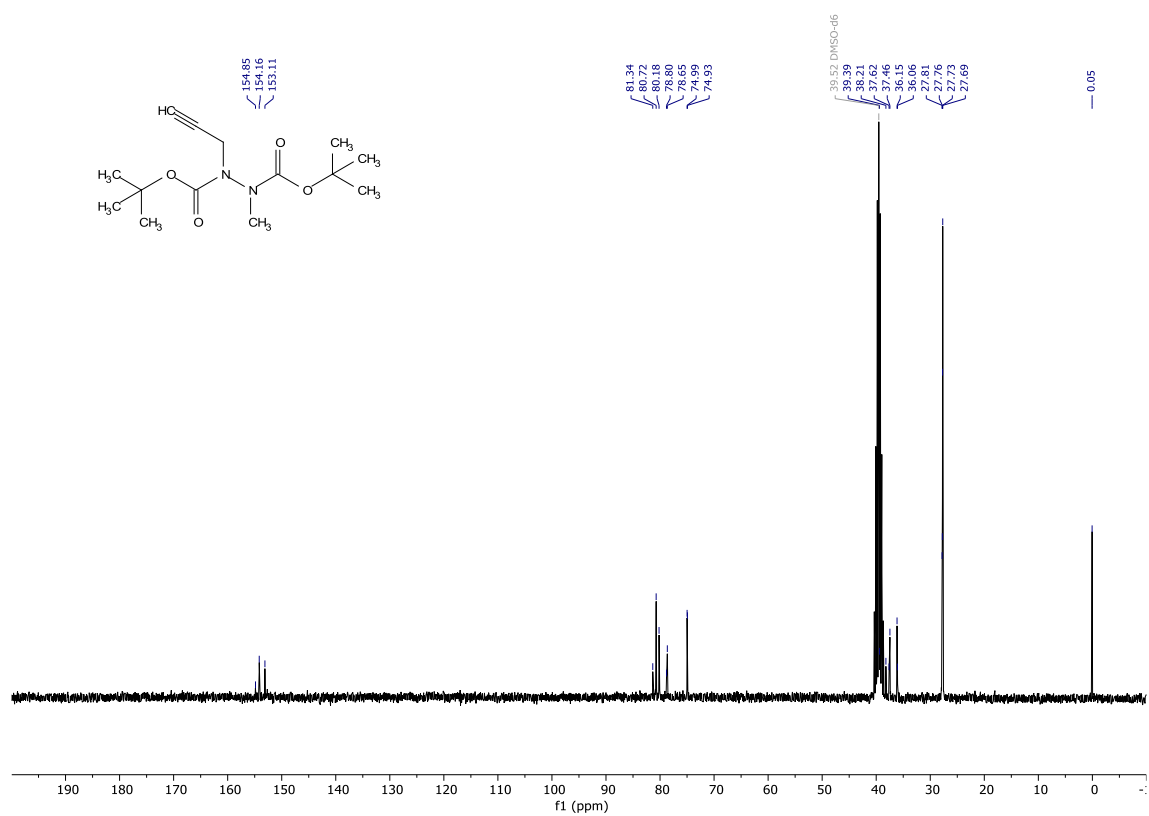
NMR spectra for final compounds

Di-*tert*-butyl 1-methylhydrazine-1,2-dicarboxylate (1)

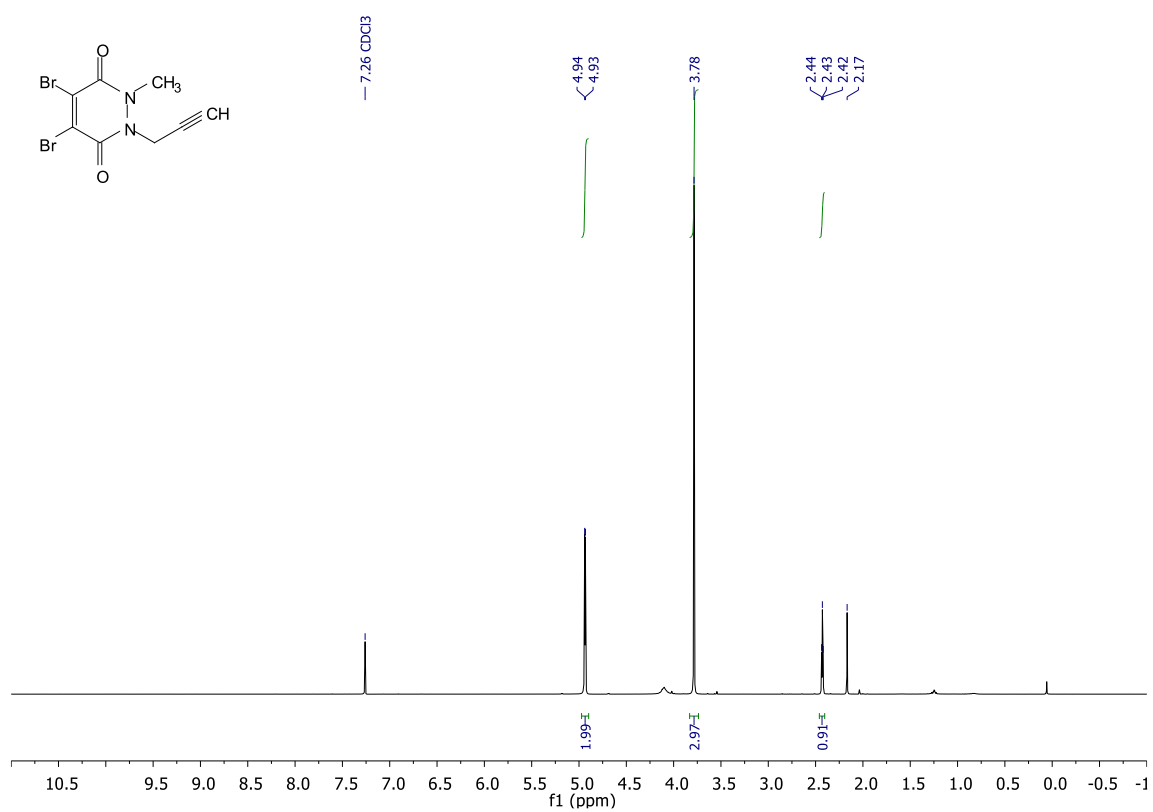


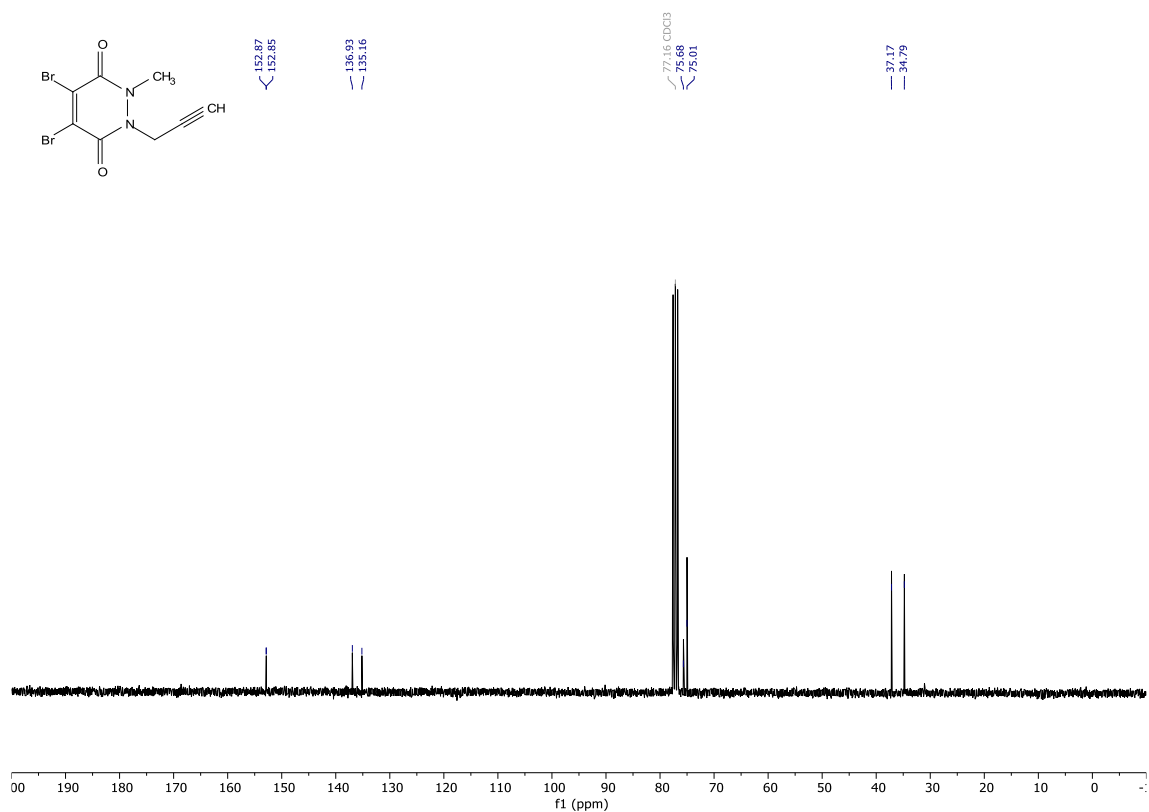
Di-*tert*-butyl 1-methyl-2-(prop-2-yn-1-yl)hydrazine-1,2-dicarboxylate (2)



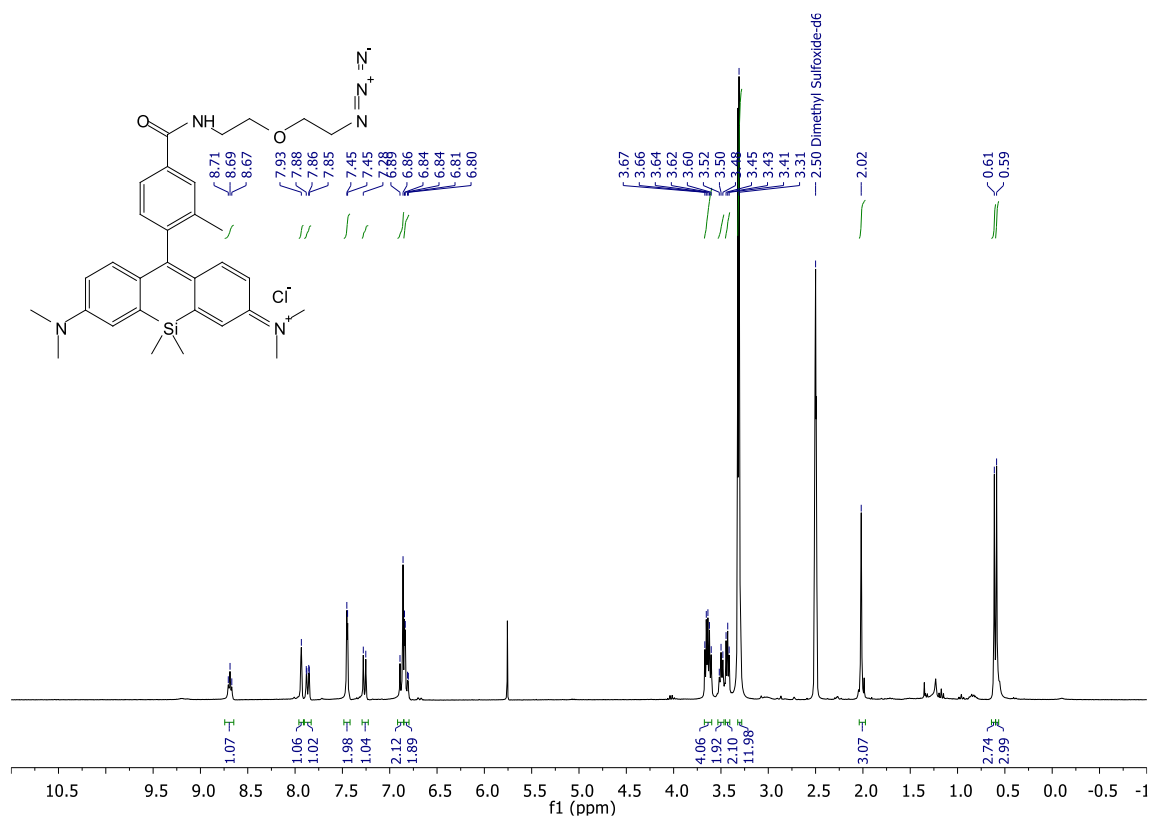


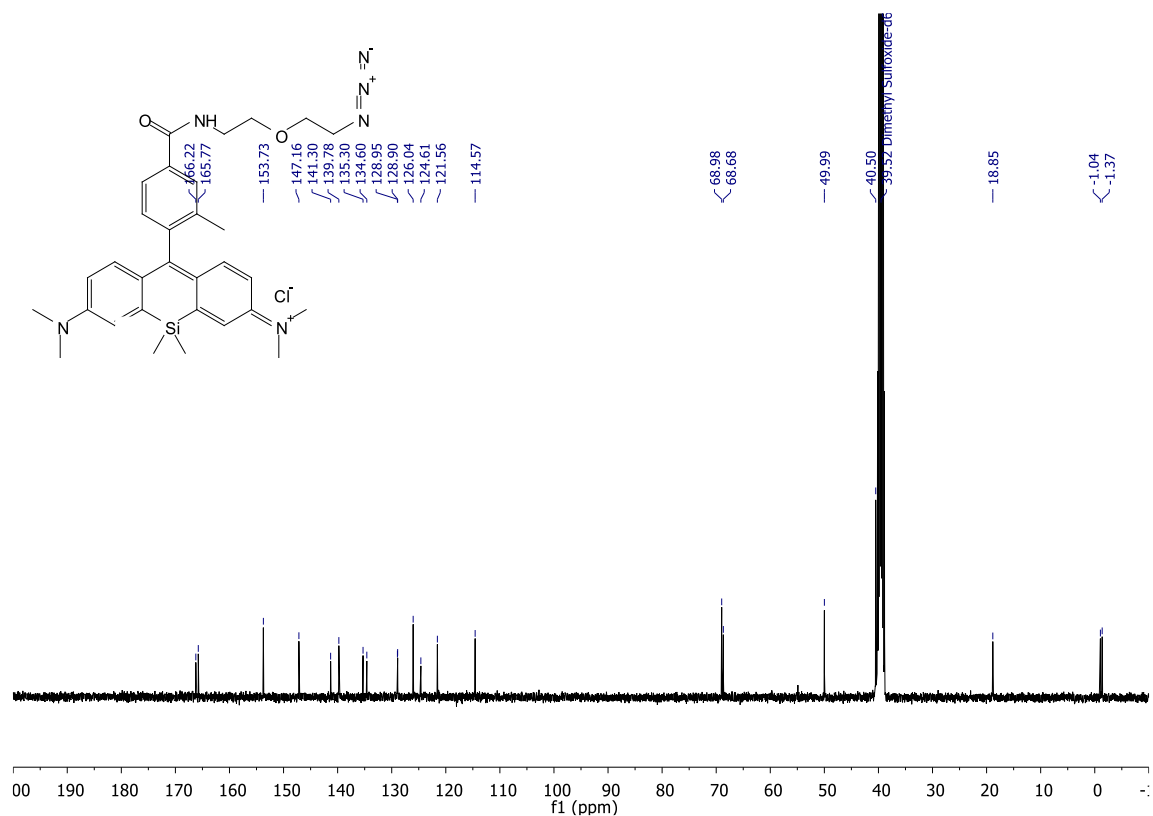
4,5-Dibromo-1-methyl-2-(prop-2-yn-1-yl)-1,2-dihydropyridazine-3,6-dione (3)



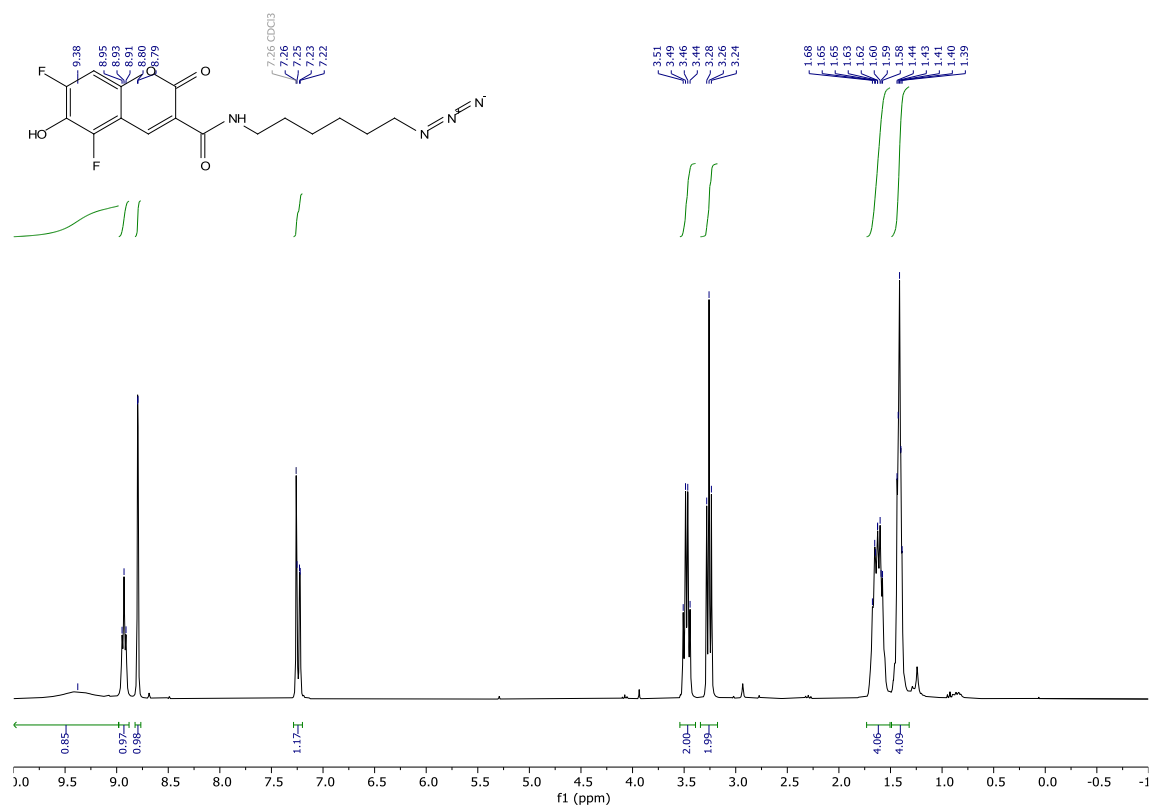


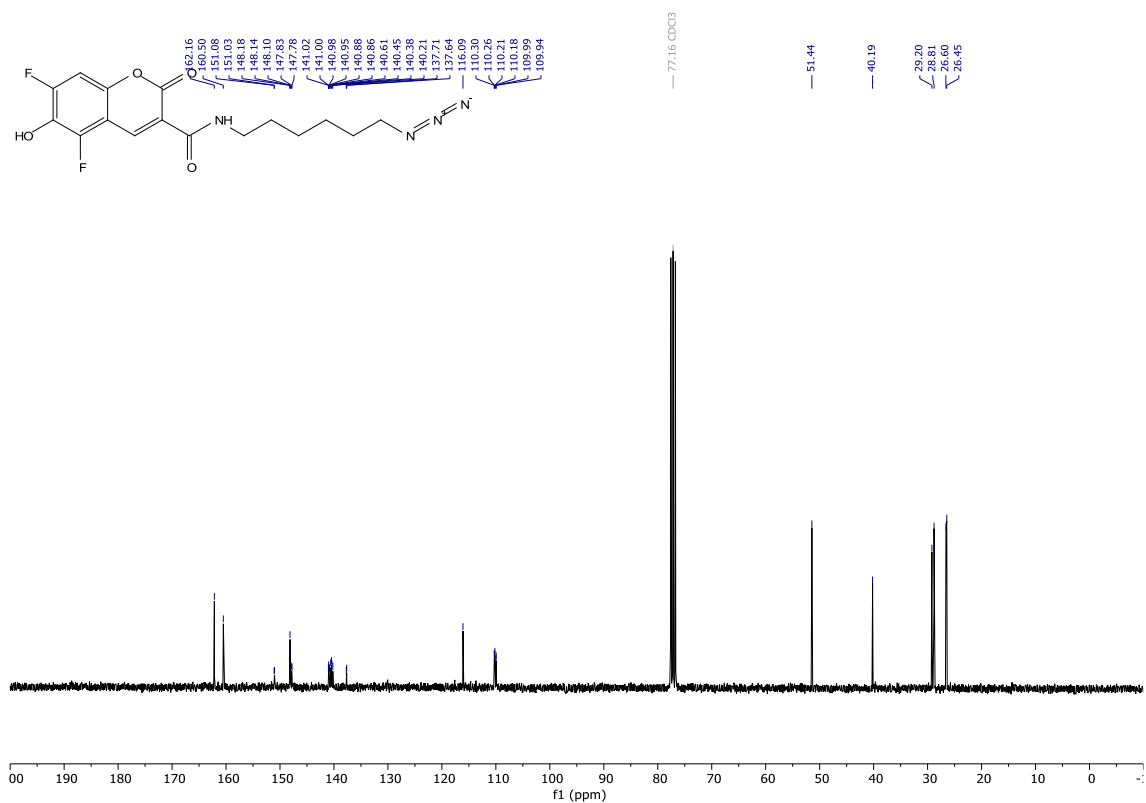
***N*-(10-(4-((2-(2-azidoethoxy)ethyl)carbamoyl)-2-methylphenyl)-7-(dimethylamino)-5,5-dimethyldibenzo[*b,e*]silin-3(*5H*)-ylidene)-*N*-methylmethanaminium chloride (4)**



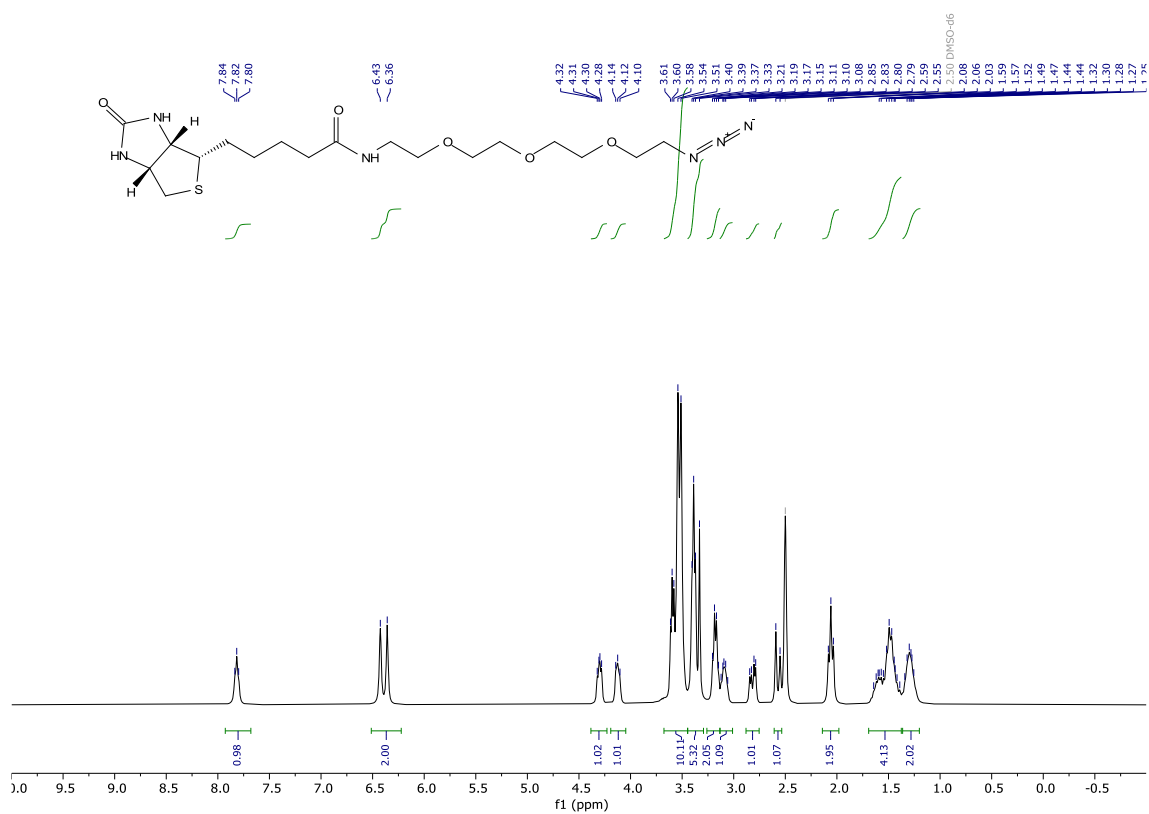


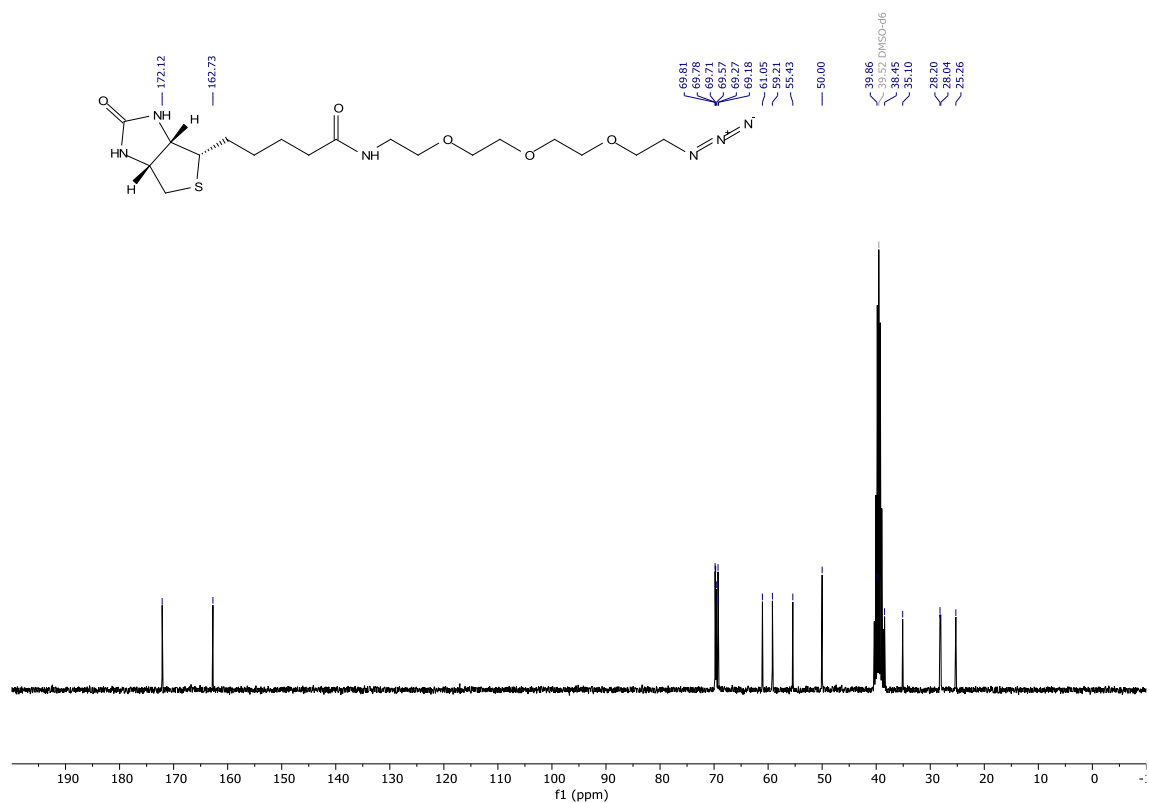
***N*-(6-azidohexyl)-5,7-difluoro-6-hydroxy-2-oxo-2*H*-chromene-3-carboxamide (6)**



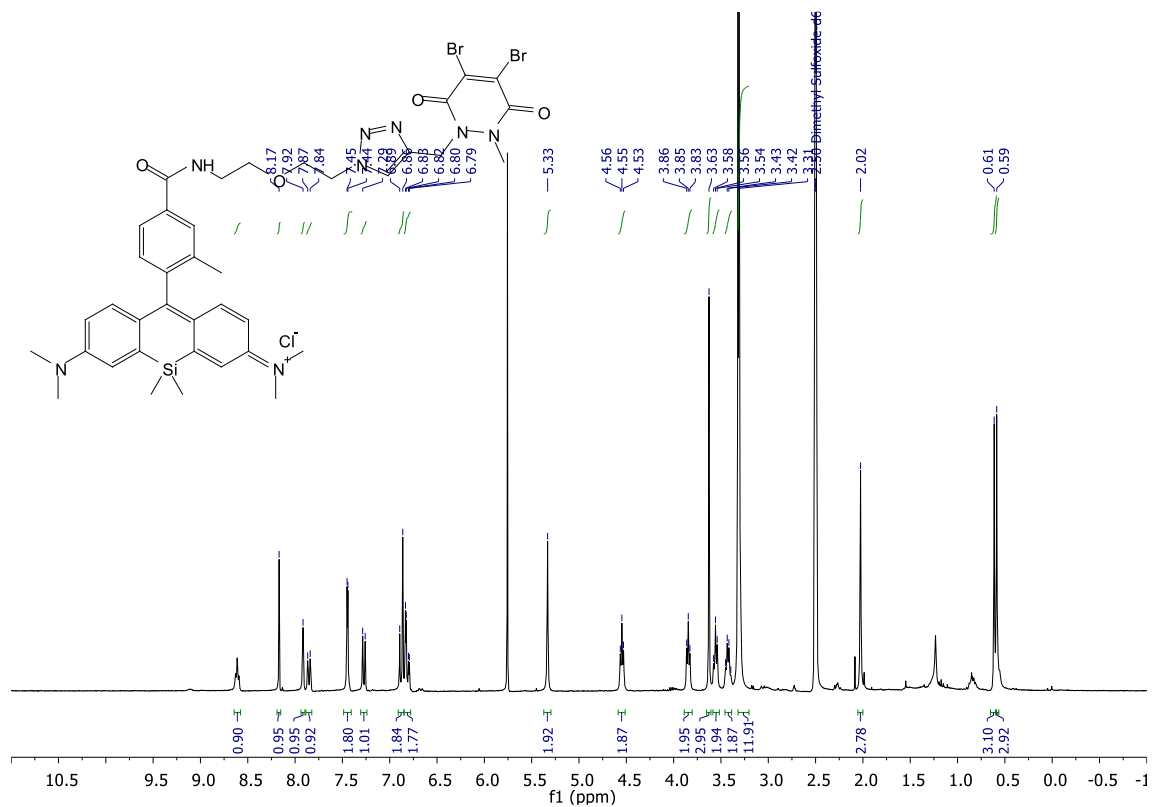


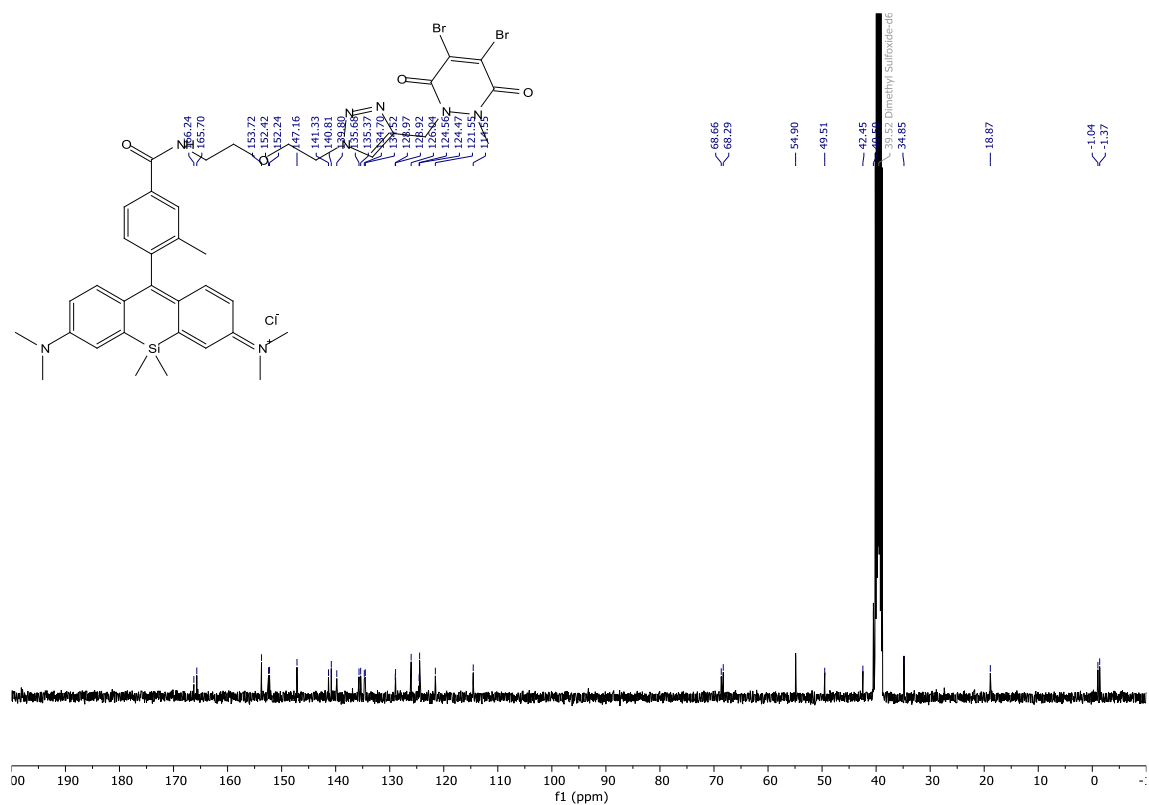
***N*-(2-(2-(2-(2-azidoethoxy)ethoxy)ethoxy)ethyl)-5-((3*a*S,4*S*,6*a*R)-2-oxohexahydro-1*H*-thieno[3,4-*d*]imidazol-4-yl)pentanamide (7)**



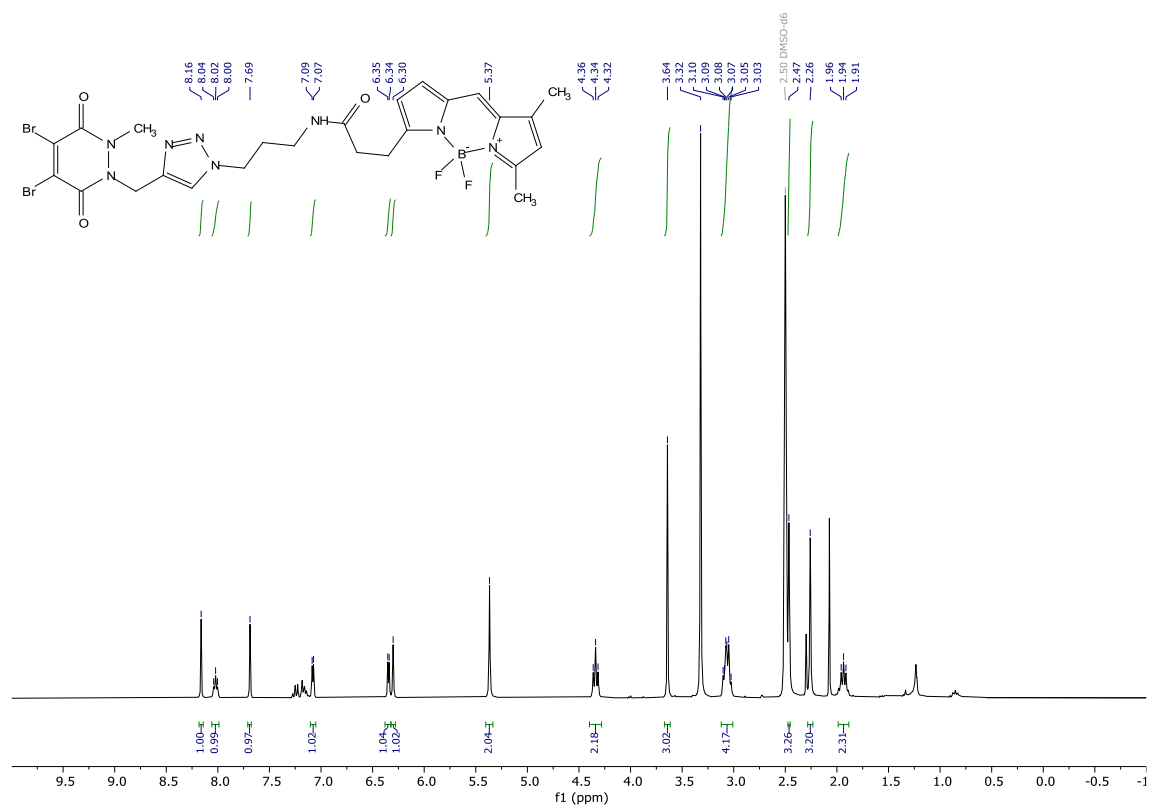


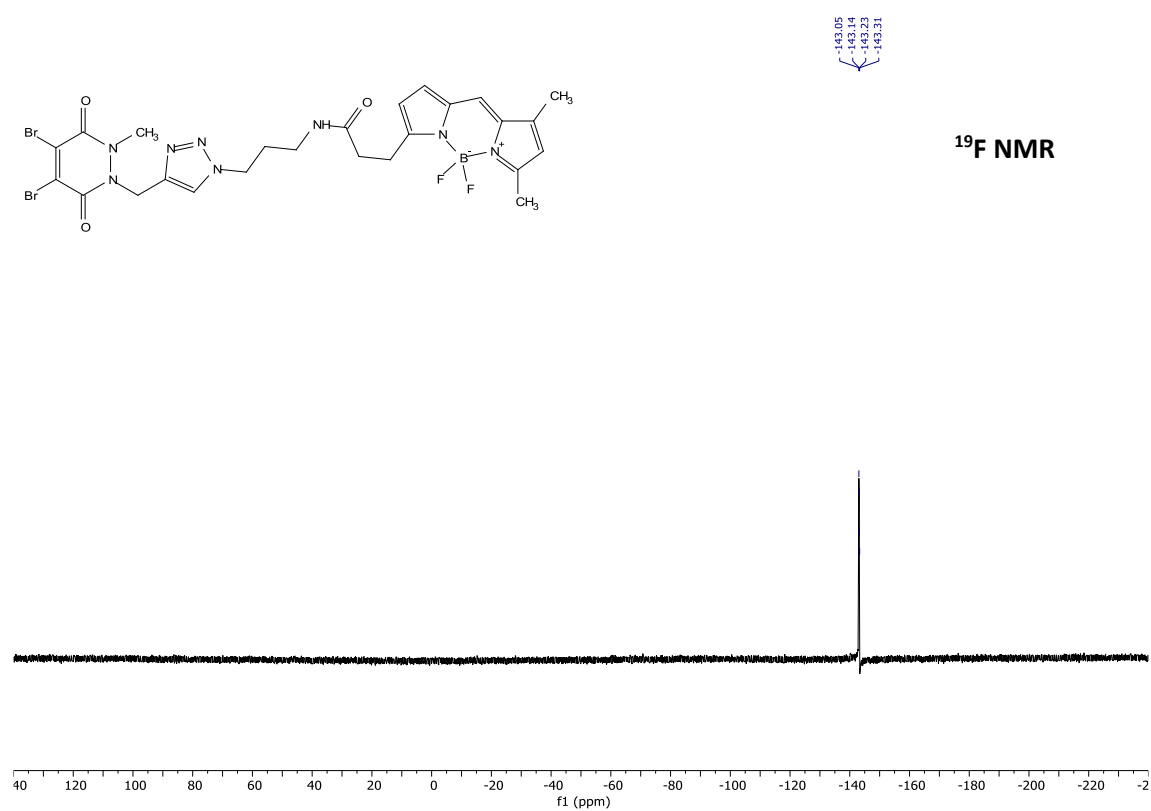
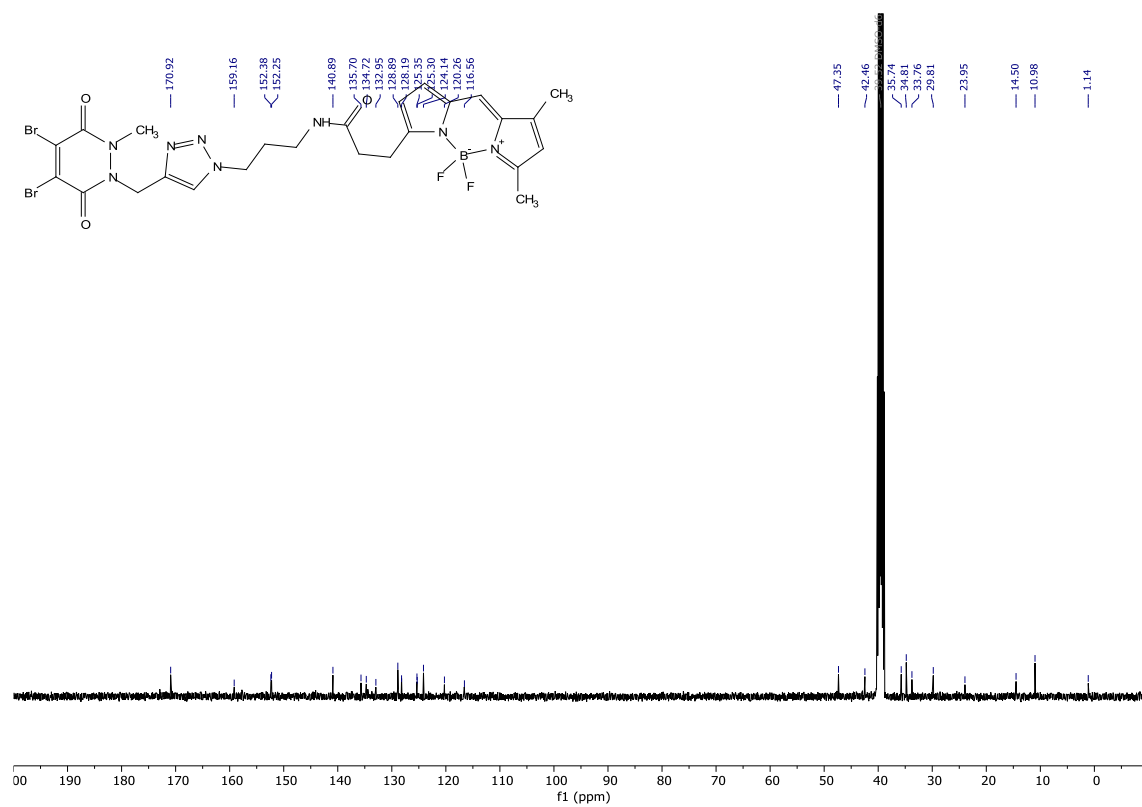
***N*-(10-(4-((2-(2-(4-((4,5-dibromo-2-methyl-3,6-dioxo-3,6-dihydropyridazin-1(2*H*)-yl)methyl)-1*H*-1,2,3-triazol-1-yl)ethoxy)ethyl)carbamoyl)-2-methylphenyl)-7-(dimethylamino)-5,5-dimethyldibenzo[*b,e*]silin-3(5*H*)-ylidene)-*N*-methylmethanaminium chloride (**8**)**

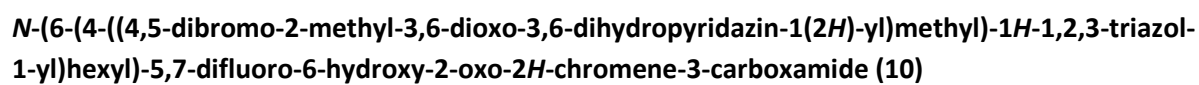


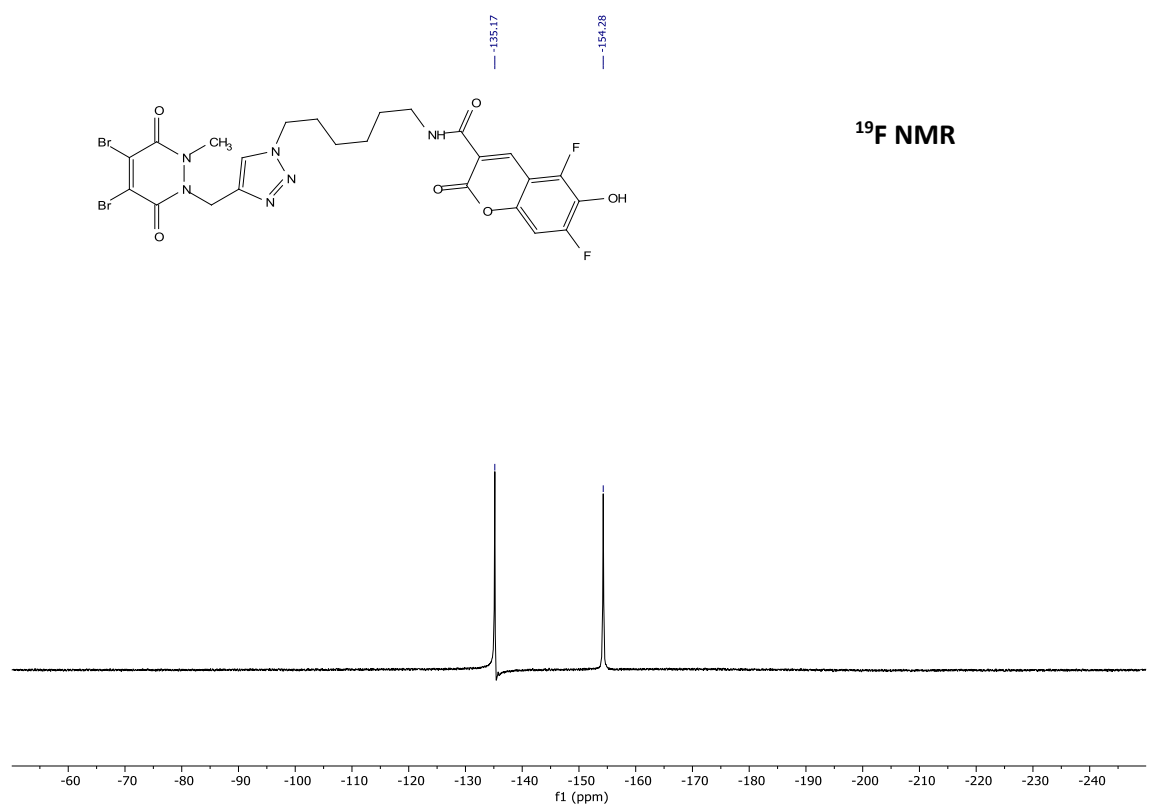
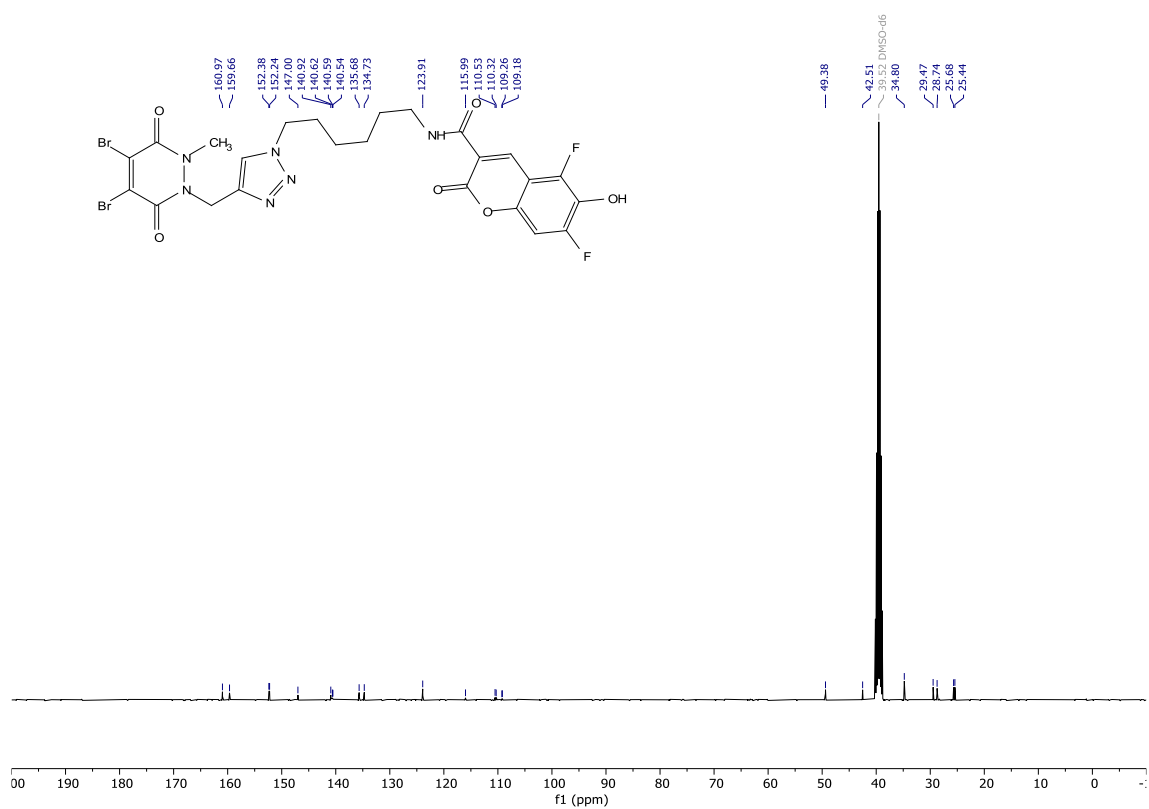


***N*-(3-(4-((4,5-dibromo-2-methyl-3,6-dioxo-3,6-dihydropyridazin-1(2*H*)-yl)methyl)-1*H*-1,2,3-triazol-1-yl)propyl)-3-(5,5-difluoro-7,9-dimethyl-5*H*-5 λ ⁴,6 λ ⁴-dipyrrolo[1,2-*c*:2',1'-*f*][1,3,2]diazaborinin-3-yl)propenamide (**9**)**

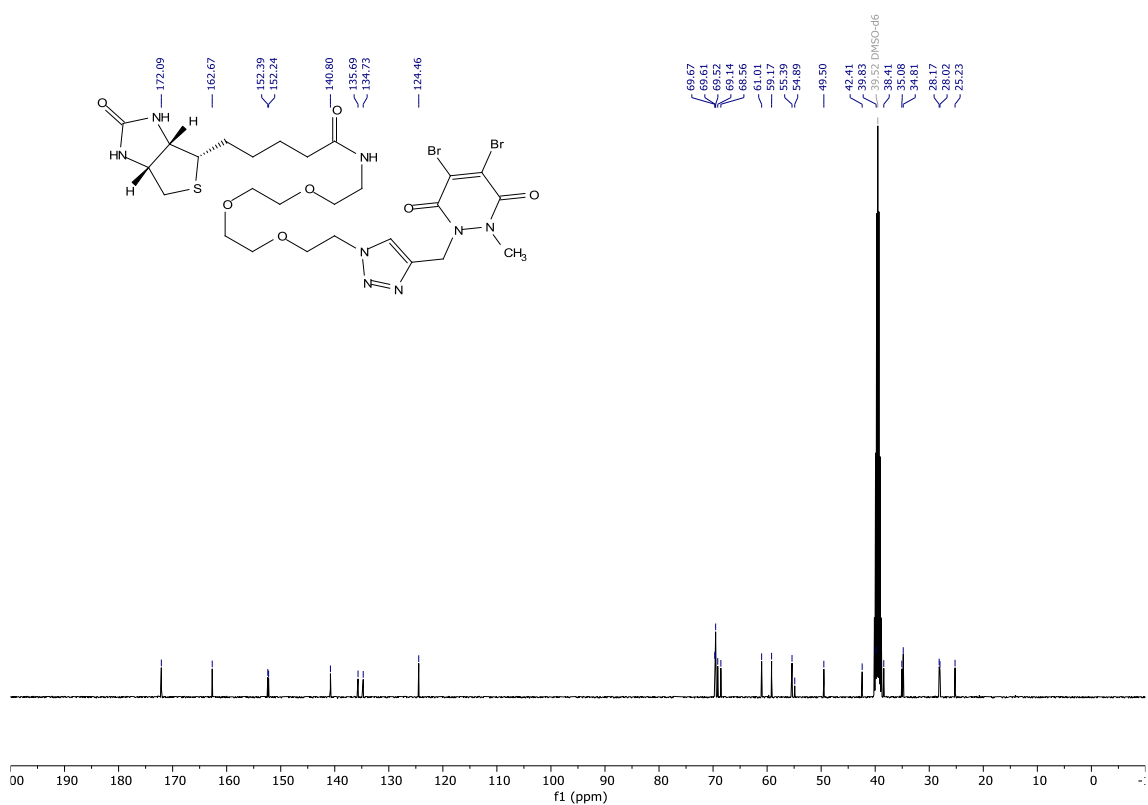
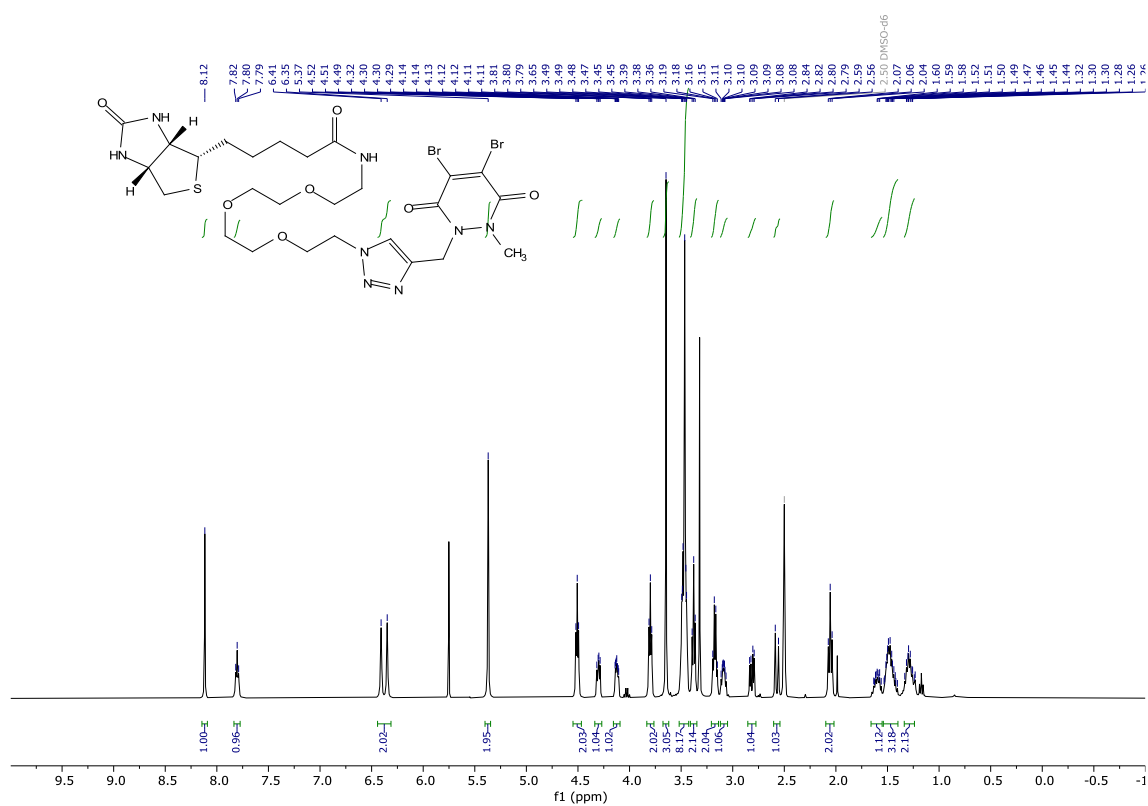








***N*-(2-(2-(2-(2-(4-((4,5-dibromo-2-methyl-3,6-dioxo-3,6-dihydropyridazin-1(2*H*)-yl)methyl)-1*H*-1,2,3-triazol-1-yl)ethoxy)ethoxy)ethoxy)ethyl)-5-((3*aS*,4*S*,6*aR*)-2-oxohexahydro-1*H*-thieno[3,4-*d*]imidazol-4-yl)pentanamide (11)**



2. Developing small molecule ligands to stabilise mitochondrial aspartate/ glutamate carrier

2.1. Introduction

Aspartate glutamate carrier *SLC25A13* citrin

The solute carrier (SLC) citrin or more commonly known as aspartate/ glutamate carrier 2 (AGC2) expressed from gene *SLC25A13* is a carrier of the mitochondrial carrier family *SLC25*. The carrier is located in the inner mitochondrial membrane (highlighted in yellow in **Figure 4**) where it transports glutamate into the mitochondrial matrix and exports aspartate from the mitochondrial matrix into the intermembrane space and subsequently into the cytosol.⁴³

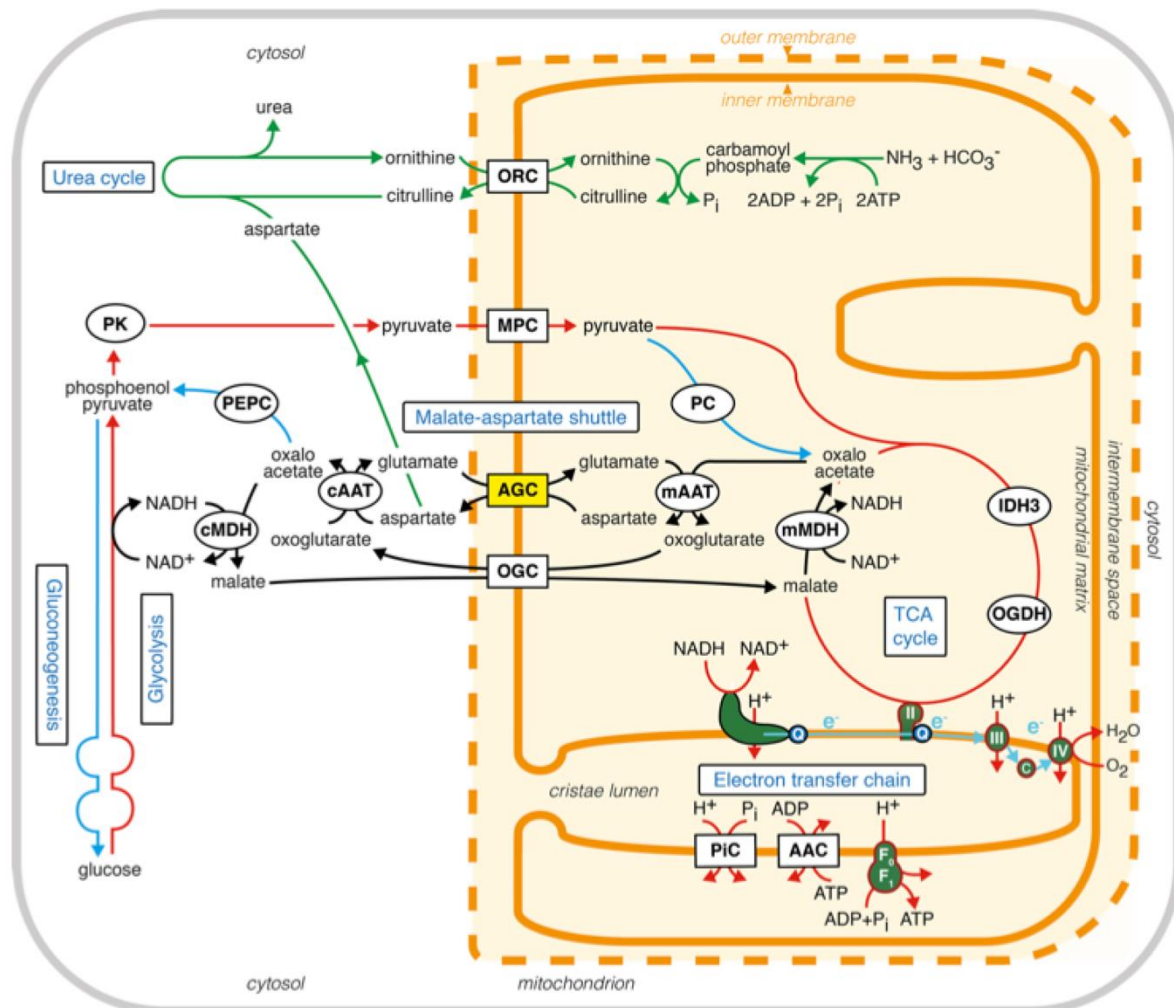


Figure 4 Location and function of the AGC within the mitochondrion

Citrin has a structural homologue (isoform) called aralar1 (*SLC25A12*, AGC1). They both transport aspartate and glutamate and fulfil mostly the same function, however they differ in their expression sites in the body. Citrin is mostly expressed in the liver, whereas aralar1 is expressed mostly in skeletal

muscle, brain and heart tissue.⁴⁴⁻⁴⁷ Both transporters are expressed in the skeletal muscles, kidneys, and pancreas.⁴⁸ Citrin shares 77.8% of its amino acid sequence with aralar1.^{45, 49}

Mutations in the gene encoding citrin are responsible for adult-onset type II citrullinemia which is an autosomal recessive inherited disease caused by citrin deficiency leading to patients suffering from disturbance of consciousness, coma and even death after a few years of onset.⁴⁵ In citrin deficiency, aspartate is not supplied to the urea cycle (**Figure 4**). As a result, the formation of argininosuccinate from aspartate and citrulline cannot be achieved. The result is an accumulation of citrulline and ammonia in the cytosol, of which the latter cannot be metabolized into urea.^{50, 51} A characteristic of the type II citrullinemia is the liver-specific deficiency.⁴⁵ As aralar1 is not present in hepatocytes it cannot compensate for the non-functional citrin. Whereas in kidneys and other tissues it is possible that aralar1 can compensate for the loss of citrin.⁵²

More than 100 pathogenic variants for citrin have been reported to date. Those include 18 splicing site-, 25 deletion- or insertion-, 21 nonsense- and 44 missense mutations.⁴³ The region having the highest prevalence of pathogenic citrin variants, is East Asia. In a recent study in China almost 30'000 new-borns were screened for 28 pathogenic variants of *SLC25A13* and around 650 individuals were identified as carriers of mutated alleles. The study estimated the carrier rate in China to be around 1:45.⁵³ Other studies found the values to be in similar range in Japan with 1:42 in Northern Japan and 1:65 in Southern Japan.⁵⁴⁻⁵⁶ In Thailand with 1:90 and Korea 1:110 the rate was assessed slightly lower.^{53, 57} **Figure 5** shows the rate of carriers and the rate of citrin deficiency affected people in East Asia. As East Asia is one of the most populated regions of the earth, the number of carriers and affected people is very high. Understanding the effect of the above-mentioned mutations would allow for rapid life-saving medical treatments. Solving the structure of citrin would greatly contribute to these efforts.

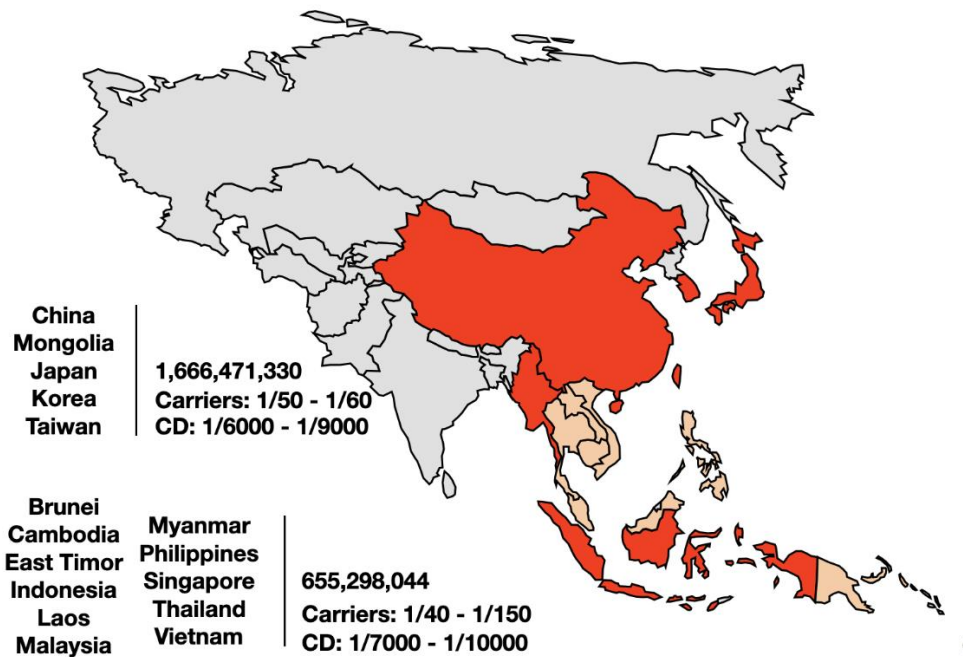


Figure 5 Disposition of carriers separated into the bundles China, Mongolia, Japan, Korea and Taiwan with higher prevalence (red) with a total population of above 1.66 billion people and Brunei, Cambodia, East Timor, Indonesia, Laos, Malaysia, Myanmar, Philippines Singapore Thailand and Vietnam with slightly lower prevalence (beige) with a total population of above 0.655 billion people

As shown in **Figure 4** citrin deficiency can negatively affect many metabolic pathways in the cell. Due to the lack of suitable model systems, the full impact of citrin deficiency has not been completely clarified yet.⁴³ A pathway greatly influenced by citrin deficiency is the malate-aspartate shuttle.⁵⁸ The malate-aspartate shuttle plays an important role in the regeneration of nicotinamide adenine dinucleotide in its reduced form (NADH) in the mitochondrial matrix. NADH is one of the products of glycolysis in the cytosol and it is itself a modulator of glycolysis and other pathways.⁵⁹ Therefore, NADH in the cytosol needs to be oxidised back to NAD^+ to be available again in the glycolytic pathway. The malate-aspartate shuttle is crucial for this oxidation in the cytosol and on the other hand is also a major player in the reduction of NAD^+ in the mitochondrion.^{58, 60} In liver tissue citrin in combination with the mitochondrial oxoglutarate carrier is important for the correct function of the malate aspartate shuttle. In a mouse model of human citrin deficiency it was suggested that the cytosolic NADH concentration in hepatocytes is increased and as a result the hepatic glycolysis is impaired.⁶¹ On the other hand in the mitochondrion the amount of electrons entering the respiratory chain is decreased, due to the decrease in mitochondrial NADH concentration. Leading to an overall decreased energy production from carbohydrates. Which is also suggested to be causing the aversion against sucrose rich foods observed by citrin deficient mice, which was not observed when saccharin was used.⁶¹

In a recent study, Rabinovich et al. hypothesised that citrin could play a role in carcinogenesis due to its role in cellular energy metabolism. They found that citrin is upregulated in several cancer types. If citrin is upregulated, elevated levels of cytosolic aspartate and NAD^+ are supported together with high concentration of mitochondrial NADH. This fuels cancer cell proliferation, migration, and invasion. Conversely, when citrin is downregulated, the available energy is reduced, promoting autophagy.⁶² This allows us to speculate, that an inhibitor for citrin could potentially be used as a new drug strategy for cancer treatment.

Structural properties of citrin

Citrin and the related carrier aralar1 consists of three domains. The hydrophilic N-terminal (35.8 kDa), a carrier domain (31.9 kDa) and a amphipathic C-terminal helix (6.5 kDa).⁶³ The transporter domain forms six α -helices, as other members of the mitochondrial carrier family do. The N- and the C-terminal are both located in the intermembrane space of the mitochondrion as it was shown experimentally that the N-terminal is in the intermembrane space.⁶⁴ The full-length carrier is dimeric which differs to other mitochondrial carriers that exist in a monomeric form. The dimerization is controlled by the N-terminal domain as it was found that the carrier domain by itself is mostly present as monomer.⁶³ The N-terminal domain or regulatory domain forms eight EF-hand motifs of which only one is involved in calcium binding and the others are assisting in the carrier dimerisation.⁶³

Through the crystallographic structure of the regulatory domain, clues about the mechanism of the Ca^{2+} regulation were found. The two carrier isoforms citrin and aralar1 are both regulated by calcium ions (Ca^{2+}) e.g., they seem to be inactive in the absence of Ca^{2+} and become activated once the Ca^{2+} concentration is rising on the external side of the inner mitochondrial membrane.^{63, 64} When Ca^{2+} binds to EF-hand 2 a conformational change is triggered where an amphipathic α -helix from the C-terminal region binds into a hydrophobic groove of the N-terminus. This change allows the substrates to enter and subsequently pass the carrier. However, the exact mechanism of this action remains unsolved.⁴³

Figure 6 depicts the regulatory domain of citrin in the Ca^{2+} (green spheres) bound form (**a**) and the regulatory domain of aralar1 with bound Ca^{2+} (**b**) and in Ca^{2+} -free state (**c**).

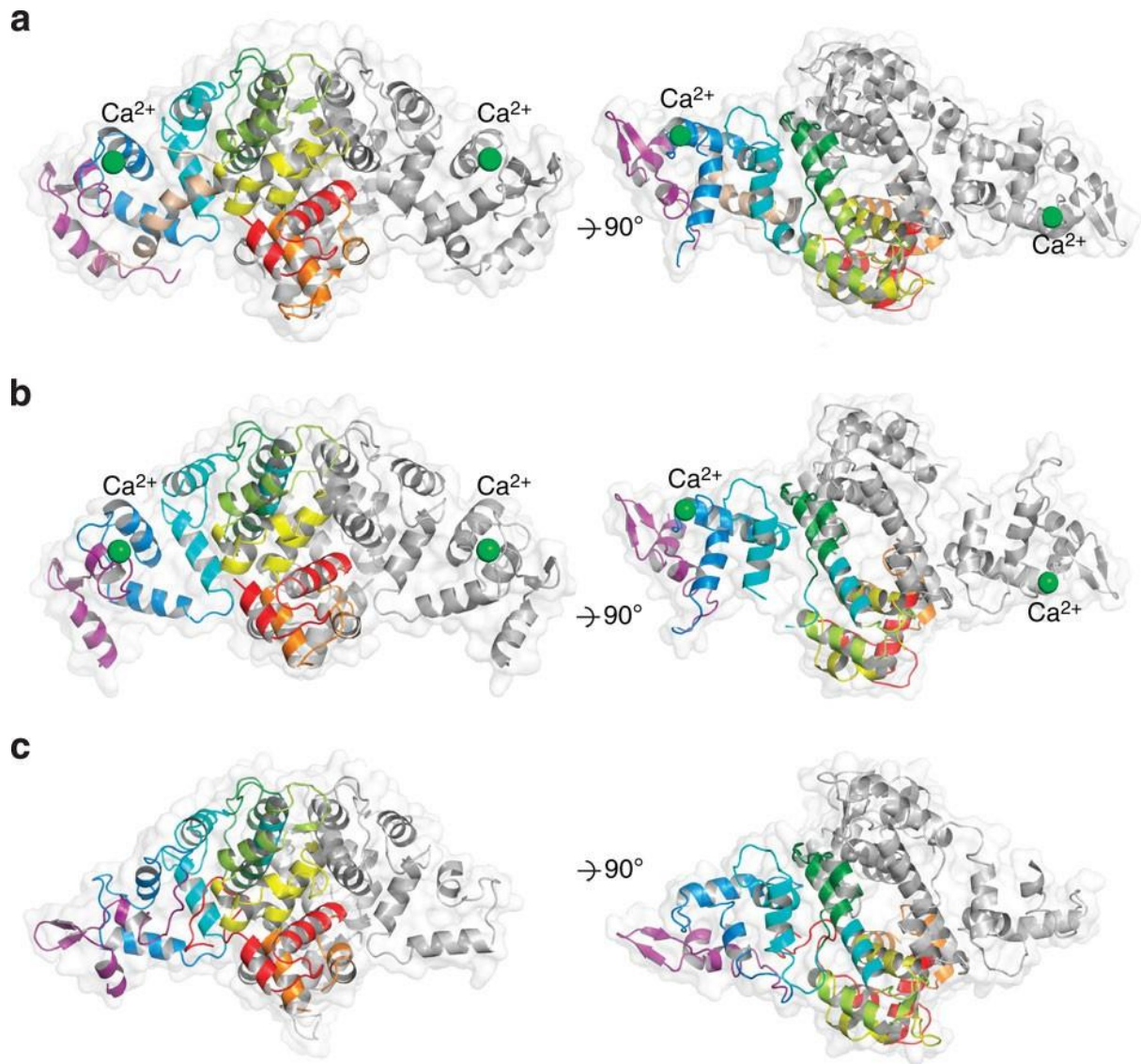


Figure 6 Structure of the N-terminal of citrin⁶³

Due to the close structural relationship to other members of the mitochondrial carrier family the structure was modelled.⁶³⁻⁶⁵ These computational studies suggested that the carrier domain cycles between two conformational states. One conformation was open to the mitochondrial matrix, which represented the m-state. The other conformation was open to the intermembrane space and consequently to the cytosol, representing the c-state.

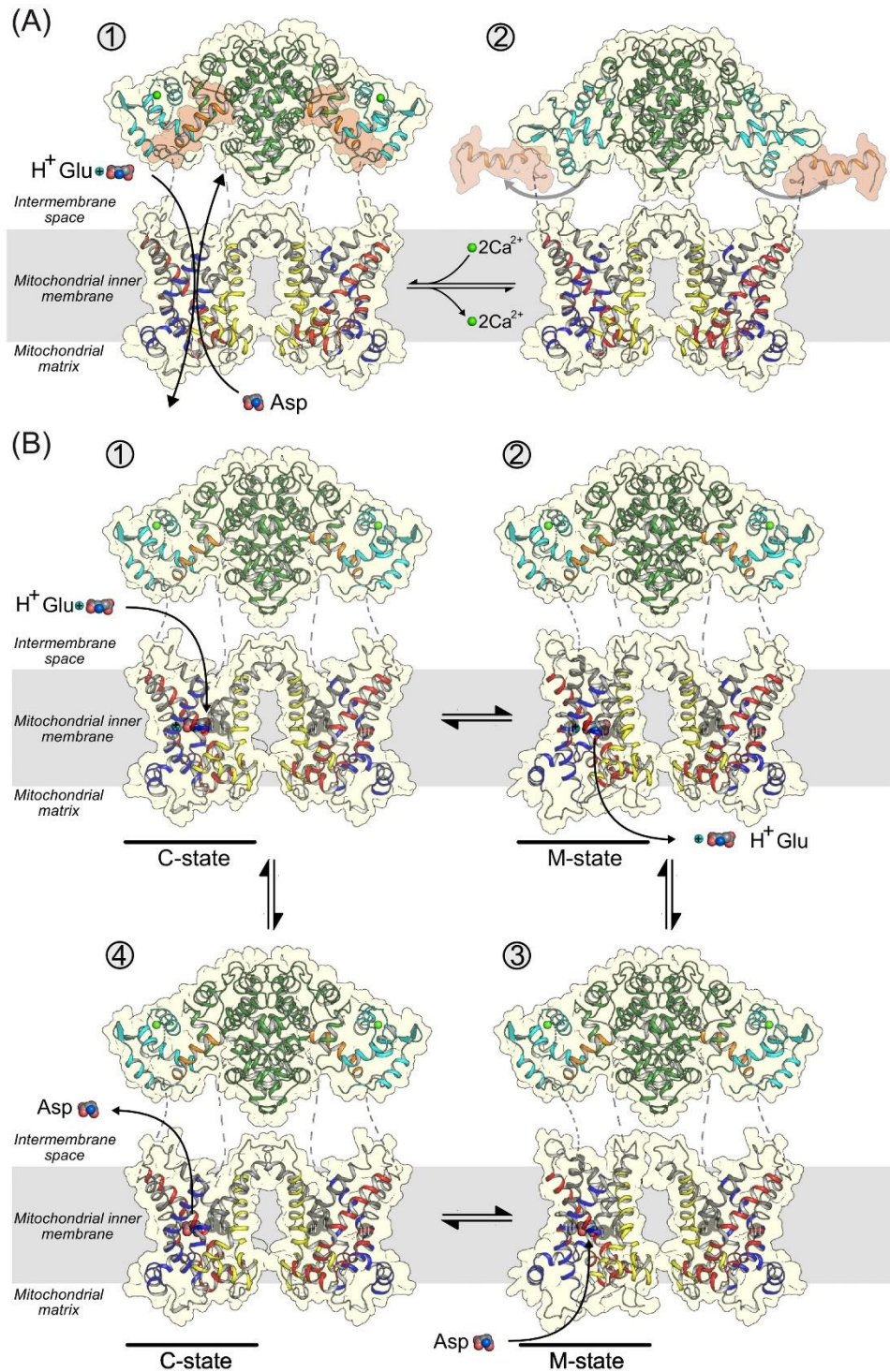


Figure 7 Mechanism of calcium regulation and transport⁴³

Figure 7 depicts the different states of the AGC that were modelled based on the structures of the mitochondrial ADP/ATP carrier in the two states. In panel (A) in the calcium bound state is shown on the left and the calcium free state on the right side. After binding of the calcium ions, the C-terminal amphipathic helix binds to the N-terminal regulatory domain allowing the carrier to transport substrates. In the calcium-free state, a conformational change in the regulatory domain leads to

release of the amphipathic helix, preventing the transport of substrates. However, the exact details of this mechanism remain unclear. In panel (B) the stages of the transport mechanism are shown. In **B-1**, a glutamate, and a proton from the intermembrane space bind to the binding site of the carrier domain in the c-state. The binding triggers a conformational change from the c-state to the m-state, going through an occluded state that is closed to both sides, allowing the glutamate and the proton to diffuse into the mitochondrial matrix (**B-2**). Aspartate can then bind to the free binding site of the carrier in the m-state (**B-3**). This aspartate binding triggers yet again a conformational change from the m-state to the c-state via an occluded state (**B-4**). The aspartate can then diffuse into the intermembrane space and continue diffusing into the cytoplasm.⁴³

Figure 8 A depicts different combinations of the carrier domains. As the transporter is dimeric each of the individual carrier domains can be in a different conformation. **Figure 8 B** illustrates the dynamic nature of the regulatory domains. These loosely attached domains can move more or less unrestrictedly with respect to the carrier domains. The combination of both dynamic factors contributes to a plethora of different confirmation states of the transporter that are exceedingly difficult to study experimentally.

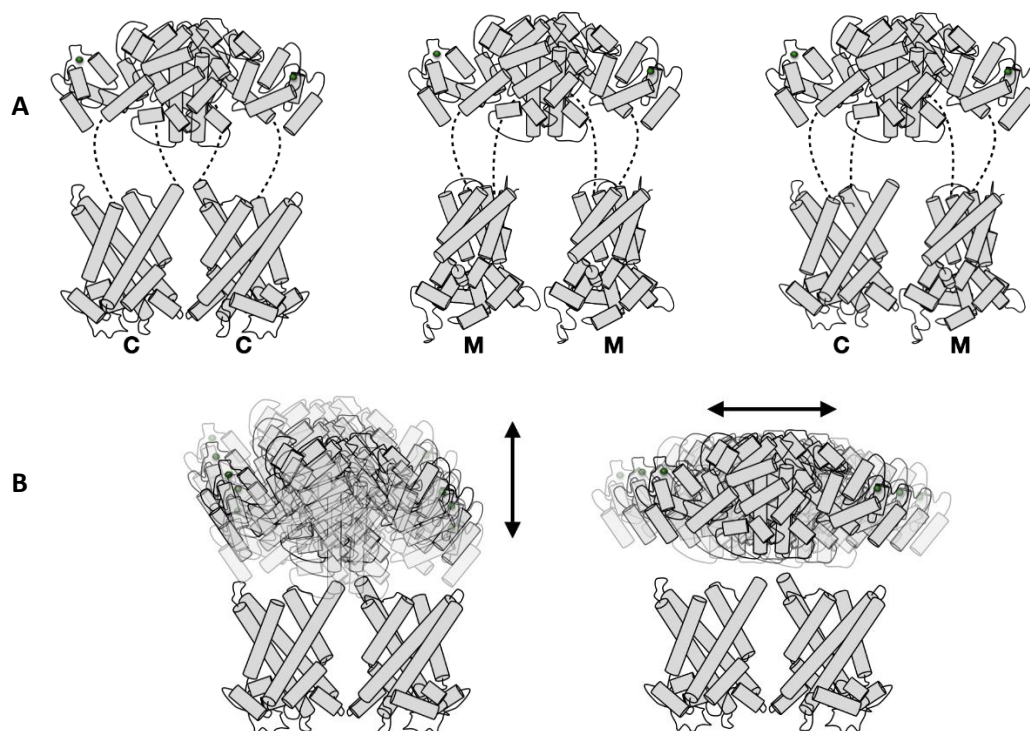


Figure 8 Dynamic nature of citrin is the main problem for structural biology efforts

Structural biology on membrane proteins

Around 30% of all proteins in the human proteome are membrane proteins. However, structural biology in this specific area still lags the rest.⁶⁶ Membrane proteins have a variety of functions such as transport, energy metabolism, signal transduction and catalysis of chemical reactions (i.e. enzymatic activity). Moreover, they present good drug targets, as over 50% of the small-molecule drugs target membrane proteins. G-protein coupled receptors are the most targeted members followed by ion channels. In recent times SLCs have increasingly come into focus. Structural biology facilitates the development of drugs against these targets by providing information about the structure and the dynamics of these proteins. Drugs candidates can also be modelled to fit into their respective target.⁶⁷ In the past decade structural biology of membrane proteins has seen a substantial rise in the number of solved structures, from around 150 solved structures in 2008⁶⁶⁻⁶⁸ to 1500⁶⁸ (**Figure 9**) structures in middle of 2022. This trend is assisted by the resolution revolution in cryo-electron microscopy (cryo-EM) leading to more and more structures being solved with this technique since the beginning of the last decade.^{67, 69, 70} For instance, transient receptor potential cation channel subfamily V member 1 (TRPV1) was the first membrane protein structure solved by cryo-EM at high resolution in 2013.⁶⁷ The other commonly used method, X-ray crystallography, can typically produce higher resolution structures. Crystallisation of membrane proteins is still not trivial and larger amounts (milligrams) of the protein of interest are required than in cryo-EM (micrograms). Therefore, cryo-EM even enables structure determination of naturally sourced membrane proteins.⁷¹ In addition, cryo-EM is better suited for highly heterogeneous structures, such as citrin, as at the image processing stage different conformations can be separated.⁷²

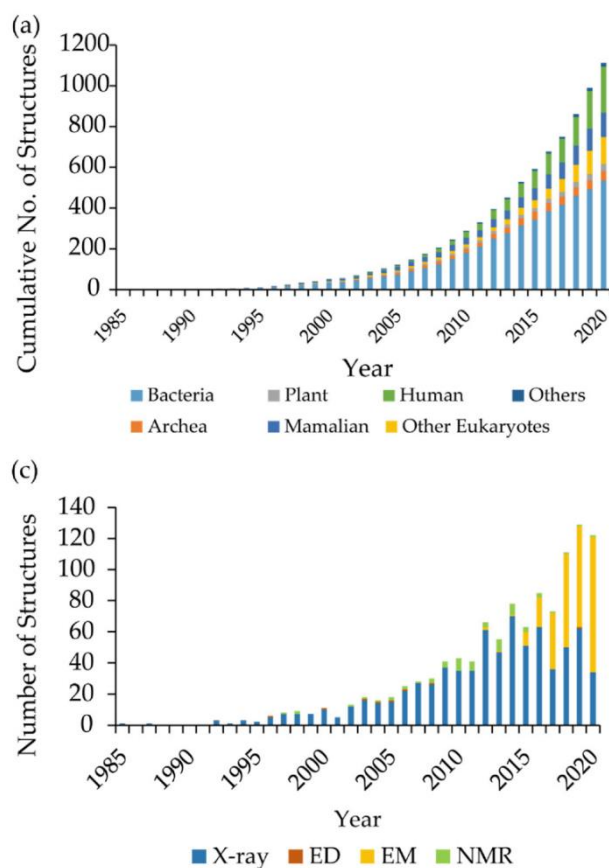


Figure 9 Solved membrane protein structures. Cumulative per year (a) and new structures per year and by method (c)⁶⁷

However, cryo-EM does not come without its own drawbacks. Especially the sample preparation for cryo-EM measurements can be tedious, presenting a similar bottleneck as the crystallisation in X-ray crystallography.^{69, 70} Despite this drawback cryo-EM appears to be better suited for the study of membrane proteins in their more or less natural lipid environment.

Inhibitors of citrin and other members of the mitochondrial SLC transporter family

The only known inhibitor for AGC was reported in 2020 by Rabinovich et al.,⁶² a γ -benzyl ester of glutamic acid (**Figure 10**). This inhibitor was initially found through a virtual screening exercise using a commercially available compound library. From this screen, L-glutamic- γ -benzyl ester (γ -BnGlu) was identified as promising candidate and found to be particularly potent. The discovered inhibitor was tested on LOX-IMVI cells overexpressing the carrier. As a control, the same cells transfected with empty vector were used. The authors found in this proof-of-concept study that in presence of γ -BnGlu, aspartate-, uracil-, lactate- and ATP levels were decreased. Moreover, the cell proliferation and invasion were decreased significantly.⁶²

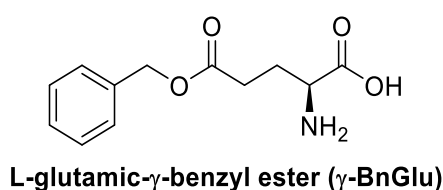


Figure 10 Inhibitor identified by Rabinovich et al.⁶²

2.2. Aim of this work

Due to the highly dynamic nature of the AGC domains the conformational states in the sample need to be stabilised to achieve a quality suitable for cryo-EM. Two approaches were considered. The first approach aimed to stabilise the structure by introduction of mutations. The second approach was to stabilise the structure by addition of a ligand, that upon binding will lock the carrier into a particular conformation. Both approaches could yield the transporter in a stable conformation suitable for cryo-EM measurements. As only one reported inhibitor structure was available, the natural substrates aspartate and glutamate, and compounds structurally related to them were chosen as starting points, together with the reported inhibitor γ -BnGlu, which itself is a glutamate derivative (**Figure 11**).

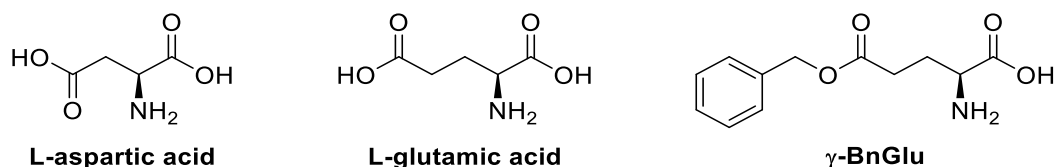


Figure 11 Starting ligand structures for this study

2.3. Methods and results

Contribution to this study

All the compounds were designed and synthesised by me. The biochemical work and the assays were done in Cambridge, in the lab of Edmund Kunji at the mitochondrial biology unit, by Denis Lacabanne.

Thermal shift assay

Two different assays were employed over the course of this project. The first was an assay based on the thermal stability of the protein-ligand construct. The assay based on this principle is called thermal shift assay (TSA). Upon binding of a ligand, the melting temperature of a protein can either be the same, increase or decrease. An increase in the melting temperature indicates strong favourable interaction of the ligand with the protein or that the carrier is forced into a conformation with a higher melting temperature, due to the interaction with the ligand. Conversely, a decrease in melting temperature suggests unfavourable interaction of the compound with the protein or that the carrier is mostly present in a conformation with a lower melting temperature. Usually, the melting curve of the protein is recorded by measuring the fluorescence of a covalently attached dye, that upon unfolding of the protein becomes fluorescent. A commonly used fluorophore for this assay is 7-diethylamino-3-(4'-maleimidylphenyl)-4-methylcoumarin which is generally referred to as coumarin phenyl maleimide or CPM dye. In **Figure 12** the dye is depicted on the left side in its non-fluorescent state. Upon reaction with a free sulfhydryl on the electrophilic position of the maleimide the compound becomes strongly fluorescent (**Figure 12**). The fluorescence intensity depends on the protein environment the CPM dye is situated in and thus it enables tracking of the thermal unfolding process using a fluorescence spectrometer.

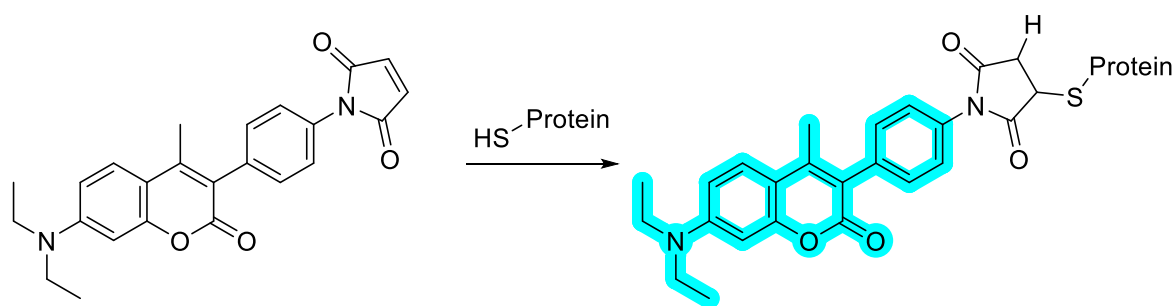


Figure 12 CPM Dye

In the assay, the free natively folded protein is mixed with the CPM dye. Then the temperature is steadily increased resulting in a progressive unfolding of the protein up to a point where most of the protein is in an unfolded state, where aggregation starts occurring. The increase of fluorescence can take place as the sulfhydryl containing cysteine are generally located on the inside of a native protein

due to their reactivity. Upon melting these cysteines successively get exposed to the surrounding media, where the sulfhydryl groups can react with the dye, which causes an increase of the fluorescence. As mentioned before, the fluorescence increases until aggregation starts occurring, at which point the proteins start to stack and quenching occurs (**Figure 13**). The melting temperature can then be read as the temperature where the fluorescence intensity was at half of the maximum measured fluorescence. However, Wang et al. suggested that the presence of free sulfhydryl groups is not required to obtain an increase in fluorescence when the protein is melting. They speculated that the increase can also be due to the fluorophore interacting with the increasing number of hydrophobic patches that get exposed upon protein unfolding.⁷³ For the employed assay highly purified citrin was obtained by expression in yeast following standard protocols.⁷⁴

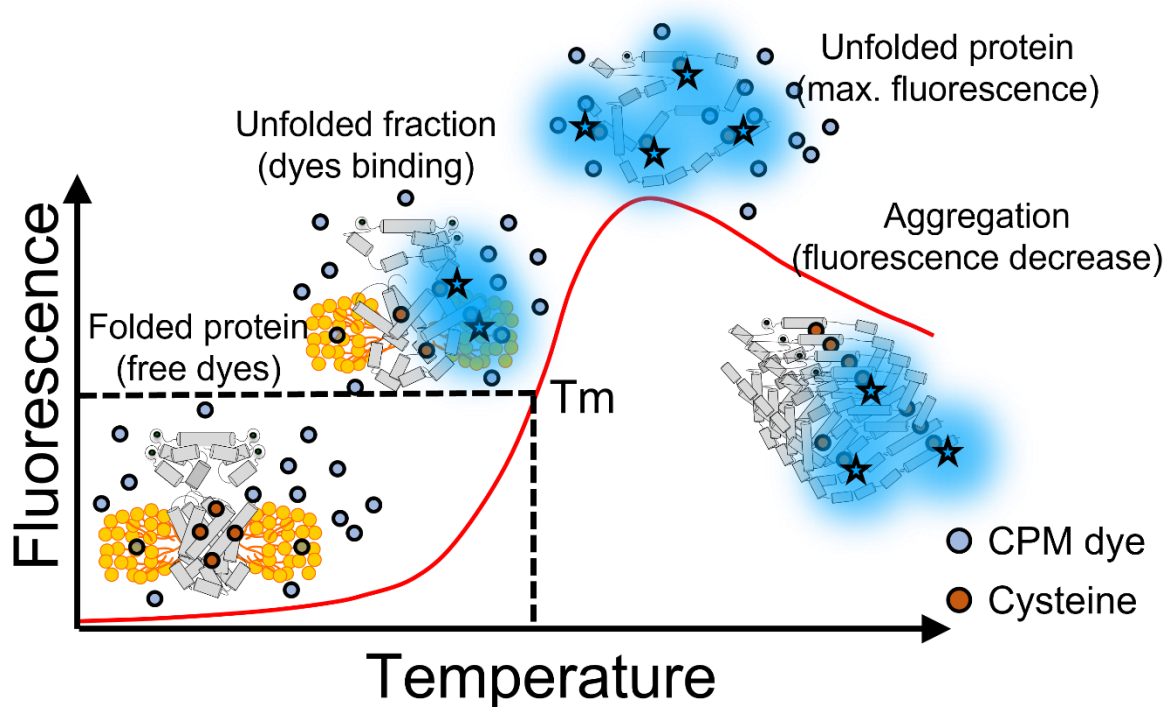


Figure 13 Thermal shift assay working principle

The derivative of the curve depicted in **Figure 13** was used for determination of the melting temperature as the point of the highest slope in the curve of **Figure 13** results in a local maximum for the derivative. In **Figure 14** the derivative of the above curve is given in red. A possible destabilisation caused by an unfavourable mutation or ligand interaction is shown in blue. And in green a favourable mutation or ligand interaction.

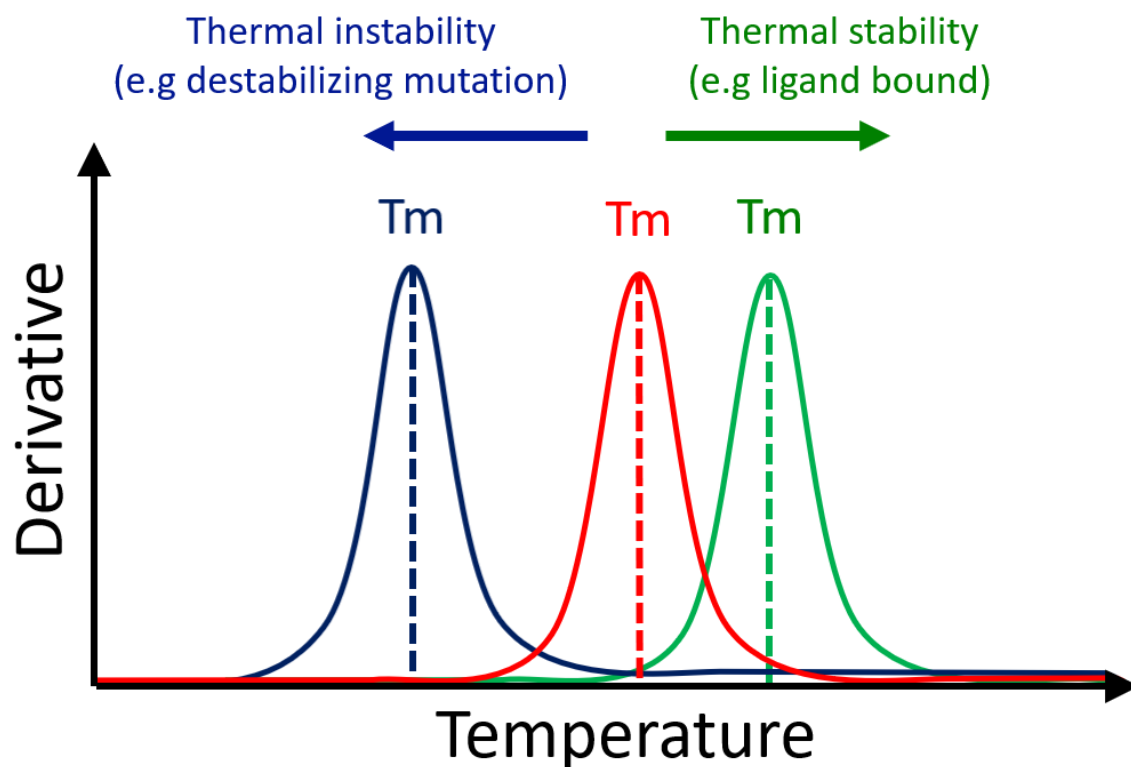


Figure 14 (red) Derivative of the red curve in **Figure 13** (blue) Effect of a destabilising mutation or ligand interaction (green) effect of a stabilising mutation or ligand interaction

The actual curves however looked different to the curves shown in **Figure 14**. Due to the highly dynamic nature of the carrier. Even in the presence of glutamate there did not appear to be one single conformation present, instead at least three different conformations were observed. In **Figure 15** the derivatives are shown. The green dotted line shows the derivative of the fluorescence curve directly after the isolation and purification. The left panel (green) shows the curve after 24 h, where apparently the carrier falls into two main conformations and does not exhibit a clear main conformation as before. This state was recoverable by addition of glutamic acid. With 5 mM (middle panel, light blue) and 10 mM (right panel, dark blue) glutamic acid the derivative of the fluorescence curve recovered to almost its original shape.

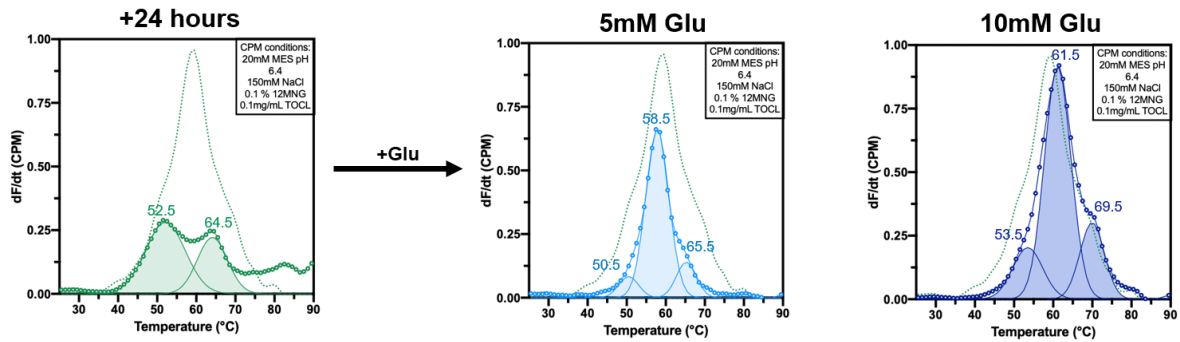


Figure 15 Actual curves of citrin with no glutamate dashed green line standing for the native state of the carrier., 5 mM glutamate & 10 mM glutamate

An ideal derivative of the fluorescence curve would be one sharp peak with no shoulders and shifted away from native state's melting temperature to higher melting temperatures. To find a ligand that yields such a curve was the aim of this work.

Transport assay

The other assay used at a later stage of the project was a transport assay. This was based on the transport of radioactively labelled aspartate across the membrane of a proteoliposome by reconstituted AGC. Through the reconstitution into the liposomes the citrin is oriented in a random 50/50 distribution, meaning that half of the citrin has the regulatory domain on the outside of the liposome and the other half has the regulatory domain on the inside. To the transporter embedded in the liposome is added ^{14}C labelled aspartate, which subsequently gets transported into the liposome in exchange for unlabelled aspartate. After certain time periods (0, 20, 40, 90, 120, 300, 600, 900, 1200, 1800 seconds) the external solution is removed, leaving just the proteoliposome with its contents. The dried proteoliposomes are dissolved with a scintillant and the radioactivity is quantified in a scintillation counter. In **Figure 16** panel **A** the principle is shown without an inhibitor. The labelled aspartates can pass readily through the membrane of the liposome via the transporter. In panel **B** however, presence of an inhibitor prevents or slows down the aspartate's uptake into the liposome, resulting in less radioactively labelled aspartate in the liposome.

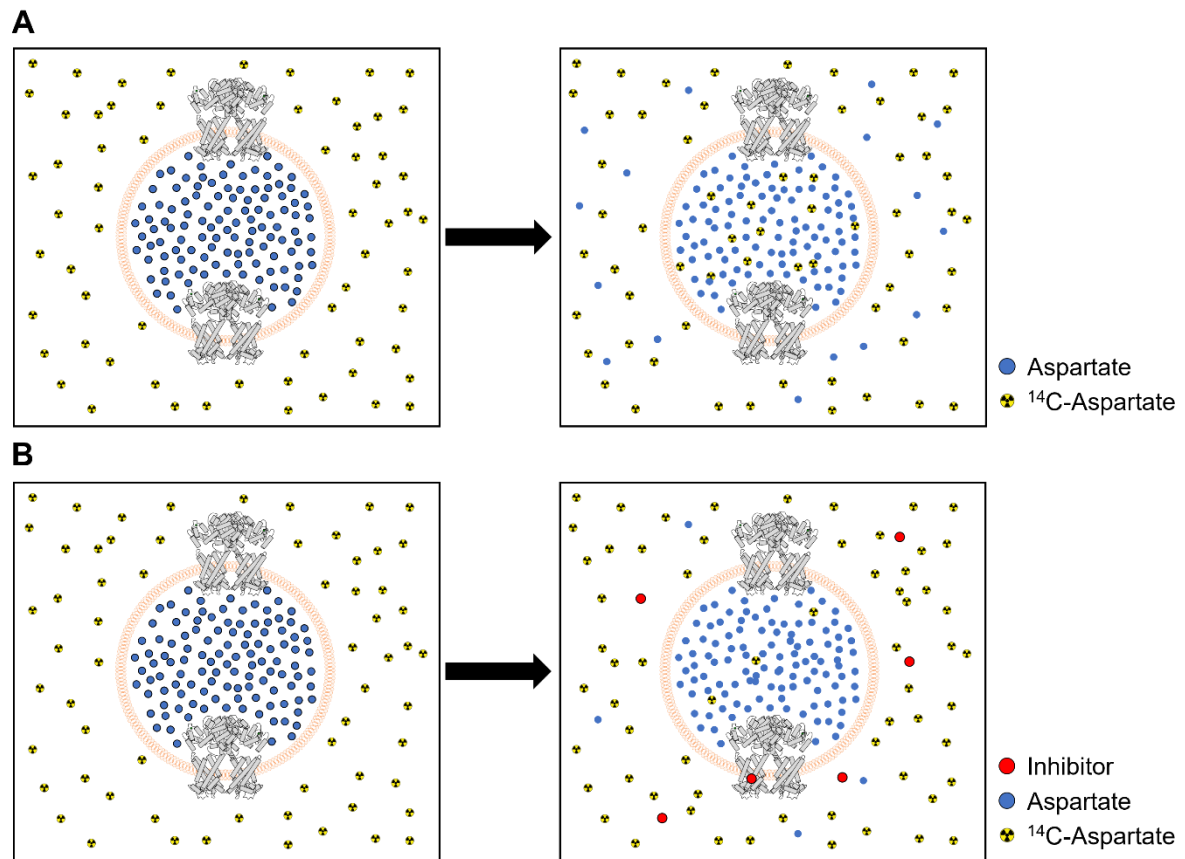


Figure 16 Principle of the transport assay

If the radioactivity at different time points of the experiment is measured and plotted against the duration of the experiment, a graph as shown in **Figure 17** is obtained. From this data the inhibition can be quantified.

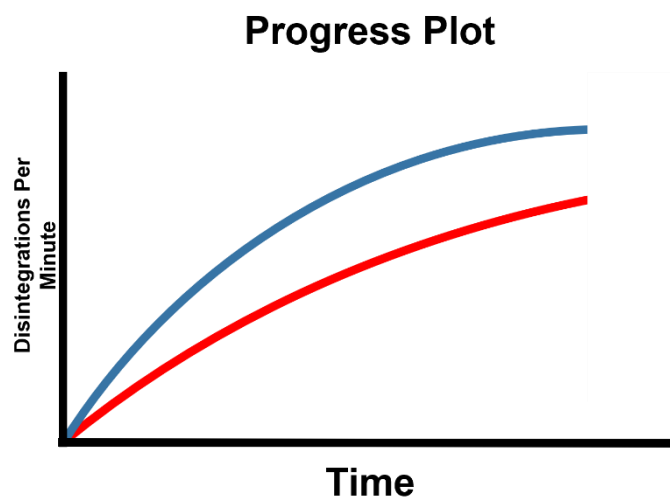


Figure 17 Schematic plot of the transport assay. **Blue** curve: [^{14}C]-aspartate uptake without inhibitor. **Red** curve: [^{14}C]-aspartate uptake in the presence of inhibitor.

In **Figure 18** an actual example of the obtained curves is shown. The curves are fitted to the data points of the individual time points at which a measurement was made. From this fit the inhibition is calculated by comparing the slope of the uninhibited transport to the slope of the inhibited transport. The relative values can be expressed as percentage of the inhibition.

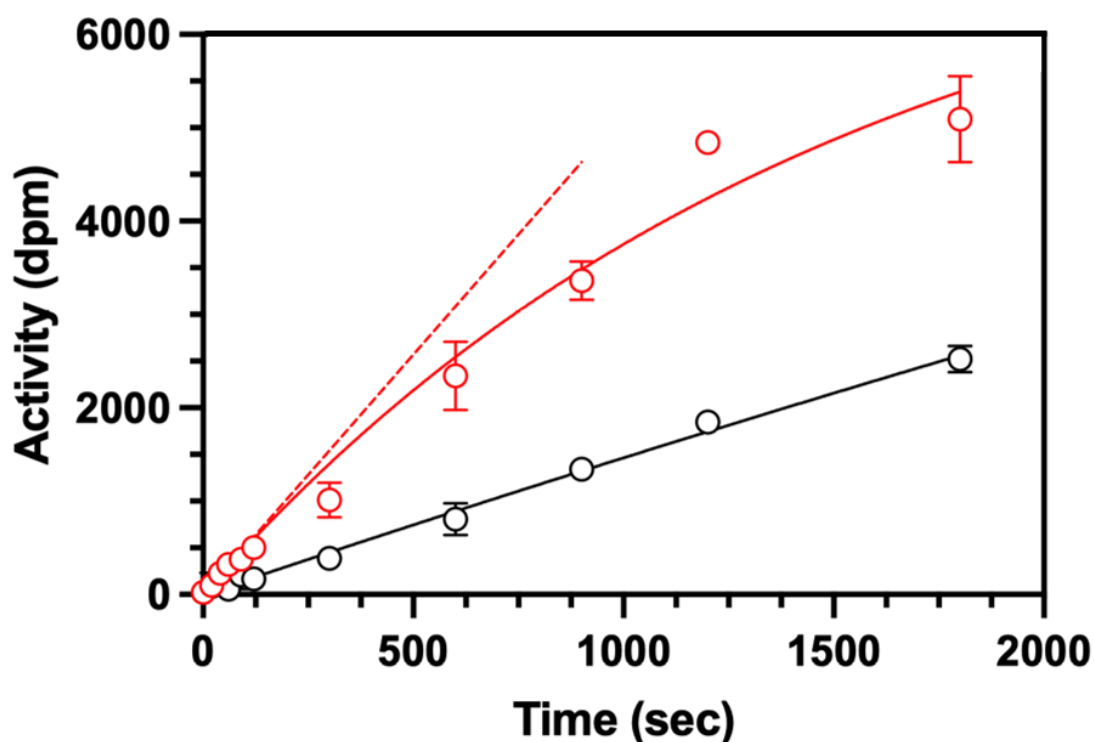
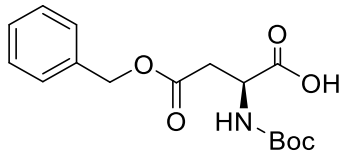
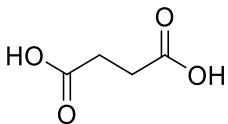
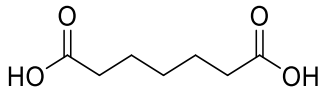
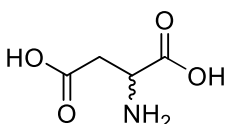
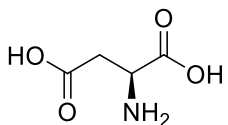
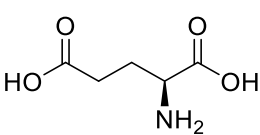
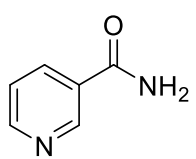
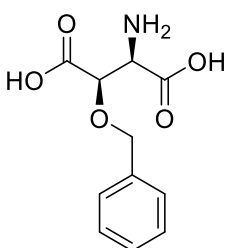
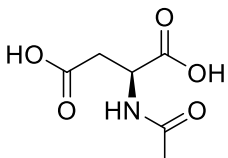


Figure 18 Example of transport assay curves with (red) uninhibited transport and (black) inhibition by PGUB81

Preliminary screening

For a first screening, compounds structurally similar to transport substrates **aspartic-** and **glutamic acid** were screened, including other amino acids such as **glutamine** or **ornithine**, as well as their protected derivatives, such as **N-Z-L-Asp-OH**. In addition, the aforementioned **γ -BnGlu** was tested as well as **DL-TBOA** which is a potent inhibitor of glutamate uptake, acting on glutamate transporters (EAATs) in brain.⁷⁵ Linear diacids, such as **succinic acid** and **pimelic acid** were also subjected to the screening. A selection of compounds and their respective thermal shift at 1 mM concentration is given in **Table 3**. The thermal shift value is given in degree Celsius compared to the native AGC without any compound.

Compound	Name	Thermal Shift [°C]
	PGUB03	+0.3
	succinic acid	+2
	pimelic acid	+1.5
	DL-aspartic acid	+1
	L-aspartic acid	+1
	L-glutamic acid	+1
	nicotinamide	+1
	DL-TBOA	+0.8
	N-acetyl-L-aspartic acid	+1

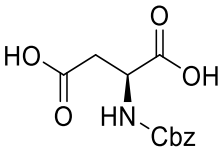
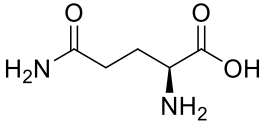
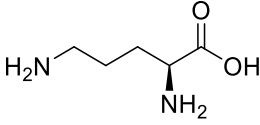
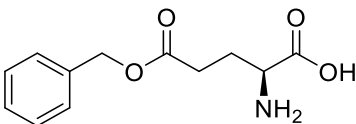
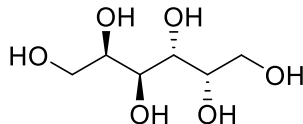
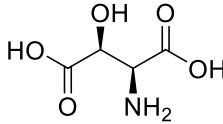
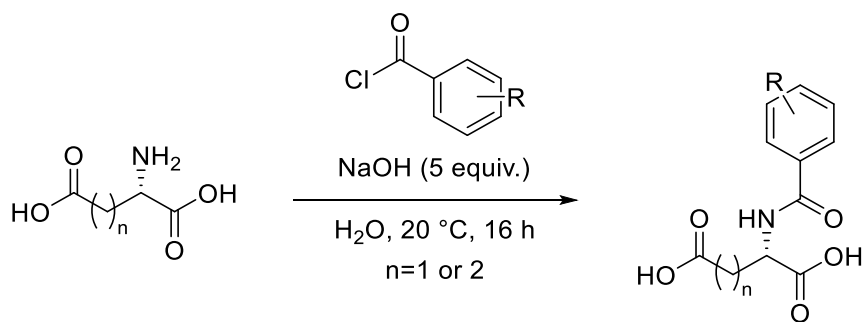
	<i>N</i> -Z-L-aspartic acid	+1
	L-glutamine	+0.3
	L-ornithine	-1
	γ -BnGlu	+0.6
	D-galactitol	-1
	PGUB02	+0.5

Table 3 Thermal shift of initially screened compounds

Interestingly, the previously reported inhibitor γ -BnGlu did perform worse than the natural substrates aspartic acid and glutamic acid. The diacids **succinic acid** and **pimelic acid** both were able to slightly increase the melting temperature. Most compounds induced a thermal shift in a similar range to the endogenous substrates aspartic- and glutamic acid.

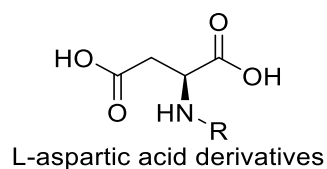
Synthesis and screening of a small library based on aspartic and glutamic acid

Based on the preliminary results we hypothesised that the diacid motif is generally an advantageous feature for the activity of the compounds and that a substitution of the amine could be potentially beneficial to increase the melting temperature. Therefore, starting from L-aspartic and L-glutamic acid various derivatives were synthesised by acylation of the amine with commercially available benzoyl chlorides or in the case of **PGUB25** using a previously prepared NHS-ester activated carboxylic acid. The general reaction scheme of the Schotten-Baumann-type reaction with the acyl chlorides is shown in **Scheme 3**. In this reaction in an alkaline aqueous environment the amine of the amino acids reacts as nucleophile attacking the electrophilic acyl chloride, resulting in the formation of an amide bond.

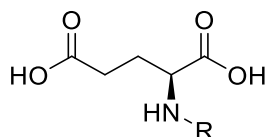


Scheme 3 General reaction scheme for a Schotten-Baumann reaction on glutamic and aspartic acid

The reactions yielded the desired compounds in poor to very good. The thermal shift results of the obtained compounds are shown in **Table 4**.



Name	Rest (R)	Thermal shift [°C]	Name	Rest (R)	Thermal shift [°C]
PGUB14	benzoyl	+1.75	PGUB22	2-trifluoromethyl benzoyl	+1.65
PGUB15	2-chlorobenzoyl	+2.15	PGUB23	3-chlorobenzoyl	-0.6
PGUB16	4-chlorobenzoyl	+2.5	PGUB24	4-bromobenzoyl	+0.5
PGUB17	2,5-difluorobenzoyl	+2	PGUB25	4-(3-(trifluoromethyl)-3H-diazirin-3-yl)benzoyl	+1.65
PGUB18	4-trifluoromethyl benzoyl	+2.15	PGUB26	4-iodobenzoyl	+1.9
PGUB19	isonicotinoyl	+1.85	PGUB31	3-iodobenzoyl	+0.4
PGUB20	picolinoyl	+1.85	PGUB33	3-bromobenzoyl	±0
PGUB21	nicotinoyl	+2.3	PGUB77	2,4-dichlorobenzoyl	±0



L-glutamic acid derivatives

Name	Rest	Thermal shift [°C]	Name	Rest	Thermal shift [°C]
PGUB27	3-chlorobenzoyl	+1.6	PGUB30	3-iodobenzoyl	+0.2
PGUB28	4-bromobenzoyl	+2.1	PGUB32	3-bromobenzoyl	+0.4
PGUB29	4-iodobenzoyl	+2	PGUB76	2,4-dichlorobenzoyl	+1.3

Table 4 Acylation derivatives of aspartic and glutamic acid

This first screening revealed compounds that were slightly more stabilising than the endogenous substrates. However, no emerging pattern was observable. Some compounds were more active as derivatives of the glutamic acid. E.g., the 3-chlorobenzoyl derivative was more stabilising when the core was the glutamic acid. Also, the 2,4-dichlorobenzoyl derivative was more active when it was the derivative of the glutamic acid. However, this first screening was not providing compounds that had stabilising properties in the wished magnitude. But by the end of the screening a serendipitous finding was made (see Serendipitous discovery: lonidamine).

Serendipitous discovery: lonidamine

Originally intended as negative control experiment for the citrin transport assay, lonidamine and zaprinast⁷⁶, known inhibitors of the mitochondrial pyruvate carrier (MPC), were used.^{76, 77} Surprisingly, both compounds showed good activity in the citrin thermal shift as well as in the radioactive uptake inhibition assay, with lonidamine giving the best results so far. The structures of lonidamine and zaprinast are shown in **Figure 19** and their respective activities in **Table 5**. Lonidamine was also synthesised according to **Scheme 5, A**, yielding a highly pure compound (**PGUB62**), which was slightly more active in the inhibition assay as well as in the thermal stabilisation compared to the commercially available lonidamine.

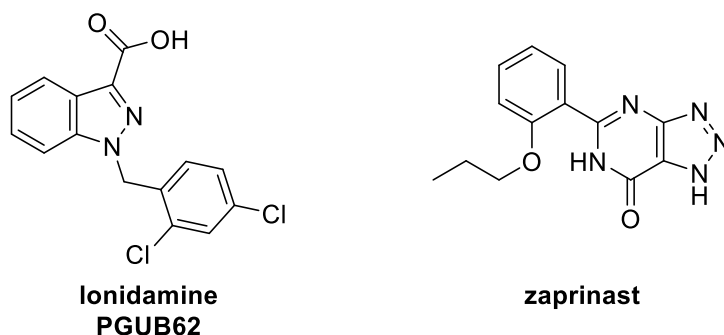


Figure 19 known mitochondrial pyruvate inhibitors also active on citrin

Name	Thermal shift [°C]	Inhibition
lonidamine	+3	75%
PGUB62	+4.75	79%
zaprinast	+2	20%

Table 5 Results for lonidamine and zaprinast

2nd generation citrin ligands

Herein, the workflow to obtain new inhibitors is described. A complete list of inhibitors and their activities is provided in **Table 6**.

Based on these serendipitous results the target structures were adapted to resemble the lonidamine scaffold. Lonidamine's core structure consists of 1*H*-indazole-3-carboxylic acid (**Figure 20**).

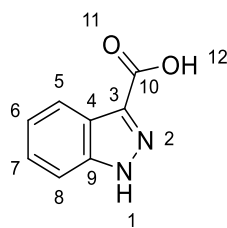


Figure 20 Indazole-1*H*-3-carboxylic acid core structure

Various derivatives of this core structure were bought or synthesised (**PGUB47, 49, 64 & 66**), and assessed using both the thermal shift and uptake assays. The first question to address was whether the substitution on the indazole *N1* nitrogen is required and how the carboxylic acid function

influences the activity. Also, indole-based structures (**PGUB64** & **PGUB66**) were evaluated. The results are given in **Table 6**.

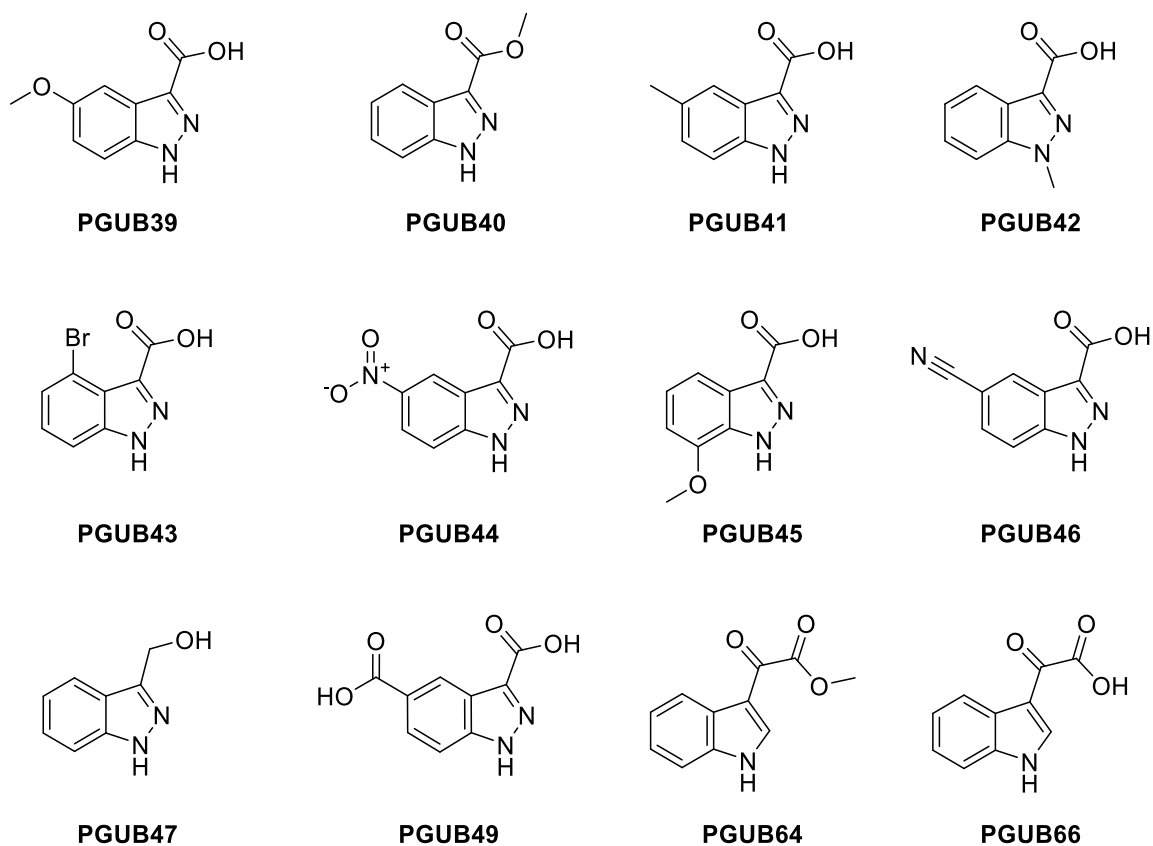


Figure 21 Indazole and indole core derivatives

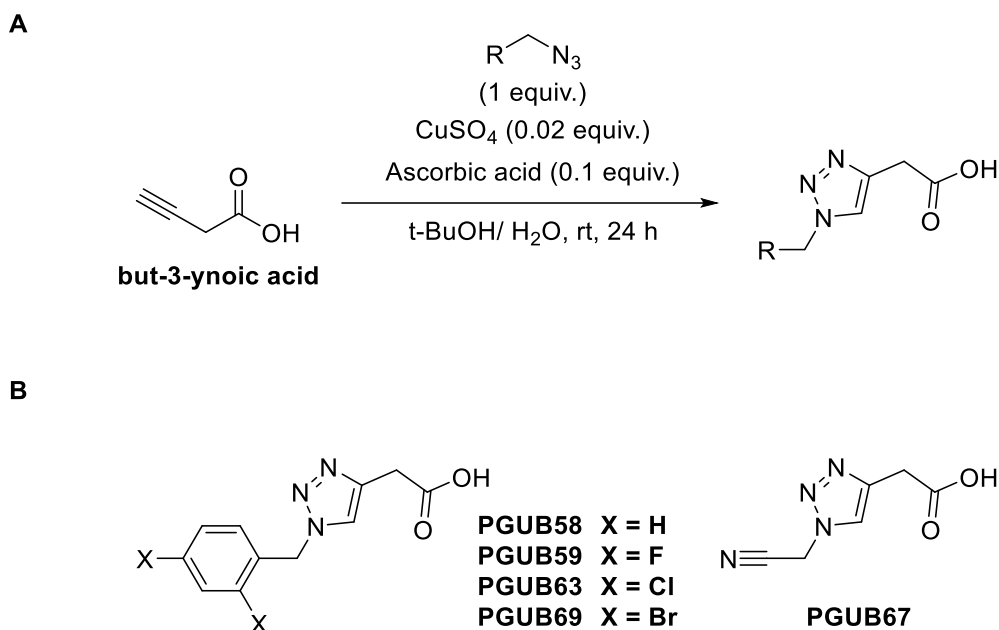
Name	Thermal shift [°C]	Inhibition
indazole 3-carboxylic acid	n/a	0%
PGUB39	+0.75	0%
PGUB40	+0.65	0%
PGUB41	+1.3	35%
PGUB42	+0.85	0%
PGUB43	+0.95	18%
PGUB44	+0.95	20%
PGUB45	+1	45%
PGUB46	+0.6	20%
PGUB47	+1.1	12%

PGUB49	n/a	15%
PGUB64	+1.25	61%
PGUB66	+2.5	60%
lonidamine	+3	75%

Table 6 Results for indazole and indole compounds in **Figure 21**

From the tested indazole compounds, the best was a 7-methoxy-indazole derivative (**PGUB45**). It showed an inhibition of the transport by almost 50%. All the other tested core structure derivatives performed worse. However, for the thermal shift assay the best result was obtained for the *N*1-methyl indazole derivative (**PGUB42**) which on the other hand performed very poorly in the inhibition assay, i.e. showing no inhibition. This indicates that the compound that increases the melting temperature the most, must not necessarily be the best transport inhibitor. This is also somewhat supported by the results of the best inhibitor in this indazole based series, **PGUB45**, which increased the melting temperature by only 1 °C, which is an above average shift slightly higher than **PGUB42**. Interestingly both indole-based structures **PGUB64** and **PGUB66** showed good activity with respect to transport inhibition. However, they differed significantly in the thermal shift assay where the methyl ester **PGUB64** performed worse than the free carboxylic acid **PGUB66**. Similarly, methyl ester indazole derivative **PGUB40** performed worse than the free carboxylic acid **PGUB47**.

Another scaffold, that is structurally related to the indazole's pyrazole core, is a triazole structure. Triazoles are readily available synthetically exploiting the unique reactivity of alkynes with azides. This reaction allows formation of triazoles in very good yields. When the reaction is catalysed by copper (I) ions, the reaction rate is greatly accelerated, and the reaction can be conducted at room temperature. **Scheme 4, A** depicts a general example for this reaction that was applied starting from but-3-ynoic acid. This so-called azide-alkyne Huisgen cycloaddition was successfully used to generate the compounds shown in **Scheme 4, B**. The biological activity results for the compounds shown in **Scheme 4, B** are listed in **Table 7**.



Scheme 4 A) General reaction scheme for the copper (I) catalysed 1,3-dipolar cycloaddition **B)** Compound library obtained using this reaction

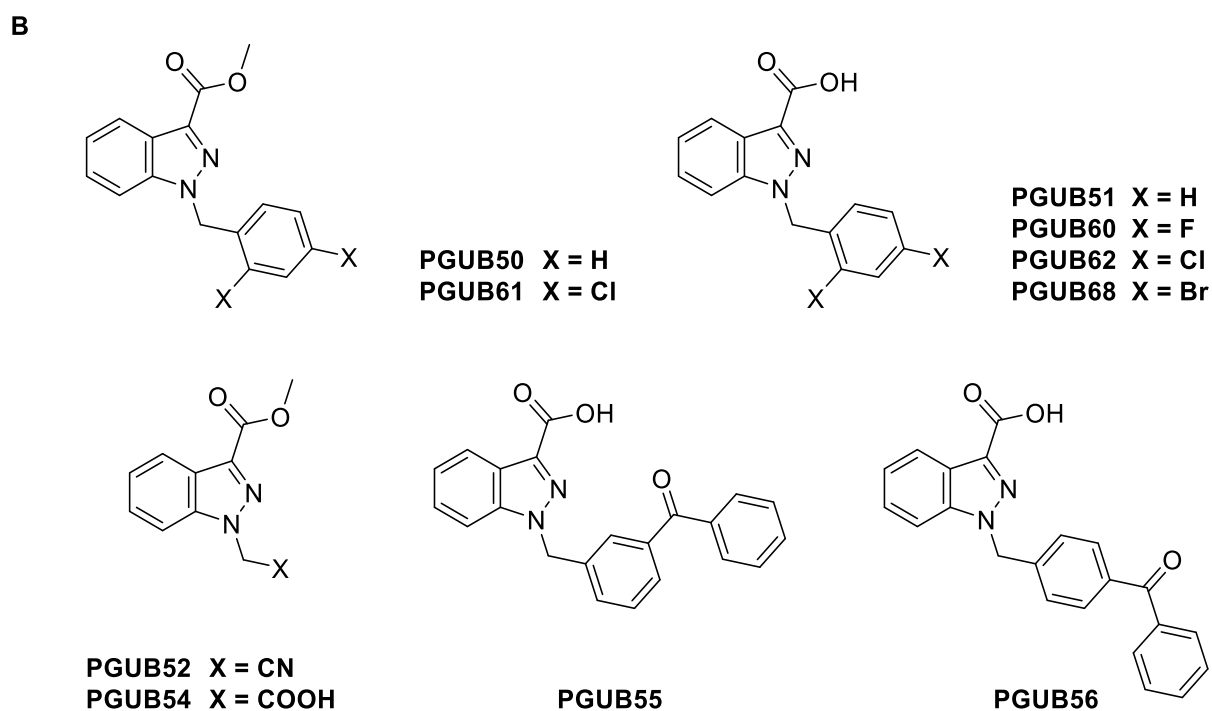
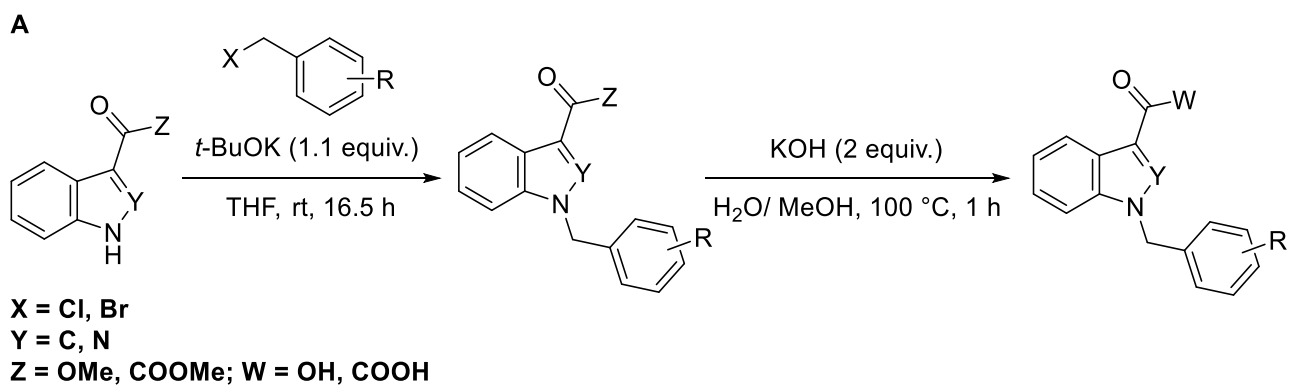
Name	Thermal shift [°C]	Inhibition
PGUB58	-0.6	49%
PGUB59	+2.5	53%
PGUB63	+2.5	60%
PGUB67	+3.35	0%
PGUB69	+4.6	0%
Ionidamine	+3	75%

Table 7 Results for compounds in **Scheme 4, B**

Some of them showed good activity in the thermal shift assay with an up to 4.6 °C increase of the melting point for the dibromo derivative **PGUB69**. Interestingly, the same compound did not show any transport inhibition. Furthermore, the nitrile derivative **PGUB67** increased the melting point significantly, but again no transport inhibition was observed. On the other hand, the unsubstituted benzyl derivative **PGUB58** decreased the melting temperature, but inhibited the transport by almost 50%. As mentioned above, this demonstrates again that a compound, which stabilises the protein significantly, does not necessarily act as a good transport inhibitor.

Modification at the *N1* position

Lonidamine is substituted with a 2,4-dichlorobenzyl moiety at the *N1* nitrogen (**Figure 20**). The *N1* position of indazoles as well as the *N1*indoles is easily alkylated with benzyl bromides or other alkyl halides by deprotonation with a moderately strong base, such as potassium tert-butoxide (*t*-BuOK), followed by subsequent nucleophilic attack on the activated carbon of the halide, resulting in the desired alkylated compounds. Some alkylation products were also tested in their ester forms (**Scheme 5, B**). The ester compounds were saponified using aq. potassium hydroxide (KOH) in a refluxing mixture of water and methanol. The addition of methanol was required to increase the solubility of the intermediate methyl esters, as they tended to be poorly soluble in water, even at reflux temperatures. An overview of the *N1*-alkylation and the following hydrolysis is shown in **Scheme 5, A** and some of the obtained compounds are depicted in **Scheme 5, B**. Compounds **PGUB52** & **54** were obtained in a similar way: Bromo-acetonitrile was used instead of an benzyl bromide, to obtain diacid compound **PGUB54**, the nitrile was hydrolysed with the methyl ester under the same conditions. It is worth noting that compounds **PGUB55** and **PGUB56** could be potentially used for photo-crosslinking. More details about this approach are shown below in the subchapter Covalent modifications.



Scheme 5 A) General reaction scheme for *N*1 modification and follow up hydrolysis **B)** Derivatives obtained by *N*1-alkylation and for some compounds subsequent hydrolysis

Name	Thermal shift [°C]	Inhibition
PGUB50	+1	0%
PGUB51	+2.45	13%
PGUB52	+0.95	32%
PGUB54	+0.1	0%
PGUB55	+2.1	80%
PGUB56	+2.1	80%
PGUB60	+3.45	65%

PGUB61	+0.1	50%
PGUB68	-4	0%
PGUB62	+4.75	79%
lonidamine	+3	75%

Table 8 Results for compounds of **Scheme 5**

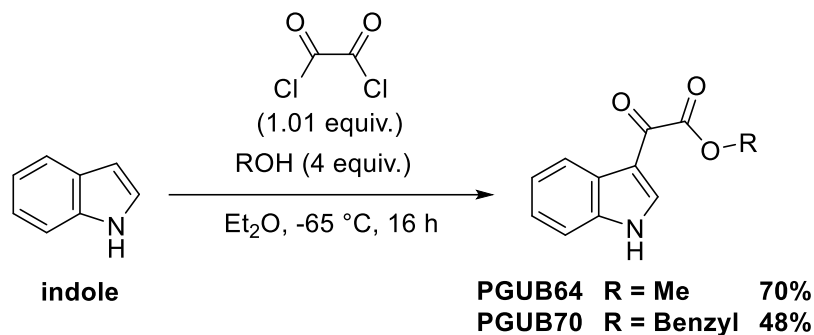
It appears that in the row of the halide substitutions from fluorine to bromine (**PGUB60, 62 & 68**) the activity increases when the fluorine is exchanged against the chlorine. However, when bromine is attached instead of the other two halogens there is no inhibitory activity, and the melting point is lowered substantially. This could be linked to the relatively bad solubility of the bromine bearing compound **PGUB68**. Even in pure DMSO the compound was hardly soluble. Compound **PGUB62** which is re-synthesised lonidamine performed well. The slight activity difference between re-synthesised and commercial lonidamine could be due to the difference in purity, with **PGUB62** having higher purity. Interestingly **PGUB51** could increase the melting point by 2.45 °C however, the inhibition was again very low. Such behaviour was already observed in some of the above-mentioned compounds. Of note, the methyl ester **PGUB50** the precursor of **PGUB51** did not show any inhibitory activity and only a slight increase in the melting temperature.

Further modifications and first hit

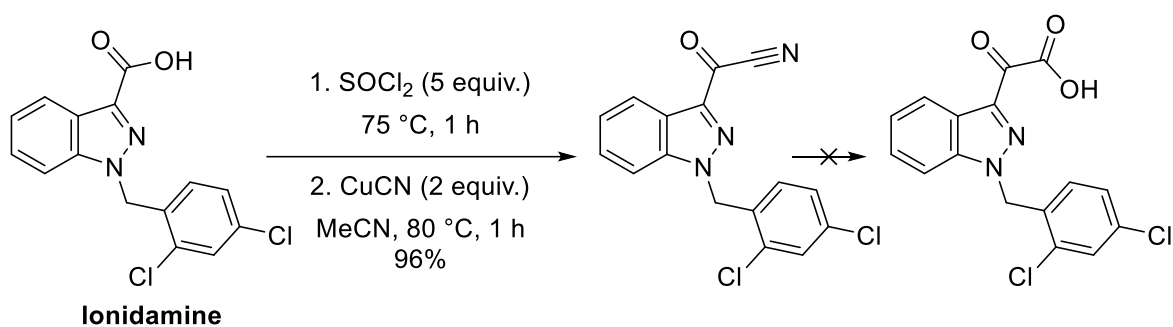
Based on the results of the previous sections and especially the 2nd generation compounds, more advanced derivatives were designed. Specifically, we wanted to study the influence of the carboxylic acid moiety on the activity and the effects of replacing this moiety with another motif. For this purpose, structures with an indole core were planned and synthesised, as indole is very easily modified at the C3 position i.e., with oxalyl chloride (**Scheme 6, A**). Reacting the acyl chloride intermediate with methanol or benzyl alcohol the corresponding esters were obtained. The resulting compounds could then be further modified by alkylation with 2,4-dichlorobenzylbromide (alkylation and hydrolysis as in **Scheme 5, A**) resulting in compound **PGUB71**. The alkylated methyl ester derivative was hydrolysed, resulting in **PGUB65** (**Scheme 6, C**). **PGUB65** is structurally similar to lonidamine but has an indole core and the α -keto-carboxylic acid motif. Attempts to synthesise a compound like **PGUB65** with an indazole core were in vain. The intermediate obtained by reaction of lonidamine with thionyl chloride followed by copper cyanide resulted in the desired but unstable keto-nitrile intermediate. The hydrolysis of the nitrile to the carboxylic acid led to decarboxylation instead and did not yield the desired α -keto-carboxylic acid. In all experiments the initial starting material lonidamine was recovered (**Scheme 6, B**). The commercially available compound **UK5099** (**Scheme 6, C**) was also

tested, to study the effects of the unsaturated C=C bond in place of the carboxylic acid part which is linked to the C3 of the indazole derivatives. **UK5099** is known to inhibit transport of pyruvate into the mitochondria by covalently binding to the mitochondrial pyruvate carrier (MPC).⁷⁸

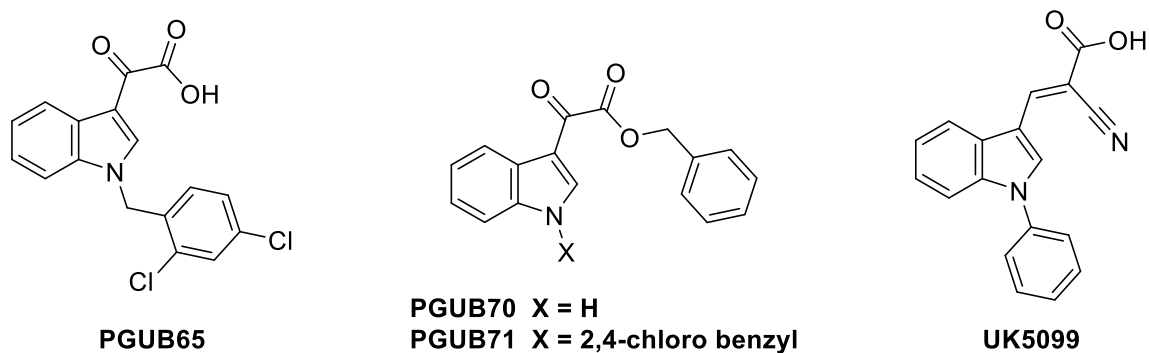
A



B



C



Scheme 6 **A)** Modification of indole on the C3 with oxalyl chloride **B)** Failed attempts to synthesise indazole based keto acid **C)** Compounds obtained with above reactions and commercially available **UK5099**

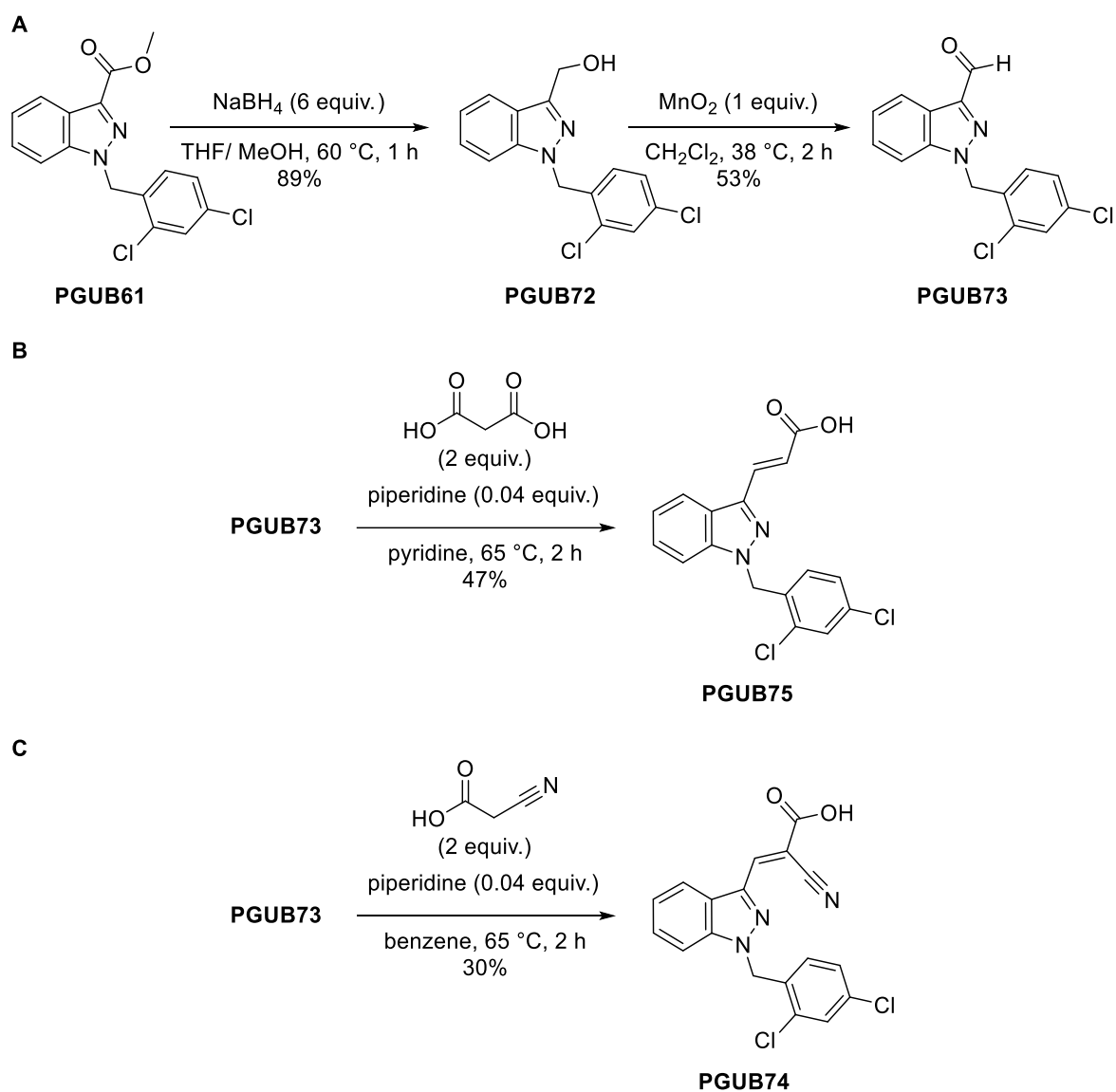
Name	Thermal shift [$^\circ\text{C}$]	Inhibition
PGUB64	+1.25	61%
PGUB65	+3	80%
PGUB70	+0.3	0%

PGUB71	+2.9	0%
UK5099	n/a	72%
lonidamine	+3	75%

Table 9 Results for compounds of **Scheme 6**

The best inhibition performance of this group was observed for **PGUB65** and **UK5099**, unfortunately the thermal shift assay did not provide results **UK5099** for this compound as the fluorescence was quenched by the compound delivering faulty readouts. However, it suggested that an unsaturation modification on the C3 could potentially increase the activity. Also, the inhibitory activity of **PGUB65** was higher than the one from lonidamine and the increase in the melting temperature was similar to lonidamine. Indicating, that the α -keto motif is also slightly improving the inhibitory effect. Benzyl esters **PGUB70** & **71** did not show high activity both in the thermal shift assay as well as in the transport assay.

Based on these results the next series of compounds was planned. Starting from the methyl ester **PGUB61** which was reduced to the alcohol **PGUB72** using sodium borohydride. Alcohol **PGUB72** was then re-oxidised to aldehyde **PGUB73**, which was subjected to a Knoevenagel reaction with either maleic acid to give unsaturated carboxylic acid derivative **PGUB75** or with cyanoacetic acid to give unsaturated nitrile-carboxylic acid derivative **PGUB74**.



Scheme 7 A) Reduction of methyl ester to alcohol followed to oxidation to alcohol **B)** Knoevenagel reaction with malonic acid **C)** Knoevenagel reaction with cyanoacetic acid

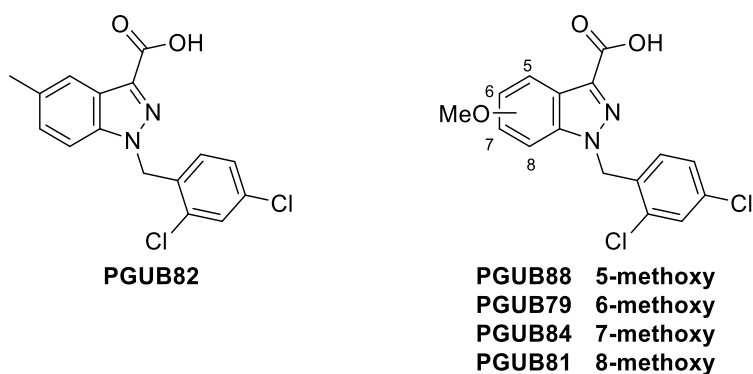
Name	Thermal shift [°C]	Inhibition
PGUB61	+0.1	50%
PGUB72	-6	28%
PGUB73	+5.3	64%
PGUB74	No signal	75%
PGUB75	+2.2	85%
Ionidamine	+3	75%

Table 10 Results for compounds of **Scheme 7**

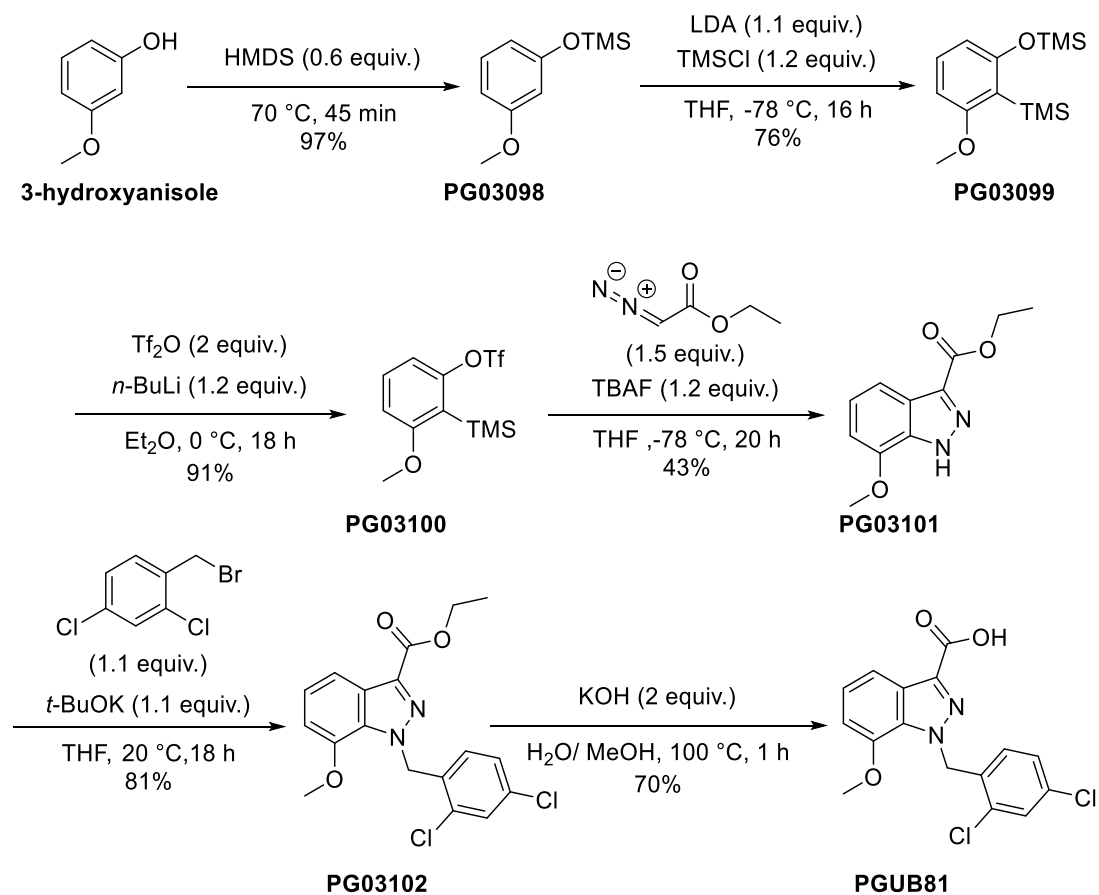
Decent inhibitory activity was observed for **PGUB74** & **75**. However, the shift in melting temperatures was not great for **PGUB75** and for **PGUB74** no signal was observed due to quenching of the CPM dye. However, it indicates that the unsaturated motif is beneficial for the inhibition as both compounds containing this motif performed better. Aldehyde **PGUB73** shifted the melting temperature relatively strongly but did exhibit moderate inhibition activity. Interestingly, even though alcohol **PGUB72** decreased the melting temperature strongly, an inhibitory activity was clearly measured.

Having the results in **Table 6**, where it was shown that a 6-methyl- or 7-methoxy indazole derivative already had slight inhibitory activity, even without the presence of the 2,4-dichlorobenzyl moiety, we aimed to explore the potential of these substitutions. Further, we aimed to synthesise all isomers bearing the methoxy substitution on the different aromatic carbons of the indazole aromatic ring. These structures, shown in **Scheme 8, A** were synthesised similarly to the reaction in **Scheme 5, A**. However, for compound **PGUB81** the core structure **PG03101** was synthesised starting from 3-hydroxyanisole in a 4-step procedure which was adapted and modified from a previous procedure that was employed in our lab.⁷⁹ The core structure was alkylated in a similar way to the previous reactions with 2,4-dichlorobenzyl bromide. However, instead of using *t*-BuOK, the intermediate **PG03101** was transformed into its sodium salt form **PG03101Na** which did not require basic conditions for its alkylation. This alkylation yielded intermediate **PG03102** in good yield. **PG03102** was successfully crystallised in a quality suitable for x-ray analysis (**Scheme 8, C**). Hydrolysis of this intermediate resulted in the desired product **PGUB81** for which also crystals in suitable quality for x-ray analysis were obtained (**Scheme 8, B & C**).

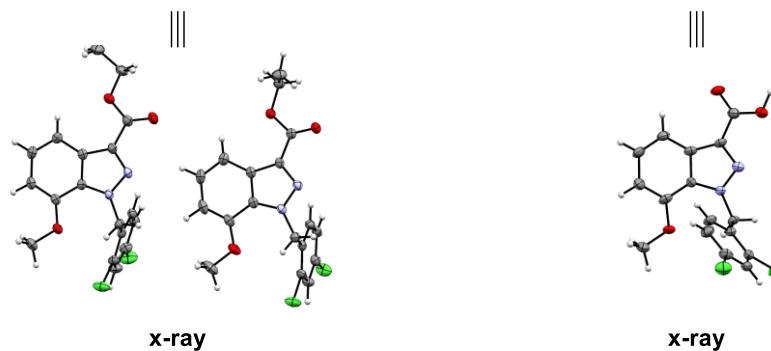
A



B



C



Scheme 8 A) Lonidamine derivatives substituted on the aromatic ring **B)** Synthetic pathway to **PGUB81** **C)** Crystal structure of intermediate **PG03102** and final compound **PGUB81**

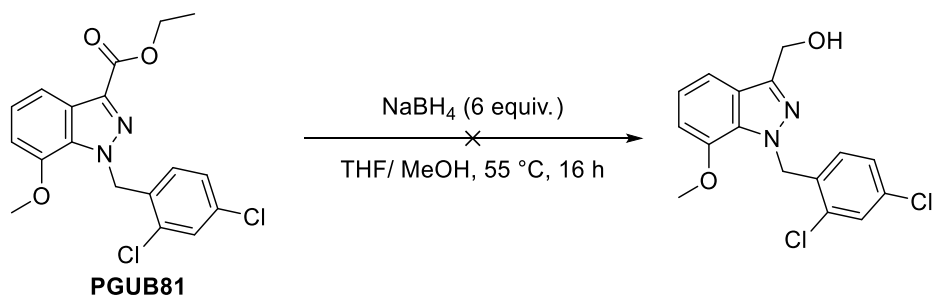
Name	Thermal shift [°C]	Inhibition
PGUB79	+4.5	80%
PGUB81	+8.5	77%
PGUB82	-0.15	69%
PGUB84	±0	45%
PGUB88	+1	25%
Ionidamine	+3	75%

Table 11 Results for compounds of **Scheme 8**

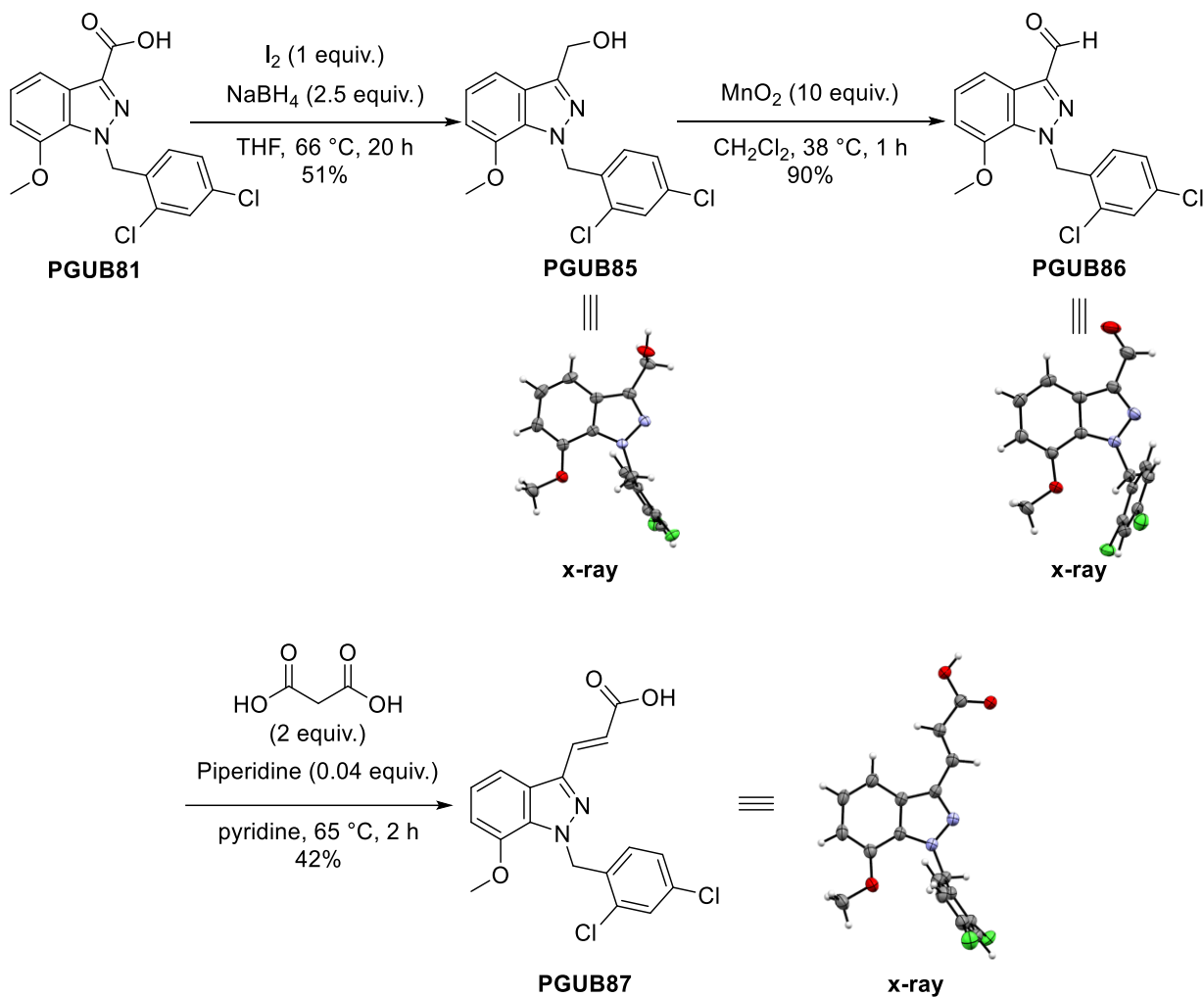
In contrast to the unsubstituted core structure **PGUB39**, which was not significantly active in both assays, **PGUB79**, which both contains the 6-methoxy substituent and the 2,4-dichlorobenzyl moiety is inhibiting the transport strongly and is also increasing the melting temperature (Table 9). Interestingly, **PGUB81** containing the core structure **PGUB45** (7-methoxy-1*H*-indazole-3-carboxylic acid), which was already moderately active in both assays, is increasing the melting temperature very strongly, shifting it by 8.5 °C. However, as already observed with previous compounds, the transport inhibition was lower than for the best compounds **PGUB74** & **75** so far (Table 10), even though the shift in melting temperature of **PGUB81** was the highest observed so far.

Based on the performance of **PGUB81** we decided to synthesise an α,β -unsaturated derivatives of it, using a similar reaction sequence as shown in **Scheme 7, A & B**. The synthesis route to **PGUB87** is shown in **Scheme 9, A & B**. Contrary to the synthesis of **PGUB74** & **75** (**Scheme 7**), the attempted reduction with sodium borohydride was unfruitful (**Scheme 9, A**). Therefore, another reduction protocol using in situ generated borane was employed. The borane is obtained by reduction of iodine with sodium borohydride. With this protocol the reduction of ethyl ester **PGUB81** to alcohol **PGUB85** was successful. The alcohol was then oxidised with activated manganese dioxide to the aldehyde **PGUB86**. The aldehyde was then reacted with malonic acid in a Knoevenagel reaction to the unsaturated carboxylic acid **PGUB87**. Compounds **PGUB85**, **86** & **87** were crystallised, and the x-ray structure was determined.

A



B



Scheme 9 A) Unsuccessful reduction B) Reaction scheme from carboxylic acid **PGUB81** to unsaturated carboxylic acid **PGUB87** structures with ellipsoid representation were obtained as x-ray crystal structures

Name	Thermal shift [°C]	Inhibition
PGUB81	+8.5	77%
PGUB85	+1.15	0%
PGUB86	+0.6	0%

PGUB87	+1.9	30%
lonidamine	+3	75%

Table 12

Unfortunately, the activity of compound **PGUB87** which was projected to be highly active, did not meet our expectations. It was lower in the transport inhibition as well as in the thermal stabilisation. Also, the intermediates that were obtained on the way to **PGUB87** were not providing the activity that was expected when comparing them to the lonidamine derivatives, which were more active with the respective functionalisation (**Scheme 7 & Table 10**).

A general trend could be that the transport inhibition and the thermal stabilisation are not arising from the same motif within the molecule, furthermore, they could possess competing properties. This idea is supported by **PGUB87** which is a combination of the motifs from the best inhibitor with the motifs of the best thermal stabiliser, performed poorly in both assays.

Covalent modifications

To stabilise the transporter structure more strongly, a promising method can be to modify covalently the target protein. A potential method is the use of photo-crosslinking ligands. Photo-activatable groups provide the advantage that they are mostly unreactive until they get activated by light. The reactivity can be harnessed at a desired time point in the experiment. Such photo-activatable groups can be for instance diazirine, azide or benzophenones derivatives.³ Another advantage is that the binding to the target protein is not solely relying on the ionic, van-der-Waals or hydrophobic interaction between the protein and the molecule. Therefore, the molecule is not able to dissociate anymore, and the overall binding is increased. Furthermore, the protein can be washed without losing the probe in the washing process. This method finds applications, especially in labelling. For the labelling various tags, such as fluorophores or radioactive groups can be used. This method is called photo-affinity labelling or PAL in short. In this case, the washing step can drastically reduce background signal by removing the unbound probe. Instead of an imaging tool also a pulldown tool can be developed with this technique by conjugating for an instance a biotin tag to the protein of interest, which allows for later isolation of the target protein by use of e.g., streptavidin beads.

In this work two different types of photo-activatable ligands were used. The first (**PGUB25**) featured a diazirine group that was conjugated to an aspartic acid derivative. Compounds (**PGUB55 & 56**) are based on benzophenone conjugates of indazole-3-carboxylic acid, the core structure of lonidamine (**Figure 19**).

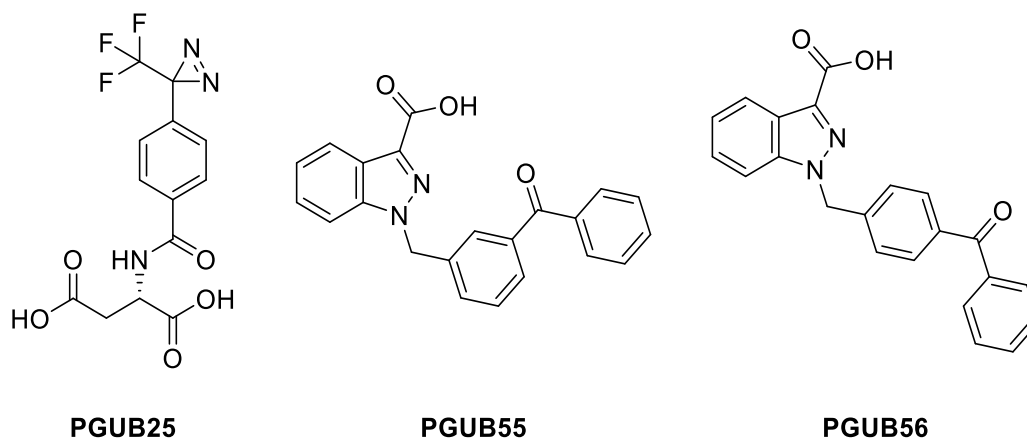


Figure 22 Photo-crosslinking compounds

The diazirine compound (**PGUB25**) generates a highly reactive carbene upon activation with UV light of around 360 nm, as depicted in **Figure 23, A**. This carbene can then undergo C-H and C-heteroatom insertion reactions and form the covalent bond to the protein of interest. The benzophenone on the other hand forms a triplet state ketyl diradical that is depicted in **Figure 23, B**. The energised electron of this activated species can then abstract a hydrogen radical and subsequent recombination of the remaining and protein-based radical forms a new covalent bond. Reactions with other active groups are also possible.³ The advantage of the benzophenones compared to the diazirines is that the activation is reversible. i.e., the excited triplet state can become deactivated and re-form the benzophenone. Whereas diazirines, when once activated as carbene, will target the closest species, leading to labelling of off-target sites. More significantly, carbenes can also be quenched by a solvent molecule (e.g., water) resulting in no covalent bond to the desired protein at all. These different properties can be chosen according to the requirements of the respective experiments. Benzophenones on the other hand can also form another form of covalent bond with amines by forming an imine species (**Figure 19, C**). This covalent imine bond formation is generally reversible and thus does not lead to permanent labelling of the protein.

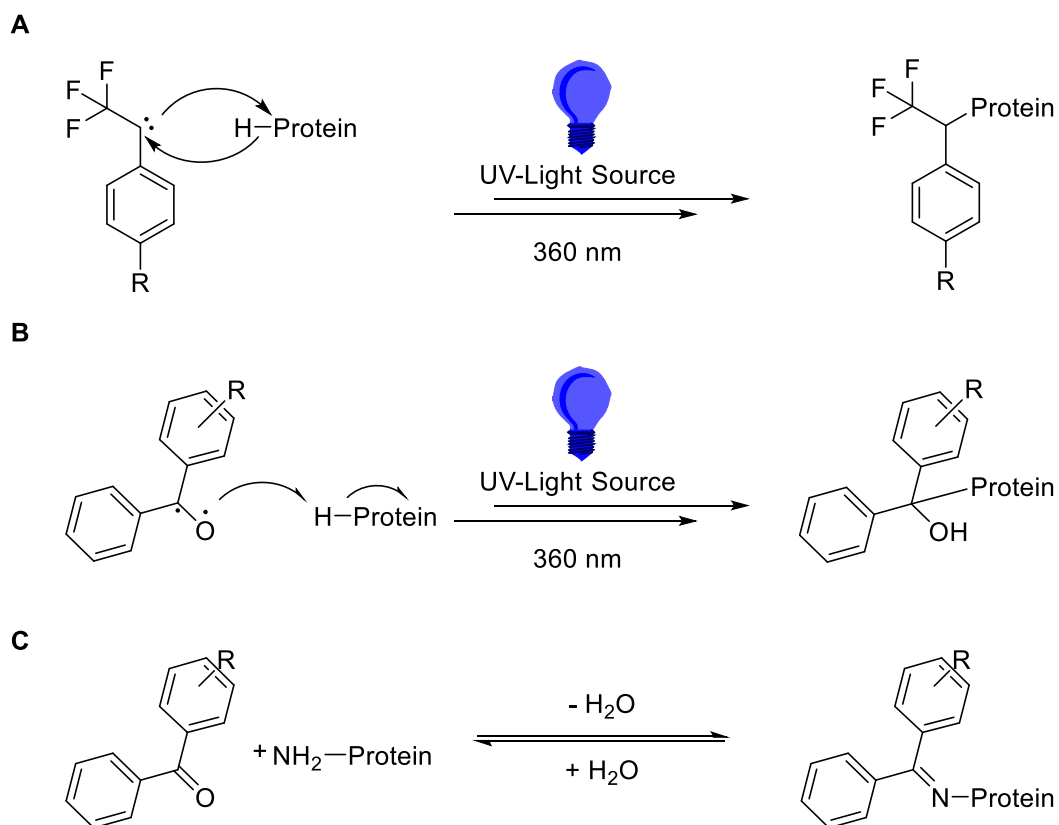


Figure 23 Reaction mechanisms of photo-activatable compounds

The diazirine derivative (**PGUB25**) was obtained by acylation of aspartic acid with the NHS-ester of the diazirine moiety (**Scheme 3**). This compound was tested under UV light irradiation. Compounds **PGUB55** & **56** were obtained by alkylation of the indazole core using the appropriate bromides (**Scheme 5**). These compounds were evaluated in the thermostability assay and transport assay without activating them with UV light. The results for these compounds are shown in **Table 13**.

Name	Thermal shift [°C]	Inhibition
PGUB25	+1.65	n/a
PGUB25+ UV	-0.35	n/a
PGUB55	+2.1	85%
PGUB56	+2.1	85%
Ionidamine	+3	75%

Table 13 Results for compounds from **Figure 22**

Astonishingly compound **PGUB25** performed worse when it was irradiated with UV light. The melting temperature was slightly decreased, compared to non-activated compound.

Other scaffolds

Axitinib is an indazole containing drug. Due to its structural similarities to the best compounds developed in this work, it was chosen to be assessed. **7ACC2** was also chosen as it was found to be inhibiting the mitochondrial pyruvate carrier.⁷⁷

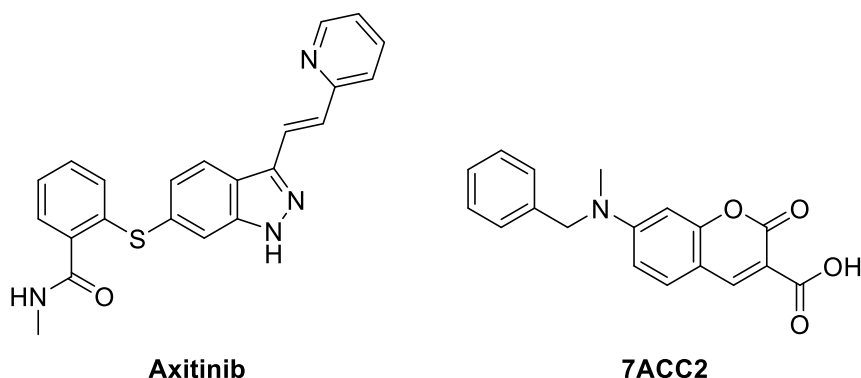


Figure 24 Axitinib and 7AAC

Name	Thermal shift [°C]	Inhibition
Axitinib	+0.5	13%
7ACC2	No signal	No signal
Ionidamine	+3	75%

Table 14 Results for Axitinib and 7ACC2

The results for **7ACC2** could not be obtained, most likely due the fluorescent properties of the coumarin core, which is known and exploited in various applications.⁸⁰ If one of these structures was active, other synthetic pathways would have to be chosen to access these alternative scaffolds. The obtained inhibition data for Axitinib did not provide evidence for high activity. Therefore, further investigation of these scaffolds did not appear reasonable for future structures.

2.4. Conclusion and outlook

Solving the structure of the carrier domain of citrin would allow to rationally develop compounds using structure-based design that bind stronger to the binding site - or possibly also other sites – reducing the required concentration required for an effective inhibition of the transporter. It could potentially be beneficial to target citrin in cancer cells as it was speculated by Rabinovich et al. that it might limit mitochondrial respiration and glycolysis.⁶² Moreover, the role of citrin in other diseases such as schizophrenia could be investigated. Also, reactivation of inactive citrin with drugs could have therapeutic benefits, depending on the underlying pathology.⁸¹

Over 80 final compounds were successfully synthesised and tested. We were pleased to discover compound **PGUB81** that caused an increase of 8.5° C in melting point in the thermal shift assay. Such a ligand-induced thermal stabilisation is promising to produce samples suitable for cryo-EM measurements. This fact was supported by the derivative of the fluorescence curve. A clear shift and no shoulders were observed. And even after 48 hours of incubation the conformation appeared to be stable over time. We will attempt first cryo-EM experiments with the carrier stabilised by **PGUB81**.

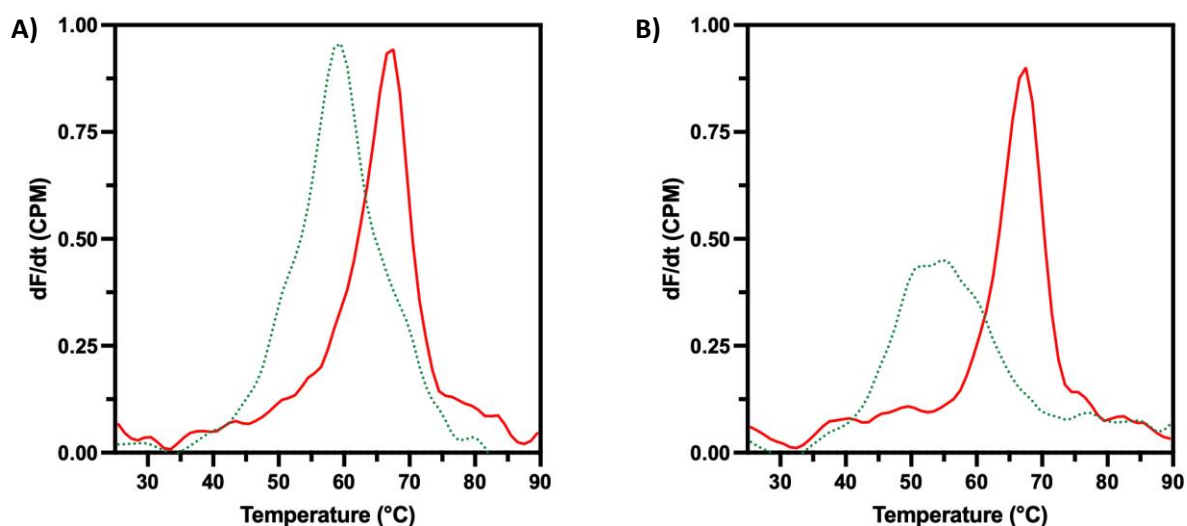


Figure 25 TSA curves for **PGUB81** for A and B the green dashed line represents the state without any ligand and the red curve represents incubation with **PGUB81**. **A)** Curve directly after incubation **B)** Curve 48 h after incubation

Despite this first success, further optimisation is still possible. We explored a lot of lonidamine based derivatives. Therefore, moving structurally away from the close similarity to lonidamine should be the next step. Probable target compounds could be conjugates of the active structures to aspartate or glutamate (**Figure 26**), either of only the core structure or with the 2,4-dichlorobenzyl moiety as shown in (**PGUBX1**, **PGUBX2** in **Figure 26**). Another suitable approach could be to demethylate the C7-attached ether (**PGUBX3** in **Figure 26**). This modification could also increase the compounds solubility in water and provide an additional hydrogen bond donor and acceptor for interactions with protein residues. A possible stumbling block could be the solubility of the *N*-alkylated indazole-3-carboxylic acid derivatives, as they are generally not soluble in organic solvents, such as dichloromethane, which are commonly used in these demethylation procedures.

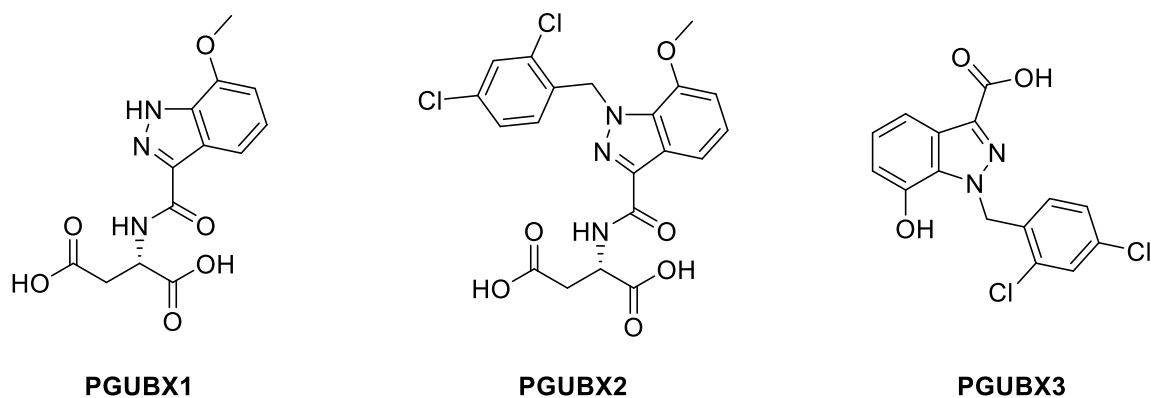


Figure 26 Possible active structures

Another scaffold that could be interesting to explore are luteorides, of which Luteoride B is shown in Figure 27. Recently a total synthesis to Luteoride B was published, starting from 7-bromo-indole, providing a route, that could be followed to synthesise derivatives.⁸²

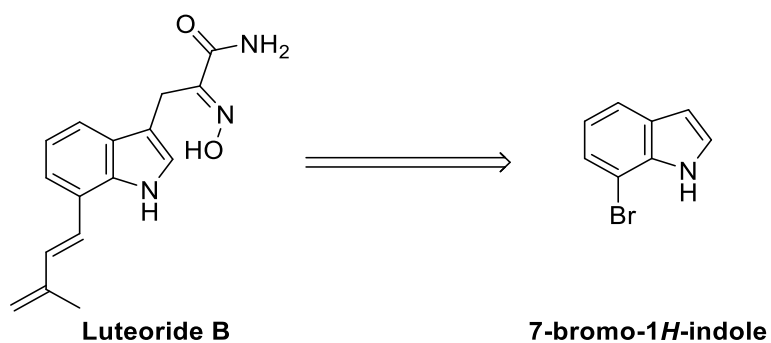


Figure 27 Retrosynthesis of Luteoride B⁸²

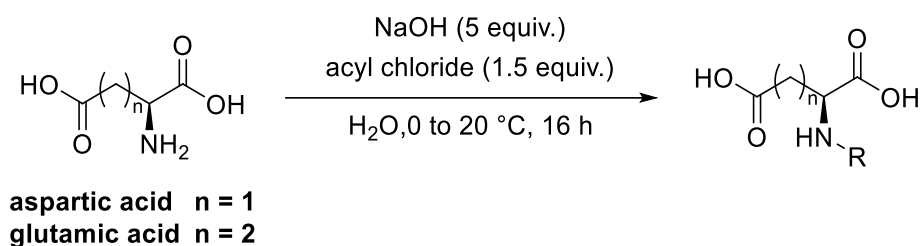
2.5. Experimental

General remarks to materials and methods

For general remarks see chapter 1.4.

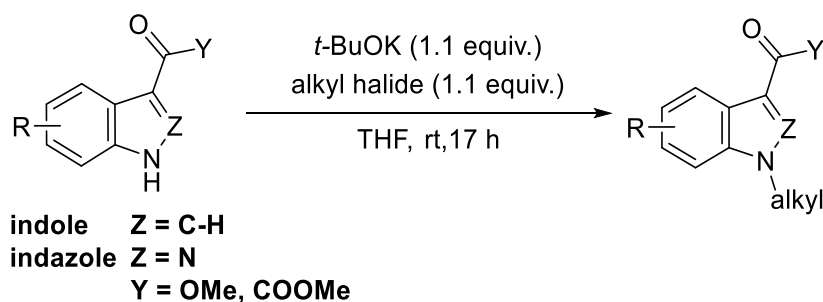
General procedures

General procedure I: Acylation of aspartic acid or glutamic acid



To a stirred solution of NaOH (5 equiv.) in water (to give 10wt% solution of amino acid) was added the amino acid (1 equiv.). The mixture was cooled to 0 °C. Then the acyl chloride (1.5 equiv.) was added. The mixture was slowly warmed to 20 °C over the course of 16 h. The clear solution was acidified with 1 M aq. HCl until a pH of about 1 was reached, causing a precipitation. To the mixture was added ethyl acetate resulting in a clear biphasic mixture. The organic phase was separated, and the aqueous phase was extracted with ethyl acetate. The combined organic phases were washed with slightly acidified brine, dried over MgSO_4 , filtered, and concentrated under reduced pressure onto silica gel. The crude was purified by flash column chromatography (cyclohexane/ (ethyl acetate/ methanol/ acetic acid 85:10:5) gradient from 1:0 to 1:1), to give the desired product.

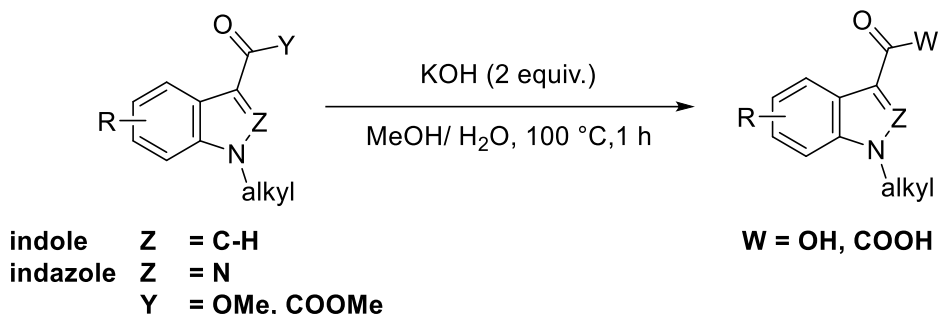
General procedure II: Alkylation of indole and indazole core structures



To a stirred solution of the alkylated indole or indazole 3-carboxy methyl ester (1 equiv.) in dry THF (to give 0.1 M solution) was added $t\text{-BuOK}$ (1.1 equiv.) for 1 h at room temperature under an argon atmosphere. Then the alkyl halide (1.1 equiv.) was added, and the mixture was stirred at room temperature for 16 h. The turbid mixture was filtered through a pad of celite. The filter cake was washed with THF, and the filtrate was concentrated onto silica gel. The crude product was purified by

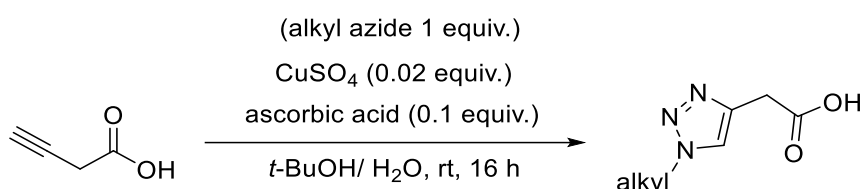
flash column chromatography (cyclohexane/ ethyl acetate gradient from 1:0 to 0:1), to give the desired product.

General procedure III: Saponification



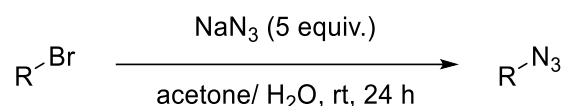
To a stirred suspension of the alkylated indole or indazole 3-carboxy methyl ester (1 equiv.) in methanol (to give 0.1 M solution) was added a solution of KOH (2 equiv.) in water (same volume as methanol). The mixture was heated to 100 °C and was stirred for 1 h. The mixture was acidified with 1 M aq. HCl until a white precipitate was formed and a pH of around 1 was obtained. To the mixture was added ethyl acetate. The organic phase was separated, and the aqueous phase was extracted with ethyl acetate (if bad solubility was encountered, little THF was added to the ethyl acetate). The combined organic phases were dried over MgSO_4 , filtered, and concentrated under reduced pressure to give the desired product.

General procedure IV: CuAAC reaction with 3-butynoic acid



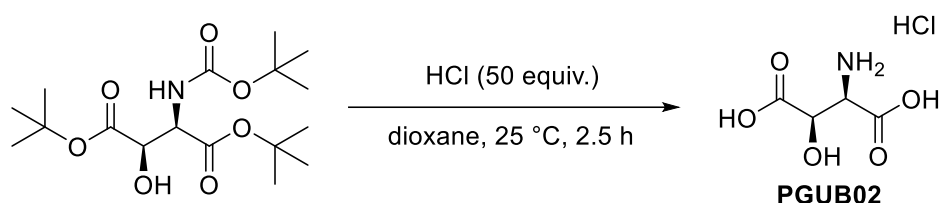
To a stirred solution of 3-butynoic acid (1 equiv.) and the alkyl azide (1 equiv.) in a mixture of *tert*-butanol (to give 0.1 M solution) was added copper sulphate (0.02 equiv.) followed by sodium ascorbate (0.1 equiv.) dissolved in water (same volume as *t*-BuOH). The mixture was left stirring for 16 h under an argon atmosphere at room temperature. To the mixture was added sodium chloride until no more dissolution was observed. Then the biphasic mixture was extracted with ethyl acetate, the combined organic layers were washed with acidified brine, dried over MgSO_4 , filtered, and concentrated under reduced pressure. The solid was then taken up in a mixture of dichloromethane and methanol and concentrated onto silica gel. The crude was purified by flash column chromatography (dichloromethane/ methanol gradient from 1:0 to 9:1), to give the desired product.

General procedure V: Azide synthesis

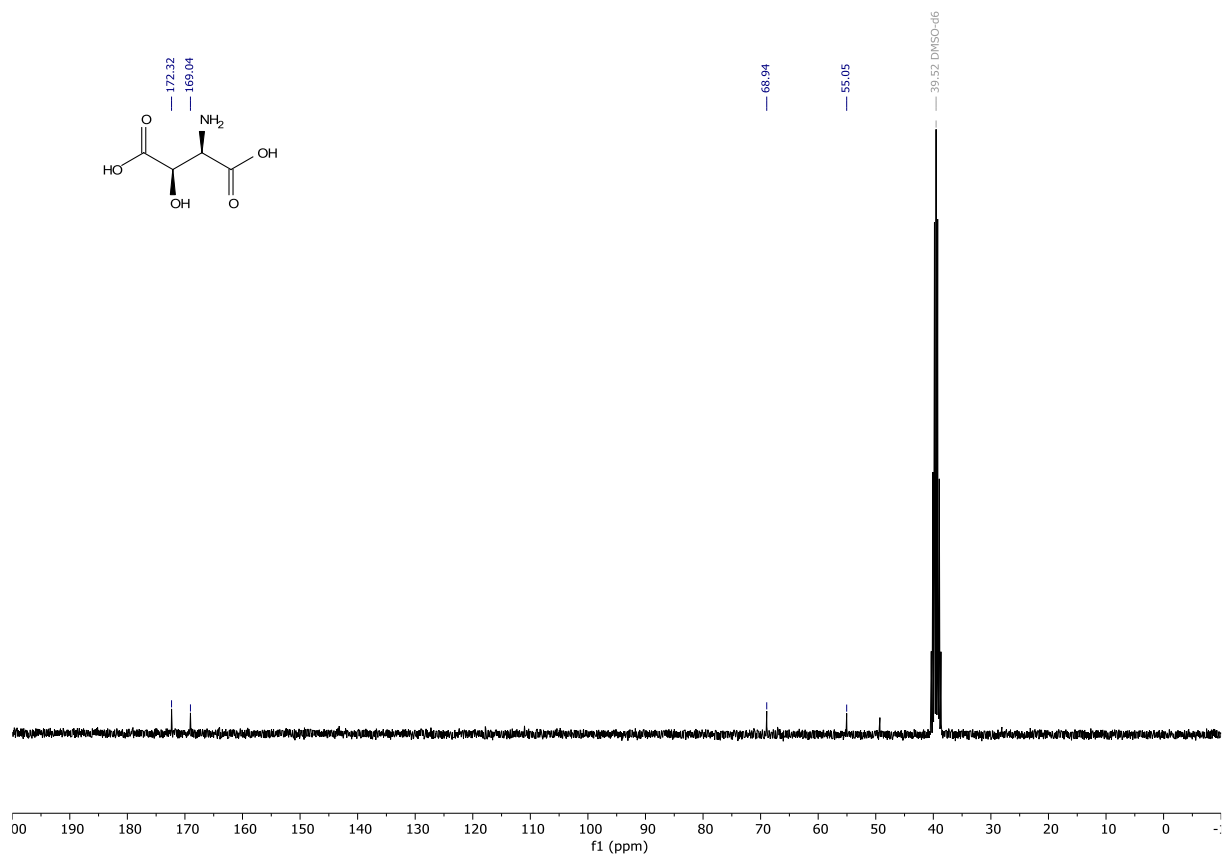
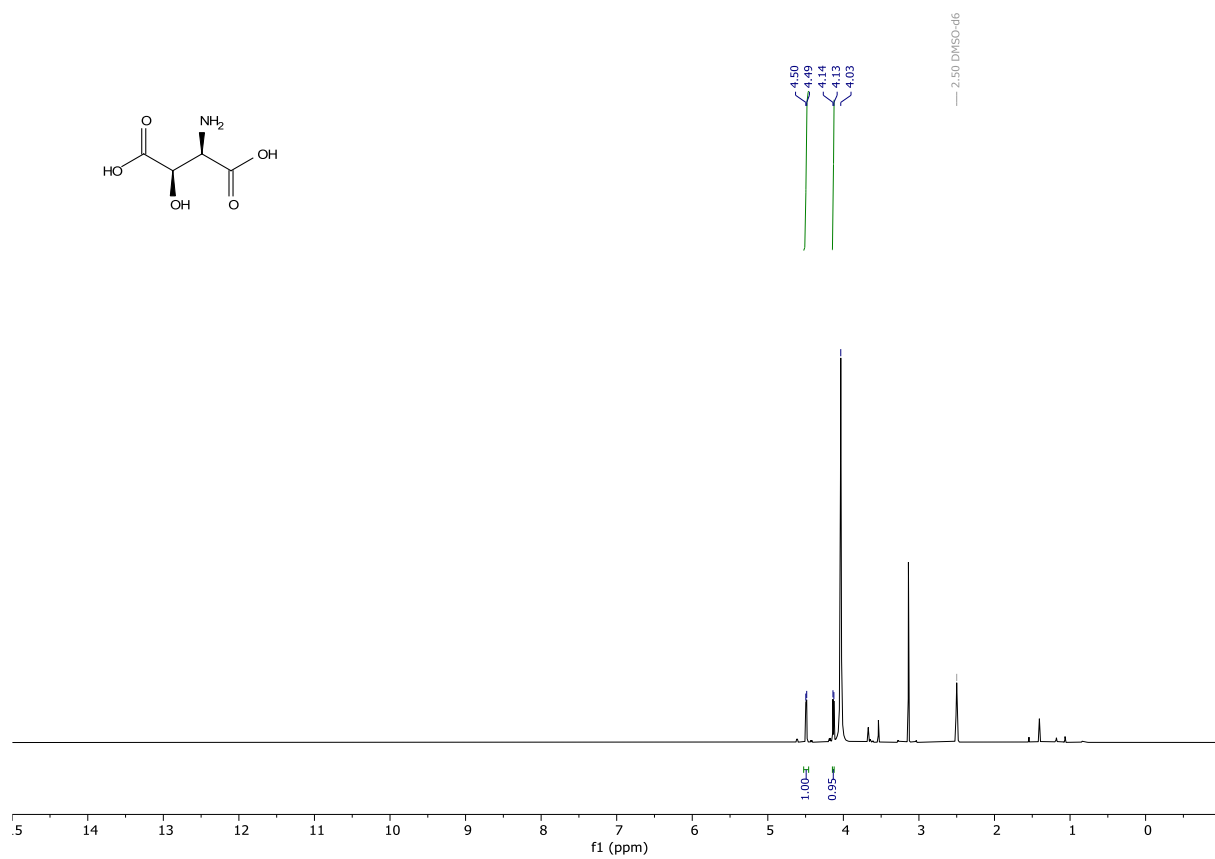


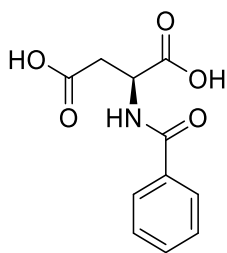
To a stirred solution of NaN₃ (5 equiv.) in a mixture of water/ acetone 1:1 (to give a 0.01 M solution of the bromide) was added slowly 1-(bromomethyl)-2,4-difluorobenzene (1 equiv.). The mixture was extracted with dichloromethane. The combined organic layers were dried with MgSO₄, filtered, and concentrated under reduced pressure. And transferred into a smaller flask. It was thoroughly dried on the high vac to give the desired product.

Synthesis



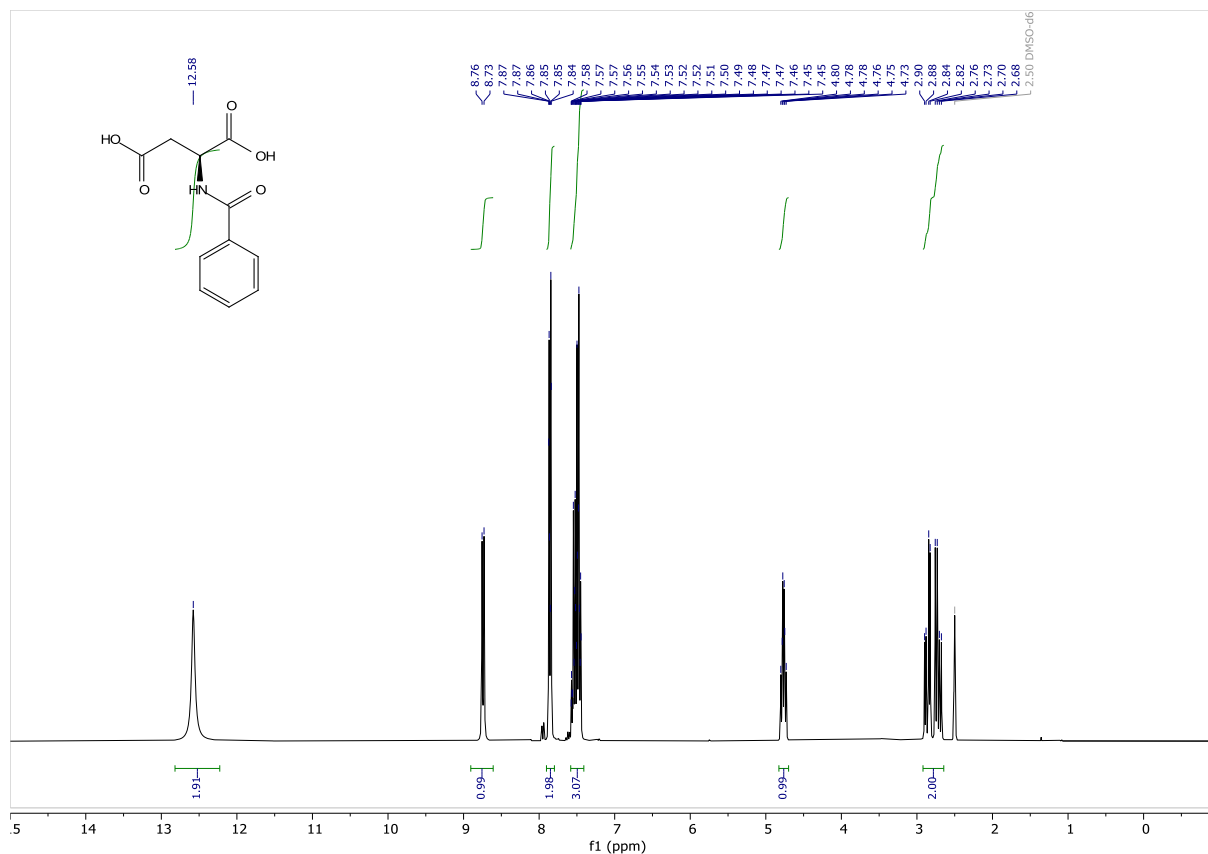
±-(2*R*,3*R*)-2-amino-3-hydroxysuccinic acid (PGUB02). To a stirred solution of di-*tert*-butyl ±-(2*R*,3*R*)-2-((*tert*-butoxycarbonyl)amino)-3-hydroxysuccinate (0.21740 g, 0.6015 mmol) in dioxane (3 mL) at 25 °C, was added HCl (4 M in dioxane, 7.5 mL, 30 mmol). The mixture was concentrated under reduced pressure. This residue was dissolved in methanol, transferred into another flask and re-concentrated to give the desired product as HCl salt in quantitative yield (0.12933 g, 0.69697 mmol). Product was very hygroscopic and contained some trace amounts of methanol. **¹H NMR** (300 MHz, DMSO-*d*₆+D₂O) δ 4.49 (d, *J* = 3.5 Hz, 1H), 4.13 (d, *J* = 3.6 Hz, 1H). **¹³C NMR** (75 MHz, DMSO) δ 172.32, 169.04, 68.94, 55.05. **HRMS** (ESI) calculated for [M+H]⁺ C₄H₈NO₅ 150.0397, found 150.0392.

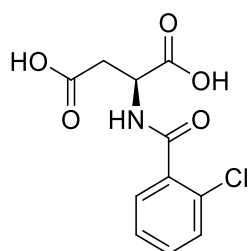
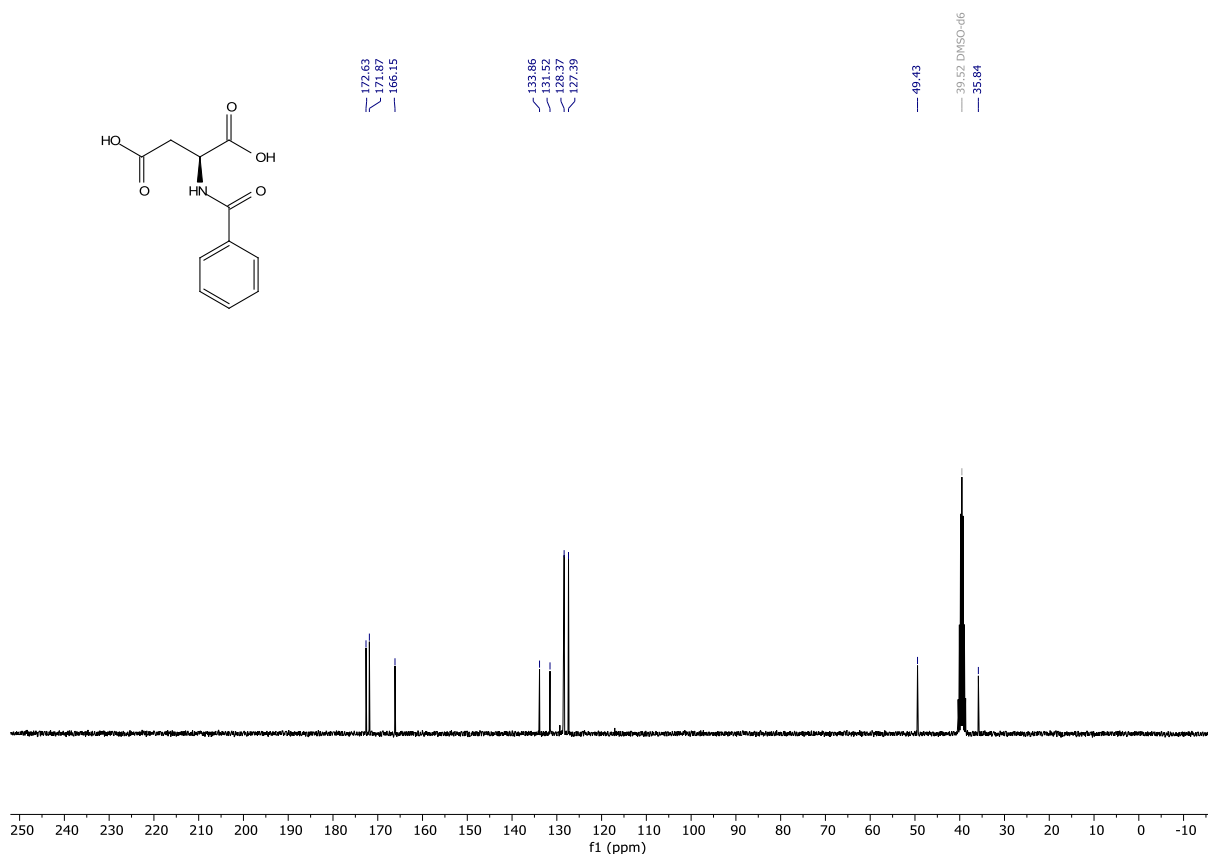




PGUB14

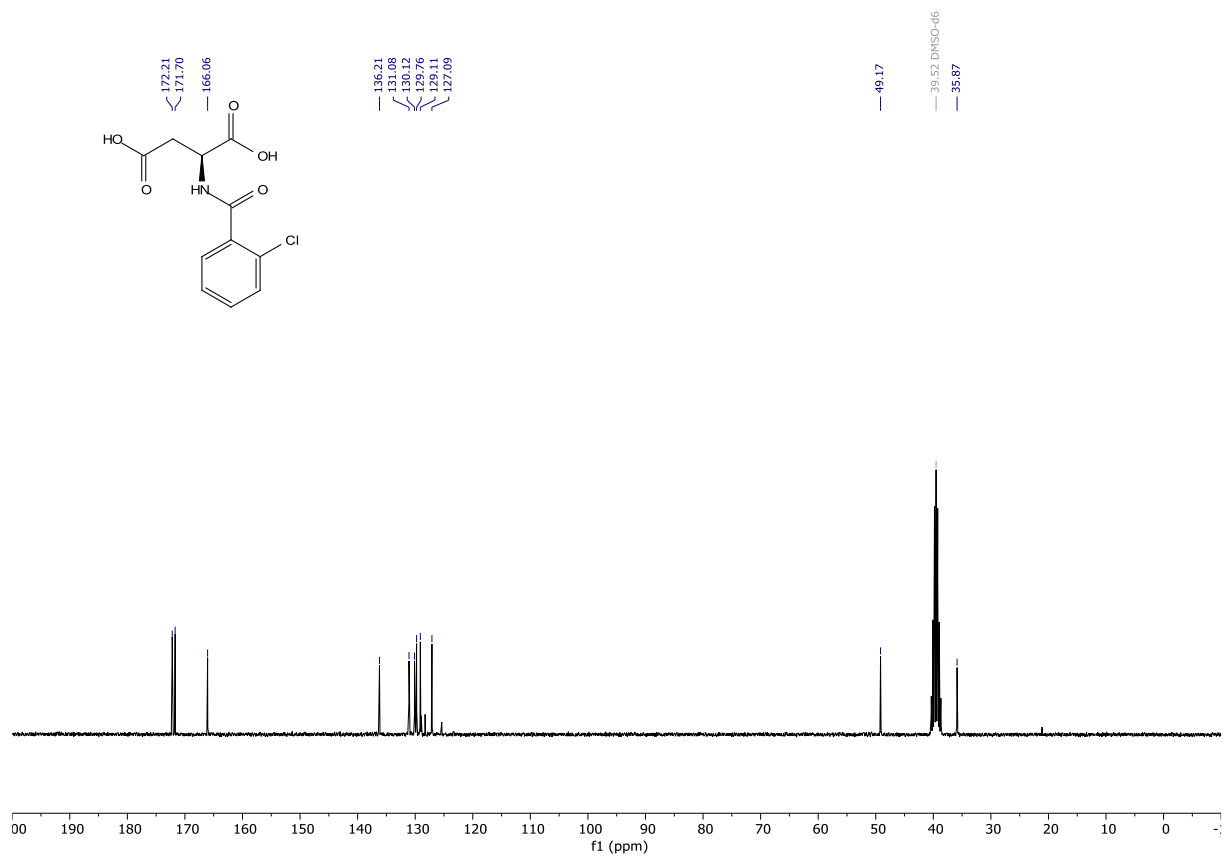
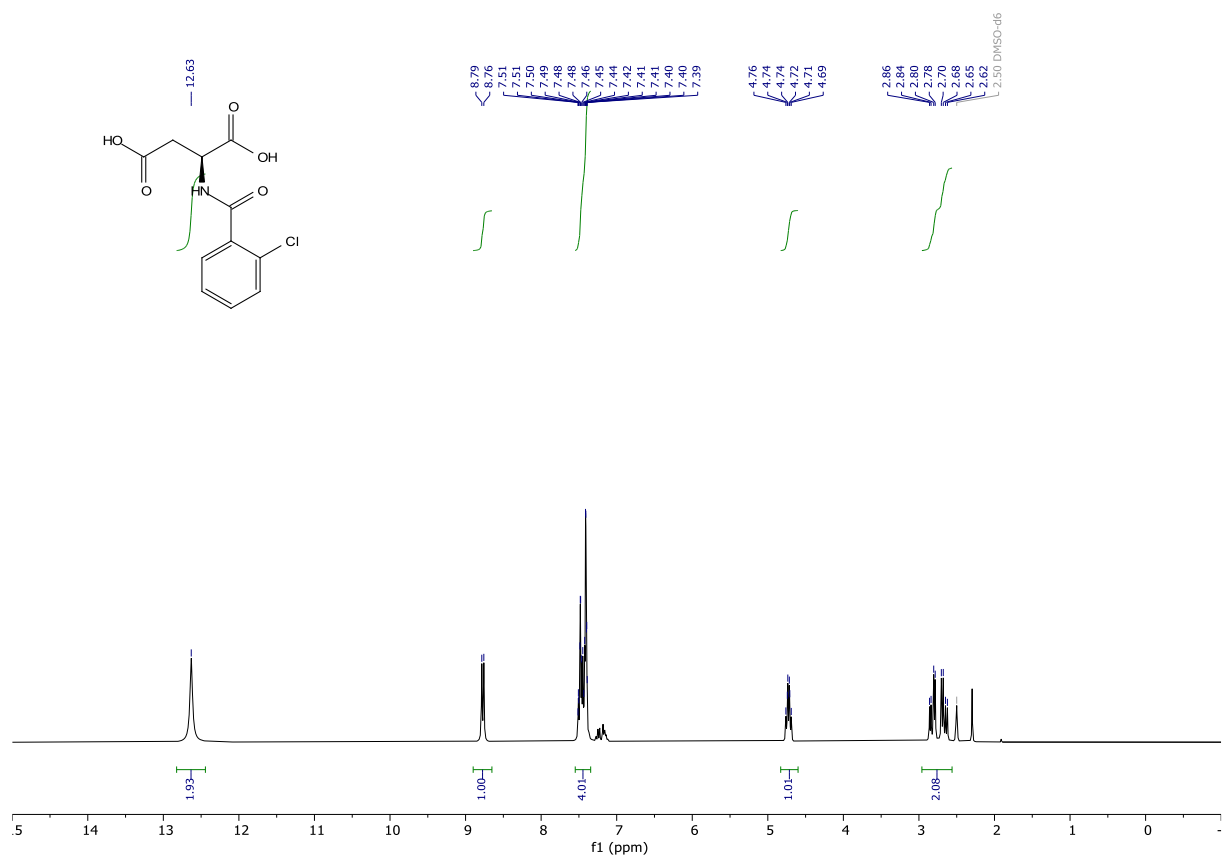
benzoyl-L-aspartic acid (PGUB14). Prepared according to general procedure I, starting from aspartic acid (0.505 g, 3.7941 mmol) using benzoyl chloride as acyl chloride, to give the desired product in 45% yield (0.40764 g, 1.7185 mmol). White solid: ^1H NMR (300 MHz, DMSO- d_6) δ 12.58 (s, 2H), 8.74 (d, J = 7.9 Hz, 1H), 7.90 – 7.80 (m, 2H), 7.58 – 7.41 (m, 3H), 4.77 (td, J = 7.9, 5.7 Hz, 1H), 2.92 – 2.64 (m, 2H). ^{13}C NMR (75 MHz, DMSO) δ 172.63, 171.87, 166.15, 133.86, 131.52, 128.37, 127.39, 49.43, 35.84. HRMS (ESI) calculated for $[\text{M}+\text{H}]^+$ $\text{C}_{11}\text{H}_{12}\text{NO}_5$ 238.0710, found 238.0713.

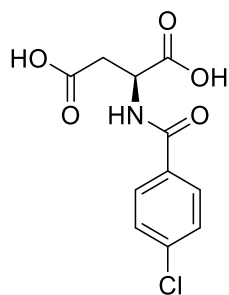




PGUB15

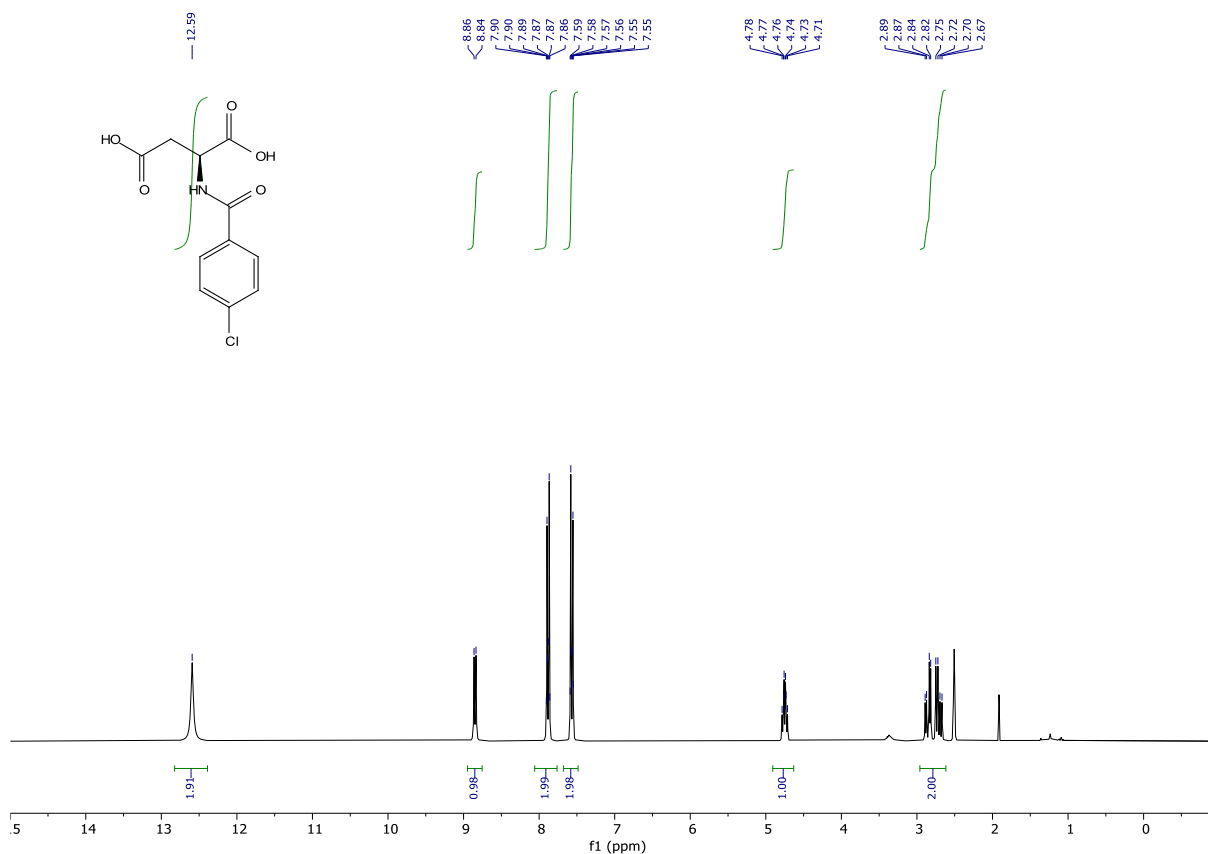
(2-chlorobenzoyl)-L-aspartic acid (PGUB15). Prepared according to general procedure I starting from aspartic acid (0.993 g, 7.4604 mmol) using 2-chlorobenzoyl chloride as acyl chloride, to give the desired product in 87% yield (1.76007 g, 6.4791 mmol). White solid: ¹H NMR (300 MHz, DMSO-*d*₆) δ 12.63 (s, 2H), 8.77 (d, *J* = 8.0 Hz, 1H), 7.55 – 7.34 (m, 4H), 4.73 (td, *J* = 7.7, 5.8 Hz, 1H), 2.96 – 2.56 (m, 2H). ¹³C NMR (75 MHz, DMSO) δ 172.21, 171.70, 166.06, 136.21, 131.08, 130.12, 129.76, 129.11, 127.09, 49.17, 35.87. HRMS (ESI) calculated for [M+H]⁺ C₁₁H₁₁NO₅Cl 272.0320, found 272.0312.

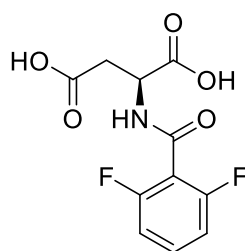
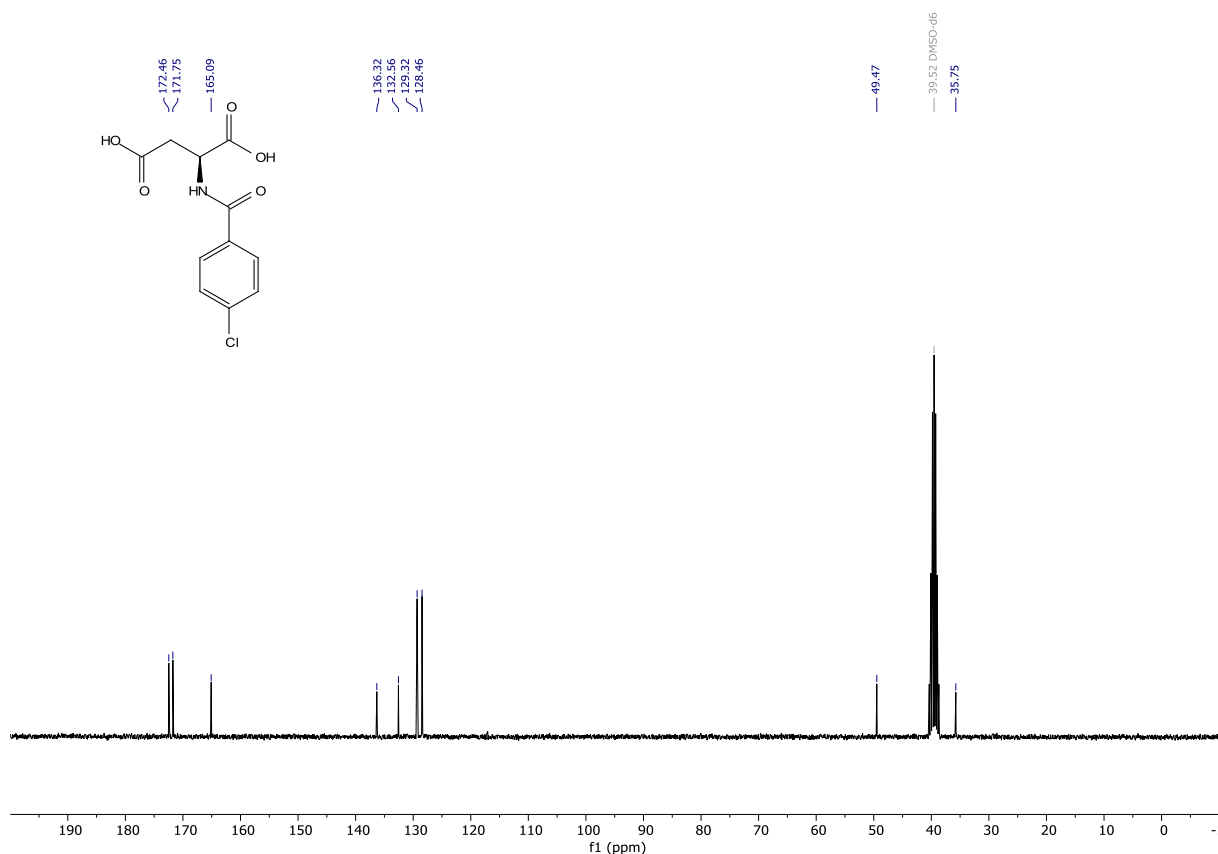




PGUB16

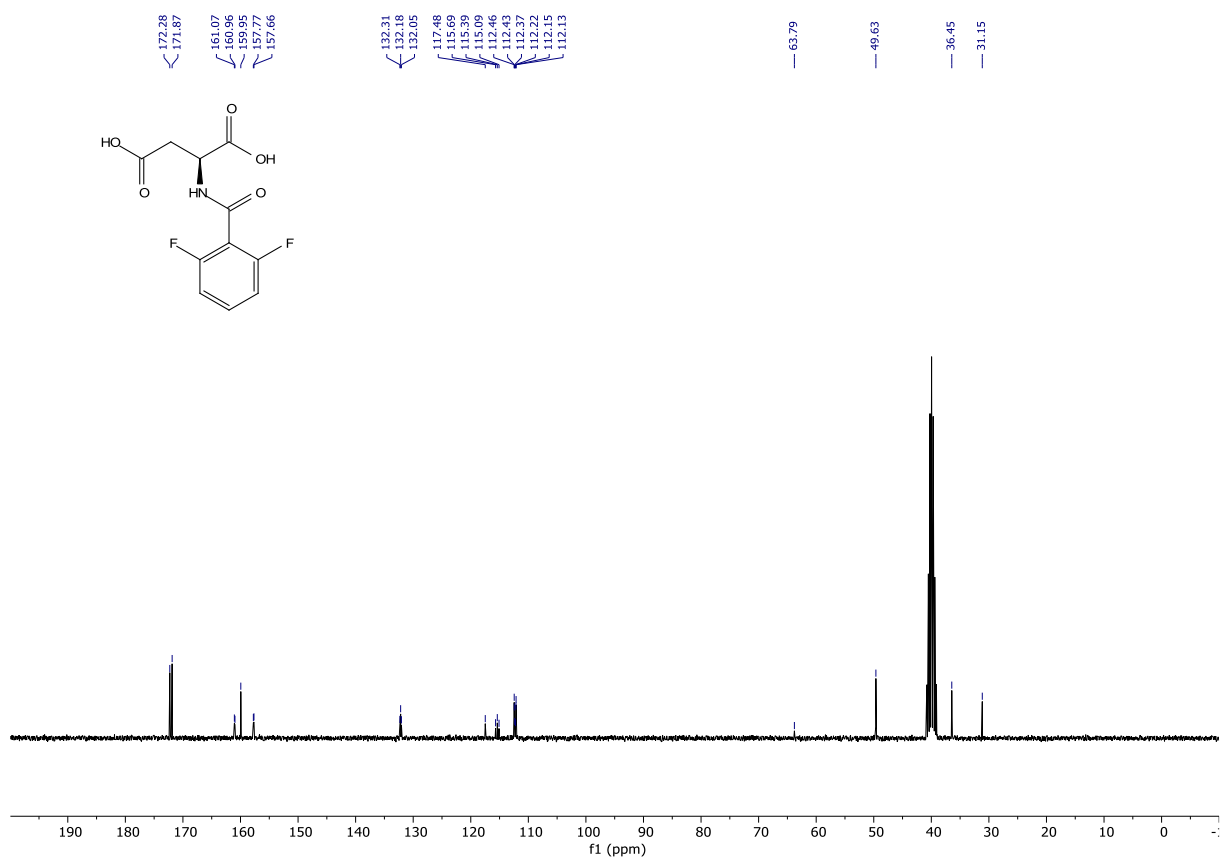
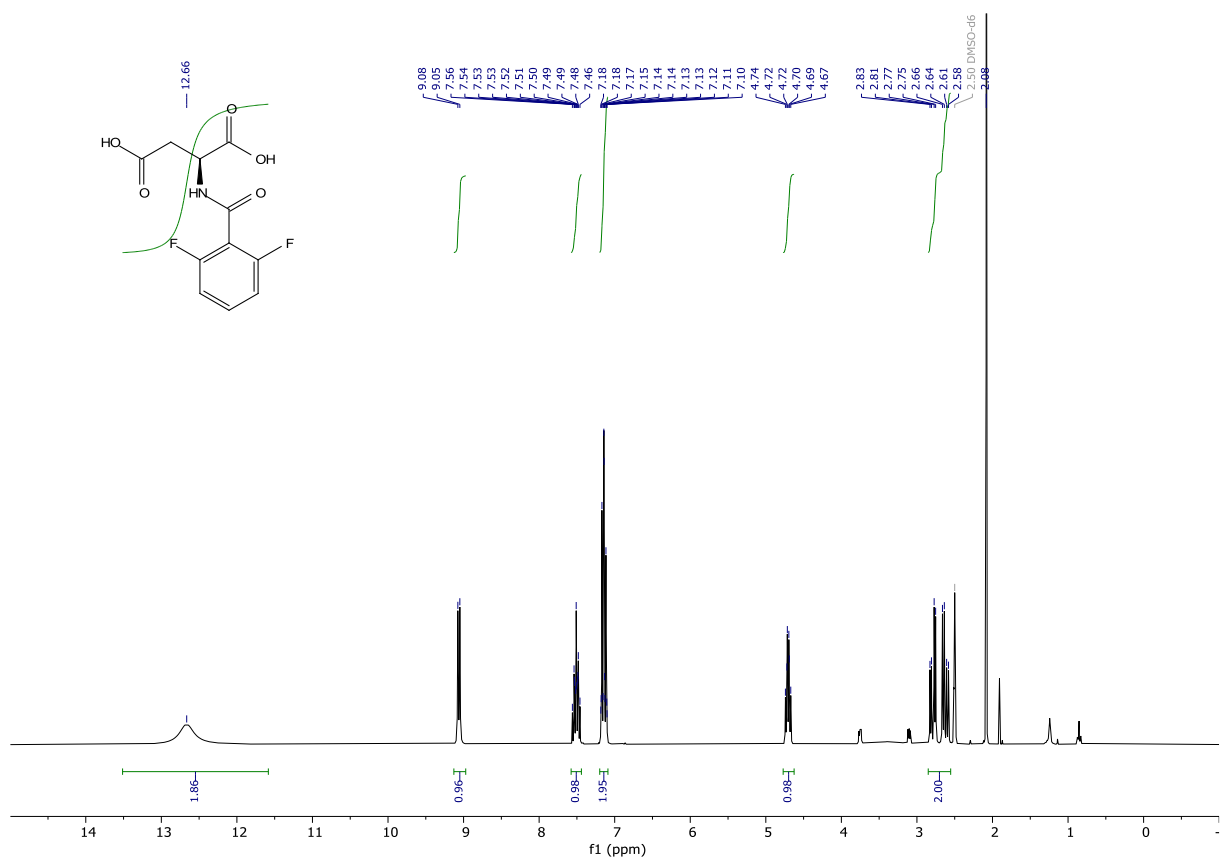
(4-chlorobenzoyl)-L-aspartic acid (PGUB16). Prepared according to general procedure I starting from aspartic acid (0.505 g, 3.7941 mmol) using 4-chlorobenzoyl chloride as acyl chloride, to give the desired product in 73% yield (0.75640 g, 2.7844 mmol). White solid: ^1H NMR (300 MHz, DMSO- d_6) δ 12.59 (s, 2H), 8.85 (d, J = 7.8 Hz, 1H), 8.06 – 7.76 (m, 2H), 7.68 – 7.48 (m, 2H), 4.75 (td, J = 8.0, 5.6 Hz, 1H), 2.96 – 2.62 (m, 2H). ^{13}C NMR (75 MHz, DMSO) δ 172.46, 171.75, 165.09, 136.32, 132.56, 129.32, 128.46, 49.47, 35.75. HRMS (ESI) calculated for $[\text{M}+\text{H}]^+$ $\text{C}_{11}\text{H}_{11}\text{NO}_5\text{Cl}$ 272.0320, found 272.0325.

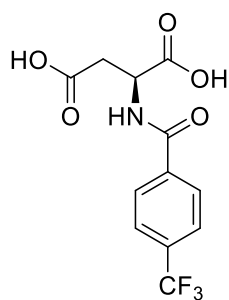
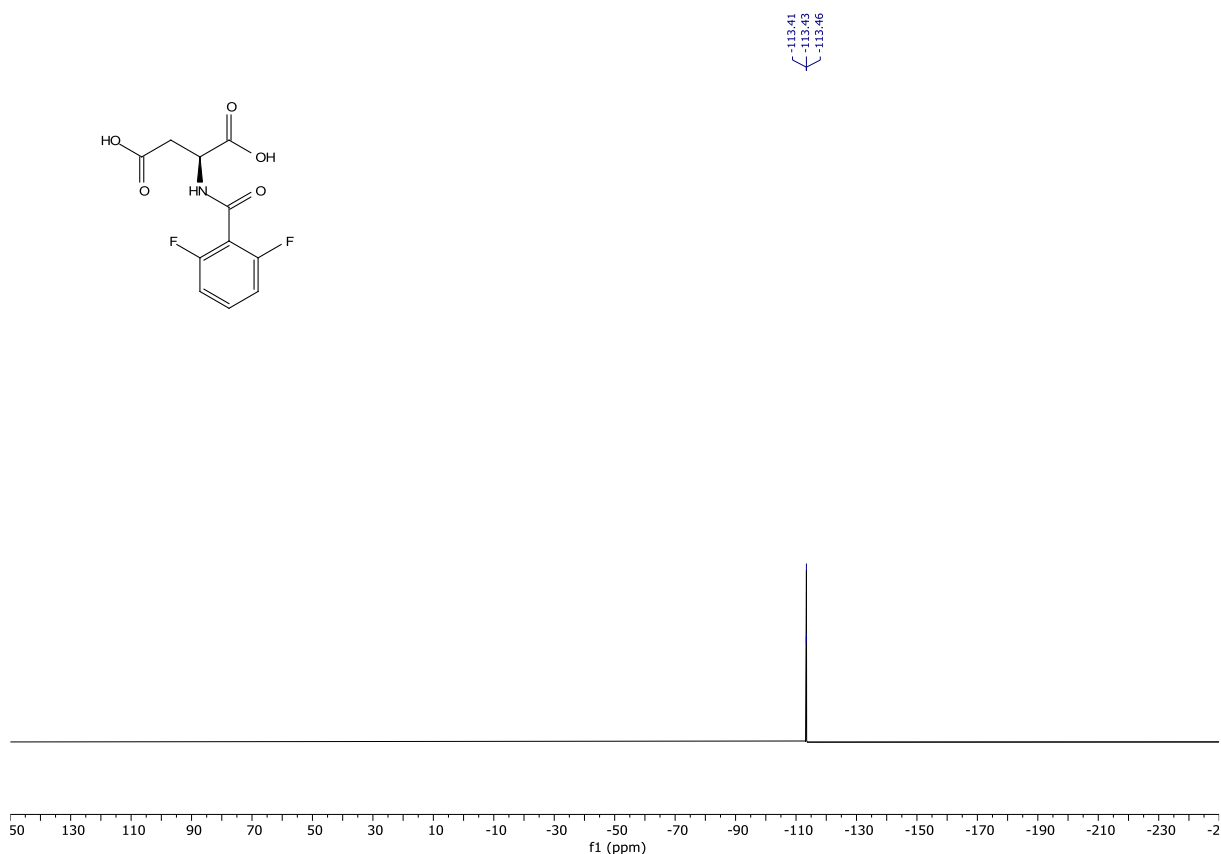




PGUB17

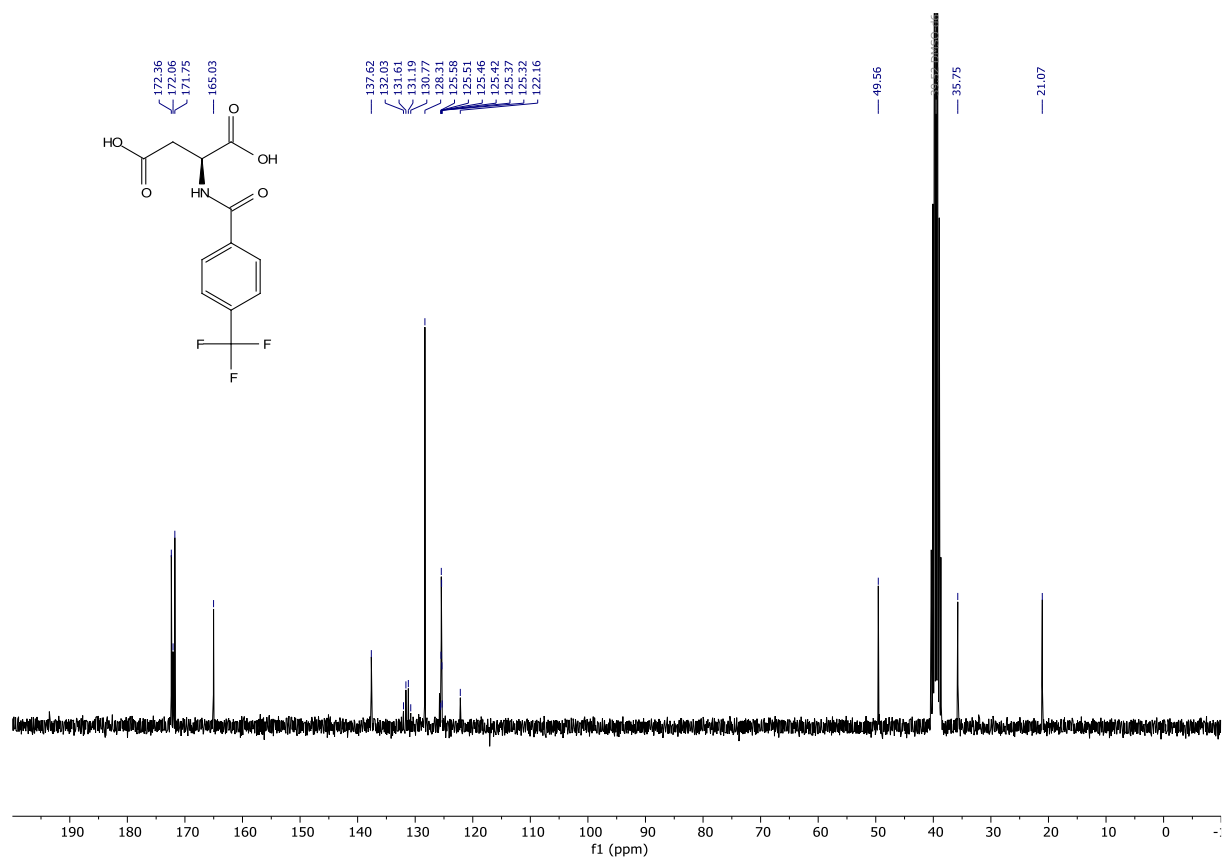
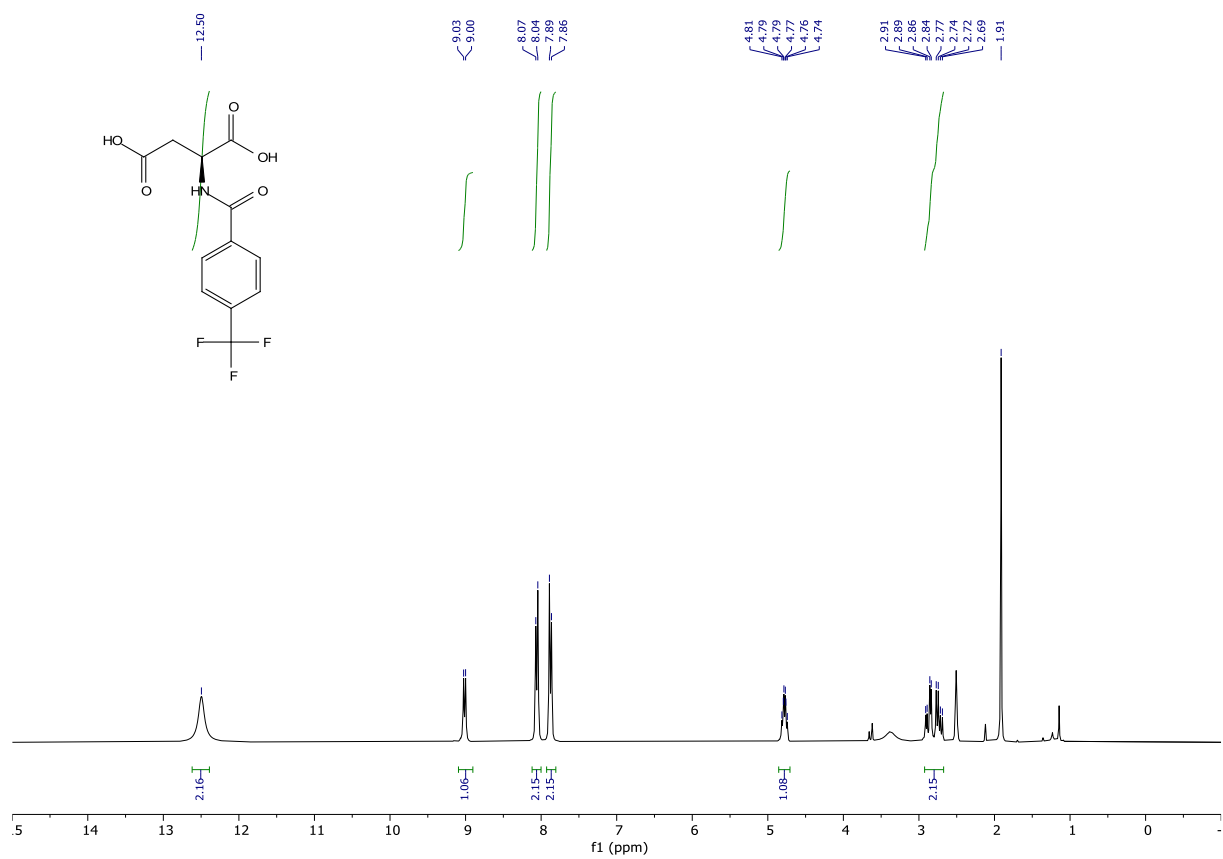
(2,6-difluorobenzoyl)-L-aspartic acid (PGUB17). Prepared according to general procedure I starting from aspartic acid (0.659 g, 4.9511 mmol) using 2,6 difluorobenzoyl chloride as acyl chloride, to give the desired product in 59% yield (0.80255 g, 2.93768 mmol). White solid, containing some little acetone: $^1\text{H NMR}$ (300 MHz, $\text{DMSO}-d_6$) δ 12.66 (s, 2H), 9.06 (d, $J = 7.9$ Hz, 1H), 7.59 – 7.43 (m, 1H), 7.21 – 7.07 (m, 2H), 4.71 (td, $J = 7.6, 5.9$ Hz, 1H), 2.86 – 2.55 (m, 2H). 2 (75 MHz, DMSO) δ 206.98, 172.28, 171.87, 161.01 (d, $J = 7.8$ Hz), 159.95, 157.71 (d, $J = 8.0$ Hz), 132.18 (t, $J = 9.9$ Hz), 117.48, 115.39 (t, $J = 22.7$ Hz), 112.96 – 111.62 (m), 63.79, 49.63, 36.45, 31.15. $^{19}\text{F NMR}$ (282 MHz, $\text{DMSO}-d_6$) δ -113.43 (t, $J = 7.1$ Hz). **HRMS** (ESI) calculated for $[\text{M}+\text{H}]^+$ $\text{C}_{11}\text{H}_{10}\text{NO}_5\text{F}_2$ 274.0522, found 274.0520.

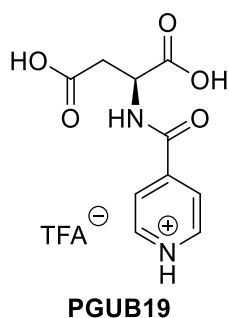




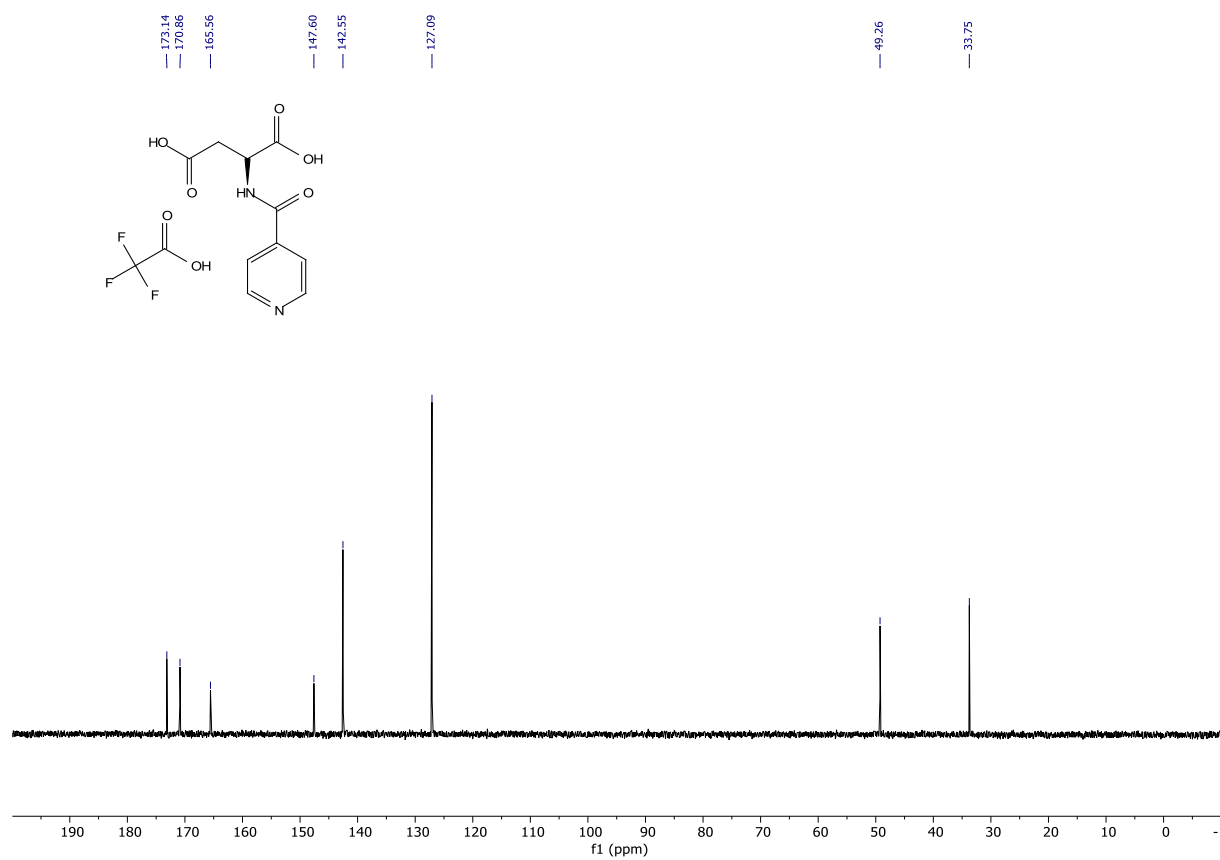
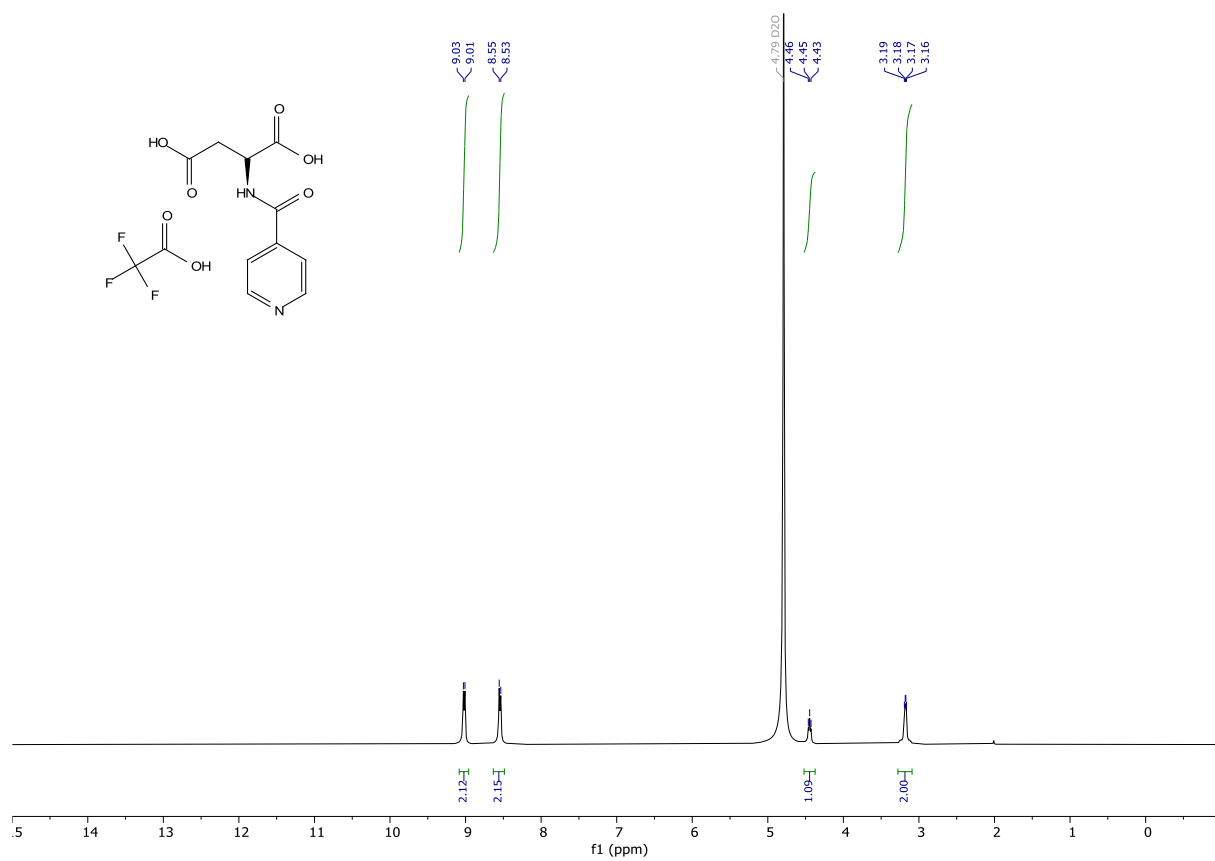
PGUB18

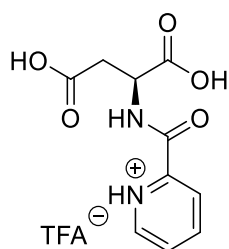
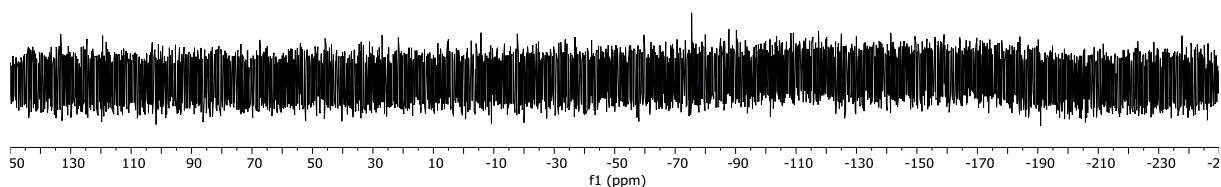
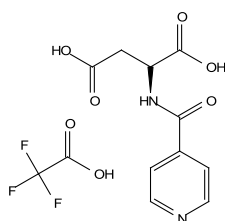
(4-trifluoromethylbenzoyl)-L-aspartic acid (PGUB18). Prepared according to general procedure I starting from aspartic acid (0.502 g, 3.7715 mmol) using 4-trifluorobenzoyl chloride as acyl chloride, to give the desired product in 67% yield (0.77318 g, 2.53328 mmol). White solid slightly impure with acetic acid: ¹H NMR (300 MHz, DMSO-d₆) δ 12.50 (s, 2H), 9.01 (d, *J* = 7.8 Hz, 1H), 8.06 (d, *J* = 8.0 Hz, 2H), 7.88 (d, *J* = 8.1 Hz, 2H), 4.78 (td, *J* = 7.9, 5.6 Hz, 1H), 3.00 – 2.61 (m, 2H). ¹³C NMR (75 MHz, DMSO) δ 172.36, 172.06, 171.75, 165.03, 137.62, 131.40 (q, *J* = 31.6 Hz), 128.31, 125.58, 125.44 (h, *J* = 4.2, 3.5 Hz), 122.16, 49.56, 35.75, 21.07. ¹⁹F NMR (282 MHz, DMSO) δ -61.36. HRMS (ESI) calculated for [M+H]⁺ C₁₂H₁₁NO₅F₃ 306.0584, found 306.0587.





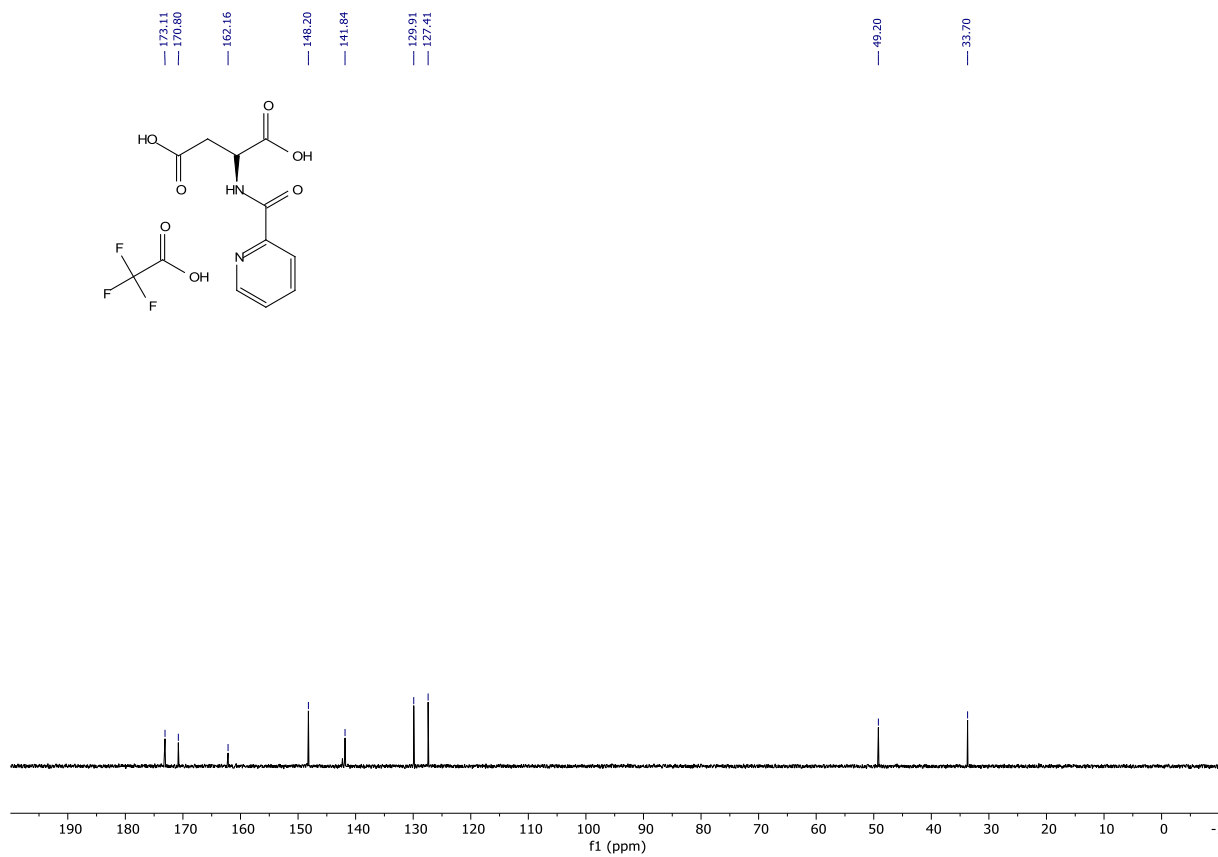
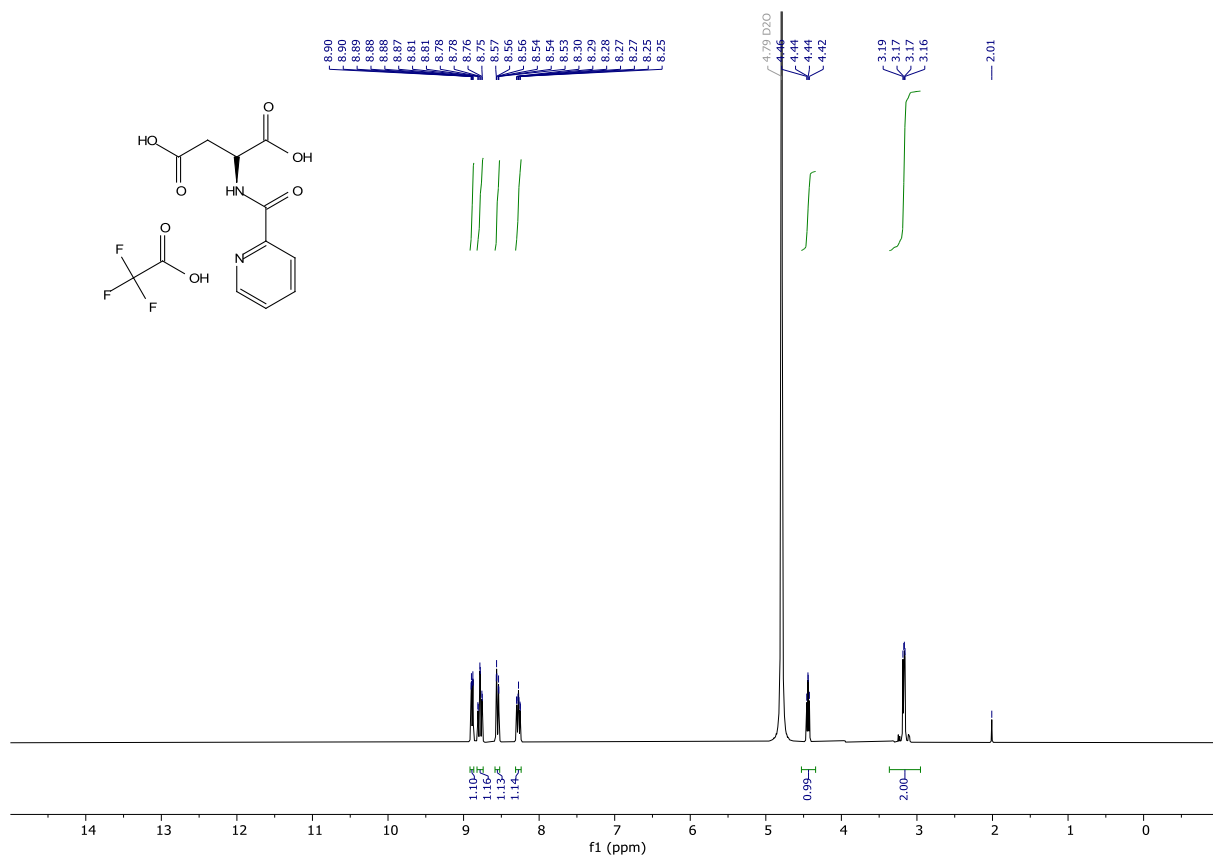
isonicotinoyl-L-aspartic acid trifluoroacetate salt (PGUB19). Except for the purification, the compound was prepared according to general procedure I starting from aspartic acid (0.744 g, 4.1795 mmol) using isonicotinoyl chloride as acyl chloride. The compound was purified by reverse phase flash column chromatography (water + 0.1% TFA/ acetonitrile + 0.1% TFA gradient from 1:0 to 0:1), to give the desired product in quantitative yield (1.78750 g, 5.07492 mmol). White hygroscopic solid: ^1H NMR (300 MHz, Deuterium Oxide) δ 9.02 (d, J = 6.2 Hz, 2H), 8.54 (d, J = 6.2 Hz, 2H), 4.45 (t, J = 5.3 Hz, 1H), 3.18 (dd, J = 5.4, 2.9 Hz, 2H). ^{13}C NMR (75 MHz, $\text{D}_2\text{O}_{\text{salt}}$) δ 173.14, 170.86, 165.56, 147.60, 142.55, 127.09, 49.26, 33.75. ^{19}F NMR (282 MHz, $\text{D}_2\text{O}_{\text{salt}}$) δ -77.39. HRMS (ESI) calculated for $[\text{M}+\text{H}-\text{TFA}]^+$ $\text{C}_{10}\text{H}_{11}\text{N}_2\text{O}_5$ 239.0662, found 239.0659.

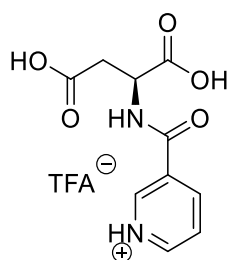
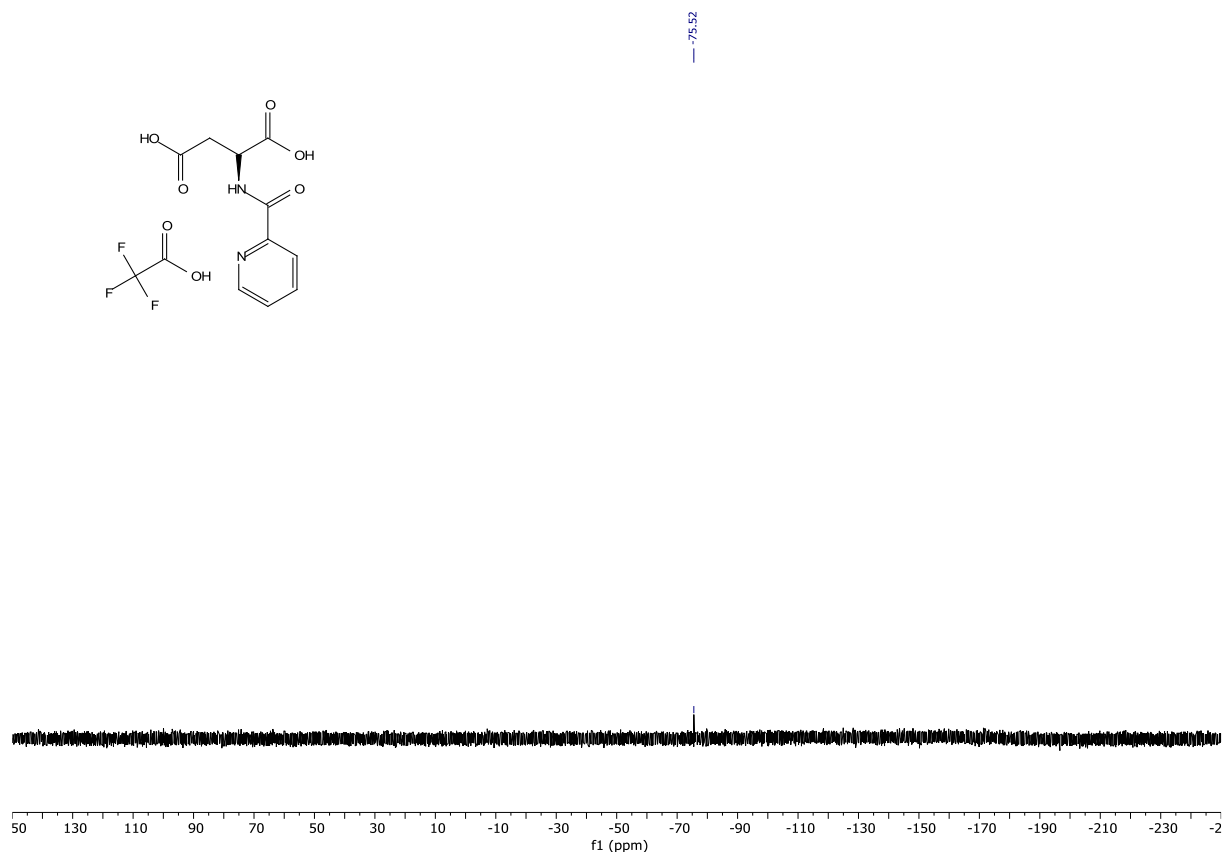




PGUB20

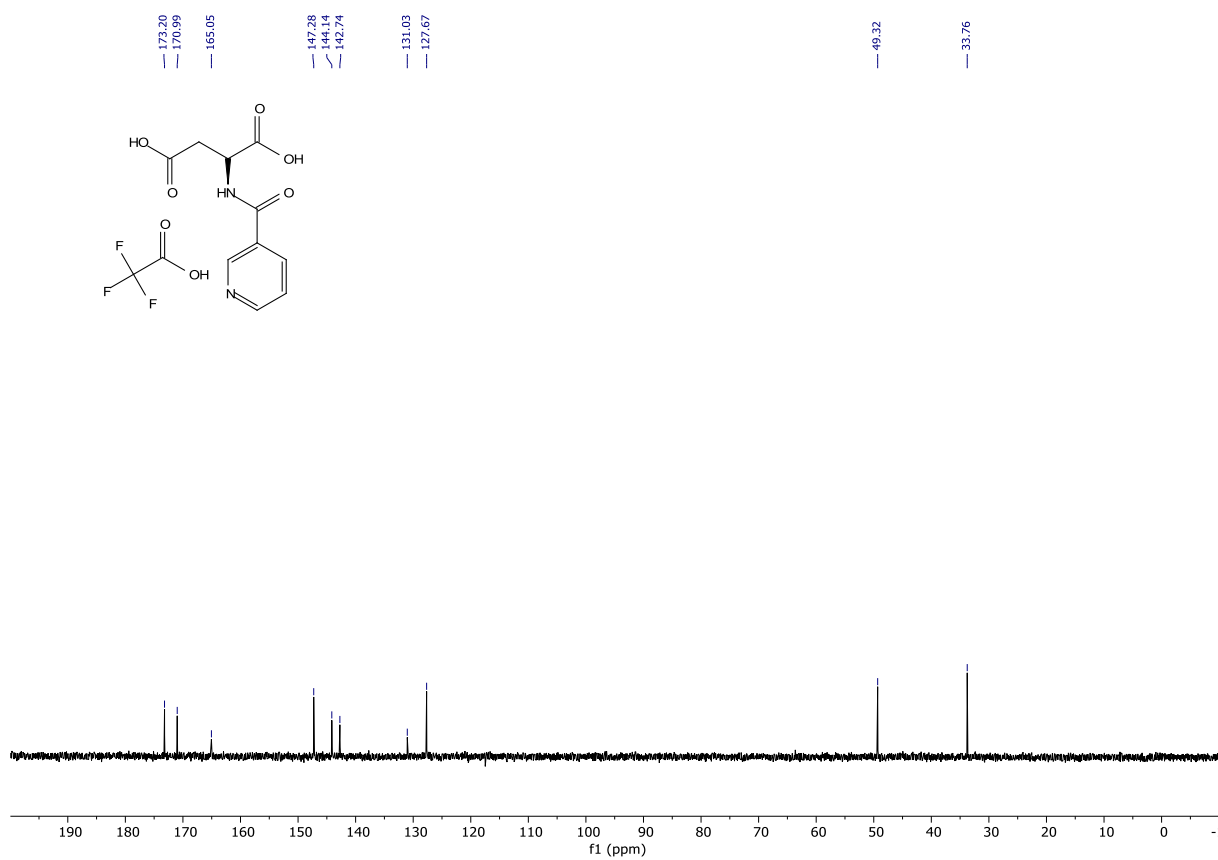
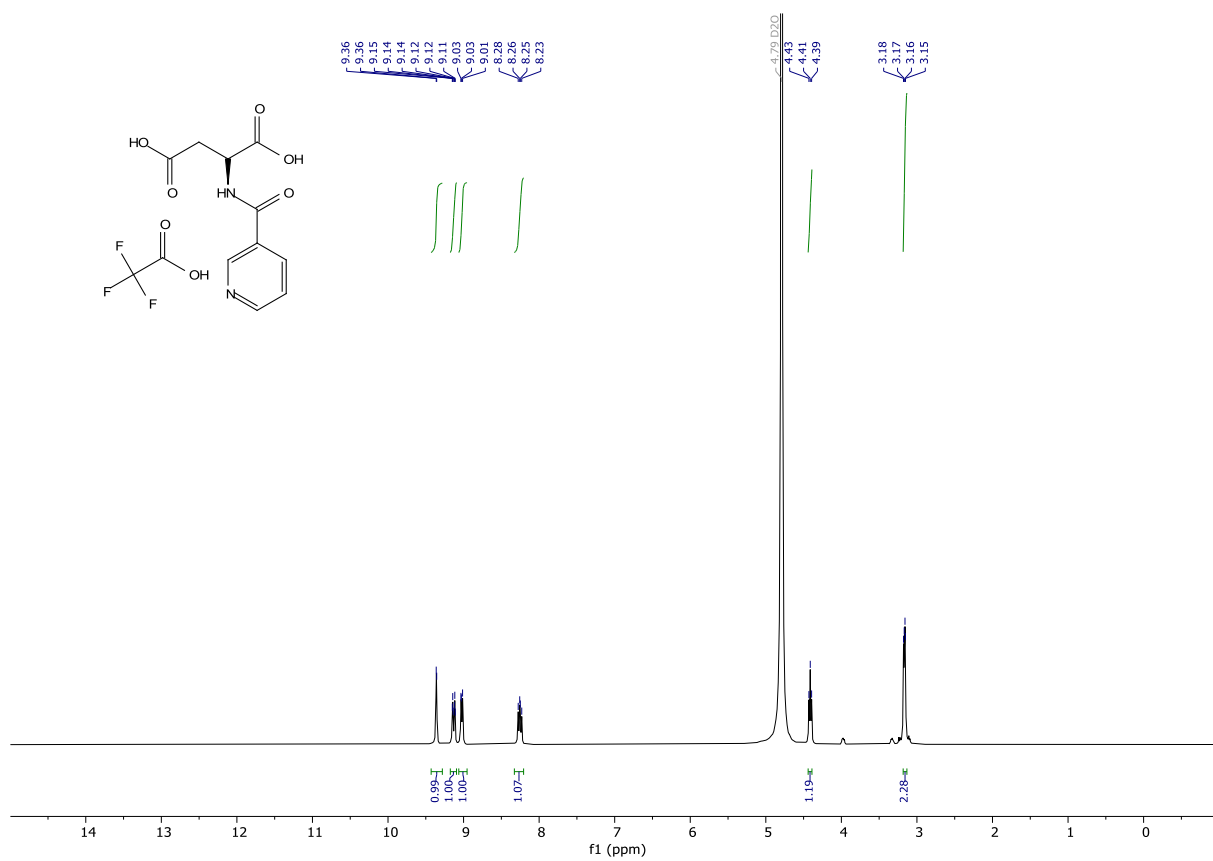
picolinoyl-L-aspartic acid trifluoroacetate salt (PGUB20). Except for the purification, the compound was prepared according to general procedure I starting from aspartic acid (0.500 g, 3.7565 mmol) using picolinoyl chloride as acyl chloride. The compound was purified by reverse phase flash column chromatography (water + 0.1% TFA/ acetonitrile + 0.1% TFA gradient from 1:0 to 0:1), to give the desired product in quantitative yield (1.32312 g, 5.10939 mmol). White hygroscopic solid: **¹H NMR** (300 MHz, Deuterium Oxide) δ 8.91 – 8.86 (m, 1H), 8.78 (td, J = 7.9, 1.5 Hz, 1H), 8.58 – 8.52 (m, 1H), 8.27 (ddd, J = 7.4, 5.8, 1.4 Hz, 1H), 4.44 (dd, J = 5.8, 4.8 Hz, 1H), 3.17 (dd, J = 5.3, 3.1 Hz, 2H). **¹³C NMR** (75 MHz, D₂O_{salt}) δ 173.11, 170.80, 162.16, 148.20, 141.84, 129.91, 127.41, 49.20, 33.70. **¹⁹F NMR** (282 MHz, D₂O_{salt}) δ -75.52. **HRMS** (ESI) calculated for [M+H-TFA]⁺ C₁₀H₁₁N₂O₅ 239.0662, desired mass was not found.

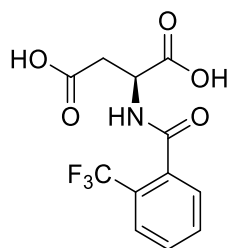




PGUB21

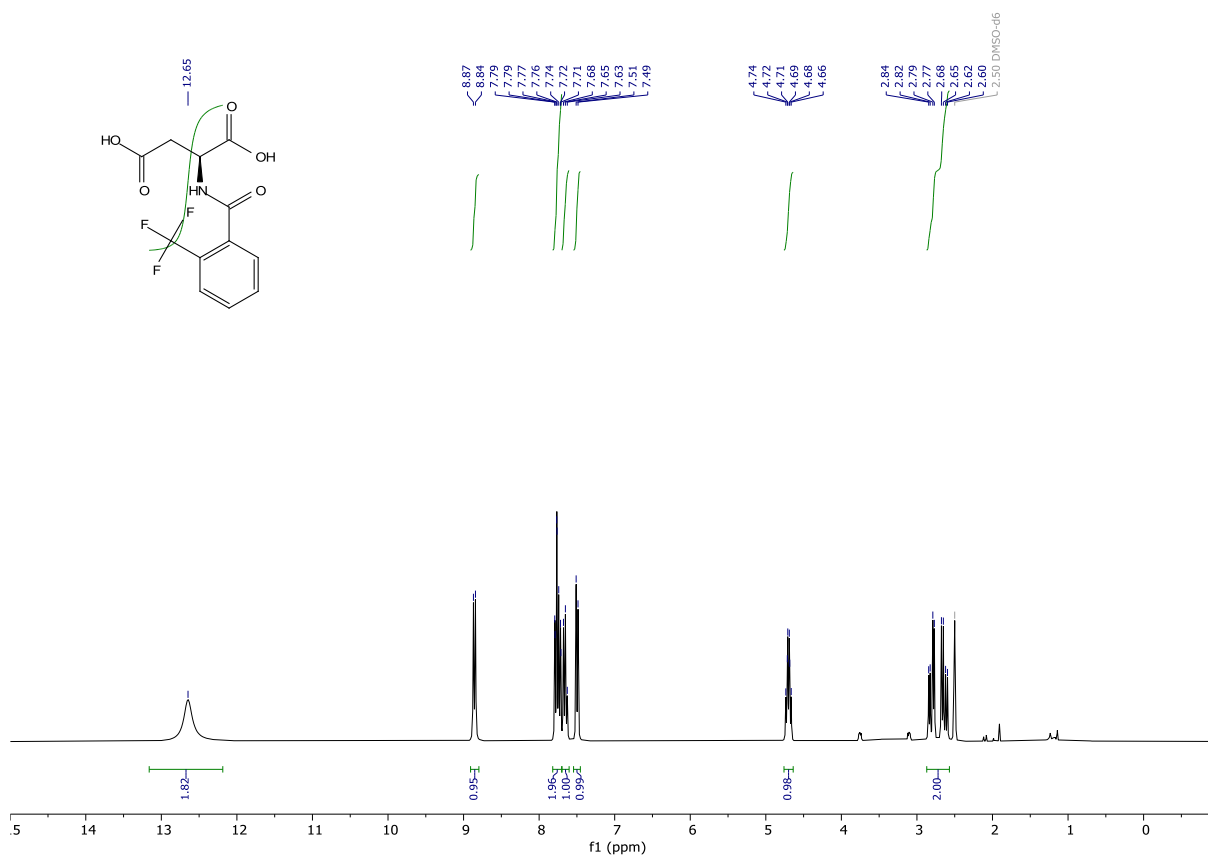
nicotinoyl-L-aspartic acid trifluoroacetate salt (PGUB21). Except for the purification, the compound was prepared according to general procedure I starting from aspartic acid (0.522 g, 3.9218 mmol) using nicotinoyl chloride as acyl chloride. The compound was purified by reverse phase flash column chromatography (water + 0.1% TFA/ acetonitrile + 0.1% TFA gradient from 1:0 to 0:1), to give the desired product in 79% yield (1.09089 g, 3.09716 mmol). White hygroscopic solid: ^1H NMR (300 MHz, Deuterium Oxide) δ 9.36 (d, J = 1.9 Hz, 1H), 9.13 (dt, J = 8.1, 1.7 Hz, 1H), 9.06 – 8.95 (m, 1H), 8.25 (dd, J = 8.2, 5.8 Hz, 1H), 4.41 (t, J = 5.3 Hz, 1H), 3.16 (dd, J = 5.4, 2.3 Hz, 2H). ^{13}C NMR (75 MHz, D₂O_salt) δ 173.20, 170.99, 165.05, 147.28, 144.14, 142.74, 131.03, 127.67, 49.32, 33.76. HRMS (ESI) calculated for $[\text{M}+\text{H}-\text{TFA}]^+$ C₁₀H₁₁N₂O₅ 239.0662, found 239.0662.

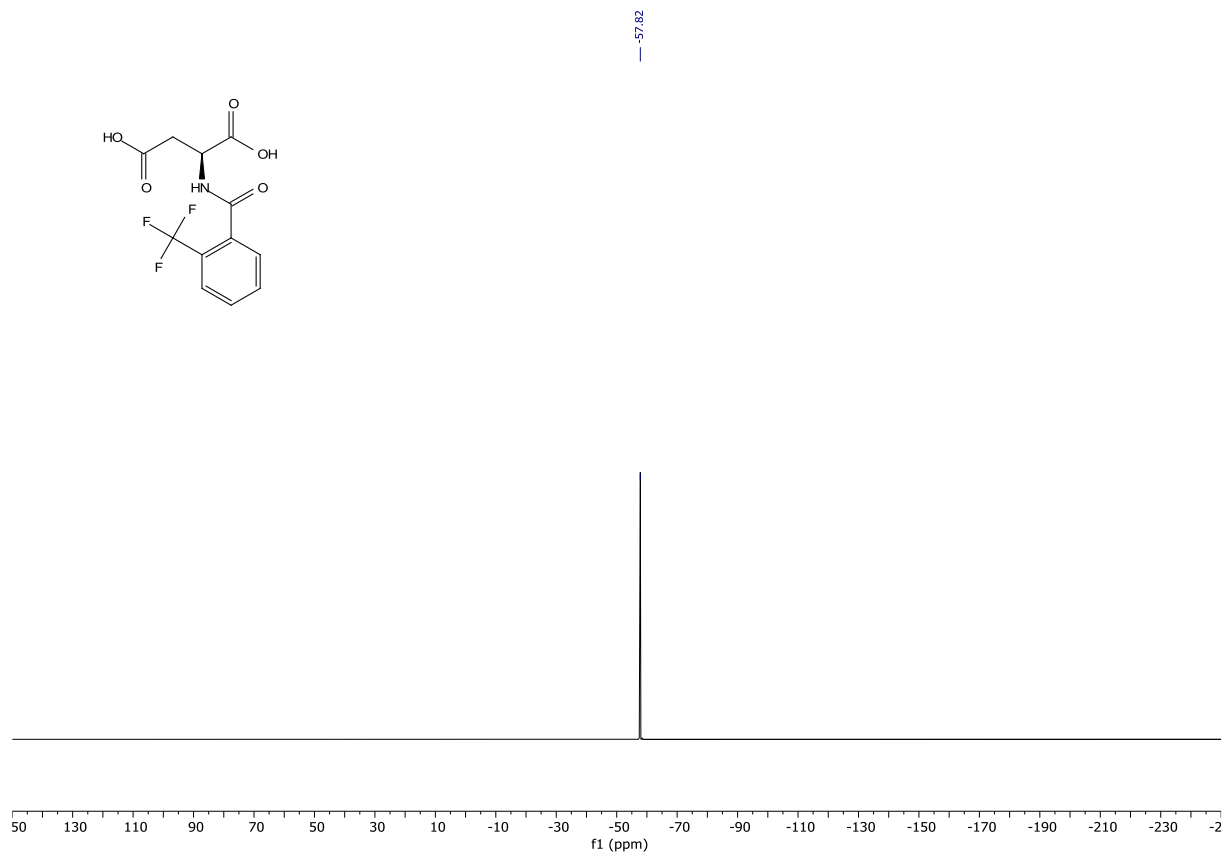
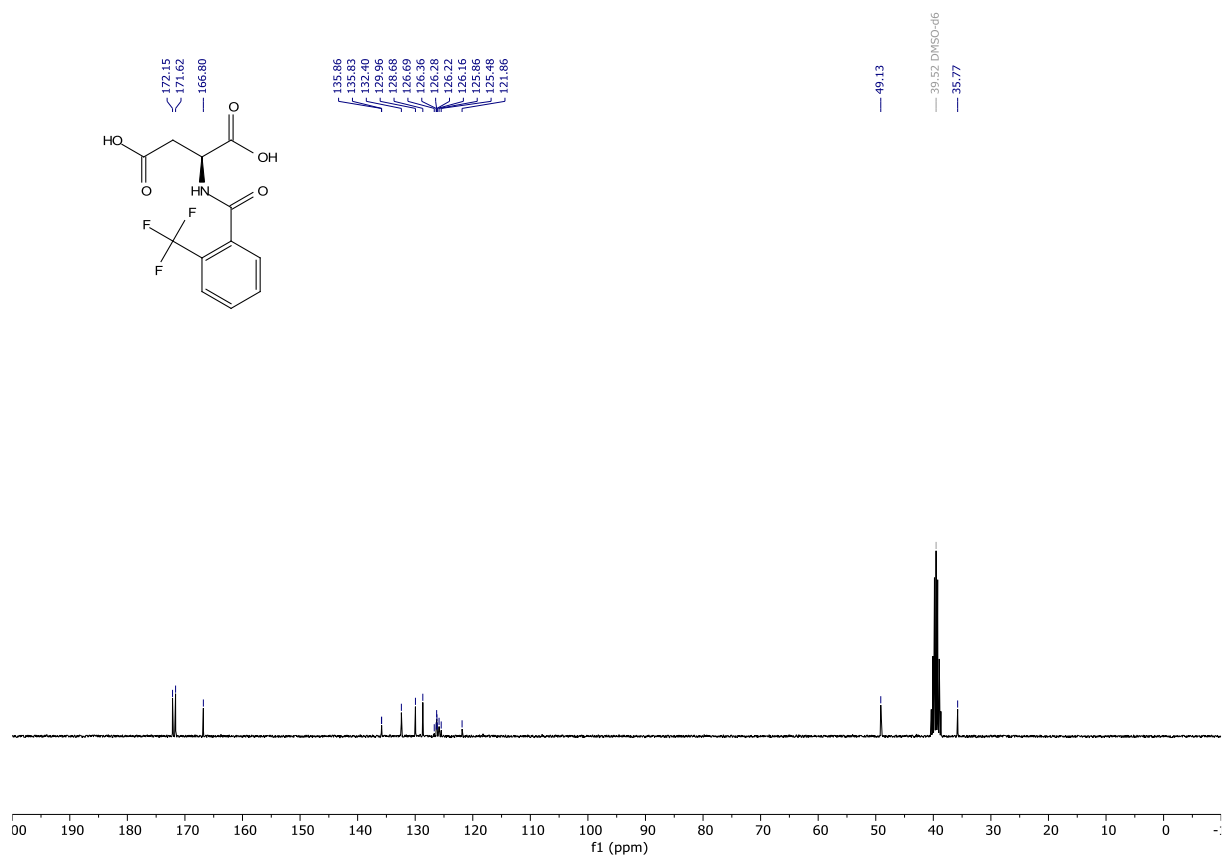


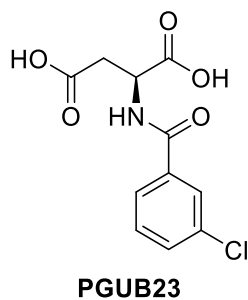


PGUB22

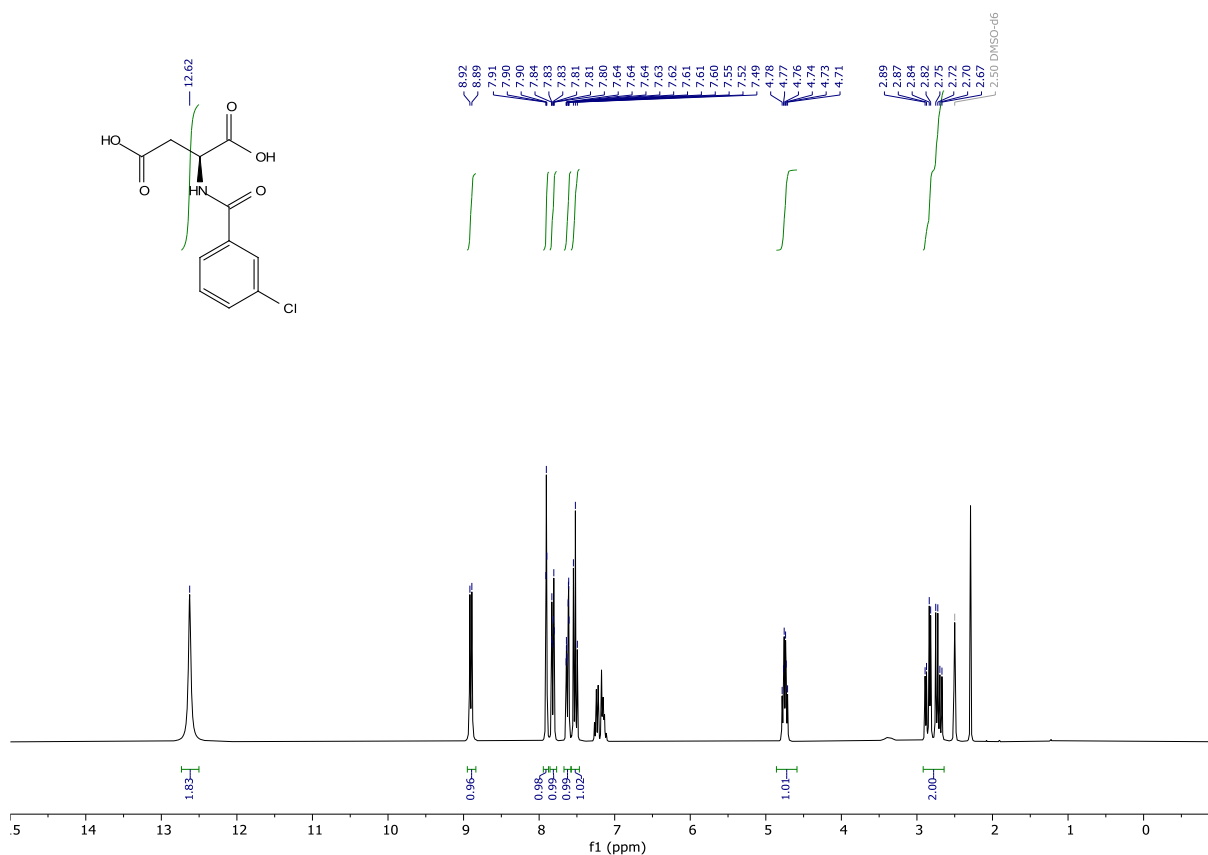
(2-trifluoromethylbenzoyl)-L-aspartic acid (PGUB22). Prepared according to general procedure I starting from aspartic acid (0.490 g, 3.6814 mmol) using 2-trifluoromethylbenzoyl chloride as acyl chloride, to give the desired product in 32% yield (0.36583 g, 1.1986205 mmol). White solid: ^1H NMR (300 MHz, DMSO- d_6) δ 12.65 (s, 2H), 8.86 (d, J = 8.1 Hz, 1H), 7.82 – 7.70 (m, 2H), 7.65 (t, J = 7.6 Hz, 1H), 7.50 (d, J = 7.4 Hz, 1H), 4.70 (td, J = 7.7, 5.9 Hz, 1H), 2.87 – 2.57 (m, 2H). ^{13}C NMR (75 MHz, DMSO) δ 172.15, 171.62, 166.80, 135.86, 135.83, 132.40, 129.96, 128.68, 126.82 – 125.36 (m), 126.25 (q, J = 5.5, 5.0 Hz). 121.86, 49.13, 35.77. ^{19}F NMR (282 MHz, DMSO) δ -57.82. **HRMS** (ESI) calculated for $[\text{M}+\text{H}]^+$ $\text{C}_{12}\text{H}_{11}\text{F}_3\text{NO}_5$ 306.0584, found 306.0581.

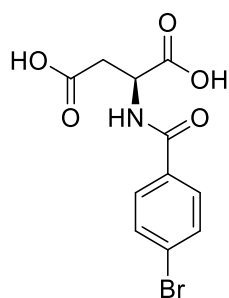
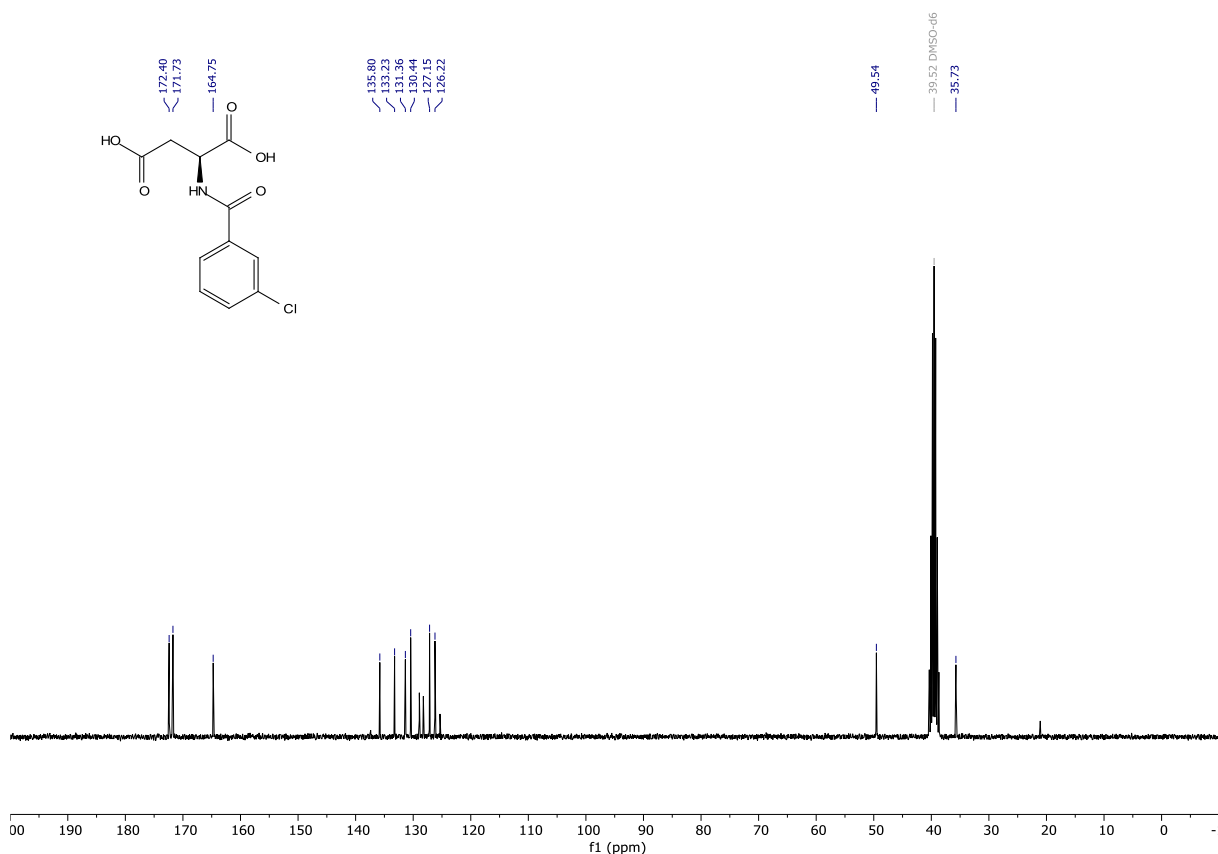






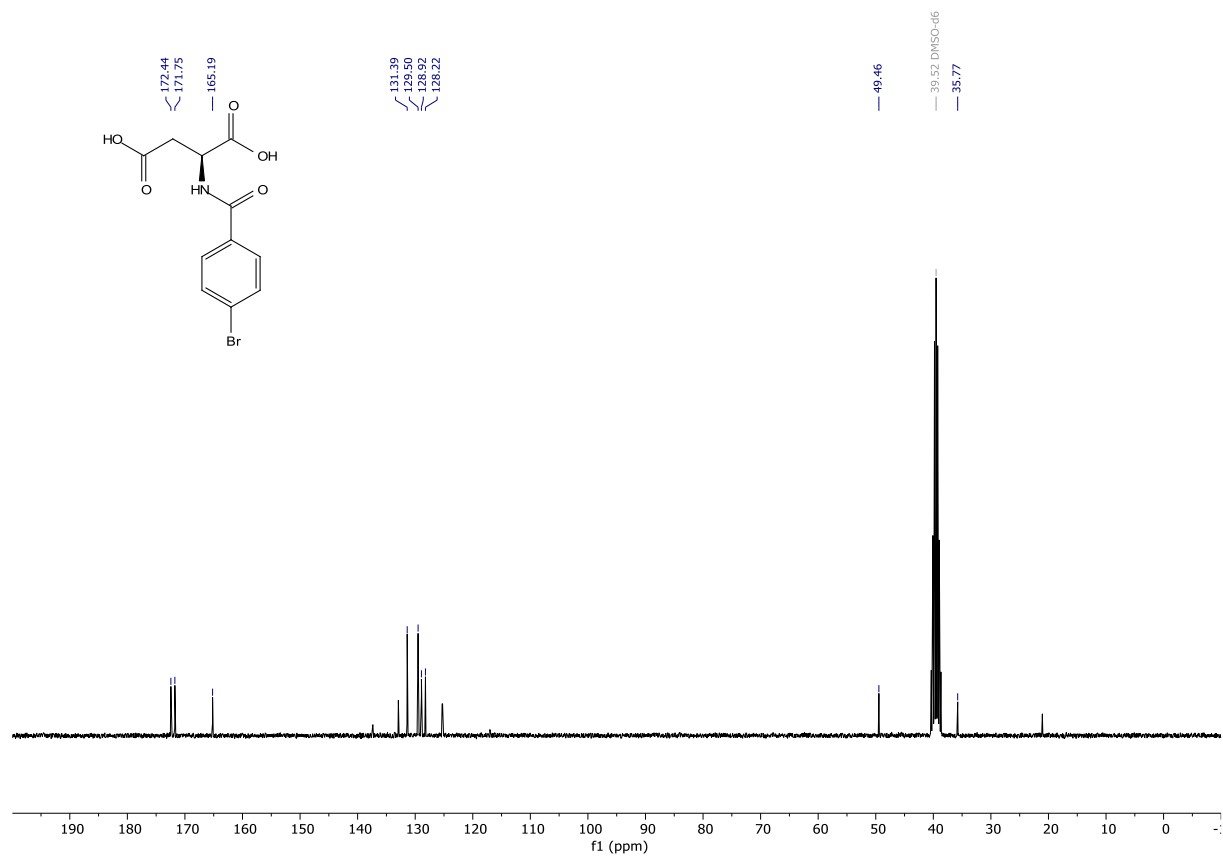
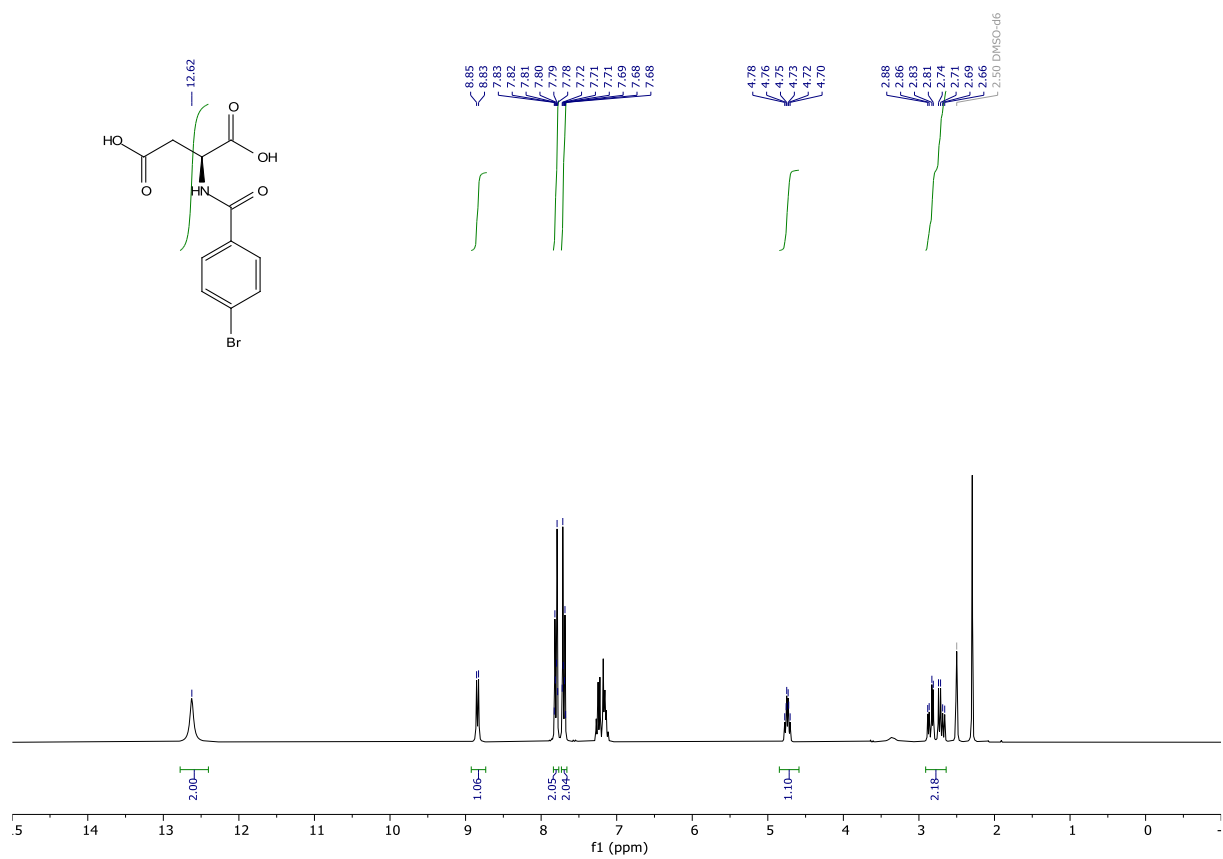
(3-chlorobenzoyl)-L-aspartic acid (PGUB23). Prepared according to general procedure I starting from aspartic acid (1.0070 g, 7.5656 mmol) using 3-chlorobenzoyl chloride as acyl chloride, to give the desired product in 72% yield (1.48086 g, 5.45129 mmol). White solid impure with toluene: ^1H NMR (300 MHz, DMSO- d_6) δ 12.62 (s, 2H), 8.90 (d, J = 7.8 Hz, 1H), 7.90 (t, J = 1.9 Hz, 1H), 7.82 (dt, J = 7.7, 1.4 Hz, 1H), 7.62 (ddd, J = 8.1, 2.2, 1.2 Hz, 1H), 7.52 (t, J = 7.8 Hz, 1H), 4.75 (td, J = 8.0, 5.6 Hz, 1H), 2.92 – 2.64 (m, 2H). ^{13}C NMR (75 MHz, DMSO) δ 172.40, 171.73, 164.75, 135.80, 133.23, 131.36, 130.44, 127.15, 126.22, 49.54, 35.73. HRMS (ESI) calculated for $[\text{M}+\text{H}]^+$ $\text{C}_{11}\text{H}_{11}\text{ClNO}_5$ 272.0320, found 272.0322.

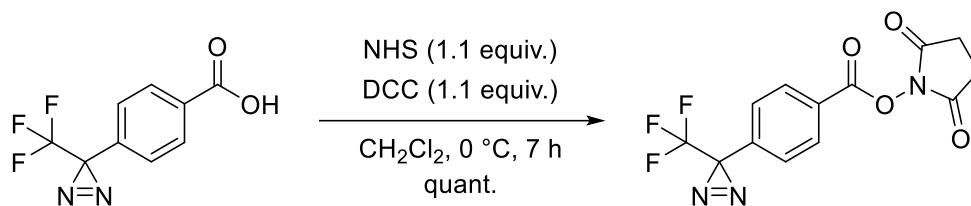




PGUB24

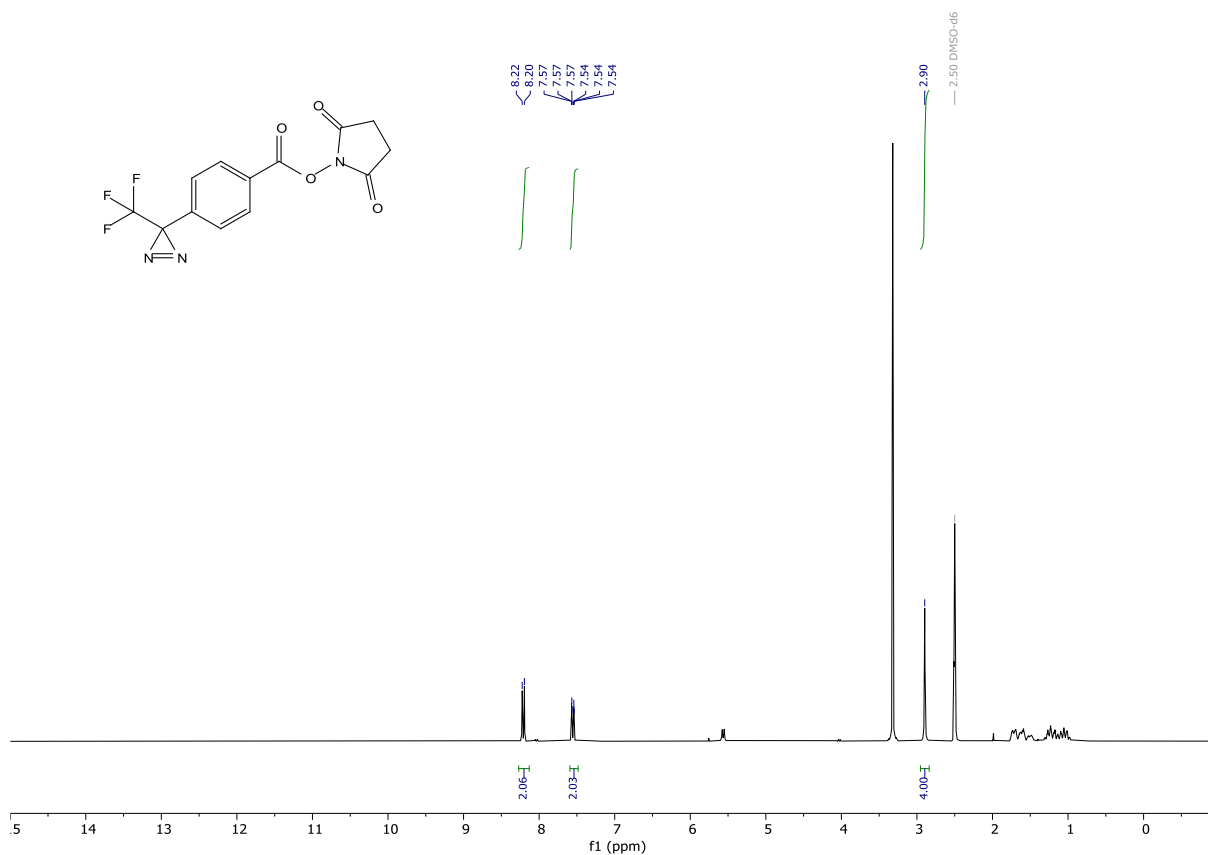
(4-bromobenzoyl)-L-aspartic acid (PGUB24). Prepared according to general procedure I starting from aspartic acid (1.044 g, 7.8435 mmol) using 4-bromobenzoyl chloride as acyl chloride, to give the desired product in 60% yield (1.488007 g, 4.70749 mmol). White solid impure with toluene: $^1\text{H NMR}$ (300 MHz, $\text{DMSO}-d_6$) δ 12.62 (s, 2H), 8.84 (d, $J = 7.8$ Hz, 1H), 7.84 – 7.77 (m, 2H), 7.73 – 7.66 (m, 2H), 4.74 (td, $J = 7.9, 5.6$ Hz, 1H), 2.91 – 2.64 (m, 2H). $^{13}\text{C NMR}$ (75 MHz, DMSO) δ 172.44, 171.75, 165.19, 131.39, 129.50, 128.92, 128.22, 49.46, 35.77. **HRMS** (ESI) calculated for $[\text{M}+\text{H}]^+ \text{C}_{11}\text{H}_{11}\text{BrNO}_5$ 315.9815, found 315.9817.

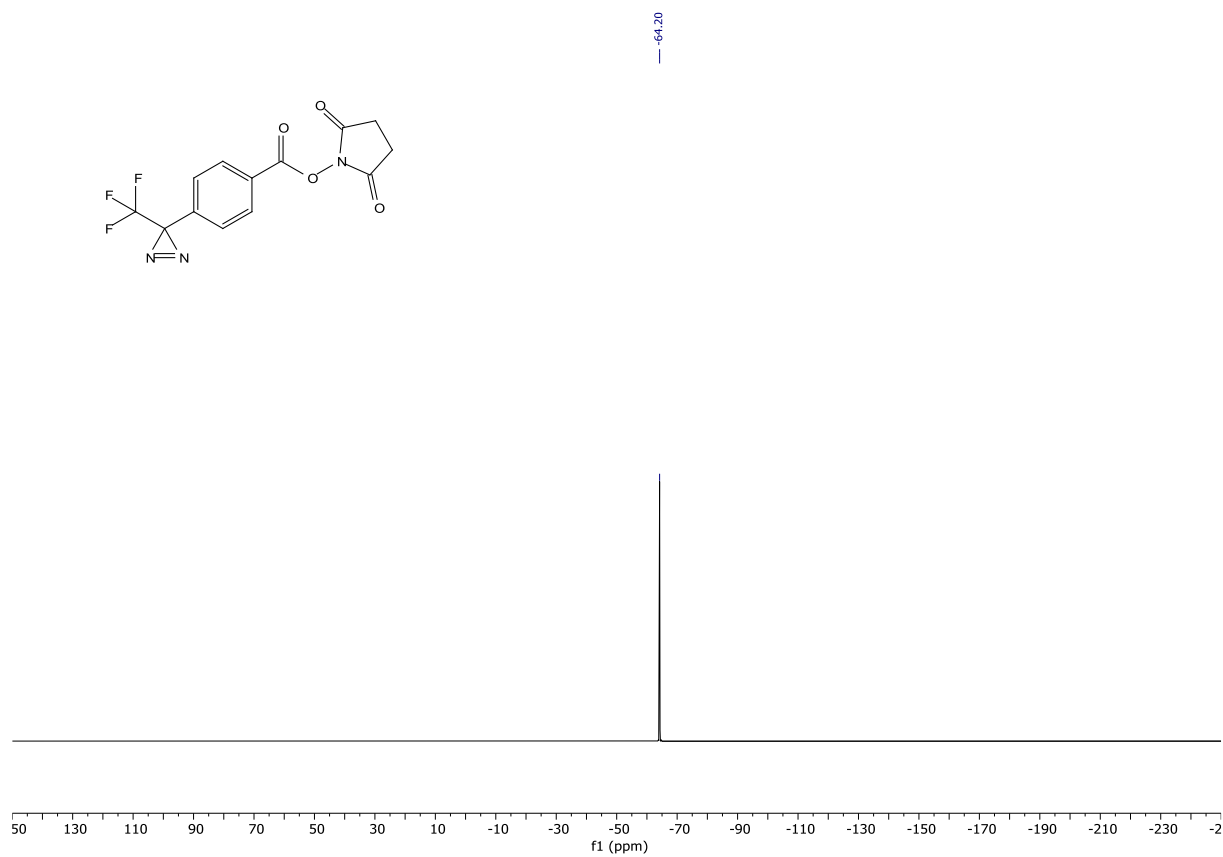
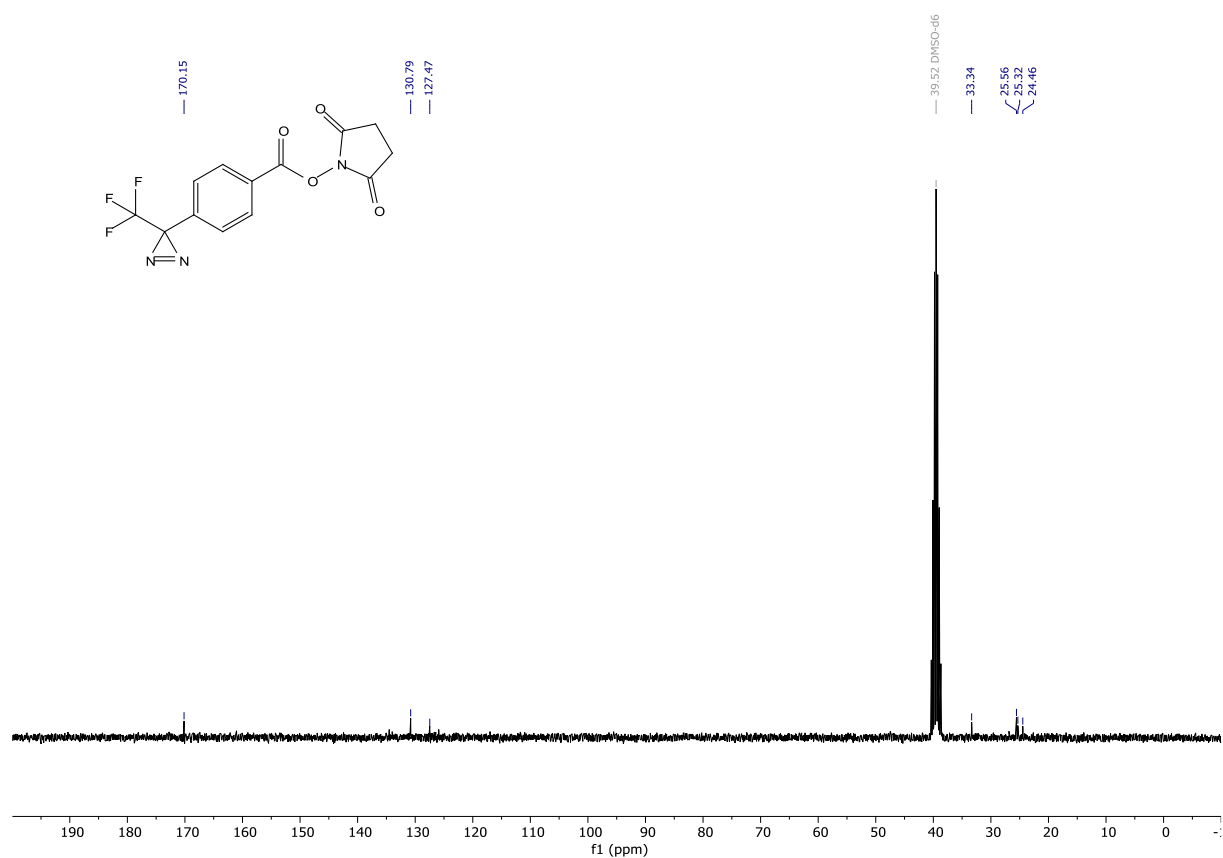


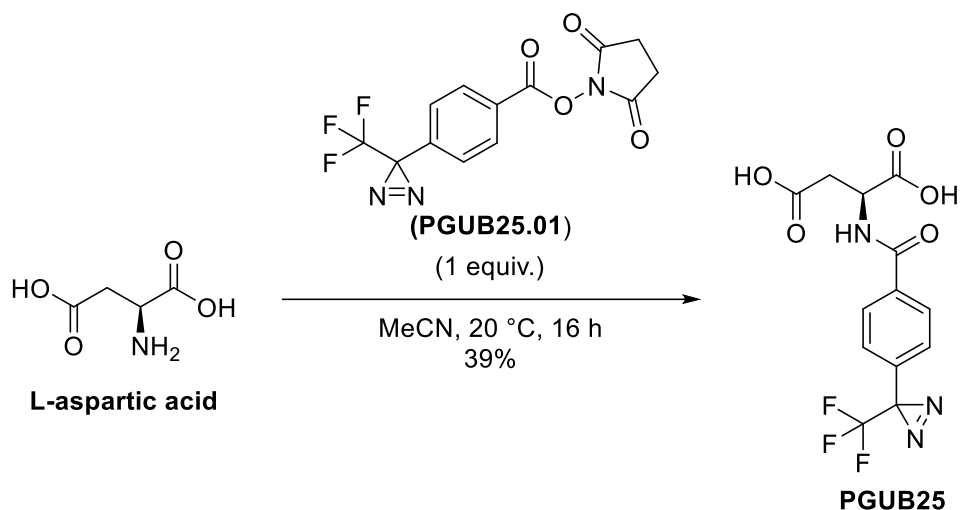


PGUB25.01

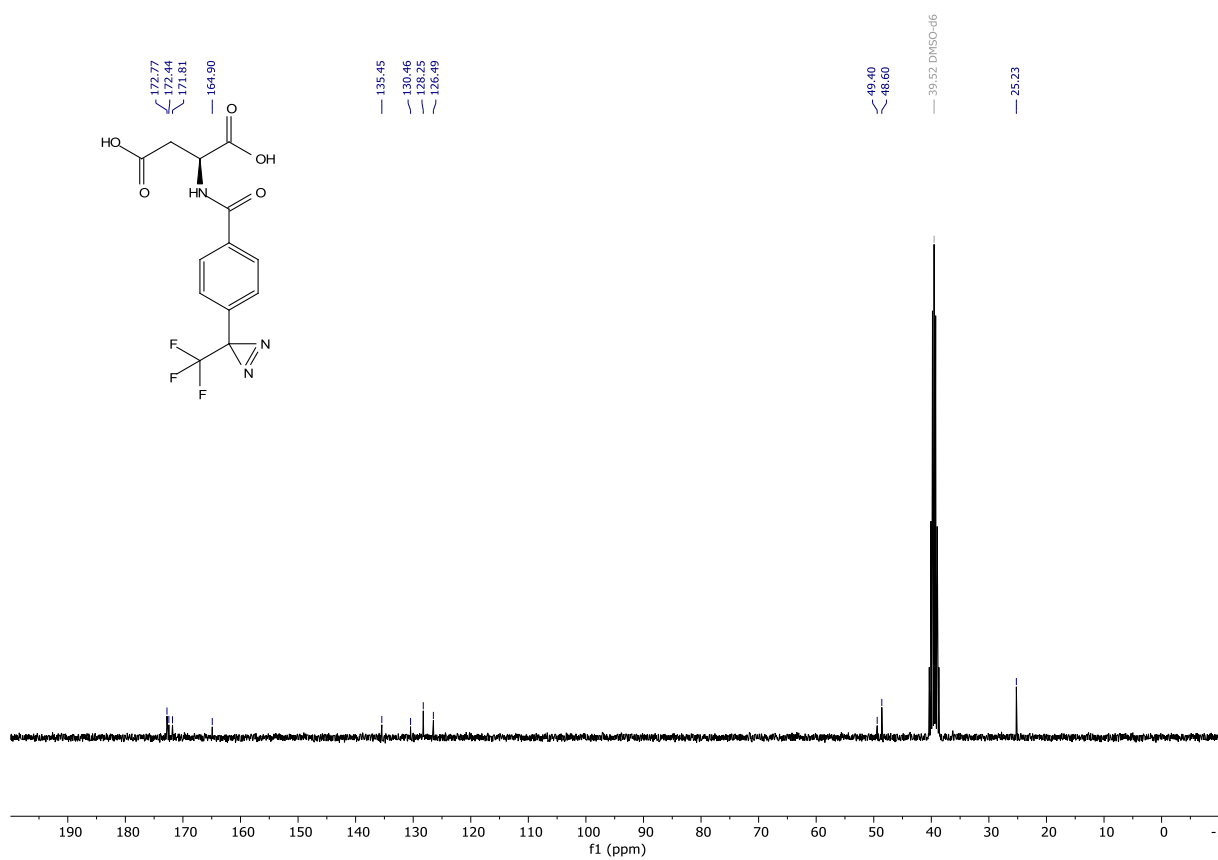
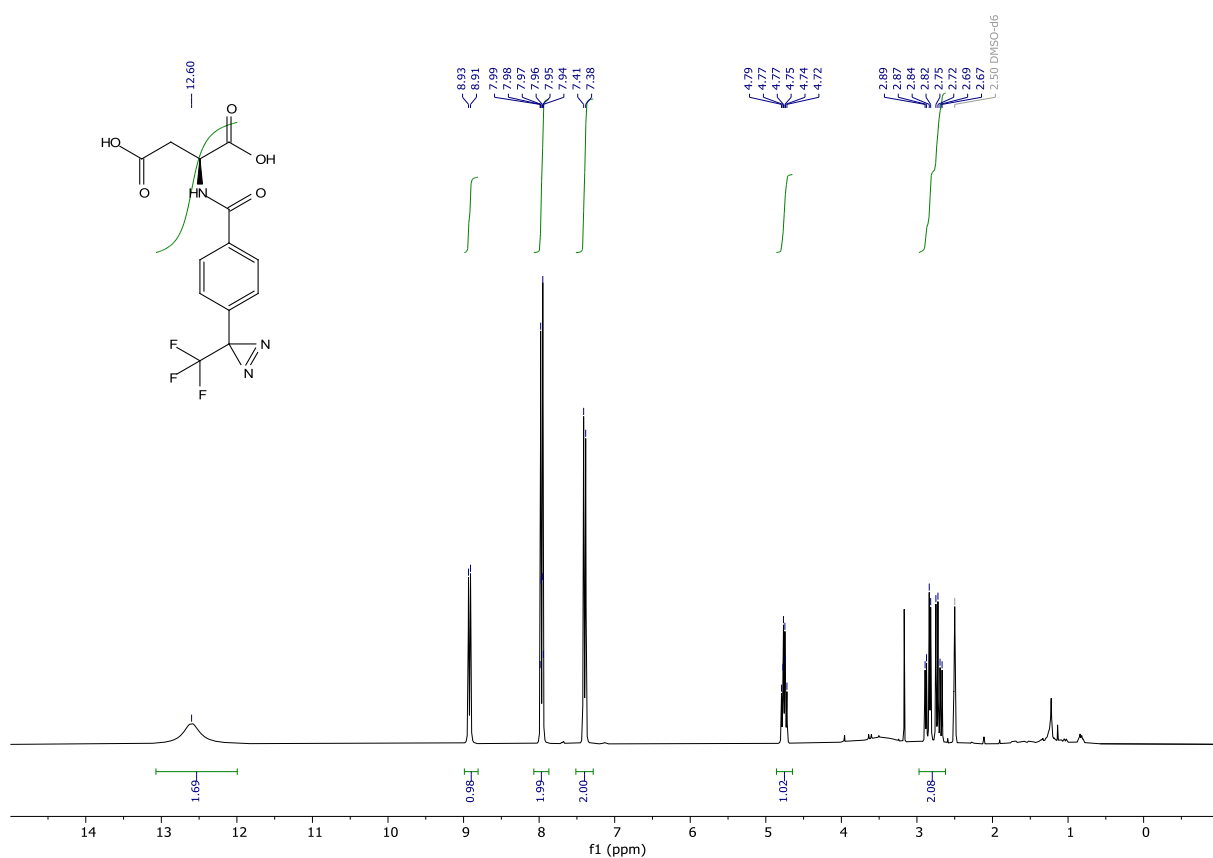
2,5-dioxopyrrolidin-1-yl 4-(3-(trifluoromethyl)-3H-diazirin-3-yl)benzoate (PGUB25.01). To a stirred solution of 4-(3-(trifluoromethyl)-3H-diazirin-3-yl)benzoic acid (0.11214 g, 0.4873 mmol) in dichloromethane (5 mL) at 0 °C was added DCC (0.11146 g, 0.5402 mmol) and NHS (0.06204 g, 0.5391 mmol). The mixture was stirred protected from light. After 7 h reaction time the mixture turned into a white suspension and it was concentrated under reduced pressure onto silica gel. The crude was purified by flash column chromatography (cyclohexane/ ethyl acetate gradient from 1:0 to 1:1), to give the desired compound in quantitative yield (0.15944 g, 0.59367 mmol). White solid impure with *N,N*-dicyclohexylurea. ¹H NMR (300 MHz, DMSO-*d*₆) δ 8.21 (d, *J* = 8.7 Hz, 2H), 7.59 – 7.48 (m, 2H), 2.90 (s, 4H). ¹³C NMR (75 MHz, DMSO) δ 170.15, 130.79, 127.47, 33.34, 25.56, 25.32, 24.46. ¹⁹F NMR (282 MHz, DMSO) δ -64.20.

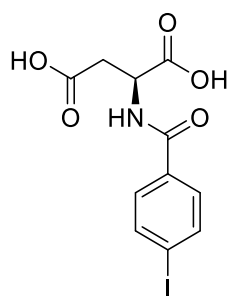






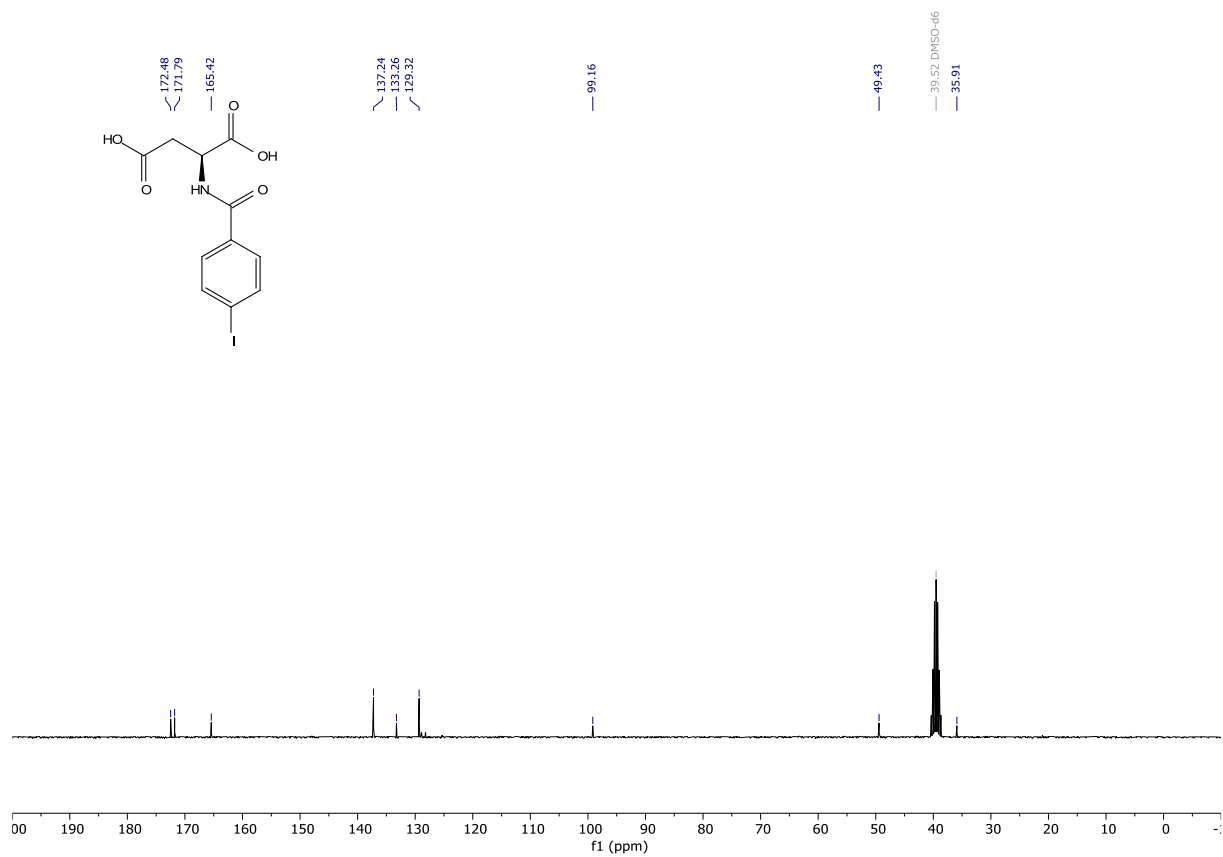
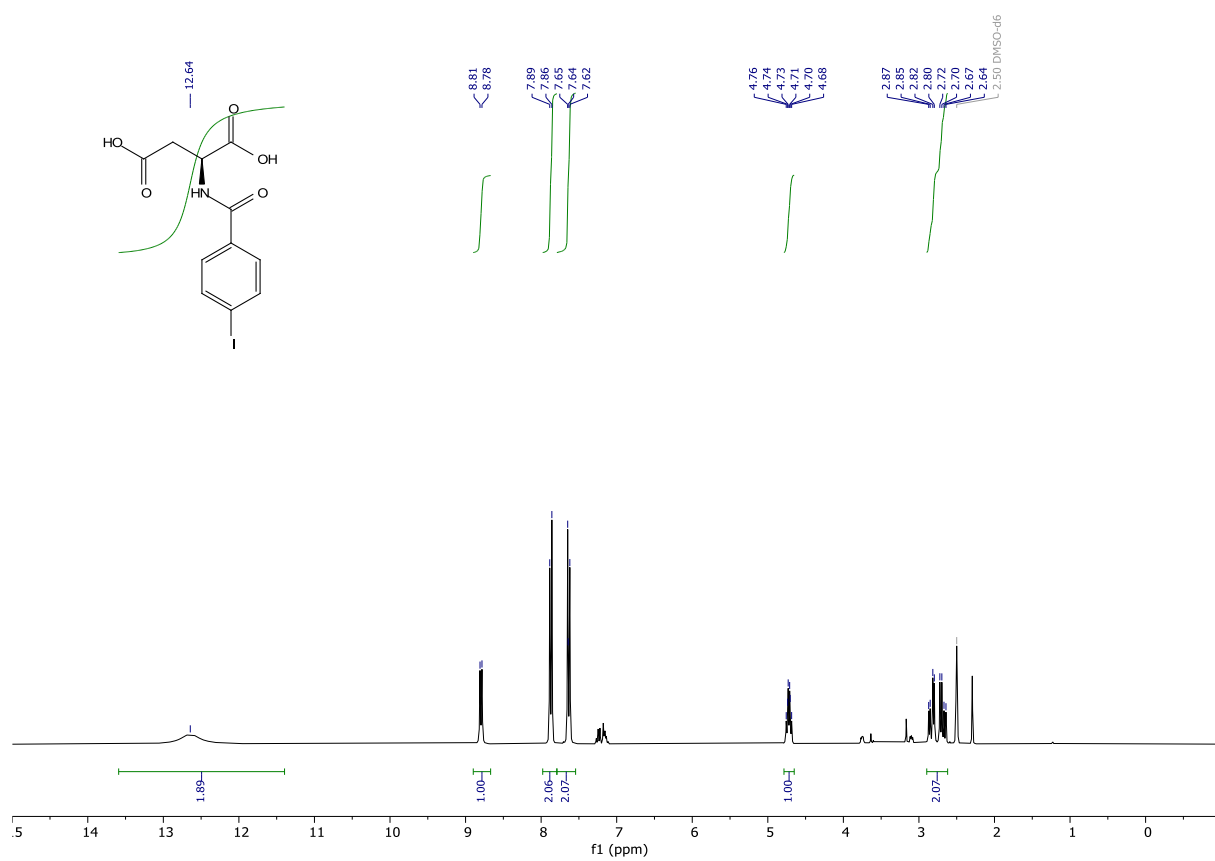
(4-(3-(trifluoromethyl)-3H-diazirin-3-yl)benzoyl)-L-aspartic acid (PGUB25). To a stirred suspension of 2,5-dioxopyrrolidin-1-yl 4-(3-(trifluoromethyl)-3H-diazirin-3-yl)benzoate (0.13934 g, 0.4258 mmol) in acetonitrile (8 mL) was added aspartic acid (0.062 g, 0.4658 mmol). The mixture was stirred for 16 h at 20 °C protected from light. After 16 h no reaction product was observed and DIPEA (3 mL) was added, and the mixture was stirred for additional 2 h. The volatiles were removed under reduced pressure. The white solid was taken up in acetone and concentrated onto silica gel. The crude was purified by flash column chromatography (cyclohexane/ (ethyl acetate/ methanol/ acetic acid 85:10:5) gradient from 1:0 to 7:3), to give an orange oil. This oil was taken up in acetone and was concentrated onto celite. It was purified by reverse phase column chromatography (water + 0.1% TFA/ acetonitrile + 0.1% TFA gradient from 1:0 to 0:1), to give the desired compound in 39% yield (0.06240 g, 0.18075 mmol). White solid: $^1\text{H NMR}$ (300 MHz, DMSO- d_6) δ 12.60 (s, 2H), 8.92 (d, J = 7.8 Hz, 1H), 8.07 – 7.87 (m, 2H), 7.40 (d, J = 8.1 Hz, 2H), 4.76 (td, J = 8.0, 5.6 Hz, 1H), 2.97 – 2.62 (m, 2H). $^{13}\text{C NMR}$ (75 MHz, DMSO) δ 172.77, 172.44, 171.81, 164.90, 135.45, 130.46, 128.25, 126.49, 49.40, 48.60, 25.23. $^{19}\text{F NMR}$ (282 MHz, DMSO) δ -64.46. **HRMS** (ESI) calculated for $[\text{M}+\text{H}]^+$ $\text{C}_{13}\text{H}_{11}\text{F}_3\text{N}_2\text{O}_5$ 346.0645, found 346.0653.

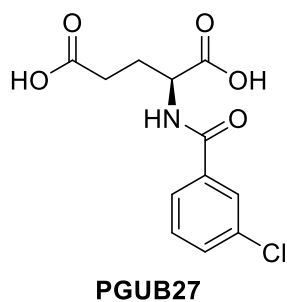




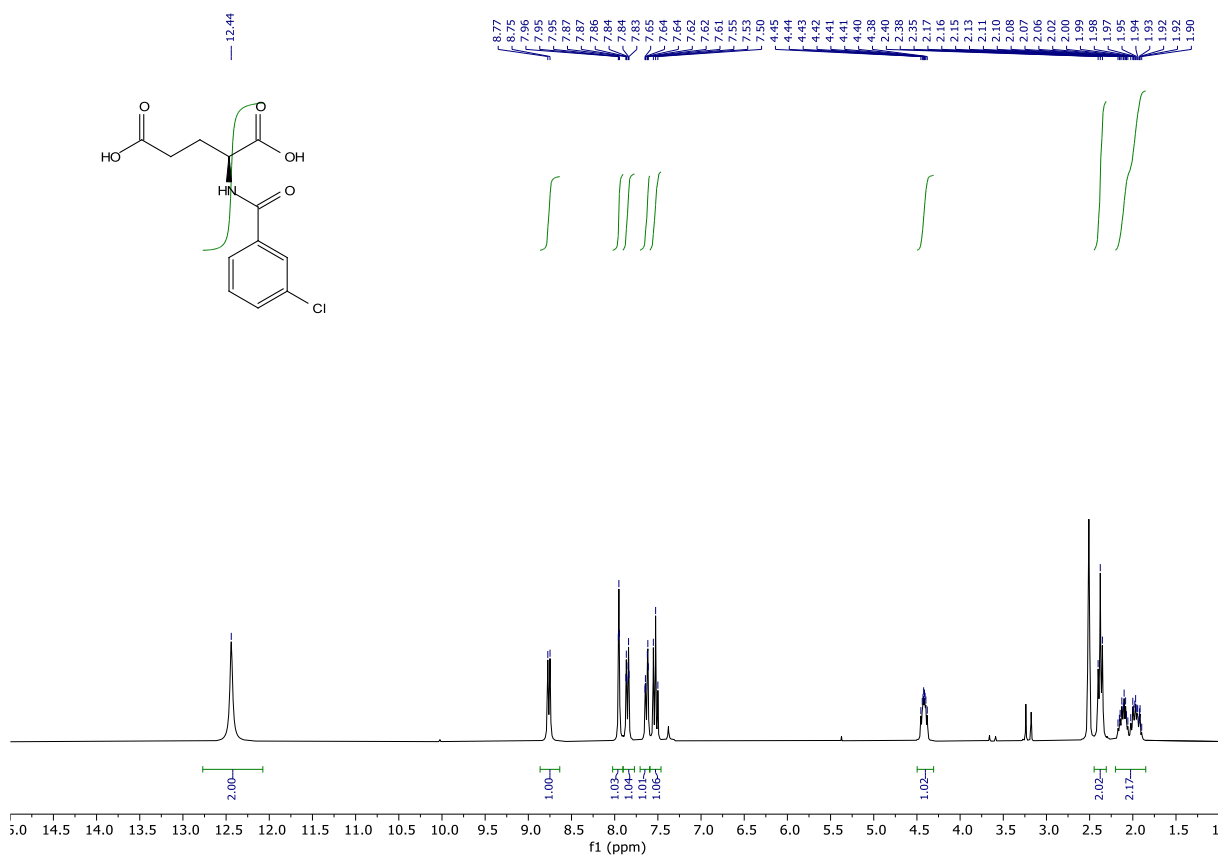
PGUB26

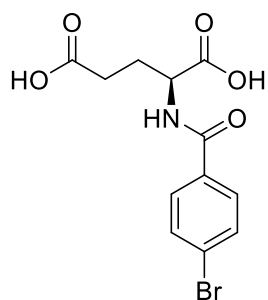
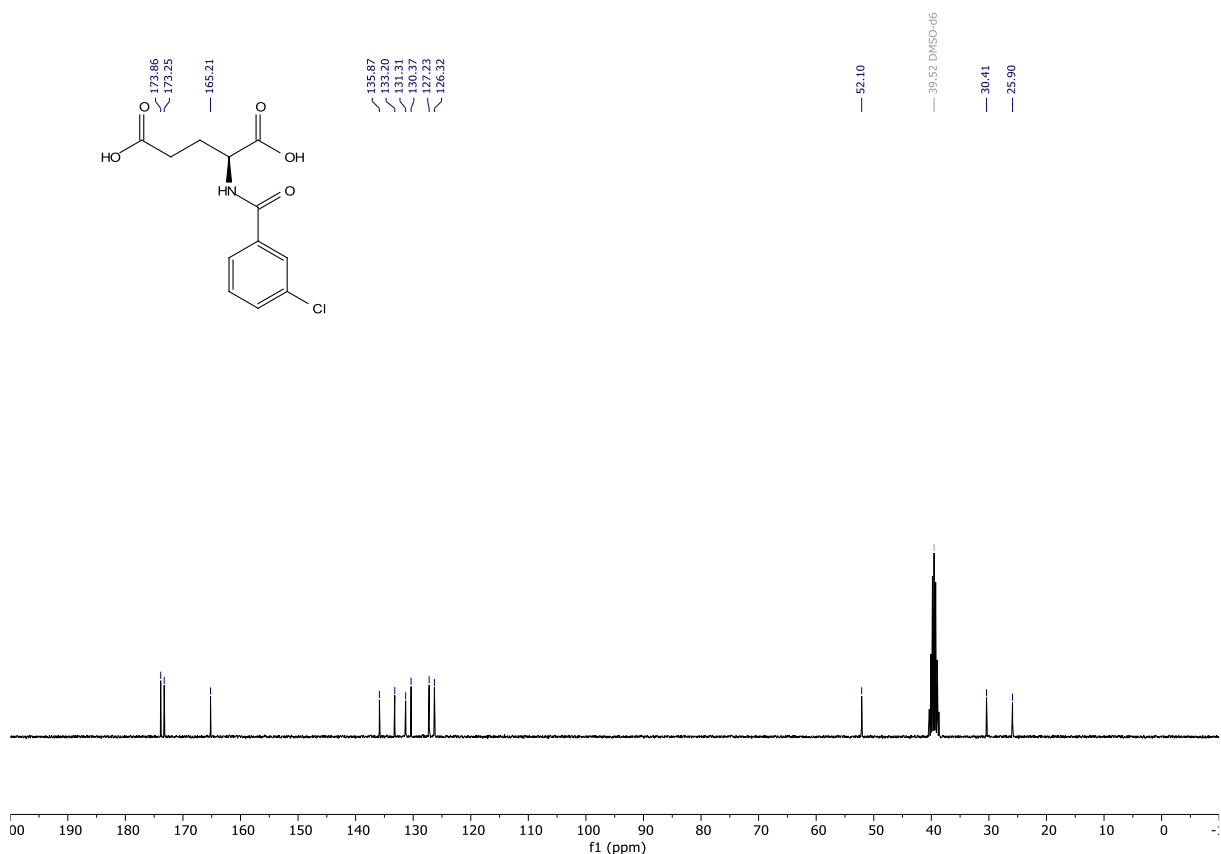
(4-iodobenzoyl)-L-aspartic acid (PGUB26). Prepared according to general procedure I starting from aspartic acid (0.496 g, 3.7264 mmol) using 4-iodobenzoyl chloride as acyl chloride, to give the desired product in 39% yield (0.53260 g, 1.46678 mmol). White solid impure with toluene: $^1\text{H NMR}$ (300 MHz, $\text{DMSO}-d_6$) δ 12.64 (s, 2H), 8.80 (d, $J = 7.8$ Hz, 1H), 7.87 (d, $J = 8.4$ Hz, 2H), 7.63 (d, $J = 8.5$ Hz, 2H), 4.72 (td, $J = 7.8, 5.8$ Hz, 1H), 2.90 – 2.62 (m, 2H). $^{13}\text{C NMR}$ (75 MHz, DMSO) δ 172.48, 171.79, 165.42, 137.24, 133.26, 129.32, 99.16, 49.43, 35.91. **HRMS** (ESI) calculated for $[\text{M}+\text{H}]^+$ $\text{C}_{11}\text{H}_{11}\text{INO}_5$ 363.9676, found 363.9684.





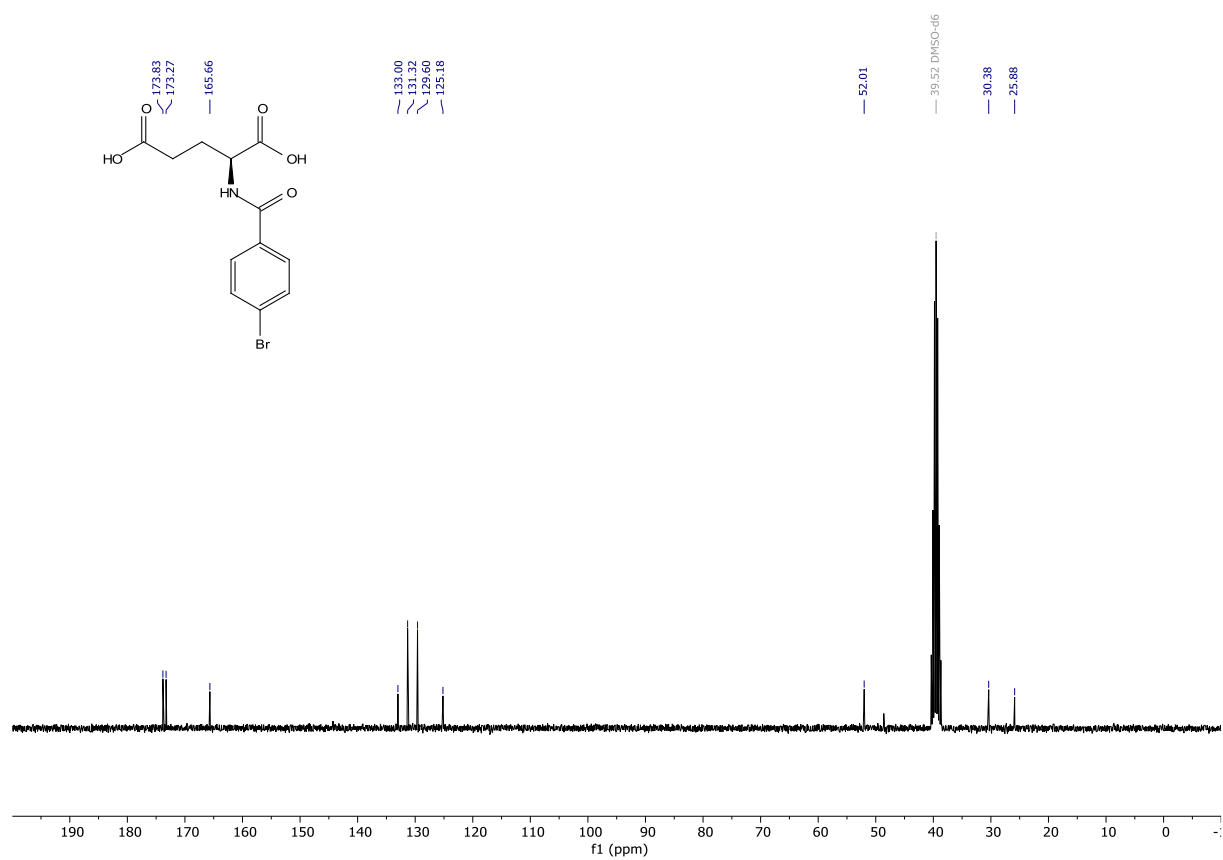
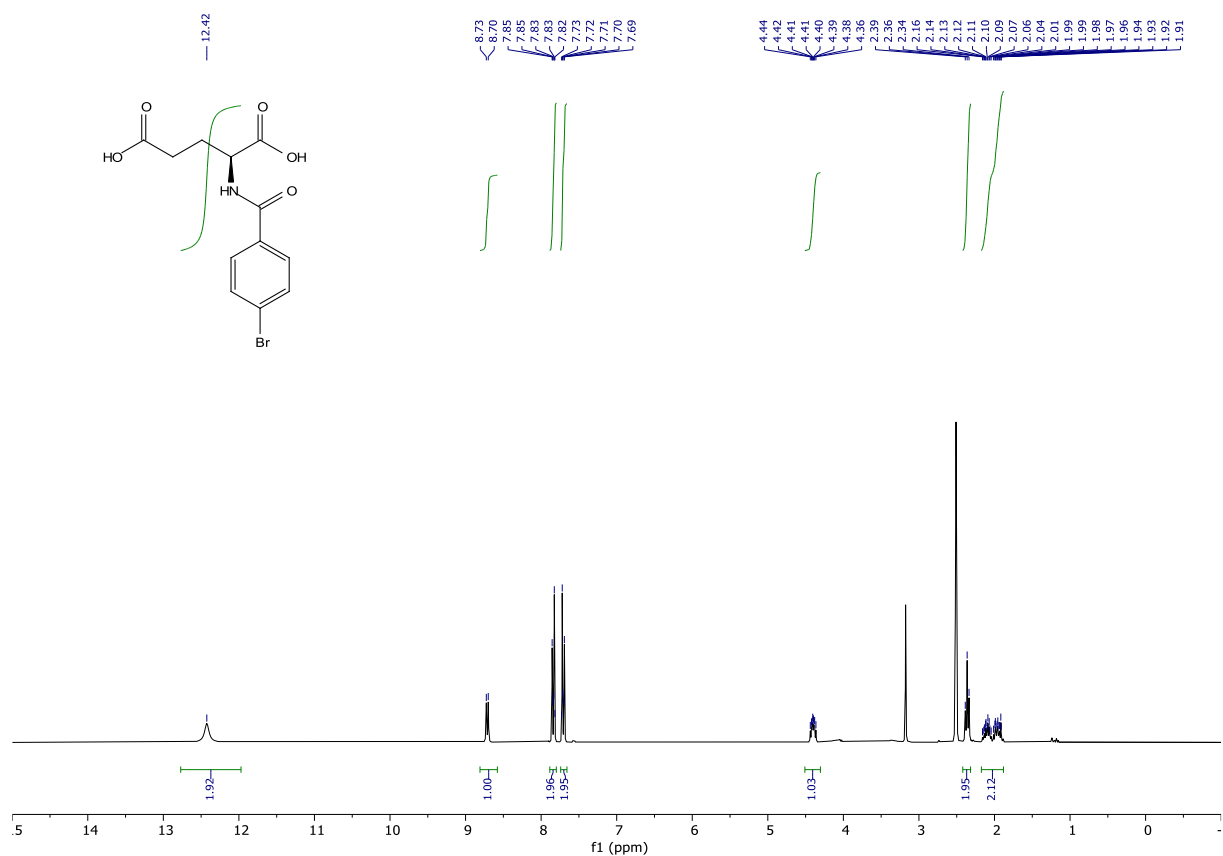
(3-chlorobenzoyl)-L-glutamic acid (PGUB27). Prepared according to general procedure I starting from glutamic acid (1.077 g, 7.3201 mmol) using 3-chlorobenzoyl chloride as acyl chloride, to give the desired product in 56% yield (1.16046 g, 4.06210 mmol). White solid: ^1H NMR (300 MHz, DMSO- d_6) δ 12.44 (s, 2H), 8.76 (d, J = 7.6 Hz, 1H), 7.95 (t, J = 1.9 Hz, 1H), 7.85 (dt, J = 7.7, 1.4 Hz, 1H), 7.63 (dt, J = 8.2, 1.4 Hz, 1H), 7.53 (t, J = 7.8 Hz, 1H), 4.42 (ddd, J = 9.7, 7.5, 4.9 Hz, 1H), 2.38 (t, J = 7.5 Hz, 2H), 2.20 – 1.85 (m, 2H). ^{13}C NMR (75 MHz, DMSO) δ 173.86, 173.25, 165.21, 135.87, 133.20, 131.31, 130.37, 127.23, 126.32, 52.10, 30.41, 25.90. HRMS (ESI) calculated for $[\text{M}+\text{H}]^+$ $\text{C}_{12}\text{H}_{13}\text{ClNO}_5$ 286.0477, found 286.0476.

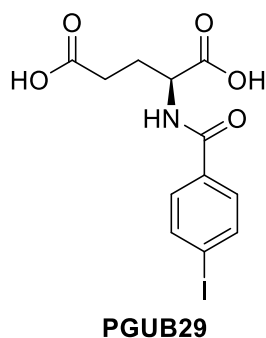




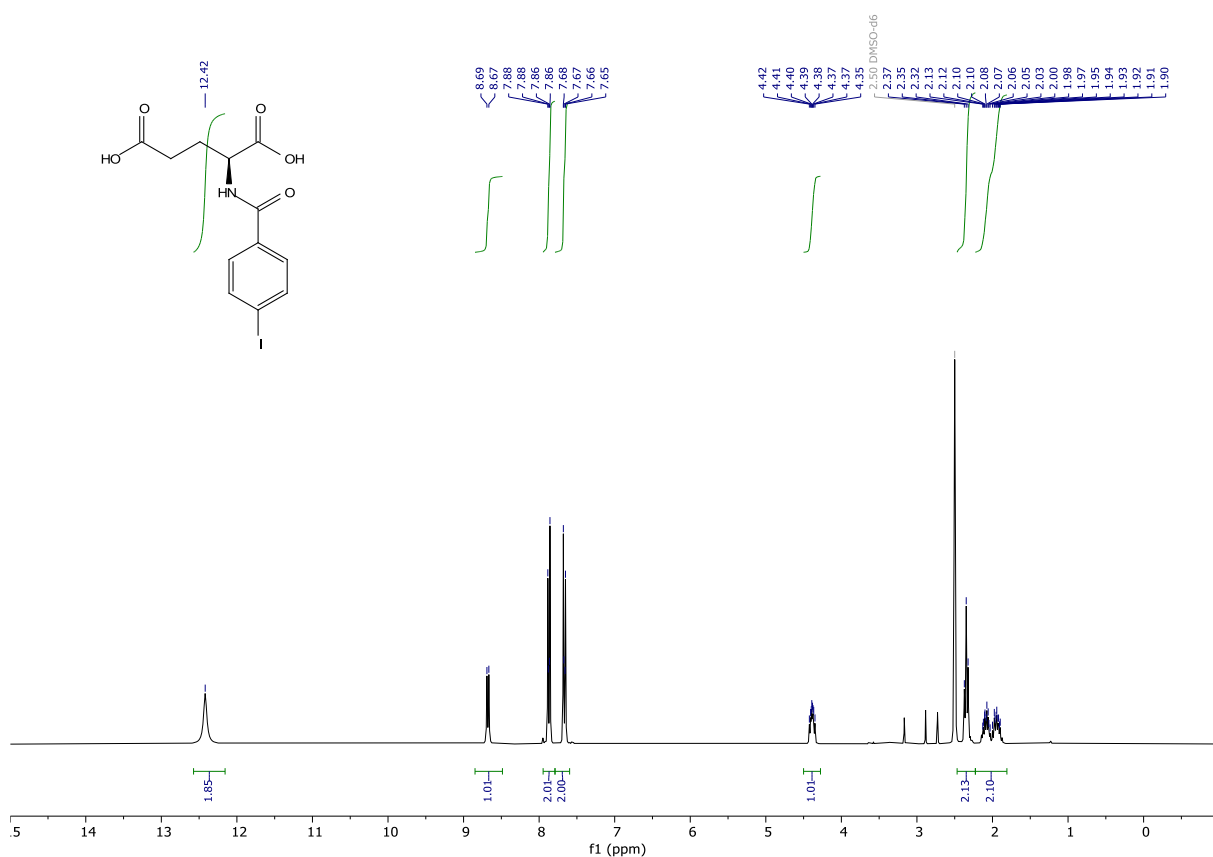
PGUB28

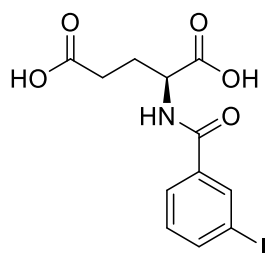
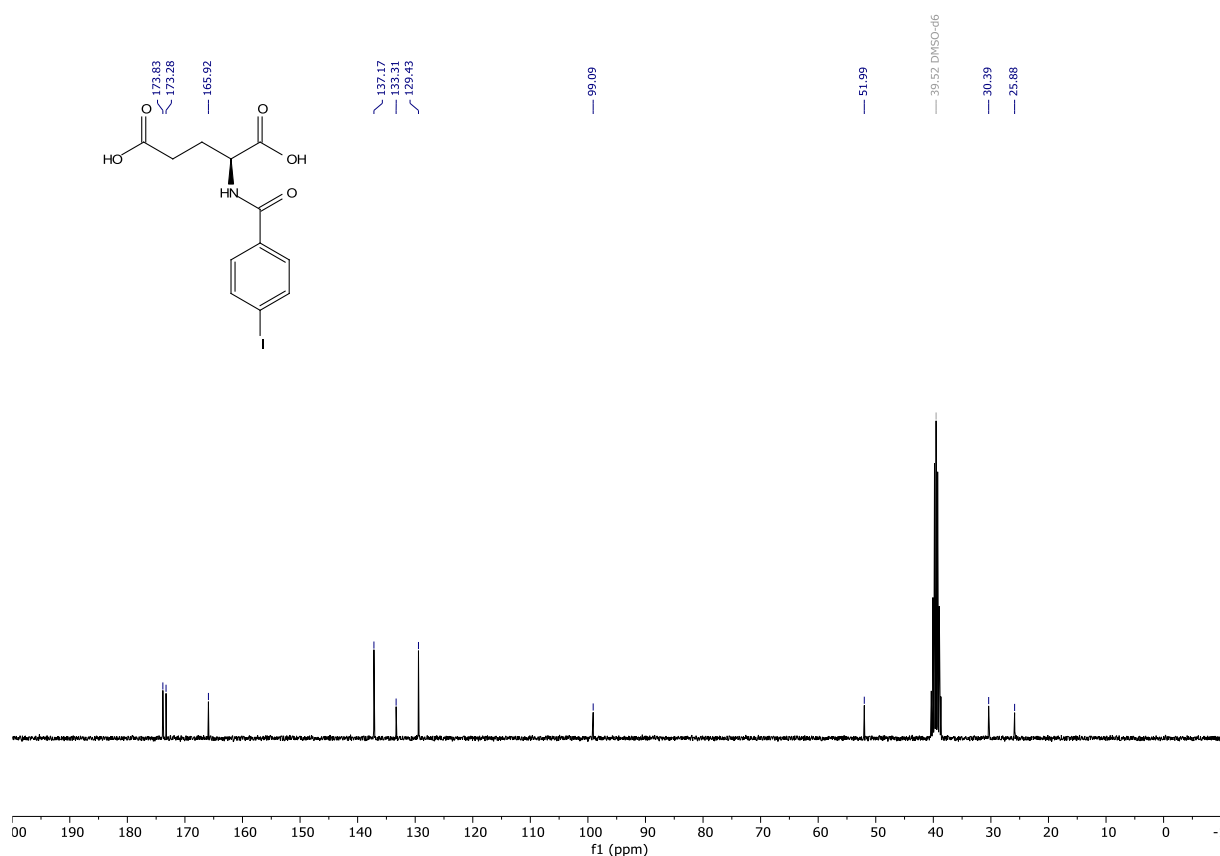
(4-bromobenzoyl)-L-glutamic acid (PGUB28). Prepared according to general procedure I starting from glutamic acid (0.546 g, 3.7110 mmol) using 4-bromobenzoyl chloride as acyl chloride, to give the desired product in 53% yield (0.64669 g, 1.95887 mmol). White solid: ^1H NMR (300 MHz, DMSO- d_6) δ 12.42 (s, 2H), 8.71 (d, J = 7.6 Hz, 1H), 7.89 – 7.80 (m, 2H), 7.74 – 7.66 (m, 2H), 4.40 (ddd, J = 9.7, 7.6, 4.9 Hz, 1H), 2.36 (t, J = 7.5 Hz, 2H), 2.17 – 1.88 (m, 2H). ^{13}C NMR (75 MHz, DMSO) δ 173.83, 173.27, 165.66, 133.00, 131.32, 129.60, 125.18, 52.01, 30.38, 25.88. HRMS (ESI) calculated for $[\text{M}+\text{H}]^+$ $\text{C}_{12}\text{H}_{13}\text{BrNO}_5$ 329.9972, found 329.9957.





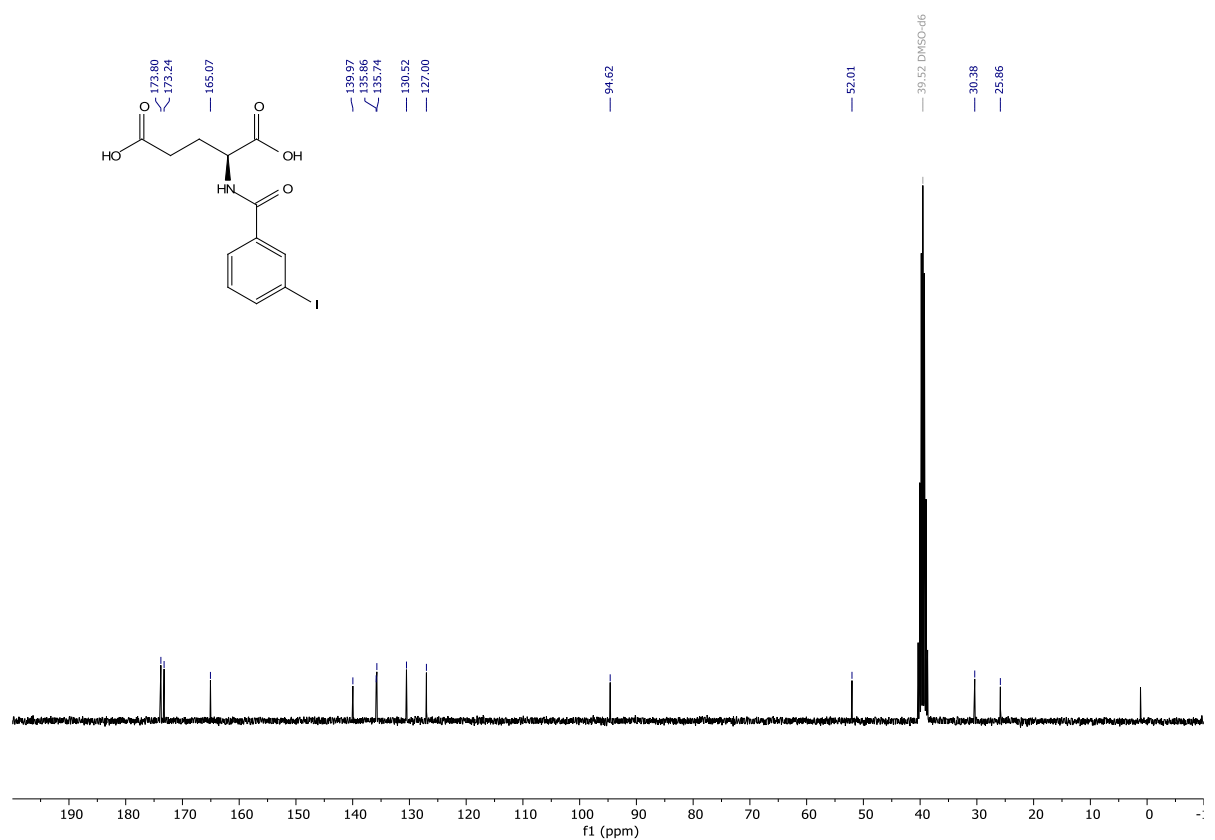
(4-iodobenzoyl)-L-glutamic acid (PGUB29). Prepared according to general procedure I starting from glutamic acid (0.504 g, 3.4255 mmol) using 4-iodobenzoyl chloride as acyl chloride, to give the desired product in 65% yield (0.83276 g, 2.20812 mmol). Slight yellowish solid: ^1H NMR (300 MHz, DMSO- d_6) δ 12.42 (s, 2H), 8.68 (d, J = 7.6 Hz, 1H), 7.95 – 7.79 (m, 2H), 7.79 – 7.60 (m, 2H), 4.39 (ddd, J = 9.7, 7.6, 4.9 Hz, 1H), 2.35 (t, J = 7.4 Hz, 2H), 2.23 – 1.81 (m, 2H). ^{13}C NMR (75 MHz, DMSO) δ 173.83, 173.28, 165.92, 137.17, 133.31, 129.43, 99.09, 51.99, 30.39, 25.88. HRMS (ESI) calculated for $[\text{M}+\text{H}]^+$ $\text{C}_{12}\text{H}_{13}\text{INO}_5$ 377.9833, found 377.9829.

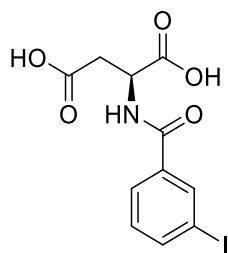




PGUB30

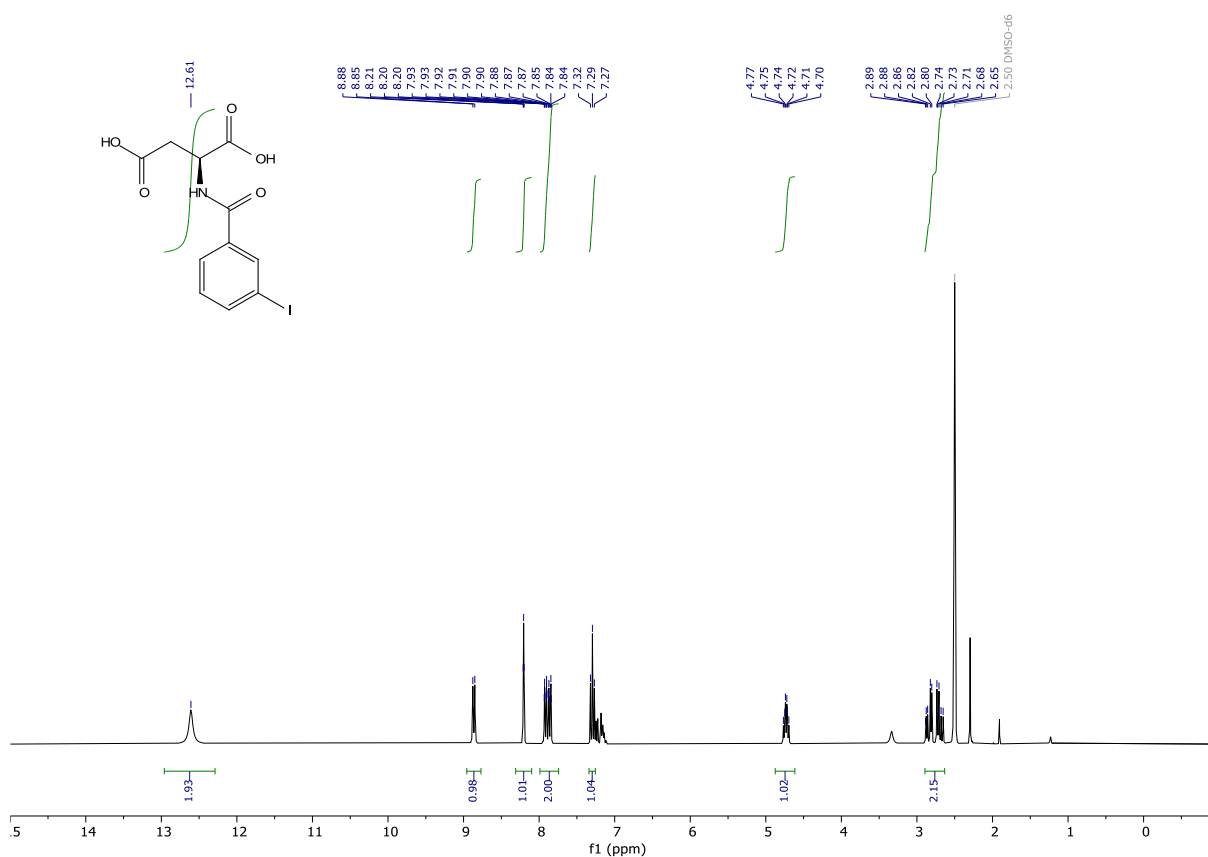
(3-iodobenzoyl)-L-glutamic acid (PGUB30). Prepared according to general procedure I starting from glutamic acid (0.513 g, 3.4867 mmol) using 3-iodobenzoyl chloride as acyl chloride, to give the desired product in 30% yield (0.39718 g, 1.05315 mmol). White solid: ^1H NMR (300 MHz, DMSO- d_6) δ 12.42 (s, 2H), 8.72 (d, J = 7.7 Hz, 1H), 8.24 (t, J = 1.7 Hz, 1H), 8.04 – 7.78 (m, 2H), 7.29 (t, J = 7.8 Hz, 1H), 4.39 (ddd, J = 9.7, 7.6, 4.9 Hz, 1H), 2.35 (t, J = 7.5 Hz, 2H), 2.15 – 1.86 (m, 2H). ^{13}C NMR (75 MHz, DMSO) δ 173.80, 173.24, 165.07, 139.97, 135.86, 135.74, 130.52, 127.00, 94.62, 52.01, 30.38, 25.86. HRMS (ESI) calculated for $[\text{M}+\text{H}]^+$ $\text{C}_{12}\text{H}_{13}\text{INO}_5$ 377.9833, found 377.9834.

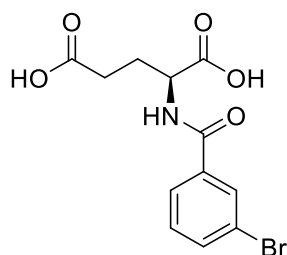
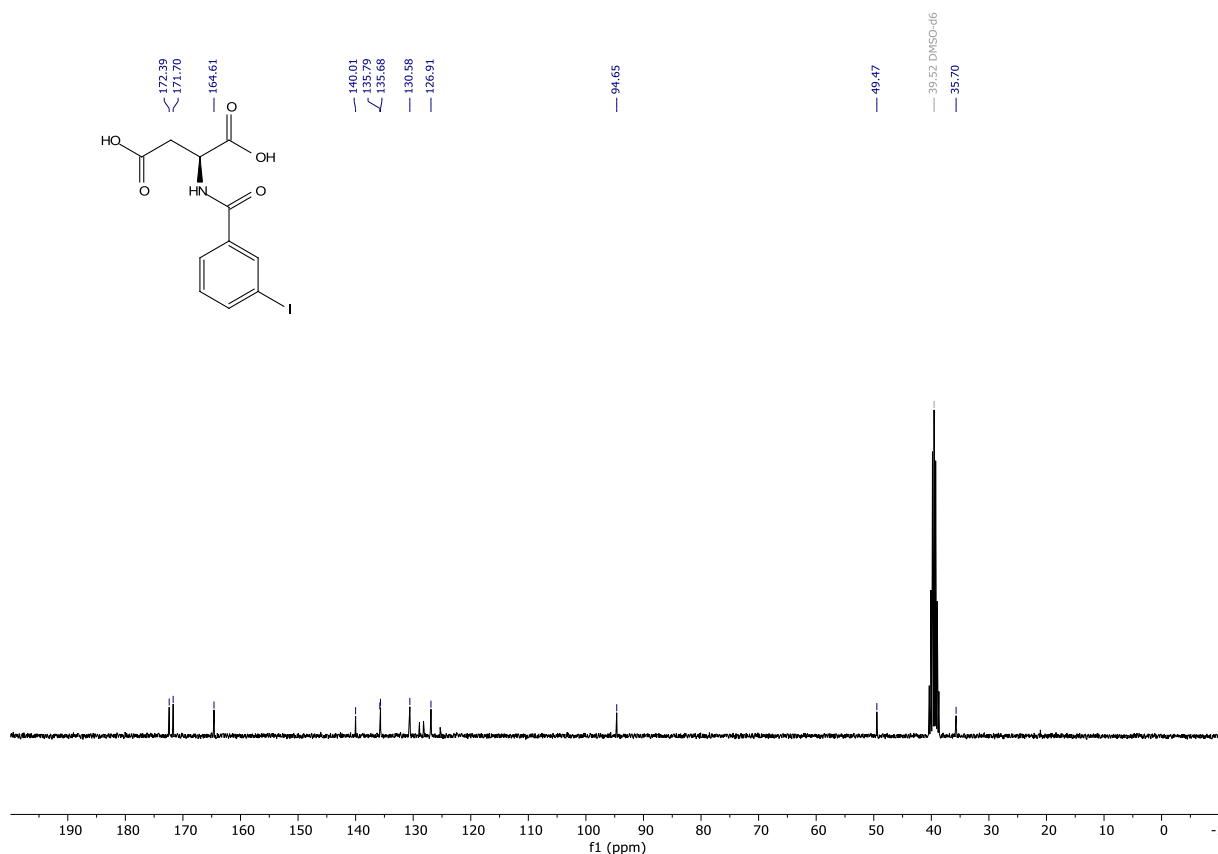




PGUB31

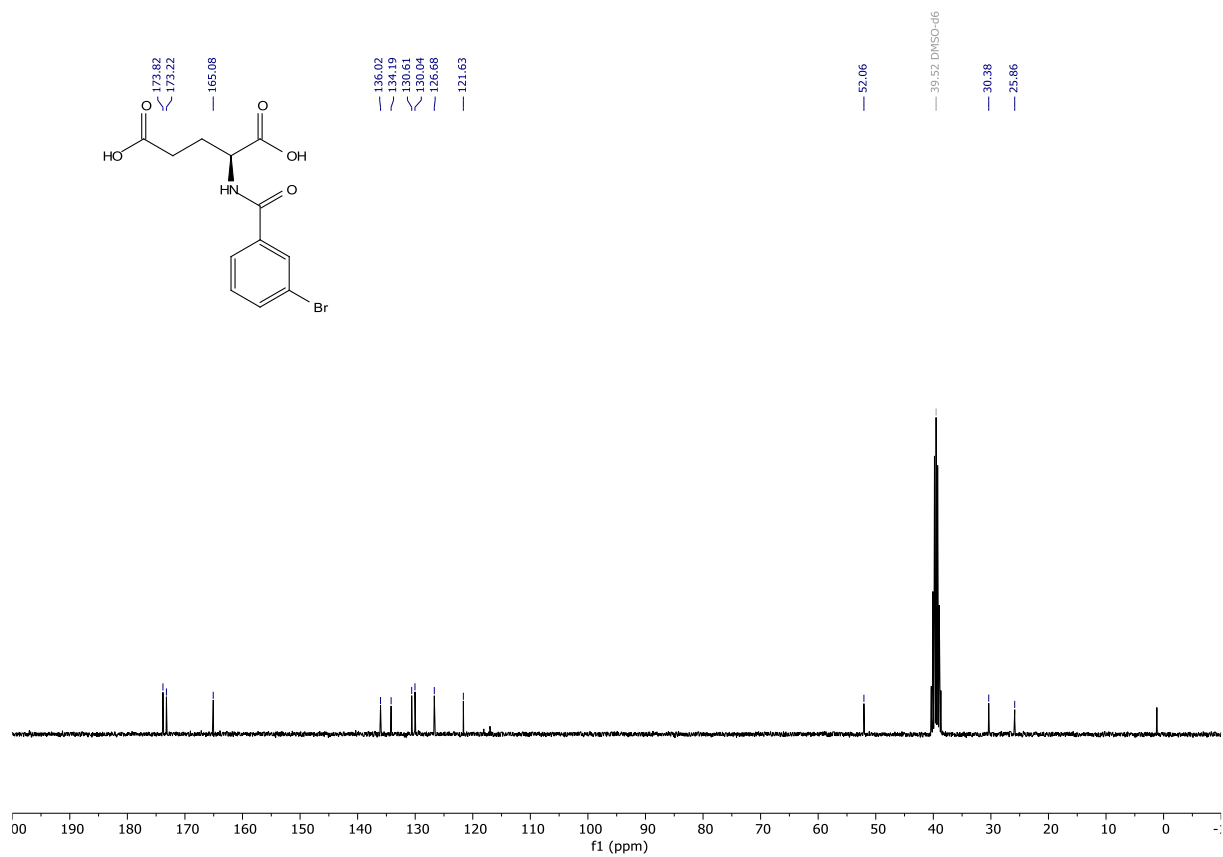
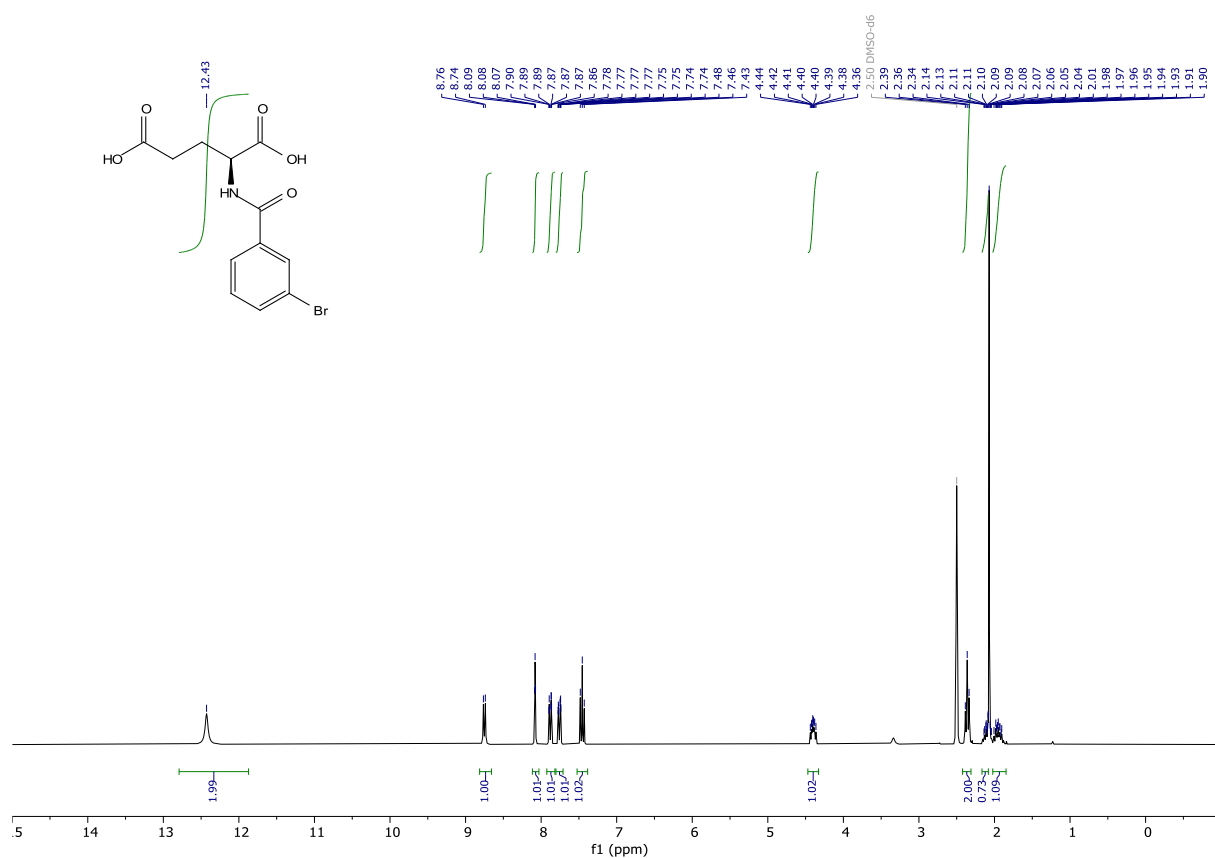
(3-iodobenzoyl)-L-aspartic acid (PGUB31). Prepared according to general procedure I starting from aspartic acid (0.513 g, 3.8542 mmol) using 3-iodobenzoyl chloride as acyl chloride, to give the desired product in 16% yield (0.23000 g, 0.63342 mmol). White solid slightly impure with toluene: ^1H NMR (300 MHz, DMSO- d_6) δ 12.61 (s, 2H), 8.86 (d, $J = 7.8$ Hz, 1H), 8.20 (t, $J = 1.7$ Hz, 1H), 7.89 (ddt, $J = 17.0$, 7.8, 1.3 Hz, 2H), 7.29 (t, $J = 7.8$ Hz, 1H), 4.73 (td, $J = 8.0$, 5.6 Hz, 1H), 2.89 – 2.63 (m, 2H). ^{13}C NMR (75 MHz, DMSO) δ 172.39, 171.70, 164.61, 140.01, 135.79, 135.68, 130.58, 126.91, 94.65, 49.47, 35.70. **HRMS** (ESI) calculated for $[\text{M}+\text{H}]^+$ $\text{C}_{11}\text{H}_{11}\text{INO}_5$ 363.9676, found 363.9682.

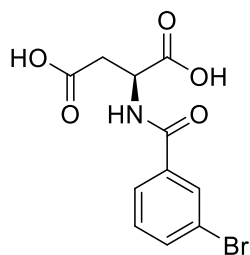




PGUB32

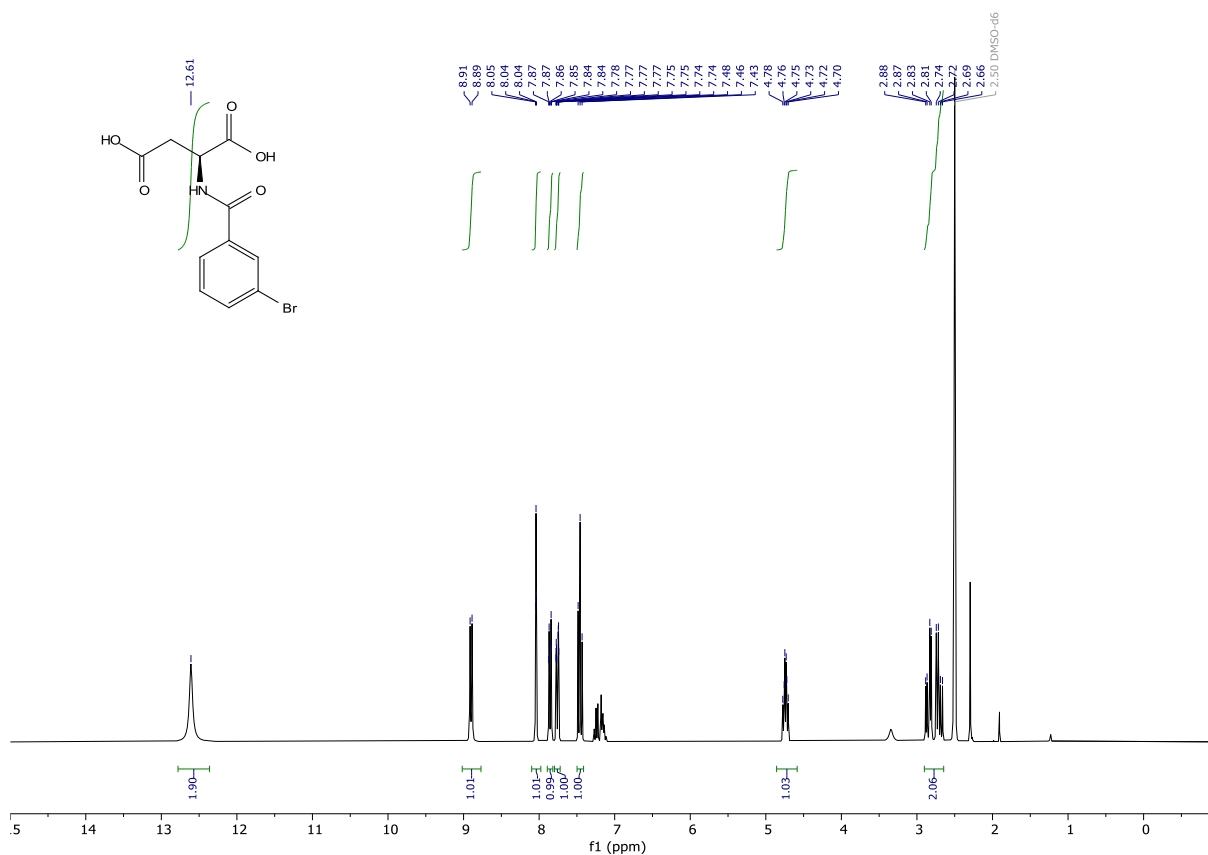
(3-bromobenzoyl)-L-glutamic acid (PGUB32). Prepared according to general procedure I starting from glutamic acid (0.570 g, 38741 mmol) using 3-bromobenzoyl chloride as acyl chloride, to give the desired product in 84% yield (1.08000 g, 3.27131 mmol). Slight yellowish solid slightly impure with acetonitrile: ^1H NMR (300 MHz, DMSO- d_6) δ 12.43 (s, 2H), 8.75 (d, J = 7.6 Hz, 1H), 8.08 (t, J = 1.8 Hz, 1H), 7.92 – 7.82 (m, 1H), 7.76 (ddd, J = 8.0, 2.0, 1.0 Hz, 1H), 7.46 (t, J = 7.9 Hz, 1H), 4.40 (ddd, J = 9.7, 7.6, 4.9 Hz, 1H), 2.36 (t, J = 7.5 Hz, 2H), 2.17 – 2.08 (m, 2H). ^{13}C NMR (75 MHz, DMSO) δ 173.82, 173.22, 165.08, 136.02, 134.19, 130.61, 130.04, 126.68, 121.63, 52.06, 30.38, 25.86. HRMS (ESI) calculated for $[\text{M}+\text{H}]^+$ $\text{C}_{12}\text{H}_{13}\text{BrNO}_5$ 329.9972, found 329.9974.

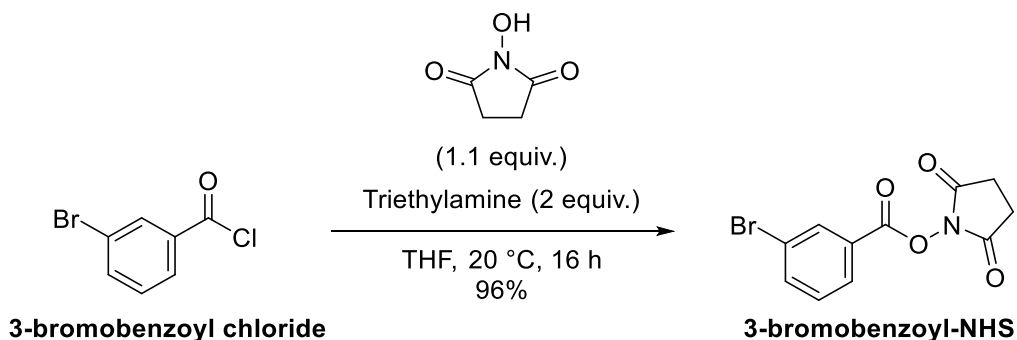
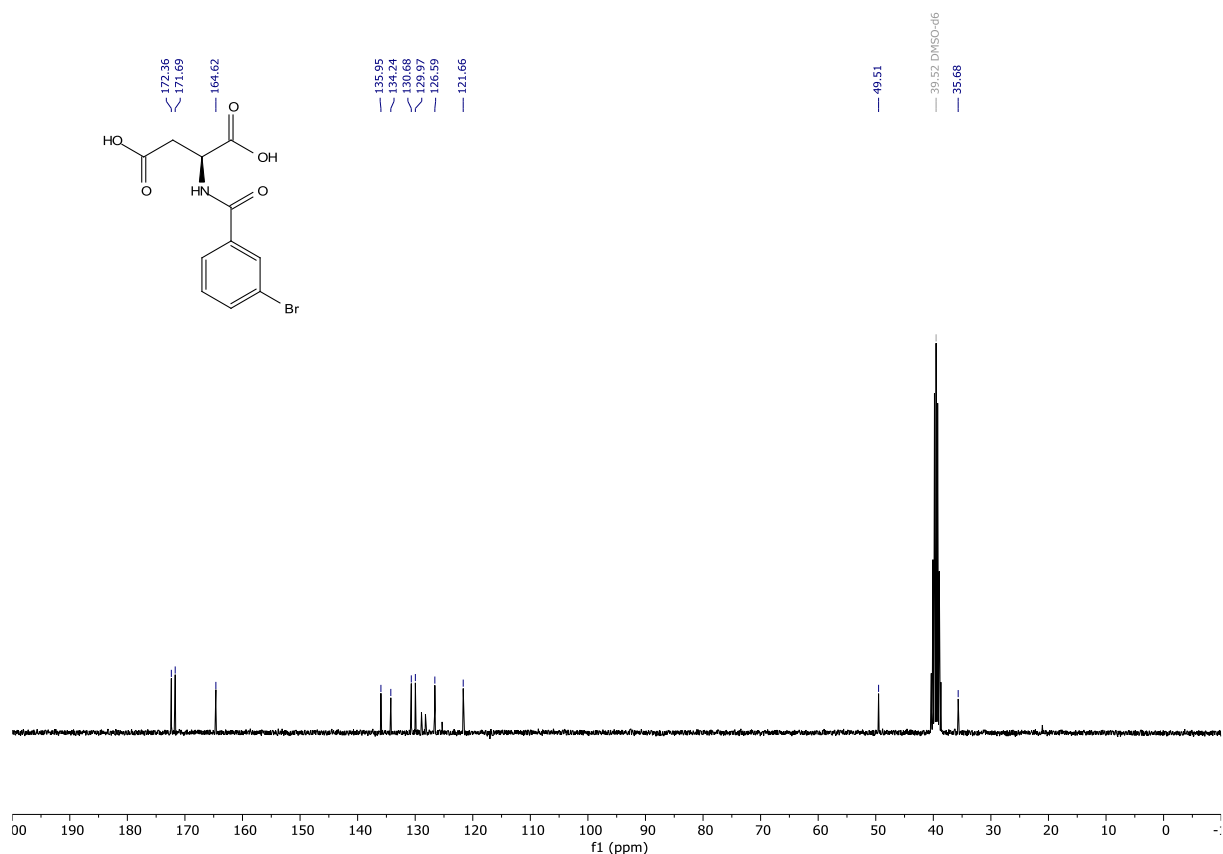




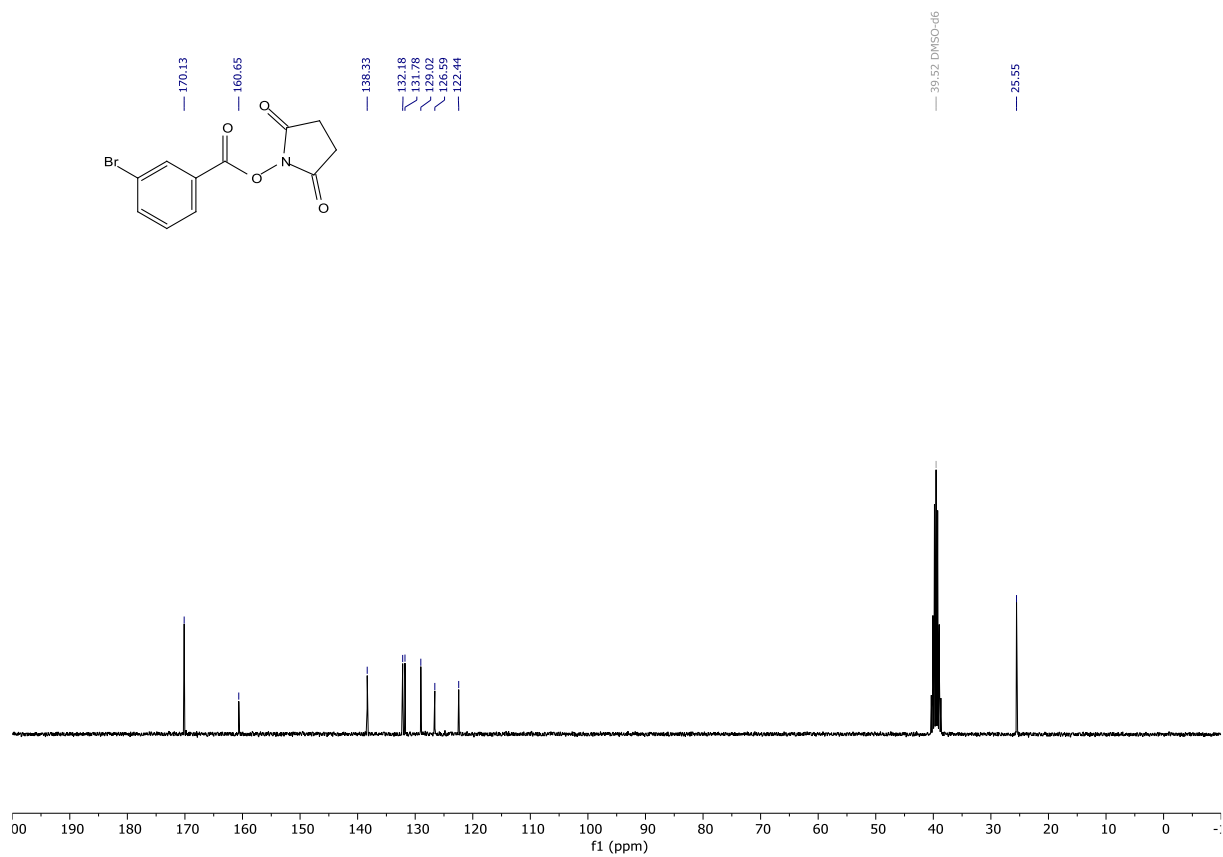
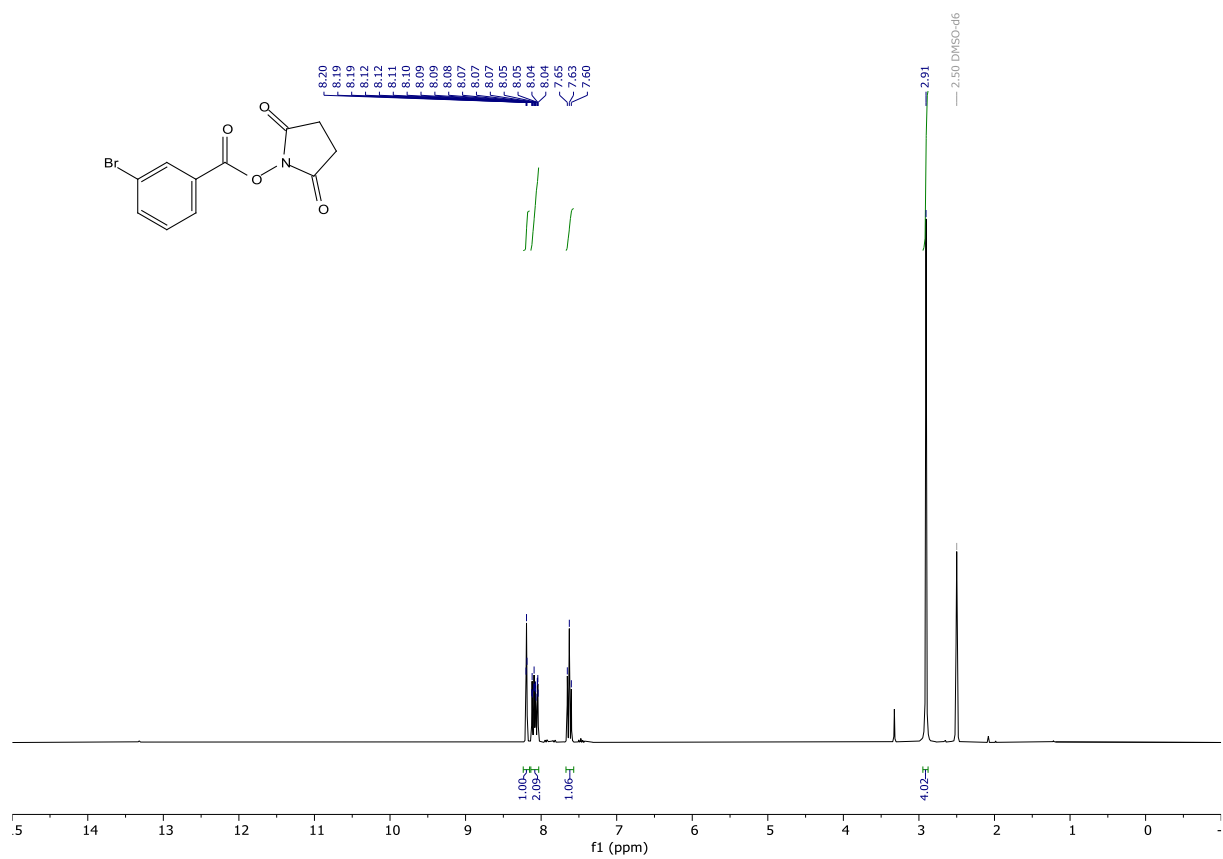
PGUB33

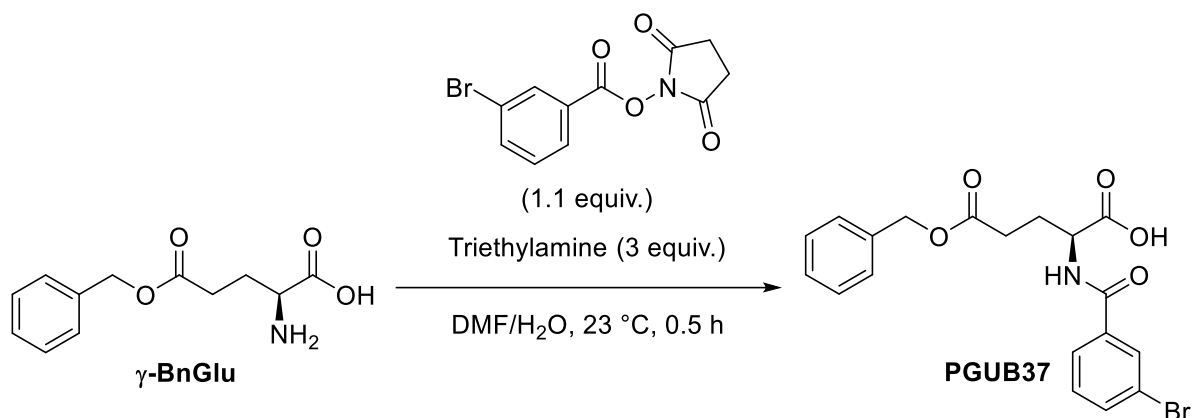
(3-bromobenzoyl)-L-aspartic acid (PGUB33). Prepared according to general procedure I starting from aspartic acid (0.568 g, 4.2674 mmol) using 3-bromobenzoyl chloride as acyl chloride, to give the desired product in 75% yield (1.01500 g, 3.21094 mmol). Slight yellowish solid slightly impure with toluene: $^1\text{H NMR}$ (300 MHz, DMSO- d_6) δ 12.61 (s, 2H), 8.90 (d, $J = 7.8$ Hz, 1H), 8.04 (t, $J = 1.8$ Hz, 1H), 7.85 (dt, $J = 7.8, 1.3$ Hz, 1H), 7.76 (ddd, $J = 8.0, 2.0, 1.0$ Hz, 1H), 7.46 (t, $J = 7.9$ Hz, 1H), 4.74 (td, $J = 8.1, 5.6$ Hz, 1H), 2.90 – 2.65 (m, 2H). $^{13}\text{C NMR}$ (75 MHz, DMSO) δ 172.36, 171.69, 164.62, 135.95, 134.24, 130.68, 129.97, 126.59, 121.66, 49.51, 35.68. **HRMS** (ESI) calculated for $[\text{M}+\text{H}]^+$ $\text{C}_{11}\text{H}_{11}\text{BrNO}_5$ 315.9815, found 315.9818.



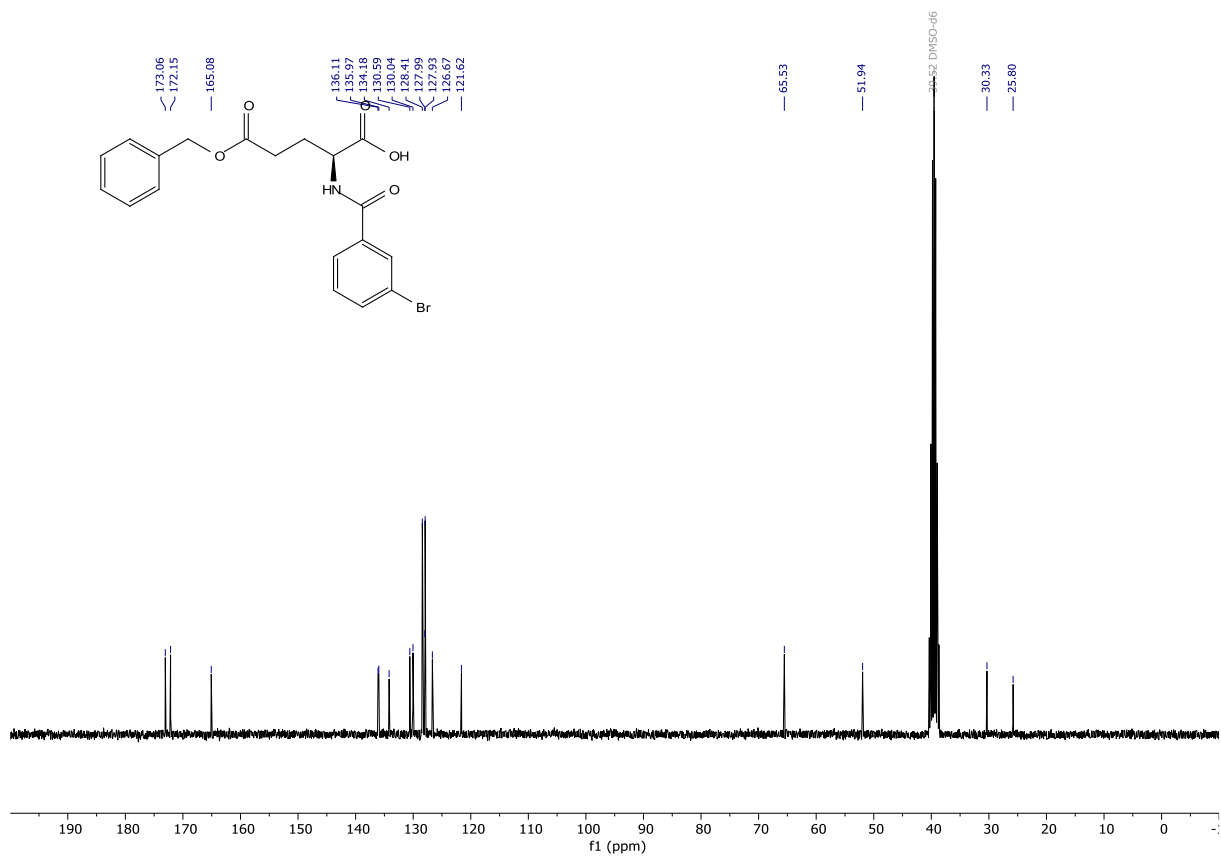
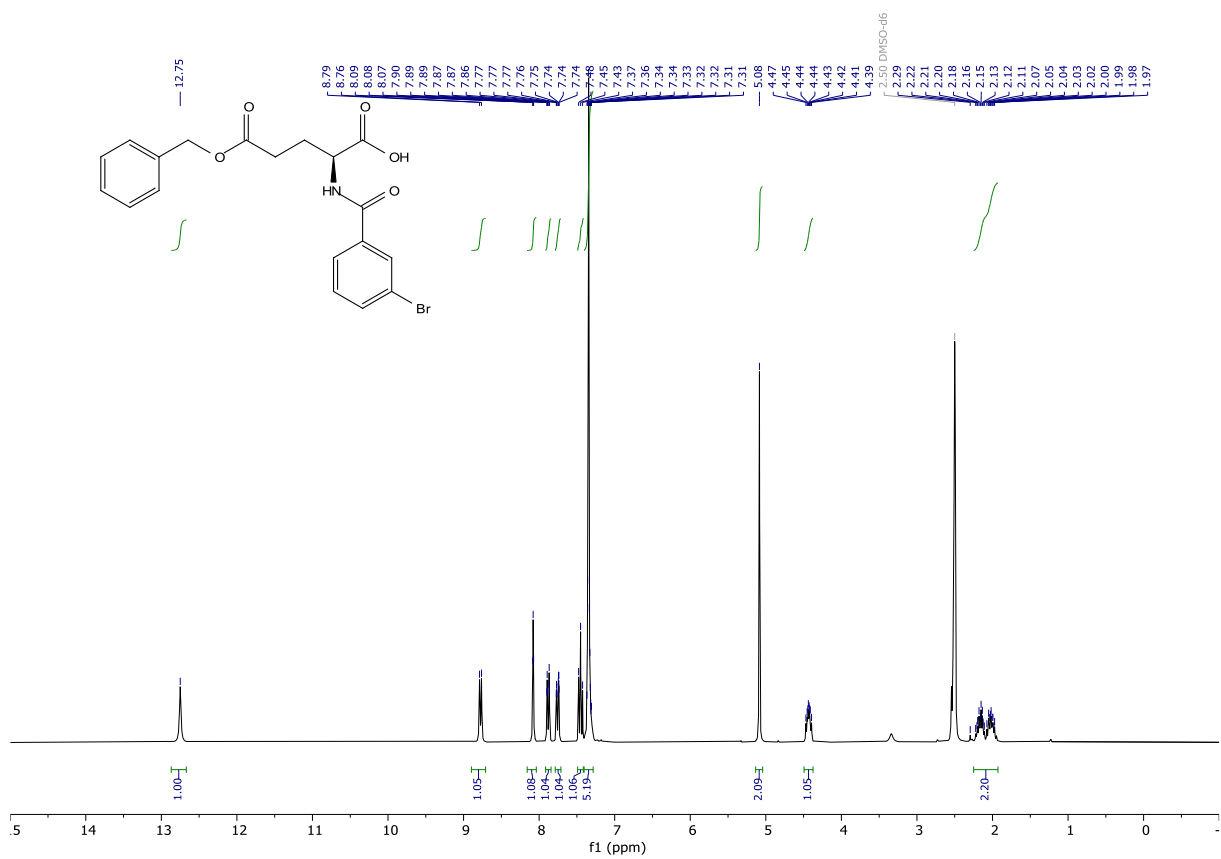


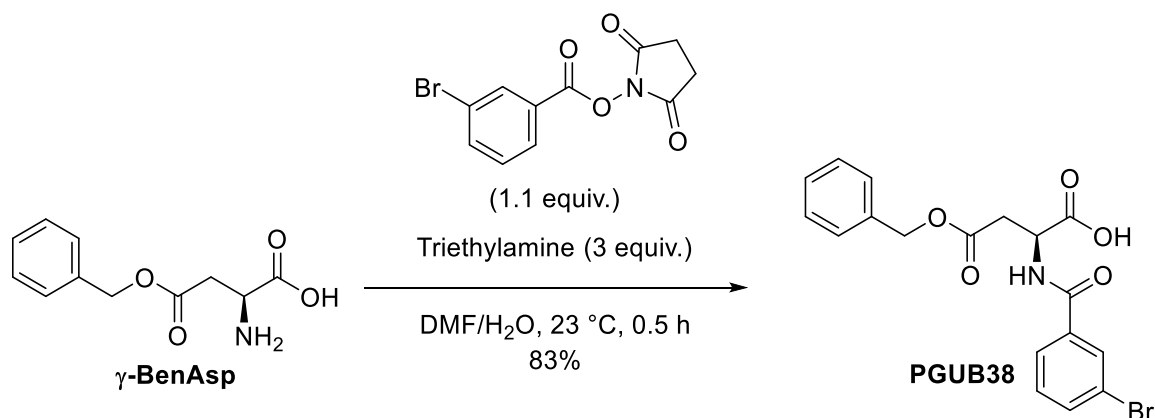
To a stirred solution of 3-Bromobenzoyl chloride (1.65 mL, 2.7456 g, 12.4053 mmol) in dry THF (10 mL) under an argon atmosphere was added *N*-hydroxysuccinimide (1.649 g, 14.3282 mmol) and then was added slowly triethylamine (4 mL, 2.92 g, 28.8566 mmol). The mixture was left stirring for 16 h. To the mixture was added water and ethyl acetate. The mixture was then extracted with ethyl acetate, leaving some white solid, that did not dissolve neither in water nor ethyl acetate. The combined organic layers were dried over MgSO_4 , filtered and concentrated under reduced pressure onto silica gel. The crude was purified by machine flash column chromatography (cyclohexane/ ethyl acetate gradient from 1:0 to 0:1), to give the desired compound in 56% yield (2.09355 g, 7.02317 mmol). Yellowish solid: ^1H NMR (300 MHz, $\text{DMSO}-d_6$) δ 8.19 (t, J = 1.9 Hz, 1H), 8.14 – 8.03 (m, 2H), 7.63 (t, J = 8.0 Hz, 1H), 2.91 (s, 4H). ^{13}C NMR (75 MHz, DMSO) δ 170.13, 160.65, 138.33, 132.18, 131.78, 129.02, 126.59, 122.44, 25.55. HRMS (ESI) calculated for $[\text{M}+\text{H}]^+$ $\text{C}_{11}\text{H}_9\text{BrNO}_4$ 315.9815, found 315.9818.



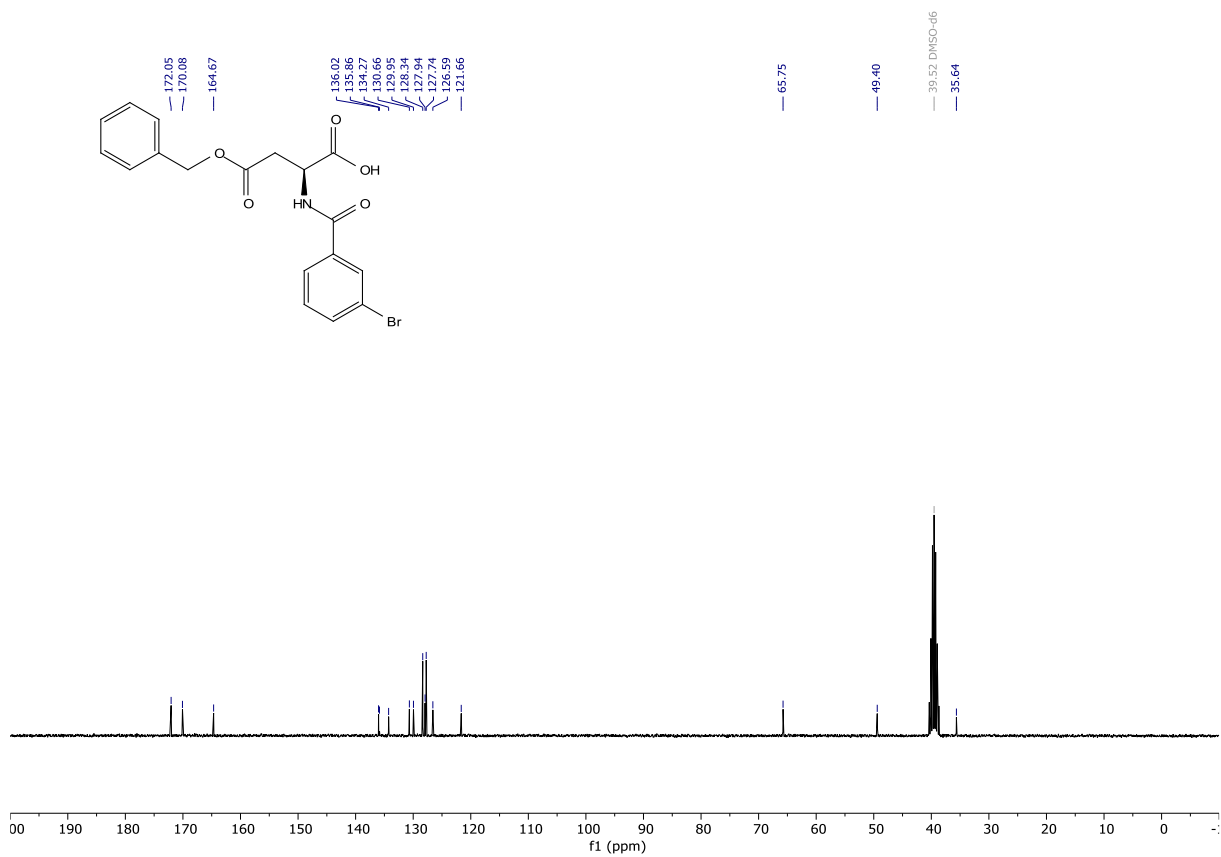
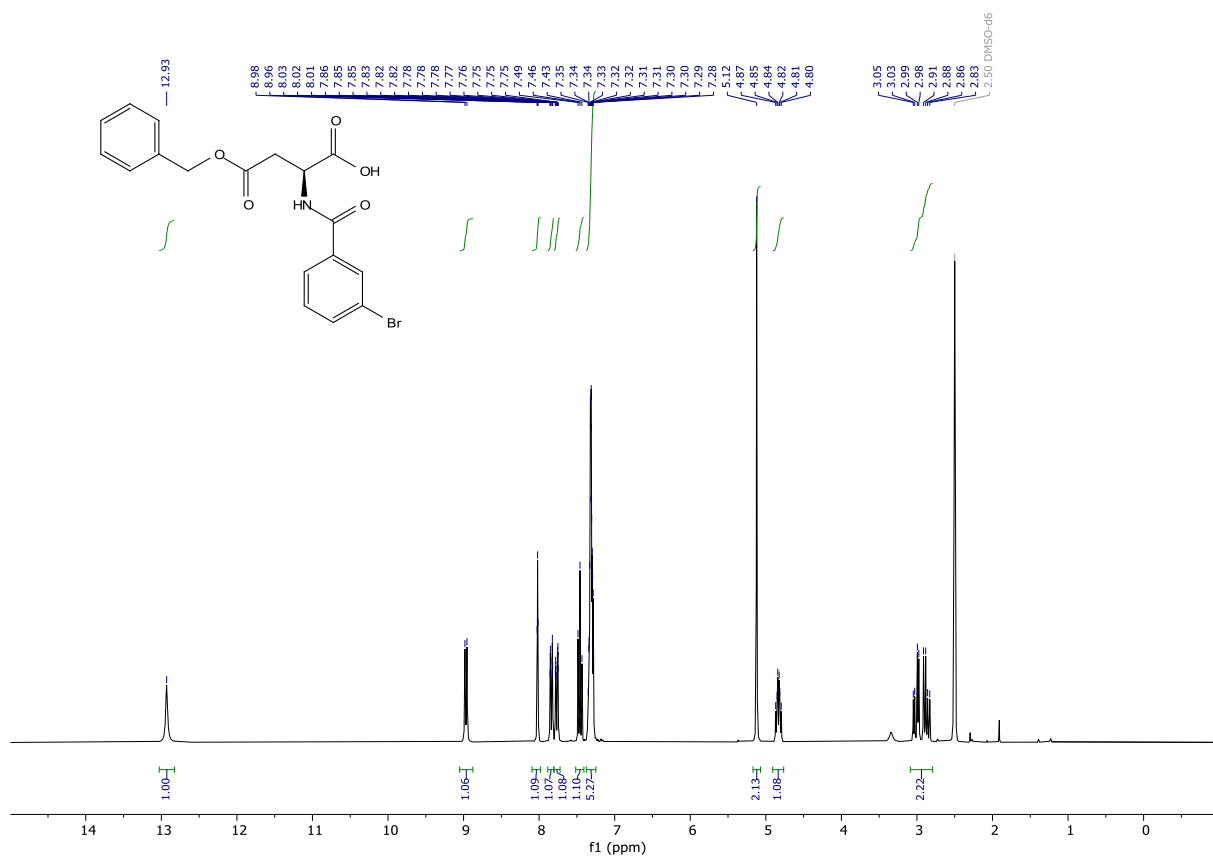


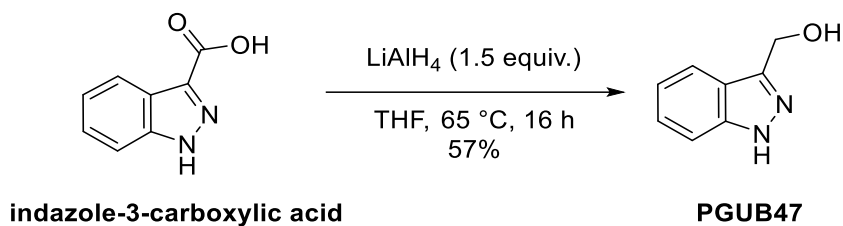
(S)-5-(benzyloxy)-2-(3-bromobenzamido)-5-oxopentanoic acid (PGUB37). To a stirred suspension of γ -BnGlu (0.46197 g, 1.9471 mmol) in DMF (10 mL) was added 3-bromobenzoyl NHS ester (0.657 g, 2.2113 mmol) followed by triethylamine (1 mL, 0.726 g, 7.1746 mmol) and water (2 mL). The mixture was stirred under an argon atmosphere for 0.5 h. The volatiles were removed under reduced pressure and the residue was taken up in dichloromethane and concentrated onto silica gel. The crude was purified by flash column chromatography (cyclohexane/ (ethyl acetate/ methanol/ acetic acid 85:10:5) gradient from 1:0 to 0:1), to give the desired product in 96% yield (0.78775 g, 1.87444 mmol). White solid: $^1\text{H NMR}$ (300 MHz, DMSO-*d*₆) δ 12.75 (s, 1H), 8.78 (d, *J* = 7.7 Hz, 1H), 8.08 (t, *J* = 1.8 Hz, 1H), 7.88 (dt, *J* = 7.9, 1.3 Hz, 1H), 7.75 (ddd, *J* = 8.0, 2.0, 1.0 Hz, 1H), 7.45 (t, *J* = 7.9 Hz, 1H), 7.34 (q, *J* = 3.0, 2.1 Hz, 5H), 5.08 (s, 2H), 4.43 (ddd, *J* = 9.7, 7.6, 4.9 Hz, 1H), 2.25 – 1.93 (m, 2H). $^{13}\text{C NMR}$ (75 MHz, DMSO) δ 173.06, 172.15, 165.08, 136.11, 135.97, 134.18, 130.59, 130.04, 128.41, 127.99, 127.93, 126.67, 121.62, 65.53, 51.94, 30.33, 25.80. **HRMS** (ESI) calculated for $[\text{M-H}]^-$ C₁₉H₁₇BrNO₅ 418.0296, found 418.0298.



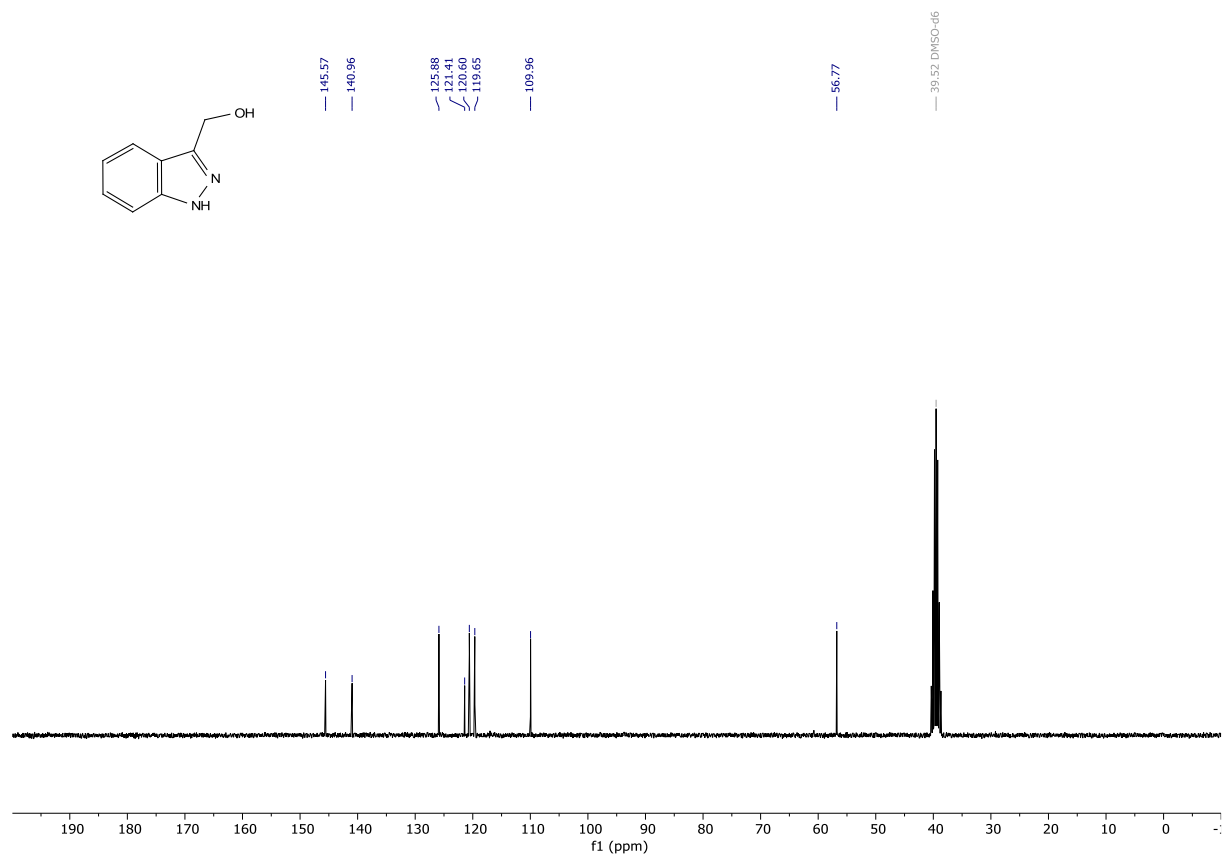
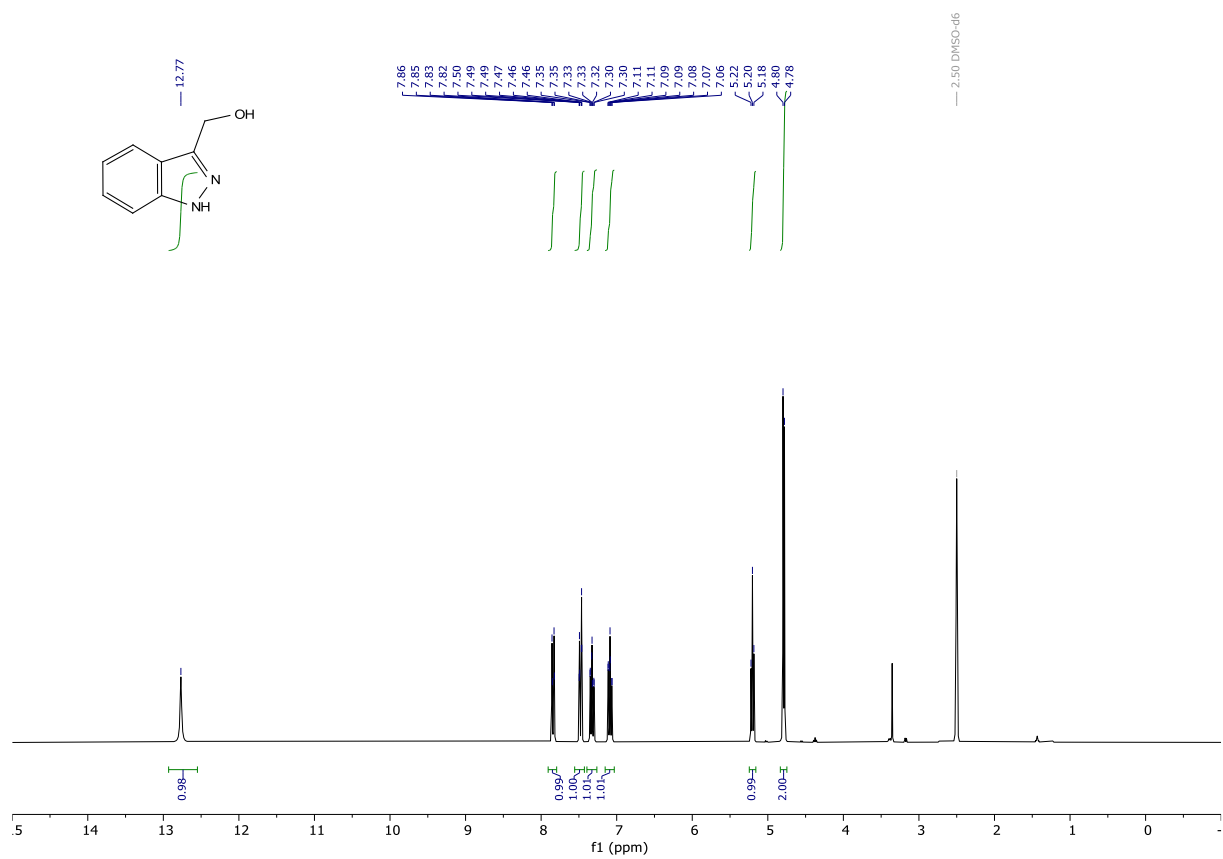


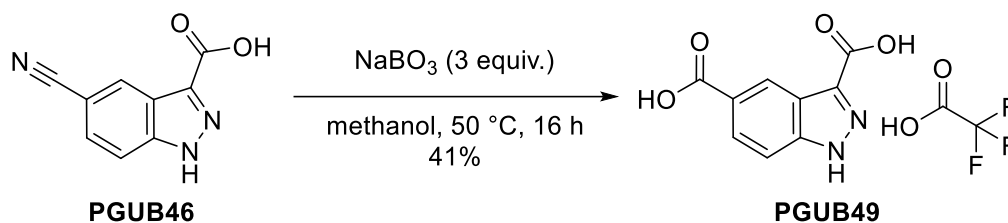
(S)-5-(benzyloxy)-2-(3-bromobenzamido)-5-oxobutanoic acid (PGUB38). To a stirred suspension of aspartic acid γ -benzyl ester (0.500 g, 2.2399 mmol) in DMF (6 mL) was added 3-bromobenzoyl NHS ester (0.740 g, 2.4907 mmol) and triethylamine (1 mL, 0.726 g, 7.1746 mmol) followed by water (2 mL). The mixture was stirred for 0.5 h at 23 °C. The volatiles were removed under reduced pressure. The oily residue was taken up in a mixture of 1 M aq. HCl and ethyl acetate. Vigorous stirring was required to get the oil to dissolve. The aqueous phase was extracted with ethyl acetate. The combined organic layers were washed with brine, dried over MgSO₄, filtered, and concentrated under reduced pressure. The resulting oil was taken up in dichloromethane and concentrated onto silica gel. The crude was purified by flash column chromatography (cyclohexane/ (ethyl acetate/ methanol/ acetic acid 85:10:5) gradient from 1:0 to 0:1), to give the desired compound in 83% yield (0.78000 g, 1.85591 mmol). White solid: ¹H NMR (300 MHz, DMSO-*d*₆) δ 12.93 (s, 1H), 8.97 (d, *J* = 7.9 Hz, 1H), 8.02 (t, *J* = 1.8 Hz, 1H), 7.84 (dt, *J* = 7.8, 1.3 Hz, 1H), 7.77 (ddd, *J* = 8.0, 2.1, 1.1 Hz, 1H), 7.46 (t, *J* = 7.9 Hz, 1H), 7.38 – 7.25 (m, 5H), 5.12 (s, 2H), 4.83 (td, *J* = 8.3, 5.6 Hz, 1H), 3.09 – 2.79 (m, 2H). ¹³C NMR (75 MHz, DMSO) δ 172.05, 170.08, 164.67, 136.02, 135.86, 134.27, 130.66, 129.95, 128.34, 127.94, 127.74, 126.59, 121.66, 65.75, 49.40, 35.64. HRMS (ESI) calculated for [M-H][−] C₁₈H₁₅BrNO₅ 404.0139, found 404.0143.



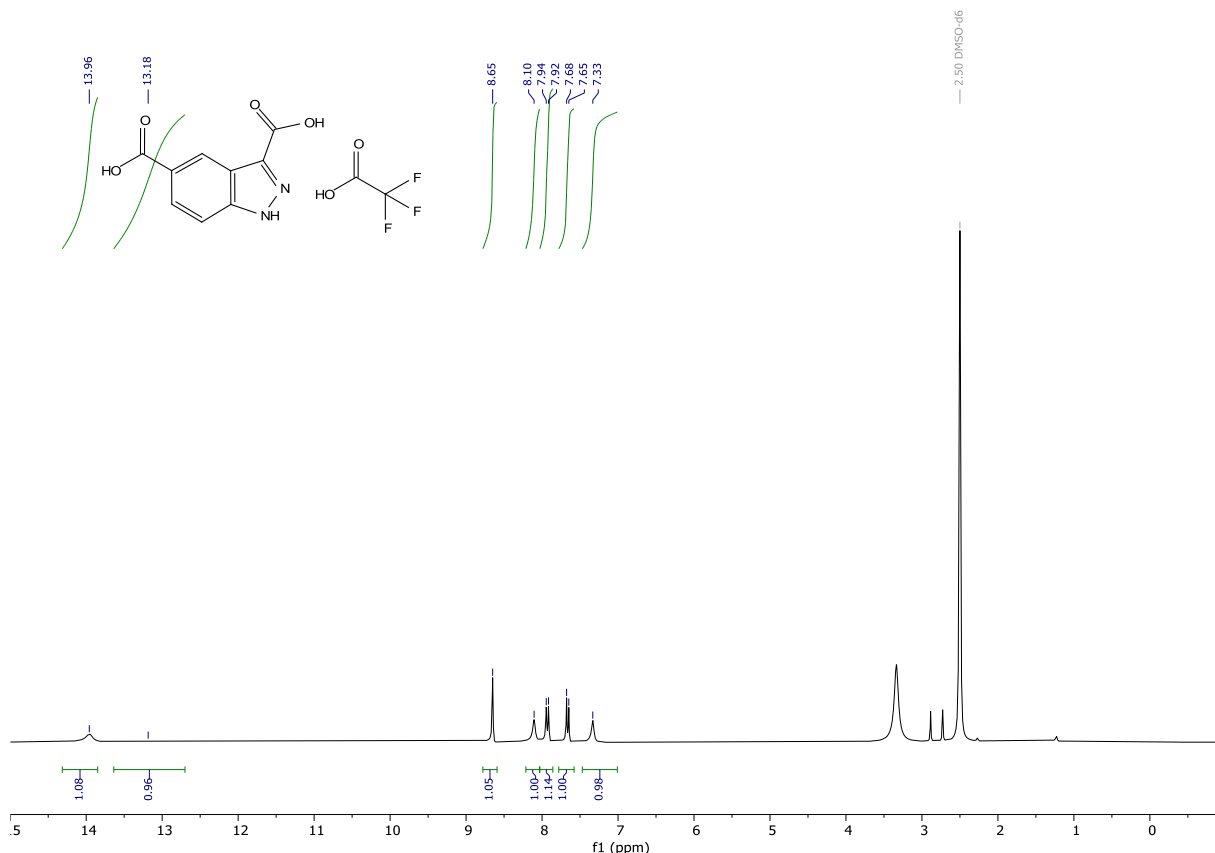


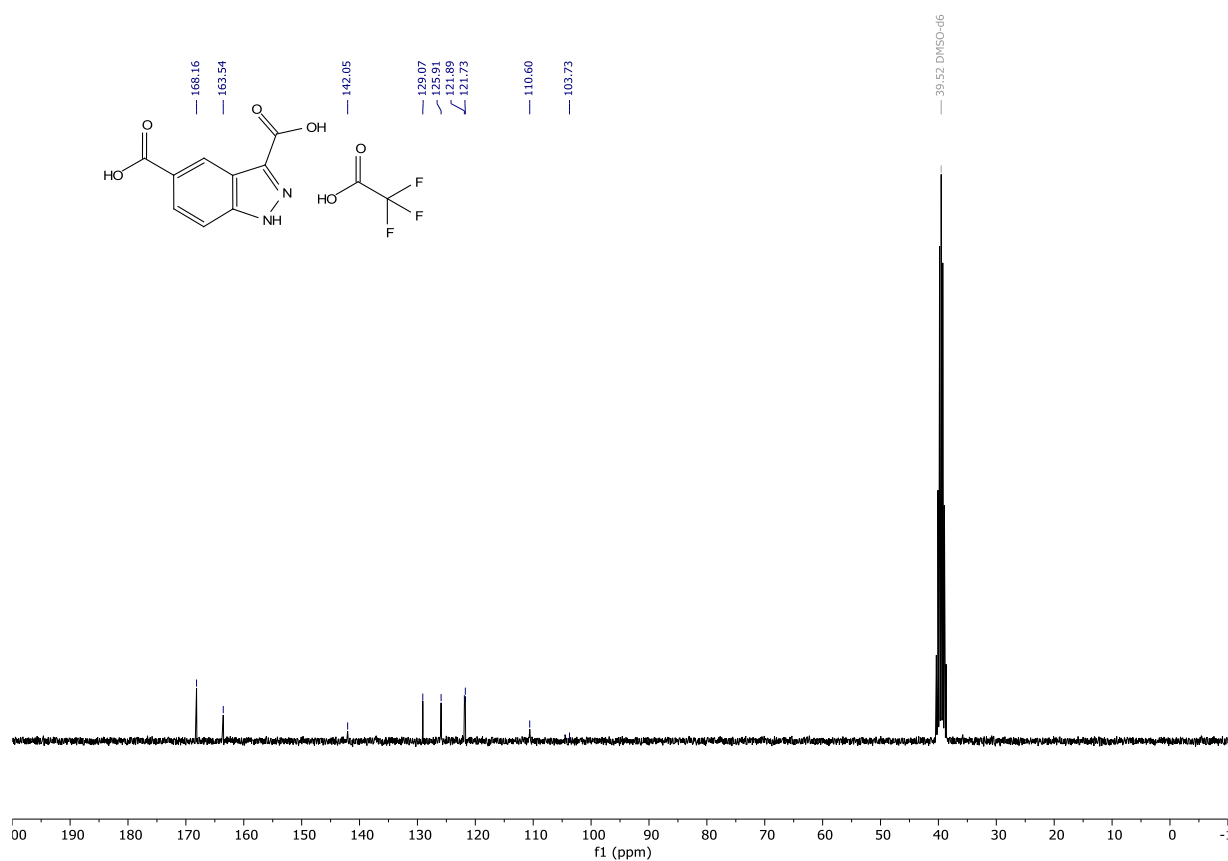
(1H-indazol-3-yl)methanol (PGUB47). To a stirred solution of LiAlH₄ (0.508 g, 13.3860 mmol) in dry THF (15 mL) at 0 °C under an argon atmosphere was added portion wise 1H-indazole-3-carboxylic acid (0.994 g, 6.1302 mmol) this resulted in vigorous gas evolution. After completed addition the ice bath was removed, and the mixture was heated to 65 °C for 16 h. The mixture was cooled to room temperature and diluted with diethyl ether. Then was added dropwise water (0.6 mL) (strong bubbling) followed by 15% aq. NaOH (0.6 mL). Then more water (10 mL) was added. The mixture was filtered through a pad of celite. The filter cake was washed with diethyl ether. The filtrate was dried over MgSO₄, filtered, and concentrated under reduced pressure onto silica gel. It was purified by flash column chromatography (dichloromethane/ methanol gradient from 1:0 to 9:1), to give the desired compound in 57% (0.51640 g, 3.48530 mmol). White crystalline solid: ¹H NMR (300 MHz, DMSO-*d*₆) δ 12.77 (s, 1H), 7.91 – 7.79 (m, 1H), 7.48 (dt, *J* = 8.4, 1.0 Hz, 1H), 7.33 (ddd, *J* = 8.3, 6.8, 1.1 Hz, 1H), 7.09 (ddd, *J* = 7.9, 6.8, 1.0 Hz, 1H), 5.20 (t, *J* = 5.8 Hz, 1H), 4.79 (d, *J* = 5.7 Hz, 2H). ¹³C NMR (75 MHz, DMSO) δ 145.57, 140.96, 125.88, 121.41, 120.60, 119.65, 109.96, 56.77. HRMS (ESI) calculated for [M-H]⁻ C₈H₉N₂O 149.0709, found 149.0710. Purity (HPLC): >96% UV₂₁₄, >98% UV₂₅₄.

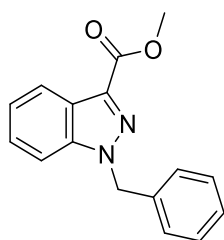




3,5-dicarboxy-1*H*-indazol-1-ium trifluoroacetate (PGUB49). To a stirred solution of sodium perborate tetrahydrate (0.17989 g, 1.1692 mmol) in water (3 mL) at 50 °C was added a solution of 5-cyano-1*H*-indazole-3-carboxylic acid (0.07266 g, 0.3882 mmol) in a mixture of methanol (3 mL) and water (6 mL) giving a yellowish solution. This solution was stirred at 50 °C for 16 h. After 16 h it was cooled to 21 °C. Most of the methanol was removed under reduced pressure. The pH was adjusted with TFA (ca. 150 μ L), which caused precipitation of a white solid. This solid was dissolved in DMF, filtered, and concentrated again under reduced pressure to give the desired product in 41% yield (0.05078g, 0.15851 mmol). Yellowish solid slightly impure with DMF: ^1H NMR (300 MHz, DMSO- d_6) δ 13.96 (s, 1H), 13.18 (s, 1H), 8.65 (s, 1H), 8.10 (s, 1H), 7.93 (d, J = 8.9 Hz, 1H), 7.66 (d, J = 8.7 Hz, 1H), 7.33 (s, 1H). ^{13}C NMR (75 MHz, DMSO) δ 168.16, 163.54, 142.05, 129.07, 125.91, 121.89, 121.73, 110.60, 103.73. ^{19}F NMR (282 MHz, DMSO) δ -73.48. HRMS (ESI) calculated for $[\text{M}+\text{H}]^+$ $\text{C}_9\text{H}_7\text{N}_2\text{O}_4$ 207.0400, mass not found. **Purity (HPLC):** >97% UV_{214} , >98% UV_{254} .

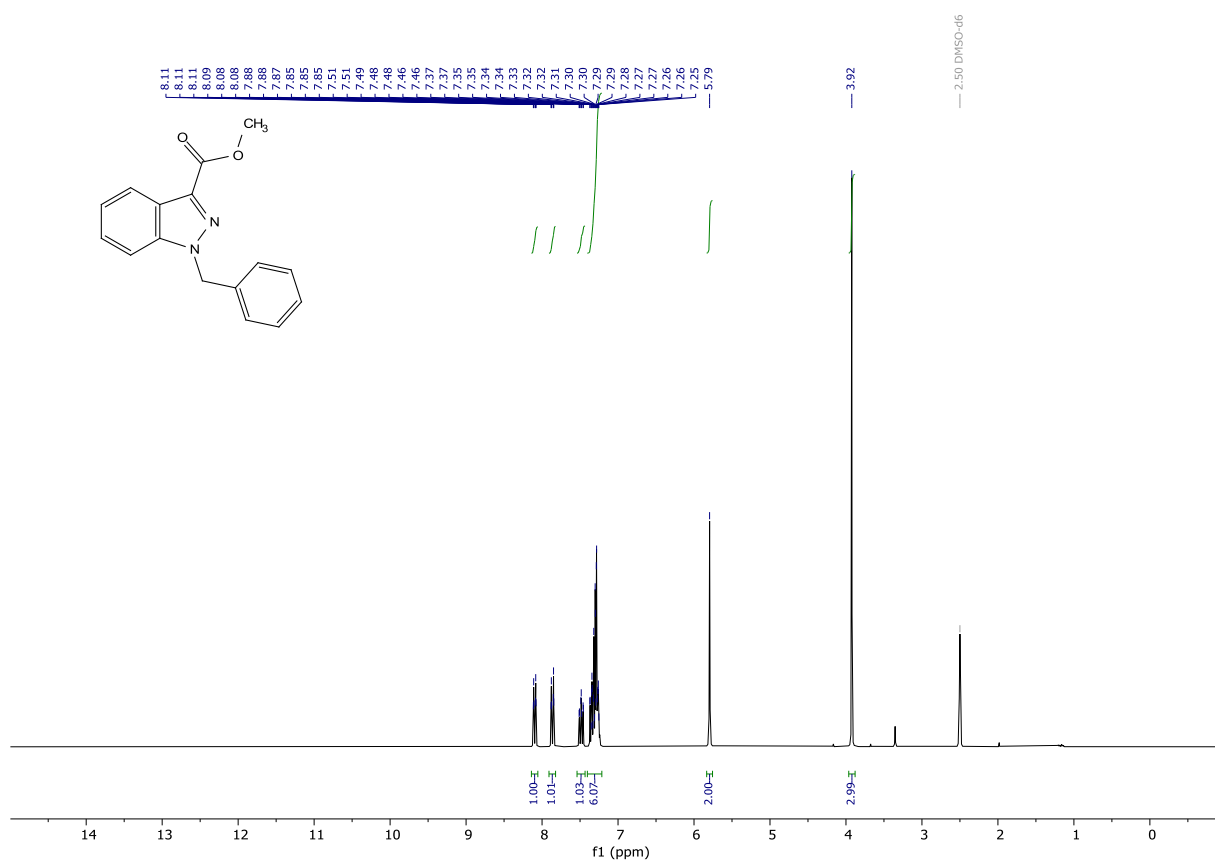


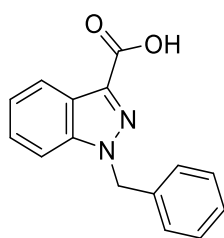
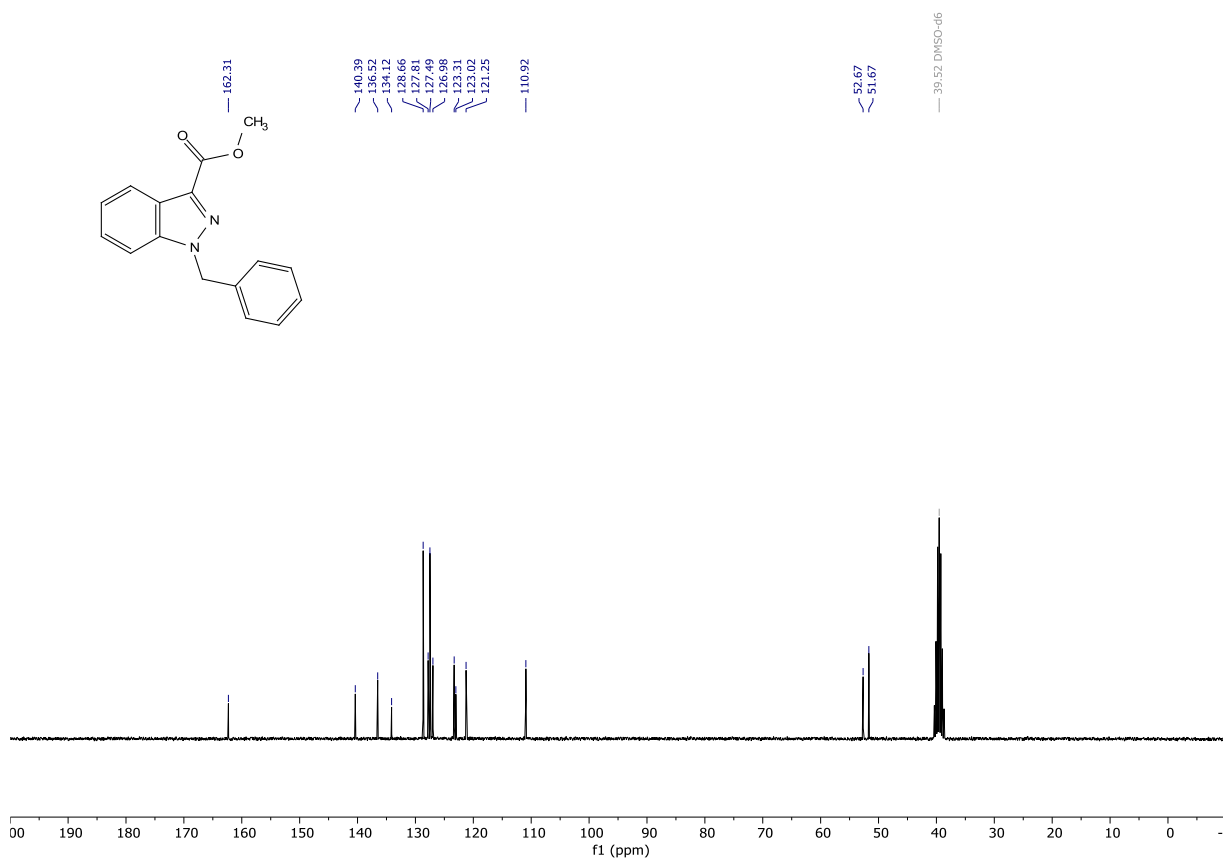




PGUB50

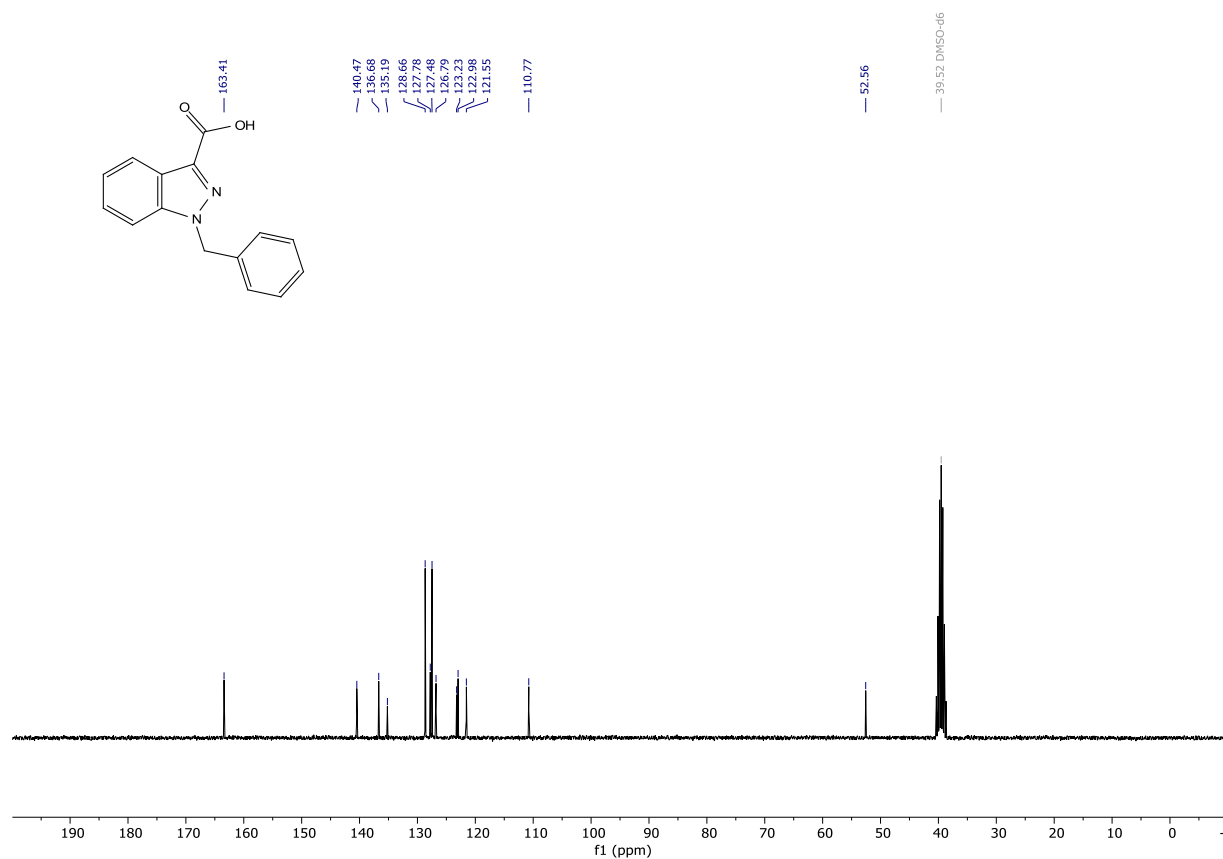
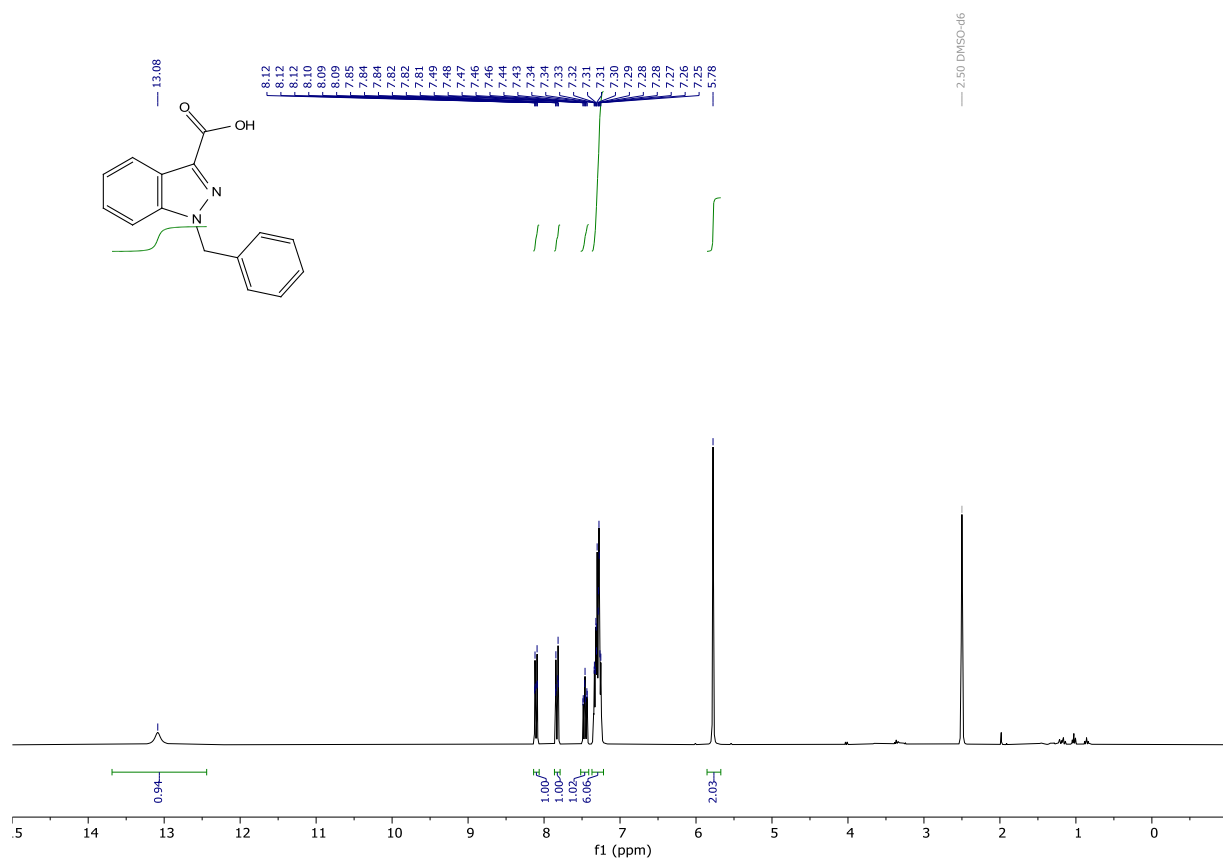
methyl 1-benzyl-1H-indazole-3-carboxylate (PGUB50) (Z = N, Y = OMe). Prepared according to general procedure II from methyl 1H-indazole-3-carboxylate (Z = N, Y = OMe, 0.31267 g, 1.7748 mmol) using benzyl bromide as alkyl halide, to give the desired product in 79% yield (0.37418 g, 1.405107 mmol). White solid: $^1\text{H NMR}$ (300 MHz, DMSO- d_6) δ 8.10 (dt, J = 8.2, 1.0 Hz, 1H), 7.86 (dt, J = 8.6, 0.9 Hz, 1H), 7.48 (ddd, J = 8.4, 6.9, 1.1 Hz, 1H), 7.40 – 7.21 (m, 6H), 5.79 (s, 2H), 3.92 (s, 3H). $^{13}\text{C NMR}$ (75 MHz, DMSO) δ 162.31, 140.39, 136.52, 134.12, 128.66, 127.81, 127.49, 126.98, 123.31, 123.02, 121.25, 110.92, 52.67, 51.67. **HRMS** (ESI) calculated for $[\text{M}+\text{H}]^+$ $\text{C}_{16}\text{H}_{15}\text{N}_2\text{O}_2$ 267.1128, found 267.1137.

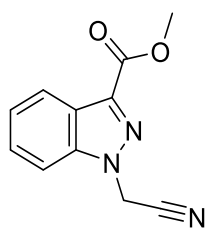




PGUB51

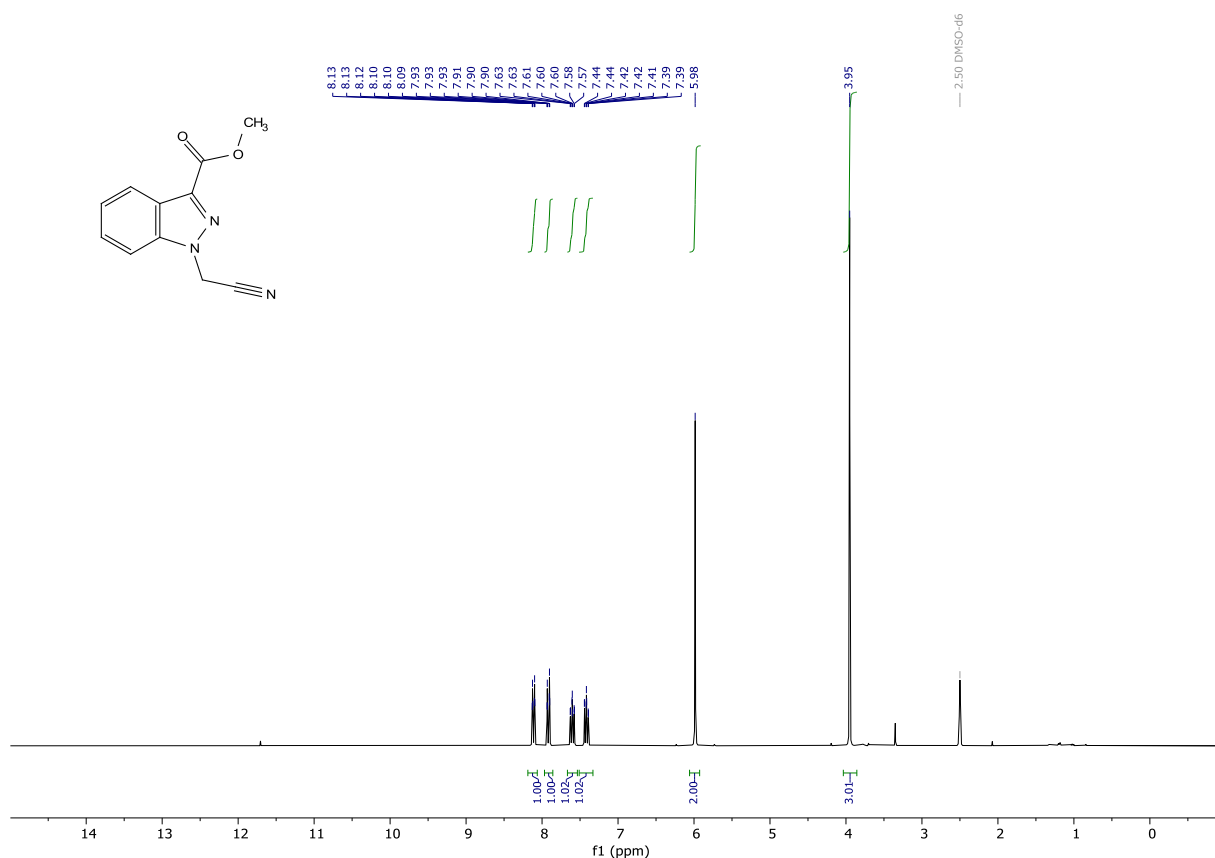
1-benzyl-1*H*-indazole-3-carboxylic acid (PGUB51) (Z = N, W = OH). Prepared according to general procedure III from methyl 1-benzyl-1*H*-indazole-3-carboxylate (Z = N, Y = OMe, 0.157 g, 0.5896 mmol), to give the desired product in quantitative yield (0.14820 g, 0.58746 mmol). White solid: **¹H NMR** (300 MHz, DMSO-*d*₆) δ 13.08 (s, 1H), 8.10 (dd, *J* = 8.1, 1.1 Hz, 1H), 7.86 – 7.79 (m, 1H), 7.46 (ddd, *J* = 8.4, 6.9, 1.2 Hz, 1H), 7.37 – 7.22 (m, 6H), 5.78 (s, 2H). **¹³C NMR** (75 MHz, DMSO) δ 163.41, 140.47, 136.68, 135.19, 128.66, 127.78, 127.48, 126.79, 123.23, 122.98, 121.55, 110.77, 52.56. **HRMS** (ESI) calculated for [M-H][−] C₁₅H₁₁N₂O₂ 251.0826, found 251.0826. **Purity (HPLC):** >98% UV₂₁₄, >97% UV₂₅₄.

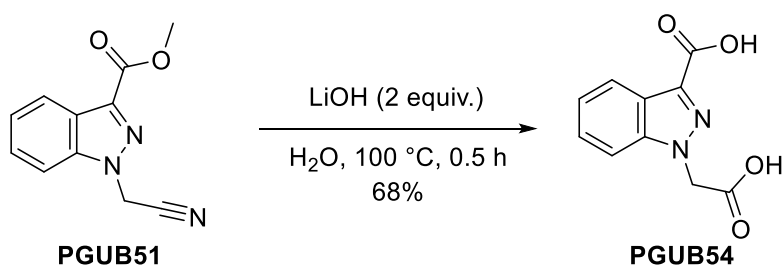
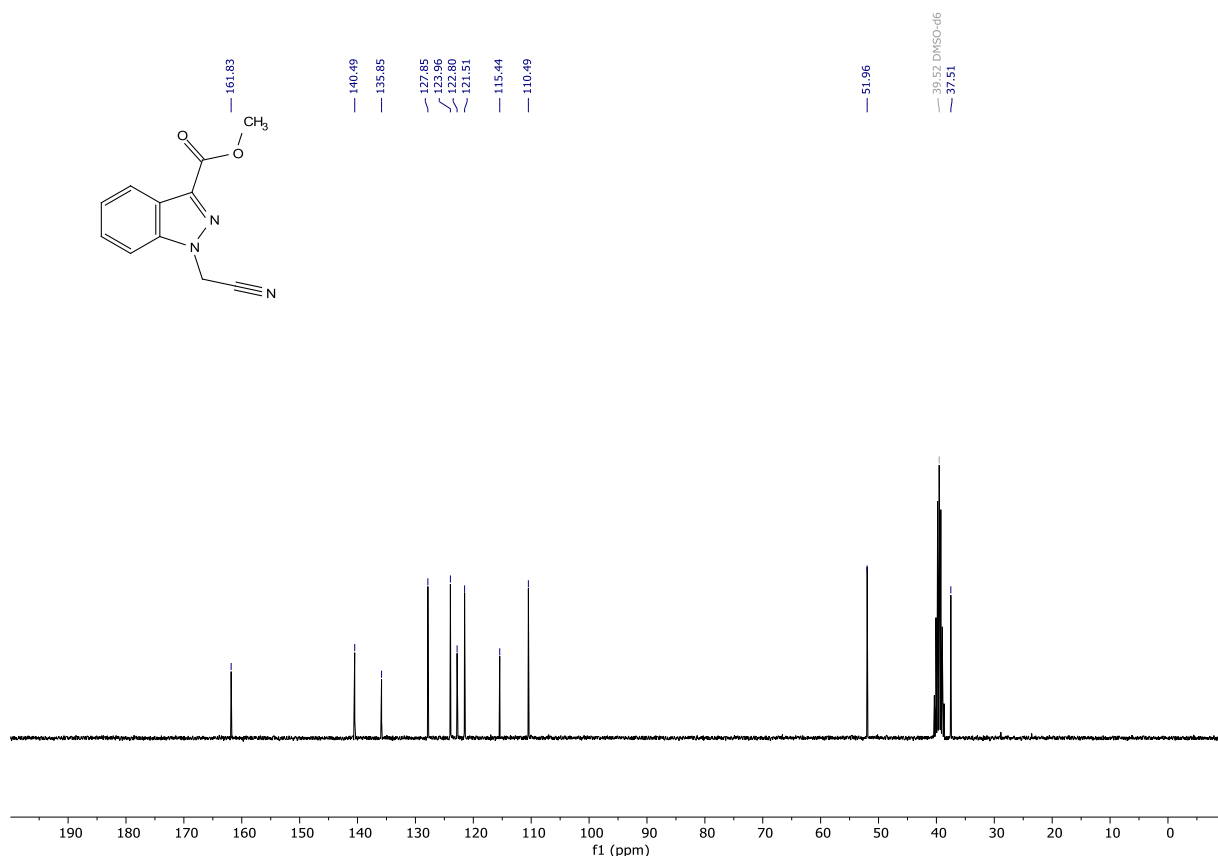




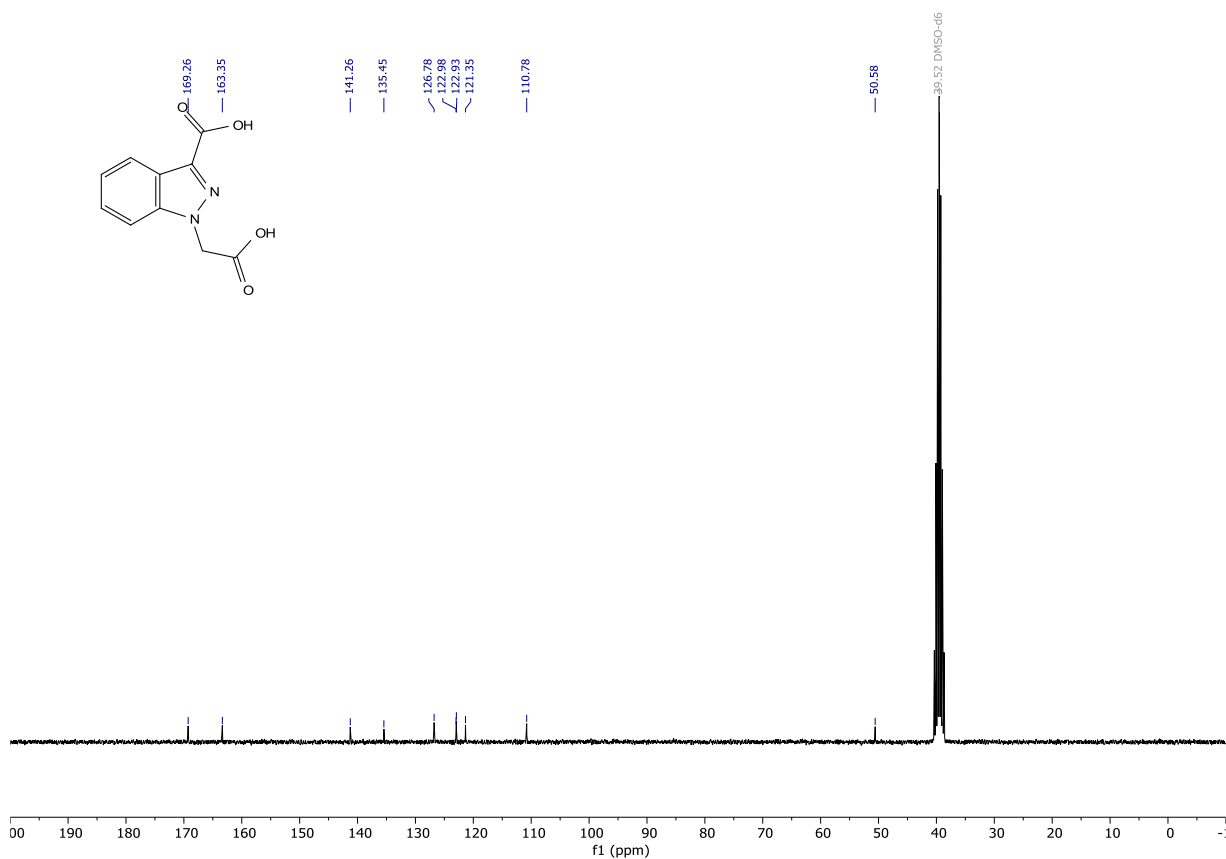
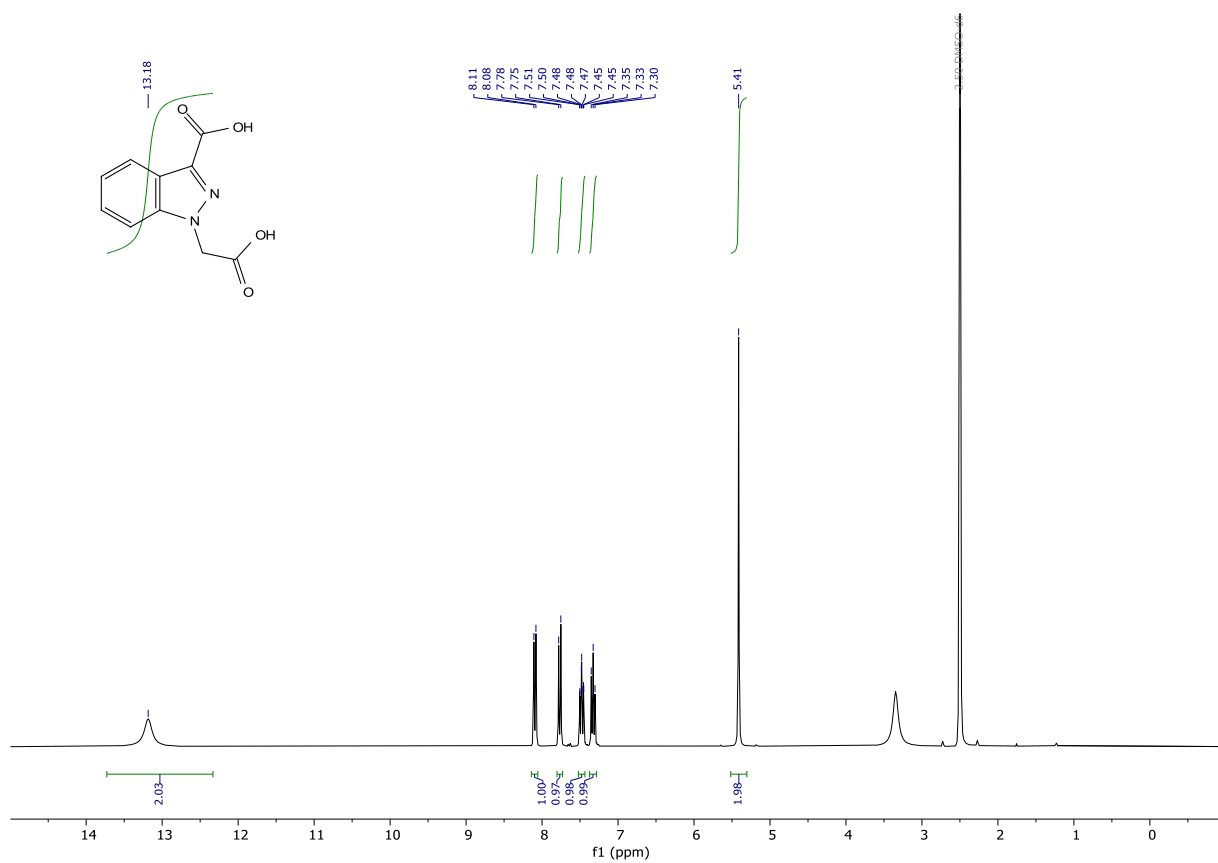
PGUB52

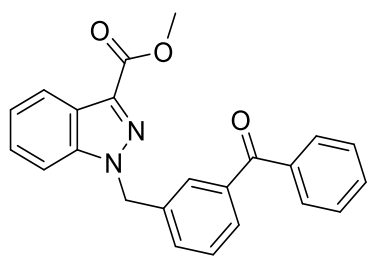
methyl 1-(cyanomethyl)-1H-indazole-3-carboxylate (PGUB50) (Z = N, Y = OMe). Prepared according to general procedure II from methyl 1H-indazole-3-carboxylate (Z = N, Y = OMe, 0.35965 g, 2.0414 mmol) using bromoacetonitrile as alkyl halide, to give the desired product in 87% yield (0.43934 g, 1.77839 mmol). White solid: ^1H NMR (300 MHz, DMSO- d_6) δ 8.11 (dt, J = 8.2, 1.0 Hz, 1H), 7.92 (dt, J = 8.6, 0.9 Hz, 1H), 7.60 (ddd, J = 8.4, 7.0, 1.1 Hz, 1H), 7.42 (ddd, J = 8.0, 6.9, 0.8 Hz, 1H), 5.98 (s, 2H), 3.95 (s, 3H). ^{13}C NMR (75 MHz, DMSO) δ 161.83, 140.49, 135.85, 127.85, 123.96, 122.80, 121.51, 115.44, 110.49, 51.96, 37.51. HRMS (ESI) calculated for $[\text{M}+\text{H}]^+$ $\text{C}_{11}\text{H}_{10}\text{N}_3\text{O}_2$ 216.0768, found 216.0774.



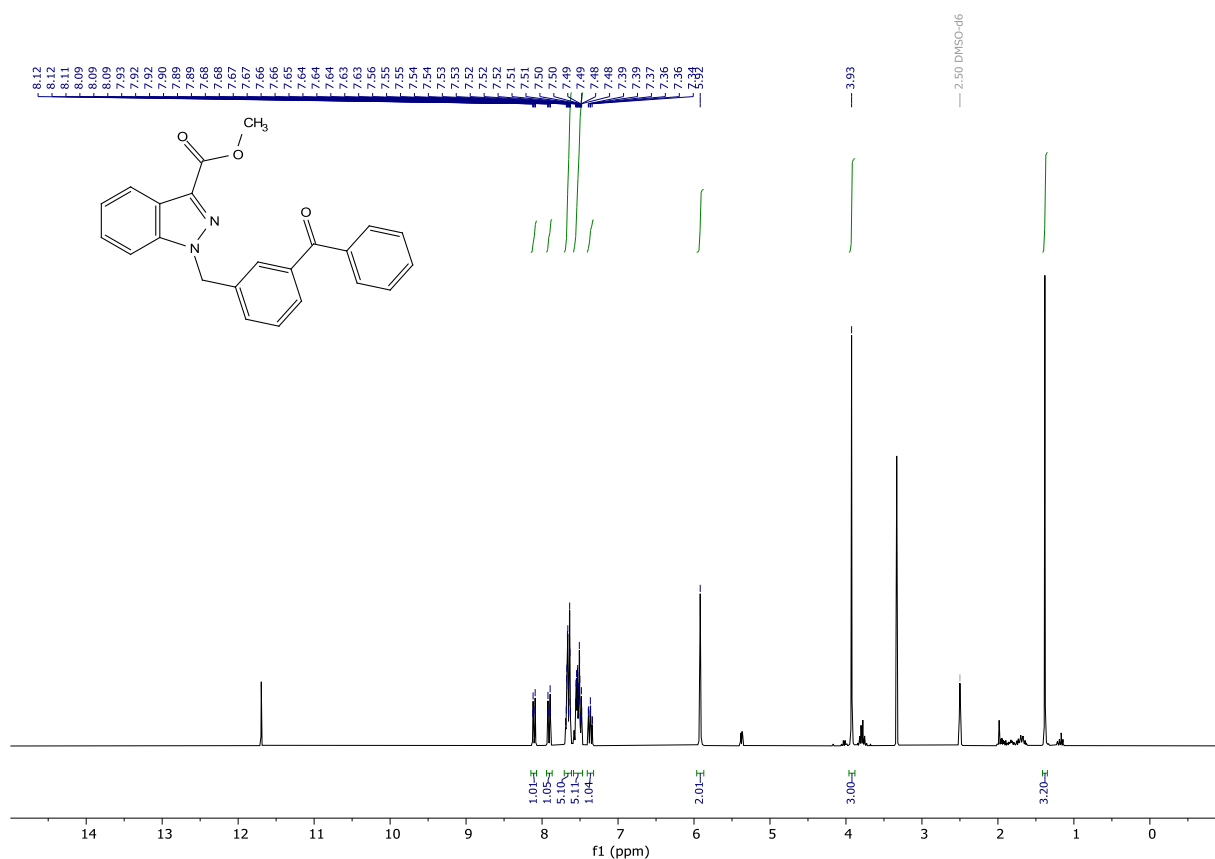


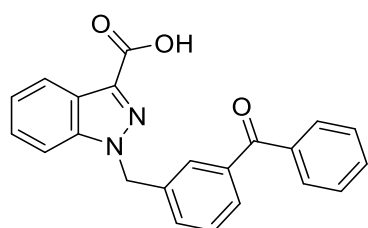
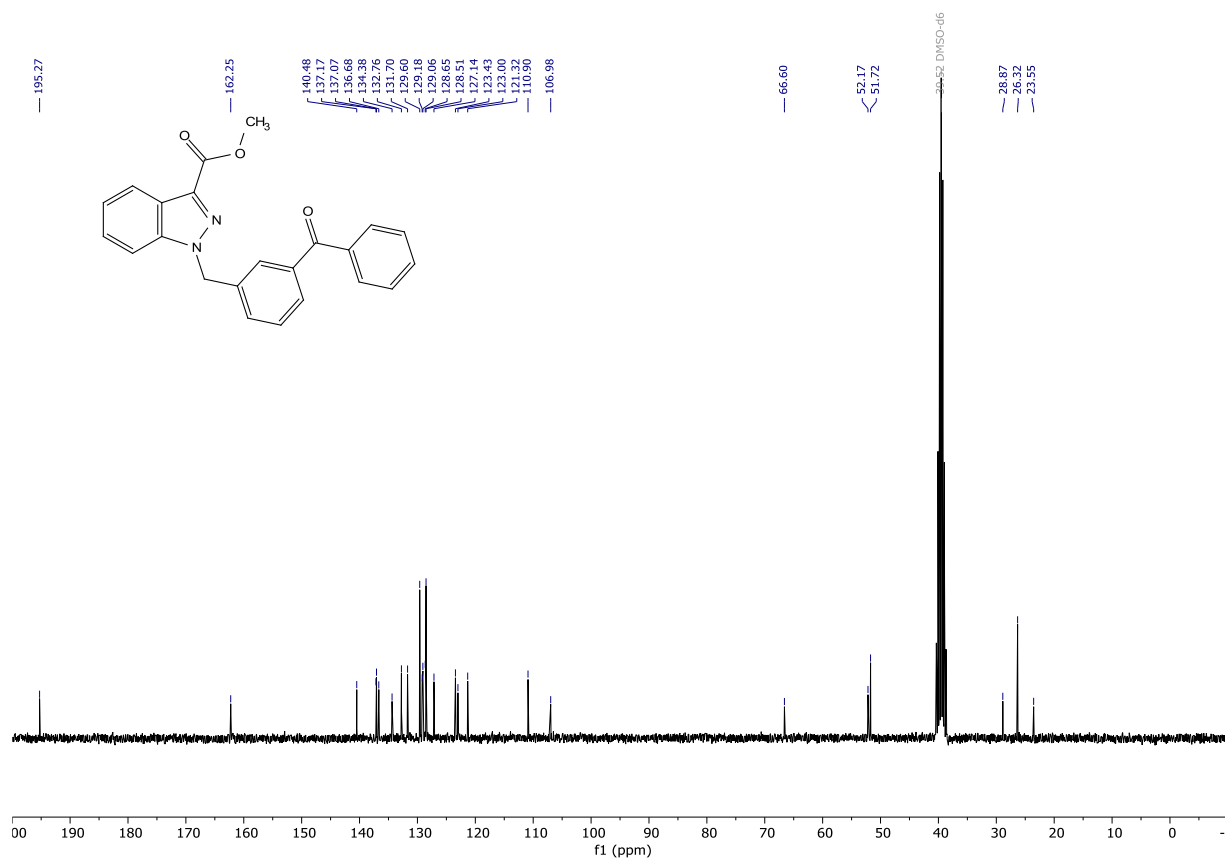
1-(carboxymethyl)-1H-indazole-3-carboxylic acid (PGUB54). To methyl 1-(cyanomethyl)-1H-indazole-3-carboxylate (PGUB51) (0.15003 g, 0.6971 mmol) was added LiOH monohydrate (0.074 g, 1.7636 mmol) in water (7 mL). The suspension was stirred and heated to 100 °C for 0.5 h. The mixture was acidified with 1 M aq. HCl and extracted with ethyl acetate. The combined organic phases were dried over MgSO₄, filtered, and concentrated under reduced pressure to give a white solid. This solid was taken up in a mixture of ethanol and acetone and was concentrated onto silica gel. The crude was purified by reverse phase column chromatography (water + 0.1% TFA/ acetonitrile + 0.1% TFA gradient from 4:1 to 0:1), to give the desired compound in 68% yield (0.10451 g, 0.47465 mmol). White solid: ¹H NMR (300 MHz, DMSO-*d*₆) δ 13.18 (s, 2H), 8.09 (d, *J* = 8.1 Hz, 1H), 7.77 (d, *J* = 8.5 Hz, 1H), 7.48 (ddd, *J* = 8.3, 6.9, 1.1 Hz, 1H), 7.33 (t, *J* = 7.5 Hz, 1H), 5.41 (s, 2H). ¹³C NMR (75 MHz, DMSO) δ 169.26, 163.35, 141.26, 135.45, 126.78, 122.98, 122.93, 121.35, 110.78, 50.58. . HRMS (ESI) calculated for [M-H]⁻ C₁₀H₇N₂O₄ 219.0411, found 219.0416. **Purity (HPLC):** >96% UV₂₁₄, >99% UV₂₅₄.





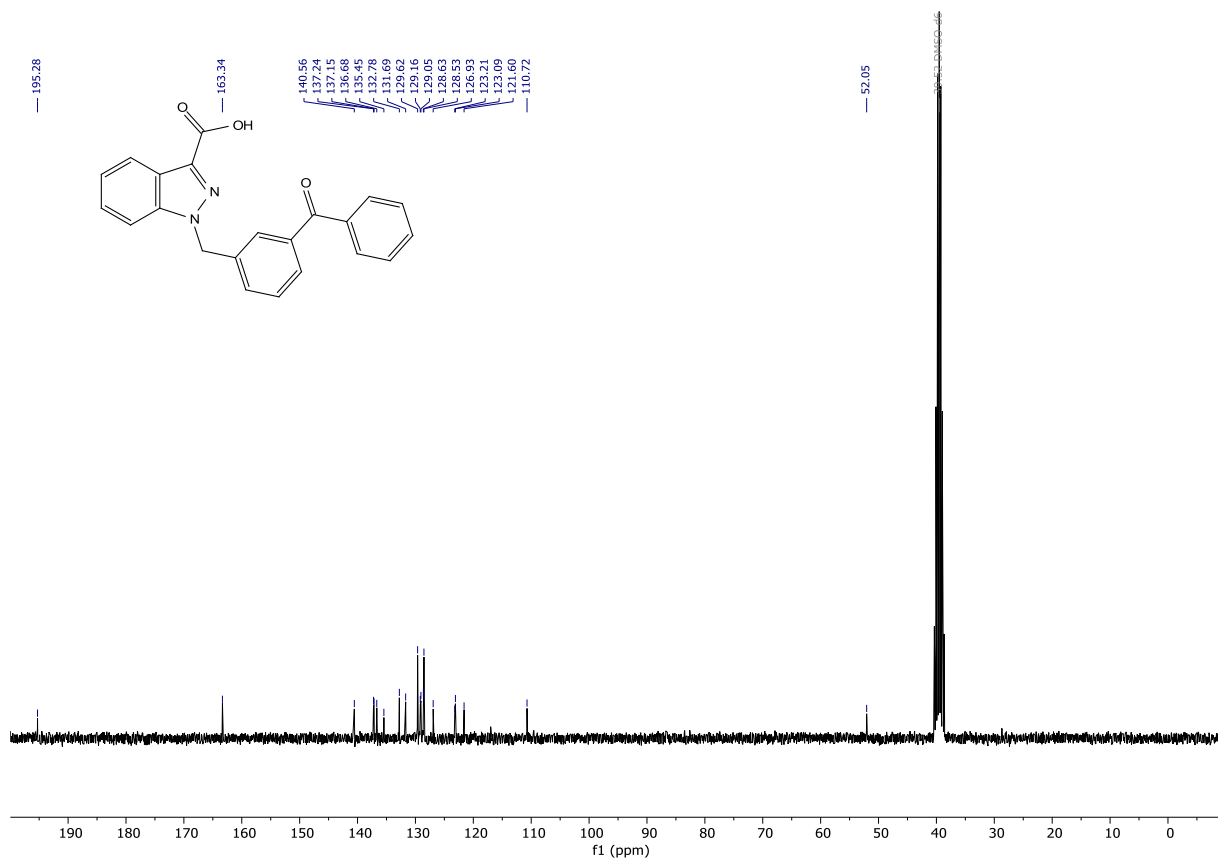
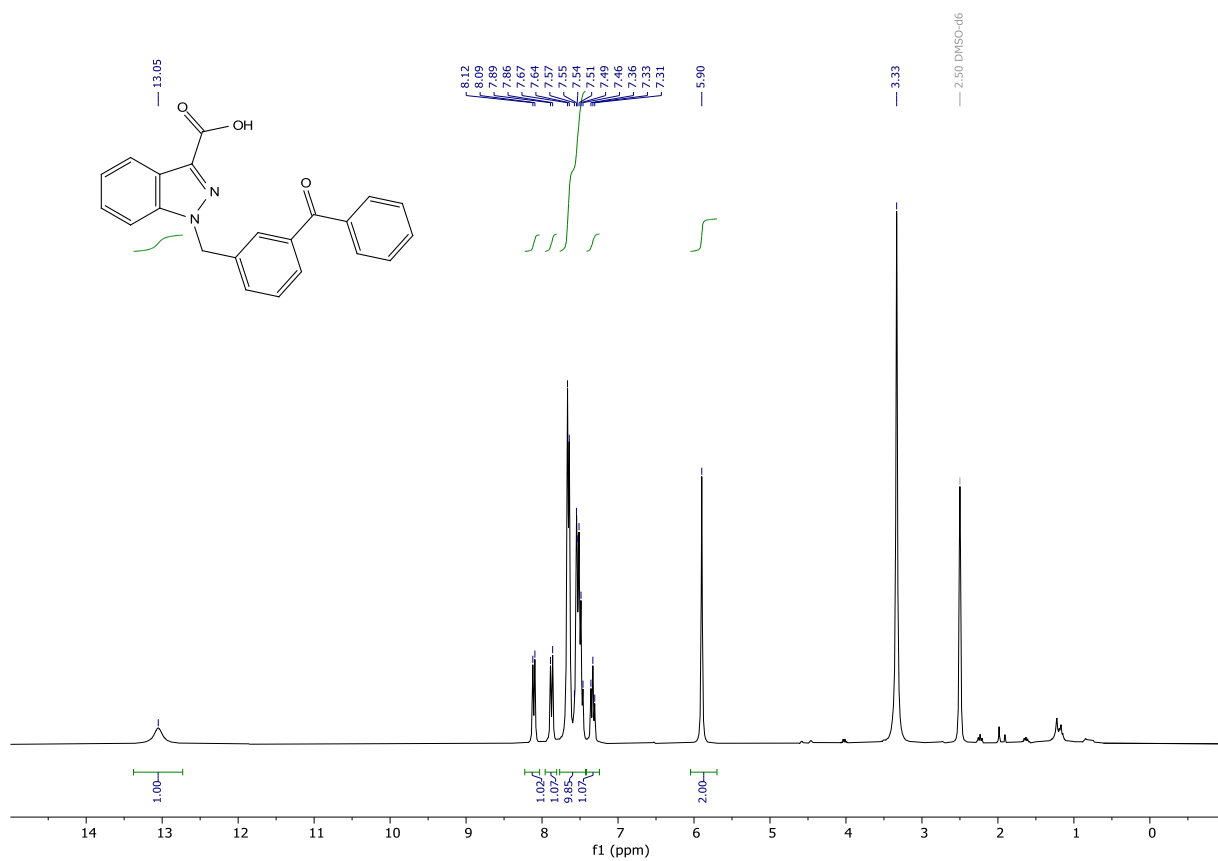
methyl 1-(3-benzoylbenzyl)-1H-indazole-3-carboxylate (Z = N, Y = OMe). Prepared according to general procedure II from methyl 1H-indazole-3-carboxylate (Z = N, Y = OMe, 0.19787 g, 1.1231 mmol) using 3-benzoylbenzyl bromide as alkyl halide, to give the desired product in 55% yield (0.22977 g, 0.62032 mmol). White solid: $^1\text{H NMR}$ (300 MHz, DMSO- d_6) δ 8.10 (dt, J = 8.2, 1.0 Hz, 1H), 7.91 (dt, J = 8.6, 1.0 Hz, 1H), 7.71 – 7.61 (m, 5H), 7.59 – 7.47 (m, 5H), 7.36 (ddd, J = 8.0, 6.9, 0.9 Hz, 1H), 5.92 (s, 2H), 3.93 (s, 3H), 1.38 (s, 3H). $^{13}\text{C NMR}$ (75 MHz, DMSO) δ 195.27, 162.25, 140.48, 137.17, 137.07, 136.68, 134.38, 132.76, 131.70, 129.60, 129.18, 129.06, 128.65, 128.51, 127.14, 123.43, 123.00, 121.32, 110.90, 106.98, 66.60, 52.17, 51.72, 28.87, 26.32, 23.55. **HRMS** (ESI) calculated for $[\text{M}+\text{H}]^+$ $\text{C}_{23}\text{H}_{19}\text{N}_2\text{O}_3$ 371.1390, found 371.1395.

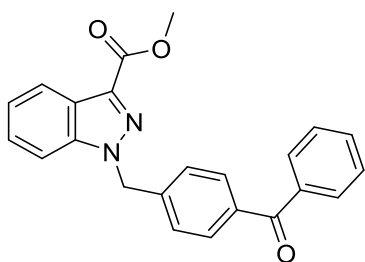




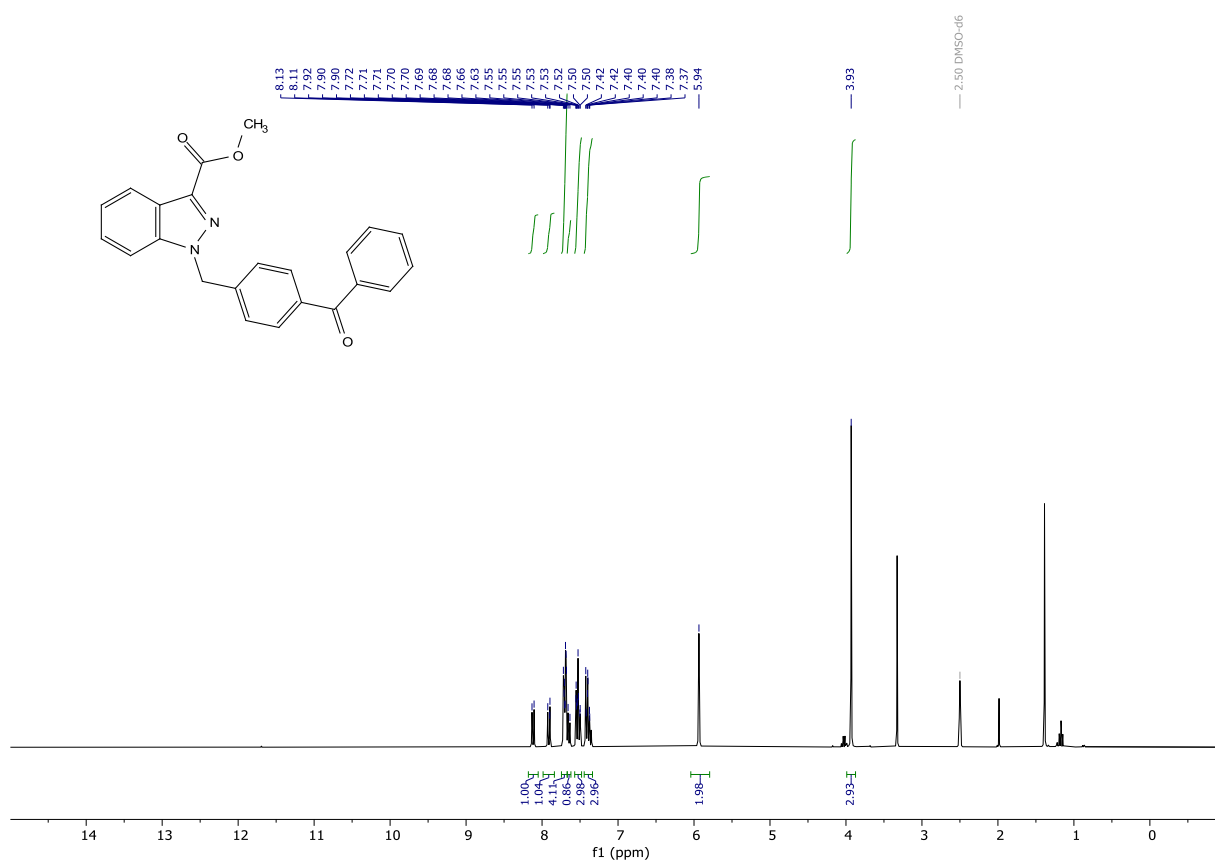
PGUB55

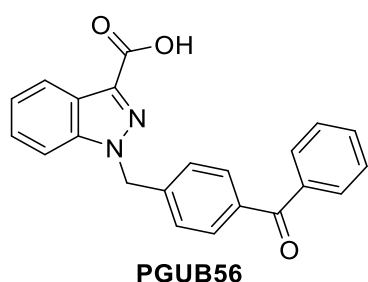
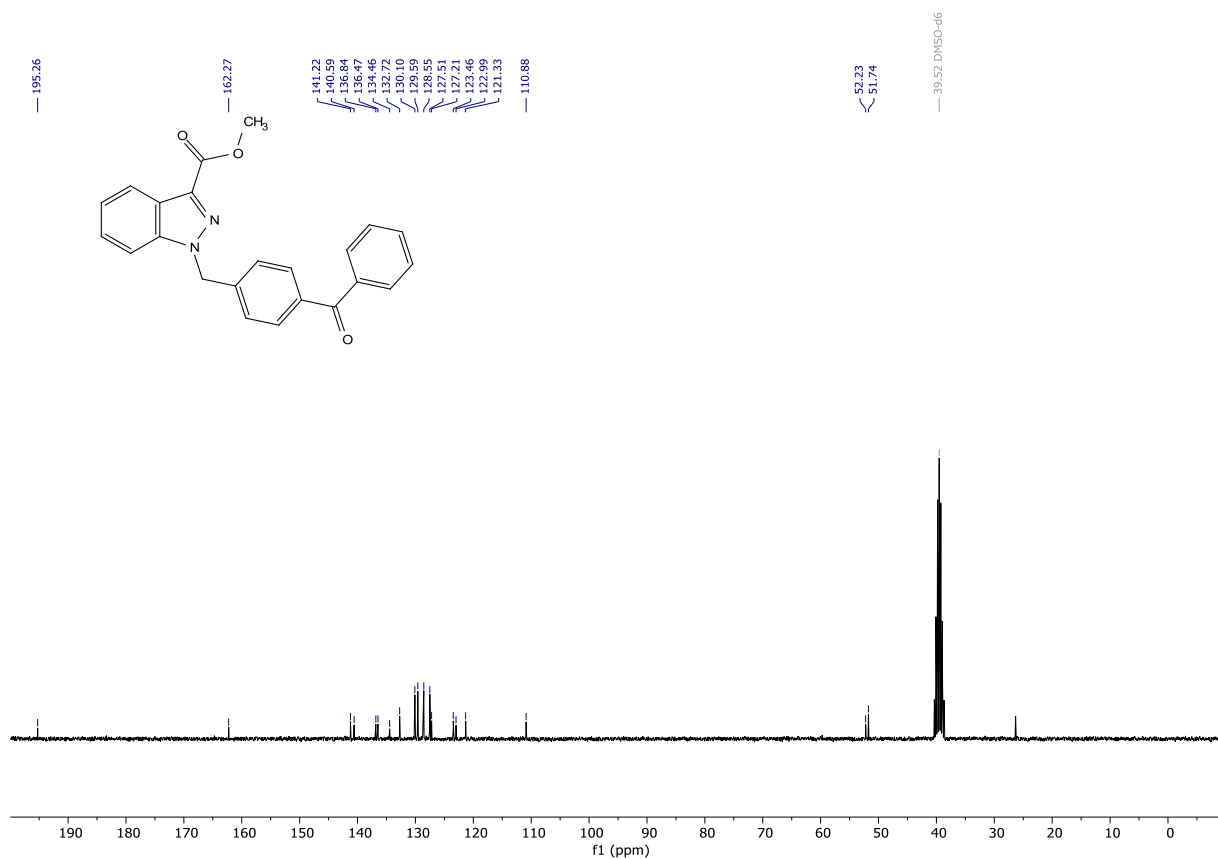
1-(3-benzoylbenzyl)-1H-indazole-3-carboxylic acid (PGUB55) (Z = N, W = OH). Prepared according to general procedure III from methyl 1-(3-benzoylbenzyl)-1H-indazole-3-carboxylate (Z = N, Y = OMe, 0.20043 g, 0.5411 mmol), to give the desired product in 89% yield (0.17120 g, 0.48039 mmol). White solid: $^1\text{H NMR}$ (300 MHz, DMSO- d_6) δ 13.05 (s, 1H), 8.11 (d, J = 8.1 Hz, 1H), 7.87 (d, J = 8.5 Hz, 1H), 7.77 – 7.43 (m, 10H), 7.33 (t, J = 7.5 Hz, 1H), 5.90 (s, 2H). $^{13}\text{C NMR}$ (75 MHz, DMSO) δ 195.28, 163.34, 140.56, 137.24, 137.15, 136.68, 135.45, 132.78, 131.69, 129.62, 129.16, 129.05, 128.63, 128.53, 126.93, 123.21, 123.09, 121.60, 110.72, 52.05. **HRMS** (ESI) calculated for $[\text{M}+\text{H}]^+$ $\text{C}_{22}\text{H}_{15}\text{N}_2\text{O}_3$ 355.1077, found 355.1087. **Purity (HPLC):** >97% UV_{214} , >99% UV_{254} .



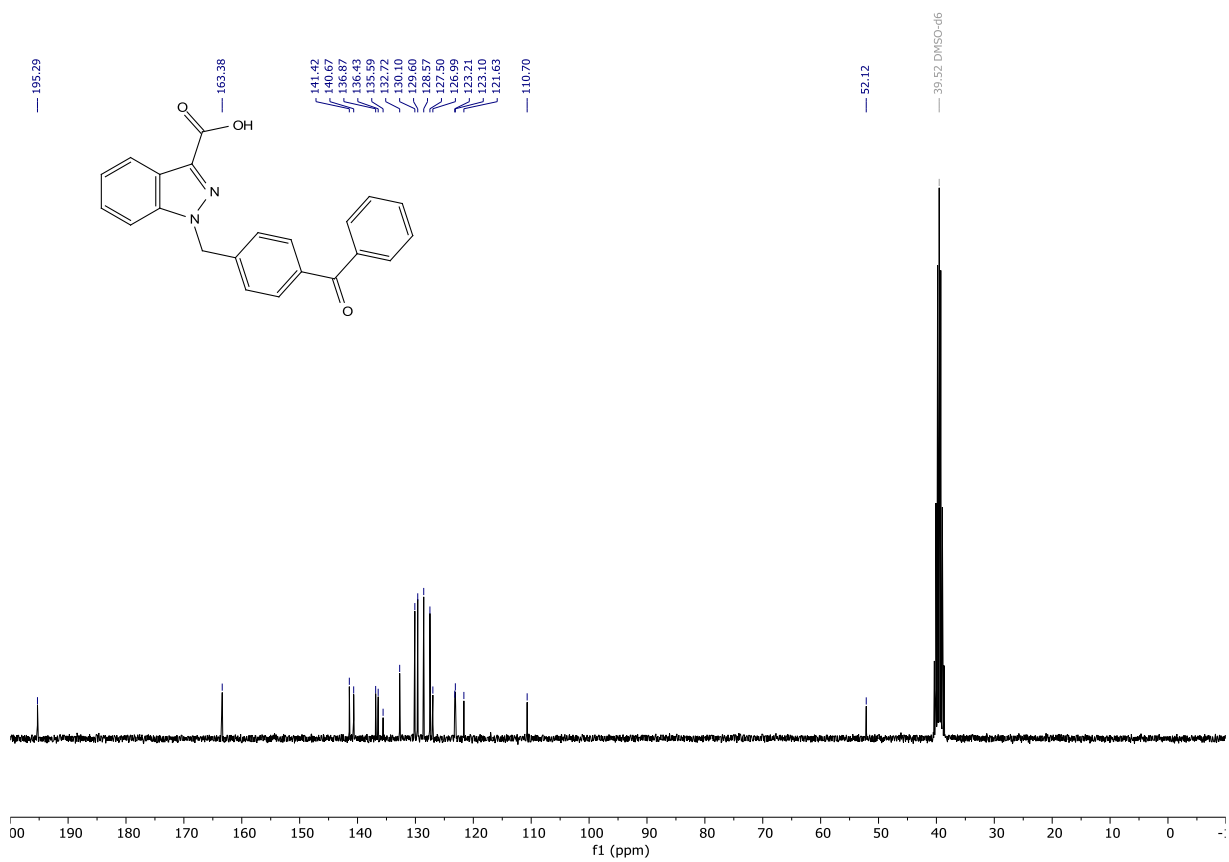
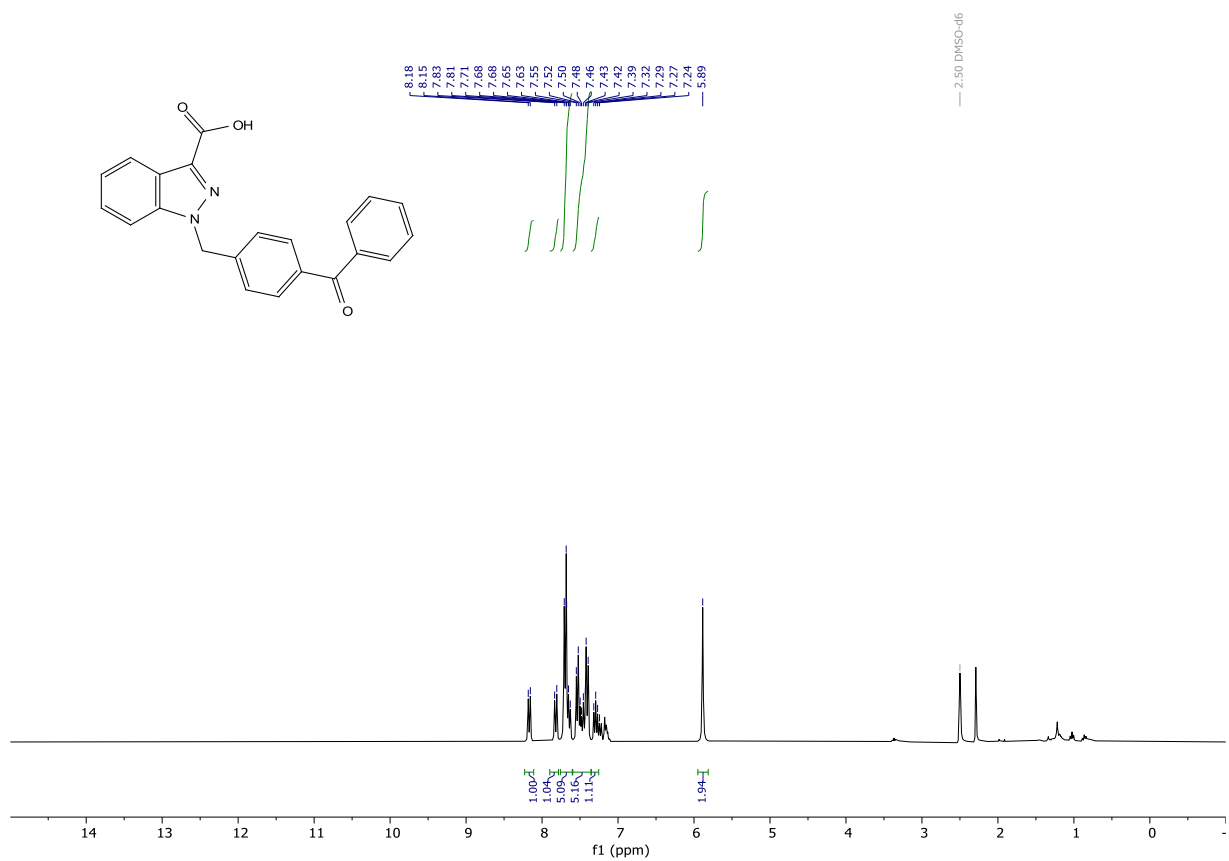


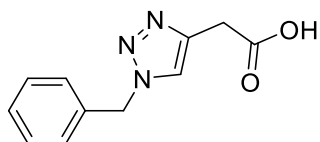
methyl 1-(4-benzoylbenzyl)-1H-indazole-3-carboxylate (Z = N, Y = OMe). Prepared according to general procedure II from methyl 1H-indazole-3-carboxylate (Z = N, Y = OMe, 0.20747 g, 1.1776 mmol) using 3-benzoylbenzyl bromide as alkyl halide, to give the desired product in 46% yield (0.20005 g, 0.54008 mmol). White solid slightly impure with cyclohexane: **¹H NMR** (300 MHz, DMSO-*d*₆) δ 8.12 (d, *J* = 8.2 Hz, 1H), 7.99 – 7.84 (m, 1H), 7.74 – 7.67 (m, 4H), 7.65 (d, *J* = 7.4 Hz, 1H), 7.57 – 7.48 (m, 3H), 7.40 (ddd, *J* = 8.0, 6.9, 1.4 Hz, 3H), 5.94 (s, 2H), 3.93 (s, 3H). **¹³C NMR** (75 MHz, DMSO) δ 195.26, 162.27, 141.22, 140.59, 136.84, 136.47, 134.46, 132.72, 130.10, 129.59, 128.55, 127.51, 127.21, 123.46, 122.99, 121.33, 110.88, 52.23, 51.74. **HRMS** (ESI) calculated for [M+H]⁺ C₂₃H₁₉N₂O₃ 371.1390, found 371.1395. **Purity (HPLC):** >97% UV₂₁₄, >99% UV₂₅₄.





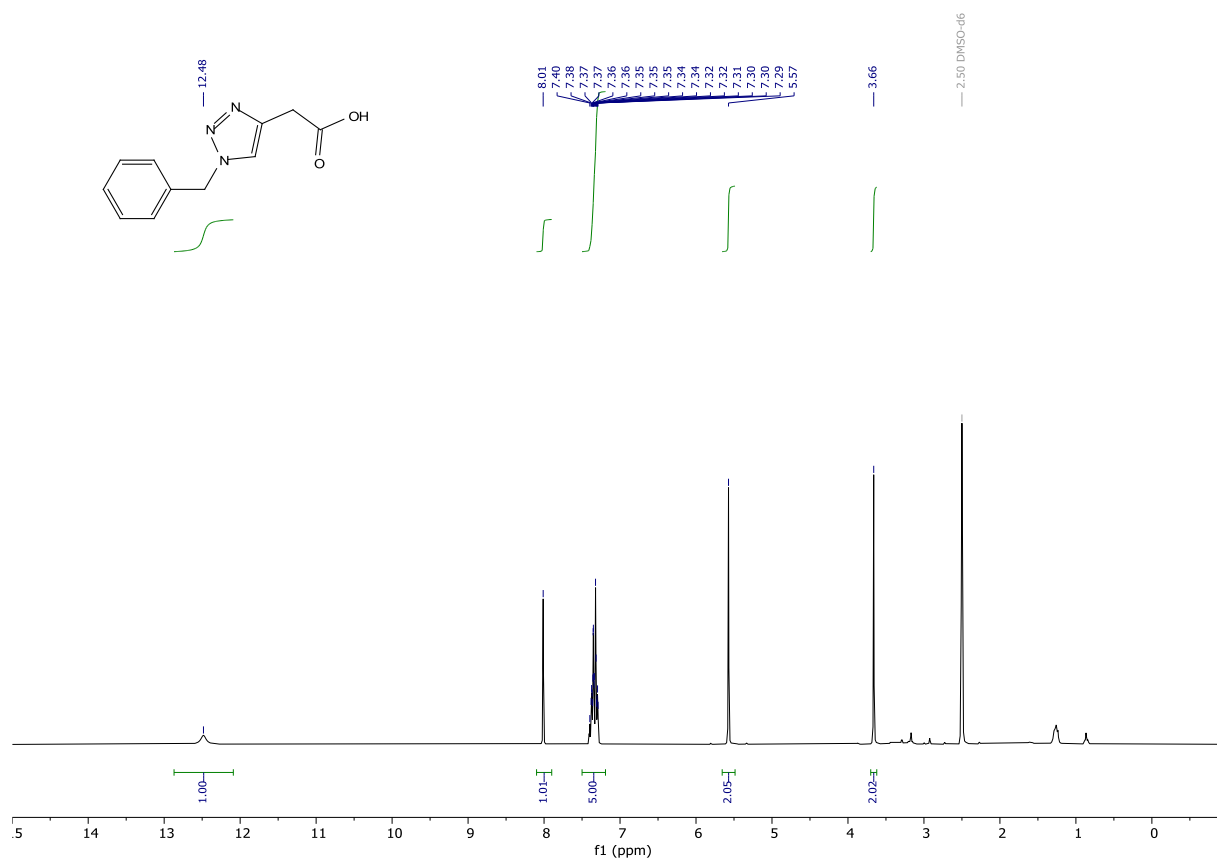
1-(4-benzoylbenzyl)-1H-indazole-3-carboxylic acid (PGUB56) (Z = N, W = OH). Prepared according to general procedure III from methyl 1-(4-benzoylbenzyl)-1H-indazole-3-carboxylate (Z = N, Y = OMe, 0.20005 g, 0.5401 mmol), to give the desired product in 73% yield (0.14443 g, 0.39529 mmol). White solid: **¹H NMR** (300 MHz, DMSO-*d*₆) δ 8.17 (d, *J* = 8.1 Hz, 1H), 7.82 (d, *J* = 8.5 Hz, 1H), 7.68 (dd, *J* = 9.2, 7.4 Hz, 5H), 7.60 – 7.35 (m, 5H), 7.36 – 7.25 (m, 1H), 5.89 (s, 2H). **¹³C NMR** (75 MHz, DMSO) δ 195.29, 163.38, 141.42, 140.67, 136.87, 136.43, 135.59, 132.72, 130.10, 129.60, 128.57, 127.50, 126.99, 123.21, 123.10, 121.63, 110.70, 52.12. **HRMS** (ESI) calculated for [M+H]⁺ C₂₂H₁₅N₂O₃ 355.1077, found 355.1085.

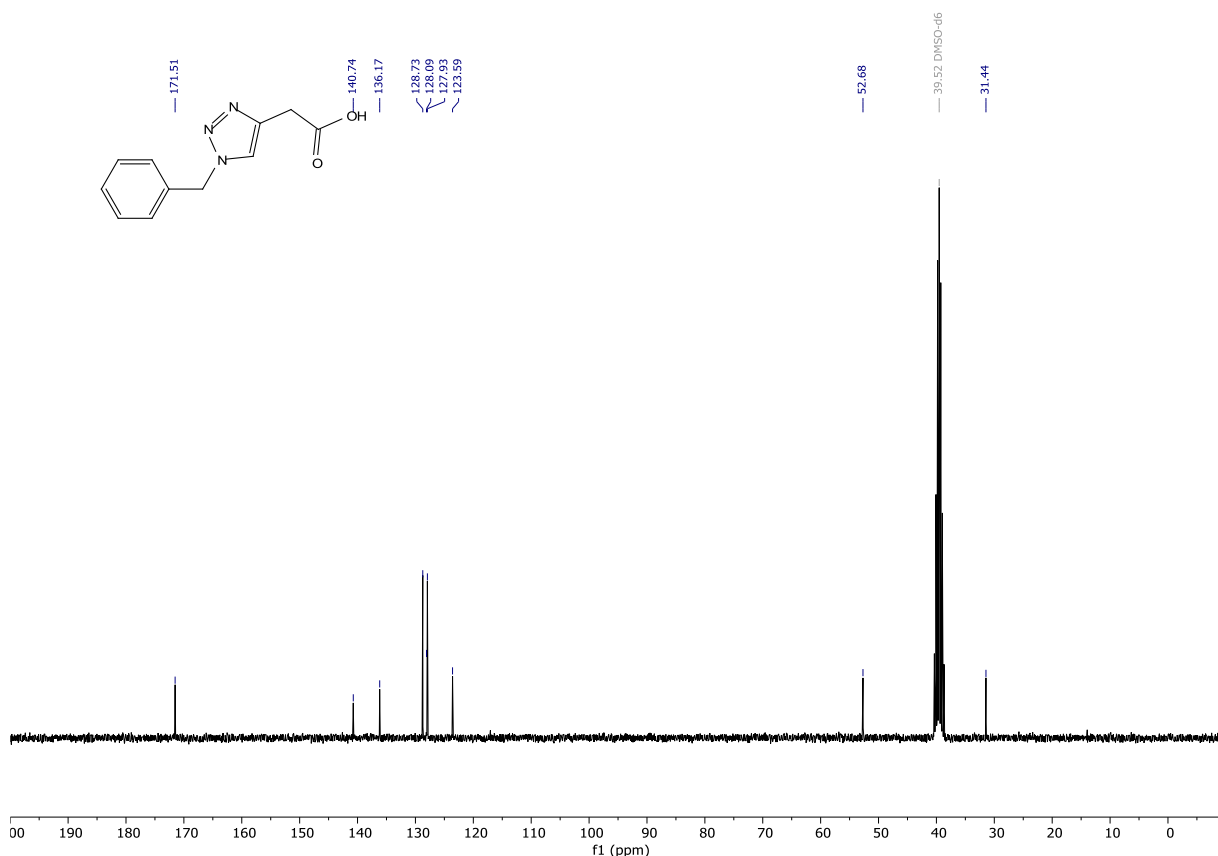




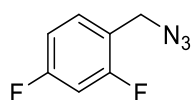
PGUB59

2-(1-benzyl-1H-1,2,3-triazol-4-yl)acetic acid (PGUB58). Prepared according to general procedure IV from 3-butynoic acid (0.04975 g, 0.5917 mmol) using benzyl azide, to give the desired product in 55% yield (0.07020 g, 0.32316 mmol). White solid: ^1H NMR (300 MHz, DMSO- d_6) δ 12.48 (s, 1H), 8.01 (s, 1H), 7.50 – 7.19 (m, 5H), 5.57 (s, 2H), 3.66 (s, 2H). ^{13}C NMR (75 MHz, DMSO) δ 171.51, 140.74, 136.17, 128.73, 128.09, 127.93, 123.59, 52.68, 31.44. HRMS (ESI) calculated for $[\text{M}+\text{H}]^+$ $\text{C}_{11}\text{H}_{10}\text{N}_3\text{O}_2$ 216.0768, found 216.0779. Purity (HPLC): >97% UV_{214} , >90% UV_{254} .





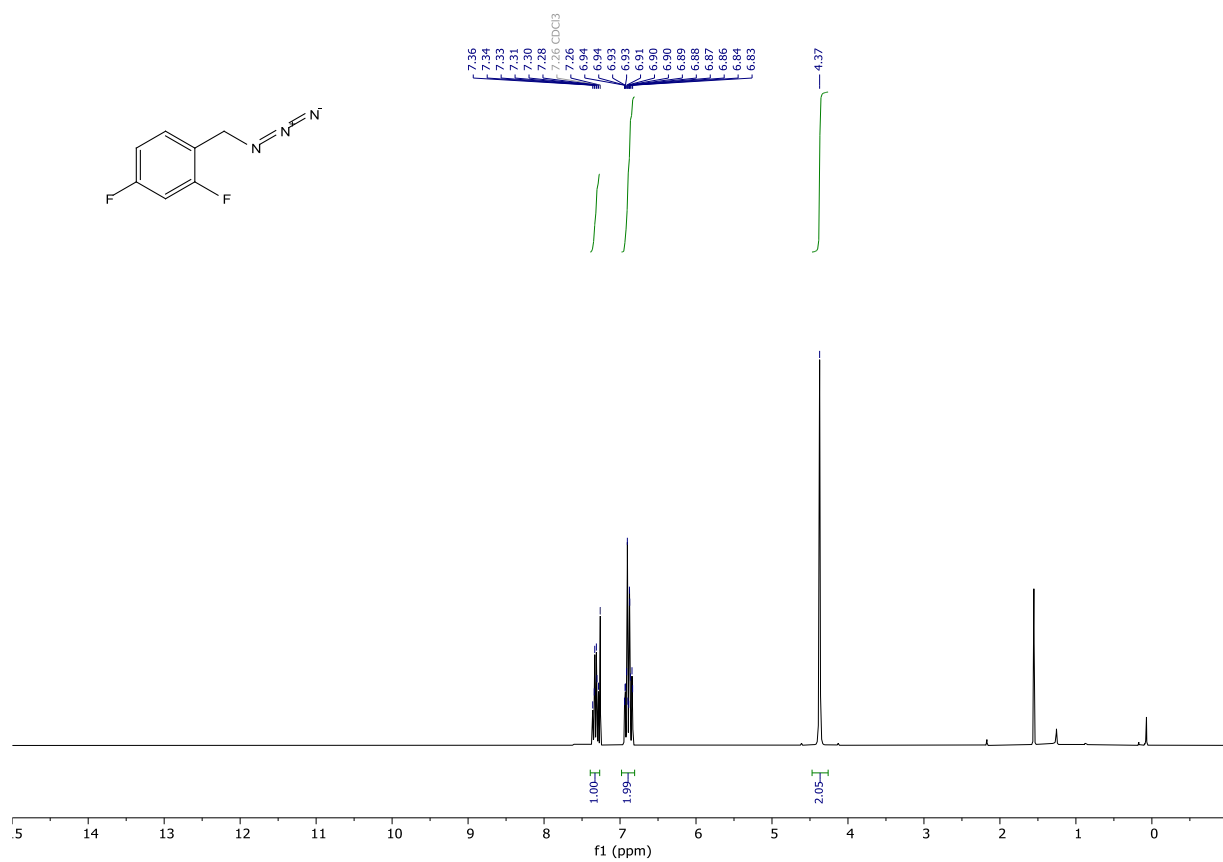
Möfflinge recipe for 4 persons. Prepared according to modified literature procedure.⁸³ The oven was preheated to 180 °C. Multigrain flour (200 g), raw cane sugar (170 g), ground almonds (130 g), cocoa powder (45 g), baking powder (12.5 g), vanilla sugar (8 g), sodium chloride (0.04 g) were thoroughly mixed. Dark chocolate (150 g) was chopped and added to the mixture. Then water (250 mL) and coconut oil (60 g) were added. The mixture was thoroughly mixed, transferred in to 12 equally sized beakers and baked in the oven at 180 °C for 0.32 h. Then chopped dark chocolate (50 g) was distributed over the 12 aliquots and the baking was continued for 0.18 h. The mixtures were removed from the oven to give the desired product in quantitative yield. Brown solid: **Taste** (averaged from 6 testers): Delicious.

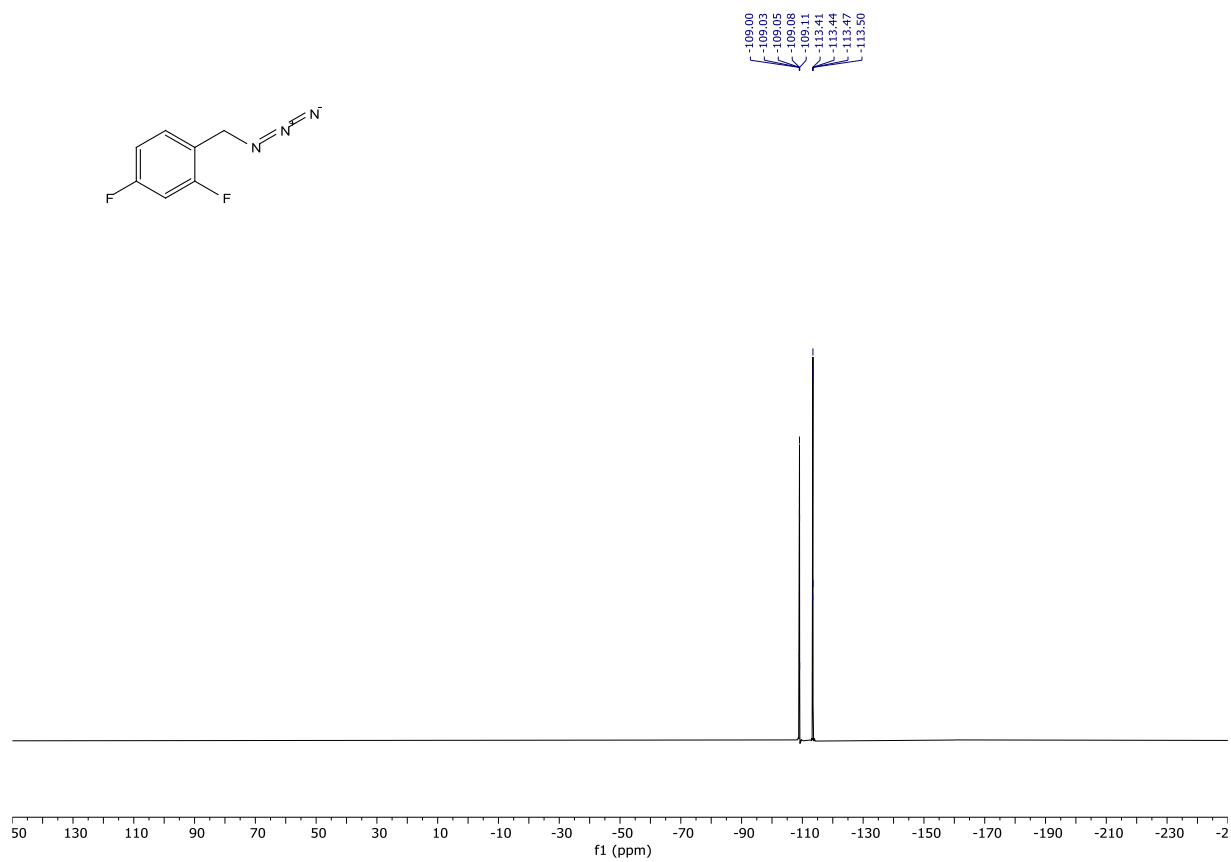
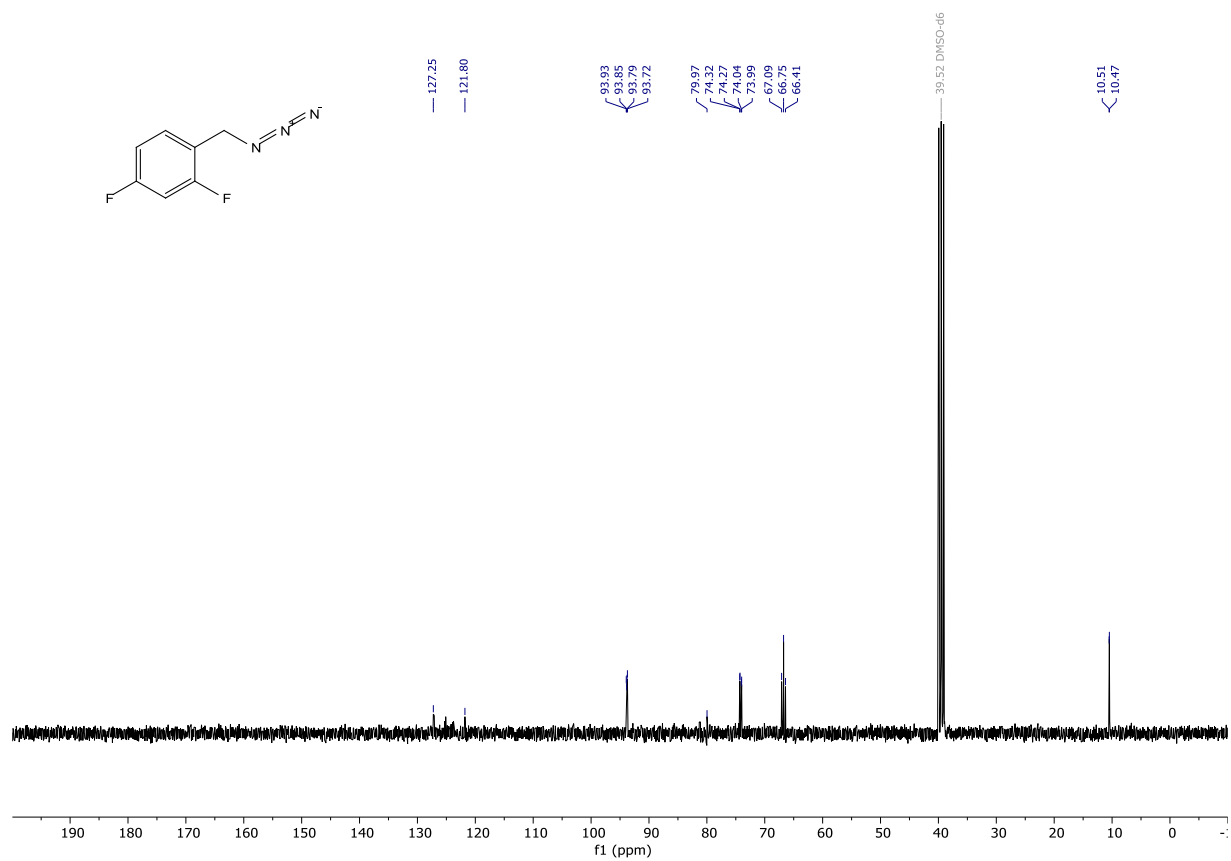


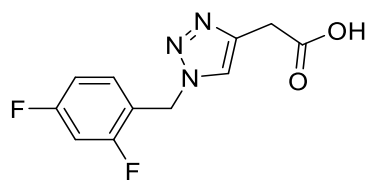
PGUB59PREC

2,4-difluorobenzyl azide (PGUB59PREC). Prepared according to general procedure V from 2,4-difluorobenzyl bromide (0.2066 g, 0.2062 mmol), to give the desired product in quantitative yield (0.18610 g, 1.10030 mmol). Brown oil: **¹H NMR** (300 MHz, Chloroform-*d*) δ 7.32 (td, J = 8.3, 6.2 Hz, 1H), 6.98 – 6.81 (m, 2H), 4.37 (s, 2H). **¹³C NMR** (75 MHz, CDCl₃) δ 127.25, 121.80, 93.93, 93.85, 93.79,

93.72, 79.97, 74.32, 74.27, 74.04, 73.99, 67.09, 66.75, 66.41, 10.51, 10.47. ^{19}F NMR (282 MHz, Chloroform- d) δ -109.05 (p, J = 7.8 Hz), -113.45 (q, J = 8.6 Hz).

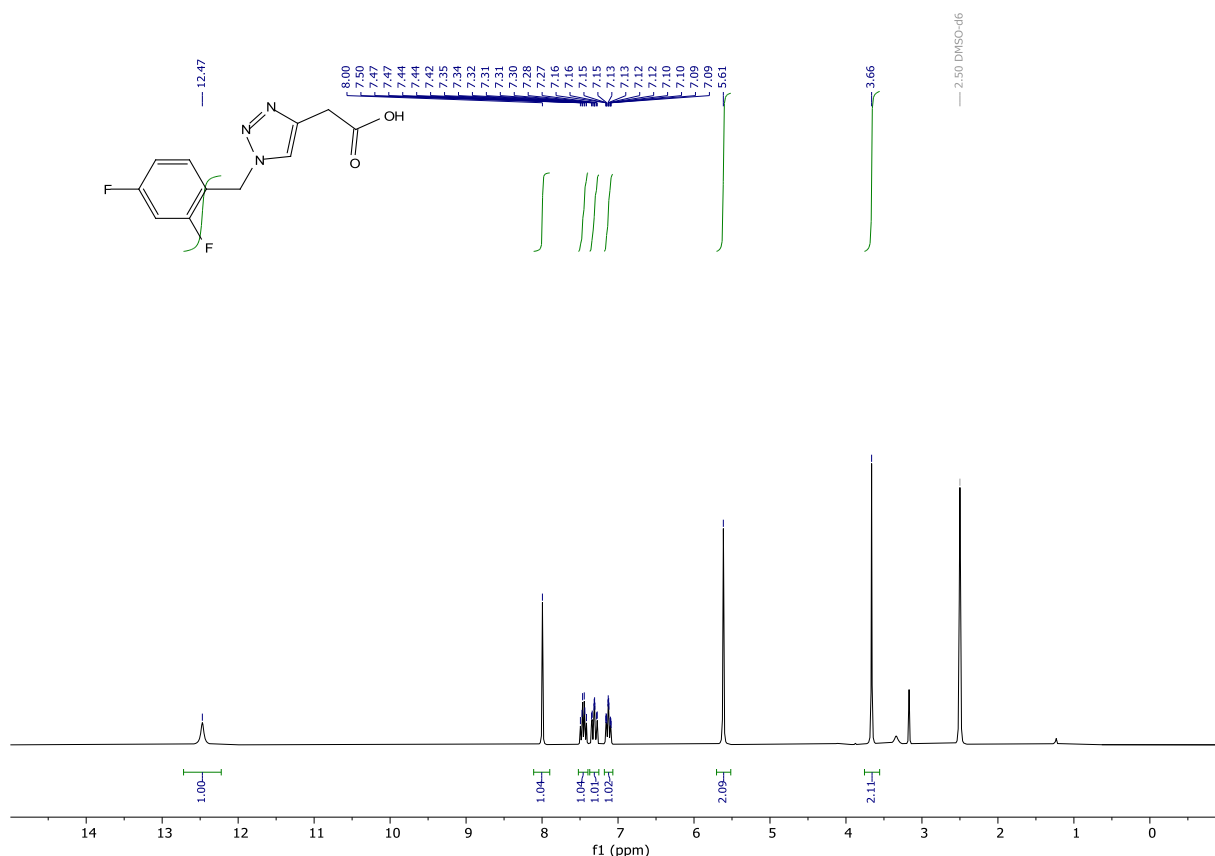


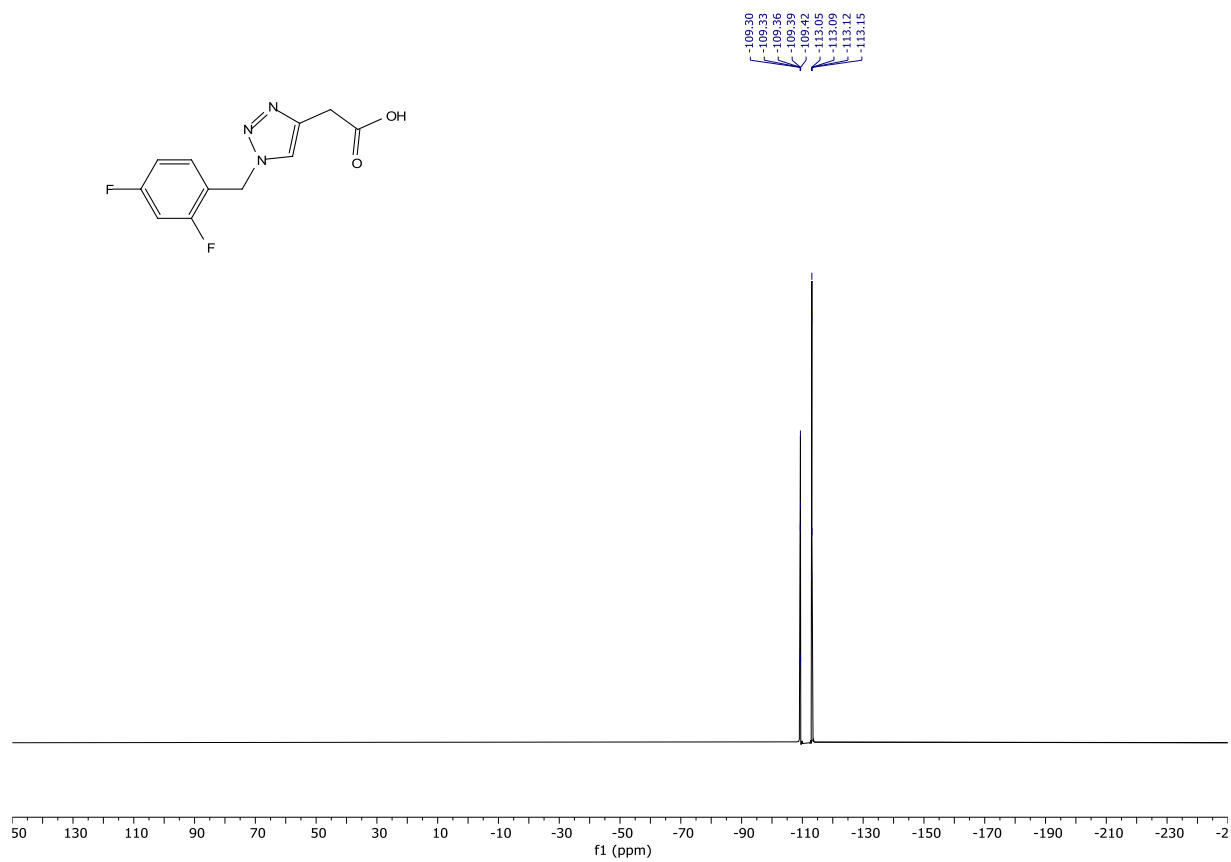
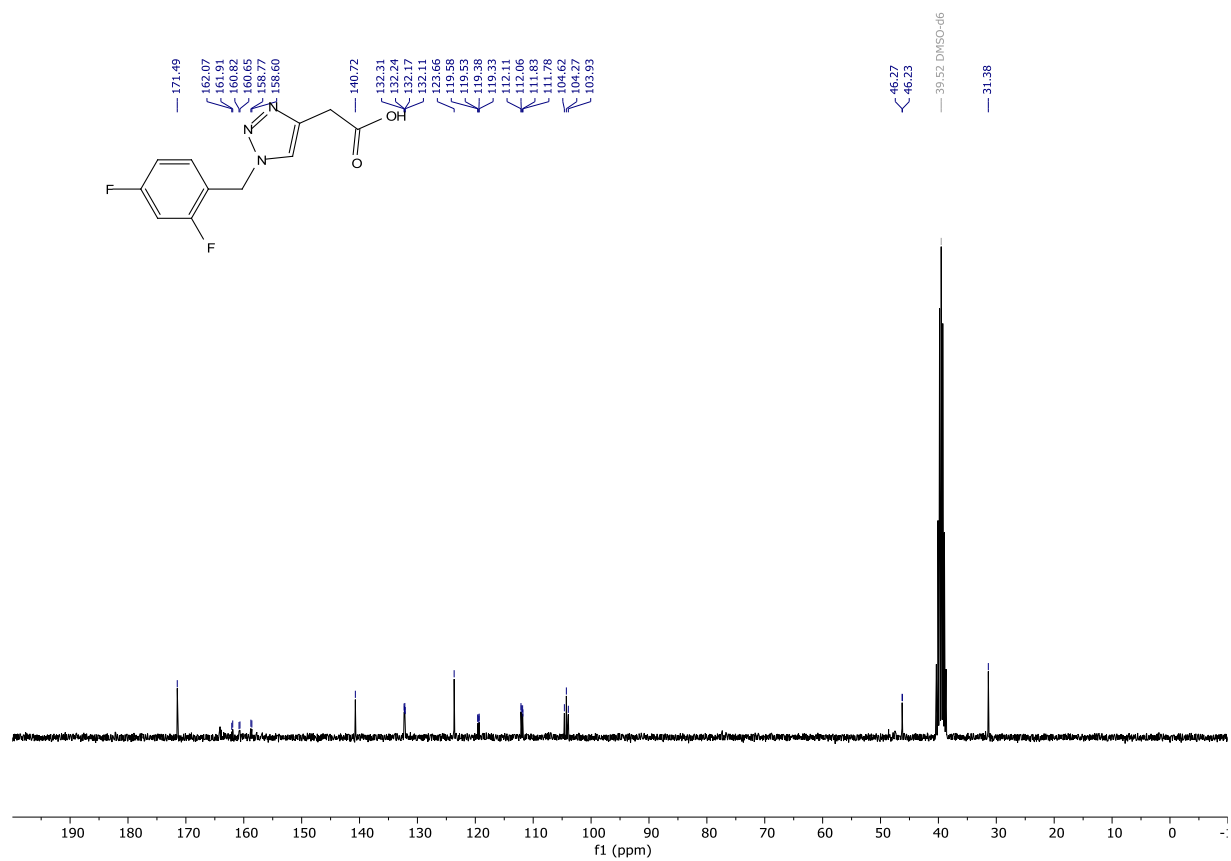


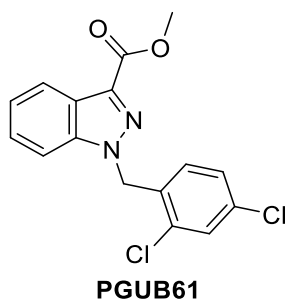


PGUB59

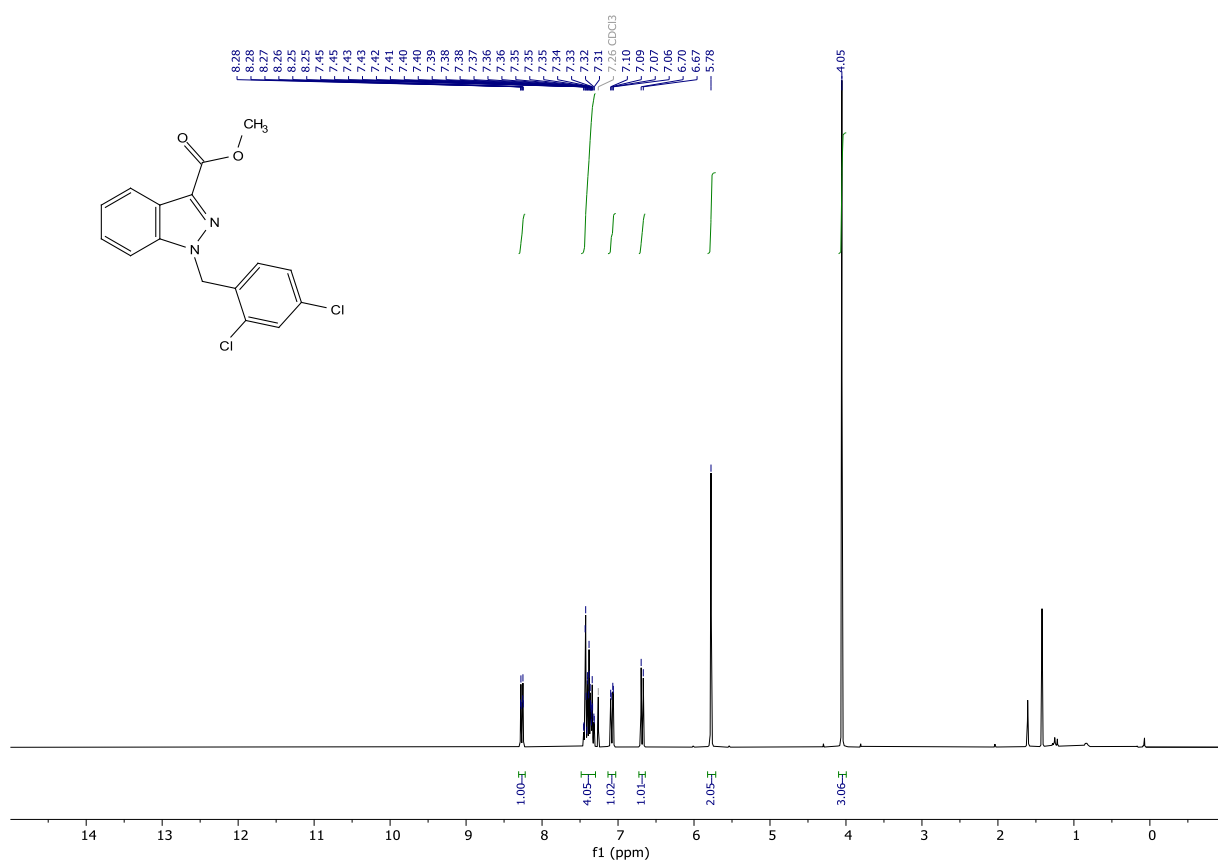
2-(1-(2,4-difluorobenzyl)-1H-1,2,3-triazol-4-yl)acetic acid (PGUB59). Prepared according to general procedure IV from 3-butynoic acid (0.0858 g, 1.0205 mmol) using 2,4-difluorobenzyl azide, to give the desired product in 91% yield (0.23582 g, 0.93133 mmol). White solid: ^1H NMR (300 MHz, DMSO- d_6) δ 12.47 (s, 1H), 8.00 (s, 1H), 7.46 (td, J = 8.7, 6.5 Hz, 1H), 7.31 (ddd, J = 10.4, 9.3, 2.6 Hz, 1H), 7.13 (tdd, J = 8.6, 2.7, 1.1 Hz, 1H), 5.61 (s, 2H), 3.66 (s, 2H). ^{13}C NMR (75 MHz, DMSO) δ 171.49, 164.01 (d, J = 12.2 Hz), 161.99 (d, J = 12.6 Hz), 160.74 (d, J = 12.3 Hz), 158.69 (d, J = 12.7 Hz), 140.73, 132.21 (dd, J = 10.1, 5.2 Hz), 123.66, 119.45 (dd, J = 15.0, 3.7 Hz), 111.95 (dd, J = 21.4, 3.7 Hz), 104.27 (t, J = 25.8 Hz), 46.25 (d, J = 3.1 Hz), 31.38. ^{19}F NMR (282 MHz, DMSO- d_6) δ -109.36 (p, J = 8.0 Hz), -113.10 (q, J = 9.1 Hz). **HRMS** (ESI) calculated for $[\text{M-H}]^-$ $\text{C}_{11}\text{H}_8\text{F}_2\text{N}_3\text{O}_2$ 252.0579, found 252.0588. **Purity (HPLC):** >99% UV_{214} , >98% UV_{254} .

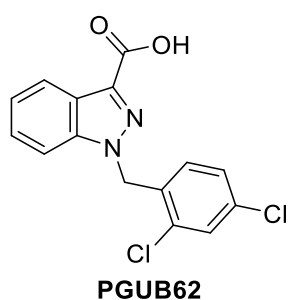
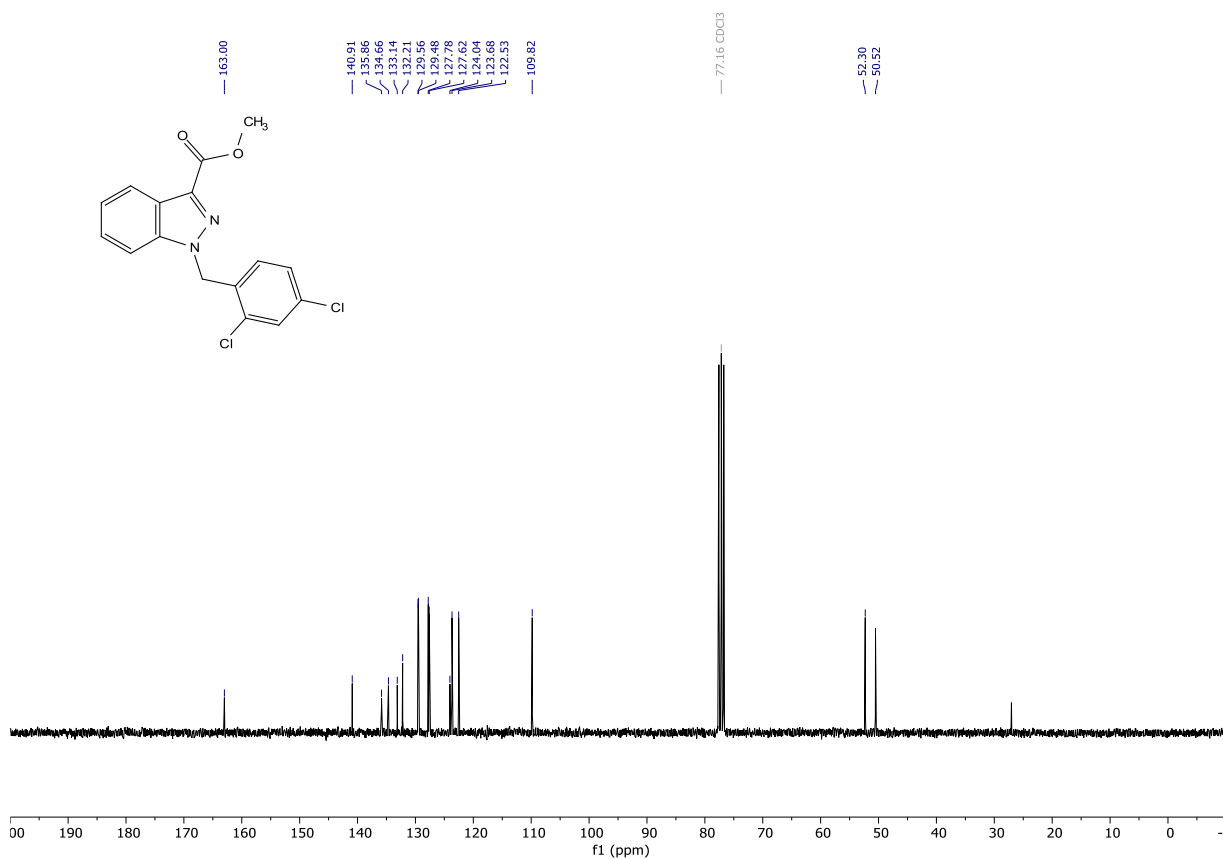




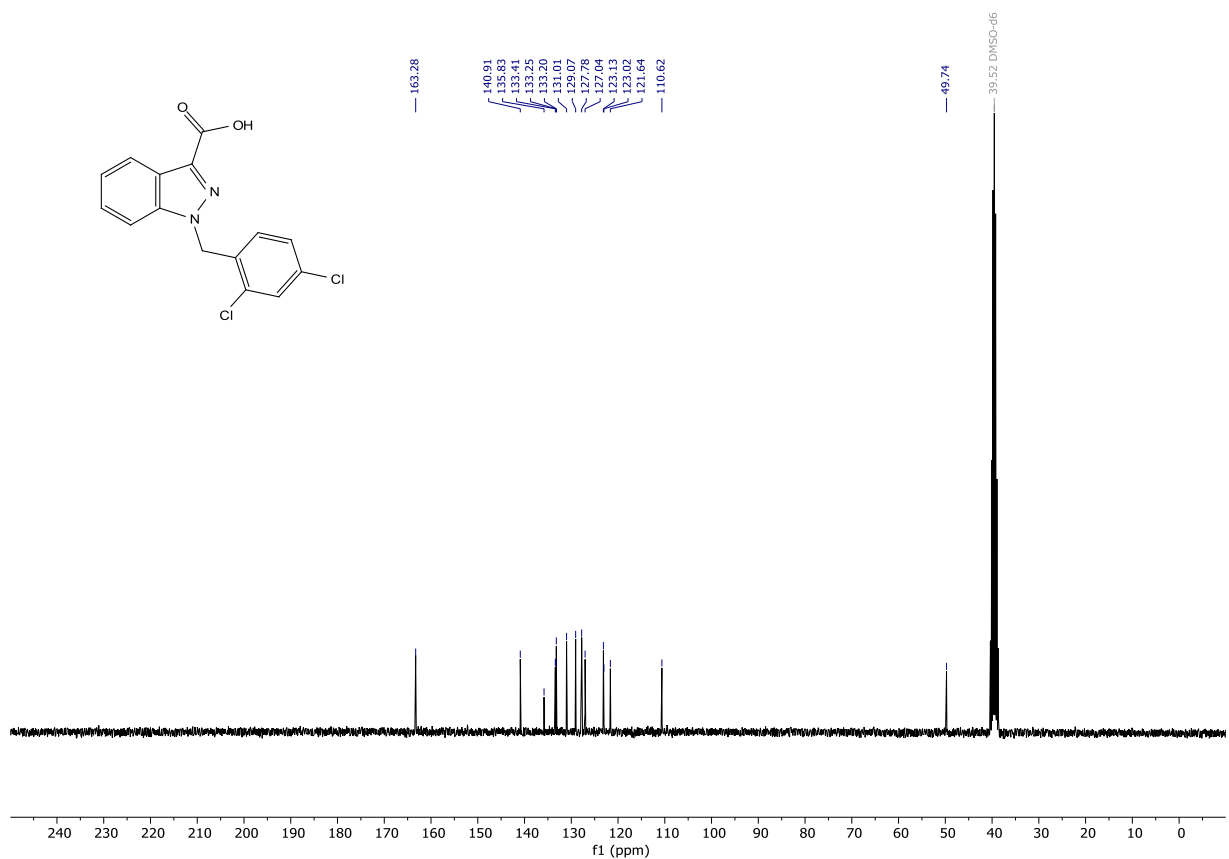
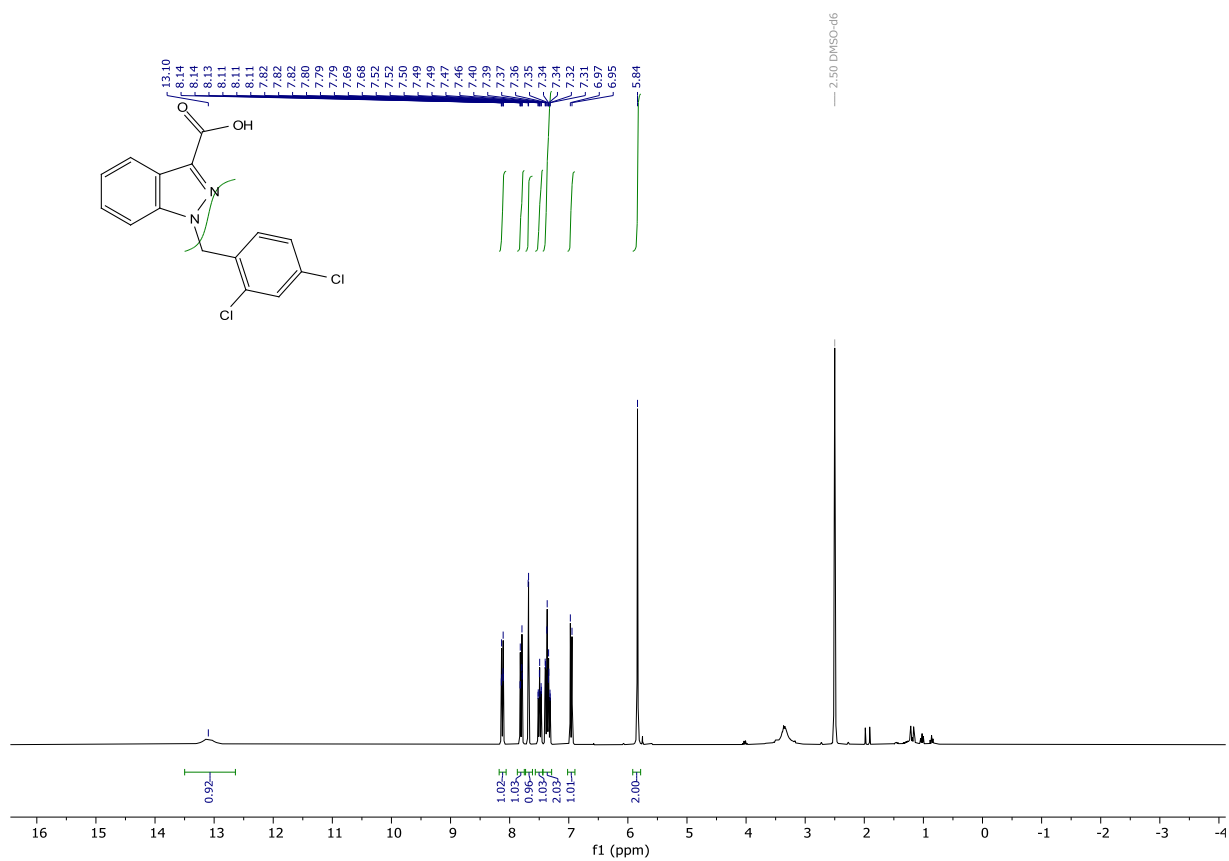


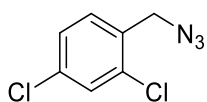
methyl 1-(2,4-dichlorobenzyl)-1H-indazole-3-carboxylate (PGUB58) (Z = N, Y = OMe). Prepared according to general procedure II from methyl 1H-indazole-3-carboxylate (Z = N, Y = OMe, 0.211 g, 1.1977 mmol) using 2,4-dichlorobenzyl bromide as alkyl halide, to give the desired product in 84% yield (0.33540 g, 1.00064 mmol). White solid slightly impure with cyclohexane: ^1H NMR (300 MHz, Chloroform-*d*) δ 8.26 (dt, J = 8.0, 1.1 Hz, 1H), 7.49 – 7.30 (m, 4H), 7.08 (dd, J = 8.4, 2.1 Hz, 1H), 6.68 (d, J = 8.4 Hz, 1H), 5.78 (s, 2H), 4.05 (s, 3H). ^{13}C NMR (75 MHz, CDCl_3) δ 163.00, 140.91, 135.86, 134.66, 133.14, 132.21, 129.56, 129.48, 127.78, 127.62, 124.04, 123.68, 122.53, 109.82, 52.30, 50.52. **HRMS** (ESI) calculated for $[\text{M}+\text{H}]^+$ $\text{C}_{16}\text{H}_{13}\text{Cl}_2\text{N}_2\text{O}_2$ 335.0349, found 335.0350. **Purity (HPLC):** >99% UV_{214} , >99% UV_{254} .





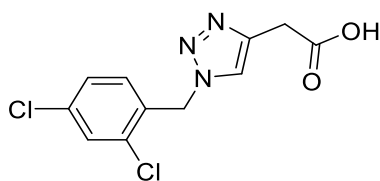
1-(2,4-dichlorobenzyl)-1H-indazole-3-carboxylic acid (PGUB62) (Z = N, W = OH). Prepared according to general procedure III from methyl 1-(4-benzoylbenzyl)-1H-indazole-3-carboxylate (PGUB61) (Z = N, Y = OMe, 0.20000 g, 0.5967 mmol), to give the desired product in quantitative yield (0.19100 g, 0.59473 mmol). White solid: **¹H NMR** (300 MHz, DMSO-*d*₆) δ 13.10 (s, 1H), 8.12 (dt, *J* = 8.2, 1.1 Hz, 1H), 7.87 – 7.75 (m, 1H), 7.68 (d, *J* = 2.1 Hz, 1H), 7.49 (ddd, *J* = 8.4, 6.9, 1.2 Hz, 1H), 7.44 – 7.29 (m, 2H), 6.96 (d, *J* = 8.3 Hz, 1H), 5.84 (s, 2H). **¹³C NMR** (75 MHz, DMSO) δ 163.28, 140.91, 135.83, 133.41, 133.25, 133.20, 131.01, 129.07, 127.78, 127.04, 123.13, 123.02, 121.64, 110.62, 49.74. **HRMS** (ESI) calculated for [M-H]⁻ C₁₅H₉Cl₂N₂O₂ 319.0047, found 319.0048. **Purity (HPLC):** >99% UV₂₁₄, >99% UV₂₅₄.





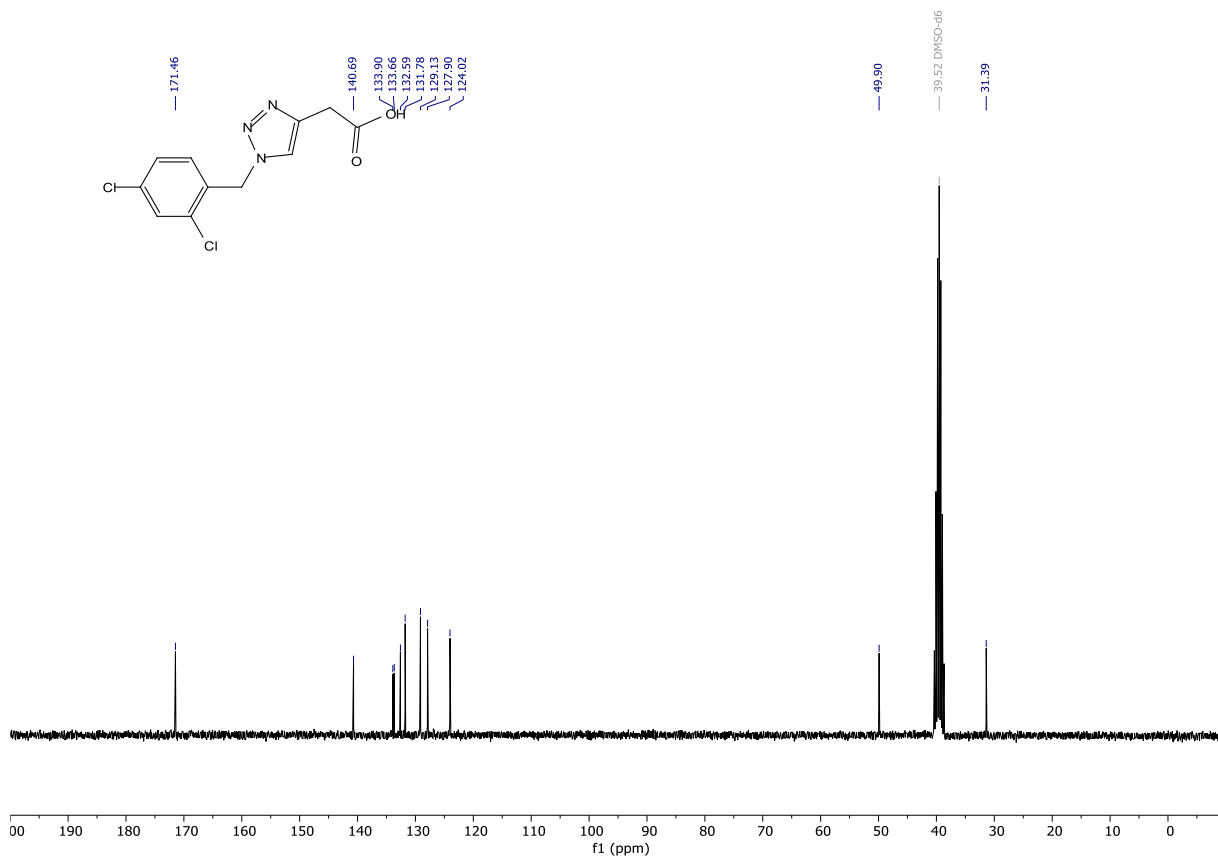
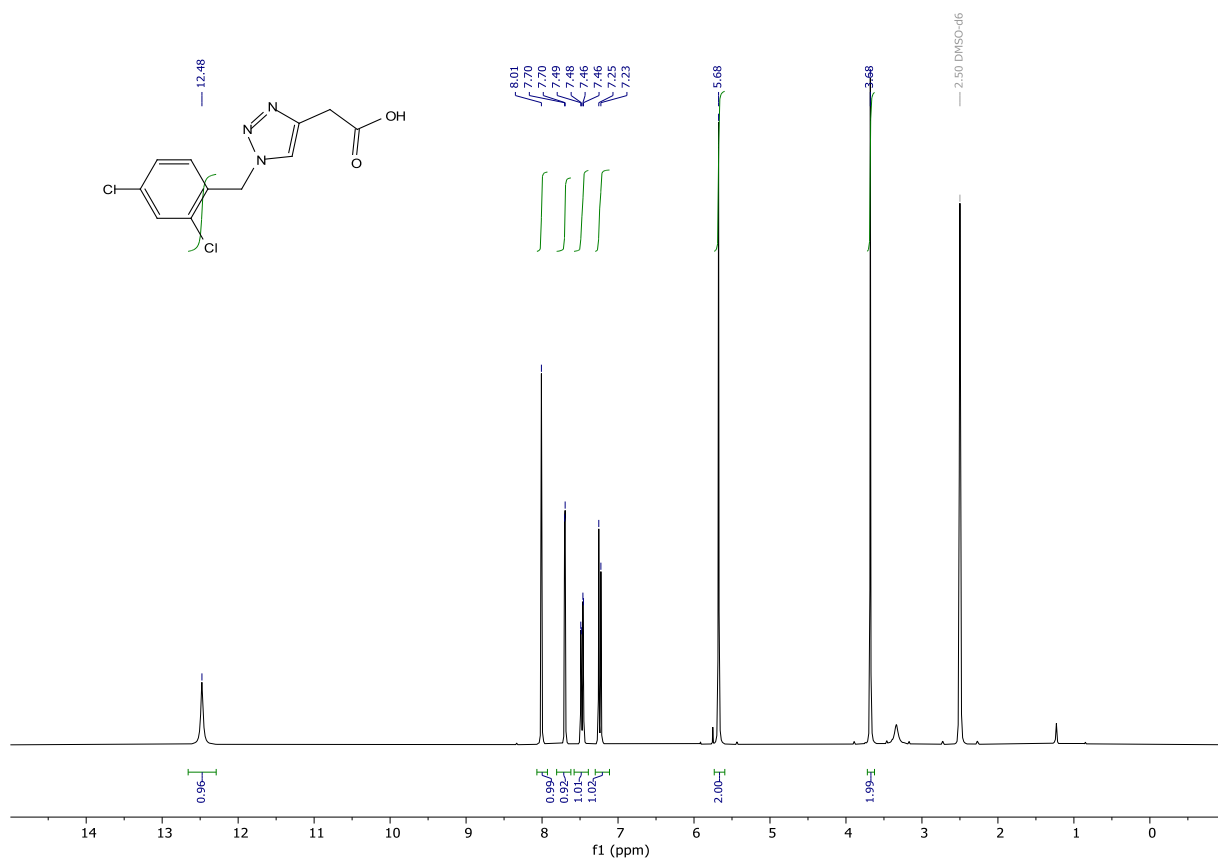
PGUB63PREC

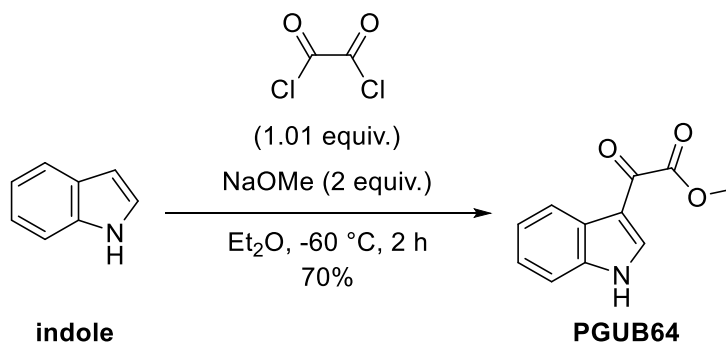
2,4-dichlorobenzyl azide (PGUB63PREC). Prepared according to general procedure V from 2,4-dichlorobenzyl bromide (0.365 g, 0.15213 mmol), to give the desired product in 98% yield (0.30110 g, 1.48998 mmol). Brown oil: $^1\text{H NMR}$ (300 MHz, Chloroform-*d*) δ 7.44 (d, J = 2.0 Hz, 1H), 7.34 (d, J = 8.2 Hz, 1H), 7.31 – 7.24 (m, 1H), 4.47 (s, 2H). $^{13}\text{C NMR}$ (75 MHz, CDCl_3) δ 134.98, 134.55, 132.12, 130.85, 129.79, 127.64, 51.85. **HRMS** (EI) calculated for $[\text{M}-\text{e}^-]^+$ $\text{C}_7\text{H}_5\text{Cl}_2\text{N}_3$ 200.9855, found 200.8955.



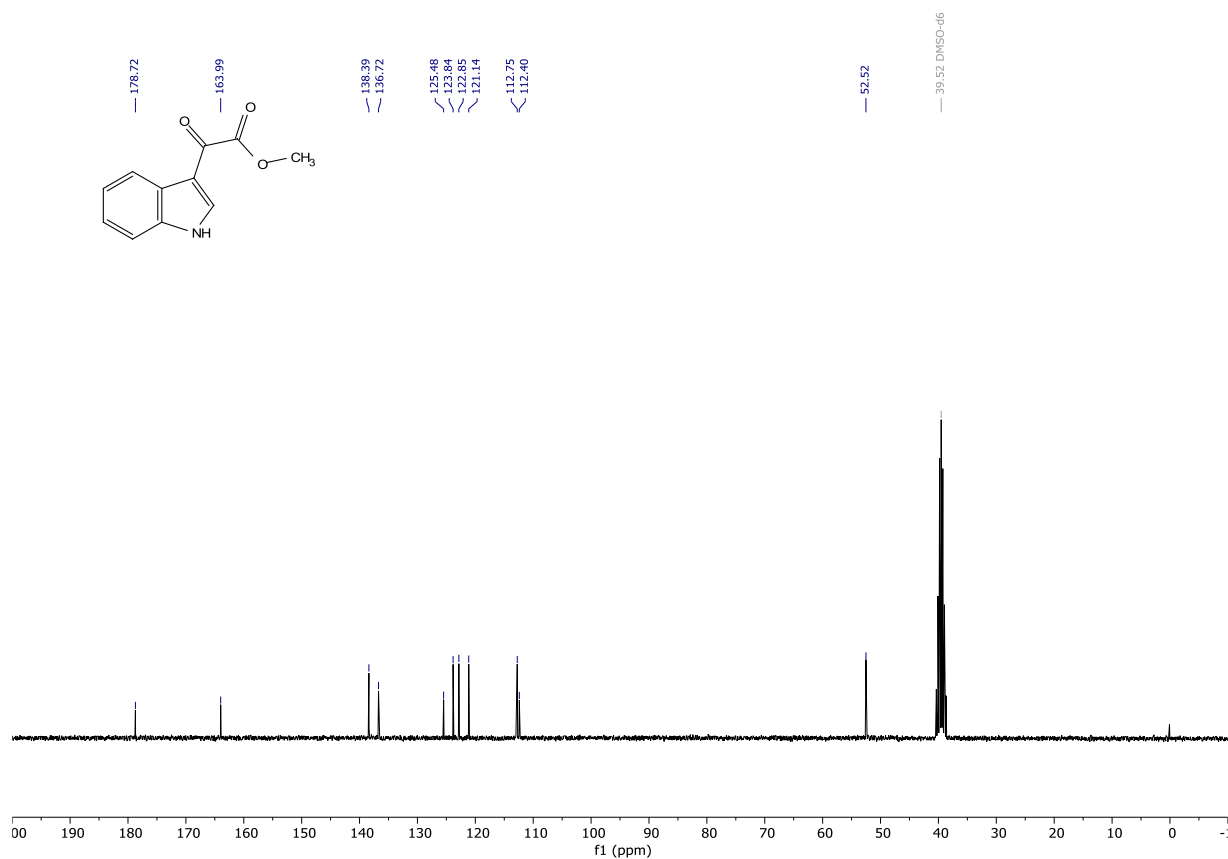
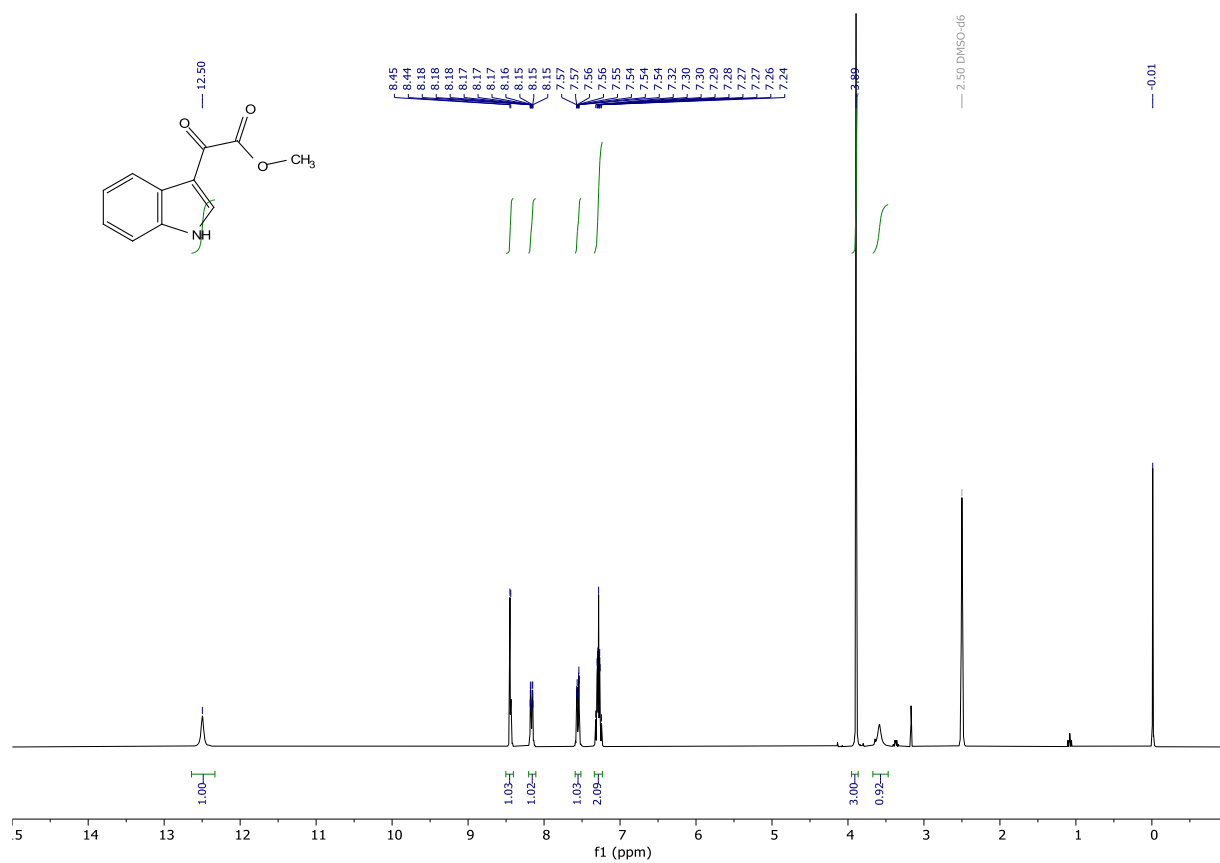
PGUB63

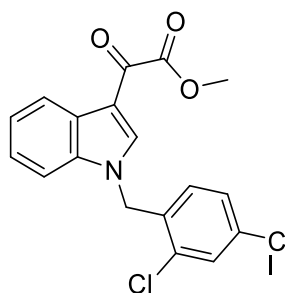
2-(1-(2,4-dichlorobenzyl)-1H-1,2,3-triazol-4-yl)acetic acid (PGUB63). Prepared according to general procedure IV from 3-butynoic acid (0.11591 g, 1.3787 mmol) using 2,4-dichlorobenzyl azide, to give the desired product in 73% yield (0.28967 g, 1.01244 mmol). White solid: $^1\text{H NMR}$ (300 MHz, DMSO-*d*₆) δ 12.48 (s, 1H), 8.01 (s, 1H), 7.70 (d, J = 2.1 Hz, 1H), 7.47 (dd, J = 8.3, 2.2 Hz, 1H), 7.24 (d, J = 8.3 Hz, 1H), 5.68 (s, 2H), 3.68 (s, 2H). $^{13}\text{C NMR}$ (75 MHz, DMSO) δ 171.46, 140.69, 133.90, 133.66, 132.59, 131.78, 129.13, 127.90, 124.02, 49.90, 31.39. **HRMS** (ESI) calculated for $[\text{M}-\text{H}]^-$ $\text{C}_{11}\text{H}_8\text{Cl}_2\text{N}_3\text{O}_2$ 293.9999, found 284.0000. **Purity (HPLC):** >99% UV_{214} , >99% UV_{254} .





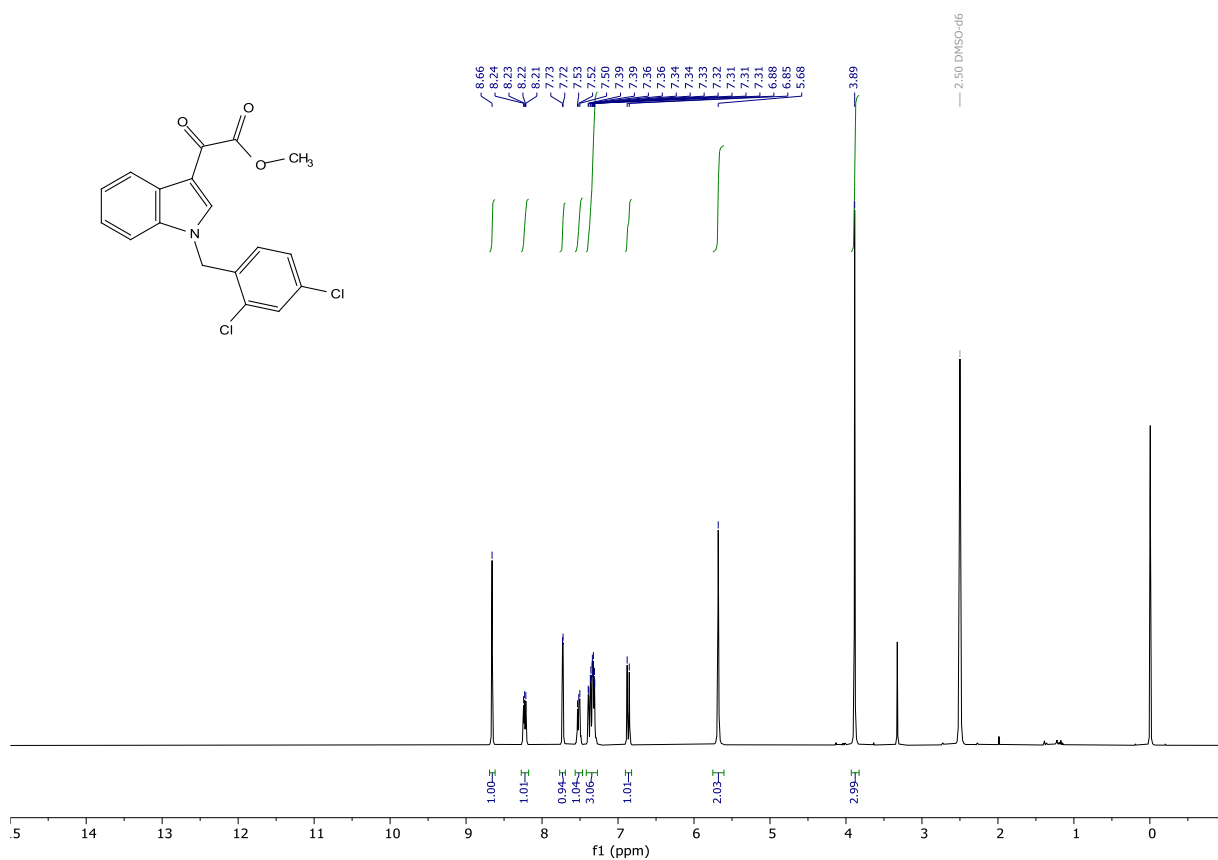
methyl 2-(1H-indol-3-yl)-2-oxoacetate (PGUB64). To a stirred solution of indole (1.563 g, 13.3418 mmol) in dry diethyl ether (15.5 mL) at 0 °C under an argon atmosphere was added slowly oxalyl chloride (1.15 ml, 1.702 g, 13.4100 mmol). The mixture gradually turned into a yellow suspension. The mixture was left stirring for 1 h. Then the mixture was cooled to -60 °C using a diisopropylether/ liquid N₂ cooling bath, and a solution of sodium methoxide (1.449 g, 26.8184 mmol) in dry methanol (6 mL) was added slowly. After the addition, the mixture was left warming to room temperature over the course of 1 h, resulting in a yellow suspension. The suspension was filtered through a por 4 frit. Giving a brownish filter cake, which was thoroughly washed with cold diethyl ether. The filter cake was thoroughly dried on the high vac. The crude was taken up in ethyl acetate and concentrated onto silica gel. It was purified by flash column chromatography (cyclohexane ethyl acetate gradient from 1:0 to 0:1), to give the desired compound in 70% (1.90944 g, 9.39699 mmol). Yellow solid: ¹H NMR (300 MHz, DMSO-*d*₆) δ 12.50 (s, 1H), 8.44 (d, *J* = 3.3 Hz, 1H), 8.20 – 8.11 (m, 1H), 7.59 – 7.52 (m, 1H), 7.34 – 7.23 (m, 2H), 3.89 (s, 3H), 3.61 (d, *J* = 17.0 Hz, 1H). ¹³C NMR (75 MHz, DMSO) δ 178.72, 163.99, 138.39, 136.72, 125.48, 123.84, 122.85, 121.14, 112.75, 112.40, 52.52. HRMS (ESI) calculated for [M+H]⁺ C₁₁H₁₀NO₃ 204.0655, found 204.0657. **Purity (HPLC):** >98% UV₂₁₄, >99% UV₂₅₄.

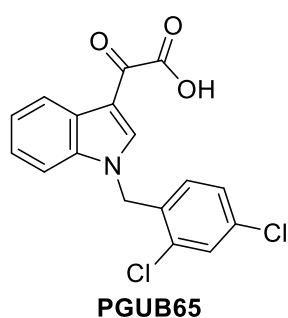
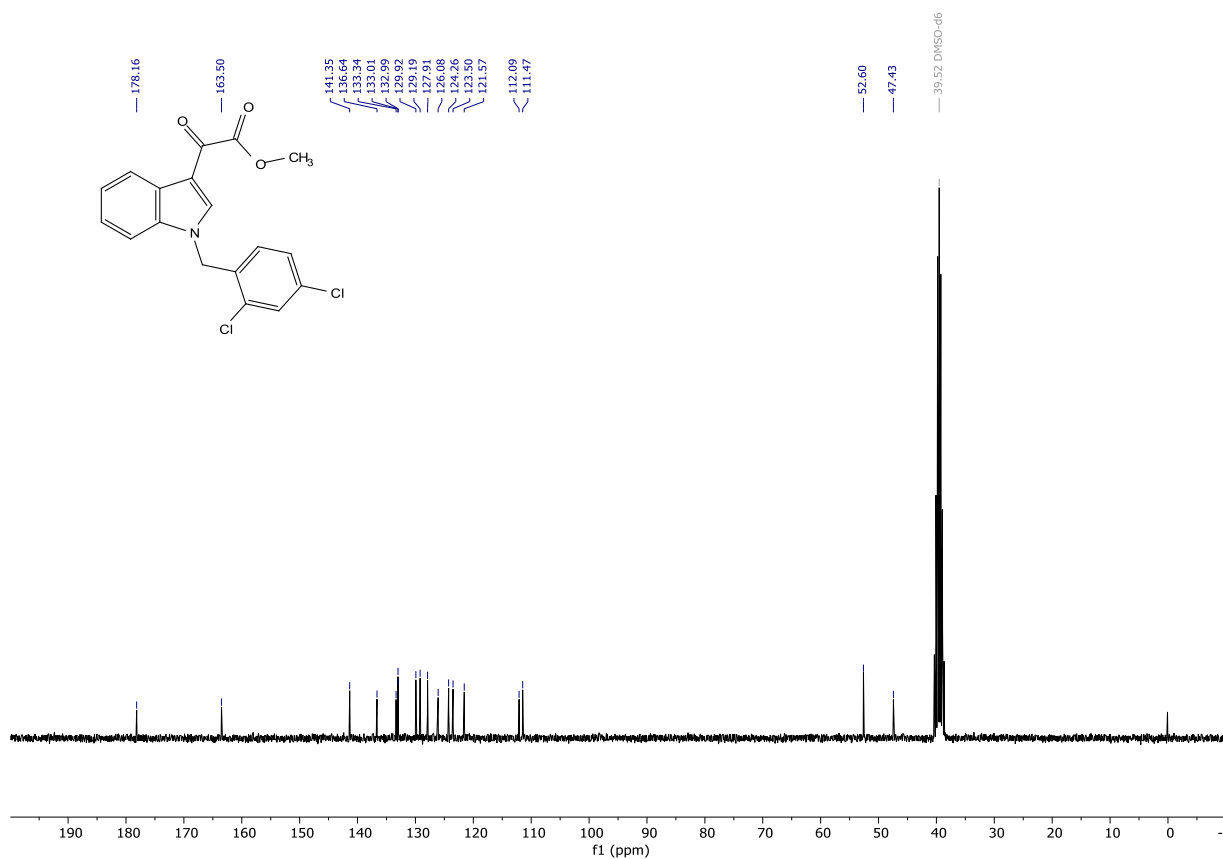




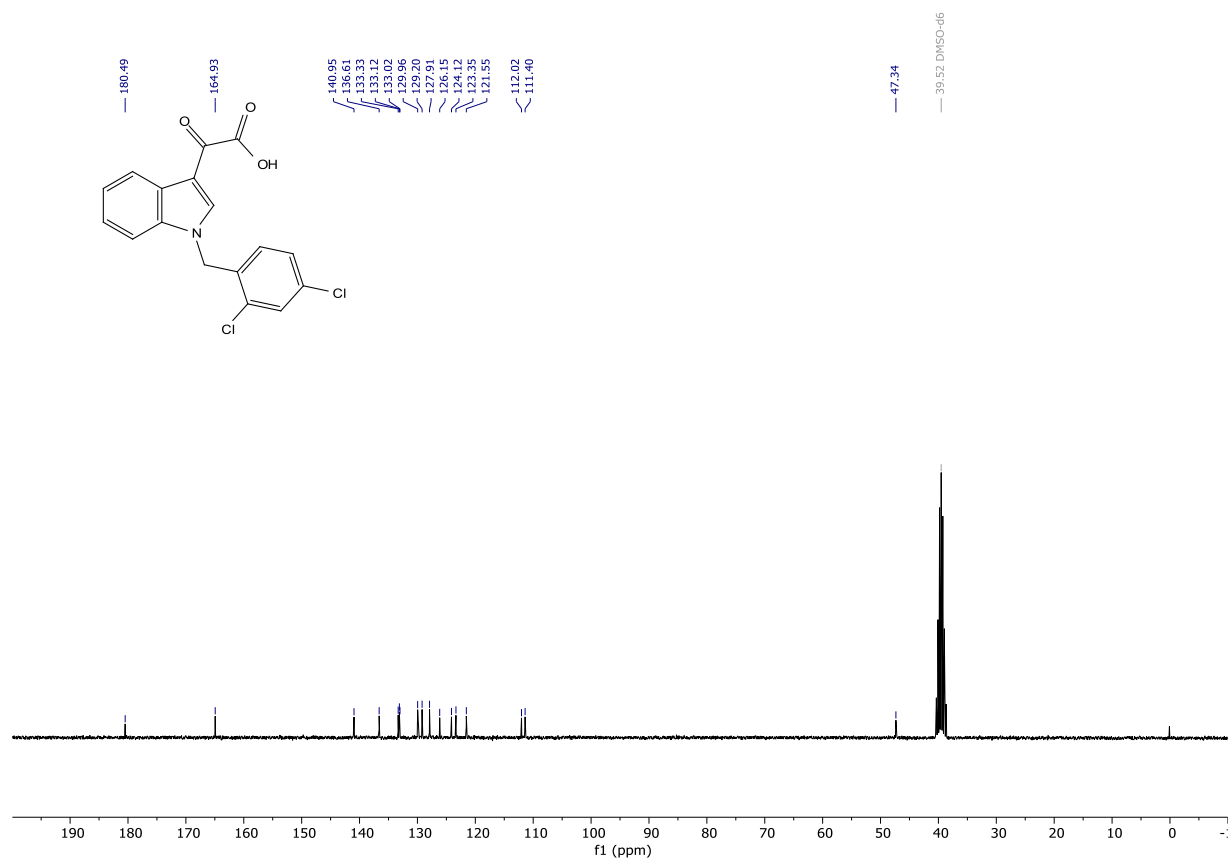
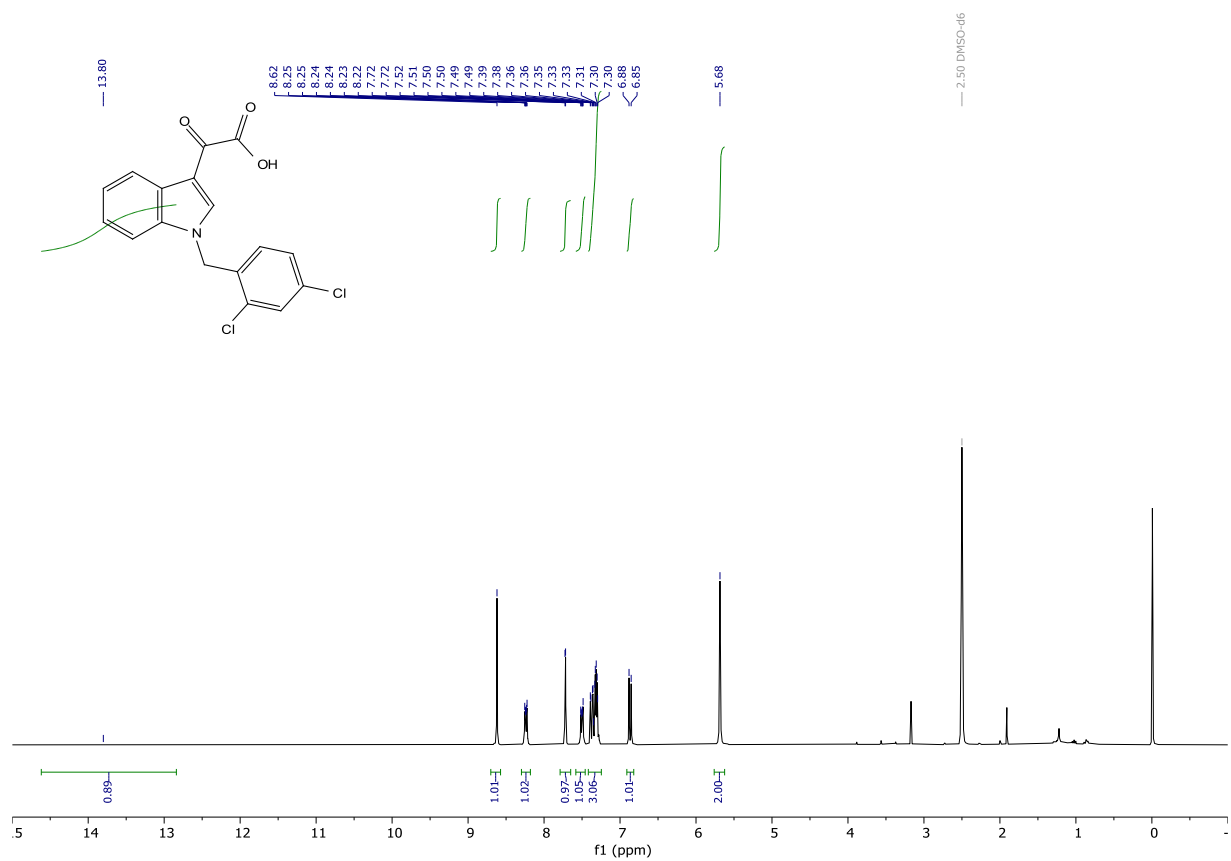
PGUB65PREC

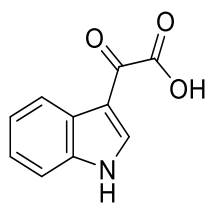
methyl 2-(1-(2,4-dichlorobenzyl)-1H-indol-3-yl)-2-oxoacetate (Z = CH, Y = COOMe). Prepared according to general procedure II from methyl 1H-indazole-3-carboxylate (Z = N, Y = OMe, 0.200 g, 0.9843 mmol) using 2,4-dichlorobenzyl bromide as alkyl halide, to give the desired product in 30% yield (0.10614 g, 0.29304 mmol). White solid: ^1H NMR (300 MHz, DMSO- d_6) δ 8.66 (s, 1H), 8.27 – 8.18 (m, 1H), 7.73 (d, J = 2.2 Hz, 1H), 7.56 – 7.47 (m, 1H), 7.42 – 7.27 (m, 3H), 6.87 (d, J = 8.4 Hz, 1H), 5.68 (s, 2H), 3.89 (s, 3H). ^{13}C NMR (75 MHz, DMSO) δ 178.16, 163.50, 141.35, 136.64, 133.34, 133.01, 132.99, 129.92, 129.19, 127.91, 126.08, 124.26, 123.50, 121.57, 112.09, 111.47, 52.60, 47.43. HRMS (ESI) calculated for $[\text{M}+\text{H}]^+$ $\text{C}_{18}\text{H}_{14}\text{Cl}_2\text{NO}_3$ 362.0345, found 362.0367.





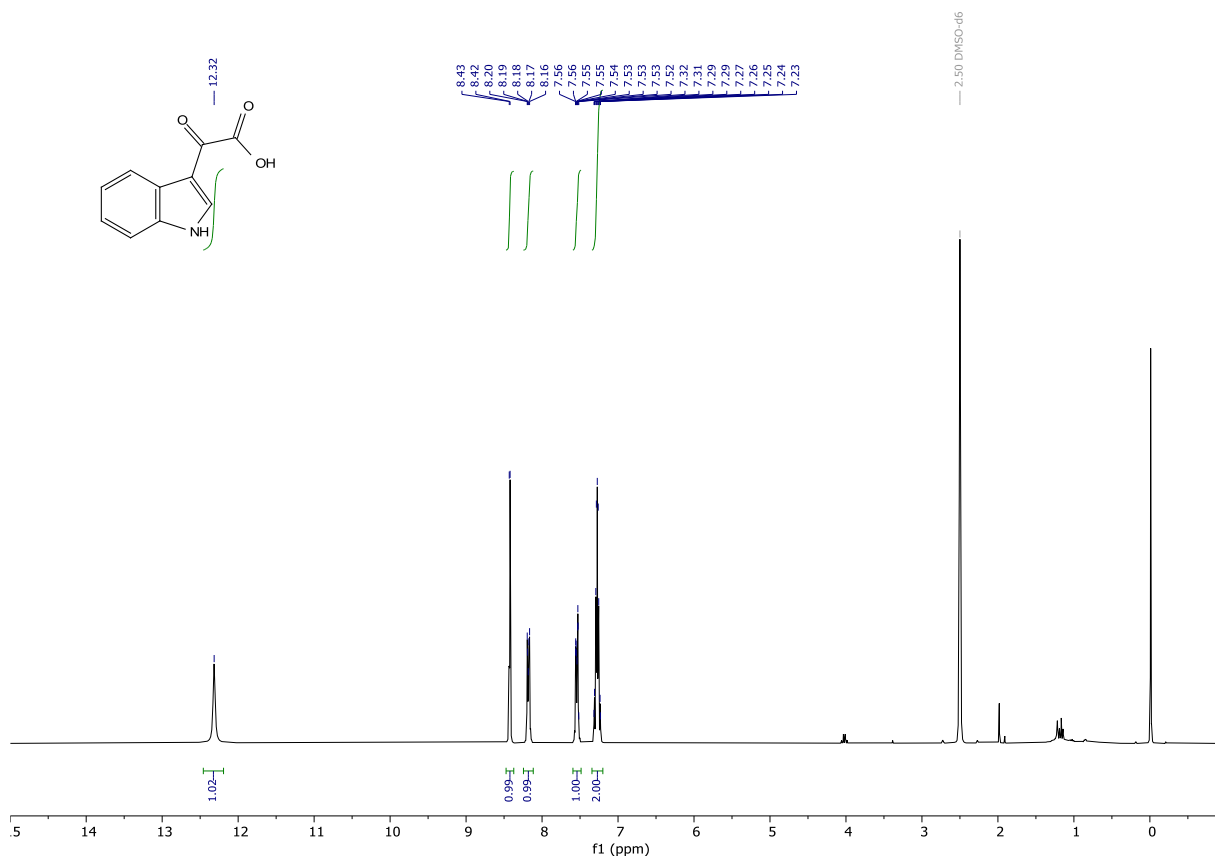
2-(1-(2,4-dichlorobenzyl)-1H-indol-3-yl)-2-oxoacetic acid (PGUB65) (Z = CH, W = COOH). Prepared according to general procedure III from methyl 2-(1-(2,4-dichlorobenzyl)-1H-indol-3-yl)-2-oxoacetate (Z = CH, Y = COOMe, 0.09354 g, 0.2583 mmol), to give the desired product in quantitative yield (0.09171 g, 0.26340 mmol). Yellow solid: $^1\text{H NMR}$ (300 MHz, DMSO- d_6) δ 13.80 (s, 1H), 8.62 (s, 1H), 8.30 – 8.18 (m, 1H), 7.72 (d, $J = 2.2$ Hz, 1H), 7.58 – 7.46 (m, 1H), 7.42 – 7.25 (m, 3H), 6.87 (d, $J = 8.4$ Hz, 1H), 5.68 (s, 2H). $^{13}\text{C NMR}$ (75 MHz, DMSO) δ 180.49, 164.93, 140.95, 136.61, 133.33, 133.12, 133.02, 129.96, 129.20, 127.91, 126.15, 124.12, 123.35, 121.55, 112.02, 111.40, 47.34. **HRMS** (ESI) calculated for $[\text{M}+\text{H}]^+$ $\text{C}_{17}\text{H}_{12}\text{Cl}_2\text{NO}_3$ 348.0189, found 348.0195. **Purity (HPLC):** >95% UV_{214} , >98% UV_{254} .

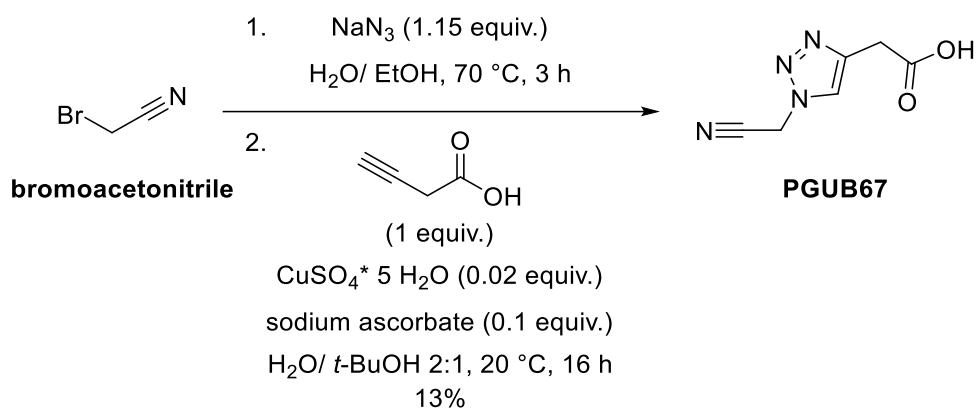
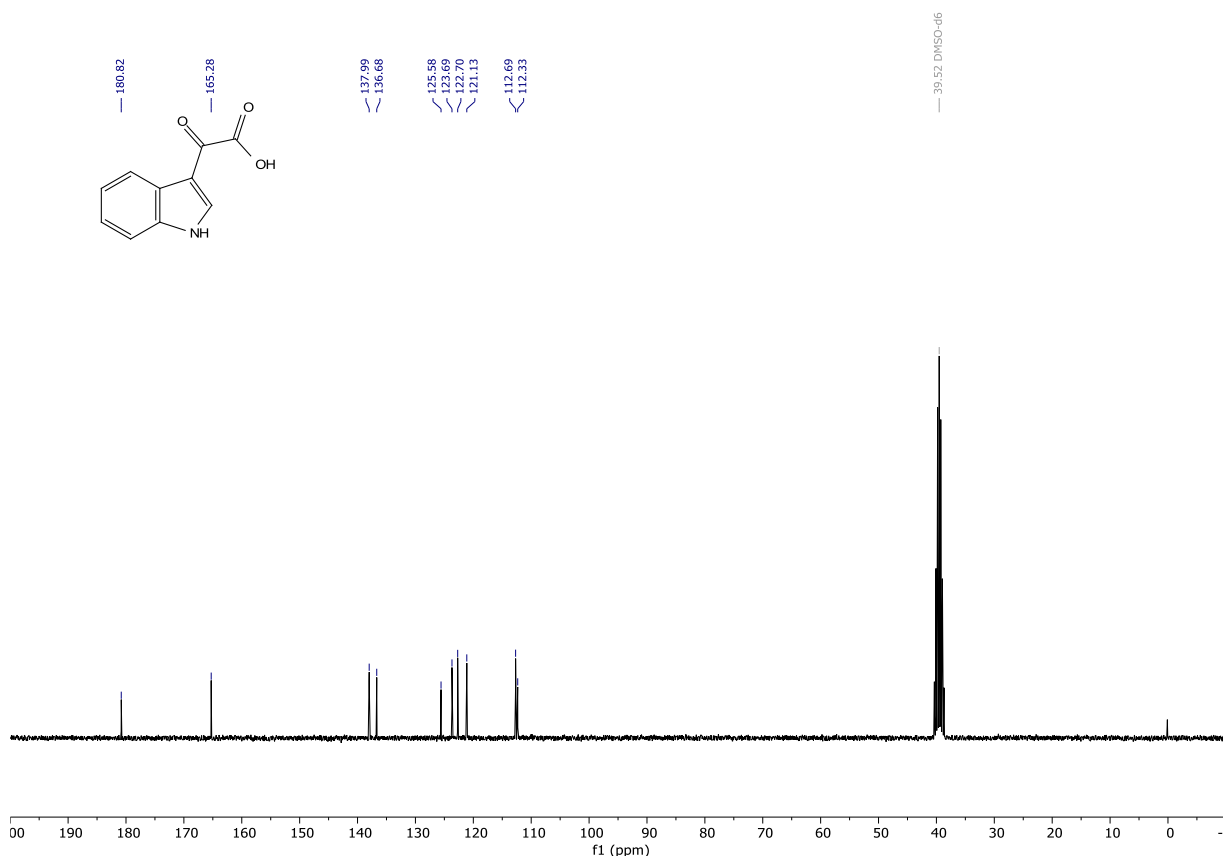




PGUB66

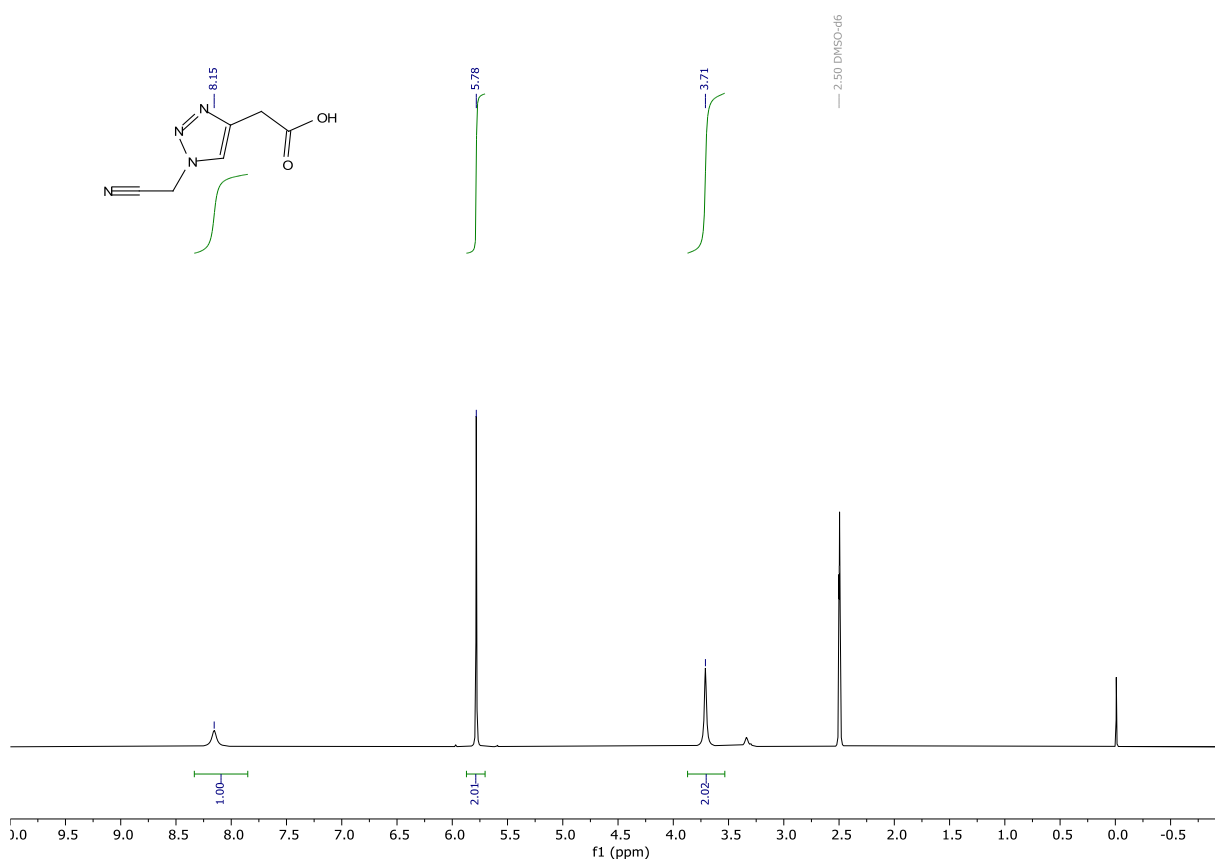
2-(1*H*-indol-3-yl)-2-oxoacetic acid (PGUB66) (Z = CH, W = COOH). Prepared according to general procedure III from methyl 2-(1*H*-indol-3-yl)-2-oxoacetate (Z = CH, Y = COOMe, 0.1015 g, 0.4995 mmol), to give the desired product in quantitative yield (0.08780 g, 0.46413 mmol). Yellow solid: **¹H NMR** (300 MHz, DMSO-*d*₆) δ 12.32 (s, 1H), 8.43 (d, *J* = 3.3 Hz, 1H), 8.24 – 8.12 (m, 1H), 7.59 – 7.49 (m, 1H), 7.34 – 7.20 (m, 2H). **¹³C NMR** (75 MHz, DMSO) δ 180.82, 165.28, 137.99, 136.68, 125.58, 123.69, 122.70, 121.13, 112.69, 112.33. **HRMS** (ESI) calculated for [M+H]⁺ C₁₀H₈NO₃ 190.0499, found 190.0503. **Purity (HPLC):** >99% UV₂₁₄, >99% UV₂₅₄.

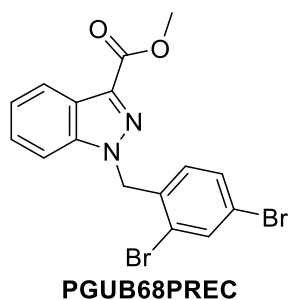
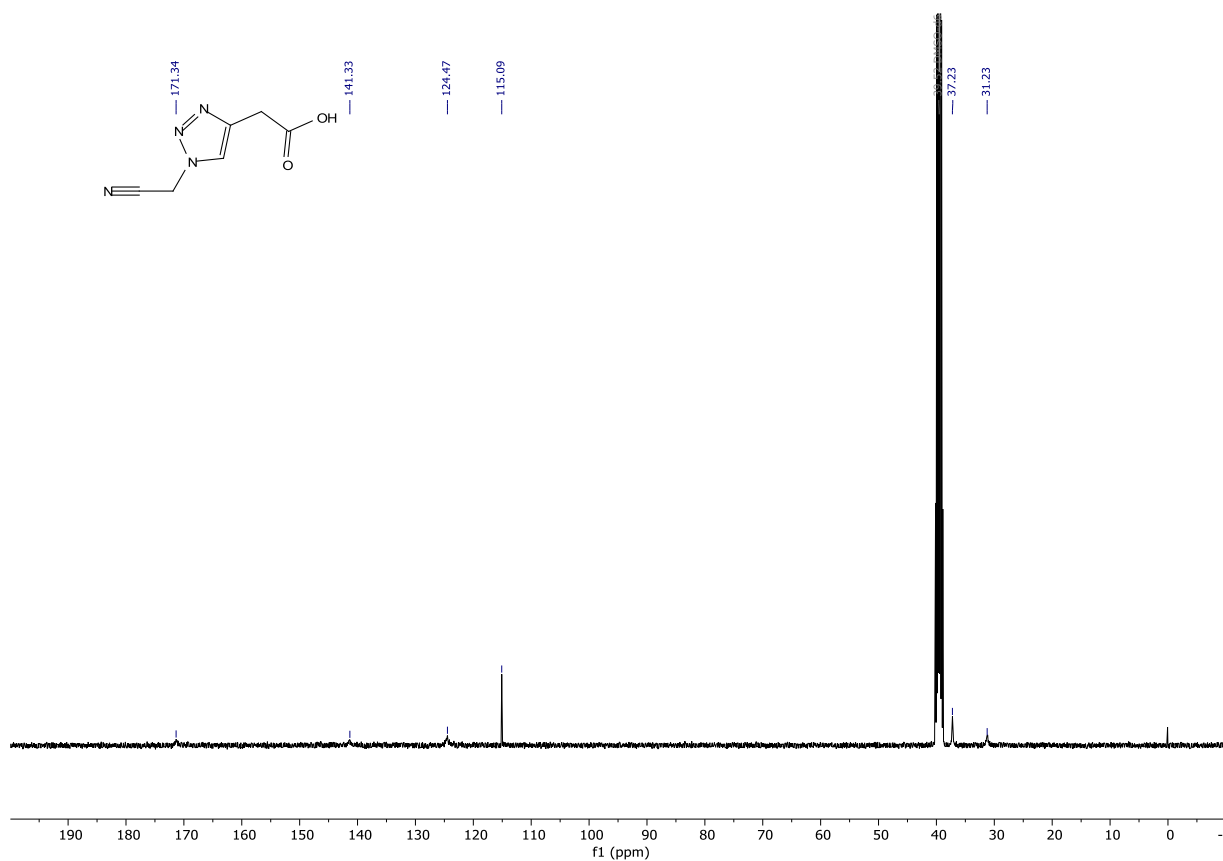




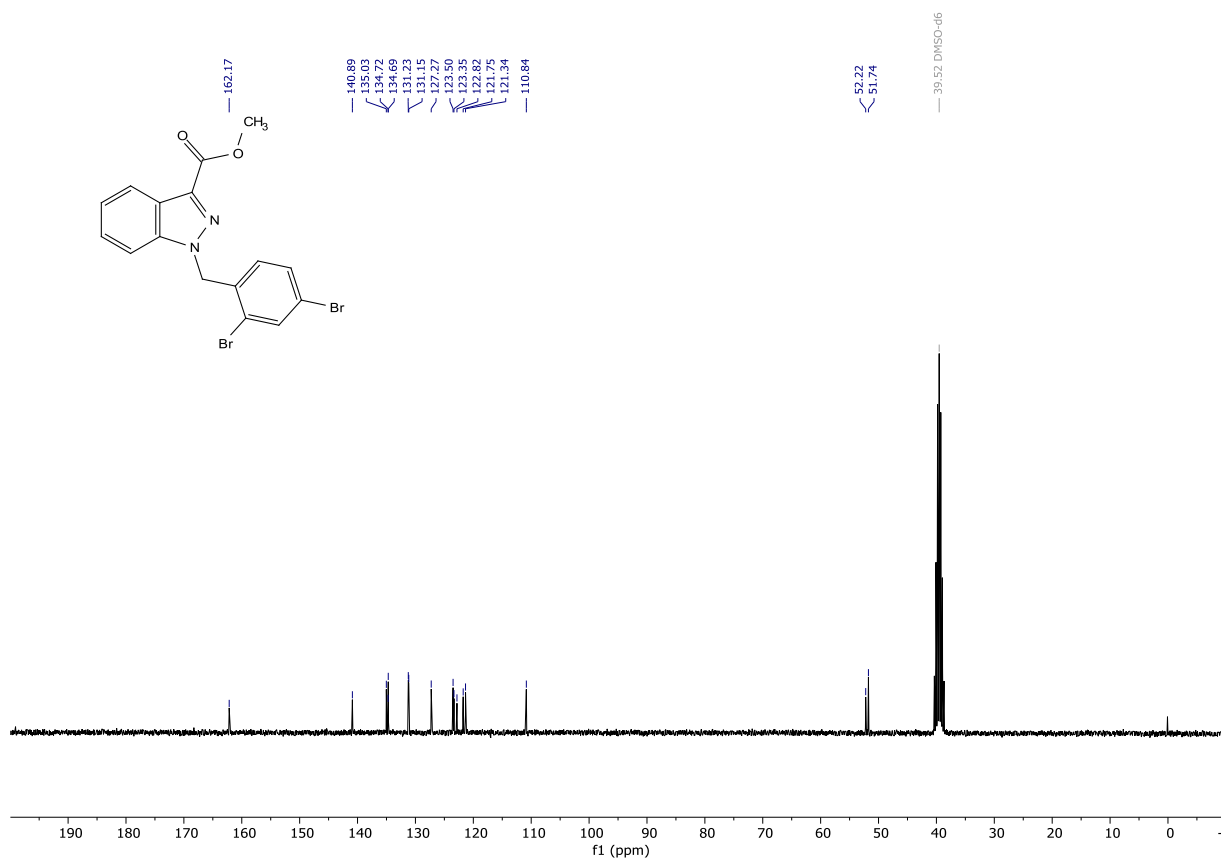
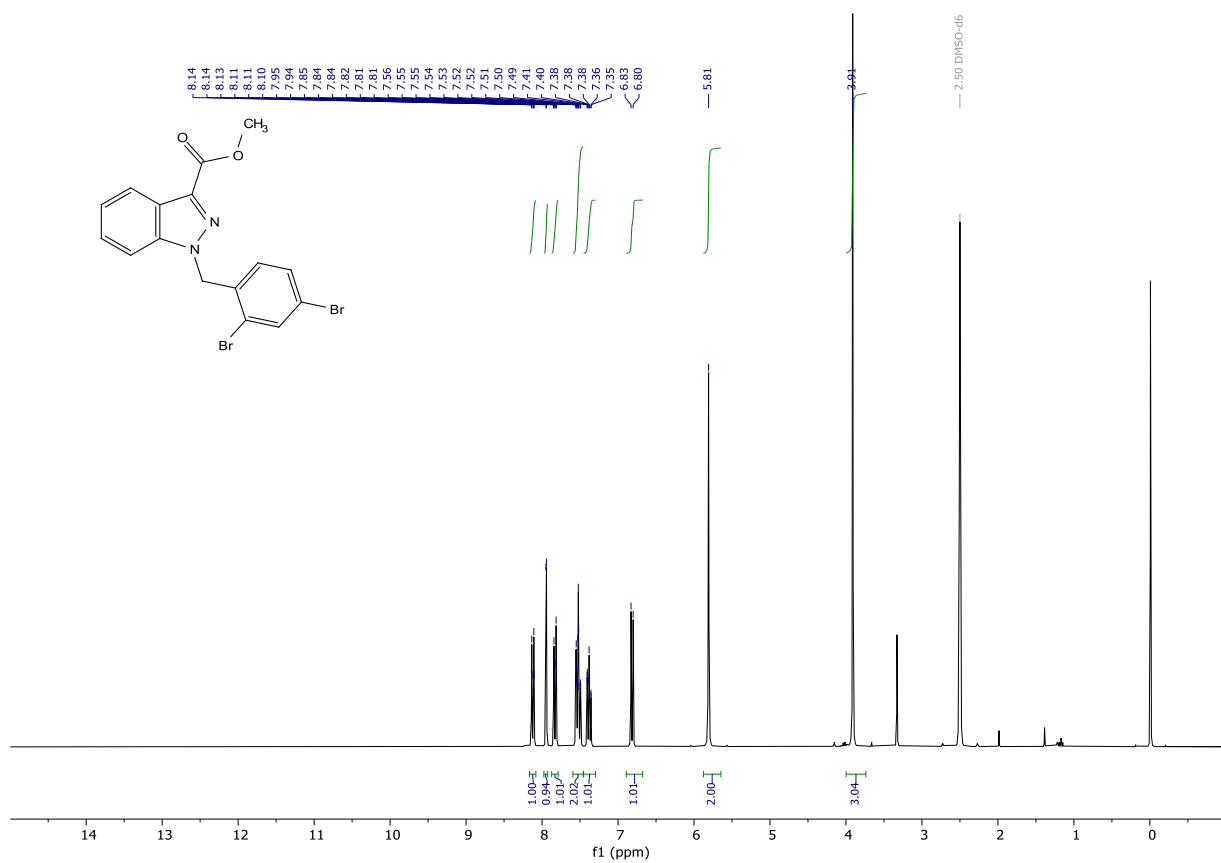
2-(1-(cyanomethyl)-1H-1,2,3-triazol-4-yl)acetic acid (PGUB67). To a stirred solution of bromoacetonitrile (0.250 mL, 0.4305 g, 3.7452 mmol) in a mixture of water and absolute ethanol was added sodium azide (0.163 g, 2.5073 mmol). The mixture was heated to 70 °C for 3.5 h. Then the mixture was diluted with water, and the aqueous phase was extracted with diethyl ether. The combined organic layers were dried over MgSO_4 , filtered, and concentrated under reduced pressure, to give 0.354 g of an orange oil. All of this was dissolved in *t*-BuOH (30 mL) and H_2O (30 mL). To the mixture was added 3-Butynoic acid (0.310 g, 3.6872 mmol), copper sulfate pentahydrate (0.018 g, 0.0721 mmol) and sodium ascorbate (0.074 g, 0.3735 mmol). The mixture was placed under an argon atmosphere and was stirred for 16 h. The mixture was acidified with 1 M HCl until a pH of 1. The

mixture was saturated with sodium chloride, extracted with ethyl acetate, the combined organic layers were washed with brine (3x) dried over MgSO_4 , filtered, and concentrated under reduced pressure, to give a white solid. The solid was taken up in a mixture of methanol and ethyl acetate and was concentrated onto silica gel. The crude was purified by reverse phase flash column chromatography (water + 0.1% TFA/ acetonitrile + 0.1% TFA gradient from 1:0 to 4:1), to give the desired product in 13% yield (0.04561 g, 0.27453 mmol). White solid: **^1H NMR** (400 MHz, $\text{DMSO}-d_6$) δ 12.54 (s, 1H), 8.15 (s, 1H), 5.78 (s, 2H), 3.71 (s, 2H). **^{13}C NMR** (101 MHz, DMSO) δ 171.34, 141.33, 124.47, 115.09, 37.23, 31.23. **HRMS** (ESI) calculated for $[\text{M}-\text{H}]^-$ $\text{C}_6\text{H}_5\text{N}_4\text{O}_2$ 165.0418, found 165.0421. **Purity (HPLC):** >99% UV_{214} , no absorption UV_{254} .





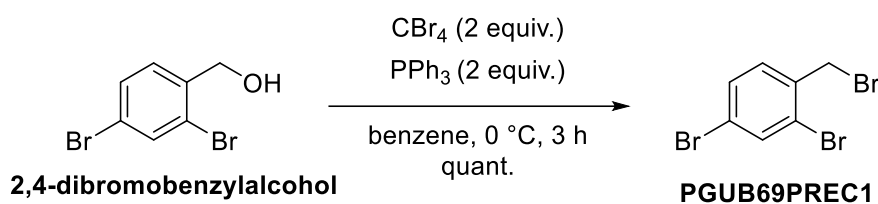
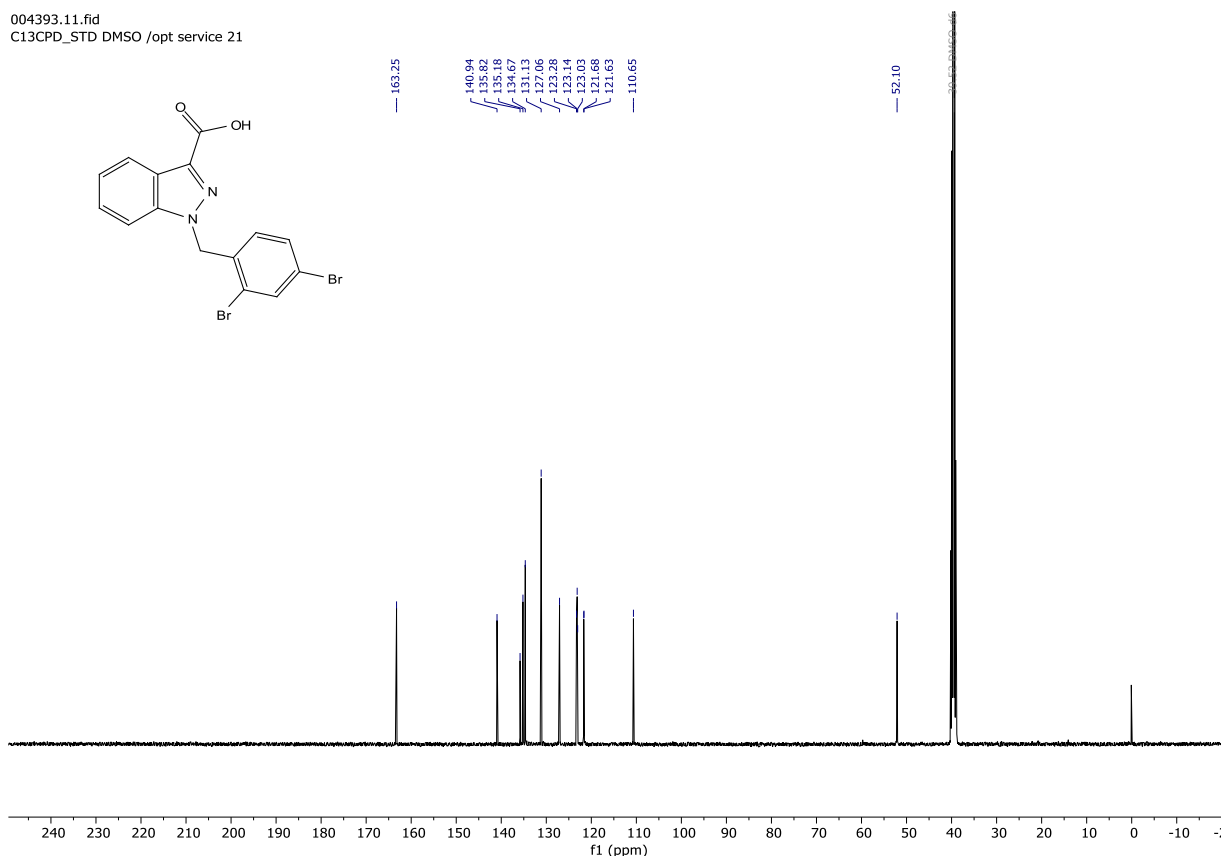
methyl 1-(2,4-dibromobenzyl)-1H-indazole-3-carboxylate (PGUB68PREC) (Z = N, Y = OMe). Prepared according to general procedure II from methyl 1H-indazole-3-carboxylate (Z = N, Y = OMe, 0.269 g, 1.5269 mmol) using 2,4-dibromobenzyl bromide as alkyl halide, to give the desired product in 48% yield (0.30800 g, 0.72626 mmol). White solid slightly impure with cyclohexane: ^1H NMR (300 MHz, DMSO- d_6) δ 8.12 (dt, J = 8.2, 1.0 Hz, 1H), 7.95 (d, J = 2.0 Hz, 1H), 7.83 (dt, J = 8.5, 0.9 Hz, 1H), 7.59 – 7.46 (m, 2H), 7.38 (ddd, J = 7.9, 6.9, 0.9 Hz, 1H), 6.81 (d, J = 8.3 Hz, 1H), 5.81 (s, 2H), 3.91 (s, 3H). ^{13}C NMR (75 MHz, DMSO) δ 162.17, 140.89, 135.03, 134.72, 134.69, 131.23, 131.15, 127.27, 123.50, 123.35, 122.82, 121.75, 121.34, 110.84, 52.22, 51.74. HRMS (ESI) calculated for $[\text{M}+\text{H}]^+$ $\text{C}_{16}\text{H}_{13}\text{Br}_2\text{N}_2\text{O}_2$ 422.9338, found 422.9338.



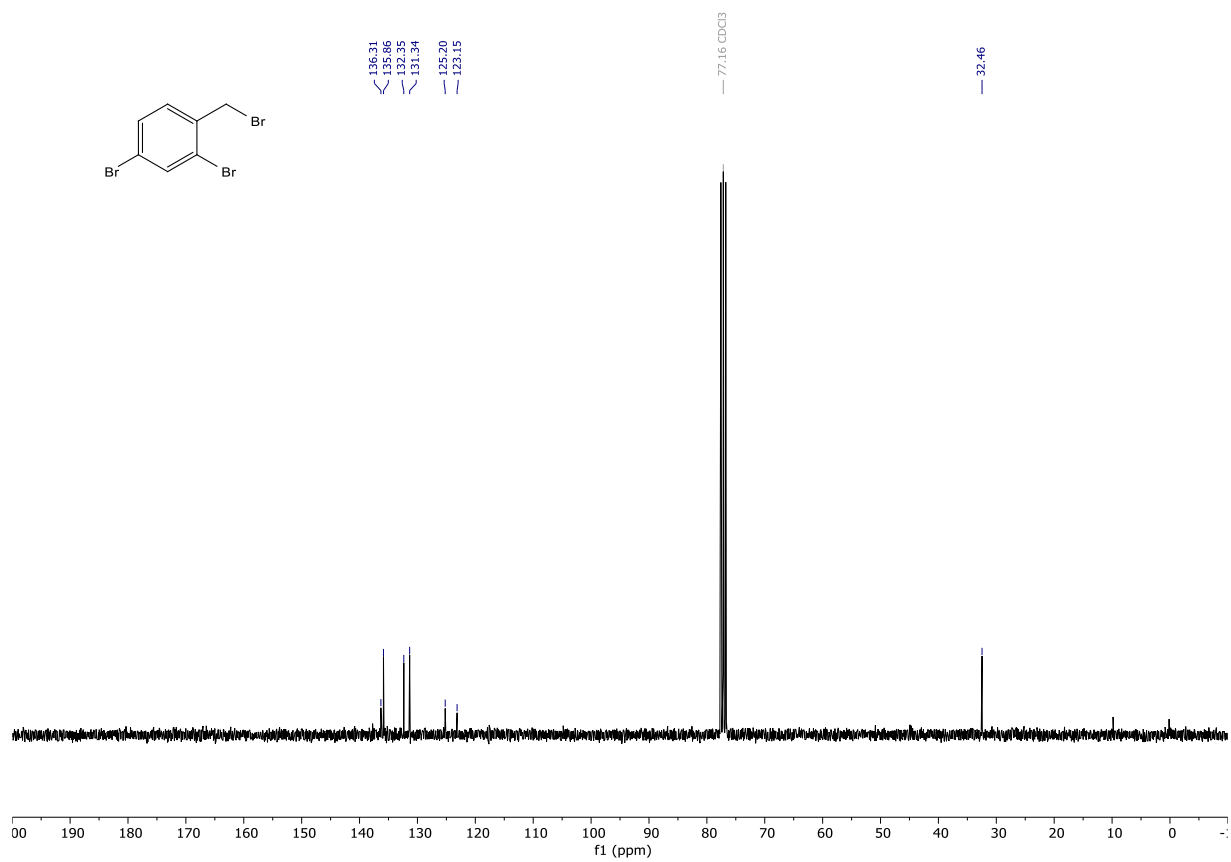
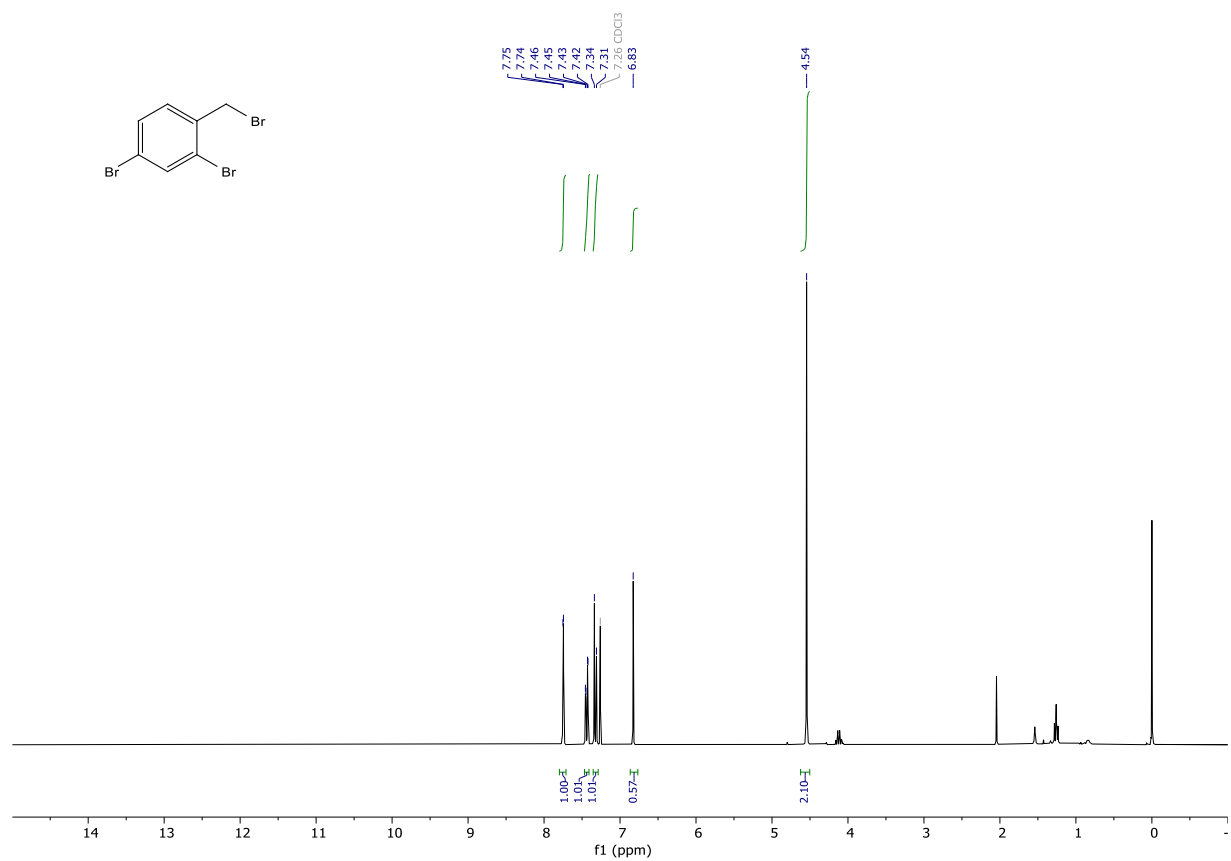


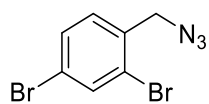
004393.10.fid
H1_STD DMSO /opt service 21





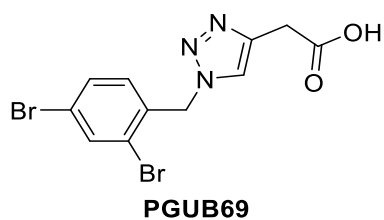
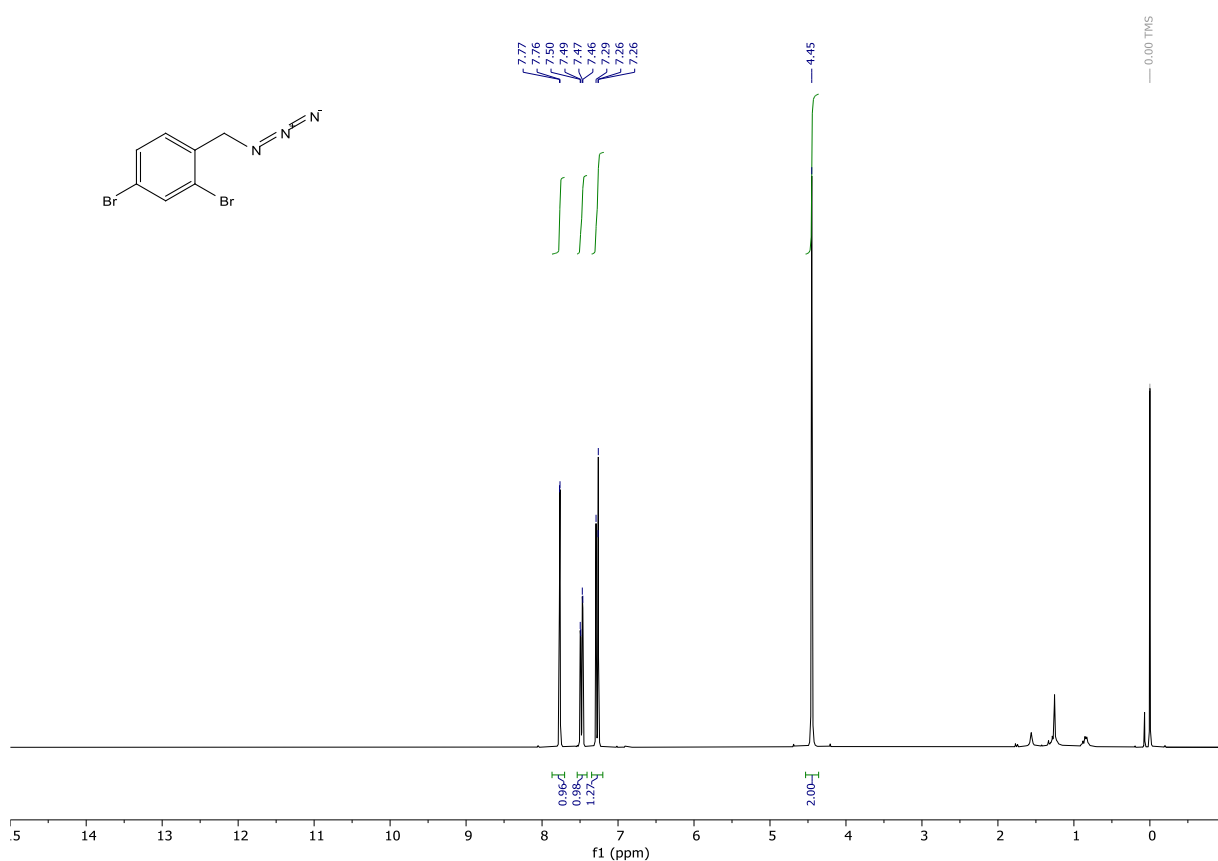
2,4-dibromobenzyl bromide (PGUB69PREC1). To a stirred solution of 2,4-Dibromophenylmethanol (1.003 g, 265.932 mmol) and CBr₄ in benzene (2.500 g, 7.5385 mmol) in benzene (40 mL) at 0 °C was added portion wise over the course of 30 minutes triphenylphosphine (1.972 g, 7.5184 mmol). The mixture turned from a yellow solution into a yellowish suspension over the course of the addition. The mixture was left stirring. The mixture was concentrated under reduced pressure. The concentrate was taken up in dichloromethane and concentrated onto silica gel. The crude was purified by flash column chromatography (cyclohexane/ ethyl acetate gradient from 1:0 to 4:1), to give the desired product in quantitative yield (1.40045 g, 4.25890 mmol). Clear colourless oil: ¹H NMR (300 MHz, Chloroform-*d*) δ 7.75 (d, *J* = 2.0 Hz, 1H), 7.44 (dd, *J* = 8.2, 2.0 Hz, 1H), 7.32 (d, *J* = 8.2 Hz, 1H), 6.83 (s, 1H), 4.54 (s, 2H). ¹³C NMR (75 MHz, CDCl₃) δ 136.31, 135.86, 132.35, 131.34, 125.20, 123.15, 32.46.





PGUB69PREC2

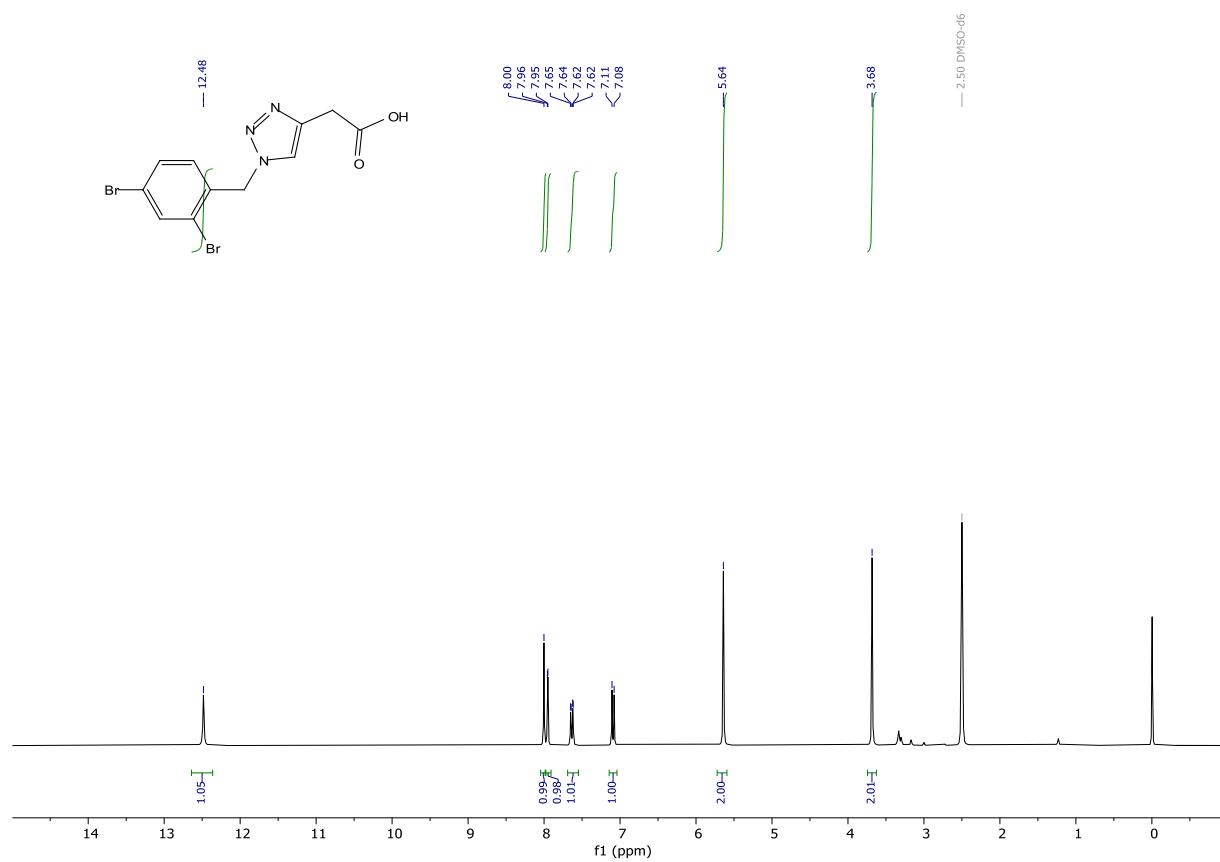
2,4-dibromobenzyl azide (PGUB69PREC2). Prepared according to general procedure V from 2,4-dibromobenzyl bromide (PGUB69PREC1) (0.688 g, 2.8676 mmol), to give the desired product in 42% yield (0.24047 g, 1.18996 mmol). Brown oil: ^1H NMR (300 MHz, Chloroform-*d*) δ 7.77 (d, J = 2.0 Hz, 1H), 7.48 (dd, J = 8.2, 2.0 Hz, 1H), 7.35 – 7.20 (m, 1H), 4.45 (s, 2H).

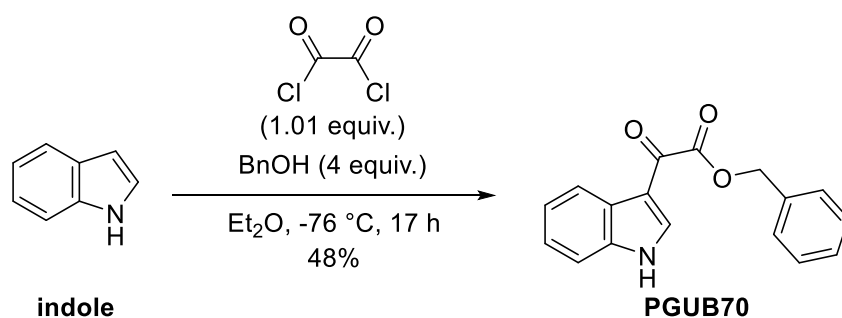
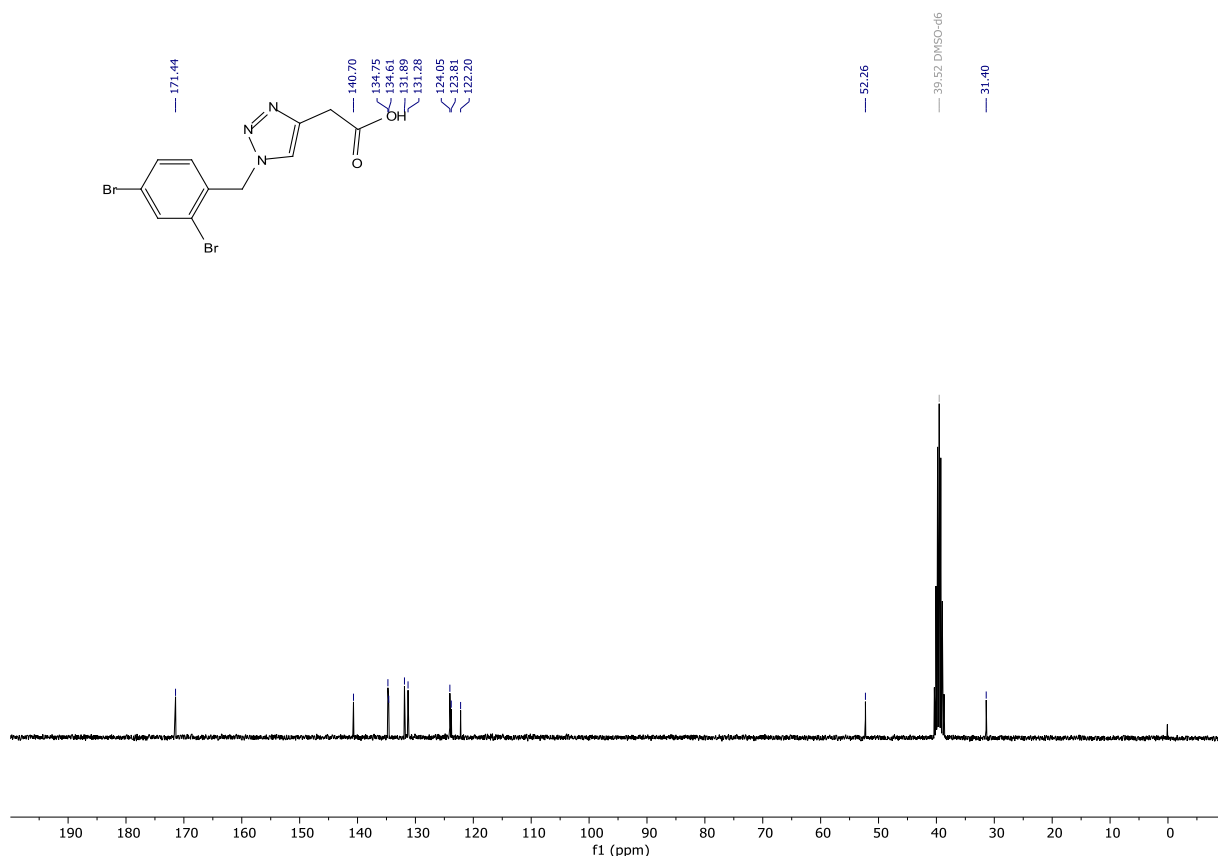


PGUB69

2-(1-(2,4-dibromobenzyl)-1H-1,2,3-triazol-4-yl)acetic acid (PGUB69). Prepared according to general procedure IV from 3-butynoic acid (0.05683 g, 0.6760 mmol) using 2,4-dibromobenzyl azide (PGUB69PREC2), to give the desired product in 56% yield (0.14180 g, 0.378113 mmol). White solid: ^1H NMR (300 MHz, DMSO-*d*₆) δ 12.48 (s, 1H), 8.00 (s, 1H), 7.95 (d, J = 2.0 Hz, 1H), 7.63 (dd, J = 8.3, 2.0 Hz, 1H), 7.09 (d, J = 8.3 Hz, 1H), 5.64 (s, 2H), 3.68 (s, 2H). ^{13}C NMR (75 MHz, DMSO) δ 171.44, 140.70,

134.75, 134.61, 131.89, 131.28, 124.05, 123.81, 122.20, 52.26, 31.40. **HRMS** (ESI) calculated for [M-H]⁻ C₁₁H₈Br₂N₃O₂ 371.8989, found 371.8996. **Purity (HPLC)**: >95% UV₂₁₄, >91% UV₂₅₄.

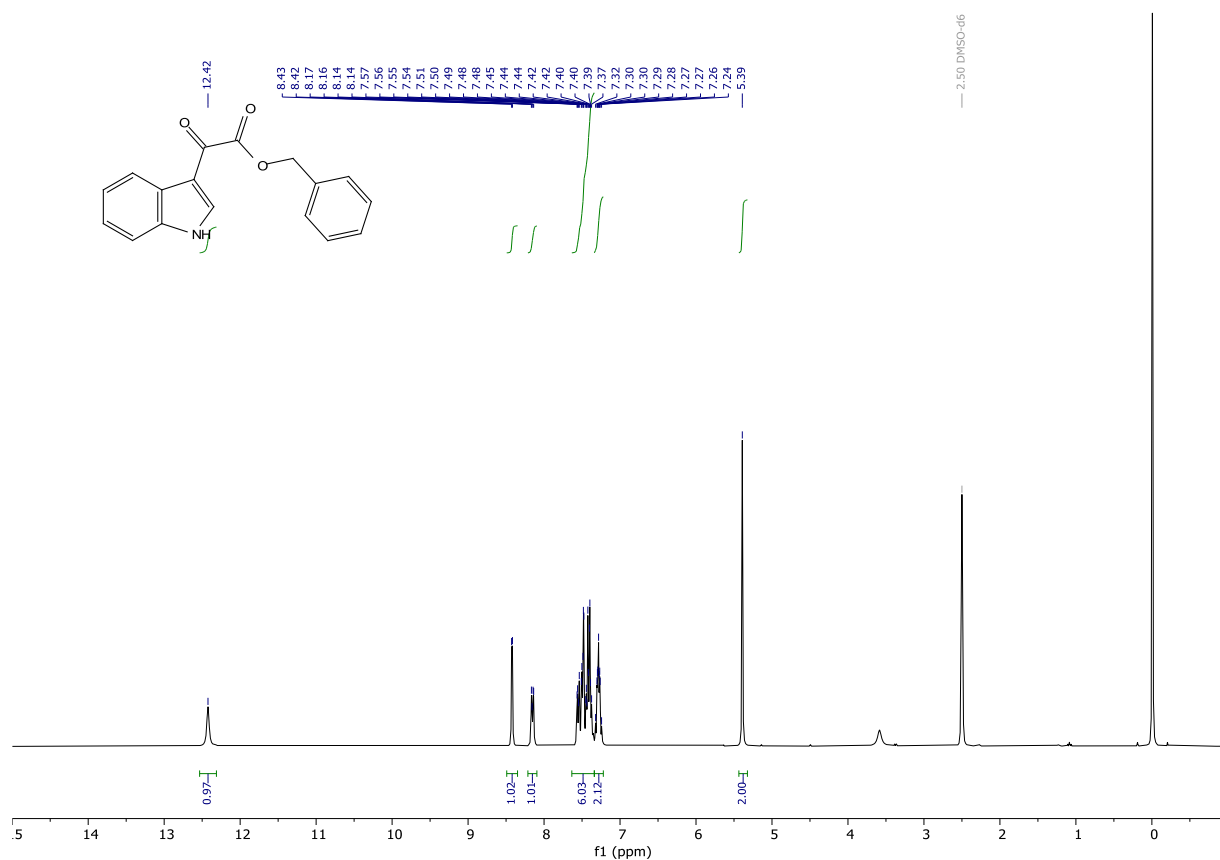


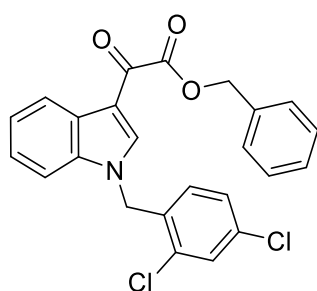
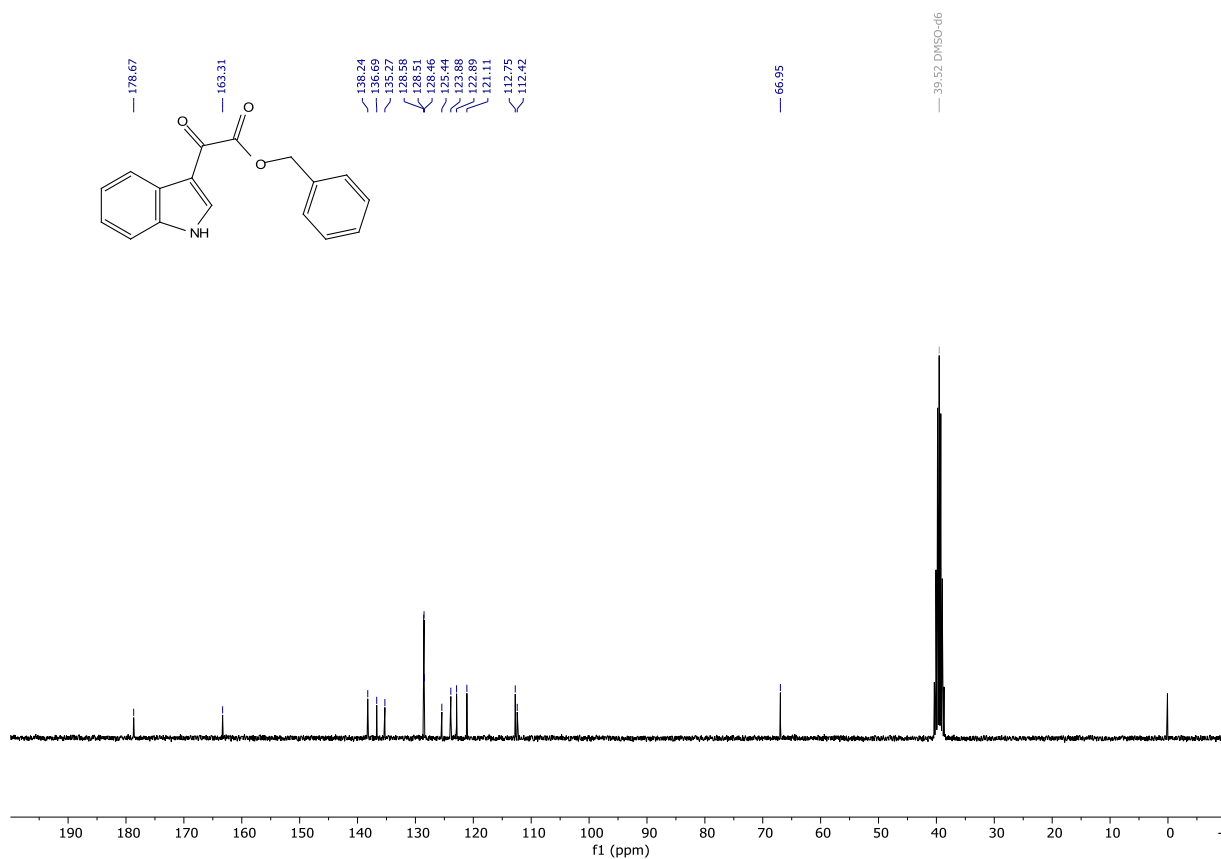


benzyl 2-(1H-indol-3-yl)-2-oxoacetate (PGUB70). To a stirred solution of indole (1.563 g, 13.3418 mmol) in dry diethyl ether (15.5 mL) at 0 °C under an argon atmosphere was added slowly oxalyl chloride (1.15 mL, 1.702 g, 13.4100 mmol). The mixture was left stirring at 0 °C for 1 h. Then the mixture was cooled to -76 °C. Then benzyl alcohol (2 mL, 2.08 g, 19.2343 mmol) was added. The mixture was left stirring while slowly warming to 21 °C over 16 h. To the mixture was added aq. sat. NaHCO₃ resulting in a precipitation. The precipitate was filtered off and was thoroughly dried to give 0.60218 g of a beige solid. This solid was taken up in a mixture of dichloromethane and methanol and was concentrated onto silica gel. The crude was purified by flash column chromatography (cyclohexane/ethyl acetate gradient from 1:0 to 0:1), to give the desired product in 48% yield (0.60218 g, 2.15607 mmol). Off white solid: ¹H NMR (300 MHz, DMSO-*d*₆) δ 12.42 (s, 1H), 8.42 (d, *J* = 3.4 Hz, 1H), 8.21 – 8.09 (m, 1H), 7.63 – 7.34 (m, 6H), 7.28 (ddd, *J* = 6.3, 3.5, 1.8 Hz, 2H), 5.39 (s, 2H). ¹³C NMR (75 MHz,

DMSO) δ 178.67, 163.31, 138.24, 136.69, 135.27, 128.58, 128.51, 128.46, 125.44, 123.88, 122.89, 121.11, 112.75, 112.42, 66.95. **HRMS** (ESI) calculated for $[M+H]^+$ $C_{17}H_{14}NO_3$ 280.0968, found 280.0957.

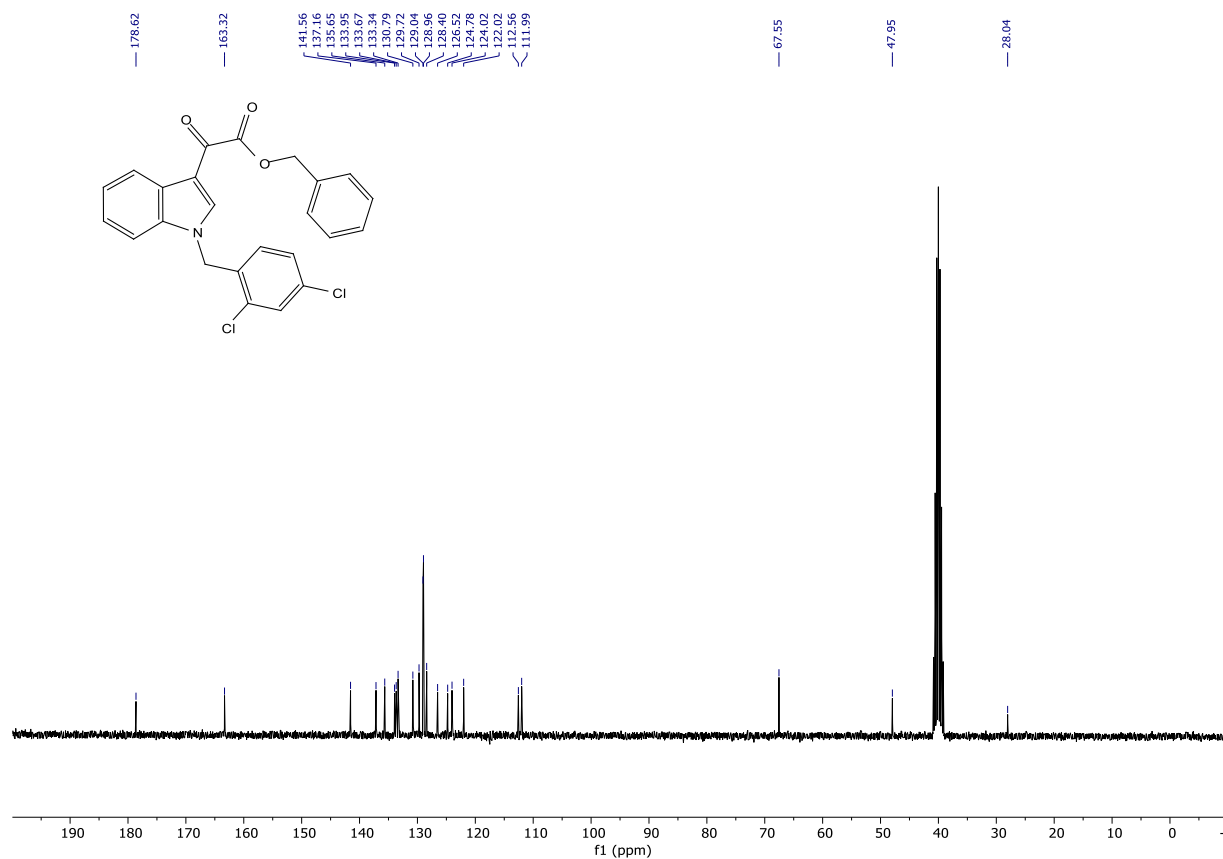
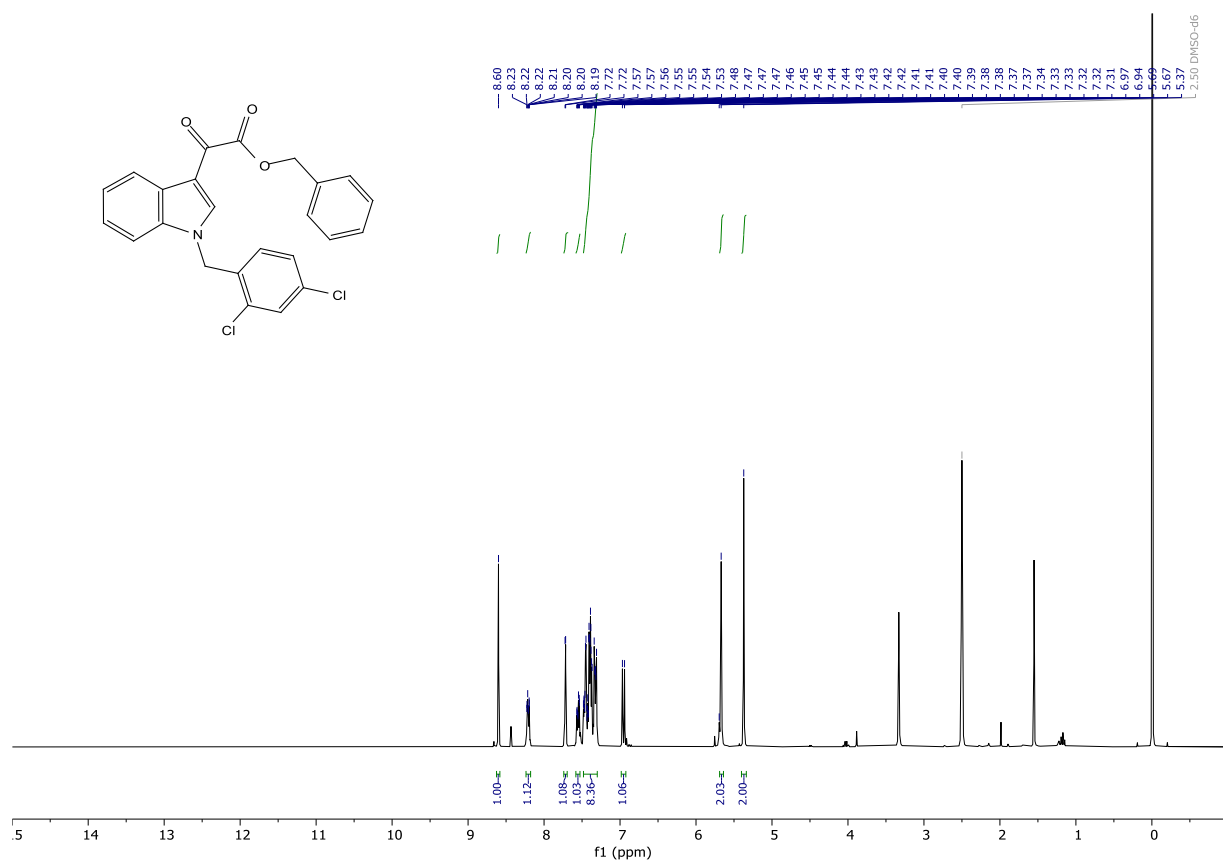
Purity (HPLC): >96% UV_{214} , >97% UV_{254} .

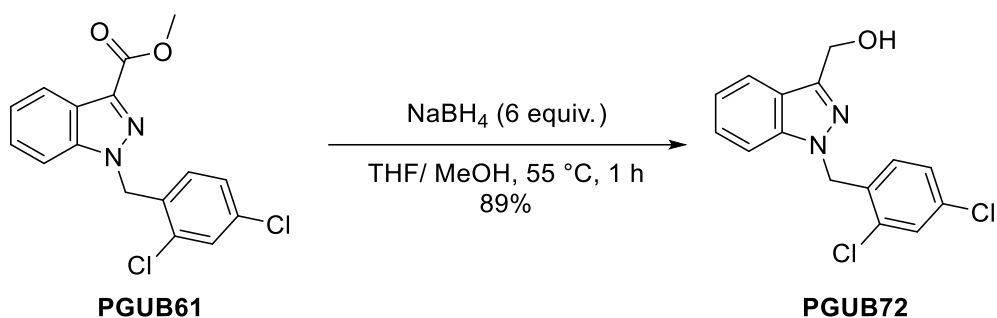




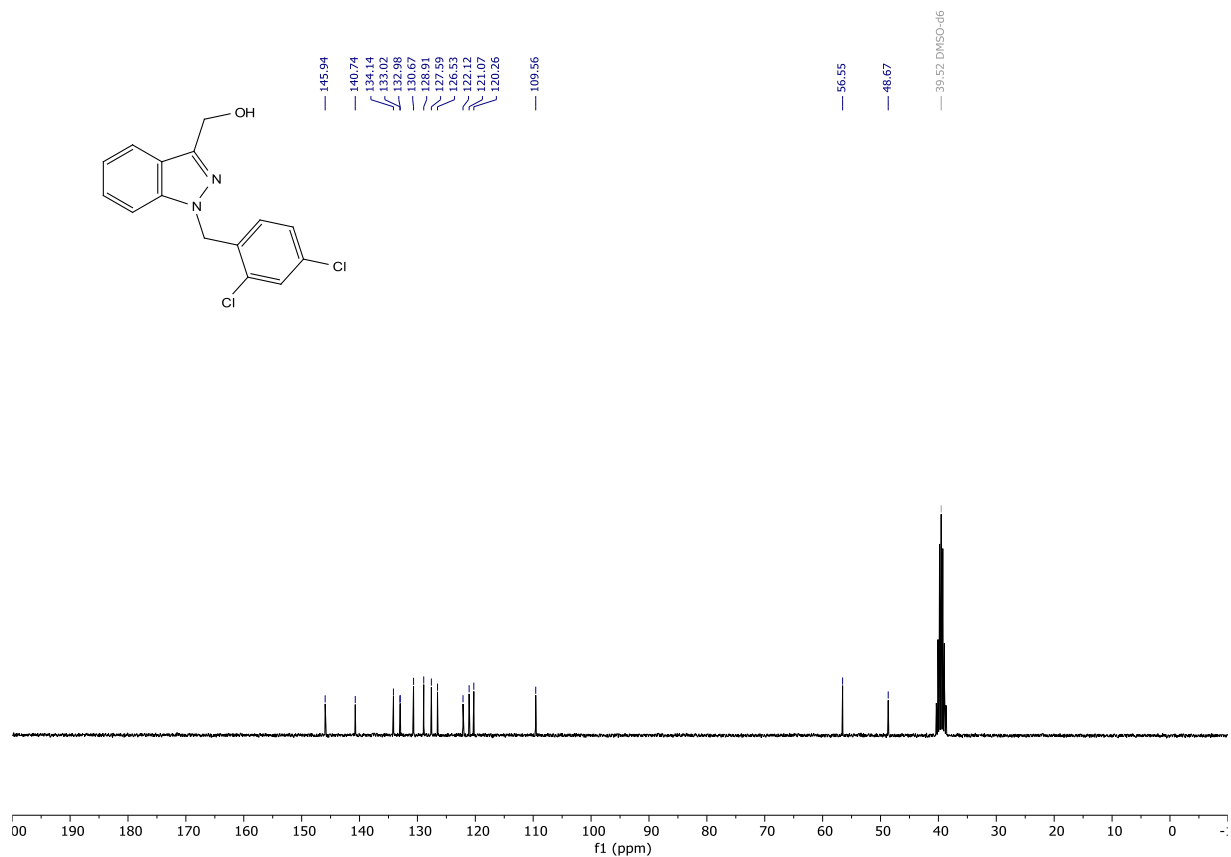
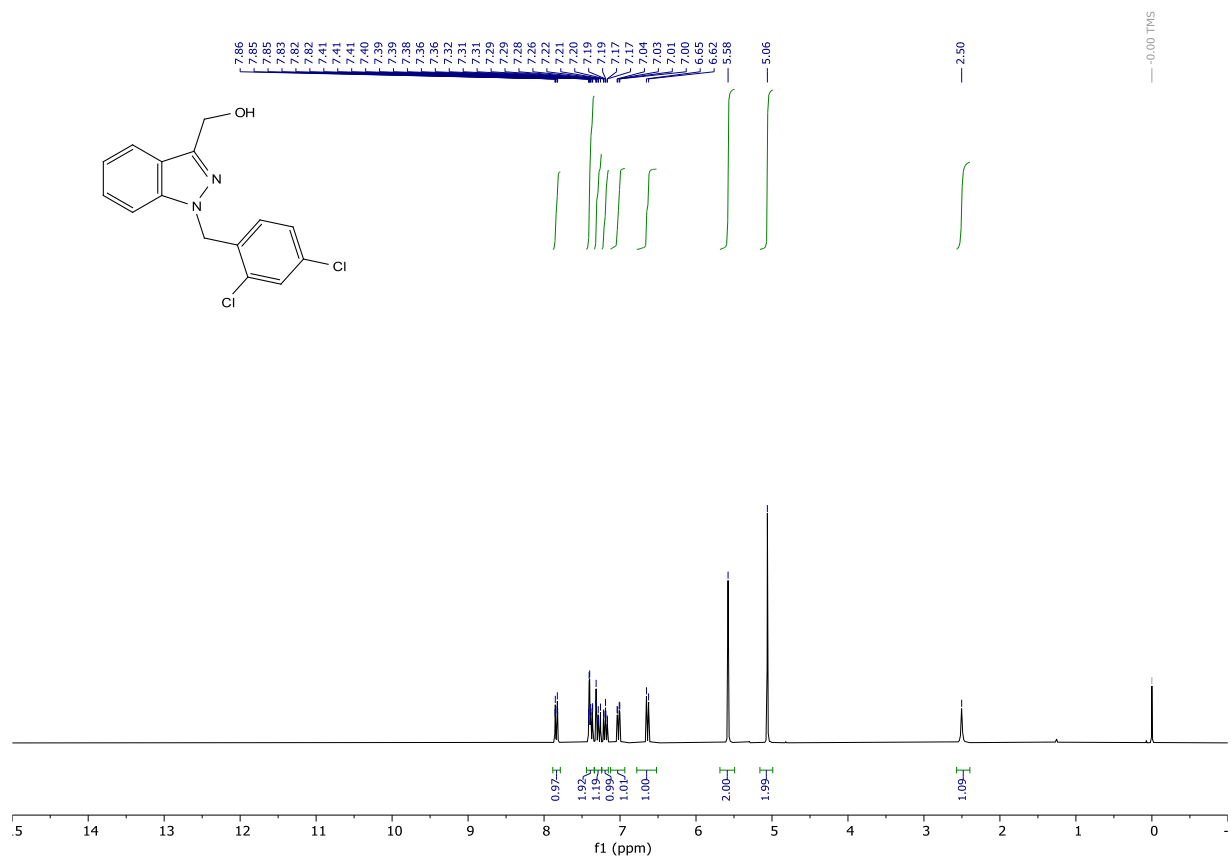
PGUB71

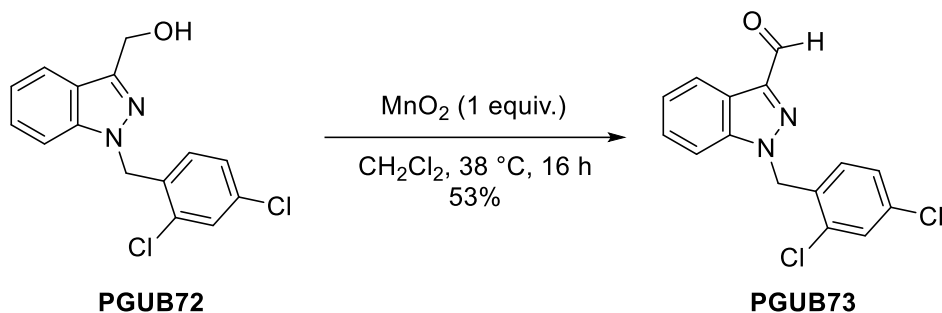
benzyl 2-(1-(2,4-dichlorobenzyl)-1H-indol-3-yl)-2-oxoacetate (PGUB71) (Z = CH, Y = OBn). Prepared according to general procedure II from benzyl 2-(1H-indol-3-yl)-2-oxoacetate (PGUB70) (Z = CH, Y = OBn, 0.300 g, 1.0741 mmol) using 2,4-dichlorobenzyl bromide as alkyl halide, to give the desired product in 57% yield (0.26936 g, 0.61455 mmol). Yellowish solid: **¹H NMR** (300 MHz, DMSO-*d*₆) δ 8.60 (s, 1H), 8.24 – 8.18 (m, 1H), 7.72 (d, *J* = 2.1 Hz, 1H), 7.58 – 7.53 (m, 1H), 7.48 – 7.30 (m, 8H), 6.95 (d, *J* = 8.3 Hz, 1H), 5.67 (s, 2H), 5.37 (s, 2H). **¹³C NMR** (75 MHz, DMSO) δ 178.62, 163.32, 141.56, 137.16, 135.65, 133.95, 133.67, 133.34, 130.79, 129.72, 129.04, 128.96, 128.40, 126.52, 124.78, 124.02, 122.02, 112.56, 111.99, 67.55, 47.95, 28.04. **HRMS** (ESI) calculated for [M+H]⁺ C₂₄H₁₈Cl₂NO₃ 438.0658, found 438.0659. **Purity (HPLC):** >97% UV₂₁₄, >97% UV₂₅₄.





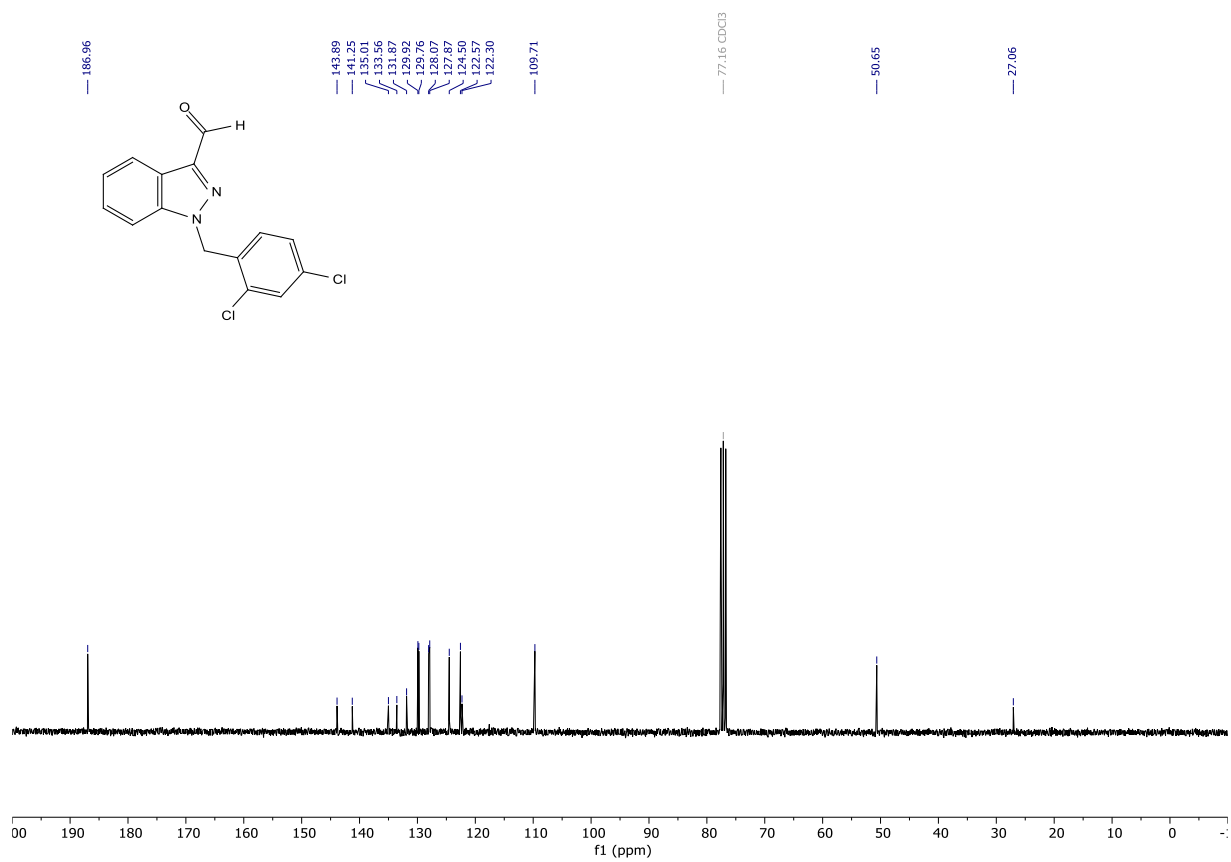
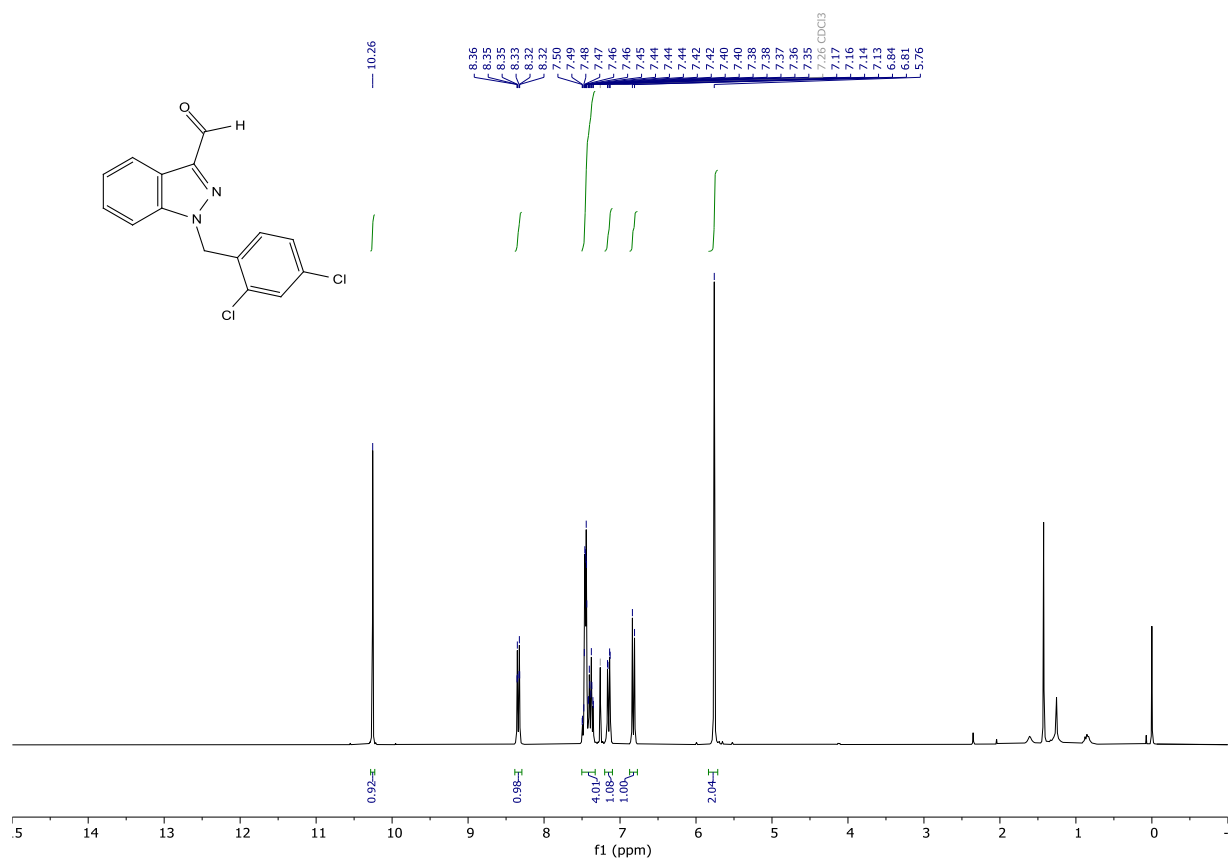
(1-(2,4-dichlorobenzyl)-1H-indazol-3-yl)methanol (PGUB72). Prepared according to modified literature procedure.⁸⁴ To a stirred solution methyl 1-(2,4-dichlorobenzyl)-1H-indazole-3-carboxylate (PGUB61) (0.65495 g, 1.9540 mmol) in THF (8 mL) was added sodium borohydride (0.44777 g, 11.8364 mmol). The mixture was heated to 55 °C. Then slow and dropwise methanol (5.2 mL) was added. This led to intense bubbling. After full addition, the mixture was stirred at 55 °C. The gas formation quickly ceased. Then the volatiles were removed under reduced pressure. The white residue was mixed with water, the aqueous phase was acidified with 2 M aq. HCl to a pH of 1. To the suspension was added dichloromethane leading to clear biphasic mixture. The aqueous phase was extracted with dichloromethane. The combined organic layers were washed with water, dried over MgSO₄, filtered, and concentrated under reduced pressure to give a white solid. This solid was stirred with n-hexane. Was filtered and the filter cake washed with little n-hexane and thoroughly dried under reduced pressure to give the desired product in 89% yield (0.53130 g, 1.72964 mmol). White solid: ¹H NMR (300 MHz, Chloroform-*d*) δ 7.84 (dt, *J* = 8.1, 1.0 Hz, 1H), 7.44 – 7.34 (m, 2H), 7.34 – 7.24 (m, 1H), 7.19 (ddd, *J* = 7.9, 6.7, 1.0 Hz, 1H), 7.02 (dd, *J* = 8.4, 2.1 Hz, 1H), 6.64 (d, *J* = 8.4 Hz, 1H), 5.58 (s, 2H), 5.06 (s, 2H), 2.50 (s, 1H). ¹³C NMR (75 MHz, DMSO) δ 145.94, 140.74, 134.14, 133.02, 132.98, 130.67, 128.91, 127.59, 126.53, 122.12, 121.07, 120.26, 109.56, 56.55, 48.67. HRMS (ESI) calculated for [M+H]⁺ C₁₅H₁₃Cl₂N₂O 307.0410, found 307.0398. **Purity (HPLC):** >96% UV₂₁₄, >99% UV₂₅₄.

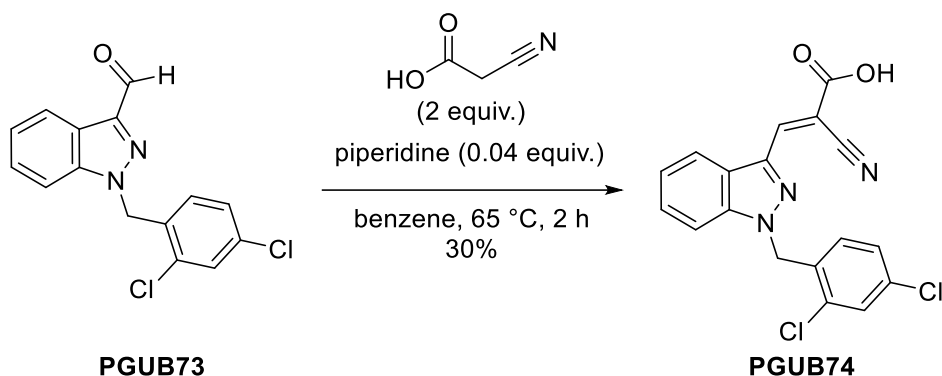




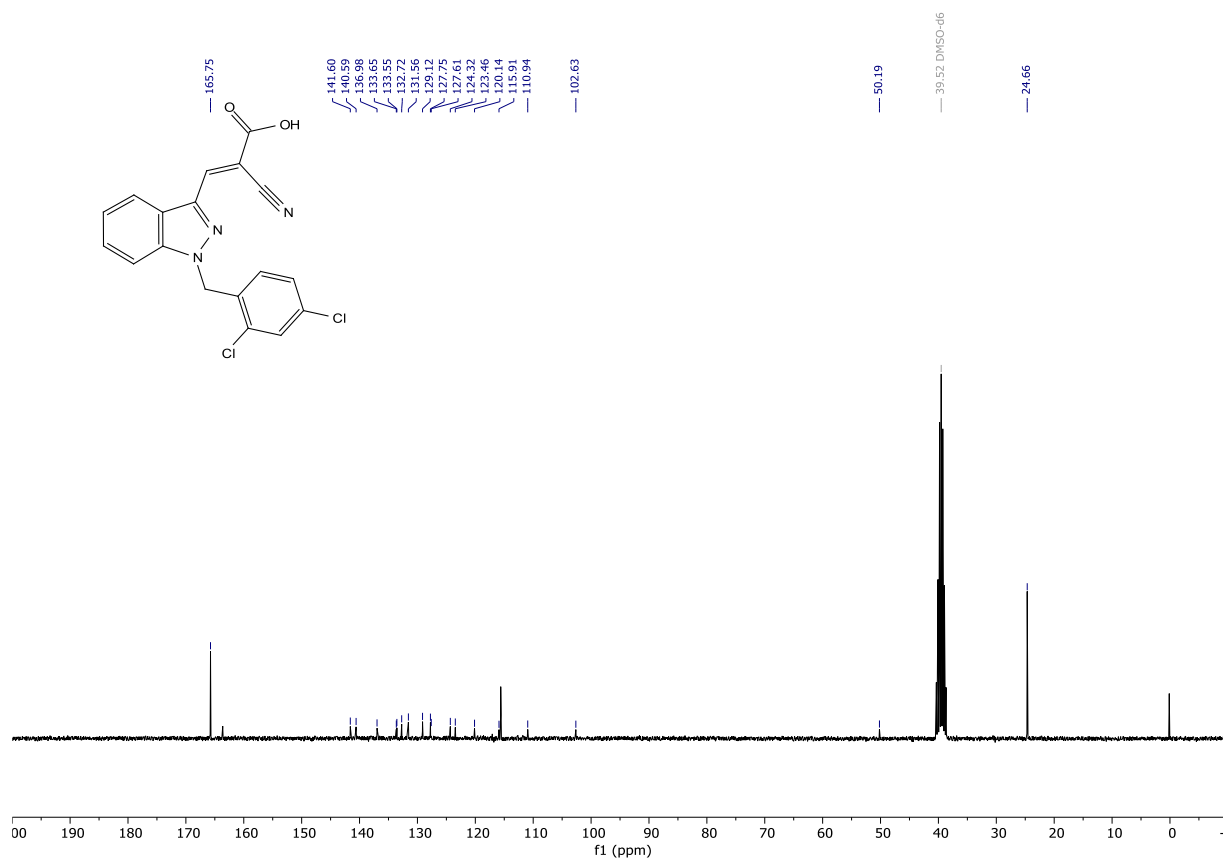
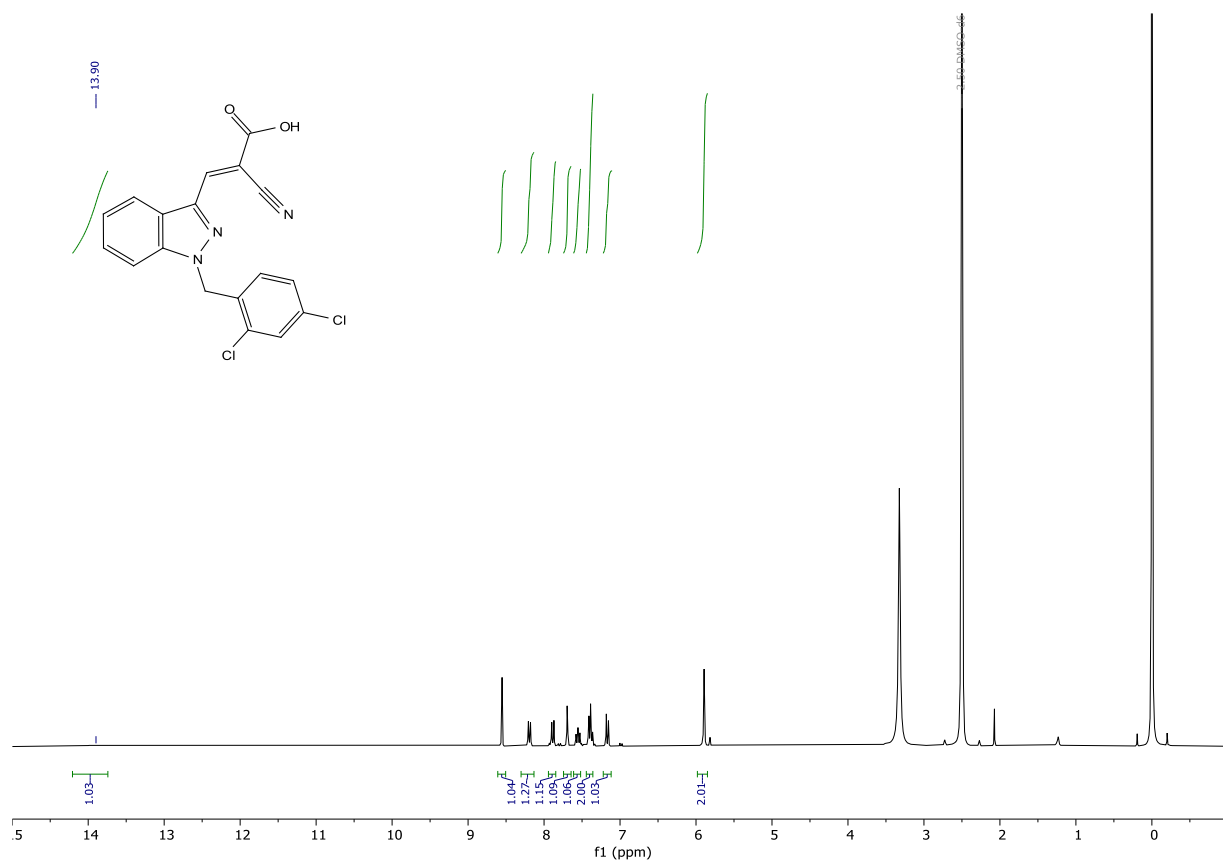
1-(2,4-dichlorobenzyl)-1H-indazole-3-carbaldehyde (PGUB73). MnO₂ was prepared according to reference literature.⁸⁵ <https://pubs.acs.org/doi/10.1021/jo00836a091>

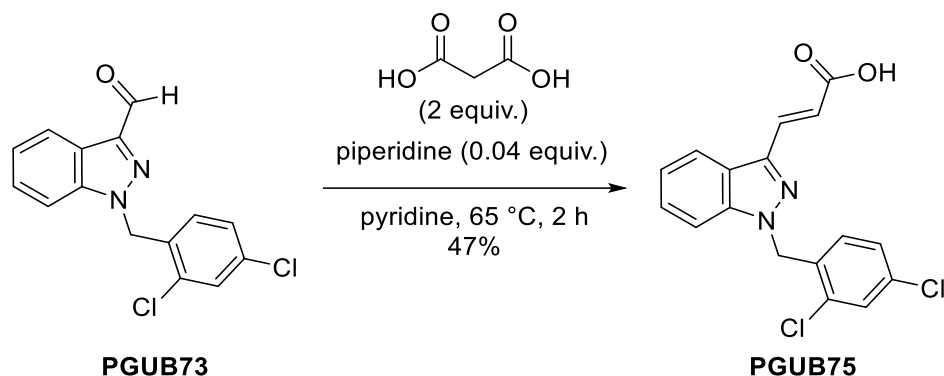
To a stirred solution of (1-(2,4-dichlorobenzyl)-1H-indazol-3-yl)methanol (PGUB72) (0.178 g, 0.5795 mmol) in dichloromethane (10 mL) was added freshly activated MnO₂ (0.503 g, 5.7856 mmol). The mixture was heated to 38 °C and stirred for 16 h. The mixture was filtered through a pad of celite leaving a clear colourless solution. This was directly concentrated onto silica gel. The crude was purified by flash column chromatography (cyclohexane/ ethyl acetate gradient from 1:0 to 0:1), to give the desired product in 53% yield (0.09351 g, 0.30643 mmol). White solid slightly impure with cyclohexane: ¹H NMR (300 MHz, Chloroform-*d*) δ 10.26 (s, 1H), 8.34 (dt, *J* = 8.0, 1.1 Hz, 1H), 7.50 – 7.33 (m, 4H), 7.15 (dd, *J* = 8.4, 2.1 Hz, 1H), 6.82 (d, *J* = 8.4 Hz, 1H), 5.76 (s, 2H), 1.42 (s, 1H). ¹³C NMR (75 MHz, CDCl₃) δ 186.96, 143.89, 141.25, 135.01, 133.56, 131.87, 129.92, 129.76, 128.07, 127.87, 124.50, 122.57, 122.30, 109.71, 50.65. HRMS (ESI) calculated for [M+H]⁺ C₁₅H₁₁Cl₂N₂O 305.0243, found 305.0245. **Purity (HPLC):** >98% UV₂₁₄, >99% UV₂₅₄.





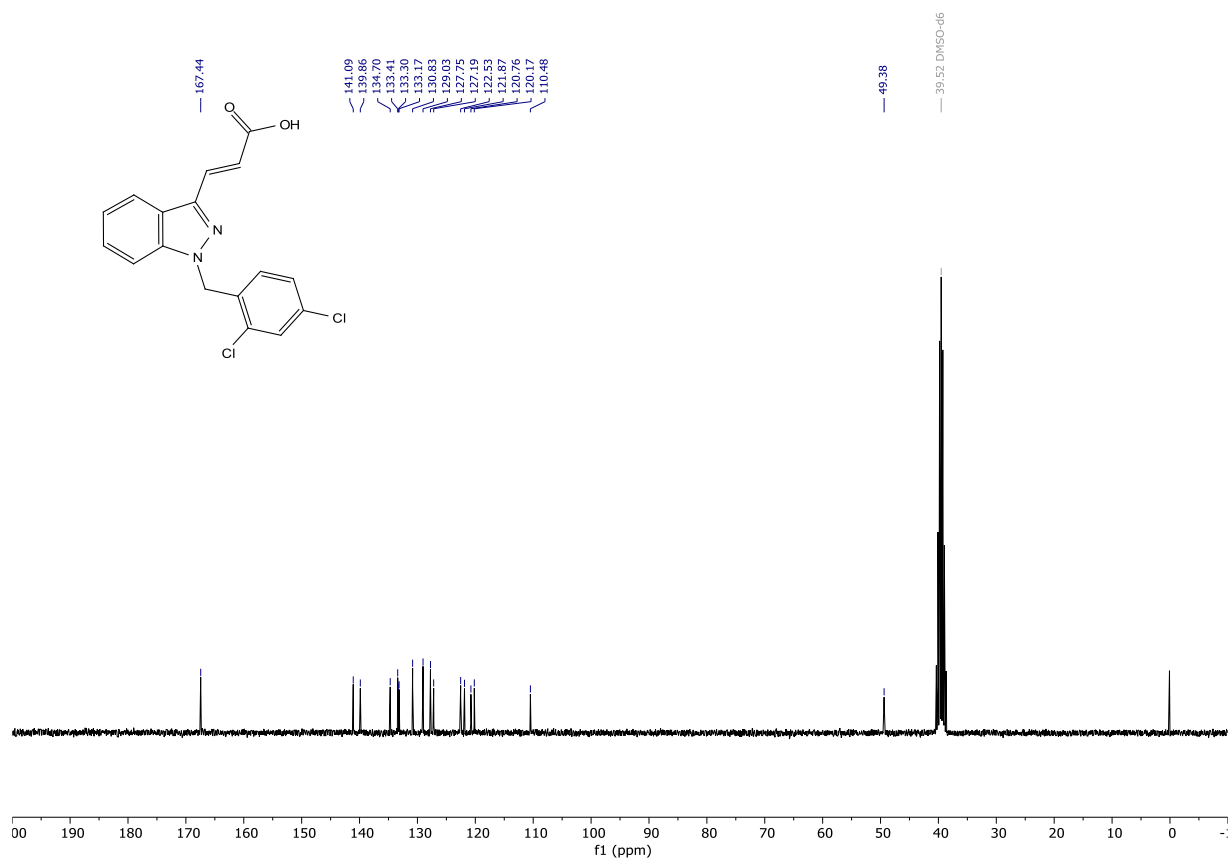
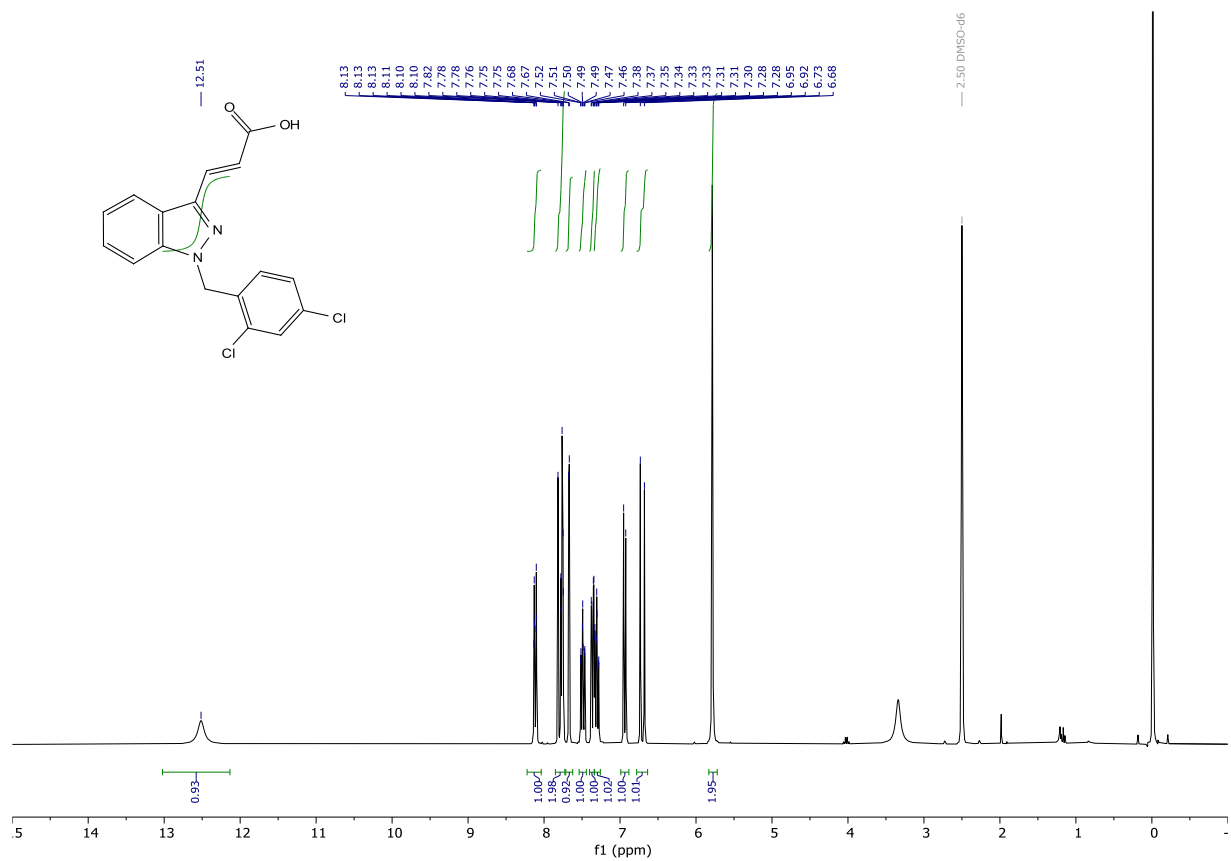
2-cyano-3-(1-(2,4-dichlorobenzyl)-1H-indazol-3-yl)acrylic acid (PGUB74). To a stirred solution of 1-(2,4-dichlorobenzyl)-1H-indazole-3-carbaldehyde (PGUB73) in benzene (5 mL) was added cyanoacetic acid (0.08735 g, 1.0269 mmol) followed by piperidine (0.010 mL, 0.00862 g, 0.1012 mmol). The mixture was stirred under an argon atmosphere for 2 h. Then the mixture was cooled to 22 °C and 0.1 M aq. HCl was added. The mixture was extracted with ethyl acetate. The combined organic layers were washed with brine, dried over MgSO_4 , filtered, and concentrated under reduced pressure onto silica gel. The crude was purified by flash column chromatography (cyclohexane/ (EtOAc/ MeOH/ AcOH 85:10:5) gradient from 1:0 to 1:1). This yielded an impure yellowish solid. The solid was taken up in a mixture of dichloromethane and methanol and concentrated onto silica gel. The mixture was purified by flash column chromatography (dichloromethane/ methanol gradient from 1:0 to 9:1). The still impure solid was purified again by reverse phase flash column chromatography (water + 0.1% TFA/ acetonitrile + 0.1% TFA gradient from 4:1 to 1:4), to give the desired product in 30% yield (0.05732 g, 0.15400 mmol). Yellow solid: $^1\text{H NMR}$ (300 MHz, $\text{DMSO}-d_6$) δ 13.90 (s, 1H), 8.55 (s, 1H), 8.30 – 8.13 (m, 1H), 7.88 (d, J = 8.6 Hz, 1H), 7.69 (d, J = 2.2 Hz, 1H), 7.55 (ddd, J = 8.3, 6.9, 1.0 Hz, 1H), 7.39 (td, J = 7.3, 6.4, 1.7 Hz, 2H), 7.17 (d, J = 8.4 Hz, 1H), 5.89 (s, 2H). $^{13}\text{C NMR}$ (75 MHz, DMSO) δ 141.60, 140.59, 136.98, 133.65, 133.55, 132.72, 131.56, 129.12, 127.75, 127.61, 124.32, 123.46, 120.14, 115.91, 110.94, 102.63, 50.19. **HRMS** (ESI) calculated for $[\text{M}+\text{H}]^+$ $\text{C}_{18}\text{H}_{12}\text{Cl}_2\text{N}_3\text{O}_2$ 372.0301, found 372.0313. **Purity (HPLC):** >80% UV_{214} , >95% UV_{254} .

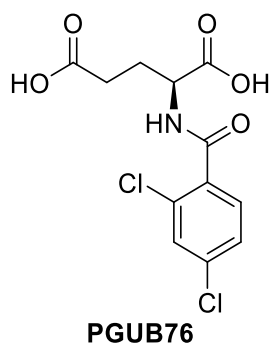




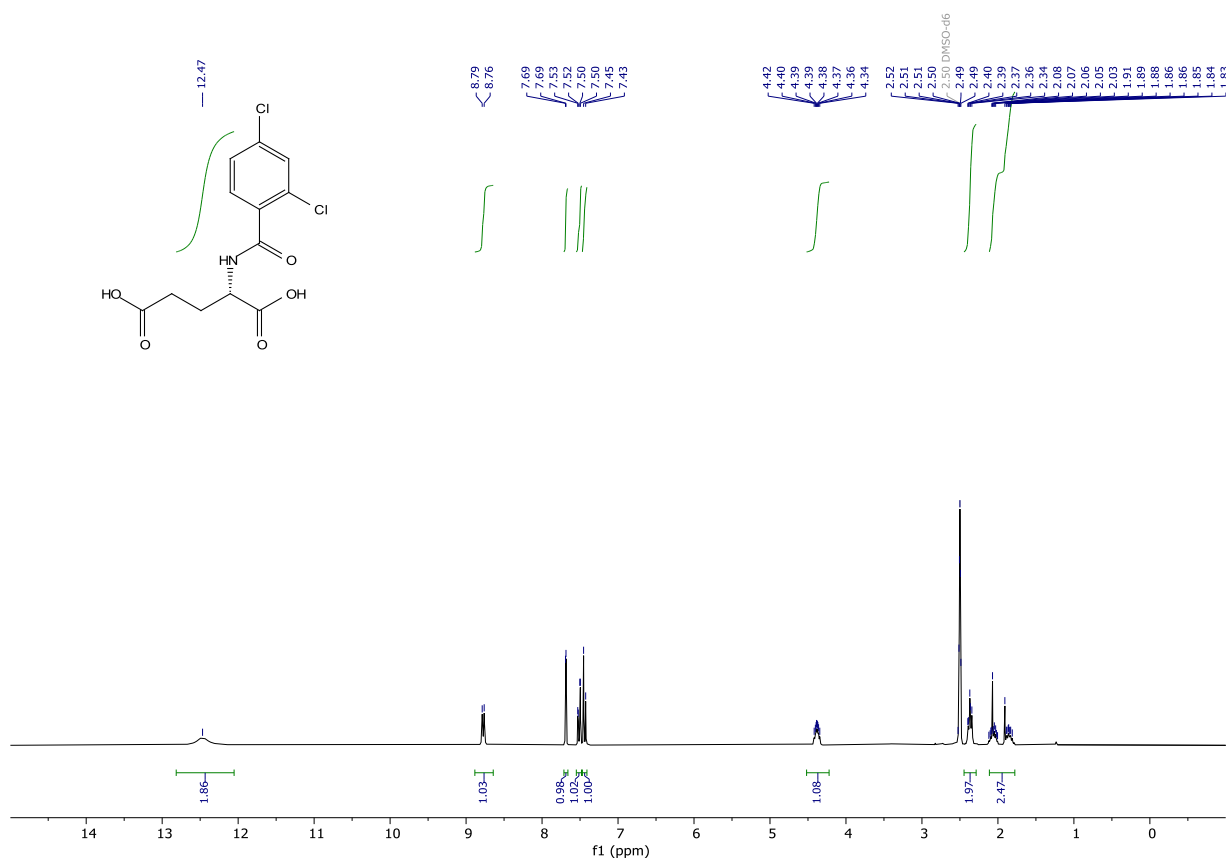
(E)-3-(1-(2,4-dichlorobenzyl)-1H-indazol-3-yl)acrylic acid (PGUB75).

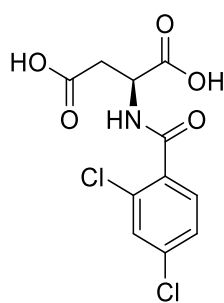
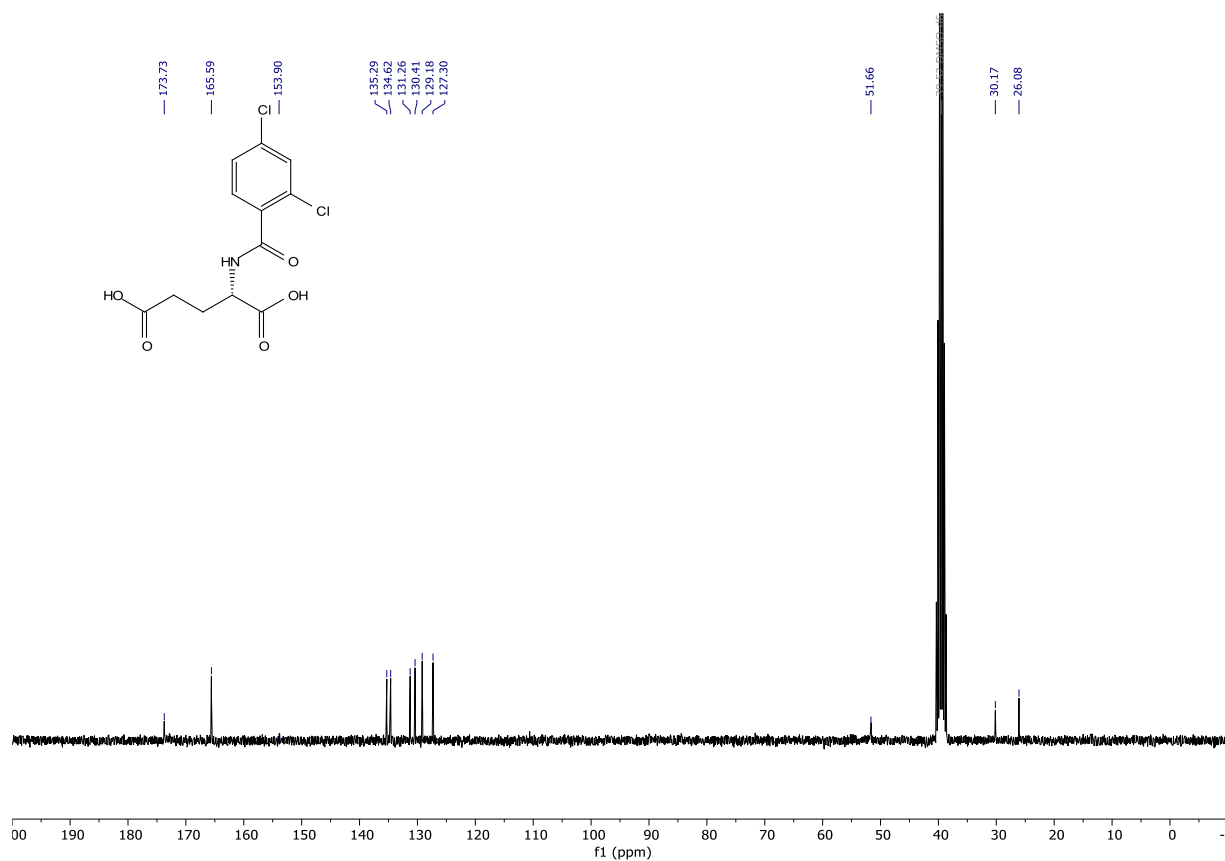
To a stirred solution of 1-(2,4-dichlorobenzyl)-1H-indazole-3-carbaldehyde (PGUB73) (0.18411 g, 0.6033 mmol) in pyridine (2 mL) was added malonic acid (0.12874 g, 1.2372 mmol) followed by piperidine (0.010 mL, 0.00862 g, 0.1012 mmol). The mixture was heated to 65 °C and was stirred for 2 h. Then the mixture was cooled to 22 °C and acidified with 1 M aq. HCl. The mixture was extracted with ethyl acetate. The combined organic layers were washed with brine, dried over MgSO₄, filtered, and concentrated under reduced pressure. The crude was taken up in a mixture of dichloromethane and methanol and concentrated onto silica gel. It was purified by flash column chromatography (cyclohexane/ ethyl acetate gradient from 1:0 to 0:1), to give the desired product in 47% yield (0.09900 g, 0.28514 mmol). White solid: **¹H NMR** (300 MHz, DMSO-*d*₆) δ 12.51 (s, 1H), 8.12 (dt, *J* = 8.2, 1.0 Hz, 1H), 7.85 – 7.73 (m, 2H), 7.67 (d, *J* = 2.2 Hz, 1H), 7.49 (ddd, *J* = 8.4, 6.9, 1.0 Hz, 1H), 7.36 (dd, *J* = 8.3, 2.2 Hz, 1H), 7.31 (ddd, *J* = 8.0, 6.9, 0.9 Hz, 1H), 6.94 (d, *J* = 8.3 Hz, 1H), 6.71 (d, *J* = 16.2 Hz, 1H), 5.79 (s, 2H). **¹³C NMR** (75 MHz, DMSO) δ 167.44, 141.09, 139.86, 134.70, 133.41, 133.30, 133.17, 130.83, 129.03, 127.75, 127.19, 122.53, 121.87, 120.76, 120.17, 110.48, 49.38. **HRMS** (ESI) calculated for [M+H]⁺ C₁₇H₁₃Cl₂N₂O₂ 347.0349, found 347.0366. **Purity (HPLC)**: >97% UV₂₁₄, >98% UV₂₅₄.





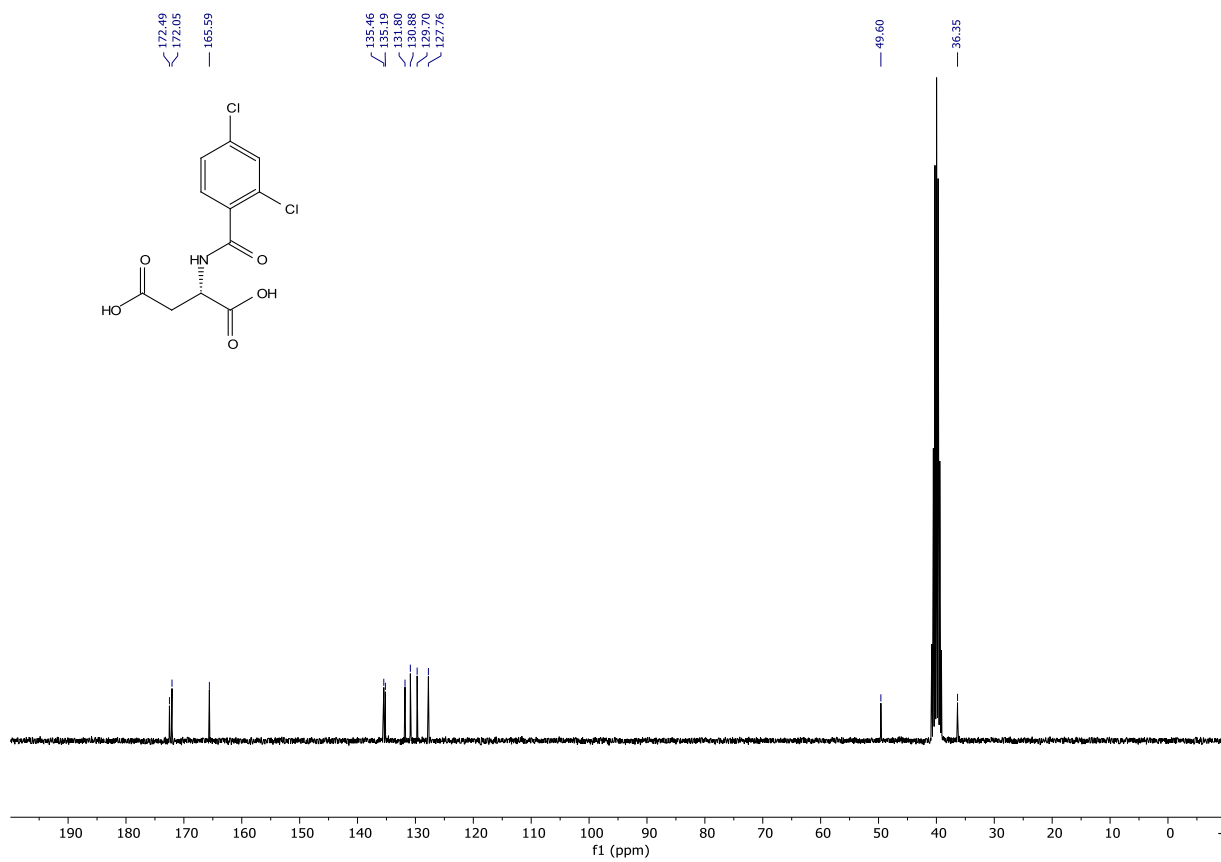
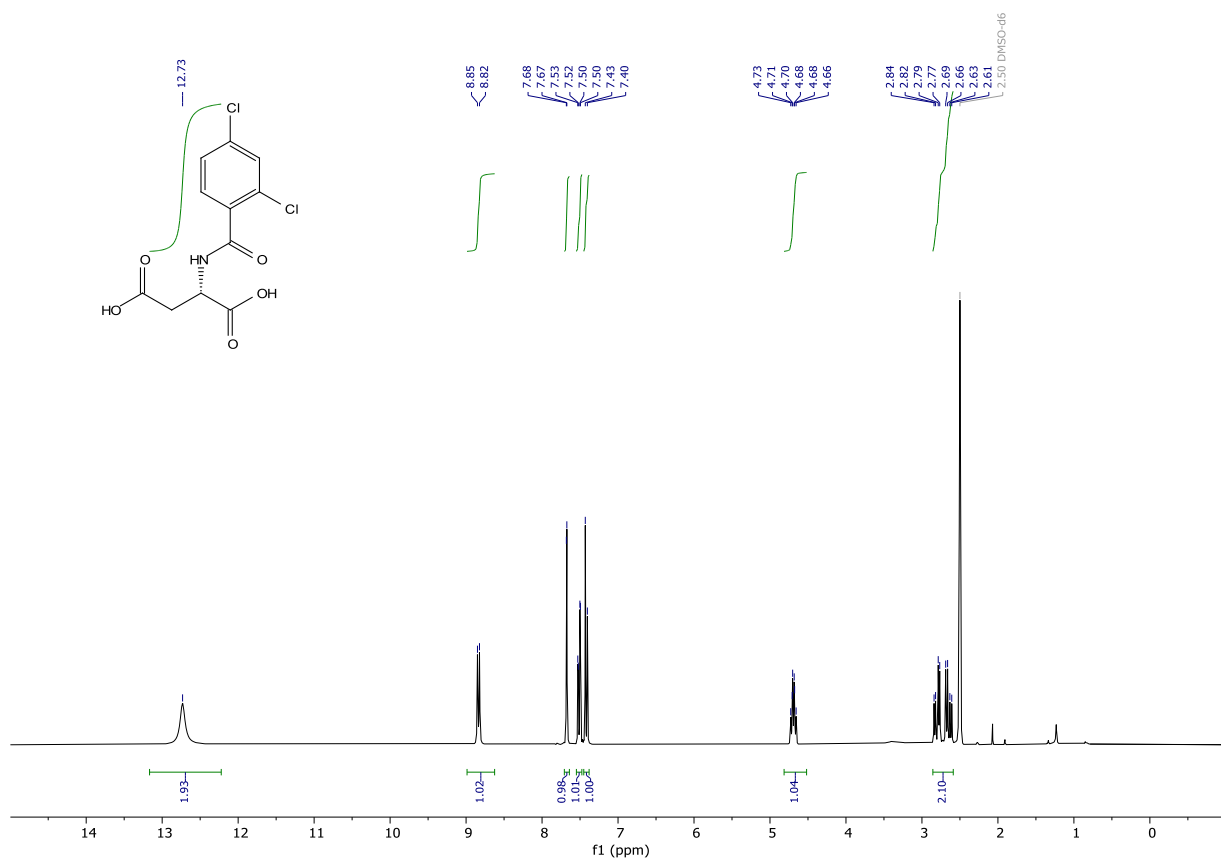
(2,4-dichlorobenzoyl)-L-glutamic acid (PGUB76). Prepared according to general procedure I starting from glutamic acid (0.49735 g, 3.3803 mmol) using 3-iodobenzoyl chloride as acyl chloride, to give the desired product in 20% yield (0.21908 g, 0.68436 mmol). White solid: ^1H NMR (300 MHz, DMSO- d_6) δ 12.47 (s, 2H), 8.77 (d, J = 7.8 Hz, 1H), 7.69 (d, J = 1.9 Hz, 1H), 7.51 (dd, J = 8.2, 2.0 Hz, 1H), 7.44 (d, J = 8.2 Hz, 1H), 4.38 (ddd, J = 9.5, 7.7, 4.8 Hz, 1H), 2.45 – 2.29 (m, 2H), 1.99 (d, J = 48.7 Hz, 2H). ^{13}C NMR (75 MHz, DMSO) δ 173.73, 165.59, 153.90, 135.29, 134.62, 131.26, 130.41, 129.18, 127.30, 51.66, 30.17, 26.08. HRMS (ESI) calculated for $[\text{M}+\text{H}]^+$ $\text{C}_{12}\text{H}_{12}\text{Cl}_2\text{NO}_5$ 320.0093, found 320.0094. Purity (HPLC): >94% UV₂₁₄, >98% UV₂₅₄.

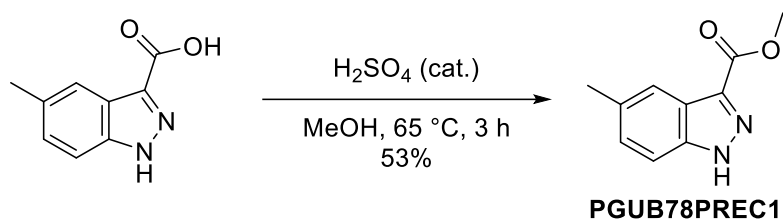




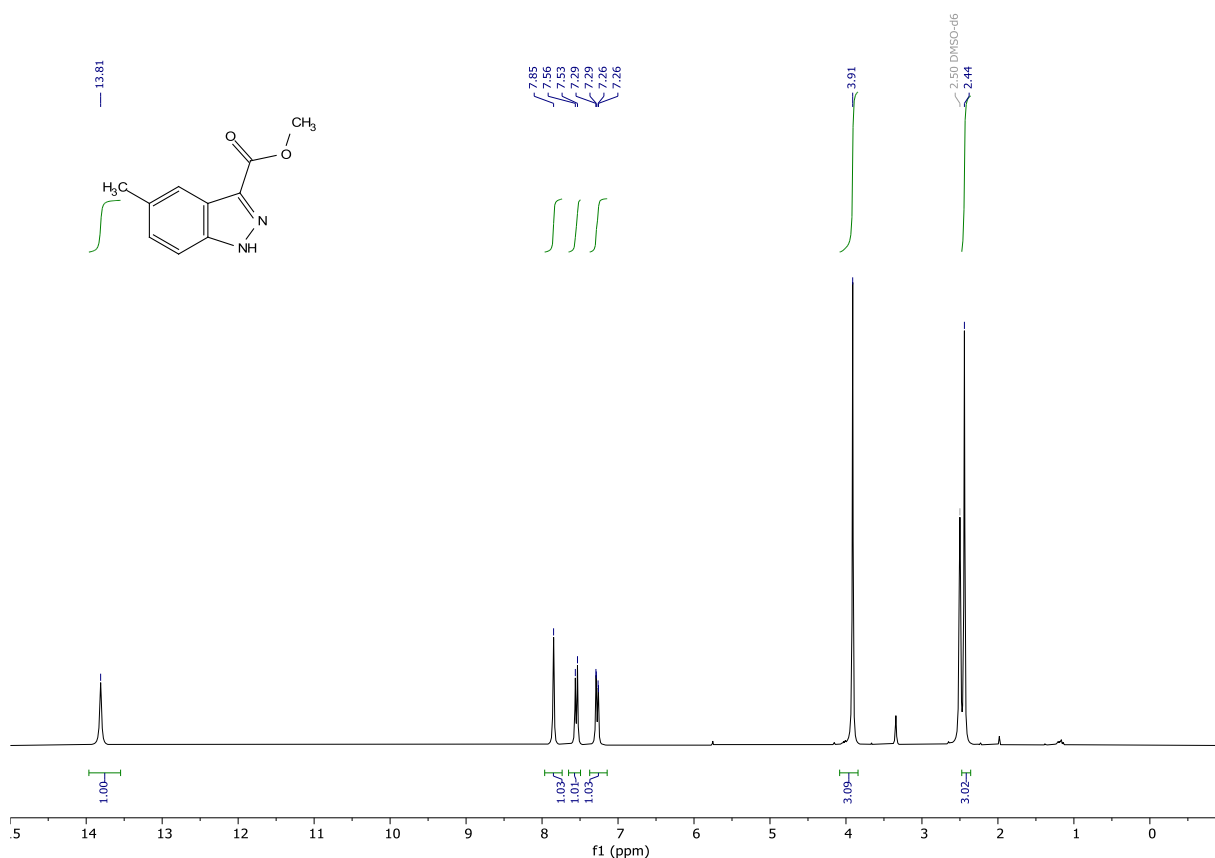
PGUB77

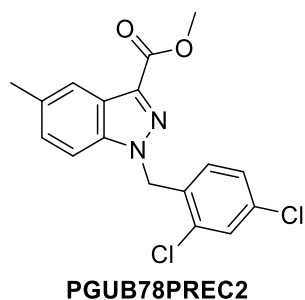
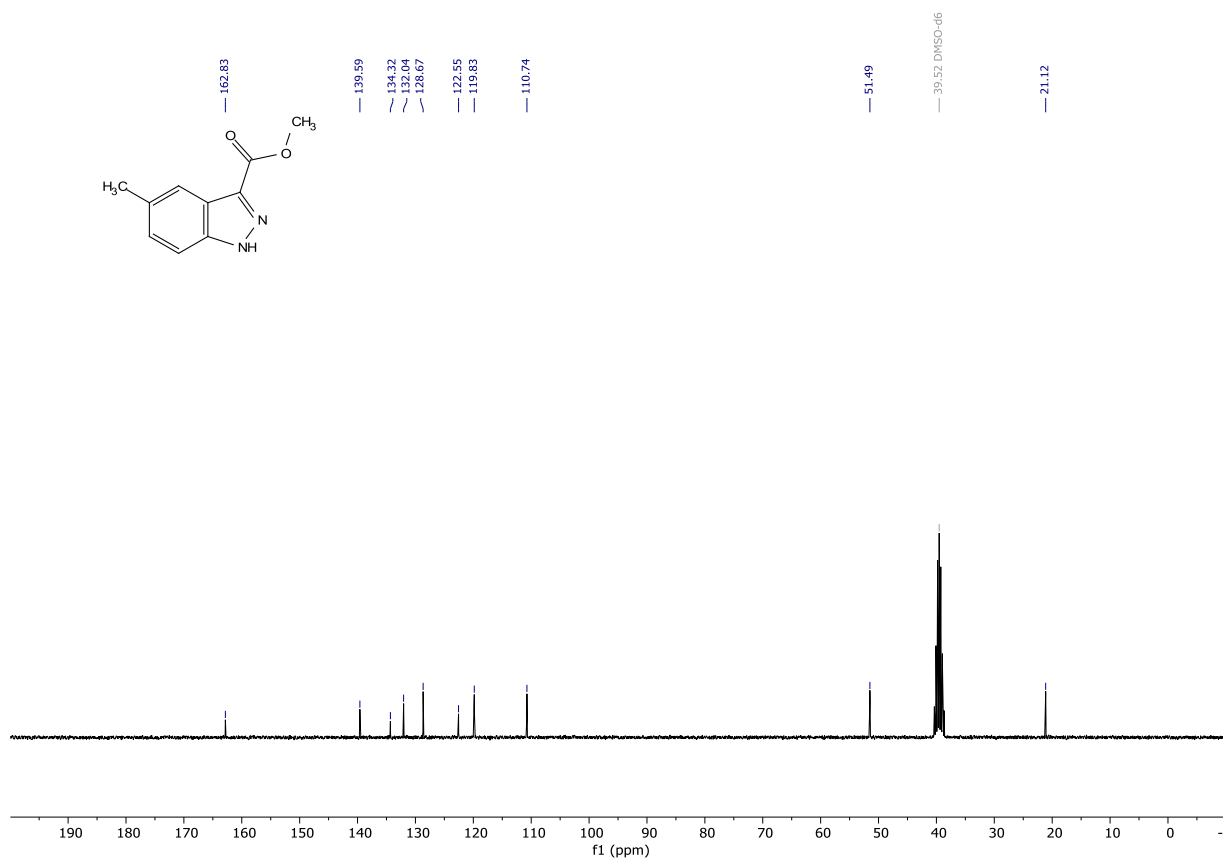
(2,4-dichlorobenzoyl)-L-aspartic acid (PGUB77). Prepared according to general procedure I starting from aspartic acid (0.49304 g, 3.7042 mmol) using 2,4-dichlorobenzoyl chloride as acyl chloride, to give the desired product in 27% yield (0.30304 g, 0.99002 mmol). White solid: ^1H NMR (300 MHz, $\text{DMSO}-d_6$) δ 12.73 (s, 2H), 8.84 (d, $J = 8.0$ Hz, 1H), 7.68 (d, $J = 1.9$ Hz, 1H), 7.51 (dd, $J = 8.3, 2.0$ Hz, 1H), 7.42 (d, $J = 8.2$ Hz, 1H), 4.69 (td, $J = 7.6, 5.8$ Hz, 1H), 2.86 – 2.59 (m, 2H). ^{13}C NMR (75 MHz, DMSO) δ 172.49, 172.05, 165.59, 135.46, 135.19, 131.80, 130.88, 129.70, 127.76, 49.60, 36.35. HRMS (ESI) calculated for $[\text{M}+\text{H}]^+$ $\text{C}_{11}\text{H}_{10}\text{Cl}_2\text{NO}_5$ 305.9936, found 305.9937. **Purity (HPLC):** >91% UV_{214} , >98% UV_{254} .



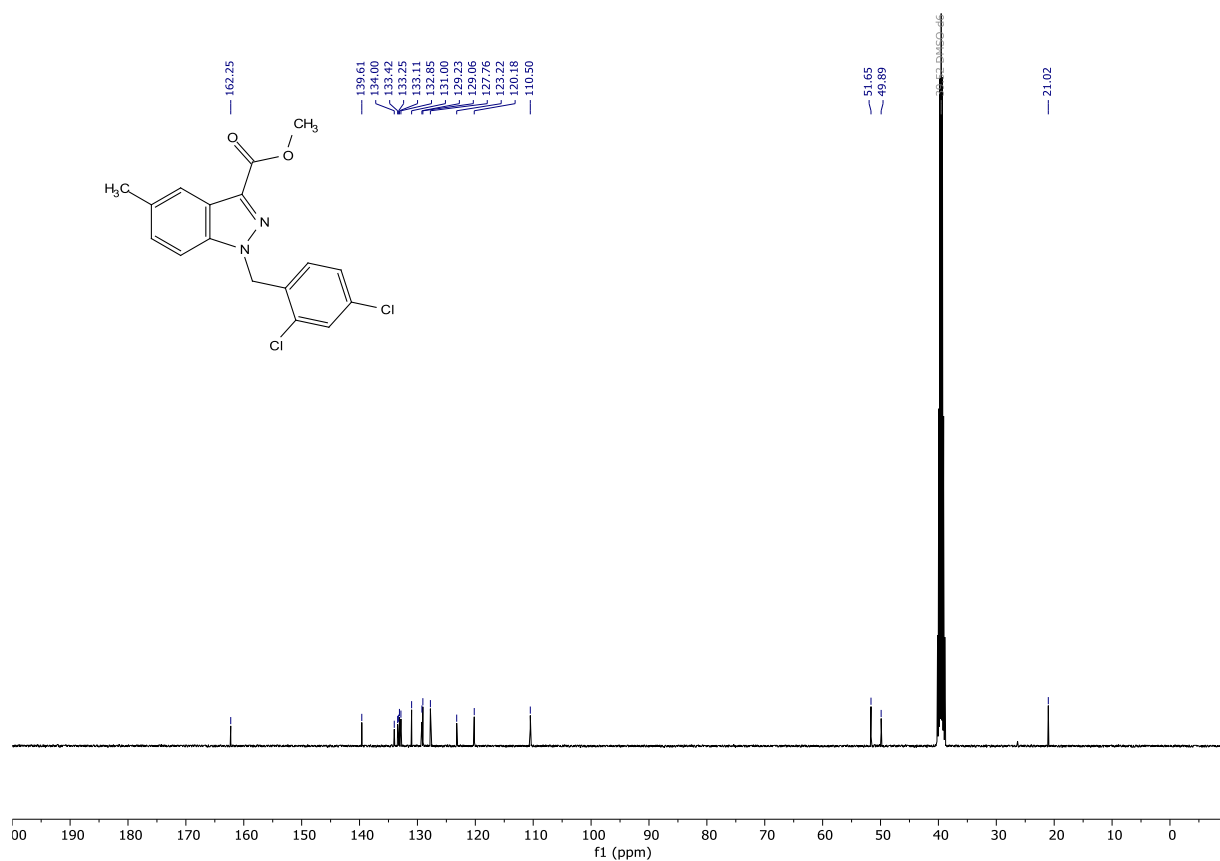
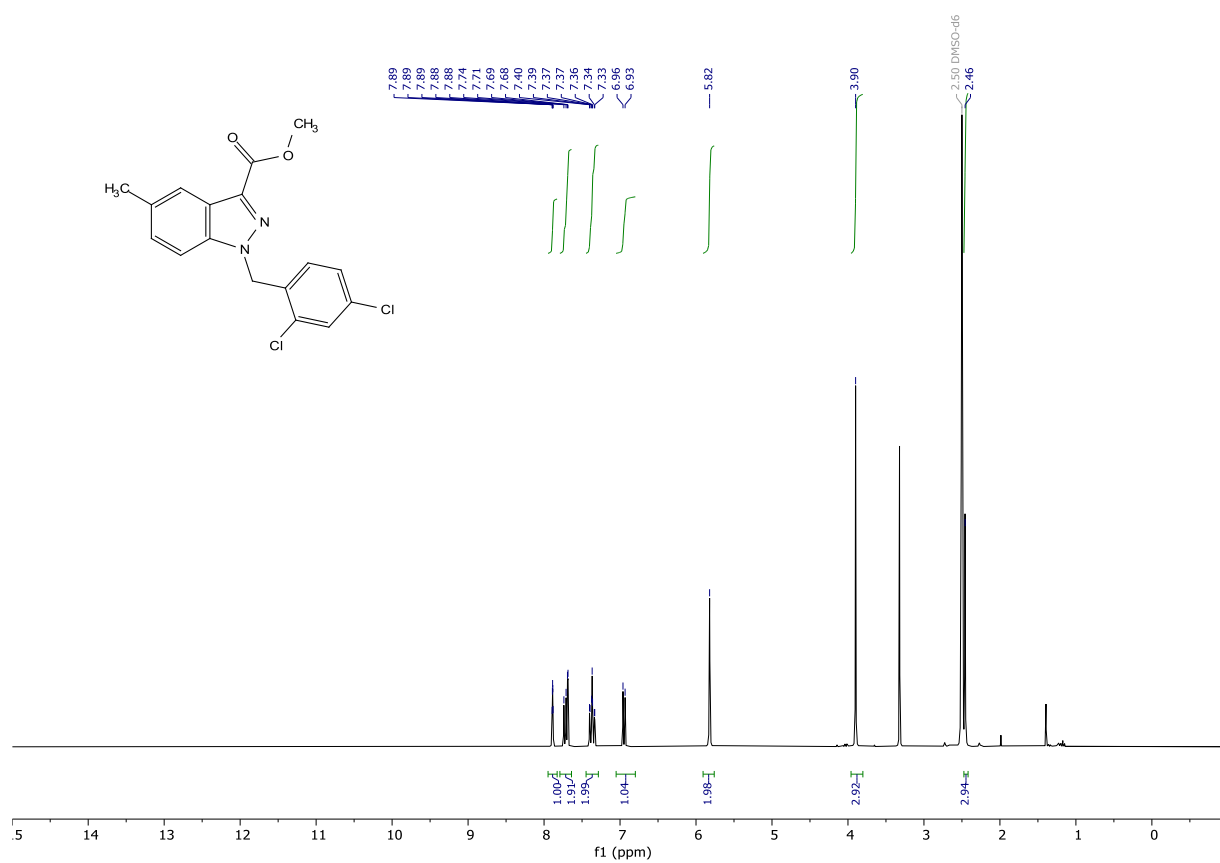


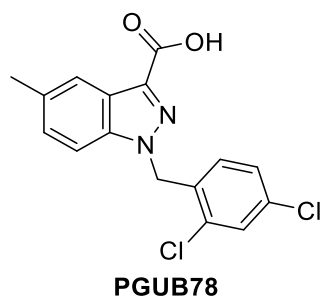
methyl 5-methyl-1H-indazole-3-carboxylate (PGUB78PREC1). To a stirred suspension of 5-methyl-1H-indazole-3-carboxylic acid (0.28943 g, 1.6429 mmol) in methanol (25 mL) was added H₂SO₄ (96%, 0.01 mL, 0.0187 mmol). The mixture was stirred at 65 °C under an argon atmosphere for 3 h. The volatiles were removed under reduced pressure. The residue was diluted with ethyl acetate. The organic phase was washed with 1 M aq. NaOH (3x) until no more colouring of the aqueous phase was observed. The organic phase was washed with brine, dried over MgSO₄, filtered, and concentrated under reduced pressure. The residue was taken up in dichloromethane and was concentrated onto silica gel. It was purified by flash column chromatography (cyclohexane/ ethyl acetate gradient from 4:1 to 0:1), to give the desired product in 53% yield (0.16582 g, 0.87181 mmol). Yellowish solid: ¹H NMR (300 MHz, DMSO-*d*₆) δ 13.81 (s, 1H), 7.85 (s, 1H), 7.55 (d, *J* = 8.5 Hz, 1H), 7.37 – 7.14 (m, 1H), 3.91 (s, 3H), 2.44 (s, 3H). ¹³C NMR (75 MHz, DMSO) δ 162.83, 139.59, 134.32, 132.04, 128.67, 122.55, 119.83, 110.74, 51.49, 21.12. HRMS (ESI) calculated for [M+H]⁺ C₁₀H₁₁N₂O₂ 191.0821, found 191.0818.



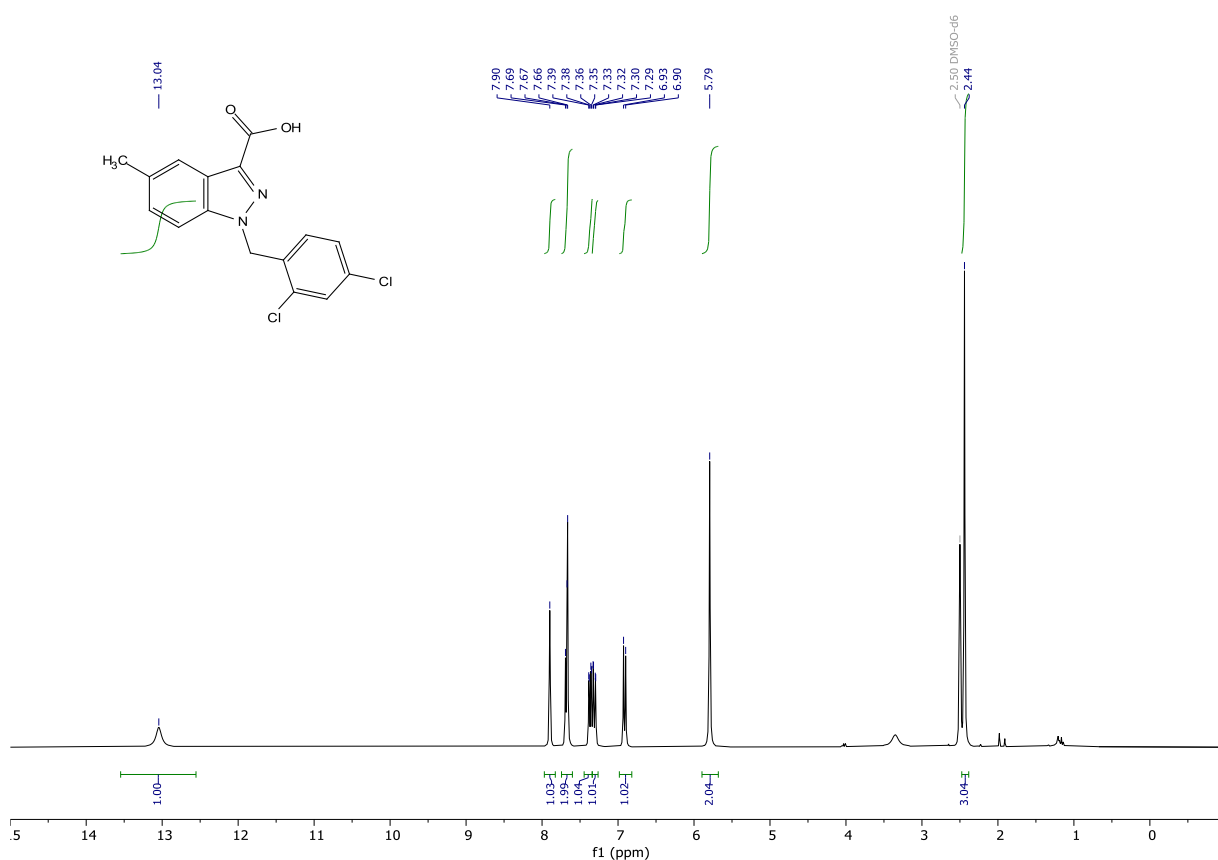


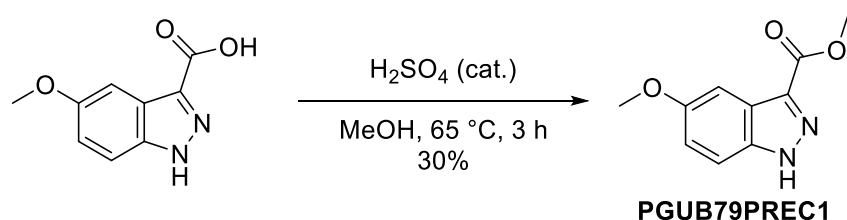
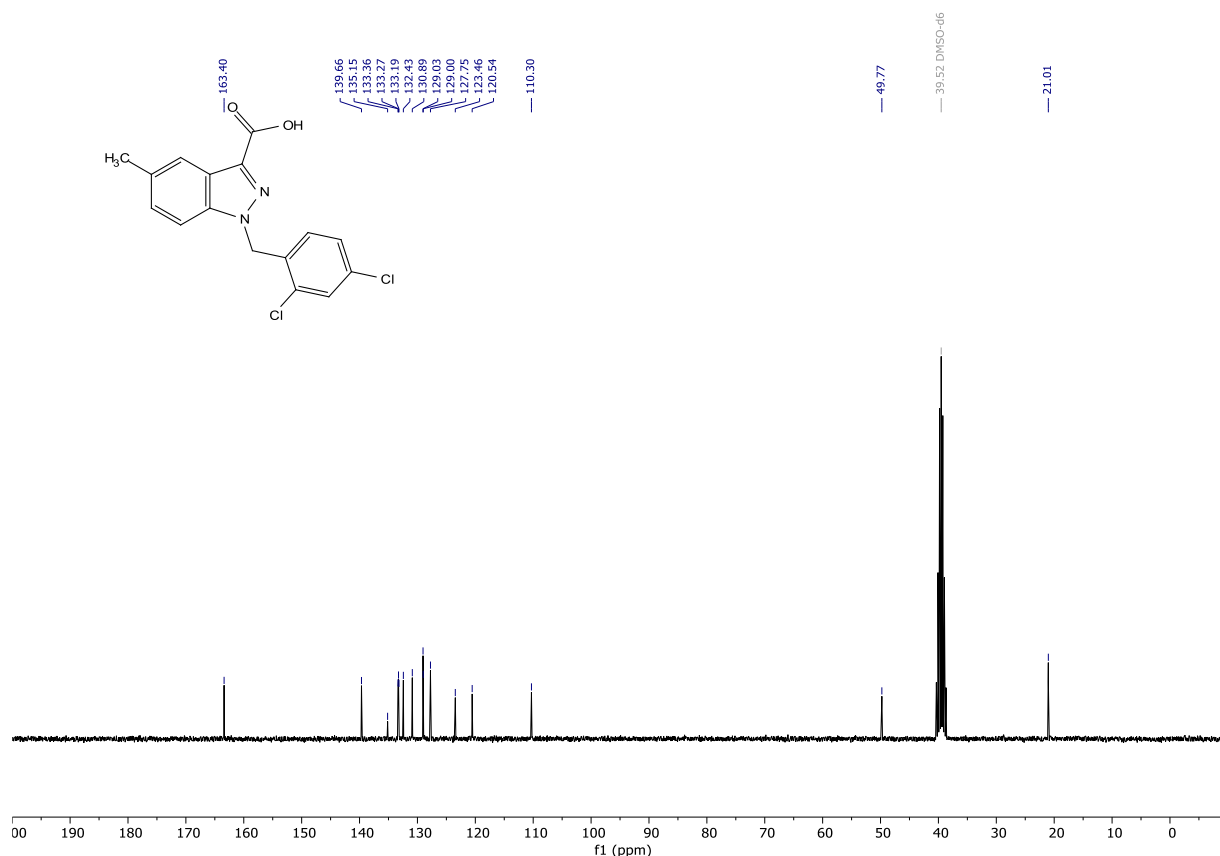
methyl 1-(2,4-dichlorobenzyl)-5-methyl-1H-indazole-3-carboxylate (PGUB78PREC2) (Z = N, Y = OMe). Prepared according to general procedure II from methyl 5-methyl-1H-indazole-3-carboxylate (PGUBPREC1) (Z = N, Y = OMe, 0.211 g, 1.1977 mmol) using 2,4-dichlorobenzyl bromide as alkyl halide, to give the desired product in 84% yield (0.23179 g, 0.66375 mmol). White solid: ^1H NMR (300 MHz, DMSO- d_6) δ 7.89 (dt, J = 1.8, 1.0 Hz, 1H), 7.79 – 7.64 (m, 2H), 7.37 (ddd, J = 10.2, 8.5, 1.9 Hz, 2H), 6.95 (d, J = 8.4 Hz, 1H), 5.82 (s, 2H), 3.90 (s, 3H), 2.46 (s, 3H). ^{13}C NMR (101 MHz, DMSO) δ 162.25, 139.61, 134.00, 133.42, 133.25, 133.11, 132.85, 131.00, 129.23, 129.06, 127.76, 123.22, 120.18, 110.50, 51.65, 49.89, 21.02. HRMS (ESI) calculated for $[\text{M}+\text{H}]^+$ $\text{C}_{17}\text{H}_{15}\text{Cl}_2\text{N}_2\text{O}_2$ 349.0505, found 349.0511.



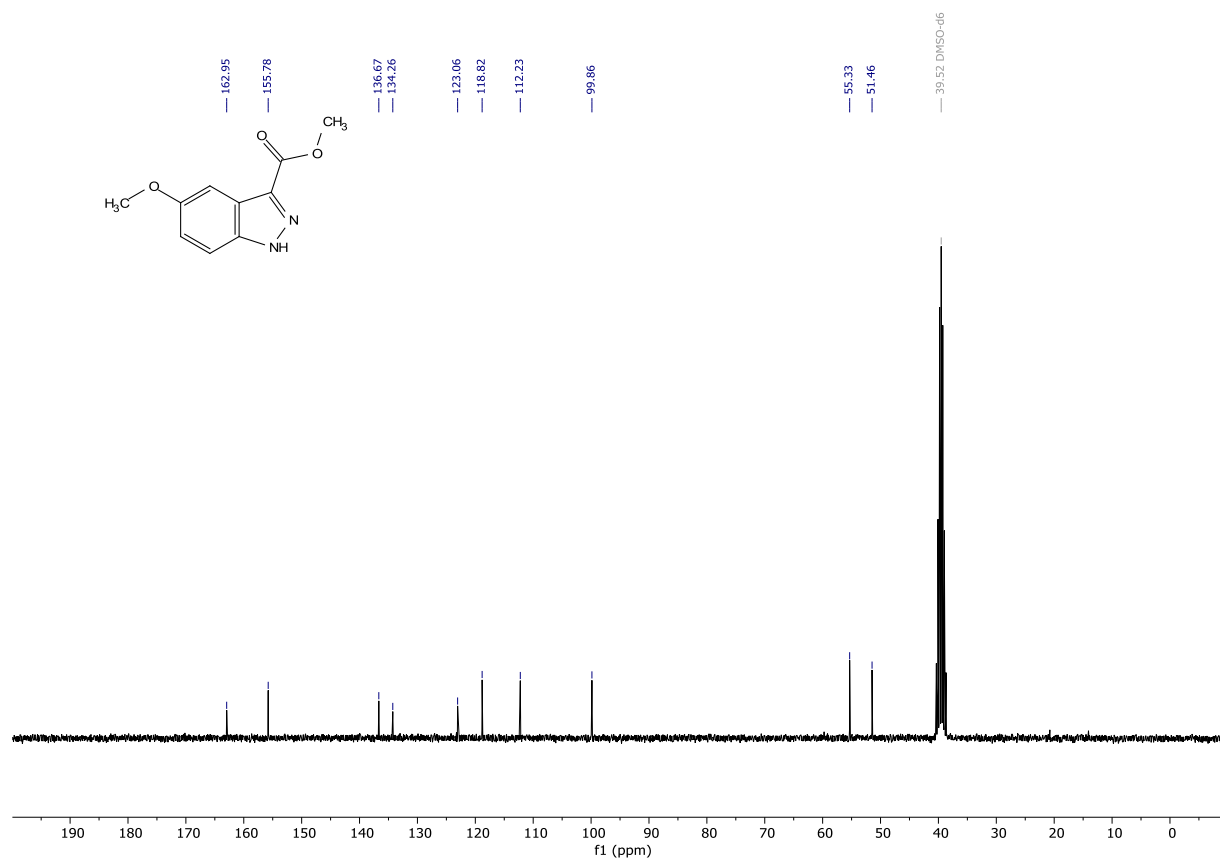
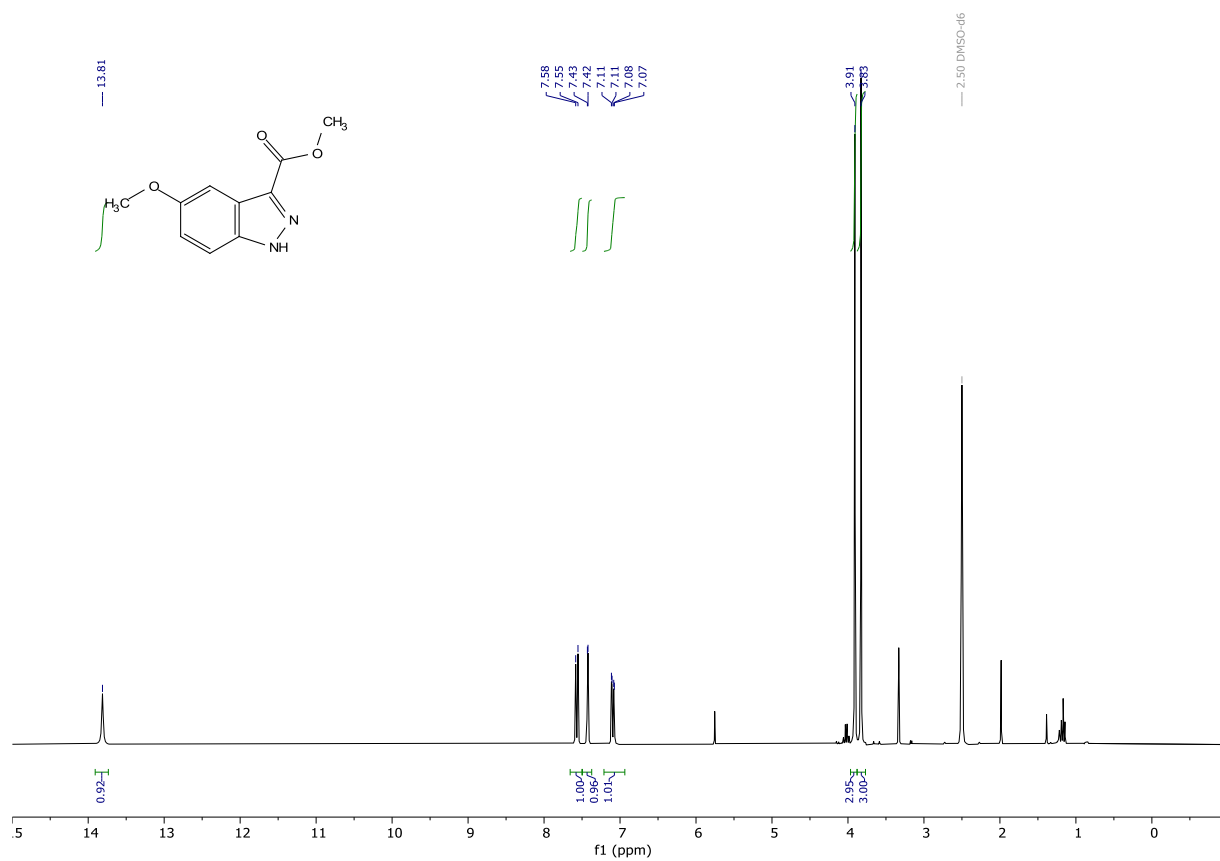


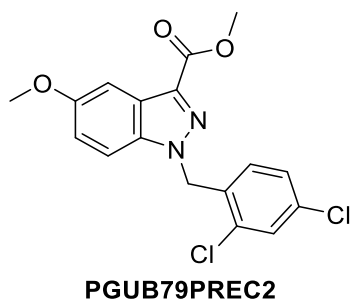
1-(2,4-dichlorobenzyl)-5-methyl-1*H*-indazole-3-carboxylic acid (PGUB68) (Z = N, W = OH). Prepared according to general procedure III from methyl 1-(2,4-dichlorobenzyl)-5-methyl-1*H*-indazole-3-carboxylate (PGUB78PREC2) (Z = N, Y = OMe, 0.22679 g, 0.6494 mmol), to give the desired product in quantitative yield (0.21779 g, 0.64976 mmol). Yellowish solid: **¹H NMR** (300 MHz, DMSO-*d*₆) δ 13.04 (s, 1H), 7.90 (s, 1H), 7.74 – 7.60 (m, 2H), 7.37 (dd, *J* = 8.4, 2.2 Hz, 1H), 7.31 (dd, *J* = 8.7, 1.7 Hz, 1H), 6.91 (d, *J* = 8.4 Hz, 1H), 5.79 (s, 2H), 2.44 (s, 3H). **¹³C NMR** (75 MHz, DMSO) δ 163.40, 139.66, 135.15, 133.36, 133.27, 133.19, 132.43, 130.89, 129.03, 129.00, 127.75, 123.46, 120.54, 110.30, 49.77, 21.01. **HRMS** (ESI) calculated for [M+H]⁺ C₁₆H₁₃Cl₂N₂O₂ 335.0349, found 335.0356. **Purity (HPLC):** >99% UV₂₁₄, >99% UV₂₅₄.



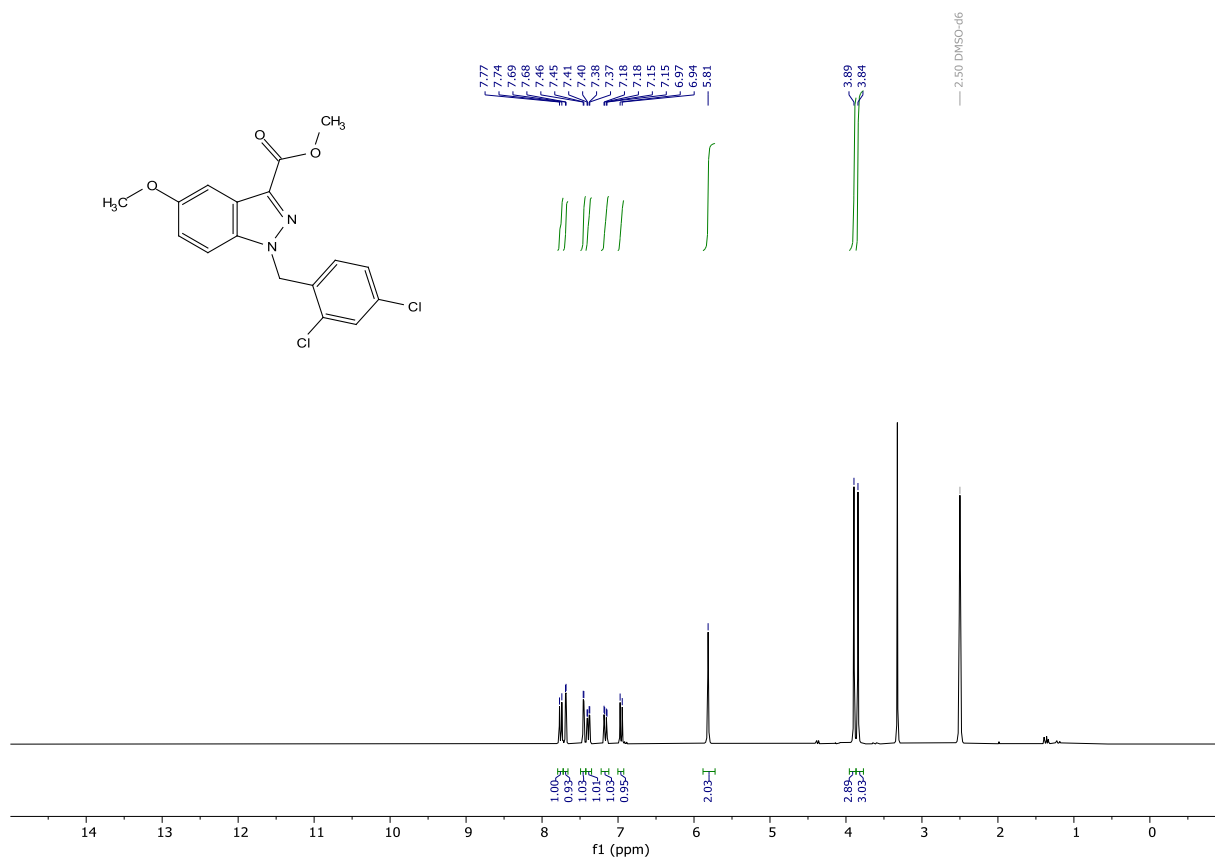


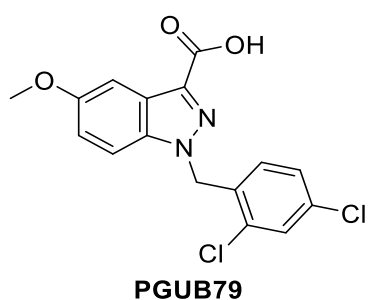
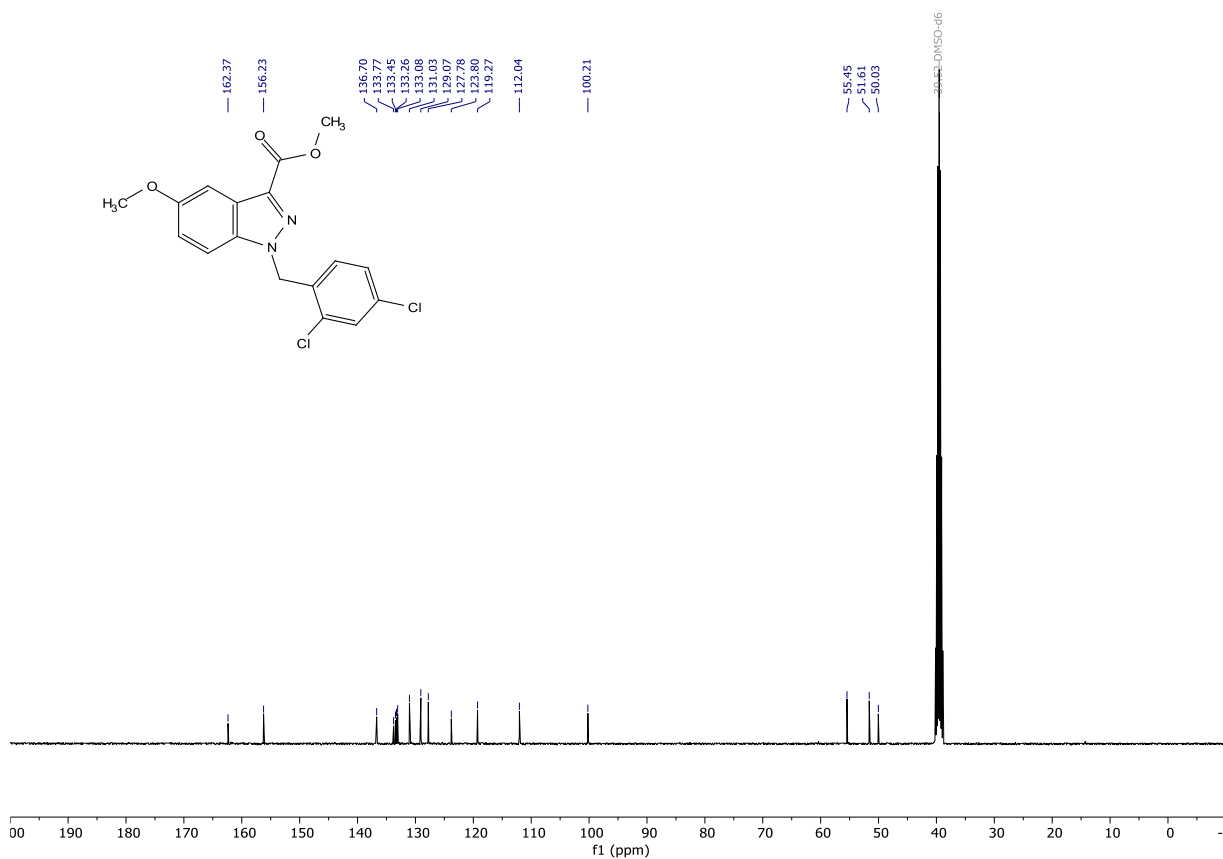
methyl 5-methoxy-1H-indazole-3-carboxylate (PGUB79PREC1). To a stirred suspension of 5-methoxy-1H-indazole-3-carboxylic acid (0.252 g, 1.3113 mmol) in methanol (25 mL) was added H₂SO₄ (96%, 0.01 mL, 0.0187 mmol). The mixture was stirred at 65 °C under an argon atmosphere for 3 h. The volatiles were removed under reduced pressure. The residue was diluted with ethyl acetate. The organic phase was washed with 1 M aq. NaOH (3x) until no more colouring of the aqueous phase was observed. The organic phase was washed with brine, dried over MgSO₄, filtered, and concentrated under reduced pressure. The residue was taken up in dichloromethane and was concentrated onto silica gel. It was purified by flash column chromatography (cyclohexane/ ethyl acetate gradient from 4:1 to 0:1), to give the desired product in 53% yield (0.16582 g, 0.87181 mmol). Yellowish solid: **¹H NMR** (300 MHz, DMSO-*d*₆) δ 13.81 (s, 1H), 7.57 (d, *J* = 9.0 Hz, 1H), 7.43 (d, *J* = 2.4 Hz, 1H), 7.09 (dd, *J* = 9.0, 2.4 Hz, 1H), 3.91 (s, 3H), 3.83 (s, 3H). **¹³C NMR** (75 MHz, DMSO) δ 162.95, 155.78, 136.67, 134.26, 123.06, 118.82, 112.23, 99.86, 55.33, 51.46. **HRMS** (ESI) calculated for [M+H]⁺ C₁₀H₁₁N₂O₃ 207.0770, found 207.0768.



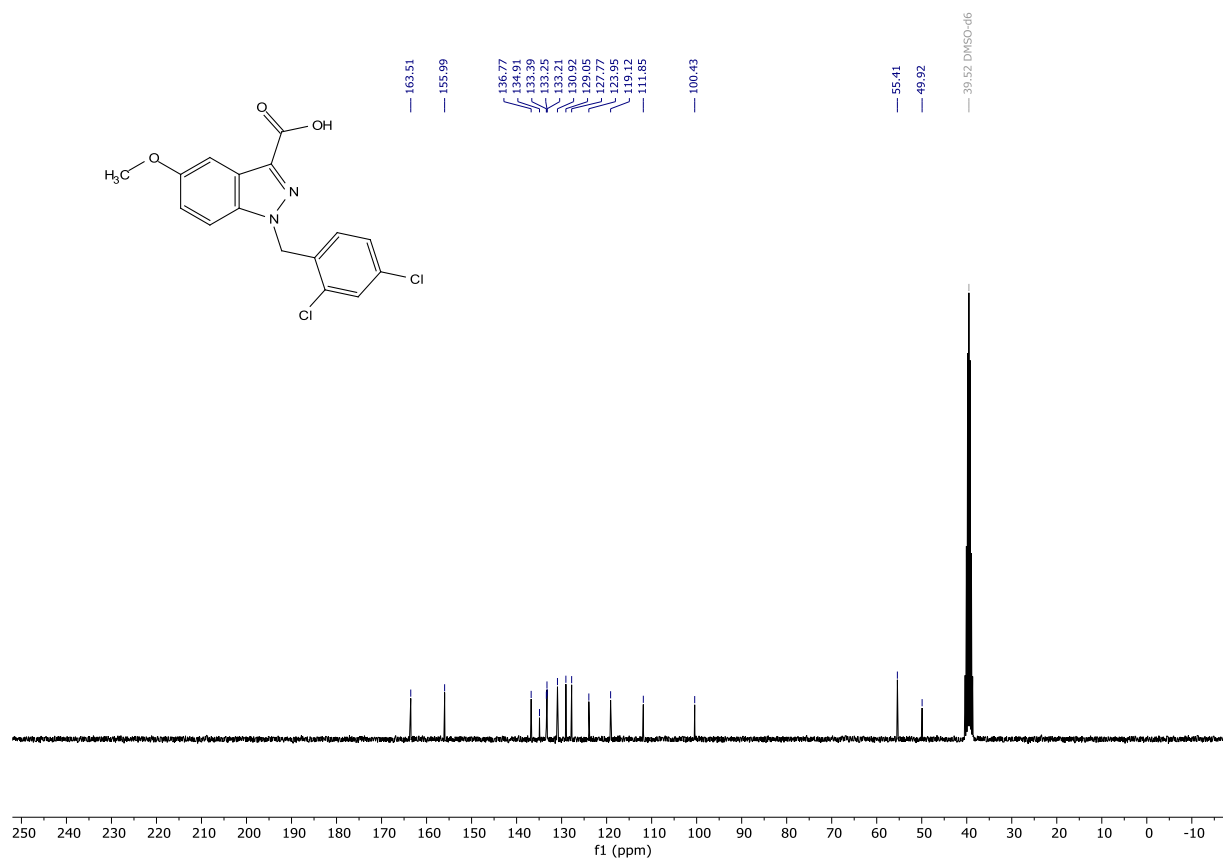
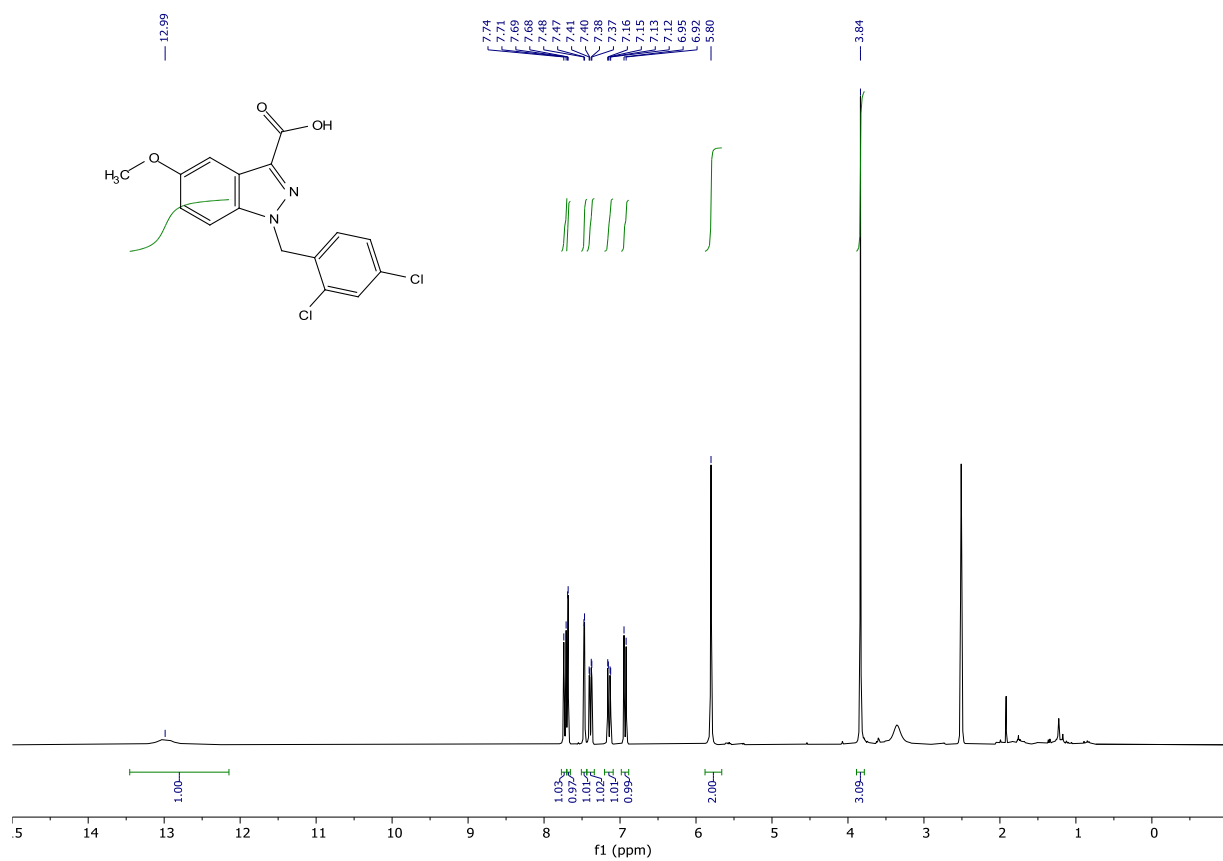


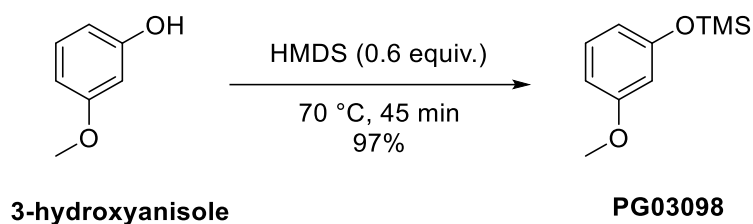
methyl 1-(2,4-dichlorobenzyl)-5-methoxy-1H-indazole-3-carboxylate (PGUB79PREC2) (Z = N, Y = OMe). Prepared according to general procedure II from methyl 5-methoxyl-1H-indazole-3-carboxylate (PGUB79PREC1) (Z = N, Y = OMe, 0.08108 g, 0.3932 mmol) using 2,4-dichlorobenzyl bromide as alkyl halide, to give the desired product in 84% yield (0.07420 g, 20317 mmol). White solid: **¹H NMR** (300 MHz, DMSO-*d*₆) δ 7.75 (d, *J* = 9.2 Hz, 1H), 7.69 (d, *J* = 2.2 Hz, 1H), 7.45 (d, *J* = 2.4 Hz, 1H), 7.39 (dd, *J* = 8.4, 2.2 Hz, 1H), 7.16 (dd, *J* = 9.2, 2.4 Hz, 1H), 6.96 (d, *J* = 8.4 Hz, 1H), 5.81 (s, 2H), 3.89 (s, 3H), 3.84 (s, 3H). **¹³C NMR** (101 MHz, DMSO) δ 162.37, 156.23, 136.70, 133.77, 133.45, 133.26, 133.08, 131.03, 129.07, 127.78, 123.80, 119.27, 112.04, 100.21, 55.45, 51.61, 50.03. **HRMS** (ESI) calculated for [M+H]⁺ C₁₇H₁₅Cl₂N₂O₃ 365.0454, found 365.0459.



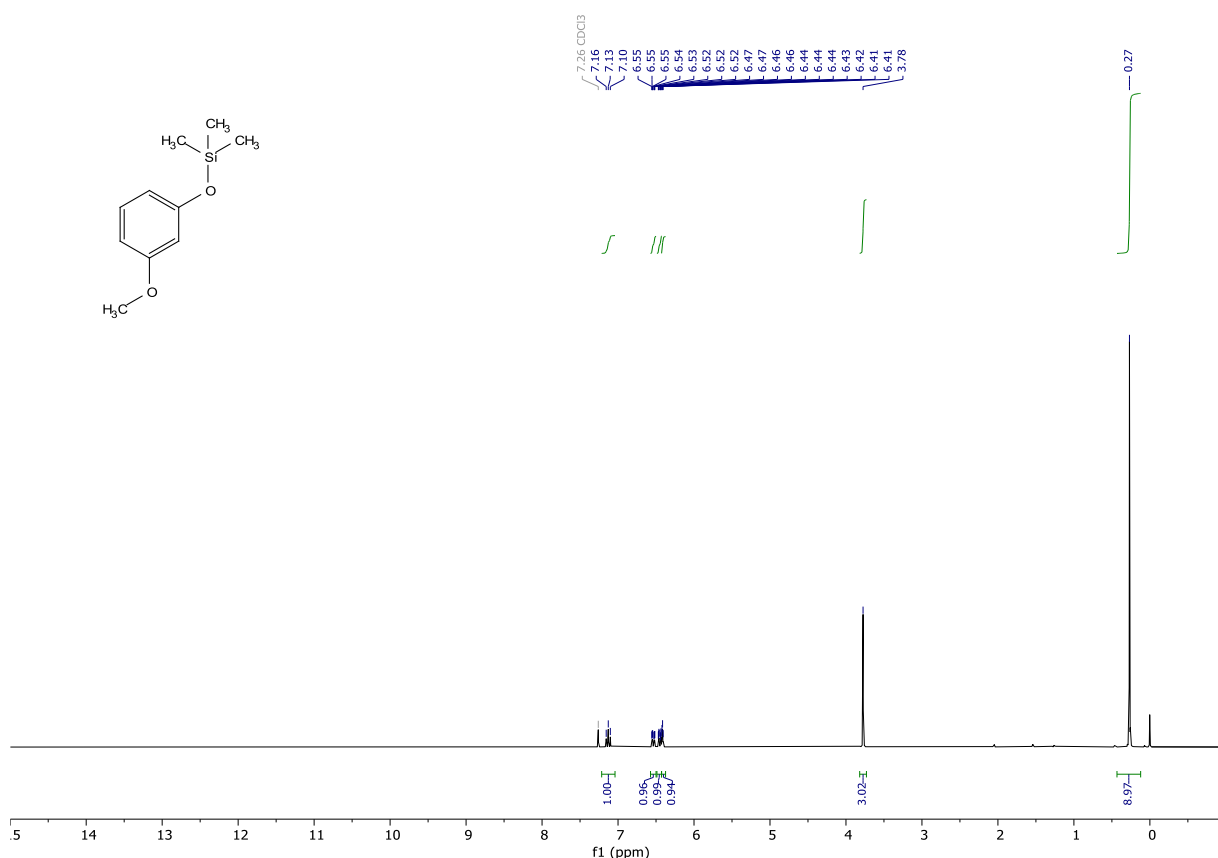


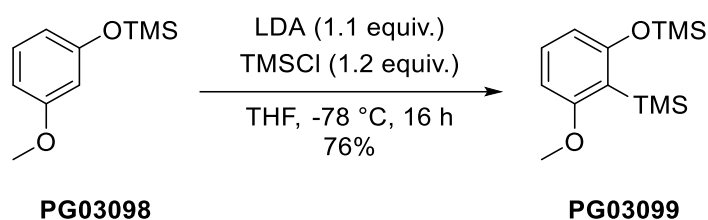
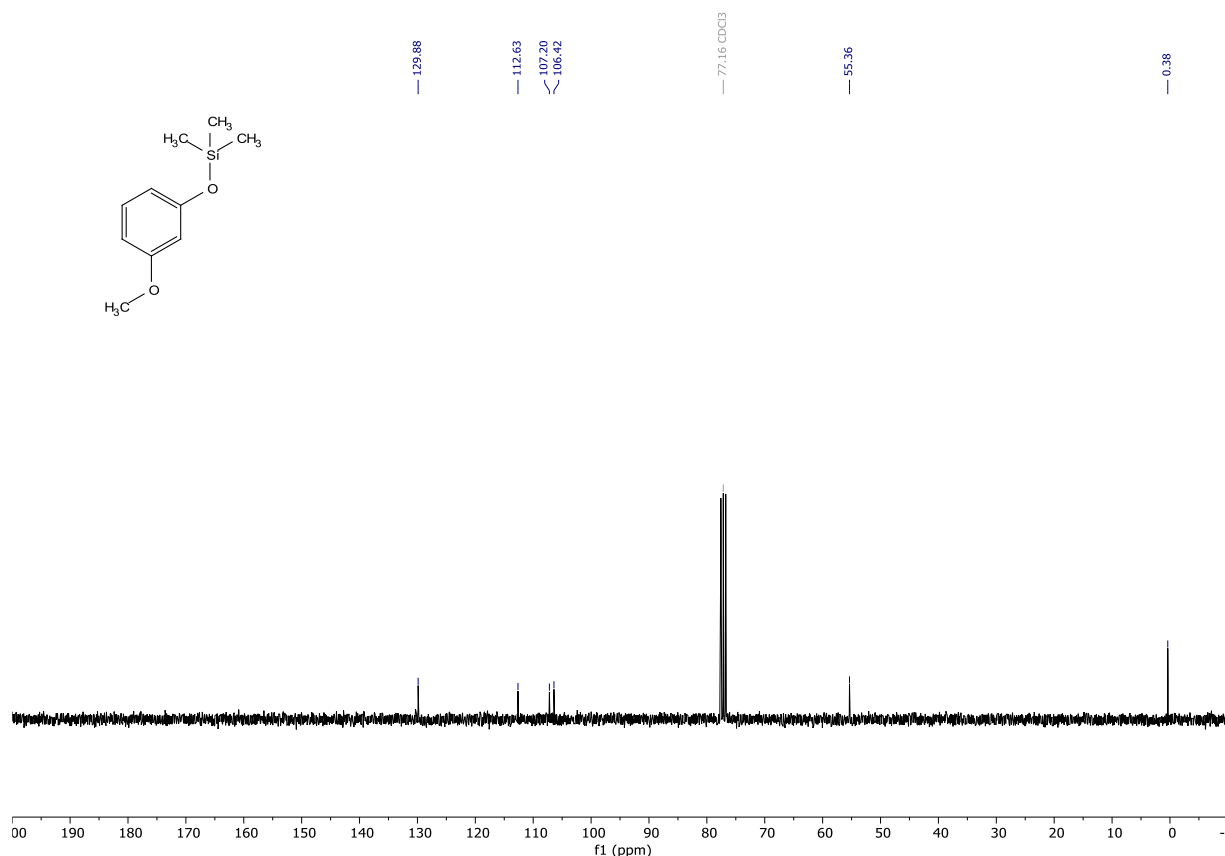
1-(2,4-dichlorobenzyl)-5-methoxy-1H-indazole-3-carboxylic acid (PGUB68) (Z = N, W = OH). Prepared according to general procedure III from methyl 1-(2,4-dichlorobenzyl)-5-methoxy-1H-indazole-3-carboxylate (PGUB79PREC2) (Z = N, Y = OMe, 0.065 g, 0.1780 mmol), to give the desired product in quantitative yield (0.06499 g, 0.18506 mmol). Yellowish solid: **¹H NMR** (300 MHz, DMSO-*d*₆) δ 12.99 (s, 1H), 7.72 (d, *J* = 9.2 Hz, 1H), 7.69 (d, *J* = 2.2 Hz, 1H), 7.47 (d, *J* = 2.4 Hz, 1H), 7.39 (dd, *J* = 8.3, 2.2 Hz, 1H), 7.14 (dd, *J* = 9.1, 2.4 Hz, 1H), 6.93 (d, *J* = 8.4 Hz, 1H), 5.80 (s, 2H), 3.84 (s, 3H). **¹³C NMR** (75 MHz, DMSO) δ 163.51, 155.99, 136.77, 134.91, 133.39, 133.25, 133.21, 130.92, 129.05, 127.77, 123.95, 119.12, 111.85, 100.43, 55.41, 49.92. **HRMS** (ESI) calculated for [M+H]⁺ C₁₆H₁₃Cl₂N₂O₃ 351.0298, found 351.0302. **Purity (HPLC):** >99% UV₂₁₄, >99% UV₂₅₄.





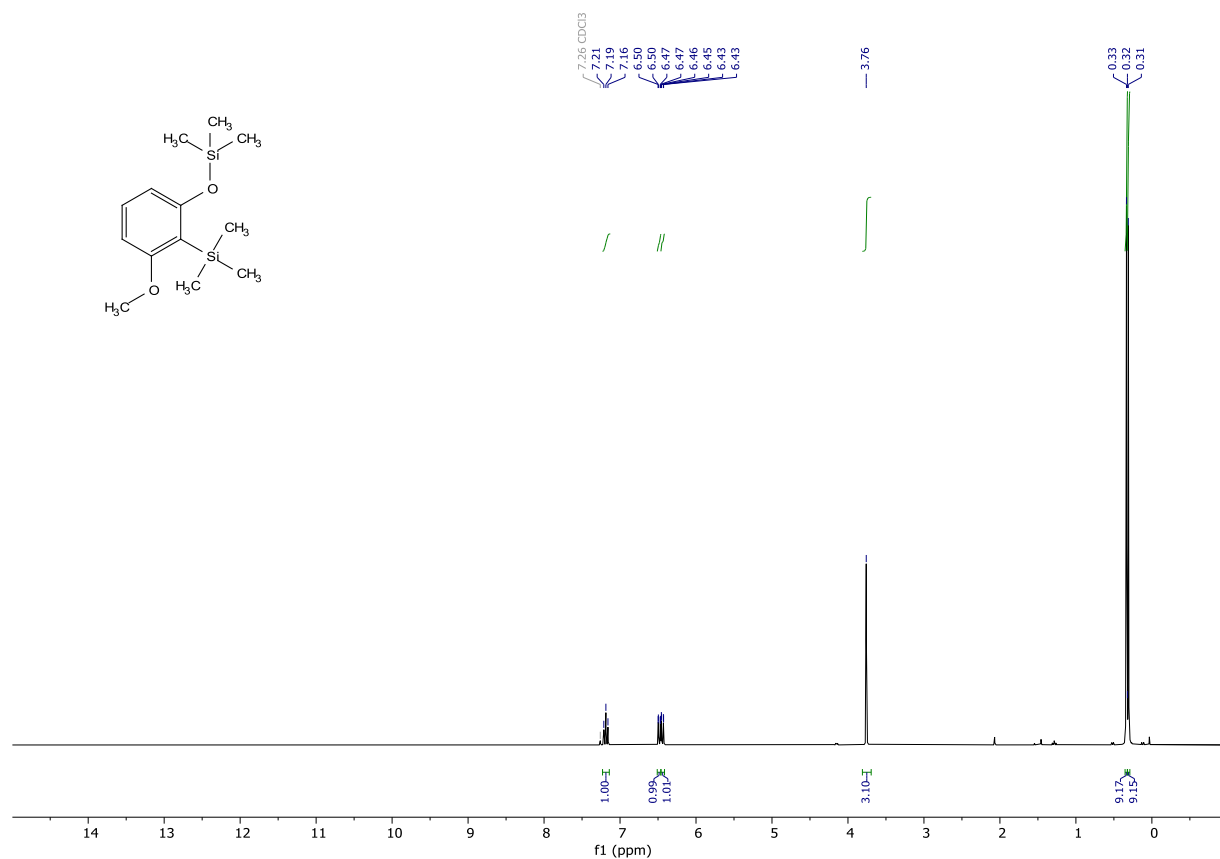
(3-methoxyphenoxy)trimethylsilane (PGUB81PREC1). To 3-methoxyphenol (3 mL, 3.393 g, 74.1447 mmol) was added HMDS (3.5 mL, 2.73 g, 16.9155 mmol) this led to gas formation. The mixture was heated to 70 °C and a constant stream of argon was blown over the mixture. The mixture was cooled to 21 °C diluted with water first, then 1 M NaOH which led to a slight bubbling. The aqueous phase was extracted with ethyl acetate. The organic phase was washed with 1 M NaOH (4 x), brine, dried over MgSO₄, filtered, and concentrated under reduced pressure to give the desired product (4.38234 g, 22.32332 mmol). Clear colourless oil: ¹H NMR (300 MHz, Chloroform-*d*) δ 7.13 (t, *J* = 8.1 Hz, 1H), 6.54 (ddd, *J* = 8.3, 2.4, 0.9 Hz, 1H), 6.45 (ddd, *J* = 8.0, 2.3, 0.9 Hz, 1H), 6.41 (t, *J* = 2.3 Hz, 1H), 3.78 (s, 3H), 0.27 (s, 9H). ¹³C NMR (75 MHz, CDCl₃) δ 129.88, 112.63, 107.20, 106.42, 55.36, 0.38. HRMS (ESI) calculated for [M+H]⁺ C₁₀H₁₆O₂Si 197.0992, found 197.0990.

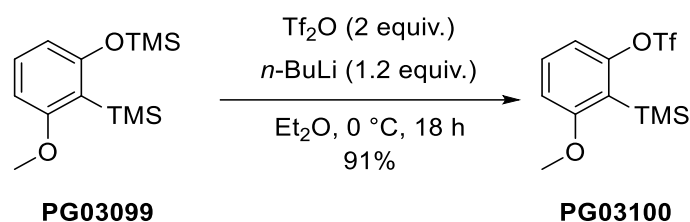
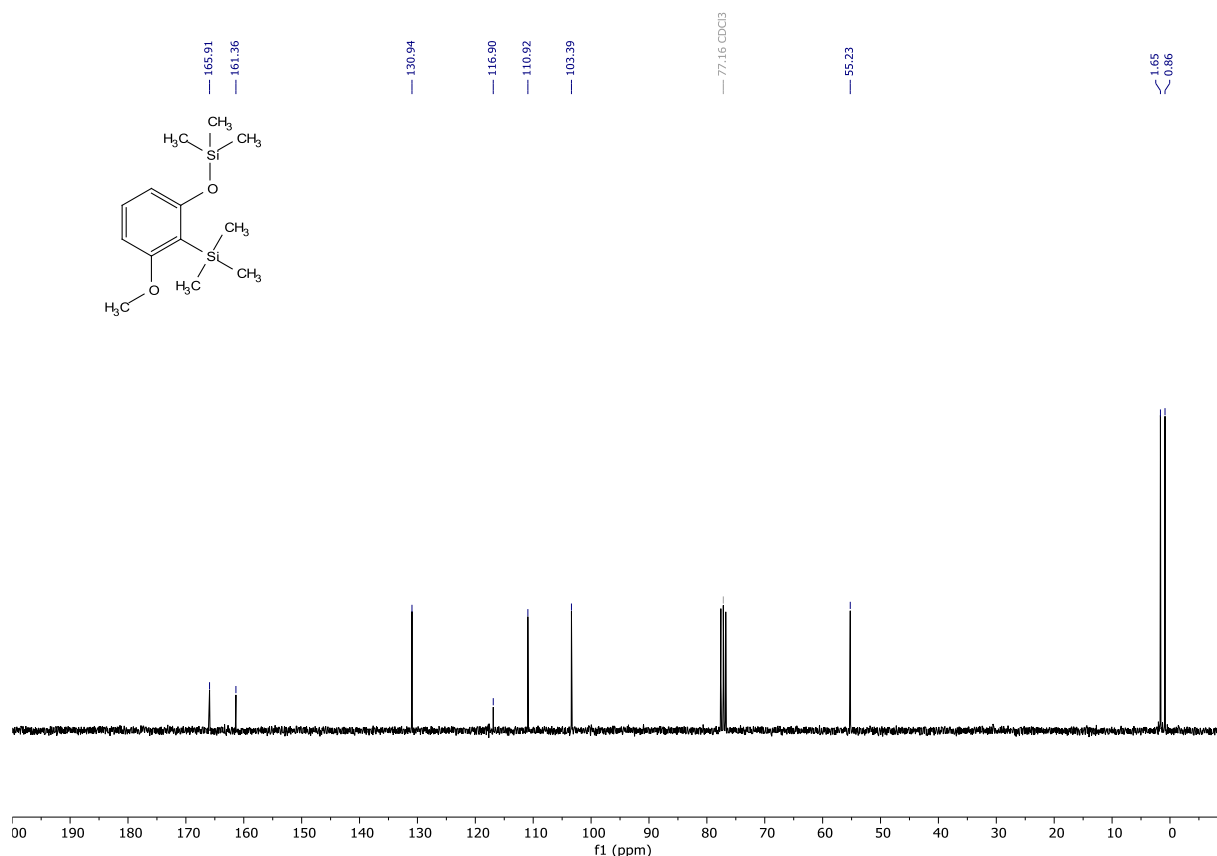




(3-methoxy-2-(trimethylsilyl)phenoxy)trimethylsilane (PGUB82PREC2). LDA was prepared prior to the reaction: To a dried flask was added dry THF (15 mL) followed by di-*iso*-propylamine (3.5 mL, 2.520 g, 24.9036 mmol). The mixture was cooled to -76 °C. Then was added dropwise *n*-BuLi (2.5 M in hexanes, 9 mL, 22.5 mmol). After full addition, the mixture was stirred for 5 minutes at -76 °C. then it was warmed to 0 °C by addition of dry THF (15 mL) and it was stirred at around 0 °C for 10 minutes. The mixture was cooled down to -76 °C then was added slowly a solution of (3-methoxyphenoxy)trimethylsilane (3.999 g, 20.3697 mmol) in dry THF (15 mL). After full addition, the mixture was warmed to 0 °C rapidly in a water bath. The mixture was stirred at room temperature for 1 h. Then it was cooled down to -76 °C and TMSCl (3.2 mL, 2.7328 g, 25.1546 mmol) was added. The mixture was slowly warmed to 20 °C over 16 h. The mixture was quenched with aq. sat. NH₄Cl solution. Then the aqueous phase was extracted with diethyl ether. The combined organic phases were washed with brine, dried over MgSO₄. And concentrated under reduced pressure to give an oily residue. This residue was taken up in dichloromethane and concentrated onto silica gel. The crude was purified by

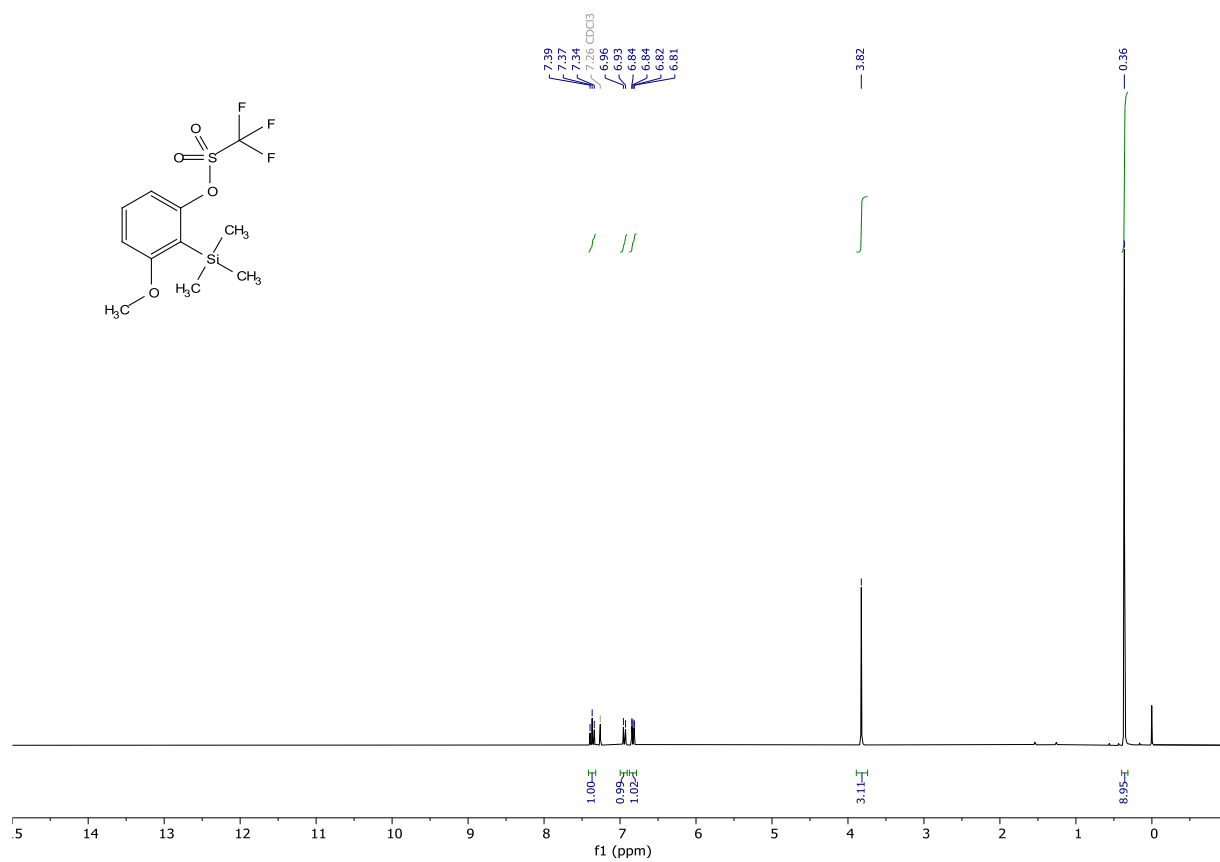
flash column chromatography (cyclohexane/ dichloromethane gradient from 1:0 to 3:1), to give the desired product in 76% (4.1594 g, 15.48936 mmol). **¹H NMR** (300 MHz, Chloroform-*d*) δ 7.19 (t, *J* = 8.2 Hz, 1H), 6.48 (dd, *J* = 8.2, 0.8 Hz, 1H), 6.44 (dd, *J* = 8.1, 0.8 Hz, 1H), 3.76 (s, 3H), 0.33 (s, 9H), 0.31 (s, 9H). **¹³C NMR** (75 MHz, CDCl₃) δ 165.91, 161.36, 130.94, 116.90, 110.92, 103.39, 55.23, 1.65, 0.86. **HRMS** (ESI) calculated for [M+H]⁺ C₁₃H₂₅O₂Si₂ 269.1388, found 269.1386.

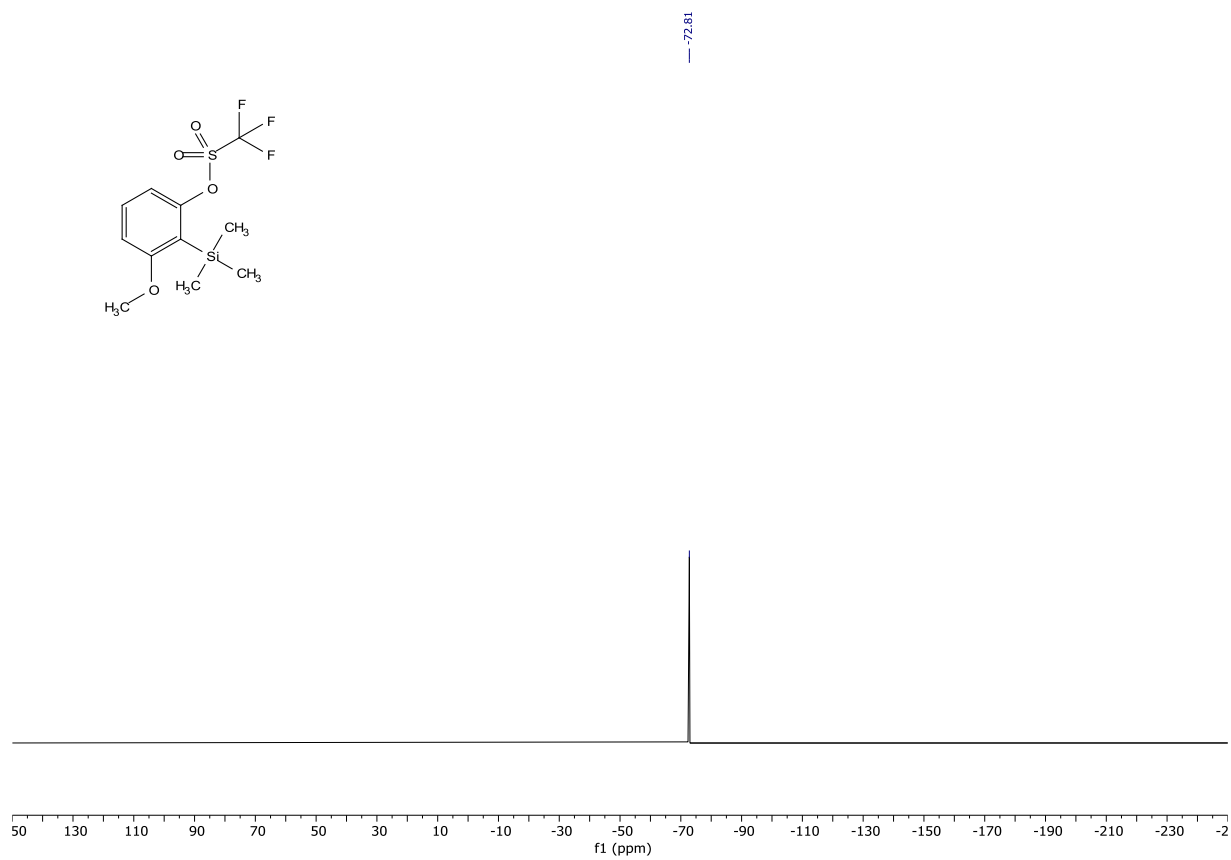
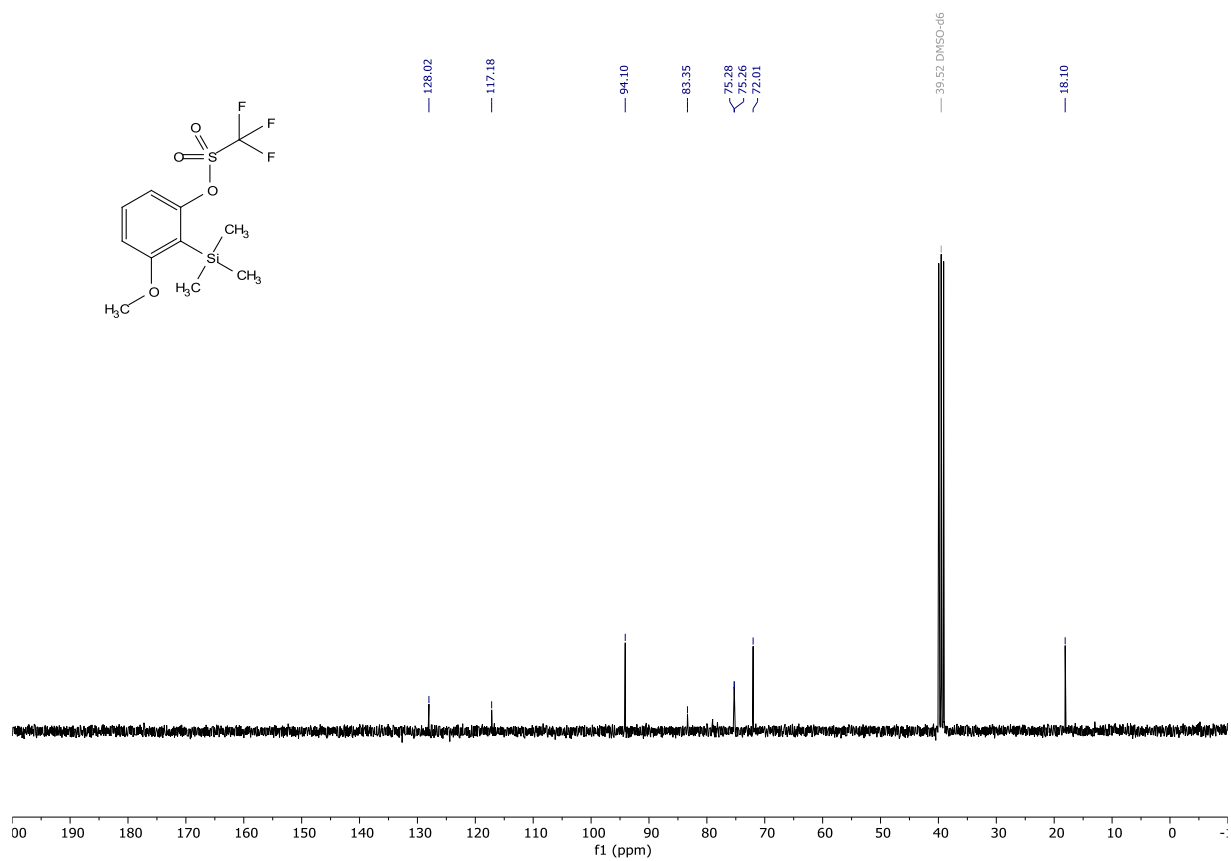


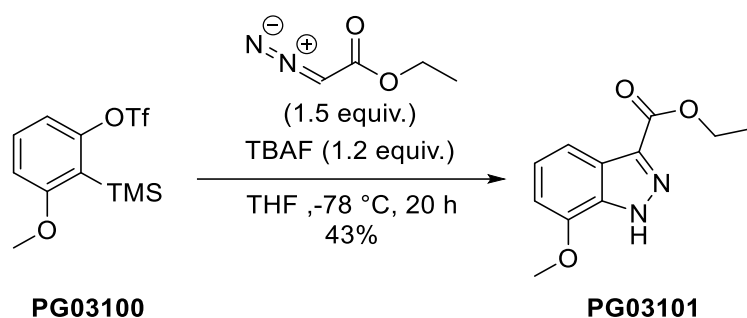


3-methoxy-2-(trimethylsilyl)phenyl trifluoromethanesulfonate (PGUB91PREC3). To a stirred solution of (3-methoxy-2-(trimethylsilyl)phenoxy)trimethylsilane (2.379 g, 8.8602 mmol) in dry diethyl ether (75 mL) at 0 °C under an argon atmosphere was added *n*-BuLi (2.5 M in hexanes, 6.8 mL, 17 mmol) was added. The ice bath was removed, and the mixture was stirred at 21 °C. After 2 h the mixture was cooled again to 0 °C and Tf₂O (5.2 mL, 8.7204 g, 30.9082 mmol) was added. The mixture was stirred for 16 h. To the mixture was added aq. NaHCO₃ clearing up the mixture resulting in a biphasic system. The aqueous phase was extracted with diethyl ether. The combined organic layers were washed with basified brine, dried over MgSO₄, filtered, and concentrated under reduced pressure. The residue was taken up in dichloromethane and was concentrated onto silica gel. The crude was purified by flash column chromatography (cyclohexane/ ethyl acetate gradient from 1:0 to 0:1), to give the desired product in 91% yield (4.57130 g, 13.920881). ¹H NMR (300 MHz, Chloroform-*d*) δ 7.37 (t, *J* = 8.3 Hz, 1H), 6.94 (d, *J* = 8.3 Hz, 1H), 6.83 (dd, *J* = 8.3, 0.8 Hz, 1H), 3.82 (s, 3H), 0.36 (s, 9H). ¹³C NMR (75 MHz, CDCl₃) δ 128.02, 117.18, 94.10, 83.35, 75.28, 75.26, 72.01, 18.10, -36.71. ¹⁹F

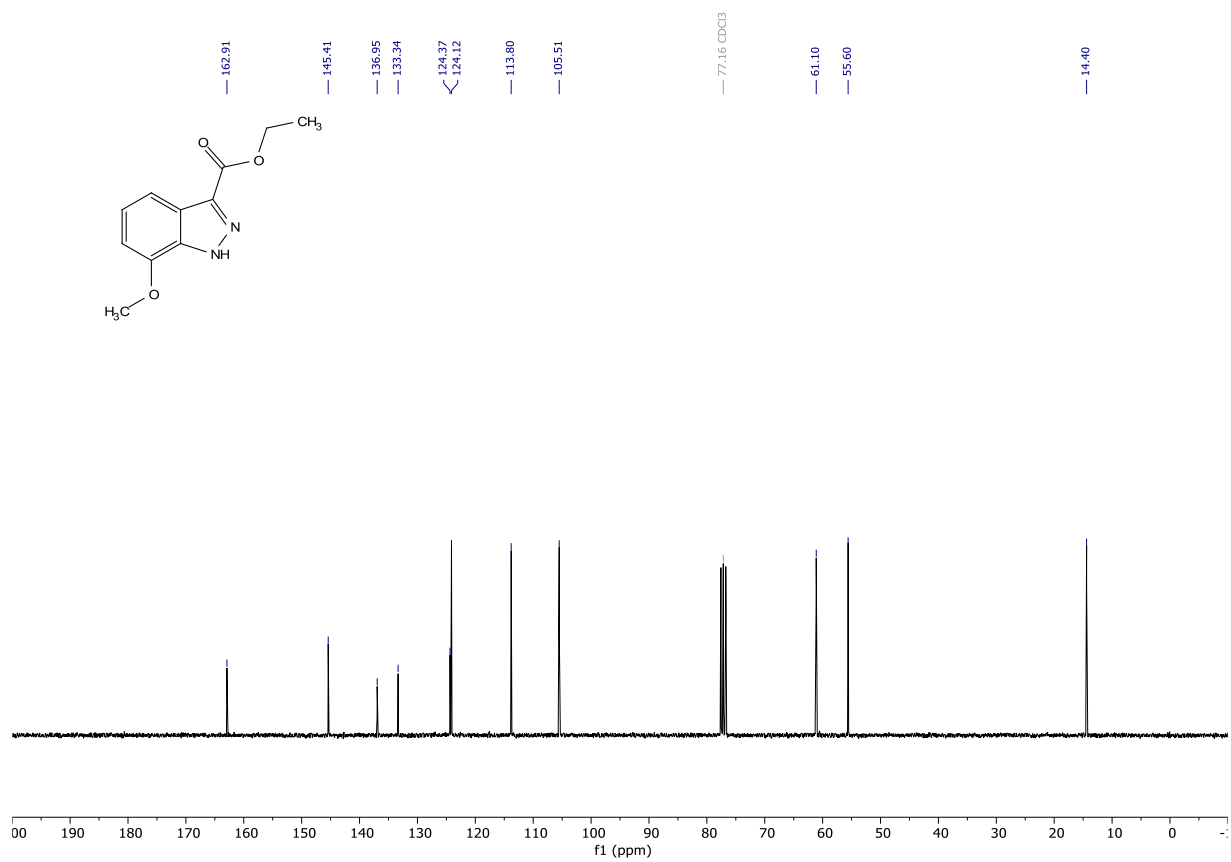
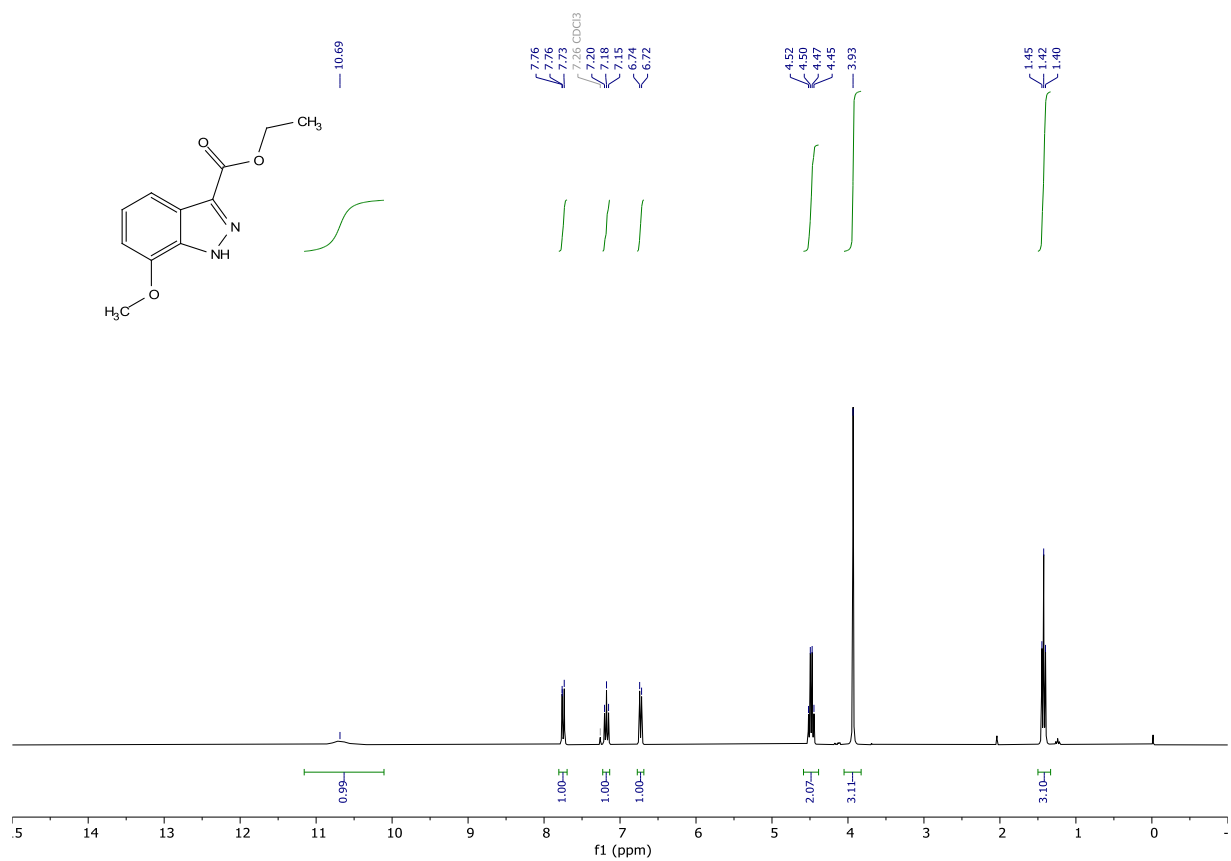
NMR (282 MHz, CDCl₃) δ -72.81. **HRMS** (EI) calculated for [M-CH₃]⁺ C₁₀H₁₂F₃O₄SSi 313.0172, found 313.0170.

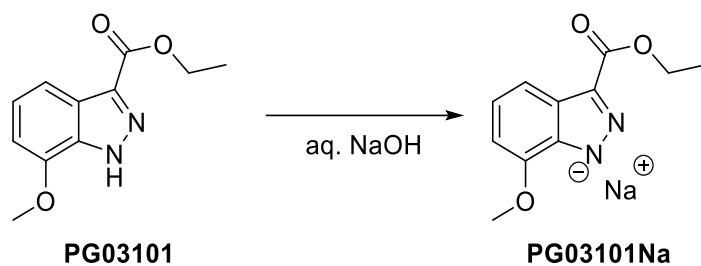




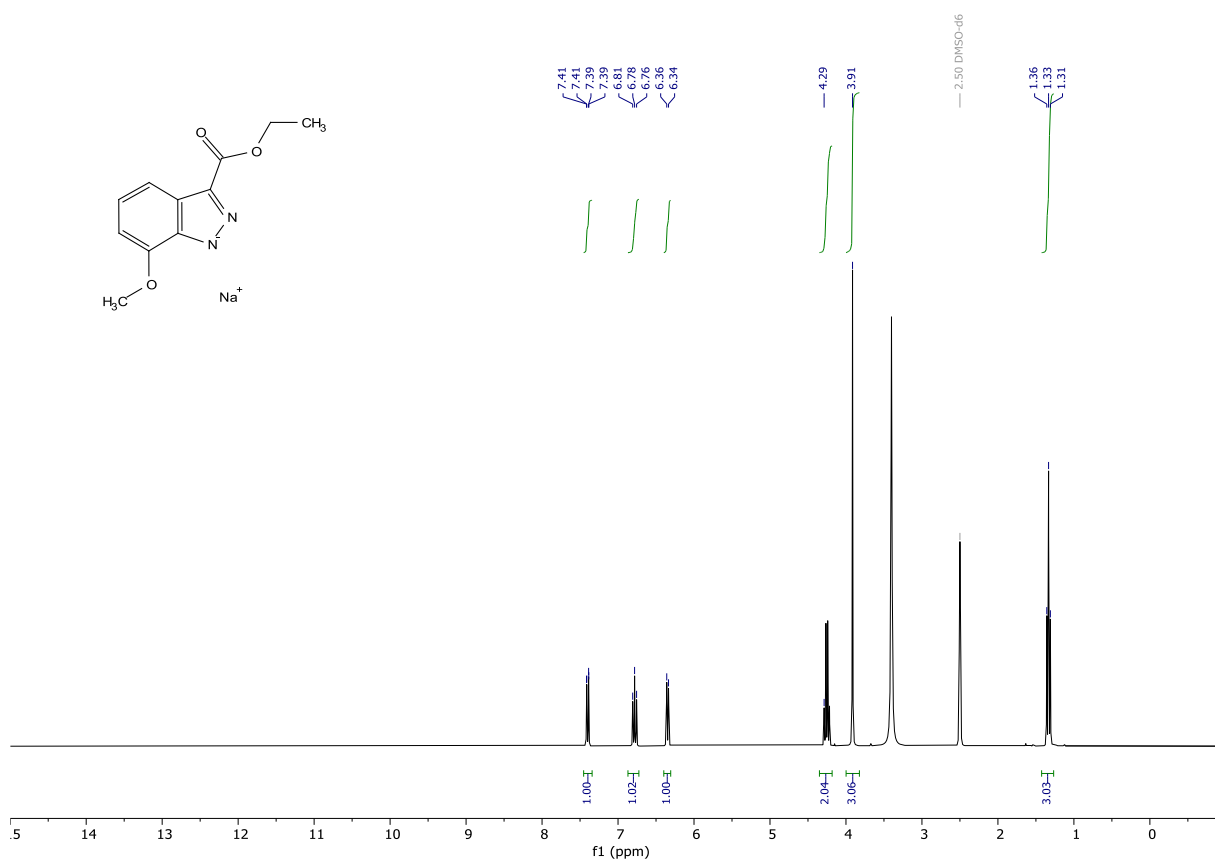


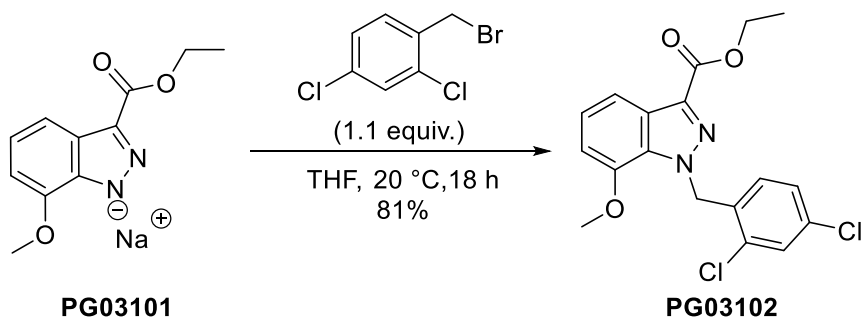
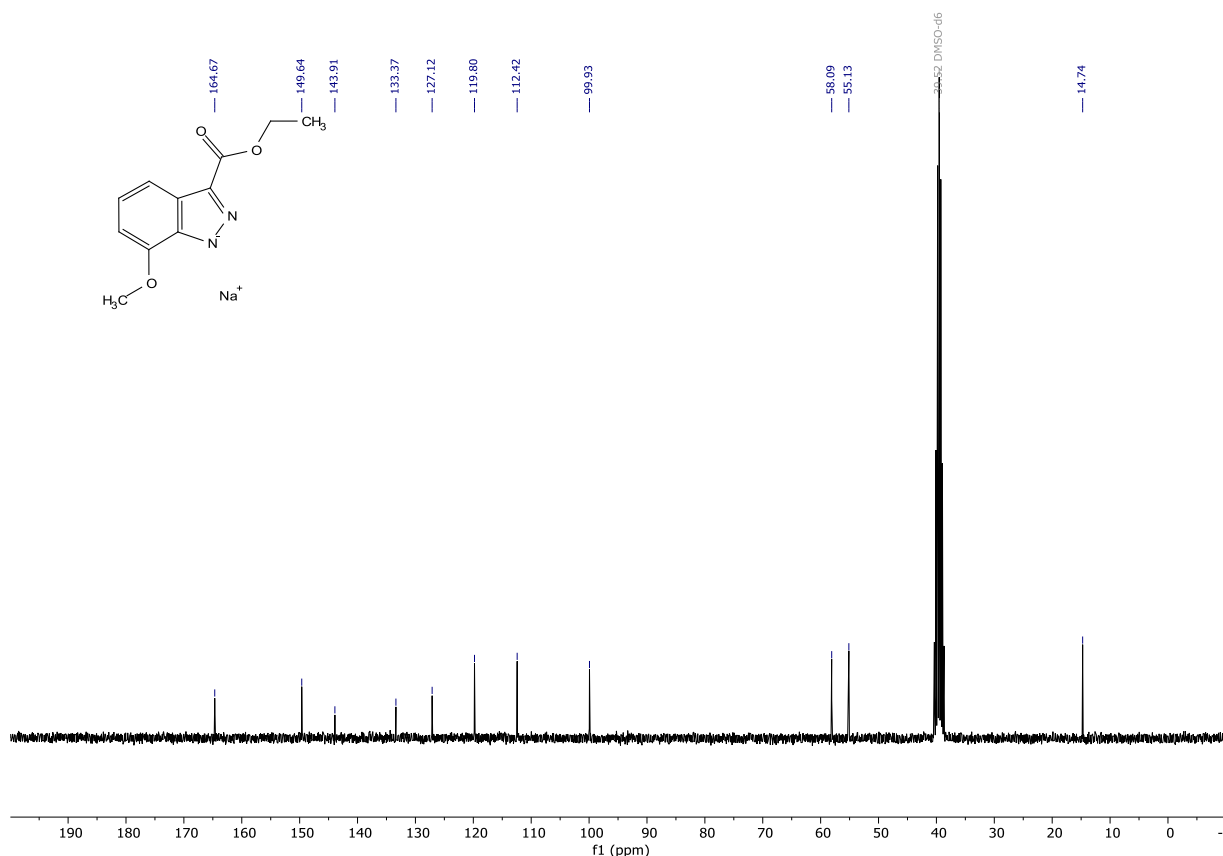
ethyl 7-methoxy-1H-indazole-3-carboxylate (PGUB81PREC4). To a stirred solution of 3-methoxy-2-(trimethylsilyl)phenyl trifluoromethanesulfonate (2.59423 g, 7.9002 mmol) in dry THF (40 mL) under an argon atmosphere was added ethyl 2-diazoacetate (15% in dichloromethane, 1.252 mL, 1.35216 g, 11.8502 mmol) was added. The mixture was cooled to -78°C . Then was added dropwise TBAF (1 M in THF, 9.5 mL, 9.5 mmol). The mixture was slowly warmed to 23°C over the course of 20 h. To the mixture was added slightly diluted brine. The aqueous phase was extracted with diethyl ether. The combined organic phases were washed with brine, dried over MgSO_4 , filtered, and concentrated under reduced pressure onto silica gel. The crude was purified by flash column chromatography (cyclohexane/ ethyl acetate gradient 1:0 to 0:1), to give the desired product in 43% yield. Brown oil: **^1H NMR** (300 MHz, Chloroform-*d*) δ 10.69 (s, 1H), 7.75 (d, $J = 8.4$ Hz, 1H), 7.18 (t, $J = 8.0$ Hz, 1H), 6.73 (d, $J = 7.6$ Hz, 1H), 4.48 (q, $J = 7.2$ Hz, 2H), 3.93 (s, 3H), 1.42 (t, $J = 7.1$ Hz, 3H). **^{13}C NMR** (75 MHz, CDCl_3) δ 162.91, 145.41, 136.95, 133.34, 124.37, 124.12, 113.80, 105.51, 61.10, 55.60, 14.40. **HRMS** (ESI) calculated for $[\text{M}+\text{H}]^+$ $\text{C}_{11}\text{H}_{13}\text{N}_2\text{O}_3$ 221.0921, found 221.0920.





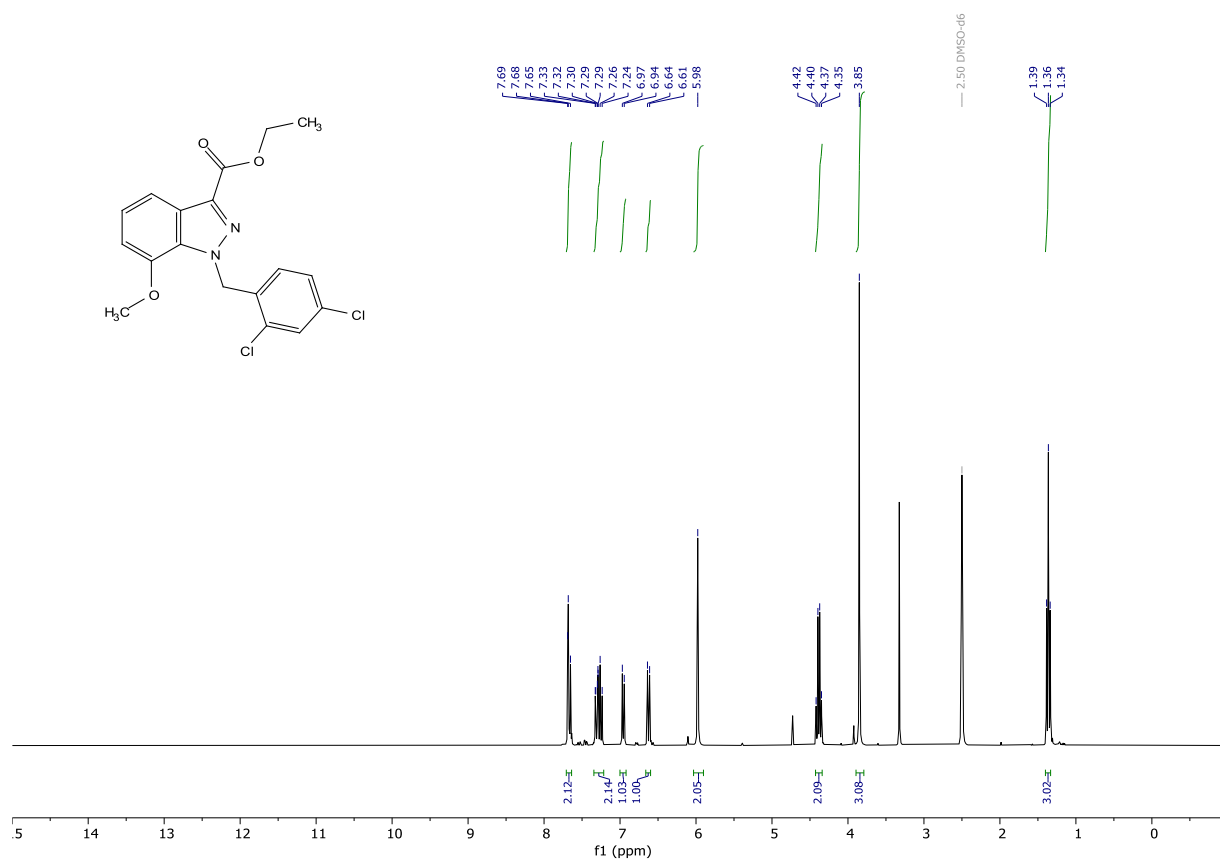
3-(ethoxycarbonyl)-7-methoxyindazol-1-ide (PGUB03101Na). A solution of PG03101 in water + 0.1% TFA was basified with 1 M NaOH. The resulting precipitate was filtered off, thoroughly washed with 1 M NaOH and diethyl ether, to give the desired product after thorough drying. White solid: ^1H NMR (300 MHz, DMSO- d_6) δ 7.45 – 7.34 (m, 1H), 6.78 (t, $J = 7.7$ Hz, 1H), 6.35 (d, $J = 7.0$ Hz, 1H), 4.29 (s, 2H), 3.91 (s, 3H), 1.33 (t, $J = 7.1$ Hz, 3H). ^{13}C NMR (75 MHz, DMSO) δ 164.67, 149.64, 143.91, 133.37, 127.12, 119.80, 112.42, 99.93, 58.09, 55.13, 14.74.

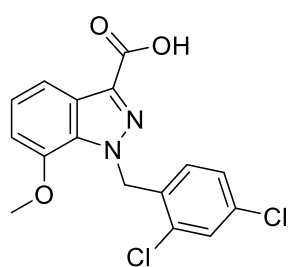
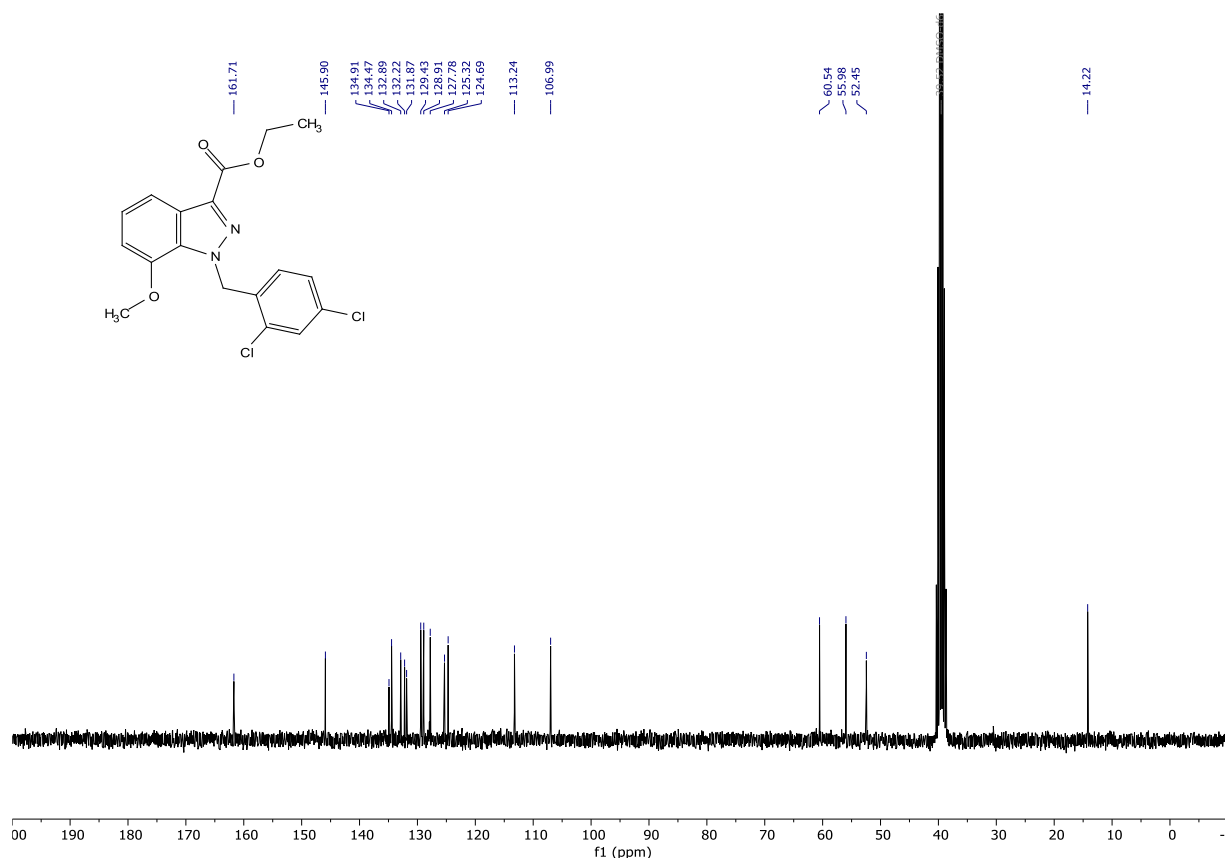




ethyl 1-(2,4-dichlorobenzyl)-7-methoxy-1H-indazole-3-carboxylate (PG03102). To a stirred suspension of sodium 3-(ethoxycarbonyl)-7-methoxyindazol-1-ide (0.2749 g, 1.1350 mmol) in dry THF (12 mL) under an argon atmosphere was added 2,4-dichlorobenzyl bromide (0.31277 g, 1.3036 mmol). The white suspension was left stirring for 18 h. The mixture was filtered through a pad of celite. The filtrate was concentrated onto silica gel. The crude was purified by flash column chromatography (cyclohexane/ ethyl acetate gradient from 1:0 to 0:1), to give the desired product in 81% yield (0.34648 g, 0.91362 mmol). A small sample was recrystallised from DMSO- d_6 and yielded single crystals of suitable quality for x-ray diffraction measurements (CCDC deposition number: 2203045). White solid: ^1H NMR (300 MHz, DMSO- d_6) δ 7.71 – 7.64 (m, 2H), 7.34 – 7.21 (m, 2H), 6.96 (d, J = 7.5 Hz, 1H), 6.62 (d, J = 8.4 Hz, 1H), 5.98 (s, 2H), 4.38 (q, J = 7.1 Hz, 2H), 3.85 (s, 3H), 1.36 (t, J = 7.1 Hz, 3H). ^{13}C NMR (75 MHz, DMSO) δ 161.71, 145.90, 134.91, 134.47, 132.89, 132.22, 131.87, 129.43, 128.91, 127.78,

125.32, 124.69, 113.24, 106.99, 60.54, 55.98, 52.45, 14.22. **HRMS** (ESI) calculated for $[M+H]^+$ $C_{18}H_{17}Cl_2N_2O_3$ 379.0611, found 379.0620.

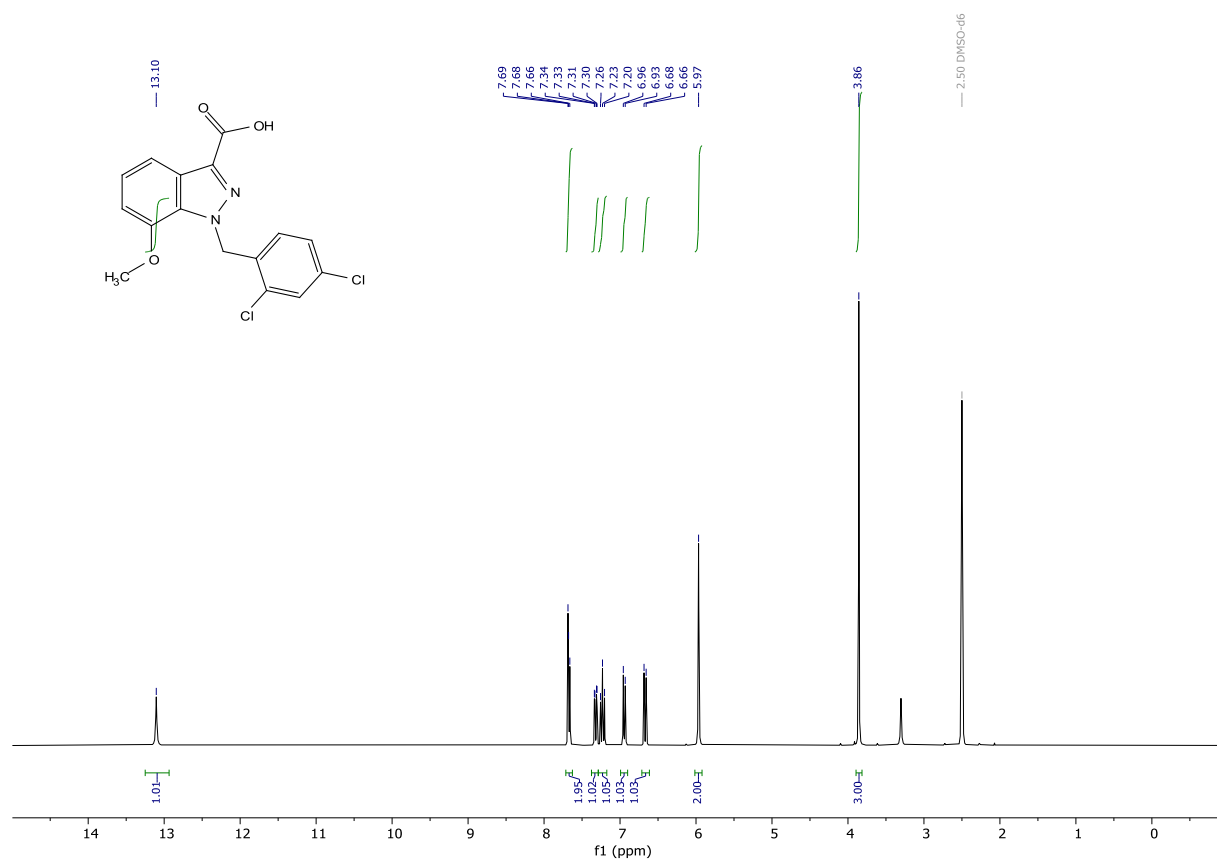


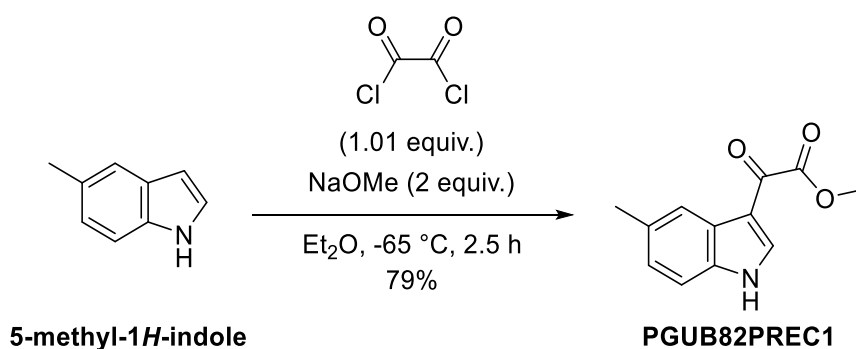
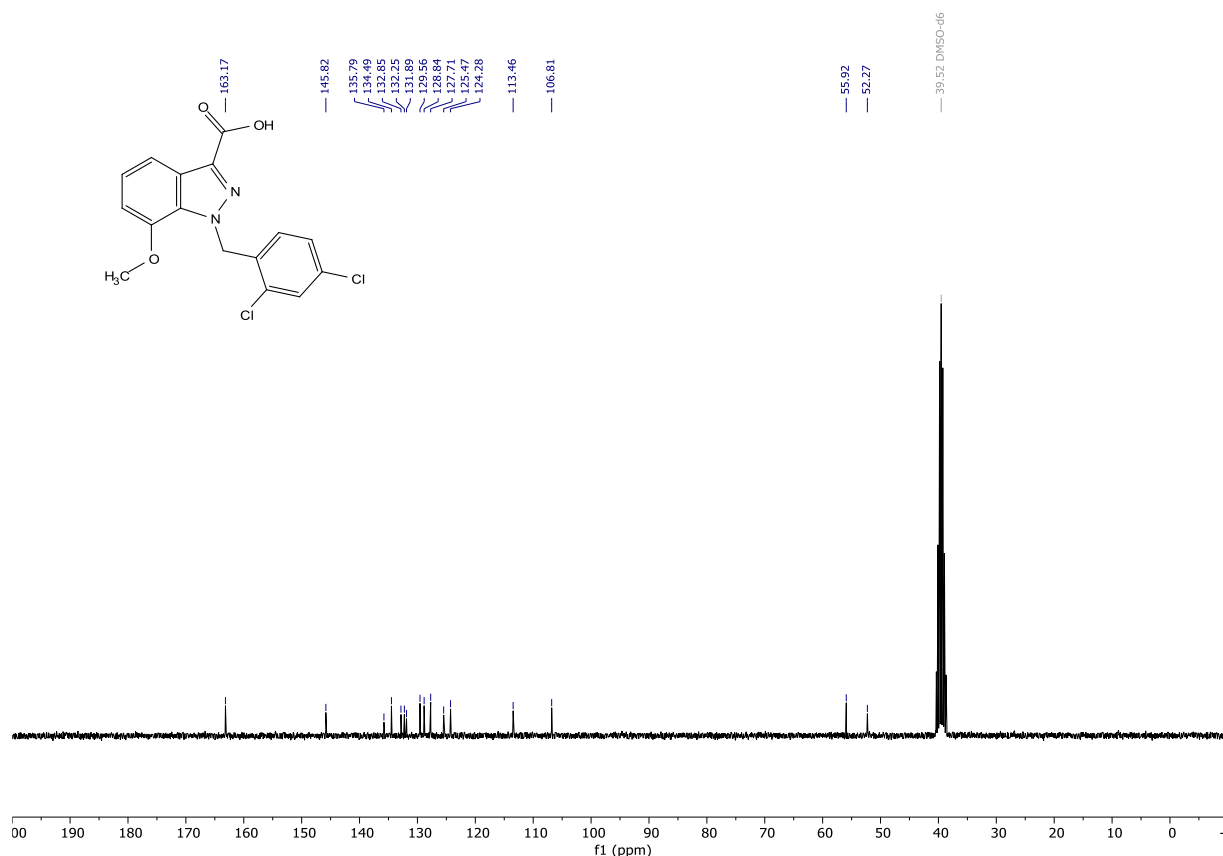


PGUB81

1-(2,4-dichlorobenzyl)-7-methoxy-1H-indazole-3-carboxylic acid (PGUB81) (Z = N, W = OH). Prepared according to general procedure III from ethyl 1-(2,4-dichlorobenzyl)-7-methoxy-1H-indazole-3-carboxylate (PGUB03102) (Z = N, Y = OEt, 0.084 g, 0.2215 mmol). The product required purification by reverse phase flash column chromatography (water + 0.1% TFA/ acetonitrile + 0.1% TFA), to give the desired product in 70% (0.05456 g, 0.15536 mmol). A small sample was recrystallised from cyclohexane/ ethyl acetate and yielded single crystals of suitable quality for x-ray diffraction measurements (CCDC deposition number: 222014). White solid: **¹H NMR** (300 MHz, DMSO-*d*₆) δ 13.10 (s, 1H), 7.71 – 7.63 (m, 2H), 7.32 (dd, *J* = 8.4, 2.1 Hz, 1H), 7.23 (t, *J* = 7.9 Hz, 1H), 6.94 (d, *J* = 7.5 Hz, 1H), 6.67 (d, *J* = 8.4 Hz, 1H), 5.97 (s, 2H), 3.86 (s, 3H). **¹³C NMR** (75 MHz, DMSO) δ 163.17, 145.82, 135.79, 134.49, 132.85, 132.25, 131.89, 129.56, 128.84, 127.71, 125.47, 124.28, 113.46, 106.81, 55.92, 52.27.

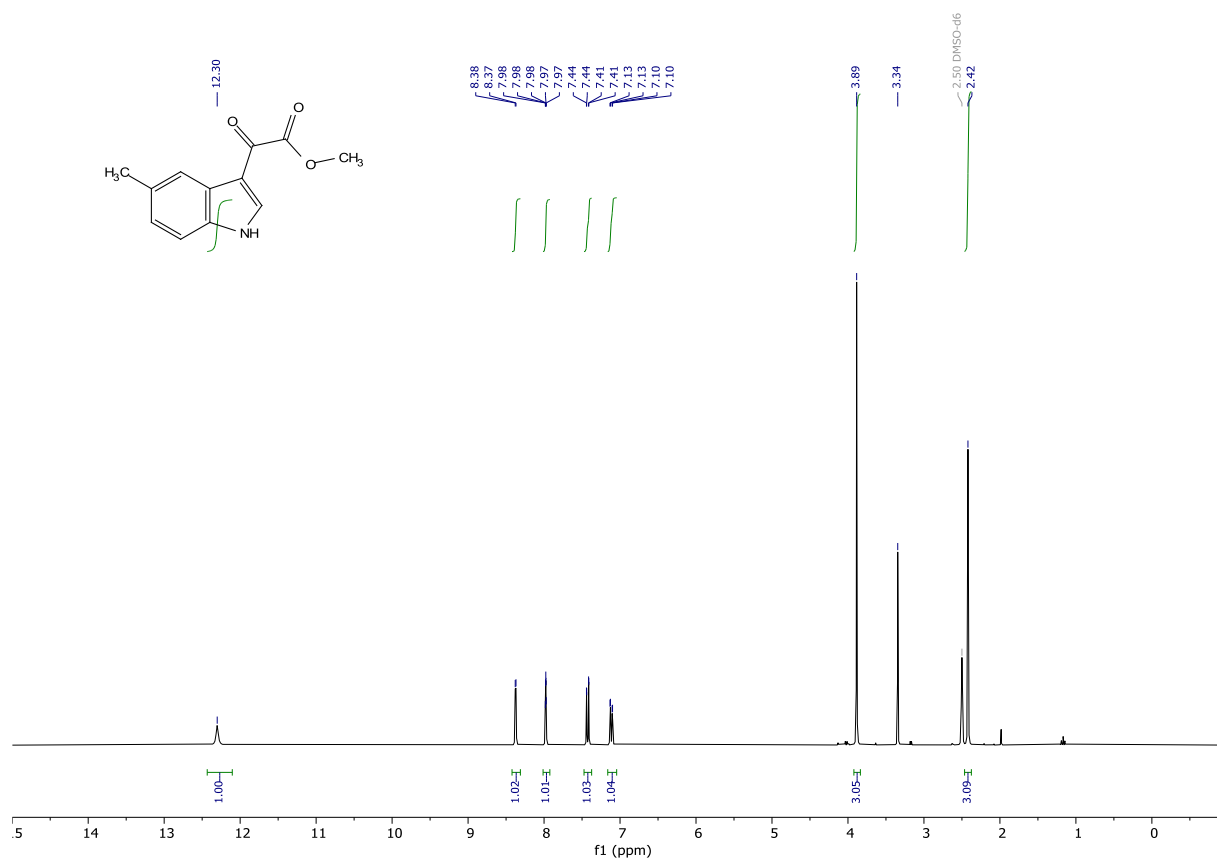
HRMS (ESI) calculated for $[M+H]^+$ $C_{16}H_{13}Cl_2N_2O_3$ 351.0298, found 351.0311. **Purity (HPLC):** >95% UV_{214} , >97% UV_{254} .

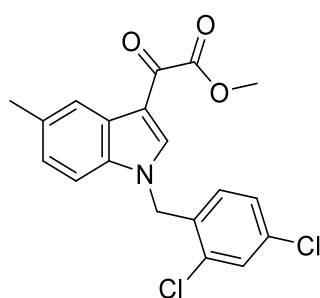
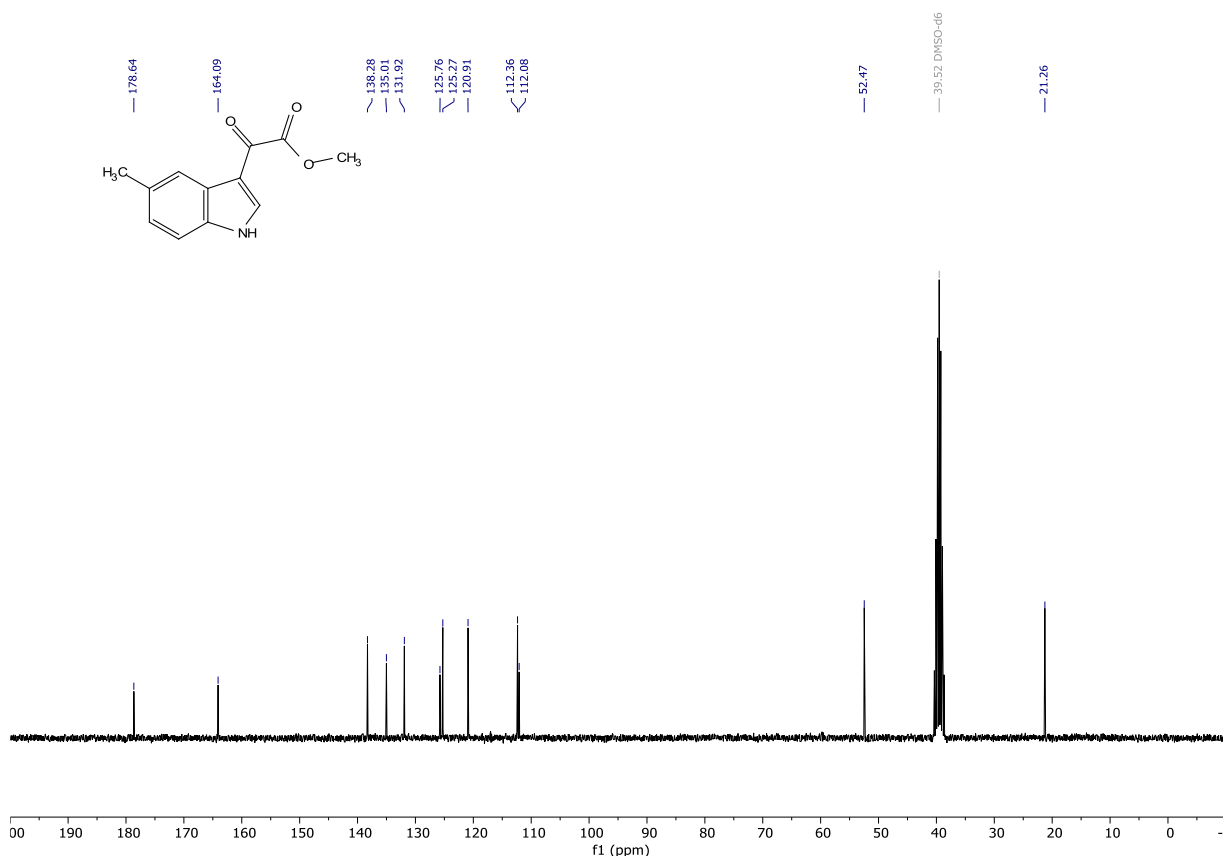




methyl 2-(5-methyl-1H-indol-3-yl)-2-oxoacetate (PGUB82PREC1). To a stirred solution of 5-methyl-1H-indole (0.51641 g, 3.9367 mmol) in dry diethyl ether (5 mL) at 0°C under an argon atmosphere was added slowly oxalyl chloride (0.35 mL, 0.518 g, 4.0813 mmol). The mixture was stirred for 1 h, then it was cooled to -76°C . A solution of sodium methoxide (0.4254 g, 7.8734 mmol) in dry methanol (5 mL) was added slowly. After the addition, the mixture was left warming to room temperature over the course of 2 h. Water was added to the mixture and the resulting suspension was filtered through a por 3 frit. Giving a brownish filter cake, which was washed with water. The filter cake was thoroughly dried on the high vac. Then it was taken up in a mixture of THF, dichloromethane, acetone, and methanol, and was concentrated onto silica gel. The crude was purified by flash column chromatography (cyclohexane/ ethyl acetate gradient from 1:0 to 0:1), to give the desired product in 79% yield (0.67210 g, 3.09404 mmol). Yellow solid: ^1H NMR (300 MHz, $\text{DMSO}-d_6$) δ 12.30 (s, 1H), 8.37

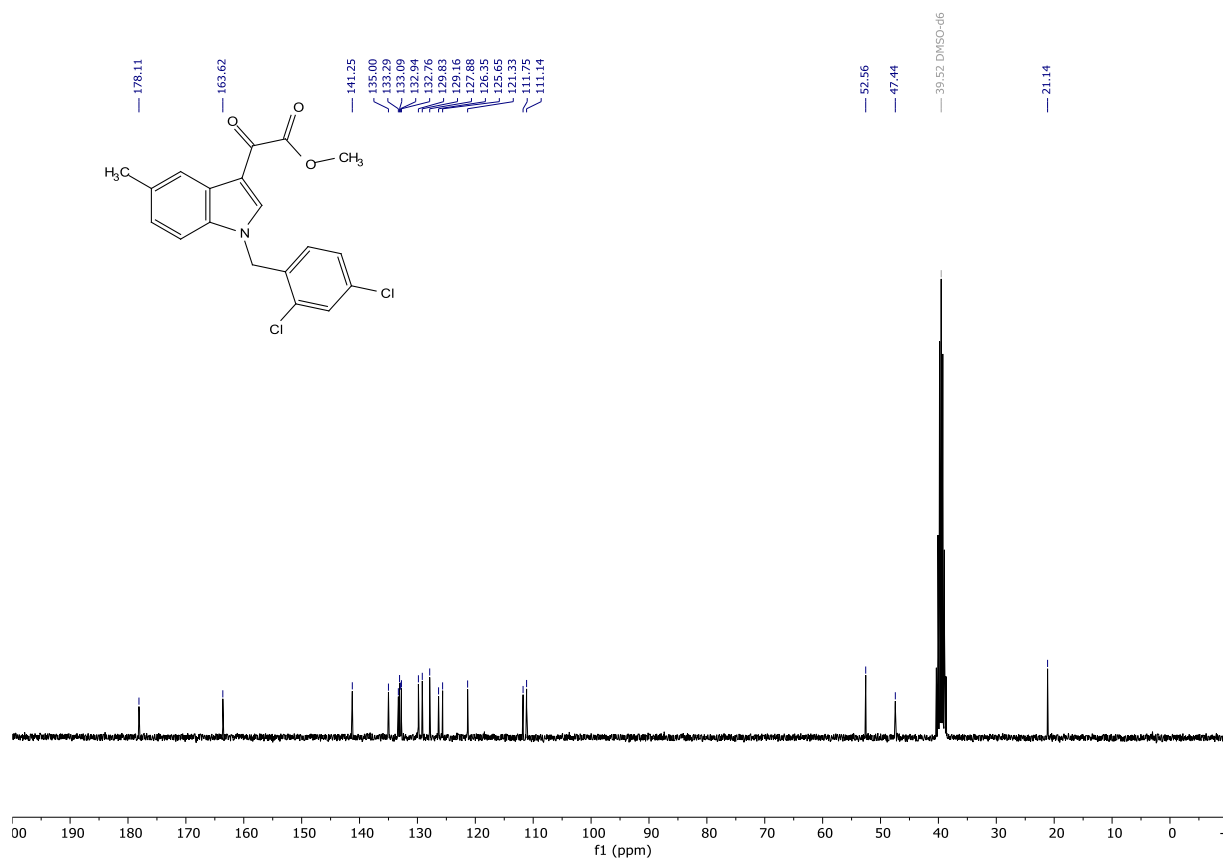
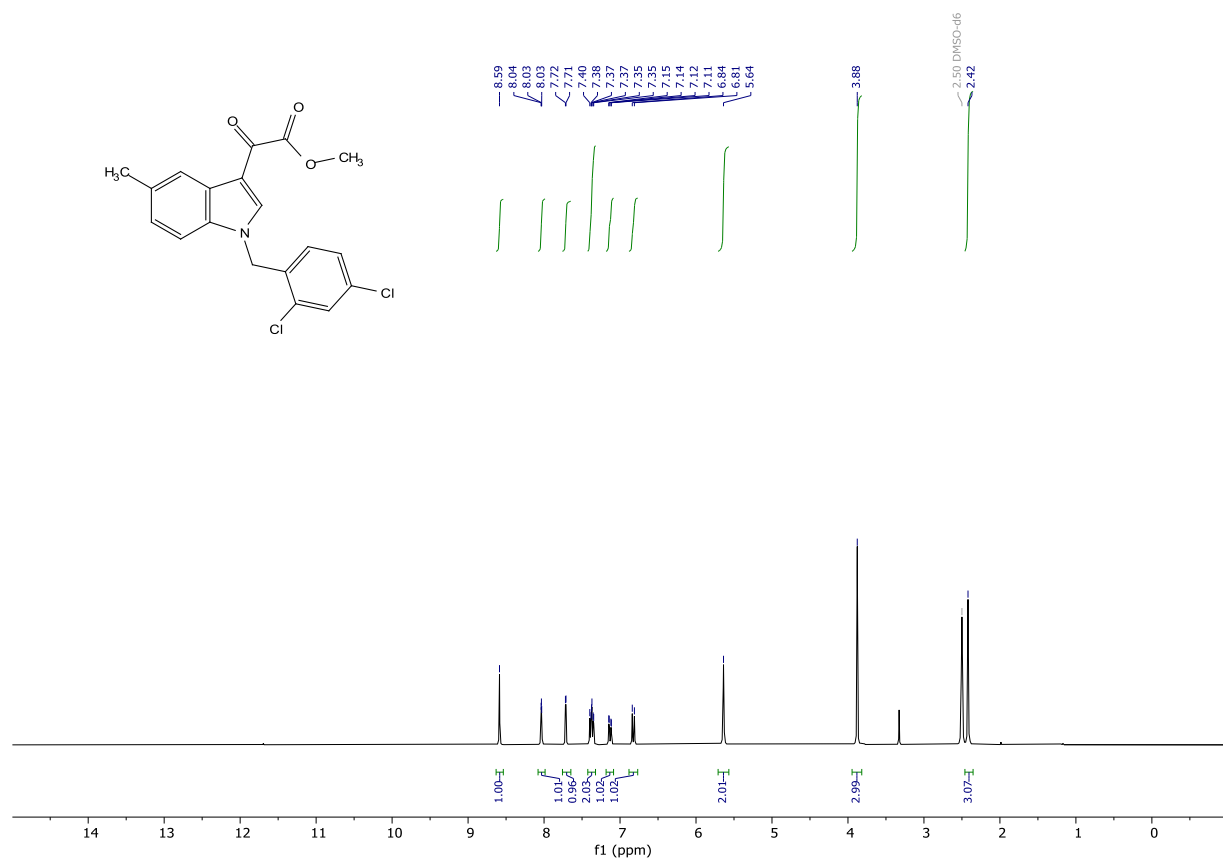
(d, $J = 3.0$ Hz, 1H), 7.98 (dt, $J = 1.7, 0.9$ Hz, 1H), 7.43 (dd, $J = 8.3, 0.7$ Hz, 1H), 7.12 (dd, $J = 8.3, 1.7$ Hz, 1H), 3.89 (s, 3H), 2.42 (s, 3H). ^{13}C NMR (75 MHz, DMSO) δ 178.64, 164.09, 138.28, 135.01, 131.92, 125.76, 125.27, 120.91, 112.36, 112.08, 52.47, 21.26. HRMS (ESI) calculated for $[\text{M}+\text{H}]^+$ $\text{C}_{12}\text{H}_{12}\text{NO}_3$ 218.0812, found 218.0816.

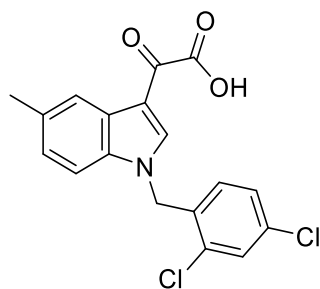




PGUB82PREC2

methyl 2-(1-(2,4-dichlorobenzyl)-5-methyl-1H-indol-3-yl)-2-oxoacetate (PGUB82PREC2) (Z = CH, Y = COOMe). Prepared according to general procedure II from methyl 2-(5-methyl-1H-indol-3-yl)-2-oxoacetate (PGUB82PREC1) (Z = CH, Y = COOMe, 0.36896 g, 1.6985 mmol) using 2,4-dichlorobenzyl bromide as alkyl halide, to give the desired product in 66% yield (0.42145 g, 1.1202 mmol). White solid: ^1H NMR (300 MHz, DMSO- d_6) δ 8.59 (s, 1H), 8.08 – 7.99 (m, 1H), 7.71 (d, J = 2.1 Hz, 1H), 7.42 – 7.32 (m, 2H), 7.13 (dd, J = 8.5, 1.7 Hz, 1H), 6.82 (d, J = 8.4 Hz, 1H), 5.64 (s, 2H), 3.88 (s, 3H), 2.42 (s, 3H). ^{13}C NMR (75 MHz, DMSO) δ 178.11, 163.62, 141.25, 135.00, 133.29, 133.09, 132.94, 132.76, 129.83, 129.16, 127.88, 126.35, 125.65, 121.33, 111.75, 111.14, 52.56, 47.44, 21.14. HRMS (ESI) calculated for $[\text{M}+\text{H}]^+$ $\text{C}_{19}\text{H}_{16}\text{Cl}_2\text{NO}_3$ 376.0502, found 376.0510.



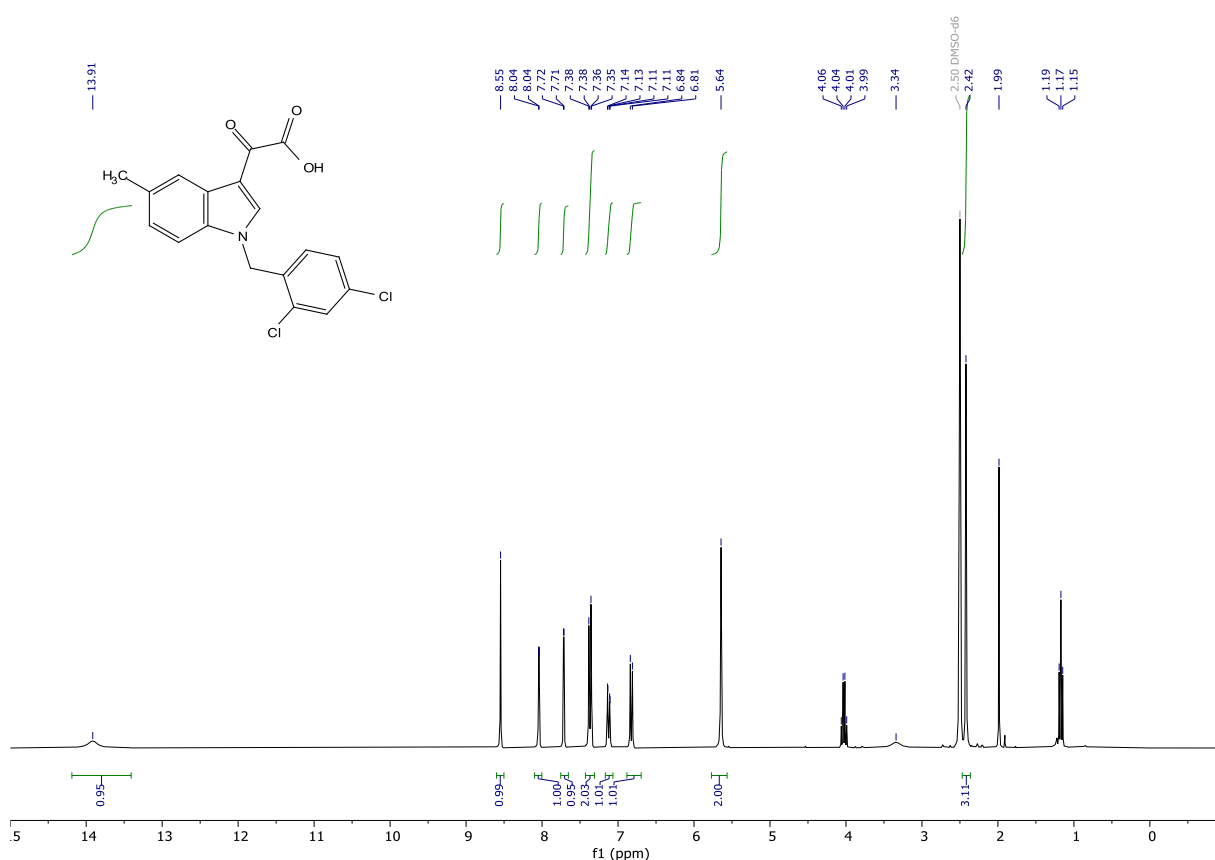


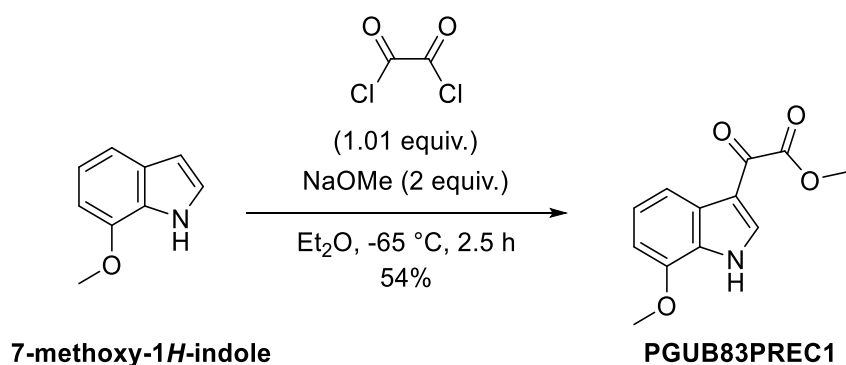
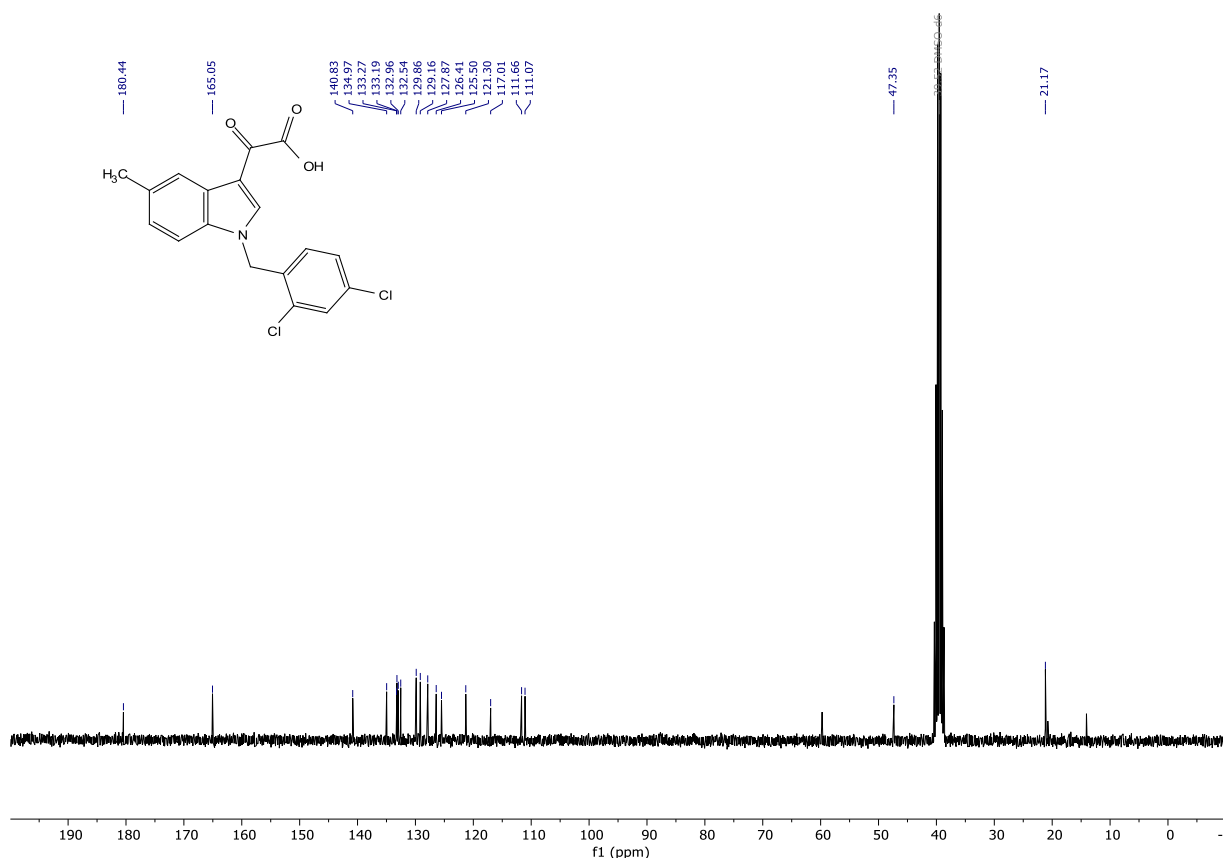
PGUB82

2-(1-(2,4-dichlorobenzyl)-5-methyl-1H-indol-3-yl)-2-oxoacetic acid (PGUB82) (Z = CH, Y = COOH).

Prepared according to general procedure III from methyl 2-(1-(2,4-dichlorobenzyl)-5-methyl-1H-indol-3-yl)-2-oxoacetate (PGUB82PREC2) (Z = CH, Y = COOMe, 0.084 g, 0.2215 mmol), to give the desired product in quantitative yield (0.12082 g, 0.33356 mmol). White solid slightly impure with diethyl ether:

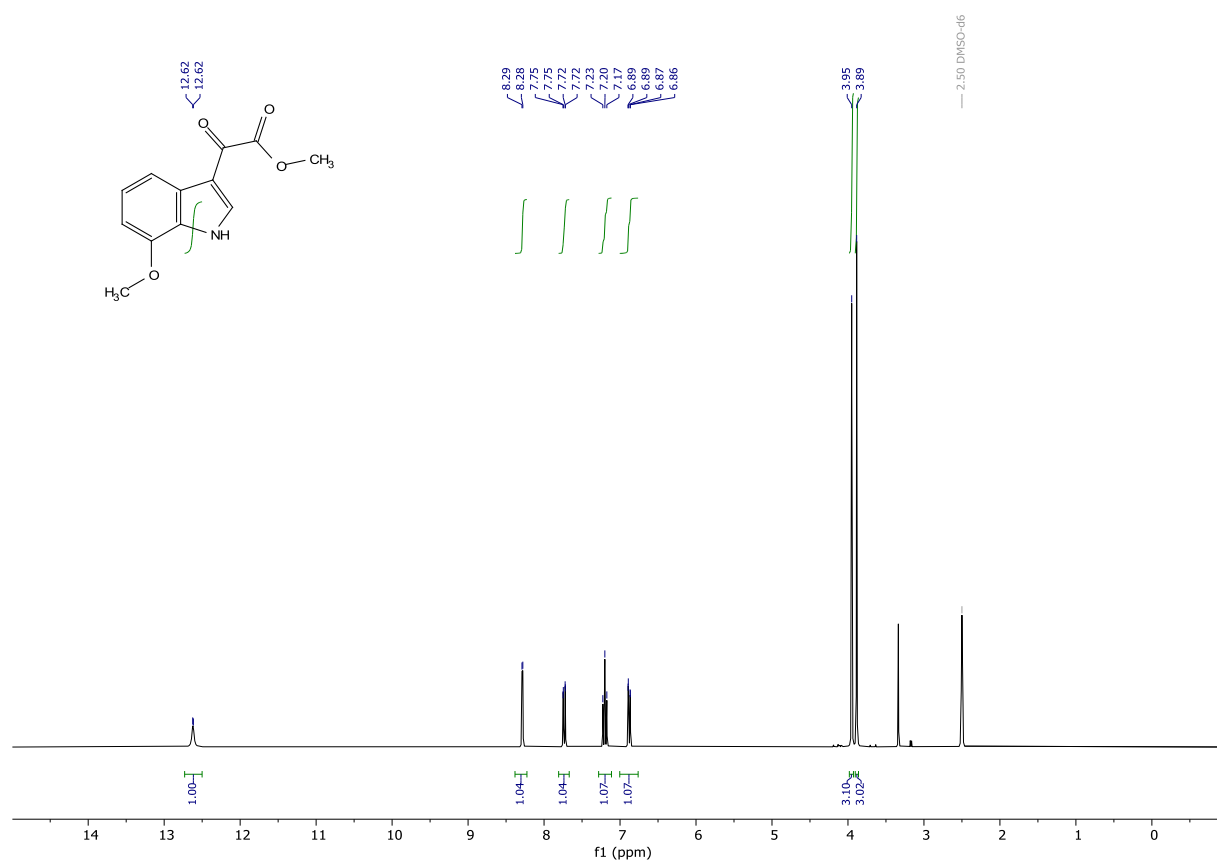
¹H NMR (300 MHz, DMSO-*d*₆) δ 13.91 (s, 1H), 8.55 (s, 1H), 8.04 (d, *J* = 1.6 Hz, 1H), 7.71 (d, *J* = 2.1 Hz, 1H), 7.37 (dd, *J* = 8.4, 2.3 Hz, 2H), 7.12 (dd, *J* = 8.4, 1.7 Hz, 1H), 6.82 (d, *J* = 8.4 Hz, 1H), 5.64 (s, 2H), 2.42 (s, 3H). **¹³C NMR** (75 MHz, DMSO) δ 180.44, 165.05, 140.83, 134.97, 133.27, 133.19, 132.96, 132.54, 129.86, 129.16, 127.87, 126.41, 125.50, 121.30, 117.01, 111.66, 111.07, 47.35, 21.17. **HRMS** (ESI) calculated for [M+H]⁺ C₁₈H₁₄Cl₂NO₃ 362.0345, found 362.0343. **Purity (HPLC):** >95% UV₂₁₄, >97% UV₂₅₄.

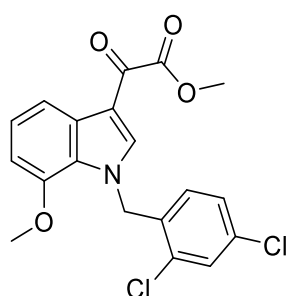
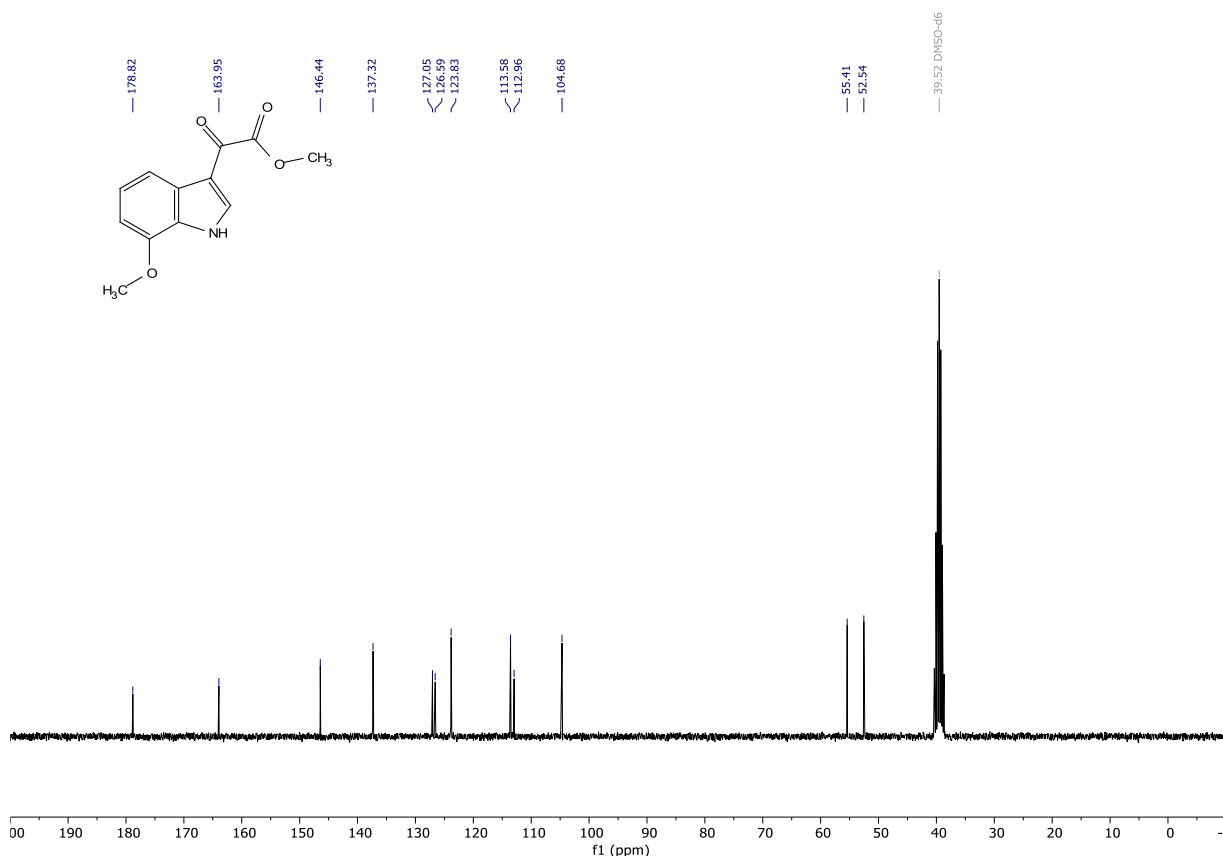




methyl 2-(7-methoxy-1*H*-indol-3-yl)-2-oxoacetate (PGUB83PREC1). To a stirred solution of 7-methoxy-1*H*-indole (0.50896 g, 3.4581 mmol) in dry diethyl ether (5 mL) at 0 °C under an argon atmosphere was added slowly oxalyl chloride (0.3 mL, 0.444 g, 3.4983 mmol). The mixture was stirred for 1 h, then it was cooled to -76 °C. A solution of sodium methoxide (0.37369 g, 6.9163 mmol) in dry methanol (5 mL) was added slowly. After the addition, the mixture was left warming to room temperature over the course of 2 h. Water was added to the mixture and the resulting suspension was filtered through a por 3 frit. Giving a brownish filter cake, which was washed with water. The filter cake was thoroughly dried on the high vac. Then it was taken up in a mixture of THF, dichloromethane, acetone, and methanol, and was concentrated onto silica gel. The crude was purified by flash column chromatography (cyclohexane/ ethyl acetate gradient from 1:0 to 0:1), to give the desired product in

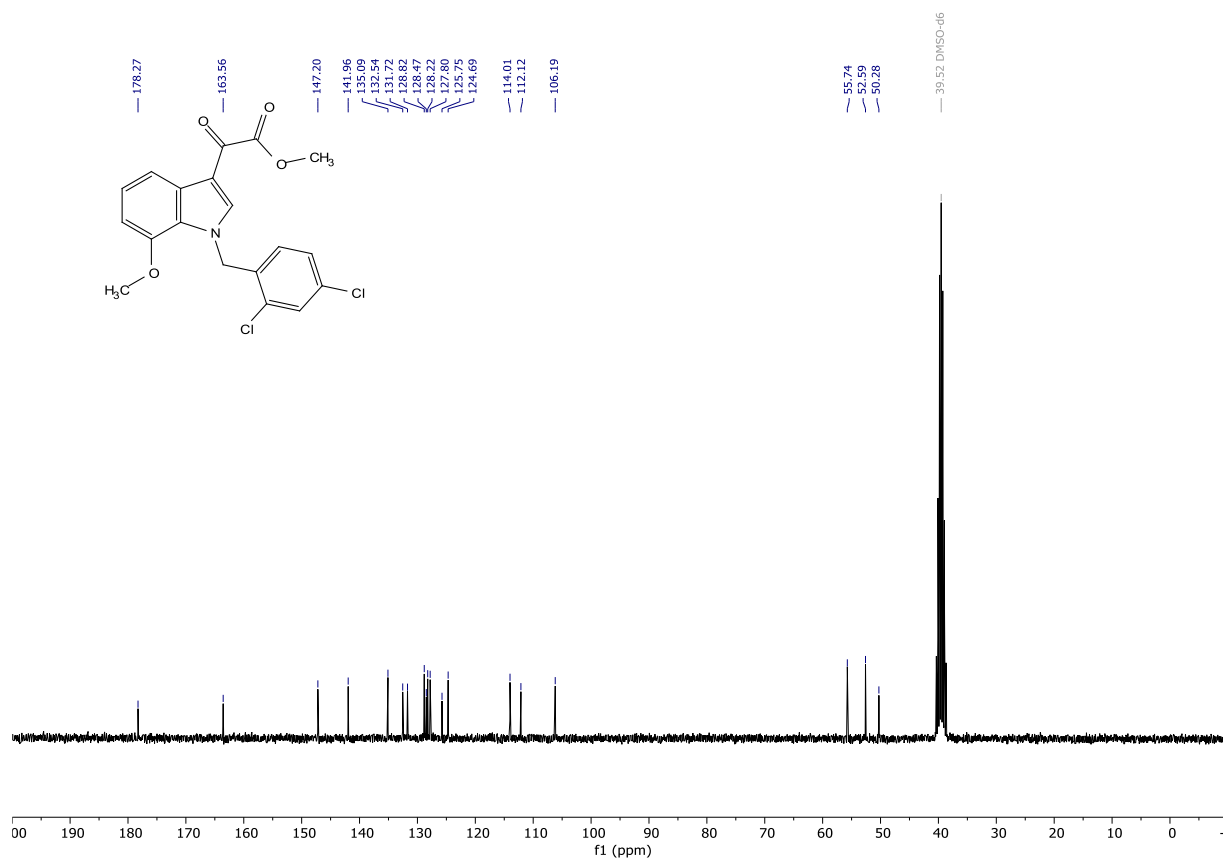
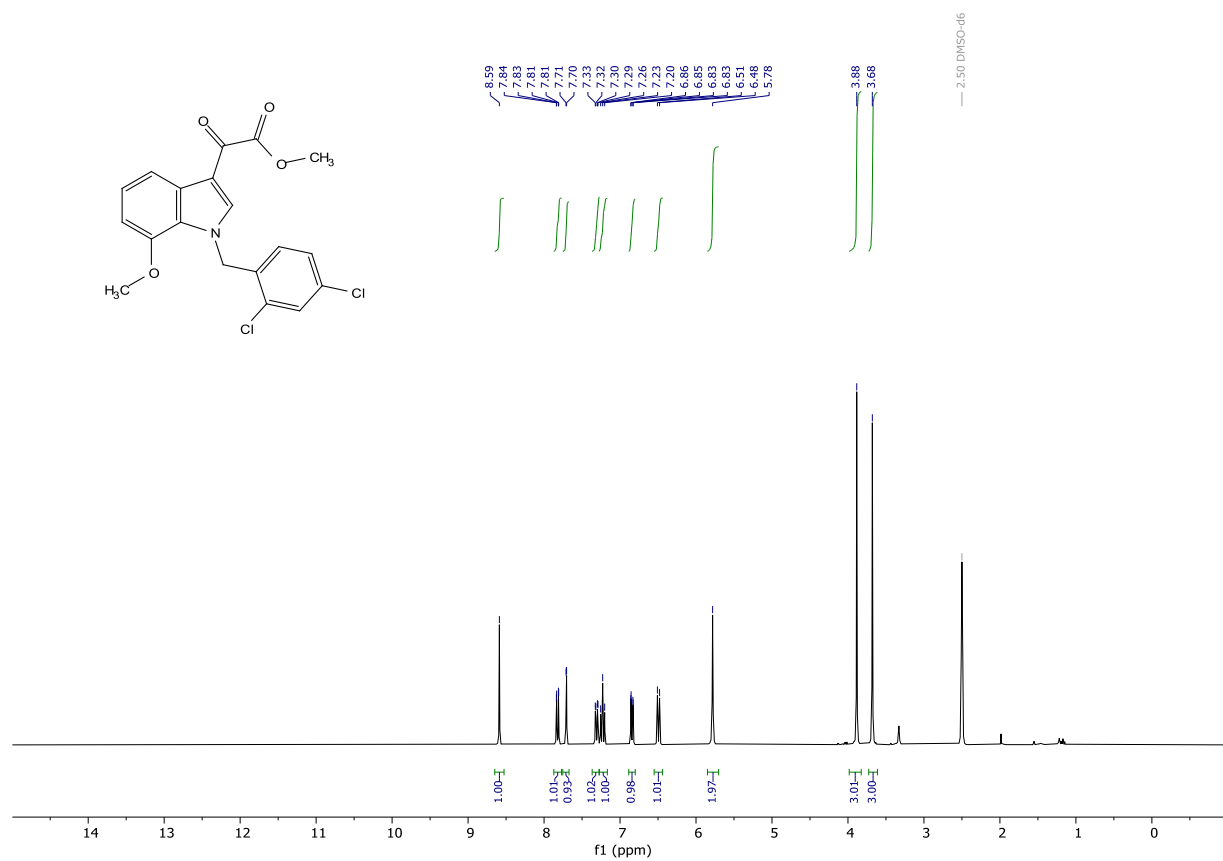
54% yield (0.42237 g, 1.81101 mmol). Orange solid: **1H NMR** (300 MHz, DMSO-*d*₆) δ 12.73 – 12.50 (m, 1H), 8.29 (d, *J* = 3.3 Hz, 1H), 7.73 (dd, *J* = 8.0, 0.9 Hz, 1H), 7.20 (t, *J* = 7.9 Hz, 1H), 6.88 (dd, *J* = 8.0, 0.9 Hz, 1H), 3.95 (s, 3H), 3.89 (s, 3H). **¹³C NMR** (75 MHz, DMSO) δ 178.82, 163.95, 146.44, 137.32, 127.05, 126.59, 123.83, 113.58, 112.96, 104.68, 55.41, 52.54. **HRMS** (ESI) calculated for [M+H]⁺ C₁₂H₁₂NO₄ 234.0761, found 234.0765.

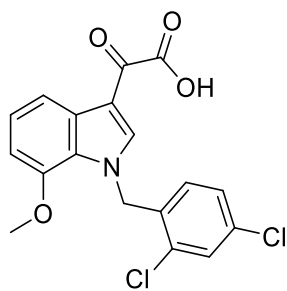




PGUB83PREC2

methyl 2-(1-(2,4-dichlorobenzyl)-7-methoxy-1H-indol-3-yl)-2-oxoacetate (PGUB82PREC2) (Z = CH, Y = COOMe). Prepared according to general procedure II from methyl 2-(7-methoxy-1H-indol-3-yl)-2-oxoacetate (PGUB83PREC1) (Z = CH, Y = COOMe, 0.14126 g, 0.6057 mmol) using 2,4-dichlorobenzyl bromide as alkyl halide, to give the desired product in 67% yield (0.15862 g, 0.40440 mmol). A small sample was recrystallised from DMSO- d_6 and yielded single crystals of suitable quality for x-ray diffraction measurements (CCDC deposition number: 2208017). White solid: ^1H NMR (300 MHz, DMSO- d_6) δ 8.59 (s, 1H), 7.82 (dd, J = 8.0, 0.9 Hz, 1H), 7.71 (d, J = 2.2 Hz, 1H), 7.31 (dd, J = 8.4, 2.2 Hz, 1H), 7.23 (t, J = 7.9 Hz, 1H), 6.89 – 6.80 (m, 1H), 6.49 (d, J = 8.4 Hz, 1H), 5.78 (s, 2H), 3.88 (s, 3H), 3.68 (s, 3H). ^{13}C NMR (75 MHz, DMSO) δ 178.27, 163.56, 147.20, 141.96, 135.09, 132.54, 131.72, 128.82, 128.47, 128.22, 127.80, 125.75, 124.69, 114.01, 112.12, 106.19, 55.74, 52.59, 50.28. HRMS (ESI) calculated for $[\text{M}+\text{H}]^+$ $\text{C}_{19}\text{H}_{16}\text{Cl}_2\text{NO}_4$ 392.0451, found 392.0453.

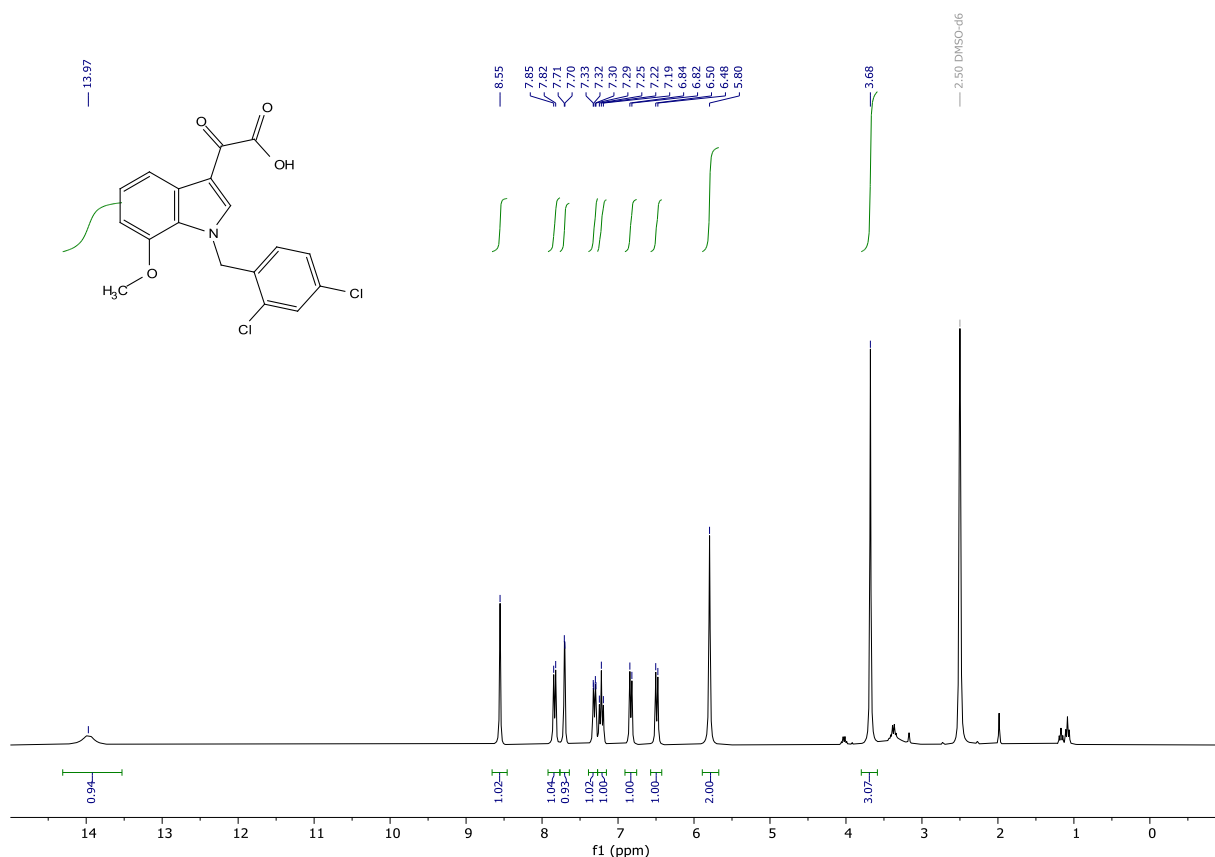


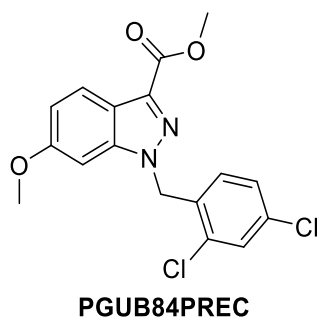
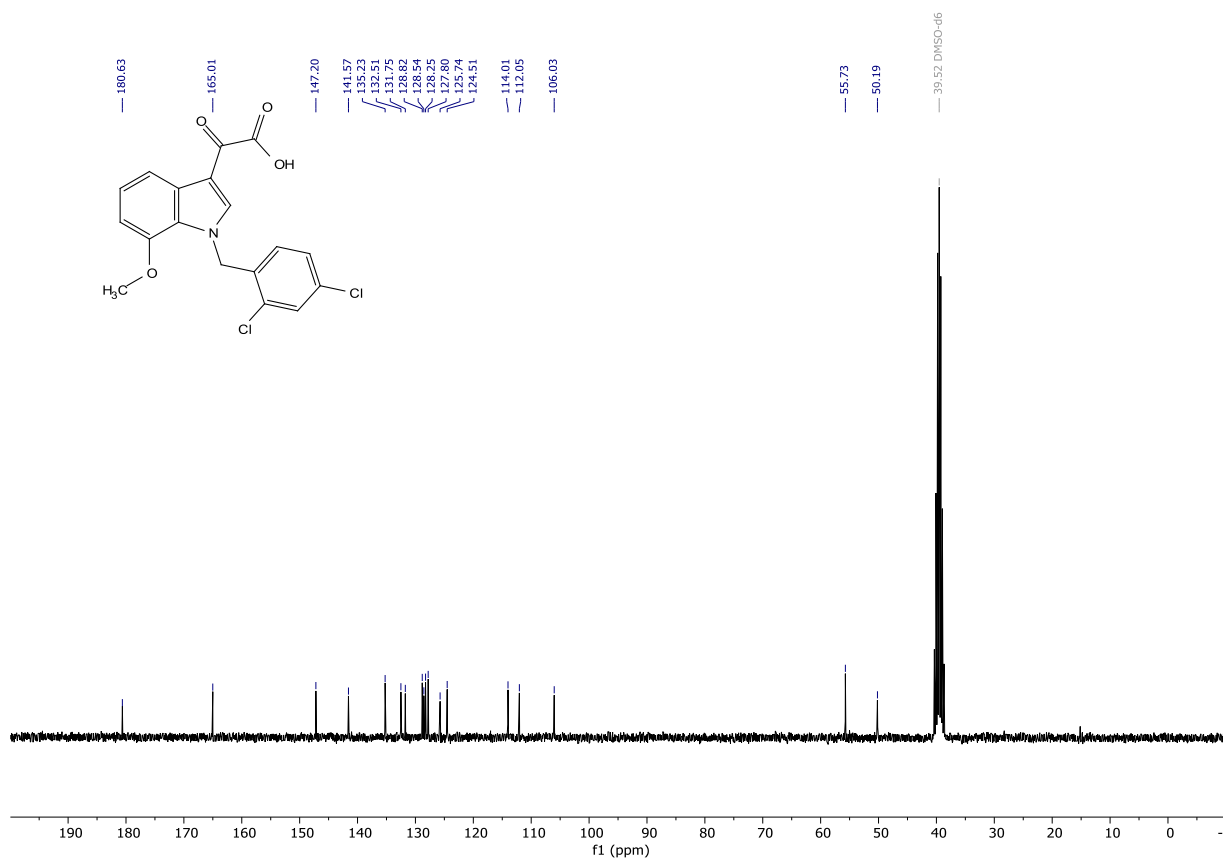


PGUB83

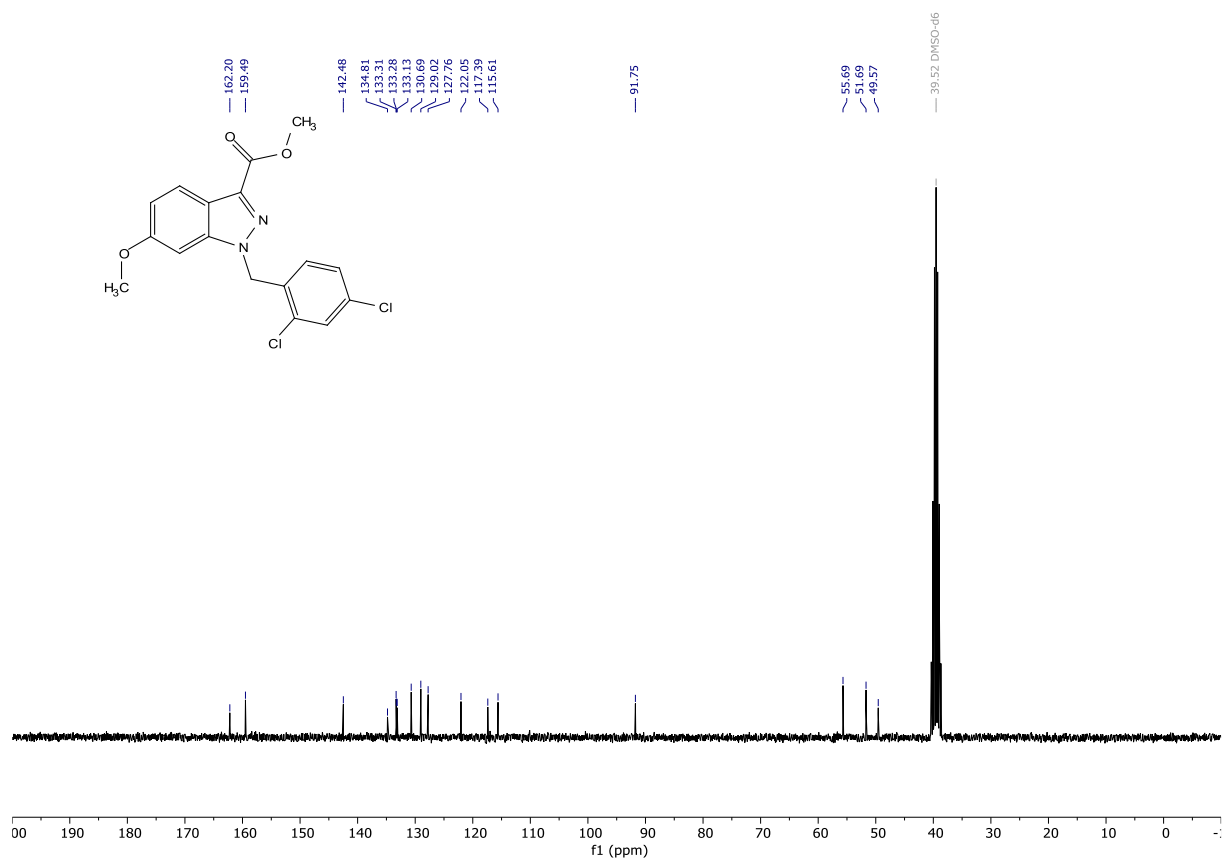
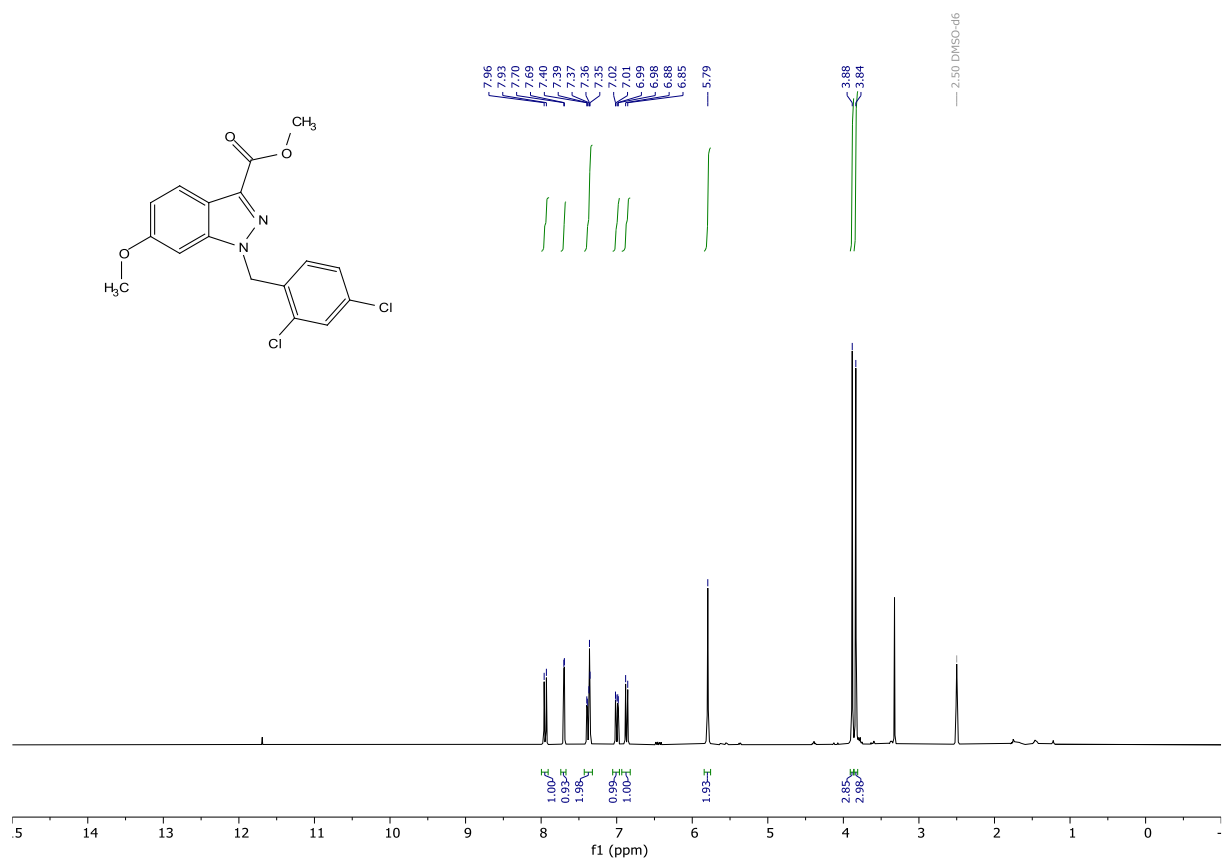
2-(1-(2,4-dichlorobenzyl)-7-methoxy-1H-indol-3-yl)-2-oxoacetic acid (PGUB83) (Z = CH, Y = COOH).

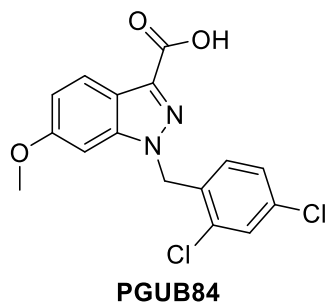
Prepared according to general procedure III from methyl 2-(1-(2,4-dichlorobenzyl)-7-methoxy-1H-indol-3-yl)-2-oxoacetate (PGUB83PREC2) (Z = CH, Y = COOMe, 0.13379 g, 0.3411 mmol), to give the desired product in 52% yield (0.06641 g, 0.17559 mmol). Yellow solid: ^1H NMR (300 MHz, DMSO- d_6) δ 13.97 (s, 1H), 8.55 (s, 1H), 7.83 (d, J = 7.9 Hz, 1H), 7.70 (d, J = 2.2 Hz, 1H), 7.31 (dd, J = 8.4, 2.2 Hz, 1H), 7.22 (t, J = 7.9 Hz, 1H), 6.83 (d, J = 7.9 Hz, 1H), 6.49 (d, J = 8.4 Hz, 1H), 5.80 (s, 2H), 3.68 (s, 3H). ^{13}C NMR (75 MHz, DMSO) δ 180.63, 165.01, 147.20, 141.57, 135.23, 132.51, 131.75, 128.82, 128.54, 128.25, 127.80, 125.74, 124.51, 114.01, 112.05, 106.03, 55.73, 50.19. HRMS (ESI) calculated for $[\text{M}+\text{H}]^+$ $\text{C}_{18}\text{H}_{14}\text{Cl}_2\text{NO}_4$ 378.0294, found 378.0299. Purity (HPLC): >98% UV_{214} , >99% UV_{254} .



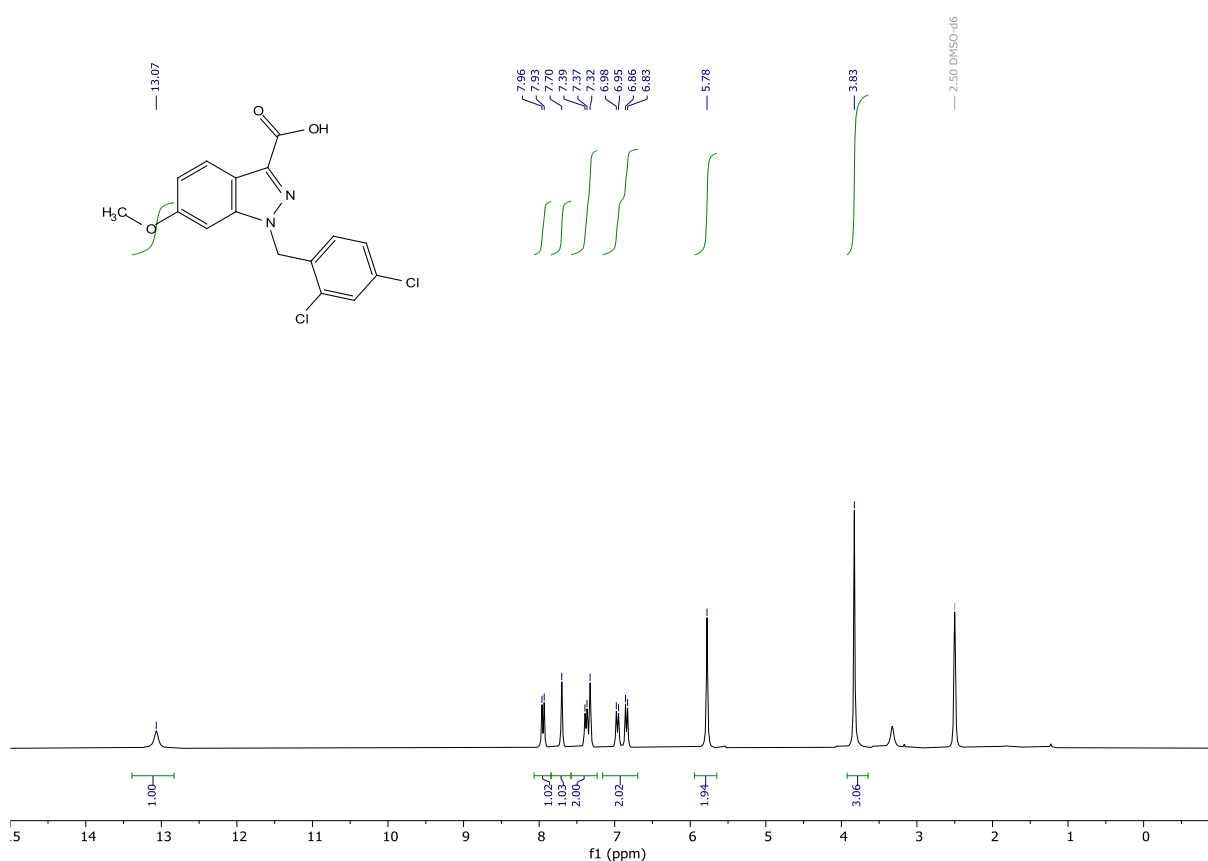


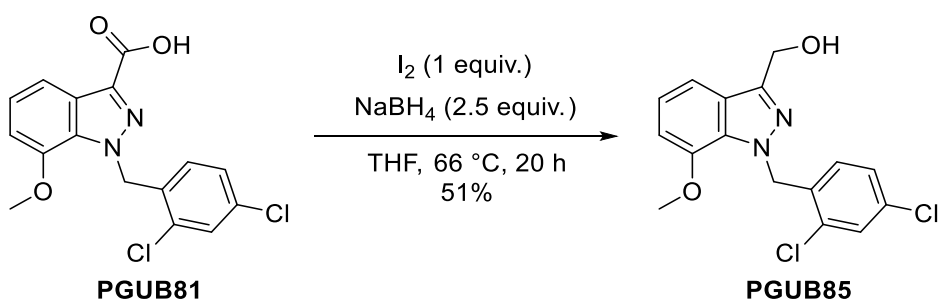
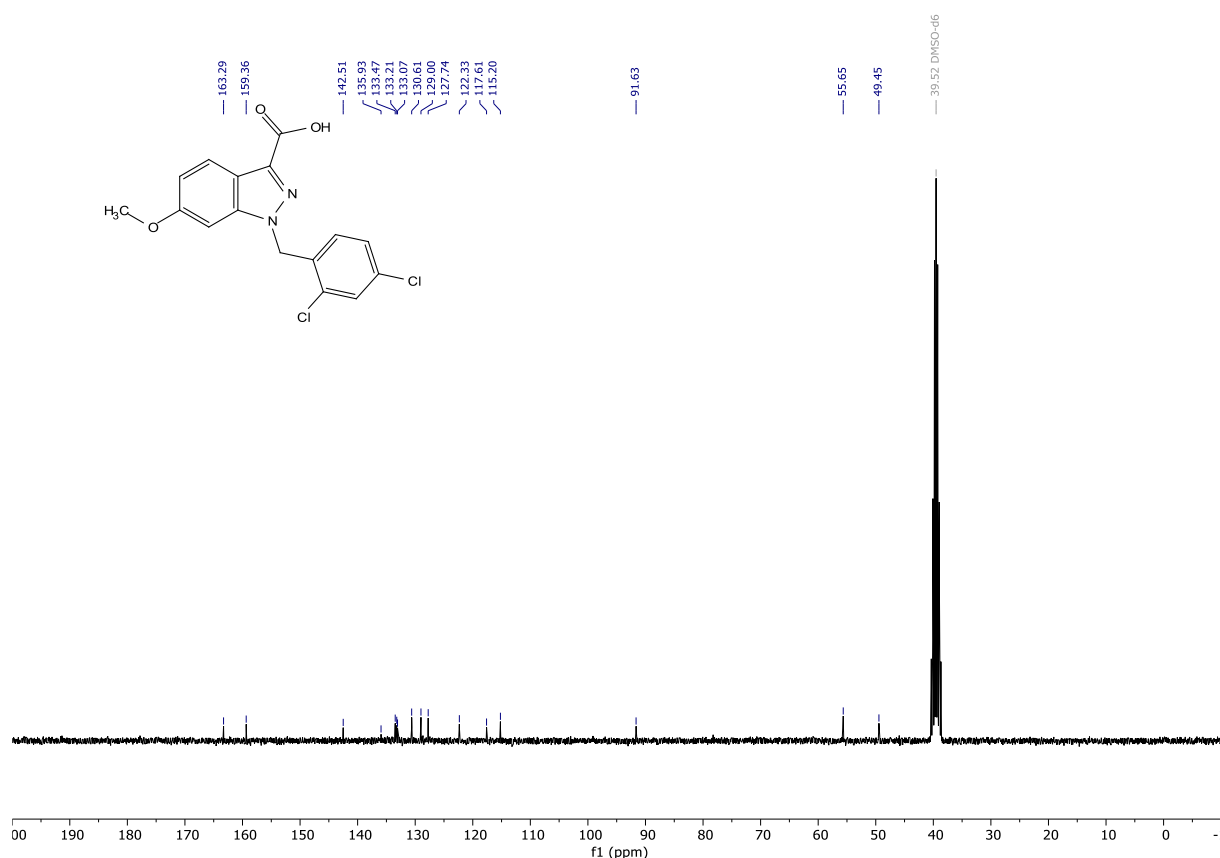
methyl 1-(2,4-dichlorobenzyl)-6-methoxy-1H-indazole-3-carboxylate (PGUB82PREC) (Z = N, Y = OMe). Prepared according to general procedure II methyl 6-methoxy-1H-indazole-3-carboxylate (Z = N, Y = OMe, 0.2464 g, 1.1950 mmol) using 2,4-dichlorobenzyl bromide as alkyl halide, to give the desired product in 84% yield (0.36614 g, 1.0025 mmol). White solid: ^1H NMR (300 MHz, DMSO- d_6) δ 7.95 (d, J = 8.9 Hz, 1H), 7.70 (d, J = 2.1 Hz, 1H), 7.43 – 7.32 (m, 2H), 7.00 (dd, J = 8.9, 2.1 Hz, 1H), 6.87 (d, J = 8.4 Hz, 1H), 5.79 (s, 2H), 3.88 (s, 3H), 3.84 (s, 3H). ^{13}C NMR (75 MHz, DMSO) δ 162.20, 159.49, 142.48, 134.81, 133.31, 133.28, 133.13, 130.69, 129.02, 127.76, 122.05, 117.39, 115.61, 91.75, 55.69, 51.69, 49.57. HRMS (ESI) calculated for $[\text{M}+\text{H}]^+$ $\text{C}_{17}\text{H}_{15}\text{Cl}_2\text{N}_2\text{O}_3$ 365.0454, found 365.0449.





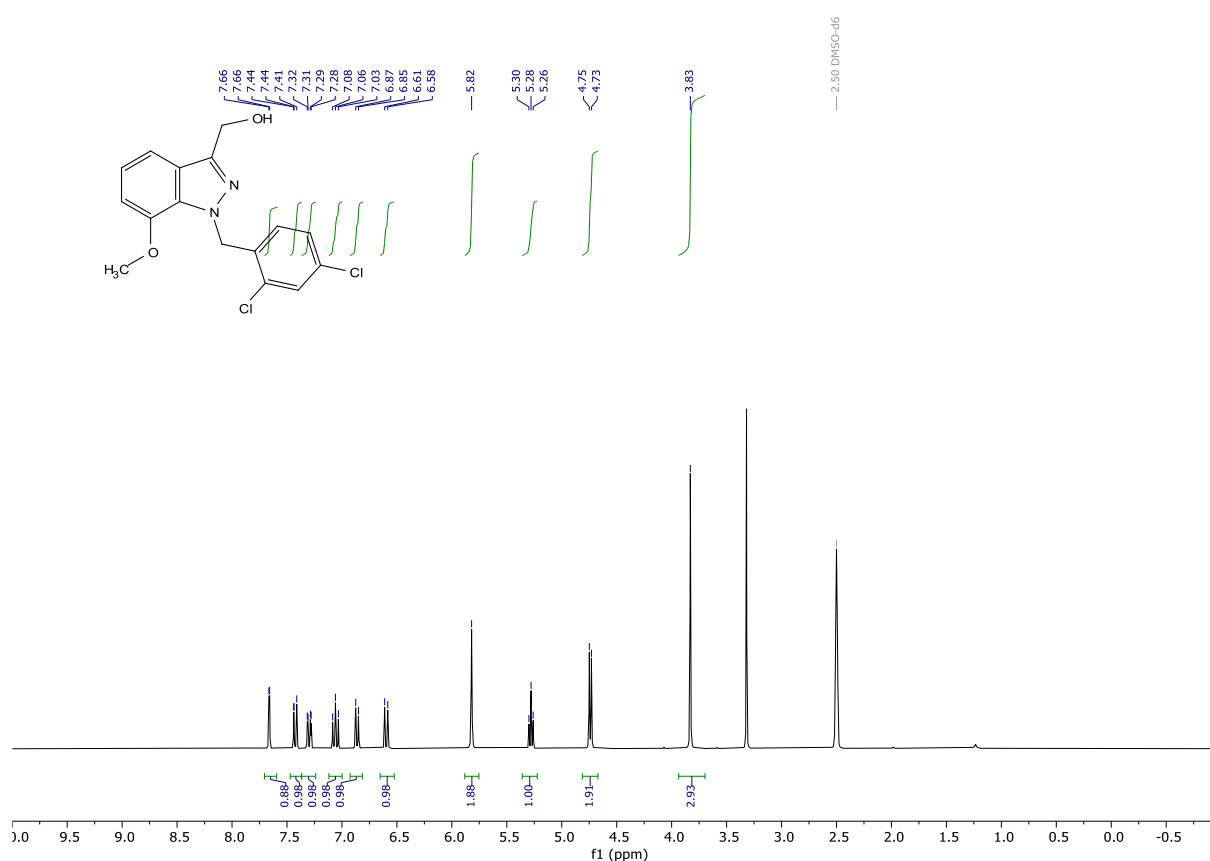
1-(2,4-dichlorobenzyl)-6-methoxy-1H-indazole-3-carboxylic acid (PGUB84) (Z = N, Y = OH). Prepared according to general procedure III from methyl 1-(2,4-dichlorobenzyl)-6-methoxy-1H-indazole-3-carboxylate (PGUB84PREC) (Z = N, Y = OMe, 0.35414 g, 0.9728 mmol), to give the desired product in 85% yield (0.29145 g, 0.829909 mmol). Beige solid: **¹H NMR** (300 MHz, DMSO-*d*₆) δ 13.07 (s, 1H), 7.95 (d, *J* = 8.9 Hz, 1H), 7.70 (s, 1H), 7.58 – 7.23 (m, 2H), 6.90 (dd, *J* = 36.4, 8.5 Hz, 2H), 5.78 (s, 2H), 3.83 (s, 3H). **¹³C NMR** (75 MHz, DMSO) δ 163.29, 159.36, 142.51, 135.93, 133.47, 133.21, 133.07, 130.61, 129.00, 127.74, 122.33, 117.61, 115.20, 91.63, 55.65, 49.45. **HRMS** (ESI) calculated for [M+H]⁺ C₁₆H₁₃Cl₂N₂O₃ 351.0298, found 351.0294. **Purity (HPLC):** >98% UV₂₁₄, >99% UV₂₅₄.

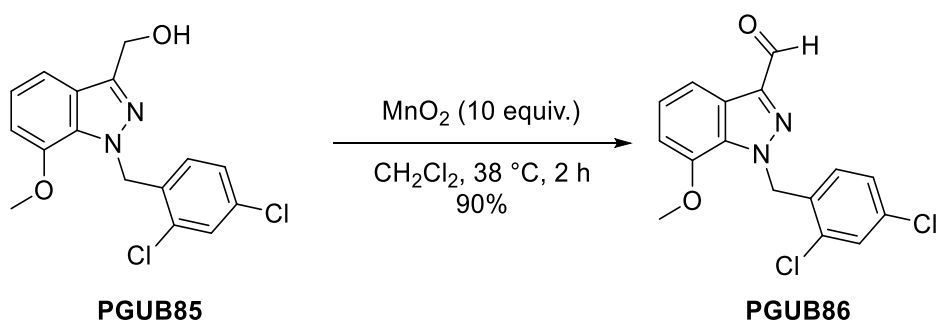
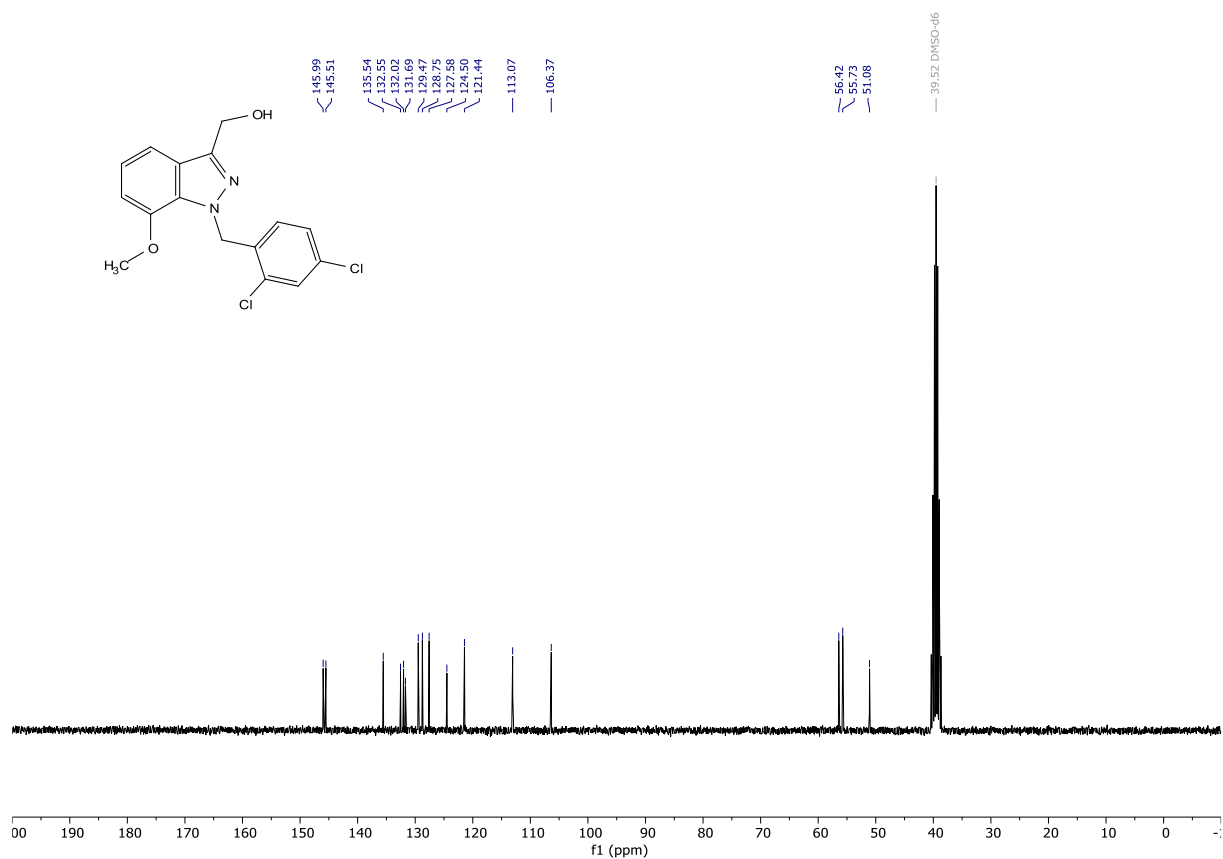




(1-(2,4-dichlorobenzyl)-7-methoxy-1H-indazol-3-yl)methanol (PGUB85). To a stirred 1-(2,4-dichlorobenzyl)-7-methoxy-1H-indazole-3-carboxylic acid (0.76099 g, 3.0296 mmol) in dry THF (15 mL) was added sodium borohydride (0.28917 g, 7.6439 mmol) under an argon atmosphere. The mixture was cooled to 0 °C at which point a solution of iodine (0.768945 g, 3.0296 mmol) in dry THF (10 mL) was slowly added. Then the mixture was heated to 60 °C and stirred for 20 h. Then the mixture was cooled to 22 °C. To the cooled mixture was carefully added methanol until no more bubbling was observed which resulted in a clear solution. This was followed by addition of 1M NaOH (15 mL). The mixture was left stirring at 45 °C for 3 h. The mixture was diluted with brine and ethyl acetate. The aqueous phase was extracted with ethyl acetate. The combined organic phases were washed with brine, dried over MgSO₄, filtered, and concentrated under reduced pressure. The residue was taken up in THF and concentrated onto silica gel. The crude was purified by flash column chromatography (cyclohexane/ ethyl acetate gradient from 1:0 to 1:1), to give the desired product in 51% yield (0.51700

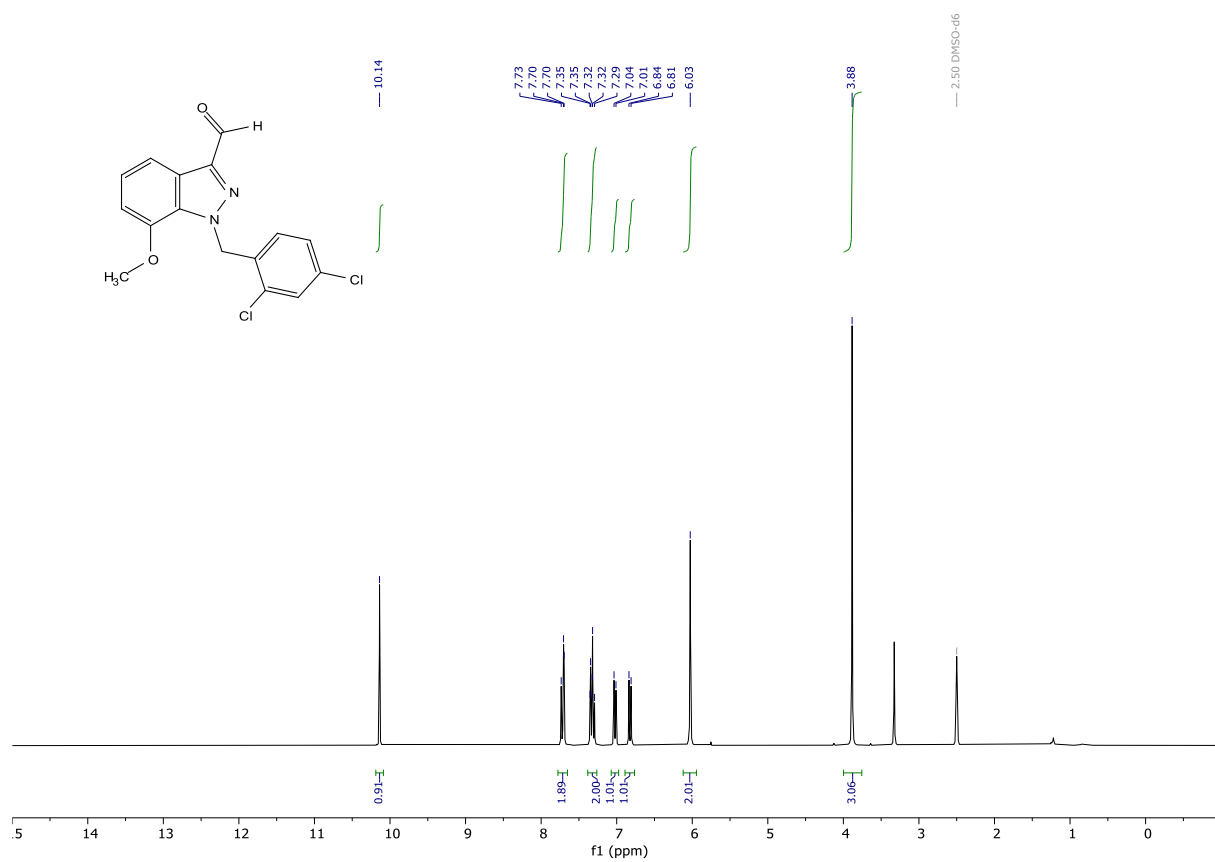
g, 1.53322 mmol). A small sample was recrystallised from cyclohexane/ ethyl acetate and yielded single crystals of suitable quality for x-ray diffraction measurements (CCDC deposition number: 2203151). White solid: **¹H NMR** (300 MHz, DMSO-*d*₆) δ 7.66 (d, *J* = 2.1 Hz, 1H), 7.47 – 7.38 (m, 1H), 7.30 (dd, *J* = 8.4, 2.1 Hz, 1H), 7.06 (t, *J* = 7.8 Hz, 1H), 6.86 (d, *J* = 7.4 Hz, 1H), 6.60 (d, *J* = 8.4 Hz, 1H), 5.82 (s, 2H), 5.28 (t, *J* = 5.8 Hz, 1H), 4.74 (d, *J* = 5.8 Hz, 2H). **¹³C NMR** (75 MHz, DMSO) δ 145.99, 145.51, 135.54, 132.55, 132.02, 131.69, 129.47, 128.75, 127.58, 124.50, 121.44, 113.07, 106.37, 56.42, 55.73, 51.08. **HRMS** (ESI) calculated for [M+H]⁺ C₁₆H₁₅Cl₂N₂O₂ 337.0505, found 337.0501. **Purity (HPLC)**: >90% UV₂₁₄, >96% UV₂₅₄.

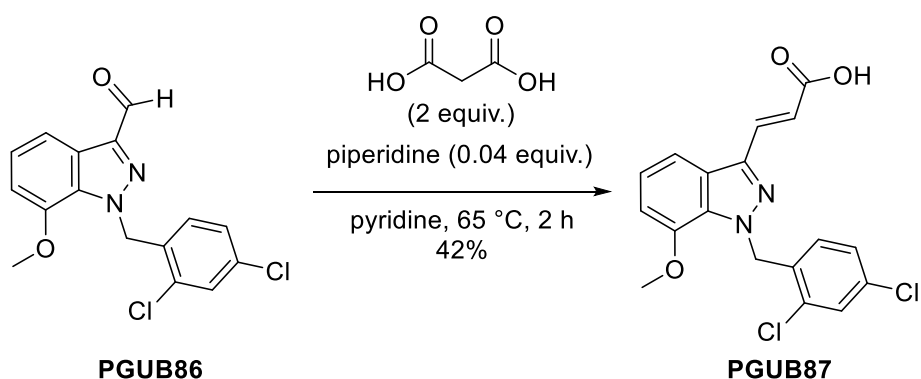
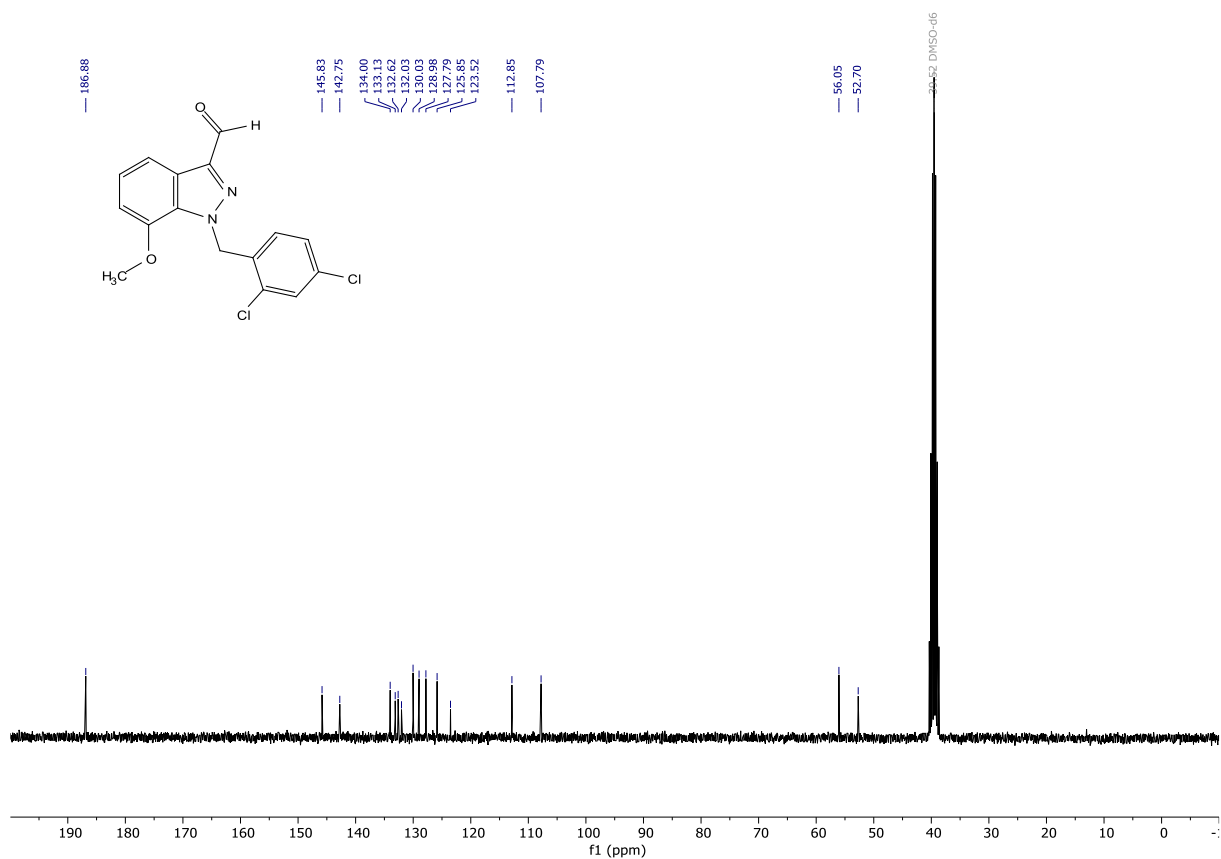




1-(2,4-dichlorobenzyl)-7-methoxy-1H-indazole-3-carbaldehyde (PGUB86). To a stirred solution of (1-(2,4-dichlorobenzyl)-7-methoxy-1H-indazol-3-yl)methanol (0.1318 g, 0.3909 mmol) in dichloromethane (15 mL) was added activated MnO_2 (0.342 g, 3.9337 mmol). The mixture was heated to 38 °C and stirred for 2 h. The mixture was concentrated onto silica gel. The crude was purified by flash column chromatography (cyclohexane/ ethyl acetate gradient from 1:0 to 0:1), to give the desired product in 90% yield (0.46120 g, 1.37596 mmol). A small sample was recrystallised from cyclohexane/ ethyl acetate and yielded single crystals of suitable quality for x-ray diffraction measurements (CCDC deposition number: 2203152). White solid: ^1H NMR (300 MHz, $\text{DMSO}-d_6$) δ 10.14 (s, 1H), 7.78 – 7.65 (m, 2H), 7.38 – 7.26 (m, 2H), 7.02 (d, J = 7.7 Hz, 1H), 6.82 (d, J = 8.4 Hz, 1H), 6.03 (s, 2H), 3.88 (s, 3H). ^{13}C NMR (75 MHz, DMSO) δ 186.88, 145.83, 142.75, 134.00, 133.13, 132.62,

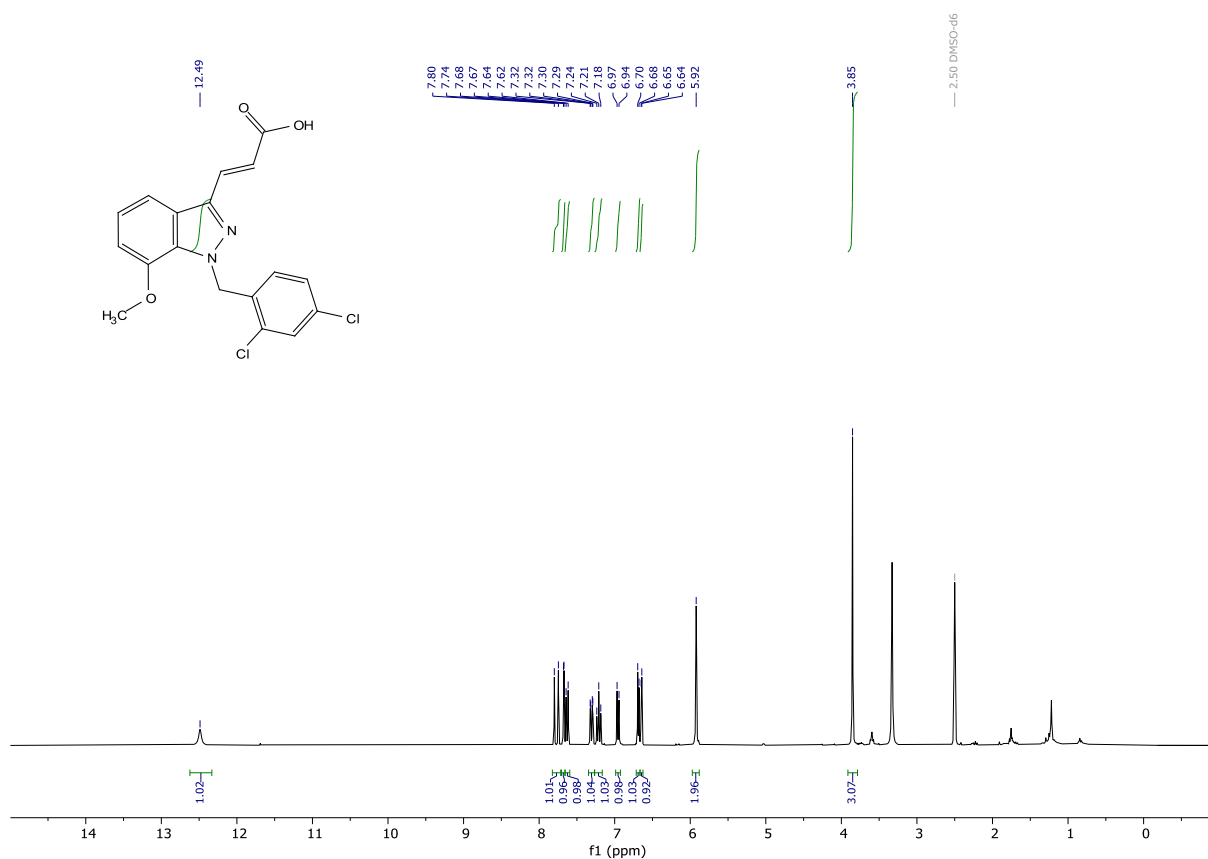
132.03, 130.03, 128.98, 127.79, 125.85, 123.52, 112.85, 107.79, 56.05, 52.70. **HRMS** (ESI) calculated for $[M+H]^+$ $C_{16}H_{13}Cl_2N_2O_2$ 335.0349, found 335.0348. **Purity (HPLC):** >97% UV₂₁₄, >98% UV₂₅₄.

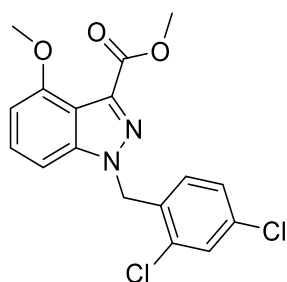
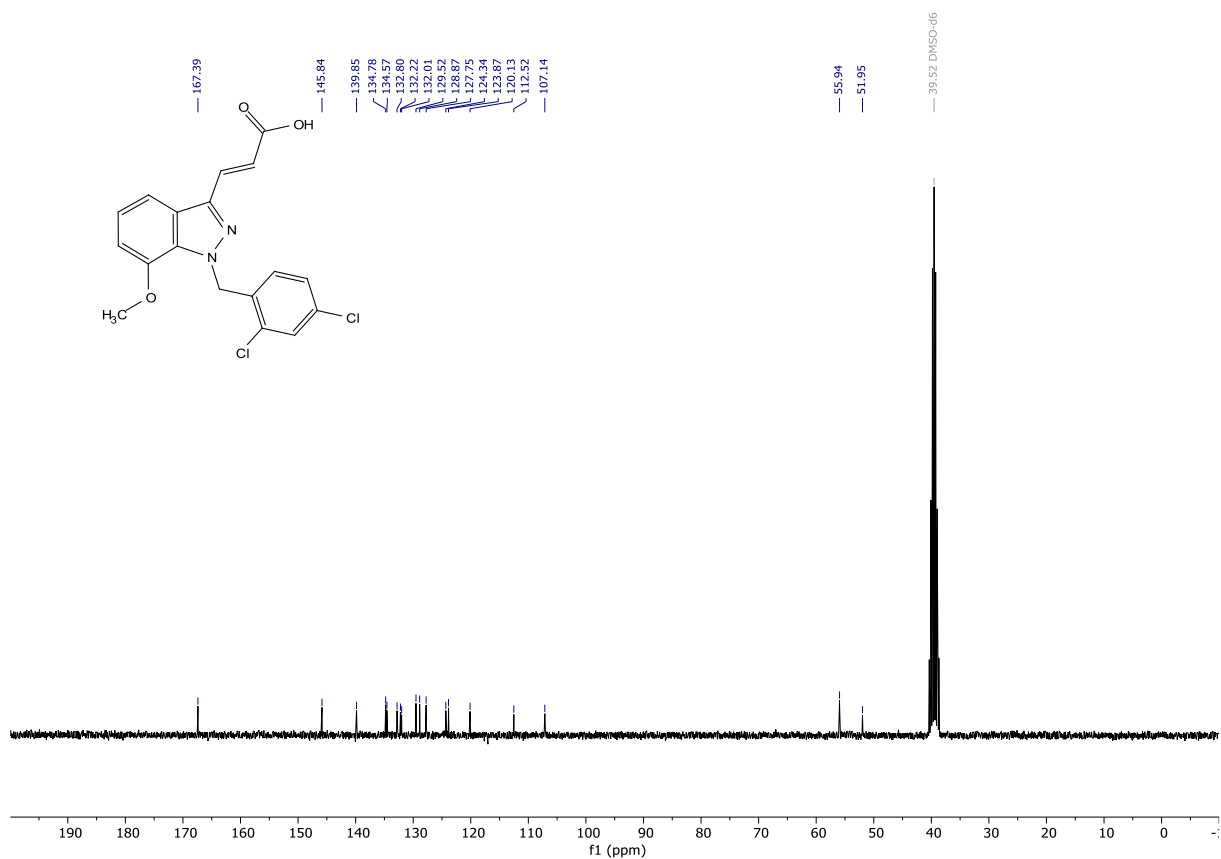




(E)-3-(1-(2,4-dichlorobenzyl)-7-methoxy-1H-indazol-3-yl)acrylic acid (PGUB87). To a stirred solution of 1-(2,4-dichlorobenzyl)-7-methoxy-1H-indazole-3-carbaldehyde (0.09365 g, 0.2794 mmol) in pyridine (2 mL) under an argon atmosphere was added malonic acid (0.05968 g, 0.5735 mmol) followed by piperidine (0.0011 mL, 0.00095 g, 0.0111 mmol). The mixture was heated to 65 °C for 1 h. Then another equivalent malonic acid (0.02388 g, 0.22948 mmol) was added. The mixture was left stirring for 1 h. The pyridine was evaporated under reduced pressure on the high vacuum. The yellow residue was taken up in THF and was acidified with AcOH (1 mL). The mixture was concentrated onto silica gel. The crude was purified flash column chromatography (cyclohexane + 2% AcOH/ ethyl acetate + 2% AcOH gradient from 1:0 to 1:1), to give the desired product in 42% yield (0.04465 g, 0.11837 mmol). A small sample was recrystallised from cyclohexane/ ethyl acetate and yielded single crystals

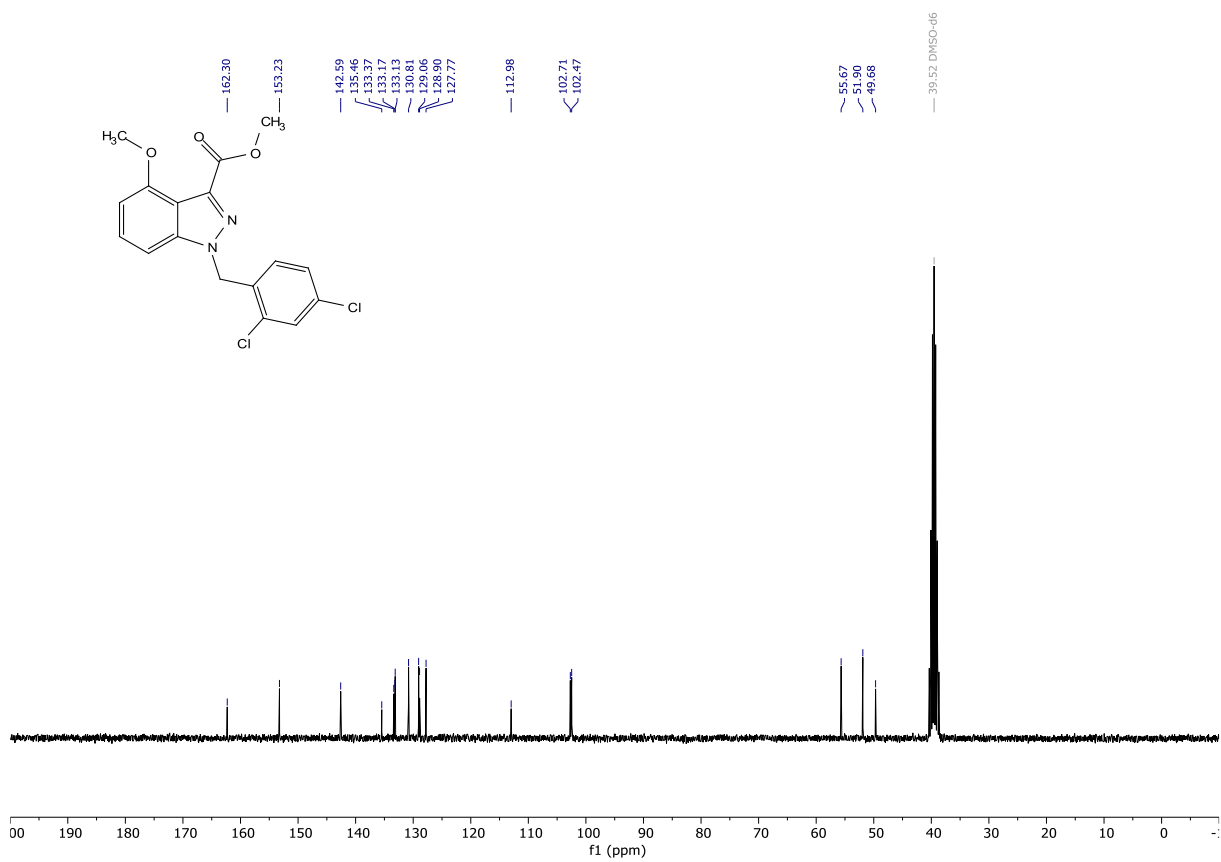
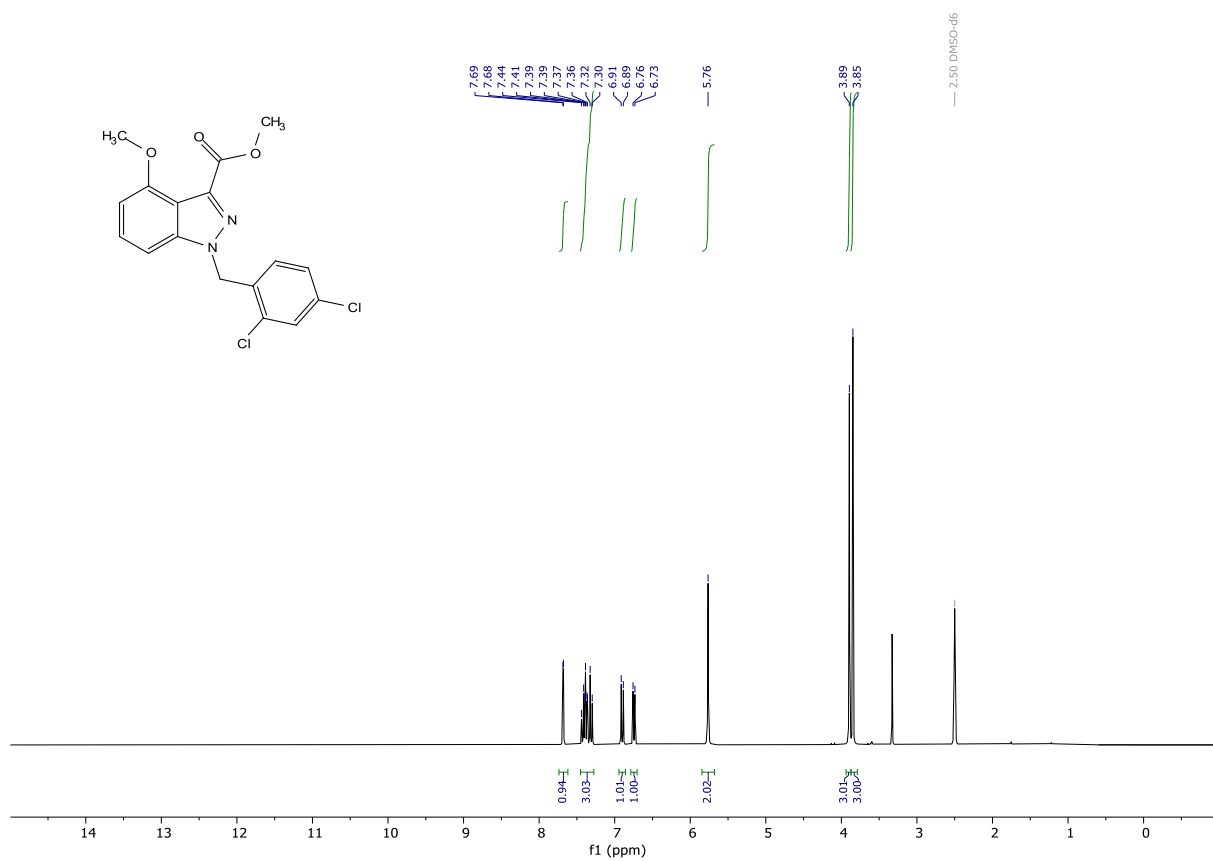
of suitable quality for x-ray diffraction measurements (CCDC deposition number: 2203158). White solid: ^1H NMR (300 MHz, $\text{DMSO-}d_6$) δ 12.49 (s, 1H), 7.77 (d, J = 16.2 Hz, 1H), 7.67 (d, J = 2.1 Hz, 1H), 7.63 (d, J = 8.1 Hz, 1H), 7.31 (dd, J = 8.4, 2.1 Hz, 1H), 7.21 (t, J = 7.9 Hz, 1H), 6.96 (d, J = 7.7 Hz, 1H), 6.69 (d, J = 5.1 Hz, 1H), 6.65 (d, J = 2.7 Hz, 1H), 5.92 (s, 2H), 3.85 (s, 3H). ^{13}C NMR (75 MHz, DMSO) δ 167.39, 145.84, 139.85, 134.78, 134.57, 132.80, 132.22, 132.01, 129.52, 128.87, 127.75, 124.34, 123.87, 120.13, 112.52, 107.14, 55.94, 51.95. HRMS (ESI) calculated for $[\text{M-H}]^-$ $\text{C}_{18}\text{H}_{13}\text{Cl}_2\text{N}_2\text{O}_3$ 375.0309, found 375.0308. Purity (HPLC): >96% UV_{214} , >97% UV_{254} .

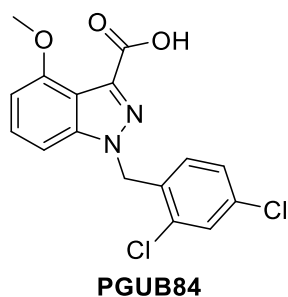




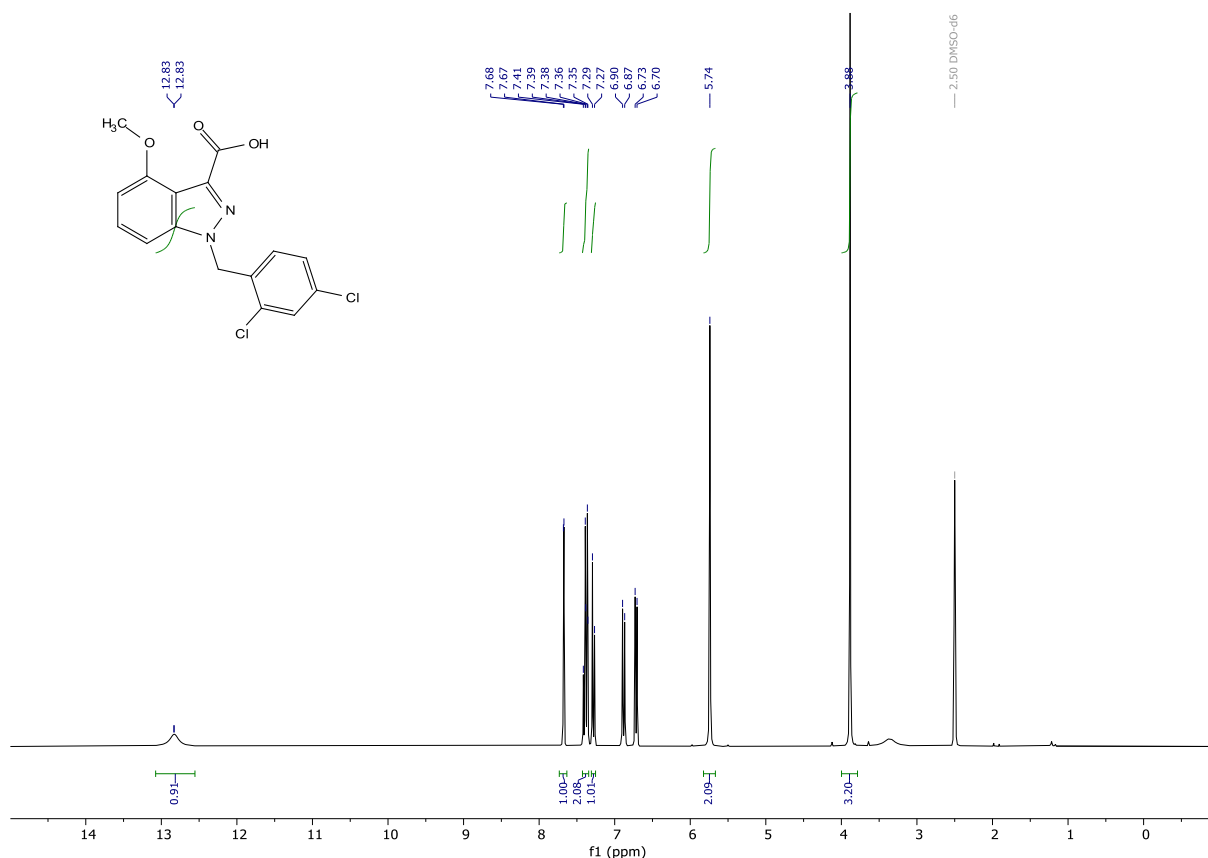
PGUB88PREC

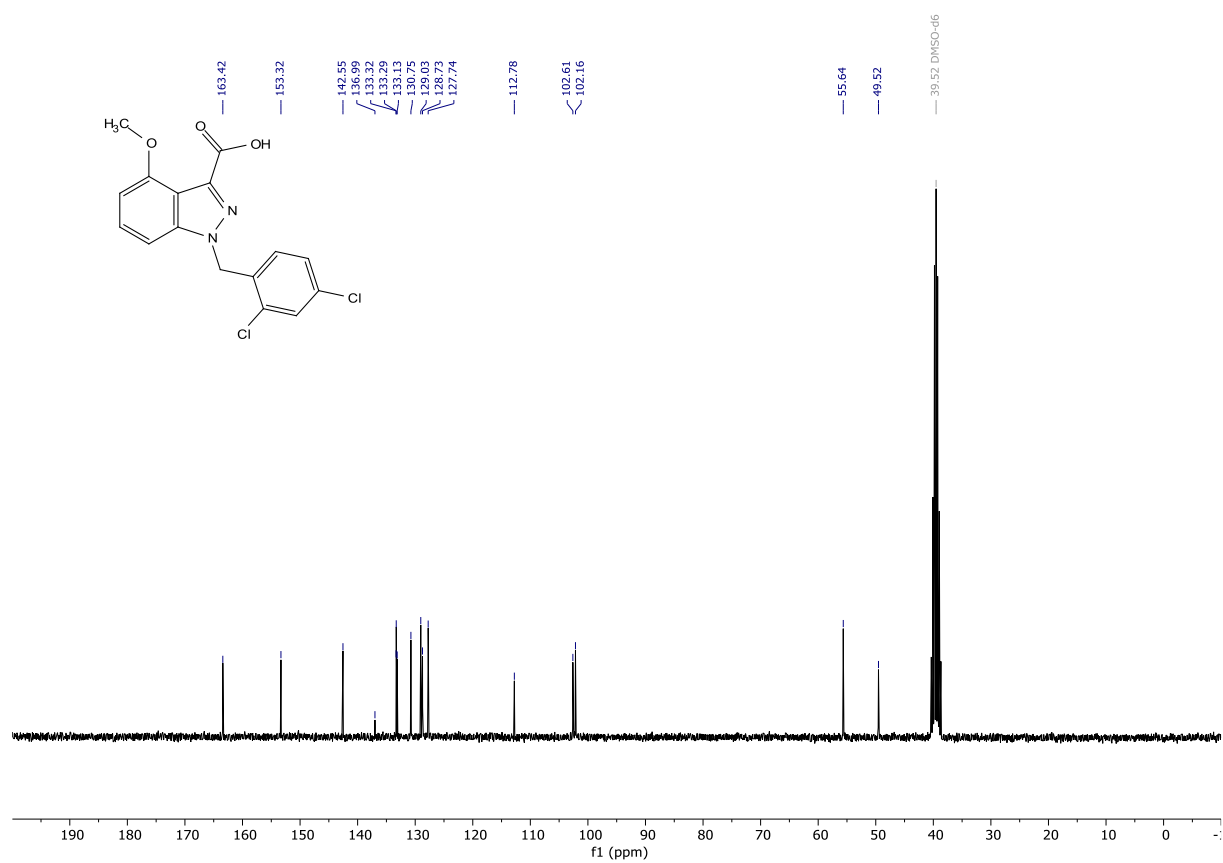
methyl 1-(2,4-dichlorobenzyl)-4-methoxy-1H-indazole-3-carboxylate (PGUB88PREC) (Z = N, Y = OMe). Prepared according to general procedure II methyl 4-methoxy-1H-indazole-3-carboxylate (Z = N, Y = OMe, 0.2504 g, 1.2143 mmol) using 2,4-dichlorobenzyl bromide as alkyl halide, to give the desired product in 90% yield (0.39992 g, 1.09504 mmol). White solid: ^1H NMR (300 MHz, DMSO- d_6) δ 7.68 (d, J = 2.1 Hz, 1H), 7.45 – 7.28 (m, 3H), 6.90 (d, J = 8.4 Hz, 1H), 6.74 (d, J = 7.5 Hz, 1H), 5.76 (s, 2H), 3.89 (s, 3H), 3.85 (s, 3H). ^{13}C NMR (75 MHz, DMSO) δ 162.30, 153.23, 142.59, 135.46, 133.37, 133.17, 133.13, 130.81, 129.06, 128.90, 127.77, 112.98, 102.71, 102.47, 55.67, 51.90, 49.68. HRMS (ESI) calculated for $[\text{M}+\text{H}]^+$ $\text{C}_{17}\text{H}_{15}\text{Cl}_2\text{N}_2\text{O}_3$ 365.0454, found 365.0458.





1-(2,4-dichlorobenzyl)-4-methoxy-1H-indazole-3-carboxylic acid (PGUB88) (Z = N, Y = OH). Prepared according to general procedure III from methyl 1-(2,4-dichlorobenzyl)-4-methoxy-1H-indazole-3-carboxylate (PGUB88PREC) (Z = N, Y = OMe, 0.37882 g, 1.0373 mmol), to give the desired product in quantitative yield (0.40030 g, 1.0399 mmol). White solid: $^1\text{H NMR}$ (300 MHz, DMSO- d_6) δ 13.08 – 12.56 (m, 1H), 7.68 (d, J = 2.1 Hz, 1H), 7.43 – 7.34 (m, 2H), 7.28 (d, J = 8.3 Hz, 1H), 5.74 (s, 2H), 3.88 (s, 3H). $^{13}\text{C NMR}$ (75 MHz, DMSO) δ 163.42, 153.32, 142.55, 136.99, 133.32, 133.29, 133.13, 130.75, 129.03, 128.73, 127.74, 112.78, 102.61, 102.16, 55.64, 49.52. **HRMS** (ESI) calculated for $[\text{M-H}]^-$ $\text{C}_{16}\text{H}_{11}\text{Cl}_2\text{N}_2\text{O}_3$ 349.0152, found 349.0163. **Purity (HPLC):** >99% UV_{214} , >98% UV_{254} .





3. Development of various molecular tools

3.1. New compounds against *Echinococcus multilocularis*

Introduction

Echinococcus multilocularis (*E. multilocularis*), which is also known as the fox tapeworm, is an endoparasite. The parasite's definite host are canids, and its intermediate hosts are small rodents. Humans can accidentally become host when eggs released by the worm are ingested. The disease caused by *E. multilocularis* is called alveolar echinococcosis and it is lethal when left untreated. The disease-causing stage of the parasite is the metacestode. The organ most affected in humans is the liver. However, at later stages of the disease the parasite can metastasise into other organs. Symptoms of alveolar echinococcosis can be similar to hepatic cancer due to the growth of the metacestode in the liver. Common symptoms are hepatomegaly cholestatic jaundice and portal hypertension.⁸⁶ Patients suffering from alveolar echinococcosis have only few treatment options. Radical surgery is the best option, but often the entire parasitic mass cannot be removed, which leaves patients only with the option of drug treatment. This is done with benzimidazole derived drugs such as albendazole or mebendazole (**Figure 28**). Benzimidazoles can have severe side effects in some patients and usually only act as a parasitostatic.⁸⁷ Thus, patients have to take the drugs for the rest of their life to prevent regrowth of the parasite.⁸⁶ Alveolar echinococcosis is a disease endemic in the northern hemisphere, including central Europe. There are also reported cases all around the northern hemisphere and especially in central Asia and eastern Russia. However, in the southern hemisphere no case of *E. multilocularis* infection have been reported neither in humans nor in animals.⁸⁸ A few decades ago, a diagnosis with alveolar echinococcosis was equal to a death sentence for the patients. The discovery of the benzimidazoles albendazole and mebendazole and progress in surgery changed this in the 1970s.^{89, 90} Benzimidazoles interact with β -tubulin, inhibiting microtubule polymerisation.⁹¹ Albendazole binds with a 100 to 1000 times higher affinity to helminth β -tubulin compared to mammalian β -tubulin.^{87, 92} It was also speculated that other, yet unidentified targets, besides microtubules can be affected by benzimidazoles.⁹³ The benzimidazole compounds are able to prolong the survival rate of the host either as single treatment or in combination with surgical removal of affected liver tissue. However, treatment with these compounds is mostly parasitostatic. Development and assessment of new chemotherapeutics is difficult also because of the ethical issues regarding randomised double-blind studies.⁹⁰ Both albendazole as well as mebendazole are administered orally. For albendazole the recommended dosage is around 10-15 mg/ kg/ day (800-1200 mg/ day for an 80 kg individual), and it should be split into two doses that are ingested together with a fat-rich meal to increase its bioavailability. For mebendazole the recommended dosage is

around 40-50 mg/ kg/ day (3200-4000 mg for an 80 kg individual) divided into three doses.⁹⁴ Adverse effects of chemotherapeutic treatment with benzimidazoles can be hepatotoxicity, leukopenia, thrombocytopenia and alopecia.^{94, 95}

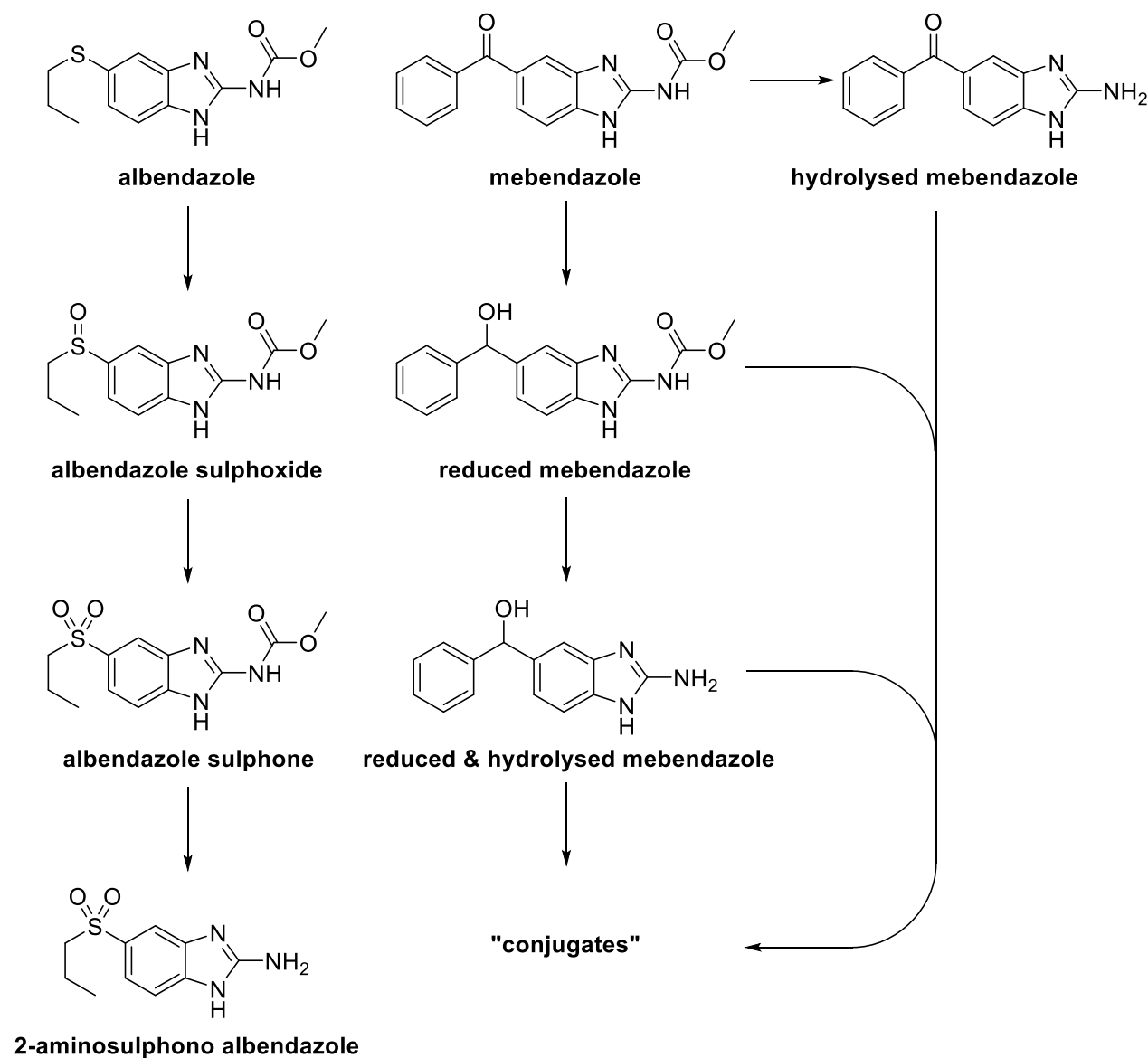


Figure 28 Metabolism of benzimidazole drugs albendazole and mebendazole

The main metabolic pathway of albendazole is the oxidation to albendazole sulfoxide followed by oxidation to the sulfone and finally hydrolysis of the carbamate to the free amine. The plasma profile of albendazole is dominated by albendazole sulfoxide and the sulfone derivatives and these are also the main metabolites found in urine. Albendazole itself was only detected in trace amounts.⁹⁶ Albendazole sulfoxide itself is also an active antihelminthic which is convenient as albendazole gets almost completely metabolised into the sulfoxide before reaching the systemic circulation.⁹⁵ For mebendazole the metabolic pathways are not as straightforward as for albendazole. Reduction of the

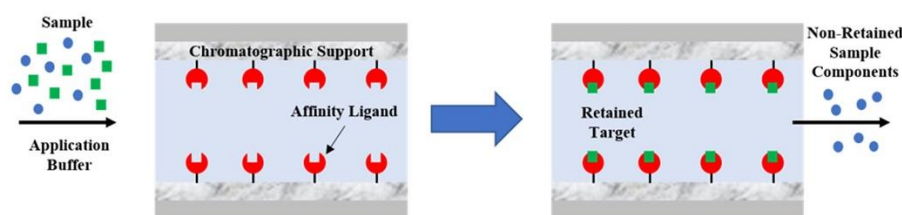
carbonyl species to an alcohol can take place, or hydrolysis of the carbamate resulting in a free amine, a pathway similar to the albendazole metabolism. Mebendazole metabolites end up as sulfate conjugates or glucuronides. These metabolites are mainly excreted in the faeces.⁹⁶

Affinity chromatography

Affinity chromatography in principle works by immobilising a biologically related agent as the stationary phase. The technique is commonly used for isolation and purification of specific targets by using the selective and reversible binding that occurs in various biological interactions. Commonly appearing interactions can be antibody/ antigen, enzyme/ substrate, or hormone/ receptor. In affinity chromatography one member of these pairs is immobilised onto a chromatographic support. The immobilised member then is called affinity ligand and should retain selectively toward its complementary partner, even when the partner is in a complex mixture, such as a whole cell lysate.⁹⁷

Figure 29 (a) depicts a common way in which affinity chromatography is used. A complex mixture is washed through a column of immobilised affinity ligand. The target is binding to the ligand and is retained, whereas the unwanted cell components get flushed through the column with no or little interaction. In this retained state the column can be washed with different eluents to remove most of the unwanted solutes. Usually, the conditions are chosen in such a way (i.e., composition of mobile phase) that the affinity ligand can form the strongest bond to the target. Among other possible variables, the pH and the ionic strength can be changed. **Figure 29 (b)** Shows possible elution methods. As mentioned above, changes in pH and ionic strength can vary the binding strength between the two partners. To elute the target from the column this principle can be exploited by changing the composition of the mobile phase. Another possibility to elute the target is to add a soluble ligand that binds more strongly to the same specific location of the target, effectively removing the target from the solid supported affinity ligand. A drawback of this method can be that the target is then strongly bound to its soluble ligand. The reversal of this principle can also be applied by using an agent that competes with the target for the binding site of the immobilised affinity ligand displacing the target. A drawback of this method can be that the competing agent elutes together with the target from the column.

(a) Application of Target and Sample onto Affinity Column



(b) Methods for Elution of Retained Target

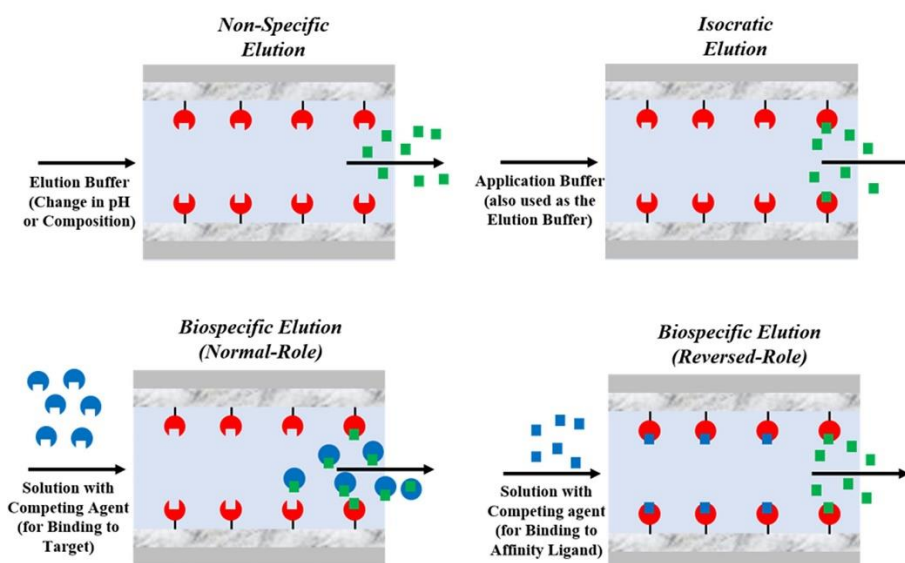


Figure 29 The (a) sample application/washing steps and (b) examples of elution methods that are used in the on/off mode of affinity chromatography. The three types of elution shown in (b) are non-specific elution, isocratic elution, and biospecific elution. Methods for biospecific elution can be further divided into normal-role elution, in which a competing agent binds to the target, and reversed-role elution, in which the competing agent binds to the immobilized affinity ligand.⁹⁷

Many different materials and matrices can be used as solid support for the columns. Often Agarose and cellulose are used, but also modified silica and synthetic polymers such as polystyrene were successfully employed.⁹⁷ Affinity ligand modified solid supports can be generated from various reactive motifs. Commonly used reactive solid support residues are amines, alcohols, and thiols. The respective counterparts can be NHS-esters (or other forms of amine reactive groups), maleimides, ketones and subsequent reductive amination, or any other reaction with a coupling agent that is orthogonal to the chemistry of the ligand and the solid support. Sometimes cleavable linkers can also be incorporated, between the solid support and the affinity ligand, allowing for removal of the target bound to the affinity ligand without the need for an alteration of the mobile phase.

Threonine dehydrogenase inhibitors

Alexander et al. published a study in *Proceedings of the National Academy of Sciences of the United States of America*,⁹⁸ where they tested approximately 200,000 drug-like synthetic chemicals in a high-throughput screen on purified, engineered mouse threonine dehydrogenase (TDH) enzyme. The protein modification was required as the full-length protein was insoluble. This problem was bypassed by deletion of 39 amino acids from the amino terminus, enabling them to produce milligram quantities of very high purity that was soluble.⁹⁸ TDH converts the co-substrate NAD^+ to NADH in presence of threonine. The conversion of NAD^+ to NADH results in an increased absorbance at 340 nm, which can be easily monitored photometrically.⁹⁸ TDH converts L-threonine to 2-amino-3-ketobutyrate which can then be further converted into glycine, catalysed by ketobutyrate CoA ligase (KBL), or undergo decarboxylation to aminoacetone (**Figure 30**).⁹⁹

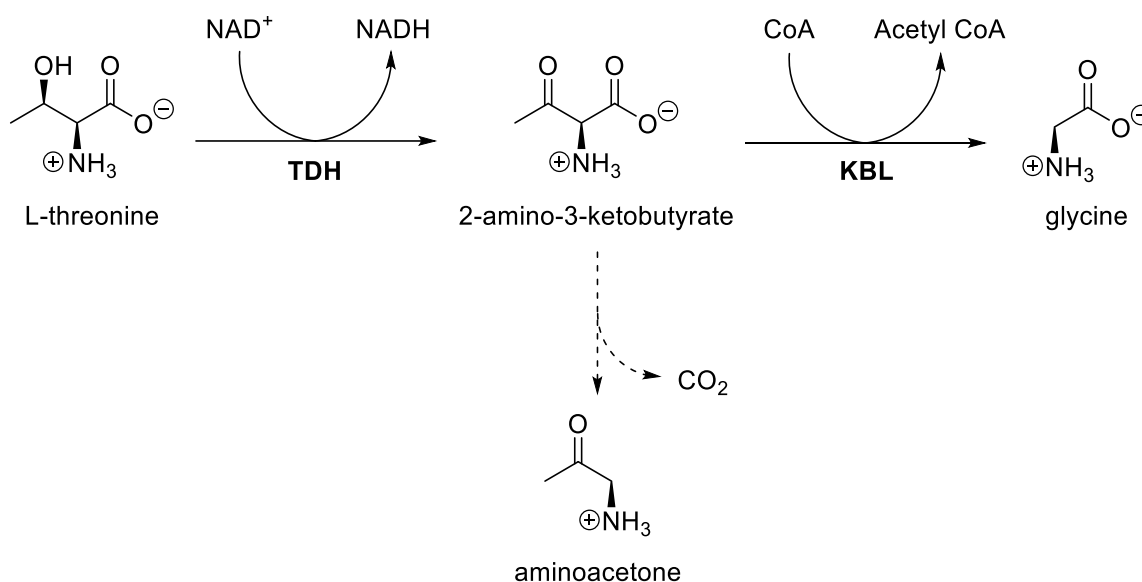


Figure 30 Conversion of L-threonine to 2-amino-3-ketobutyrate and following reactions⁹⁹

From the 200,000 structures evaluated in the high-throughput screen six compounds that were closely related were chosen for further study due to the promising activity found. The structures of these six quinazolinecarboxamide (Qc) compounds are shown in (**Figure 31**). Mouse embryonic stem cells exist in a state of high dependency from threonine and also the quantification of messenger RNA revealed unusually high expression of the TDH encoding gene.¹⁰⁰ Therefore, inhibition of TDH induced a form of cellular autophagy that led to cell death specifically in mouse embryonic stem cells. To check for off target toxicity, they assessed the identified six Qc compounds on human cancer cells (HeLa) and 3T3 fibroblasts which do not express TDH. It was found that the Qc compounds did not inhibit proliferation of the HeLa and 3T3 cells at 10 μM , a concentration that was sufficient to inhibit the proliferation of mouse embryonic stem cells.⁹⁸

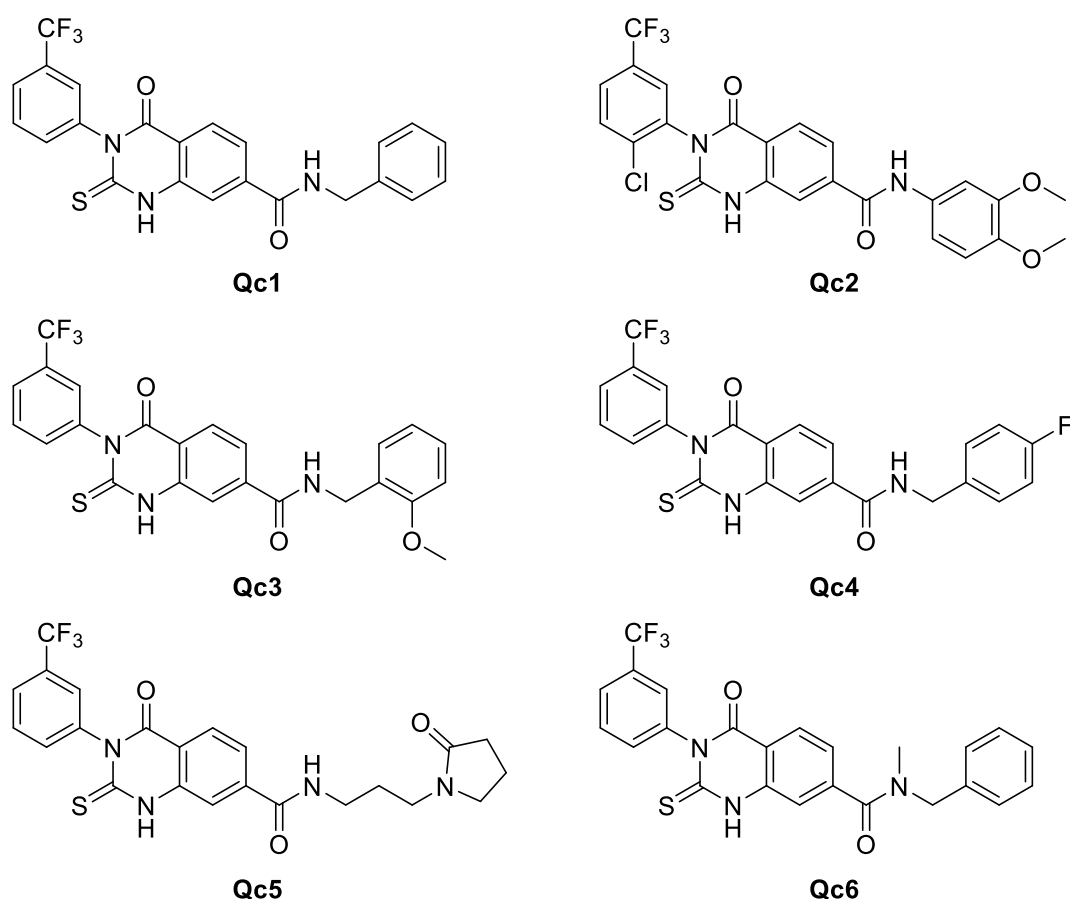


Figure 31 Inhibitors of the threonine dehydrogenase⁹⁸

By thorough investigation using ¹H-NMR, HPLC and enzymatic assays, Ritler et al. could show in 2019 that *E. multilocularis* metacystodes consume mostly glucose and threonine from the culture medium. They also found that the *E. multilocularis* metacystodes only excrete traces of aspartate, glutamate and glycine into the medium,¹⁰¹ correlating with the results of another study, which found transcriptomic information on the synthesis pathways of all amino acids, except alanine, aspartate, glutamate and glycine.¹⁰² Interestingly, threonine was not found to be heavily used for protein synthesis. Thus, they speculated that threonine is used for the synthesis of acetyl-CoA and glycine (as shown in **Figure 30**) and therefore subsequently for purine synthesis, DNA-replication and energy generation.¹⁰¹ Therefore, *E. multilocularis* TDH (EmTDH) was proposed as new target to kill off the parasite.

Aim of this work

Solid supported albendazole

The aim of this work was to generate compounds derived from albendazole and/or mebendazole that are suitable for conjugation to a solid support. This construct could then be used for an affinity column to purify proteins of *E. multilocularis* and specially to obtain the targets that the benzimidazoles are binding, as there are most likely other mechanisms than just binding to tubulin as mode of action for the benzimidazole compounds.

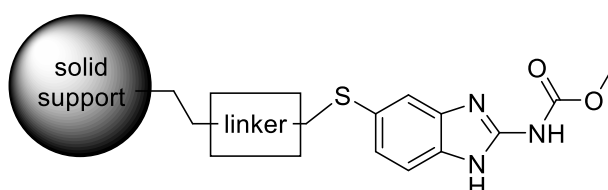


Figure 32 Solid supported albendazole

TDH inhibitors

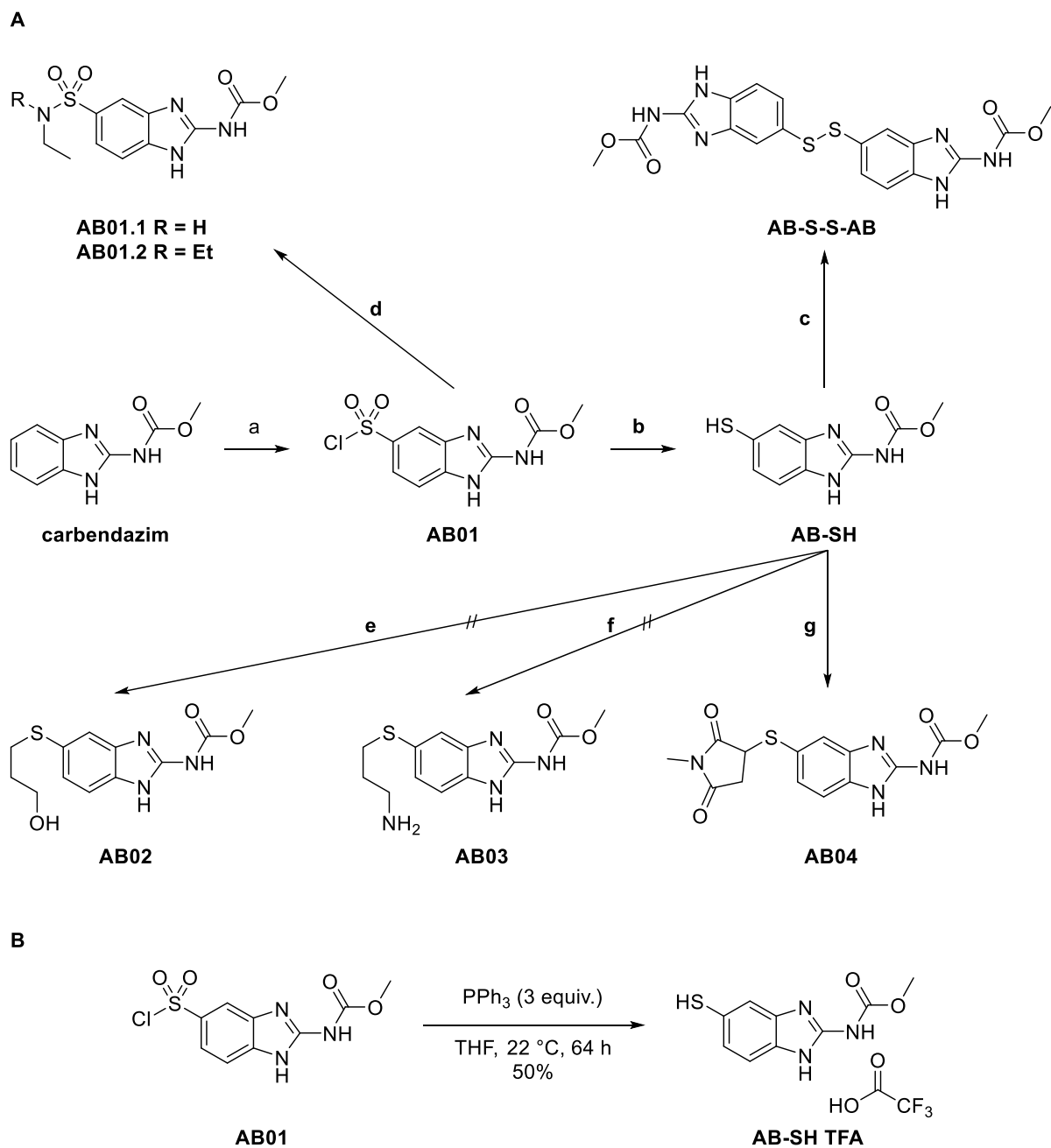
The second aim was to elaborate a synthetic route to efficiently generate the Qc compounds found by Alexander et al.⁹⁸, as synthesis information for these compounds was neither published nor available in chemical reaction databases (Sci-Finder and Reaxys). The synthesised Qc compounds should then be tested as suggested in the study by Ritler et al.¹⁰¹, i.e. the testing should be carried out on metacestodes as well as on purified recombinant *E. multilocularis* TDH.

Results

Solid supported albendazole

For the **solid supported albendazole**, the idea was to first start with the synthesis of compounds that could be reacted to a solid support at a later stage but form stable intermediates that can be tested and assessed for their qualities as antihelmintics. The synthesis of albendazole derivatives started from cheap, commercially available carbendazim. This was sulfonylated with chlorosulfonic acid to give carbendazim sulfonyl chloride (**AB01**, **Scheme 10, A**). From this intermediate, dialkyl sulfonamides (**AB01.1**, **AB01.2**, **Scheme 10, A**) were easily obtained by reaction with the corresponding dialkylamines. The reaction of the sulfonyl chloride with an amine to yield a sulfonamide can potentially be used to couple **AB01** to an amine-modified solid support. **AB01.2** is structurally like albendazole's propyl moiety in respect of the length of the alkyl chain. Reduction of the sulfonyl chloride intermediate generated a thiol (**AB-SH**) that was isolated after many failed attempts, where oxidation to the disulfide (**AB-S-S-AB**, **Scheme 10, A**) or degradation of the product was observed. Reduction, work-up and purification conditions were optimised to reliably generate the desired thiol (**AB-SH**, **Scheme 10, A & B**), stabilised by trifluoroacetic acid to prevent subsequent reaction or decomposition of the thiol into undesired products such as the disulfide bridged dimer (**AB-S-S-AB**, **Scheme 10, A**). The best reaction condition out of 24 attempts is shown in **Scheme 10, B** some examples of less successful attempts are given in **Table 15**. Entry 1 was following a protocol found in a Chinese patent using iron as reducing agent.¹⁰³ This reduction procedure was unsuccessful in our hands. In entry 2 reduction using zinc as electron donor was attempted, following a literature procedure for similar arylthiols¹⁰⁴, resulting in traces of the desired compound. In entry 3, a published general procedure for synthesis of arylthiols¹⁰⁵ was adapted, using triphenylphosphine in DMF. In entry 4, similar conditions in toluene were tested and although trace formation of the product was observed, no desired product could be isolated. The experiment was repeated in entry 5 and the reaction was worked up by directly concentrating it, which resulted in undesired formation of dimer compound **AB-S-S-AB**. Similar conditions were tried using THF as solvent in entry 6. This successfully produced a small amount of the desired compound, which was then isolated by reverse phase column chromatography as trifluoroacetate salt **AB-SH TFA**. In entry 7, triphenylphosphine was replaced by tris-(2-carboxyethyl)-phosphine (TCEP). Using this substitution and water as solvent, no product formation was observed. However, when the previously formed dimer **AB-S-S-AB** of entry 5 was treated with TCEP, cleavage of the disulfide bridge and formation of the desired product was observed as shown in entry 8. The reaction conditions from entry 6 were applied to generate the material used for the subsequent reactions shown in **Scheme 10, A**. From thiol **AB-SH**, alcohol (**AB02**, **Scheme 10, A**), amine (**AB03**, **Scheme 10, A**) and maleimide conjugate (**AB04**, **Scheme 10, A**) were successfully

generated by alkylation or conjugation, isolated and characterised. Alcohol **AB02** was obtained by reaction of the free thiol with (2-bromoethoxy)(*tert*-butyl)dimethylsilane followed by deprotection with tetrabutylammonium fluoride (TBAF) resulting in the free alcohol. Similarly, the amino derivative was obtained by alkylation of the thiol with *tert*-butyl 2-bromoethylcarbamate. The amine was then deprotected using trifluoroacetic acid resulting in the amine **AB03**. Both alcohol **AB02** as well as amine **AB03** can be coupled to a solid support with the respective reactivity. Reaction of the free thiol with *N*-methylmaleimide resulted in thioether compound **AB04**. This reaction represents a generic coupling reaction of thiols to a maleimide modified solid support.



Scheme 10 A) Synthesis of AB-SH and its derivatives: **a)** chlorosulfonic acid, 22 °C, 1.5 h **b)** see Table 15 entry 6 **c)** see Table 15 entry 5 **d)** amine neat, 22 °C, 0.5-16 h **e)** 1) 2-bromoethoxy)(*tert*-butyl)dimethylsilane, K₂CO₃, DMF, 25 °C, 3 h 2) TBAF, 25 °C, 16 h **f)** 1) 2-(Boc-amino)ethyl bromide, DMF; 25 °C, 1 h 2) CH₂Cl₂/TFA 10:1, 21 °C, 1 h **g)** *N*-Methylmaleimide, K₂CO₃, DMF, 25 °C, 0.5 h **B)** Best reaction conditions for the reduction of the sulfonyl chloride to the thiol

Entry	Reducing agent	Additive	Solvent	Temperature	Time	Purification	Yield
1	Fe (3 equiv.)	H ₂ SO ₄ (3 equiv.)	H ₂ O	22 °C	16 h	- ^a	np
2	Zn (3.5 equiv.)	DMA (3 equiv.) SiMe ₂ Cl ₂ (3 equiv.)	DCE	75 °C	16 h	- ^a	traces
3	PPh ₃ (3 equiv.)	-	DMF	rt	16 h	- ^a	np
4	PPh ₃ (3 equiv.)	-	Toluene	rt	16 h	- ^a	traces
5	PPh ₃ (3 equiv.)	-	Toluene	rt	16 h	dc	62% ^b
6	PPh₃ (3 equiv.)	-	THF	rt	64 h	rpcc	50%
7	TCEP (3 equiv.)	-	H ₂ O	rt	16 h	- ^a	np
8 ^c	TCEP (3 equiv.)	-	H ₂ O	rt	16 h	rpcc	21%

Table 15 Selected entries for sulfonyl chloride reduction **dc**) direct concentration **rpcc**) reverse phase column chromatography **np**) no product **a**) no purification was done as no product formation was observed **b**) product was the disulfide bridged **AB-S-S-AB** **c**) reduction starting from **AB-S-S-AB**

The compounds were transferred to the group of Britta Lundström-Stadelmann at the Institute of Parasitology in the Vetsuisse Faculty at the University of Bern, where they were evaluated in a PGI-assay, in which the phosphoglucose isomerase (PGI) of *E. multilocularis* (EmPGI) is used as marker for metacystode vesicle damage *in vitro*. The enzyme EmPGI is part of the glycolysis pathway where it converts D-fructose-6-phosphate to D-glucose-6-phosphate. This activity and the fact that the enzyme is normally found in the vesicle fluid of metacystodes are exploited for this assay. When the vesicles rupture, the enzyme is released into the supernatant. The presence of the EmPGI is measured indirectly by adding its substrate D-fructose-6-phosphate to the supernatant which gets converted to D-glucose-6-phosphate. The D-glucose-6-phosphate then is transformed into 6-phosphogluconolactone by the enzyme glucose-6-phosphate dehydrogenase which uses nicotinamide adenine dinucleotide (NAD⁺) as a co-factor. The NAD⁺ is converted into NADH of which the absorption at 340 nm light can be measured by a spectrophotometer (Figure 33). The obtained values can then be employed to calculate the abundance of EmPGI in the supernatant.^{87, 106, 107}

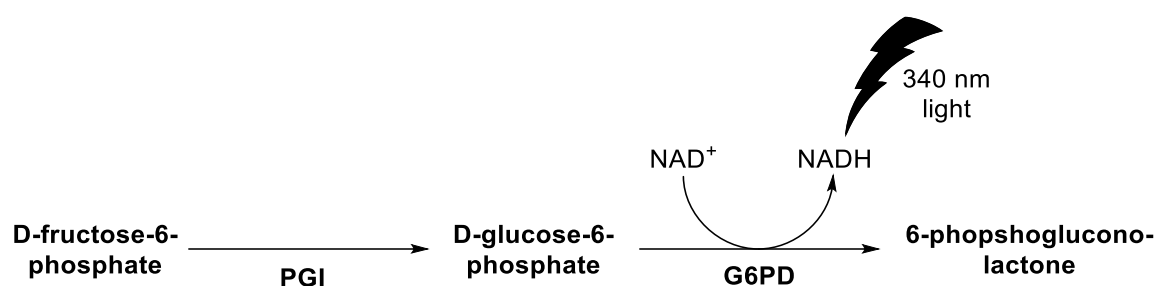


Figure 33 Working principle of the PGI-assay

A drawback of the PGI-assay is that it only detects activity of drugs, which harm the vesicle's integrity and lead to leakage of fluid into the supernatant. Filling this gap, the CellTiterGlo[®] assay can determine the viability of the cells by the measurement of bioluminescence emission caused by reaction of cell-derived adenosine triphosphate (ATP) with luciferase.^{87, 108}

In the PGI-assay Triton X-100 is used as positive control and DMSO as negative control. **Figure 34** shows the results of the PGI-assay normalised to Triton X-100.

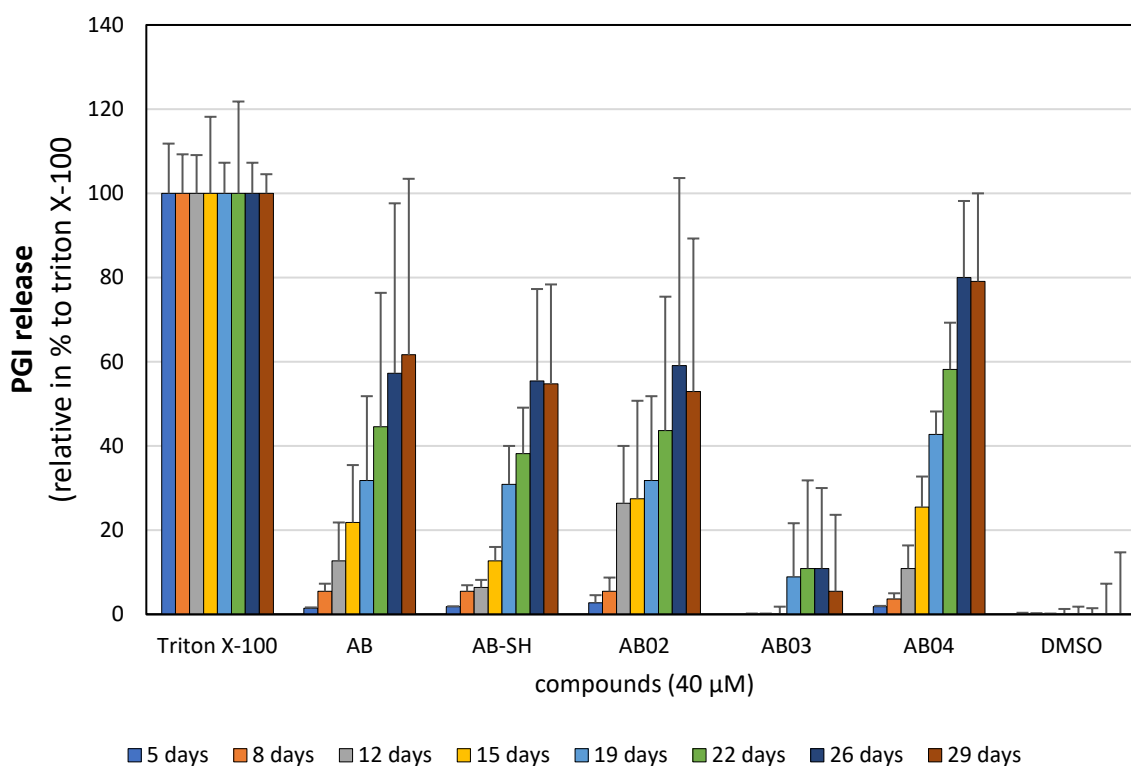


Figure 34 Results for the albendazole derivatives in the PGI-assay on *E. multilocularis* metacestodes. Data from Tobias Kämpfer, Institute of Parasitology, University of Bern

The assay revealed weak activity for **AB03** compared to the negative control. For the other compounds, the activity appeared to be in a similar range to the unmodified **albendazole** (AB).

To further evaluate the compounds, they were tested in the cell viability assay which was normalised to Triton X-100 that manages to effectively kill cells due to its action as surfactant. As negative control DMSO was used, in which the compounds are dissolved for the assay.

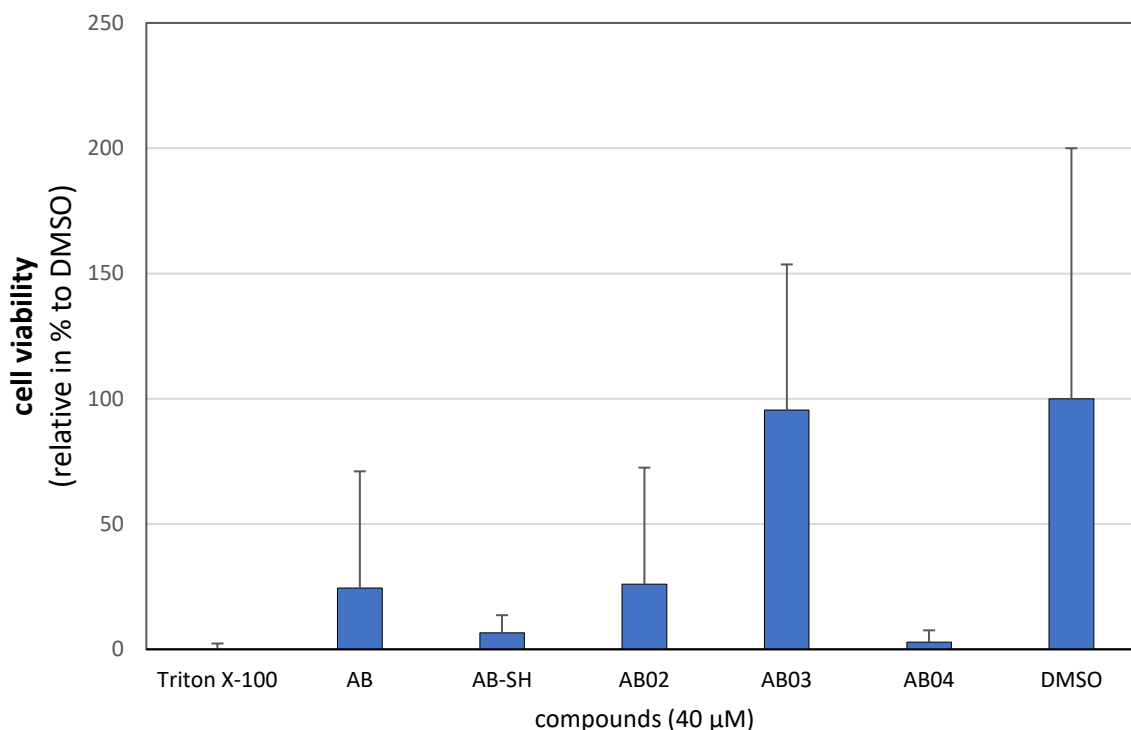
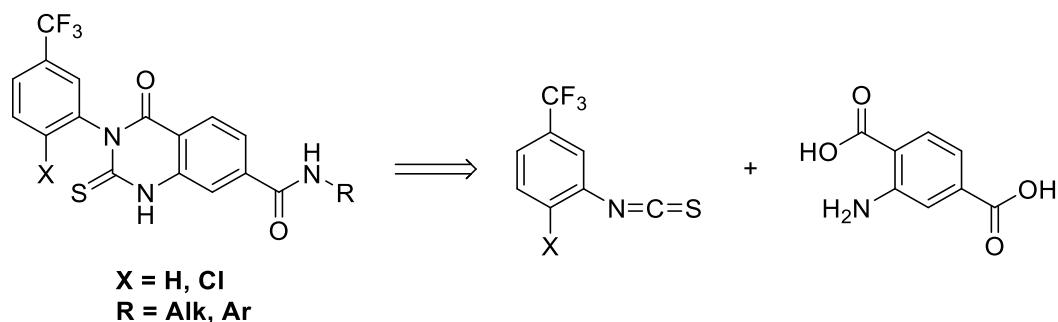


Figure 35 Results for the CellTiterGlo®/ cell viability assay for the albendazole derivatives, normalised to Triton X-100 on *E. multilocularis* metacystodes. Albendazole (AB) for the compounds AB-SH, AB-02, AB03 & AB04 see **Scheme 10**. Data from Tobias Kämpfer, Institute of Parasitology, University of Bern

AB-SH and maleimide-based derivative **AB04** appear to be more effective as **albendazole** (AB). Alcohol **AB02** is in a similar range to albendazole and the amine bearing **AB03** appears to be inactive, being very close to the negative control DMSO.

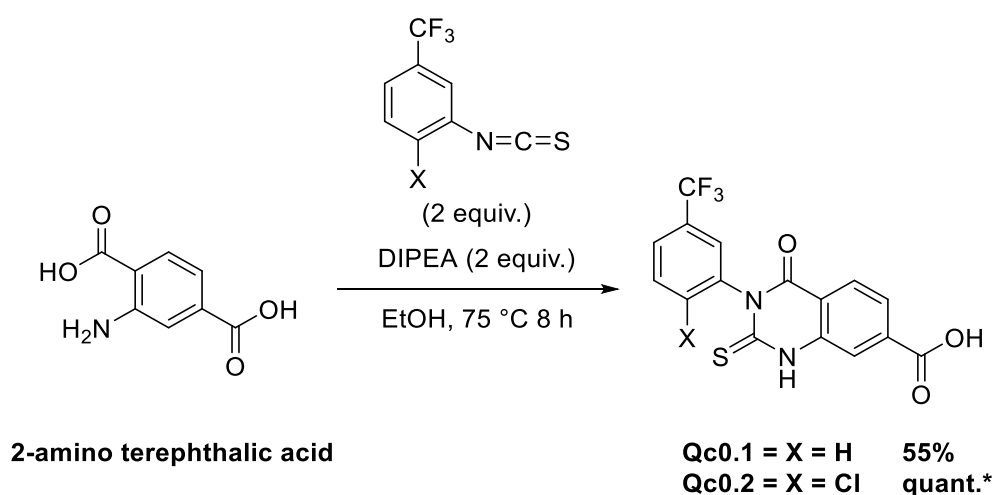
TDH inhibitors

The **Qc** target structures were retro-synthetically analysed and the most feasible way, inspired by a review article by El-Hiti et al. about the synthesis of thioxoquinazolines compounds, was the use of isothiocyanate building blocks.¹⁰⁹ Based on this a synthetic pathway was designed as shown in **Scheme 11**.



Scheme 11 Retrosynthesis of quinazoline carboxamides

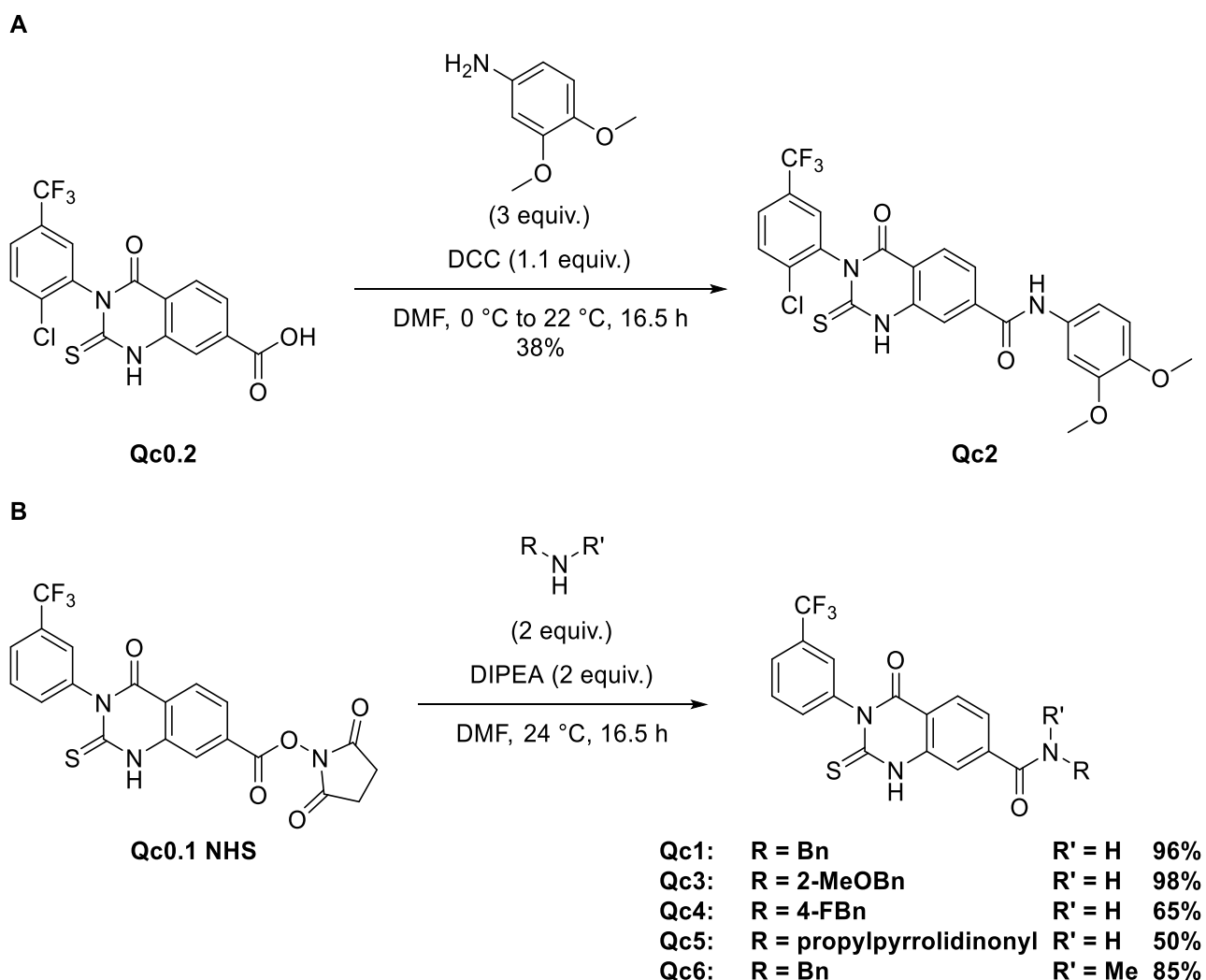
Two commercially available starting materials were found having the correct building block structure for accessing the desired target Qc derivatives. The 2-amino terephthalic acid can be used for all the core structures **Qc1-6** (**Figure 31**). The corresponding alkyl and aromatic R groups for **Qc1-6** need to be coupled individually. For the central building block, 2-amino terephthalic acid was reacted with 3-trifluoromethylphenyl isothiocyanate to give in **Qc0.1** or with 2-chloro-5-trifluoromethylphenyl isothiocyanate to give **Qc0.2** (**Scheme 12**).



Scheme 12 Reactions to the access the **Qc** core structure *product contained toluene as impurity

The subsequent amide formation reaction was achieved using two different approaches. First a coupling procedure using *N,N'*-dicyclohexylmethanediimine (DCC) was used to transform the carboxylic acid intermediate **Qc0.1** to activated *N*-hydroxysuccinimide (NHS) ester **Qc0.1 NHS**. The

advantage of NHS-activated esters as intermediates is the convenient amide formation, which can be achieved by mixing the NHS-ester with the corresponding amine in the presence of *N,N*-diisopropylethylamine (DIPEA). This led efficiently to the desired amides with NHS as only side product that can easily be removed by chromatography. Applying the NHS-ester method compounds **Qc1**, **Qc3-6** were successfully synthesised in moderate to excellent yield (**Scheme 13, B**). Using DCC as the coupling agent, **Qc2** was successfully synthesised, albeit in low yield (**Scheme 13, A**).



Scheme 13 A) Coupling with *N,N'*-dicyclohexylmethanediimine (DCC) **B)** Reaction with NHS activated ester

The compounds **Qc1-Qc6** and carboxylic acid **Qc0.1** were evaluated in a PGI-assay and cell viability assay (see above). The results for the PGI assay are shown in **Figure 36**. The results are given as percentage relative to Triton X-100 (positive control) for low (1 g/L) and high (4.5 g/L) glucose in the medium.

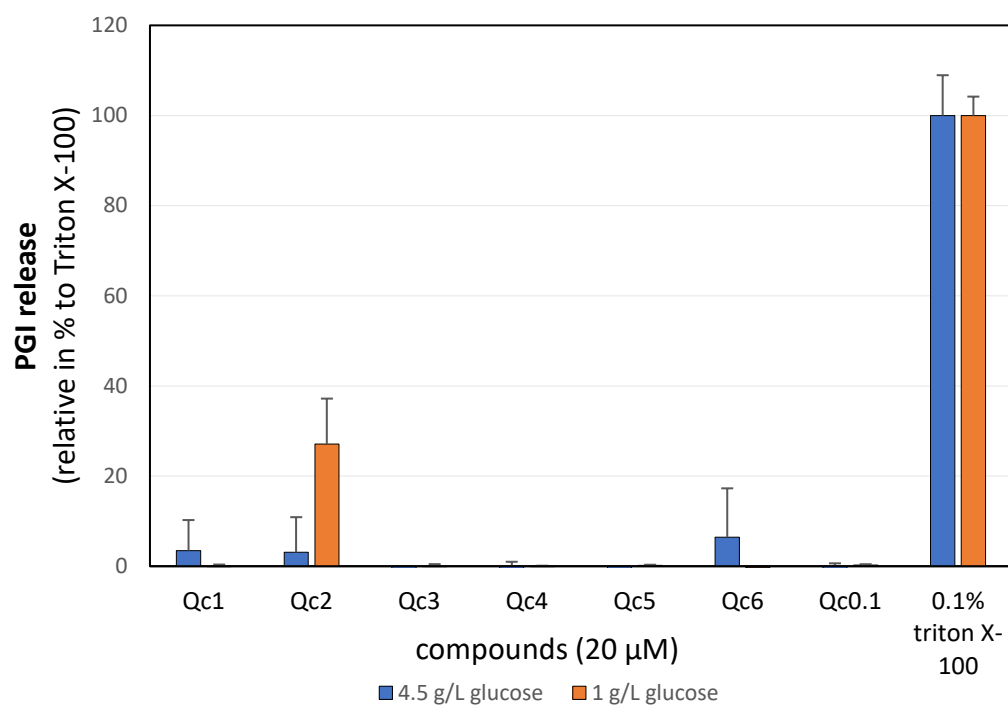


Figure 36 Results for the PGI assay of the Qc derivatives relative to Triton X-100. Data from Marc Kaethner, Institute of Parasitology, University of Bern

Of all the Qc derivatives tested in the assay, **Qc2** showed to be effective at 20 µM concentration in low glucose medium. In high glucose medium however, the compound was not effective. The other compounds did not appear to be effective. The compounds were also evaluated in the CellTiterGlo® assay on metacestodes under low glucose conditions. The results are shown in **Figure 37**.

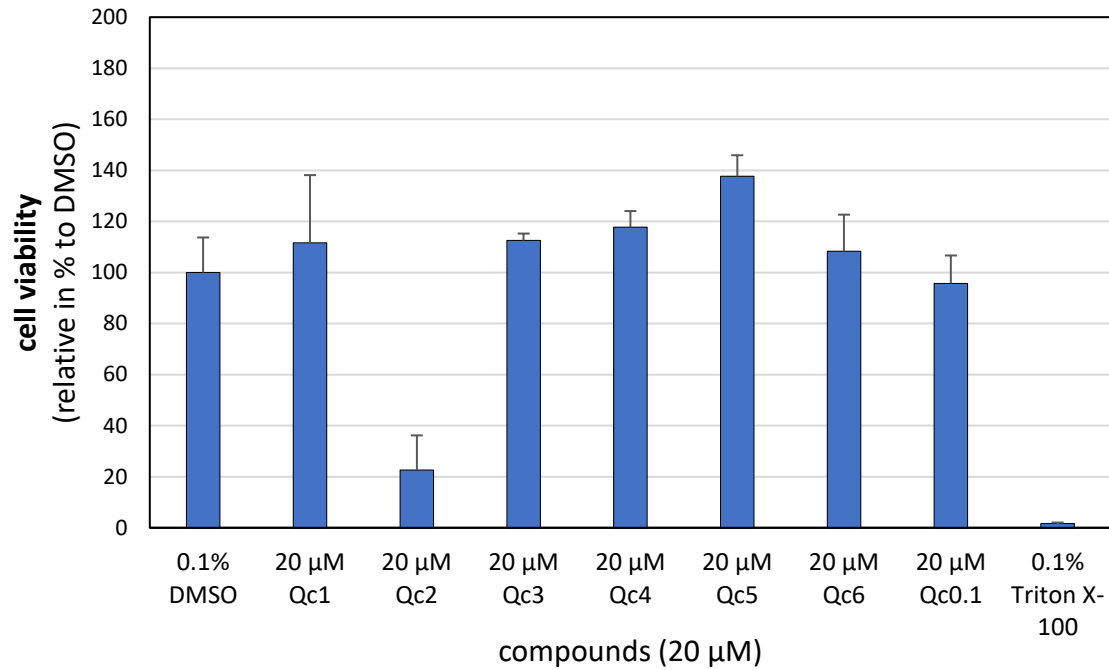


Figure 37 Results for the cell viability assay on metacestodes with Qc derivatives after 12 days of incubation under microaerobic conditions via CellTiterGlo® assay relative to DMSO. Data from Marc Kaethner, Institute of Parasitology, University of Bern

With 20 µM **Qc2** only 20% of the cells survived compared to the DMSO incubation. Showing a similar result to the previous PGI assay.

The supernatant of the metacestodes was measured by HPLC to determine the concentration of amino acids after 5 days of incubation with the Qc compounds. **Figure 38** shows the results of the measurements.

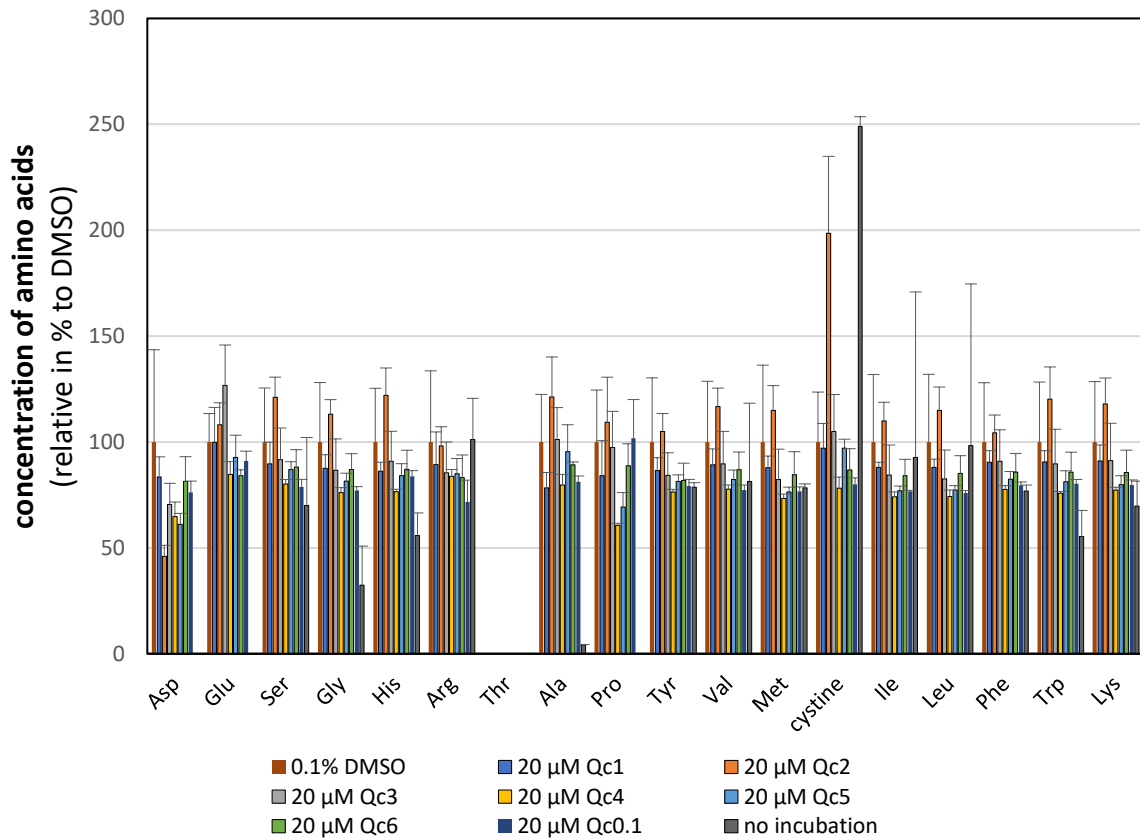


Figure 38 Concentration of amino acids in the medium supernatant of *E. multilocularis* metacystodes treated with Qcs. Data from Marc Kaethner, Institute of Parasitology, University of Bern. Measurement performed by lab of S. Schürch, DCB, University of Bern

The data show that for **Qc2**-incubated metacystodes the consumption of cystine decreased significantly and the consumption of aspartic acid increased significantly. For the other **Qc** derivatives, the amino acid concentrations in the supernatant remained at similar levels as to control incubation with DMSO.

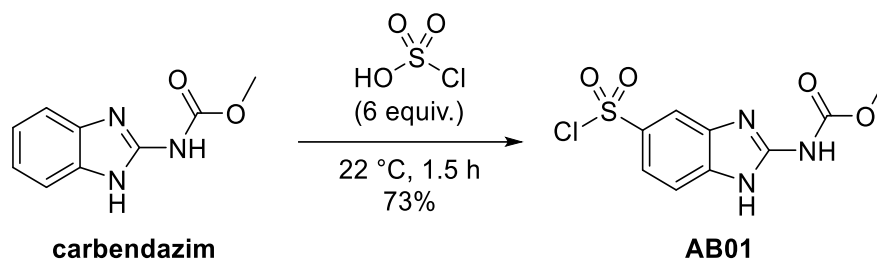
Conclusion and outlook solid supported albendazole

Conclusion and outlook TDH inhibitors

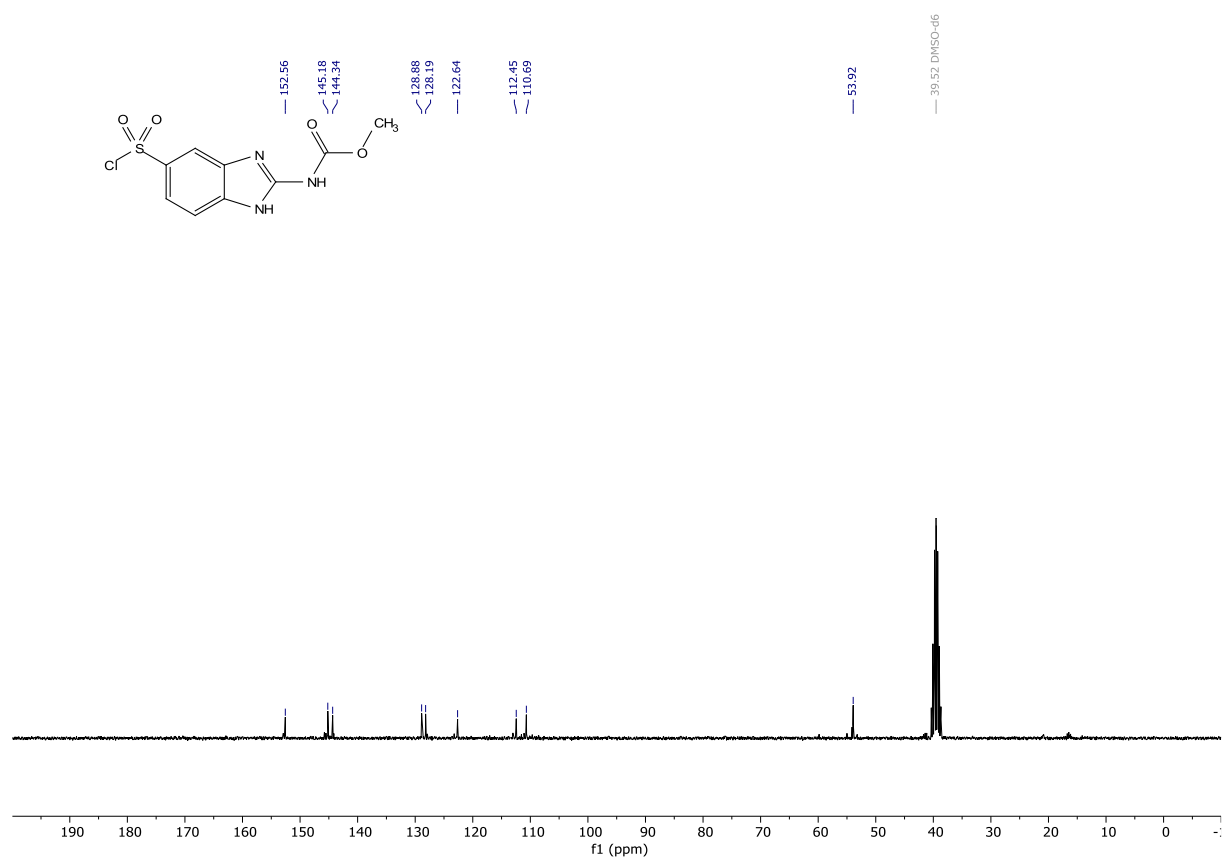
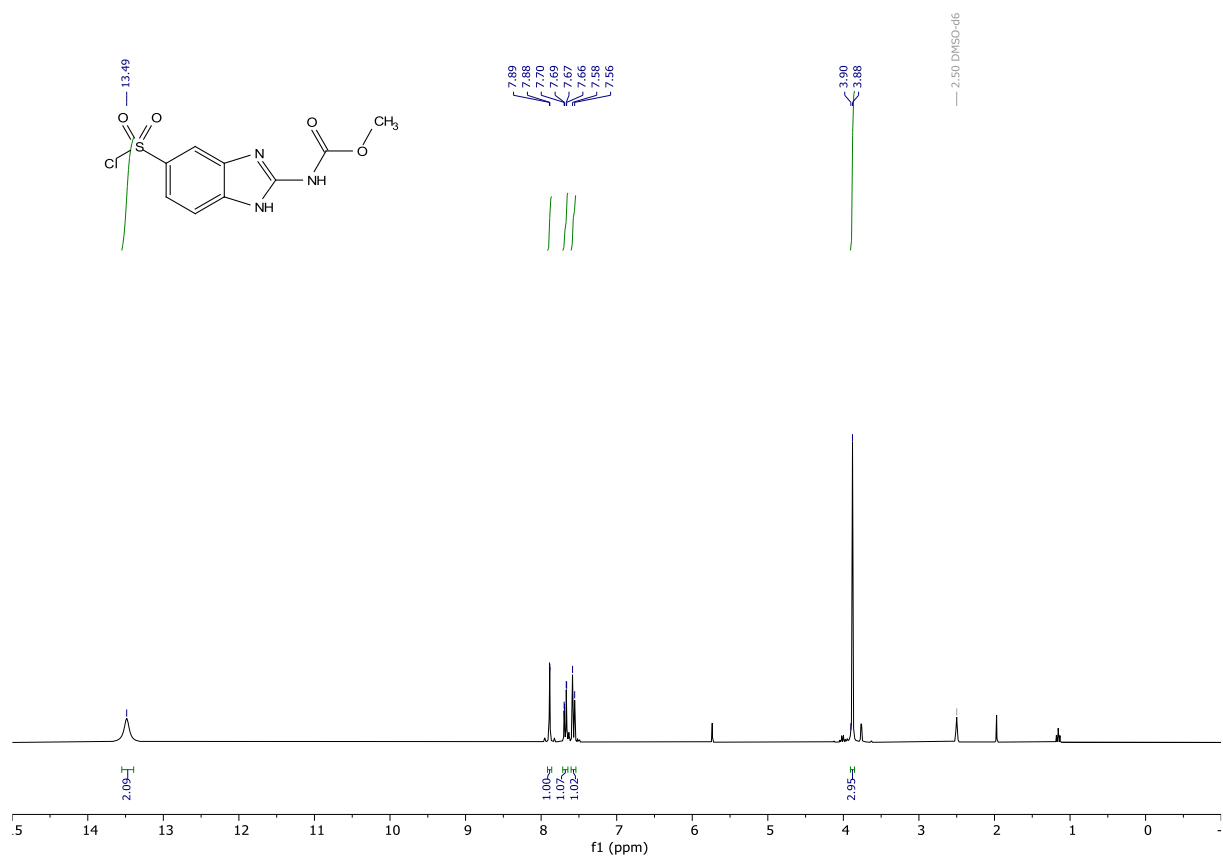
From the experiments, it appears that **Qc2** is active on the metacestodes. However, the activity does not seem to arise from its interaction with the EmTDH as the HPLC experiments showed consumption of the threonine. To find an inhibitor that is specific for the EmTDH the protein will be recombinantly expressed and the compounds will be assessed in an in vitro assay on purified EmTDH. However, **Qc2** appears to be, could still be an interesting compound to investigate further as it showed some activity, and it would be interesting to identify its target(s) in the parasite.

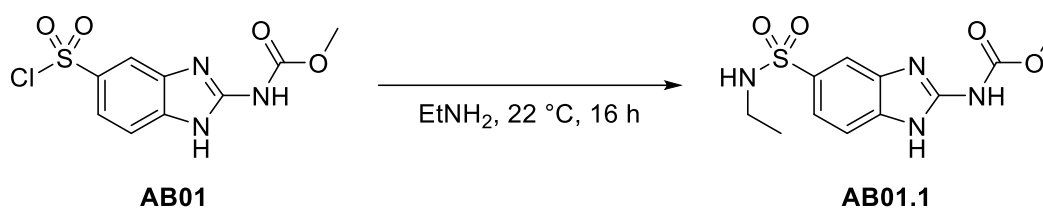
Synthesis

Synthesis of albendazole derivatives

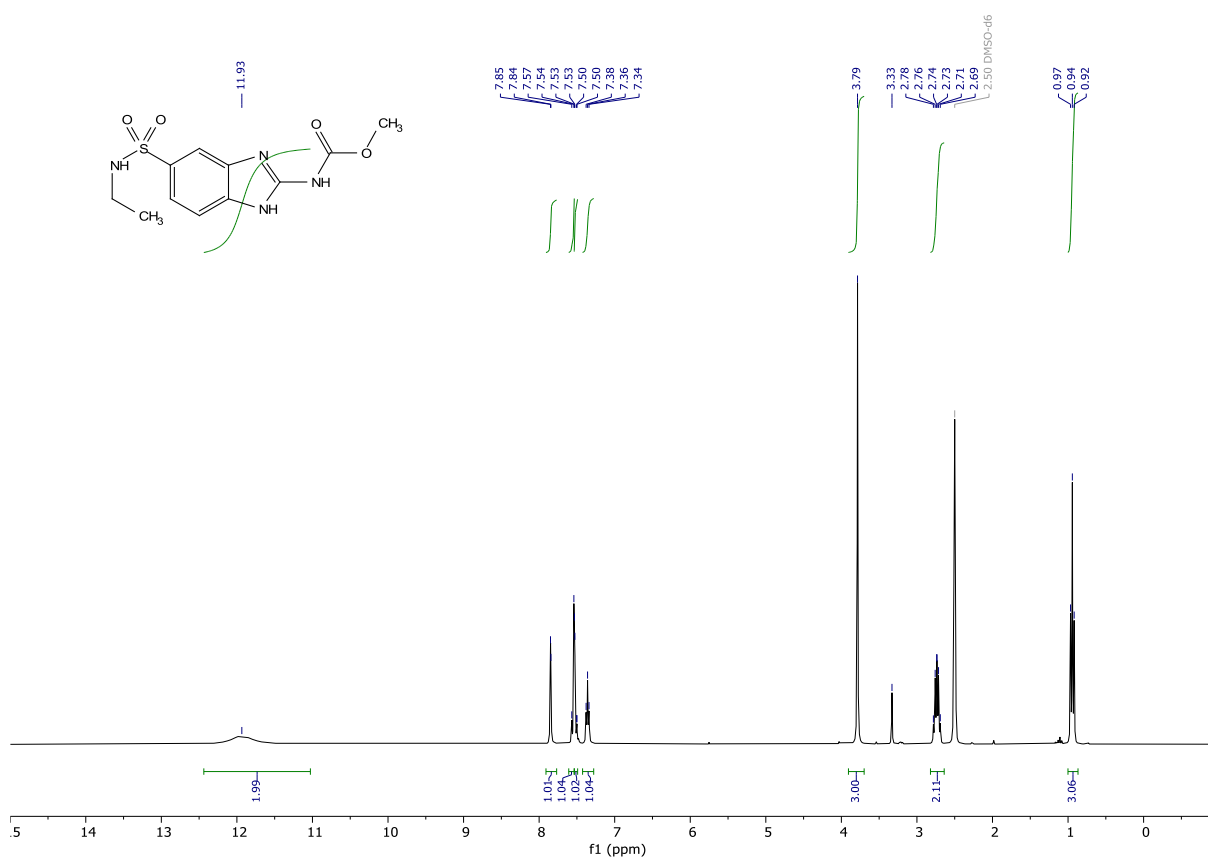


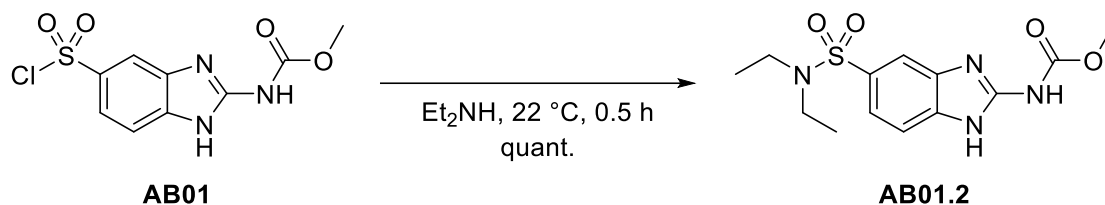
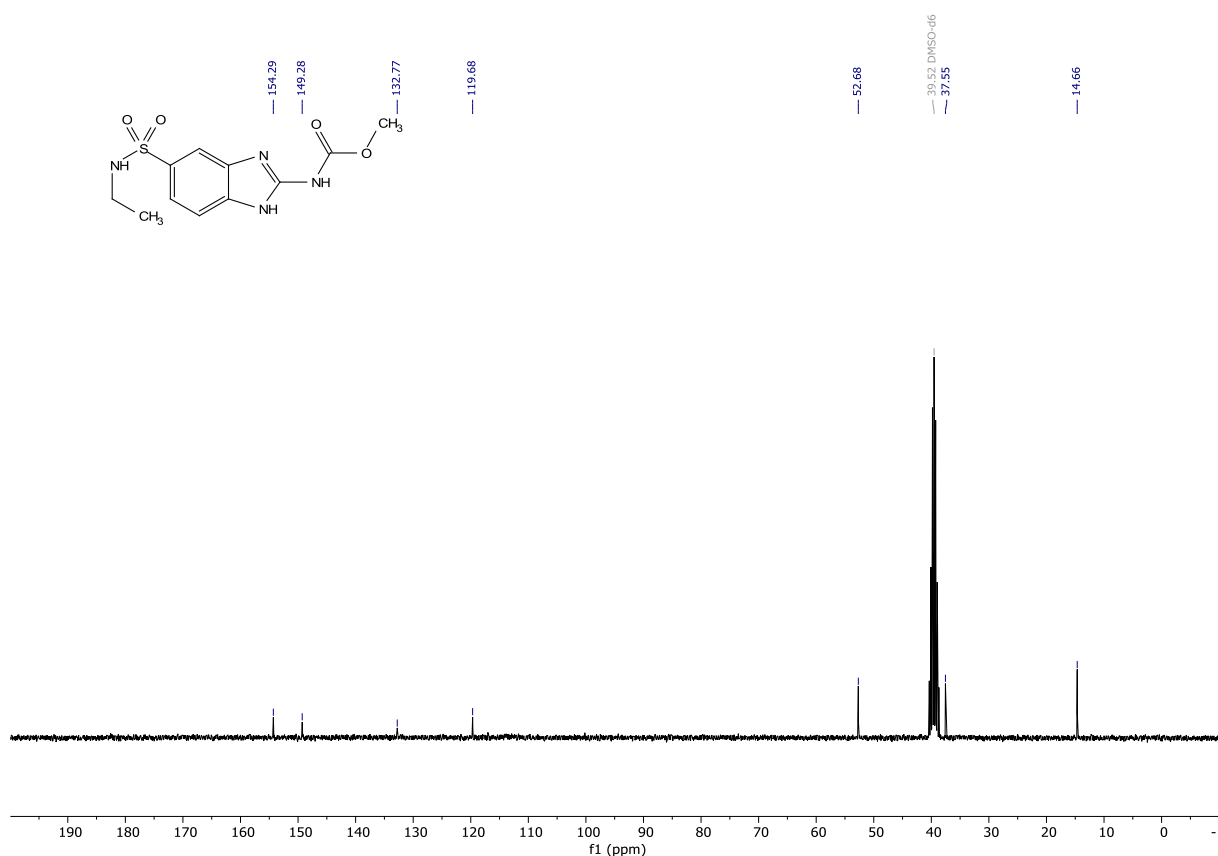
methyl (5-(chlorosulfonyl)-1H-benzo[d]imidazol-2-yl)carbamate (AB01). To carbendazim (5.000 g, 26.1520 mmol) in a beaker chlorosulfonic acid was added (12 mL, 21.036 g, 180.54 mmol). Upon addition of the chlorosulfonic acid, the mixture started bubbling and smoke formation was observed. A brown solution formed immediately. The mixture was stirred at room temperature for 1.5 h. Then it was poured onto ice, which led to an off-white precipitate. This was filtered off with a por 4 frit and it was washed with water several times and thoroughly dried on the filter. Then it was further dried in high vacuum and in the Kugelrohr at 80 °C for 3 h, to give the desired product in 73% yield (5.541 g, 19.1273 mmol). Grey powder: $^1\text{H NMR}$ (300 MHz, $\text{DMSO}-d_6$) δ 13.49 (bs, 2H), 7.89 (d, $J = 1.5$ Hz, 1H), 7.68 (dd, $J = 8.4, 1.5$ Hz, 1H), 7.57 (d, $J = 8.4$ Hz, 1H), 3.88 (s, 3H). $^{13}\text{C NMR}$ (75 MHz, DMSO) δ 152.56, 145.18, 144.34, 128.88, 128.19, 122.64, 112.45, 110.69, 53.92. **HRMS** (ESI) calculated for $[\text{M}+\text{H}]^+$ $\text{C}_9\text{H}_9\text{N}_3\text{O}_4\text{ClS}$ 289.9997, found 289.9991.





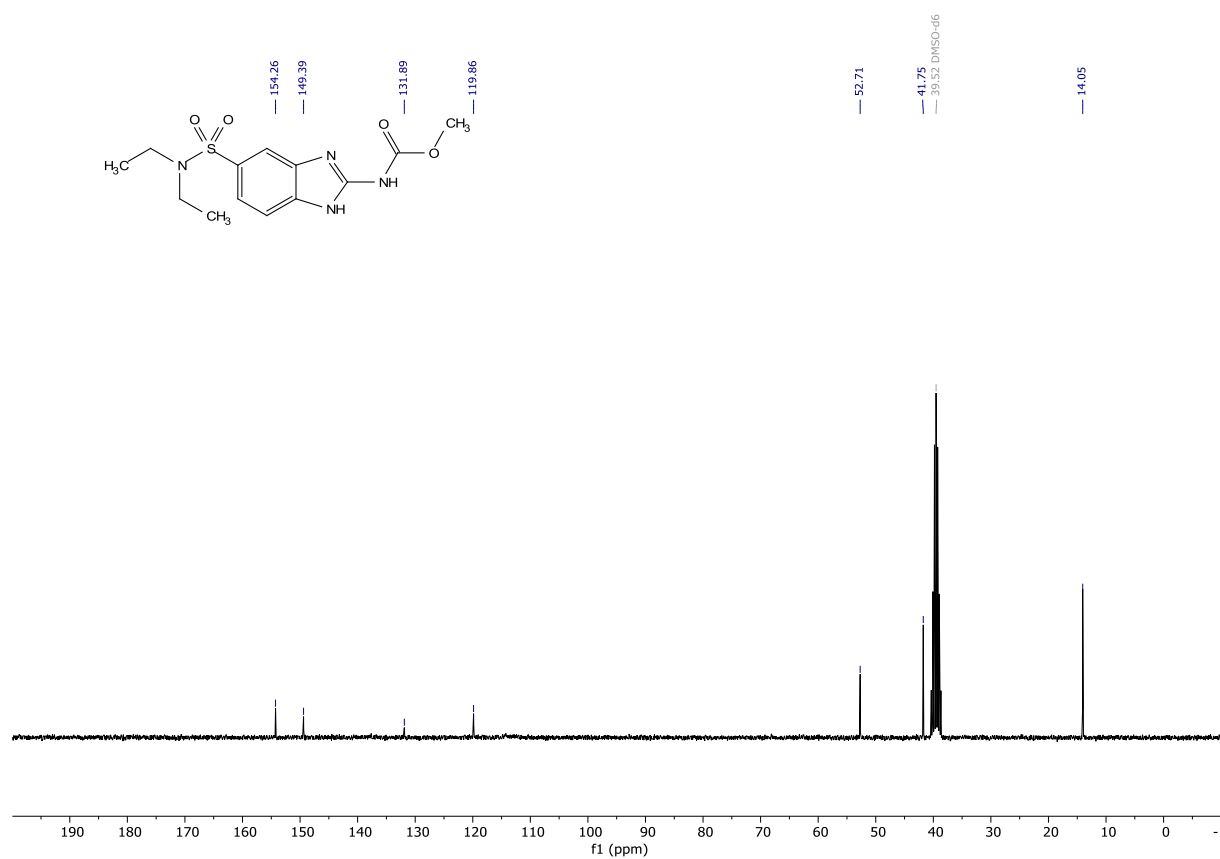
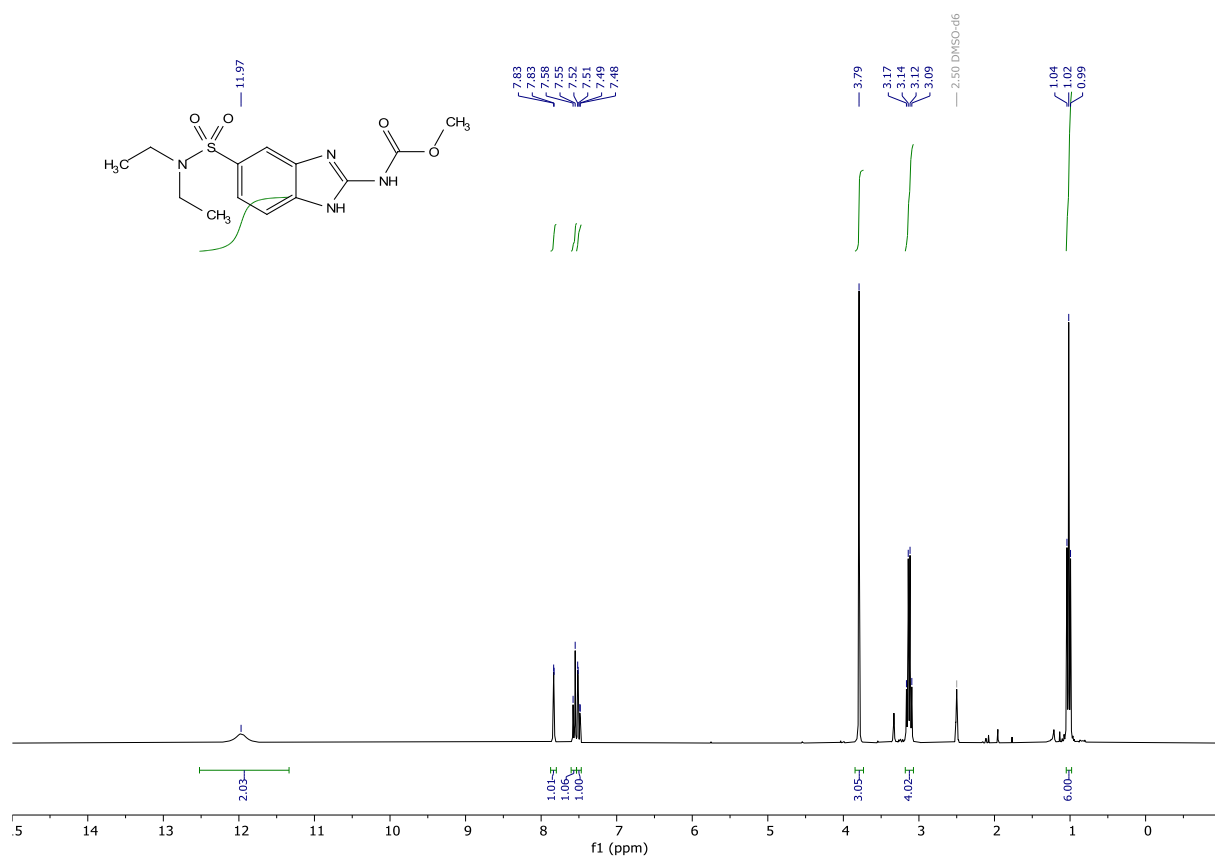
methyl (5-(*N*-ethylsulfamoyl)-1*H*-benzo[*d*]imidazol-2-yl)carbamate (AB01.1). To methyl (5-(chlorosulfonyl)-1*H*-benzo[*d*]imidazol-2-yl)carbamate (AB01) (0.255 g, 0.8803 mmol) was added ethylamine (70% in water, 5 mL). The mixture was stirred for 16 h. Then the volatiles were removed under reduced pressure to give a white solid. It was attempted to dissolve this solid in a mixture of water and ethyl acetate, but it was not possible to get a clear solution. It was therefore filtered through a por 3 frit. The filter cake was thoroughly washed with water to give the desired compound in 53% yield (0.13875 g, 0.46511 mmol). White solid: **¹H NMR** (300 MHz, DMSO-*d*₆) δ 11.93 (s, 2H), 7.85 (d, *J* = 1.6 Hz, 1H), 7.55 (d, *J* = 8.4 Hz, 1H), 7.52 (dd, *J* = 8.4, 1.6 Hz, 1H), 7.36 (t, *J* = 5.7 Hz, 1H), 3.79 (s, 3H), 2.82 – 2.64 (m, 2H), 0.94 (t, *J* = 7.2 Hz, 3H). **¹³C NMR** (75 MHz, DMSO) δ 154.29, 149.28, 132.77, 119.68, 117.02, 52.68, 37.55, 14.66. **HRMS** (ESI) calculated for [M+H]⁺ C₁₁H₁₅N₄O₄S 299.0809, found 299.0804.

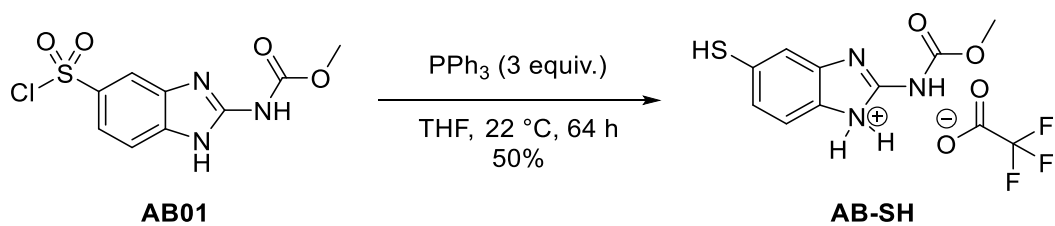




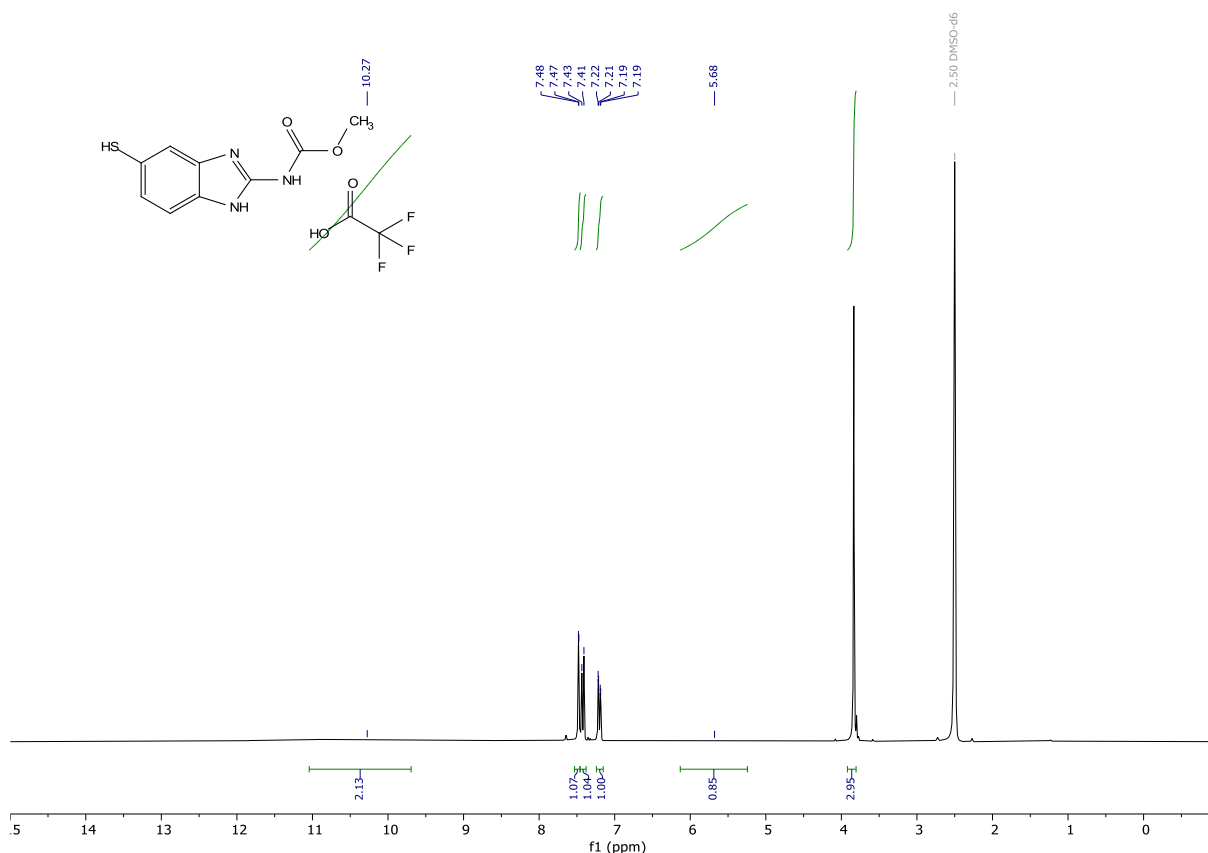
methyl (5-(N,N-diethylsulfamoyl)-1H-benzo[d]imidazol-2-yl)carbamate (AB01.2). To carbendazim sulfonyl chloride (AB01) (0.0547 g, 0.1888 mmol) was added diethylamine (5 mL, 3.55 g, 48.5377 mmol). The originally turbid mixture cleared up immediately after the addition of the amine, just to turn turbid the next instant. The mixture was left stirring for 30 minutes at 22 °C. The mixture was filtered through a pad of silica. The pad was washed several times with dichloromethane/ methanol 9:1 and little diethylamine. The volatiles were removed under reduced pressure leaving a yellow residue. This residue was dissolved in acetone and concentrated onto silica gel. The crude was purified by flash column chromatography (dichloromethane/ methanol gradient from 1:0 to 9:1), to give the desired compound in quantitative yield (0.06387 g, 0.19569 mmol). White solid: ^1H NMR (300 MHz, DMSO- d_6) δ 11.97 (bs, 2H), 7.83 (d, J = 1.7 Hz, 1H), 7.56 (d, J = 8.4 Hz, 1H), 7.50 (dd, J = 8.4, 1.8 Hz, 1H), 3.79 (s, 3H), 3.13 (q, J = 7.1 Hz, 4H), 1.02 (t, J = 7.1 Hz, 6H). ^{13}C NMR (75 MHz, DMSO) δ 154.26, 149.39,

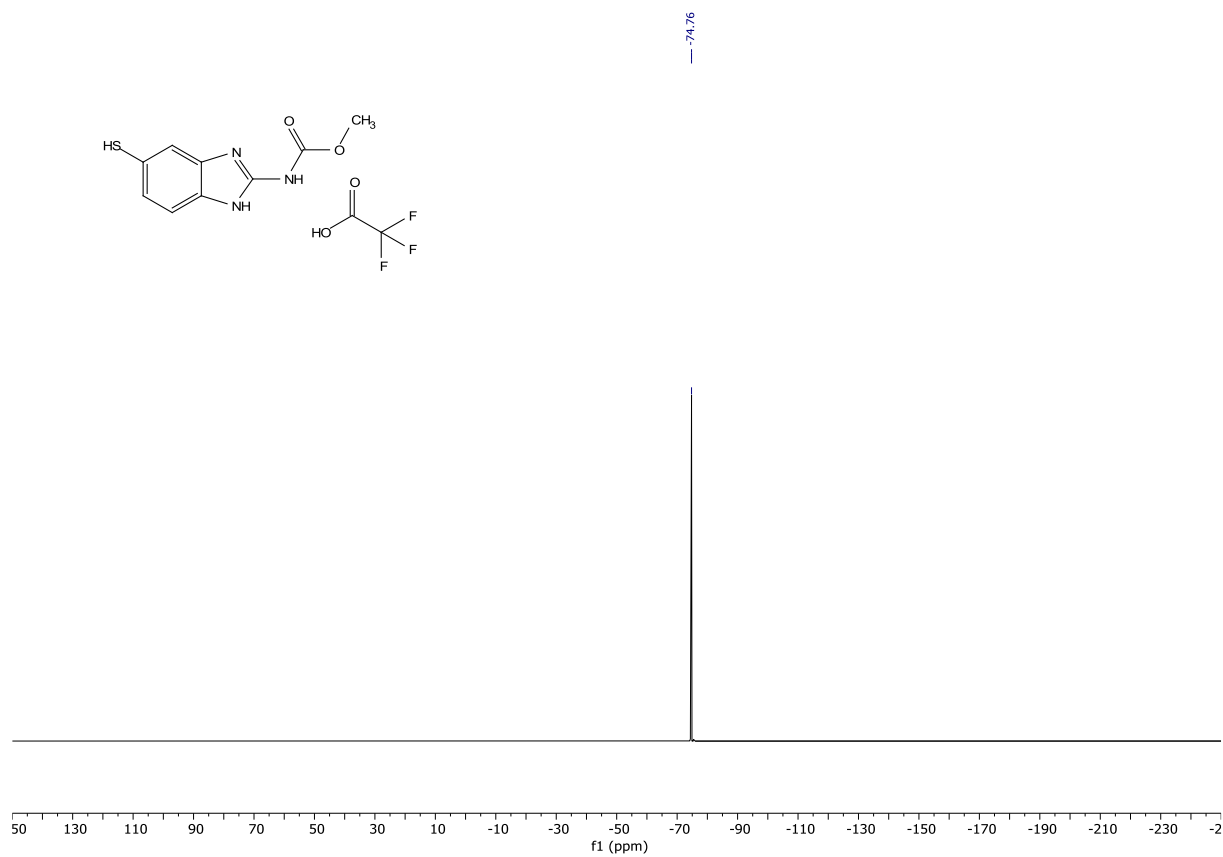
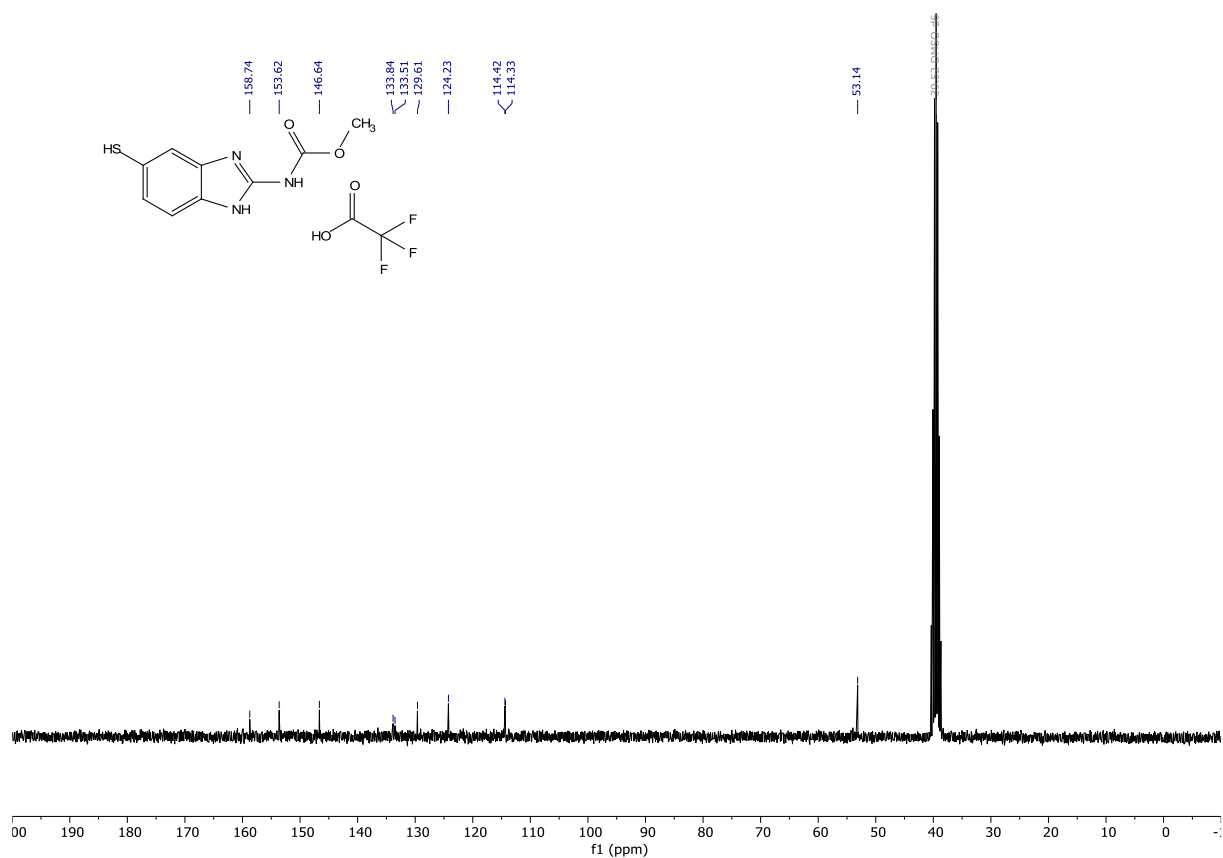
131.89, 119.86, 52.71, 41.75, 14.05. **HRMS** (ESI) calculated for $[M+H]^+$ $C_{13}H_{19}N_4O_4S$ 327.1132, found 327.1118.

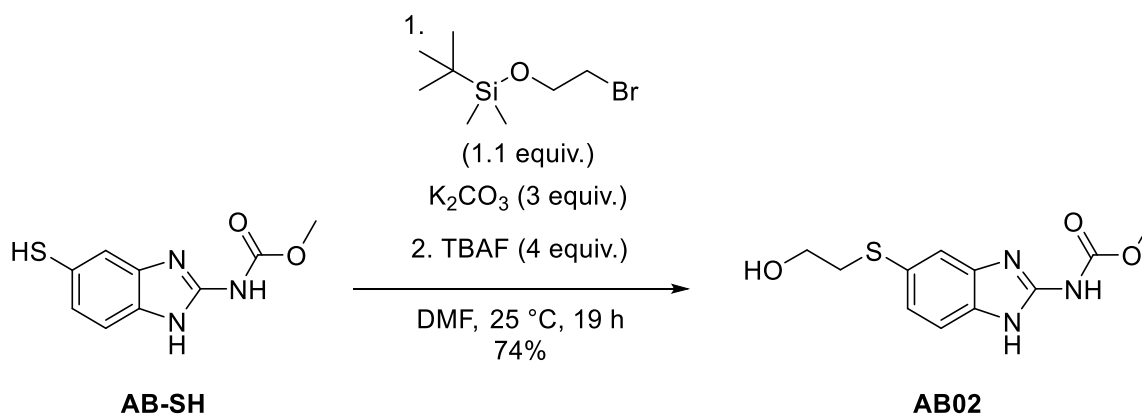




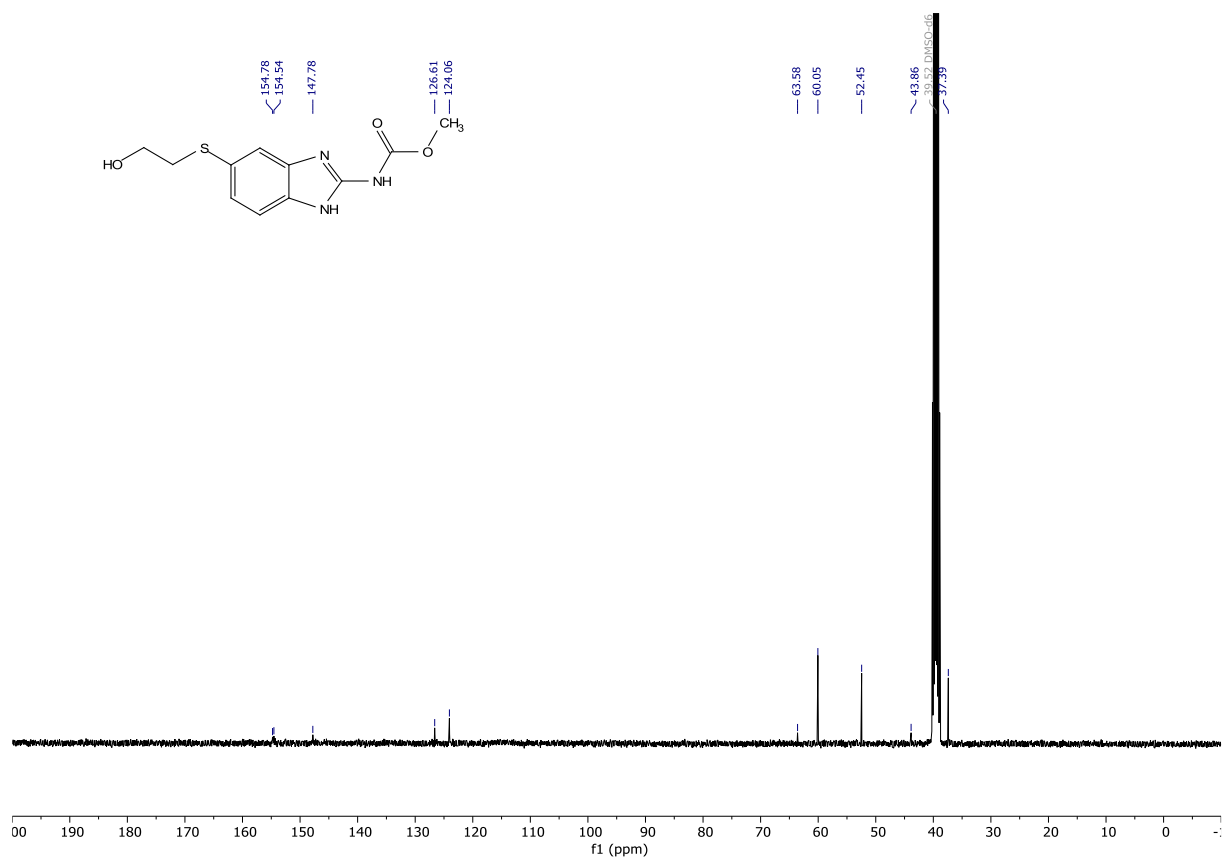
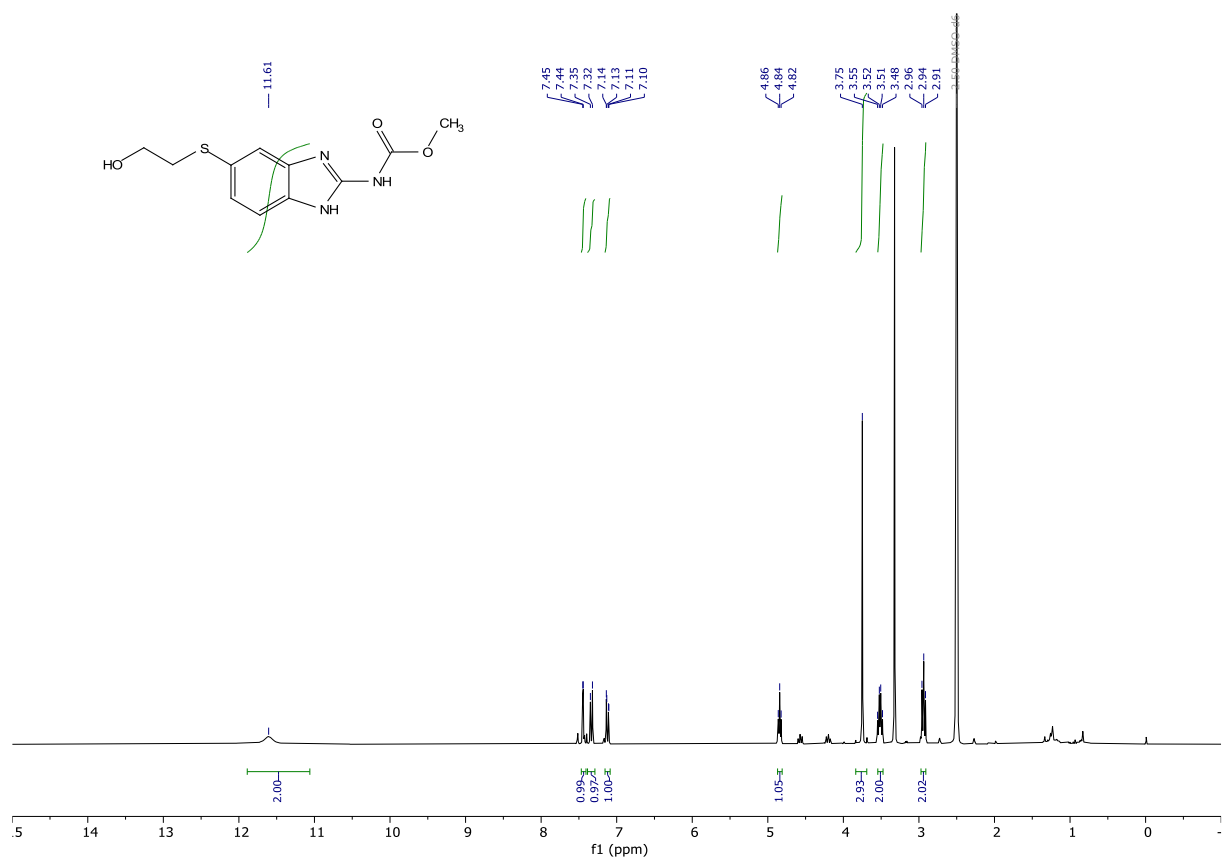
5-mercapto-2-((methoxycarbonyl)amino)-1H-benzo[d]imidazol-1-ium 2,2,2-trifluoroacetate (AB-SH). To a stirred suspension of carbendazim sulfonyl chloride (0.447 g, 1.5430 mmol) in THF (10 mL) was added triphenylphosphine (1.488 g, 5.6731 mmol). The mixture was stirred for 64 h, after which it was diluted with water + 0.1% TFA and filtered through a pad of celite. The filtrate was then directly injected as a liquid in the reverse phase flash column chromatography (water + 0.1% TFA / acetonitrile + 0.1% TFA). The fractions containing the product were concentrated under argon atmosphere (to prevent oxidation to the disulfide), to give the desired compound as TFA salt in 50% yield. (0.2583 g, 0.765848 mmol). White solid: $^1\text{H NMR}$ (300 MHz, DMSO- d_6) δ 10.27 (bs, 2H), 7.48 (d, $J = 1.7$ Hz, 1H), 7.42 (d, $J = 8.4$ Hz, 1H), 7.20 (dd, $J = 8.4, 1.8$ Hz, 1H), 5.68 (s, 1H), 3.83 (s, 3H). $^{13}\text{C NMR}$ (75 MHz, DMSO) δ 158.74, 153.62, 146.64, 133.84, 133.69 – 133.38 (m), 129.61, 124.23, 114.42, 114.33, 53.14. $^{19}\text{F NMR}$ (282 MHz, DMSO) δ -74.76. **HRMS** (ESI) calculated for $[\text{M}+\text{H}]^+$ $\text{C}_9\text{H}_{10}\text{N}_3\text{O}_2\text{S}$ 224.0488, found 224.0479.

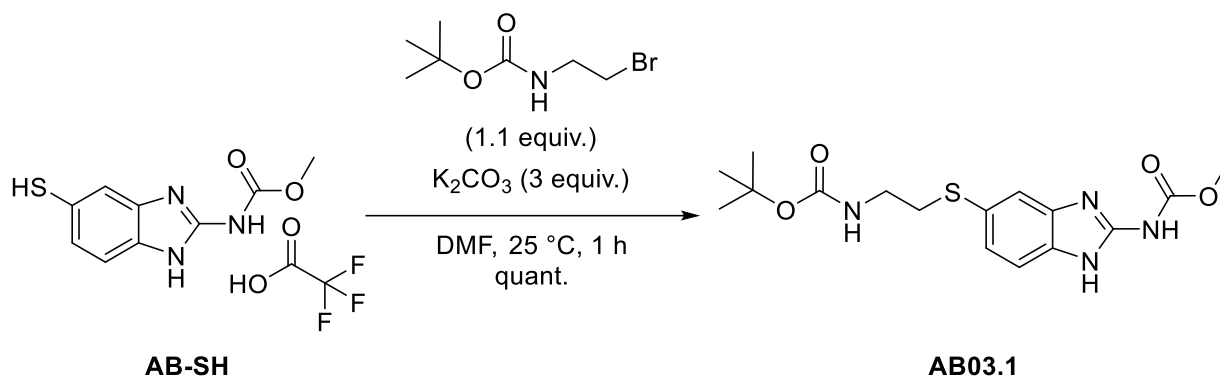




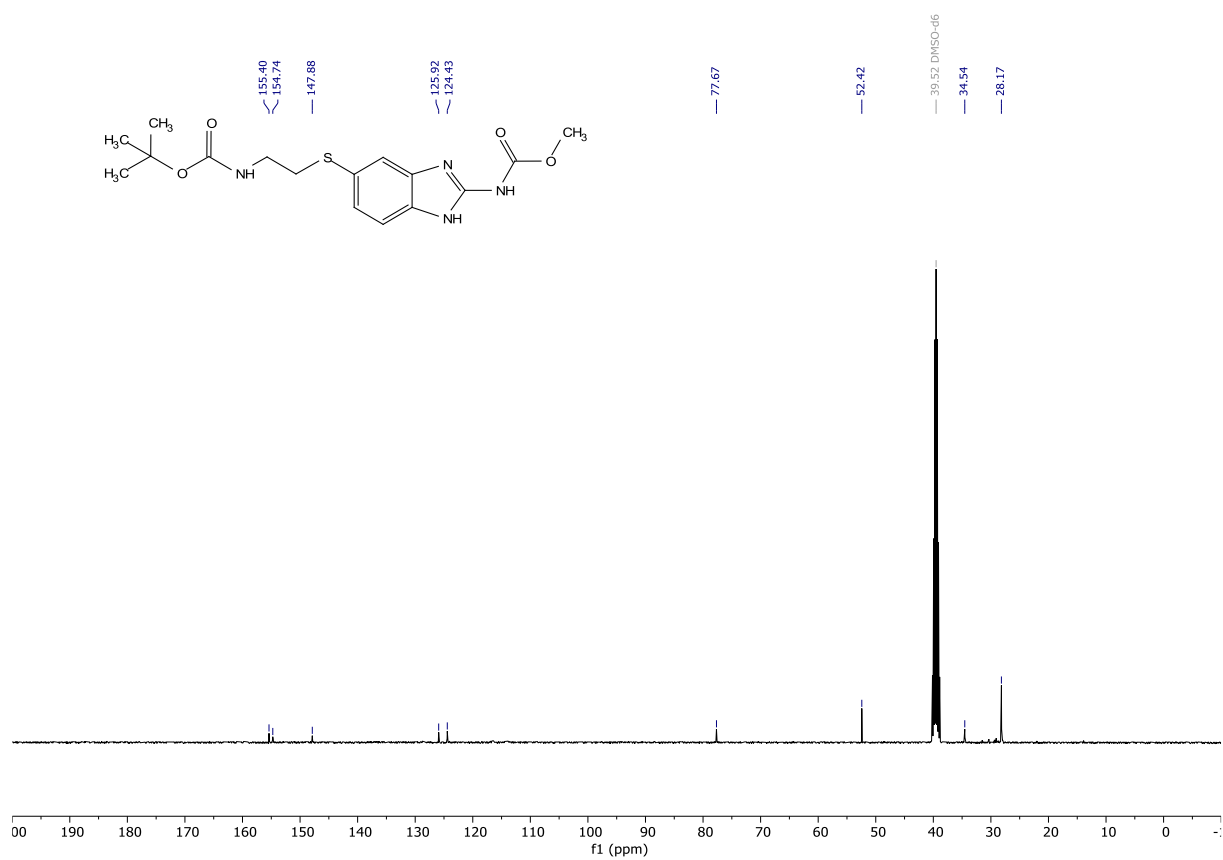
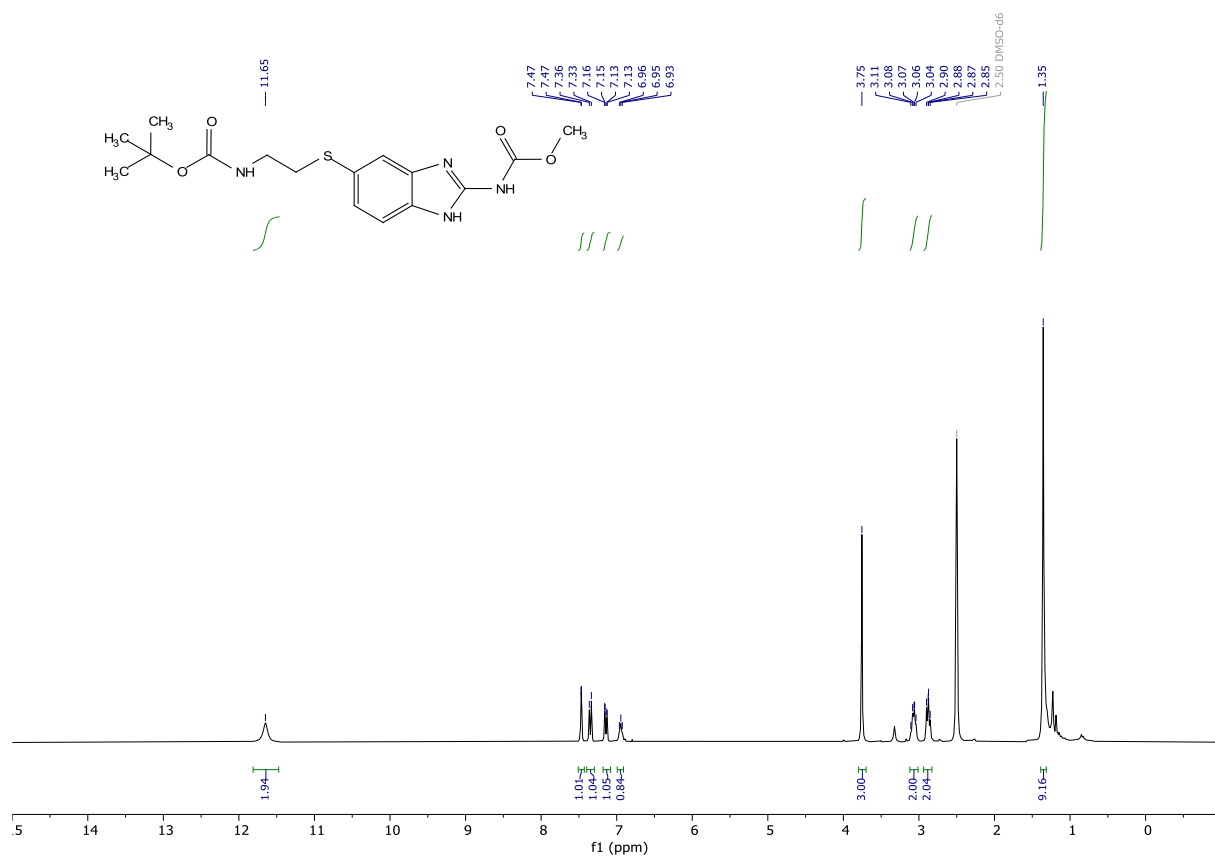


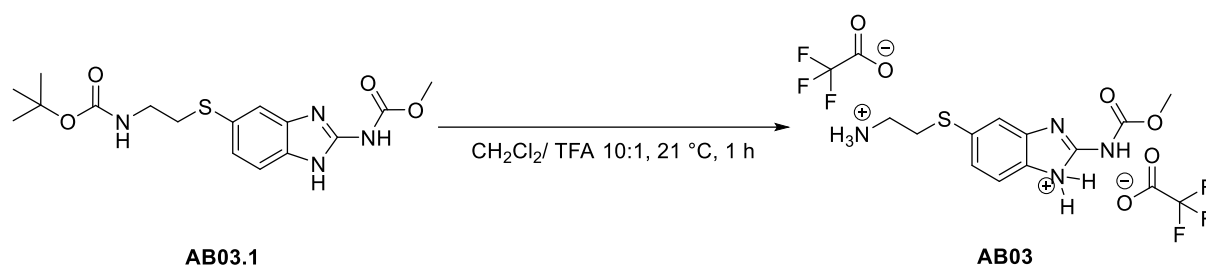
methyl (5-((2-hydroxyethyl)thio)-1H-benzo[d]imidazol-2-yl)carbamate (AB02). To a stirred solution of (5-mercapto-1H-benzo[d]imidazol-2-yl)carbamate (0.051 g, 0.1512 mmol) in dry DMF (2 mL) under an argon atmosphere was added (2-bromoethoxy)(*tert*-butyl)dimethylsilane (0.04 mL, 0.0446 g, 0.4586 mmol) to give a clear solution. To which was added potassium carbonate (0.06338 g, 4586 mmol). The mixture was stirred at 21 °C for 3 h. Then TBAF (1 M in THF, 0.2 mL, 2 mmol) was added and the mixture was stirred for 16 h. The mixture was diluted with water and ethyl acetate, the aqueous phase was slightly basified with dilute aq. NaOH. The aqueous phase was extracted with ethyl acetate. The combined organic layers were washed with brine (5x), dried over MgSO₄, filtered, and concentrated under reduced pressure. The mixture was then taken up in dichloromethane, and concentrated onto silica. The crude was purified by flash column chromatography (dichloromethane/methanol gradient 1:0 to 9:1) to give the desired compound in 74% yield (0.04248 g, 0.11133 mmol). White solid: ¹H NMR (300 MHz, DMSO-*d*₆) δ 11.61 (bs, 2H), 7.45 (d, *J* = 1.7 Hz, 1H), 7.33 (d, *J* = 8.2 Hz, 1H), 7.12 (dd, *J* = 8.3, 1.8 Hz, 1H), 4.84 (t, *J* = 5.6 Hz, 1H), 3.75 (s, 3H), 3.56 – 3.48 (m, 2H), 2.94 (t, *J* = 7.0 Hz, 2H). ¹³C NMR (101 MHz, DMSO) δ 154.78, 154.54, 147.78, 126.61, 124.06, 63.58, 60.05, 52.45, 43.86, 37.39. HRMS (ESI) calculated for [M+H]⁺ C₁₁H₁₃N₃O₃S 268.0750, found 268.0752.



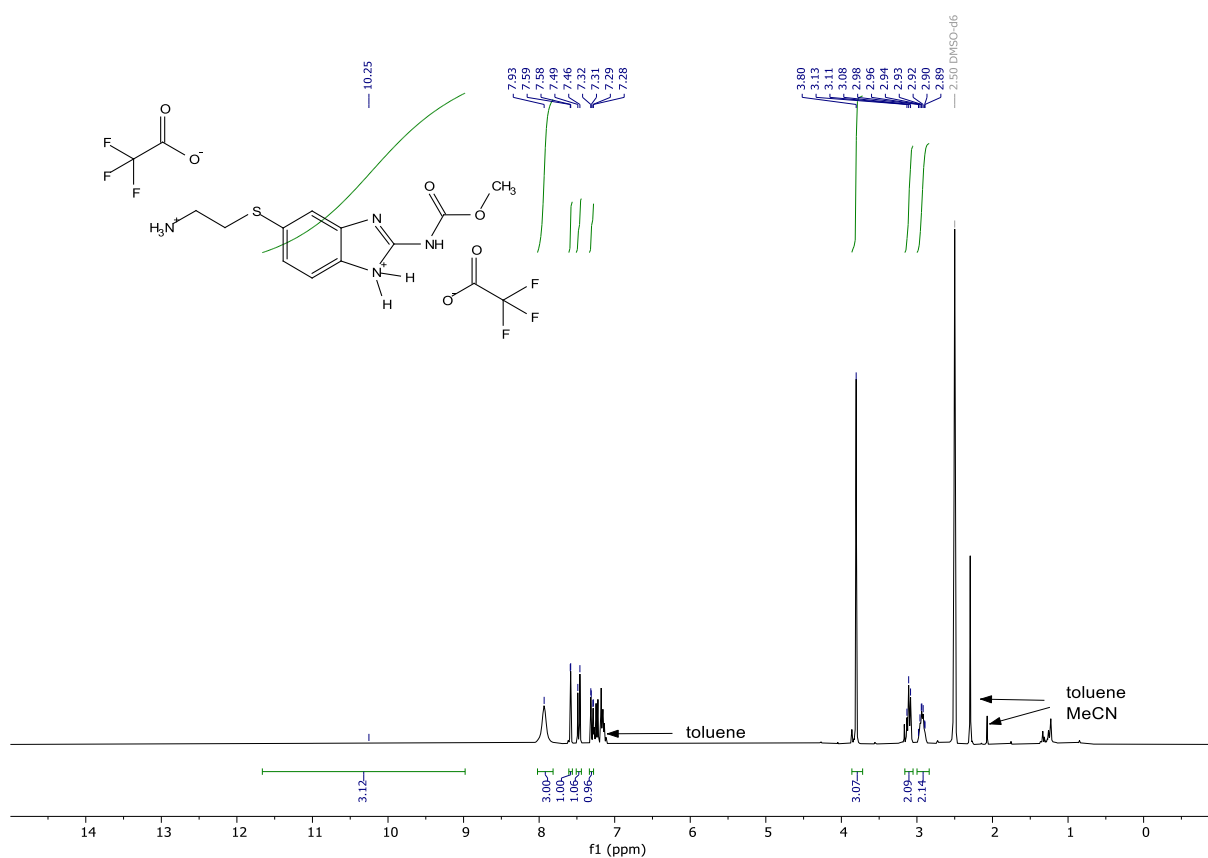


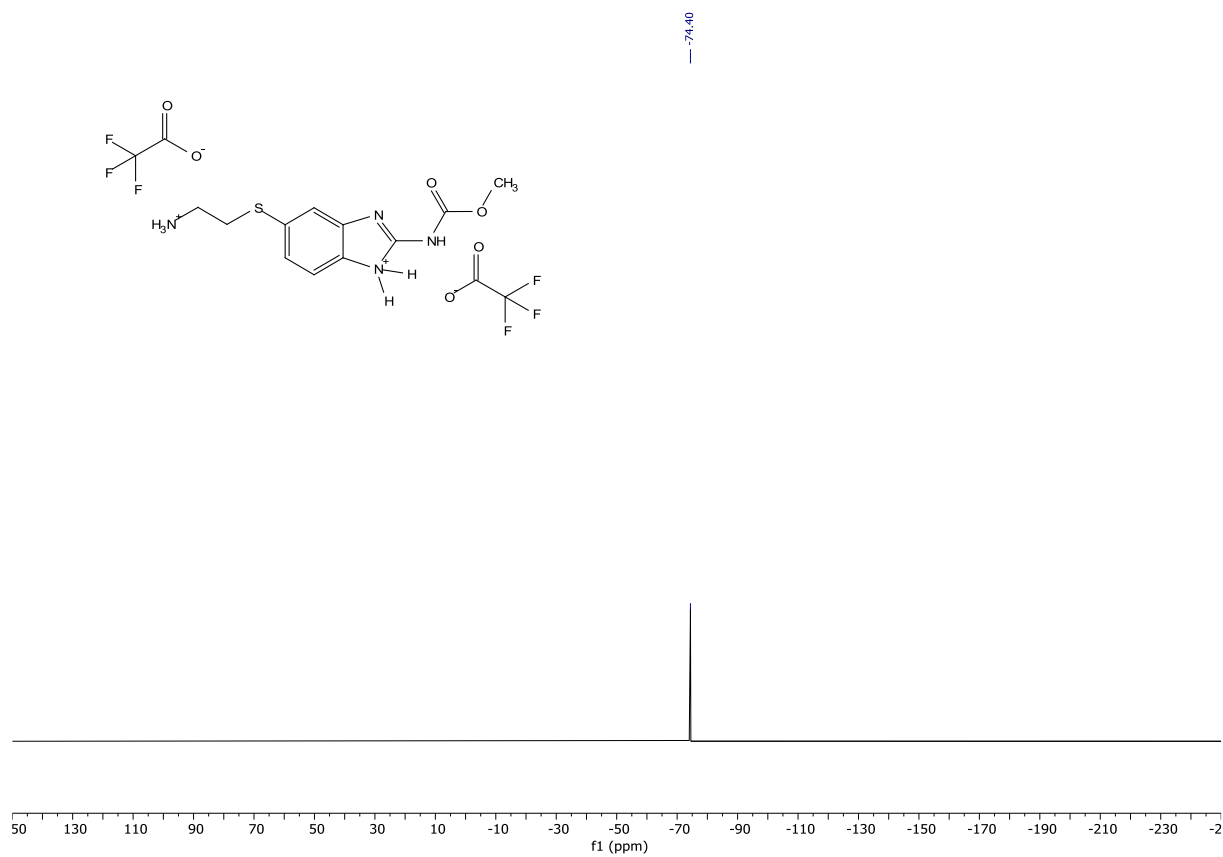
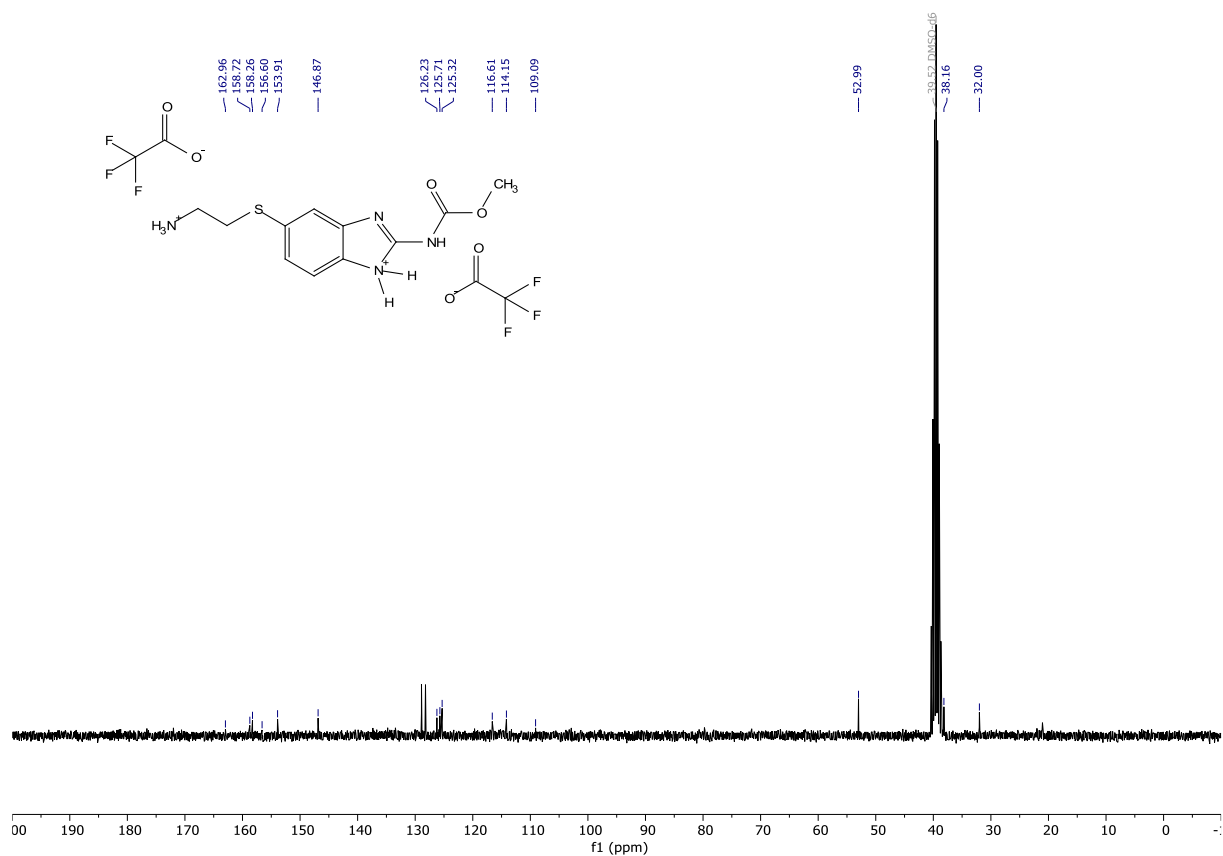
methyl (5-((2-((tert-butoxycarbonyl)amino)ethyl)thio)-1H-benzo[d]imidazol-2-yl)carbamate (AB03.1). (5-mercapto-1H-benzo[d]imidazol-2-yl)carbamate (0.09934 g, 0.2945 mmol) and 2-(Boc-amino)ethyl bromide (0.07693 g, 1.6957 mmol) was mixed in DMF (3 mL) to give a clear solution. To this was added potassium carbonate (0.477 g, 3.4514 mmol). The mixture was stirred at 21 °C for 1 h. The volatiles were removed under reduced pressure. The residue was taken up in a mixture of dichloromethane and methanol and filtered through a pad of celite. Then it was concentrated onto silica gel. The crude was purified by flash column chromatography (dichloromethane/ methanol gradient from 1:0 to 9:1). An impure product was isolated. Therefore, the mixture was concentrated onto silica gel and purified by flash column chromatography (cyclohexane/ ethyl acetate gradient from 1:0 to 0:1) giving the desired product in quantitative yield (0.10917 g, 0.29791 mmol). White solid: ¹H NMR (300 MHz, DMSO-*d*₆) δ 11.65 (bs, 2H), 7.47 (d, *J* = 1.7 Hz, 1H), 7.35 (d, *J* = 8.2 Hz, 1H), 7.14 (dd, *J* = 8.3, 1.8 Hz, 1H), 6.95 (t, *J* = 5.7 Hz, 1H), 3.75 (s, 3H), 3.14 – 3.01 (m, 2H), 2.94 – 2.82 (m, 2H), 1.35 (s, 9H). ¹³C NMR (101 MHz, DMSO) δ 155.40, 154.74, 147.88, 125.92, 124.43, 77.67, 52.42, 34.54, 28.17. HRMS (ESI) calculated for [M+Na]⁺ C₁₆H₂₁N₄NaO₄S 389.1254, found 389.1241.

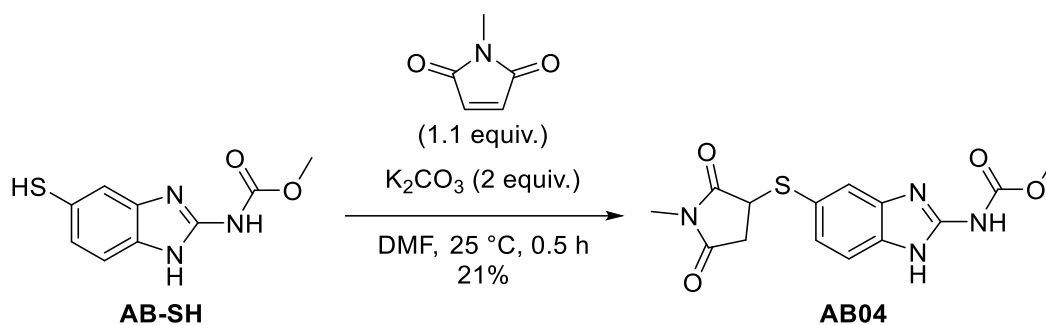




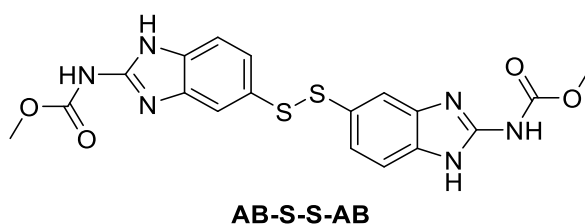
5-((2-ammonioethyl)thio)-2-((methoxycarbonyl)amino)-1H-benzo[d]imidazol-1-ium 2,2,2-trifluoroacetate (AB03). To a stirred suspension of methyl 5-((2-((*tert*-butoxycarbonyl)amino)ethyl)thio)-1H-benzo[d]imidazol-2-yl)carbamate in dichloromethane (5 mL) was added trifluoroacetic acid (0.5 mL, 0.74 g, 6.4901 mmol) which immediately gave a clear colourless solution. The mixture was stirred at room temperature for 1 h. The volatiles were removed under reduced pressure, to give the desired product in 91% yield (0.11264 g, 0.29615 mmol). White solid: $^1\text{H NMR}$ (300 MHz, DMSO- d_6) δ 10.25 (bs, 3H), 7.93 (s, 3H), 7.59 (d, $J = 1.7$ Hz, 1H), 7.47 (d, $J = 8.3$ Hz, 1H), 7.30 (dd, $J = 8.3, 1.8$ Hz, 1H), 3.80 (s, 3H), 3.16 – 3.05 (m, 2H), 3.01 – 2.84 (m, 2H). $^{13}\text{C NMR}$ (75 MHz, DMSO) δ 162.96, 158.72, 158.26, 156.60, 153.91, 146.87, 126.23, 125.71, 125.32, 116.61, 114.15, 109.09, 52.99, 38.16, 32.00. $^{19}\text{F NMR}$ (282 MHz, DMSO) δ -74.40. (NMR spectra contain acetonitrile and toluene as the compound was not fully dry yet). **HRMS** (ESI) calculated for $[\text{M}+\text{H}]^+$ $\text{C}_{11}\text{H}_{15}\text{N}_3\text{O}_2\text{S}$ 267.0910, found 267.0905.



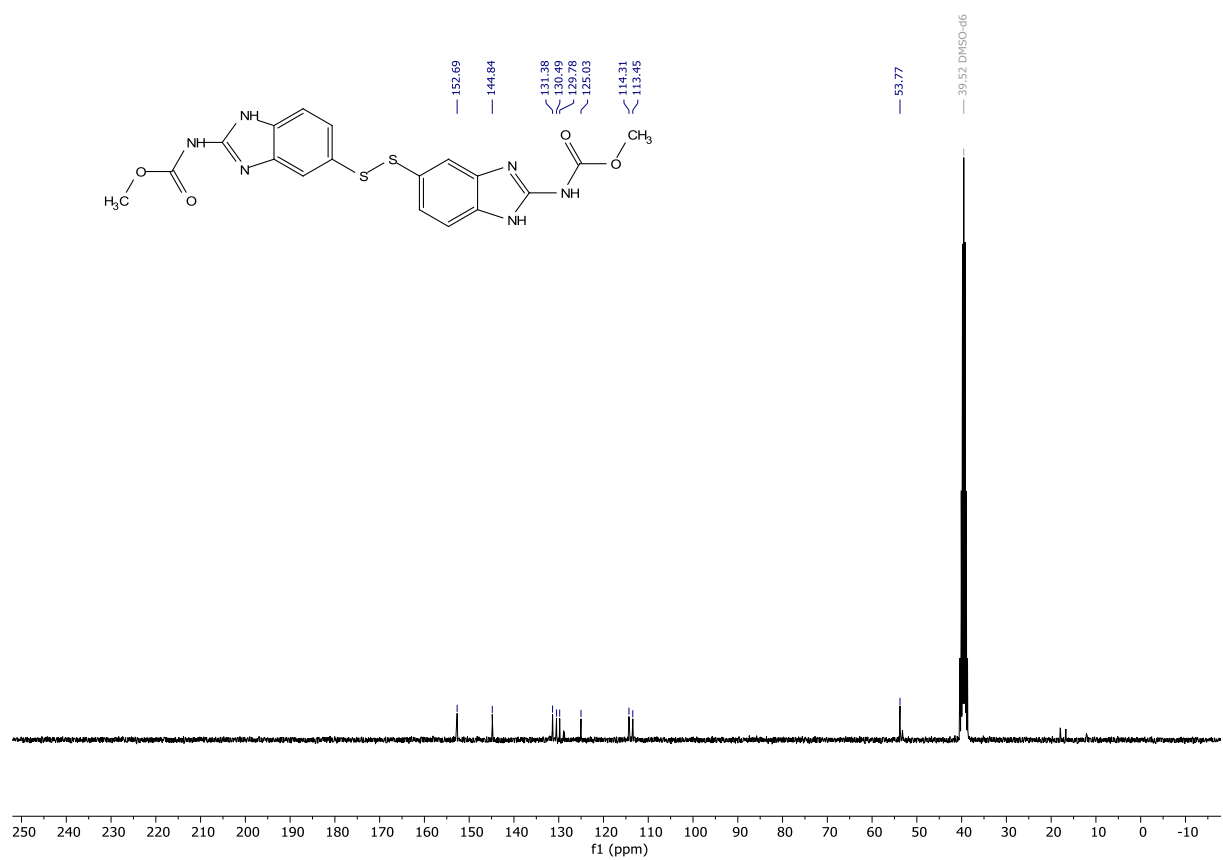
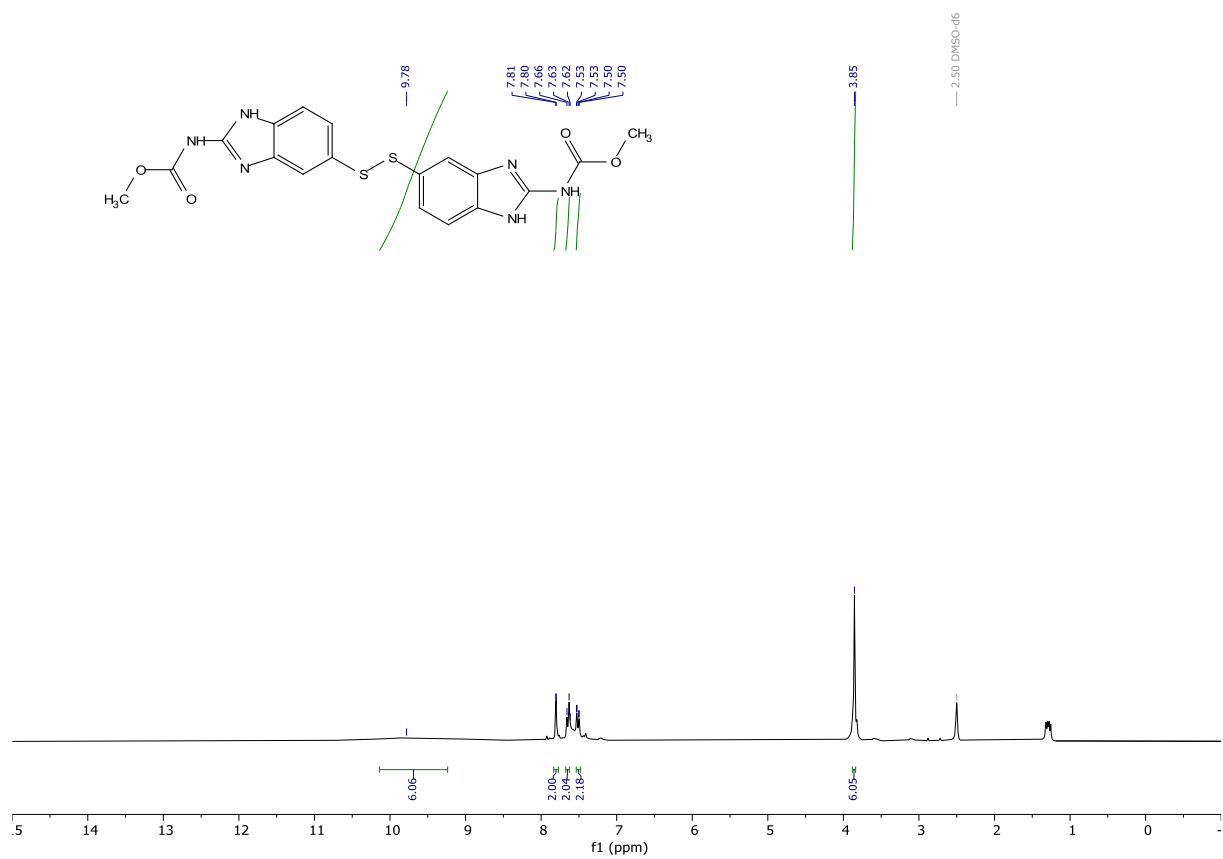




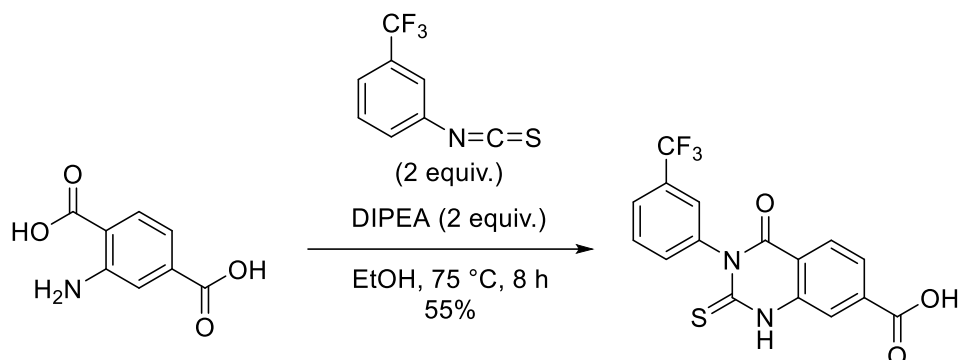
methyl (5-((1-methyl-2,5-dioxopyrrolidin-3-yl)thio)-1H-benzo[d]imidazol-2-yl)carbamate (AB04). To a stirred solution of (5-mercapto-1H-benzo[d]imidazol-2-yl)carbamate (0.06202 g, 0.1839 mmol) in dry DMF (2 mL) under an argon atmosphere was added *N*-Methylmaleimide (0.0244 g, 0.2196 mmol) to give a clear solution. To this was added potassium carbonate (0.05113 g, 0.3700 mmol). The mixture was stirred at 21 °C for 0.5 h. The volatiles were removed under reduced pressure. The residue was taken up in methanol and concentrated onto silica gel. The crude was purified by flash column chromatography (dichloromethane/ (methanol + 0.1% NEt₃) gradient from 1:0 to 9:1) to give the desired compound in 21% yield (0.01300 g, 0.03888 mmol). Off white solid: **NMR** was not measured due to the small amount obtained. **HRMS** (ESI) calculated for [M+H]⁺ C₁₁H₁₅N₄O₄S 335.0809, found 335.0787. **Purity (HPLC):** >95% UV₂₁₄, >95% UV₂₅₄.



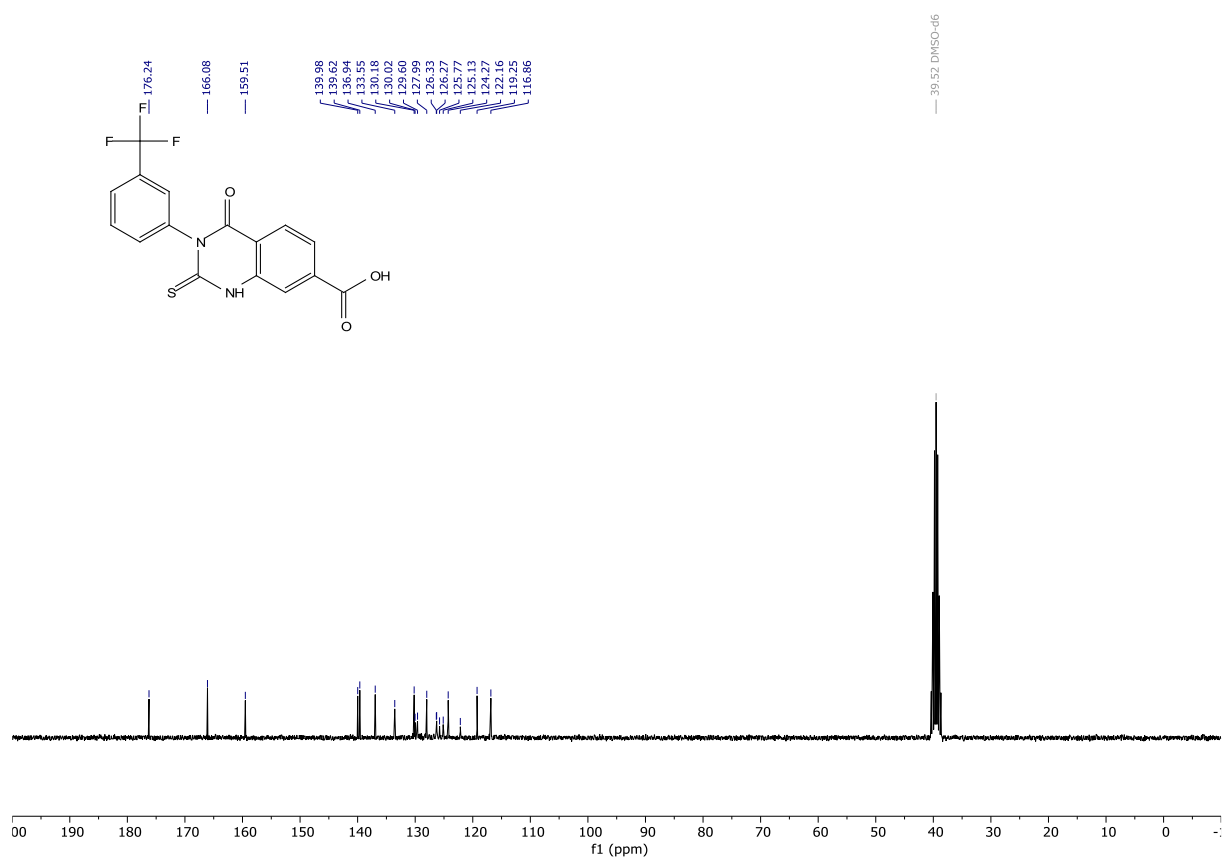
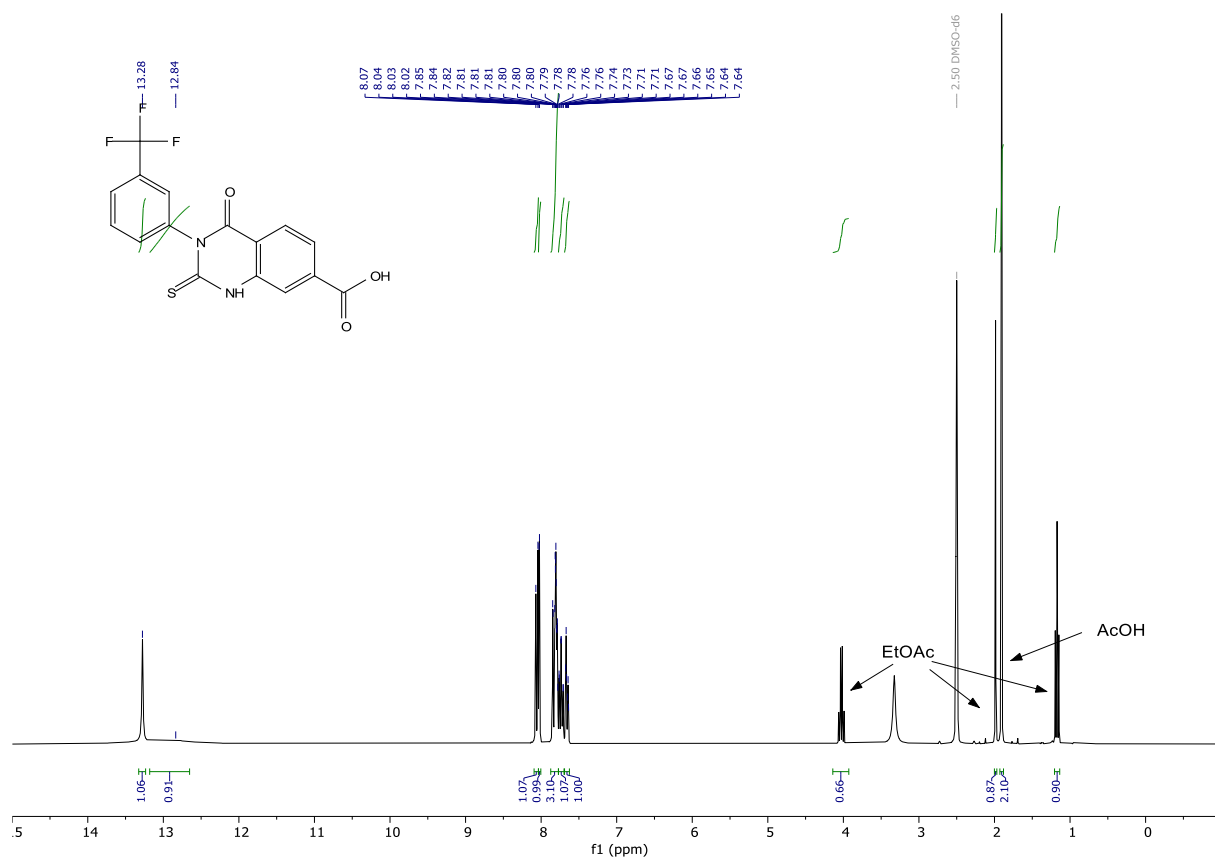
dimethyl (disulfanediyldis(1H-benzo[d]imidazole-5,2-diyl))dicarbamate (AB-S-S-AB). The product was isolated as a side product. White amorphous solid: **¹H NMR** (300 MHz, DMSO-*d*₆) δ 9.78 (bs, 6H), 7.80 (s, 2H), 7.64 (d, *J* = 8.4 Hz, 2H), 7.51 (dd, *J* = 8.5, 1.8 Hz, 2H), 3.85 (s, 6H). **¹³C NMR** (75 MHz, DMSO) δ 152.69, 144.84, 131.38, 130.49, 129.78, 125.03, 114.31, 113.45, 53.77. **HRMS** (ESI) calculated for [M+H]⁺ C₁₈H₁₇N₆O₄S 445.0747, found 445.0734.

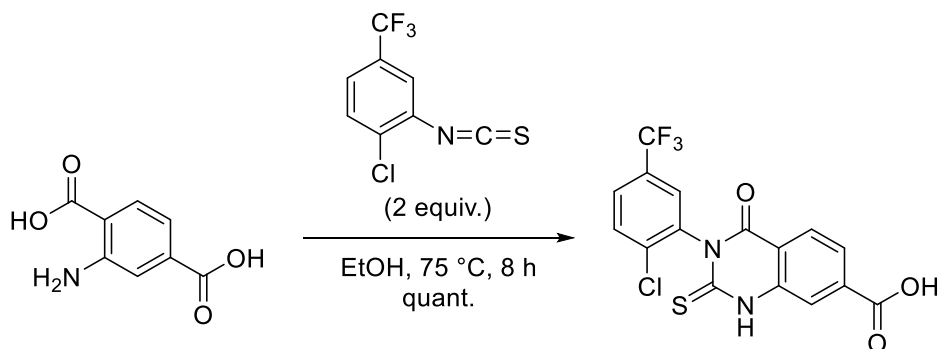


Synthesis of quinazolinecarboxamides Qc1-6



4-oxo-2-thioxo-3-(3-(trifluoromethyl)phenyl)-1,2,3,4-tetrahydroquinazoline-7-carboxylic acid (Qc0.1). To a stirred suspension of 2-aminoterephthalic acid (0.5079 g, 2.8038 mmol) in absolute ethanol (6 mL) at 75 °C DIPEA was added (1 mL, 0.76 g, 5.88 mmol), followed by 3-(trifluoromethyl)phenyl thioisocyanate (0.8 mL, 1.068 g, 5.25 mmol) the mixture was placed under an argon atmosphere and stirred for 8 h. The mixture was concentrated under reduced pressure. The residue was taken up in acetone and concentrated onto silica gel. The crude was purified by flash column chromatography (cyclohexane/ (ethyl acetate/ acetic acid 9:1) gradient from 1:0 to 0:1). The fractions containing the desired product were concentrated and co-evaporated with toluene to remove the acetic acid, to give the desired product in 55% yield (0.56025 g, 1.52942 mmol). Product was contaminated with ethyl acetate and acetic acid (purity ~83%, NMR) White solid: **¹H NMR** (300 MHz, DMSO-*d*₆) δ 13.28 (s, 1H), 12.84 (s, 1H), 8.06 (d, *J* = 8.2 Hz, 1H), 8.02 (d, *J* = 1.4 Hz, 1H), 7.87 – 7.77 (m, 3H), 7.77 – 7.70 (m, 1H), 7.66 (dt, *J* = 7.7, 1.8 Hz, 1H). **¹³C NMR** (75 MHz, DMSO) δ 176.24, 166.08, 159.51, 139.98, 139.62, 136.94, 133.55, 130.18, 130.02, 129.60, 127.99, 126.33, 126.27, 125.77, 125.13, 124.27, 122.16, 119.25, 116.86. **¹⁹F NMR** (282 MHz, DMSO) δ -60.97. **HRMS** (ESI) calculated for [M+H]⁺ C₁₆H₁₀F₃N₂O₃S 367.0359, found 367.0342.



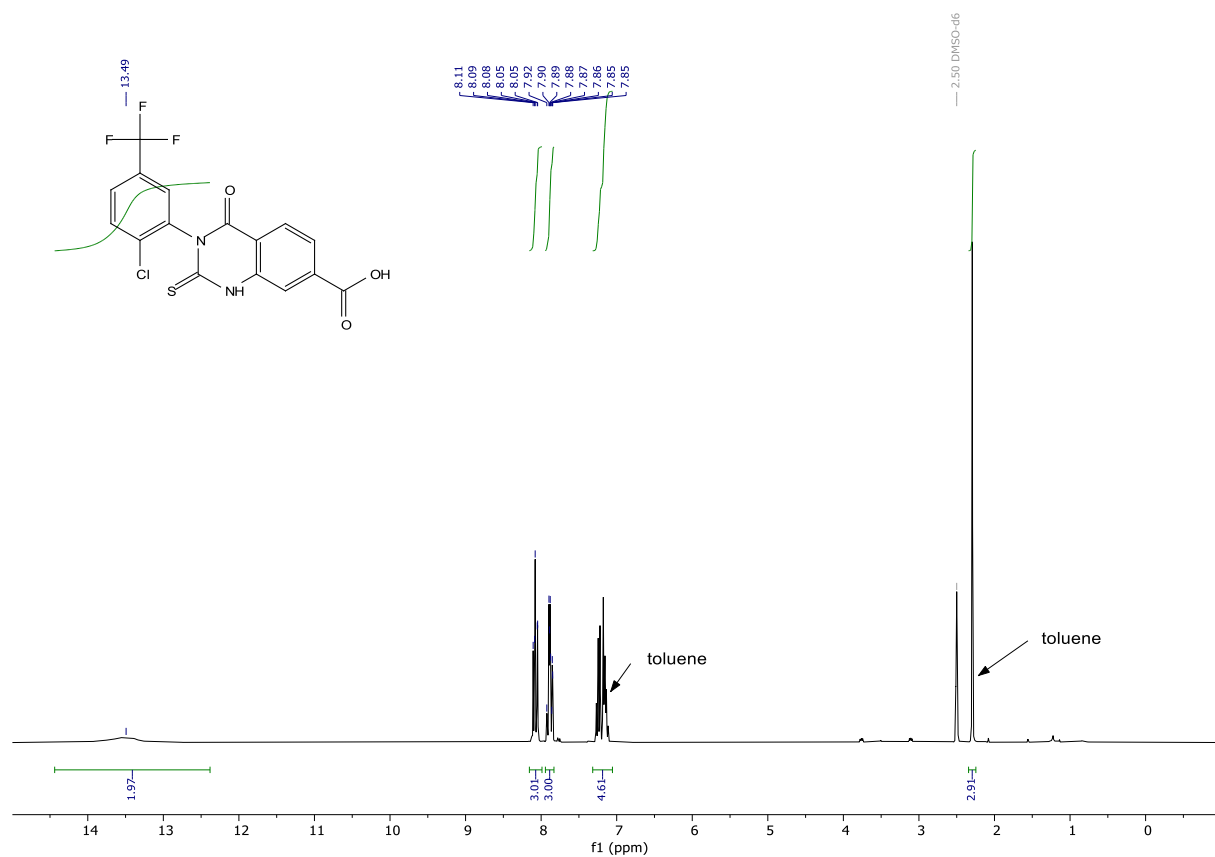


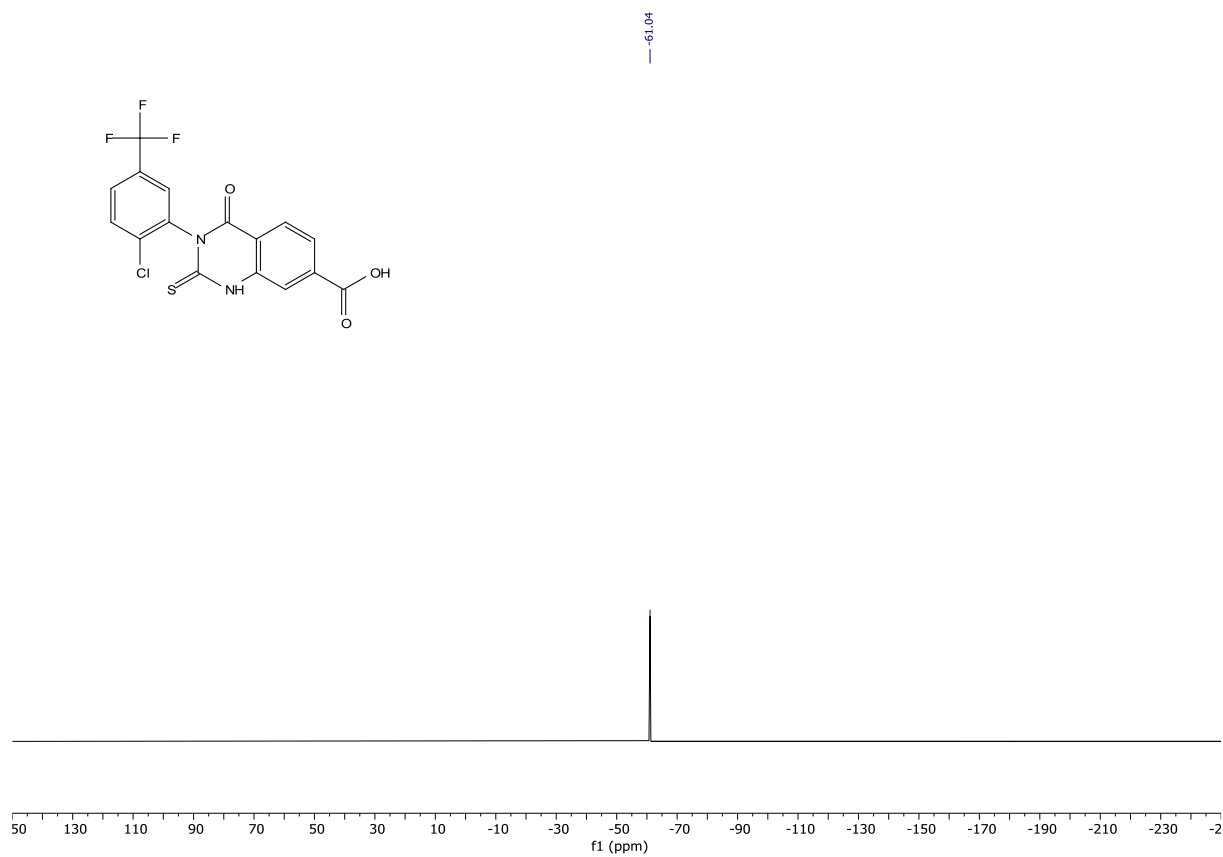
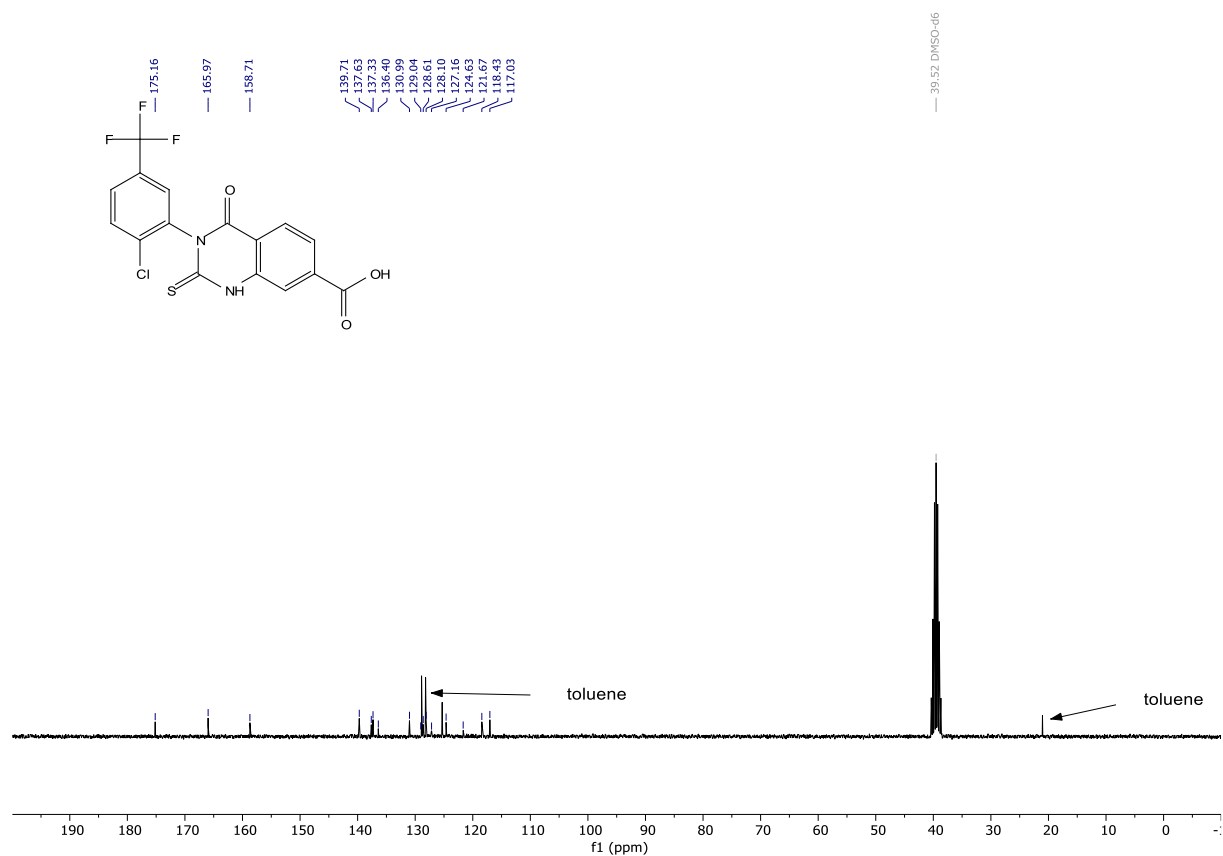
2-amino terephthalic acid

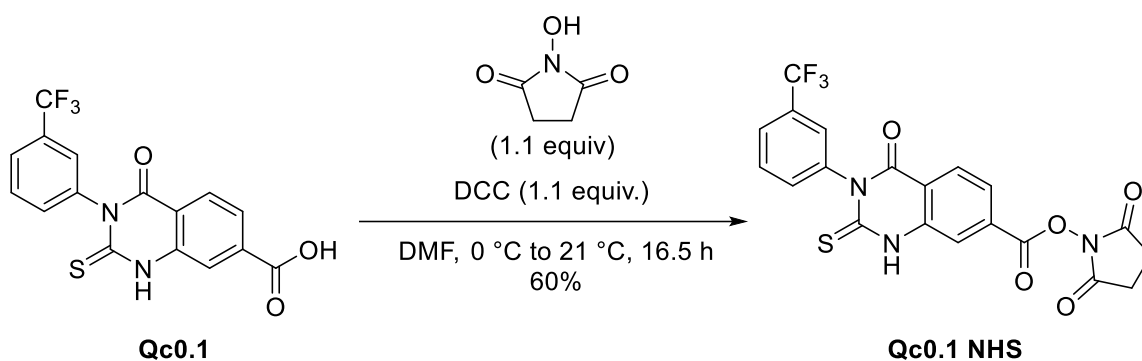
Qc0.2

3-(2-chloro-5-(trifluoromethyl)phenyl)-4-oxo-2-thioxo-1,2,3,4-tetrahydroquinazoline-7-carboxylic acid (Qc0.2). To a stirred suspension of 2-aminoterephthalic acid (0.11331 g, 0.6255 mmol) in absolute ethanol (2 mL), DIPEA (0.180 μL , 0.1368 g, 1.058 mmol) and 1-chloro-2-isothiocyanato-4-(trifluoromethyl)benzene (0.180 μL , 0.261 g, 1.098 mmol) was added. The mixture was heated to 75 °C and stirred for 8 h. The mixture was concentrated under reduced pressure. The residue was taken up in acetone and concentrated onto silica gel. The crude was purified by flash column chromatography (cyclohexane/ (ethyl acetate/ acetic acid 9:1) gradient from 1:0 to 0:1). The fractions containing the desired product were concentrated and co-evaporated with toluene to remove the acetic acid, to give the desired product in 131% yield (0.32843 g, 0.81953 mmol). Product was contaminated with toluene (purity ~80% NMR). Yellow solid: ^1H NMR (300 MHz, DMSO- d_6) δ 13.49 (s,

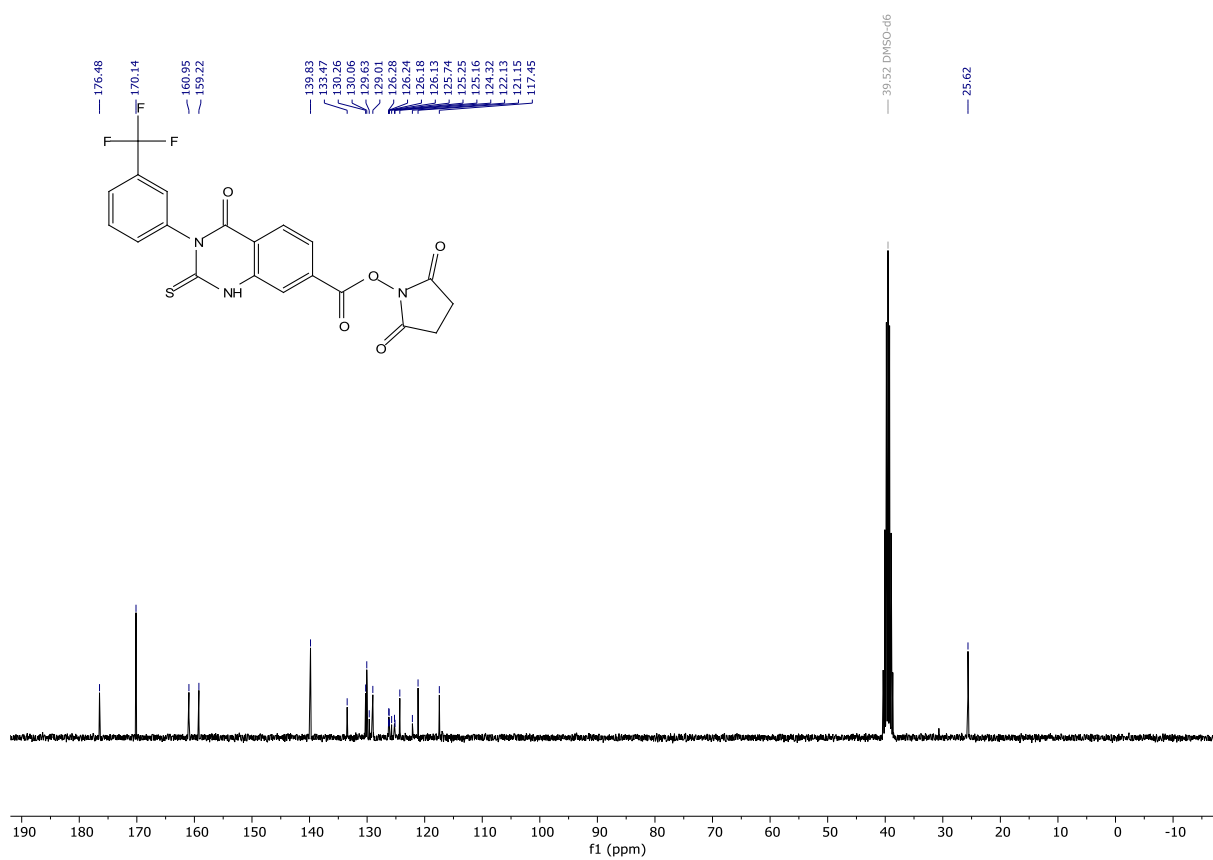
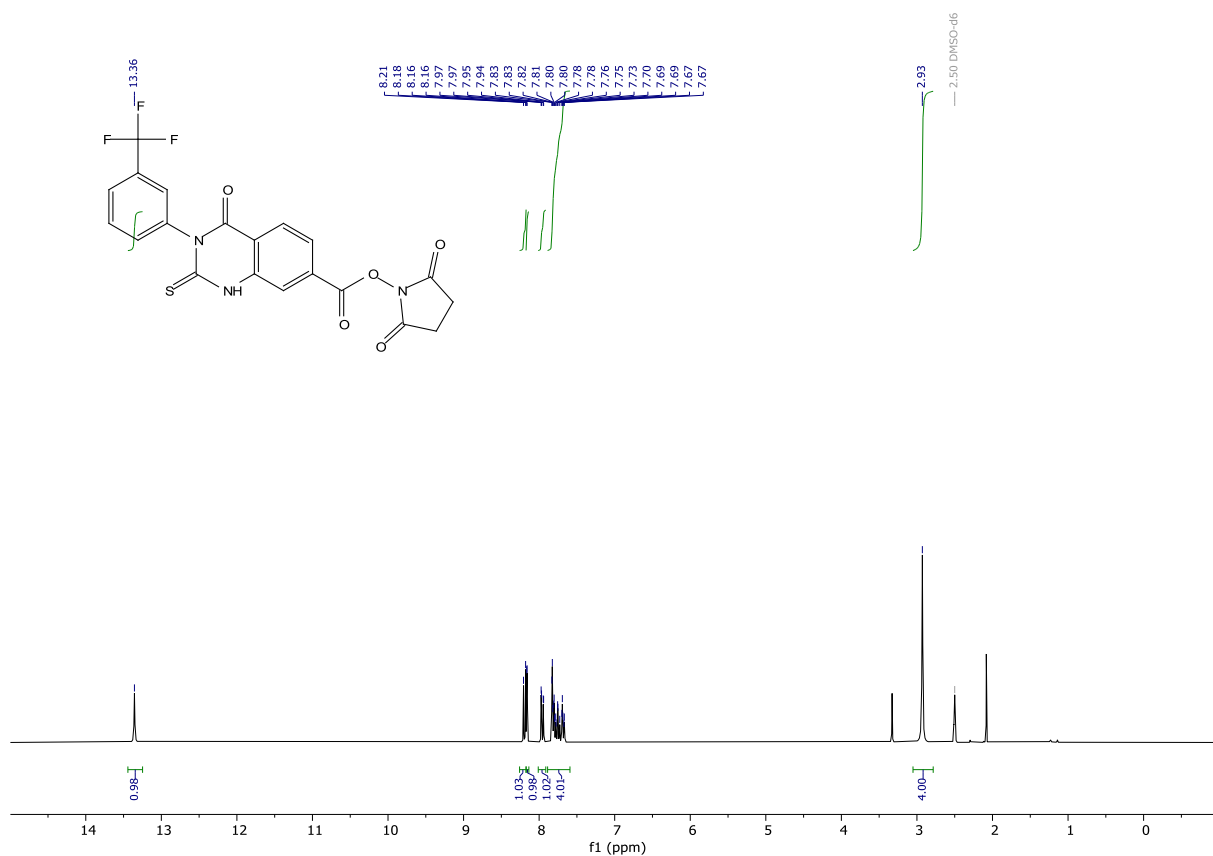
2H), 8.16 – 7.99 (m, 3H), 7.94 – 7.83 (m, 3H). **¹³C NMR** (75 MHz, DMSO) δ 175.16, 165.97, 158.71, 139.71, 137.63, 137.33, 136.40, 130.99, 129.04, 128.61, 128.10, 127.16, 124.63, 121.67, 118.43, 117.03. **¹⁹F NMR** (282 MHz, DMSO) δ -61.04. **HRMS** (ESI) calculated for [M+H]⁺ C₁₆H₉ClF₃N₂O₃S 400.9969, found 400.9957.

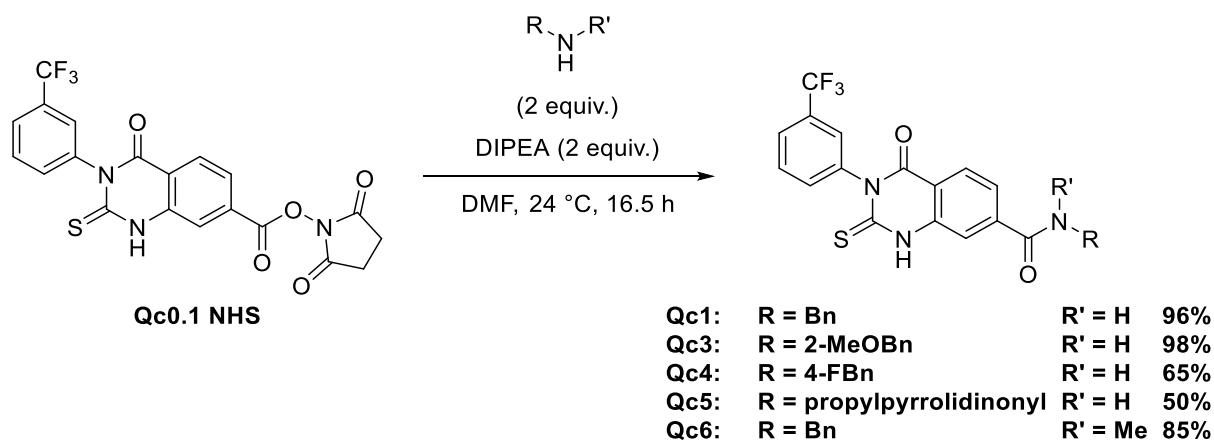






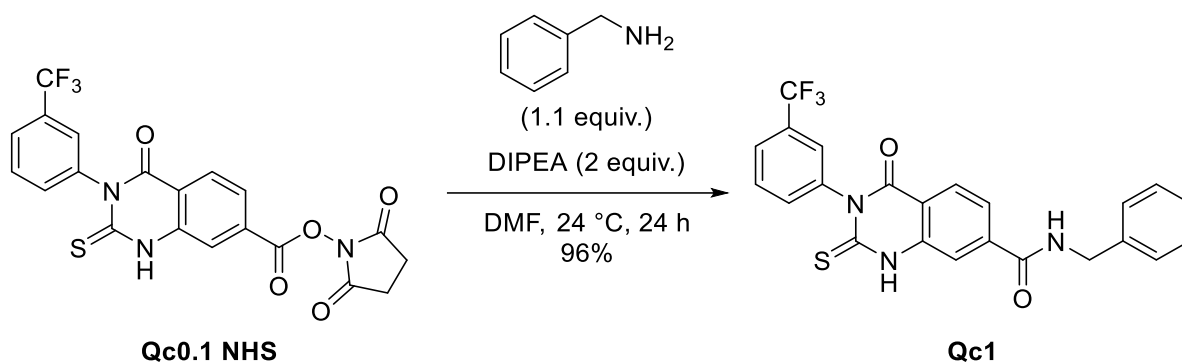
2,5-dioxopyrrolidin-1-yl 4-oxo-2-thioxo-3-(3-(trifluoromethyl)phenyl)-1,2,3,4-tetrahydroquinazoline-7-carboxylate (Qc0.1 NHS). To a stirred solution of 4-oxo-2-thioxo-3-(3-(trifluoromethyl)phenyl)-1,2,3,4-tetrahydroquinazoline-7-carboxylic acid (0.20167 g, 0.5504 mmol) in dry DMF at 0 °C under an argon atmosphere was added DCC (0.12390 mg, 0.6006 mmol). The mixture was stirred for 30 minutes. Then was added *N*-hydroxysuccinimide (0.0931 g, 0.80893 mmol). The mixture was stirred for 16 h. The volatiles were removed under reduced pressure. The residue was taken up in acetone and concentrated onto silica gel. The crude was purified by flash column chromatography (cyclohexane/ ethyl acetate gradient from 1:0 to 0:1) to give the desired product in 94% (0.23975 g, 0.51738 mmol). Product was contaminated with cyclohexane and ethyl acetate (purity ~64%, NMR) White solid: $^1\text{H NMR}$ (300 MHz, DMSO- d_6) δ 13.36 (s, 1H), 8.19 (d, J = 8.3 Hz, 1H), 8.16 (d, J = 1.6 Hz, 1H), 7.96 (dd, J = 8.3, 1.6 Hz, 1H), 7.89 – 7.59 (m, 4H), 2.93 (s, 4H). $^{13}\text{C NMR}$ (75 MHz, DMSO) δ 176.48, 170.14, 160.95, 159.22, 139.83, 133.47, 130.26, 130.06, 129.63, 129.01, 126.21 (q, J = 3.9 Hz), 125.74, 125.25 (m), 124.32, 122.13, 121.15, 117.45, 25.62. $^{19}\text{F NMR}$ (282 MHz, DMSO) δ -60.98. **HRMS** (ESI) calculated for $[\text{M}+\text{H}]^+$ $\text{C}_{20}\text{H}_{13}\text{F}_3\text{N}_3\text{O}_5\text{S}$ 464.0523, found 464.0511.





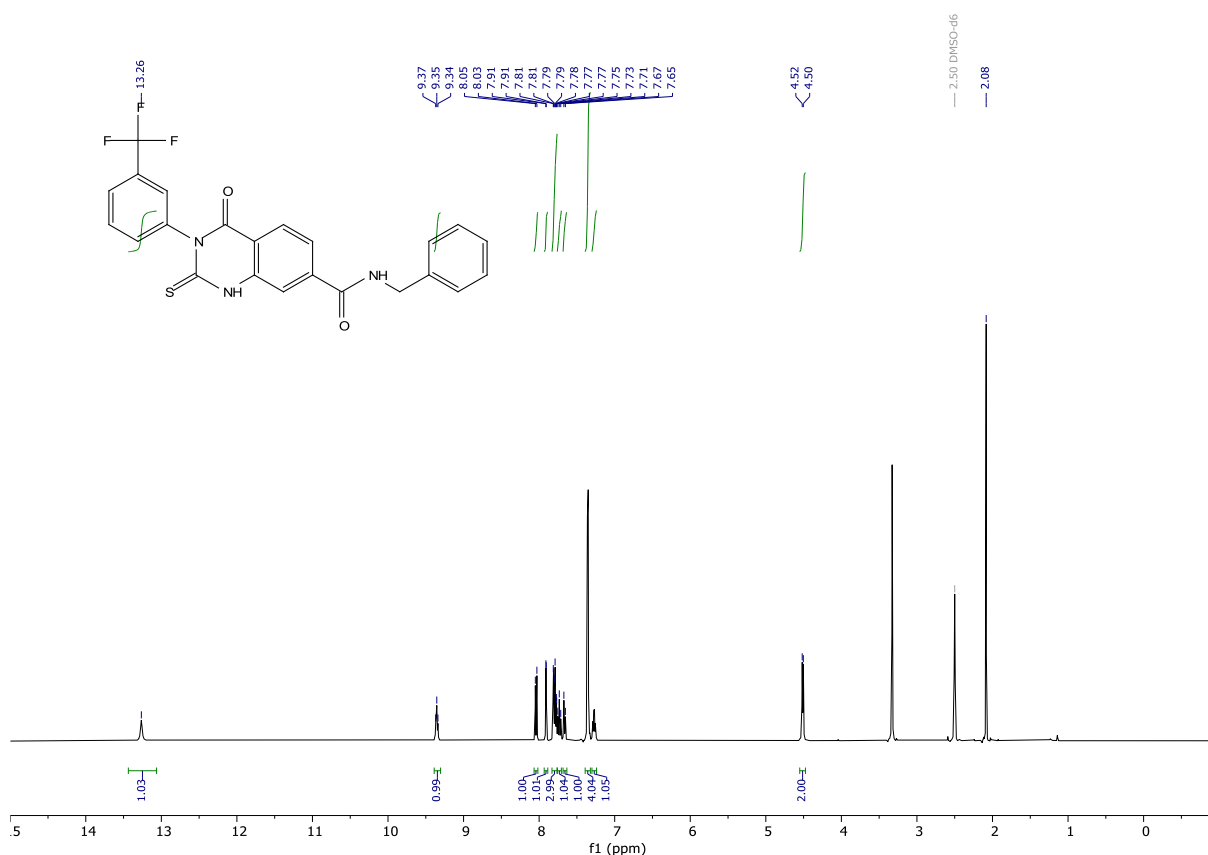
General procedure I: Synthesis of Qc amides from Qc0.1 NHS

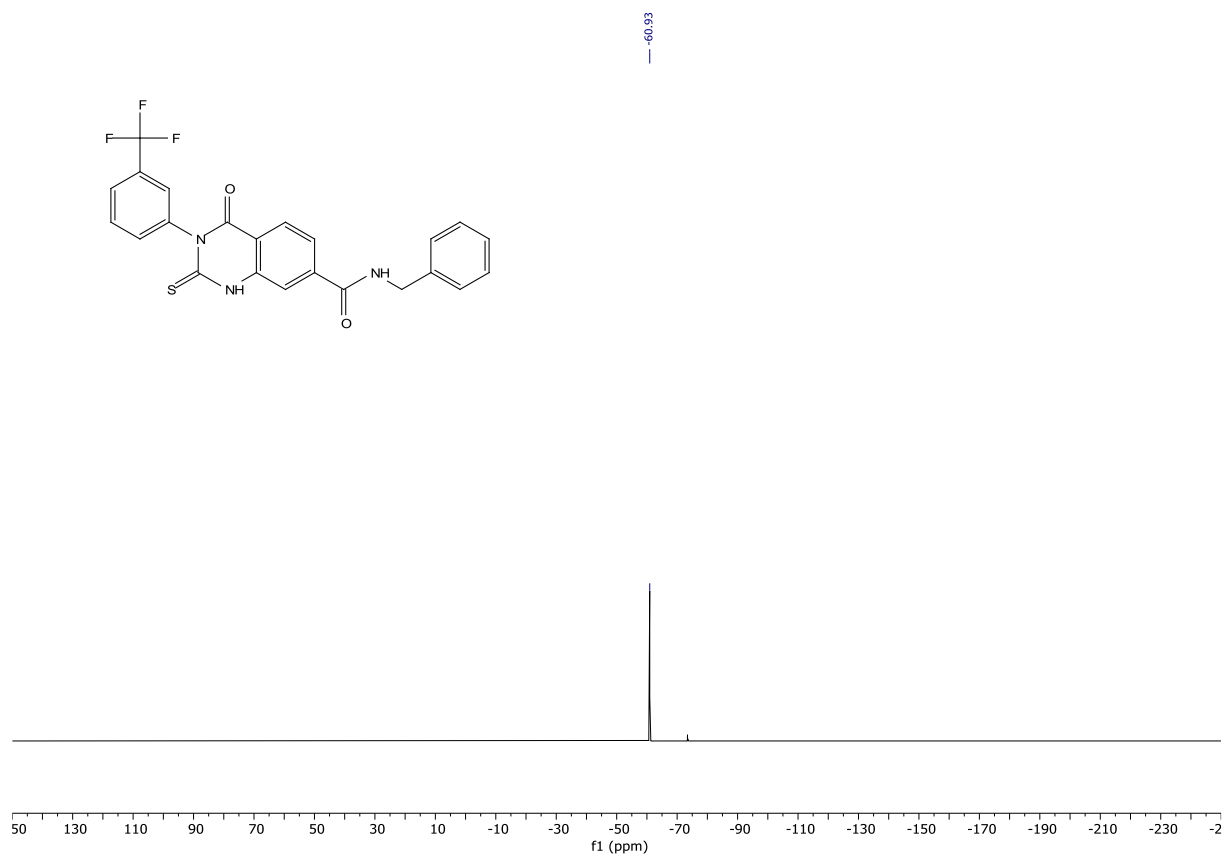
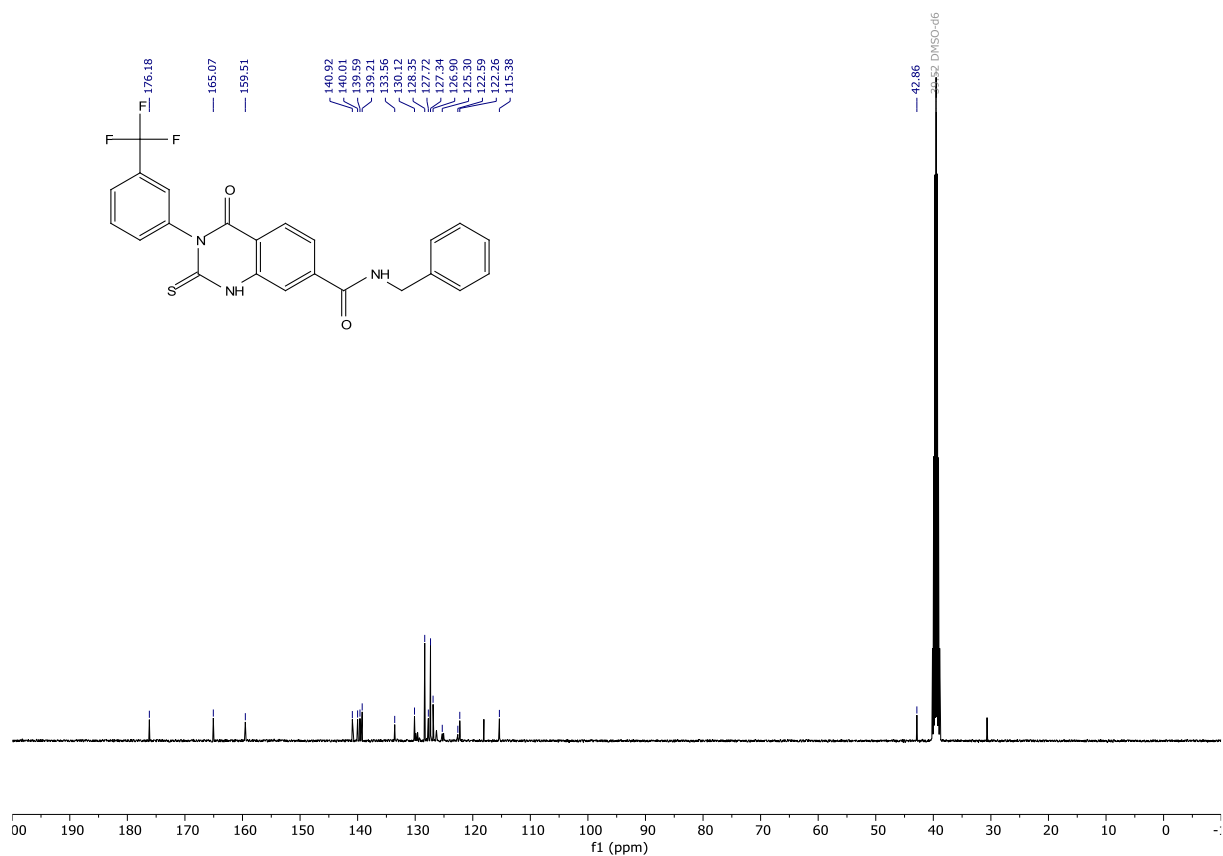
To a stirred solution of 2,5-dioxopyrrolidin-1-yl 4-oxo-2-thioxo-3-(3-(trifluoromethyl)phenyl)-1,2,3,4-tetrahydroquinazoline-7-carboxylate (Qc0.1 NHS) in dry dimethylformamide (0.1 M) at 24 °C under an argon atmosphere was added *N,N*-Diisopropylethylamine (2 equiv.). Then the corresponding amine (2 equiv.) was added. The mixture was stirred for 24 h. The volatiles were removed. The residue was taken up in a mixture of acetonitrile and methanol and concentrated onto silica gel. The crude was purified by reverse phase flash column chromatography (water +0.1% TFA/ acetonitrile 0.1% TFA gradient from 1:0 to 0:1), to give the desired product.

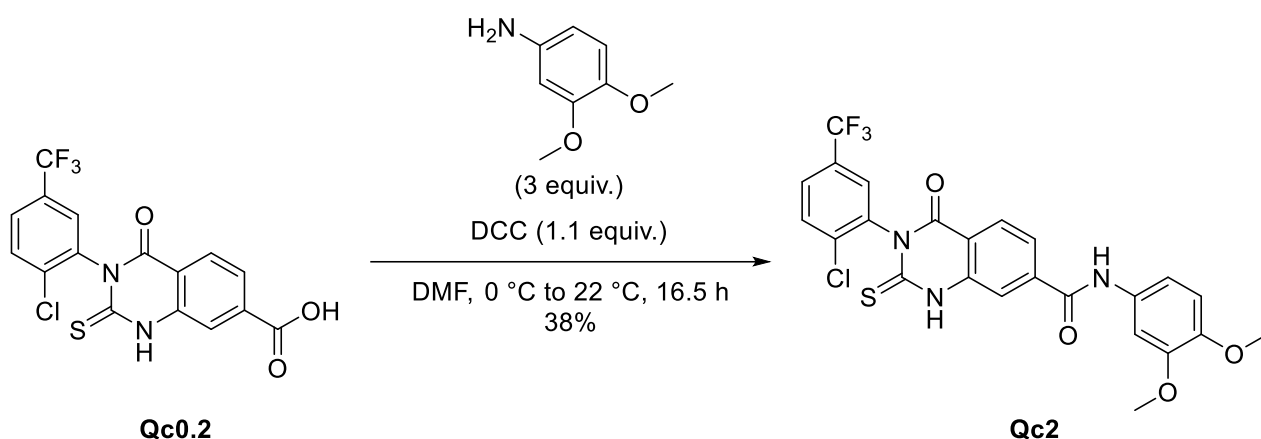


***N*-benzyl-4-oxo-2-thioxo-3-(3-(trifluoromethyl)phenyl)-1,2,3,4-tetrahydroquinazoline-7-**

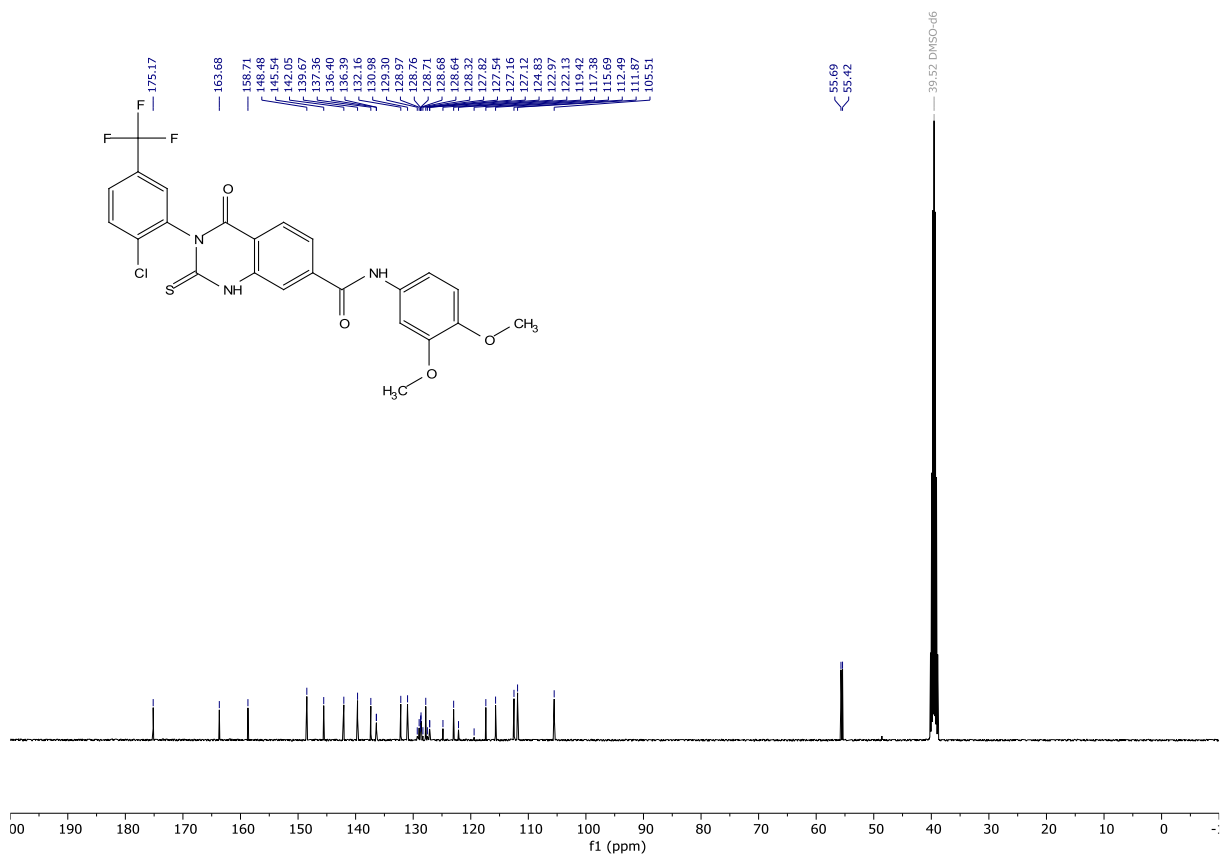
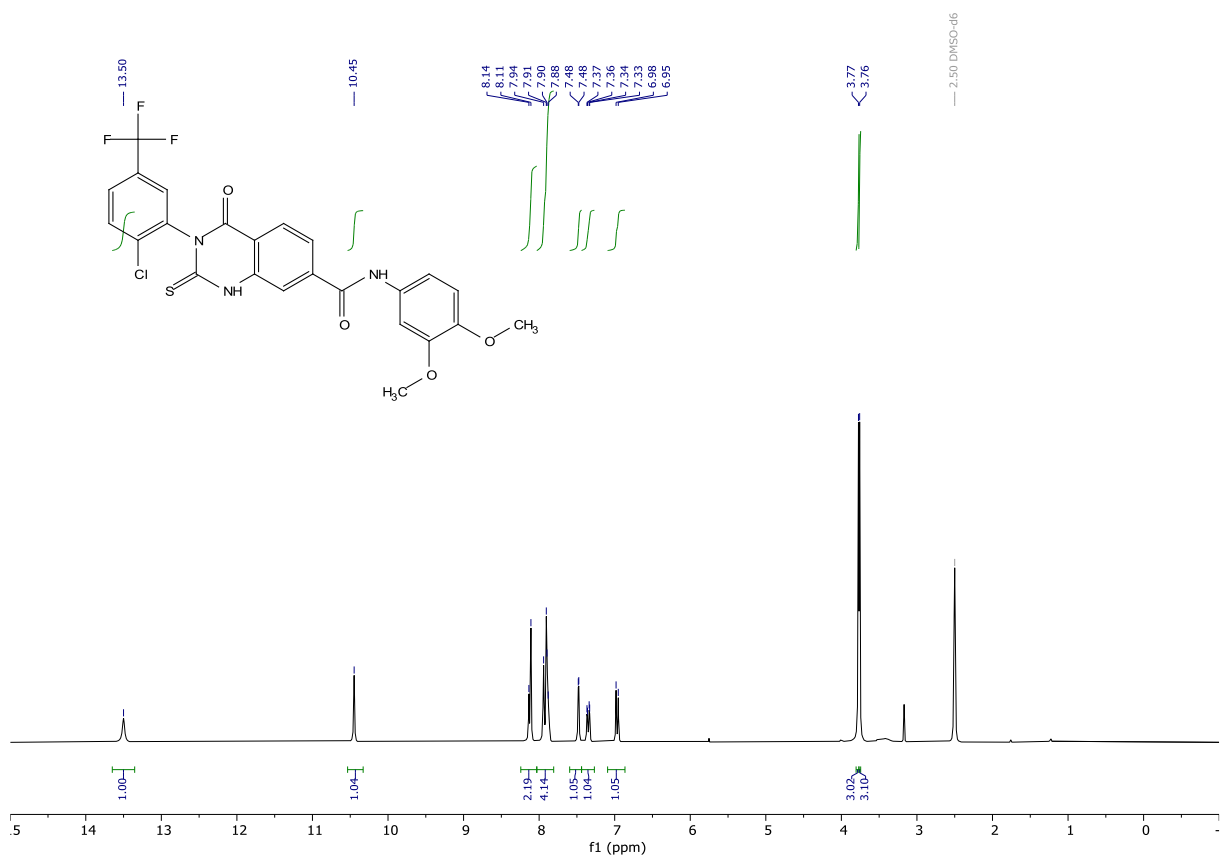
carboxamide (Qc1). According to general procedure I: 96% yield (0.09529 g, 0.2094 mmol). White solid: ^1H NMR (400 MHz, DMSO- d_6) δ 13.26 (s, 1H), 9.35 (t, J = 6.0 Hz, 1H), 8.04 (d, J = 8.2 Hz, 1H), 7.91 (d, J = 1.5 Hz, 1H), 7.83 – 7.76 (m, 3H), 7.73 (t, J = 7.7 Hz, 1H), 7.66 (d, J = 8.1 Hz, 1H), 7.36 (d, J = 4.3 Hz, 4H), 7.30 – 7.24 (m, 1H), 4.51 (d, J = 5.9 Hz, 2H). ^{13}C NMR (101 MHz, DMSO) δ 176.18, 165.07, 159.51, 140.92, 140.01, 139.59, 139.21, 133.56, 130.12, 129.74 (q, J = 32.1 Hz), 128.35, 127.72, 127.34, 126.90, 126.43 – 126.17 (m), 125.30, 125.06 (d, J = 3.4 Hz), 122.59, 122.26, 115.38, 42.86, 30.67. ^{19}F NMR (282 MHz, DMSO) δ -60.93. HRMS (ESI) calculated for $[\text{M}+\text{H}]^+$ $\text{C}_{23}\text{H}_{17}\text{F}_3\text{N}_3\text{O}_2\text{S}$ 456.0988, found 456.0979.

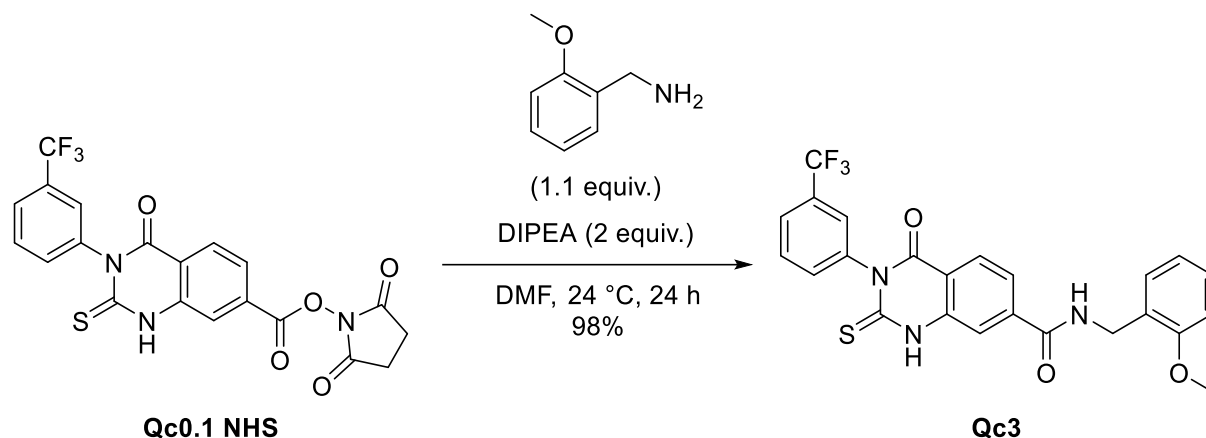
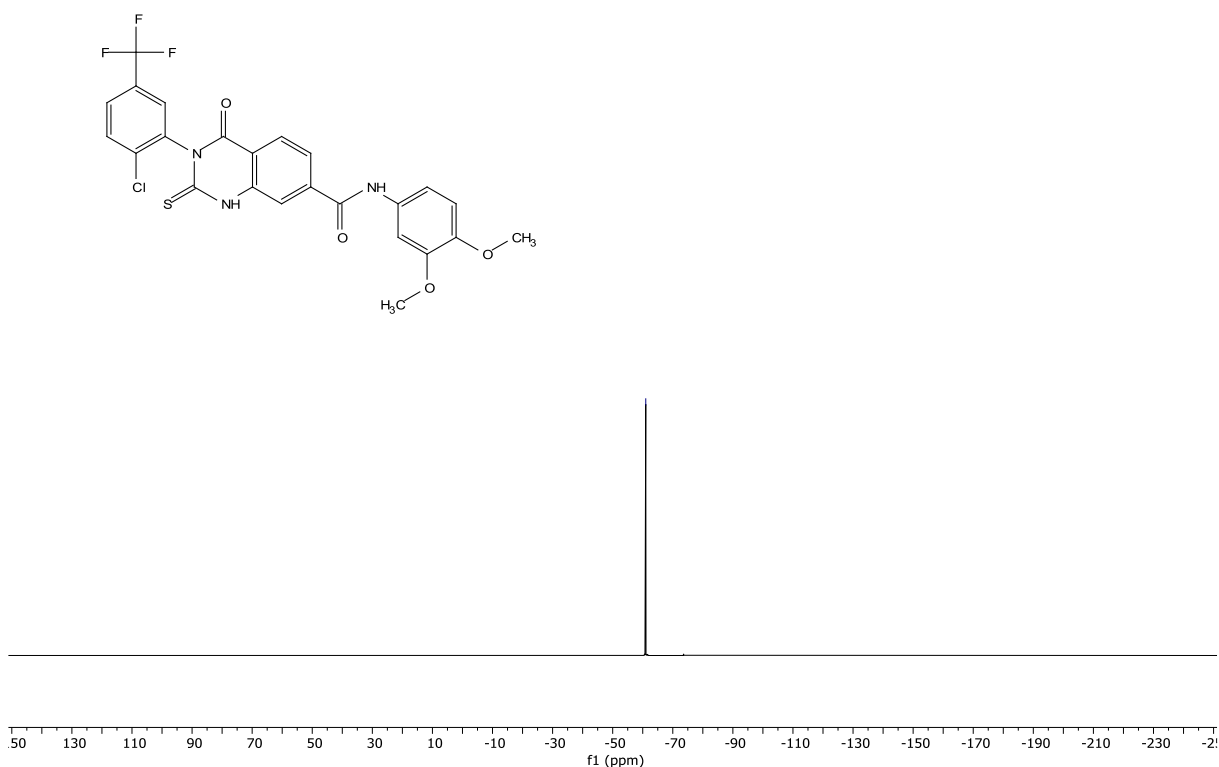






3-(2-chloro-5-(trifluoromethyl)phenyl)-N-(3,4-dimethoxyphenyl)-4-oxo-2-thioxo-1,2,3,4-tetrahydroquinazoline-7-carboxamide (Qc2). To a stirred solution of 3-(2-chloro-5-(trifluoromethyl)phenyl)-4-oxo-2-thioxo-1,2,3,4-tetrahydroquinazoline-7-carboxylic acid (0.1169 g, 0.2917 mmol) in dry DMF (2 mL) at 0 °C under an argon atmosphere was added DCC (0.077 g, 0.3732 mmol) and the mixture was stirred for 30 minutes. Then was added 3,4-Dimethoxyaniline (0.133 g, 0.8683 mmol) and the mixture was stirred for 16 h whilst warming to 22 °C. Then the volatiles were removed. The residue was taken up in a mixture of acetonitrile/ water with little TFA. The crude was purified by reverse phase flash column chromatography (water + 0.1% TFA/ MeCN + 0.1% TFA gradient from 1:0 to 0:1), to give the desired compound in 38% yield (0.05885 g, 0.1098 mmol). Yellow solid: ¹H NMR (300 MHz, DMSO-*d*₆) δ 13.50 (s, 1H), 10.45 (s, 1H), 8.12 (d, *J* = 8.1 Hz, 2H), 8.03 – 7.81 (m, 4H), 7.48 (d, *J* = 2.0 Hz, 1H), 7.35 (dd, *J* = 8.7, 2.0 Hz, 1H), 6.97 (d, *J* = 8.8 Hz, 1H), 3.77 (s, 3H), 3.76 (s, 3H). ¹³C NMR (101 MHz, DMSO) δ 175.65, 164.16, 159.19, 148.96, 146.03, 142.53, 140.15, 137.84, 136.88, 136.87, 132.64, 131.46, 129.29 (q, *J* = 32.9 Hz), 129.18 (q, *J* = 7.6, 3.8 Hz), 127.76 – 127.45 (m), 128.30, 123.96 (q, *J* = 272.3 Hz), 123.46, 117.86, 116.17, 112.98, 112.35, 105.99, 56.18, 55.90. ¹⁹F NMR (282 MHz, DMSO) δ -61.01. HRMS (ESI) calculated for [M+H]⁺ C₂₄H₁₇ClF₃N₃O₄S 536.0653, found 536.0620. Purity (HPLC) >93% (at 214 nm), >96% (at 254 nm).

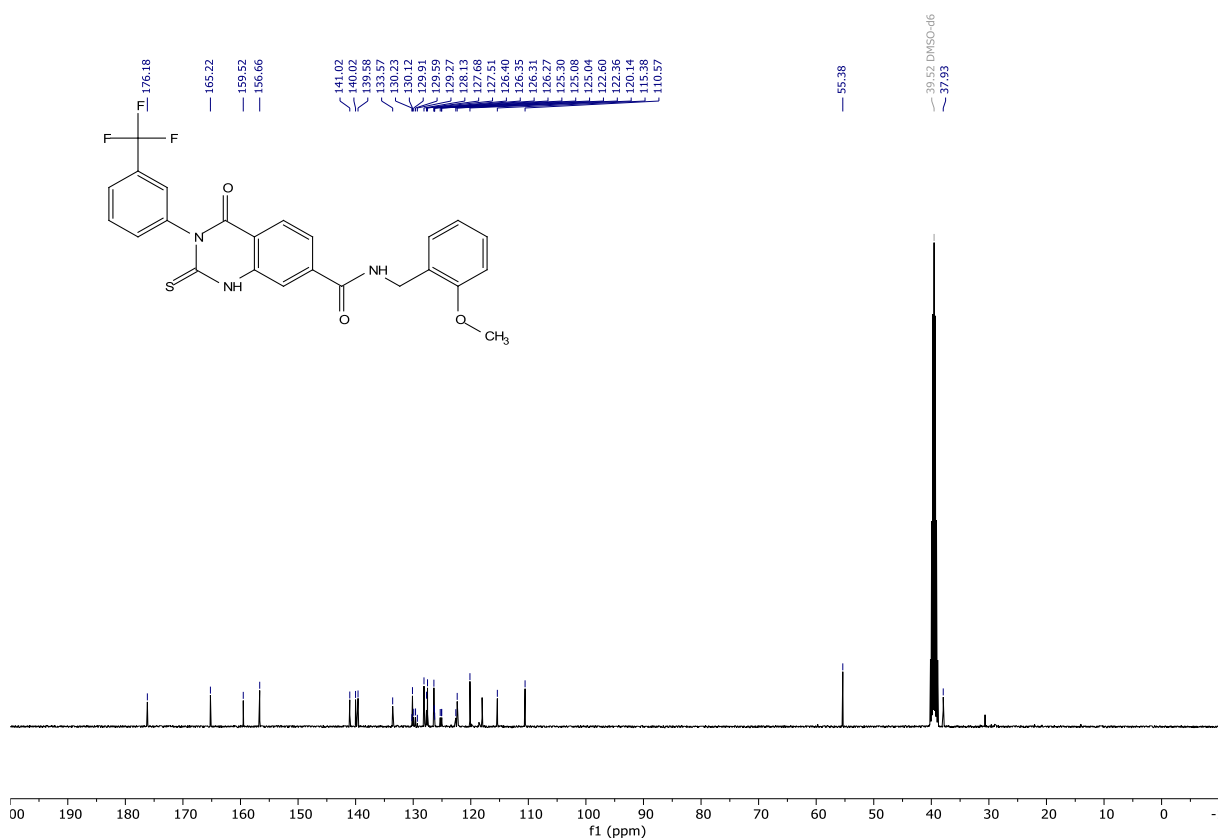
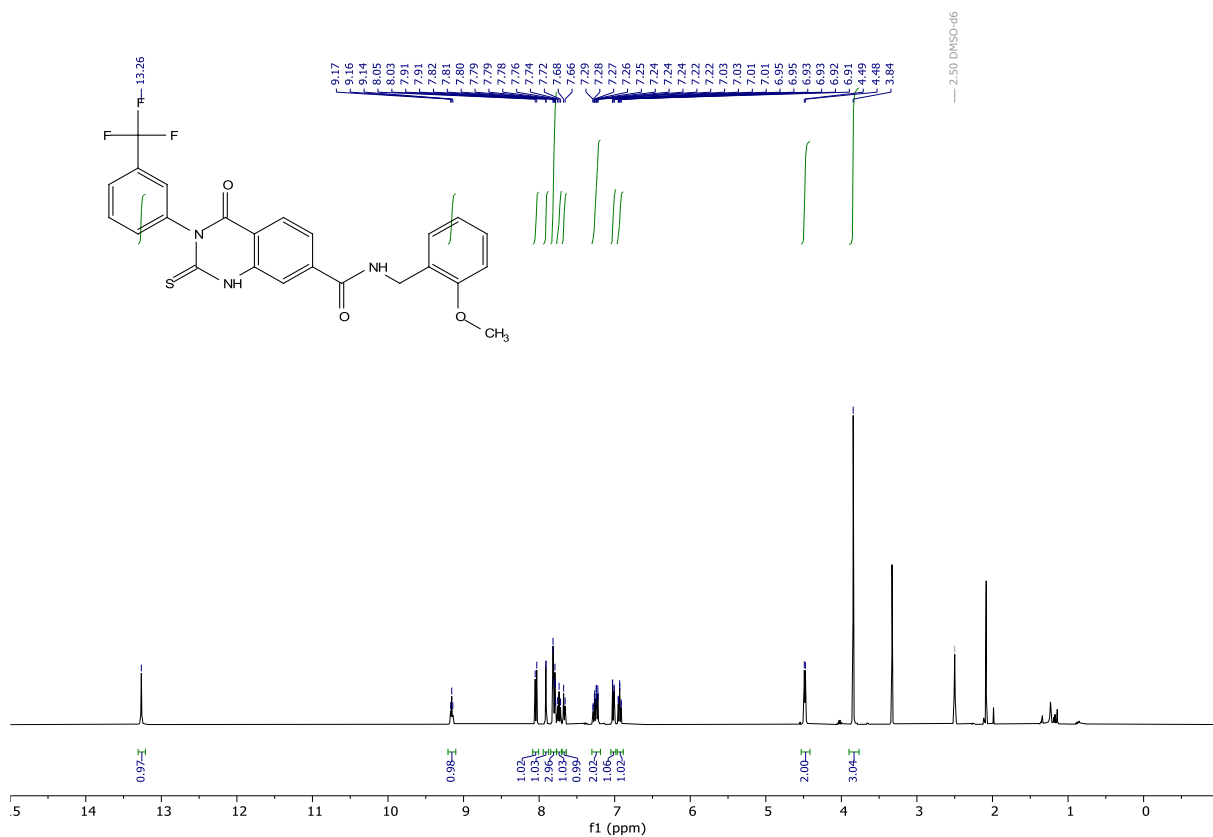


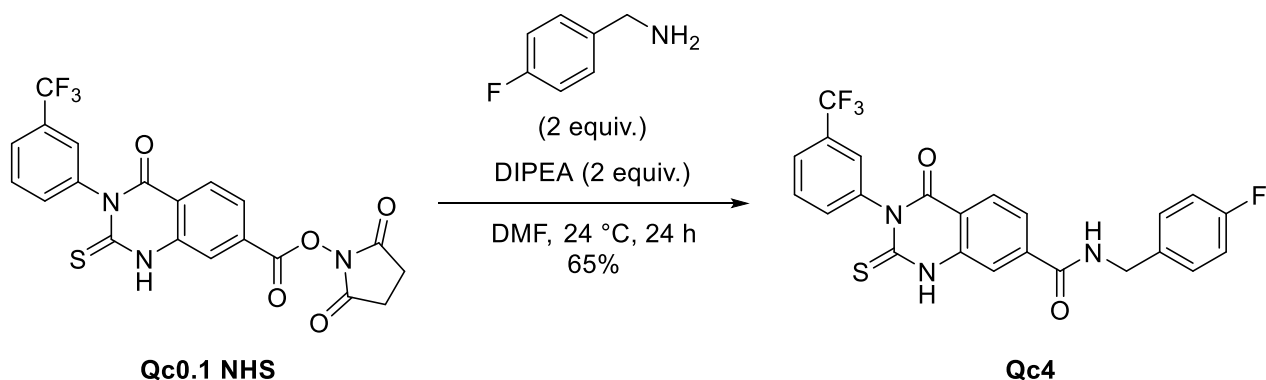


***N*-(2-methoxybenzyl)-4-oxo-2-thioxo-3-(3-(trifluoromethyl)phenyl)-1,2,3,4-tetrahydroquinazoline-7-carboxamide (Qc3).** According to general procedure I: 98% yield (0.10493 g, 0.21614 mmol). White solid: ¹H NMR (400 MHz, DMSO-*d*₆) δ 13.26 (s, 1H), 9.16 (t, *J* = 5.8 Hz, 1H), 8.04 (d, *J* = 8.3 Hz, 1H), 7.91 (d, *J* = 1.6 Hz, 1H), 7.80 (dd, *J* = 9.9, 1.7 Hz, 3H), 7.74 (t, *J* = 7.8 Hz, 1H), 7.67 (d, *J* = 7.8 Hz, 1H), 7.30 – 7.19 (m, 2H), 7.02 (dd, *J* = 8.2, 1.1 Hz, 1H), 6.93 (td, *J* = 7.4, 1.1 Hz, 1H), 4.48 (d, *J* = 5.7 Hz, 2H), 3.84 (s, 3H). ¹³C NMR (101 MHz, DMSO) δ 176.18, 165.22, 159.52, 156.66, 141.02, 140.02, 139.58, 133.57, 130.12, 129.75 (q, *J* = 32.1 Hz), 128.13, 127.68, 127.51, 126.51 – 126.20 (m), 126.40, 125.30, 125.22 –

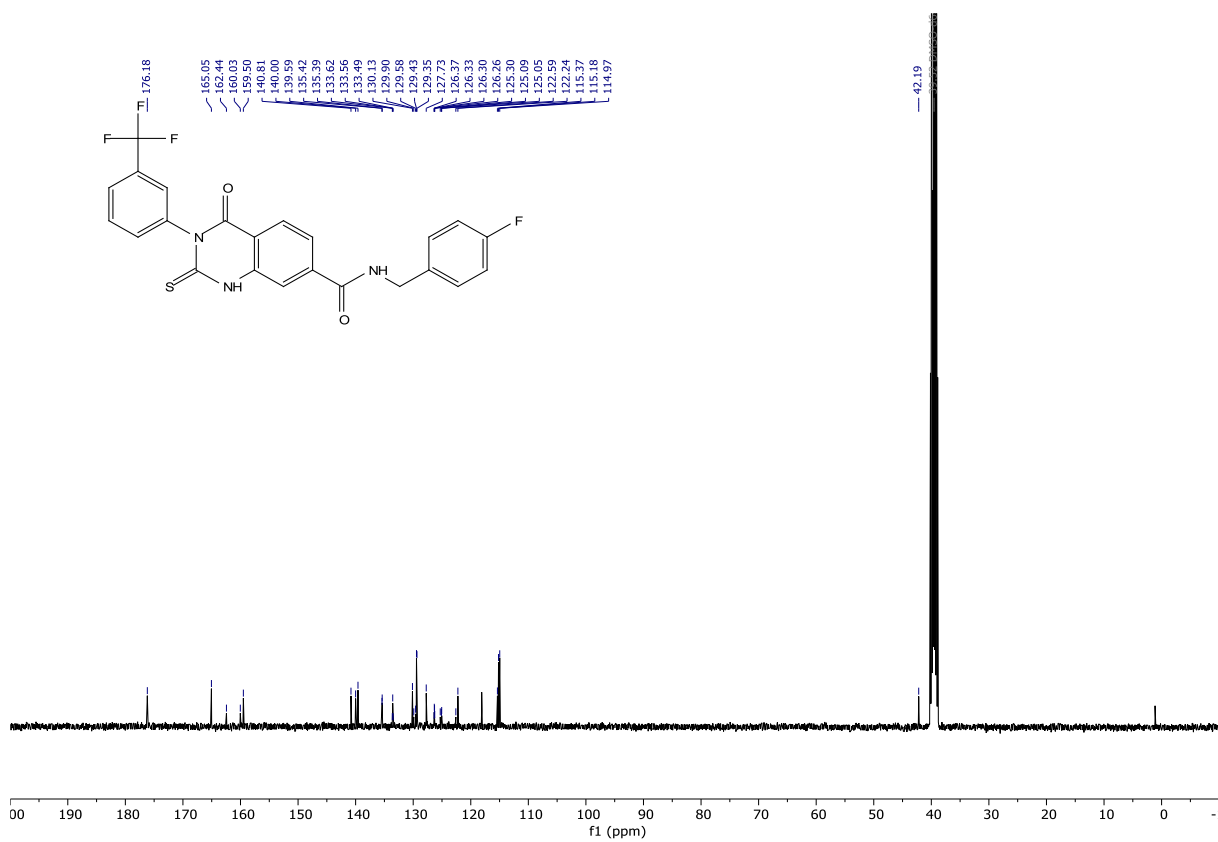
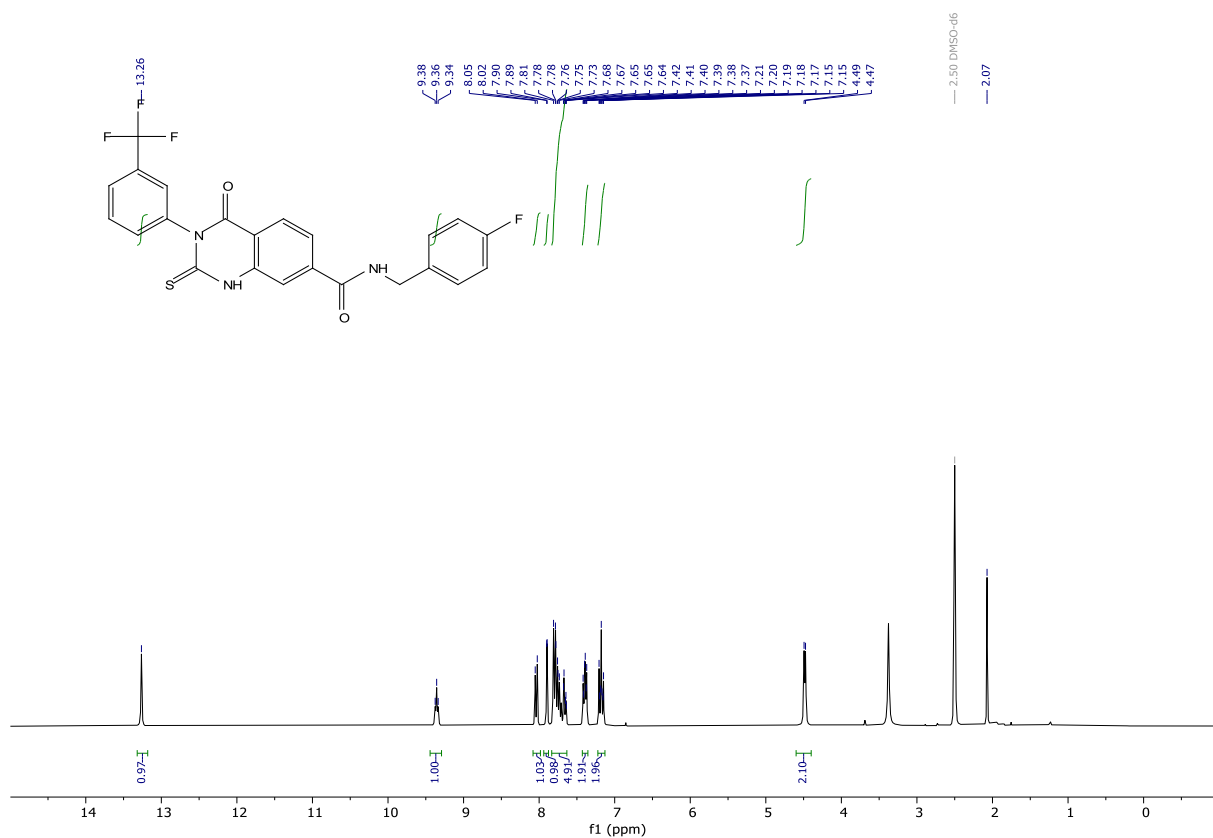
124.87 (m), 122.60, 122.36, 120.14, 115.38, 110.57, 55.38, 37.93. ^{19}F NMR (282 MHz, DMSO) δ -60.93.

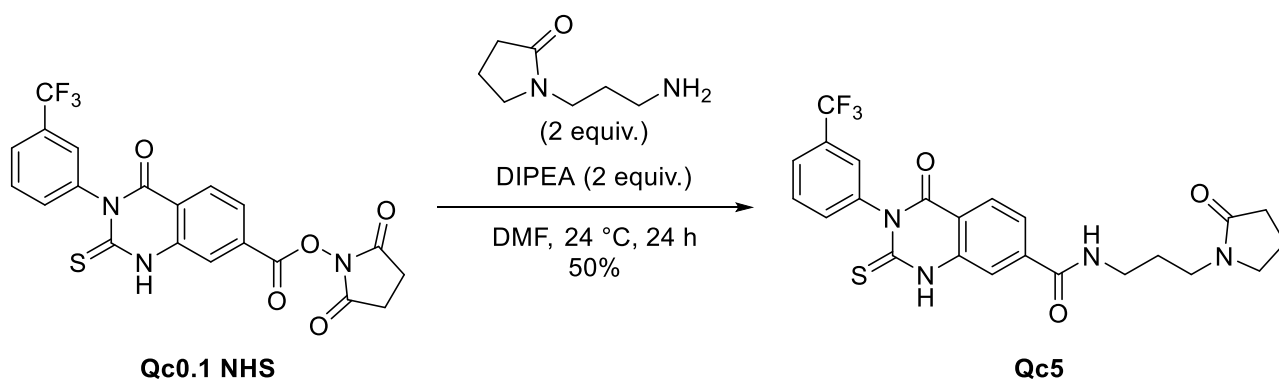
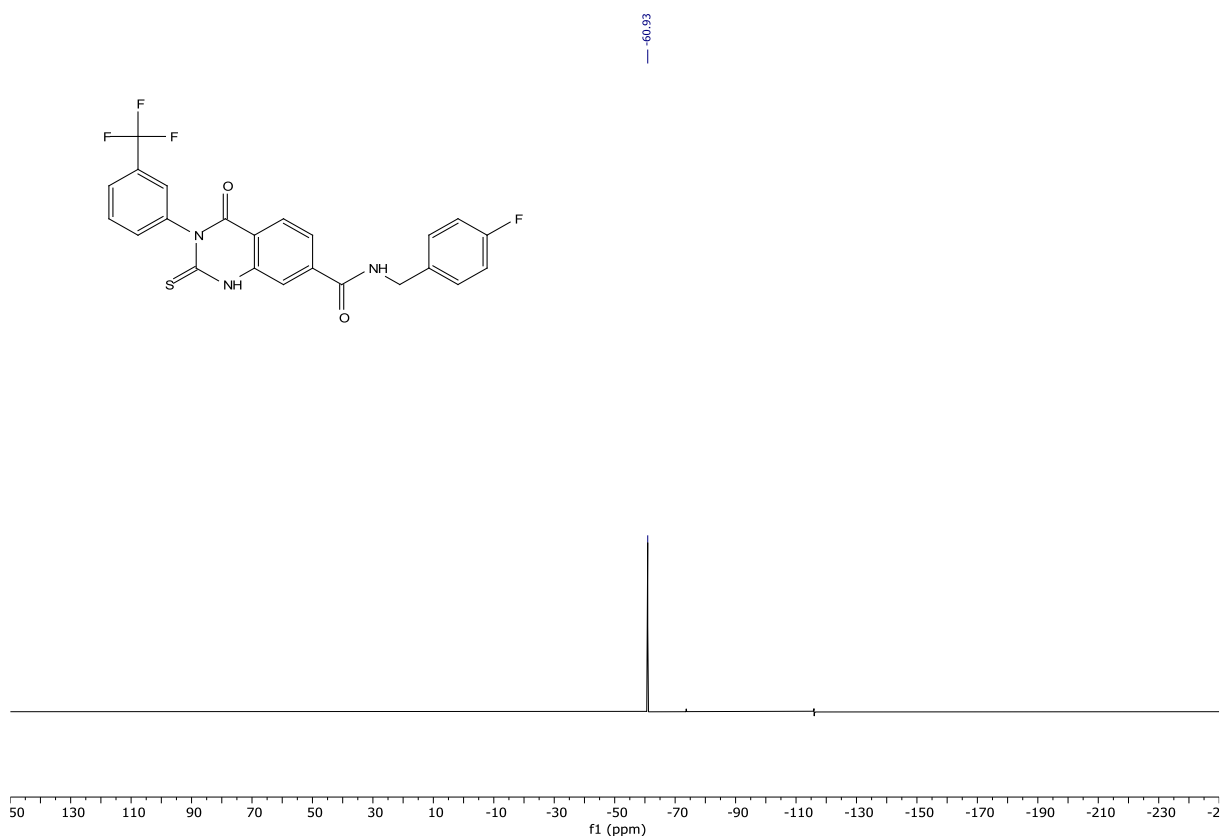
HRMS (ESI) calculated for $[\text{M}+\text{H}]^+$ $\text{C}_{24}\text{H}_{19}\text{F}_3\text{N}_3\text{O}_3\text{S}$ 486.1094, found 486.1081.



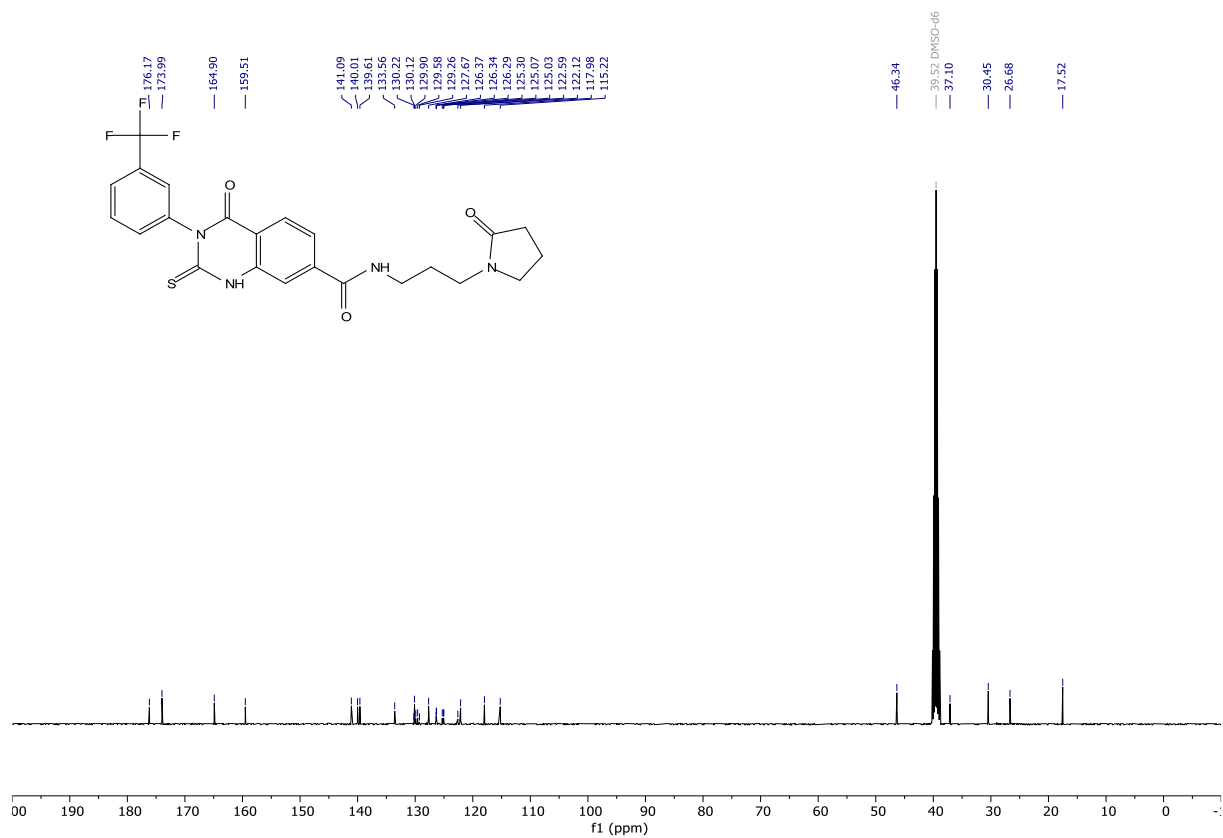
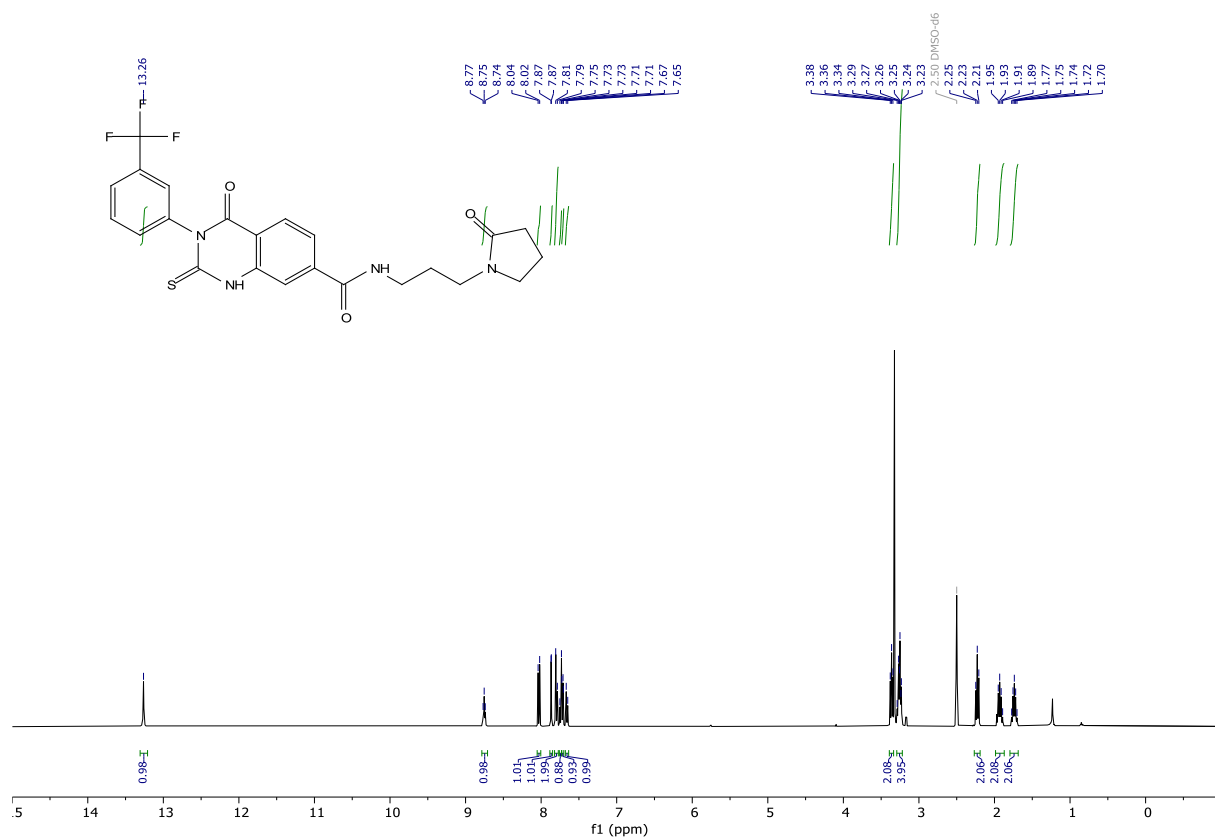


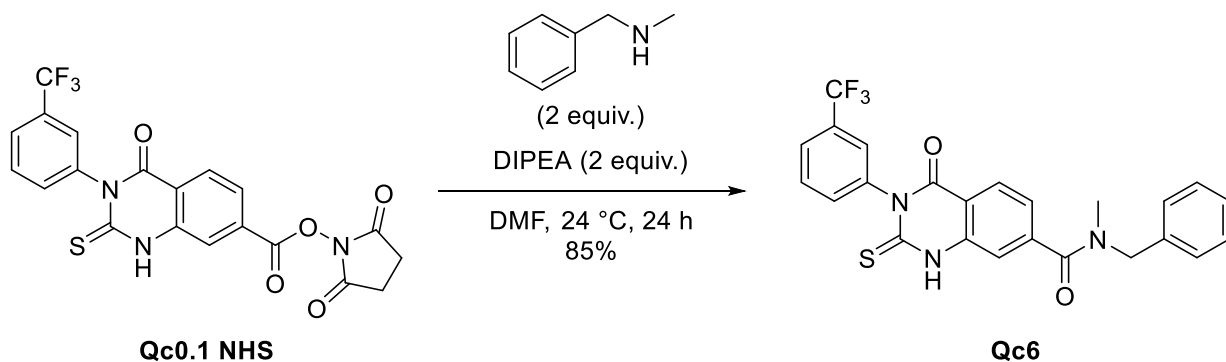
***N*-(4-fluorobenzyl)-4-oxo-2-thioxo-3-(3-(trifluoromethyl)phenyl)-1,2,3,4-tetrahydroquinazoline-7-carboxamide (Qc4).** According to general procedure I: 65% yield (0.06704 g, 0.14160 mmol). Yellowish solid: $^1\text{H NMR}$ (300 MHz, $\text{DMSO}-d_6$) δ 13.26 (s, 1H), 9.36 (t, $J = 6.0$ Hz, 1H), 8.04 (d, $J = 8.2$ Hz, 1H), 7.90 (d, $J = 1.5$ Hz, 1H), 7.84 – 7.61 (m, 5H), 7.39 (dd, $J = 8.5, 5.7$ Hz, 2H), 7.24 – 7.12 (m, 2H), 4.48 (d, $J = 5.8$ Hz, 2H). $^{13}\text{C NMR}$ (101 MHz, DMSO) δ 176.18, 165.05, 162.44, 160.03, 159.50, 140.81, 140.00, 139.59, 135.56 – 135.30 (m), 133.82 – 133.37 (m), 130.13, 129.90, 129.58, 129.43, 129.35, 127.73, 126.32 (q, $J = 3.6$ Hz), 125.30, 125.21 – 124.88 (m), 122.59, 122.24, 115.37, 115.18, 114.97, 42.19. $^{19}\text{F NMR}$ (282 MHz, DMSO) δ -60.93. **HRMS** (ESI) calculated for $[\text{M}+\text{H}]^+$ $\text{C}_{23}\text{H}_{16}\text{F}_4\text{N}_3\text{O}_2\text{S}$ 474.0894, found 474.0881.



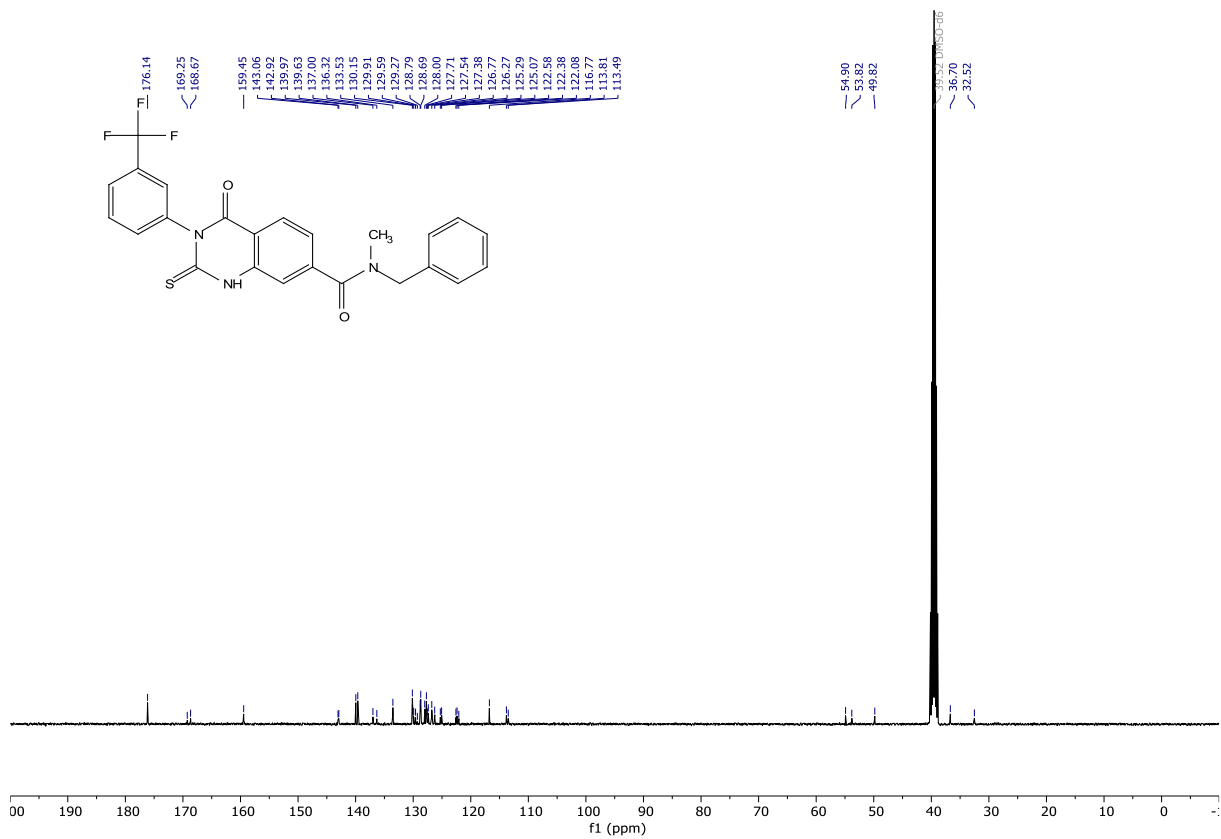
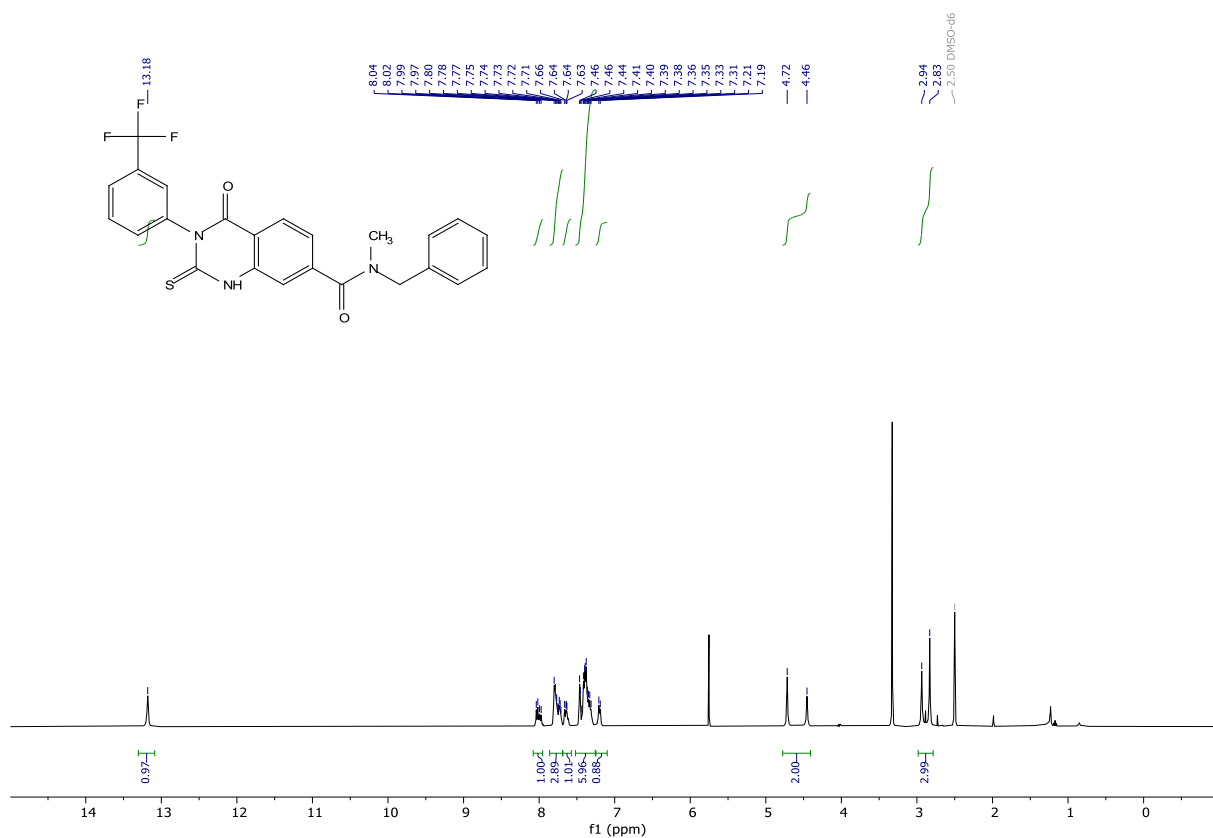


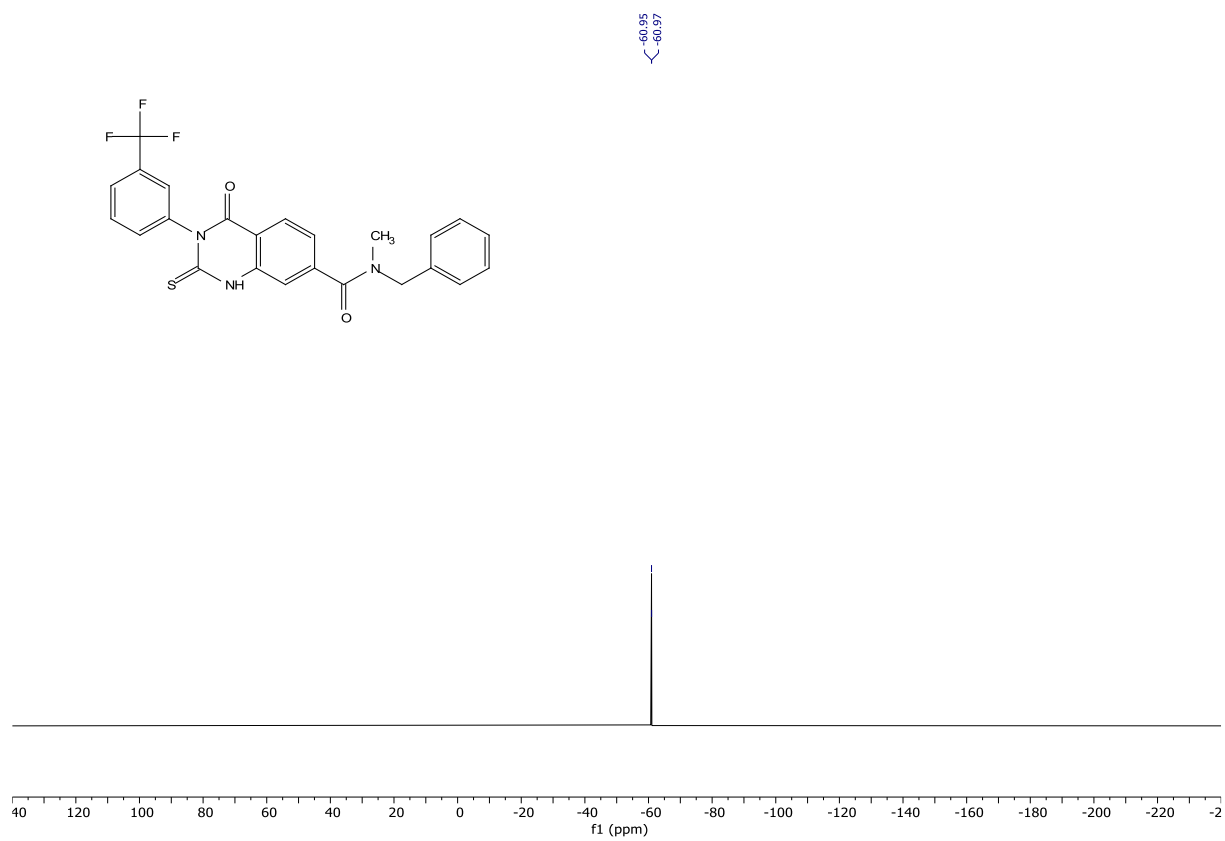
4-oxo-N-(3-(2-oxopyrrolidin-1-yl)propyl)-2-thioxo-3-(3-(trifluoromethyl)phenyl)-1,2,3,4-tetrahydroquinazoline-7-carboxamide (Qc5). According to general procedure I: 50% yield (0.05538 g, 0.11299 mmol). White solid: $^1\text{H NMR}$ (400 MHz, $\text{DMSO}-d_6$) δ 13.26 (s, 1H), 8.75 (t, $J = 5.6$ Hz, 1H), 8.03 (d, $J = 8.2$ Hz, 1H), 7.87 (d, $J = 1.5$ Hz, 1H), 7.80 (d, $J = 8.8$ Hz, 2H), 7.74 (d, $J = 8.1$ Hz, 1H), 7.73 – 7.70 (m, 1H), 7.66 (d, $J = 7.9$ Hz, 1H), 3.36 (t, $J = 7.0$ Hz, 2H), 3.29 – 3.22 (m, 4H), 2.23 (t, $J = 8.0$ Hz, 2H), 1.92 (q, $J = 7.7$ Hz, 2H), 1.74 (p, $J = 7.1$ Hz, 2H). $^{13}\text{C NMR}$ (101 MHz, DMSO) δ 176.17, 173.99, 164.90, 159.51, 141.09, 140.01, 139.61, 133.56, 130.12, 129.74 (q, $J = 32.1$ Hz), 127.67, 126.49 – 126.08 (m), 125.30, 125.18 – 124.94 (m), 122.59, 122.12, 117.98, 115.22, 46.34, 37.10, 30.45, 26.68, 17.52. $^{19}\text{F NMR}$ (282 MHz, DMSO) δ -60.93. **HRMS** (ESI) calculated for $[\text{M}+\text{H}]^+$ $\text{C}_{23}\text{H}_{22}\text{F}_3\text{N}_4\text{O}_3\text{S}$ 491.1359, found 491.1351.





***N*-benzyl-*N*-methyl-4-oxo-2-thioxo-3-(3-(trifluoromethyl)phenyl)-1,2,3,4-tetrahydroquinazoline-7-carboxamide (Qc6).** According to general procedure I: 85% yield (0.08755 g, 0.18648 mmol). Yellow solid: Mixture of rotamers, ^1H NMR (400 MHz, DMSO- d_6) δ 13.18 (s, 1H), 8.08 – 7.95 (m, 1H), 7.86 – 7.69 (m, 3H), 7.69 – 7.57 (m, 1H), 7.52 – 7.26 (m, 6H), 7.20 (d, J = 7.5 Hz, 1H), 4.78 – 4.41 (m, 2H), 2.98 – 2.79 (m, 3H). ^{13}C NMR (101 MHz, DMSO) δ 176.14, 169.25, 168.67, 159.45, 143.06, 142.92, 139.97, 139.63, 137.00, 136.32, 133.53, 130.15, 129.91, 129.59, 129.27, 128.79, 128.69, 128.00, 127.71, 127.54, 127.38, 126.77, 126.27, 125.29, 125.07, 122.58, 122.38, 122.08, 116.77, 113.81, 113.49, 54.90, 53.82, 49.82, 36.70, 32.52. ^{19}F NMR (376 MHz, DMSO) δ -60.95, -60.97. HRMS (ESI) calculated for $[\text{M}+\text{H}]^+$ $\text{C}_{24}\text{H}_{19}\text{F}_3\text{N}_3\text{O}_2\text{S}$ 470.1145, found 470.1136.



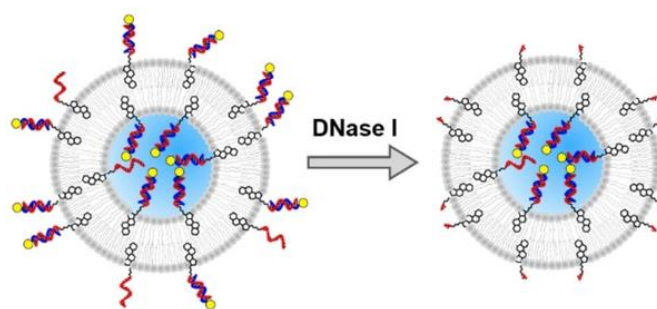


3.2. pH-Dependent fluorophores

Introduction

To study the function of reconstituted membrane proteins, pH-sensitive dyes can be used. They react to changes in the concentration of H^+ -ions. These H^+ -ions play very vital roles in cellular processes such as determining the pH ($pH = -\log_{10}(c(H^+))$) or regulating enzymatic activity and stability. Moreover, H^+ -ions contribute to transport processes through membranes, i.e., by establishing an electrochemical gradient across the membrane or by serving as coupling ions to substrates that can be transported across membranes using this gradient. Readout of the H^+ -ion concentration can be used to study the function of membrane transporters that interact with H^+ -ions. Particularly important examples for this interaction are found in the members of the respiratory chain and in the ATP synthase, which are found in the inner membrane of mitochondria or in the cytoplasmic membrane of bacteria. To study such proteins, they are usually purified and then reconstituted into liposomes, which mimics their native environment for functional analysis. Recently, Dolder et al. described a procedure to introduce pH-sensitive fluorophores into liposomes. They coupled pH sensitive dyes to a DNA oligomer, which in turn was attached to a lipophilic cholesterol. In this way, a construct was obtained having on one side a fluorophore and on the other side a lipophilic anchor, separated by a DNA duplex strand. When the dye is introduced into the liposome, a ratio of 50/50 is achieved with half of the membrane anchored dye on the outside and the other half on the inside of the liposome. Applying DNase on the outside of the liposome removes this half of the dye, allowing for measurement of the concentration of H^+ -ions on the inside of the liposome. A schematic process of this is shown in

Scheme 14.¹¹⁰



Scheme 14 Formation of liposomes with DNA attached dye on the inside¹¹⁰

They state that this method avoids the low incorporation yields by having almost quantitative incorporation. Also, employing this method one does not need to bleach or quench the dye on the outside as there is no longer any dye present. This prevents interaction of the bleaching/ quenching

chemicals with the proteins of interest. They also highlight, that the anchoring of the dye prevents the passive leakage of the dye across the liposome membrane. Furthermore, the DNA linker with its hydrophilic nature makes it unlikely that the DNA-dye construct flips from the inner to the outer side.¹¹⁰

Recently, formation of giant unilamellar vesicles (GUV) under different conditions and the effect of immobilisation on the vesicle structure and membrane tightness against proton and dye diffusion was studied.¹¹¹ For further studies a system with a fluorophore, that is ratiometric or a fluorophore that is coupled to DNA as shown above are desired. The fluorophores should ideally be photostable and have the correct pK_a for the proteins of interest that are studied. In our case, the required pK_a should be around 7. However, the pK_a of a fluorophore can shift when coupled to a protein or a lipid, i.e. it typically increases.¹¹²

Aim of this work

We aimed to synthesise fluorophores, that could either be attached to lipids or proteins by practical, bio-orthogonal reactions such as copper-catalysed click reaction (CuAAC) or by preparing an activated NHS-ester that upon reacting with an amine would result in an amide with minimal side products formed. For this, we based the fluorophore on a compound that was published in 2017 by Niu et al.¹¹³, who used their lysosomal targeted fluorophore for tracking of pH changes in the lysosome. The generic target structure **hNR-R** is shown in **Figure 40, A** with R standing for the reactive alkyne or NHS-ester groups.

Another approach was to take trisodium 8-hydroxypyrene-1,3,6-trisulfonat (HPTS or pyranine) dye and attach hydrophobic tails to it resulting in **C₁₂-HPTS**. This synthesis was based on two different descriptions of Finkler et al.¹¹⁴ and Amdursky et al.¹¹⁵ The target structure is shown in **Figure 40, B**.

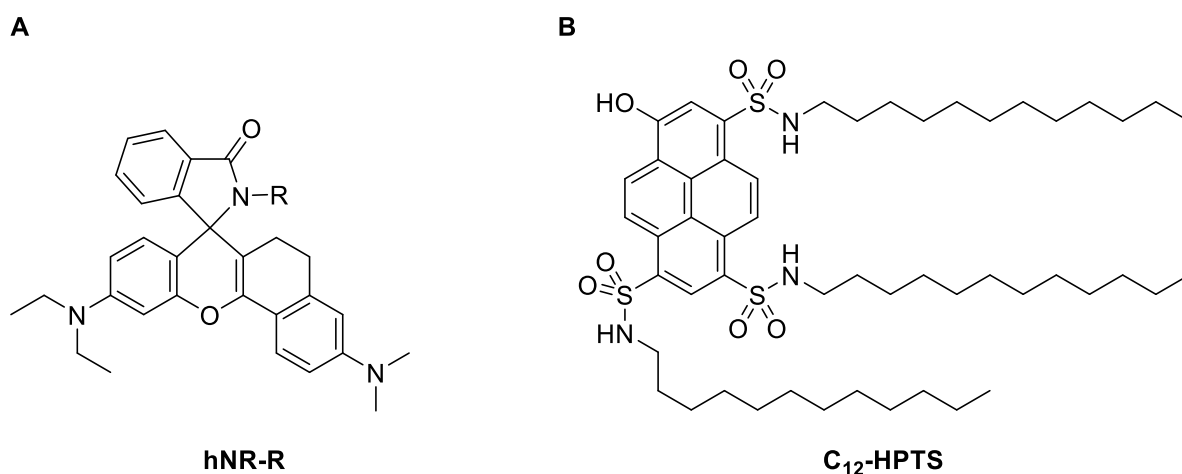
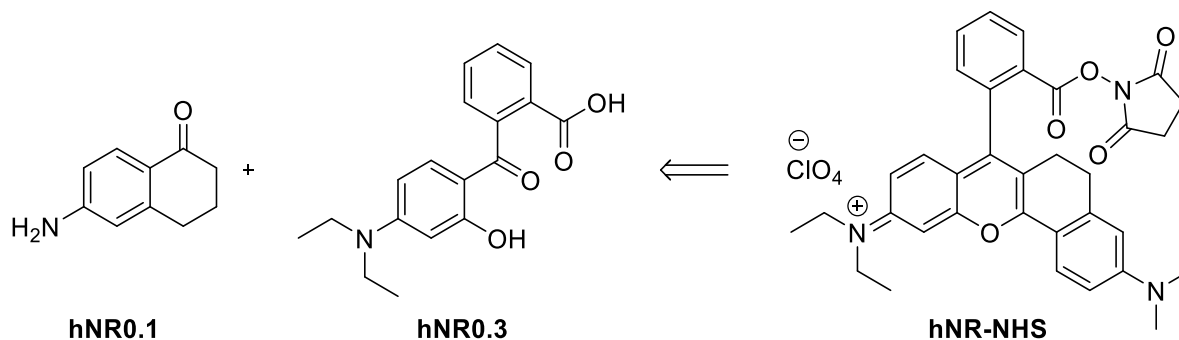


Figure 40 Target fluorophores

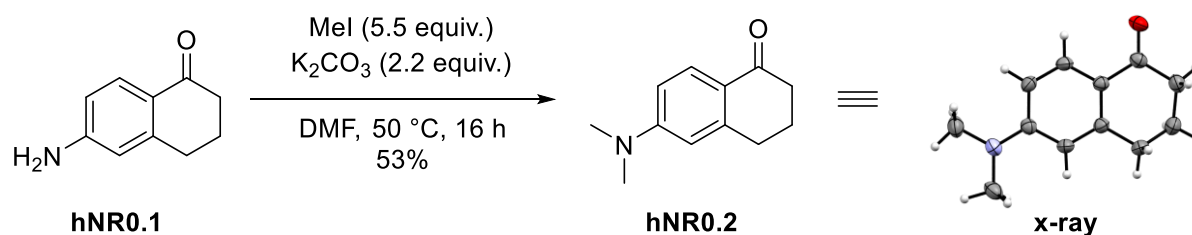
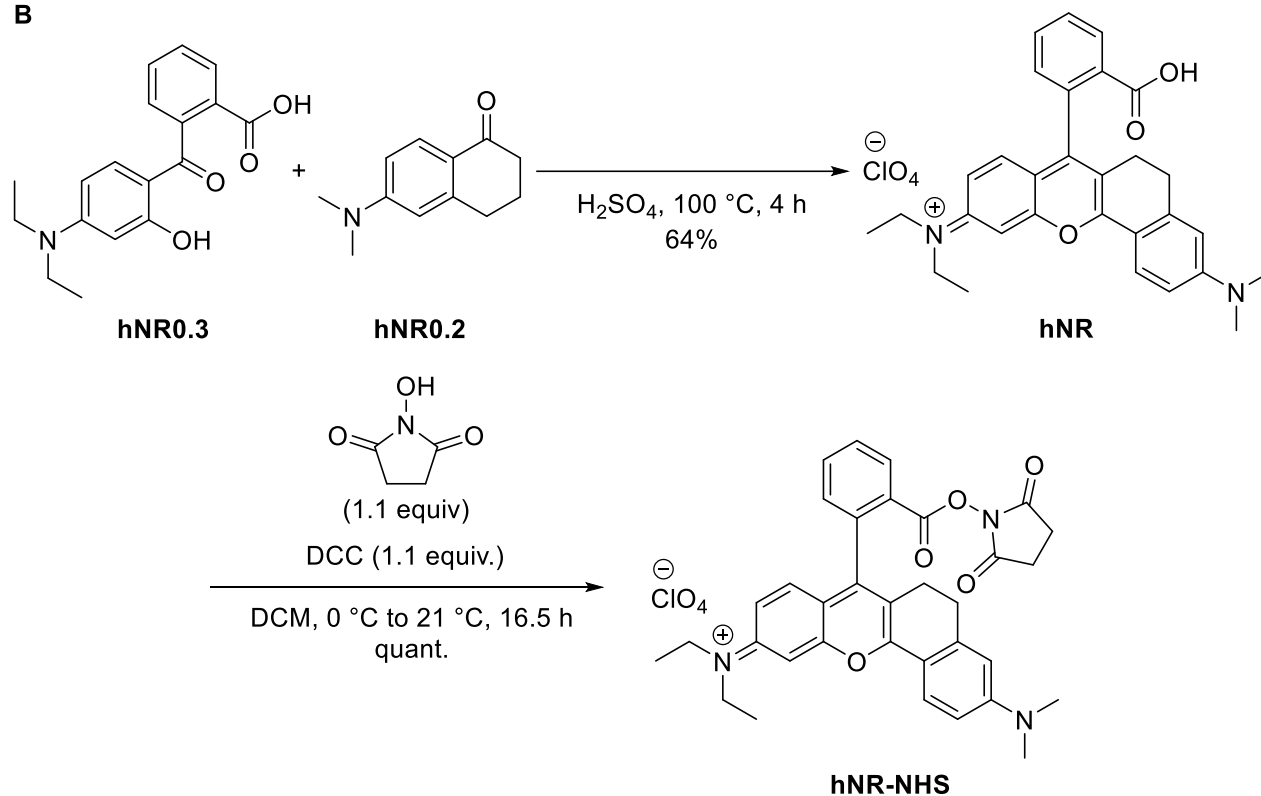
Results

As a first versatile intermediate compound, the NHS activated ester (**hNR-NHS**, in **Scheme 15**) of the described **hNR** fluorophore by Niu et al.¹¹³ was chosen. The retrosynthetic approach from **hNR0.1** and **hNR0.3** is shown in **Scheme 15**.



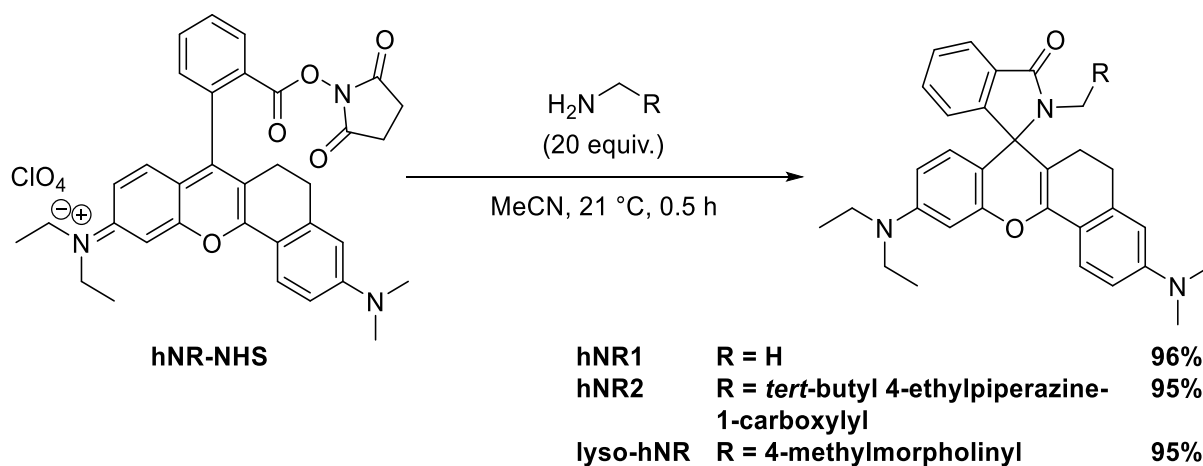
Scheme 15 Retrosynthetic approach to the versatile intermediate **hNR-NHS**

The commercially available **hNR0.1** was converted to **hNR0.2** by methylation using methyl iodide in DMF at 50 °C, resulting in the desired methylated product (**Scheme 16, A**). This product was successfully crystallised, and the x-ray structure was obtained. The product was then reacted with **hNR0.3** in sulfuric acid at 100 °C to yield **hNR**, which was then coupled to *N*-hydroxysuccinimide using DCC as coupling agent, giving the desired **hNR-NHS** ester in quantitative yield (**Scheme 16, B**).

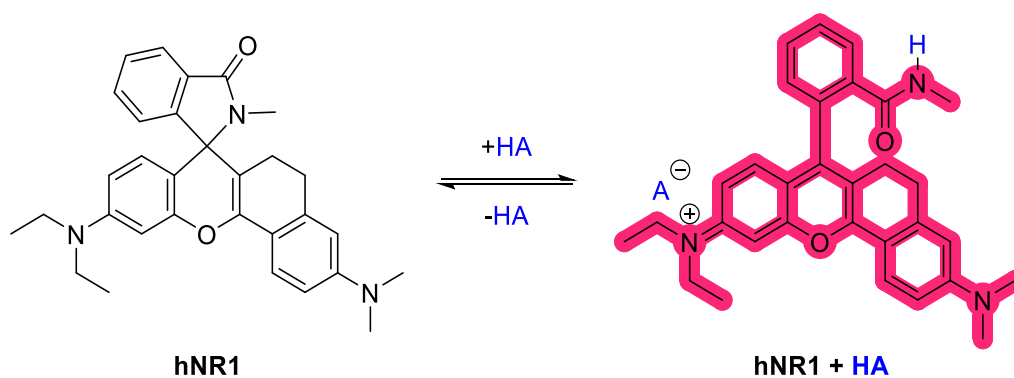
A**B****Scheme 16 A)** Methylation reaction **B)** Reaction cascade to hNR-NHS

From this versatile precursor various products were obtained by reaction of the NHS ester with different amines resulting in the formation of amides **hNR1**, **hNR2** and **lyso-hNR** (**Scheme 17, A**). **hNR1** was used as a model compound, to check whether the desired ring opening takes place at acidic conditions and whether the lactam formation is observed at basic conditions e.g., by addition of dilute sodium hydroxide solution. Due to the reversibility of the reaction, addition of e.g., dilute acetic acid could restore the fluorescent form of the compound. The equilibrium is depicted in **Scheme 17, B**. For lyso-hNR the pK_a was measured to be around 5.0.

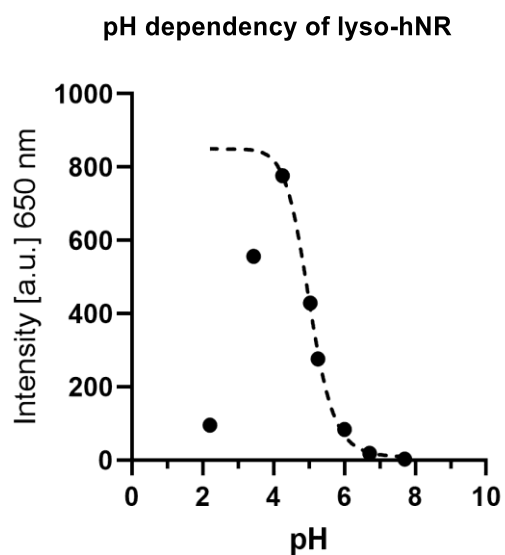
A



B

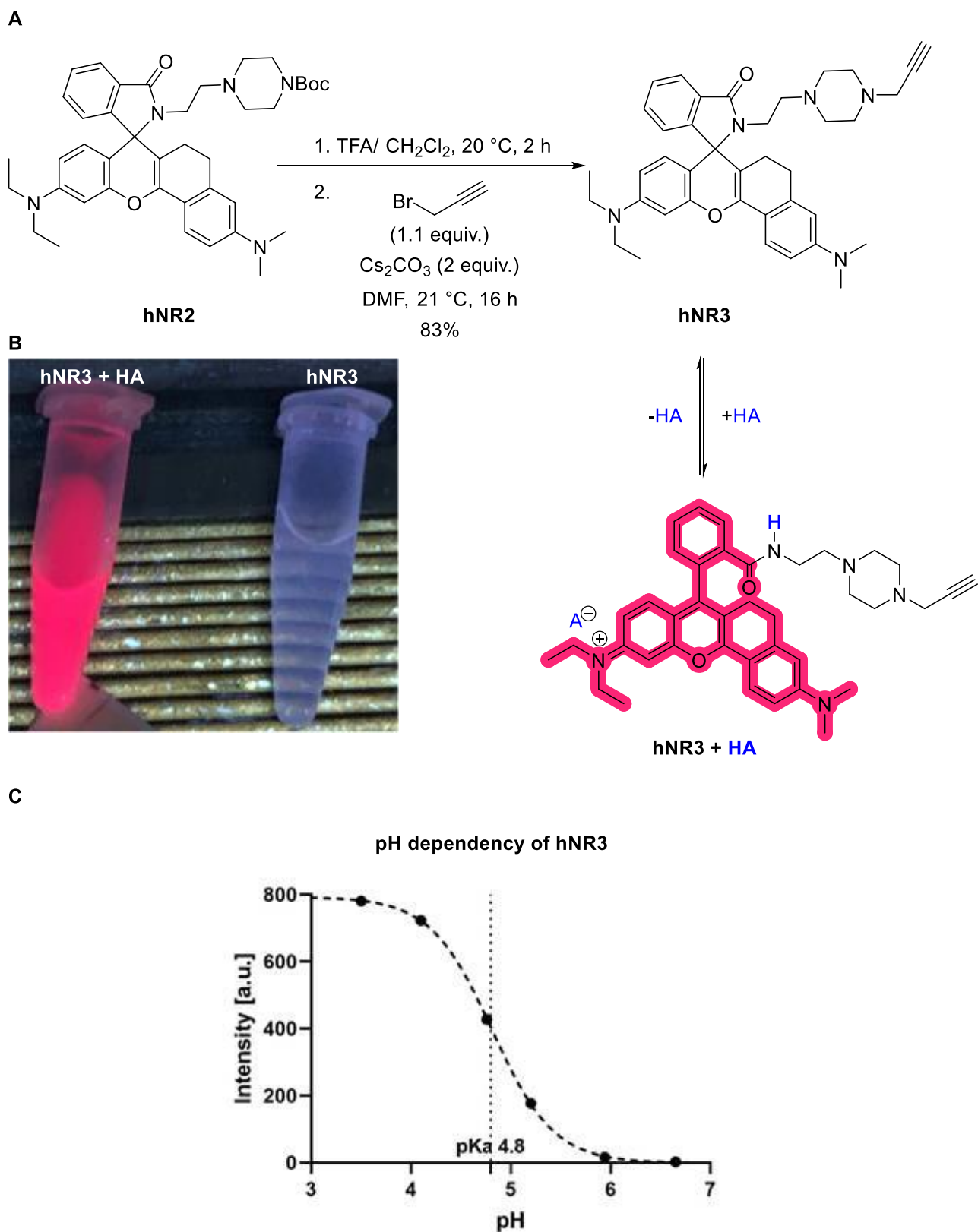


C



Scheme 17 A) Reaction of the NHS-ester with various amines **B)** Equilibrium changed by acid **C)** Absorption @650 nm vs. pH for lyso-hNR. Data from Nicolas Dolder, Department of Chemistry Biochemistry and Pharmacy, University of Bern

hNR2 containing a *N*-Boc protection group on the piperazine moiety, was deprotected in trifluoroacetic acid and dichloromethane. The residue was directly used for the subsequent alkylation with propargyl bromide, which gave the alkyne bearing **hNR3** (**Scheme 18, A**). **Scheme 18, A** depicts the equilibrium between the open and the closed form. In **Scheme 18, B** a representative image of an acidified and basified sample of **hNR3** is shown. The pK_a of **hNR3** was measured to be around 4.8 (**Scheme 18, C**).

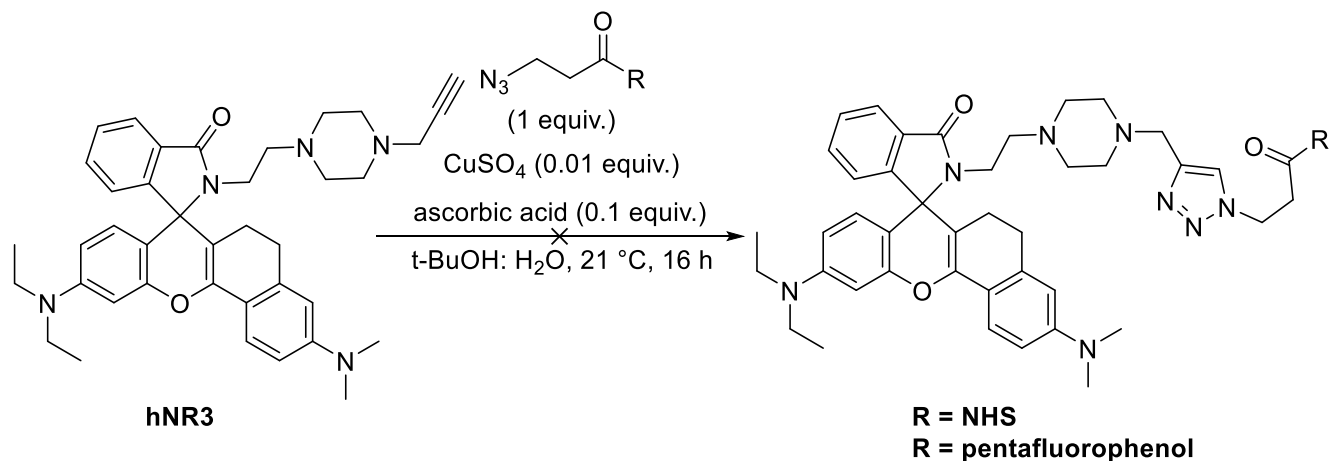


Scheme 18 A) Propargylation deprotection and subsequent alkylation hNR2 **B)** Image of two samples of hNR3. The left acidified with dilute acetic acid. The right basified with dilute aq. NaOH. The samples were excited with UV light of 366 nm. **C)** Absorption @650 nm vs. pH for hNR3. Data from Nicolas Dolder, Department of Chemistry Biochemistry and Pharmacy, University of Bern

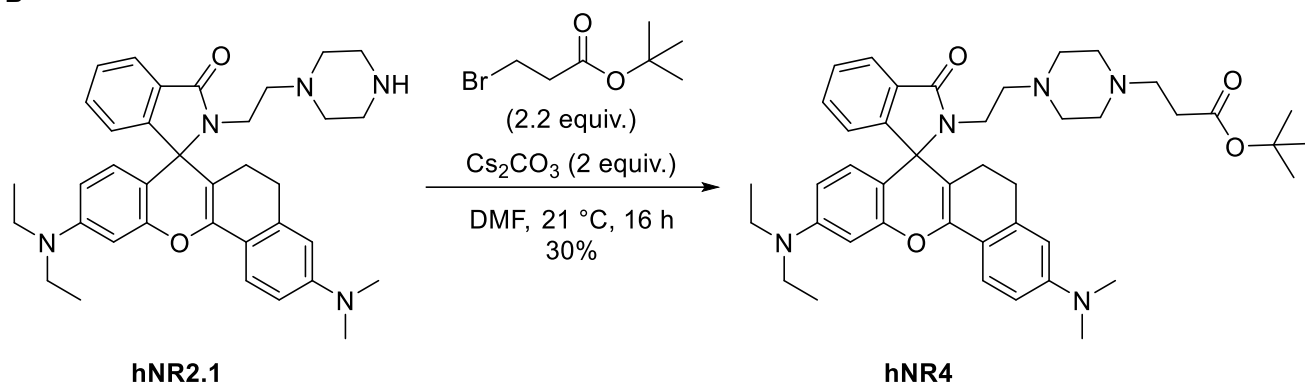
hNR3 is currently under evaluation for its suitability to be applied as pH sensitive dye in GUVs.

Other approaches were used to synthesise an activated ester or azide functionalised derivative of the **hNR**. Some attempts are given in Scheme 19. Panel **A** depicts an approach where either a pentafluorophenol- or NHS-activated ester was tried to be clicked in a CuAAC reaction to **hNR3**. However, despite several attempts, the desired products were never isolated. Only decomposition of the starting material giving complex mixtures was observed. Pentafluorophenol was chosen due to its UV-absorbing properties, making it easier to track than the NHS-ester activated 3-azidopropionic acid. Panel **B** shows successful alkylation of the free deprotected piperazine derivative **hNR2.1** with 3-bromopropionic acid *tert*-butyl ester. Whilst the alkylation was successful, the desired product was isolated in low yield. All subsequent deprotection and functionalisation attempts were in vain. Panel **C** shows another approach where **hNR** conjugation with an azide bearing linker was attempted. Again, this protocol resulted in decomposition. However, it must be noted that the target molecule could eventually be obtained by reaction of the amino-azide linker with the **hNR-NHS** ester. Since **hNR3** had already some useful functional features, further attempts to synthesise piperazine containing activated esters was postponed.

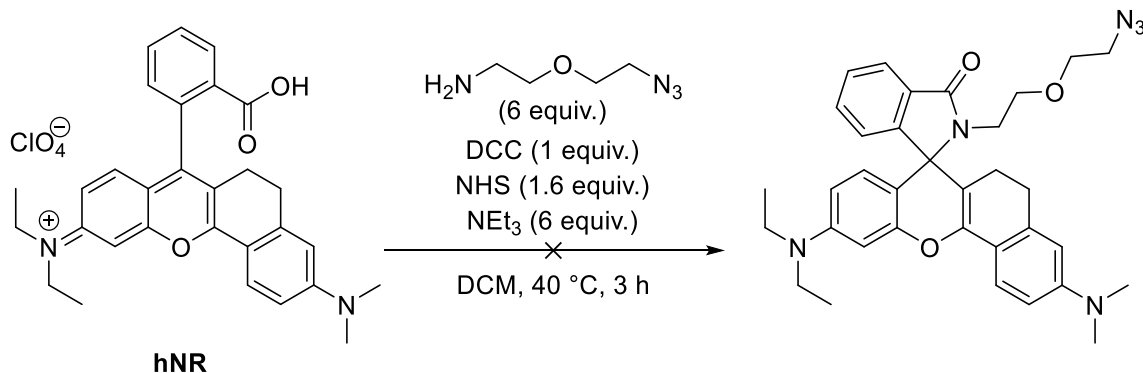
A



B



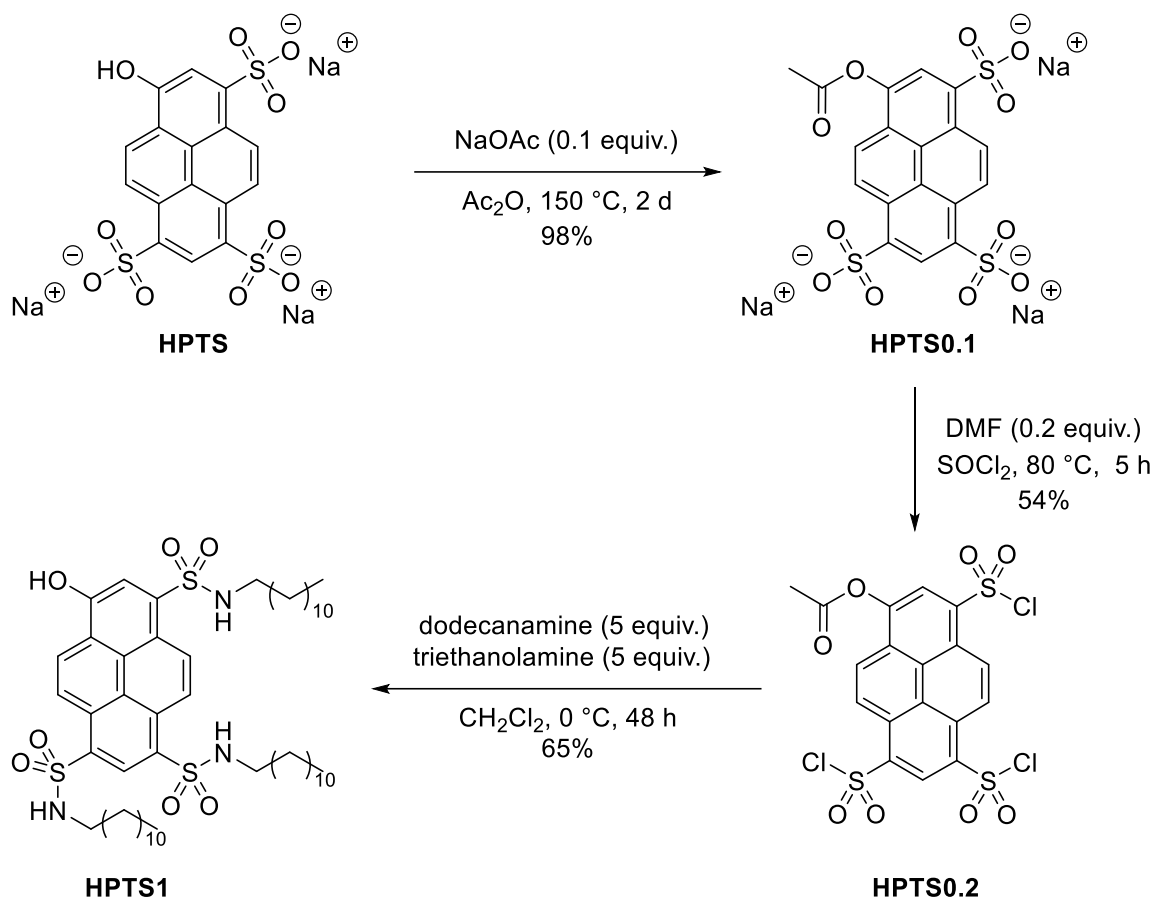
C



Scheme 19 Failed attempts for the synthesis of an activated ester

HPTS1 was synthesised following modified literature procedures.^{114, 115} From commercially available trisodium **HPTS**, the hydroxy group was acylated with acetic anhydride and sodium acetate over the course of two days at reflux resulting almost quantitatively in the protected intermediate **HPTS0.1**. This intermediate was then subjected to refluxing thionyl chloride with a catalytic amount of *N,N*-dimethylformamide resulting in the tris sulfonyl chloride **HPTS0.2**. This electrophilic compound was

then transformed into the tris sulfonamide with dodecanamine in the presence of triethanolamine as base, resulting in the target compound **HPTS1** (Scheme 20).



Scheme 20 Synthesis of HPTS1 from HPTS

Whilst the synthesis and characterisation of the fluorophore is completed, the evaluation of this membrane bound fluorophore in the GUVs is ongoing.

Conclusion and outlook

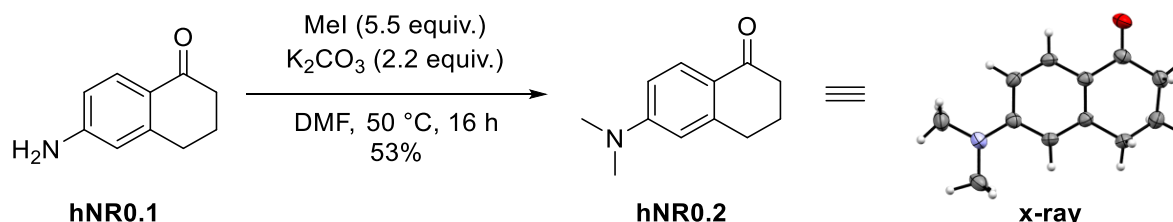
The synthesised compound **hNR3** represents an interesting fluorescent probe for the study of pH changes in biological systems. Due to its alkyne moiety, the fluorophore can be attached to targets of interest bearing an azide group, by employing a copper catalysed azide alkyne cycloaddition. While the pK_a of the free **hNR3** lies below the targeted value of around 7, it is well possible that when bound to a lipid, the pK_a value can shift to the desired region.

The synthesis and characterisation of **HPTS1** was conducted. The biochemical assessment of the compound in GUVs is currently ongoing.

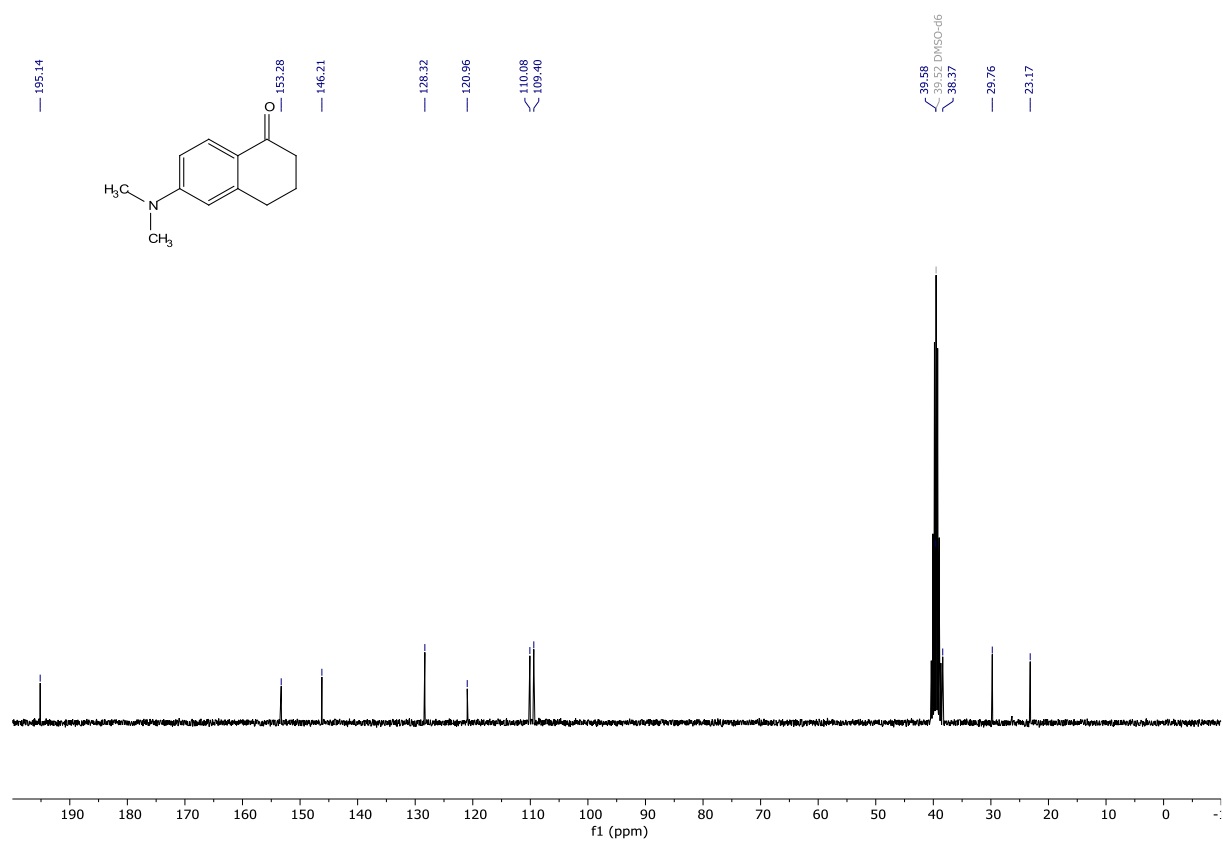
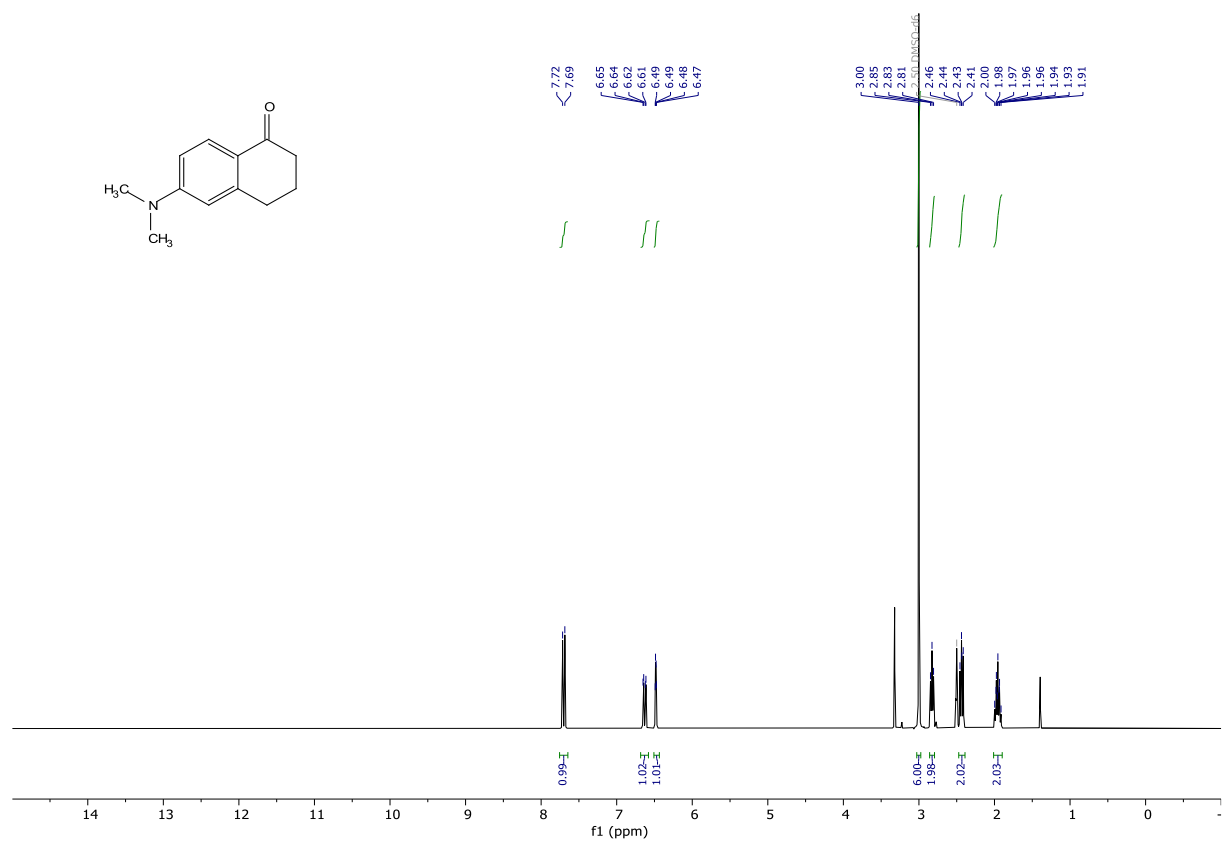
General remarks to materials & methods

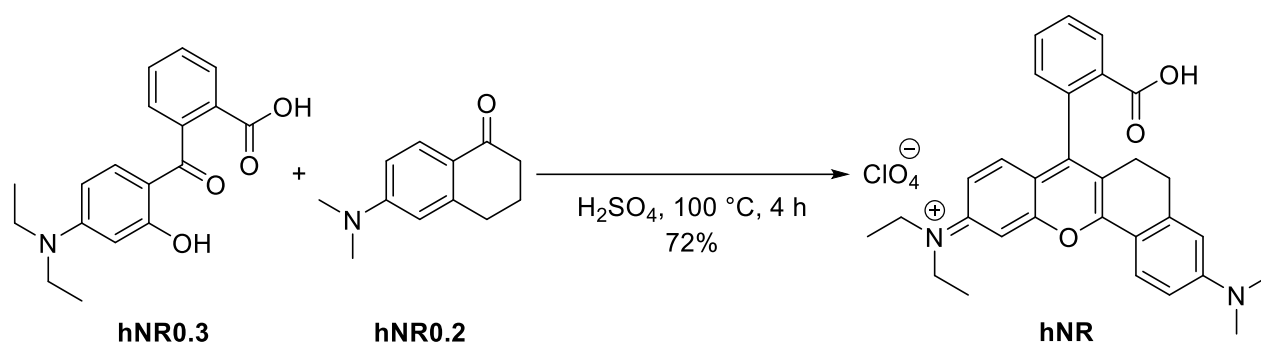
For general remarks see chapter 1.4.

Synthesis

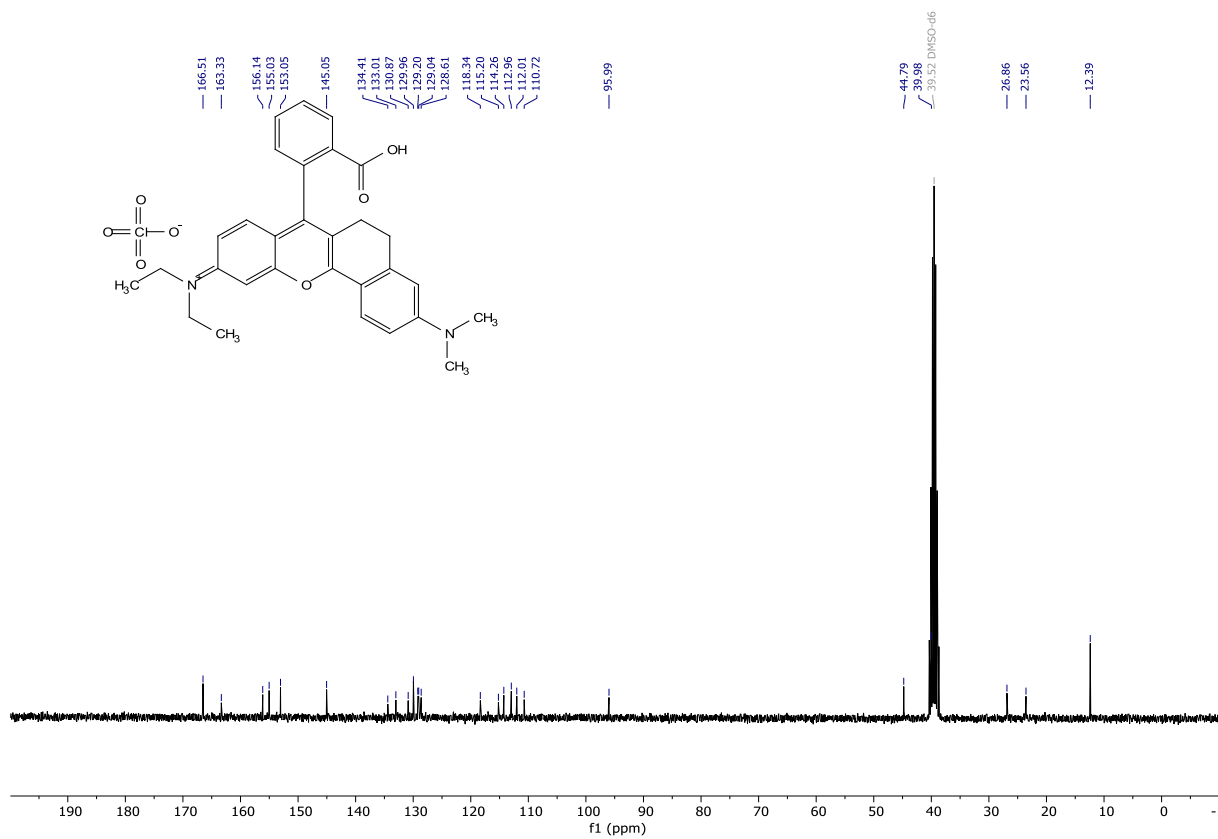
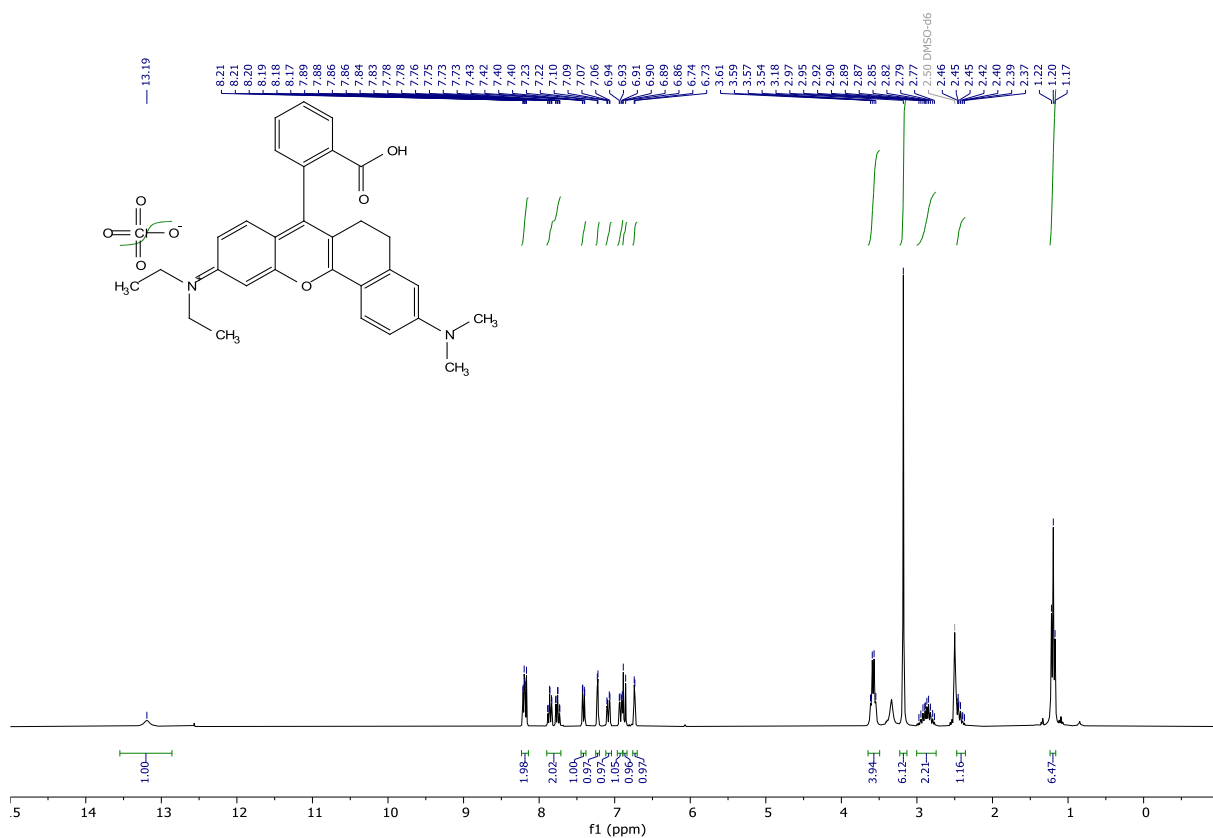


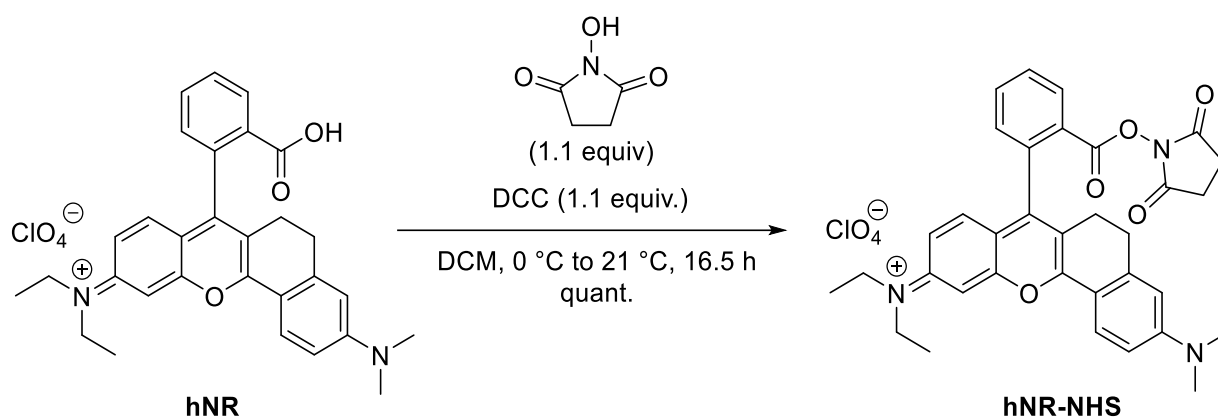
6-(dimethylamino)-3,4-dihydronaphthalen-1(2H)-one (hNR0.2). To a stirred solution of 6-amino-3,4-dihydronaphthalen-1(2H)-one (2.006 g, 12.4439 mmol) in DMF (80 mL) was added K₂CO₃ (3.768 g, 27.2648 mmol) and Iodomethane (4.2 mL, 9.576 g, 67.4653 mmol). The mixture was placed under an argon atmosphere, and it was heated to 50 °C. To the mixture was added brine and ethyl acetate and the aqueous phase was extracted with ethyl acetate. The combined organic phases were washed with brine, dried over MgSO₄, filtered, and concentrated under reduced pressure. The residue was redissolved in dichloromethane and concentrated onto silica gel. The crude was purified by flash column chromatography (cyclohexane/ ethyl acetate gradient from 1:0 to 0:1) to give the desired compound in 53% yield (1.2439 g, 6.5727 mmol). A small sample was recrystallised from *n*-hexane and ethyl acetate, giving crystals suitable for x-ray diffraction measurements (CCDC deposition number: 2195852). Clear crystalline solid: ¹H NMR (300 MHz, DMSO-*d*₆) δ 7.70 (d, *J* = 8.9 Hz, 1H), 6.63 (dd, *J* = 8.9, 2.6 Hz, 1H), 6.51 – 6.44 (m, 1H), 3.00 (s, 6H), 2.83 (t, *J* = 6.1 Hz, 2H), 2.43 (dd, *J* = 7.1, 5.7 Hz, 2H), 2.01 – 1.90 (m, 2H). ¹³C NMR (75 MHz, DMSO) δ 195.14, 153.28, 146.21, 128.32, 120.96, 110.08, 109.40, 39.58, 38.37, 29.76, 23.17. HRMS (ESI) calculated for [M+H]⁺ C₁₂H₁₆O 190.1226, found 190.1221.



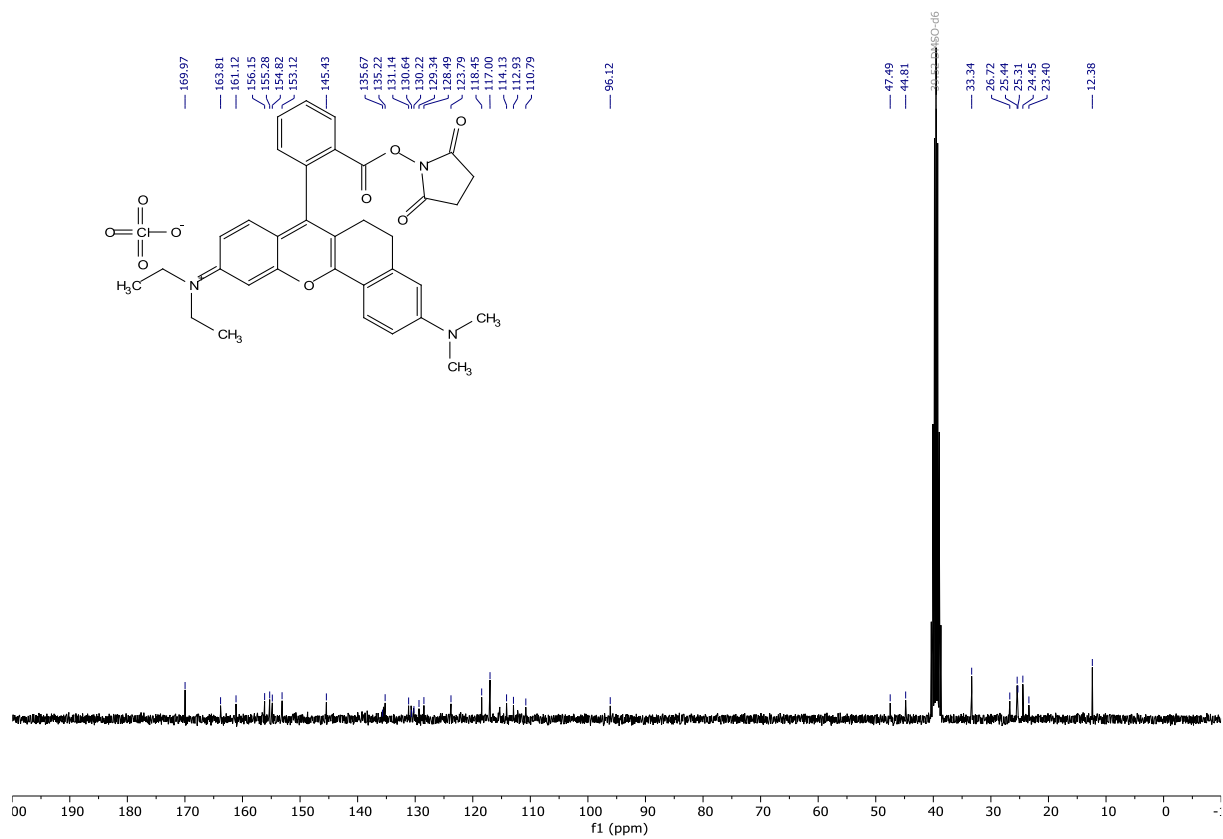
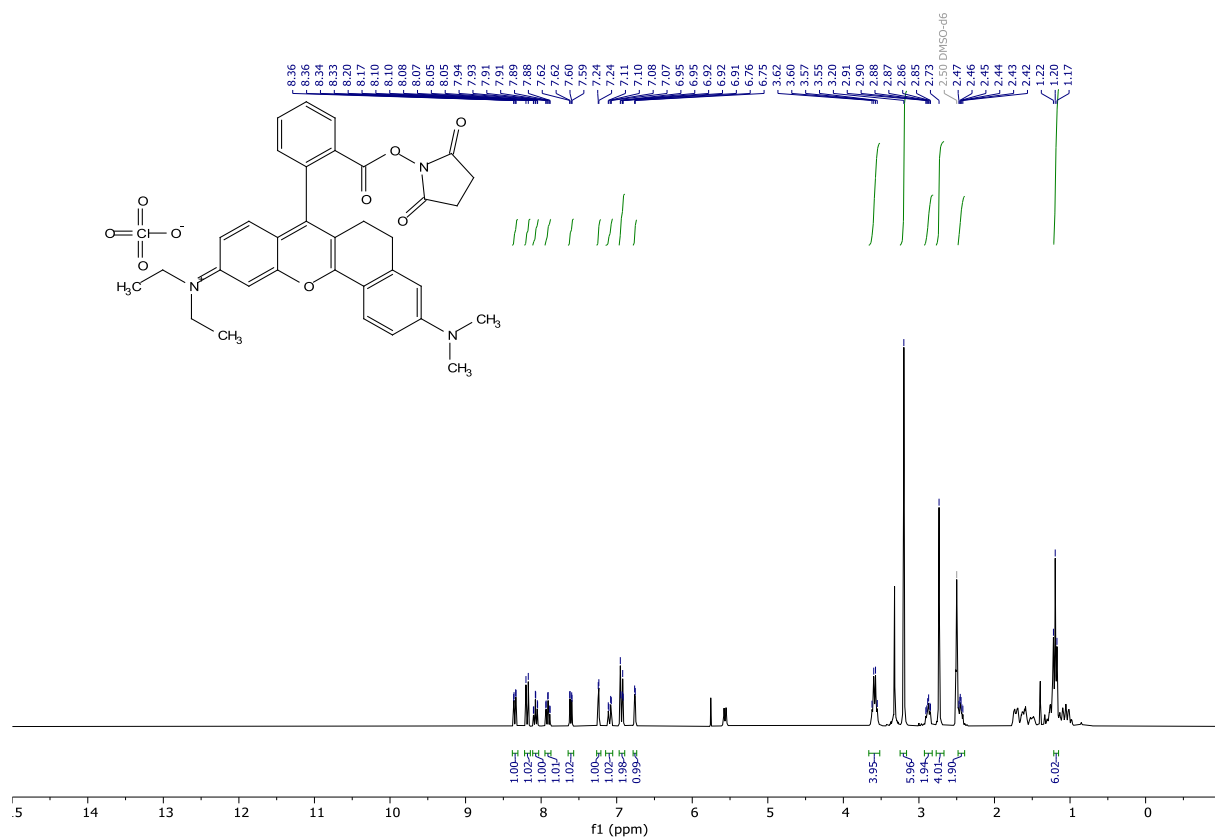


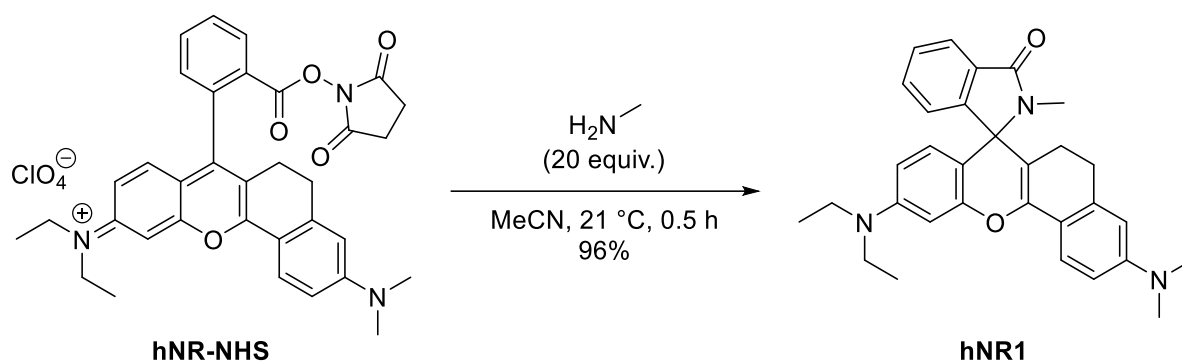
***N*-(7-(2-carboxyphenyl)-3-(dimethylamino)-5,6-dihydro-10*H*-benzo[*c*]xanthen-10-ylidene)-*N*-ethylethanaminium perchlorate (hNR).** To sulfuric acid (96%, 16.5 mL) was added 6-(dimethylamino)-3,4-dihydronaphthalen-1(2*H*)-one (0.257 g, 0.8202 mmol) and 2-(4-(diethylamino)-2-hydroxybenzoyl)benzoic acid (0.157 g, 0.8296 mmol). The bright red mixture was heated to 100 °C and stirred for 4 h. After 4 h the mixture was cooled in an ice bath to 0 °C. Then it was poured into 50 mL of ice water, which led to the formation of an intense blue/ purple colour. To this mixture was carefully added perchloric acid (50%, 2 mL). The precipitate was filtered off, washed with little water and perchloric acid, and dried under reduced pressure. The crude was taken up in dichloromethane and concentrated onto silica gel. The crude was purified by flash column chromatography (dichloromethane/ methanol gradient from 1:0 to 9:1) to give the desired compound in 72% yield (0.33629 g, 0.59396 mmol). Green solid: ¹**H NMR** (300 MHz, DMSO-*d*₆) δ 13.19 (s, 1H), 8.24 – 8.14 (m, 2H), 7.81 (dtd, *J* = 31.8, 7.6, 1.4 Hz, 2H), 7.41 (dd, *J* = 7.6, 1.3 Hz, 1H), 7.23 (d, *J* = 2.4 Hz, 1H), 7.08 (dd, *J* = 9.5, 2.5 Hz, 1H), 6.92 (dd, *J* = 9.2, 2.5 Hz, 2H), 6.87 (d, *J* = 9.4 Hz, 1H), 6.74 (d, *J* = 2.5 Hz, 1H), 3.58 (q, *J* = 7.0 Hz, 4H), 2.86 (ddq, *J* = 23.3, 15.9, 7.6, 7.0 Hz, 2H), 2.49 – 2.34 (m, 2H), 1.20 (t, *J* = 7.1 Hz, 7H). ¹³**C NMR** (75 MHz, DMSO) δ 166.51, 163.33, 156.14, 155.03, 153.05, 145.05, 134.41, 133.01, 130.87, 129.96, 129.20, 129.04, 128.61, 118.34, 115.20, 114.26, 112.96, 112.01, 110.72, 95.99, 44.79, 39.98, 26.86, 23.56, 12.39. **HRMS** (ESI) calculated for [M+ClO₄]⁺ C₃₀H₃₁N₂O₃ 467.2329, found 467.2314 .





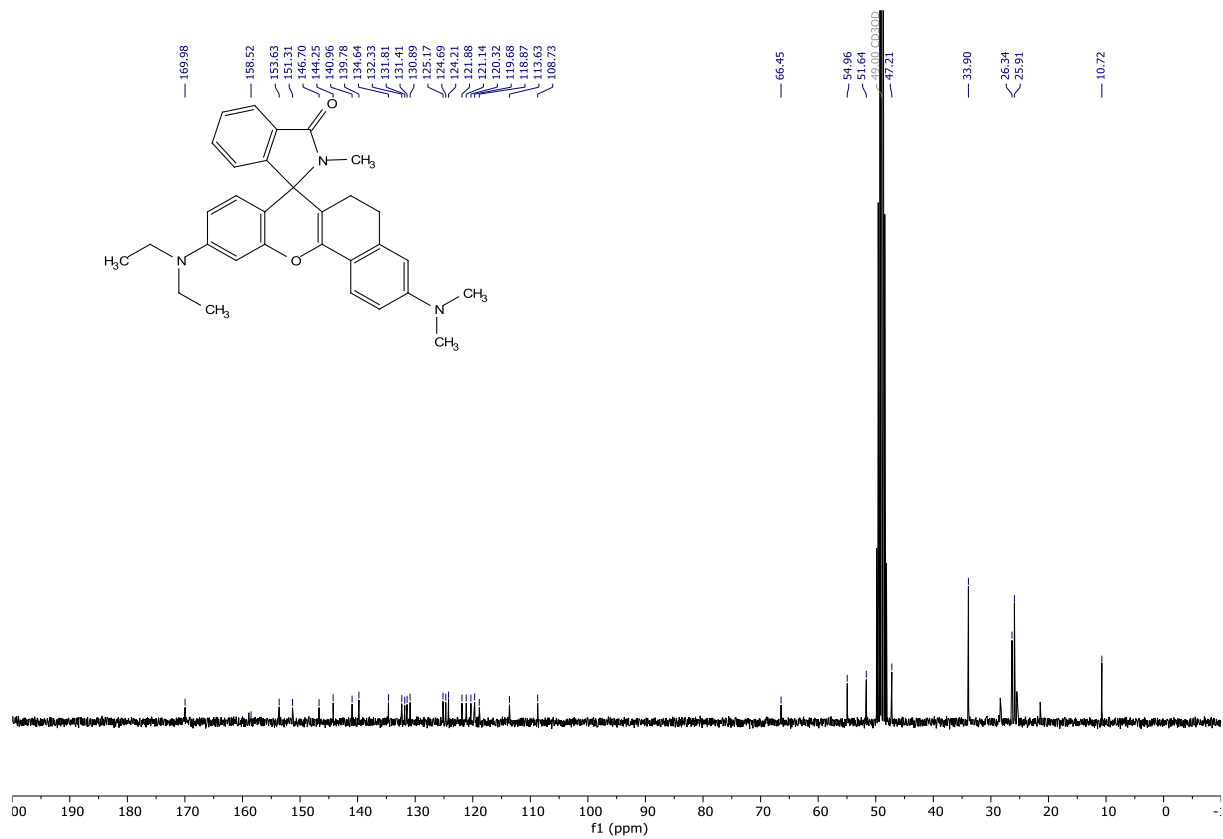
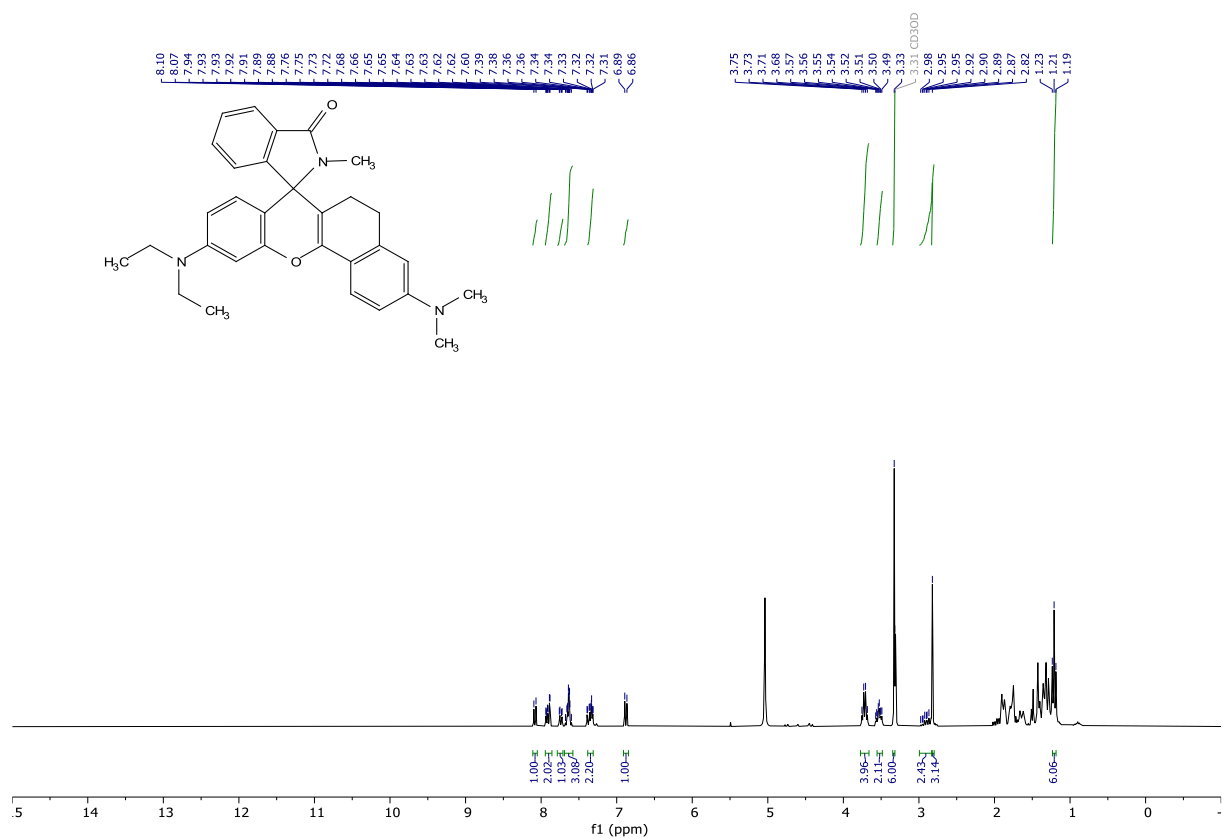
***N*-(3-(dimethylamino)-7-(2-(((2,5-dioxopyrrolidin-1-yl)oxy)carbonyl)phenyl)-5,6-dihydro-10*H*-benzo[*c*]xanthen-10-ylidene)-*N*-ethylethanaminium perchlorate (hNR-NHS).** To a stirred solution of *N*-(7-(2-carboxyphenyl)-3-(dimethylamino)-5,6-dihydro-10*H*-benzo[*c*]xanthen-10-ylidene)-*N*-ethylethanaminium (0.260 g, 0.4585 mmol) in dichloromethane (15 mL) at 0 °C under an argon atmosphere was added *N,N'*-Dicyclohexylmethanediimine (0.116 g, 0.5622 mmol). The mixture was stirred for 30 minutes and *N*-Hydroxysuccinimide (0.06290 g, 0.5465 mmol) was added. The mixture was stirred for 16 h slowly warming to 21 °C. The mixture was filtered, and the filtrate was concentrated onto silica gel under reduced pressure. The crude was purified by flash column chromatography (dichloromethane/ methanol gradient from 1:0 to 9:1) to give the desired product in quantitative yield (0.30333 g, 0.45675 mmol). Purple solid contaminated with *N,N'*-dicyclohexylurea: ¹**H NMR** (300 MHz, DMSO-*d*₆) δ 8.35 (dd, *J* = 7.9, 1.2 Hz, 1H), 8.19 (d, *J* = 9.2 Hz, 1H), 8.07 (td, *J* = 7.6, 1.3 Hz, 1H), 7.91 (td, *J* = 7.7, 1.3 Hz, 1H), 7.61 (dd, *J* = 7.7, 1.2 Hz, 1H), 7.24 (d, *J* = 2.4 Hz, 1H), 7.09 (dd, *J* = 9.4, 2.4 Hz, 1H), 6.98 – 6.88 (m, 2H), 6.76 (d, *J* = 2.5 Hz, 1H), 3.59 (q, *J* = 6.9 Hz, 4H), 3.20 (s, 6H), 2.88 (m, 2H), 2.73 (s, 4H), 2.45 (m, 2H), 1.18 (d, *J* = 6.9 Hz, 8H). ¹³**C NMR** (75 MHz, DMSO) δ 169.97, 163.81, 161.12, 156.15, 155.28, 154.82, 153.12, 145.43, 135.67, 135.22, 131.14, 130.64, 130.22, 129.34, 128.49, 123.79, 118.45, 117.00, 114.13, 112.93, 110.79, 96.12, 47.49, 44.81, 33.34, 26.72, 25.44, 25.31, 24.45, 23.40, 12.38. **HRMS** (ESI) calculated for [M+ClO₄]⁺ C₃₄H₃₄N₃O₅ 564.2493, found 564.2481.

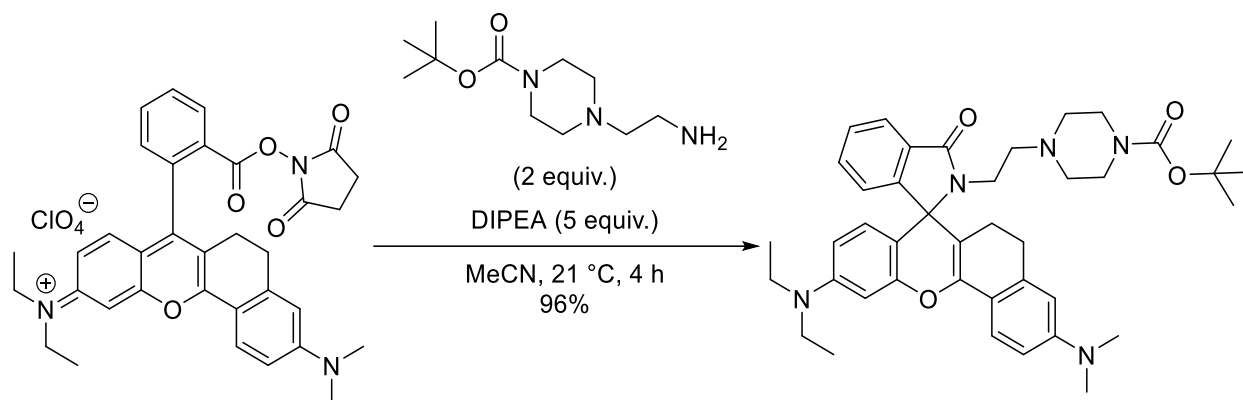




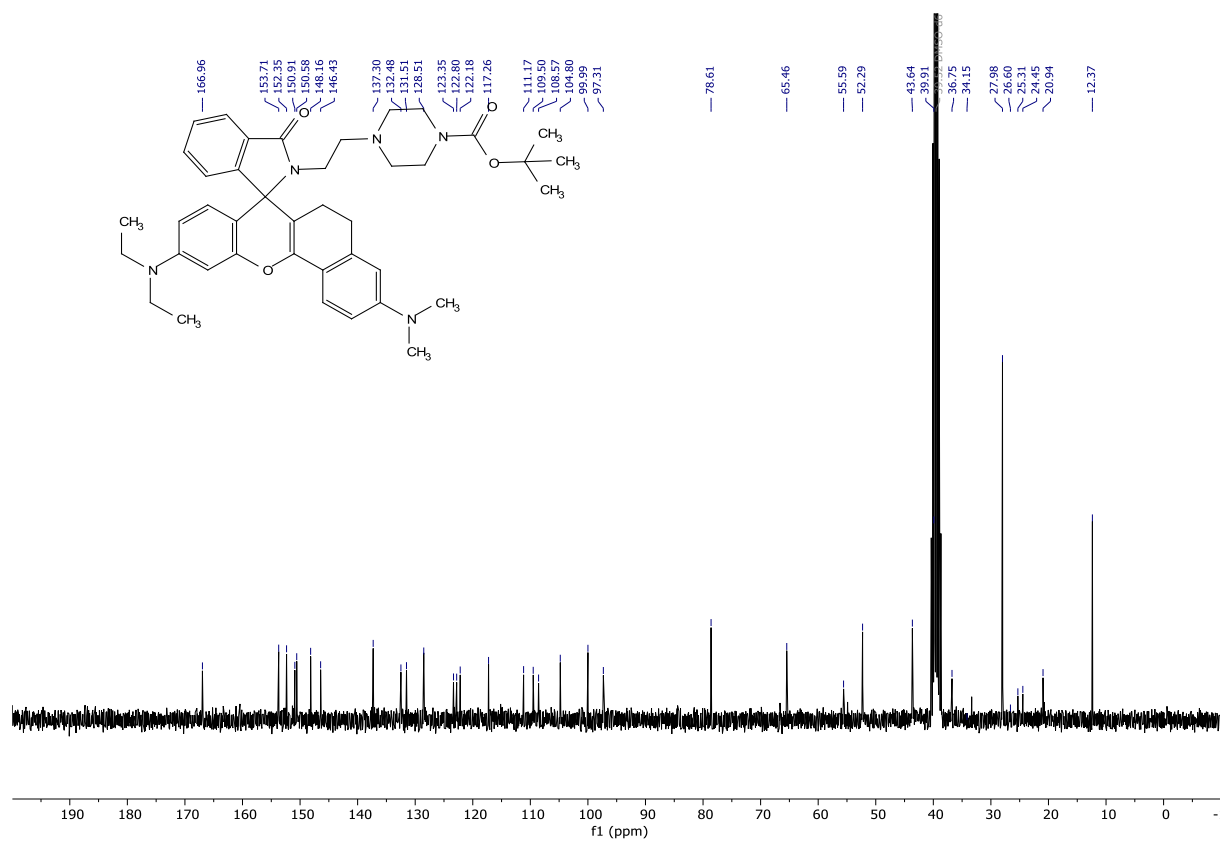
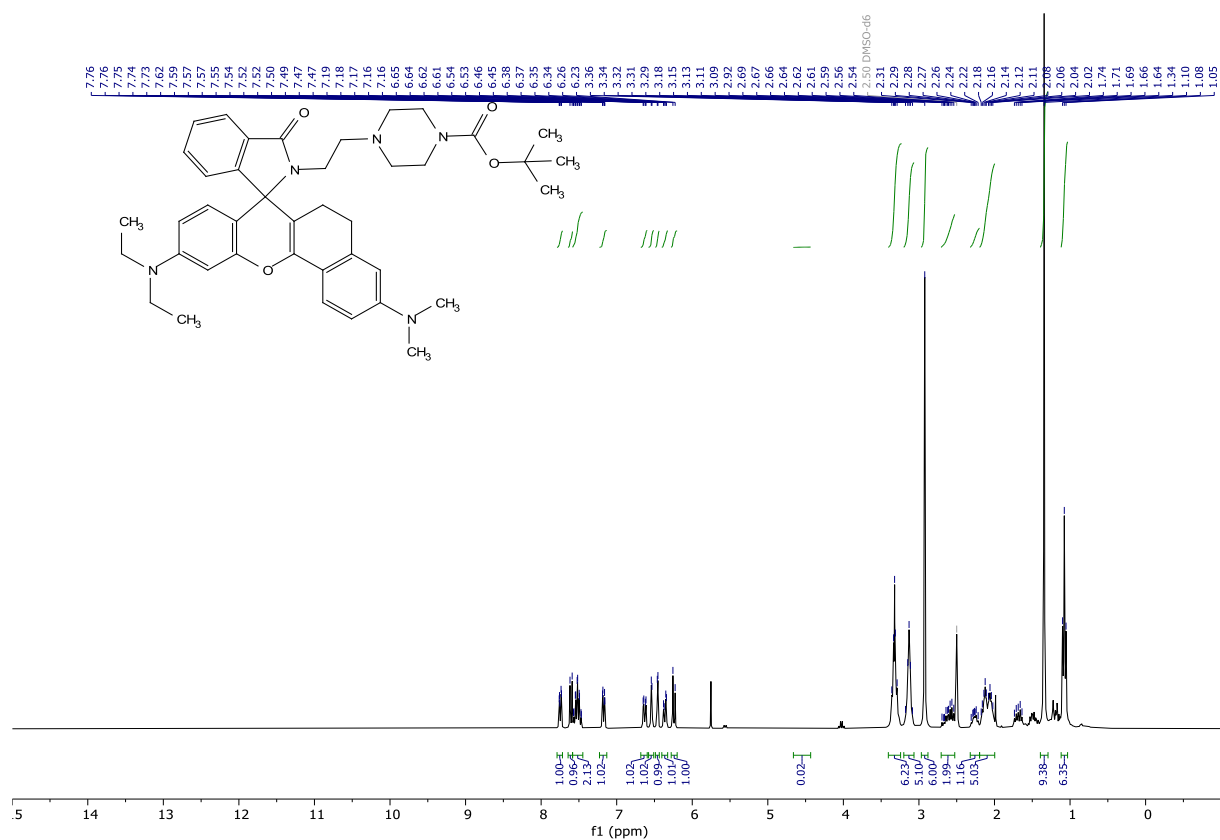
10-(diethylamino)-3-(dimethylamino)-2'-methyl-5,6-dihydrospiro[benzo[c]xanthene-7,1'-

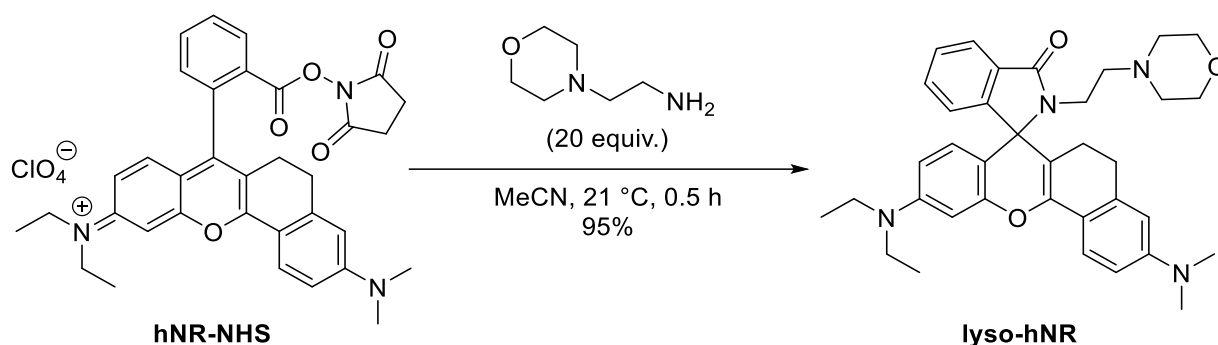
isoindolin]-3'-one (hNR1). To a stirred solution of *N*-(3-(dimethylamino)-7-(2-(((2,5-dioxopyrrolidin-1-yl)oxy)carbonyl)phenyl)-5,6-dihydro-10*H*-benzo[*c*]xanthene-10-ylidene)-*N*-ethylethanaminium perchlorate (0.06814 g, 0.1026 mmol) in acetonitrile (10 mL) was added methylamine (40wt% in water, 0.2 mL, 0.089186 g, 2.871 mmol). After 30 minutes the mixture was concentrated under reduced pressure to give a blueish solid. This solid was readily dissolved in a mixture of water and dichloromethane. The dichloromethane was separated, and the aqueous phase was extracted with dichloromethane. The combined organic layers were washed with 2M NaOH and brine, dried over MgSO₄, filtered, and concentrated under reduced pressure onto silica gel. The crude was purified by flash column chromatography (cyclohexane/ ethyl acetate gradient from 1:0 to 0:1) to give the desired product in 96% yield (0.30333 g, 0.45675 mmol). White solid contaminated with *N,N'*-dicyclohexylurea: ¹**H NMR** (300 MHz, Methanol-*d*₄) δ 8.08 (d, *J* = 8.5 Hz, 1H), 7.94 – 7.86 (m, 2H), 7.74 (dd, *J* = 8.5, 2.4 Hz, 1H), 7.69 – 7.58 (m, 3H), 7.38 – 7.31 (m, 2H), 6.88 (d, *J* = 8.6 Hz, 1H), 3.72 (q, *J* = 7.2 Hz, 4H), 3.60 – 3.46 (m, 2H), 3.33 (s, 6H), 2.99 – 2.82 (m, 2H), 2.82 (s, 3H), 1.21 (t, *J* = 7.2 Hz, 6H). ¹³**C NMR** (75 MHz, MeOD) δ 169.98, 158.52, 153.63, 151.31, 146.70, 144.25, 140.96, 139.78, 134.64, 132.33, 131.81, 131.41, 130.89, 125.17, 124.69, 124.21, 121.88, 121.14, 120.32, 119.68, 118.87, 113.63, 108.73, 66.45, 54.96, 51.64, 47.21, 33.90, 26.34, 25.91, 10.72. **HRMS** (ESI) calculated for [M+H]⁺ C₃₁H₃₄N₃O₂ 480.2646, found 480.2633.



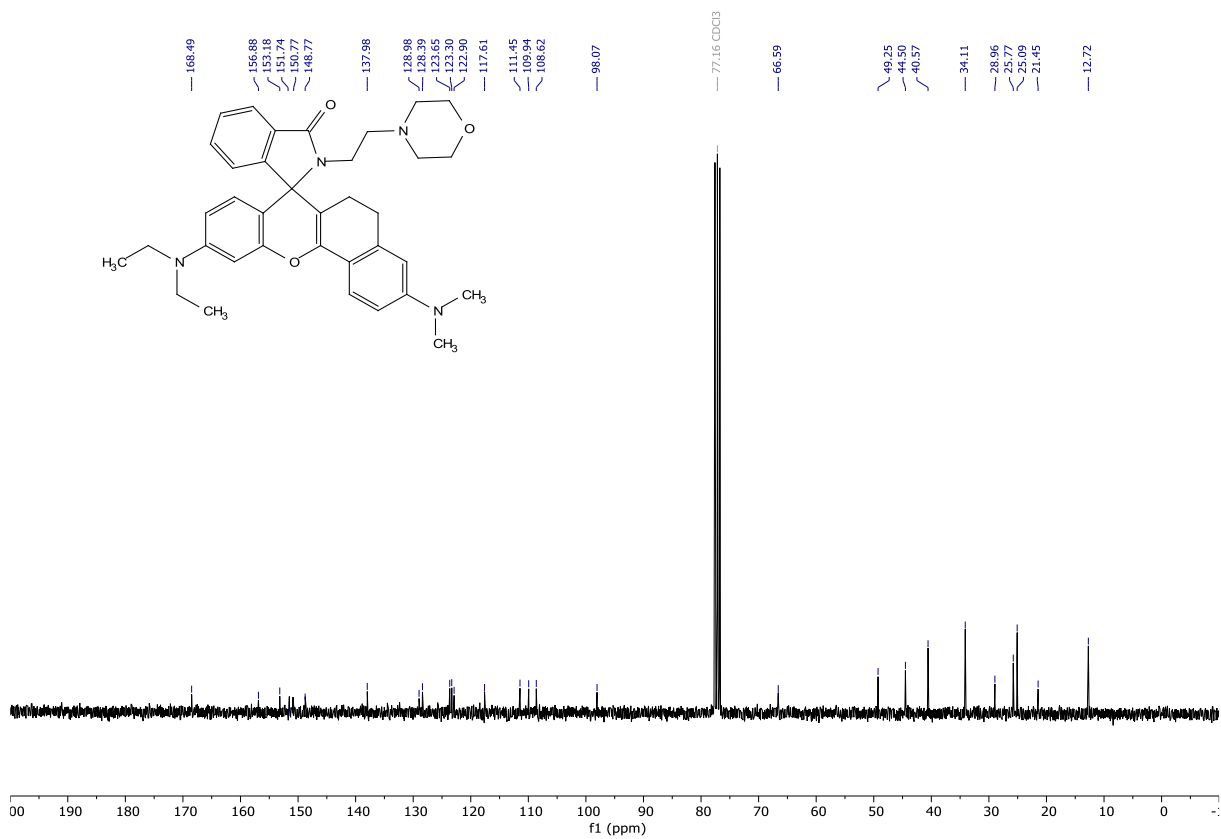
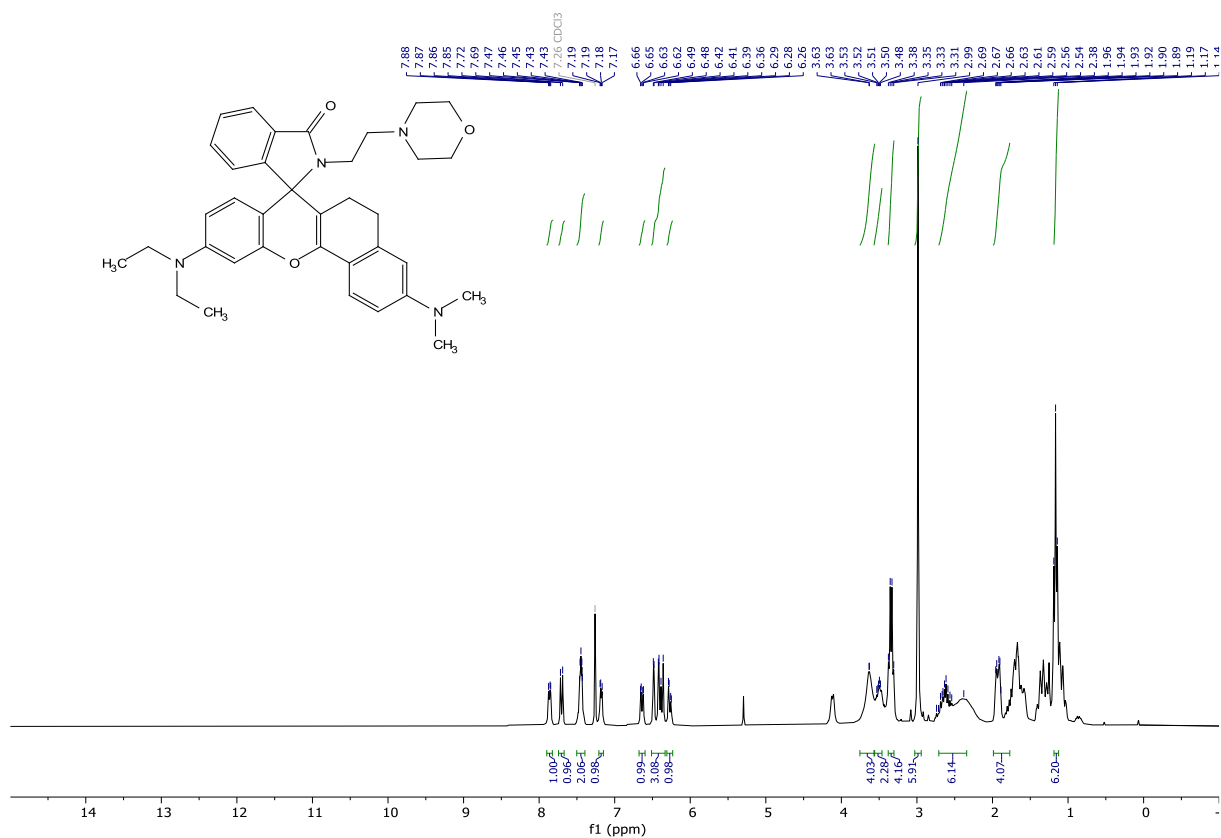


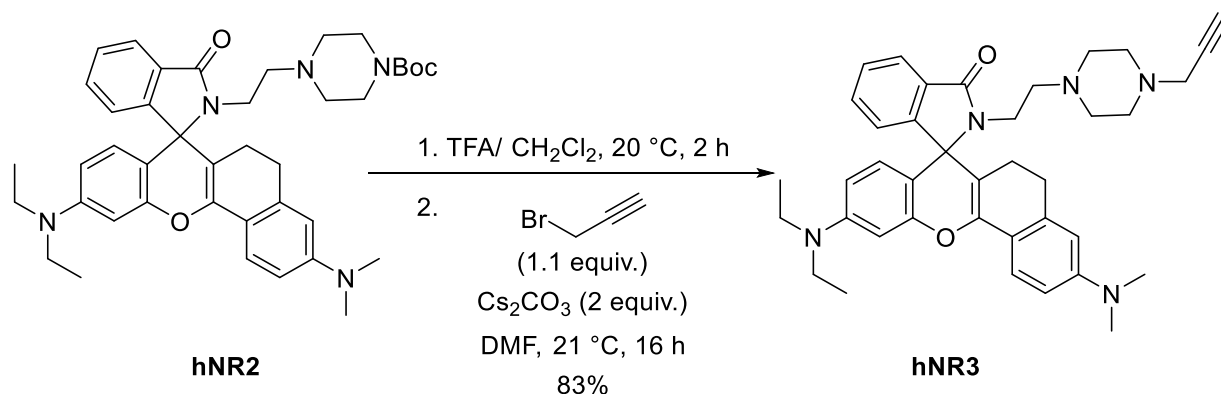
tert-butyl 4-(2-(10-(diethylamino)-3-(dimethylamino)-3'-oxo-5,6-dihydrospiro[benzo[c]xanthene-7,1'-isoindolin]-2'-yl)ethyl)piperazine-1-carboxylate (hNR2). To a stirred solution of *N*-(3-(dimethylamino)-7-(2-(((2,5-dioxopyrrolidin-1-yl)oxy)carbonyl)phenyl)-5,6-dihydro-10*H*-benzo[c]xanthene-10-ylidene)-*N*-ethylethanaminium perchlorate (0.23124, 0.3482) in acetonitrile (20 mL) was added DIPEA (0.303 mL, 0.2250 g, 1.7408 mmol) and *tert*-butyl 4-(2-aminoethyl)piperazine-1-carboxylate (0.14600 g, 0.6367 mmol). After 4 h the solvent was removed under reduced pressure. The slight blue residue was taken up in a mixture of dichloromethane and water. The aqueous phase was extracted with dichloromethane, the combined organic layers were dried over MgSO_4 , filtered, and concentrated under reduced pressure onto silica gel. The crude was purified by flash column chromatography (cyclohexane/ ethyl acetate gradient from 1:0 to 0:1) to give the desired product in 96% yield. Light blue solid: $^1\text{H NMR}$ (300 MHz, $\text{DMSO}-d_6$) δ 7.79 – 7.72 (m, 1H), 7.60 (d, J = 8.6 Hz, 1H), 7.52 (pd, J = 7.3, 1.4 Hz, 2H), 7.23 – 7.13 (m, 1H), 6.63 (dd, J = 8.7, 2.6 Hz, 1H), 6.54 (d, J = 2.5 Hz, 1H), 6.46 (d, J = 2.5 Hz, 1H), 6.36 (dd, J = 8.9, 2.6 Hz, 1H), 6.24 (d, J = 8.8 Hz, 1H), 3.40 – 3.24 (m, 6H), 3.14 (q, J = 7.1, 5.3 Hz, 5H), 2.92 (s, 6H), 2.71 – 2.53 (m, 2H), 2.32 – 2.20 (m, 1H), 2.20 – 2.00 (m, 5H), 1.77 – 1.61 (m, 1H), 1.34 (s, 9H), 1.08 (t, J = 6.9 Hz, 6H). $^{13}\text{C NMR}$ (75 MHz, DMSO) δ 166.96, 153.71, 152.35, 150.91, 150.58, 148.16, 146.43, 137.30, 132.48, 131.51, 128.51, 123.35, 122.80, 122.18, 117.26, 111.17, 109.50, 108.57, 104.80, 99.99, 97.31, 78.61, 65.46, 55.59, 52.29, 43.64, 39.91, 36.75, 34.15, 27.98, 26.60, 25.31, 24.45, 20.94, 12.37. **HRMS** (ESI) calculated for $[\text{M}+\text{H}]^+$ $\text{C}_{41}\text{H}_{52}\text{N}_5\text{O}_4$ 678.4014, found 678.4015.





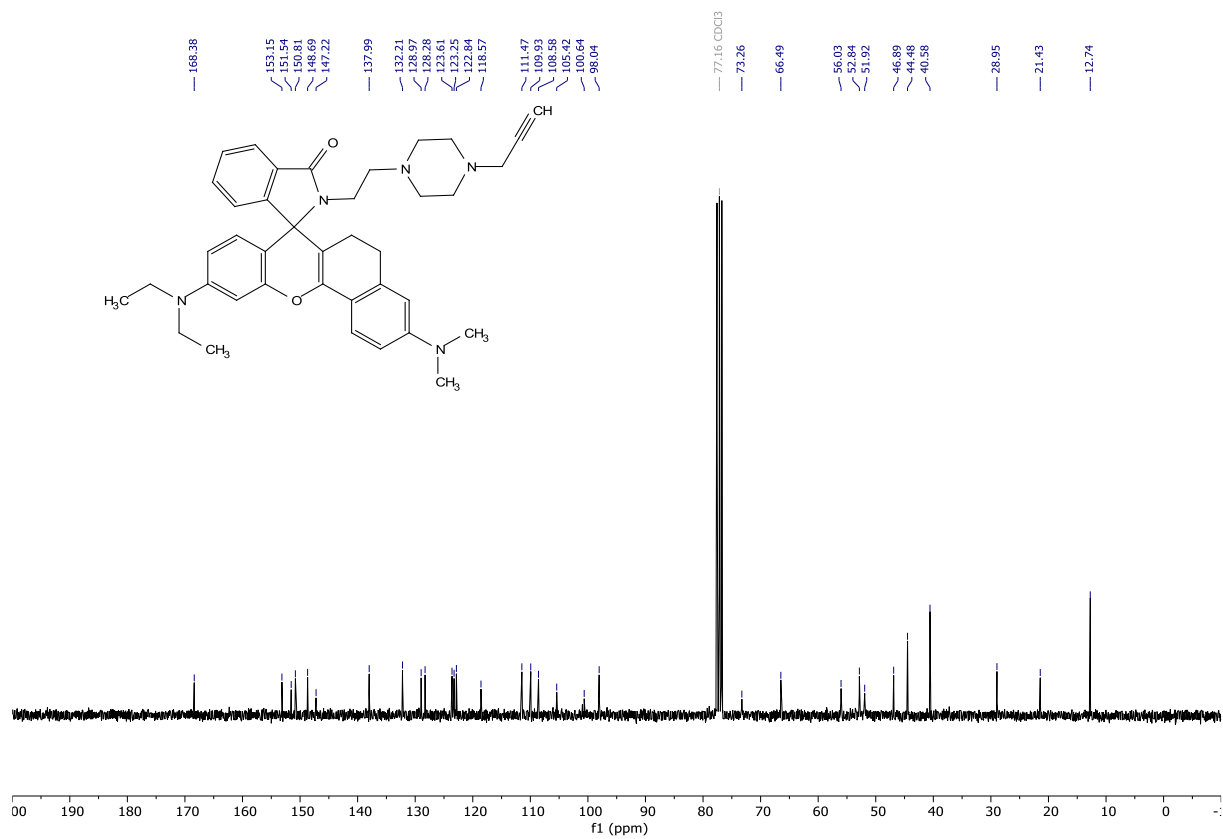
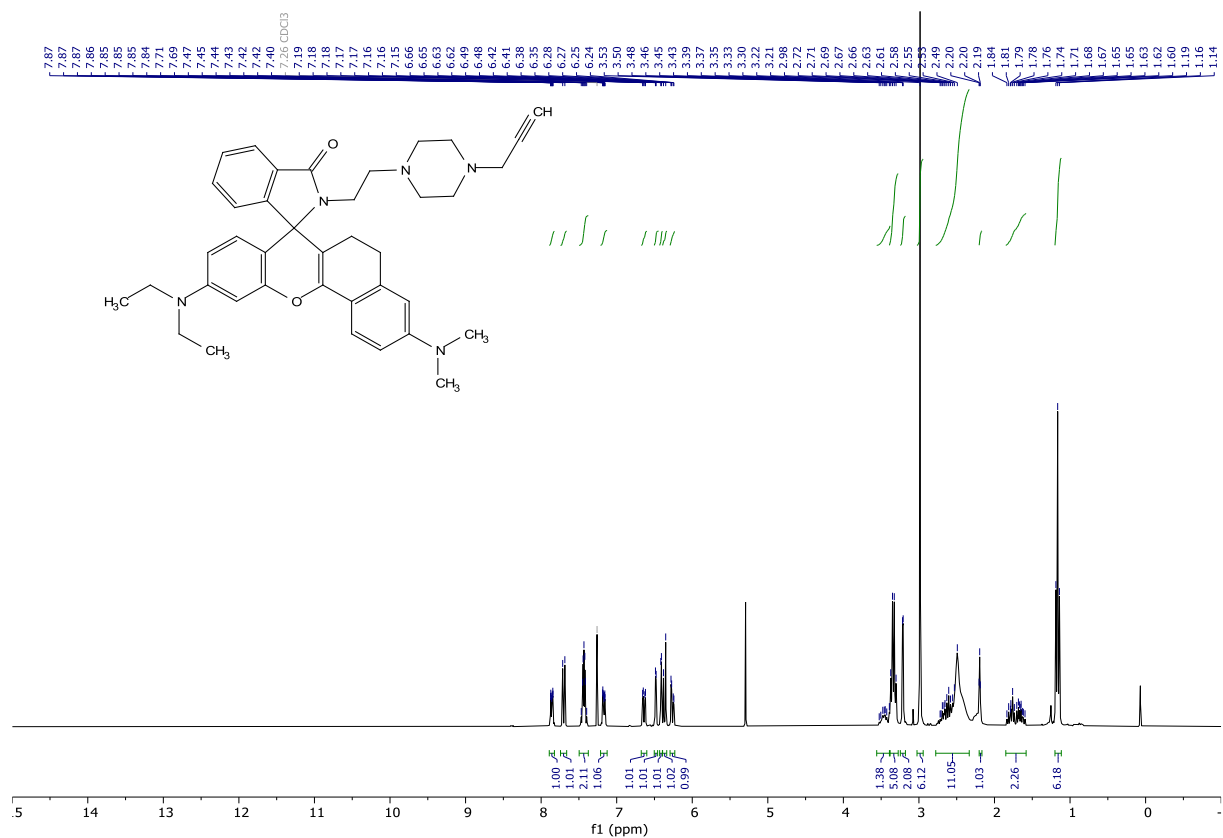
10-(diethylamino)-3-(dimethylamino)-2'-(2-morpholinoethyl)-5,6-dihydrospiro[benzo[*c*]xanthene-7,1'-isoindolin]-3'-one (lyso-hNR). To a stirred solution of *N*-(3-(dimethylamino)-7-(2-(((2,5-dioxopyrrolidin-1-yl)oxy)carbonyl)phenyl)-5,6-dihydro-10*H*-benzo[*c*]xanthen-10-ylidene)-*N*-ethylethanaminium perchlorate (0.07114 g, 0.1071 mmol) in acetonitrile (10 mL) was added 4-(2-aminoethyl)morpholine (0.3 mL, 0.2967 g, 2.2772 mmol). The mixture was stirred for 30 minutes. Then the mixture was concentrated under reduced pressure to give a blueish solid. This solid was readily dissolved in a mixture of water and dichloromethane. The aqueous phase was extracted with dichloromethane. The combined organic layers were washed with 2M NaOH and brine, dried over MgSO₄, filtered, and concentrated under reduced pressure onto silica gel. The crude was purified by flash column chromatography (cyclohexane/ ethyl acetate gradient from 1:0 to 0:1) to give the desired product in 95% (0.05892 g, 0.101804 mmol). White solid: ¹H NMR (300 MHz, Chloroform-*d*) δ 7.90 – 7.82 (m, 1H), 7.70 (d, *J* = 8.6 Hz, 1H), 7.45 (dt, *J* = 5.6, 2.1 Hz, 2H), 7.21 – 7.15 (m, 1H), 6.64 (dd, *J* = 8.6, 2.6 Hz, 1H), 6.51 – 6.33 (m, 3H), 6.27 (dd, *J* = 8.9, 2.6 Hz, 1H), 3.75 – 3.56 (m, 4H), 3.57 – 3.46 (m, 2H), 3.34 (q, *J* = 7.0 Hz, 4H), 2.99 (s, 6H), 2.71 – 2.34 (m, 6H), 1.99 – 1.77 (m, 4H), 1.17 (t, *J* = 6.9 Hz, 8H). ¹³C NMR (75 MHz, CDCl₃) δ 168.49, 156.88, 153.18, 151.74, 150.77, 148.77, 137.98, 128.98, 128.39, 123.65, 123.30, 122.90, 117.61, 111.45, 109.94, 108.62, 98.07, 66.59, 49.25, 44.50, 40.57, 34.11, 28.96, 25.77, 25.09, 21.45, 12.72. HRMS (ESI) calculated for [M+H]⁺ C₃₆H₄₃N₄O₃ 579.3330, found 579.3317.

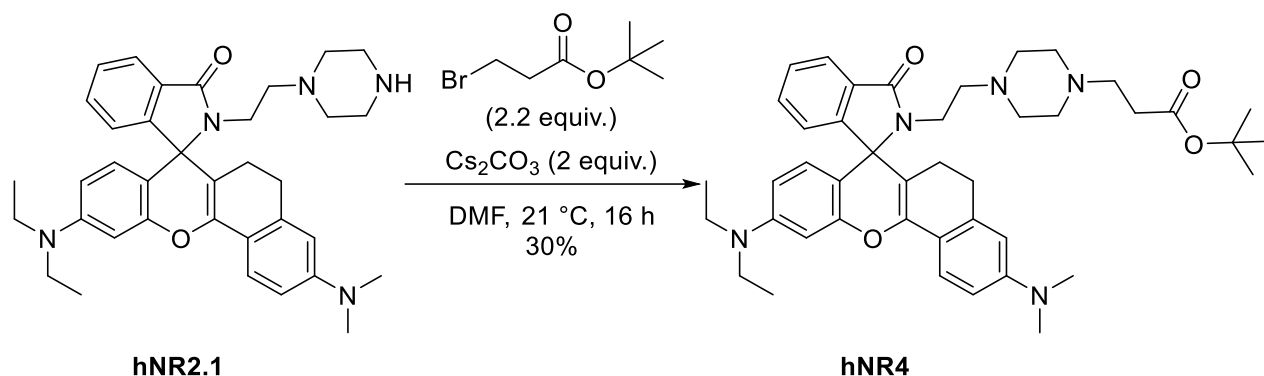




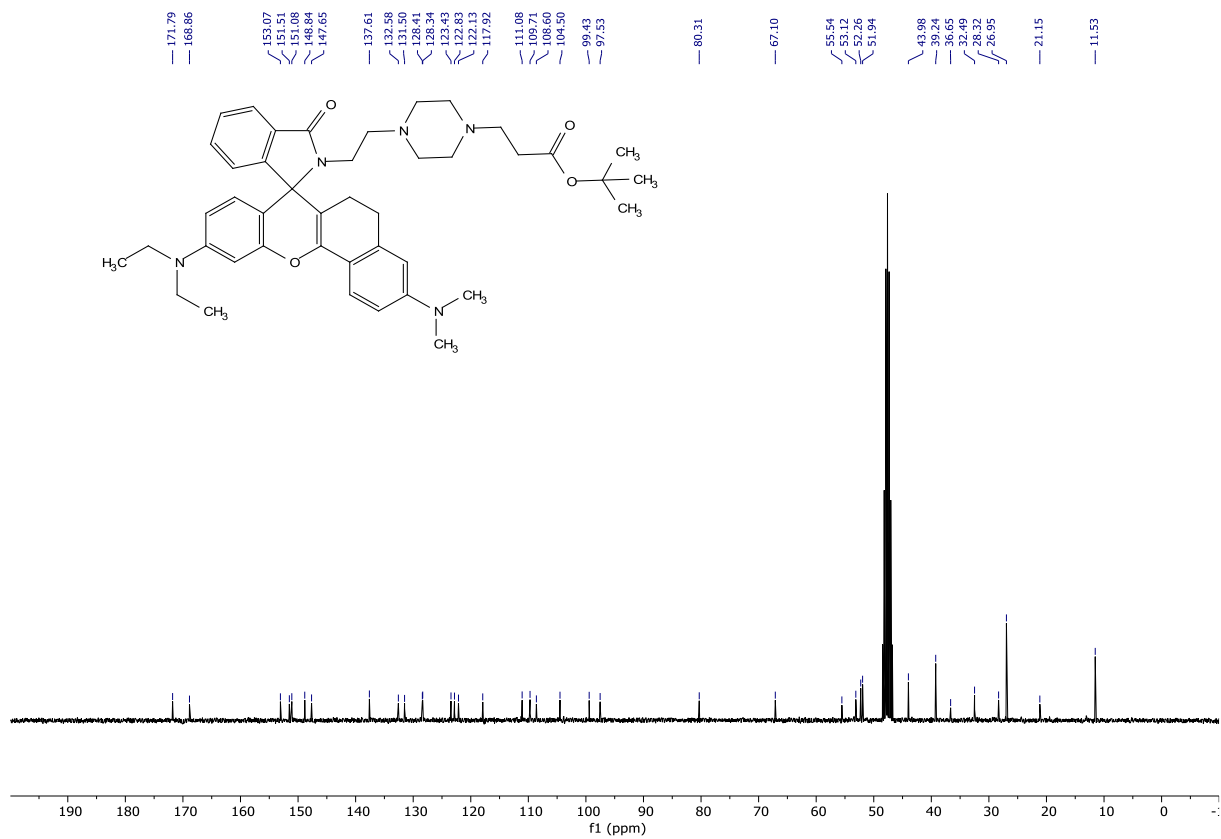
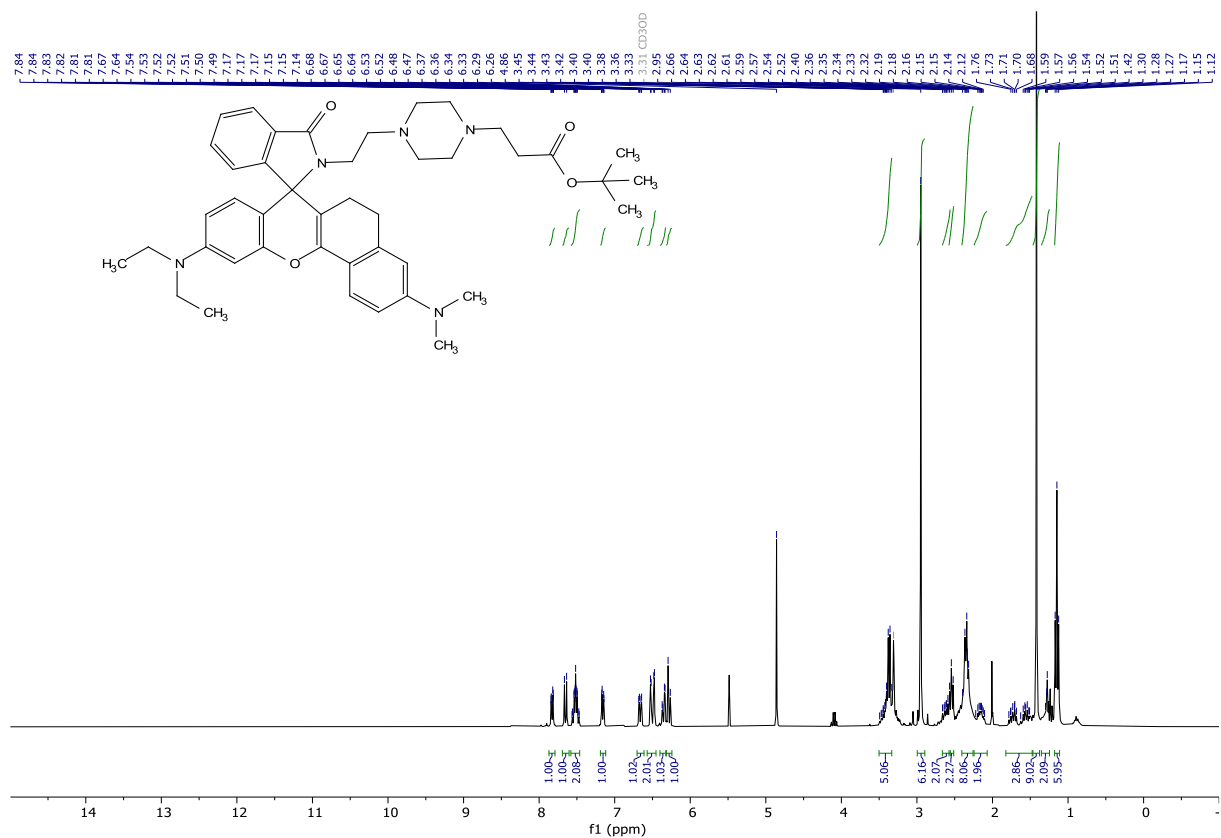
10-(diethylamino)-3-(dimethylamino)-2'-(2-(4-(prop-2-yn-1-yl)piperazin-1-yl)ethyl)-5,6-

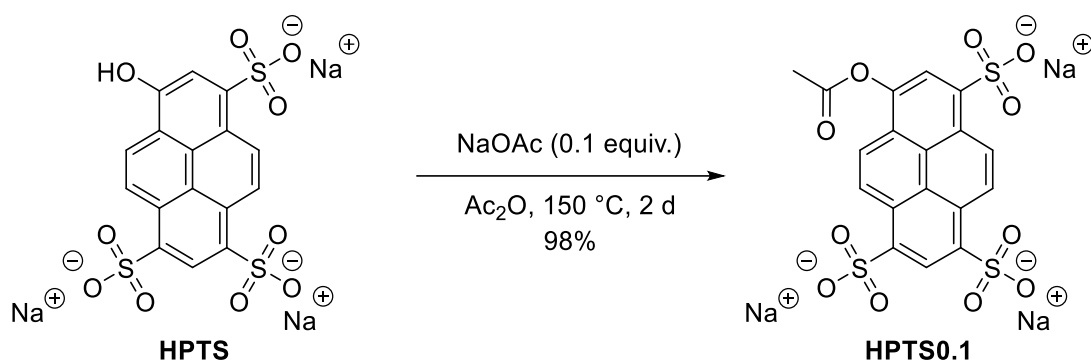
dihydrospiro[benzo[c]xanthene-7,1'-isoindolin]-3'-one (hNR3). To a stirred solution of *tert*-butyl 4-(2-(10-(diethylamino)-3-(dimethylamino)-3'-oxo-5,6-dihydrospiro[benzo[c]xanthene-7,1'-isoindolin]-2'-yl)ethyl)piperazine-1-carboxylate (0.24901 g, 0.36732 mmol) in dichloromethane (5 mL) was added trifluoroacetic acid (2 mL). After 2 h, the mixture was diluted with water and the organic phase was washed with dilute NaOH. The aqueous phase was extracted with dichloromethane, the combined organic phases were dried over MgSO₄, filtered, and concentrated under reduced pressure. The obtained solid was dissolved in DMF (5 mL) and to the solution was added CsCO₃ (0.24094 g, 0.7395 mmol) and propargyl bromide (80% in toluene, 0.05 mL, 0.0534g, 0.448 mmol). The mixture was stirred under an argon atmosphere for 16 h. Then the DMF was removed under reduced pressure. The beige solid was dissolved in a mixture of water and dichloromethane. The aqueous phase was extracted with dichloromethane. The combined organic layers were dried over MgSO₄, filtered, and concentrated under reduced pressure onto silica gel. The crude was purified by flash column chromatography (dichloromethane/ methanol gradient from 1:0 to 9:1), to give the desired compound in 83% yield (0.1846 g, 0.30441 mmol). White solid: ¹H NMR (300 MHz, Chloroform-*d*) δ 7.89 – 7.82 (m, 1H), 7.70 (d, *J* = 8.6 Hz, 1H), 7.50 – 7.38 (m, 2H), 7.21 – 7.13 (m, 1H), 6.64 (dd, *J* = 8.7, 2.6 Hz, 1H), 6.48 (d, *J* = 2.6 Hz, 1H), 6.41 (d, *J* = 2.5 Hz, 1H), 6.37 (d, *J* = 8.9 Hz, 1H), 6.26 (dd, *J* = 8.9, 2.6 Hz, 1H), 3.56 – 3.38 (m, 1H), 3.34 (q, *J* = 7.1 Hz, 5H), 3.21 (d, *J* = 2.5 Hz, 2H), 2.98 (s, 6H), 2.78 – 2.33 (m, 11H), 2.20 (t, *J* = 2.4 Hz, 2H), 1.85 – 1.58 (m, 2H), 1.16 (t, *J* = 7.0 Hz, 6H). ¹³C NMR (75 MHz, CDCl₃) δ 168.38, 153.15, 151.54, 150.81, 148.69, 147.22, 137.99, 132.21, 128.97, 128.28, 123.61, 123.25, 122.84, 118.57, 111.47, 109.93, 108.58, 105.42, 100.64, 98.04, 73.26, 66.49, 56.03, 52.84, 51.92, 46.89, 44.48, 40.58, 28.95, 21.43, 12.74. HRMS (ESI) calculated for [M+H]⁺ C₃₉H₄₆N₅O₂ 616.3622, found 616.3626.



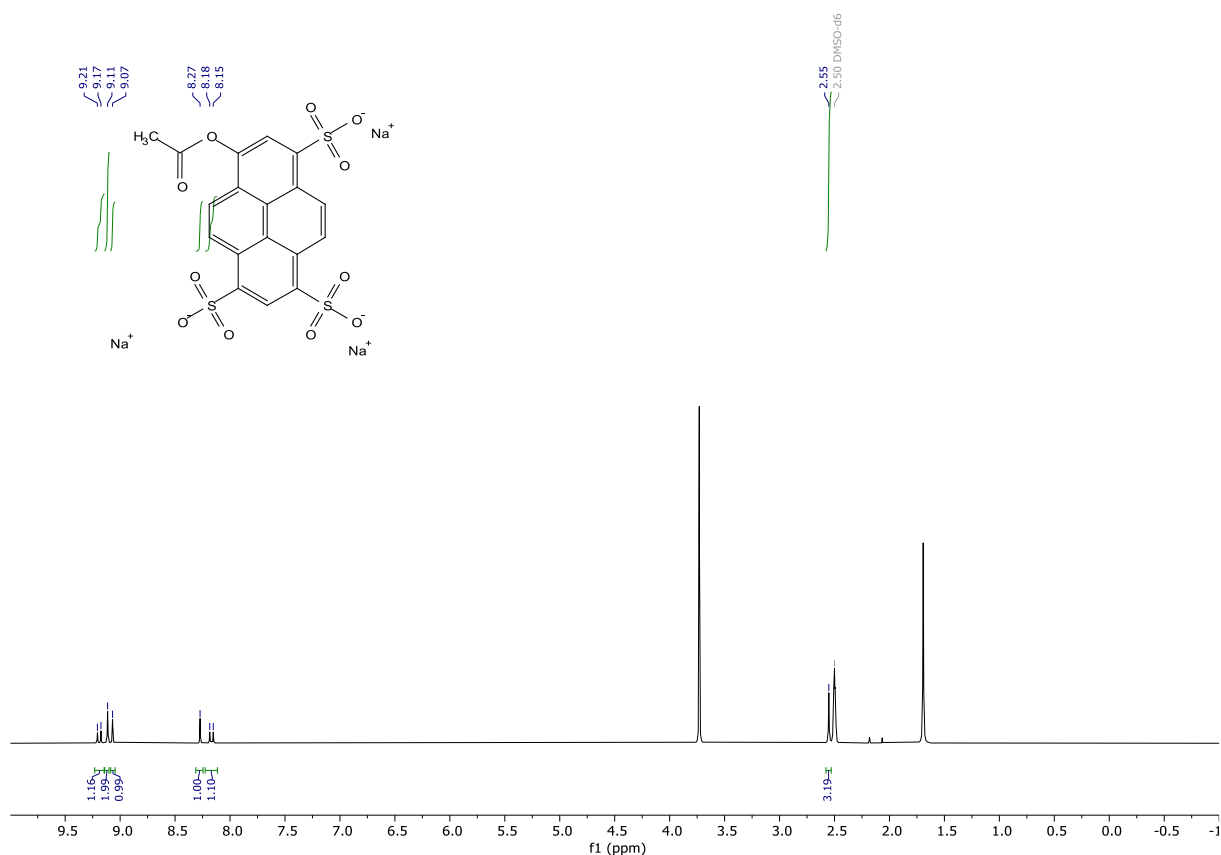


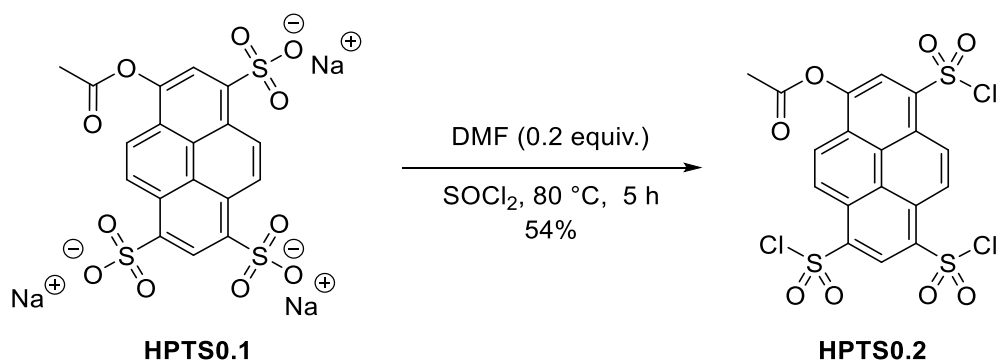
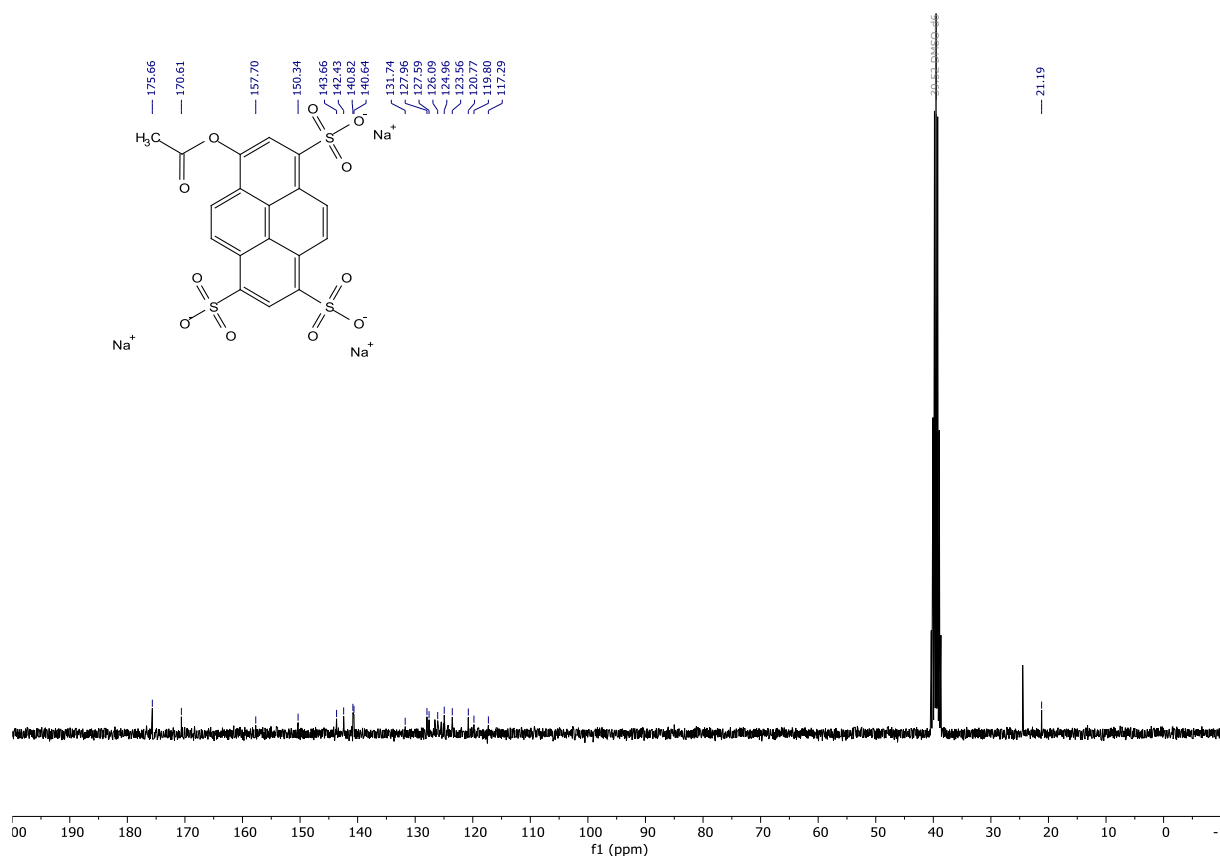
tert-butyl 3-(4-(2-(10-(diethylamino)-3-(dimethylamino)-3'-oxo-5,6-dihydrospiro[benzo[c]xanthene-7,1'-isoindolin]-2'-yl)ethyl)piperazin-1-yl)propanoate (hNR4). To a stirred solution of 10-(diethylamino)-3-(dimethylamino)-2'-(2-(piperazin-1-yl)ethyl)-5,6-dihydrospiro[benzo[c]xanthene-7,1'-isoindolin]-3'-one (0.09955 g, 0.1723 mmol) in DMF (5 mL) at 20 °C was added caesium carbonate (0.1150 g, 0.3530) followed by *tert*-butyl 3-bromopropanoate (0.040 mL, 0.05012 g, 0.23886 mmol). After 16 h, more *tert*-butyl 3-bromopropanoate (0.040 mL, 0.05012 g, 0.23886 mmol) was added. The mixture was stirred for 5 h. Then the reaction was stopped by adding water and dichloromethane. The aqueous phase was extracted with dichloromethane. The combined organic phases were washed with brine (3x), dried over MgSO_4 , filtered, and concentrated under reduced pressure onto silica gel. The crude was purified by flash column chromatography (dichloromethane/ methanol gradient from 1:0 to 9:1) to give the desired product in 30% yield (0.03677 g, 0.05209 mmol). White solid: $^1\text{H NMR}$ (300 MHz, Methanol- d_4) δ 7.87 – 7.79 (m, 1H), 7.65 (d, J = 8.7 Hz, 1H), 7.58 – 7.46 (m, 2H), 7.19 – 7.12 (m, 1H), 6.66 (dd, J = 8.7, 2.6 Hz, 1H), 6.50 (dd, J = 13.3, 2.5 Hz, 2H), 6.35 (dd, J = 8.9, 2.5 Hz, 1H), 6.28 (d, J = 8.9 Hz, 1H), 3.50 – 3.33 (m, 5H), 2.95 (s, 6H), 2.69 – 2.56 (m, 2H), 2.54 (t, J = 7.1 Hz, 3H), 2.41 – 2.26 (m, 8H), 2.24 – 2.07 (m, 2H), 1.82 – 1.47 (m, 3H), 1.42 (s, 9H), 1.35 – 1.25 (m, 2H), 1.15 (t, J = 7.0 Hz, 6H). $^{13}\text{C NMR}$ (75 MHz, MeOD) δ 171.79, 168.86, 153.07, 151.51, 151.08, 148.84, 147.65, 137.61, 132.58, 131.50, 128.41, 128.34, 123.43, 122.83, 122.13, 117.92, 111.08, 109.71, 108.60, 104.50, 99.43, 97.53, 80.31, 67.10, 55.54, 53.12, 52.26, 51.94, 43.98, 39.24, 36.65, 32.49, 28.32, 26.95, 21.15, 11.53. **HRMS** (ESI) calculated for $[\text{M}+\text{H}]^+$ $\text{C}_{43}\text{H}_{55}\text{N}_5\text{O}_4$ 706.4327, found 706.4340.



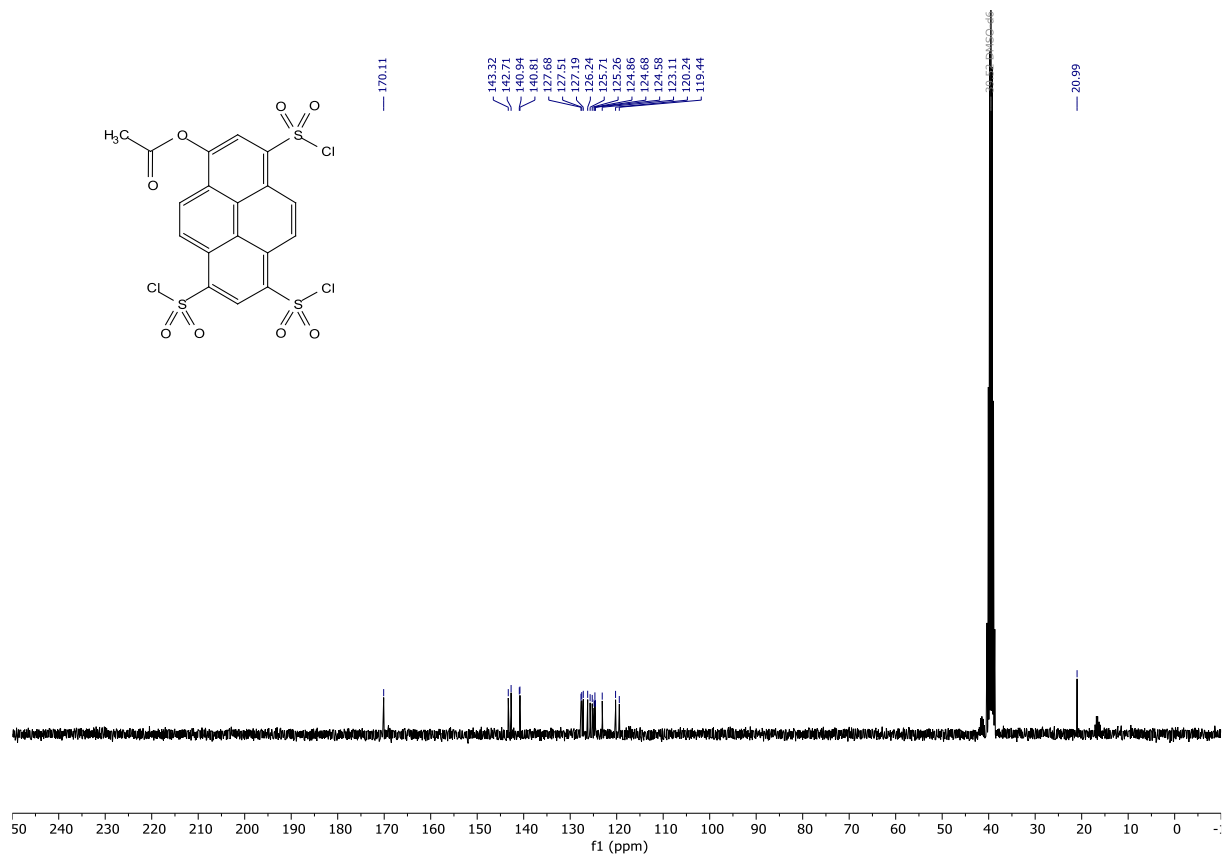
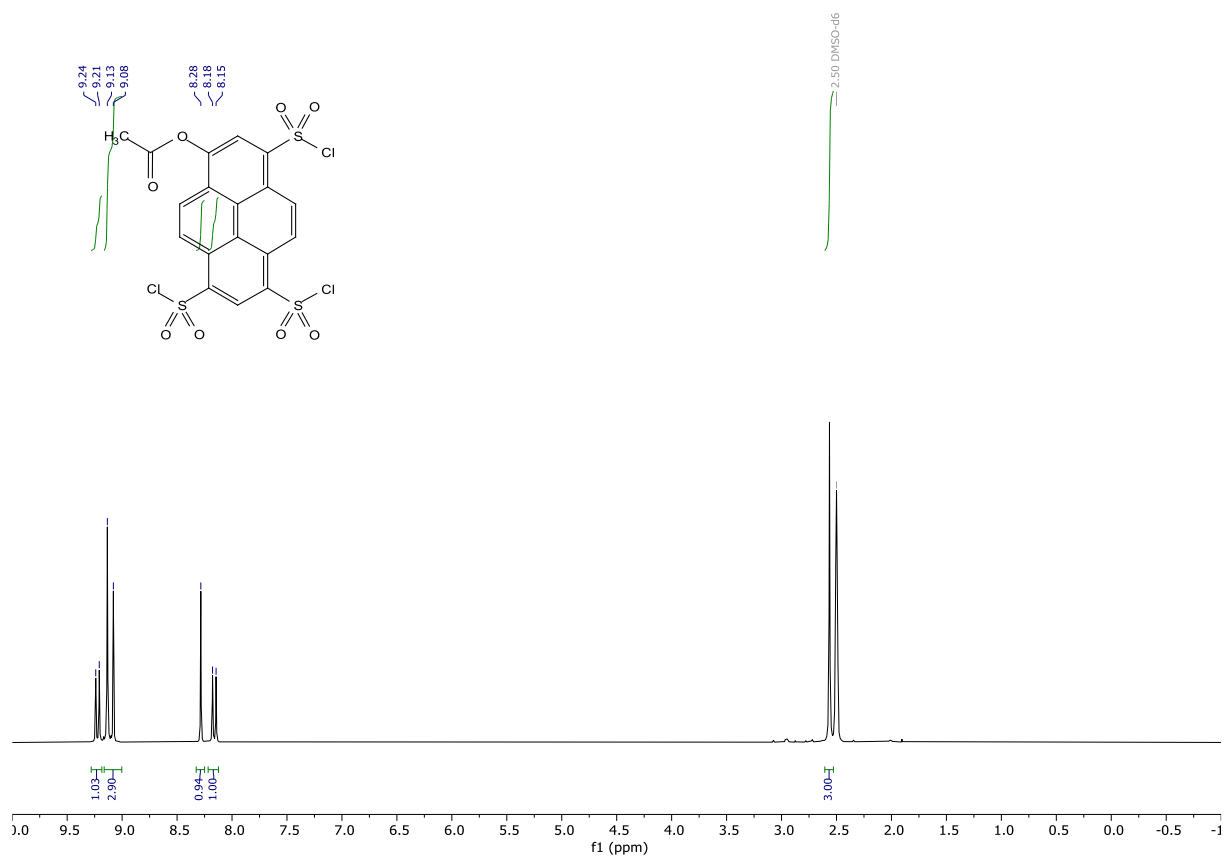


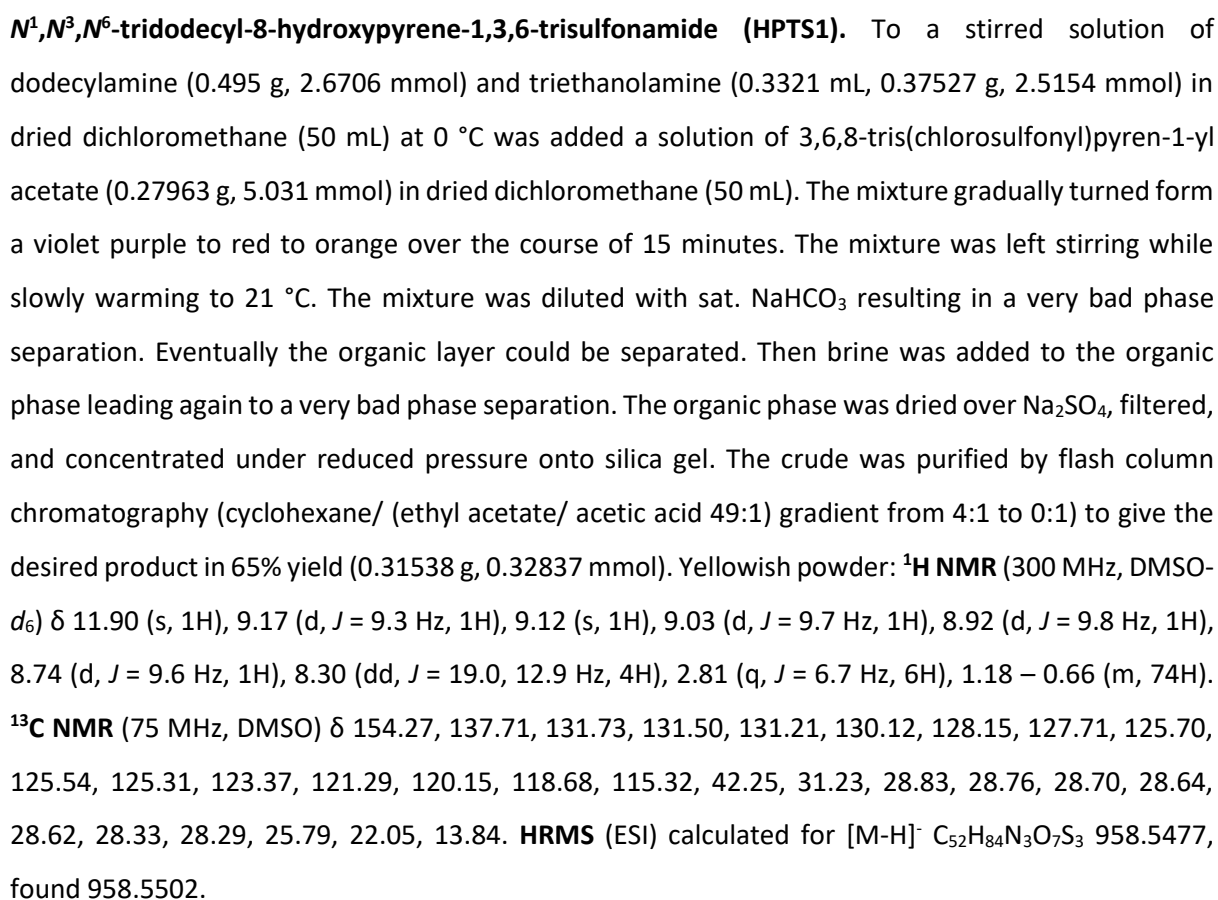
sodium 8-acetoxypyrene-1,3,6-trisulfonate (HPTS0.1). Trisodium 8-hydroxypyrene-1,3,6-trisulfonic acid (0.54872 g, 1.0464 mmol) and sodium acetate (0.00885 g, 0.1079 mmol) were suspended in acetic anhydride (10 mL) under an argon atmosphere. The mixture was heated to 120 °C. After 40 h reaction time, the mixture was cooled to 21 °C. Then THF (25 mL) was added to the grey suspension. The mixture was filtered through a por 4 frit. The filter cake was washed with acetone (25 mL) and the orange filtrate was discarded. The filter cake was thoroughly dried under high vac, to give the desired product in 98% yield (0.58150 g, 1.02665 mmol). Greyish solid (impure): ¹H NMR (300 MHz,) δ 9.19 (d, *J* = 9.7 Hz, 1H), 9.11 (s, 2H), 9.07 (s, 1H), 8.27 (s, 1H), 8.17 (d, *J* = 9.6 Hz, 1H), 2.55 (s, 3H). ¹³C NMR (75 MHz, DMSO) δ 175.66, 170.61, 157.70, 150.34, 143.66, 142.43, 140.82, 140.64, 131.74, 127.96, 127.59, 126.09, 124.96, 123.56, 120.77, 119.80, 117.29, 21.19. HRMS (ESI) calculated for [M-Na]⁺ C₁₈H₉Na₂O₁₁S₃ 542.9108, found 542.9126.

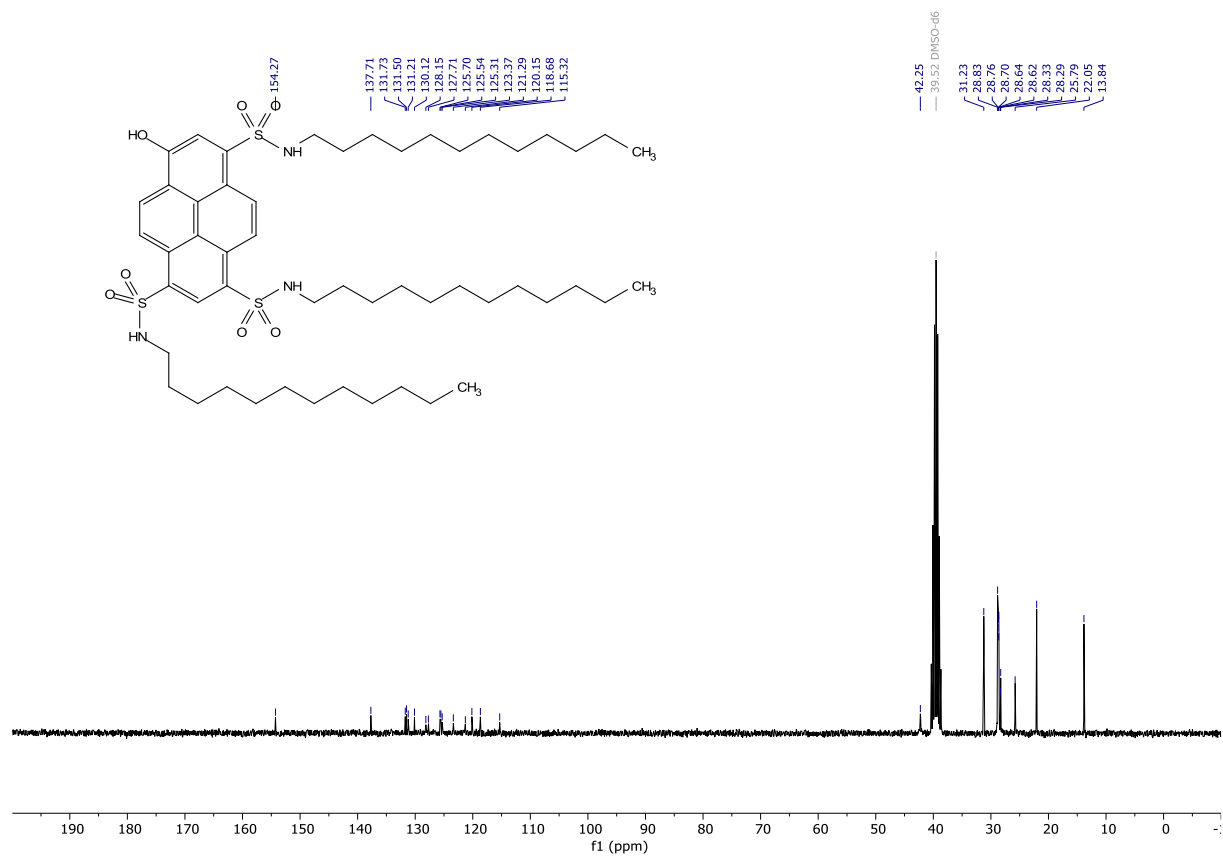
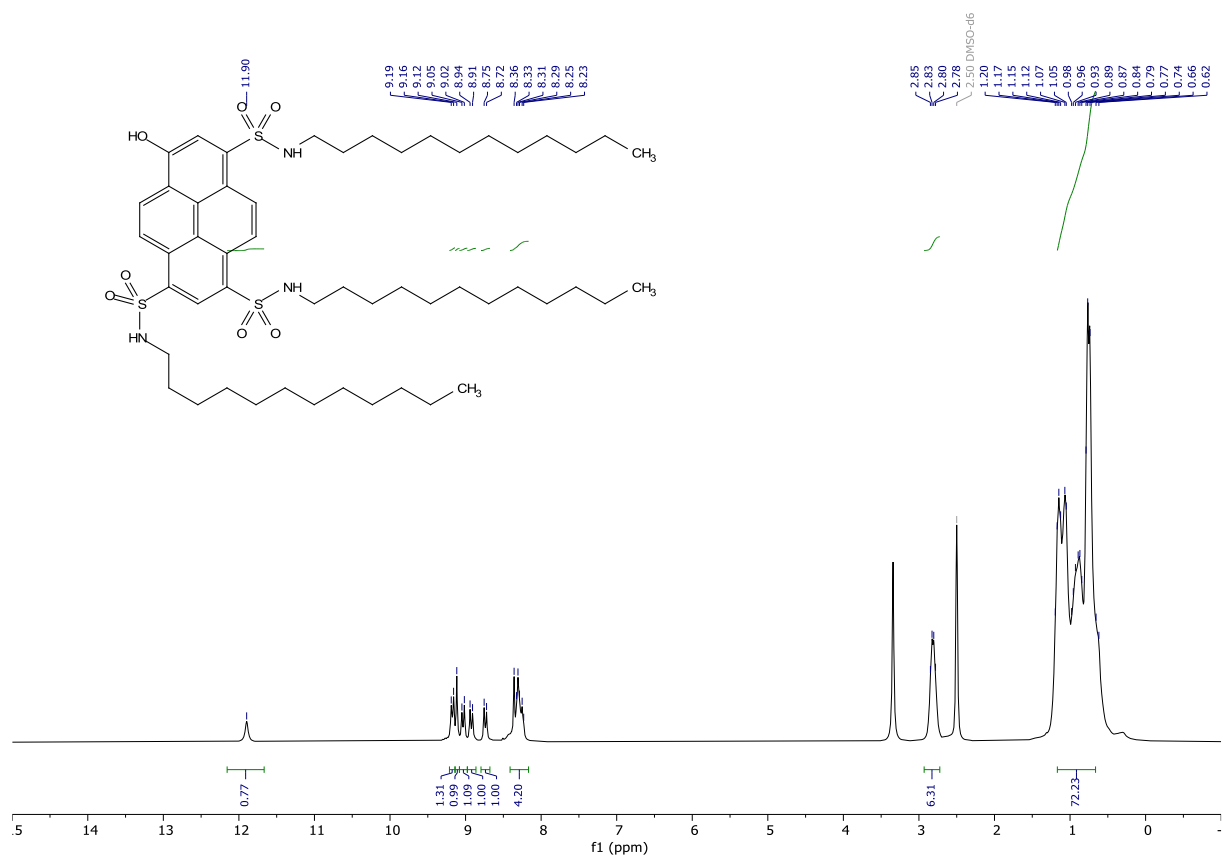




3,6,8-tris(chlorosulfonyl)pyrene-1-yl acetate (HPTS0.2). To sodium 8-acetoxypyrene-1,3,6-trisulfonate (0.56687 g, 1.0008 mmol) was added thionyl chloride (5 mL) followed by DMF (0.015 mL). The mixture was placed under an argon atmosphere, and was heated to 80 °C. The mixture was poured onto ice leading to an orange precipitate, which was filtered off through a por3 frit. The filter cake was washed thoroughly with water and dried in high vacuum to give the desired product in 54% (0.29963 g, 0.53911 mmol). Orange, brown solid: $^1\text{H NMR}$ (300 MHz, DMSO- d_6) δ 14.48 (s, 2H), 9.22 (d, J = 9.6 Hz, 1H), 9.11 (d, J = 16.4 Hz, 3H), 8.28 (s, 1H), 8.16 (d, J = 9.6 Hz, 1H), 2.56 (s, 3H). $^{13}\text{C NMR}$ (75 MHz, DMSO) δ 170.11, 143.32, 142.71, 140.94, 140.81, 127.68, 127.51, 127.19, 126.24, 125.71, 125.26, 124.86, 124.68, 124.58, 123.11, 120.24, 119.44, 20.99. **HRMS** (ESI) calculated for $[\text{M}-\text{Cl}+\text{O}]^-$ $\text{C}_{18}\text{H}_9\text{Cl}_2\text{O}_9\text{S}_3$ 534.8791, found 534.8806.







3.3. Trifunctional probe

Background and aim

Biotinylated or fluorescent probes are widely used in biochemistry labs. The use of biotinylated probes in combination with its binder avidin or streptavidin allows for selective pull-down of target proteins from lysates or other complex mixtures.¹¹⁶ On the other hand, fluorescent probes are ubiquitously used to localise and monitor targets in equally complex mixtures.¹¹⁷ A polyfunctional chemical biology probe that combines several useful properties (e.g. biotin, fluorophore and bioorthogonal handle/anchor **Figure 41**) can be a very powerful research tool in target identification and proteomic projects. Amino acids represent convenient scaffolds for multifunctional probe development but lengthy syntheses and protection/deprotection strategies can complicate access to such probes. A possible way to avoid these issues is to use cysteine as scaffold. The advantage of cysteine is that it already provides three different reacting moieties. We aimed to explore this unique feature by developing a reaction cascade using “click reactions” that sequentially couples a fluorophore, biotin, and an azide. The azide is used for selective reaction to an alkynylated target in the “complex mixture”.

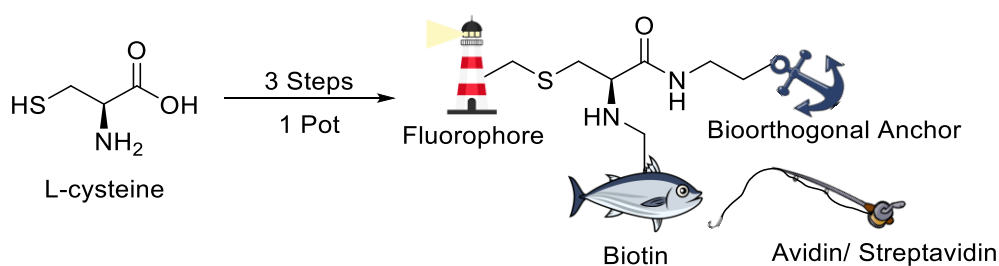


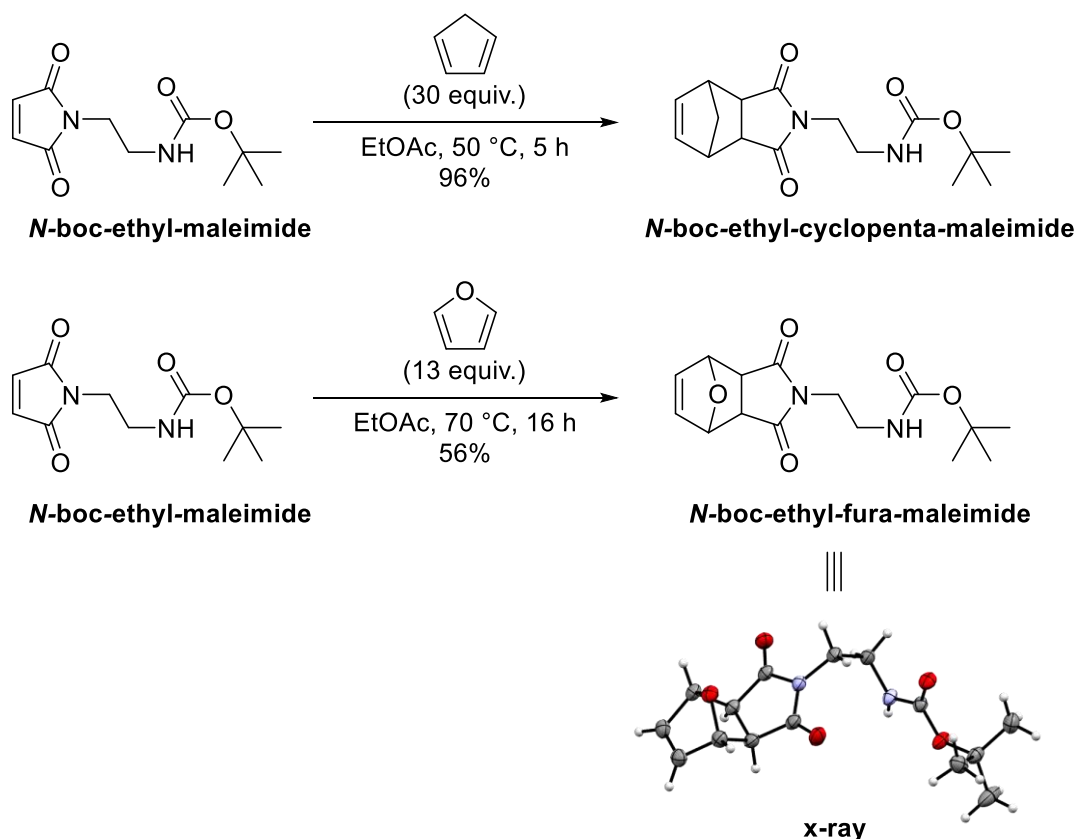
Figure 41 Cartoon depiction of the trifunctional probe

Results

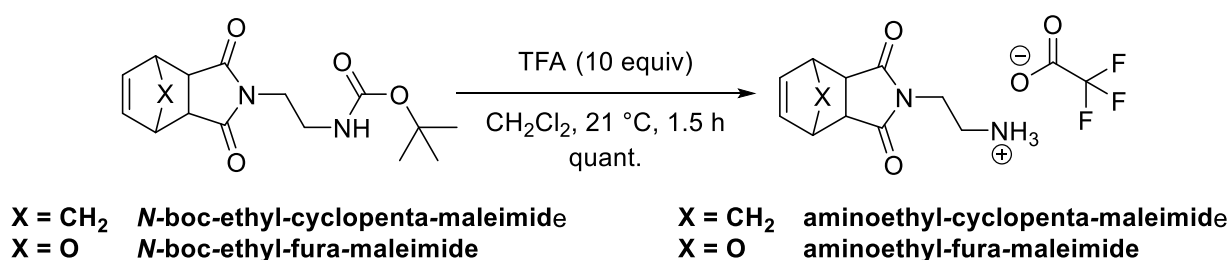
As the protection free synthesis of the probe is based on the reactivity of the three functional groups of cysteine, reaction partners that are orthogonal to the other functional moieties are required. The sulfhydryl of the cysteine is reactive towards maleimides that possess an electrophilic Michael acceptor position. Therefore, the fluorophore could contain a maleimide to react selectively with the sulfhydryl. A possible route to a silicon rhodamine with a maleimide motif was described by a previous PhD student in our group.¹¹⁸ We planned to synthesise the SiR-maleimide starting from SiR-NHS ester that was previously synthesised and described in 1.5, by coupling it with a maleimide-amine. Maleimides tend to react willingly with nucleophiles at their electrophilic Michael acceptor position. Therefore, protection of the maleimide was required. We chose a Diels-Alder reaction to protect the maleimide as shown in **Scheme 21**. The deprotection and reformation of the maleimide was projected by a retro-Diels-Alder reaction. Starting from a boc-protected maleimide (*N*-Boc-ethyl-maleimide in

Scheme 21, A) the maleimide was reacted with cyclopentadiene or furane. It is interesting to note that the reaction with cyclopentadiene was faster and gave higher yields compared to the reaction with the furane. Both boc protected intermediates were deprotected in dichloromethane with trifluoroacetic acid (**Scheme 21, B**).

A



B

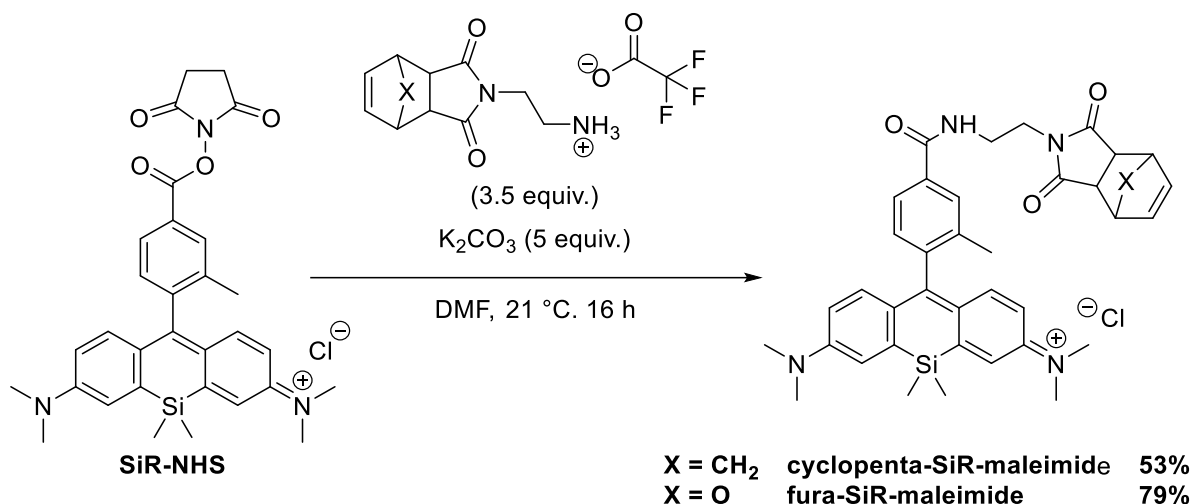


Scheme 21 A) Diels-Alder reaction with cyclopentadiene and furane. *N*-boc-ethyl-fura-maleimide the crystal structure was obtained **B)** Boc deprotection with TFA

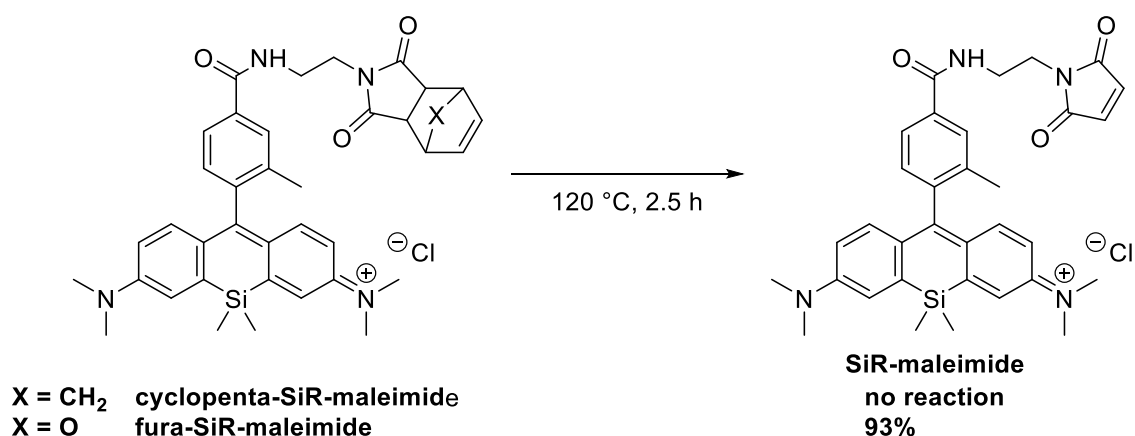
Both compounds were successfully coupled to the SiR-NHS ester in dimethylformamide using potassium carbonate as base (**Scheme 22, A**). However, in the deprotection reaction of the precursors to the final **SiR-maleimide** only decomposition was observed for the cyclopentadiene protected intermediate (**Scheme 22, B**). Conversely, for the furane protected species clean conversion was

achieved. This is in line with the results observed in the protection reaction, where the efficiency was higher for the cyclopentadiene, indicating that the cyclopentadiene product is energetically more stable than the furane-protected one.

A



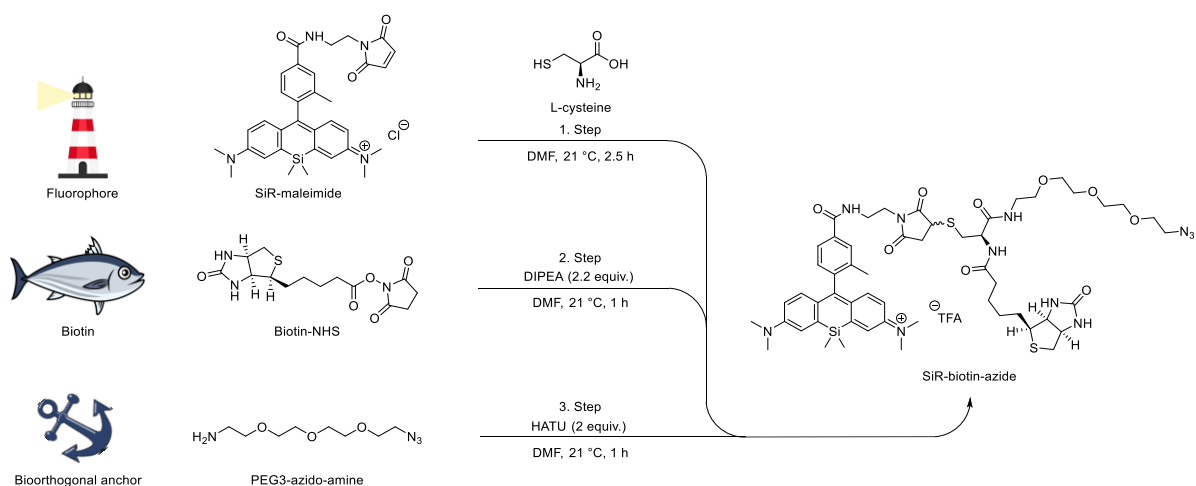
B



Scheme 22 A) Coupling to the SiR-NHS **B)** Retro Diels-Alder reaction

On the cysteine, another reactive moiety is the amine. Activated NHS-esters react very quickly and cleanly with free amines forming amides and *N*-hydroxysuccinimide as a side product, which is easily removed by chromatography. An available NHS-ester was biotin, which was also previously synthesised and described in chapter 1.5. The remaining free carboxylic acid is functionalised by its reaction with a coupling agent such as 1-[bis(dimethylamino)methylene]-1*H*-1,2,3-triazolo[4,5-*b*]pyridinium 3-oxide hexafluorophosphate (HATU). The *N*-hydroxysuccinimide, which was formed as a side product in the previous reaction should not interfere with these coupling reactions. If the NHS leaving group would react with the activated carboxylic acid, an activated NHS-ester would be formed, which could still react with an amine and form the desired amide.

Starting from L-cysteine the thiol was first reacted with a SiR-maleimide in equimolar amount in DMF at 21 °C for 2.5 h. This reaction was found to be fast and clean as it was followed by HPLC analysis. The reaction did not produce side products and/ or impurities based on the chromatogram. Therefore, the product was directly subjected to the next reaction with biotin-NHS ester in an equimolar amount and adding *N,N*-diisopropylethylamine (2.2 equiv.) as a base to adjust the pH suitable for the reaction at 21 °C, at which it was stirred for 1 h. This also resulted in a clean and fast reaction as observed by HPLC, producing only the *N*-hydroxysuccinimide as side product. To the reaction was then added HATU (2 equiv.) and the PEG3-azido-amine (2 equiv.). This final reaction produced some side products as observed by HPLC. However, reverse phase flash column chromatography could separate the impurities from the desired product as observed in the HPLC fractions. However, upon concentration of the desired fractions the product appeared to decompose, which resulted in a very heterogeneous mixture as observed by HPLC (all HPLC traces shown in **Figure 42**).



Scheme 23 Reaction scheme for the trifunctional modification of L-cysteine

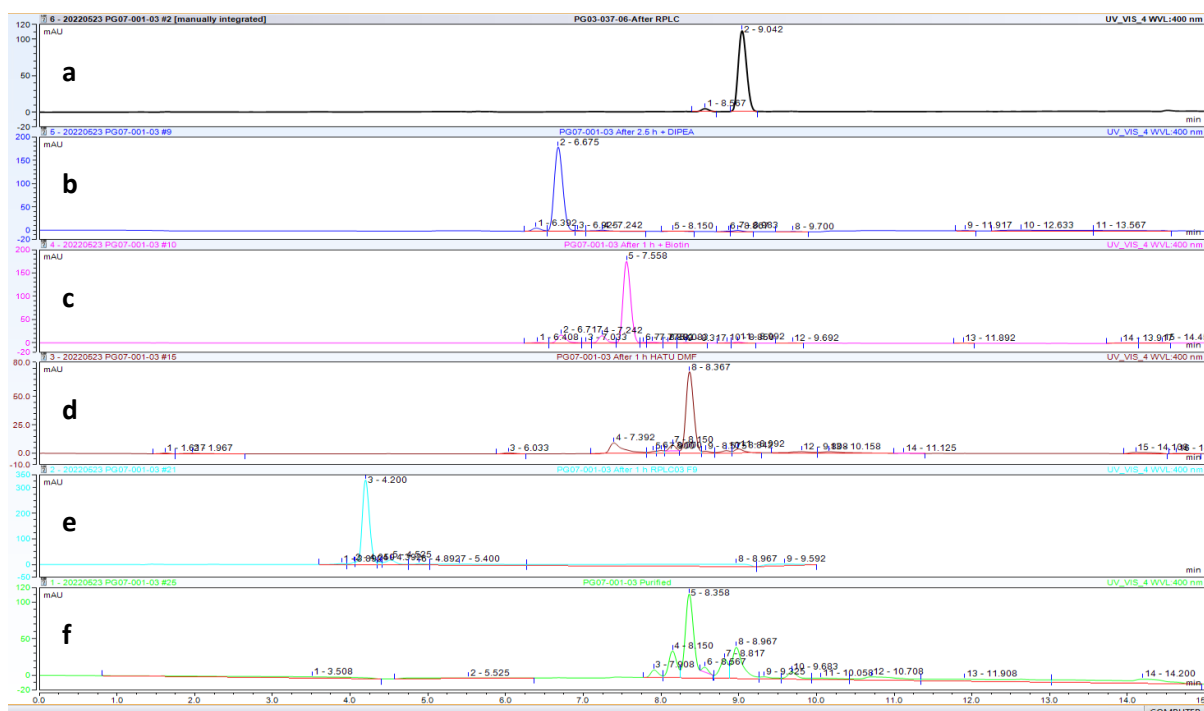
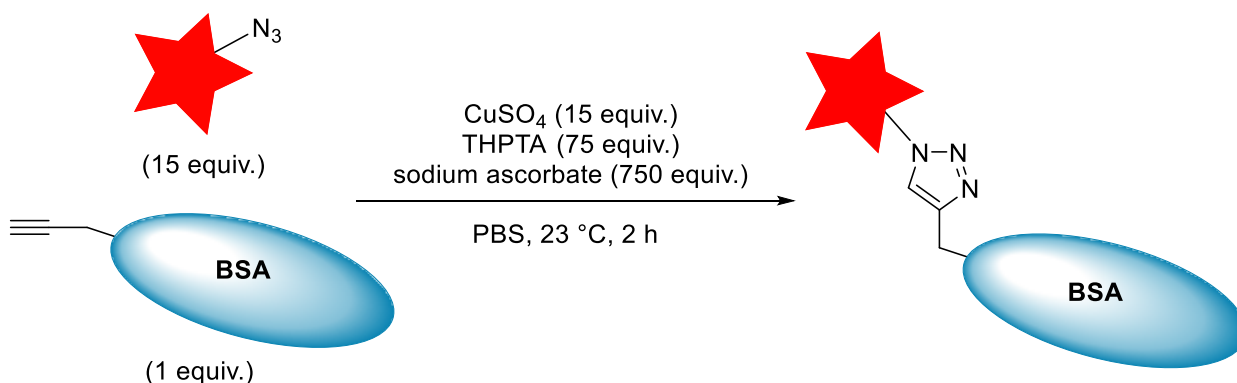


Figure 42 HPLC **a**) Silicon rhodamine maleimide conjugate **b**) reaction mixture (rm) after reaction with L-cysteine **c**) rm after reaction with biotin-NHS **d**) rm after coupling to azide linker **e**) product after purification before evaporation of fractions **f**) product after concentration and drying of fractions

This decomposition of the desired product after purification could arise from an isomerisation and opening of the succinimide, which has been observed under certain conditions.¹¹⁹ This opening could be induced by the TFA, that was used for the reverse phase purification.

To test the functional integrity of the final probe, it was first conjugated to an alkyne-modified BSA model protein (Scheme 15).



Scheme 24 Coupling of the trifunctional probe to alkyne modified bovine serum albumin

The reaction was monitored by sodium dodecyl sulfate polyacrylamide gel electrophoresis (SDS-PAGE) as shown in **Figure 43**. The SDS-PAGE showed that the CuAAC-reaction successfully conjugated the

trifunctional probe to alkynylated BSA, compared to control reactions (e.g., omitting Cu(I)) and to native BSA. We therefore concluded that the one-pot reaction sequence on unprotected cysteine to obtain the final probe did affect neither the clicking moiety (azide) nor the fluorophore.

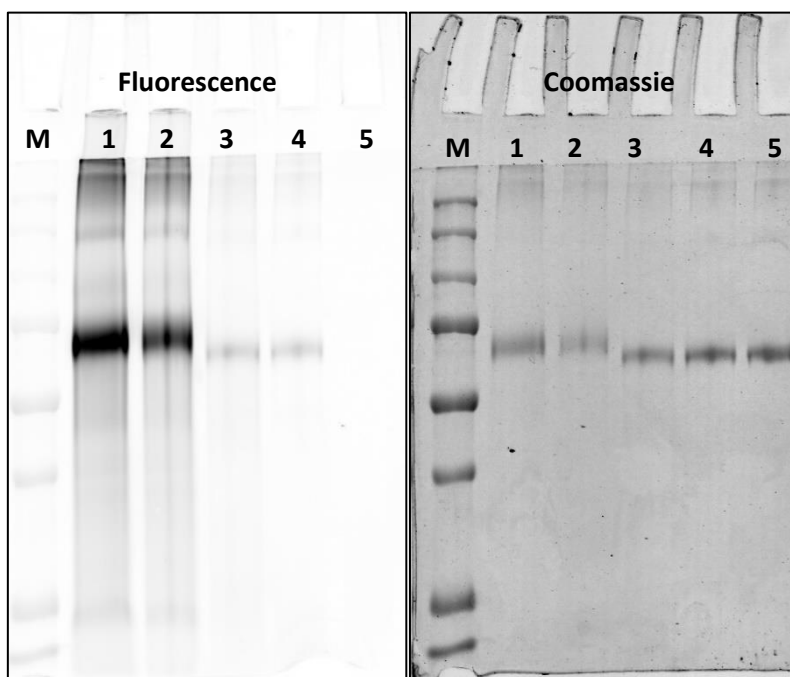


Figure 43 SDS-PAGE analysis of the trifunctionally labelled BSA. **M**: Protein marker **1**: SiR-biotin-azide-labelled BSA **2**: SiR-biotin-azide-labelled BSA (sample loaded at half concentration as in lane 1) **3**: no Cu added in conjugation reaction **4**: SiR-biotin-azide mixed with native BSA **5**: native BSA

Conclusion & outlook

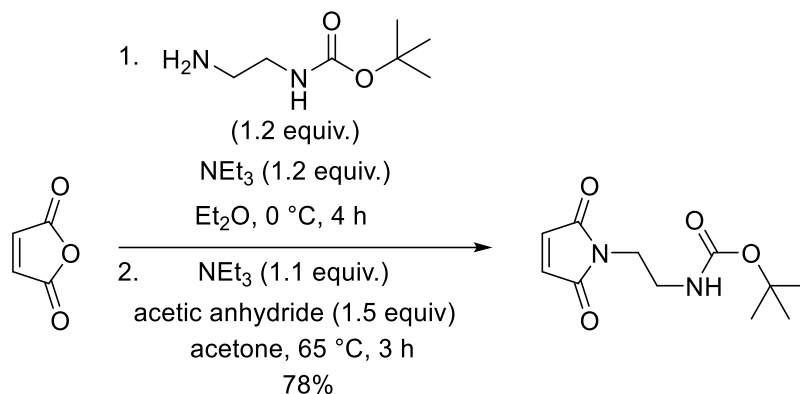
Based on the initial results on the SDS-PAGE the coupling is effective. The biotin moiety was not evaluated for its functionality yet. This is planned as a next step by fishing out the alkynylated BSA from a complex cell lysate and testing by western blot if a fluorescently labelled streptavidin can selectively bind to the biotin. For this application, it must be ensured that the fluorophore employed is not emitting in a similar wavelength range as the SiR-fluorophore that is attached to the probe. A streptavidin derivative that fits this requirement could be with conjugated FITC or Alexa488 fluorescent dyes.

General remarks to materials & methods

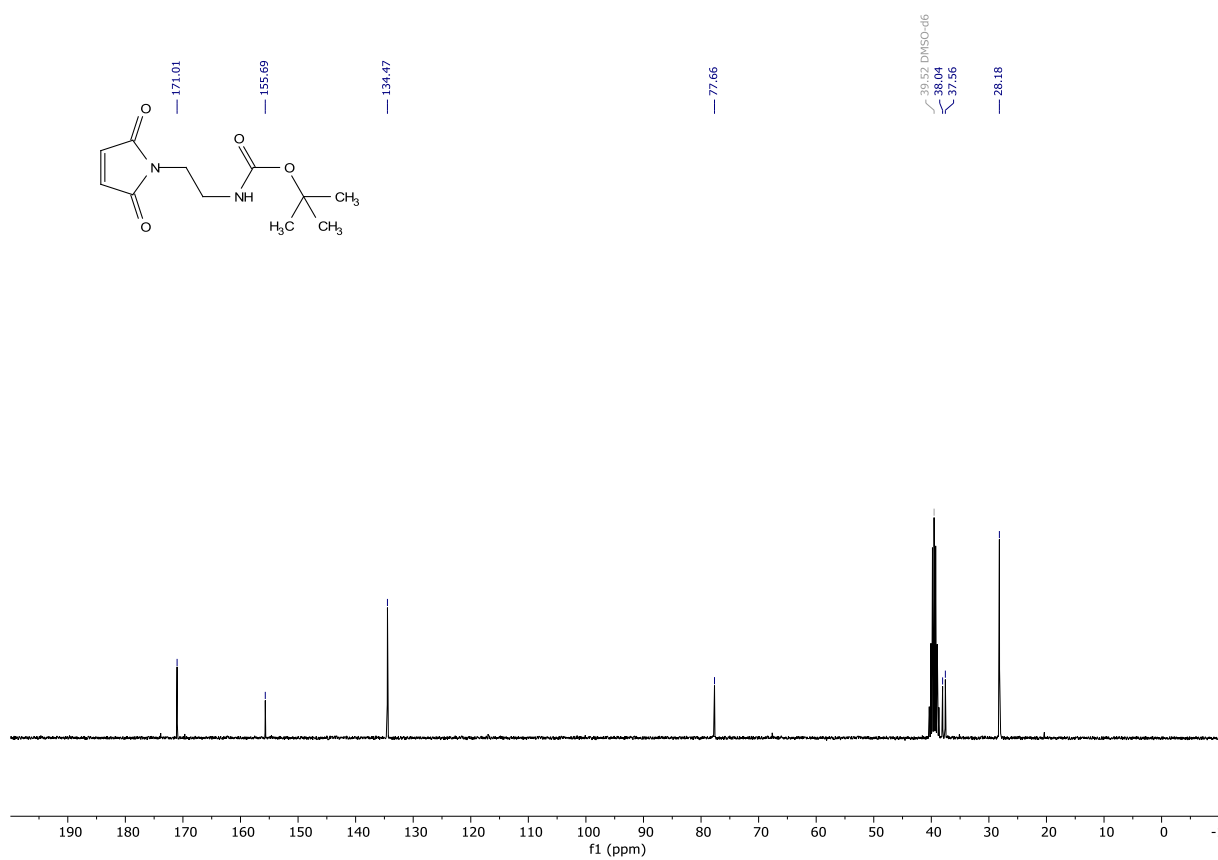
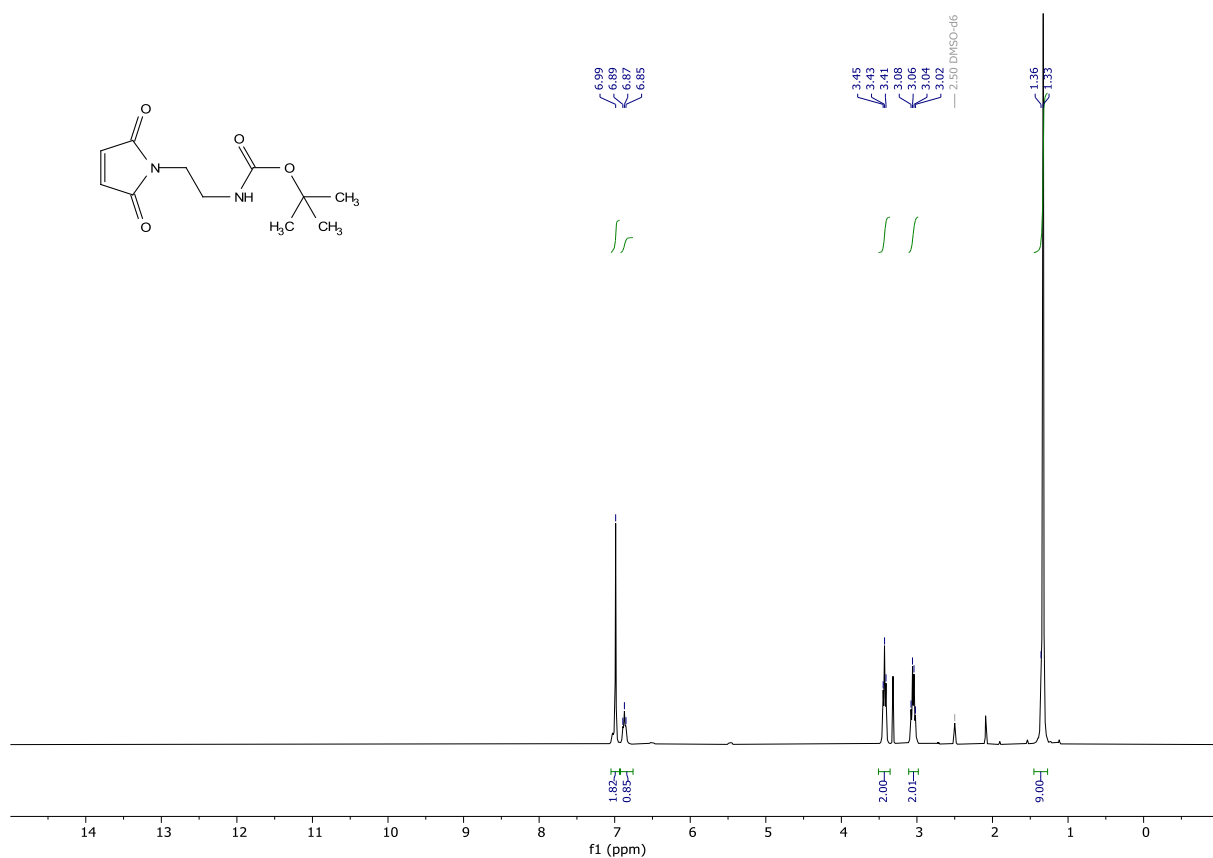
For general remarks see chapter 1.4.

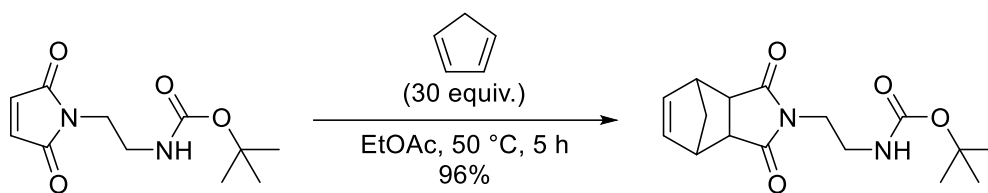
Synthesis

The synthesis of the biotin-NHS, and the amino azide linker & SiR-NHS is described under 1.5.

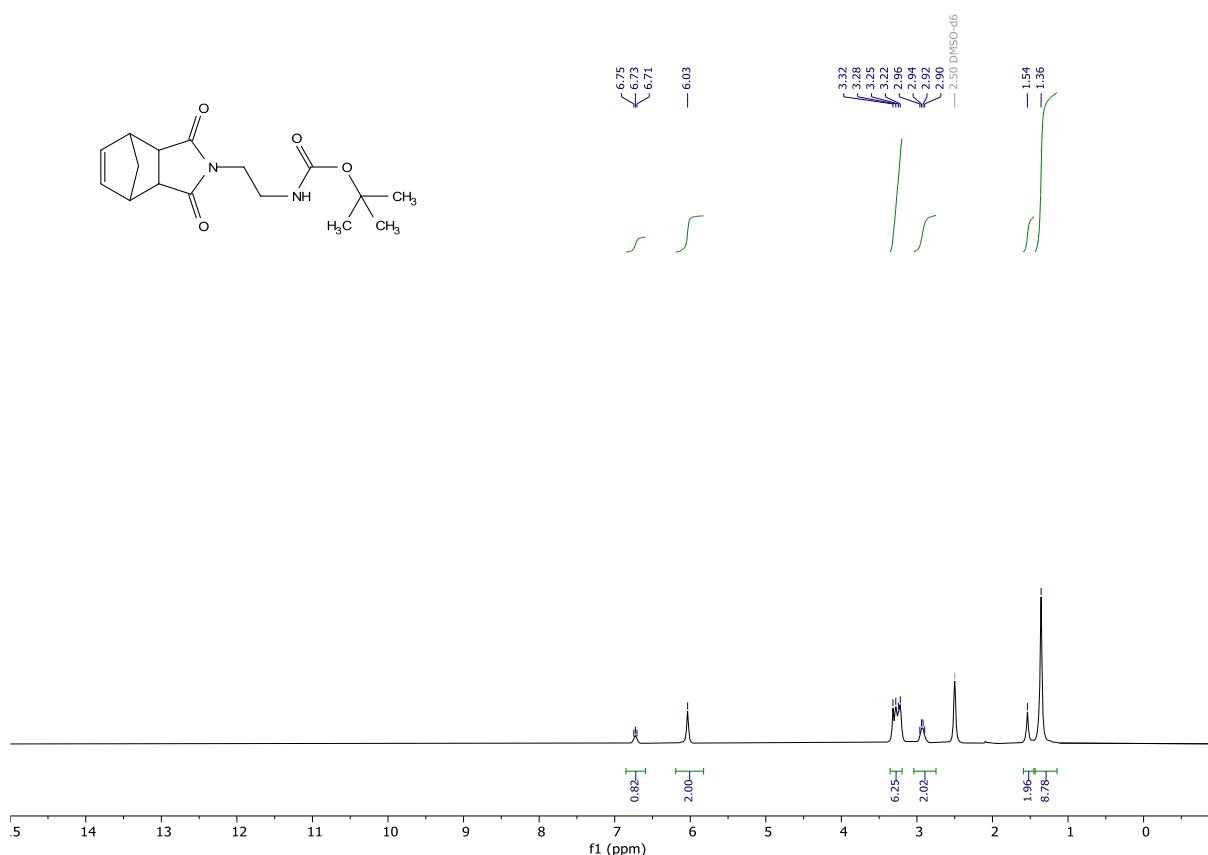


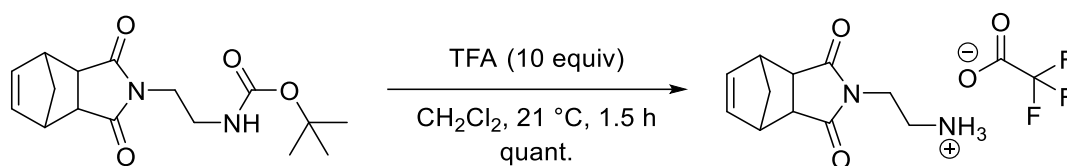
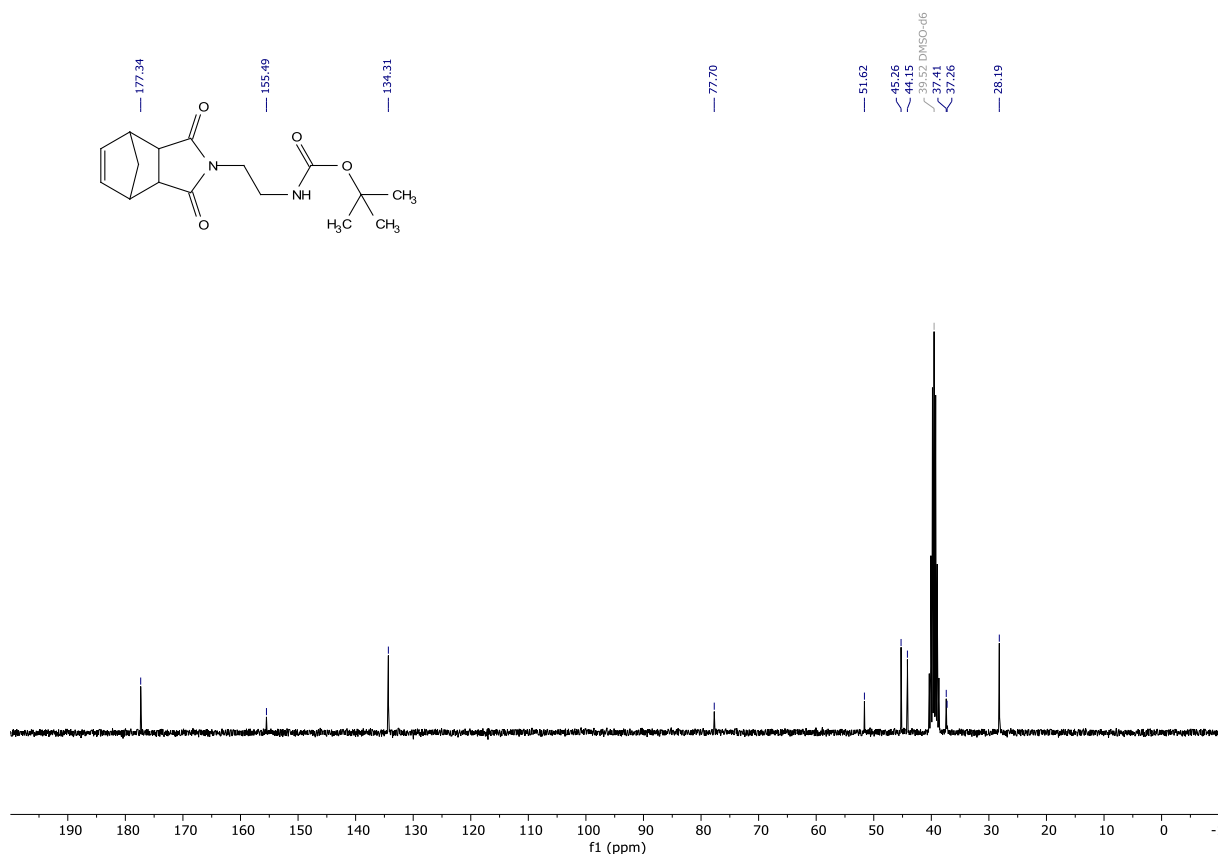
***tert*-Butyl (2-(2,5-dioxo-2,5-dihydro-1H-pyrrol-1-yl)ethyl)carbamate.** To a stirred solution of *tert*-butyl (2-aminoethyl)carbamate (5.259 g, 32.8242 mmol) in diethyl ether (60 mL) was added triethylamine (6.8 mL, 4.9368 g 48.7874 mmol). The clear colourless mixture was cooled to 0 °C. To this mixture was added dropwise via an addition funnel a solution of maleic anhydride (3.225 g, 32.8890 mmol) in diethyl ether (50 mL). The mixture was left stirring for 4 h. The volatiles were removed under reduced pressure (650 mbar) leading to a clear orange viscous oil. The oil was taken up in acetone (150 mL) and triethylamine (10 mL, 7.26 g, 71.7462 mmol) and acetic anhydride (5 mL, 5.4 g, 52.8945 mmol) were added. The mixture was heated to 80 °C for 16 h. The volatiles were removed under reduced pressure. The resulting off white solid was taken up in dichloromethane. The dichloromethane was washed with 1 M HCl, dried over MgSO_4 , filtered, and concentrated under reduced pressure onto silica gel. The crude was purified by flash column chromatography (cyclohexane/ ethyl acetate gradient from 1:0 to 0:1), to give the desired product in 78% yield (6.12357 g, 25.48737 mmol). White solid: ^1H NMR (300 MHz, $\text{DMSO}-d_6$) δ 6.99 (s, 2H), 6.87 (t, J = 6.3 Hz, 1H), 3.43 (t, J = 5.7 Hz, 2H), 3.05 (q, J = 5.9 Hz, 2H), 1.33 (s, 9H). ^{13}C NMR (75 MHz, DMSO) δ 171.01, 155.69, 134.47, 77.66, 38.04, 37.56, 28.18. HRMS (ESI) calculated for $[\text{M}+\text{H}]^+$ $\text{C}_{11}\text{H}_{17}\text{N}_2\text{O}_4$ 241.1183, found 241.1181.





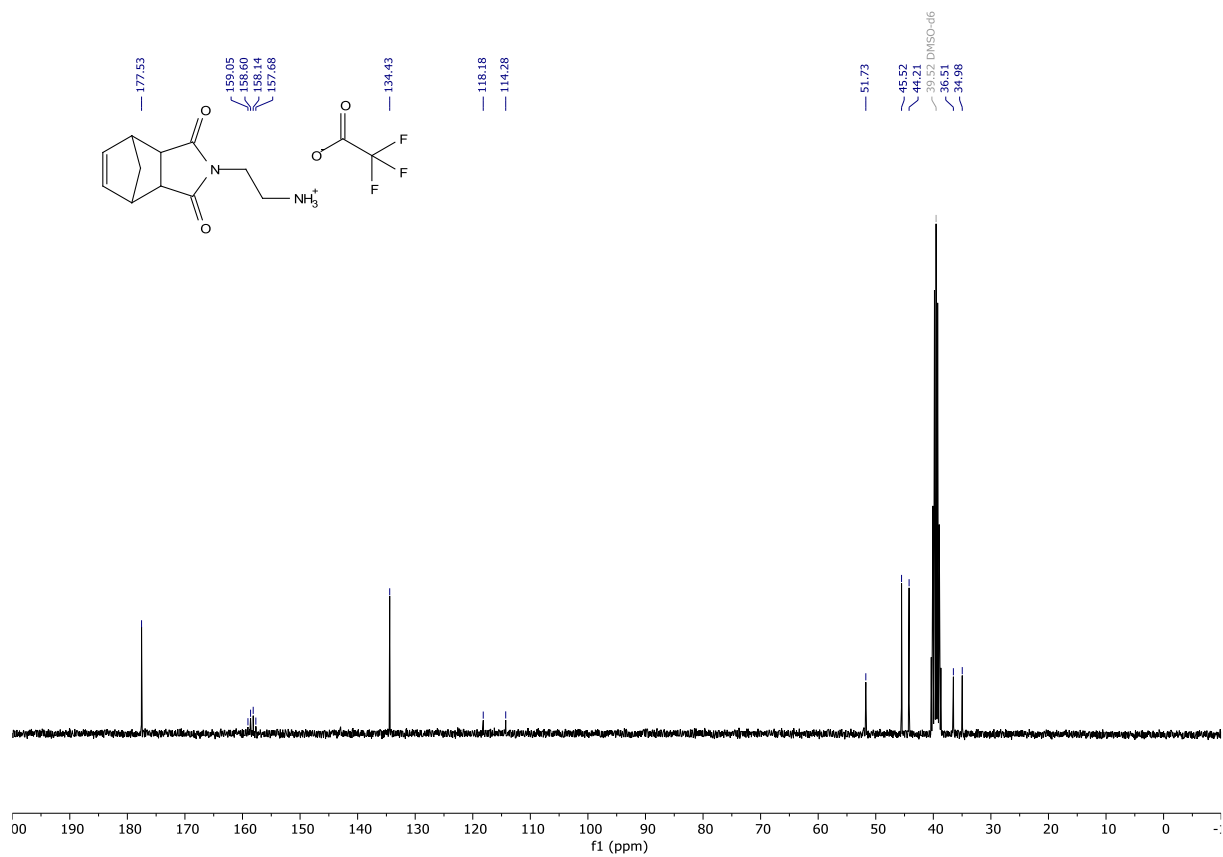
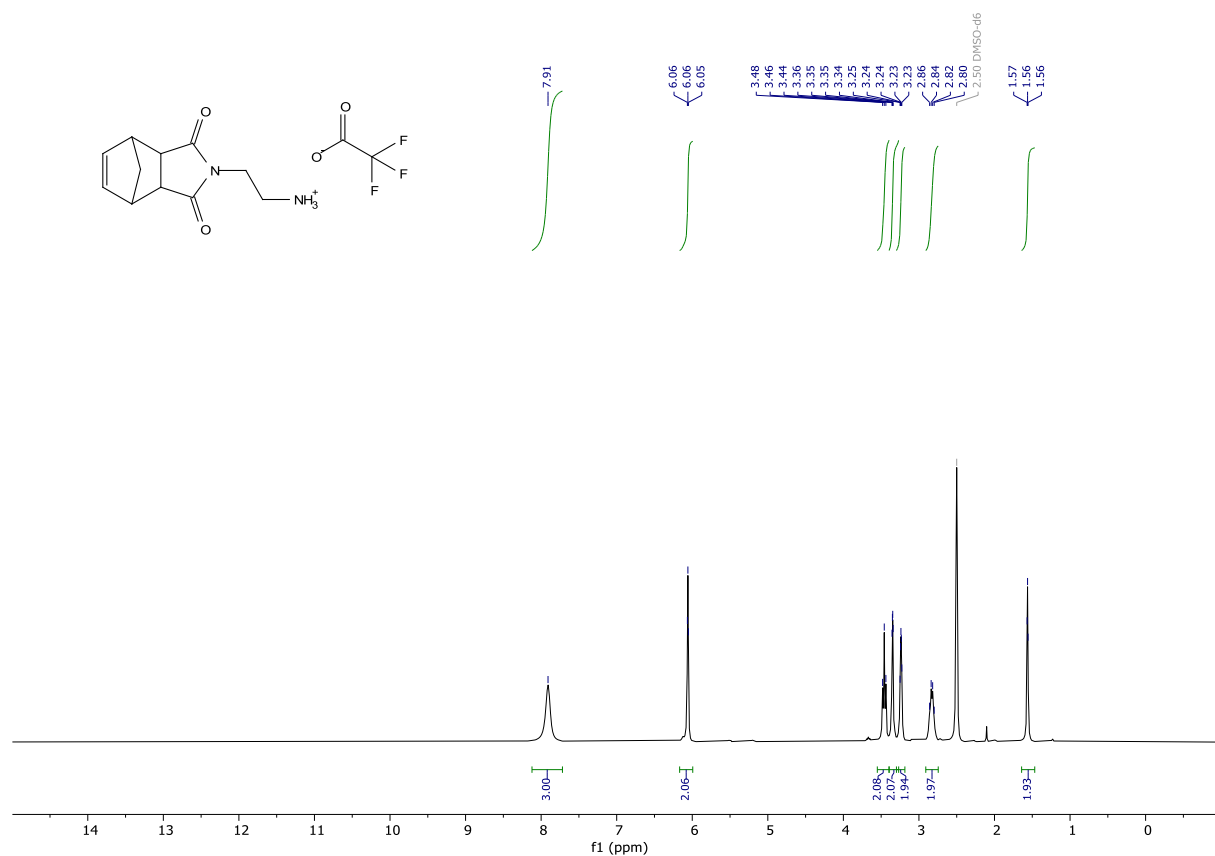
tert-Butyl (2-(1,3-dioxo-1,3,3a,4,7,7a-hexahydro-2H-4,7-methanoisoindol-2-yl)ethyl)carbamate. To a stirred solution of *tert*-butyl (2-(2,5-dioxo-2,5-dihydro-1H-pyrrol-1-yl)ethyl)carbamate (0.509 g, 2.1185 mmol) in ethyl acetate (7 mL) at 50 °C was added freshly distilled cyclopentadiene (2.5 mL, 1.965 g, 29.7263 mmol). The clear solution was stirred under an argon atmosphere for 5 h. The volatiles were removed under reduced pressure. The residue was taken up in dichloromethane and concentrated onto silica gel. The crude was purified by flash column chromatography (cyclohexane/ethyl acetate gradient from 1:0 to 0:1), to give the desired compound in 96% yield (0.62112 g, 2.02741 mmol). White solid: ^1H NMR (300 MHz, DMSO- d_6) δ 6.73 (t, J = 6.2 Hz, 1H), 6.03 (s, 2H), 3.35 – 3.20 (m, 6H), 2.93 (q, J = 6.4 Hz, 2H), 1.54 (s, 2H), 1.36 (s, 9H). ^{13}C NMR (75 MHz, DMSO) δ 177.34, 155.49, 134.31, 77.70, 51.62, 45.26, 44.15, 37.41, 37.26, 28.19. HRMS (ESI) calculated for $[\text{M}+\text{H}]^+$ $\text{C}_{16}\text{H}_{23}\text{N}_2\text{O}_4$ 307.1652, found 307.1654.

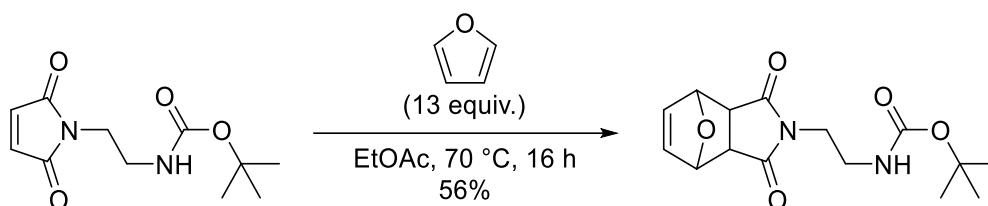
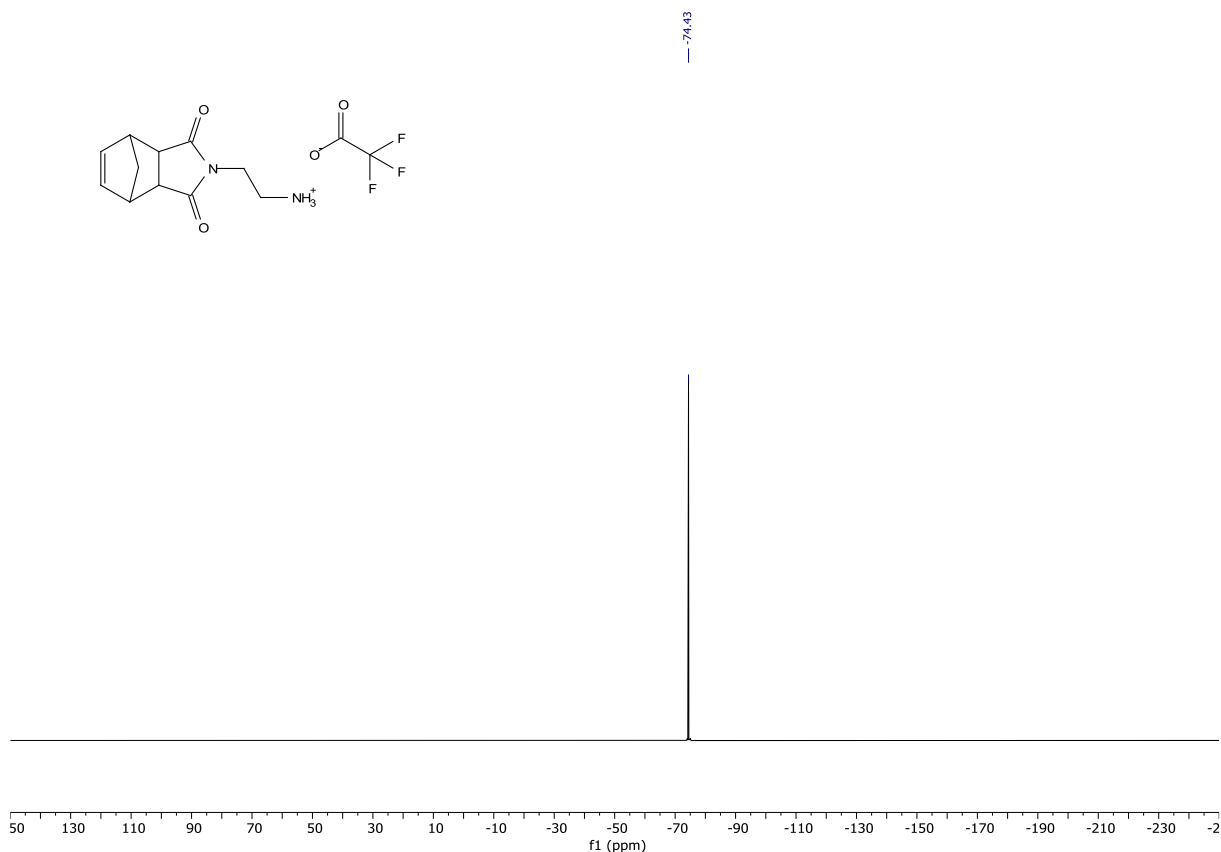




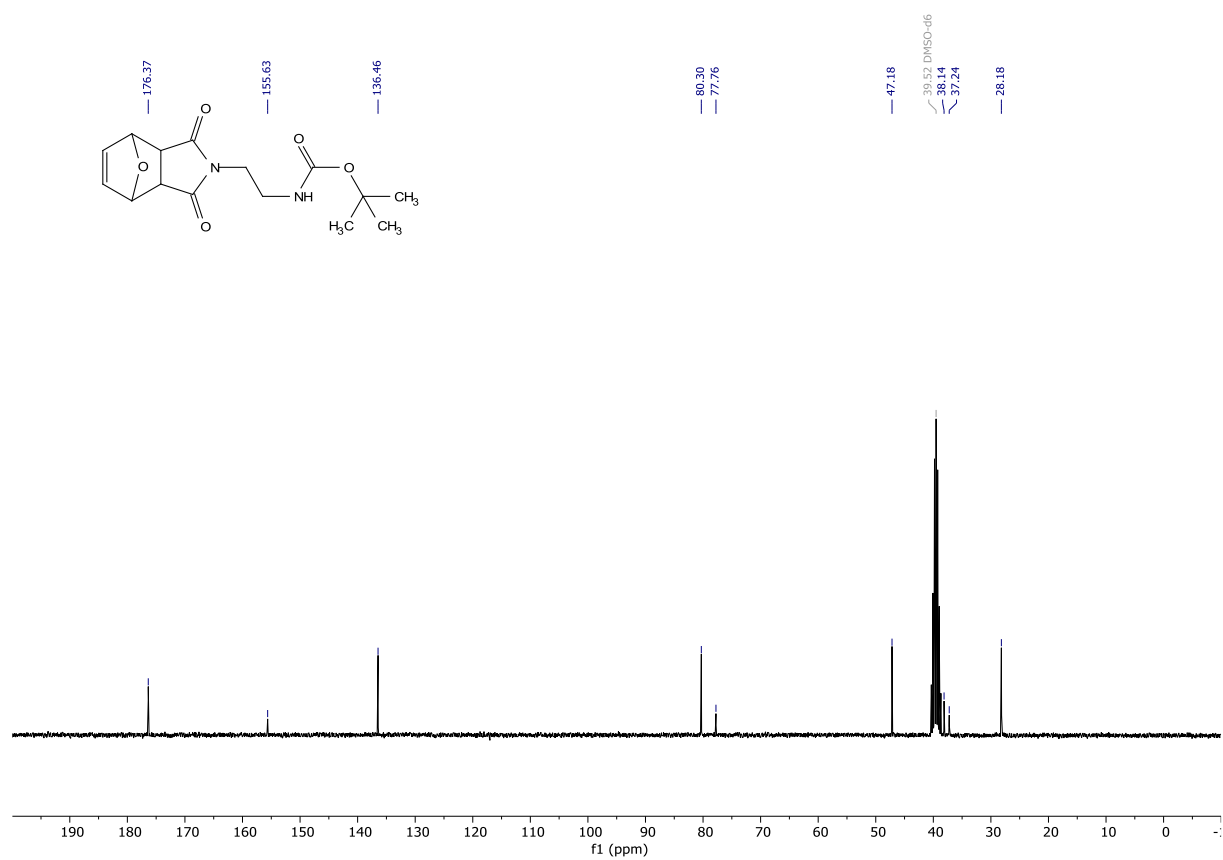
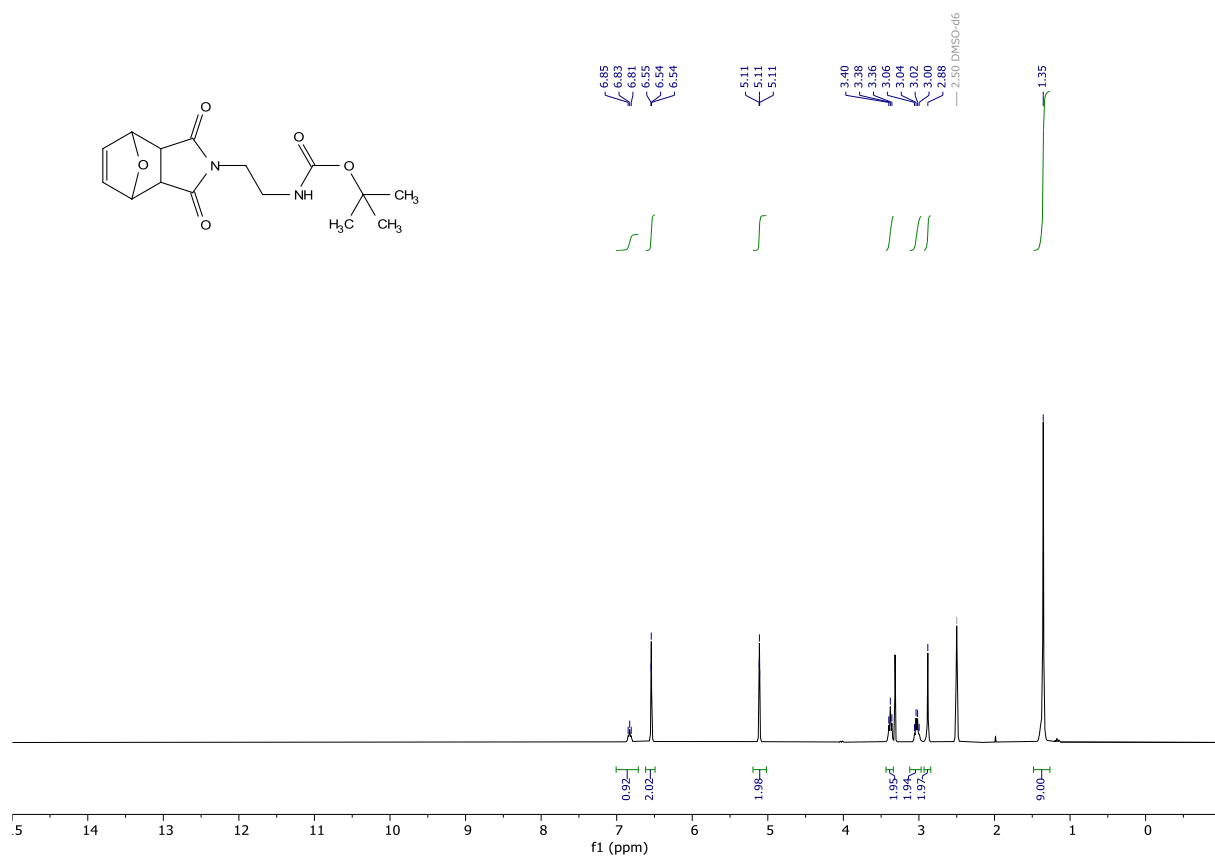
2-(1,3-dioxo-1,3,3a,4,7,7a-hexahydro-2H-4,7-methanoisindol-2-yl)ethan-1-aminium

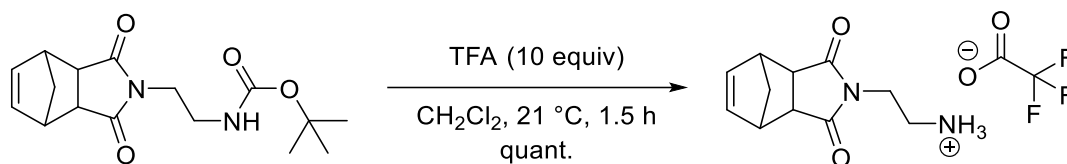
trifluoroacetate. *tert*-butyl (2-(1,3-dioxo-1,3,3a,4,7,7a-hexahydro-2H-4,7-methanoisindol-2-yl)ethyl)carbamate (0.72683 g, 2.3502 mmol) was dissolved in dichloromethane (10 mL) and to the solution was added trifluoro acetic acid (2 mL, 2.96 g, 25.9604 mmol). The mixture was stirred for 1,5 h, then the volatiles were removed under reduced pressure whilst heating to 35 °C, to give the desired product in quantitative yield (0.75365 g, 2.3502 mmol). Brownish solid: **¹H NMR** (300 MHz, DMSO-*d*₆) δ 7.91 (s, 3H), 6.06 (t, *J* = 1.9 Hz, 2H), 3.46 (t, *J* = 6.5 Hz, 2H), 3.39 – 3.27 (m, 2H), 3.30 – 3.19 (m, 2H), 2.83 (q, *J* = 6.1 Hz, 2H), 1.64 – 1.47 (m, 2H). **¹³C NMR** (75 MHz, DMSO) δ 177.53, 158.37 (q, *J* = 34.5 Hz), 134.43, 116.23 (d, *J* = 294.4 Hz), 51.73, 45.52, 44.21, 36.51, 34.98. **¹⁹F NMR** (282 MHz, DMSO) δ -74.43. **HRMS** (ESI) calculated for [M+H]⁺ C₁₁H₁₅N₂O₂ 207.1128, found 207.1126.





tert-butyl (2-(1,3-dioxo-1,3,3a,4,7,7a-hexahydro-2H-4,7-epoxyisoindol-2-yl)ethyl)carbamate. To a stirred solution of *tert*-butyl (2-(2,5-dioxo-2,5-dihydro-1H-pyrrol-1-yl)ethyl)carbamate (0.2826 g, 1.1762 mmol) in ethyl acetate (3.5 mL) at 70 °C was added furan (1.3 mL, 1.2168 g, 17.8744 mmol). The clear solution was stirred under an argon atmosphere for 16 h. The solvent evaporated overnight leaving a white solid. The residue was taken up in little ethyl acetate and filtered through a por4 frit. This left a crystalline white solid, which was thoroughly dried under reduced pressure to give the desired compound in 56% yield (0.20260 g, 0.65701 mmol). A small sample was recrystallised from ethyl acetate and yielded single crystals of suitable quality for x-ray diffraction analysis (CCDC deposition number: 2205406). White solid: $^1\text{H NMR}$ (300 MHz, DMSO- d_6) δ 6.83 (t, J = 6.1 Hz, 1H), 6.54 (d, J = 1.0 Hz, 2H), 5.11 (d, J = 0.9 Hz, 2H), 3.38 (t, J = 6.2 Hz, 2H), 3.03 (q, J = 6.2 Hz, 2H), 2.88 (s, 2H), 1.35 (s, 9H). $^{13}\text{C NMR}$ (75 MHz, DMSO) δ 176.37, 155.63, 136.46, 80.30, 77.76, 47.18, 38.14, 37.24, 28.18. **HRMS** (ESI) calculated for $[\text{M}+\text{H}]^+$ $\text{C}_{15}\text{H}_{21}\text{N}_2\text{O}_5$ 309.1445, found 309.1446.

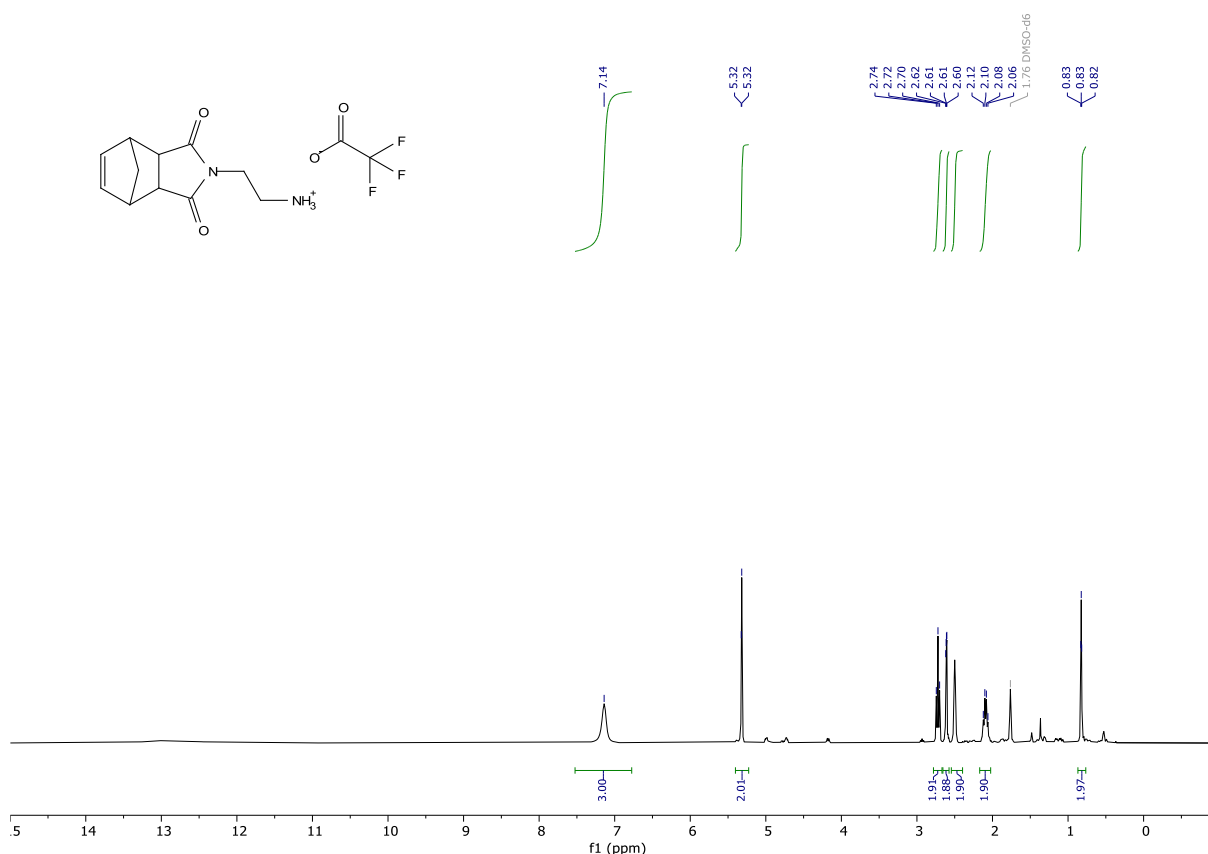


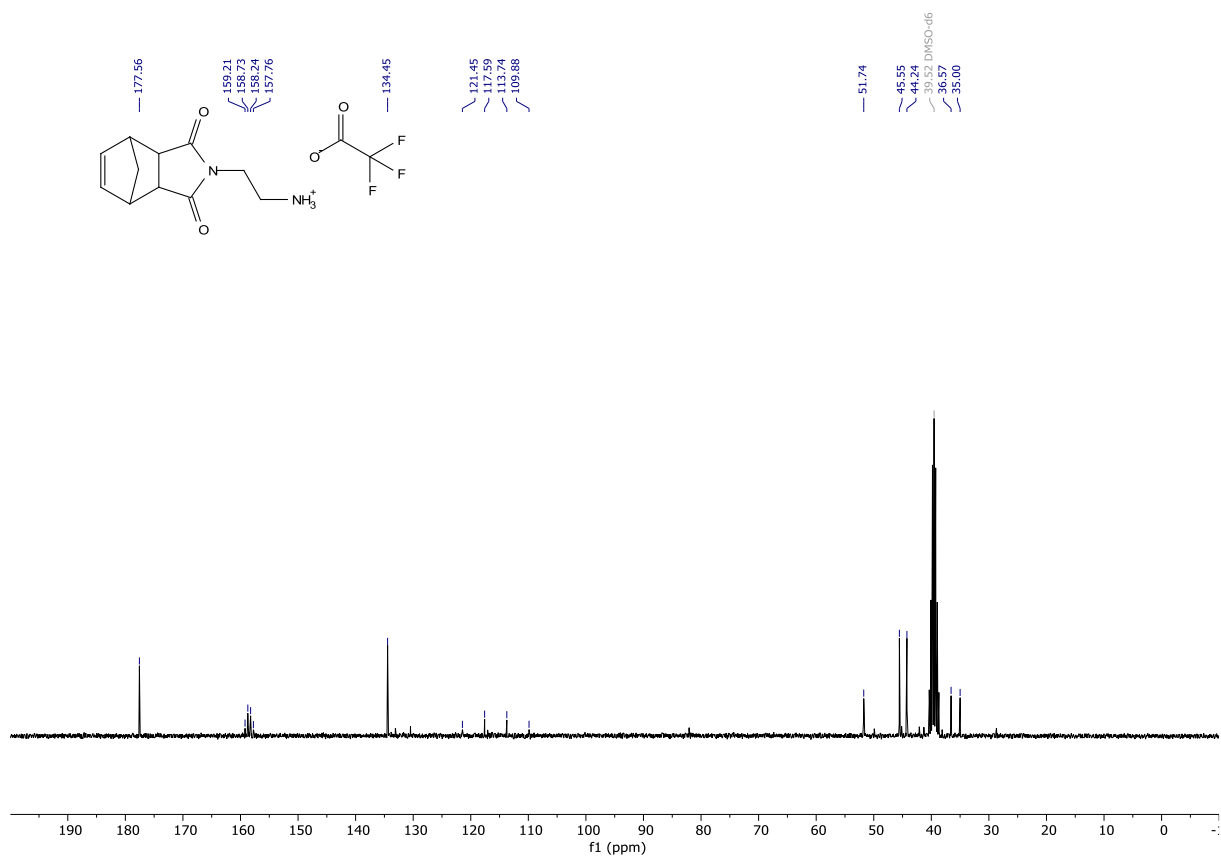


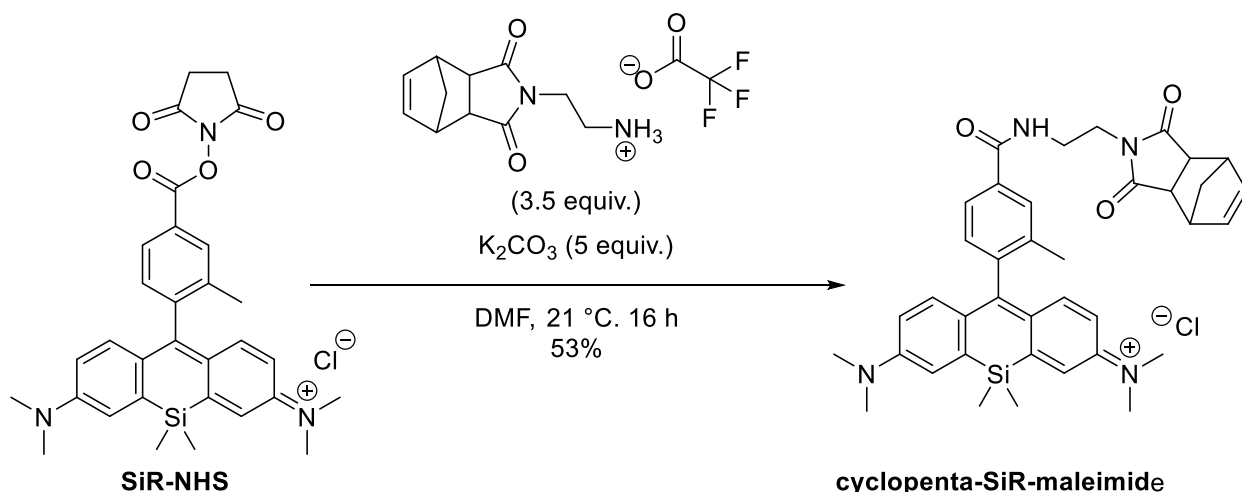
2-(1,3-dioxo-1,3,3a,4,7,7a-hexahydro-2H-4,7-methanoisindol-2-yl)ethan-1-aminium

trifluoroacetate.

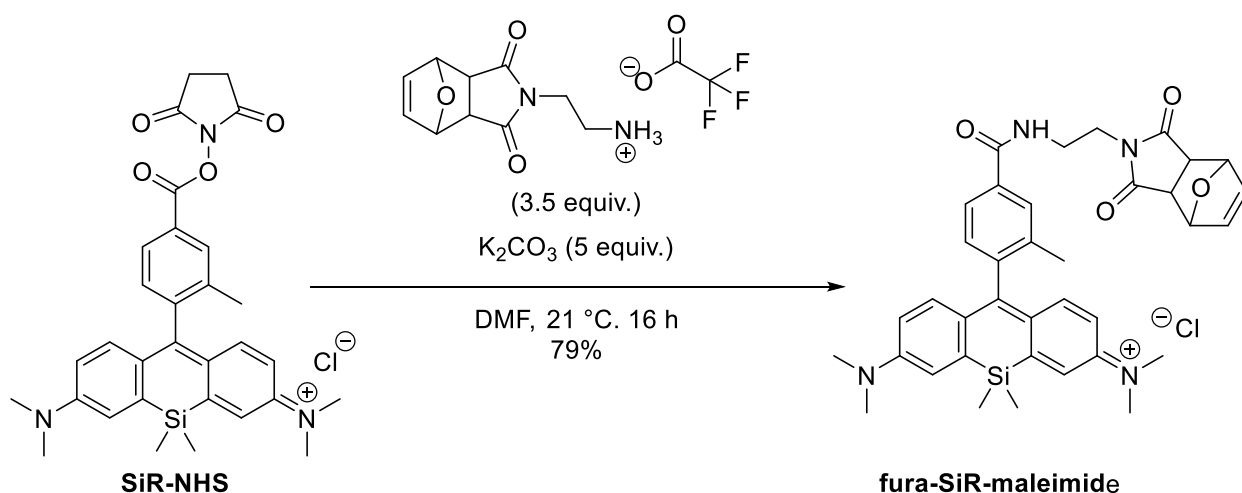
tert-Butyl-(2-(1,3-dioxo-1,3,3a,4,7,7a-hexahydro-2H-4,7-methanoisindol-2-yl)ethyl)carbamate (0.72683 g, 2.3725 mmol) was dissolved in dichloromethane (10 mL) and to the clear colourless solution was added trifluoro acetic acid (2 mL, 2.96 mmol, 25.9604 mmol). The mixture was stirred for 1.5 h and the volatiles were removed under reduced pressure whilst heating to 35 °C, to give the desired product in quantitative yield. Brown solid: **¹H NMR** (300 MHz, DMSO-*d*₆) δ 7.14 (s, 3H), 5.32 (d, *J* = 1.9 Hz, 2H), 2.72 (t, *J* = 6.6 Hz, 2H), 2.61 (dd, *J* = 3.0, 1.5 Hz, 2H), 2.50 (dq, *J* = 3.4, 1.8 Hz, 2H), 2.09 (q, *J* = 6.2 Hz, 2H), 0.83 (t, *J* = 1.6 Hz, 2H). **¹³C NMR** (75 MHz, DMSO) δ 177.56, 158.49 (q, *J* = 36.5 Hz), 134.45, 115.67 (q, *J* = 291.1 Hz), 51.74, 45.55, 44.24, 36.57, 35.00. **¹⁹F NMR** (282 MHz, DMSO) δ -74.92. **HRMS** (ESI) calculated for [M+H]⁺ C₁₁H₁₅N₂O₅ 207.1128, found 207.1126.



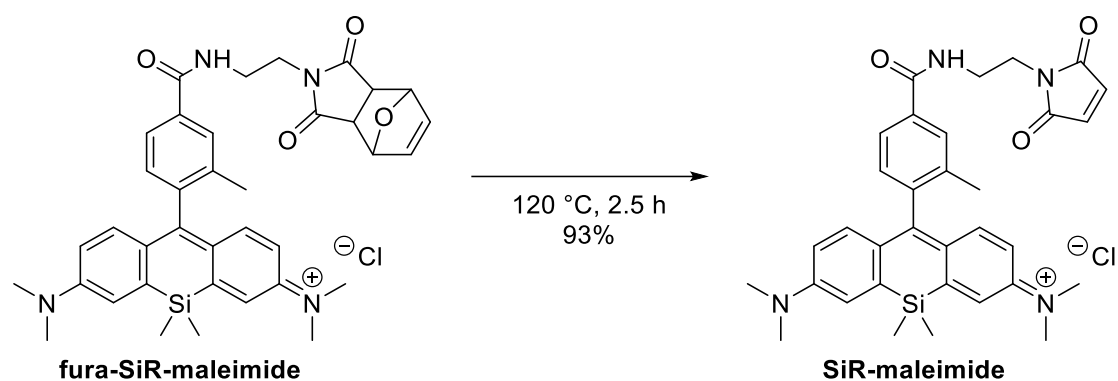




***N*-(7-(dimethylamino)-10-(4-((2-(1,3-dioxo-1,3,3a,4,7,7a-hexahydro-2*H*-4,7-methanoisindol-2-yl)ethyl)carbamoyl)-2-methylphenyl)-5,5-dimethyldibenzo[*b,e*]silin-3(5*H*)-ylidene)-*N*-methylmethanaminium chloride (cyclopenta-SiR-maleimide).** To a stirred solution of *N*-(7-(dimethylamino)-10-(4-(((2,5-dioxopyrrolidin-1-yl)oxy)carbonyl)-2-methylphenyl)-5,5-dimethyldibenzo[*b,e*]silin-3(5*H*)-ylidene)-*N*-methylmethanaminium chloride (0.149 g, 0.2586 mmol) and 2-(1,3-dioxo-1,3,3a,4,7,7a-hexahydro-2*H*-4,7-methanoisindol-2-yl)ethan-1-aminium trifluoroacetate (0.131 g, 0.4090 mmol) in DMF (8) at 21 °C was added potassium carbonate (0.088 g, 10.6367 mmol). The mixture was stirred for 16 h. The mixture was acidified with 2 M HCl (1.5 mL), then the volatiles were removed under reduced pressure. The crude was taken up in dichloromethane and concentrated onto silica gel. The crude was purified by flash column chromatography (dichloromethane/ methanol gradient from 1:0 to 9:1), to give the desired compound in 53% yield (0.09086 g, 0.13616 mmol). Purple solid: No NMR data was recorded for this compound. **HRMS** (ESI) calculated for $[\text{M}-\text{Cl}]^+ \text{C}_{38}\text{H}_{43}\text{N}_4\text{O}_3\text{Si}$ 631.3099, found 631.3088.

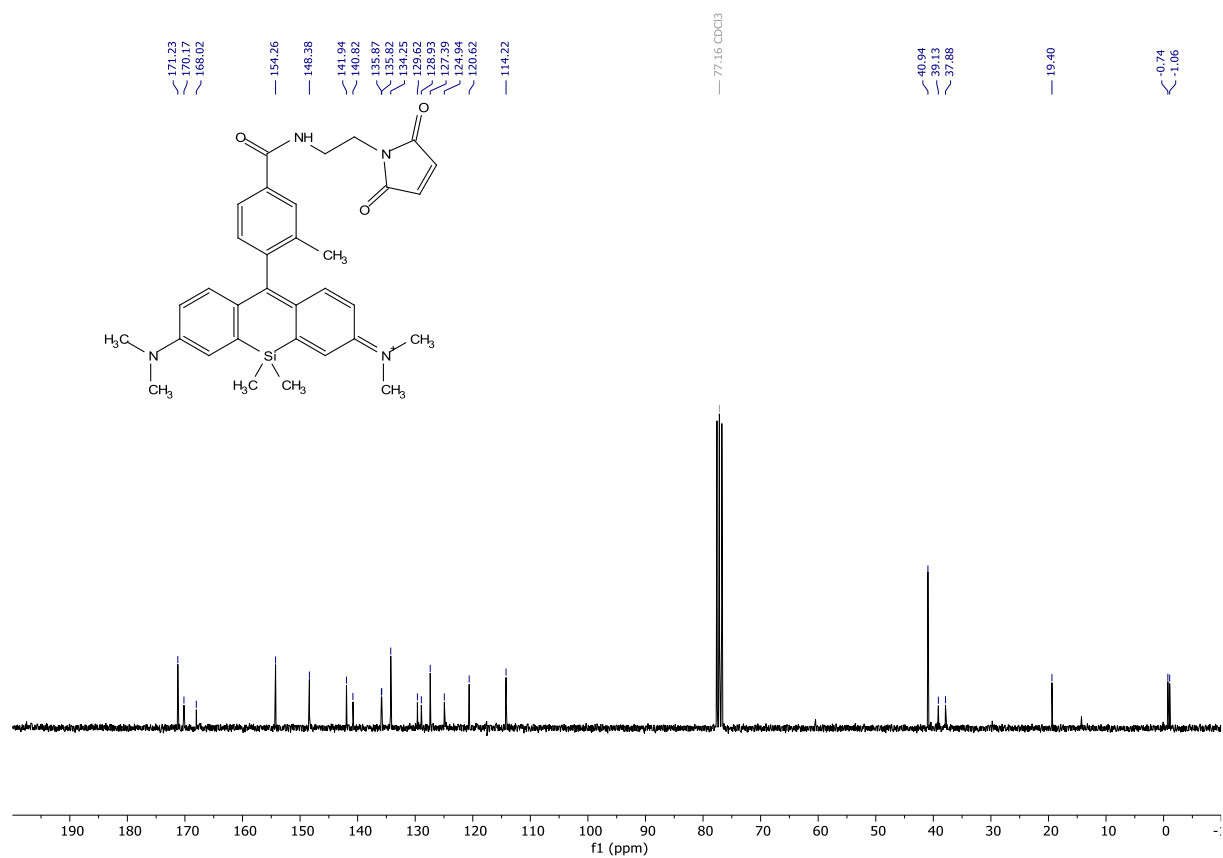
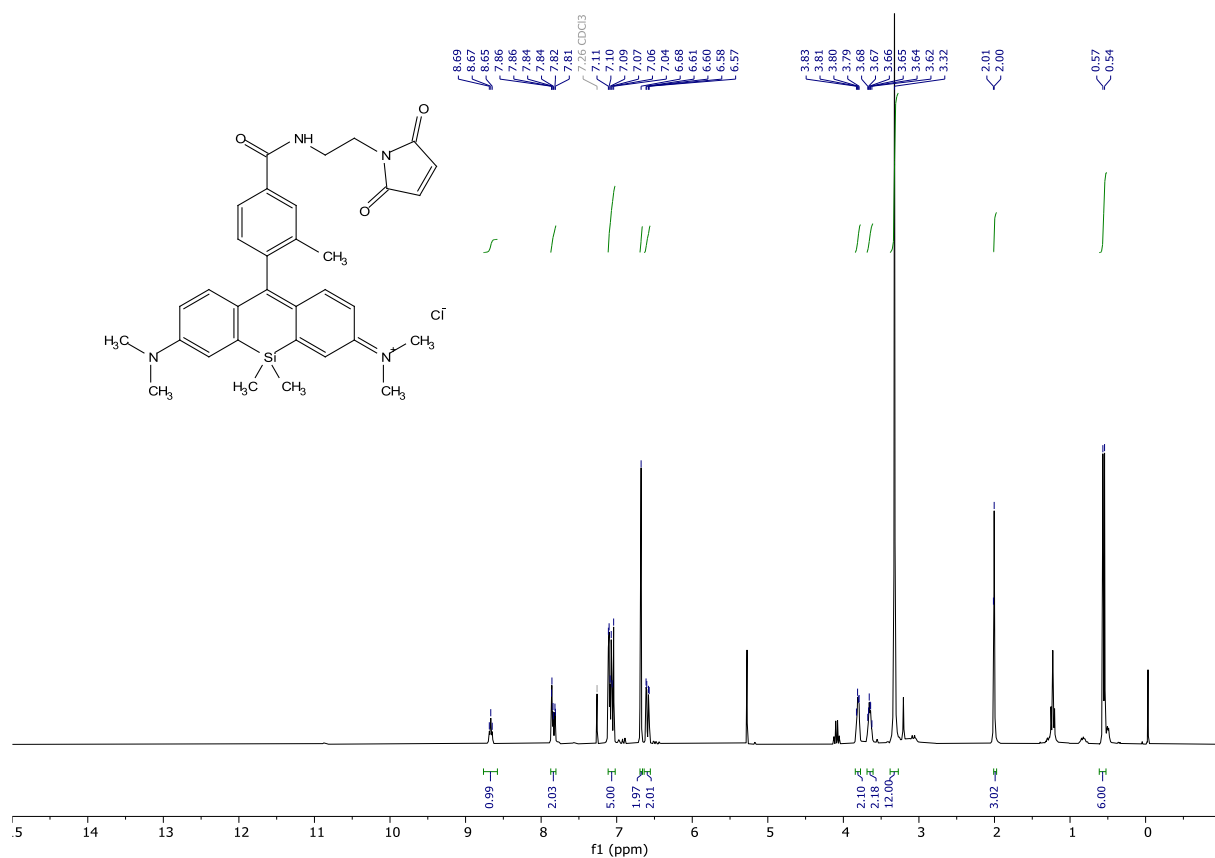


***N*-(7-(dimethylamino)-10-(4-((2-(1,3-dioxo-1,3,3a,4,7,7a-hexahydro-2*H*-4,7-epoxyisoindol-2-yl)ethyl)carbamoyl)-2-methylphenyl)-5,5-dimethyldibenzo[*b,e*]silin-3(5*H*)-ylidene)-*N*-methylmethanaminium chloride (fura-SiR-maleimide).** To a stirred solution of *N*-(7-(dimethylamino)-10-(4-(((2,5-dioxopyrrolidin-1-yl)oxy)carbonyl)-2-methylphenyl)-5,5-dimethyldibenzo[*b,e*]silin-3(5*H*)-ylidene)-*N*-methylmethanaminium chloride (0.08225 g, 0.1428 mmol) and 2-(1,3-dioxo-1,3,3a,4,7,7a-hexahydro-2*H*-4,7-epoxyisoindol-2-yl)ethan-1-aminium trifluoroacetate (0.15852 g, 0.4919 mmol) in DMF (3 mL) at 21 °C was added potassium carbonate (0.10044 g, 0.7236 mmol). The mixture was stirred for 16 h then the mixture was concentrated under reduced pressure to give a reddish residue that was taken up in a mixture of dichloromethane and 1 M aq. HCl, turning its colour back into a very intense blue. The aqueous phase was extracted with dichloromethane, the combined organic phases were dried over MgSO₄, filtered, and concentrated under reduced pressure onto silica gel. The crude was purified by flash column chromatography (dichloromethane/ methanol gradient 1:0 to 9:1), to give the desired compound in 79% yield (0.07526 g, 0.11278 mmol). Purple solid: ¹H NMR (300 MHz, Chloroform-*d*) δ 8.65 (t, *J* = 5.8 Hz, 1H), 7.84 (d, *J* = 1.6 Hz, 1H), 7.80 (dd, *J* = 7.8, 1.7 Hz, 1H), 7.18 – 6.98 (m, 5H), 6.58 (dd, *J* = 9.6, 2.8 Hz, 2H), 6.43 (s, 2H), 5.17 (d, *J* = 0.9 Hz, 2H), 3.75 (dd, *J* = 6.8, 3.4 Hz, 2H), 3.71 – 3.58 (m, 2H), 3.32 (s, 12H), 3.04 (s, 2H), 1.99 (s, 3H), 0.55 (d, *J* = 6.7 Hz, 6H). ¹³C NMR (75 MHz, CDCl₃) δ 177.14, 170.28, 167.94, 154.23, 148.36, 141.96, 140.72, 136.46, 135.88, 135.82, 129.58, 128.89, 127.38, 124.88, 120.58, 114.16, 80.88, 47.84, 40.90, 38.83, 38.22, 19.36, -0.77, -1.08. HRMS (ESI) calculated for [M+H]⁺ C₃₇H₄₁N₄O₄Si 633.2892, found 633.2887. Purity (HPLC) >91% UV_{214 nm}, >95% UV_{254 nm}.

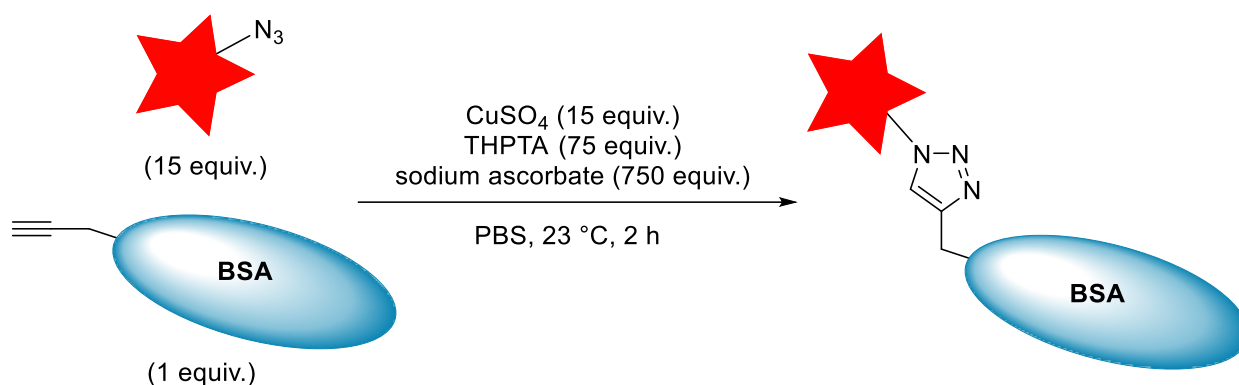


***N*-(7-(dimethylamino)-10-(4-((2-(2,5-dioxo-2,5-dihydro-1*H*-pyrrol-1-yl)ethyl)carbamoyl)-2-methylphenyl)-5,5-dimethyldibenzo[*b,e*]silin-3(5*H*)-ylidene)-*N*-methylmethanaminium chloride (SiR-maleimide).**

N-(7-(dimethylamino)-10-(4-((2-(1,3-dioxo-1,3,3a,4,7,7a-hexahydro-2*H*-4,7-epoxyisoindol-2-yl)ethyl)carbamoyl)-2-methylphenyl)-5,5-dimethyldibenzo[*b,e*]silin-3(5*H*)-ylidene)-*N*-methylmethanaminium chloride (0.09109 g, 0.1361 mmol) was evenly coated onto a 25 mL round bottom flask by evaporation from dichloromethane on a rotavapor. Then the flask was placed in a 120 °C oil bath and vacuum ~1mbar was applied for 2,5 h. The oil bath was removed, and the vacuum application was continued until 21 °C were reached, to give the desired compound in 93% yield (0.07639 g, 0.12706 mmol). Purple solid: **¹H NMR** (300 MHz, Chloroform-*d*) δ 8.67 (t, *J* = 5.7 Hz, 1H), 7.87 – 7.80 (m, 2H), 7.11 – 7.02 (m, 5H), 6.68 (s, 2H), 6.59 (dd, *J* = 9.6, 2.8 Hz, 2H), 3.81 (dd, *J* = 6.7, 3.9 Hz, 2H), 3.69 – 3.61 (m, 2H), 3.32 (s, 12H), 2.00 (s, 3H), 0.55 (d, *J* = 6.7 Hz, 6H). **¹³C NMR** (75 MHz, CDCl₃) δ 171.23, 170.17, 168.02, 154.26, 148.38, 141.94, 140.82, 135.87, 135.82, 134.25, 129.62, 128.93, 127.39, 124.94, 120.62, 114.22, 40.94, 39.13, 37.88, 19.40, -0.74, -1.06. **HRMS** (ESI) calculated for [M+H]⁺ C₃₃H₃₇N₄O₃Si 565.2629, found 565.2629. **Purity (HPLC)** >96% UV_{214 nm}, >96% UV_{254 nm}.



Conjugation reaction to alkyne modified BSA



The procedure was adapted from Presolski et al.¹²⁰ Stock solutions were prepared from the individual reagents. The mixtures were placed in Eppendorf tubes that were flushed with argon prior to closing after addition of all the reagents. The ascorbic acid solution was prepared freshly prior to the experiment.

The order of addition was

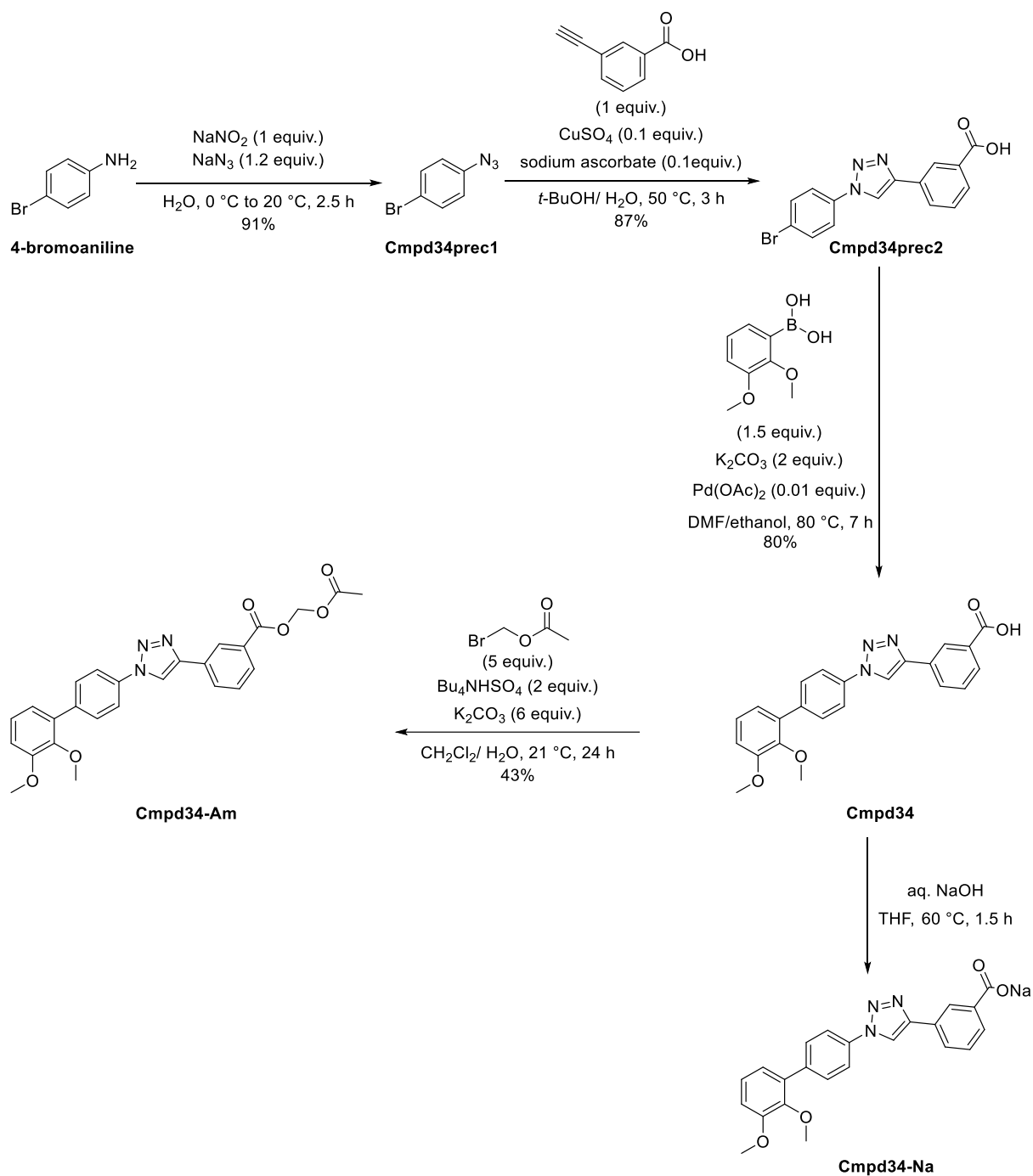
- 1) 50 μL of the alkyne modified BSA (1 mg/ mL in 0.5x PBS) 1 equiv.
- 2) 2.245 μL of the Azide (5 mM in water + DMSO 1%) 15 equiv.
- 3) 1.684 μL of a mixture with 1/3 CuSO_4 (20 mM) 15 equiv. and 2/3 THPTA (50 mM) 75 equiv.
- 4) 5.613 μL of Sodium Ascorbate solution (100 mM) 750 equiv.

The mixtures were left without stirring at 23 °C for 2 h.

From these mixtures the SDS-PAGE analysis was directly performed. The aliquots of the reaction mixtures were diluted with the appropriate amount of 4x reducing loading buffer and incubated at 37 °C for 15 minutes. The 10% polyacrylamide gel was run at 90 V for 15 minutes and then at 120 V until the bromophenol blue indicator exited the gel after ca. 2,5 h.

3.4. New SOCE inhibitors

Store operated calcium entry (SOCE) was previously studied in our group using various tool compounds.¹²¹⁻¹²³ For a new SOCE project it was planned to study a new inhibitor scaffold that was recently published. For these preliminary small studies **compound 34** (Cmpd34) published by Serafini et al.¹²⁴ was synthesised accordingly. The sodium salt of **Cmpd34** was successfully obtained by precipitation from THF. Another interesting tool compound **Cmpd34-Am** was synthesised as well. This acetoxymethyl (AM) ester can potentially permeate easier through membranes by diffusion. In the cytosol esterase activity then removes the acetyl group, leaving a hemiacetal, which quickly fragments to release formaldehyde and the carboxylic acid. The synthesised compounds were tested in still ongoing studies conducted by the group of Mathias Hediger at the Department for Biomedical Research (DBMR) in the Faculty of Medicine of the University of Bern. The preliminary results were used for a grant proposal that was recently accepted by the Swiss national science foundation (SNF). The synthesis of **Cmpd34**, **Cmpd34-Na** and **Cmpd34-AM** is shown in **Scheme 25**.

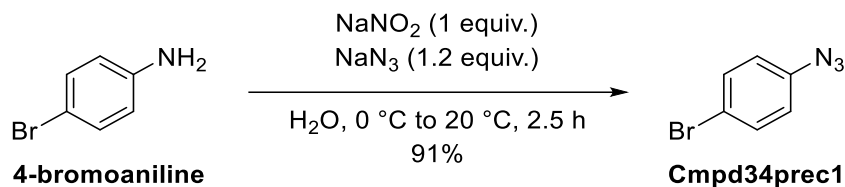


Scheme 25 Synthesis of Cmpd34 and its sodium salt derivative Cmpd34-Na and AM ester derivative Cmpd34-AM

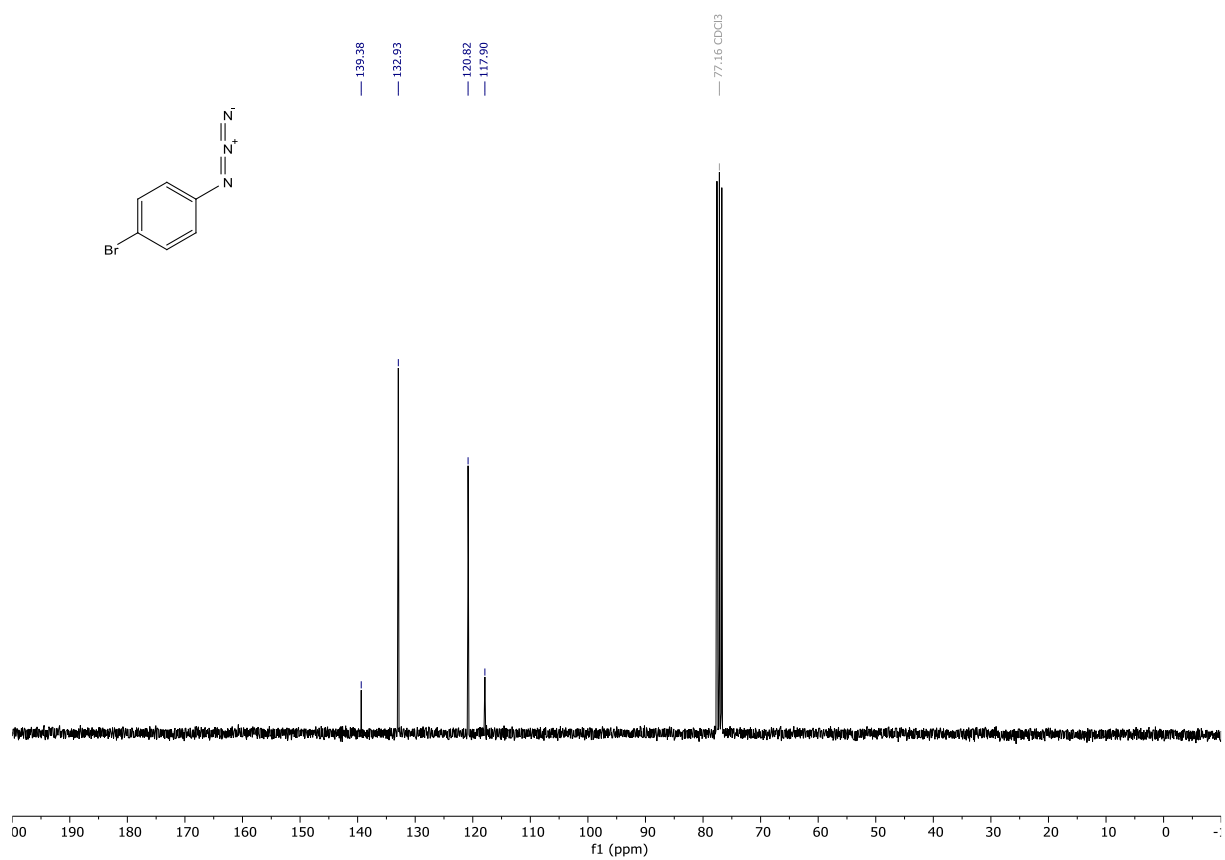
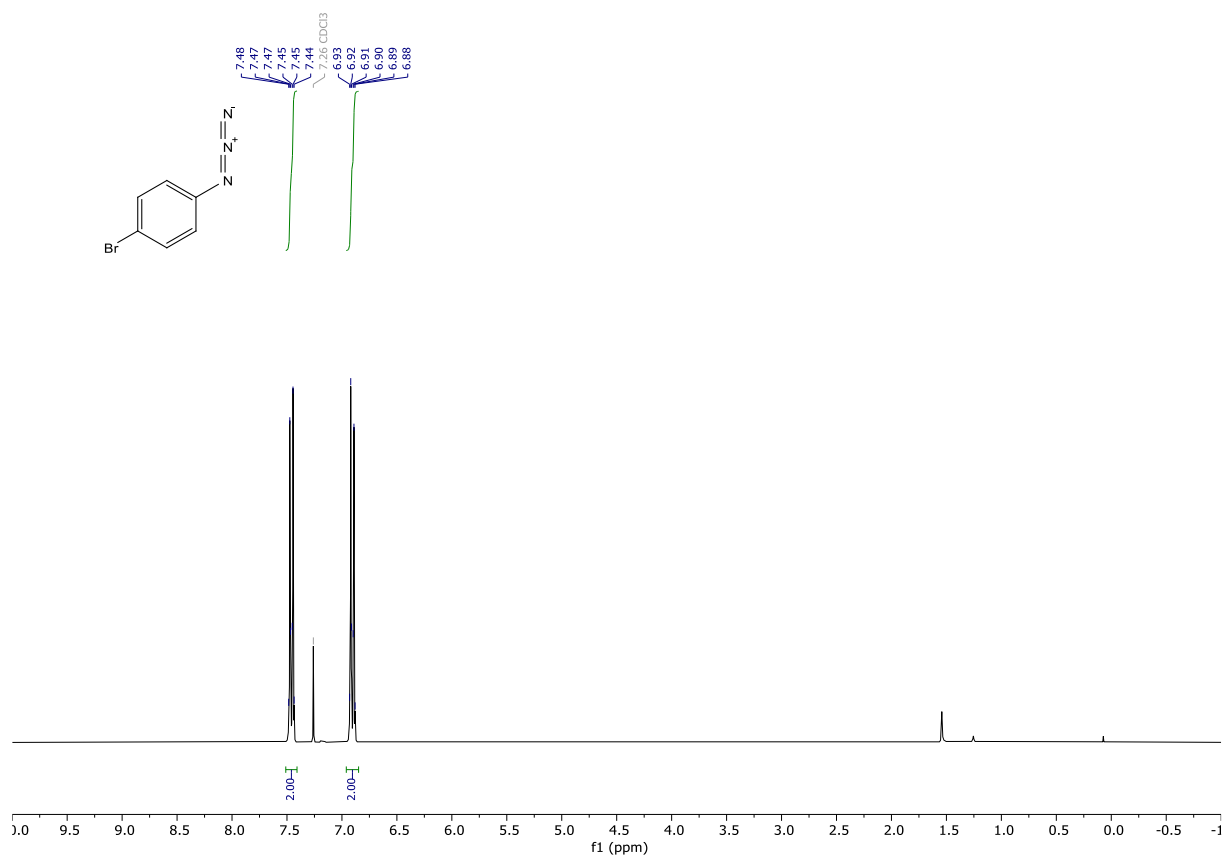
General remarks to materials & methods

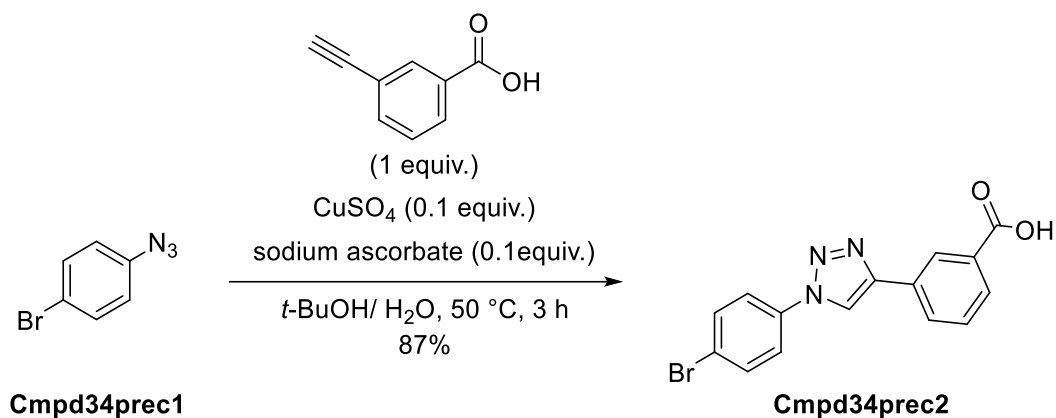
For general remarks see chapter 1.4.

Synthesis

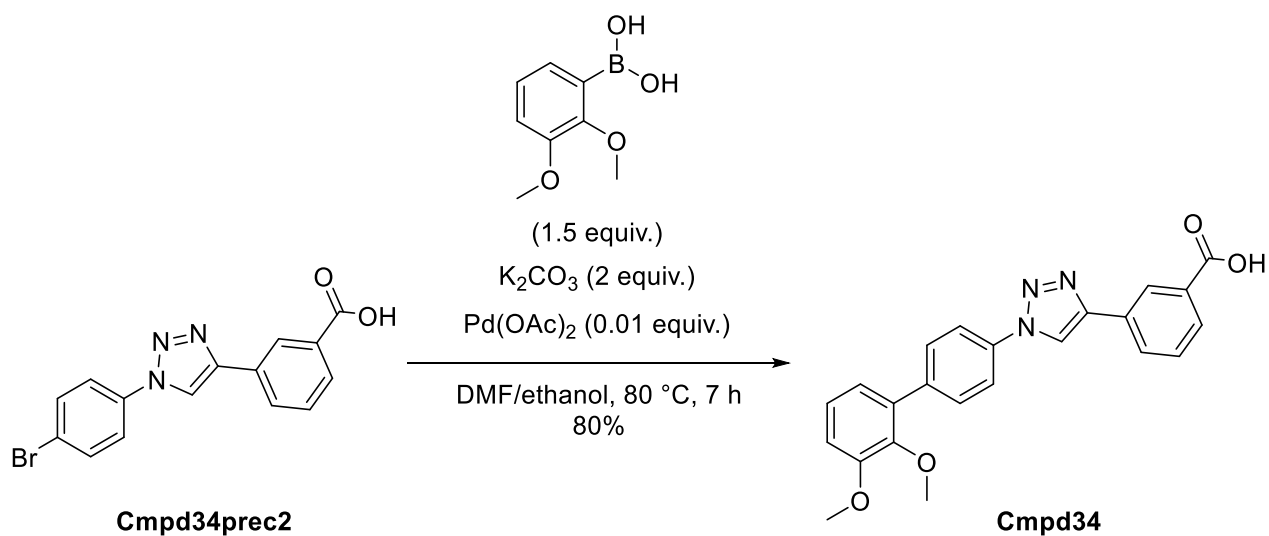
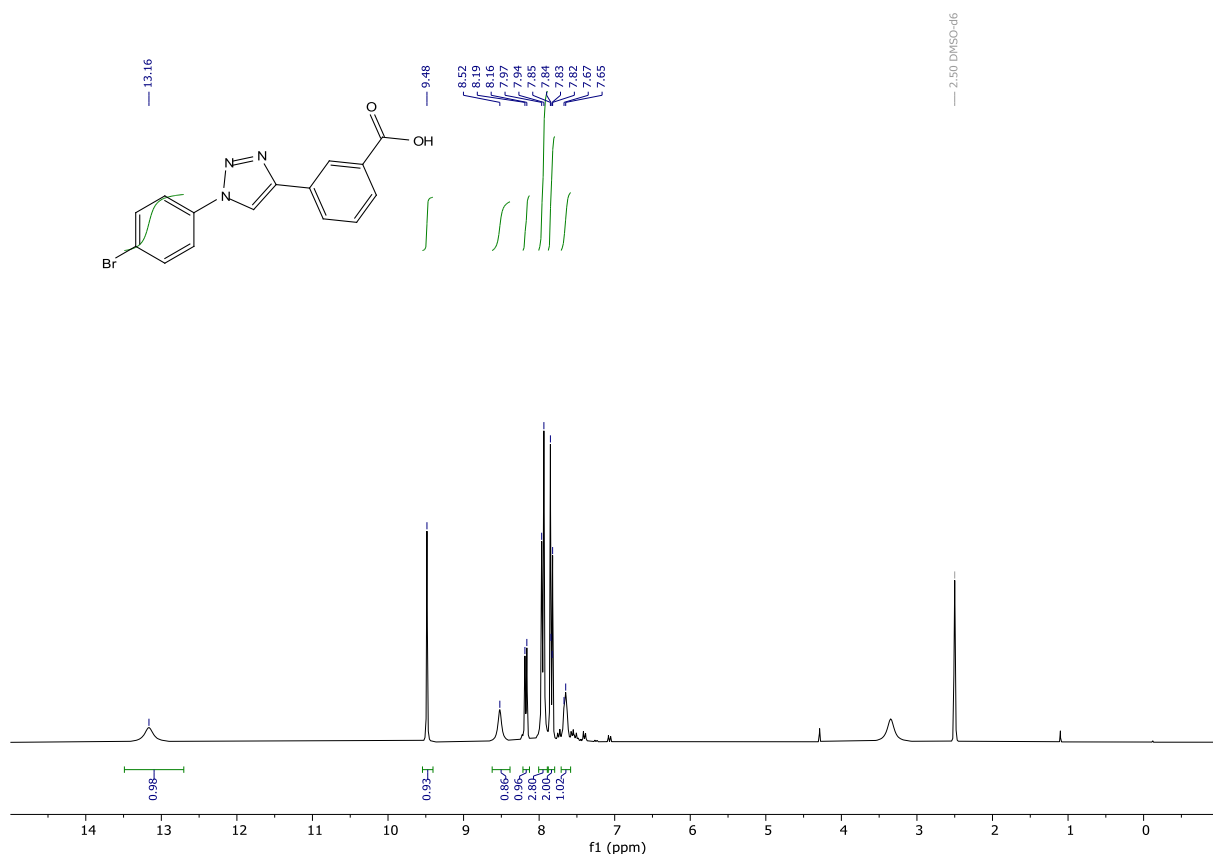


1-azido-4-bromobenzene (Cmpd34prec1). The compound was synthesised according to modified literature procedure.¹²⁴ To a stirred suspension of 4-Bromoaniline (3.002 g, 17.4510 mmol) in water (70 mL) at 0 °C, was added HCl 18.5% (15 mL). This led to a clear colourless solution. This solution was left to cool back down to 0 °C. Then was added slowly a solution of sodium nitrite (1.2056 g, 17.4750 mmol) in water (3 mL). The mixture was left stirring for 30 minutes at 0 °C. Then was added sodium azide (1.36144 g, 20.9420 mmol). This led to an immediate white precipitate that interrupted the stirring. Ethyl acetate was therefore added resulting in solvation of the precipitate. This solution was stirred for 2 h slowly warming to room temperature. (Careful: Addition of acid to mixtures containing sodium azide can lead to formation of HN_3 , a highly toxic a potentially explosive substance). Then the mixture was extracted with ethyl acetate. The combined organic layers were washed with water, brine, dried over MgSO_4 , filtered, and concentrated under reduced pressure onto silica gel. It was purified by flash column chromatography (cyclohexane/ ethyl acetate gradient from 1:0 to 9:1), to give the desired compound in 91% yield (3.12857 g, 15.79902 mmol). Yellow solid with low melting point: $^1\text{H NMR}$ (300 MHz, Chloroform-*d*) δ 7.51 – 7.41 (m, 2H), 6.96 – 6.85 (m, 2H). $^{13}\text{C NMR}$ (75 MHz, CDCl_3) δ 139.38, 132.93, 120.82, 117.90. **HRMS** (ESI/EI) no data could be obtained for this compound.



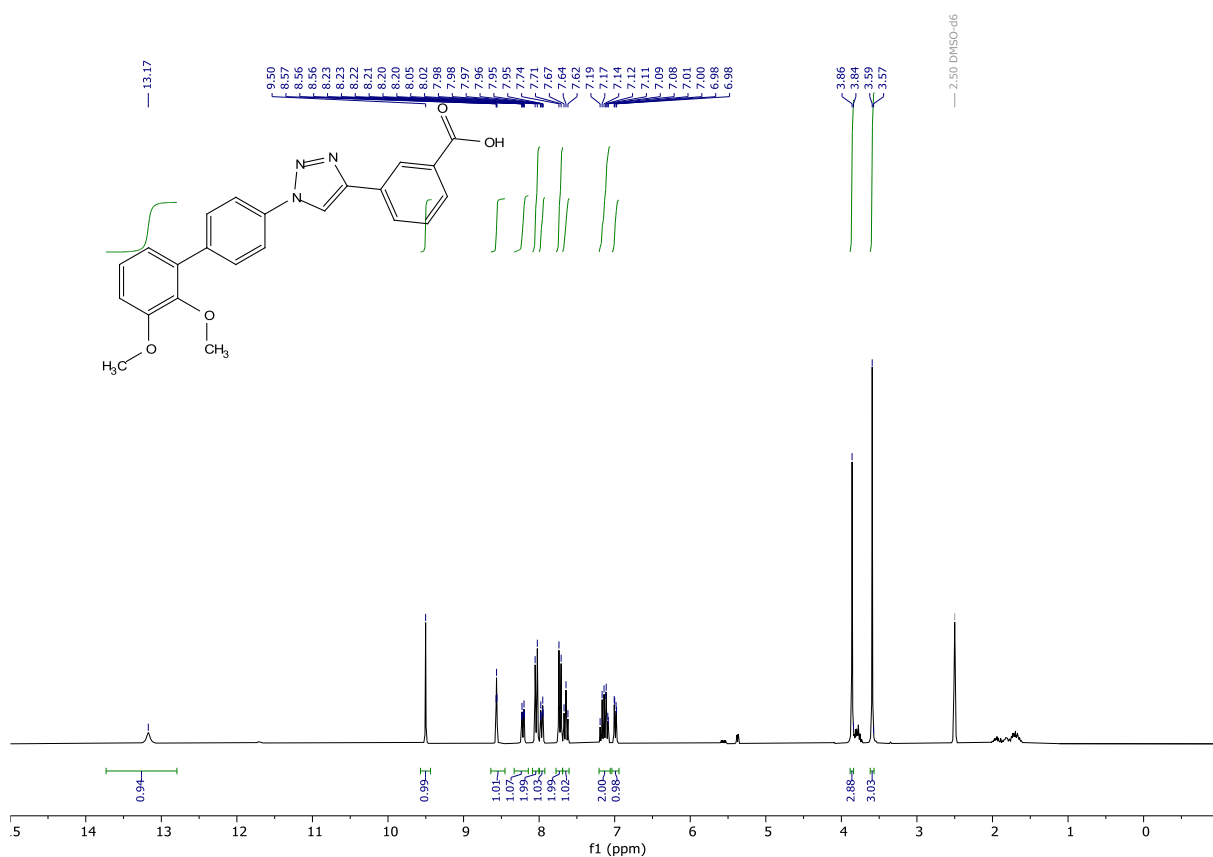


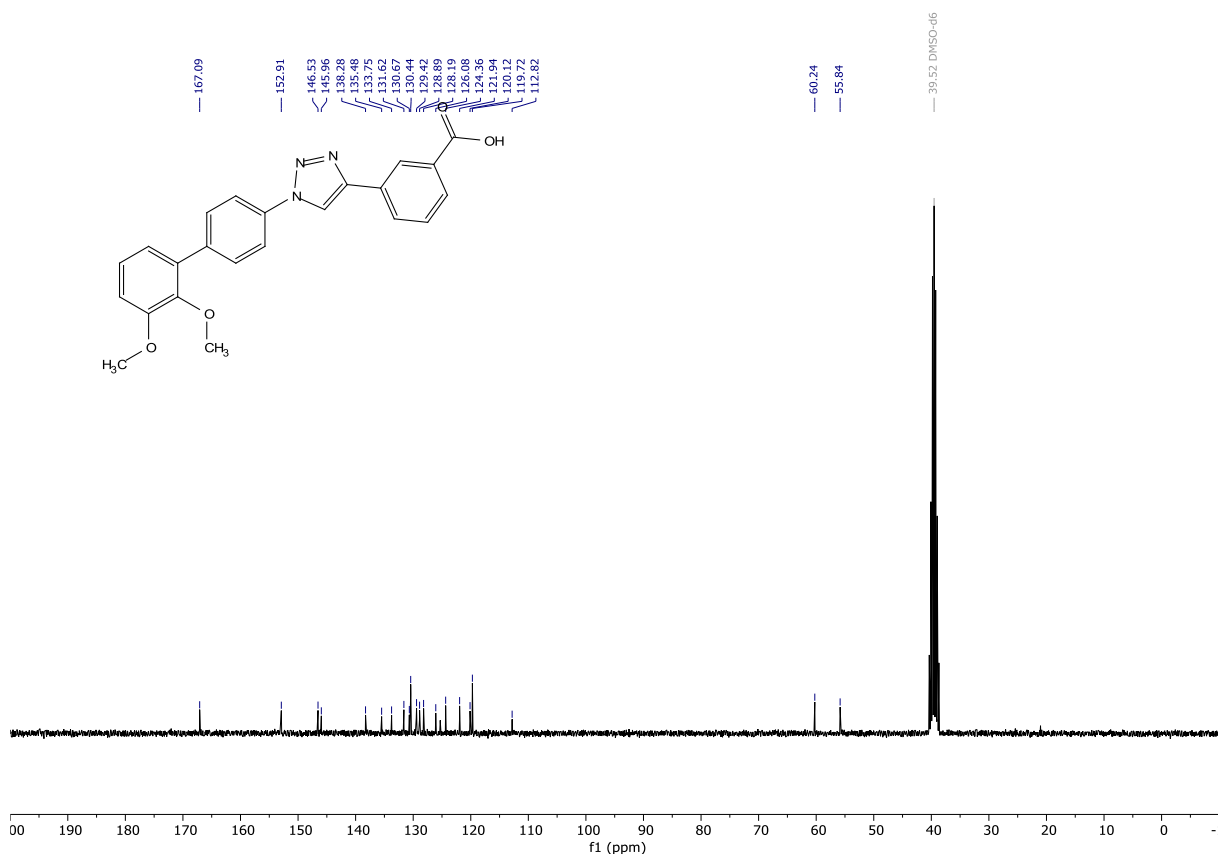
3-(1-(4-bromophenyl)-1H-1,2,3-triazol-4-yl)benzoic acid (Cmpd34prec2). The compound was prepared according to modified literature procedure.¹²⁴ To a stirred solution of 1-azido-4-bromobenzene (Cmpd34prec1) (2.94913 g, 14.8929 mmol) in *t*-BuOH (30 mL) was added water (30 mL) this gave a suspension to which was added 3-ethynylbenzoic acid (2.17515 g, 14.8835 mmol). The resulting mixture was warmed to 50 °C. Then was added copper sulfate pentahydrate (0.0743 g, 0.2976 mmol) and sodium ascorbate (0.31716 g, 1.6009 mmol). Upon addition, the mixture instantaneously precipitated a yellow solid. The mixture was left stirring for 3 h, during which stirring became increasingly difficult due to the amount of precipitate. It was cooled to 0°C and filtered. The filter cake was thoroughly washed with ice cold, slightly acidified (HCl) water. Then it was dried on the filter applying suction and transferred into a round bottom flask. To this was added toluene to remove the water by azeotropic co-evaporation. The obtained powder was dried under high vacuum to give the desired product in 87% yield (4.44000 g, 12.90068 mmol). Physical and spectral data in accordance with literature.¹²⁴ Yellow solid: $^1\text{H NMR}$ (300 MHz, DMSO-*d*₆) δ 13.16 (s, 1H), 9.48 (s, 1H), 8.52 (s, 1H), 8.18 (d, *J* = 7.6 Hz, 1H), 7.95 (d, *J* = 8.8 Hz, 3H), 7.84 (d, *J* = 8.8 Hz, 2H), 7.66 (d, *J* = 6.7 Hz, 1H). **HRMS** (ESI) calculated for $[\text{M}+\text{H}]^+$ C₁₅H₁₁BrN₃O₂ 344.0029, found 344.0039.



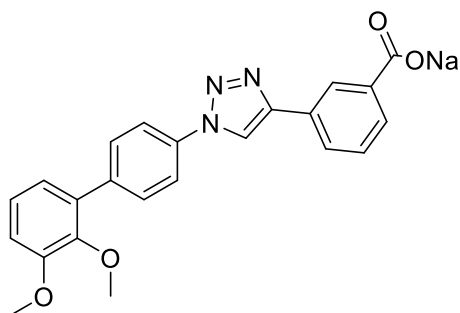
3-(1-(2',3'-dimethoxy-[1,1'-biphenyl]-4-yl)-1H-1,2,3-triazol-4-yl)benzoic acid (Cmpd34). The compound was prepared according to modified literature procedure.¹²⁴ A stirred solution of 3-(1-(4-bromophenyl)-1H-1,2,3-triazol-4-yl)benzoic acid (Cmpd34prec2) (0.518 g, 1.5051 mmol), (2,3-dimethoxyphenyl)boronic acid (0.455 g, 2.5002 mmol), K₂CO₃ (0.424 g, 3.0679 mmol) and Pd(II) acetate (0.006 g, 0.0267 mmol) in a mixture of dimethylformamide (3.6 mL) and ethanol (3.6 mL) was heated to 80 °C under an argon atmosphere. The yellowish mixture quickly became a dark brown solution. After 7 h the volatiles were removed under reduced pressure. The mixture was taken up in

methanol and was concentrated onto silica gel. The crude was purified by flash column chromatography (cyclohexane/ (ethyl acetate/ methanol/ acetic acid 85:10:5) gradient from 1:0 to 0:1). The obtained solid was impure and thus it was taken up in THF and concentrated onto silica gel. It was purified by reverse phase flash column chromatography (water + 0.1% TFA/ acetonitrile + 0.1% TFA gradient from 1:0 to 0:1) to give the desired compound in 80% yield (0.48220 g, 1.201230 mmol). Yellow solid: **¹H NMR** (300 MHz, DMSO-*d*₆) δ 13.17 (s, 1H), 9.50 (s, 1H), 8.56 (t, *J* = 1.7 Hz, 1H), 8.21 (dt, *J* = 7.8, 1.5 Hz, 1H), 8.04 (d, *J* = 8.7 Hz, 2H), 7.97 (dt, *J* = 7.7, 1.4 Hz, 1H), 7.72 (d, *J* = 8.6 Hz, 2H), 7.64 (t, *J* = 7.8 Hz, 1H), 7.22 – 7.05 (m, 2H), 6.99 (dd, *J* = 7.4, 1.8 Hz, 1H), 3.86 (s, 3H), 3.59 (s, 3H). **¹³C NMR** (75 MHz, DMSO) δ 167.09, 152.91, 146.53, 145.96, 138.28, 135.48, 133.75, 131.62, 130.67, 130.44, 129.42, 128.89, 128.19, 126.08, 124.36, 121.94, 120.12, 119.72, 112.82, 60.24, 55.84. **HRMS** (ESI) calculated for [M+H]⁺ C₂₃H₂₀N₃O₄ 402.1448, found 402.1433.





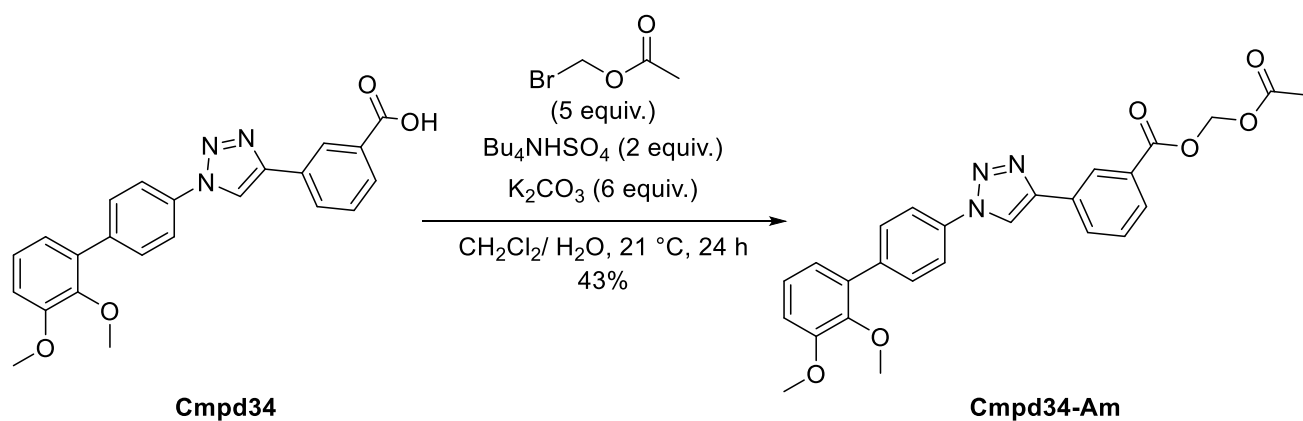
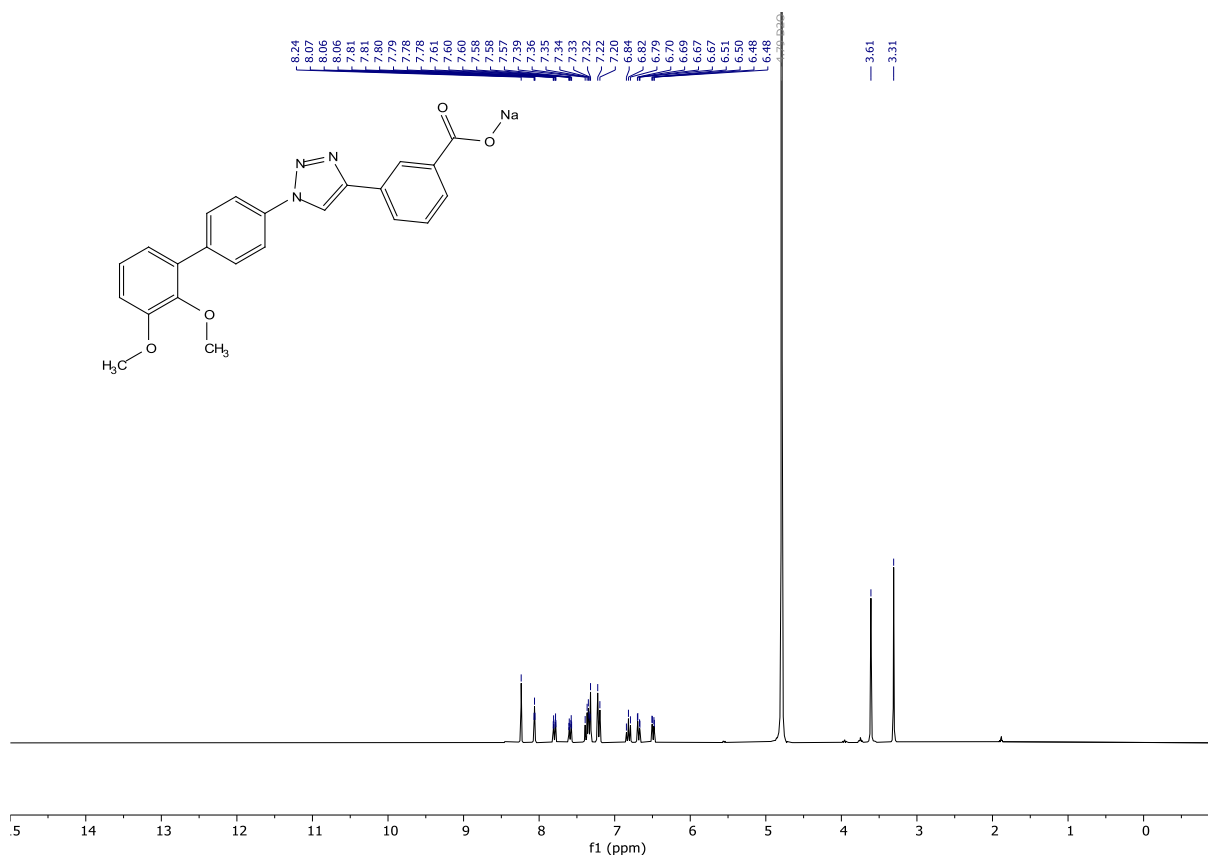
Preparation of the sodium Salt (Cmpd34-Na)



Cmpd34-Na

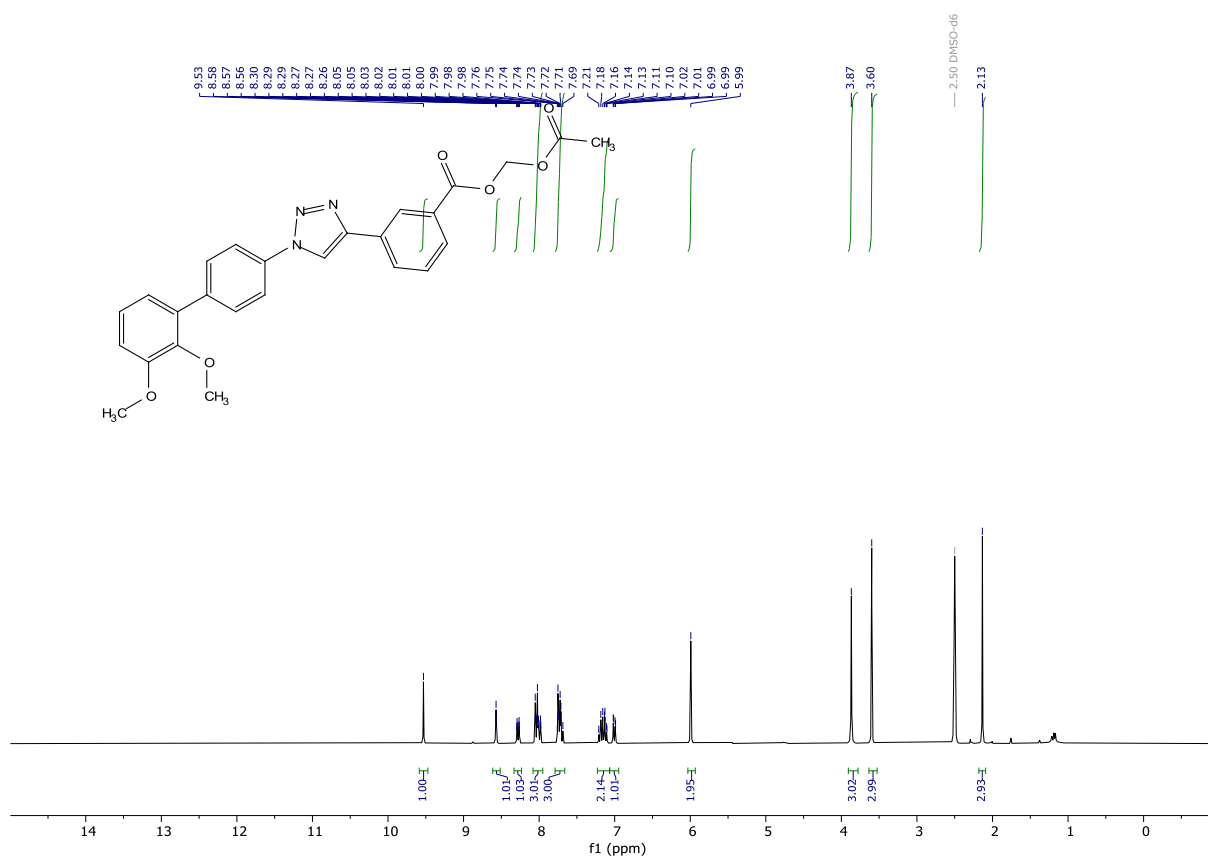
sodium 3-(1-(2',3'-dimethoxy-[1,1'-biphenyl]-4-yl)-1H-1,2,3-triazol-4-yl)benzoate (Cmpd34-Na). 3-(1-(2',3'-dimethoxy-[1,1'-biphenyl]-4-yl)-1H-1,2,3-triazol-4-yl)benzoic acid (0.21251 g, 0.5294 mmol) was dissolved in THF (2 mL) and the mixture was heated to 60 °C giving a clear yellow solution. To this was added NaOH (50% in water, 22 µL). This gave an immediate precipitate. The mixture was stirred at 60 °C for 0.5 h. Then the mixture was slowly cooled to 21 °C while stirring. After 1 h the precipitate was filtered through a por 4 frit. This gave a yellow filter cake and a yellow solution. The filter cake was washed with little THF (3x). This removed a lot of the colour to give an off-white powder. This powder was thoroughly dried on the High vacuum. Off white solid: ¹H NMR (300 MHz, Deuterium Oxide) δ 8.24 (s, 1H), 8.06 (t, *J* = 1.7 Hz, 1H), 7.80 (dt, *J* = 7.7, 1.4 Hz, 1H), 7.59 (dt, *J* = 7.7, 1.5 Hz, 1H),

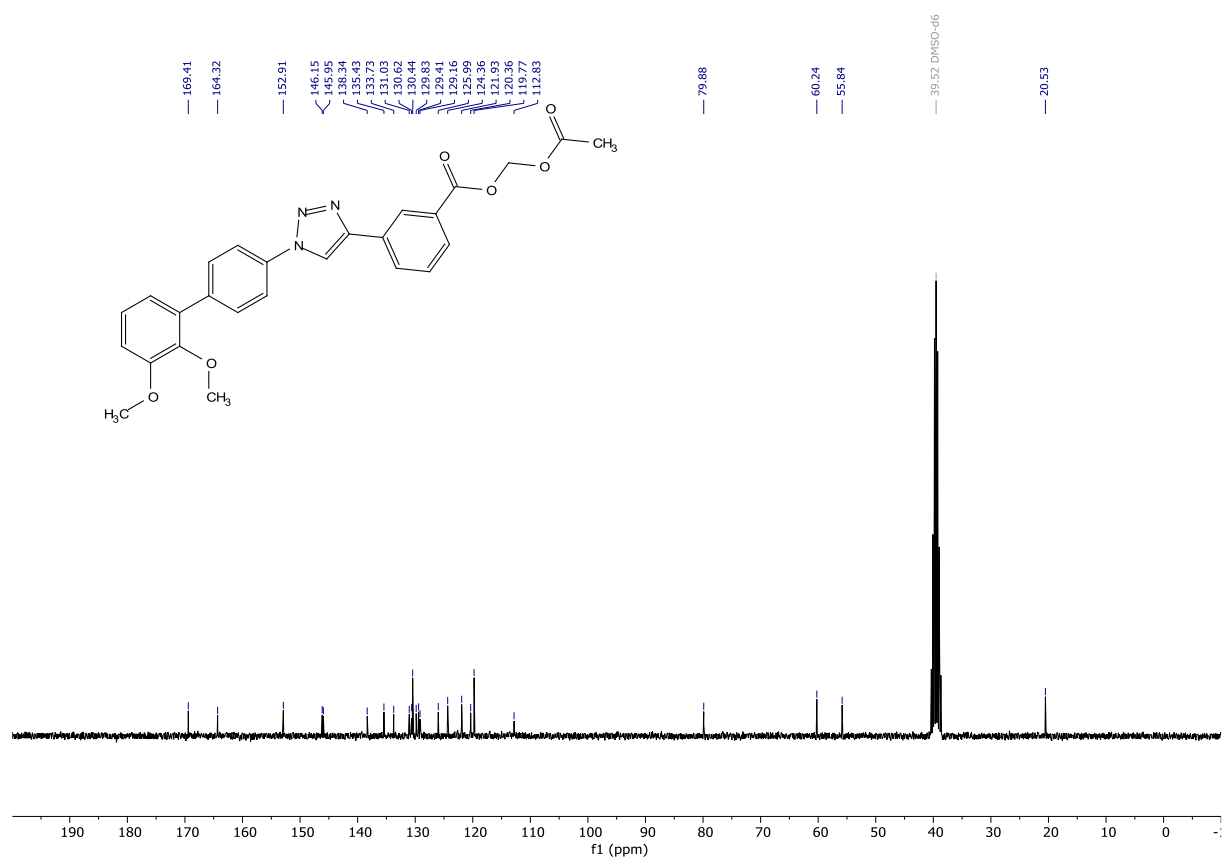
7.42 – 7.29 (m, 3H), 7.21 (d, $J = 8.6$ Hz, 2H), 6.82 (t, $J = 8.0$ Hz, 1H), 6.68 (dd, $J = 8.3, 1.4$ Hz, 1H), 6.49 (dd, $J = 7.8, 1.5$ Hz, 1H), 3.61 (s, 3H), 3.31 (s, 3H).



acetoxymethyl 3-(1-(2',3'-dimethoxy-[1,1'-biphenyl]-4-yl)-1H-1,2,3-triazol-4-yl)benzoate (Cmpd34-Am). This synthesis was based on a procedure, in which other carboxylic acids were esterified.¹²⁵ To a stirred suspension of 3-(1-(2',3'-dimethoxy-[1,1'-biphenyl]-4-yl)-1H-1,2,3-triazol-4-yl)benzoic acid (0.08542 g, 0.2128 mmol) in water (2 mL) was added potassium carbonate (0.15357 g, 1.2807 mmol). This was followed by addition of tetrabutyl ammonium hydrogensulfate (0.15357 g, 0.4523 mmol) in dichloromethane (1 mL). This gave a clear biphasic solution with a yellowish coloured organic layer. To this was added bromomethyl acetate (0.1 mL, 0.156 g, 1.0198 mmol). The mixture was stirred

vigorously at 21 °C. The mixture was extracted with dichloromethane, the combined organic layers were dried over MgSO_4 , filtered, and concentrated under reduced pressure onto silica gel. The crude was purified by flash column chromatography (cyclohexane/ ethyl acetate gradient from 1:0 to 0:1) to give an oily product. The product was taken up in acetonitrile + 0.1% TFA to which was added water + 0.1% TFA. The addition of water led to a white precipitate. The volatiles were removed under reduced pressure to give the desired product in 43% yield (0.04322 g, 0.09128 mmol). Yellow solid: **^1H NMR** (300 MHz, $\text{DMSO}-d_6$) δ 9.53 (s, 1H), 8.57 (t, $J = 1.7$ Hz, 1H), 8.28 (dt, $J = 7.8, 1.4$ Hz, 1H), 8.08 – 7.95 (m, 3H), 7.79 – 7.66 (m, 3H), 7.23 – 7.07 (m, 2H), 7.00 (dd, $J = 7.4, 1.8$ Hz, 1H), 5.99 (s, 2H), 3.87 (s, 3H), 3.60 (s, 3H), 2.13 (s, 3H). **^{13}C NMR** (75 MHz, DMSO) δ 169.41, 164.32, 152.91, 146.15, 145.95, 138.34, 135.43, 133.73, 131.03, 130.62, 130.44, 129.83, 129.41, 129.16, 125.99, 124.36, 121.93, 120.36, 119.77, 112.83, 79.88, 60.24, 55.84, 20.53. **HRMS** (ESI) calculated for $[\text{M}+\text{H}]^+$ $\text{C}_{26}\text{H}_{24}\text{N}_3\text{O}_6$ 474.1660, found 474.1654.





3.5. MIPS-521

Background

In recent years, our group developed selective adenosine A₁ receptor (A₁R) agonists.¹²⁶⁻¹²⁸ These agonists are based on the endogenous nucleoside adenosine and bind to the orthosteric site of the G protein-coupled A₁R. Likewise, allosteric modulators offer the possibility to modulate receptor function in the presence of endogenous ligand by binding to a different (allosteric) site. Thiophene compound **MIPS521** (**Figure 44**) was recently published as a potent positive A₁R allosteric modulator.¹²⁹ Our collaborators were interested to test this novel compound in their cellular A₁R assay. Furthermore, we were interested to explore if the **MIPS521** scaffold would be suitable for synthetic modifications with the aim of creating conjugates and bitopic ligands (i.e. by linking **MIPS521** with orthosteric ligands), guided by some recent structural information from cryo-EM.¹³⁰

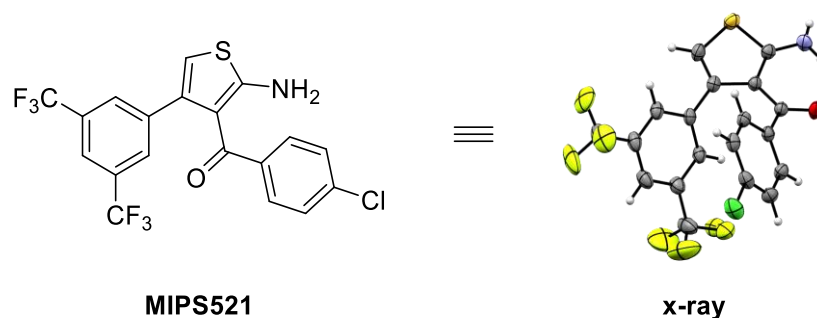
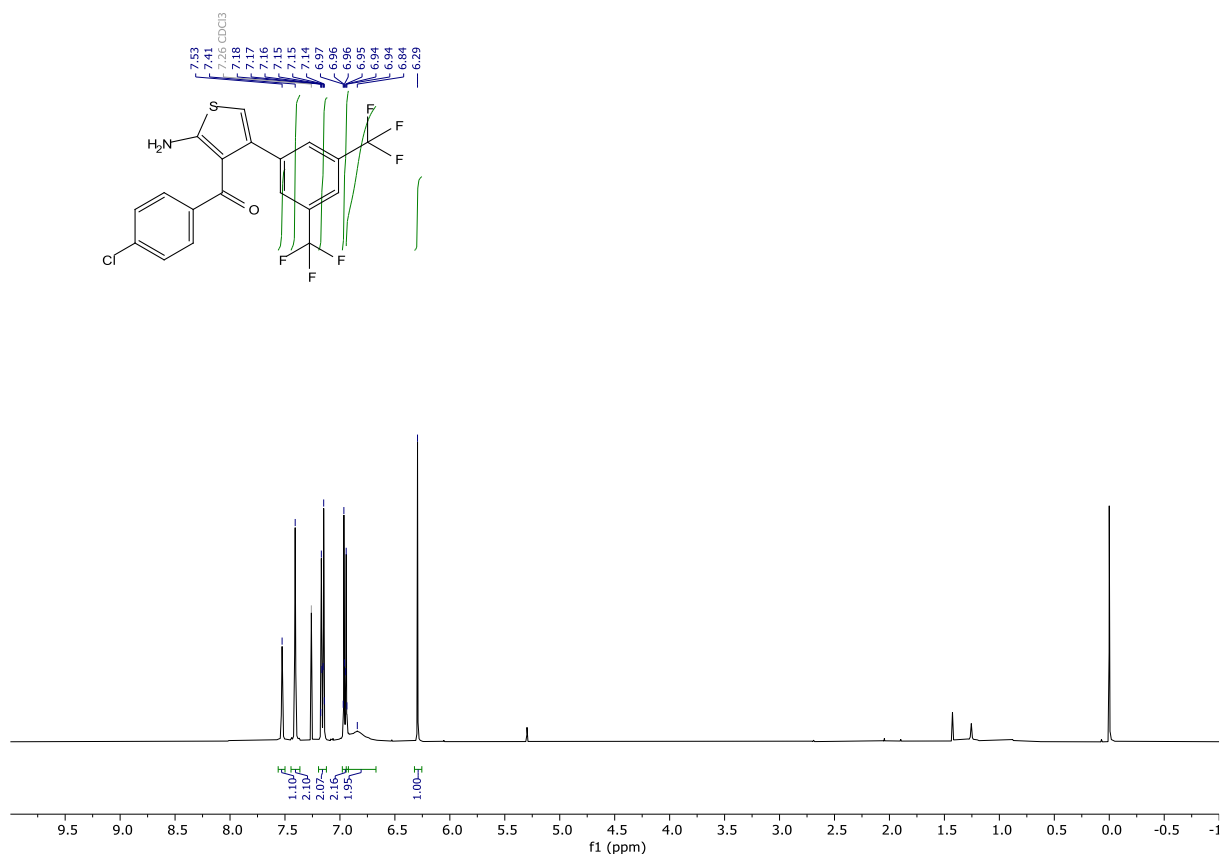
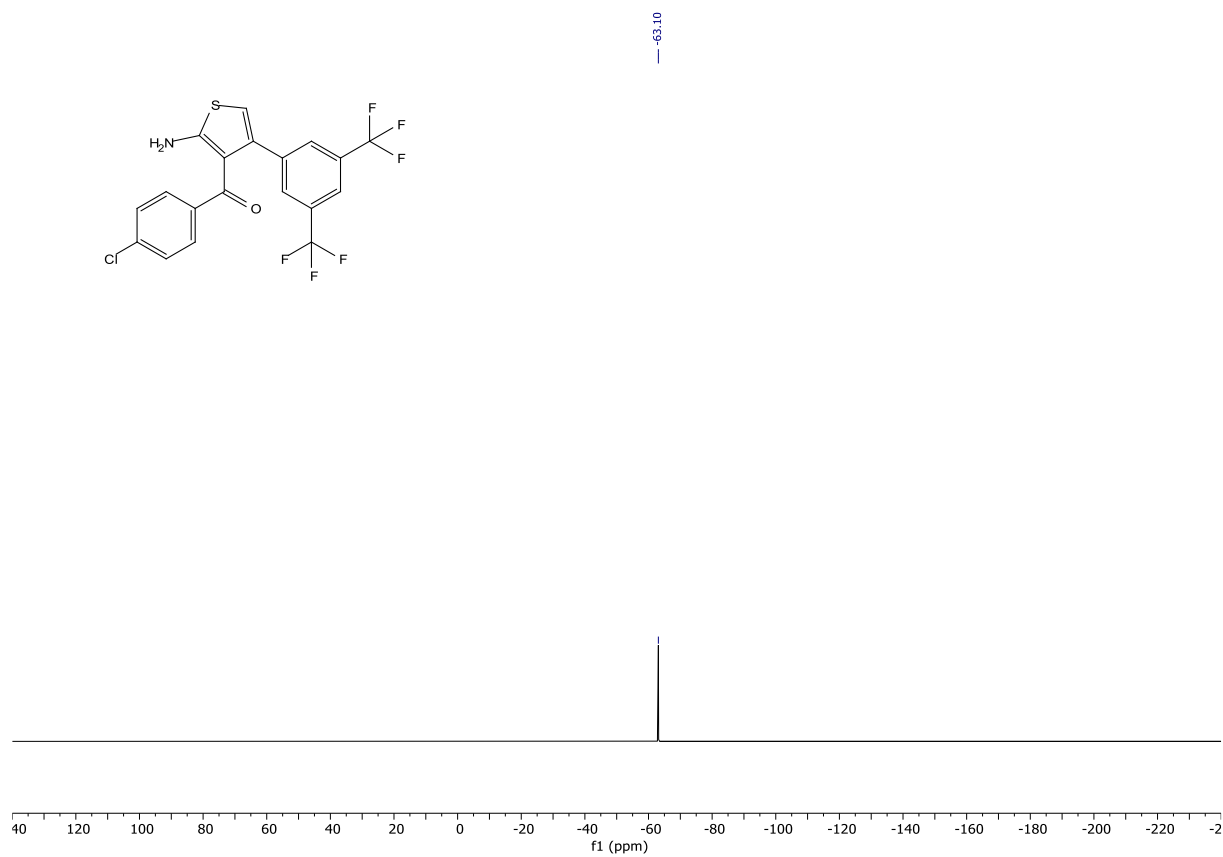
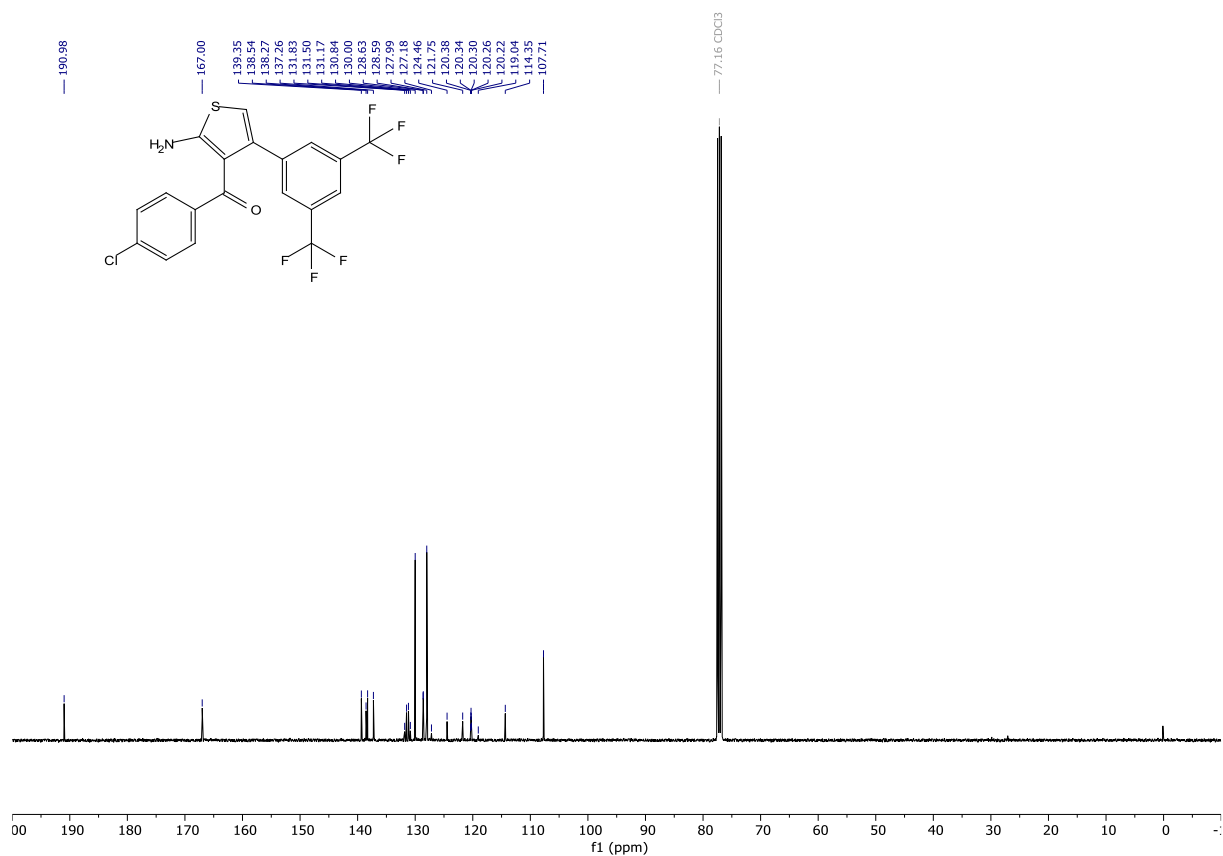


Figure 44 MIPS521 Structure & x-ray crystal structure

crystals of suitable quality for x-ray diffraction measurements (CCDC deposition number: 2192327). Yellow crystalline solid: **¹H NMR** (300 MHz, CDCl₃) δ 7.53 (s, 1H), 7.41 (s, 2H), 7.21 – 7.11 (m, 2H), 7.00 – 6.92 (m, 2H), 6.84 (bs, 2H), 6.29 (s, 1H). **¹³C NMR** (101 MHz, CDCl₃) δ 190.98, 167.00, 139.35, 138.54, 138.27, 137.26, 131.34 (q, *J* = 33.3 Hz), 130.00, 128.61 (d, *J* = 3.7 Hz), 127.99, 123.11 (q, *J* = 272.8 Hz), 120.30 (p, *J* = 3.8 Hz), 114.35, 107.71. **¹⁹F NMR** (376 MHz, CDCl₃) δ -63.10. **HRMS** (ESI) calculated for [M+H]⁺ C₁₉H₁₀ClF₆NOS 450.0149, found 450.0140. **Purity (HPLC)** >95% UV₂₁₄ nm, >95% UV₂₅₄ nm.





4. Functional design of bacterial superoxide: quinone oxidoreductase

Overview

This project was a collaborative effort together with the groups of Prof. Dr. Christoph von Ballmoos at the department of chemistry, biochemistry, and pharmaceutical sciences (DCBP) at the university of Bern and of Prof. Dr. Martin Högbom at the institute of biochemistry and biophysics at the university of Stockholm. The results of this effort were published in *Biochimica et Biophysica Acta (BBA) – Bioenergetics*. The chemical synthesis of the employed ubiquinone derivatives was carried out in our labs and the biochemical testing and data interpretation was carried out in the von Ballmoos and Högbom Labs. The compounds were tested on the cytochrome b_{561} enzyme, that catalyses the oxidation of superoxide (O_2^-) to molecular oxygen (O_2) transferring the electrons onto ubiquinones reducing them to ubiquinols. The compounds were used, amongst others to test the enzyme's reactions as well as its redox behaviour. In the following subchapters, the focus is put on our contribution to this study, i.e. the chemical synthesis of the ubiquinones. The main text containing the biochemical questions addressed, and the results can be found online. (<https://doi.org/10.1016/j.bbabbio.2022.148583>).

To give the reader an idea of the biochemical experiments the abstract of the article is presented below, followed by schemes, which depict the synthetic pathway to obtain the derivatives.

Contribution to this study

Ubiquinones Q_1 , Q_2 and decylubiquinone were synthesised by me. The synthesis was adapted and modified from procedures published by Lu et al.¹³¹ The rest of the study was conceived, designed and carried out by the other authors. The study was published in the journal *Biochimica et Biophysica Acta (BBA) – Bioenergetics*. Accessible under: <https://doi.org/10.1016/j.bbabbio.2022.148583>

Abbas Abou-Hamdan*, Roman Mahler*, **Philipp Grossenbacher**, Olivier Biner, Dan Sjöstrand, **Martin Lochner**, Martin Högbom, Christoph von Ballmoos, Functional design of bacterial superoxide:quinone oxidoreductase, *Biochimica et Biophysica Acta (BBA) - Bioenergetics*, Volume 1863, Issue 7, 2022, 148583.

*Authors contributed equally to the study.

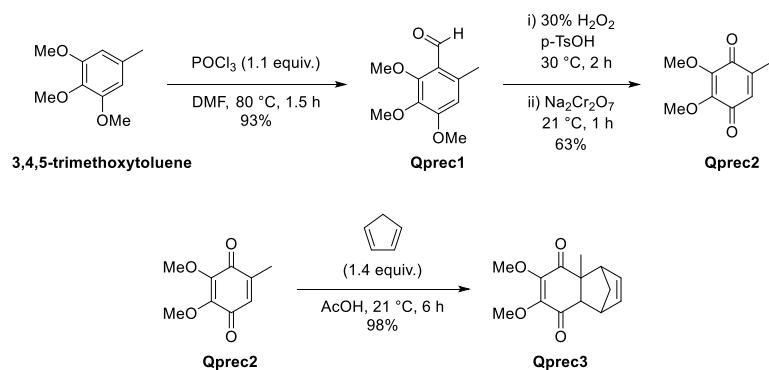
Abstract

The superoxide anion - molecular oxygen reduced by a single electron - is produced in large amounts by enzymatic and adventitious reactions. It can perform a range of cellular functions, including bacterial warfare and iron uptake, signalling and host immune response in eukaryotes. However, it also serves as precursor for more deleterious species such as the hydroxyl anion or peroxynitrite and defense mechanisms to neutralize superoxide are important for cellular health. In addition to the soluble proteins superoxide dismutase and superoxide reductase, recently the membrane embedded diheme cytochrome *b*₅₆₁ (CybB) from *E. coli* has been proposed to act as a superoxide:quinone oxidoreductase. Here, we confirm superoxide and cellular ubiquinones or menaquinones as natural substrates and show that quinone binding to the enzyme accelerates the reaction with superoxide. The reactivity of the substrates is in accordance with the here determined midpoint potentials of the two *b* hemes (+48 and -23 mV / NHE). Our data suggest that the enzyme can work near the diffusion limit in the forward direction and can also catalyse the reverse reaction efficiently under physiological conditions. The data is discussed in the context of described cytochrome *b*₅₆₁ proteins and potential physiological roles of CybB.

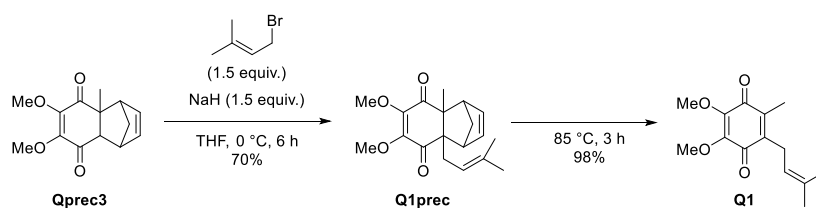
Synthesis overview

In **Scheme 26** an overview of the synthesis to **Q1**, **Q2** and **decylubiquinone** is depicted. Starting from 3,4,5-trimethoxytoluene transforming it in 3 steps into the versatile protected precursor **Qprec3** (**Scheme 26, A**). From there the ubiquinones were accessed via alkylation and subsequent retro Diels-Alder deprotection. **Q1** and **decylubiquinone** were accessed over two steps from **Qprec3** (**Scheme 26, B and D**). To access **Q2** a preliminary transformation of geraniol to geranyl bromide via an Appel reaction was required (**Scheme 26, C**). Reverse phase flash chromatography yielded very pure ubiquinones.

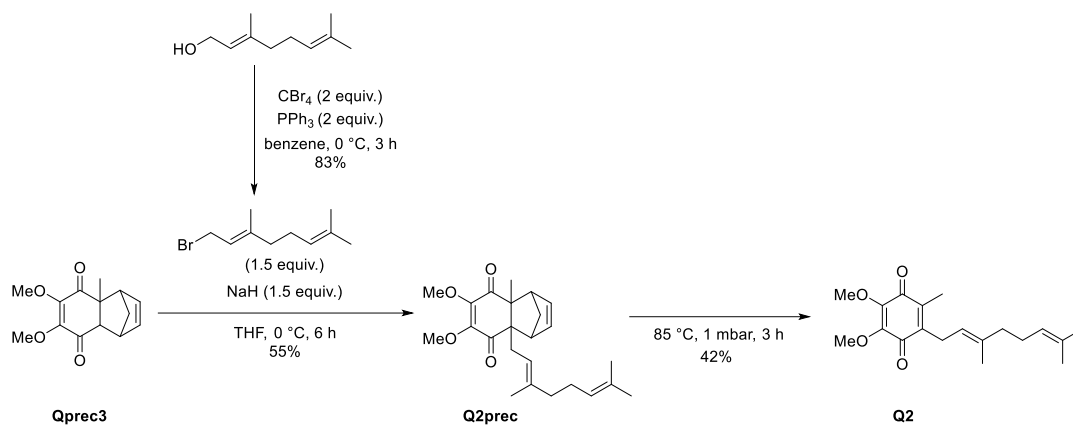
A



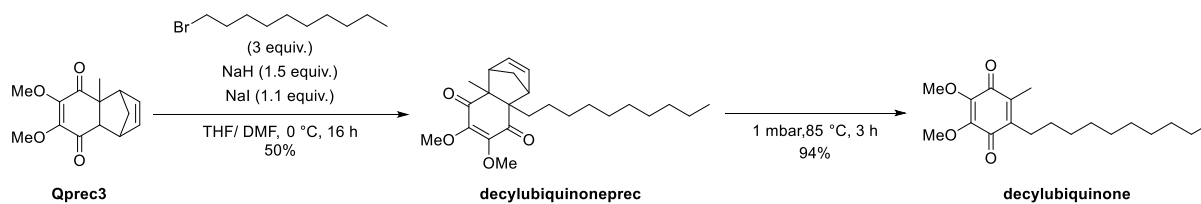
B



C



D

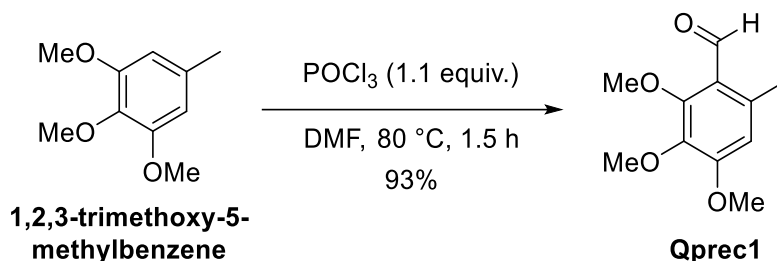


Scheme 26 A) Synthesis of the versatile precursor Qprec3 **B)** Synthesis of Q1 from Qprec3 **C)** Synthesis of Q2 from Qprec3 **D)** Synthesis of decylubiquinone from Qprec3

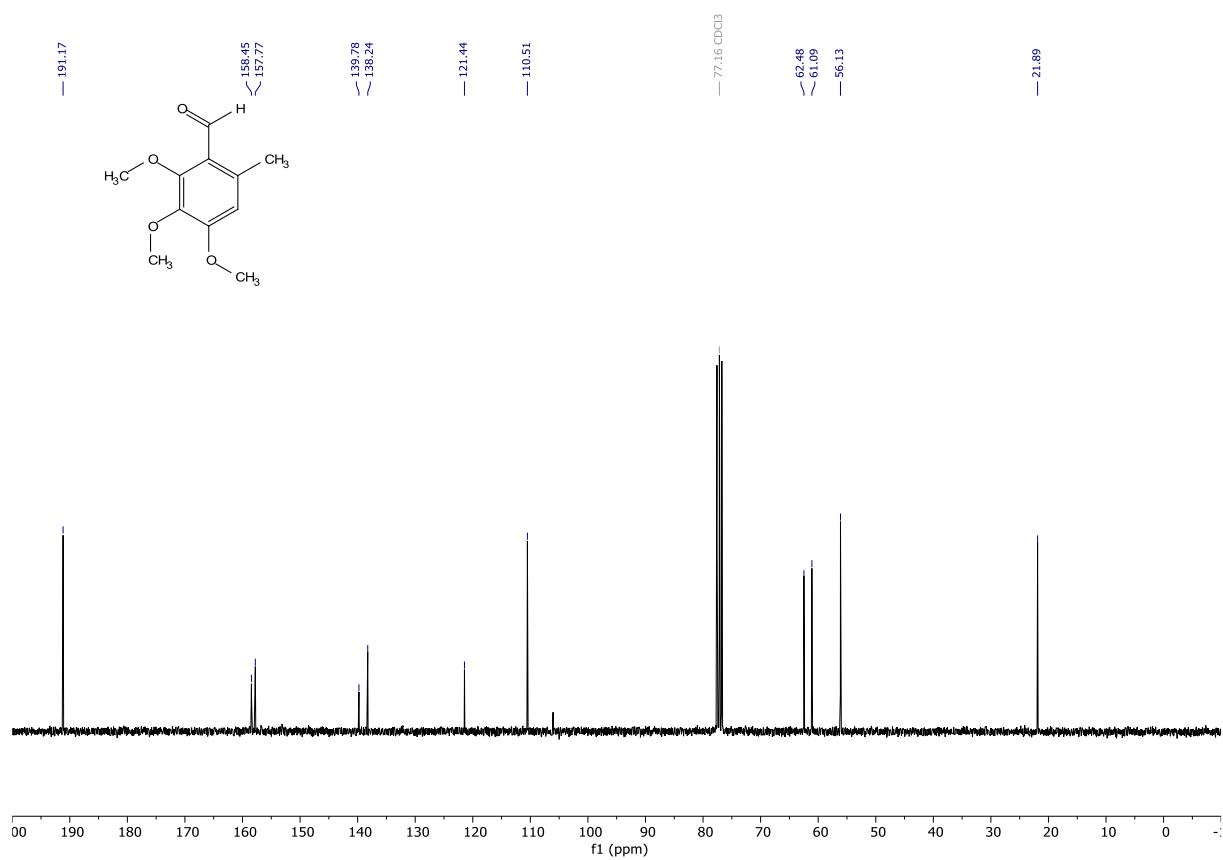
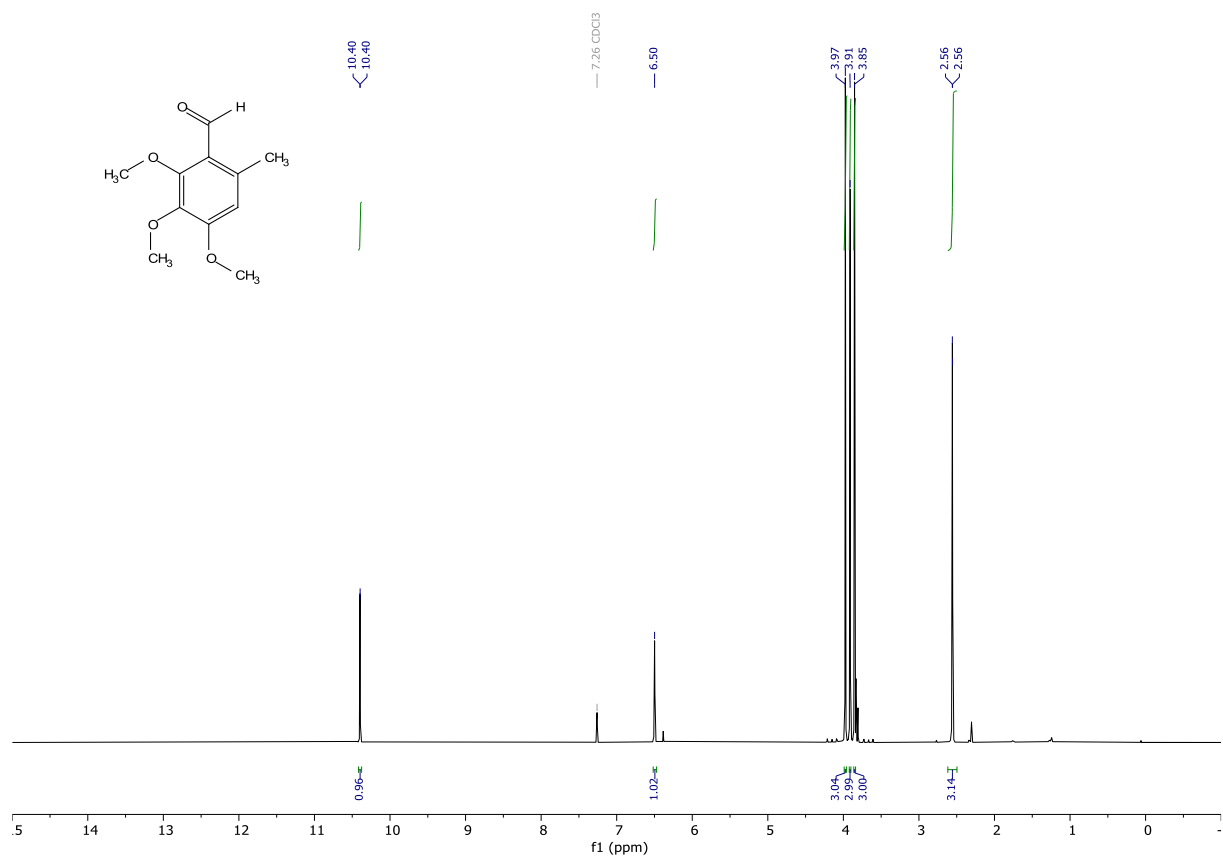
General remarks to materials & methods

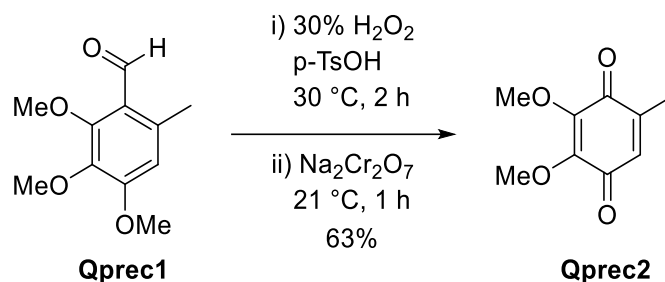
For general remarks see chapter 1.4.

Synthesis

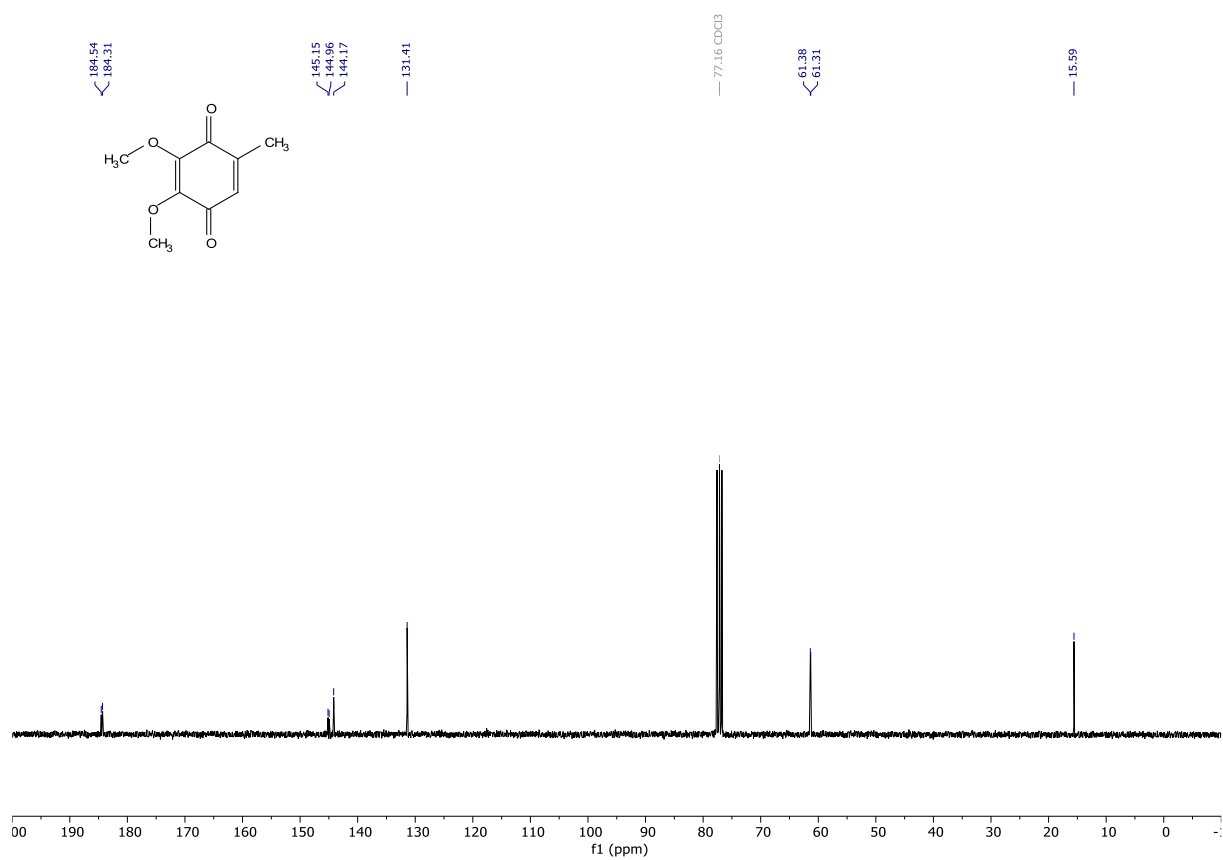
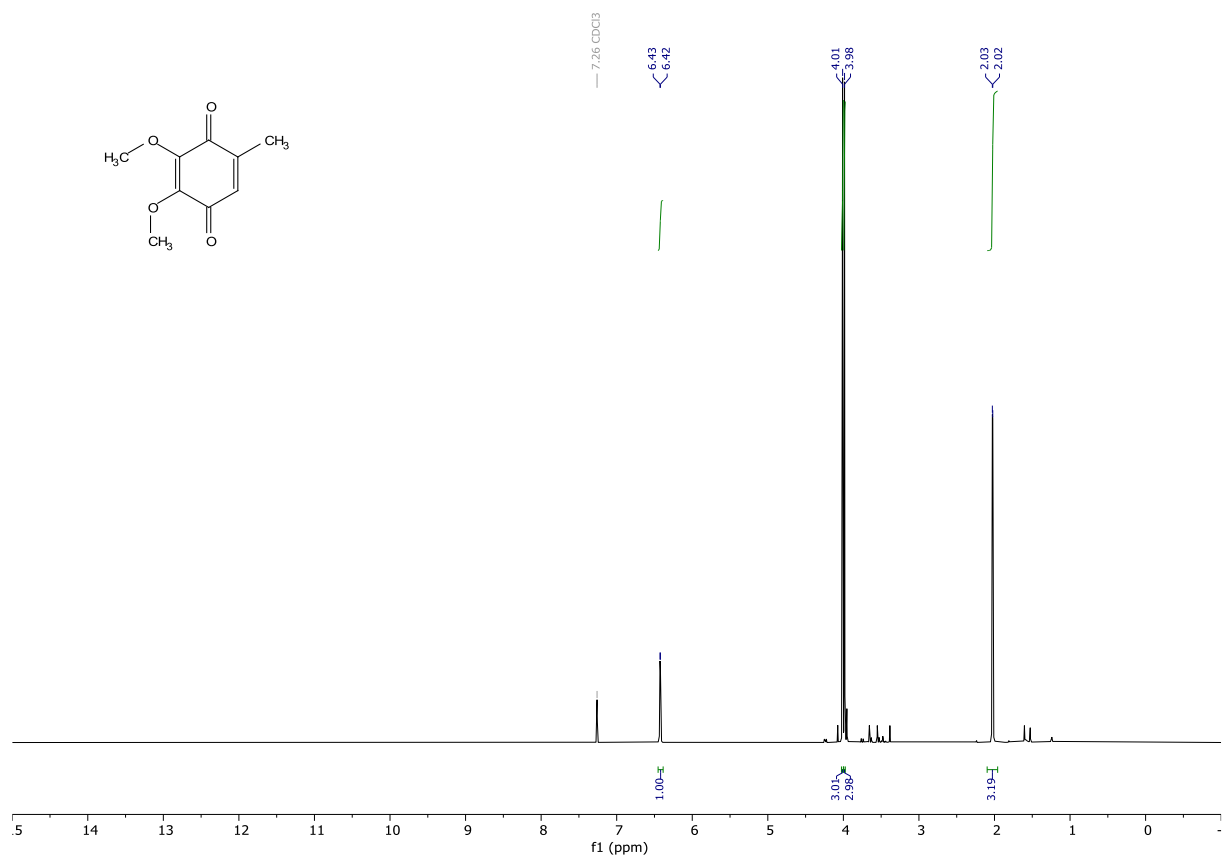


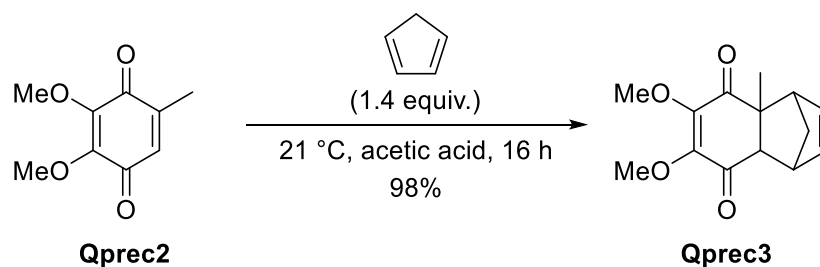
2,3,4-trimethoxy-6-methylbenzaldehyde (Qprec1). To a stirred solution of 3,4,5-trimethoxytoluene (10.047 g, 55.137 mol) in DMF (10 mL) POCl₃ (5.8 mL, 9.512 g, 62.036 mmol) was added dropwise over a period of 30 minutes through an addition funnel at 45 °C. Then the reaction mixture was warmed to 80 °C and stirred for 1.5 h. The mixture was cooled to 21 °C using an ice bath. Then the mixture was poured onto approximately 100 mL of wet ice. The pH was adjusted to ≈ 7 using aq. NaOH (ca. 100 mL 2 M NaOH). A mixture of ethyl acetate and dichloromethane was added to this solution. The layers were separated, and the aqueous phase was extracted with a mixture of ethyl acetate and dichloromethane. The combined organic phases were washed with brine (3x), dried over MgSO₄, filtered, and concentrated under reduced pressure. The title compound was obtained in 93% yield (10.832 g, 51.525 mmol) as yellowish solid. **¹H NMR** (300 MHz, CDCl₃) δ 10.40 (d, J = 0.6 Hz, 1H), 6.50 (s, 1H), 3.97 (s, 3H), 3.91 (s, 3H), 3.85 (s, 3H), 2.56 (d, J = 0.7 Hz, 3H). **¹³C NMR** (75 MHz, CDCl₃) δ 191.17, 158.45, 157.77, 139.78, 138.24, 121.44, 110.51, 62.48, 61.09, 56.13, 21.89. **HRMS** (ESI) calculated for [M+H]⁺ 211.0965, found 211.0959.



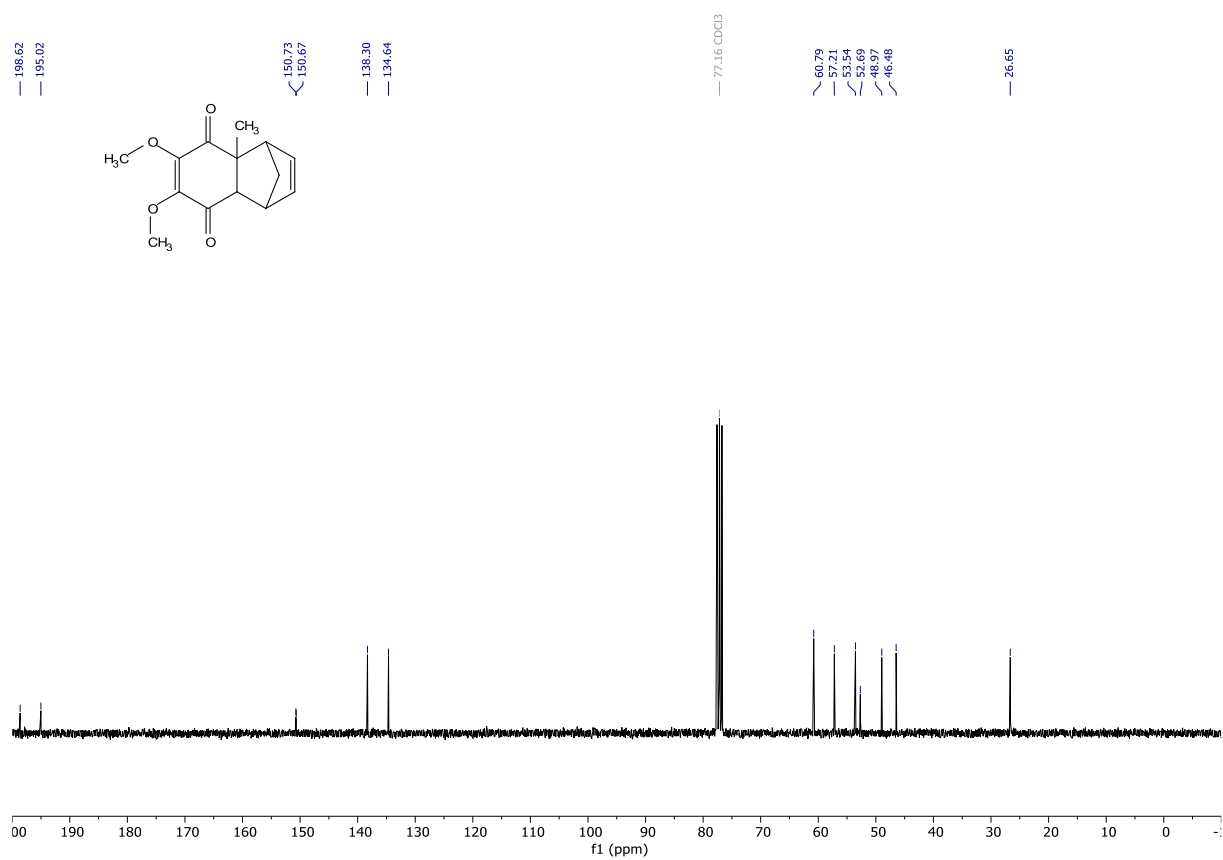
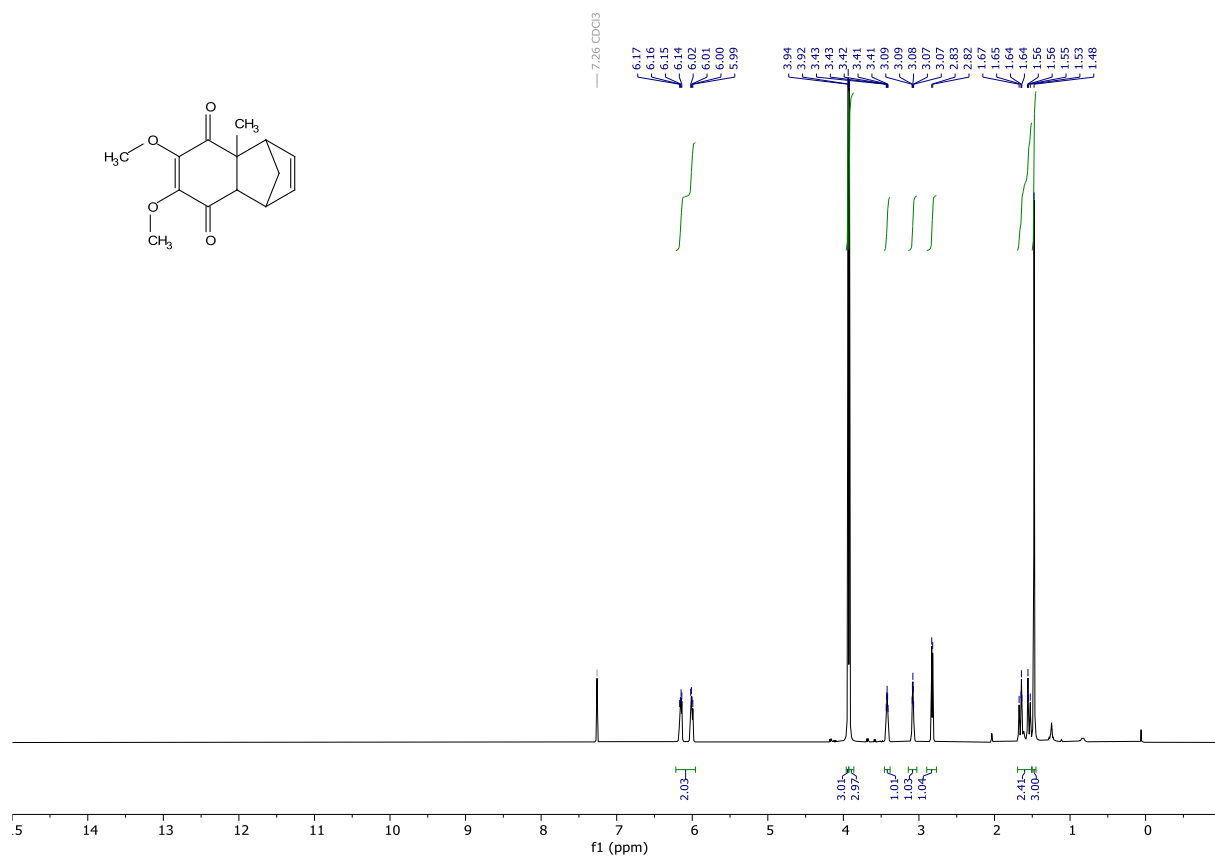


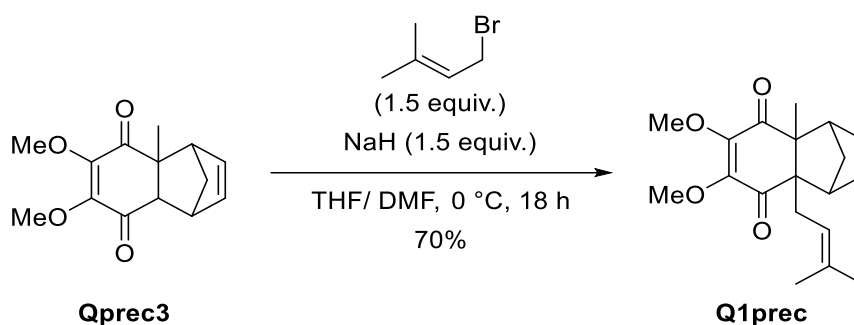
2,3-dimethoxy-5-methylcyclohexa-2,5-diene-1,4-dione (Qprec2). To a stirred solution of 2,3,4-trimethoxy-6-methylbenzaldehyde (Qprec1) (1.0000 g, 4.7567 mmol) and *p*-TsOH monohydrate (0.4520 g, 2.3762 mmol) in methanol (5 mL) at 30 °C hydrogen peroxide (30% in water, 0.6 mL, 6.4603 mmol) was added slowly. After stirring for 2 h at 30 °C to the orange mixture sodium dichromate (0.3931 g, 1.3188 mmol) was added. This immediately led to the formation of a greenish-black solution. The mixture was stirred for 1 h at room temperature and its colour changed to brown. Petrol ether (bp 50-70 °C) was added, the layers separated, which resulted in an orange-coloured organic phase. The aqueous phase was extracted with petrol ether (bp 50-70 °C). The combined organic layers were washed with brine, dried over MgSO₄, filtered, and concentrated under reduced pressure. The title compound was obtained in 63% yield (0.54240 g, 2.9773 mmol) as a red solid. The physical appearance and the spectral data were in accordance with literature values. ¹H NMR (300 MHz, CDCl₃) δ 6.42 (d, *J* = 1.6 Hz, 1H), 4.01 (s, 3H), 3.98 (s, 3H), 2.03 (d, *J* = 1.7 Hz, 3H). ¹³C NMR (75 MHz, CDCl₃) δ 184.54, 184.31, 145.15, 144.96, 144.17, 131.41, 61.38, 61.31, 15.59. HRMS (ESI) calculated for [M+H]⁺ 183.0652, found 183.0650.



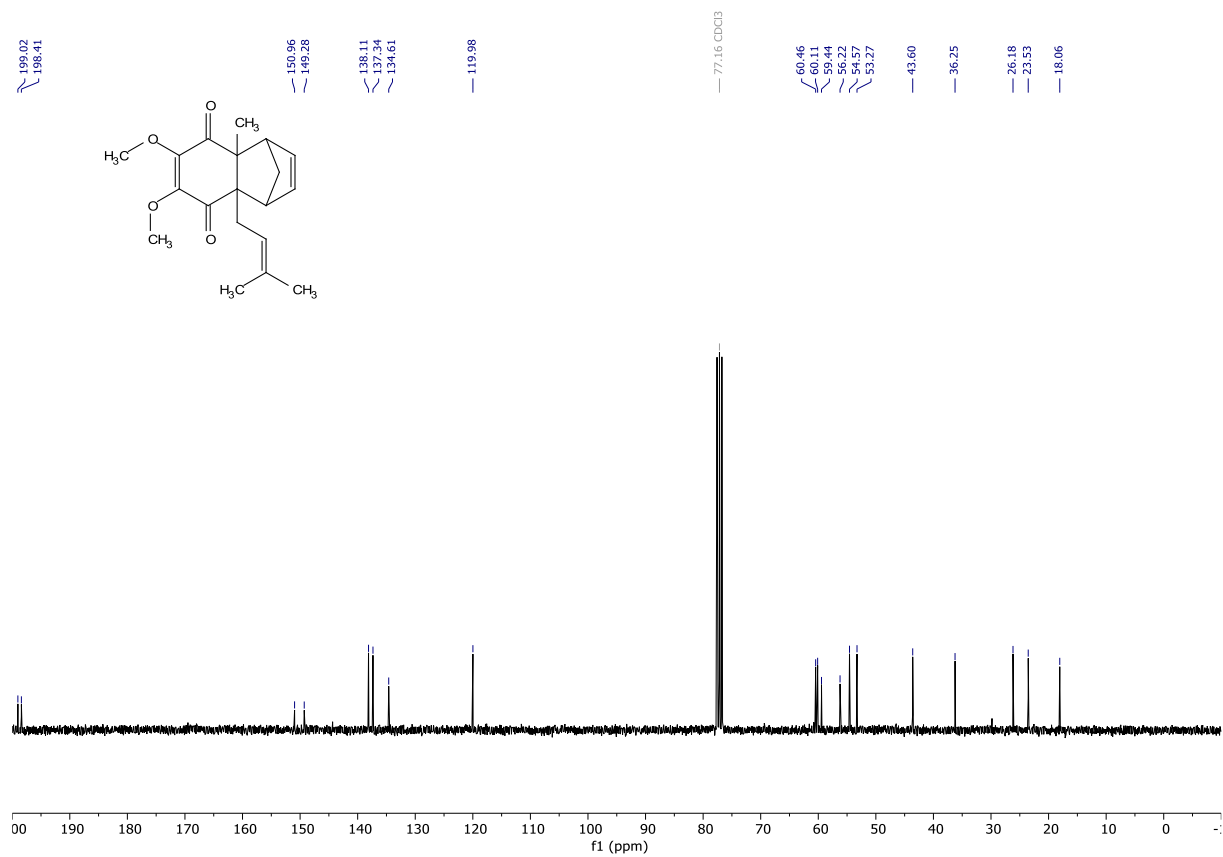
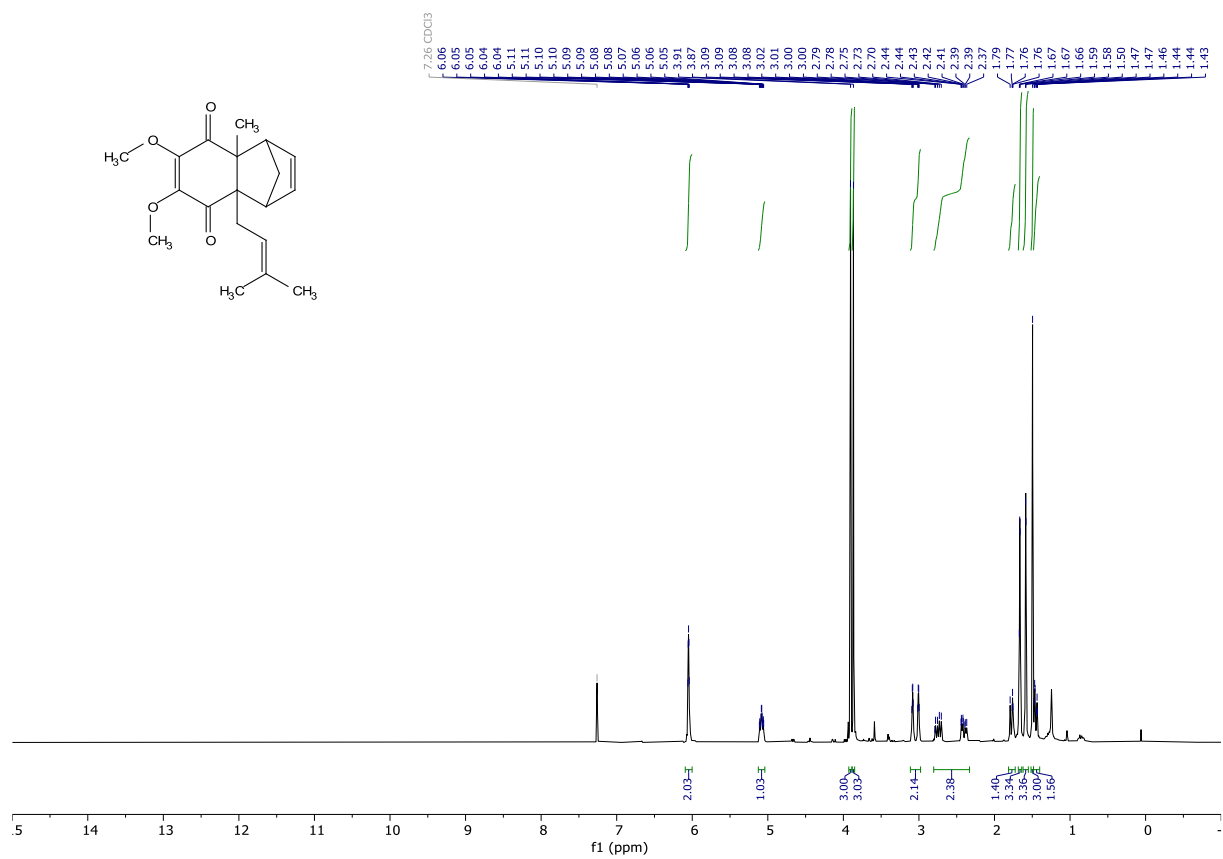


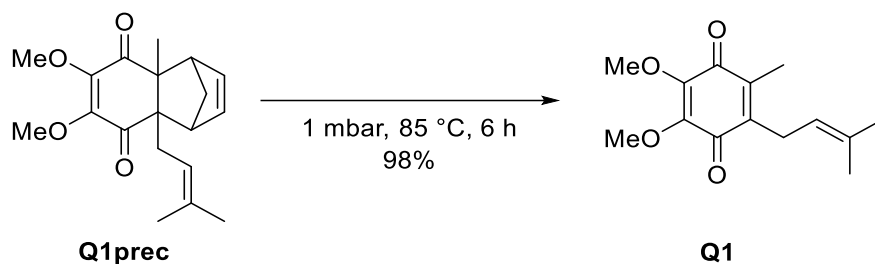
6,7-dimethoxy-4a-methyl-1,4,4a,8a-tetrahydro-1,4-methanonaphthalene-5,8-dione (Qprec3). To a stirred solution of dimethoxy benzoquinone (Qprec2) (3.34458 g, 18.3592 mmol) in acetic acid (8 mL) freshly distilled cyclopentadiene (2.2 mL, 1.76 g, 26.6251 mmol) was added and the red mixture was stirred under an argon atmosphere at 21 °C for 16 h. The red colour slowly changed into a faint orange. After 16 h of reaction time, the mixture was concentrated under reduced pressure, then taken up in dichloromethane and concentrated onto silica gel. The crude was purified by flash column chromatography (cyclohexane/ ethyl acetate gradient from 1:0 to 7:3). The title compound was obtained in 98% yield (4.45771 g, 17.9540 mmol) as a yellow oil. The physical appearance and the spectral data were in accordance with literature values. ¹H NMR (300 MHz, CDCl₃) δ 6.08 (ddd, *J* = 43.7, 5.7, 2.9 Hz, 2H), 3.94 (s, 3H), 3.92 (s, 3H), 3.42 (p, *J* = 1.6 Hz, 1H), 3.14 – 3.03 (m, 1H), 2.82 (d, *J* = 3.9 Hz, 1H), 1.69 – 1.51 (m, 2H), 1.48 (s, 3H). ¹³C NMR (75 MHz, CDCl₃) δ 198.62, 195.02, 150.73, 150.67, 138.30, 134.64, 60.79 (2 C), 57.21, 53.54, 52.69, 48.97, 46.48, 26.65. HRMS (ESI) calculated for [M+Na]⁺ 271.0941, found 271.0935.



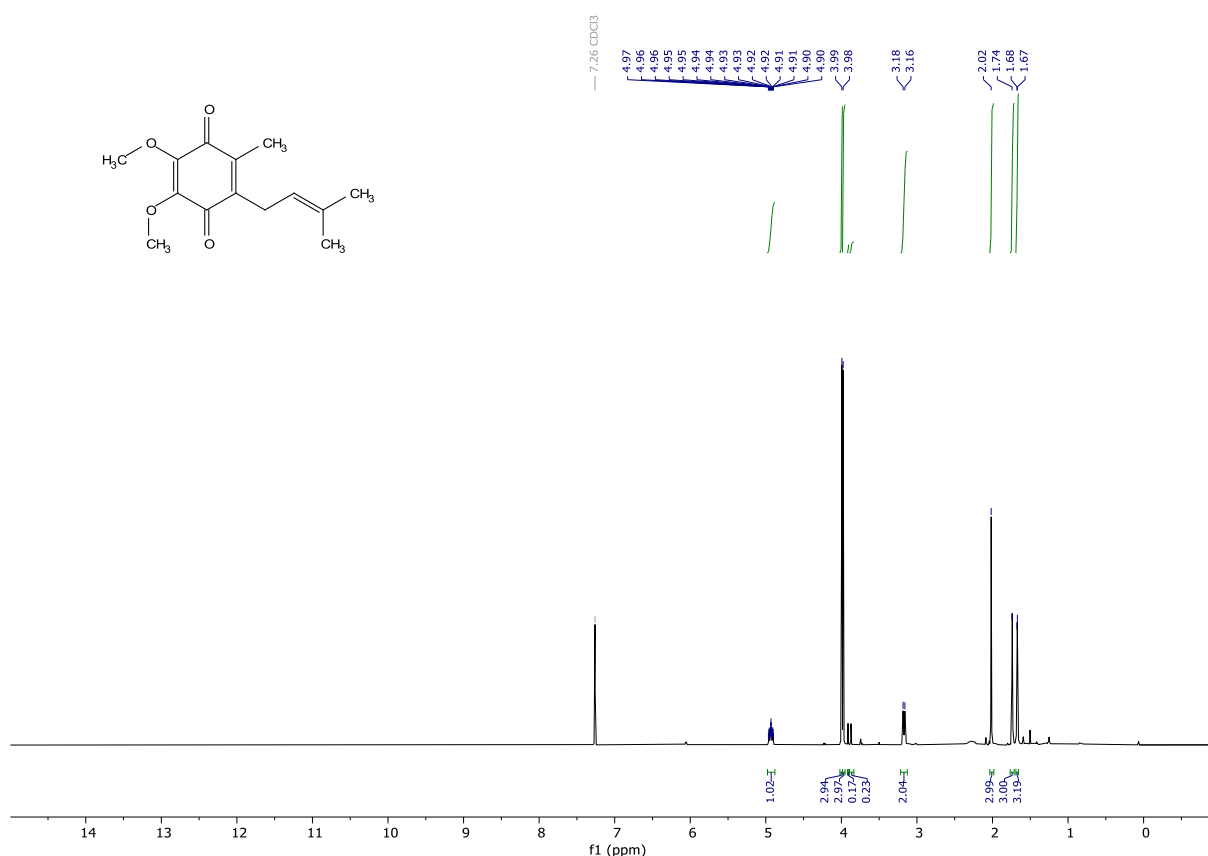


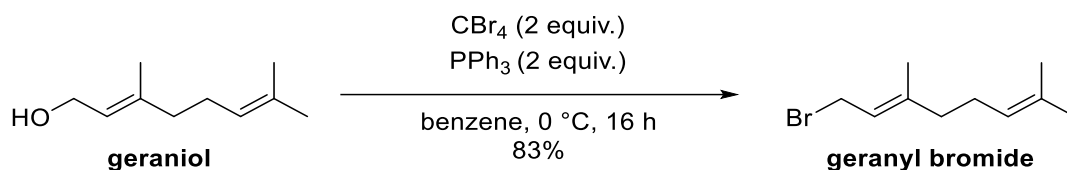
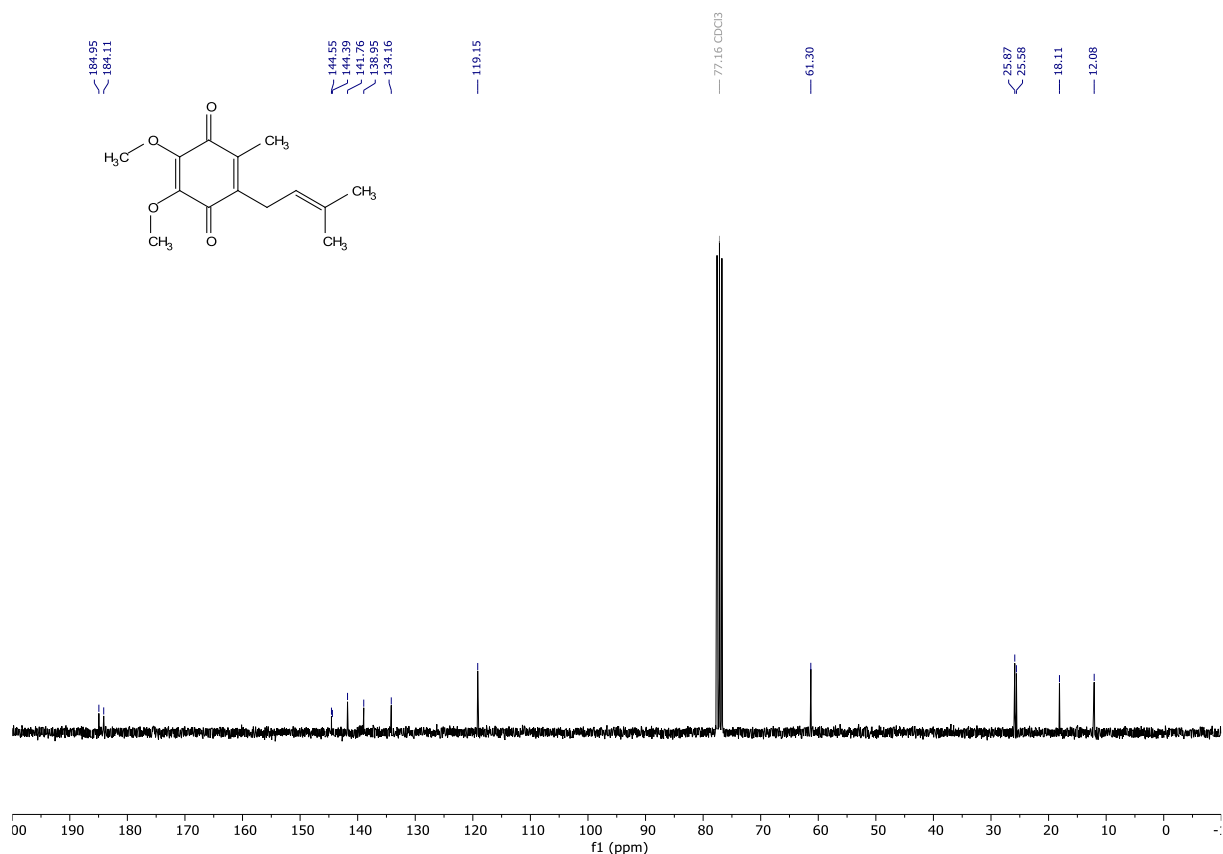
6,7-dimethoxy-4a-methyl-8a-(3-methylbut-2-en-1-yl)-1,4,4a,8a-tetrahydro-1,4-ethanonaphthalene-5,8-dione (Q1prec). To a stirred solution of 6,7-dimethoxy-4a-methyl-1,4,4a,8a-tetrahydro-1,4-methanonaphthalene-5,8-dione (Qprec3) (0.2638 g, 1.0625 mmol) in dry THF (2 mL) at 0 °C NaH (60% dispersion in paraffin, 0.0498 g, 2.0759 mmol) was added. The mixture was stirred for 60 minutes at 0 °C giving a brown slurry. After 1 h stirring at 0 °C, 1-bromo-3-methyl-2-butene (1.0 mL, 1.29 g, 8.6559 mmol) was added dropwise. The mixture gradually turned into a yellowish slurry. It was left stirring for 16 h at room temperature. Then DMF (2 mL) was added, and the mixture was stirred for another 1 h. The reaction was carefully quenched with water. The aqueous phase was extracted with ethyl acetate. The combined organic layers were dried over MgSO_4 , filtered, and concentrated under reduced pressure. The crude was taken up in dichloromethane and concentrated onto silica gel. The crude was purified by flash column chromatography (cyclohexane/ ethyl acetate gradient from 1:0 to 3:2). The title compound was obtained in 70% yield (0.23552 g, 0.7444 mmol) as yellow oil. **^1H NMR** (300 MHz, CDCl_3) δ 6.05 (dt, J = 2.6, 1.2 Hz, 2H), 5.08 (tdd, J = 6.3, 2.9, 1.4 Hz, 1H), 3.91 (s, 3H), 3.87 (s, 3H), 3.05 (dq, J = 23.6, 1.8 Hz, 2H), 2.80 – 2.33 (m, 2H), 1.81 – 1.73 (m, 1H), 1.67 (s, 3H), 1.58 (s, 3H), 1.50 (s, 3H), 1.48 – 1.40 (m, 2H). **^{13}C NMR** (75 MHz, CDCl_3) δ 199.02, 198.41, 150.96, 149.28, 138.11, 137.34, 134.61, 119.98, 60.46, 60.11, 59.44, 56.22, 54.57, 53.27, 43.60, 36.25, 26.18, 23.53, 18.06. **HRMS** (ESI) calculated for $[\text{M}+\text{H}]^+$ 317.1747, found 317.1750.



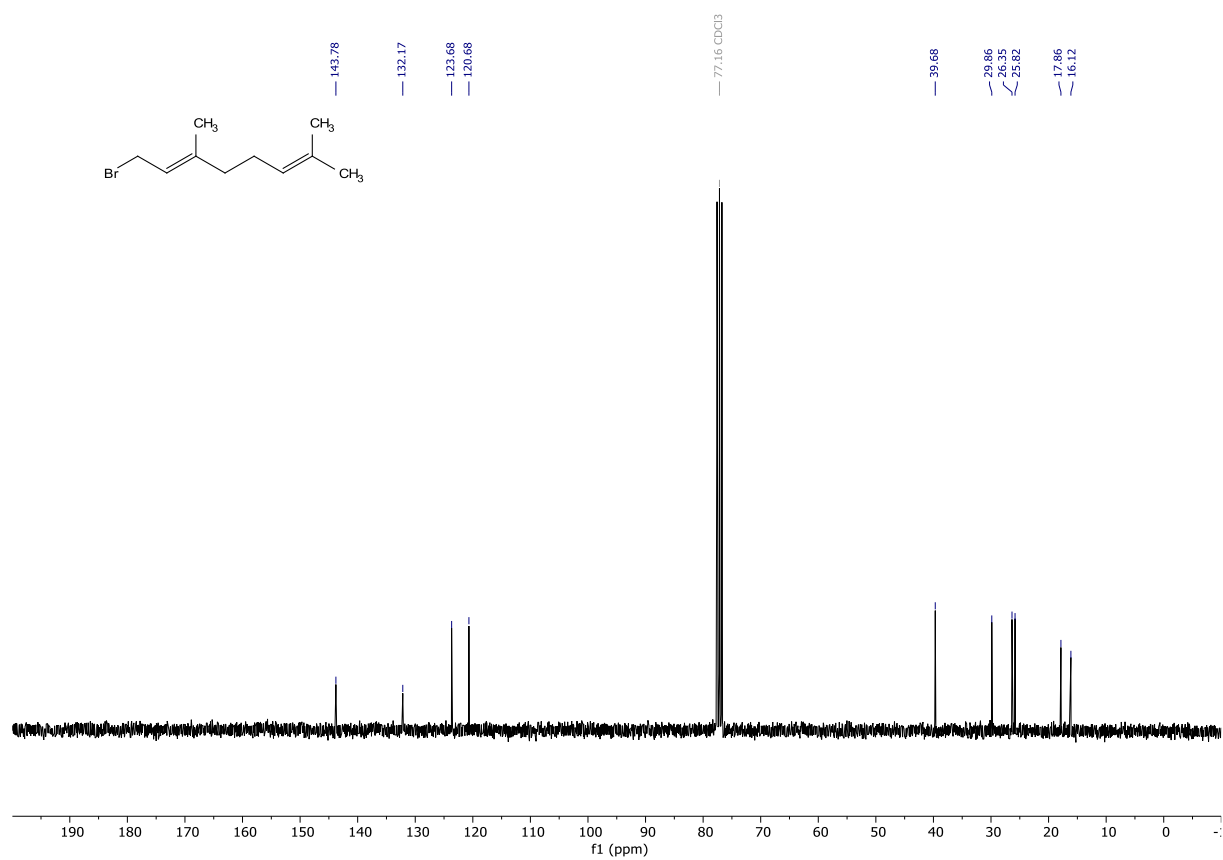
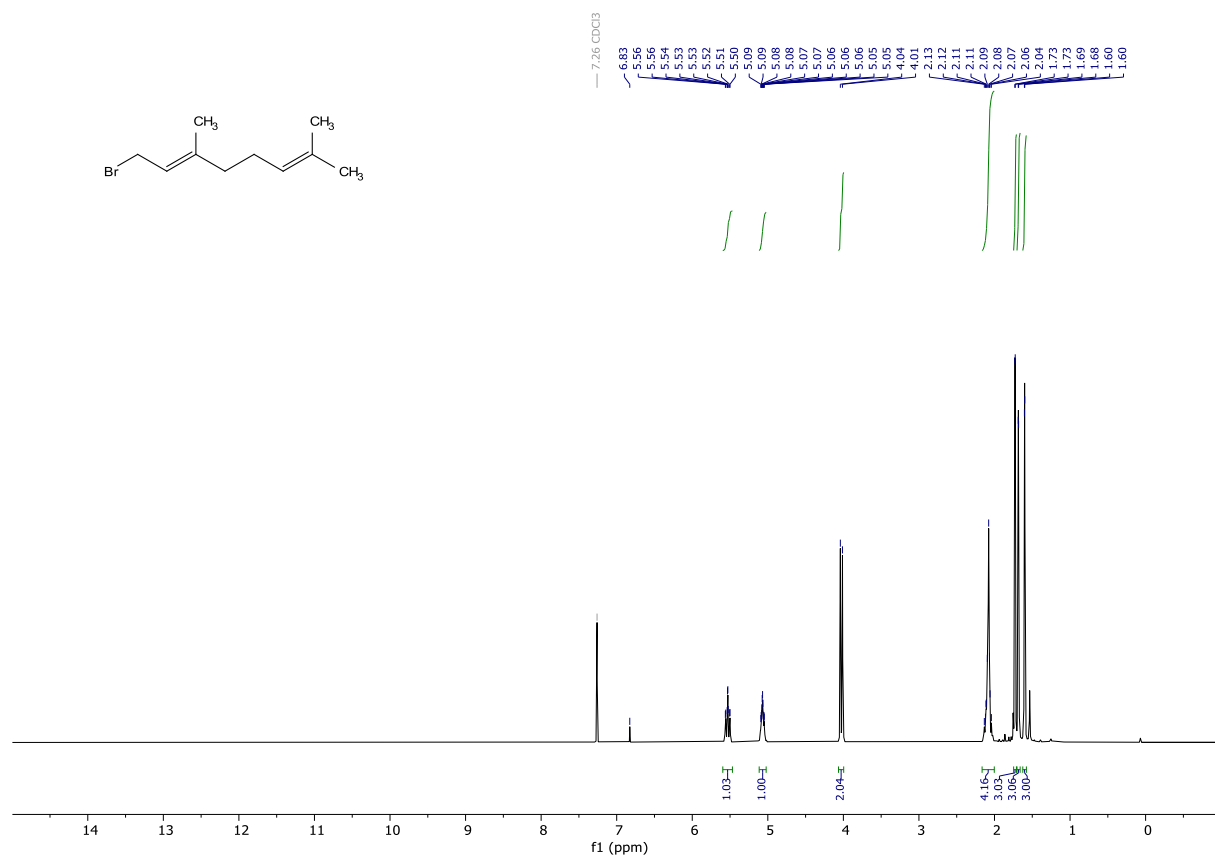


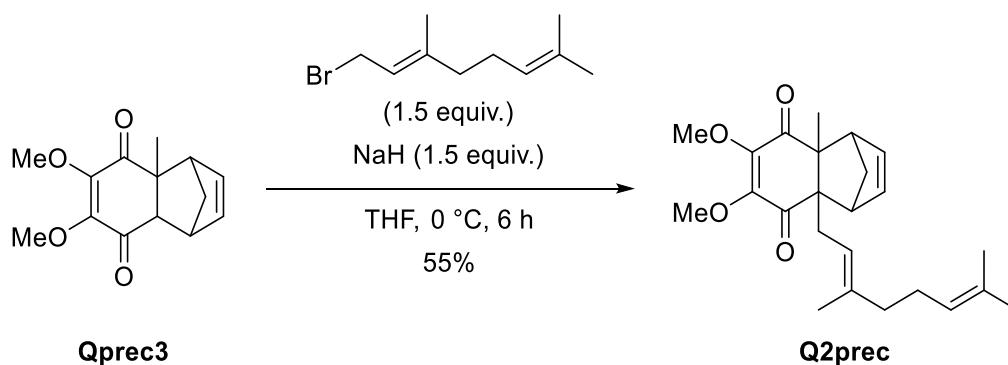
2,3-dimethoxy-5-methyl-6-(3-methylbut-2-en-1-yl)cyclohexa-2,5-diene-1,4-dione (Q1). 6,7-dimethoxy-4a-methyl-8a-(3-methylbut-2-en-1-yl)-1,4,4a,8a-tetrahydro-1,4-methanonaphthalene-5,8-dione (0.22311 g, 0.7052 mmol) was heated to 85 °C under reduced atmosphere (~1 mbar). The mixture was protected from light with tinfoil. The orange oil gradually changed its colour to an intense red. After 6 h the compound was cooled to room temperature. The crude was purified by reverse phase flash column chromatography (C18, H₂O + 0.1% TFA/ MeCN + 0.1% TFA gradient from 1:0 to 0:1). The title compound was obtained in 98% yield (0.17247 g, 0.6890 mmol) as a red oil. **¹H NMR** (300 MHz, CDCl₃) δ 4.93 (tp, *J* = 7.1, 1.4 Hz, 1H), 3.99 (s, 3H), 3.98 (s, 3H), 3.17 (d, *J* = 7.1 Hz, 2H), 2.02 (s, 3H), 1.74 (s, 3H), 1.67 (d, *J* = 1.4 Hz, 3H). **¹³C NMR** (75 MHz, CDCl₃) δ 184.95, 184.11, 144.55, 144.39, 141.76, 138.95, 134.16, 119.15, 61.30, 25.87, 25.58, 18.11, 12.08. **HRMS** (ESI) calculated for [M+H]⁺ 251.1278, found 251.1287. **Purity (HPLC):** 93% (at 214 nm), 96% (at 254 nm).



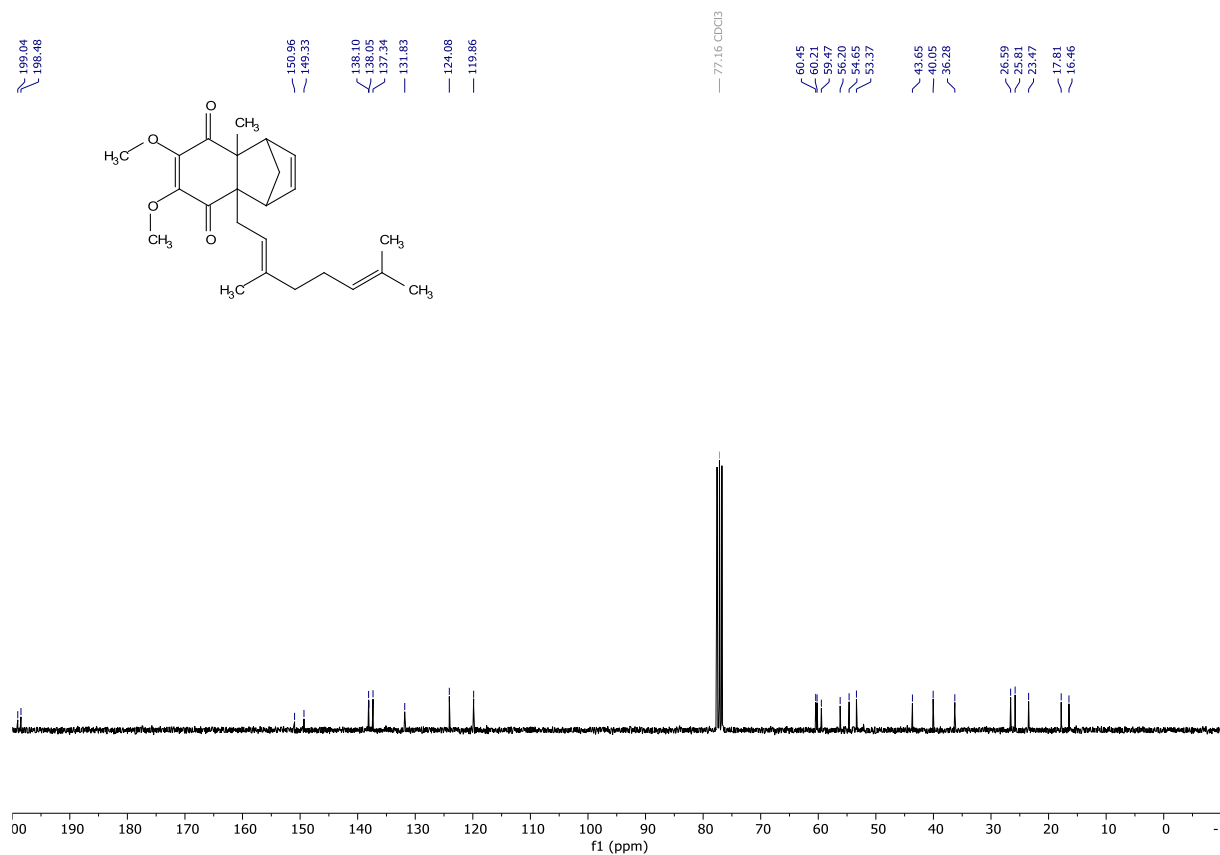
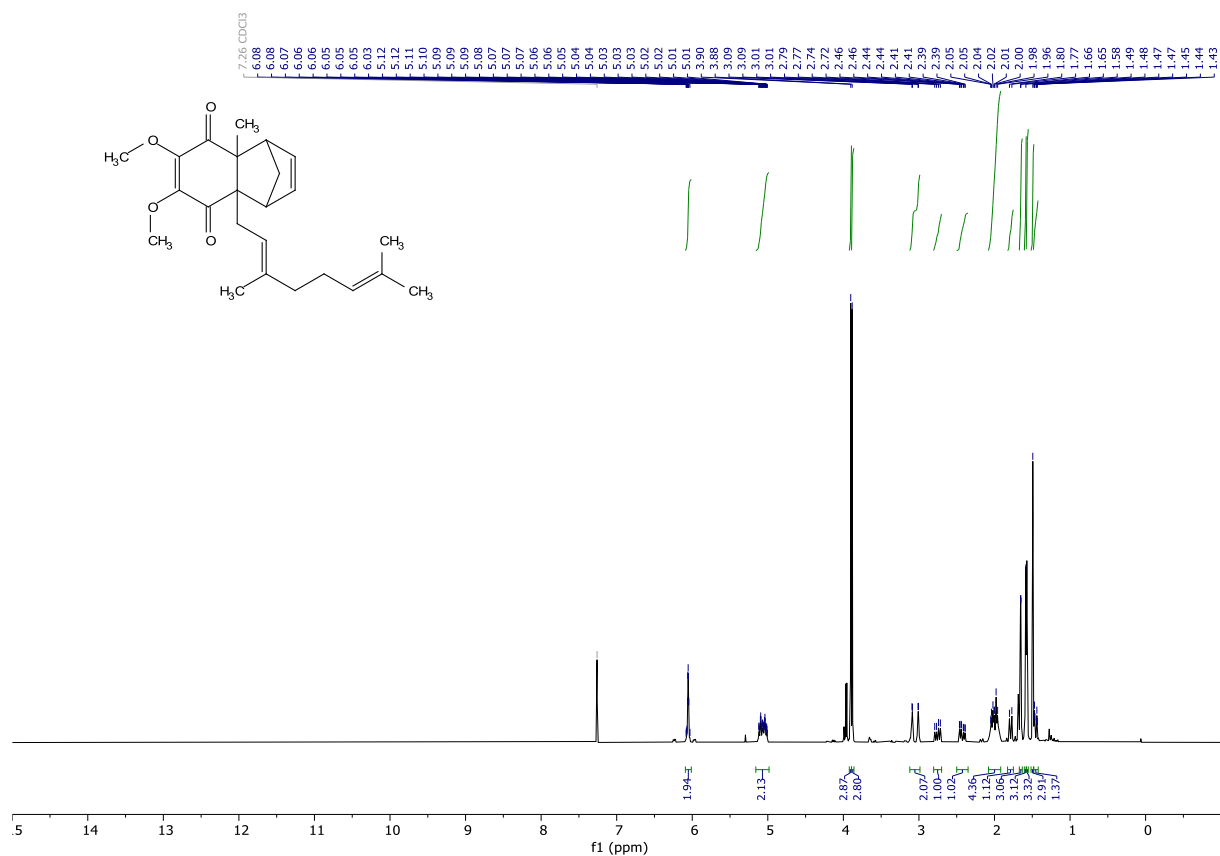


(E)-1-bromo-3,7-dimethylocta-2,6-diene (geranyl bromide). To a stirred solution of geraniol (2.501 g, 16.2136 mmol) and tetrabromomethane (10.818 g, 32.6027 mmol) in benzene (50 mL) at 0 °C triphenylphosphine (8.533 g, 32.5327 mmol) was added in portions. The mixture was stirred at 0 °C. It was stirred for another 16 h while slowly warming to 20 °C. To the mixture was added petrolether (bp 50-70 °C). This led to a brown solid. This solid was filtered off, and the filtrate was concentrated under reduced pressure. To the resulting clear colourless liquid residue petrolether (bp 50-70 °C) was added. This led to a lot of white precipitate. This mixture was filtered through a pad of celite. The filtrate was concentrated under reduced pressure. The crude was distilled twice in a Kugelrohr apparatus at ~1mbar and 120 °C. The title compound was obtained in 83% yield (2.93063 g, 13.4959 mmol) of a clear colourless low viscosity oil. ¹H NMR (300 MHz, CDCl₃) δ 5.60 – 5.47 (m, 1H), 5.09 – 5.05 (m, 1H), 4.03 (d, *J* = 8.4 Hz, 2H), 2.16 – 2.00 (m, 4H), 1.73 (d, *J* = 1.4 Hz, 3H), 1.68 (s, 3H), 1.60 (s, 3H). ¹³C NMR (75 MHz, CDCl₃) δ 143.78, 132.17, 123.68, 120.68, 39.68, 29.86, 26.35, 25.82, 17.86, 16.12. HRMS (ESI, EI) Ionisation of the compound was not achieved with the instrumentation and methods used.

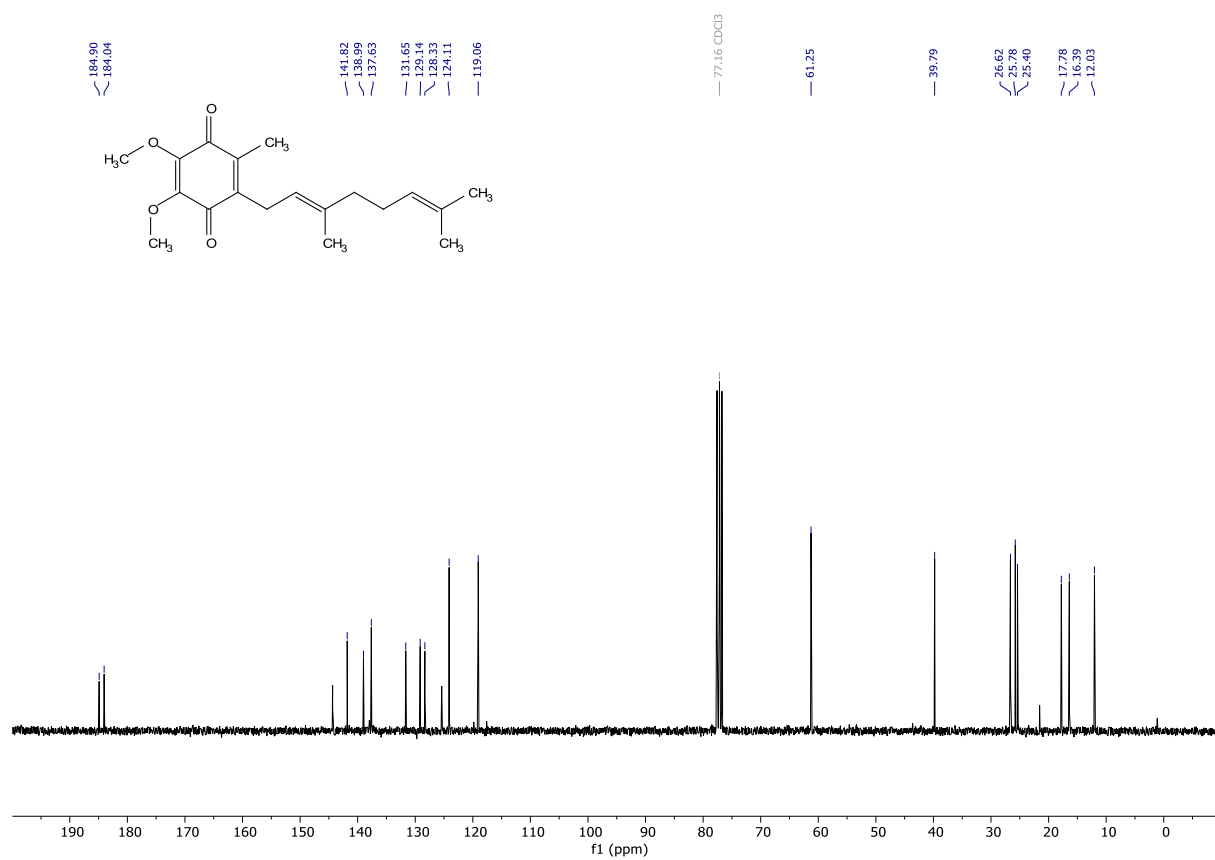
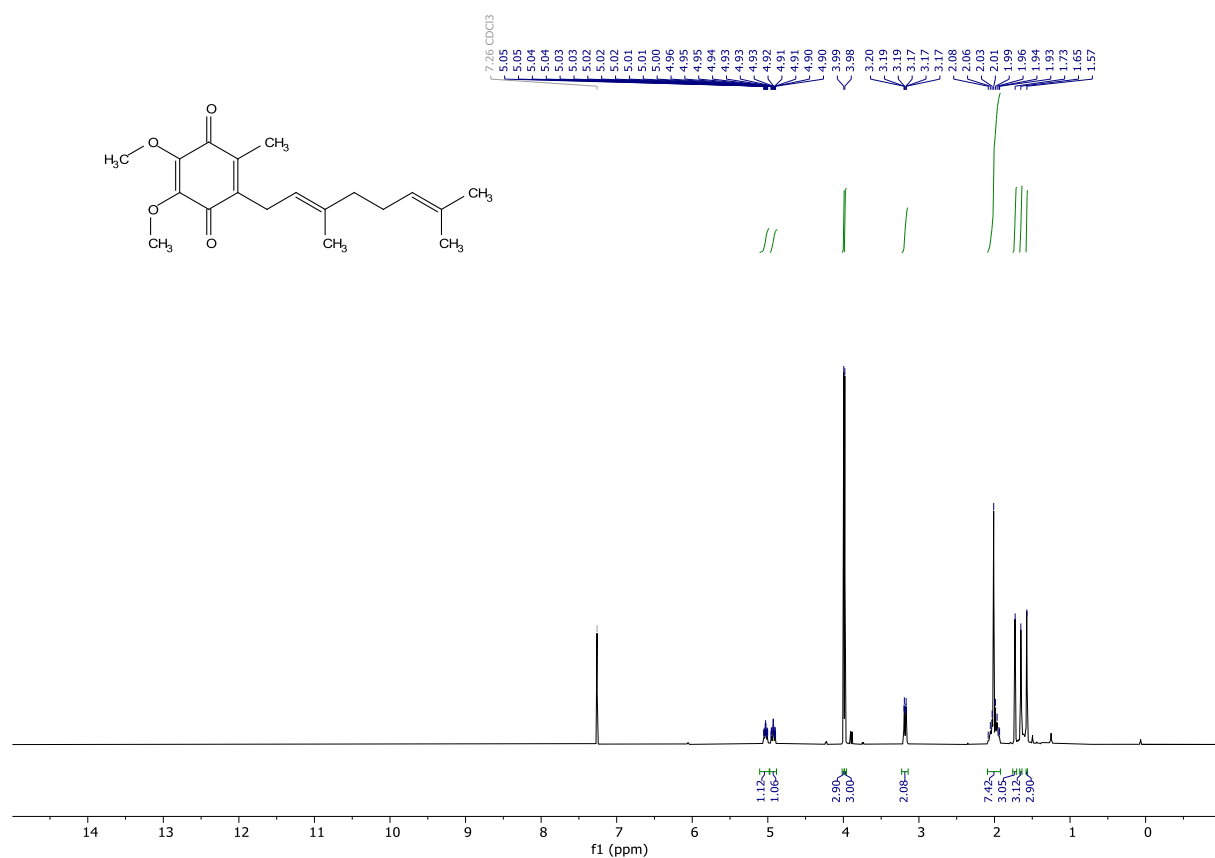


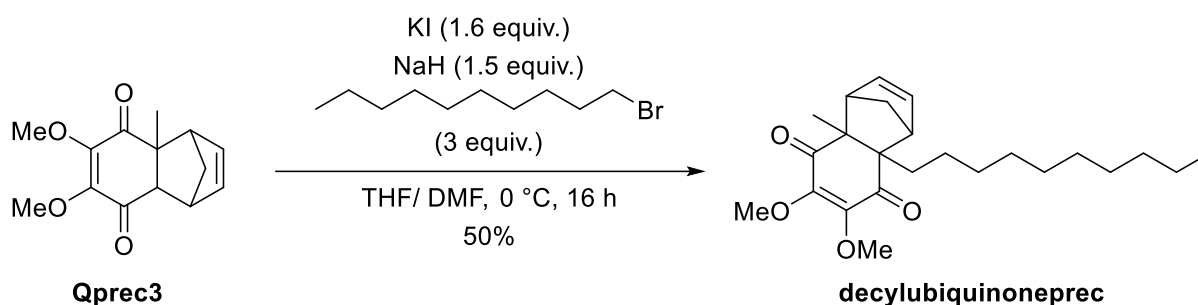


(E)-4a-(3,7-dimethylocta-2,6-dien-1-yl)-6,7-dimethoxy-8a-methyl-1,4,4a,8a-tetrahydro-1,4-methanonaphthalene-5,8-dione (Q2prec). To a stirred solution of 6,7-dimethoxy-4a-methyl-1,4,4a,8a-tetrahydro-1,4-methanonaphthalene-5,8-dione (Qprec3) (1.0099 g, 4.0676 mmol) in dry THF (5 mL) at 0 °C NaH (60% dispersion in paraffin, 0.290 g, 7.2530 mmol) was added. The mixture was stirred for 30 minutes at 0 °C, resulting in a white suspension. To this was added (*E*)-1-bromo-3,7-dimethylocta-2,6-diene (1.497 g, 6.8939 mmol) and DMF (1 mL). The mixture was slowly warmed to 21 °C and stirred for 16 h. The yellow solution was carefully quenched with water. The aqueous phase was extracted with ethyl acetate. The combined organic layers were washed with brine, dried over MgSO₄, filtered, and concentrated under reduced pressure to give a brown oil. The oil was taken up in dichloromethane and concentrated onto silica gel. The crude was purified by flash column chromatography (cyclohexane/ ethyl acetate gradient from 1:0 to 1:1). The title compound was obtained in 55% yield (0.85634 g, 2.2271 mmol) as orange oil. ¹H NMR (300 MHz, CDCl₃) δ 6.08 – 6.03 (m, 2H), 5.12 – 5.01 (m, 2H), 3.90 (s, 3H), 3.88 (s, 3H), 3.05 (dd, *J* = 23.9, 1.7 Hz, 2H), 2.75 (dd, *J* = 15.2, 7.3 Hz, 1H), 2.43 (dd, *J* = 14.5, 5.8 Hz, 1H), 2.05 – 1.96 (m, 4H), 1.79 (d, *J* = 9.4 Hz, 1H), 1.65 (s, 3H), 1.58 (s, 3H), 1.60 – 1.54 (m, 3H), 1.49 (s, 3H), 1.46 (dt, *J* = 9.5, 1.7 Hz, 1H). ¹³C NMR (75 MHz, CDCl₃) δ 199.04, 198.48, 150.96, 149.33, 138.10, 138.05, 137.34, 131.83, 124.08, 119.86, 60.45, 60.21, 59.47, 56.20, 54.65, 53.37, 43.65, 40.05, 36.28, 26.59, 25.81, 23.47, 17.81, 16.46. HRMS (ESI) calculated for [M+Na]⁺ 407.2193, found 407.2198.



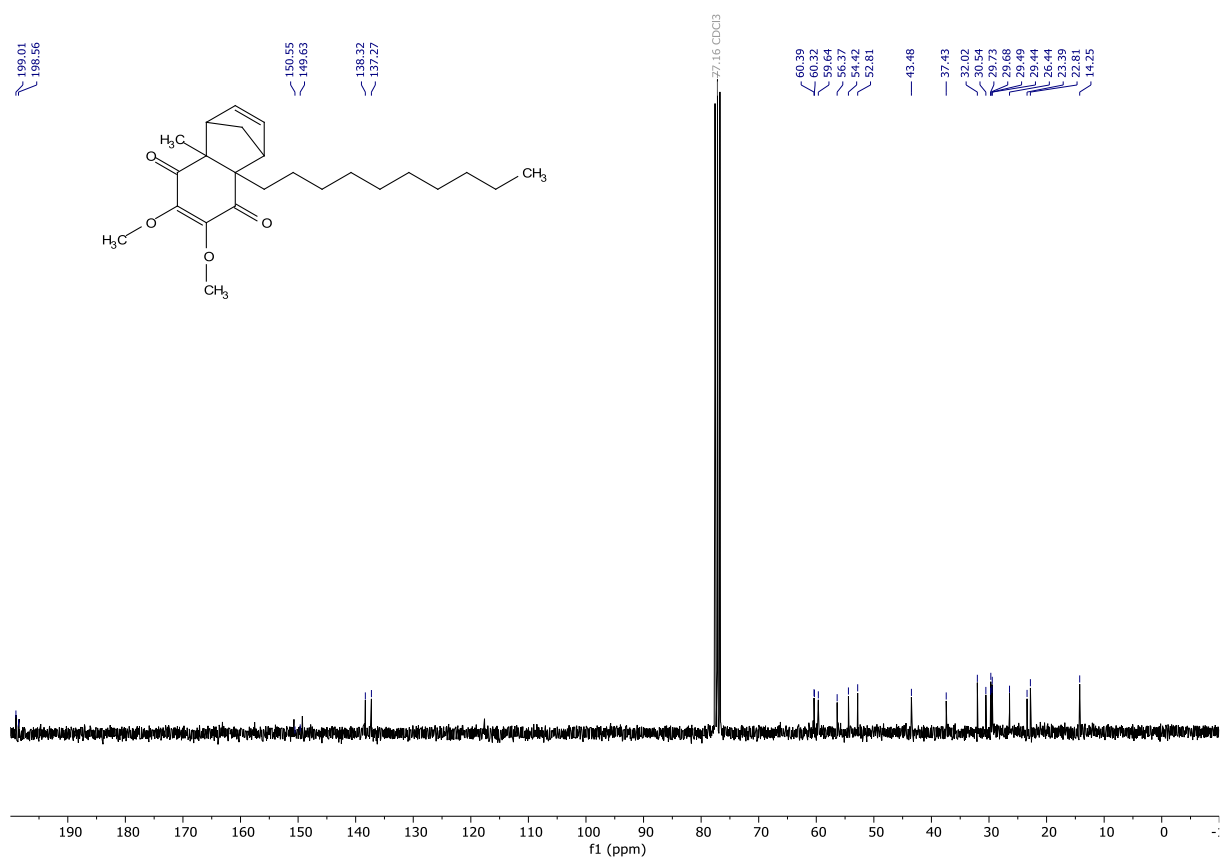
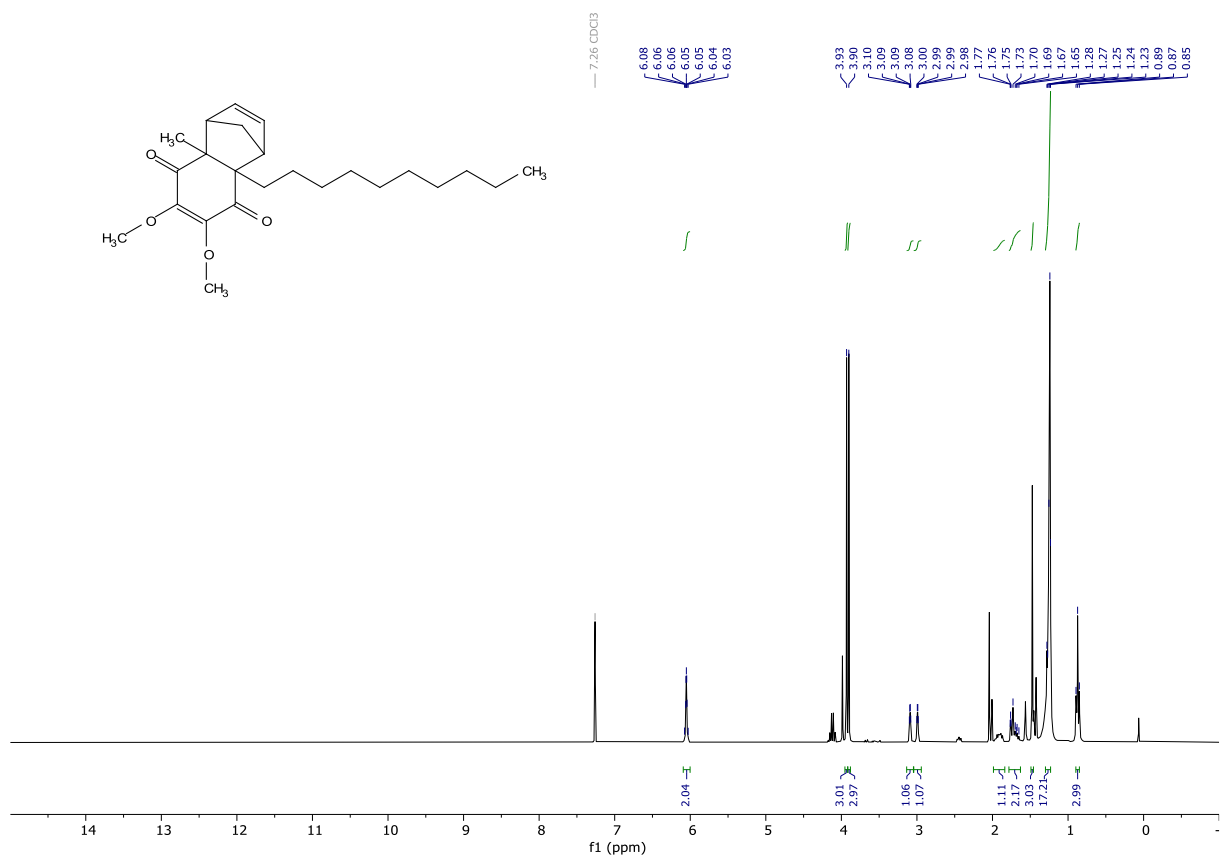
393

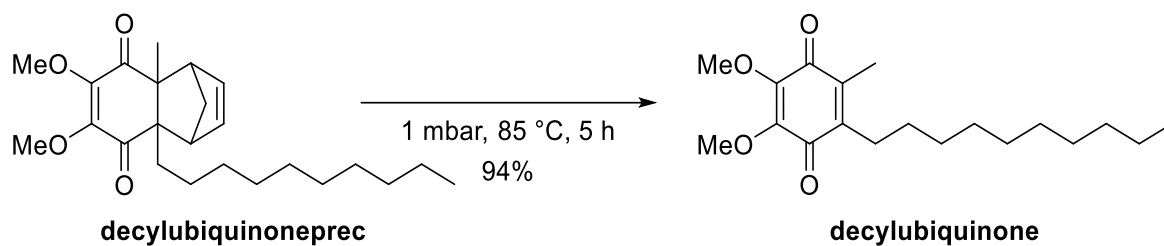




4a-decyl-6,7-dimethoxy-8a-methyl-1,4,4a,8a-tetrahydro-1,4-methanonaphthalene-5,8-dione

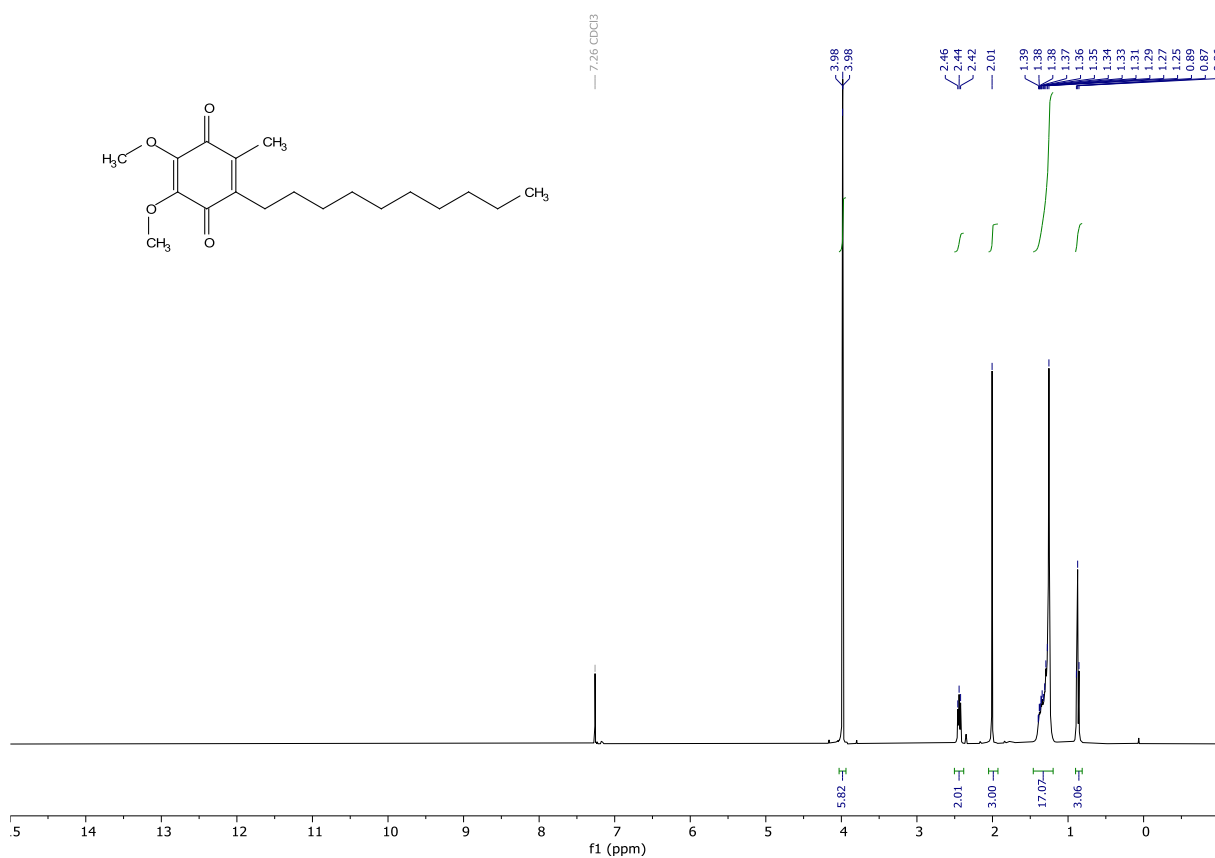
(decylubiquinoneprec). To a stirred solution of 6,7-dimethoxy-4a-methyl-1,4,4a,8a-tetrahydro-1,4-methanonaphthalene-5,8-dione (Qprec3) (1.17549 g, 4.7346 mmol) in dry THF (2.5 mL) at 0 °C NaH (60% dispersion in paraffin, 0.250 g, 6.4277 mmol) was added. The mixture was stirred for 45 minutes at 0 °C, giving a brown slurry. To this was added 1-bromodecane (2 mL, 2.132 g, 9.6391 mmol) and a solution of KI (0.250 g, 1.5058 mmol) in dry DMF (2.5 mL). The mixture was stirred at 0 °C for 15 minutes, after which it was slowly warmed to 21 °C. Then additional KI (0.86345 g, 5.2008 mmol) was added, and the mixture was stirred for another 15 h, resulting in a brownish semi-solid mixture. To this was added a mixture of water and ethyl acetate with little $\text{Na}_2\text{S}_2\text{O}_3$. The aqueous phase was extracted with ethyl acetate, the combined organic layers were washed with brine, dried over MgSO_4 , filtered, and concentrated under reduced pressure. The mixture was taken up in dichloromethane and concentrated onto silica gel. The crude was purified by flash column chromatography (cyclohexane/ethyl acetate gradient from 1:0 to 4:1). The title compound was obtained in 50% yield (0.79448 g, 2.04455 mmol) as orange oil. $^1\text{H NMR}$ (300 MHz, CDCl_3) δ 6.08 – 6.03 (m, 2H), 3.93 (s, 3H), 3.90 (s, 3H), 3.10 – 3.08 (m, 1H), 3.00 – 2.98 (m, 1H), 1.94 – 1.87 (m, 1H), 1.77 – 1.65 (m, 2H), 1.47 (s, 3H), 1.27 – 1.23 (m, 17H), 0.90 – 0.85 (m, 3H). $^{13}\text{C NMR}$ (75 MHz, CDCl_3) δ 199.01, 198.56, 150.55, 149.63, 138.32, 137.27, 60.39, 60.32, 59.64, 56.37, 54.42, 52.81, 43.48, 37.43, 32.02, 30.54, 29.73, 29.68, 29.49, 29.44, 26.44, 23.39, 22.81, 14.25. **HRMS** (ESI) calculated for $[\text{M}+\text{H}]^+$ 389.2686, found 389.2682.

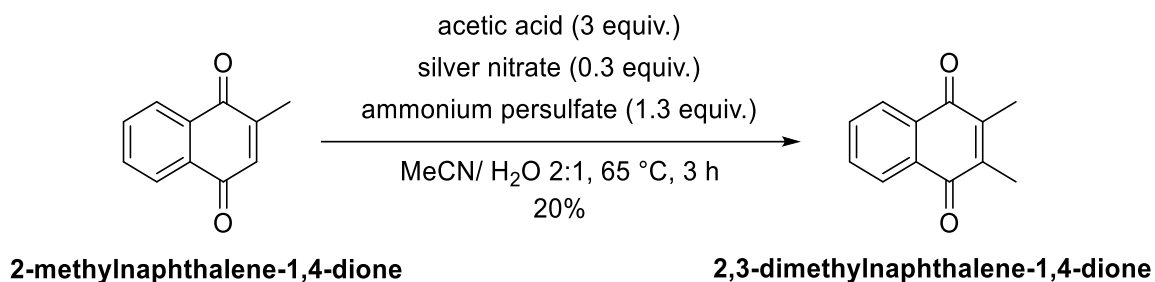
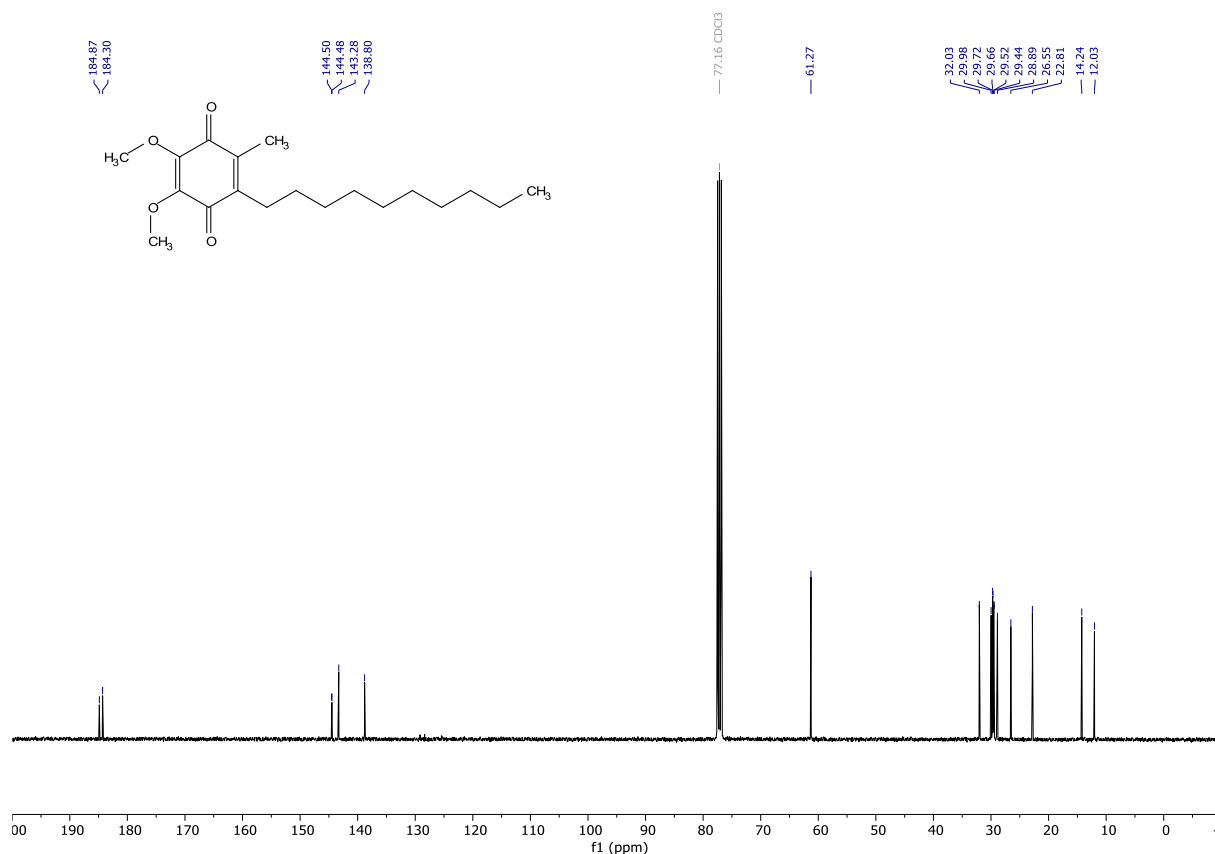




2-decyl-5,6-dimethoxy-3-methylcyclohexa-2,5-diene-1,4-dione (decylubiquinone). 4a-decyl-6,7-dimethoxy-8a-methyl-1,4,4a,8a-tetrahydro-1,4-methanonaphthalene-5,8-dione

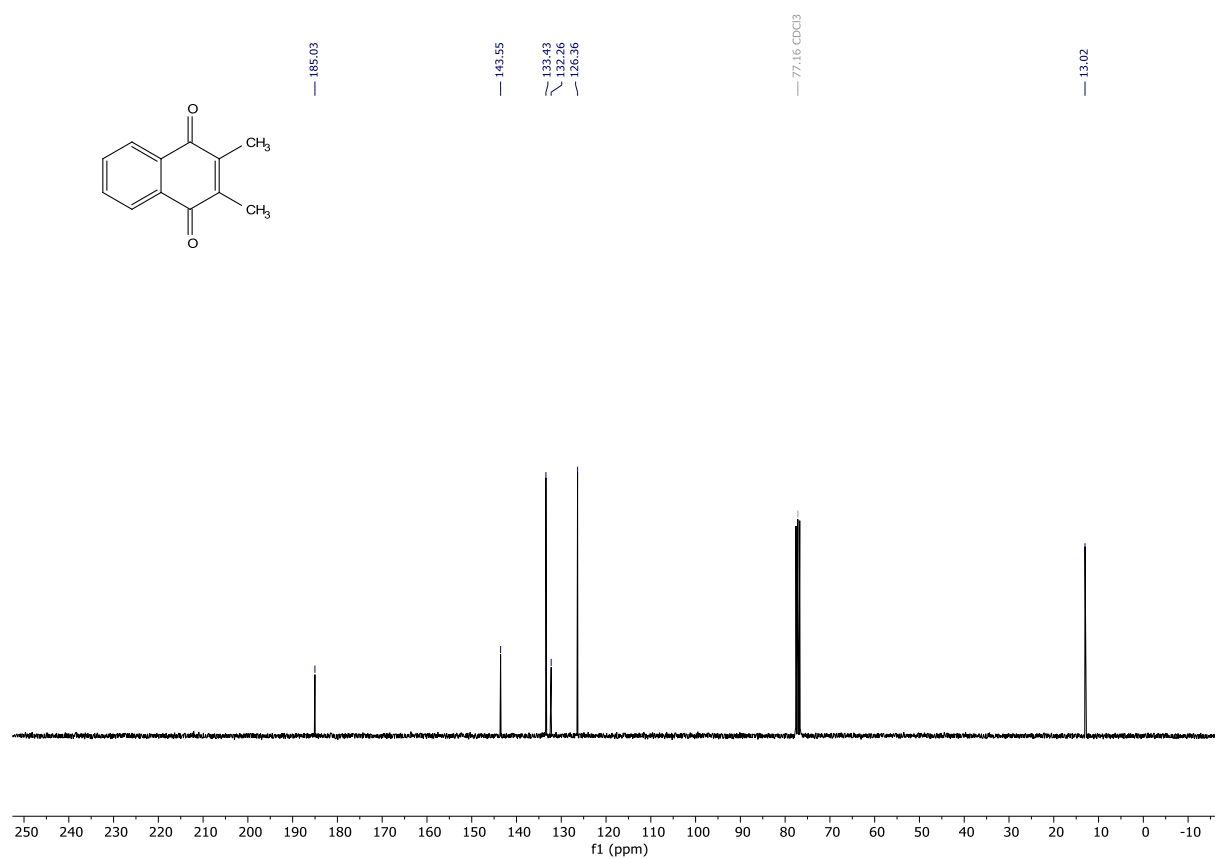
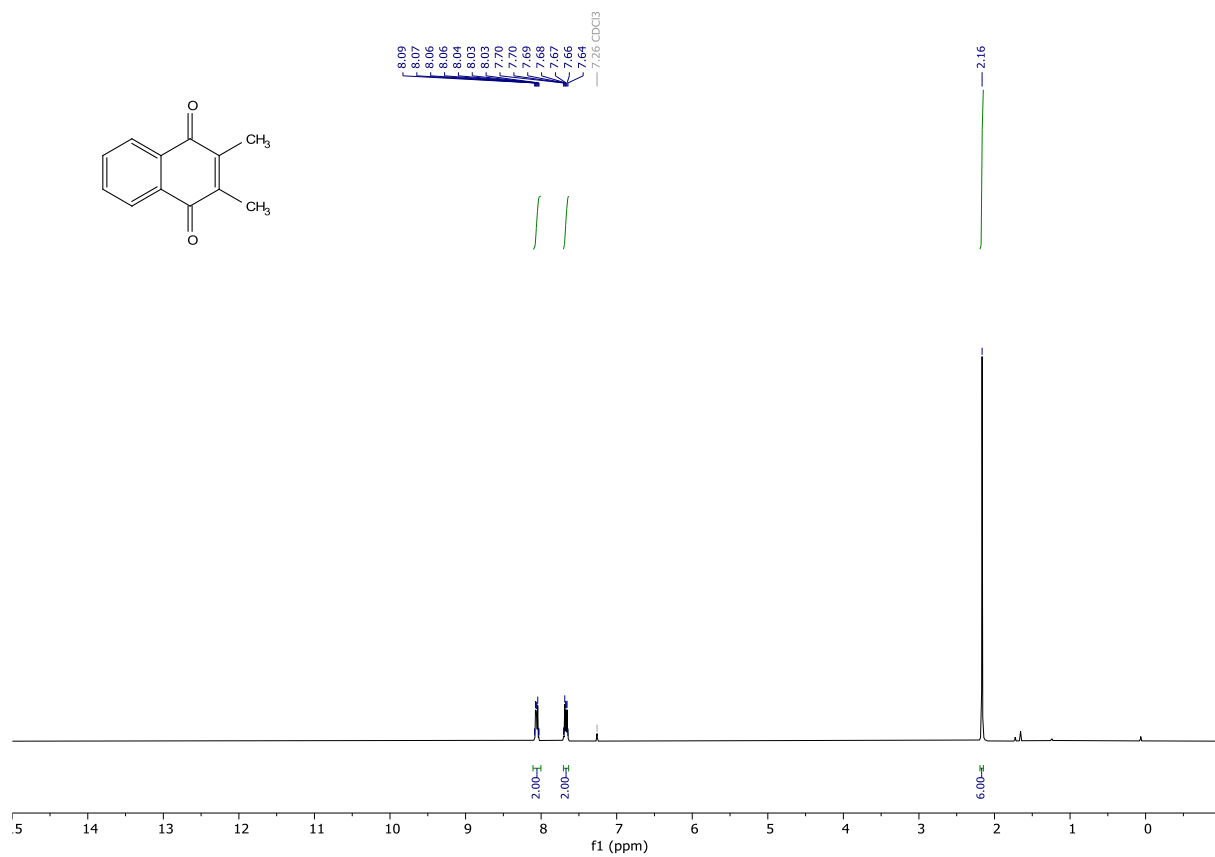
(decylubiquinoneprec) (0.28314 g, 0.7287 mmol) was heated to 85 °C at ~1 mbar atmosphere for 5 h. The mixture gradually turned dark red. The red oil was diluted with dichloromethane and concentrated onto silica gel. The crude was purified by reverse phase flash column chromatography (C18, H₂O + 0.1% TFA/ MeCN + 0.1% TFA gradient from 1:0 to 0:1). The title compound was obtained in 94% yield (0.62001 g, 1.9228 mmol) as red oil. **¹H NMR** (400 MHz, CDCl₃) δ 3.98 (m, 6H), 2.44 (t, J = 7.4 Hz, 2H), 2.01 (s, 3H), 1.39 – 1.25 (m, 16H), 0.87 (t, J = 6.8 Hz, 3H). **¹³C NMR** (101 MHz, CDCl₃) δ 184.87, 184.30, 144.50, 144.48, 143.28, 138.80, 61.27 (2C), 32.03, 29.98, 29.72, 29.66, 29.52, 29.44, 28.89, 26.55, 22.81, 14.24, 12.03. **HRMS** (ESI) calculated for [M+H]⁺ 323.2217, found 323.2211. **Purity (HPLC)**: 99% (at 214 nm), 98% (at 254 nm).





2,3-dimethylnaphthalene-1,4-dione. 2-methylnaphthalene-1,4-dione (0.99951 g, 5.8020 mmol) was dissolved in a mixture of MeCN and water (2:1, 58 mL), and to this mixture acetic acid (0.995 mL, 1.04475 g, 17.3974 mmol) was added. The mixture was heated to 65°C and silver nitrate (0.30959 g, 1.8225 mmol) was added. Over the course of 2 h a solution of ammonium persulfate (1.7325 g, 7.5927 mmol) in water (5 mL) was added dropwise. After completed addition the mixture was stirred for 1 h at 65°C. The mixture was diluted with water, cooled, and extracted with dichloromethane. The combined organic layers were washed with brine, dried over MgSO₄, filtered, and concentrated under reduced pressure onto silica gel. The crude was purified by flash column chromatography (cyclohexane/ dichloromethane gradient from 9:1 to 1:1). The title compound was obtained in 20% yield (0.21456 g, 1.1523 mmol) as yellow crystals. The physical appearance and the spectral data were in accordance with literature values. ¹H NMR (300 MHz, CDCl₃) δ 8.11 – 8.00 (m, 2H), 7.70 – 7.64 (m, 2H), 2.16 (s, 6H). ¹³C NMR (75 MHz, CDCl₃) δ 185.03 (2 C), 143.55 (2 C), 133.43 (2 C), 132.26 (2 C),

126.36 (2 C), 13.02 (2 C). **HRMS** (ESI) calculated for $[M+H]^+$ 187.0754, found 187.0753 (molecular ion peak low intensity). **Purity (HPLC)**: 98% (at 214 nm), 99% (at 254 nm).



5. Summary, conclusion, and outlook

Molecular tools for biochemists and biologists are of high importance and use. The availability of such tools is generally limited to generic derivatives. Access to highly specific tools is either expensive or requires a specialised team of chemists that can provide these tools. In this work we described the synthesis of a tool that allowed for a site specific bioorthogonal site-selective conjugation of fluorescent dyes to antibodies. Specifically, dibromopyridazinedione re-bridging compounds were synthesised and coupled with fluorescent dyes. The whole construct was then incorporated into the disulfide bridges of IgG antibodies, rendering them fluorescent whilst theoretically maintaining their ability to specifically bind their antigen. We demonstrated successful incorporation of the re-bridging compounds into various antibodies. Furthermore, we explored their activity in western blot and fluorescence microscopy applications. The developed method worked well for some antibodies whilst for others a successful labelling was observed but the modified antibodies could not detect their antigen anymore. We could not observe a pattern that allowed us to predict for which antibodies a successful modification was possible. However, this method provides a new and useful tool for quick access to fluorescently labelled antibodies starting from commercially available non-labelled antibodies. In the wake of this project a concise and efficient synthesis of a silicon-rhodamine dye was established. (See chapter 1)

Another focus of the work was the development of small molecule compounds that can stabilise the conformation of the mitochondrial aspartate glutamate carrier 2. In the ideal case, only one conformation of the carrier should be obtained which can then be subsequently analysed by cryogenic electron microscopy, to solve the structure of the carrier. The solved structure would assist to assess the effect of mutations on the structure and the function of the carrier. As the aspartate glutamate carrier 2 plays a role in cancer cell metabolism, solving the structure of the carrier would also assist in discovering new cancer remedies. In this work over 80 final compounds were synthesised and tested for their ability to lock the carrier in one specific conformation. From these compounds, the synthesised compound **PGUB81** was able to lock the carrier into a conformation that had an approximately 8.5 °C higher melting temperature compared to the native state, as found in a thermal shift assay. Employing this compound, attempts for solving the structure are ongoing. (See chapter 2)

In further work, various smaller projects were pursued to build tools that were employed in different biological applications. In the most extensive of these projects, new compounds against the parasite *echinococcus multilocularis* were designed, synthesised, and tested. For one part of the project new structures based on the known drug Albendazole were explored in order to find a derivative that could be coupled to a solid support, and subsequently be used in affinity chromatography to elucidate the

molecular target(s) of albendazole-derived structures. Four scaffolds were synthesised that could subsequently be used to be coupled to a solid support. One of the structures provided decent activity in a similar range to the known drug Albendazole, when tested in vitro. Another approach focused on the parasite's metabolism, where its excessive threonine consumption in the metacystode state could be targeted. To achieve this, six known inhibitors of threonine dehydrogenase were synthesised, as no established synthetic route to obtain the inhibitors was known. A concise synthesis was developed, including an activated *N*-hydroxysuccinimide ester as versatile intermediate compound. This allowed for easy synthesis of the six inhibitors but would also allow for further expansion of the library of inhibitors. These inhibitors were tested in vitro revealing mild activity for one of the six synthesised compounds. However, the activity appeared not to be based on inhibition of the threonine dehydrogenase as the parasite was still able to consume threonine from the growth medium in presence of the inhibitors. In future experiments the inhibitors will be tested on purified threonine dehydrogenase. (See chapter 3.1)

In a smaller subproject, pH-sensitive fluorophores were synthesised based on the previously published structure **hNR**. The fluorophores were modified with different reactive groups, such as *N*-hydroxysuccinimide ester, alkynes, and azides. These reactive group allow for conjugation to modified lipids. Another approach used the known pyranine dye as base scaffold, to which lipophilic alkyl amines were conjugated providing a membrane anchored dye. The synthesised fluorophores are employed in evaluating the proton gradient across membranes of proteoliposomes. Conjugation and analysis are ongoing. (See chapter 3.2)

As a versatile probe a trifunctional construct based on unprotected L-cysteine was designed and synthesised. The three functions included an azide anchor, a fluorescent dye and a biotin tag that were attached to cysteine in a simple three step, one pot reaction, exploiting the different reactivities of the three functional groups of cysteine. Starting with the modification of the thiol, followed by conjugation to the amine, and finally formation of an amide from the carboxylic acid. The biological utility of the final probe is currently evaluated by conjugation of the trifunctional probe to an alkyne-modified bovine serum albumin (BSA) and subsequent analysis of the modified BSA. (See chapter 3.3)

In a last part three ubiquinone derivatives with different alkyl chain lengths (**Q₁**, **Q₂** & **decylubiquinone**) were synthesised by partially following literature procedures and developing new and efficient synthetic protocols. The synthesised derivatives were used to characterise *E. coli* cytochrome *b*₅₆₁, an enzyme that catalyses the oxidation of superoxide to oxygen and transfers the electrons onto ubiquinone derivatives, reducing them to ubiquinols. The three ubiquinones were used

to study the reactions and the redox behaviour of the enzyme. The synthesised derivatives as well as a new ubiquinone derivative will be used for further studies. (See chapter 4)

6. Bibliography

1. P. Khongorzul, C. J. Ling, F. U. Khan, A. U. Ihsan and J. Zhang, *Mol. Cancer Res.*, 2020, **18**, 3-19.
2. S. J. Walsh, J. D. Bargh, F. M. Dannheim, A. R. Hanby, H. Seki, A. J. Counsell, X. Ou, E. Fowler, N. Ashman, Y. Takada, A. Isidro-Llobet, J. S. Parker, J. S. Carroll and D. R. Spring, *Chem. Soc. Rev.*, 2021, **50**, 1305-1353.
3. G. T. Hermanson, *Bioconjugate Techniques*, Academic Press, 3rd edn., 2013.
4. V. Chudasama, A. Maruani and S. Caddick, *Nat. Chem.*, 2016, **8**, 114-119.
5. J. R. Junutula, H. Raab, S. Clark, S. Bhakta, D. D. Leipold, S. Weir, Y. Chen, M. Simpson, S. P. Tsai, M. S. Dennis, Y. Lu, Y. G. Meng, C. Ng, J. Yang, C. C. Lee, E. Duenas, J. Gorrell, V. Katta, A. Kim, K. McDorman, K. Flagella, R. Venook, S. Ross, S. D. Spencer, W. Lee Wong, H. B. Lowman, R. Vandlen, M. X. Sliwowski, R. H. Scheller, P. Polakis and W. Mallet, *Nat. Biotechnol.*, 2008, **26**, 925-932.
6. B.-Q. Shen, K. Xu, L. Liu, H. Raab, S. Bhakta, M. Kenrick, K. L. Parsons-Repointe, J. Tien, S.-F. Yu, E. Mai, D. Li, J. Tibbitts, J. Baudys, O. M. Saad, S. J. Scales, P. J. McDonald, P. E. Hass, C. Eigenbrot, T. Nguyen, W. A. Solis, R. N. Fuji, K. M. Flagella, D. Patel, S. D. Spencer, L. A. Khawli, A. Ebens, W. L. Wong, R. Vandlen, S. Kaur, M. X. Sliwowski, R. H. Scheller, P. Polakis and J. R. Junutula, *Nat. Biotechnol.*, 2012, **30**, 184-189.
7. F. A. Liberatore, R. D. Comeau, J. M. McKearin, D. A. Pearson, B. Q. Belonga, S. J. Brocchini, J. Kath, T. Phillips, K. Oswell and R. G. Lawton, *Bioconjugate Chem.*, 1990, **1**, 36-50.
8. R. B. Del Rosario, R. L. Wahl, S. J. Brocchini, R. G. Lawton and R. H. Smith, *Bioconjugate Chem.*, 1990, **1**, 51-59.
9. D. Wei, Y. Mao, Z. Xu, J. Chen, J. Li, B. Jiang and H. Chen, *Bioorg. Med. Chem.*, 2021, **51**, 116497.
10. O. Koniev, I. Dovgan, B. Renoux, A. Ehkirch, J. Eberova, S. Cianférani, S. Kolodych, S. Papot and A. Wagner, *Med. Chem. Commun.*, 2018, **9**, 827-830.
11. B. Shi, M. Wu, Z. Li, Z. Xie, X. Wei, J. Fan, Y. Xu, D. Ding, S. H. Akash, S. Chen and S. Cao, *Cancer Med.*, 2019, **8**, 1793-1805.
12. Q.-Y. Hu and H. Imase, *Methods for making conjugates from disulfide-containing proteins*, WO2014/083505, 2014.
13. F. F. Schumacher, J. P. M. Nunes, A. Maruani, V. Chudasama, M. E. B. Smith, K. A. Chester, J. R. Baker and S. Caddick, *Org. Biomol. Chem.*, 2014, **12**, 7261-7269.
14. J. P. M. Nunes, M. Morais, V. Vassileva, E. Robinson, V. S. Rajkumar, M. E. B. Smith, R. B. Pedley, S. Caddick, J. R. Baker and V. Chudasama, *Chem. Commun.*, 2015, **51**, 10624-10627.

15. M. Morais, J. P. M. Nunes, K. Karu, N. Forte, I. Benni, M. E. B. Smith, S. Caddick, V. Chudasama and J. R. Baker, *Org. Biomol. Chem.*, 2017, **15**, 2947-2952.
16. A. Maruani, M. E. B. Smith, E. Miranda, K. A. Chester, V. Chudasama and S. Caddick, *Nat. Commun.*, 2015, **6**, 6645.
17. A. Maruani, H. Savoie, F. Bryden, S. Caddick, R. Boyle and V. Chudasama, *Chem. Commun.*, 2015, **51**, 15304-15307.
18. M. T. W. Lee, A. Maruani, D. A. Richards, J. R. Baker, S. Caddick and V. Chudasama, *Chem Sci*, 2017, **8**, 2056-2060.
19. E. Robinson, J. P. M. Nunes, V. Vassileva, A. Maruani, J. C. F. Nogueira, M. E. B. Smith, R. B. Pedley, S. Caddick, J. R. Baker and V. Chudasama, *RSC Adv.*, 2017, **7**, 9073-9077.
20. C. Bahou, D. A. Richards, A. Maruani, E. A. Love, F. Javaid, S. Caddick, J. R. Baker and V. Chudasama, *Org. Biomol. Chem.*, 2018, **16**, 1359-1366.
21. S. Shao, M.-H. Tsai, J. Lu, T. Yu, J. Jin, D. Xiao, H. Jiang, M. Han, M. Wang and J. Wang, *Bioorg. Med. Chem. Lett.*, 2018, **28**, 1363-1370.
22. F. Javaid, C. Pilotti, C. Camilli, D. Kallenberg, C. Bahou, J. Blackburn, J. R. Baker, J. Greenwood, S. E. Moss and V. Chudasama, *RSC Chem. Biol.*, 2021, **2**, 1206-1220.
23. S. J. Walsh, S. Omarjee, W. R. J. D. Galloway, T. T. L. Kwan, H. F. Sore, J. S. Parker, M. Hyvönen, J. S. Carroll and D. R. Spring, *Chem. Sci.*, 2019, **10**, 694-700.
24. S. J. Walsh, S. Omarjee, F. M. Dannheim, D.-L. Couturier, D. Bexheti, L. Mendil, G. Cronshaw, T. Fewster, C. Gregg, C. Brodie, J. L. Miller, R. Houghton, J. S. Carroll and D. R. Spring, *Chem. Commun.*, 2022, **58**, 1962-1965.
25. A. R. Hanby, S. J. Walsh, A. J. Counsell, N. Ashman, K. T. Mortensen, J. S. Carroll and D. R. Spring, *Chem. Commun.*, 2022, **58**, 9401-9404.
26. C. Bahou, E. A. Love, S. Leonard, R. J. Spears, A. Maruani, K. Armour, J. R. Baker and V. Chudasama, *Bioconjugate Chem.*, 2019, **30**, 1048-1054.
27. M. T. W. Lee, A. Maruani, J. R. Baker, S. Caddick and V. Chudasama, *Chem. Sci.*, 2016, **7**, 799-802.
28. Y. Koide, Y. Urano, K. Hanaoka, T. Terai and T. Nagano, *ACS Chem. Biol.*, 2011, **6**, 600-608.
29. C. Nicholls, H. Li and J.-P. Liu, *Clin. Exp. Pharmacol. Physiol.*, 2012, **39**, 674-679.
30. M. A. Sirover, *Biochim. Biophys. Acta, Protein Struct. Mol. Enzymol.*, 1999, **1432**, 159-184.
31. M. A. Sirover, *Biochim. Biophys. Acta, Gen. Subj.*, 2011, **1810**, 741-751.
32. The Universal Protein Resource (UniProt), <https://www.uniprot.org/uniprot/P16858>, (accessed 01.04.2022).

33. H. Liu and K. May, *mAbs*, 2012, **4**, 17-23.
34. G. Vidarsson, G. Dekkers and T. Rispens, *Front. Immunol.*, 2014, **5**.
35. L. C. Ozhathil, J.-S. Rougier, P. Arullampalam, M. C. Essers, D. Ross-Kaschitzka and H. Abriel, *Int. J. Mol. Sci.*, 2021, **22**, 3401.
36. T. Pastierik, P. Sebej, J. Medalova, P. Stacko and P. Klan, *J Org Chem*, 2014, **79**, 3374-3382.
37. C. Fischer and C. Sparr, *Angew Chem Int Ed Engl*, 2018, **57**, 2436-2440.
38. J. B. Grimm, T. A. Brown, A. N. Tkachuk and L. D. Lavis, *ACS Cent Sci*, 2017, **3**, 975-985.
39. A. N. Butkevich, G. Lukinavicius, E. D'Este and S. W. Hell, *J Am Chem Soc*, 2017, **139**, 12378-12381.
40. R. Sato, J. Kozuka, M. Ueda, R. Mishima, Y. Kumagai, A. Yoshimura, M. Minoshima, S. Mizukami and K. Kikuchi, *J Am Chem Soc*, 2017, **139**, 17397-17404.
41. Y. Cui, Y. Li, Q. Duan and T. Kakuchi, *Applied Biochemistry and Biotechnology*, 2013, **169**, 239-249.
42. A. W. Schwabacher, J. W. Lane, M. W. Schiesher, K. M. Leigh and C. W. Johnson, *Journal of Organic Chemistry*, 1998, **63**, 1727-1729.
43. S. Tavoulari, D. Lacabanne, C. Thangaratnarajah and E. R. S. Kunji, *Trends Endocrinol Metab*, 2022, DOI: 10.1016/j.tem.2022.05.002.
44. A. del Arco and J. Satrustegui, *J Biol Chem*, 1998, **273**, 23327-23334.
45. K. Kobayashi, D. S. Sinasac, M. Iijima, A. P. Boright, L. Begum, J. R. Lee, T. Yasuda, S. Ikeda, R. Hirano, H. Terazono, M. A. Crackower, I. Kondo, L. C. Tsui, S. W. Scherer and T. Saheki, *Nat Genet*, 1999, **22**, 159-163.
46. A. Del Arco, M. Agudo and J. Satrustegui, *Biochem J*, 2000, **345 Pt 3**, 725-732.
47. M. Iijima, A. Jalil, L. Begum, T. Yasuda, N. Yamaguchi, M. Xian Li, N. Kawada, H. Endou, K. Kobayashi and T. Saheki, *Adv Enzyme Regul*, 2001, **41**, 325-342.
48. SLC Tables on AGC2, <http://slc.bioparadigms.org/protein?GeneName=SLC25A13>, (accessed 29.07.2022).
49. A. del Arco, M. Agudo and J. Satrustegui, *Biochem J*, 2000, **345**, 725-732.
50. T. Saheki, K. Kobayashi and I. Inoue, *Rev Physiol Biochem Pharmacol*, 1987, **108**, 21-68.
51. K. Kobayashi, H. Kakinoki, T. Fukushige, N. Shaheen, H. Terazono and T. Saheki, *Human Genetics*, 1995, **96**, 454-463.

52. M. Iijima, M. A. Jalil, L. Begum, T. Yasuda, N. Yamaguchi, M. X. Li, N. Kawada, H. Endou, K. Kobayashi and T. Saheki, *Advances in Enzyme Regulation*, Vol 41, 2001, **41**, 325-342.
53. Y. Lin, Y. Liu, L. Zhu, K. Le, Y. Shen, C. Yang, X. Chen, H. Hu, Q. Ma, X. Shi, Z. Hu, J. Yang, Y. Shen, C. H. Lin, C. Huang and X. Huang, *J Inherit Metab Dis*, 2020, **43**, 467-477.
54. A. Tabata, J. S. Sheng, M. Ushikai, Y. Z. Song, H. Z. Gao, Y. B. Lu, F. Okumura, M. Iijima, K. Mutoh, S. Kishida, T. Saheki and K. Kobayashi, *J Hum Genet*, 2008, **53**, 534-545.
55. A. Kikuchi, N. Arai-Ichinoi, O. Sakamoto, Y. Matsubara, T. Saheki, K. Kobayashi, T. Ohura and S. Kure, *Mol Genet Metab*, 2012, **105**, 553-558.
56. Y. B. Lu, K. Kobayashi, M. Ushikai, A. Tabata, M. Iijima, M. X. Li, L. Lei, K. Kawabe, S. Taura, Y. Yang, T. T. Liu, S. H. Chiang, K. J. Hsiao, Y. L. Lau, L. C. Tsui, D. H. Lee and T. Saheki, *J Hum Genet*, 2005, **50**, 338-346.
57. P. Wongkittichote, C. Sukasem, A. Kikuchi, W. Aekplakorn, L. T. Jensen, S. Kure and D. Wattanasirichaigoon, *World J Gastroenterol*, 2013, **19**, 7735-7742.
58. P. Borst, *IUBMB Life*, 2020, **72**, 2241-2259.
59. A. K. Hopp, P. Gruter and M. O. Hottiger, *Cells*, 2019, **8**.
60. J. B. Chappell, *Br Med Bull*, 1968, **24**, 150-157.
61. T. Saheki, K. Inoue, H. Ono, Y. Fujimoto, S. Furuie, K. I. Yamamura, E. Kuroda, M. Ushikai, A. Asakawa, A. Inui, K. Eto, T. Kadowaki, M. Moriyama, D. S. Sinasac, T. Yamamoto, T. Furukawa and K. Kobayashi, *Mol Genet Metab*, 2017, **120**, 306-316.
62. S. Rabinovich, A. Silberman, L. Adler, S. Agron, S. Levin-Zaidman, A. Bahat, Z. Porat, E. Ben-Zeev, I. Geva, M. Itkin, S. Malitsky, A. Buchaklian, D. Helbling, D. Dimmock and A. Erez, *Oncogene*, 2020, **39**, 164-175.
63. C. Thangaratnarajah, J. J. Ruprecht and E. R. Kunji, *Nat Commun*, 2014, **5**, 5491.
64. L. Palmieri, B. Pardo, F. M. Lasorsa, A. del Arco, K. Kobayashi, M. Iijima, M. J. Runswick, J. E. Walker, T. Saheki, J. Satrustegui and F. Palmieri, *EMBO J*, 2001, **20**, 5060-5069.
65. J. J. Ruprecht, M. S. King, T. Zogg, A. A. Aleksandrova, E. Pardon, P. G. Crichton, J. Steyaert and E. R. S. Kunji, *Cell*, 2019, **176**, 435-447 e415.
66. E. P. Carpenter, K. Beis, A. D. Cameron and S. Iwata, *Curr Opin Struct Biol*, 2008, **18**, 581-586.
67. J. Birch, H. Cheruvara, N. Gamage, P. J. Harrison, R. Lithgo and A. Quigley, *Biology (Basel)*, 2020, **9**.

68. Membrane Proteins of Known 3D Structure Database, <https://blanco.biomol.uci.edu/mpstruc/>, (accessed 15.07.2022).
69. S. C. Shoemaker and N. Ando, *Biochemistry*, 2018, **57**, 277-285.
70. G. Weissenberger, R. J. M. Henderikx and P. J. Peters, *Nat Methods*, 2021, **18**, 463-471.
71. R. Nygaard, J. Kim and F. Mancia, *Curr Opin Struct Biol*, 2020, **64**, 26-33.
72. W. Kuhlbrandt, *Science*, 2014, **343**, 1443-1444.
73. Z. Wang, C. Ye, X. Zhang and Y. Wei, *Anal Bioanal Chem*, 2015, **407**, 3683-3691.
74. M. S. King and E. R. S. Kunji, in *Expression, Purification, and Structural Biology of Membrane Proteins*, eds. C. Perez and T. Maier, Springer US, New York, NY, 2020, DOI: 10.1007/978-1-0716-0373-4_4, pp. 47-61.
75. D. Jambaudon, K. Shimamoto, Y. Yasuda-Kamatani, M. Scanziani, B. H. Gähwiler and U. Gerber, *Proc Natl Acad Sci U S A*, 1999, **96**, 8733-8738.
76. W. T. Hodges, C. Jarasvaraparn, D. Ferguson, K. Griffett, L. E. Gill, Y. Chen, M. X. G. Ilagan, L. Hegazy, B. Elgendy, K. Cho, G. J. Patti, K. S. McCommis and B. N. Finck, *J Biol Chem*, 2022, **298**, 101554.
77. S. Tavoulari, T. J. J. Schirris, V. Mavridou, C. Thangaratnarajah, M. S. King, D. T. D. Jones, S. Ding, I. M. Fearnley and E. R. S. Kunji, *Mol Metab*, 2022, **60**, 101469.
78. J. C. Hildyard, C. Ammala, I. D. Dukes, S. A. Thomson and A. P. Halestrap, *Biochim Biophys Acta*, 2005, **1707**, 221-230.
79. J. Simonin, S. K. Vernekar, A. J. Thompson, J. D. Hothersall, C. N. Connolly, S. C. Lummis and M. Lochner, *Bioorg Med Chem Lett*, 2012, **22**, 1151-1155.
80. X. Y. Sun, T. Liu, J. Sun and X. J. Wang, *Rsc Adv*, 2020, **10**, 10826-10847.
81. N. D. Amoedo, G. Punzi, E. Obre, D. Lacombe, A. De Grassi, C. L. Pierri and R. Rossignol, *Biochim Biophys Acta*, 2016, **1863**, 2394-2412.
82. J. Song, G. Lu, B. Yang, M. Bai, J. Li, F. Wang, T. Lei and S. Jiang, *Tetrahedron*, 2022, **122**, 132933.
83. Schokolade-Muffins, https://www.bettybossi.ch/de/Rezept/ShowRezept/BB_VEG130401_0279A-40-de, (accessed 03.10.2022).
84. A. Veerareddy, G. Surendrareddy and P. K. Dubey, *Synthetic Communications*, 2013, **43**, 2236-2241.
85. L. A. Carpino, *Journal of Organic Chemistry*, 1970, **35**, 3971-&.
86. J. Eckert and P. Deplazes, *Clin Microbiol Rev*, 2004, **17**, 107-135.
87. L. Dick, Master Thesis, University of Bern, 2018.

88. D. A. Vuitton, H. Zhou, S. Bresson-Hadni, Q. Wang, M. Piarroux, F. Raoul and P. Giraudoux, *Parasitology*, 2003, **127**(S1), S87-107.
89. J. Horton, *The Efficacy of Anthelmintics: Past, Present, and Future, Controlling Disease Due to Helminth Infections*, World Health Organisation, Genf, 2004.
90. R. W. Ammann, A. Fleiner-Hoffmann, F. Grimm and J. Eckert, *J Hepatol*, 1998, **29**, 994-998.
91. P. A. Friedman and E. G. Platzer, *Biochim Biophys Acta*, 1978, **544**, 605-614.
92. E. Lacey, *Parasitol Today*, 1990, **6**, 112-115.
93. B. Lundstrom-Stadelmann, R. Rufener, D. Ritler, R. Zurbriggen and A. Hemphill, *Food Waterborne Parasitol*, 2019, **15**, e00040.
94. E. Brunetti, P. Kern, D. A. Vuitton and W.-I. Writing Panel for the, *Acta Trop*, 2010, **114**, 1-16.
95. T. Junghanss, A. M. da Silva, J. Horton, P. L. Chiodini and E. Brunetti, *Am J Trop Med Hyg*, 2008, **79**, 301-311.
96. D. W. Gottschall, V. J. Theodorides and R. Wang, *Parasitol Today*, 1990, **6**, 115-124.
97. E. L. Rodriguez, S. Poddar, S. Iftekhar, K. Suh, A. G. Woolfork, S. Ovbude, A. Pekarek, M. Walters, S. Lott and D. S. Hage, *J Chromatogr B Analyt Technol Biomed Life Sci*, 2020, **1157**, 122332.
98. P. B. Alexander, J. Wang and S. L. McKnight, *Proc Natl Acad Sci U S A*, 2011, **108**, 15828-15833.
99. A. Bowyer, H. Mikolajek, J. W. Stuart, S. P. Wood, F. Jamil, N. Rashid, M. Akhtar and J. B. Cooper, *J Struct Biol*, 2009, **168**, 294-304.
100. J. Wang, P. Alexander, L. Wu, R. Hammer, O. Cleaver and S. L. McKnight, *Science*, 2009, **325**, 435-439.
101. D. Ritler, R. Rufener, J. V. Li, U. Kampfer, J. Muller, C. Buhr, S. Schurch and B. Lundstrom-Stadelmann, *Sci Rep*, 2019, **9**, 19438.
102. I. J. Tsai, M. Zarowiecki, N. Holroyd, A. Garcarrubio, A. Sanchez-Flores, K. L. Brooks, A. Tracey, R. J. Bobes, G. Frago, E. Sciutto, M. Aslett, H. Beasley, H. M. Bennett, X. Cai, F. Camicia, R. Clark, M. Cucher, N. De Silva, T. A. Day, P. Deplazes, K. Estrada, C. Fernandez, P. W. H. Holland, J. Hou, S. Hu, T. Huckvale, S. S. Hung, L. Kamenetzky, J. A. Keane, F. Kiss, U. Koziol, O. Lambert, K. Liu, X. Luo, Y. Luo, N. Macchiaroli, S. Nichol, J. Paps, J. Parkinson, N. Pouchkina-Stantcheva, N. Riddiford, M. Rosenzvit, G. Salinas, J. D. Wasmuth, M. Zamanian, Y. Zheng, C. Taenia solium Genome, J. Cai, X. Soberon, P. D. Olson, J. P. Laclette, K. Brehm and M. Berriman, *Nature*, 2013, **496**, 57-63.
103. *CN Pat.*, CN1147507A, 1997.

104. H. Uchiro and S. Kobayashi, *Tetrahedron Lett*, 1999, **40**, 3179-3182.
105. E. V. Bellale, M. K. Chaudhari and K. G. Akamanchi, *Synthesis-Stuttgart*, 2009, DOI: 10.1055/s-0029-1216955, 3211-3213.
106. B. Stadelmann, M. Spiliotis, J. Muller, S. Scholl, N. Muller, B. Gottstein and A. Hemphill, *Int J Parasitol*, 2010, **40**, 1563-1574.
107. B. Stadelmann, S. Scholl, J. Muller and A. Hemphill, *J Antimicrob Chemother*, 2010, **65**, 512-519.
108. B. Stadelmann, R. Rufener, D. Aeschbacher, M. Spiliotis, B. Gottstein and A. Hemphill, *PLoS Negl Trop Dis*, 2016, **10**, e0004535.
109. G. A. El-Hiti, A. Hussain, A. S. Hegazy and M. H. Alotaibi, *J Sulfur Chem*, 2011, **32**, 361-395.
110. N. Dolder and C. von Ballmoos, *Chembiochem*, 2020, DOI: 10.1002/cbic.202000146.
111. N. Dolder, PhD Thesis, University of Bern, 2022.
112. G. C. Kemmer, S. A. Bogh, M. Urban, M. G. Palmgren, T. Vosch, J. Schiller and T. G. Pomorski, *Analyst*, 2015, **140**, 6313-6320.
113. G. Niu, P. Zhang, W. Liu, M. Wang, H. Zhang, J. Wu, L. Zhang and P. Wang, *Anal Chem*, 2017, **89**, 1922-1929.
114. B. Finkler, C. Spies, M. Vester, F. Walte, K. Omlor, I. Riemann, M. Zimmer, F. Stracke, M. Gerhards and G. Jung, *Photochem Photobiol Sci*, 2014, **13**, 548-562.
115. N. Amdursky, Y. Lin, N. Aho and G. Groenhof, *Proc Natl Acad Sci U S A*, 2019, **116**, 2443-2451.
116. B. J. Leslie and P. J. Hergenrother, *Chem Soc Rev*, 2008, **37**, 1347-1360.
117. E. M. Sletten and C. R. Bertozzi, *Angew Chem Int Ed Engl*, 2009, **48**, 6974-6998.
118. D. Tscherrig, PhD Thesis, Universität Bern, 2019.
119. K. Zheng, Y. Chen, J. Wang, L. Zheng, M. Hutchinson, J. Persson and J. Ji, *J Pharm Sci*, 2019, **108**, 133-141.
120. S. I. Presolski, V. P. Hong and M. G. Finn, *Curr Protoc Chem Biol*, 2011, **3**, 153-162.
121. A. Schild, R. Bhardwaj, N. Wenger, D. Tscherrig, P. Kandasamy, J. Dernic, R. Baur, C. Peinelt, M. A. Hediger and M. Lochner, *Int J Mol Sci*, 2020, **21**.
122. S. Kappel, T. Kilch, R. Baur, M. Lochner and C. Peinelt, *Int J Mol Sci*, 2020, **21**.
123. A. Hofer, G. Kovacs, A. Zappatini, M. Leuenberger, M. A. Hediger and M. Lochner, *Bioorg Med Chem*, 2013, **21**, 3202-3213.

124. M. Serafini, C. Cordero-Sanchez, R. Di Paola, I. P. Bhela, S. Aprile, B. Purghe, R. Fusco, S. Cuzzocrea, A. A. Genazzani, B. Riva and T. Pirali, *J Med Chem*, 2020, **63**, 14761-14779.
125. L. D. Lavis, T. Y. Chao and R. T. Raines, *Chem Sci*, 2011, **2**, 521-530.
126. A. Knight, J. L. Hemmings, I. Winfield, M. Leuenberger, E. Frattini, B. G. Frenguelli, S. J. Dowell, M. Lochner and G. Ladds, *J Med Chem*, 2016, **59**, 947-964.
127. G. Deganutti, K. Barkan, B. Preti, M. Leuenberger, M. Wall, B. G. Frenguelli, M. Lochner, G. Ladds and C. A. Reynolds, *ACS Pharmacol Transl Sci*, 2021, **4**, 314-326.
128. M. J. Wall, E. Hill, R. Huckstepp, K. Barkan, G. Deganutti, M. Leuenberger, B. Preti, I. Winfield, S. Carvalho, A. Suchankova, H. Wei, D. Safitri, X. Huang, W. Imlach, C. La Mache, E. Dean, C. Hume, S. Hayward, J. Oliver, F. Y. Zhao, D. Spanswick, C. A. Reynolds, M. Lochner, G. Ladds and B. G. Frenguelli, *Nat Commun*, 2022, **13**, 4150.
129. L. Aurelio, C. Valant, B. L. Flynn, P. M. Sexton, A. Christopoulos and P. J. Scammells, *J Med Chem*, 2009, **52**, 4543-4547.
130. C. J. Draper-Joyce, R. Bhola, J. Wang, A. Bhattarai, A. T. N. Nguyen, I. Cowie-Kent, K. O'Sullivan, L. Y. Chia, H. Venugopal, C. Valant, D. M. Thal, D. Wootten, N. Panel, J. Carlsson, M. J. Christie, P. J. White, P. Scammells, L. T. May, P. M. Sexton, R. Danev, Y. Miao, A. Glukhova, W. L. Imlach and A. Christopoulos, *Nature*, 2021, **597**, 571-576.
131. L. Lu and F. Chen, *Synthetic Communications*, 2004, **34**, 4049-4053.

7. Curriculum Vitae

Philipp Grossenbacher

List of publications

2022 Grossenbacher, Philipp, et al. "Bioorthogonal site-selective conjugation of fluorescent dyes to antibodies: method and potential applications" *RSC Advances* 2022, **12**, 28306-28317. <https://doi.org/10.1039/d2ra05580e>

Abou-Hamdan, Abbas, et al. "Functional design of bacterial superoxide: Quinone oxidoreductase." *Biochimica et Biophysica Acta (BBA)-Bioenergetic* 2022, **7**,148583. <https://doi.org/10.1016/j.bbabi.2022.148583>

2021 Máille, Gearóid M. Ó., et al. "Modulation of N[^] N'-bidentate chelating pyridyl-pyridylidene amide ligands offers mechanistic insights into Pd-catalysed ethylene/methyl acrylate copolymerisation." *Dalton transactions* ,2021, **50**, 6133-6145. <https://doi.org/10.1039/D1DT00389E>

*red bull oder rotwy, darling, mängisch muess me sech entscheide, nid
aus wird besser, we mes mischt, obschon me mängisch scho chly
schtuunt, was e mönsch so aues vertreit*

Kreissaal – Patent Ochsner

8. Declaration of Originality

Last name, first name: Grossenbacher, Philipp

Matriculation number: 11-127-669

I hereby declare that this thesis represents my original work and that I have used no other sources except as noted by citations.

All data, tables, figures, and text citations which have been reproduced from any other source, including the internet, have been explicitly acknowledged as such.

I am aware that in case of non-compliance, the Senate is entitled to withdraw the doctorate degree awarded to me based on the present thesis, in accordance with the “Statut der Universität Bern (Universitätsstatut; UniSt)”, Art. 69, of 7 June 2011.

Place, date Bern, 16.12.2022

Signature Philipp Grossenbacher

A handwritten signature in black ink, consisting of a stylized 'P' followed by a horizontal line and a vertical stroke.